DEVELOPMENT OF A PERFORMANCE-BASED SEISMIC DESIGN PHILOSOPHY FOR MID-RISE WOODFRAME CONSTRUCTION

NEESWOOD

SEISMIC TESTING OF A FULL-SCALE MID-RISE BUILDING: THE NEESWOOD CAPSTONE TEST



By

Shiling Pei, John W. van de Lindt, Steven E. Pryor, Hidemaru Shimizu, Hiroshi Isoda and Douglas R. Rammer

Technical Report MCEER-10-0008 ▪ December 1, 2010

This research was conducted at Colorado State University and was supported by the National Science Foundation under Grant No. CMMI-0529903 (NEES Research) and CMMI-0402490 (NEES Operations).

Sponsored by the
National Science Foundation
NSF Grant Number CMMI-0529903 and CMMI-0402490

Project Title
Development of a Performance-Based Seismic Design
Philosophy for Mid-Rise Woodframe Construction

Project Team
Colorado State University
University of Delaware
University at Buffalo, State University of New York
Rensselaer Polytechnic Institute
Texas A&M University

Web Site
http://jwv.eng.ua.edu/neeswood_reports.html

DISCLAIMER

NEESWood Report No. 4

Seismic Testing of a Full-Scale Mid-Rise Building: The NEESWood Capstone Test

by

Shiling Pei,[1] John W. van de Lindt,[2] Steven E. Pryor,[3] Hidemaru Shimizu,[4]
Hiroshi Isoda[5] and Douglas Rammer[6]

Publication Date: December 1, 2010
Submittal Date: September 30, 2010

Technical Report MCEER-10-0008

NSF Grant Numbers CMMI-0529903 and CMMI-0402490
George E. Brown, Jr. Network for Earthquake Engineering Simulation (NEES)
Program of the National Science Foundation

1 Assistant Professor, Department of Civil and Environmental Engineering, South Dakota State University; former Post-Doctoral Researcher, Department of Civil Engineering, Colorado State University
2 Professor and Garry Neil Drummond Endowed Chair in Civil Engineering, Department of Civil, Construction, and Environmental Engineering, The University of Alabama; former Associate Professor, Department of Civil Engineering, Colorado State University
3 Building Systems Research and Development Manager, Simpson Strong-Tie Company
4 Research Associate, Hyogo Earthquake Engineering Research Center of Japan's National Research Institute for Earth Science and Disaster Prevention (NIED)
5 Associate Professor, Department of Architecture & Civil Engineering, Shinshu University, Japan
6 Research General Engineer, Forest Products Laboratory, USDA Forest Service

MCEER
University at Buffalo, State University of New York
Red Jacket Quadrangle, Buffalo, NY 14261
Phone: (716) 645-3391; Fax (716) 645-3399
E-mail: *mceer@buffalo.edu*; WWW Site: *http://mceer.buffalo.edu*

Project Overview

NEESWood: Development of a Performance-Based Seismic Design Philosophy for Mid-Rise Woodframe Construction

While woodframe structures have historically performed well with regard to life safety in regions of moderate to high seismicity, these types of low-rise structures have sustained significant structural and nonstructural damage in recent earthquakes. To date, the height of woodframe construction has been limited to approximately four stories, mainly due to a lack of understanding of the dynamic response of taller (mid-rise) woodframe construction, nonstructural limitations such as material fire requirements, and potential damage considerations for nonstructural finishes. Current building code requirements for engineered wood construction around the world are not based on a global seismic design philosophy. Rather, wood elements are designed independently of each other without considering the influence of their stiffness and strength on the other structural components of the structural system. Furthermore, load paths in woodframe construction arising during earthquake shaking are not well understood. These factors, rather than economic considerations, have limited the use of wood to low-rise construction and, thereby, have reduced the economical competitiveness of the wood industry in the U.S. and abroad relative to the steel and concrete industry. This project sought to take on the challenge of developing a direct displacement based seismic design philosophy that provides the necessary mechanisms to safely increase the height of woodframe structures in active seismic zones of the U.S. as well as mitigating damage to low-rise woodframe structures. This was accomplished through the development of a new seismic design philosophy that will make mid-rise woodframe construction a competitive option in regions of moderate to high seismicity. Such a design philosophy falls under the umbrella of the performance-based design paradigm.

In Year 1 of the NEESWood Project, a full-scale seismic benchmark test of a two-story woodframe townhouse unit that required the simultaneous use of the two three-dimensional shake tables at the University of Buffalo's NEES node was performed. As the largest full-scale three-dimensional shake table test ever performed in the U.S., the results of this series of shake table tests on the townhouse serve as a benchmark for both woodframe performance and nonlinear models for seismic analysis of woodframe structures. These efficient analysis tools provide a platform upon which to build the direct displacement based design (DDBD) philosophy. The DDBD methodology relies on the development of key performance requirements such as limiting inter-story deformations. The method incorporates the use of economical seismic protection systems such as supplemental dampers and base isolation systems in order to further increase energy dissipation capacity and/or increase the natural period of the woodframe buildings.

The societal impacts of this new DDBD procedure, aimed at increasing the height of woodframe structures equipped with economical seismic protection systems, is also investigated within the scope of this NEESWood project. Following the development of the DDBD philosophy for mid-rise (and all) woodframe structures, it was applied to the seismic design of a mid-rise (six-story) multi-family residential woodframe condominium/apartment building. This mid-rise woodframe structure was constructed and tested at full-scale in a series of shake table tests on the E-Defense (Miki) shake table in Japan. The use of the E-Defense shake table, the largest 3-D shake table in the world, was necessary to accommodate the height and payload of the mid-rise building.

This report describes the seismic testing of a full-scale seven-story mid-rise wood frame building. The building was designed using a new performance-based seismic design (PBSD) philosophy developed within the NEESWood project. It was constructed at the E-Defense facility in Miki, Japan over a four-month period with construction materials shipped from the U.S. and Canada. A series of shake table tests were carried out, first on a seven-story hybrid structure with a steel moment frame at the first story. In the second phase, the steel moment frame story was "locked down" with cross bracing members and the six-story wood-only structure was subjected to three seismic tests, with maximum ground motion intensity approximately corresponding to a 2,475 year return period. The building performed very well with maximum averaged inter-story drifts of about 2% and suffered only minor nonstructural damage. The testing program, called the Capstone test program, was the largest wood frame building shake table test to date and provided a landmark data set for the performance of mid-rise woodframe buildings during earthquakes, and validated the effectiveness of the PBSD procedure developed in the NEESWood project.

Project Team

John W. van de Lindt, Ph.D., Principal Investigator: Professor and Garry Neil Drummond Endowed Chair, Department of Civil, Construction and Environmental Engineering, The University of Alabama, Box 870205, Tuscaloosa, AL 35487-0205; *jwvandelindt@eng.ua.edu;* formerly of Colorado State University.

Rachel A. Davidson, Ph.D., Co-Principal Investigator: Associate Professor, Department of Civil and Environmental Engineering, University of Delaware, Newark, DE 19716-3120; *rdavidso@udel.edu.*

Andre Filiatrault, Ph.D. Eng., Co-Principal Investigator: Professor Department of Civil, Structural, and Environmental Engineering, State University of New York at Buffalo, Buffalo, NY 14261; *af36@buffalo.edu*.

David V. Rosowsky, Ph.D., Co-Principal Investigator: Professor and Dean of Engineering, Department of Civil and Environmental Engineering, Rensselaer Polytechnic Institute, 110 8th Street, Troy, NY 12180-3590; *rosowd@rpi.edu*; formerly of Texas A&M University.

Michael D. Symans, Ph.D., Co-Principal Investigator: Associate Professor, Department of Civil and Environmental Engineering, Rensselaer Polytechnic Institute, 110 8th Street, Troy, NY 12180-3590; *symans@rpi.edu*.

Abstract

This report presents the results of a shake table testing program of a full-scale mid-rise light-frame wood apartment building tested at the world's largest shake table in Miki, Japan as part of the NEESWood project funded by U.S. National Science Foundation. The objectives of the test program were to (1) demonstrate that the performance-based seismic design procedure developed as part of the NEESWood project worked on the full scale building, i.e., validate the design philosophy to the extent one test can; and (2) gain a better understanding of how mid-rise light-frame wood buildings respond, in general, to a major earthquake while providing a landmark data set to the seismic engineering research community. The six-story building (with an additional steel moment frame story at bottom) consisted of 1350 square meters of living space and had twenty-three apartment units; approximately half one-bedroom units and half two-bedroom units. The building was constructed over a 14 week period and lifted to the shake table where it was subjected to three earthquakes ranging from seismic intensities corresponding to the 72 year event to the 2500 year event for Los Angeles, CA. The building was instrumented with just over 300 sensors and 50 LED optical tracking points to measure the component and global responses, respectively. The building was found to perform excellently with little damage even following the 2500 year earthquake. The inter-story drift was well controlled thus validating the effectiveness of the performance-based seismic design philosophy developed in the NEESWood project.

Acknowledgments

The authors are grateful to the co-investigators of the NEESWood project team including David V. Rosowsky, Andre Filiatrault, Rachel A. Davidson, and Michael D. Symans. Thank you also to Weichiang Pang of Clemson University for his participation in the design portion of the NEESWood Capstone building.

Thank you to NSF REU's Doug Allen and Kathryn Pfrefzschner, researchers Izumi Nakamura, Chikahiro Minowa, N. Kawai, and Mikio Koshihara at the University of Tokyo. Two graduate students, Kazuki Tachibana and Tomoya Okazaki, contributed to the construction and instrumentation of the NEESWood Capstone building and a former Ph.D. student, Kimberly Cronin, assisted with the architectural design of the Capstone building early in the project. Kelly Cobeen performed the original IBC design of the building in collaboration with Kimberly Cronin.

Thank you also to Tim Ellis of Simpson Strong Tie Co., David Clyne and Mr Yumoto of Maui Homes USA. Technical collaborators beyond the authors affiliation included the U.S. Forest Product Laboratory, FP Innovations-Forintek Division, and Maui Homes U.S.A. Financial and in-kind product and personal donations were provided by Simpson Strong Tie, Maui Homes, B.C. Ministry of Housing and Social Development, Stanley Bostitch, Strocal Inc., Structural Solutions Inc., Louisiana Pacific Corp., Natural Resources Canada, Forestry Innovation Investment, APA-The Engineered Wood Association, American Forest and Paper Association, Canadawood, Howdy, Ainsworth, Calvert Glulam, and the 2x4 Association of Japan.

Table of Contents

Table of Contents (Cont'd)

Table of Contents (Cont'd)

List of Figures

List of Figures (Cont'd)

List of Tables

Chapter 1 Introduction

Light-frame wood buildings represent the vast majority of the building stock in North America. Most of these buildings are single- and multi-family dwellings with a moderate percentage being light commercial construction. Historically, light-frame wood buildings have performed relatively well during earthquakes from a life-safety standpoint but not necessarily from a damage and property loss standpoint. Much of the damage following the 1994 Northridge earthquake was felt to be the result of excessive inter-story drifts. Since that time significant progress in better understanding and modeling the seismic response of light-frame wood buildings has been made by researchers essentially laying the foundation to move to performance-based seismic design (PBSD) of wood frame buildings. The performance of mid-rise wood frame buildings during earthquakes had not been adequately examined. As a result, the NEESWood project was funded through the George E. Brown Jr. Network for Earthquake Engineering Simulation (NEES) program of the National Science Foundation to address the challenge specifically better understanding the behavior of mid-rise woodframe construction within the framework of performance-based seismic design. The contents of this report summarize the preparation, shake table testing and results of the NEESWood Capstone test building, a seven-story condominium building designed using the performance-based seismic design procedures developed within the NEESWood project. Testing took place in the summer of 2009 at the world's largest shake table, known as E-Defense, in Miki, Japan.

Full-scale seismic testing, i.e. shake table testing, is one of the most reliable investigation methods used by researchers to study the seismic performance of building structures. For woodframe buildings, full-scale seismic testing has only been performed a handful of times worldwide. During the CUREE Caltech Woodframe project, Filiatrault et al (2001) tested a rectangular two-story house with an integrated one car garage. The building was limited by the size of the available shake table, but provided state of the art testing results nonetheless. The building was subjected to two 1994 Northridge recordings, i.e. the Canoga Park and Rinaldi stations. It was concluded that overall the performance was adequate and that non-structural finishes such as gypsum wall board (GWB) and stucco significantly contributed in increasing both the strength and stiffness of the system (Filiatrault et al, 2004). Another shake table test during the CUREE Caltech Woodframe project was of a three-story apartment building with a tuck under garage (Mosalam, 2003). The results of that series of tests confirmed that these types of structures were prone to torsional response and soft story collapse mechanisms. In the first year of the NEESWood project (van de Lindt et al, 2006), Filiatrault et al (2010) conducted full-scale tri-axial tests of a two-story three-bedroom 160m^2 (1800 sq ft) townhouse with an integrated two-car garage utilizing the twin shake tables at the State University of New York at Buffalo's SEESL laboratory. That report is also available as part of the NEESWood report series (NW-01, 2007). This building, called the Benchmark structure, was designed to the 1988 Uniform Building Code (UBC, 1988) and was intended to benchmark the seismic performance of existing buildings in California and other high seismic regions. The benchmark structure performed relatively well by seemingly protecting life safety of would-be occupants, but suffered substantially costly damage. Filiatrault et al (2010) was also able to validate the earlier conclusion that non-structural elements such as GWB and exterior stucco significantly increase the strength and stiffness thereby contributing to the seismic performance of wood frame buildings. The NEESWood Capstone test summarized in this report is the first time a full scale light-frame wood building exceeding three stories has ever been tested on a shake table.

1.1 Description of the NEESWood Project

The NEESWood project seeks to take on the challenge of developing a performance based seismic design philosophy and providing the necessary design procedures to safely increase the height of woodframe structures in active seismic zones of the U.S. as well as providing a mechanism to mitigate damage to low-rise woodframe buildings. This will be accomplished through a variety of research and development tasks including numerical investigation, shake table testing, wood frame building performance evaluation, and development of a performance based seismic design procedure.

In Year 1 of the NEESWood Project, a full-scale seismic benchmark tests of a two-story woodframe townhouse that requiring simultaneous use of the two three-dimensional shake tables at the SUNY-Buffalo NEES node was performed. As the largest full-scale three-dimensional shake table test ever performed in the U.S., the results of this series of shake table tests on the townhouse served as a benchmark for both woodframe performance and nonlinear models for seismic analysis of woodframe structures. Innovative seismic protection systems, i.e. supplemental dampers, were also incorporated into one of the test phases of the Benchmark test. A full study on dampers in woodframe building is also available on a separate NEESWood report (Shinde and Symans, 2010).

Numerical models and tools were developed and calibrated with the Benchmark test results. These efficient analysis tools provided a platform upon which to build the performance-based seismic design (PBSD) philosophy. The PBSD methodology developed in NEESWood project focuses on limiting damage and relies on the design constraints related to key performance requirements such as limiting inter-story drifts. The methodology also provides for the incorporation of economical seismic protection systems such as supplemental dampers and base isolation systems as options. These types of seismic protective systems further increase energy dissipation capacity and/or increase the natural period of woodframe buildings.

The societal impacts of this new PBSD procedure, aimed at limiting earthquake induced damage to woodframe structures was also investigated within the scope of the NEESWood project.

As a verification for the PBSD procedure for mid-rise (and all) woodframe structures developed in the NEESWood project, the procedure was applied to the seismic design of a mid-rise (six-story) multi-family residential woodframe apartment building. The PBSD procedure known as “direct displacement design” is detailed in another NEESWood report (Pang and Rosowsky, 2009). This mid-rise woodframe structure, with an optional steel moment frame first story, was constructed and tested at full-scale in a series of shake table tests on the E-Defense (Miki) shake table in Japan as detailed herein. The use of the E-Defense shake table, the largest 3-D shake table in the world, was necessary to accommodate the height and payload of the mid-rise building. The testing program, called the Capstone test program, represented the largest wood frame building shake table test to date and provides a landmark data set for the performance of mid-rise woodframe buildings during earthquakes and validates the effectiveness of the performance-based seismic design procedure developed in the NEESWood project.

1.2 Description of NEESWood Capstone Testing Program

The Capstone test buildings’ architecture was based on a realistic multi-family apartment building or condominium that might be typical of an urban infill building in Northern or Southern California. The building has seven stories total: six-stories of light-frame wood containing twenty-three living units and a bottom story Steel Special Moment Frame (SMF) at level 1. The architectural concept of the Capstone test building is shown in Figure 1.1, with relative size of the building to the shake table also illustrated. The building was tested in two different configurations during two phases of the test program:

Phase I: The seven-story mixed-use building, investigating the viability of incorporating a steel moment frame bottom story for multi-story wood frame construction.

Phase II: The SMF was locked down with tightened cross bracing to become an extension of the shake table and the six-story light-frame wood building was tested.

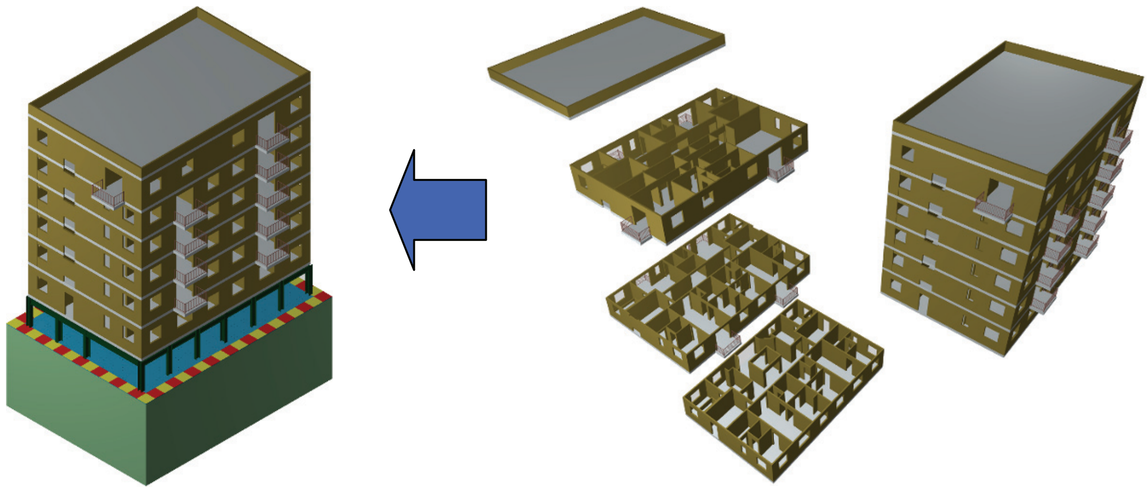

Figure 1.1: NEESWood Capstone test building

The height of the Capstone test building from the ground level to the roof (including the height of the SMF) was 66.3 ft and its total weight was 797.4 kips. The foot print of the floor plan was approximately 40x60 ft. Shear walls within the building were sheathed with 15/32" thick OSB panels. Half inch thick gypsum wallboard was installed on the inside of the building and the ceiling. The exterior walls of the building were not finished, i.e. no stucco or siding.

Multiple seismic tests were conducted for the two configurations of the Capstone test building described earlier. The first configuration included the interaction of the SMF and wood superstructure. The second configuration included only the wood frame structure since the SMF were adequately locked down by diagonal bracing members to behave as a fixed base. A total of five seismic tests were included in the test program. Low amplitude uni-axial white noise tests were also conducted between the seismic tests to identify any change in the dynamic characteristics of the test building in each direction. The test building was inspected for damage after each test. No repairs were conducted in between the tests since the structure was designed to survive most of the tests with only minor damage. Additional seismic weight was placed in the test building at all levels to bring the weight to the design weight which remained the same for all tests (see Appendix F for details).

One set of tri-axial historical ground motions were used for all seismic tests: an ordinary ground motion recorded during the Northridge earthquake at the Canoga Park recording station was used. The ground motion was scaled to represent a somewhat frequent earthquake having a probability of exceedance of 50% in 50 years, a Design Basis Earthquake (DBE) having a probability of exceedence of 10% in 50 years (10%/50 years), and a Maximum Credible Earthquake (MCE) having a probability of exceedence of 2% in 50 years (2%/ 50 years), or a return period of 2475 years. There was also a test conducted in Phase I with an intensity level between DBE and MCE event, corresponding to a 665 year return period (7%/50 years).

The Capstone test building was instrumented with over 300 channels of displacement, acceleration, and strain measurements during the various tests. A separate optical tracking system was employed to measure the absolute displacement of 50 points on the exterior of the building during the tests. Due to the limitation on the number of high speed cameras available for the optical tracking system, only three sides of the structure could be optically tracked for absolute deformation during the test.

Chapter 2 Capstone Test Building and Testing Objectives

This chapter provides a description of the Capstone test building, and information on the experimental set-up that was used to conduct the series of shake table tests. A brief summary of the testing objectives of each test phase is included in the last section.

2.1 Description of Capstone Test building

The test building was a six-story wood frame apartment building with one additional (optional) steel moment frame (SMF) story at the bottom, with a floor plan representative of a typical residential multi-story condominium in California. It was constructed at full scale with twenty-three living units for the wood portion providing approximately 14,400ft^2 of residential living space. The optional bottom steel story had 2,400ft^2 of retail commercial space. The dead load of the building was estimated based on a force-based design of the same architectural plan per IBC (2006), including finishing materials such as floor tile, insulation, air conditioning units, wiring, and plumbing. Although the building was actually designed using PBSD, this dead load was used. During the test, supplemental seismic weights in the form of steel plates were attached to the structure at each floor to bring the actual seismic weight for each story to the design weight. The height of the wood six-story structure was 55.7 ft. The SMF story was 10.5 ft in height. With all the supplement weight included, the total weight of the wood only six-story building was 628 kips (285 metric tons). The total weight of the seven-story wood-steel hybrid building was 797 kips (361 metric tons)

There was no exterior finishing material installed on the exterior of the building. For all interior walls, 1/2 in. thick gypsum wallboard was installed with #6 x 1.625" bugle head screws at 16" spacing everywhere on both sides (i.e. not a "float" drywall installation) except for walls in the stair well (only had drywall on one side) and the double mid-ply walls which will be described later (do not have drywall installed). The drywall panels were purchased in Japan, with a unit weight of approximately 2lb/ft^2 and was "normal" strength Japanese drywall (Note: Drywall in Japan is available in three different strengths). The drywall was installed with tape and putty on all joints except the wall-to-ceiling joints and corners. Finishing as many joints as possible was desirable in order to provide realistic damage inspection results. The first wood story (hereafter referred to as Story 2 in this report) floor plan of the test building is shown in Figure 2.1, with the boundary of the E-defense shake table also shown. Similarly, Figures 2.2 shows the floor plan for Story 3 to 6. The floor plan of the top story, Story 7, is shown in Figure 2.3. The steel moment frame grid at the top of Story 1 is shown in Figure 2.4. Figure 2.5 shows elevation views of the test building. The detailed architectural and structural plans for the test building can be found in Appendix A. The structural details of all shear walls in the buildings are included in Appendix B of this report.

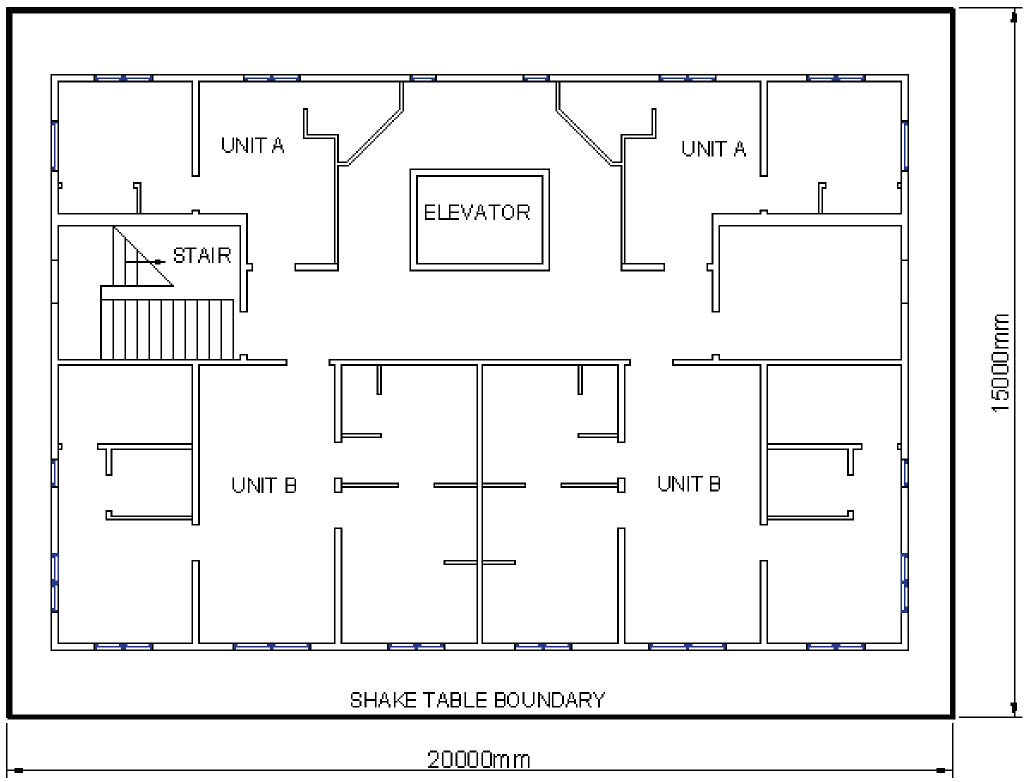

Figure 2.1: Floor plan for Story 2 of the Capstone test building

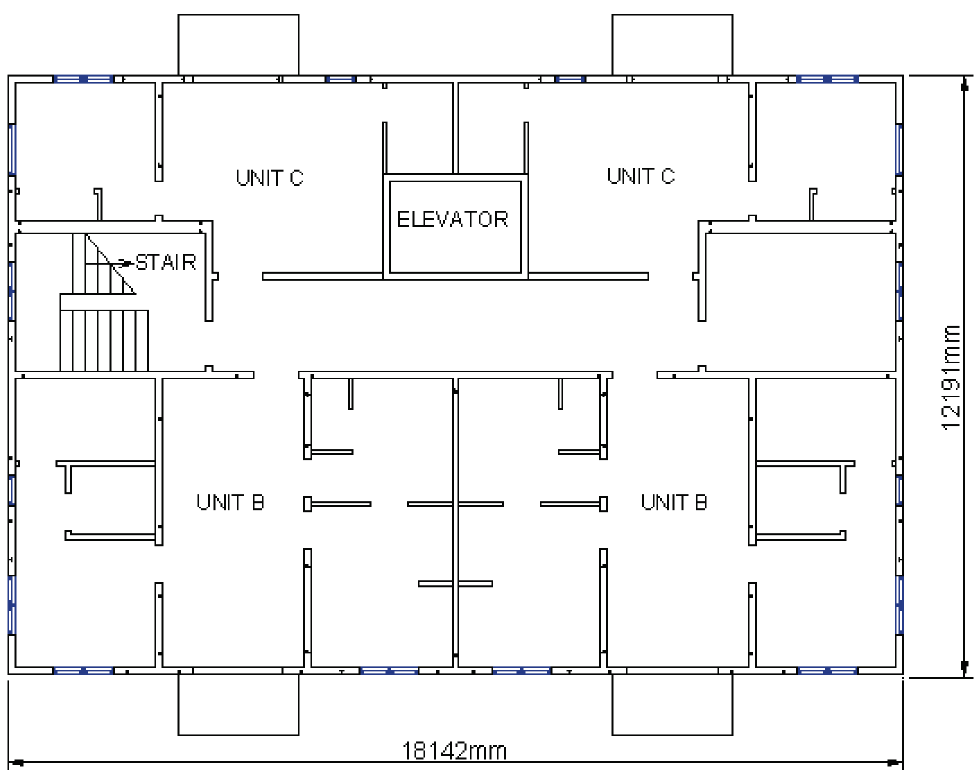

Figure 2.2: Floor plan for Story 3~6 of the Capstone test building

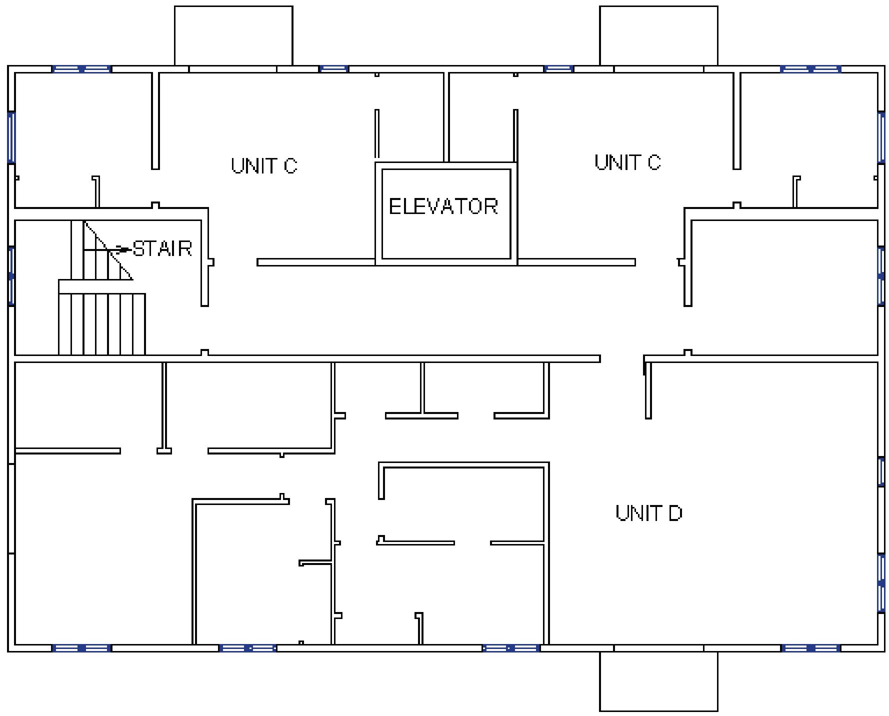

Figure 2.3: Floor plan for Story 7 of the Capstone test building

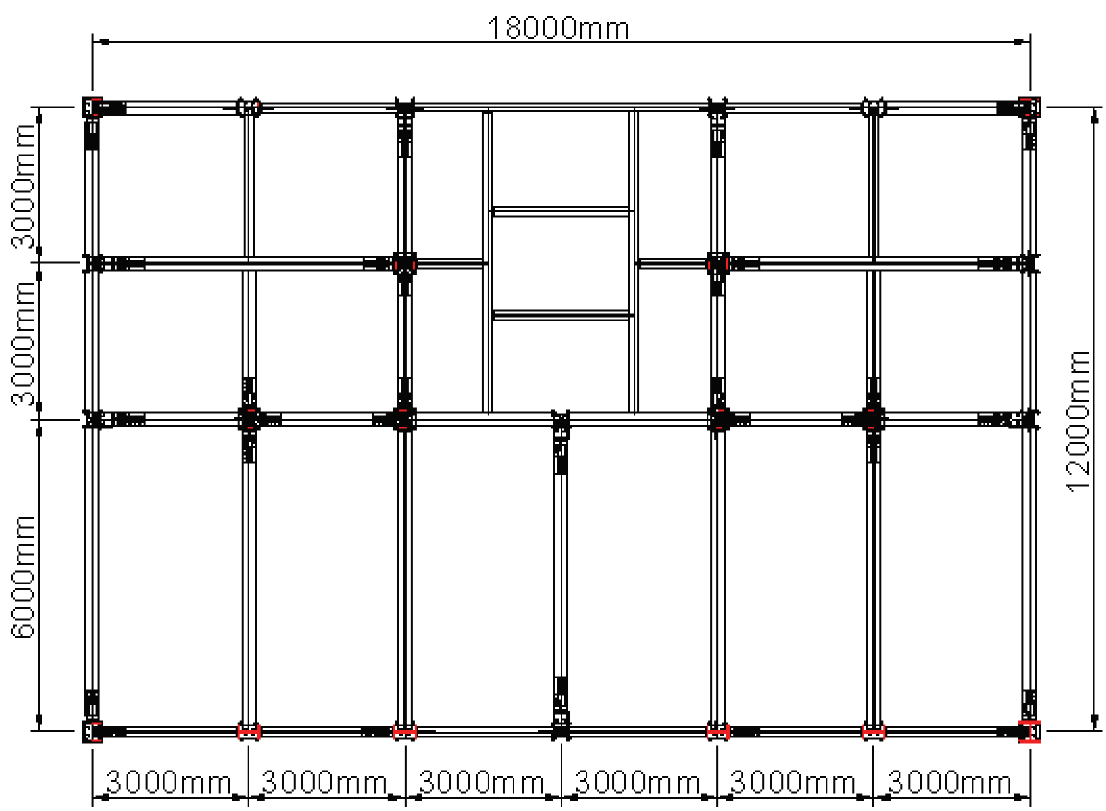

Figure 2.4: Plan view of the SMF grid of the Capstone test building

Figure 2.5: Elevation view of the Capstone test building (Steel cross bracings not shown)

Most of framing materials for the shear walls of the Capstone test building were 2x6 dimensional lumber. The sill plates were 3x6 dimensional lumbers (please refer to Appendix B for detailed designation of sill plate type, wood species, sheathing nail pattern, and framing layout). Some 2x8 dimensional lumber was used to construct the end-studs for double Midply shear walls at each story. The single Midply shear wall is a concept that originated in Canada and was expanded to a double Midply shear wall during the design of the test building. Wall B1 in Appendix B show the design configuration details for these walls. Additional information on Midply walls can be found in Pei et al. (2010). The top plates for regular shear walls consisted of double 2x6 members, while the sill plate and the interior studs are single members. Regular studs were spaced at 16 in. on center wherever possible. There were also compression stud packs installed for each shear wall that consisted of 8 to 12 2x6 studs depending on the amount of compression force imposed on shear wall ends in the design. Two different wood species were used in construction. Douglas Fir-Larch North (DFL-N) was used for the bottom 3 wood stories and all sill plates. Machine rated (MR) SPF 1650 was used for top 3 wood stories.

The floor system for the Capstone test building consisted of 9-1/2” LP Joists installed between 5-1/8” x 9” glulam shear collectors with top-mount joist hangers. A slice of half inch (15/32”) thick OSB was attached to the bottom of the 5x9” glulam so that the glulam had the same height as the joist. The roof was constructed with 14” LP Joist and LVL rim-board of the same height. Standard 18mm (23/32 inch) T&G Oriented Strand Board (OSB) was used for floor and roof sheathing. Air driven 10d common nail was used for floor and roof nailing. A nail pattern of 4”/12” was used for the floor sheathing for first 3 floors, and the rest of the floors and the roof had a 6”/12” nail pattern. There were framing straps used at certain locations on the floor in order to provide load transferring continuity. Details for all straps can be found in the framing tie drawings in Appendix A.

Continuous Anchor Tie-down Systems (ATS) from Simpson Strong-Tie Company were installed at both ends of every shear wall in the building, together with shrinkage compensation devices also from Simpson. The system served as the hold-down mechanism for stacked shear walls to limit the uplift and rocking of these walls. The sheathing-to-framing connectors were gun driven 10d common Stanley Bostitch nails.

The steel moment frame story was designed by Simpson Strong-Tie company in collaboration with Colorado State University. The frame was manufactured in California by Strocal Inc of Stockton and assembled in Japan by Simpson Strong-Tie. The SMF also served as the lifting frame for the entire structure after it was constructed. Detailed construction drawings for the SMF can also be found in Appendix A.

Figure 2.6 shows a photo of the completed Capstone test building at the building site in the E-defense laboratory prior to being lifted on to the shake table. A more detailed description of the materials used in construction of the Capstone test building and the details involved in the construction process can be found in Chapter 5 of this report.

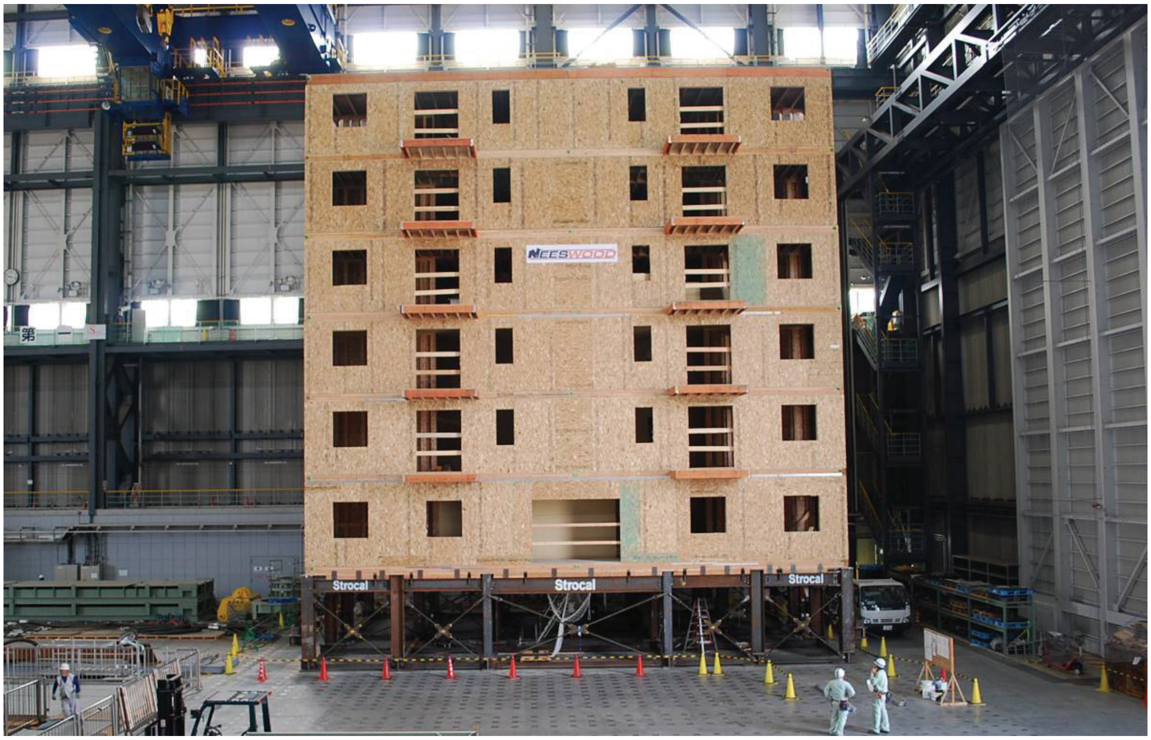

Figure 2.6: Completed Capstone test building at the construction site inside the E-Defense laboratory

2.2 Experimental Set-up

Shake table testing of a building the size of the Capstone test specimen necessitated the use of the E-Defense shake table in Miki City, Japan. This shake table is the largest (tri-axial) shake table in the world with a payload capacity of 2.5 million pounds and the ability to reproduce the largest recorded records from many of the world's large earthquakes. The facility was built following the 1995 Kobe earthquake and opened in 2004. The NEESWood Capstone test was the first U.S. led test conducted at E-Defense and represents the largest building structure ever tested at full scale on a shake table. Figure 2.7 shows a picture of the E-defense facility shortly after it opened in 2004.

Figure 2.7: Aerial image of the E-Defense facility in 2004.

The shake table is shown in Figure 2.8 from the first floor balcony inside the E-defense laboratory. It is approximately 50ft x 65ft and has the ability to operate in either acceleration or displacement control. For safety it was necessary to have approximately one meter clear space around the perimeter of the shake table. For the installation of the test specimen on the table, it was critical to align the walls (and steel frame under the walls) with the shake table bolt pattern. Based on these constraints the floor plan layout superimposed on the E-Defense shake table pattern is shown in Figure 2.9 (with the floor plan of Story 2 shown in the figure).

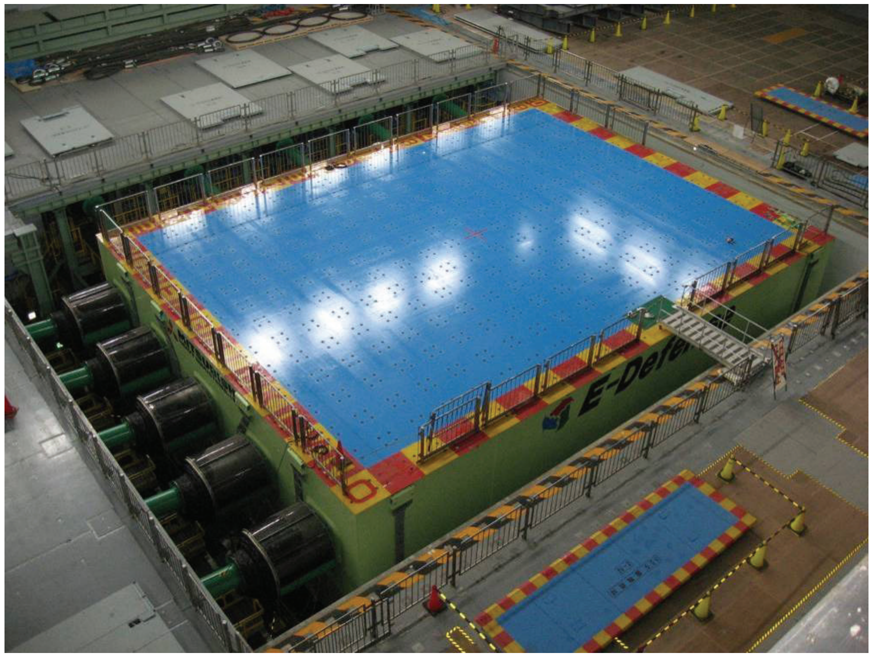

Figure 2.8: E-Defense shake table with actuator CV joints shown exposed on left side

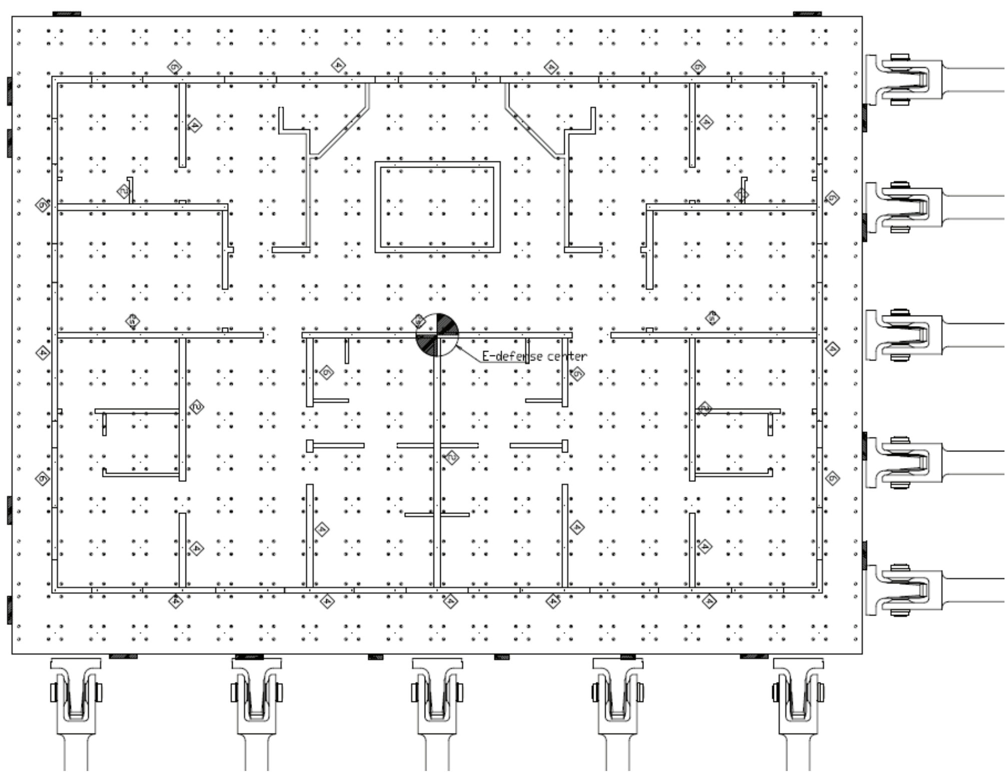

Figure 2.9: Layout of building walls with shake table bolt pattern superimposed

The Capstone test building was attached to the shake table with special anchor rods connecting the existing hole pattern on the shake table and steel moment frame pedestals at the base of each column. Figure 2.10 shows a detail for the seating of the building by the overhead cranes on to the shake table.

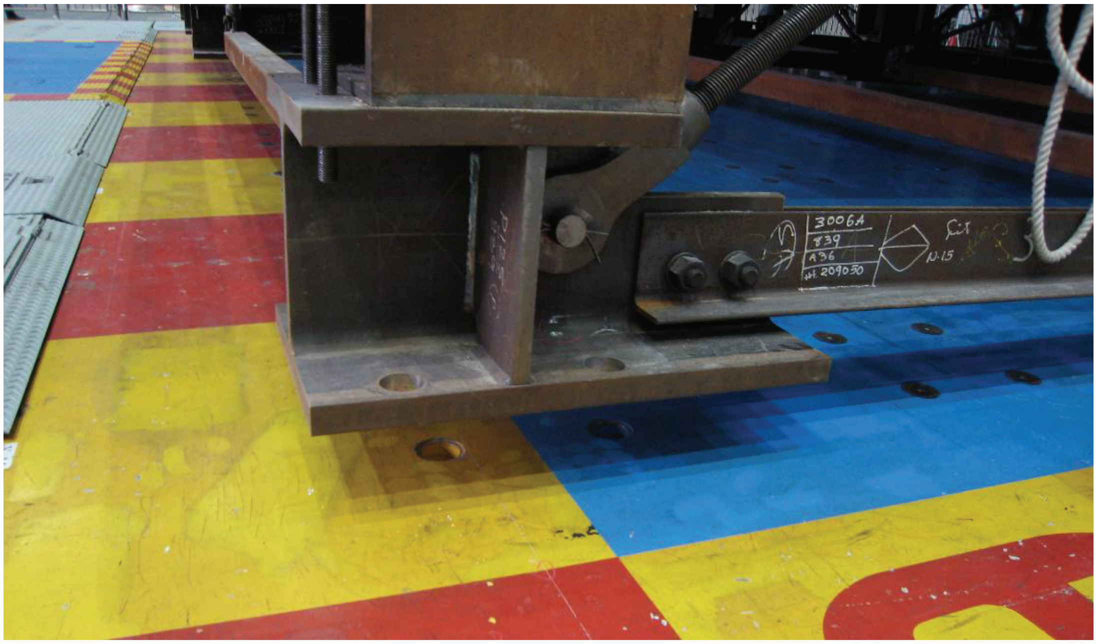

Figure 2.10: Seating of the specimen on the E-defense table

2.3 Test Objectives

The NEESWood Capstone tests at E-Defense had three (3) major objectives:

Objective 1: To confirm that a representative mid-rise woodframe structure designed using the NEESWood PBSD philosophy satisfies the performance objectives, as pre-defined during the design process. These performance objectives were developed as part of the project and seek to limit damage and losses while protecting life safety.

Objective 2: Provide a general understanding of the behavior of a mid-rise woodframe structure similar to those currently in place in the Western U.S. and provide a full-scale data set for verification and calibration of nonlinear dynamic models.

Objective 3: Confirm that a representative mixed-use seven-story steel-woodframe mixed-use building designed using the NEESWood design philosophy satisfies the performance objectives, as pre-defined during the design process. Obtain a better understanding of how to combine wood and steel to provide more building options in areas of high seismicity.

Recall that there were two test phases in the Capstone test program; each with a different building configuration. The first configuration involved loosening all cross bracings for the SMF, allowing the SMF to act as the first story of the 7-story wood-steel hybrid building structure. This configuration focused on Objective 3 listed above. Then the cross bracings were tightened to make the SMF essentially an extension of the shake table, allowing the testing of a six-story wood frame building in Phase II. The Phase II testing focused on objective 1 and 2 above. A detailed description of the instrumentation set up for the Capstone test building is summarized in Chapter 4 of this report. The data obtained from these tests is the first database for a mid-rise woodframe test at full scale, thus providing the first database for mid-rise Woodframe building numerical model development and calibration. In addition to the instrumentation, detailed damage inspections were performed following each seismic test. These damage inspections provided key information which was used to verify damage control as the result of PBSD and also to establish the correlation between building performance and seismic intensity levels.

The shear wall configuration for Capstone test building was designed using the Direct Displacement Design (DDD) approach (Pang and Rosowsky, 2009) which had certain prescribed performance expectations at different seismic intensity levels. The NEESWood project team, with input from the project advisory committee, defined the four seismic intensity levels as:

Level 1: Earthquake intensity having a 50% chance of being exceeded in 50 years. This corresponds to a 72 year return period.
Level 2: Earthquake intensity having a 10% chance of being exceeded in 50 years. This corresponds to a 475-year return period. Corresponds *approximately* to the Design-Basis Earthquake (DBE).

Level 3: Earthquake intensity having a 2% chance of being exceeded in 50 years. This corresponds to a 2500-year return period. Corresponds to the Maximum Credible Earthquake (MCE).
Level 4: Optional Near Fault: Un-scaled near-fault ground motions. This is an optional seismic hazard for use depending on the location of a building with respect to the fault and/or the owner's desired performance expectation.

Each of the seismic intensity levels described above was combined with a particular performance expectation. Table 2.1 presents the performance expectations from Christovasillis et al. (2007) which were developed based on the Benchmark tests at the University at Buffalo. The Benchmark test report is available in NEESWood Project report NW-01.

Table 2.1. Performance Expectations (Derived from Christovasilis et al, 2007)

Performance Expectations	**Corresponding Peak Inter-story Drift (%)**	**Wood Framing and OSB/Plywood Sheathing**	**Gypsum Wall Board (GWB)**
Level A	0.1 – 1.0%	Minor Splitting and cracking of sill plates (some propagation) Slight sheathing nail withdraw	Slight cracking of GWB Diagonal propagation from door/window openings Partial screw withdraw Cracking at ceiling-to-wall interface
Level B	1.0 - 2.0%	Permanent differential movement of adjacent panels Corner sheathing nail pullout Cracking/splitting of sill/top plates	Crushing at corners of GWB Cracking of GWB taped/mud joints
Level C	2.0 - 4.0%	Splitting of sill plates equal to anchor bolt diameter Cracking of studs above anchor bolts Possible failure of anchor bolts	Separation of GWB corners in ceiling Buckling of GWB at openings
Level D	4.0 - 7.0%	Severe damage across edge nail lines, separation of sheathing Vertical posts uplifted Failure of anchor bolts	Large pieces separated from framing Entire joints separated and dislodged

Each performance level is specified by a probability of non-exceedance (NE) of an inter-story drift limit at a specified level of seismic hazard as shown in Table 2.2. For example, at seismic intensity level 1 the building should not exceed a median inter-story drift of 1%. At a level 3 seismic intensity the non-exceedance percentile was moved from the 50^{th} percentile, i.e. median, to the 80^{th} percentile because the 4% drift limit was close to what was felt to be the threshold between repairable damage and collapse. Thus it was assumed to be more critical during the design.

Table 2.2. Capstone test building design expectations

	Seismic hazard (Intensity) Level			
Performance Expectations	**Level 1**	**Level 2**	**Level 3**	**Level 4**
Level A (1%)	**50% NE**			
Level B (2%)		**50% NE**		
Level C (4%)			**80% NE**	
Level D (7%)				**50% NE**

Chapter 3 Description of Shake Table Tests

This chapter describes the two types of shake table tests that were performed on the Capstone test building; specifically the white noise excitation tests and the seismic tests. The characteristics of the input motions that were used for each type of tests are reported, along with information on the synchronizing of the displacement (optical tracking) data with the other instrumentation. In addition, the seismic weight added to the Capstone test building is also introduced.

3.1 Test Protocols

3.1.1 White Noise Excitation Tests

The main objective of the white noise excitation tests was to identify the natural period of the building and monitor for possible degradation of the building stiffness indicative of damage during the seismic tests. Additional analysis on the white noise excitation test results can be performed to obtain other characteristics of the structure including mode shapes and modal damping ratios. But these analyses are not included in the scope of this report. All seismic and white noise result data is available to the public at NEES website.

The input excitation was an acceleration-controlled random noise with a frequency band between 0.1-10 Hz provided by the E-defense. The acceleration record was scaled to have a maximum value of 0.05g and was applied to the X, Y, and Z direction of the building separately (uni-axial) during a period of about 2 minutes. The sampling rate of the recorded data was 200 Hz (this is the sampling rate for all measurements except for the optical tracking measurements, which has a sampling rate of 100 Hz). No additional filtering was applied to the raw data. The time history of input acceleration is shown in Figure 3.1.

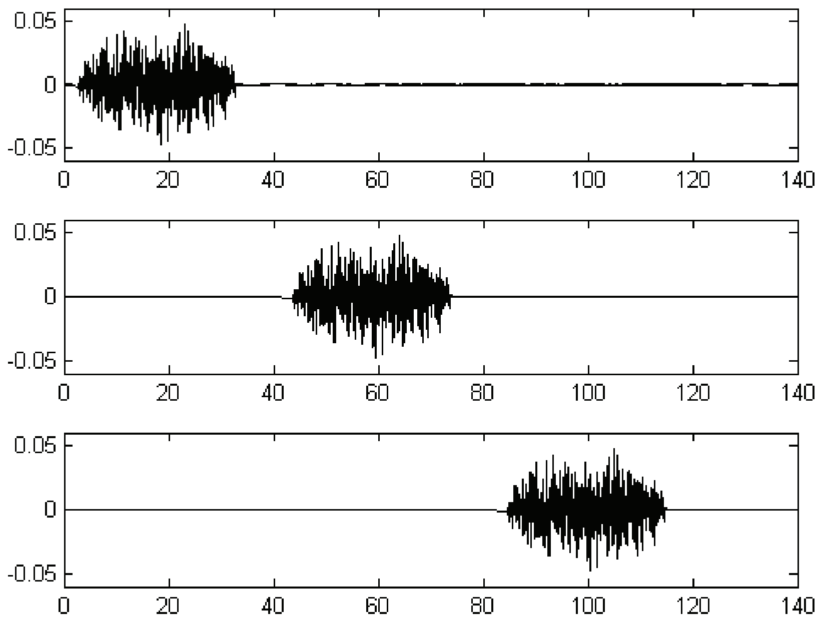

Figure 3.1: Input white noise record used in the test

White noise tests described above were conducted at the beginning of the test program, in between seismic tests, and at the end of the test program. There were a total of 9 white noise tests conducted for the Capstone test building, as listed in Table G.1 in Appendix G. Also listed in the table are the resulting fundamental periods of the building obtained from the spectral analysis of the averaged acceleration measurement at the roof level. WN3 test was performed after WN2 due to the tightening of the ATS anchor nuts at the steel moment frame level which were found to be loose after the WN2 test. WN8 was conducted after WN7 because Test 5 was conducted on a different day than Test 4 and WN7.

3.1.2 Seismic Tests

The main objective of the seismic tests was to determine the performance of the Capstone test building under several levels of seismic intensity. The input motions used for the seismic tests were selected from the recorded 1994 Northridge Earthquake ground motions in California. Canoga Park ground motion, recorded at Topanga Canyon (USC Station 90053) which was located at a distance of 15.8 km from the fault rupture. This record was used as the input motion for all seismic tests in the Capstone test program. The acceleration time-histories of the three components of the Canoga Park record are shown in Figure 3.2. The acceleration response spectra of the three un-scaled components of the Canoga Park record for 5% damping are presented in Figure 3.3. Through application of different scaling factors, the ground motion represents different seismic hazard levels used in the NEESWood project. A scaling factor of 0.53 was used to represent a seismic event with 50% probability of exceedance in 50 years (72 year return period). The ground motion with an amplitude-scaling factor of 1.20 was considered to represent a Design Basis Earthquake (DBE) event with a 10% probability of exceedance in 50 years or a return period of 475 years. A scaling factor of 1.80 was used in this study to represent a Maximum Credible Earthquake (MCE) with a 2% probability of exceedance in 50 years or a return period of 2475 years. In addition to these three hazard levels, the Canoga Park ground motions were scaled to produce an additional level of 7%/50 years (665 year return period) in order to adequately engage the steel moment frame participation during the end of Phase I testing and at the same time limit damage to the wood frame structure above.

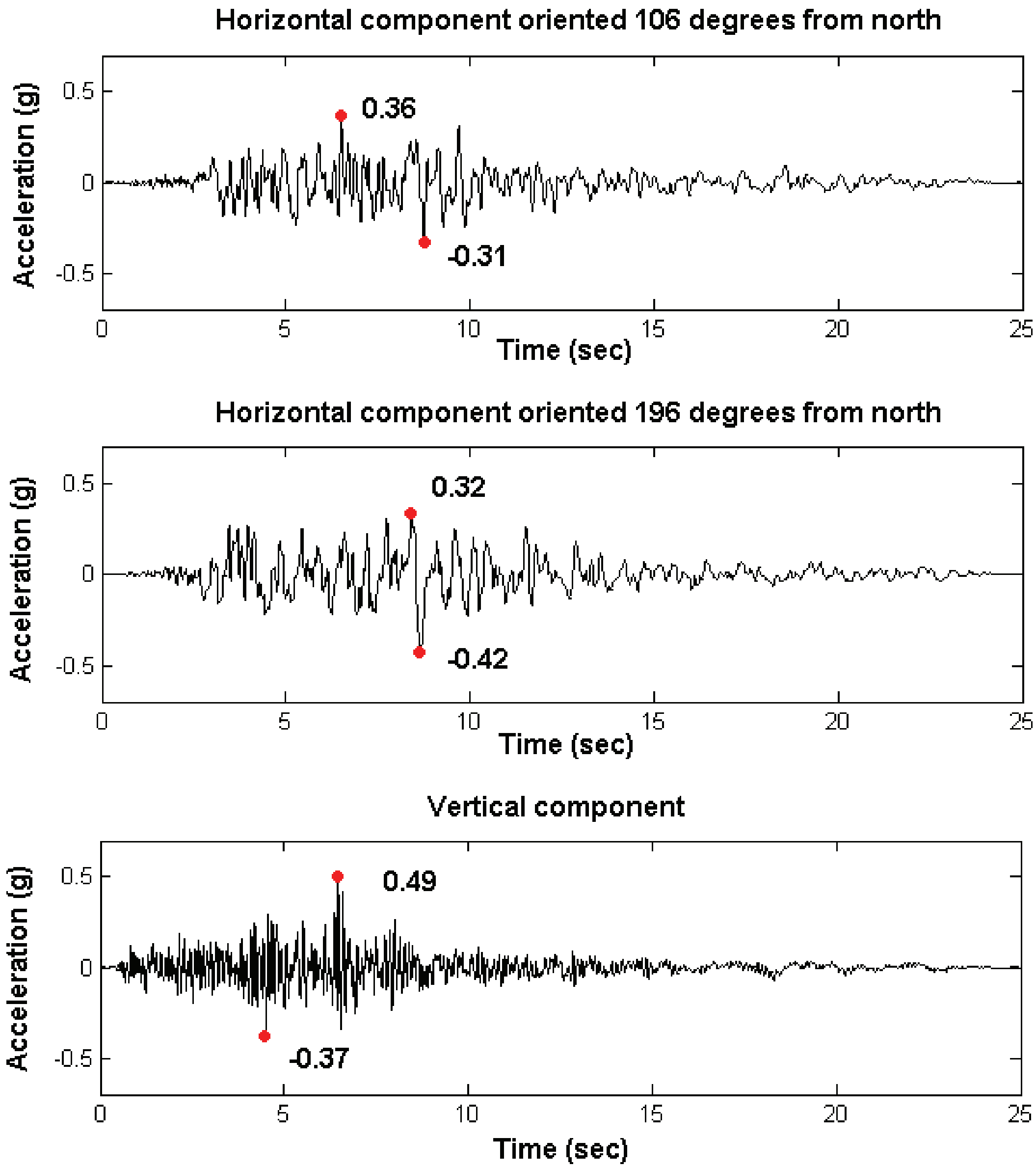

Figure 3.2: Three components of the unscaled Northridge Canoga Park ground motion record

The horizontal component oriented 106 degree from North (CP 106 and RN 318) was applied in the short (X) direction of the Capstone test building, while the horizontal component oriented 196 degree from North (CP 196 and RN 228) was applied in the long (Y) direction. The vertical component was applied in the vertical direction of the Capstone test building. The amplitude scaling factors and the resulting peak ground accelerations for each component are listed in Table 3.1 for all levels of seismic intensity.

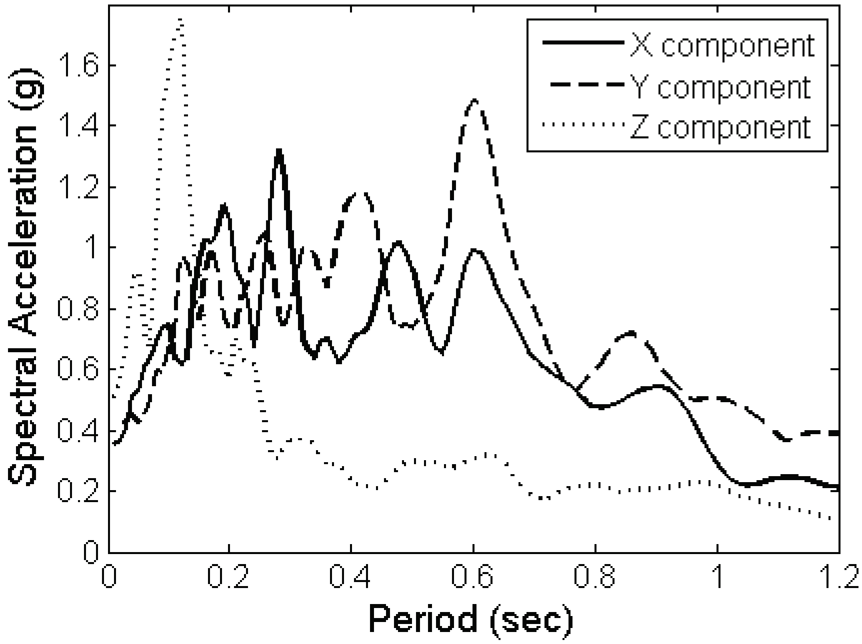

Figure 3.3: Acceleration response spectra of unscaled Canoga Park record for 5% damping

Table 3.1: Ground motions for seismic tests

Seismic test	Test date	Structure	Hazard level	Scaling factor	PGA (g)		
					X	Y	Z
1	6/30/2009	Wood-Steel	50%/50 yr	0.53	0.19	0.22	0.26
2			7%/50 yr	1.40	0.50	0.58	0.69
3	7/6/2009	Wood-only	50%/50 yr	0.53	0.19	0.22	0.26
4			10%/50 yr	1.20	0.43	0.50	0.59
5	7/14/2009		2%/50 yr	1.80	0.65	0.75	0.88

In summary, there were five seismic tests performed on three separate days. The input ground motions were four scaled versions of the Canoga Park record from the 1994 Northridge Earthquake. All of the five tests were tri-axial tests that simulate all of the ground motion components. It should be noted that there was no repair or modifications of the structure during the entire testing program.

3.2 Structural Configurations for Shake Table Tests

The two seismic tests conducted for the seven-story mixed-use building configuration in Phase I were both on June 30th, 2009, as shown in Table 3.1. The second configuration in Phase II was the six-story wood-only configuration, in which the cross bracing members for the steel moment frame were tightened so that the steel moment frame served as an extension of the shake table and the six story wood frame building above. There were three seismic tests conducted for this configuration on July 6th, 2009 and July 14th, 2009, as shown in Table 3.1.

3.3 Data Acquisition and Synchronization

Except for the optical tracking displacement data, all of the data from white noise and seismic tests were collected through the high speed data acquisition system at the E-Defense laboratory. The sampling rate for all data was 200 Hz and there was no additional filter applied to these data. The optical tracking displacement data was captured with a 100 Hz sampling rate, and there was no additional filter applied to these data.

The synchronization of the optical tracking data and the E-Defense system data was done using a synchronization signal at the beginning of each test. The E-Defense data acquisition system recorded data before the optical track system data acquisition was started. As the E-Defense data acquisition system became active, a sustained 5 volt signal was fed to the computer controlling the optical tracking system. Then before the ground motion started, this signal will drop from 5 to 0 volt, which triggered the beginning of the optical tracking data acquisition. The first record in the optical tracking data should be synchronized with the E-Defense data point 1/100 second after the voltage signal went from 5 to 0 volts. The synchronizing signal can be found in the 05.csv file for every seismic and white noise test data files under the column entitled “PARUSU”.

3.4 Description of Shake Table Tests

The Capstone test program consisted of a total of five (5) shake table tests conducted on three separate test days. After the test specimen was successfully moved to the table on the June 22nd,2009, it took about a week to connect all instrumentation, rearrange and attach seismic weights, loosen all steel moment bracing members, and testing all the data acquisition systems.

The first two seismic tests (test ID 1 and 2) and 4 white noise tests were conducted on June 30th, 2009 with the hybrid seven story building configuration. After the first seismic test, there was a 90 minute window for damage inspection teams to record the damage with sketches and photos. The damage teams were made up of volunteer researchers and students. It was discovered that there were some loose anchor nuts on the steel moment frame that held the ATS rods (they were designed to be snug-tight nuts without pretension). These nuts were re-tightened to their design condition. An additional white noise test (WN3) was conducted after this change in the structure. The second seismic test was conducted in the afternoon on the same day, but the damage inspection for seismic test 2 was performed the next day.

Following the June 30th tests, the diagonal truss members on the SMF were tightened sufficiently in order to remove the participation of the steel moment frame for Phase II of the program. The procedure for test 3 and 4 for the July 6th tests followed the same sequence as the June 30th tests, with the exception that there was no additional white noise test conducted on that day.

The last seismic test (Test 5) was conducted on July 14th. In order to observe the effect of earthquake acceleration in the building, one of the rooms in the seventh story was furnished with simple furniture (see Figure 3.4). Damage inspection following this last test was conducted in two subsequent days following the test.

Figure 3.4: A furnished room on the 7th story of Capstone test building for test 5

3.5 Design Weight Distribution and Total Weight of Capstone Test Building

Additional weights were installed in the Capstone test building to bring the weight of the test building up to the design weight. This included approximately 25psf floor dead load and 16psf roof dead load. The as-built structural dead weights were calculated for each story and compared with the force-based design seismic weight in order to find the amount of supplemental weight for each story. Extra gypsum wall panels and building materials (studs, OSB) left in each story after completion of the building were all re-arranged and fixed to the floor based on the amount of weight needed at each story. The total building weights are provided in Table F.1 in Appendix F. The total weight reading of the cranes from the lifting of the building onto the shake table confirmed the accuracy of the as-built building weight estimation.

Appendix F contains all the information related to the supplemental weights for the Capstone test building for all test levels. All of these weights were effectively anchored on the floor using customized wood frames, SDS screws (a special type of self-tapping wood screw from Simpson Strong-Tie Company), and nails. There were six types of supplemental weight used in the test. Each of the weight types are listed in Appendix F with detailed information on their weight and shape. Figures F.1 to F.7 shows the location and quantity of each weight type throughout the Capstone test building.

Chapter 4 Shake Table Tests and Instrumentation

The Capstone test building was instrumented with approximately 240 sensors (over 300 data acquisition channels) during the shake table tests. Various types of sensors were selected to measure acceleration, displacement, and strain in the structure during white noise and seismic testing. Appendix D contains detailed information related to various sensor types. It also provides a list of the data acquisition channels in the test data file and their corresponding physical measurements (Tables D.2). The instrumentation plans of the locations of each specific instrument are also included in Appendix D with a photo of each type of mounting scheme. This Chapter provides an overall description and general location of each type of instrument.

4.1 Types of Instrumentation for Shake Table Tests

4.1.1 Acceleration Measurements

There were a total of 33 tri-axial accelerometers installed in the Capstone test building to measure absolute accelerations during the shake table tests. Each accelerometer had three (3) output channels corresponding to the X, Y, and Z direction. There were five (5) accelerometers for each floor and the roof level, all directly attached to the wood floor at each of the four corners and the center of the floor plan. There was one accelerometer mounted on the center of the shake table to record the shake table motion. One accelerometer was attached to the center location of the steel special moment frame in order to quantify any differences between the steel moment frame acceleration and the acceleration of the shake table. Another accelerometer was attached to a seismic mass steel plate on the roof as a safety precaution.

The shake table acceleration record was obtained directly from the E-defense shake table control system and included in the output data file.

4.1.2 Displacement Measurements

Displacement measurements were obtained using Linear Variable Differential Transformer (LVDT) sensors and string potentiometers. There were three types of displacement measurements taken during the tests.

The first type displacement sensor was for the purpose of measuring the diagonal displacements between two points at the beginning and at the end of selected shear walls, recording diagonally from one bottom corner to the opposite top corner of the wall. There were a total of 33 walls in the building instrumented with diagonal gages, 17 in the 2nd story, and 3 walls for the 3rd to 6th story, and 4 walls on the 7th story. The locations of these walls in the floor plan were illustrated in Appendix D. The 3 walls instrumented from the 3rd to 6th story are all parts of three shear wall stacks running from the 2nd story to the 6th story. This instrumentation arrangements ware intended to capture most of the wall deformation in the 2nd story and also monitor the behavior of 3 five-story high shear wall stacks in the test building. The diagonal measurements were obtained by building a wooden support which keeps a LVDT or string-pot sensor at the correct angle close to the lower corner of the target shear wall. Then for the string-pot, the end of the string was attached to an SDS screw attached to the upper corner of the wall. For the LVDTs were not spring loaded, it was necessary to attach the upper end of the moving core of the

LVDT to the upper corner of the wall (also using an SDS screw) with a string, and then attach the lower end of LVDT core to another SDS screw at the lower corner of the wall with a spring that provided pretension force for the set-up. In order to prevent disturbance of the measurement from the movement of the sheathing panels, a hole of about 1" diameter was cut through the OSB and drywall panels at the location of SDS screws. Thus the measured diagonal deformation is directly from the framing members behind the sheathing. Figure 4.1 shows an example of the diagonal gage set-up for the test building.

Figure 4.1: Diagonal deformation measurements using string-pod or LVDT

The second type of displacement sensor was used to measure the uplift of the end studs for selected walls in the 2nd and 7th story. There were a total of 4 walls gauged with the end stud uplift measurement. Two of them in story 2 and two on story 7. The locations of these walls in the floor plan are presented in Appendix D. The LVDT sensors were attached upside-down to a wooden frame fixed on the floor near the end-stud. The spring loaded LVDT core was pressed against an extended surface from the end stud. A smooth plastic surface layer served as the contact surface as shown in the photograph of Figure 4.2.

Figure 4.2: End stud uplift measurements

The third type of displacement measurement was the relative vertical deformation between the 2nd and the 3rd floor diaphragms. The measurement was conducted by building wood extension frames from both the ceiling and the floor. A spring loaded LVDT sensor was installed to the top of the extension frame on the floor, with its measuring end pressed against a smooth surface attached to the bottom of the extension frame on the ceiling. This instrumentation setup is shown in the photograph of Figure 4.3. There were a total of 13 vertical deformation measurements at different locations in the floor plan. These locations and other details associated with these gages can be found in Appendix D.

Figure 4.3: Relative vertical deformation between story diaphragm measurement

The shake table motion feedback including acceleration, velocity, and displacement was obtained directly from the E-defense shake table control system and included in the output data file.

4.1.3 Strain Measurements

All strain measurements for the Capstone test were simple one channel output quarter or half bridge measurements. The unit for strain measurements in all output channels was μ (10^{-6}). There are two types of strain measurement. The first type was the strain measurement for the ATS rods at both ends of selected shear walls. Every shear wall that had diagonal deformation measurement also had ATS strains recorded. Locations of all the 78 ATS rod strain measurements are shown in the floor plan in Appendix D. The second type was the strain measurement for the steel moment frame moment connections. The strain gages were attached to the moment connection plates designed to yield during a strong earthquake before the yielding of the beam thus forcing the plastic hinge to form at this point in the connection. There are two reduced section plates for every beam to column connection, one on the top flange and one on the bottom flange of the beam. Each plate had two strain gage attached to it, one on each side. So there were 4 strain measurements for one moment connection. Figure 4.4 shows one of the moment connections with strain measurements attached. Only 17 moment connections were monitored during the test, slightly more than half of the total moment connections. The location of these connections can also be found in Appendix D.

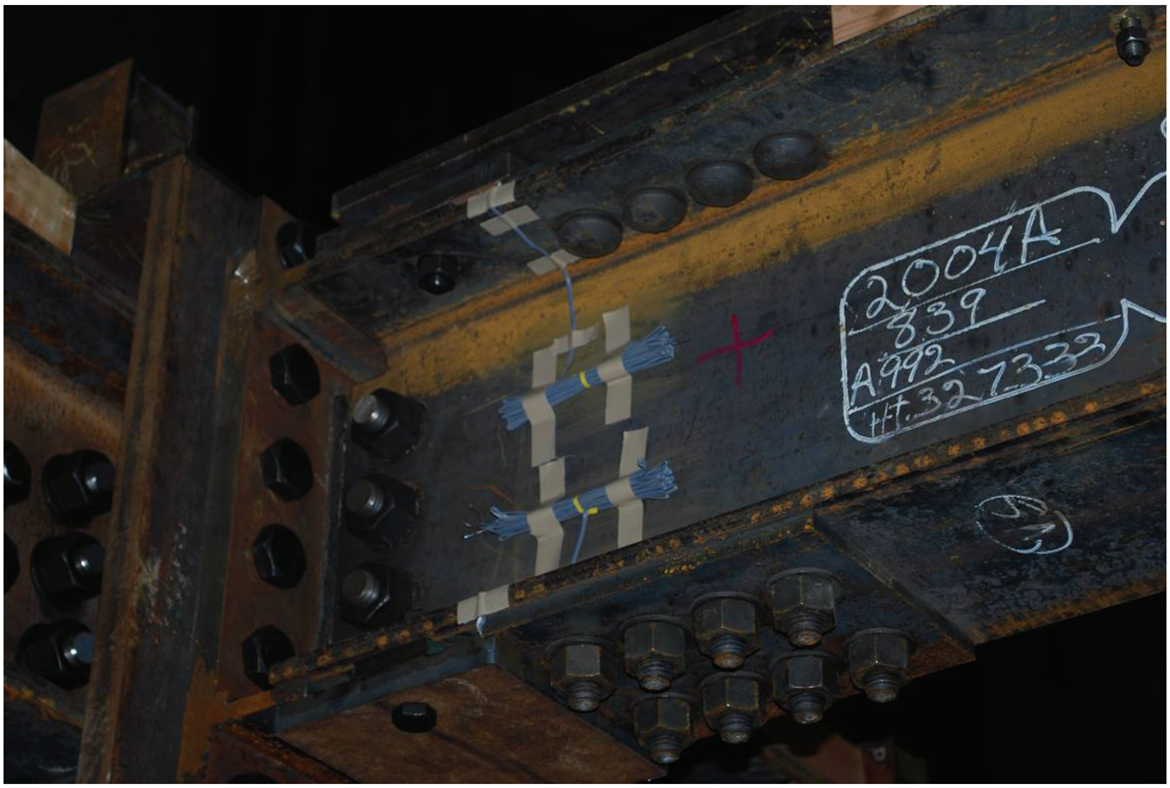

Figure 4.4: Strain gage attached to moment connection (actual gages are covered)

All the strain gages were installed as the construction progressed. The connection of the gages to the data acquisition system was conducted after the building was moved on to the table. The initial strain information was not available due to an accidental initialization operation for all data channels to an arbitrary zero value by data acquisition system at E-defense (which was repeated after the seismic test 1 before caught to the attention of the researchers).

4.1.4 Optical Tracking Measurements

Because of the size of the Capstone test building, it would be quite difficult to find a physical fixed reference target to instrument the absolute motion of the structure with traditional displacement gages. An optical tracking measurement system was employed in the test program to capture the absolute building displacements. Seven high speed cameras were located in the laboratory capturing the motion of the building from different angles. Then the recorded motion was analyzed with proprietary software to produce three dimensional displacement time histories of the points of interest on the exterior of the building. A total of 50 LED light markers were attached to the exterior of the building. Seven markers were installed for each diaphragm level and one marker was installed at the mid-point on one of the steel moment frame columns at a corner. Only three sides of the building were monitored because of availability of cameras in combination with the test building size. The location of these markers is shown in the schematic of Figure 4.5. A more detailed list and locations for each of these markers can be found in Appendix D.

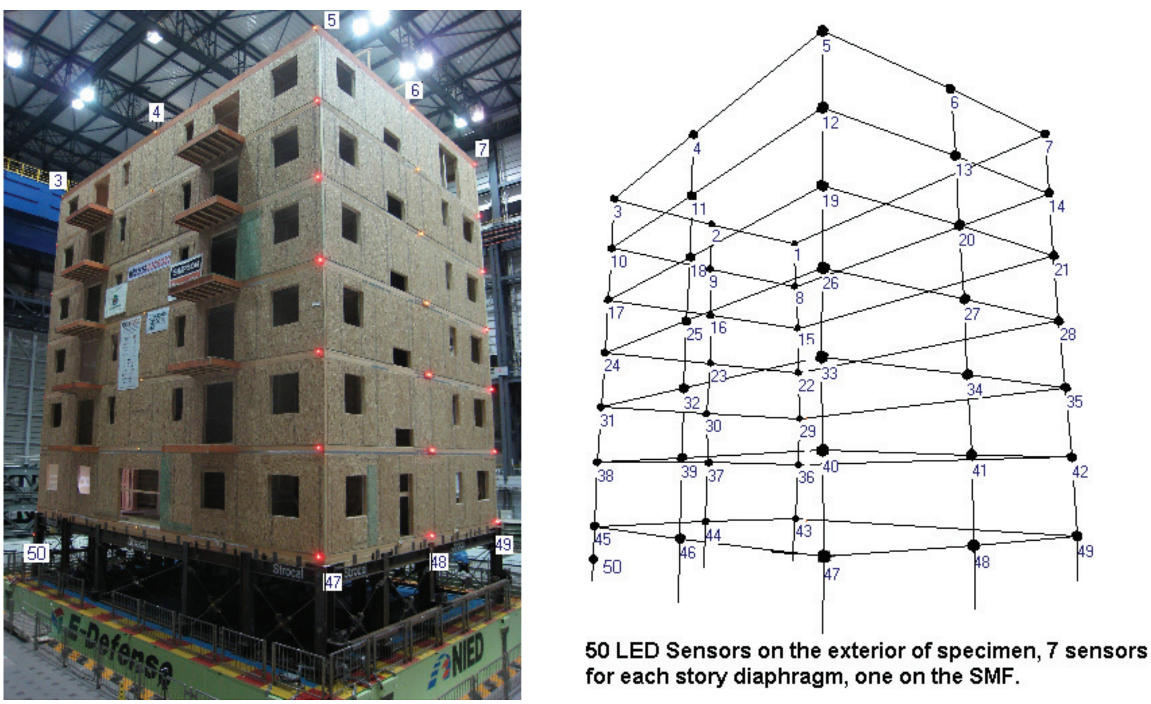

Figure 4.5: LED sensors for optical tracking of absolute displacements on the exterior of the specimen

The accuracy of the optical tracking measurement can be quite high for locations with good visibility and without disturbance from other light sources. The measurements for some of the points were relatively noisy.

4.2 Sign Convention and Instrumentation Summary

The sign convention discussed in this section applies to only the original raw output data, which is available from The NEES website under the NEESWood Capstone Test Program folder. For most of the measurements, the data was collected to conform to the coordinate system shown in Figure 4.6, including the accelerations, displacements measured with

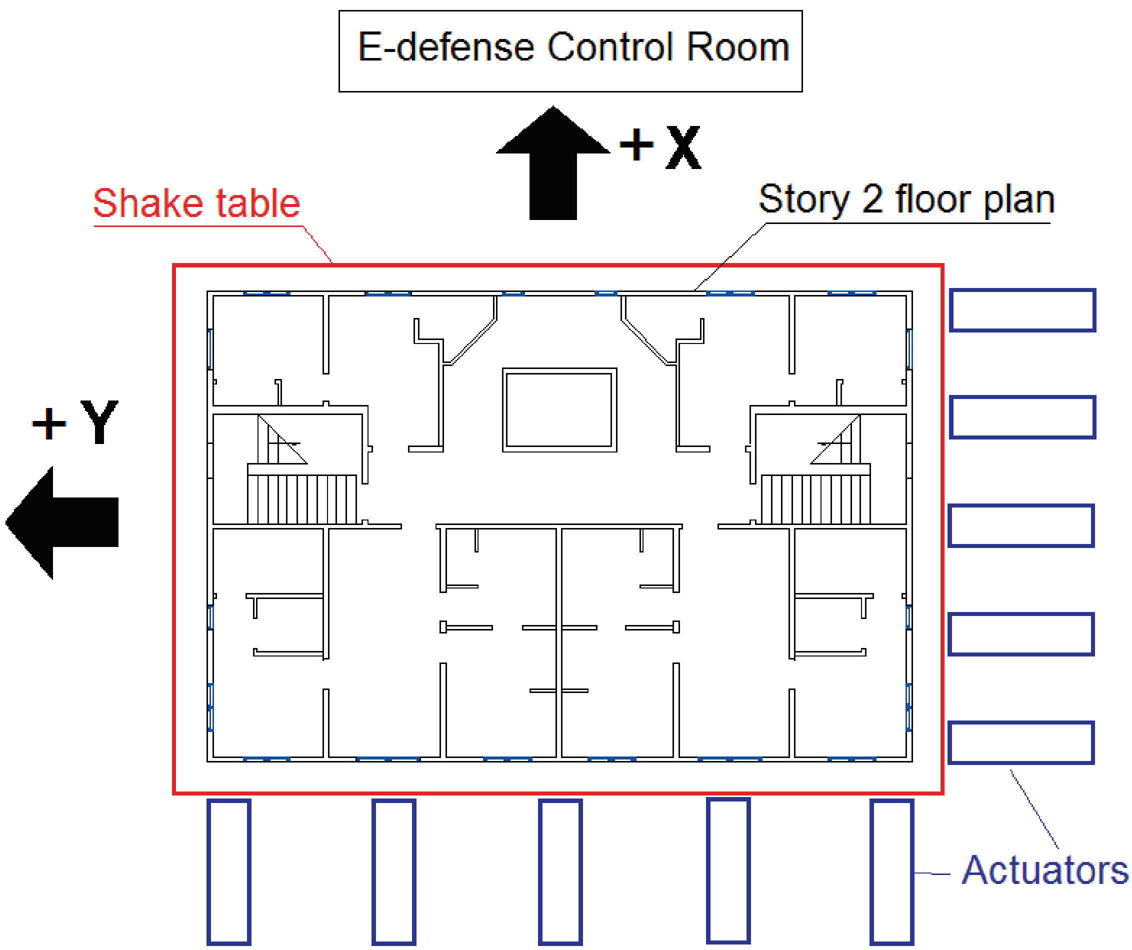

Figure 4.6: Sign convention for displacement and acceleration measurements

optical tracking, and diaphragm out-of-plane deformation measurements. The end-stud uplift measurement is negative when the stud uplifts due to the positioning of the LVDT's. As for the diagonal measurements of shear wall deformation, the sign convention depends on the orientation of the gage. The uniform orientation of all gages is not possible due to some space restrictions on site. Thus a detailed sign convention for each shear wall diagonal measurement is listed in Chapter 7.

Table 4.1 provides a summary of the type and total number of sensors that were recording data during all shake table tests. In total 288 sensors were used to effectively capture the detailed seismic response of the test building.

Table 4.1 Summary of all instrumentations for Capstone test

Measurement	Location	Type	Number
Absolute acceleration	Each Floor	3D-acceleration	38
Diagonal shear wall drift	Selected shear walls	LVDT	33
Out of plane diaphragm deformation	Third floor diaphragm	LVDT	13
Shear wall end stud uplift	Selected shear walls	LVDT	8
ATS hold-down strain	Selected shear walls	Strain gage	78
SMF connection strain	Moment connections	Strain gage	68
Absolute displacement	Building exterior	3D Optical tracking	50

Chapter 5 Materials and Construction of Capstone Test Building

This chapter explains the materials and construction process for the Capstone test building. The specimen was constructed following North American light frame construction practice with additional details associated with the increased capacity as a result of the PBSD. Two Japanese carpenter crews were hired for the construction: One team from Osaka and one team from Kobe, Japan. Almost all construction materials were shipped from the U.S. and Canada as detailed below.

5.1 Construction Materials

The Capstone test building was constructed mostly with construction materials readily available in North America. These materials were either donated or purchased in the U.S. and Canada and shipped to the E-defense laboratory via 18 40-foot long shipping containers. Table 5.1 shows a brief summary of the major materials used in the construction and their approximate quantities. Detailed quantities for each type of material can be obtained from the structural drawings provided in Appendix A.

Table 5.1 Summary of Capstone construction materials

Component	Product	Description	Quantity
Floor system	Glulam	5-1/8"x9" DFL glulams as shear collectors under wall lines	3100 ft
	Joist	LP joists, 9-1/2" for floor systems and 14" for roof	9900 ft
	LVL	For patio and roof framing	1900 ft
	OSB	23/32" thick for floor sheathing	16800 ft^2
	Drywall	½" GWB for ceiling	14400 ft^2
Wall system	Dimension lumber	Mostly 2x6	47000 ft
	Structural sheathing	15/32" thick for wall panels	28000 ft^2
	Drywall	½" GWB for drywall	24000 ft^2
Other	ATS system	Steel tie-down rods running through multiple stories	Installed in 30 5~6 story shear wall stacks
	Structural Steel	Special moment frame served as the optional first story	140 kips

The following is a detailed description for the property and usage of each construction materials:

<u>Dimension lumber</u>:

Most of the dimension lumber used for the project was 2x6 lumber with exact dimensions of 1.5" x 5.5". This lumber was primarily provided by FP Innovations – Forintek Division through a grant from the B.C. Forestry Innovation Initiative (FII) and shipped to Japan by the end of 2008. The lumber was kiln-dryed but was kept wrapped outside the laboratory during the construction process due to space limitations in the laboratory. The moisture content of the lumber was not monitored during the construction process. The wood was Douglas Fir Larch - North (No.2 or higher) for the first three wood stories (story 2~4) and SPF 1650 MR (No.2 or higher) for the upper stories (story 5~7). Finally, all sill plates that were 3x6 were DFL-N and were purchased in Japan. Their moisture content was high upon delivery but they were allowed to dry as the project progressed bring them into a reasonable range.

<u>Wall and floor sheathing</u>:

One type of shear wall sheathing material was used throughout the project. It was 12mm (15/32 inch) OSB purchased at a reduced rate from Ainsworth. The span rating of the sheathing panel was 16”/32”. The floor and roof sheathing was standard 18mm (23/32 inch) T&G Oriented Strand Board (OSB) also from Ainsworth.

<u>Floor and roof Joists</u>:

All floor and roof joists were purchased from LP. The 9-1/2” joists were used for floor framing and the 14” joists were used for the roof. LVL rim-boards of the same height from LP were also used in places within the building such as patio cantilever framing, roof rim board, and some of the drag members within the floor framing plan.

<u>Gypsum drywall board</u>

All gypsum drywall board was purchased in Japan. The board thickness was ½” and the same material was used for both the walls and ceiling. The grade of the board was GB-R: Gypsum-Board Regular-type (Japanese industrial standard, JIS A6901) with fire-proof condition designation as NM-8612. This “standard” strength drywall was approximately equal to U.S. drywall but slightly lighter at 64 lbs/sheet.

<u>Glulam member</u>:

In order to adequately handle the high shear demand and stability under extreme seismic loading, most of the collectors (headers) in the Capstone test building framing plan were glulam members (DFL-North, grade 2400F-V4, no camber). The material was purchased at a reduced cost from Calvert Glulam. The glulams were also stored wrapped outside the laboratory during the construction.

<u>Nails and drywall screws</u>:

All of the sheathing nails used in the project were 10d common (0.131 inch diameter, 2-5/8 inch long) donated by Stanley Bostich. The framing was constructed using 16d common (0.162 inch diameter, 3-1/2 inch long) nails. In several places where 2x6’s were toe nailed to form stud packs for compression at the ends of shear walls three 16d sinker nails were used in place of two 16d common nails. The nail guns used in construction were either brought from U.S. or adjusted to comply with the U.S. construction practice.

The drywall screws used in the project were #6 x 1.625" bugle head screws donated by Simpson Strong-Tie Company along with several QuickDrive guns for driving the screws.

Connector Hardware:

A self-tapping high strength screw known as an SDS screw was used throughout the construction for shear critical connections. The screw was a standard product for the Simpson Strong-Tie Company and thousands were donated for the project. Both the 4 inch and 6 inch long SDS screws have a nominal diameter of 1/4 inch and an ultimate shear capacity of about 1kip/screw given that the connector was adequately engaged. One of the major usages of the screw was to transfer shear force from the shear wall sill plate to the glulams. Joist hangers, floor system drag straps, hold downs for tension transfer, shear clips, and other hardware was all donated by Simpson Strong-Tie Company. In addition, a special type of “channel” connection for extreme shear load transfer was custom made for shear transfer from the wall top plate to floor system. It was essentially an extruded post tie down but extruded to 60 inches in length.

Anchor Tiedown System (ATS):

Simpson Strong-Tie Company donated all of the ATS hardware for the building, together with the shrinkage compensation devices. The ATS was installed by the Japanese carpenter teams under the supervision of Simpson Strong-Tie representatives on site. Most of the ATS donated were standard off-the-shelf products with the exception of one wall with 2” diameter tie-down rods in the lower stories, which were custom made for the project. Properties of the ATS rods can be found in Simpson Strong-Tie product Catalog and related specifications.

Steel Special Moment Frame (SMF)

The entire steel special moment frame and the bracing members were donated by Simpson Strong-Tie. The frame was first manufactured in California by Strocal, then shipped to Japan for assemble in E-defense laboratory. Strocal donated the fabrication of the frame.

Miscellaneous items

There were miscellaneous items that were purchased in Japan such as the steel connection plate and 16mm bolts used for connection between SMF and wood story, tape and mud for the gypsum wall board, and materials used to furnish a room on top floor before Seismic Test 5. These materials are consistent with materials that can easily be found and manufactured in the U.S.

In summary, the materials used for the construction of the Capstone test building were selected so that they are readily available by U.S. construction suppliers and comply with wood frame building practices in the U.S.

5.2 Construction of Structural Assemblies

Preparation for construction began in early 2008 with a joint meeting including the CSU research team, the contractor Maui Homes USA, and representatives from Simpson Strong-Tie Company. The construction materials were shipped from the U.S. and Canada to Japan in 18 containers at the end of 2008 and beginning of 2009. From the first piece of steel lifting frame being laid on the ground to the move of the specimen onto the shake table, the construction of the test specimen last exactly four months, from February 23rd 2009 to June 22nd 2009.

5.2.1 Preparation and shipment of construction materials

Following the planning of the construction and determination of the testing schedule, construction materials purchased or donated in the U.S. and Canada were shipped to the shake table site in Miki, Japan (see map in Figure 5.1), in shipping containers from the ports of Seattle, Vancouver B.C., and Los Angeles.

Figure 5.1 Location of Miki City and E-defense

The first shipment left the U.S. in October, 2008. By the start of construction in February 2009, the majority of the materials had been delivered to the E-defense site. The majority of the lumber was wrapped and stored outside the shake table laboratory but the structural panels were stored indoors because of rain. Figure 5.2 shows the arrival of the first few shipments by truck from the Port of Osaka and the lumber being stacked for subsequent cutting. In order to avoid excessive dust and debris inside the E-defense laboratory, most of the precutting was carried out outside the lab based on detailed stick drawings for each shear wall prepared by researchers at Colorado State University.

Figure 5.2: Arrival of the construction materials

5.2.2 Steel Moment Frame Erection

Recall that the SMF served as the first story of the structure during the first two seismic tests as well as the lifting frame. As such, the steel special moment frame designed by Simpson Strong-Tie Company was the first part of the structure to be erected. Initially the column pedestals that facilitate the connection of the test specimen to the shake table were laid out on the designated construction space. Specifically, these pedestals were carefully leveled in order to provide a flat foundation surface for the entire building. The erection of the frame was completed in 10 working days. Figure 5.3 shows several photos from the steel moment frame erection.

Figure 5.3: Erection of steel moment frame base

The steel moment frame was characterized by special proprietary moment connections that were designed to yield and provide ductility at design drift levels without introducing plastic hinge formation on the beam members. The concept of this special connection is shown in Figure 5.4. The flange of the beam section was connected to the column through dog-bone shaped steel plates on each side whose dimensions are determined based on the ductility demand desired at the connection. The shear tab connection on the beam web was designed to allow sufficient rotation by using slotted bolt holes at all but the center location thus transferring shear only. For some locations, additional bolts were installed on the beams in order to transfer the axial load when the frame was used to lift the building, but was taken out after the specimen was installed on the table.

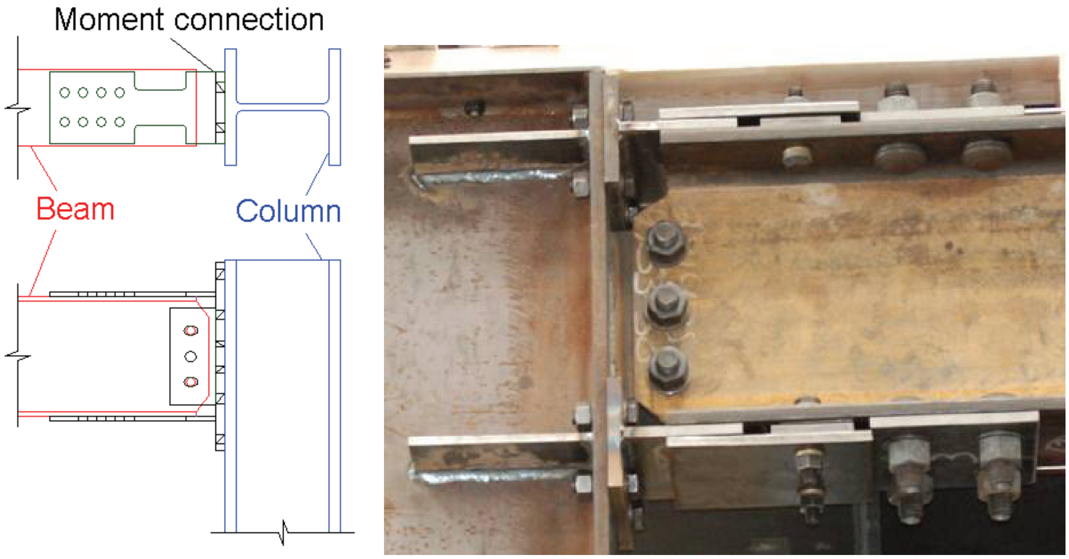

Figure 5.4: Ductile moment connection configuration

On the upper flange of the steel beams, staggered bolt holes were drilled for the installation of wood nailer as the wood-steel connection interface. The steel “cages” that receive the ATS tie-down steel rods had been welded to the upper flange during initial fabrication of the frame members. Stiffeners were welded under the ATS locations to avoid local yielding at the flange due to the large anticipated uplift forces. The wood nailers discontinue at these cage locations. The size of the wood nailer was 6”x6” nominal, Another layer of 2x6 dimension lumber was placed on top of the nailer (connected to the nailer with 16d common nails in order to provide a uniform wood material surface over the top of the steel moment frame). The finished steel SMF story is shown in Figure 5.5.

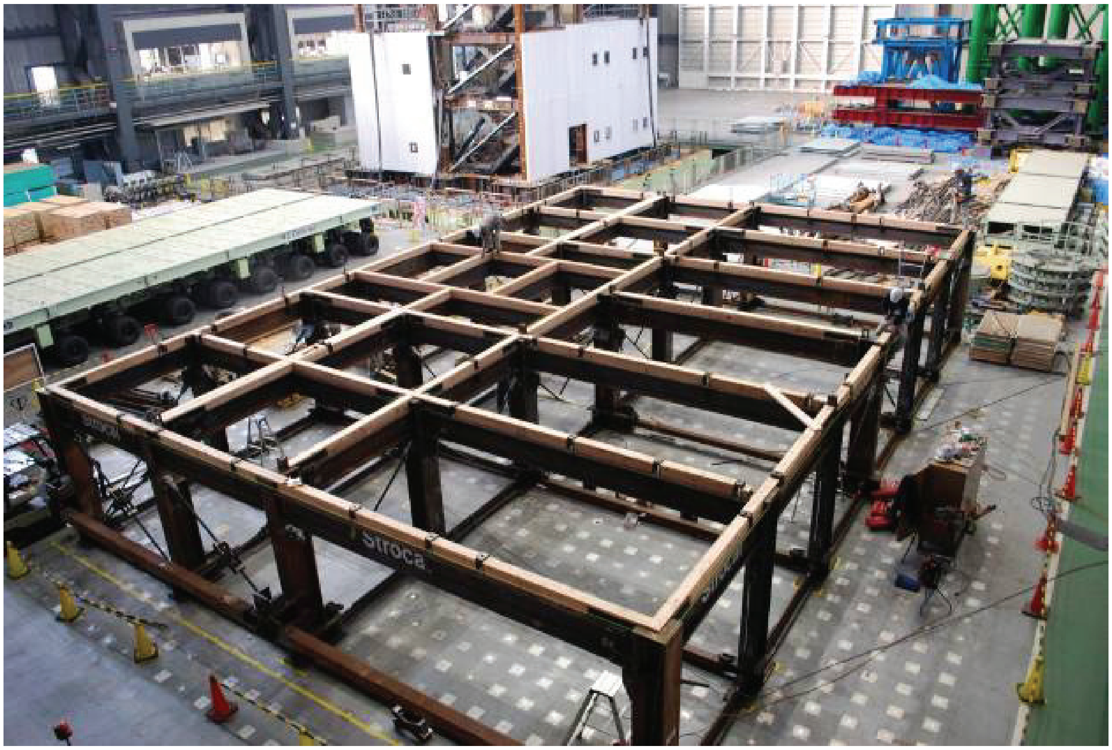

Figure 5.5: Steel special moment frame with nailer installed on top

5.2.3 Construction of the Woodframe Building

The Capstone test building differs from traditional low-rise light frame wood buildings in a number of details that allow the structure to perform well at high seismic intensity levels. This increased seismic demand is due to the increase in the height of the structure as well as the increased earthquake return period it was designed for, i.e. the Maximum Credible Earthquake having a 2500 year return period. These design details can be summarized into three categories, namely floor system details, shear wall details, and anchor tie-down system details.

The most significant difference between the Capstone test buildings' floor system and a traditional floor system was the use of glulam members as shear collectors due to the amount of shear force that needed to be transferred from the shear walls to the floor system at each story. As shown in the detailing plans in Appendix A, 5-1/8"x9" glulam members were used under every wall line to form the main diaphragm framing. Because the height of floor joist was 9-1/2", a layer of half inch OSB strip was attached to every glulam to match this height. Glulam hangers from the Simpson Strong-Tie catalog were used to connect them at the point of intersection. A photo of the floor system is shown in Figure 5.6. At particular splice locations along the glulam framing, steel straps and hold-down hardware were used to ensure the continuity of the collector force transfer, as shown in Figure 5.7 and 5.8 and also in framing tie plans in Appendix A. The steel straps and glulam splices were designed using the design shear wall forces transferred to the collectors.

Figure 5.6: Construction of the floor system

Figure 5.7: Steel strap installed at glulam splice

Figure 5.8: Tension transfer connector for glulam collectors

At the location of the double midply shear wall (wall B1 and B2), two glulam members were placed side-by-side due to the thickness of the double midply wall. The floor joists were attached to the main framing by top joist hangers, as shown earlier in Figure 5.5.

For the roof level, since the shear force demand for the framing collector decreases, 2x14 LVL rim boards were used as the main framing member. The height of the roof joist was 14" because of the increased span of the joist from the change in floor plan for the top story, story 7. The original architectural floor plan for the top story had a patio on the short side of the building. This patio was built but found to interfere with the lifting cables and was therefore removed prior to lifting the test building onto the shake table.

Wood shear walls were all framed with 2x6 members. The framing and sheathing details for all wall segments in Capstone test building are detailed in Appendix B. There were a significant number of members in the stud packs at the lower stories. These were installed at each end of the wall in order to resist the design compression force during dynamic loading, i.e. wall racking. The number of compression studs in the stud packs was calculated based on force demand. The studs were nailed together at 12" with one another to avoid buckling of individual member. Most stud packs were installed after the sill and top plates of the wall were connected adequately to the floor and ceiling collector members. The stud packs were only toe-nailed to the sill and top plates because they were designed to resist compression force only.

Many shear walls in the Capstone test building were double sided shear walls with relatively close nail spacing. In order to avoid over damage to the framing member because of the amount of nailing needed from both sides, sill plates in lower stories for double sided walls were 3x6 members instead of 2x6. This was not a problem for top plates and the end studs since there were at least double 2x6 plates at these locations.

Nailing for the 2/12 pattern was specified to be staggered, while other nailing schedules were nailed in a single line. All the wall segments with no nailing specification were nailed with a 6/12 pattern, single sided.

A special type of shear wall system, called a Double Midply wall, was incorporated into the Capstone test building design and construction. The concept of a single Midply wall is to place the sheathing panel in between two layers of framing members constructed with framing members oriented with their long edge against the sheathing. Then the nails can be driven through both framing members and through the sheathing, engaging each shear connector in double shear as the panel racks. The Midply wall was intended to provide approximately double the amount of shear capacity compared to a regular shear wall with the same nailing pattern. The Double Midply wall essentially places two standard Midply walls side-by-side. The detailed configuration of double Midply wall can be found in Appendix B. The installation of a double Midply shear wall in the Capstone test building was more challenging than traditional shear walls or a standard Midply wall. Special details such as staggered bolts through the end posts had to be used in order to prevent buckling of the end studs under a high level of compression. Figure 5.9 shows a photo of a completed Double Midply wall in the building.

Figure 5.9: Completed Double Midply wall in the Capstone test building

With maximum design ultimate wall shear exceeding 4 kips/ft for most walls in lower story, special shear transfer detailing was employed for the sill and top plate connections. Two special shear connection details were used in Capstone test building: one uses a 1/4 inch diameter self-tapping wood screw that has about 1 kip ultimate shear capacity (SDS screw, Simpson Strong-Tie Company), drilled upward through the top plates into Glulam collector; the other is a specially designed channel that is capable of providing 5 kip/ft shear between shear wall top plates and glulam floor framing collectors. The concept of this channel connection detail is shown in Figure 5.10. The shear wall drawings in Appendix A provide the shear transfer detail for each of the walls in the building by specifying either SDS screws at certain spacing or a channel section with the length equal to the length of shear wall segment.

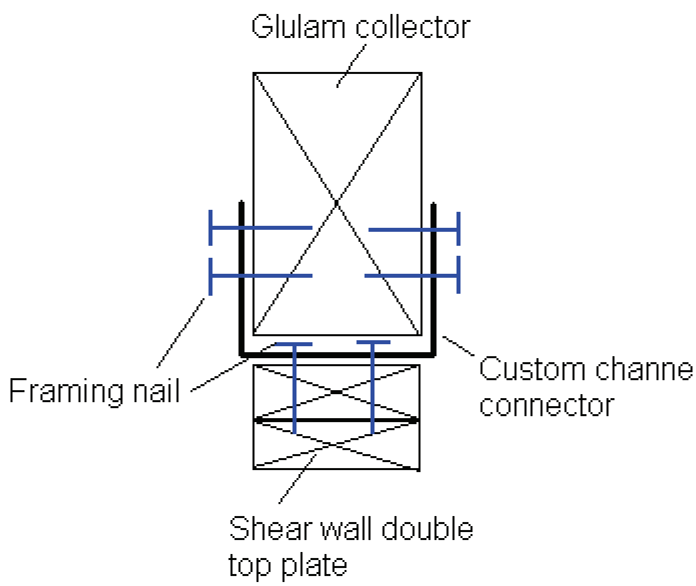

Figure 5.10: Concept of channel connection for shear wall top plates

In order to install the compression stud packs after fastening the sill and top plates to the floor system, the SDS screws were all counter-sunk about half an inch into the plates. Figure 5.11 illustrated the counter-sinking of the screws before the installation of the stud packs.

Figure 5.11: Shear transfer detail: Counter-sunk SDS screws on a 3x6 sill plate

Shear transfer between the steel moment frame and the wood first story was achieved through specially designed shear transferring plates. Recall that a 6x6 nailer was connected to the top flange of steel beam by anchor bolts with the capacity exceeding the design ultimate shear demand. Thus as long as the wood first story was adequately connected to the nailer, a continuous shear transfer load path was established. The shear plate detail included 1/4 inch steel plates on each side with eight 16mm diameter bolts, providing more than 16 kips shear transfer capacity for each connection based on a nonlinear finite element analysis of the connection. These plates were installed at approximately 4 ft spacing along every glulam framing collector at the bottom story, with spacing irregular when a steel cage or other detail interfered with the placement. The dimensions for this connection detail are shown in Figure 5.12. A photo of a plate installed at the base of the building is shown in Figure 5.13.

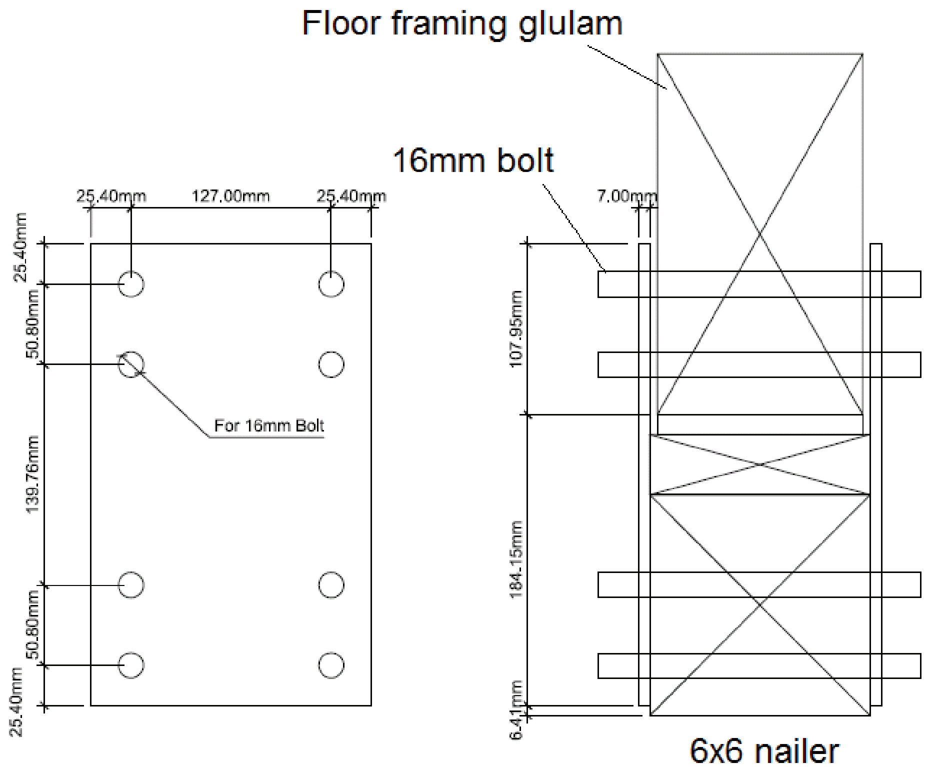

Figure 5.12: Shear transfer plate for steel-wood interface

Figure 5.13: Installed shear plate on Capstone test building

At roof level, LVL rim boards were used as the shear collectors instead of glulam members. Another shear detail was assigned based on the design roof diaphragm shear. HGA10 angle connectors from the Simspon Strong-Tie Company were installed at 2 ft along the LVL board, as shown in Figure 5.14.

Figure 5.14: Shear transfer detail for the roof level.

Another important feature for multi-story wood frame buildings is the use of continuous hold down systems, in the present case the anchor tie-down system (ATS). Unlike traditional hold-down devices installed at the corners of wood shear walls, the anchor tie-down system (ATS) utilizes a continuous run of steel rods that runs through the entire height of shear wall stacks and is anchored at each story with an intermediate anchor plate for bearing. This allows the difference in tension force between two adjacent stories in the wall stack to be used in the calculation of the bearing plate size. The steel rod sizes were selected based on desired anchor force and stiffness and included a design stipulation that the rods elongate no more than ¼ inch for any single story for MCE level earthquake. The rod size typically decreased going up the building, with reduced uplift demand. This configuration has been used in current multi-story wood frame building construction in California, but the elongation limit is typically not as stringent. Thus the ATS system used in the Capstone test building is a readily available product, with the exception of some oversized tie-down rods (2" diameter rods) specified for the bottom story. A detailed description of the location and size of the ATS rods is provided in the structural drawings in Appendix A.

As shown in Figure 5.15 and 5.16, all ATS rods in the Capstone test building were anchored to the top of the steel moment frame through welded "cages". The nuts were only snug-tightened to avoid pre-stressing the rods, because snug tight is the intent of the design. Stiffeners for steel beam flange were added at the anchor locations to avoid local rupture or yielding.

Figure 5.15: ATS connecting to the top of steel moment frame

Figure 5.16: Steel anchor detail for ATS rods on SMF

Figure 5.17 shows the intermediate anchor plate installed at each story sill plate. One can also see in the photo there is a special hex nut that joins ATS rods with different diameters together. In between the small steel plates shown in the photo was a special shrinkage compensation device, which can automatically keep the rod in snug-tightened condition to eliminate most of the slag in the system caused by shrinkage, settling, and creep deformation of the wood members over time.

Figure 5.17: Intermediate anchor plate for the ATS system

Figure 5.18 shows the ATS rod running across multiple stories at a wall stack near the stairwell. Figure 5.19 shows a typical shear wall with several ATS rods. Not all ATS rods ran through the entire height of the building. Some ATS runs stopped at the top of the sixth story, in this case, the wall in the seventh story was not a shear wall.

Figure 5.18: ATS continues over the entire height of stacked wall system

Figure 5.19: Shear wall installed with ATS

In order to achieve a realistic representation of typical multi-story wood frame construction, non-structural material that contributes to the building strength and stiffness was also included in the test building. For all interior walls, drywall boards were attached with drywall screws at 16" spacing (including top and bottom, i.e. not a floating construction style). The gypsum wall board ceiling was also installed since the drywall panels contribute to diaphragm stiffness and mass. Finally drywall boards installed were tape-and-mudded. Figure 5.20 shows some photos during the installation of gypsum wall board panels.

Figure 5.20: Installation of drywall panels for walls and ceiling

Different stages of construction are shown in Figure 5.21. After the construction was completed, the scaffold was removed, the steel frame was braced and the building was lifted on to the shake table. Most of the instrumentation has been installed in the building before the move.

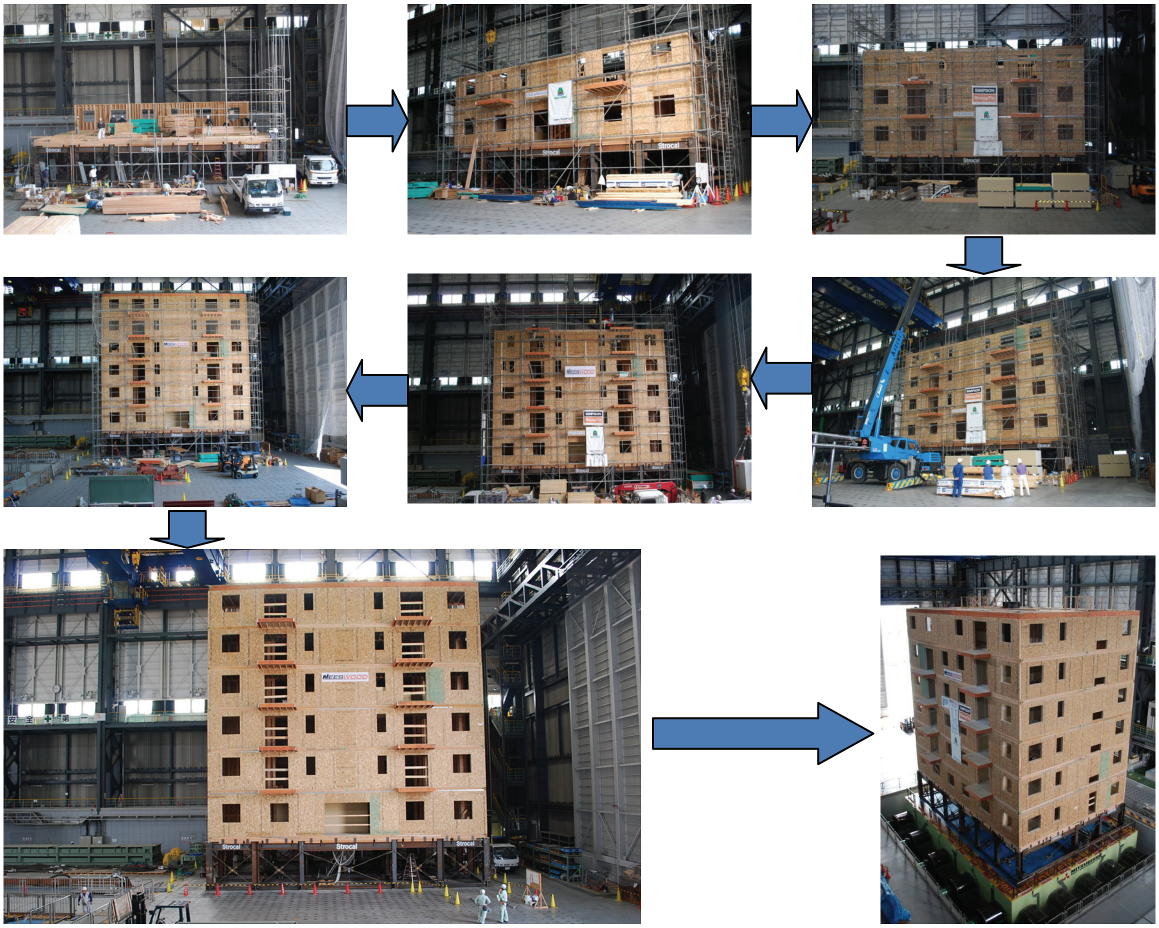

Figure 5.21: Construction of the Capstone test building

There was no construction activity conducted on Capstone test building after it was moved and fixed to the table except fastening of some seismic weights and installation of the GWB.

The building was moved to the table on June 22, 2009 using the steel moment frame at story 1 as a space truss for lifting. Cross bracing members designed for the lift (see Figure 5.22) were tightened for the lift. The original design for lift did not include the spreader bar which became available between the time the design was performed and the day of the lift. A six-point lift was conducted using twin 400 metric ton cranes and is depicted in Figure 5.23. The crane reading after the building was lifted was approximately 161 metric tons for both cranes, indicating a total lifting weight of 322 tons, which confirmed the dead weight of the structure at that stage (the roof supplemental mass was not added until the specimen is on the table).

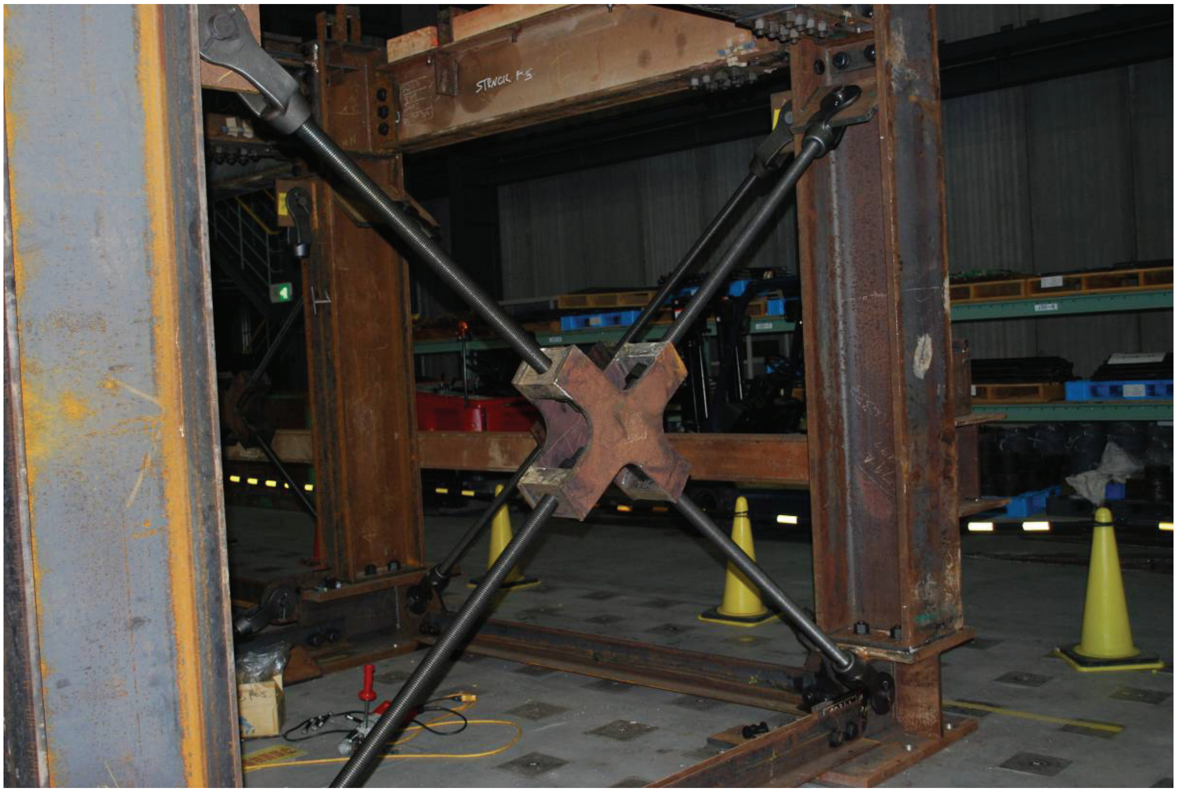

Figure 5.22: Cross bracing member added for SMF

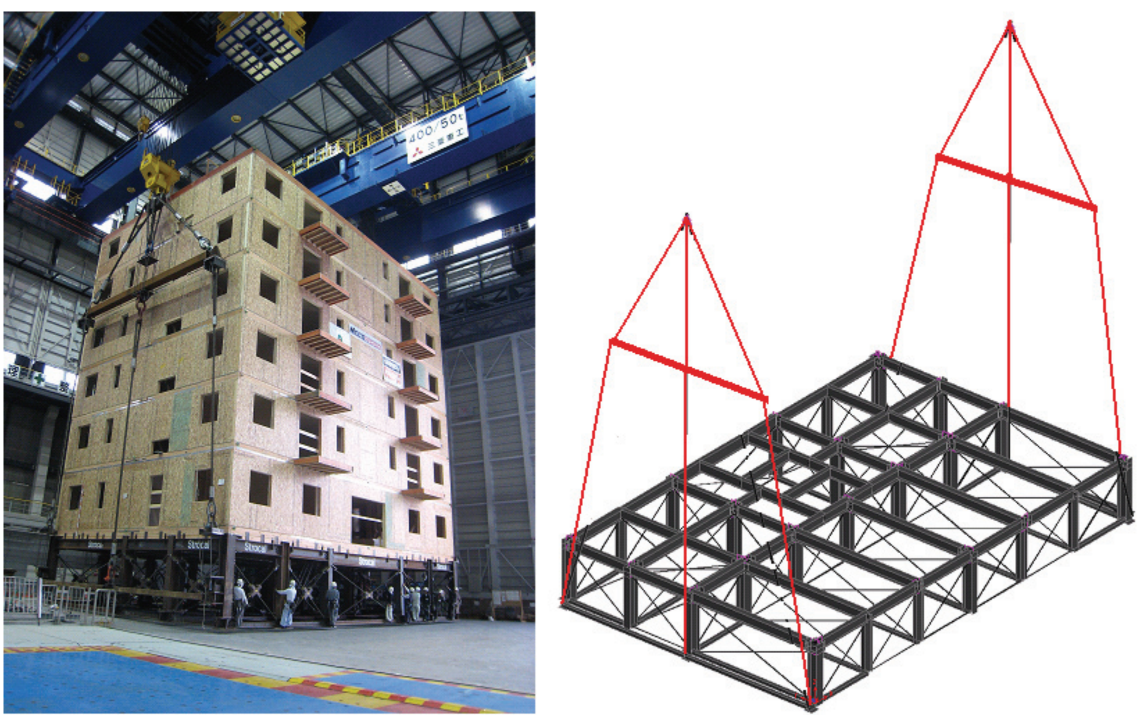

Figure 5.23: Lifting of the Capstone test building on to the shake table

After the building was installed on the shake table, the braces were loosened for the first phase of the test with 7-story mixed use structure. Then for Phase 2, the braces for the steel moment frame were tightened enabling the lifting frame to behave as an extension of the shake table. In other words the SMF did not participate in the subsequent wood frame building tests within Phase 2.

5.3 Quality Control

The construction quality of the shearwalls in the building was closely monitored during the construction process. Since the shear walls are the major lateral force resisting components in the building, it was very important to make sure the nailing pattern, studs lay out, anchor tie-down system, and the shear transfer details at the top and sill plates were correctly installed. As each wall was erected, the stud layout and shear connection for the top and sill plates were first checked. Then the ATS rods were installed and checked. Finally the sheathing panels were applied and the nail pattern was inspected. This process was performed for every structural wall in the building. Any error in construction was documented and corrected. In some cases shear walls were sheathed on one side while ATS hardware was shipped from the U.S., then the other side was sheathed after the ATS system was installed and inspected.

In the early stages of construction, NEESWood project PI Dr. John W. van de Lindt travelled to Japan eight times and conducted the most critical part of the quality inspection during the construction phases including the construction and correction of the first Midply wall system. During the construction, graduate student researchers from Japanese universities oversaw and checked the details for all of the shear wall construction with the detailed wall configuration check sheets developed by the CSU design team (an example of a wall check sheet is shown in Figure 5.24). For the final two months of the construction, the CSU design team (including Dr. John W. van de Lindt and Dr. Shiling Pei) and collaborator from Simpson Strong-Tie Company (Steven E. Pryor, SE) stayed on site and supervised the completion of the construction and lifting of the specimen on to the shake table.

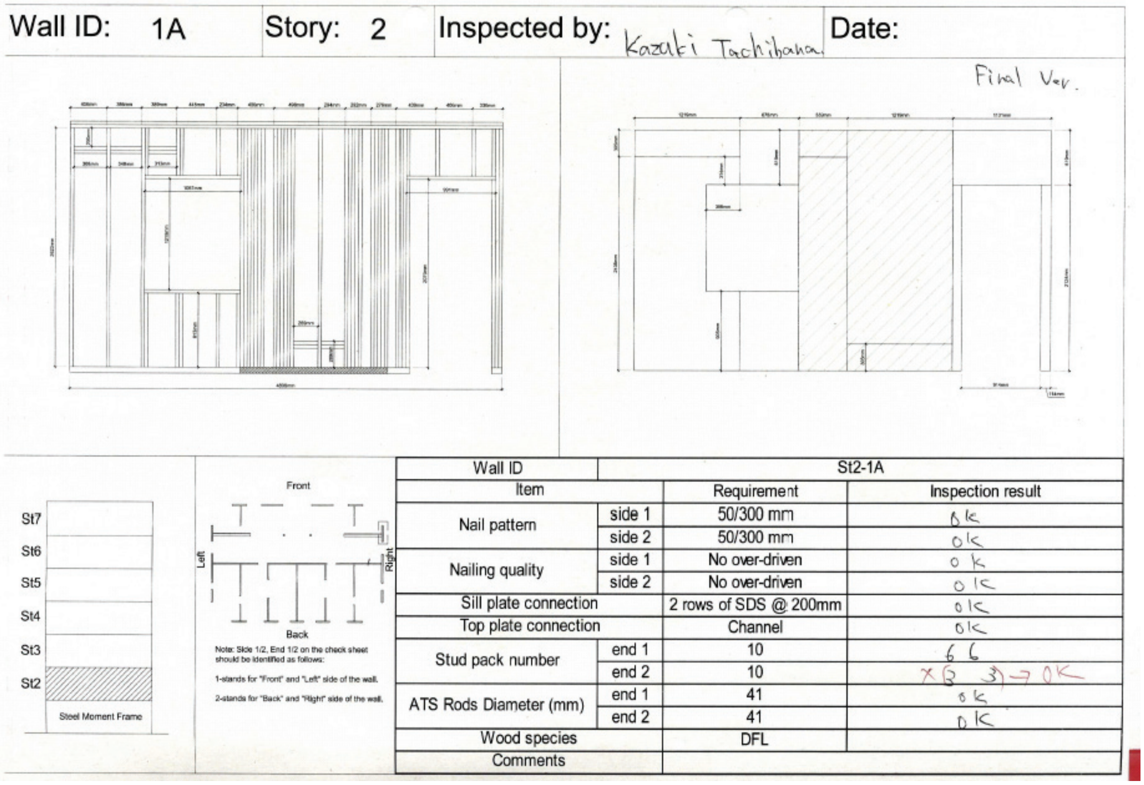

Wall ID: 1A | Story: 2 | Inspected by: Kazuki Tachibana | Date:

Final Ver.

St7
St6
St5
St4
St3
St2
Steel Moment Frame

Front
Left
Right
Back

Note: Side 1/2, End 1/2 on the check sheet should be identified as follows:
1-stands for "Front" and "Left" side of the wall.
2-stands for "Back" and "Right" side of the wall.

Wall ID		St2-1A	
Item		Requirement	Inspection result
Nail pattern	side 1	50/300 mm	ok
	side 2	50/300 mm	ok
Nailing quality	side 1	No over-driven	ok
	side 2	No over-driven	ok
Sill plate connection		2 rows of SDS @ 200mm	ok
Top plate connection		Channel	ok
Stud pack number	end 1	10	6 6
	end 2	10	×(3 3)→OK
ATS Rods Diameter (mm)	end 1	41	ok
	end 2	41	ok
Wood species		DFL	
Comments			

Figure 5.24: Onsite check sheet for shear wall construction

Chapter 6 Results of White Noise Excitation Tests

This chapter presents the results from the white noise excitation tests. White noise tests in the Capstone program were employed to identify possible damage between different seismic tests. Because the repair of the specimen was not feasible between the tests, it was desirable that the building did not experience much damage during earlier tests. Comparison of the building period measured from uniaxial excitation in three orthogonal directions confirmed the integrity of the specimen.

6.1 Data Analysis

For all white noise excitation tests, the absolute acceleration data from five accelerometers attached at the roof level were averaged first to provide the average acceleration at the roof. Then power spectral density (PSD) function for the average acceleration time history for each direction was generated. The natural frequency of the building was determined as the frequency value corresponding to the maximum value of the power spectral density function.

The software program Matlab was used to produce the power spectral density function. The PSD estimation was conducted using Welch's method through function “pwelch”. The window size was 500 data points with 2/3 window overlap. The NFFT value used in the analysis was 20000.

6.2 Natural frequencies

Following the analysis procedure described in section 6.1, the power spectral density plot for each white noise test is shown in Figure 6.1 to 6.9 with the frequency value corresponding to the first peak of the PSD curve for each direction marked out. The corresponding natural periods were listed in Table 6.1.

Table 6.1 Natural periods of the test building at different configurations

Test ID	Natural Period (sec)		
	X	Y	Z
WN1	0.42	0.41	0.13
1	Test Level 1-Seismic (SMF)		
WN2	0.48	0.48	0.13
WN3	0.48	0.48	0.13
2	Test Level 2 plus-Seismic (SMF)		
WN4	0.48	0.49	0.14
SMF Tie down			
WN5	0.41	0.42	0.13
ST3	Test Level 1-Seismic		
WN6	0.41	0.42	0.13
ST4	Test Level 2-Seismic		
WN7	0.41	0.42	0.13
WN8	0.41	0.42	0.13
ST5	Test Level 3-Seismic		
WN9	0.47	0.49	0.14

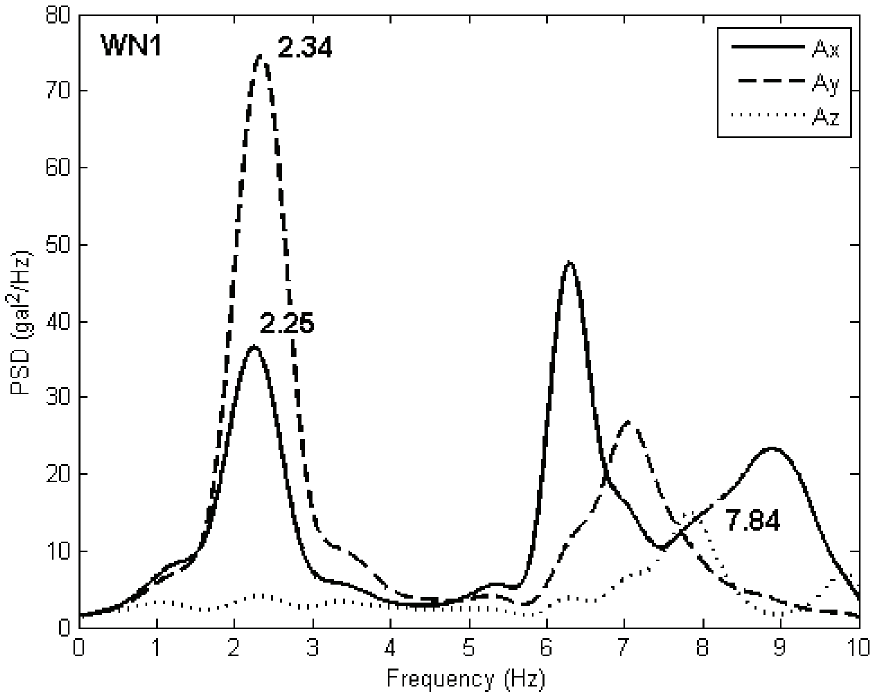

Figure 6.1: Roof acceleration power spectral density for WN1

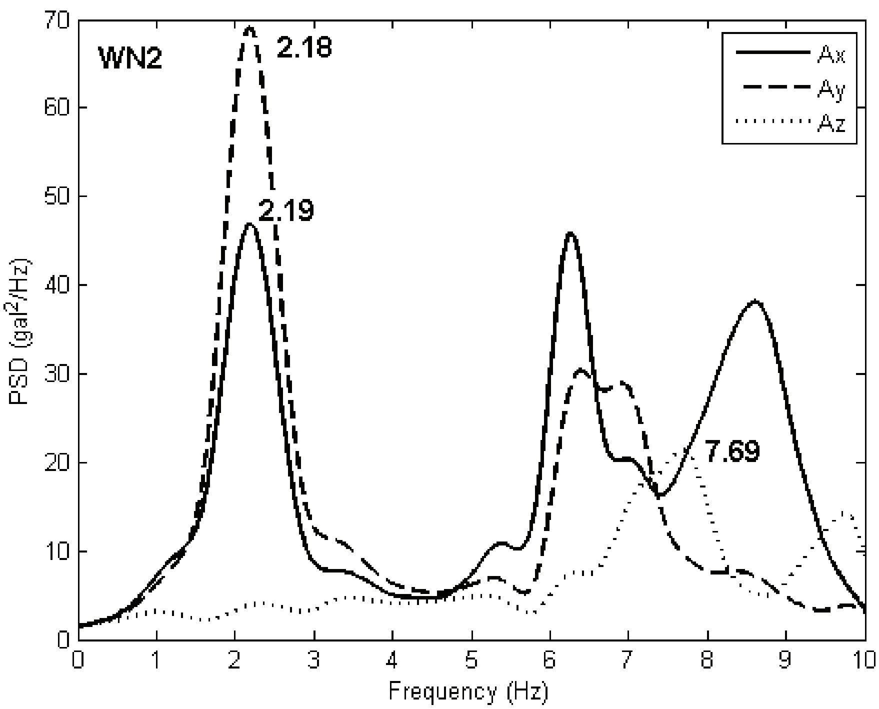

Figure 6.2: Roof acceleration power spectral density for WN2

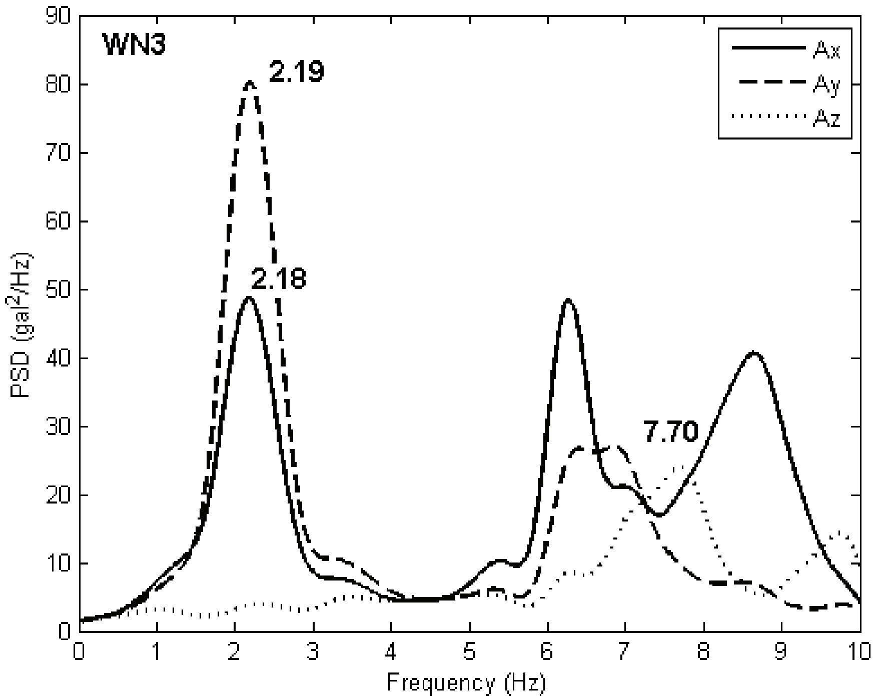

Figure 6.3: Roof acceleration power spectral density for WN3

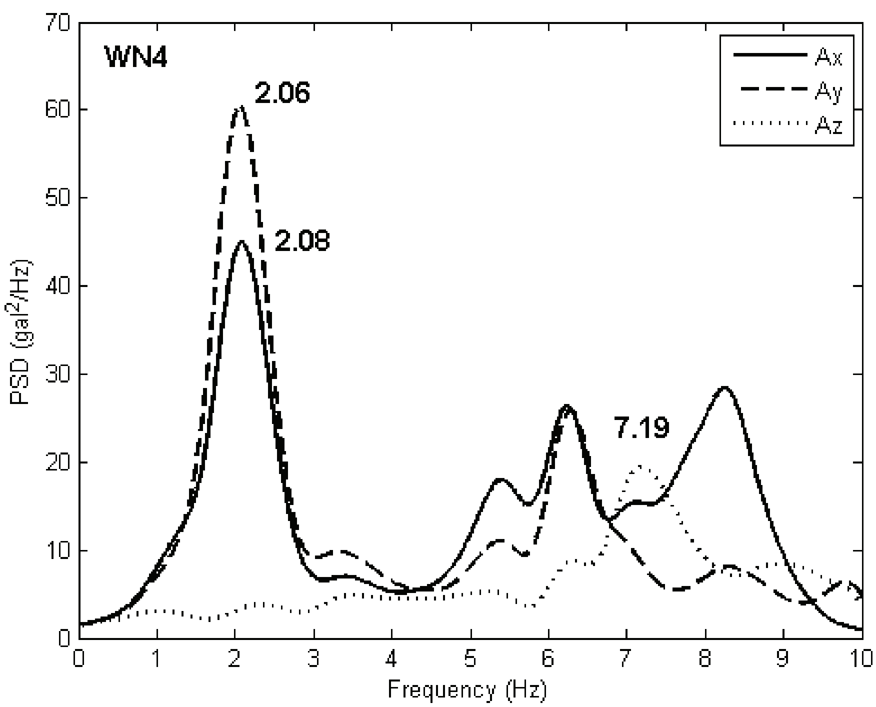

Figure 6.4: Roof acceleration power spectral density for WN4

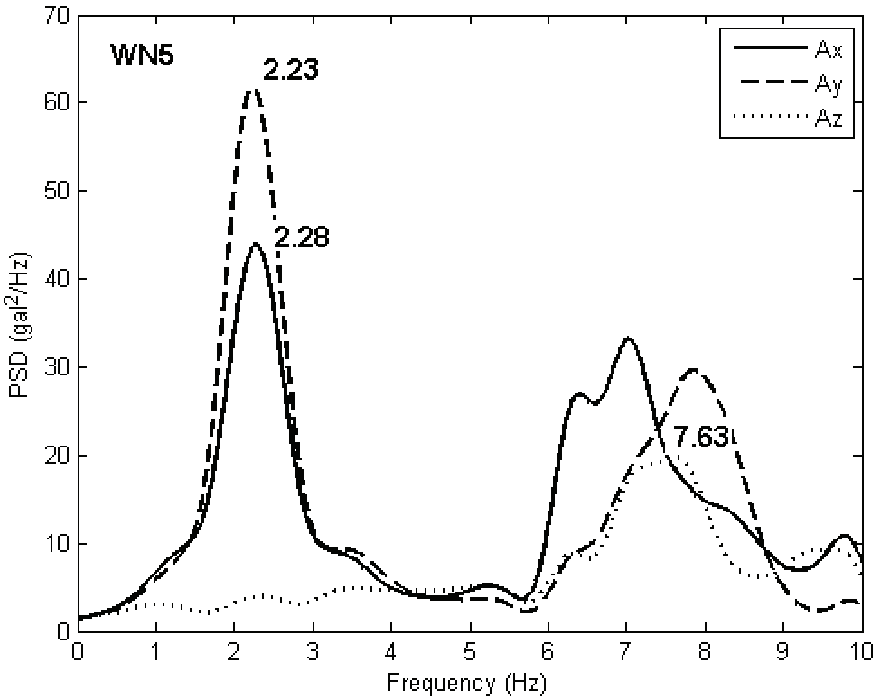

Figure 6.5: Roof acceleration power spectral density for WN5

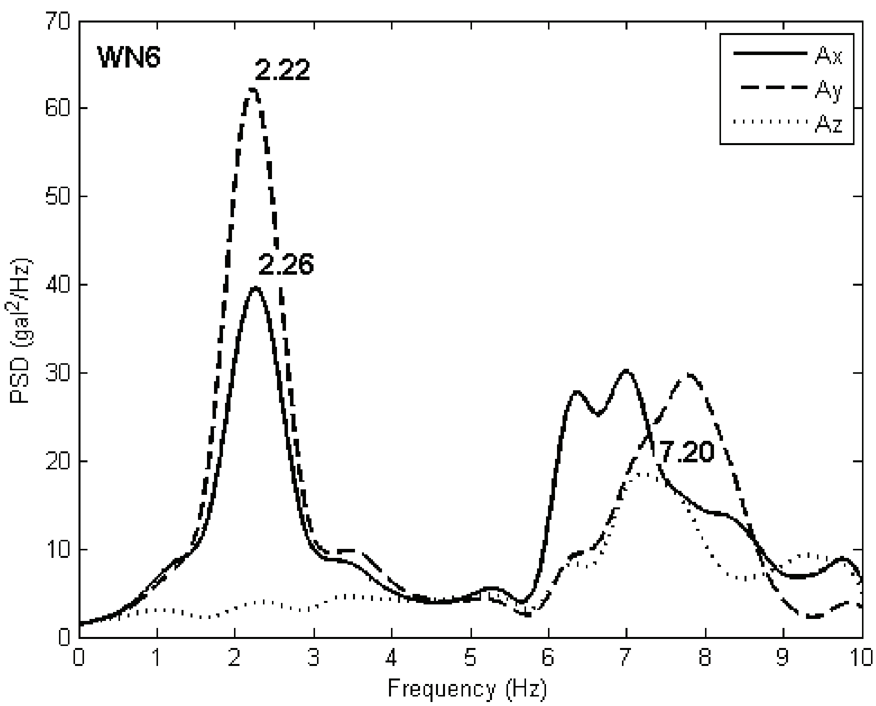

Figure 6.6: Roof acceleration power spectral density for WN6

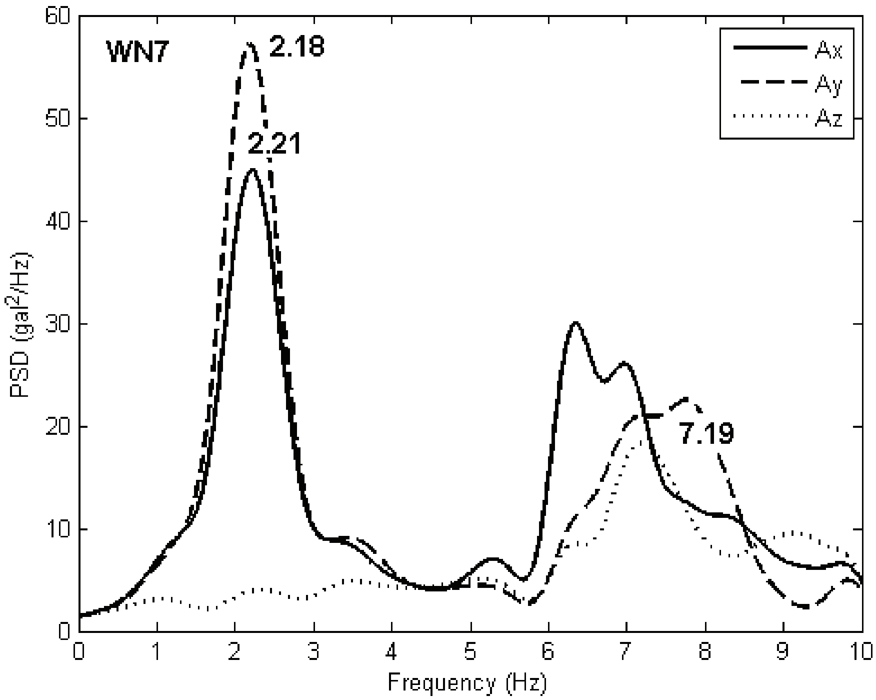

Figure 6.7: Roof acceleration power spectral density for WN7

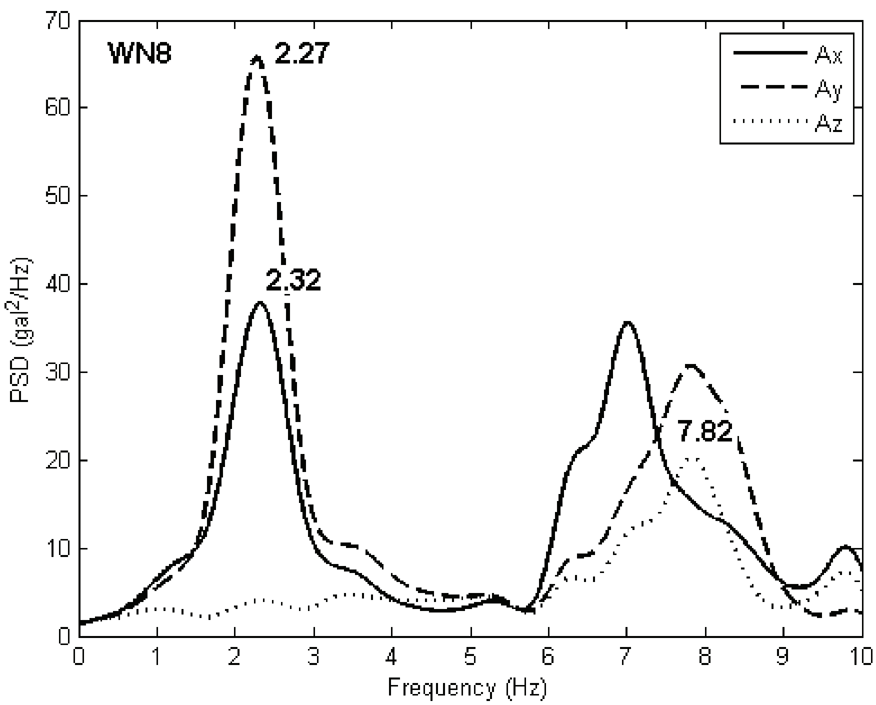

Figure 6.8: Roof acceleration power spectral density for WN8

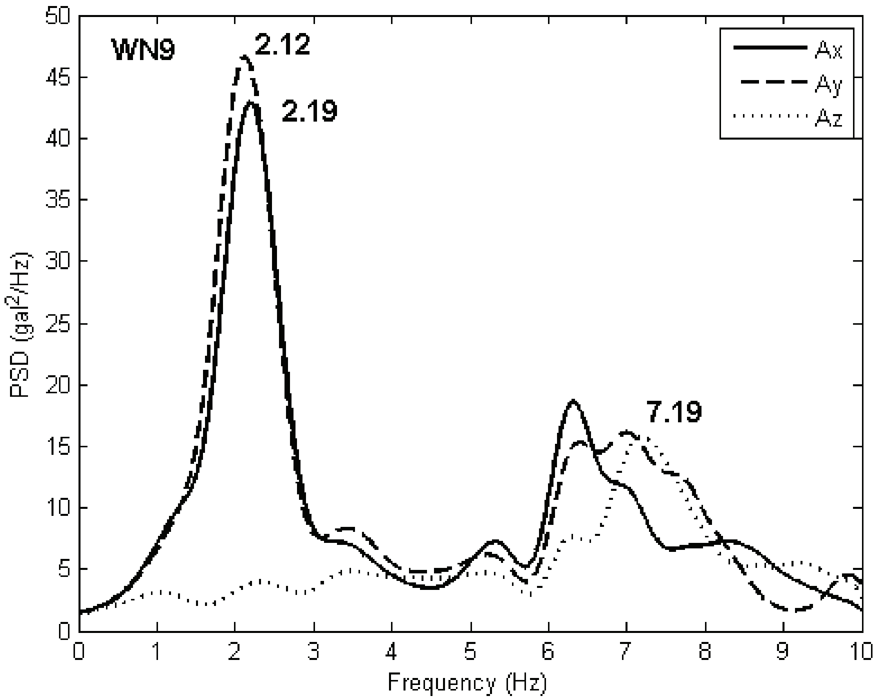

Figure 6.9: Roof acceleration power spectral density for WN9

Chapter 7 Results of the Seismic Tests

This chapter presents a summary of the results from the seismic tests with all results available in the Appendices. As discussed earlier, the main objectives of the seismic tests was to examine the performance of the Capstone test building under several levels of seismic intensity as well as quantify the agreement between measured seismic performance and the PBSD expectations. Recall the test program consisted of two major phases, therefore the experimental results of both the mixed-use 7-story building (Test 1 and 2) and wood-only 6-story building (Test 3, 4, and 5) are presented in this Chapter. In order to avoid confusion on the story numbering, all test results are presented using the numbering convention of the 7-story building, i.e. story 1 through story 7.

First, the shake table fidelity is discussed based on the correlation between the desired and the recorded shake table motions. Different measurements that reflect the performance of the Capstone test building are then presented in terms of various recorded intensity measures, which have been incorporated in the appendices of this report.

7.1 Shake Table Fidelity

One important aspect of shake table testing is the ability to accurately reproduce the simulated ground motions. It is significant to acquire a good match between the recorded and the desired shake table motions in the frequency range of interest, especially when input motions of different levels of shaking intensities are part of the testing program.

The recorded acceleration time histories of the shake table during the test in the three orthogonal directions were used to calculate the acceleration response spectra for each direction and they were compared with the target acceleration response spectra of each specific seismic test. Appendix H contains plots of the 5% damped response spectra that were generated from the recorded motions along with the desired response spectra of the given seismic test. In general, the shake table fidelity was felt to be reasonable over different intensities used in the NEESWood Project Capstone testing. One general observation is that in most of the cases the ground motion in Y direction from the table exceeded the desired spectral acceleration value near the building fundamental frequency while the motion in X direction had slightly smaller spectral values. The table fidelity was better for the vertical components than for horizontal components. The desired PGA for each test level and the table feedback PGA values were listed in Table 7.1. Figure 7.1 illustrated the comparison of the measured ground motion response spectra with 5% damping and the input ground motion response spectra. One can see some difference in the Y direction component.

Table 7.1: PGA for the input ground motion and shake table feedback

Seismic Test	X		Y		Z	
	Target	Feedback	Target	Feedback	Target	Feedback
1	0.19	0.20	0.22	0.32	0.26	0.17
2	0.5	0.56	0.58	1.00	0.69	0.63
3	0.19	0.19	0.22	0.31	0.26	0.22
4	0.43	0.47	0.5	0.85	0.59	0.61
5	0.65	0.72	0.75	1.43	0.88	0.88

The measured maximum table rotation for all seismic tests in all directions did not exceed 0.02 degree, which can be neglected in the data analysis.

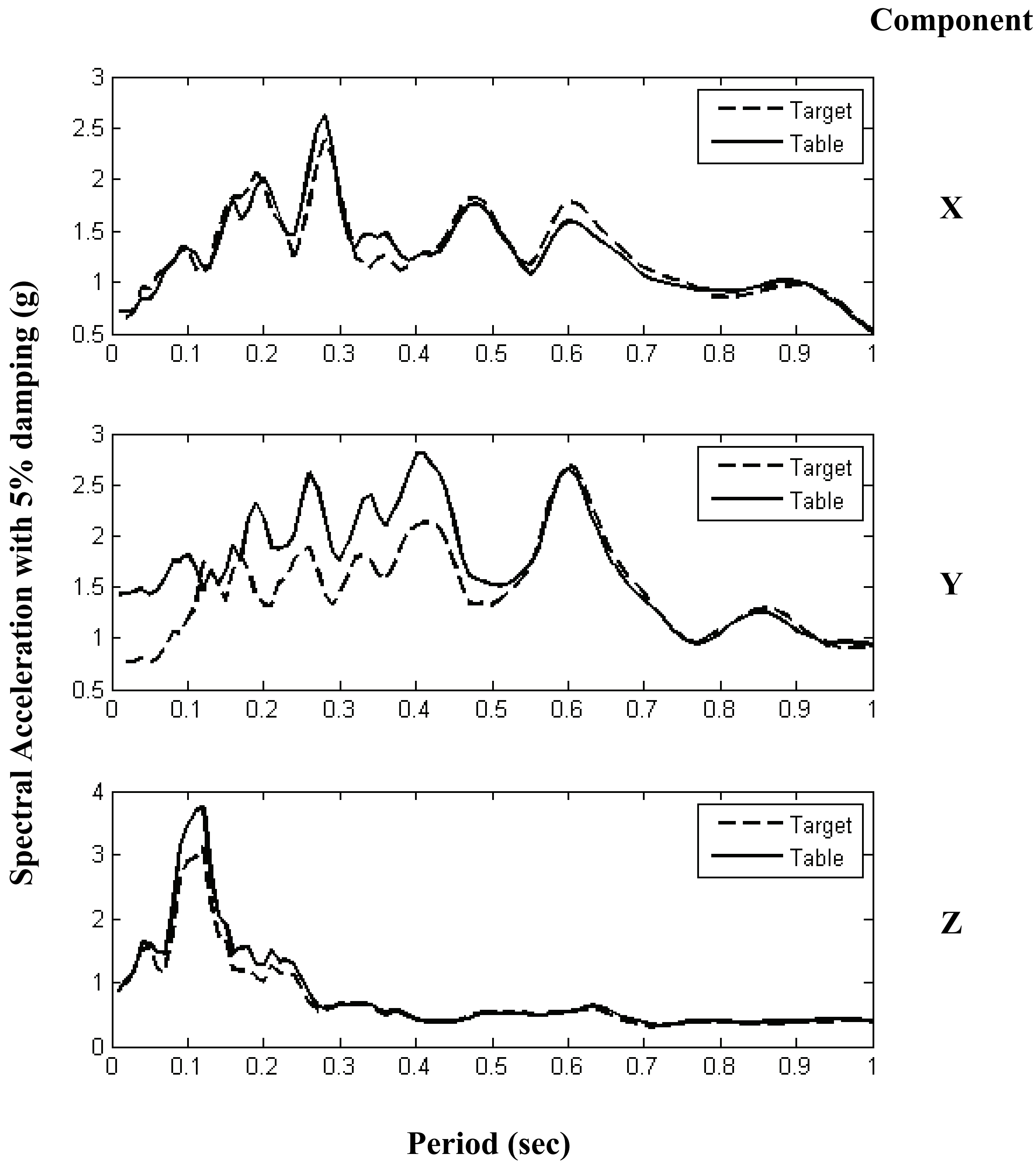

Figure 7.1: Response spectra of ground motion input and table feedback for Seismic Test 5

7.2 Damage Observations

Visual damage inspections were performed after each seismic test. Appendix I contains selected photos that represent the major types of damage observed in the building interior, which was identified in each test phase. The full portfolio with several thousands of photos is available on the NEES website. Table 7.2 summarizes the types of damage observed in each seismic test.

Table 7.2: Visual damage check description after each seismic test

Seismic Test	Damage observation
1	Minor cracking on drywall near corner of openings; no detectable damage to structural members or panels.
2	Propagation of existing cracks, some cracks extended to the edge of the drywall panel; damage to ceiling GWB panel near elevator walls; no detectable damage to structural members
3	Very limited propagation of existing cracks; most cracks remained unchanged; cracking on exposed compression studs of Midply wall was observed but there is no sign of propagation; no detectable damage to structural members
4	Limited propagation of existing cracks; most cracks remained unchanged; minor cracking on ceiling GWB panel at very limited locations; no detectable damage to structural members
5	Propagation of existing cracks; local buckling of GWB panel near wall openings; new cracks observed on exposed compression studs of Midply wall; several nails showed sign of pulling out on Midply wall studs; the exterior shear wall panels were examined after the test, no structural damage was observed based on the inspection.

In general, the damage to the test specimen from all seismic tests was not felt to be significant. There was no visible significant damage to any structural components or assemblies of the building, with damage limited to the gypsum wall board (GWB). The GWB damage was observed primarily around the corners of openings as shown in the photographs in Figure 7.2.

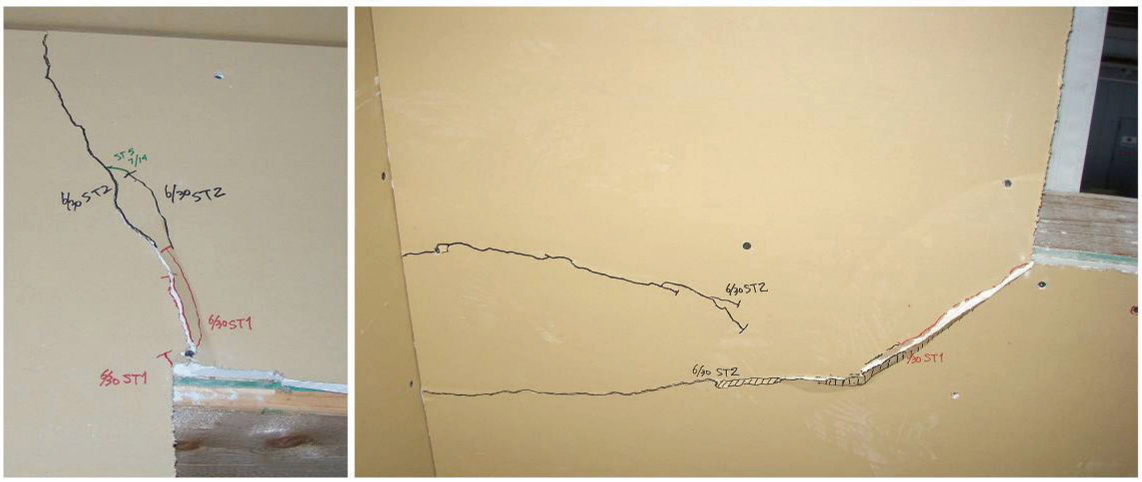

Figure 7.2: Typical visual damage inspection photo

Although the inter-story drift was small for most of the seismic tests, correlation was still observed between the damage and story drift. The cracking of gypsum wall board was more severe for stories with larger inter-story drift as would be expected. For example, the overall damage observed on the upper floors with greater average inter-story drifts (e.g., 5^{th} and 6^{th}) was more severe than the damage observed on the 2^{nd} floor.

7.3 Optical Tracking Measurements

There were 50 points on the exterior of the Capstone test building that were monitored during the seismic tests using an optical tracking displacement measurement system. This optical tracking data was used to compute the global displacement response and inter-story displacement of the Capstone test building. For each point, the raw data from the optical tracking system was tri-axial absolute displacement. The accuracy of the measurement in ideal conditions could be controlled within a few millimeters, although the exact accuracy is not constant for all points on the building since it is a function of camera distance and often visibility. The measurement can also be affected by lighting conditions, thus there are several points that exhibited more noise than others.

The optical tracking measurements were synchronized with the shake table displacement measurements. By subtracting the table motion from the optical tracking time history, the displacement of each point relative to the shake table was obtained and is presented in its entirety in Appendix E. These relative displacements are the basis for computing the building responses including roof displacement, inter-story drifts, torsional response, and overall building deformation profile.

Sign convention for the optical tracking measurements is shown in Chapter 4 (Figure 4.6). The point on the Capstone test building that experienced the maximum amount of movement relative to the shake table was located at corner D on the roof level (see Figure 7.3).

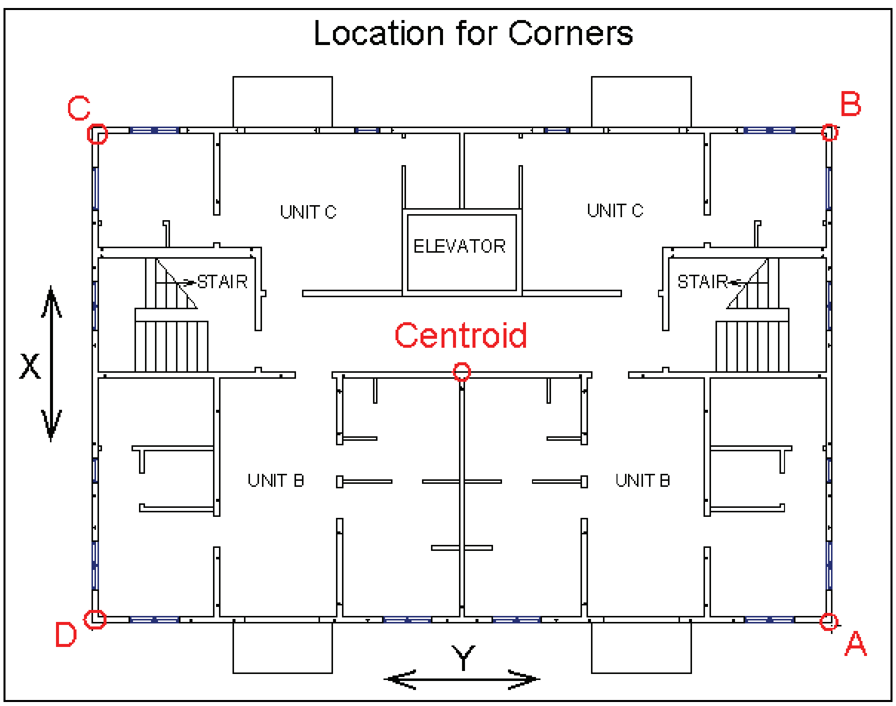

Figure 7.3: Location of the corners and centroid for each story diaphragm (roof)

By averaging measurements from all seven optical tracking points (see Appendix E for tracking points locations), the average floor displacement response was obtained and is termed "averaged displacement". The roof level experienced the maximum averaged displacement relative to shake table. The time history for the roof averaged responses is illustrated in Figure 7.4. Figure 7.5 shows the average lateral response of the roof displacement during seismic test 5 (MCE) together with the response of the two opposite corners at the roof. It is apparent that torsion was present in the Capstone test building's lateral response since there was a significant difference in the responses at opposite corners. Table 7.3 lists the maximum displacement values (relative to the building foundation) for the centroid and four corners of each floor level for all seismic tests.

Table 7.3: Maximum displacements on the roof level

Test Date	30-Jun				6-Jul				14-Jul	
Centroid										
Max Displacement (inch)	Test 1		Test 2		Test 3		Test 4		Test 5	
Direction	X	Y	X	Y	X	Y	X	Y	X	Y
SMF	0.21	0.35	0.37	0.56	0.13	0.11	0.18	0.31	0.34	0.37
Story 2	0.46	0.71	0.93	1.52	0.28	0.50	0.61	1.12	0.92	1.52
Story 3	0.63	1.23	1.59	2.54	0.54	0.88	1.14	2.10	1.74	2.88
Story 4	0.86	1.59	2.20	3.69	0.72	1.38	1.61	3.06	2.50	4.46
Story 5	1.17	2.00	3.03	4.90	0.94	1.78	2.36	4.20	3.55	5.88
Story 6	1.41	2.31	3.66	5.97	1.26	2.23	2.93	5.23	4.51	7.70
Story 7 (roof)	1.67	2.57	4.38	6.52	1.55	2.37	3.65	5.76	5.58	8.62
Corner A										
SMF	0.45	0.56	0.83	0.87	0.52	0.20	0.58	0.36	0.94	0.58
Story 2	0.75	1.01	1.18	1.95	0.54	0.65	0.69	1.33	1.28	1.84
Story 3	0.69	1.35	1.22	3.19	0.49	1.14	0.97	2.42	1.54	3.54
Story 4	0.87	1.88	1.74	4.58	0.55	1.78	1.12	3.86	1.99	5.38
Story 5	0.92	2.41	2.17	5.51	0.69	2.45	1.64	4.83	3.05	6.63
Story 6	1.32	2.69	2.31	7.02	0.67	2.83	1.72	6.24	3.30	9.15
Story 7 (roof)	1.13	3.06	2.54	7.68	0.73	2.98	1.75	6.90	3.25	10.15
Corner B										
SMF	0.19	0.27	0.39	0.46	0.18	0.12	0.24	0.24	0.22	0.39
Story 2	0.27	0.56	0.80	1.44	0.24	0.51	0.50	1.07	0.68	1.51
Story 3	0.45	1.08	1.03	2.30	0.39	0.72	0.71	1.95	1.26	2.68
Story 4	0.57	1.38	1.32	3.38	0.45	1.16	1.07	2.68	1.65	4.04
Story 5	0.73	1.74	1.69	4.25	0.58	1.55	1.18	3.69	2.28	5.38
Story 6	0.87	1.94	1.95	5.20	0.68	1.78	1.46	4.63	2.85	6.92
Story 7 (roof)	0.99	2.40	2.37	5.74	0.70	2.01	1.74	5.15	3.01	7.83
Corner C										
SMF	0.36	0.28	0.63	0.54	0.17	0.31	0.33	0.39	0.40	0.38
Story 2	0.63	0.69	1.44	1.34	0.52	0.46	1.02	0.94	1.38	1.39
Story 3	1.03	1.11	2.44	2.36	0.94	0.83	1.84	1.85	2.57	2.67
Story 4	1.40	1.38	3.34	3.22	1.28	1.22	2.66	2.65	3.94	3.78
Story 5	1.81	1.77	4.40	4.32	1.65	1.52	3.64	3.62	5.26	5.24
Story 6	2.10	2.08	5.31	5.13	2.06	1.84	4.46	4.36	6.35	6.23
Story 7 (roof)	2.47	2.28	6.07	5.84	2.39	2.12	5.34	5.08	7.96	7.58
Corner D										
SMF	0.47	0.49	0.76	0.70	0.61	0.41	0.64	0.44	1.06	0.57
Story 2	1.71	1.53	1.60	1.71	0.99	0.58	1.10	1.33	1.41	1.80
Story 3	1.15	1.27	2.62	3.13	1.02	1.23	2.05	2.59	3.03	3.67
Story 4	1.53	1.85	3.47	4.38	1.34	1.75	2.75	3.66	4.36	5.50
Story 5	1.98	2.32	4.58	5.89	1.63	2.14	4.11	5.07	5.62	6.27
Story 6	2.16	2.73	5.78	7.31	2.30	2.87	4.97	6.67	7.22	9.19
Story 7 (roof)	2.59	2.79	6.98	7.72	2.68	2.93	5.95	6.73	8.28	9.89

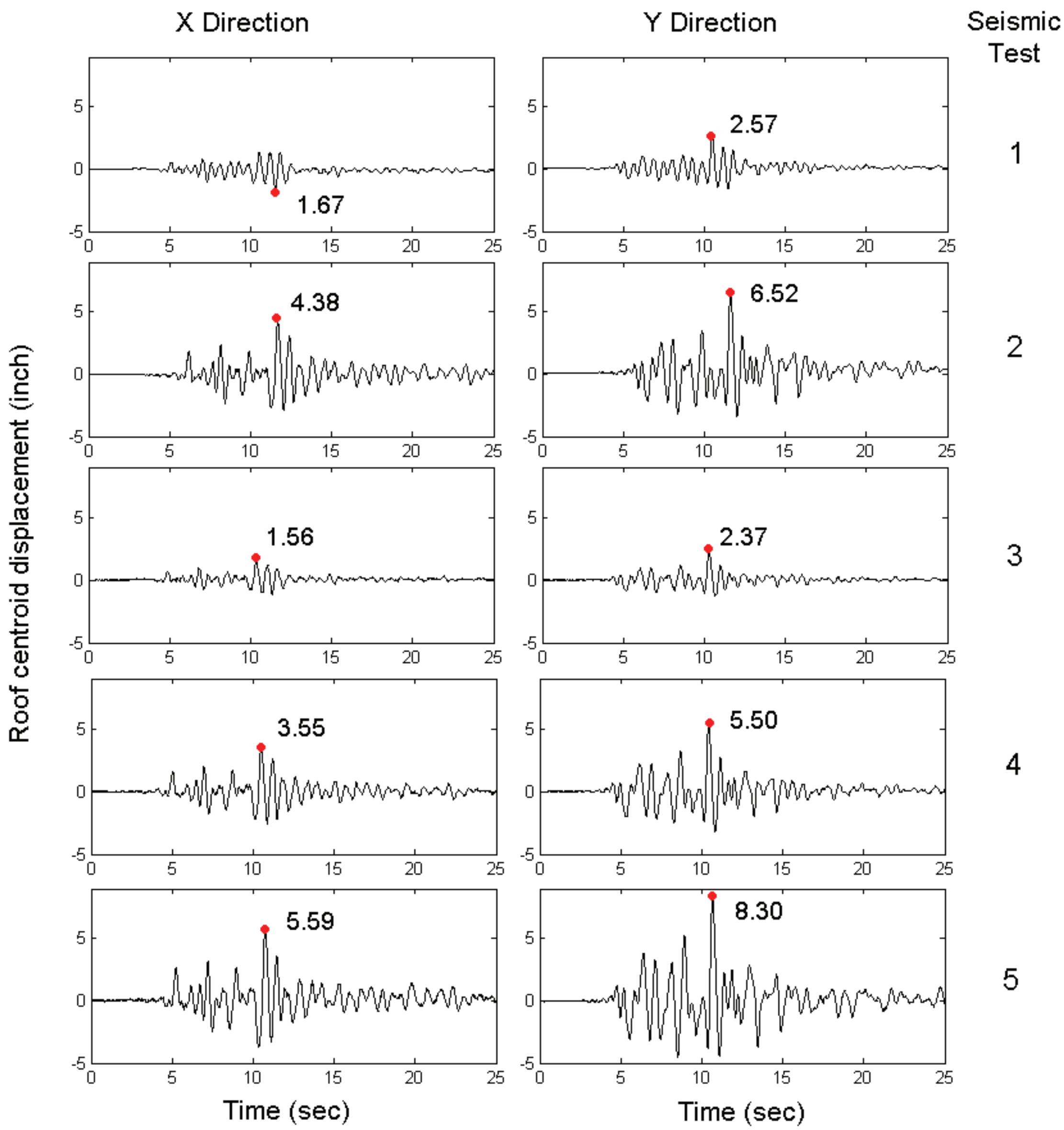

Figure 7.4: Roof displacement relative to ground during seismic tests

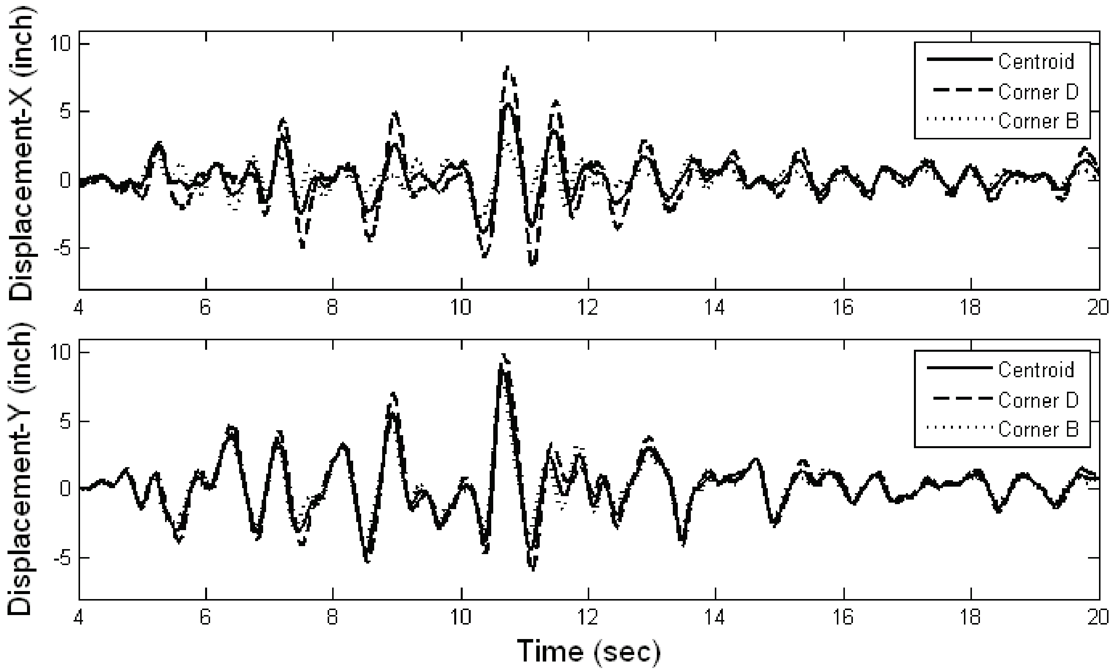

Figure 7.5: Displacement time history of roof centroid and corners

The inter-story time-history displacement responses of the Capstone test building, generated from the averaged floor displacements, are presented in Appendix J, for each seismic test conducted. These time histories were computed by subtracting the lower floor averaged displacement from current floor averaged displacement. Dividing the resulted average inter-story displacement by the story height then results in the averaged inter-story drift. The maximum averaged inter-story drifts for each story for each of the seismic tests are listed in Table 7.4, together with the story height used for the drift calculation. The height of the story was taken as the height of the shear walls for that story. It can be noted that the maximum inter-story drift did not occur at the bottom story.

Table 7.4: Maximum inter-story drift for each story

Test Date		30-Jun				6-Jul				14-Jul	
Inter-story Drift (%)		Test 1		Test 2		Test 3		Test 4		Test 5	
Story	Height (ft)	X	Y	X	Y	X	Y	X	Y	X	Y
SMF	9.1	0.19	0.32	0.34	0.51	0.12	0.10	0.16	0.28	0.31	0.34
Story 2	9	0.35	0.38	0.60	0.91	0.26	0.44	0.49	0.77	0.84	1.12
Story 3	8	0.41	0.58	0.77	1.14	0.35	0.42	0.63	1.05	0.97	1.46
Story 4	8	0.35	0.41	0.75	1.20	0.29	0.54	0.64	1.02	0.89	1.64
Story 5	8	0.36	0.45	0.92	1.31	0.30	0.44	0.77	1.22	1.10	1.48
Story 6	8	0.33	0.35	0.83	1.15	0.36	0.46	0.64	1.14	1.00	1.88
Story 7	8	0.38	0.29	0.96	0.65	0.40	0.21	0.88	0.58	1.35	1.11

The inter-story drift for each individual wall line can be estimated using the optical tracking point data directly located at that wall line. The torsional response means that the inter-story drift at a wall line can be quite different than the averaged floor inter-story drift. Table 7.5 lists the maximum inter-story drifts calculated using the Corner D displacements, which was the maximum observed inter-story drift (with the X direction corresponding to wall line 11, and the Y direction corresponding to wall line E). The story heights used for the drift calculation were the same as that used in average inter-story drift. The difference between the inter-story drifts for the entire story and individual wall line confirmed the presence of torsion.

Table 7.5: Maximum inter-story drift derived from Corner D displacements

Test Date	30-Jun				6-Jul				14-Jul	
	Test 1		Test 2		Test 3		Test 4		Test 5	
	X	Y	X	Y	X	Y	X	Y	X	Y
SMF	0.19	0.32	0.34	0.51	0.12	0.10	0.16	0.28	1.09	0.59
Story 2	1.70	1.37	1.48	1.11	0.91	0.64	1.09	1.02	1.40	1.50
Story 3	1.88	2.04	1.87	1.50	1.25	0.82	1.20	1.41	1.90	2.10
Story 4	0.66	0.78	1.28	1.43	0.69	0.75	1.21	1.18	1.57	2.00
Story 5	0.73	0.75	1.40	1.64	0.60	0.62	1.69	1.69	1.62	2.35
Story 6	0.54	0.63	1.28	1.63	0.74	0.80	1.29	1.90	1.82	3.08
Story 7	0.70	0.53	1.40	0.63	0.69	0.63	1.18	0.71	1.63	0.83

Average story torsion was calculated based on the optical tracking measurements at four corners of the story diaphragm. The formula used to calculate torsion angle is shown in Figure 7.6. Maximum torsion amount (R, in rad) at each story for different seismic tests are listed in Table 7.6.

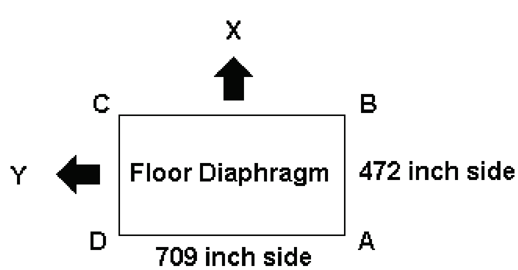

$$R = \left(\frac{(X_A + X_B) - (X_C + X_D)}{709} + \frac{(Y_C + Y_B) - (Y_A + Y_D)}{472} \right) \Big/ 4$$

Figure 7.6: Torsional response calculation

Table 7.6: Maximum torsional response (R) for each story (x10^{-3} rad)

Date	30-Jun		6-Jul		14-Jul
Test	Test 1	Test 2	Test 3	Test 4	Test 5
SMF	0.75	0.98	0.80	0.69	1.01
Story 2	1.25	1.70	0.87	1.46	1.65
Story 3	1.24	2.80	1.31	2.46	3.05
Story 4	1.67	4.04	1.84	3.64	4.67
Story 5	2.15	4.99	2.25	4.87	6.12
Story 6	2.31	5.84	2.78	5.63	7.77
Roof	2.35	6.13	2.82	6.15	8.11

Using the optical tracking displacement data from the exterior of the building, it was possible to plot the deformed shape of the building at any point in time for the seismic test. Figure 7.7 illustrates the deformed shape of Capstone test building during seismic test 5, the MCE level test. Note that it is significantly amplified to be able to see the shape. It can also be seen that lateral and torsional deformation was distributed approximately uniformly along the height of the structure, indicating a first-mode dominant response and lack of a soft story. Note that there was recording noise in some of the optical tracking points, resulting in a distorted shape of the building grid at certain locations.

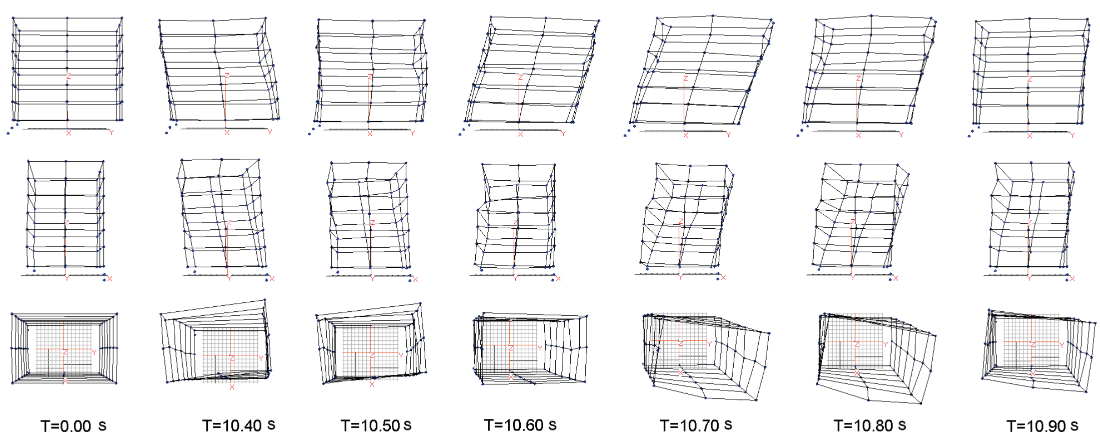

Figure 7.7: Building deformation profile during MCE level test

7.4 Absolute Acceleration Measurements

The absolute acceleration time-histories, recorded at 5 points (see Appendix K) on each floor of the Capstone test building are presented in Appendix K, for each seismic test conducted. Based on these measurements, the average floor acceleration was calculated using weighted average among five accelerometers on the floor, with the accelerometer at the center carrying twice the weight of the accelerometers at the corners. The maximum value for the averaged floor acceleration is summarized in Table 7.7, together with the recorded ground acceleration produced by the shake table.

Table 7.7: Averaged peak acceleration measured at each floor and the ground (g)

Date	Test	Direction	Ground	SMF	Story 2	Story 3	Story 4	Story 5	Story 6	Roof
30-Jun	Test1	X	0.20	0.20	0.20	0.21	0.26	0.32	0.41	0.53
		Y	0.32	0.27	0.26	0.31	0.38	0.49	0.62	0.66
		Z	0.17	0.19	0.24	0.25	0.26	0.29	0.29	0.34
	Test2	X	0.56	0.64	0.59	0.56	0.57	0.65	0.89	1.24
		Y	1.00	0.91	0.86	0.89	0.87	0.93	1.28	1.43
		Z	0.63	0.69	0.78	0.84	0.88	1.02	1.03	1.12
6-Jul	Test3	X	0.19	0.19	0.18	0.20	0.21	0.26	0.35	0.45
		Y	0.31	0.27	0.23	0.22	0.28	0.34	0.51	0.60
		Z	0.22	0.22	0.25	0.27	0.27	0.29	0.31	0.37
	Test4	X	0.47	0.52	0.46	0.52	0.52	0.59	0.91	1.24
		Y	0.85	0.79	0.71	0.77	0.77	0.87	1.27	1.61
		Z	0.61	0.64	0.75	0.80	0.86	0.96	1.03	1.18
14-Jul	Test5	X	0.72	0.77	0.69	0.84	0.87	0.81	1.26	1.52
		Y	1.43	1.27	1.18	1.35	1.33	1.40	1.55	2.06
		Z	0.88	1.02	1.07	1.17	1.33	1.52	1.44	1.76

As one might expect, it can be seen that the floor acceleration increases as story gets higher. The maximum acceleration reached just over 1.5 g for top floor. Excessive acceleration on higher floors of a multi-story building sometimes will results in contents damage and injury to occupants. The level of acceleration measured in the Capstone test building indicated that special fixture details might be needed in preventing damage to contents at higher story levels in multi-story wood frame buildings. Note that the values in the table were the average acceleration for the entire floor. The acceleration at certain locations on the floor (presented in Appendix L) can be higher due to torsion.

7.5 Wall Deformation Measurements

Appendix M presents the displacement time-histories derived from the diagonal string potentiometers that were installed across selected wood shear walls in the Capstone test building, for all seismic tests conducted. The recorded data were modified to transform the diagonal deformations of each instrumented wall, measured by the diagonally oriented string potentiometers, to the equivalent horizontal inter-story displacement. Table 7.8 contains the angle of inclination, ϕ, for each diagonal potentiometer with respect to the horizontal direction, as well as the final scale factor (SF) that was applied to the test data to yield the correct horizontal displacement. The wall numbering for shear walls with diagonal measurements is presented in Figure 7.8. Equation (7.1) shows how ϕ and the SF were computed based on the horizontal and vertical distances L and H, respectively, between the two ends of each string potentiometer. The potentiometers that measured the wall deformations were attached to the center of the top and bottom plates of the walls.

$$SF = 1/\cos(\phi) = 1/\cos(\tan^{-1}(H/L)) \tag{7.1}$$

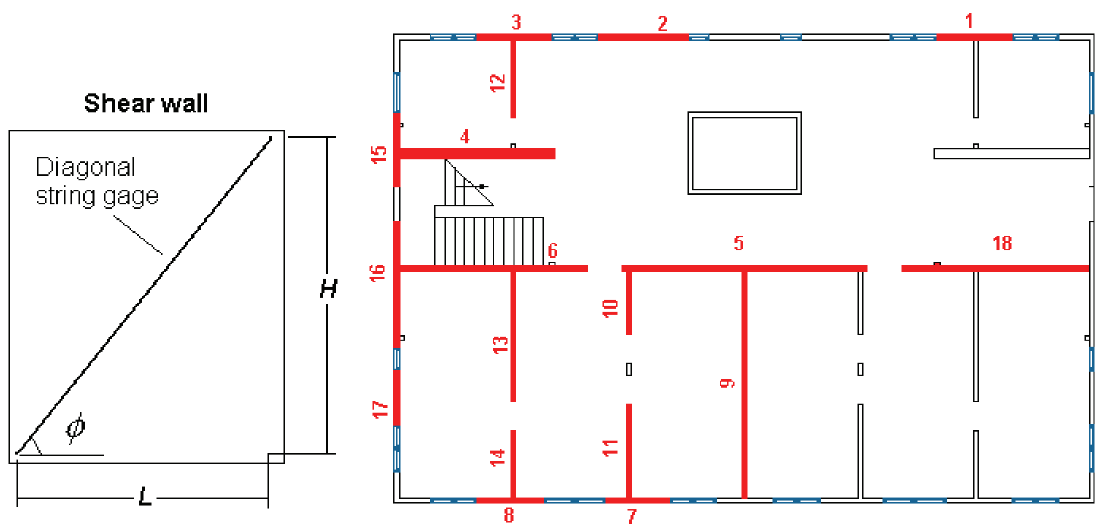

Figure 7.8: Typical configuration of a string potentiometer and numbering of shear walls with diagonal string gage measurements

Table 7.8: Angle of inclination and scale factor for each diagonal string potentiometer

Story	Wall	H (inch)	L (inch)	ϕ (degree)	Sign convention*	SF
2	1	108.75	75.50	55.2	+	1.75
	2	108.75	91.30	50.0	-	1.56
	3	108.75	75.50	55.2	+	1.75
	4	108.75	157.50	34.6	+	1.22
	5	108.75	250.00	23.5	-	1.09
	6	108.75	191.00	29.7	-	1.15
	7	108.75	64.50	59.3	+	1.96
	8	108.75	67.50	58.2	+	1.90
	9	108.75	231.00	25.2	-	1.11
	10	108.75	64.00	59.5	-	1.97
	11	108.75	95.00	48.9	-	1.52
	12	108.75	78.60	54.1	+	1.71
	13	108.75	132.00	39.5	-	1.30
	14	108.75	68.50	57.8	-	1.88
	15	108.75	66.50	58.6	+	1.92
	16	108.75	121.50	41.8	+	1.34
	17	108.75	55.00	63.2	-	2.22
3	4	96.75	157.50	31.6	-	1.17
	9	96.75	231.00	22.7	-	1.08
	17	96.75	55.00	60.4	-	2.02
4	4	96.75	157.50	31.6	-	1.17
	9	96.75	231.00	22.7	+	1.08
	17	96.75	55.00	60.4	+	2.02
5	4	96.75	157.50	31.6	-	1.17
	9	96.75	231.00	22.7	+	1.08
	17	96.75	55.00	60.4	+	2.02
6	4	96.75	157.50	31.6	-	1.17
	9	96.75	231.00	22.7	+	1.08
	17	96.75	55.00	60.4	+	2.02
7	5	96.75	250.00	21.2	+	1.07
	6	96.75	191.00	26.9	+	1.12
	12	96.75	78.60	50.9	-	1.59
	18	96.75	191.00	26.9	+	1.12

* Note: Sign convention indicates the direction of positive reading on diagonal measurements with respect to global coordinate system showing in Figure 4.6.

Table 7.9 lists the maximum wall deformation measured during all seismic tests. One can see from the maximum values that the shear wall deformation was not significant even for the MCE level test, i.e. seismic test 5. This result is consistent with visual damage inspection results indicating that only limited damage to non-structural components occurred.

Table 7.9: Maximum wall shear deformation for all seismic tests

Story	Wall	Shear deformation (inch)				
		Test 1	Test 2	Test 3	Test 4	Test 5
2	1	0.08	0.25	0.10	0.27	0.43
	2	0.19	0.58	0.20	0.51	0.78
	3	0.17	0.52	0.19	0.50	0.75
	4	0.15	0.36	0.12	0.28	0.49
	5	0.24	0.65	0.27	0.62	0.80
	6	0.16	0.55	0.20	0.49	0.72
	7	0.29	0.63	0.28	0.68	0.90
	8	0.52	0.92	0.40	0.88	1.17
	9	0.10	0.32	0.11	0.29	0.52
	10	0.06	0.29	0.05	0.26	0.48
	11	0.11	0.36	0.09	0.34	0.53
	12	0.13	0.35	0.12	0.29	0.47
	13	0.12	0.32	0.14	0.36	0.58
	14	0.21	0.43	0.16	0.40	0.63
	15	0.18	0.45	0.22	0.51	0.79
	16	0.17	0.51	0.22	0.49	0.79
	17	0.17	0.56	0.21	0.55	0.87
3	4	0.13	0.46	0.16	0.38	0.66
	9	0.08	0.24	0.08	0.22	0.39
	17	0.16	0.65	0.22	0.58	0.82
4	4	0.09	0.33	0.14	0.31	0.54
	9	0.07	0.33	0.10	0.29	0.50
	17	0.14	0.53	0.21	0.54	0.90
5	4	0.06	0.31	0.12	0.33	0.65
	9	0.05	0.26	0.07	0.24	0.42
	17	0.12	0.46	0.19	0.50	0.90
6	4	0.15	0.21	0.07	0.27	0.60
	9	0.03	0.19	0.05	0.18	0.31
	17	0.05	0.27	0.11	0.32	0.62
7	5	0.06	0.28	0.10	0.30	0.51
	6	0.02	0.08	0.02	0.09	0.19
	12	0.04	0.35	0.09	0.35	0.73
	18	0.03	0.07	0.02	0.10	0.22

The shear wall displacement measured by the diagonal potentiometers is associated primarily with the shear (racking) deformation of the wall, composed of shear in the sheathing panels, slipping of the nails, and (usually moderate) bending deformations of the framing, which can be observed in walls with relatively high aspect (height over length) ratios. Components of the total inter-story displacements that are not measured by the diagonal potentiometers are any slippage of the bottom sill plate and the top plate (which were not believed to have occurred in the Capstone test building due to the shear connection type) and the rotation of the shear wall as a whole due to shear wall stack bending. The comparison of shear wall deformation with the averaged inter-story deformation obtained from optical tracking measurements indicated that the wall deformation measured using diagonal potentiometers is always smaller than the total inter-story deformation, as it should be. Table 7.10 lists the maximum inter-story drift for the three shear wall stacks obtained from diagonal measurement compared with the inter-story drifts for these wall lines estimated using optical tracking measurements. From the deformation of the shear wall stacks, one can also see that the shear deformation of these walls was distributed quite uniformly along the height of the building.

Table 7.10: Maximum shear and total deformation for shear wall stacks (inch)

Story	Test 1		Test 2		Test 3		Test 4		Test 5	
	Diagonal	Total	Diagonal	Total	Diagonal	Total	Diagonal	Total	Diagonal	Total
	Wall stack 4									
2	0.15	0.48	0.36	0.92	0.12	0.44	0.28	0.81	0.49	1.30
3	0.13	0.47	0.46	1.04	0.16	0.46	0.38	0.98	0.66	1.30
4	0.09	0.44	0.33	1.04	0.14	0.52	0.31	0.97	0.54	1.39
5	0.06	0.43	0.31	1.38	0.12	0.41	0.33	1.02	0.65	1.59
6	0.15	0.45	0.21	0.97	0.07	0.53	0.27	1.09	0.60	1.54
	Wall stack 9									
2	0.10	1.03	0.32	0.92	0.11	0.50	0.29	0.70	0.52	1.22
3	0.08	1.01	0.24	1.01	0.08	0.62	0.22	0.66	0.39	1.16
4	0.07	0.59	0.33	0.86	0.10	0.47	0.29	0.63	0.50	1.02
5	0.05	0.48	0.26	1.28	0.07	0.48	0.24	0.97	0.42	1.49
6	0.03	0.50	0.19	1.21	0.05	0.67	0.18	1.03	0.31	1.49
	Wall stack 17									
2	0.17	1.03	0.56	1.08	0.21	0.81	0.55	1.08	0.87	1.39
3	0.16	0.99	0.65	1.01	0.22	0.62	0.58	0.98	0.82	1.47
4	0.14	0.51	0.53	1.14	0.21	0.57	0.54	1.10	0.90	1.53
5	0.12	0.57	0.46	1.29	0.19	0.52	0.50	1.40	0.90	1.64
6	0.05	0.60	0.27	1.14	0.11	0.61	0.32	1.07	0.62	1.38

The comparison of total inter-story drift and inter-story shear drift clearly indicates that only a portion of the inter-story drift between two adjacent floors is due to wall racking deformations. Therefore, results of racking (shear) tests of wall specimens must be interpreted carefully, since the behavior of the wall specimen, dictated by the tests, is different than the real behavior when the wall is incorporated into a large (system-level) structure.

7.6 Wall End Stud Uplift

Appendix N presents the peak uplift displacements recorded at the end studs of four shear walls in the second and seventh floor, for all seismic tests conducted. Since the LVDT sensors used to measure stud uplift were attached to the floor near the wall corners, the total uplift displacement consisted of two components. The first component was the uplift of the end stud with respect to the sill plate. The second component was the vertical movement of the shear wall corner relative to the nearby floor. These two components were not distinguishable from one the other because only 1 LVDT was used for each corner. As the LVDT was oriented upside-down, negative readings in the raw data file should be interpreted as uplift.

The uplift deformations during the tests were very small even for the MCE level earthquake, e.g. on the order of 0.3 inches. It was not unusual for a wall to develop an unbalanced uplift, which means one side of the wall uplifts much more than the other side. This can be attributed mainly to ground motion and unsymmetrical lateral shear wall deformation. Also, the measurement showed that for most of the studs, the end stud actually can "push" into the floor system during dynamic loading, resulting in a positive reading from the LVDT. But the amount of movement in that direction was generally less than the uplift movement during uplift. The maximum uplift of the studs relative to their initial location (in order to remove the effect of residual deformation from previous tests) is listed in Table 7.11.

Table 7.11: Maximum uplift for selected walls at different intensity levels (inches)

Story	2				7			
Wall	10A		B1		10A		D2	
End	a	b	a	b	a	b	a	b
Test 1	0.04	0.03	0.02	0.08	0.01	0.01	0.02	0.03
Test 2	0.07	0.09	0.06	0.17	0.08	0.12	0.05	0.10
Test 3	0.03	0.04	0.01	0.07	0.02	0.04	0.02	0.03
Test 4	0.06	0.09	0.06	0.15	0.09	0.14	0.04	0.08
Test 5	0.10	0.13	0.06	0.17	0.16	0.27	0.07	0.14

Good correlation between end studs uplift and tension forces in the steel rod anchoring tie-down system was observed. For example, Figure 7.9 shows the time history of stud uplift at one end of the second floor Midply wall and the tension force in the ATS rod near the same location during seismic test 5. Note that the tension force and uplift displacement were both normalized by their maximum value respectively so they could appear on one plot. The peaks of the two time history series can be seen to be closely in phase with one other.

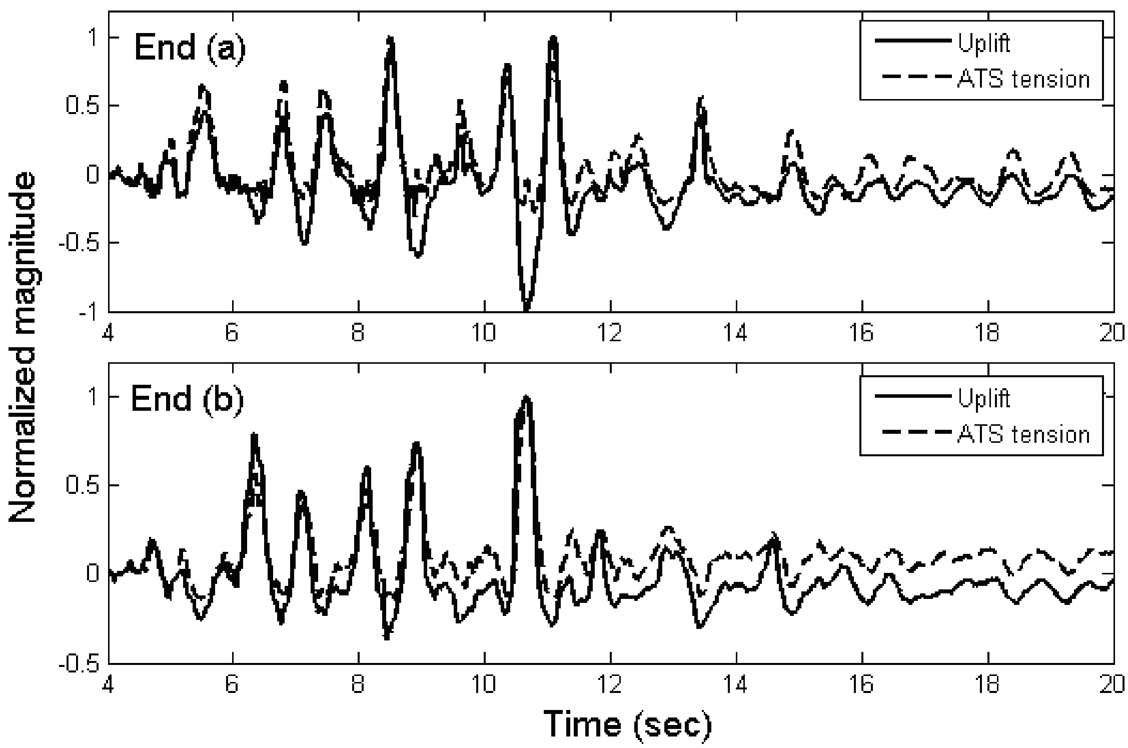

Figure 7.9: Midply wall (B1) stud uplift and rod tension time history comparison

.

7.7 Global Hysteresis Loops

Appendix P presents the global hysteresis loops, in terms of base shear force and building roof central relative displacement, recorded along the two principal orthogonal directions, for all seismic tests conducted. Note that the base shear force for seismic test 1 and 2 was the shear force resisted by the steel moment frame. For test 3, 4, and 5, the shear force of the first wood story (story 2) was used since the SMF was locked down during those tests. Similarly, Appendix Q contains the inter-story hysteresis loops, in terms of story shear force and story central relative displacement, recorded along the two principal directions, for all seismic tests conducted. The forces at each floor level were computed by multiplying the average story absolute acceleration measurements by the tributary mass of the story. As a result, the calculated forces include both the resisting force generated by the structural components and the damping force that is inherent in the system. The displacements were calculated based on optical tracking measurements as described in Section 7.3. Average displacements were used for all hysteresis loops. The maximum and minimum force and displacement values are indicated on each figure of Appendices P and Q by a black circle. Note that the maximum (or minimum) displacement and force may not occur at the same time, thus the point indicated by the circle may not appear to be part of the hysteresis loop data. Figure 7.10 Shows the global hysteresis loop in both directions for Seismic Test 5.

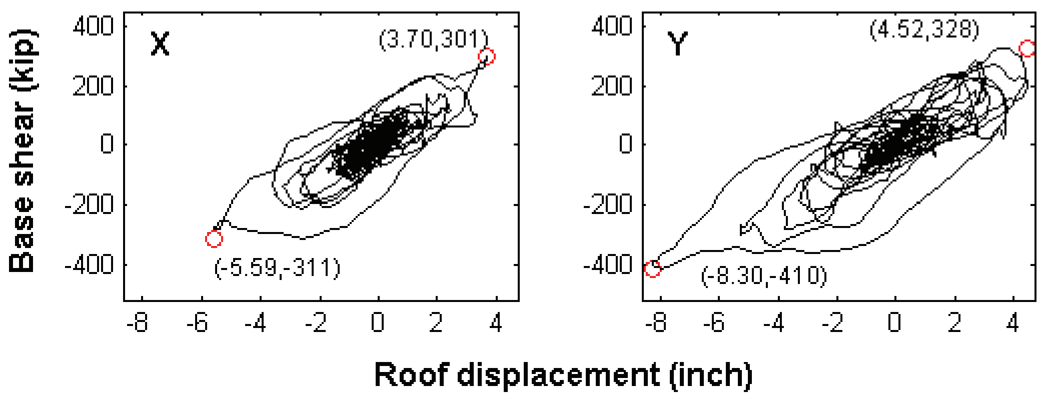

Figure 7.10: Global hysteresis loop from Seismic Test 5

The global hysteresis presented in Appendix P were all similar in shape because the same ground motion record was used for all the tests with different scaling factors. The maximum base shear during the MCE event exceeded 60% of building total weight. More hysteretic energy dissipation was observed (represented by the area surrounded by the hysteretic loops) as the seismic intensity increases for both building configurations.

The shape of the hysteresis for the SMF story changed drastically after seismic test 2 because of the addition of the bracing members, essentially makes it a layer with very high lateral stiffness. The behavior of the SMF story in test 1 and 2 was close to a linear response, which was expected for the SMF considering the level of seismic intensity during those tests. Inspection of the hysteresis loops for the wood stories shows that similar behavior occurred for most stories. The amount of inter-story displacement was close for each story, while the hysteretic energy dissipation and maximum shear forces decreased as story gets higher, i.e. going up the building. The seventh story almost behaved linearly with very little energy dissipation compared to the other stories. Table 7.12 lists the maximum values for story shear and displacement for each story during all seismic tests.

Table 7.12: Maximum story shear force and displacement during all test levels

Story	Test 1		Test 2		Test 3		Test 4		Test 5	
Force (kip)	Fx	Fy	Fx	Fy	Fx	Fy	Fx	Fy	Fx	Fy
SMF	154	229	287	370	112	159	244	317	355	398
Story 2	141	223	282	366	107	161	232	325	311	410
Story 3	134	212	266	362	102	154	227	323	316	405
Story 4	123	192	251	329	94	143	224	307	308	387
Story 5	105	159	222	294	84	125	212	274	281	359
Story 6	76	109	173	220	65	93	157	221	206	292
Story 7	35	43	80	93	29	39	80	104	99	134
Displacement (inch)	Dx	Dy	Dx	Dy	Dx	Dy	Dx	Dy	Dx	Dy
SMF	0.21	0.35	0.37	0.56	0.13	0.11	0.18	0.31	0.34	0.37
Story 2	0.38	0.41	0.65	0.99	0.29	0.48	0.53	0.83	0.92	1.22
Story 3	0.39	0.56	0.75	1.10	0.34	0.41	0.61	1.01	0.94	1.41
Story 4	0.34	0.39	0.72	1.16	0.28	0.53	0.62	0.99	0.86	1.58
Story 5	0.35	0.43	0.89	1.27	0.29	0.43	0.75	1.18	1.07	1.43
Story 6	0.32	0.34	0.80	1.12	0.35	0.44	0.62	1.10	0.97	1.82
Story 7	0.37	0.28	0.93	0.63	0.39	0.20	0.85	0.56	1.30	1.08

7.8 Anchor Tie-down Force Measurements

During seismic tests, strain measurement time histories for the anchor tie-down rods were recorded at selected locations throughout the Capstone test building, mostly in shear walls in the 2nd story. Appendix M presents the time histories of the rod forces derived from these strain measurements for all instrumented rods for all seismic tests conducted. The maximum rod forces at the 2nd story for each seismic test are also presented in Appendix M. The rod forces were calculated based on rod cross sectional area and modulus of elasticity of steel (29,000ksi). The actual rod diameter used in calculating section area is listed in Table 7.13.

Table 7.13: Actual rod diameter for rod force calculation

Story	Wall	Rod size	
		Diameter (inch)	Area (inch2)
2	1	1.15	1.04
	2	1.75	2.41
	3	1.15	1.04
	4	1.75	2.41
	5	1.75	2.41
	6	1.75	2.41
	7	1.75	2.41
	8	1.75	2.41
	9	1.75	2.41
	10	1.75	2.41
	11	1.75	2.41
	12	1.75	2.41
	13	1.75	2.41
	14	1.75	2.41
	15	1.75	2.41
	16	1.75	2.41
	17	1.75	2.41
3	4	1.02	0.82
	9	1.75	2.41
	17	1.75	2.41
4	4	0.80	0.50
	9	1.02	0.82
	17	1.02	0.82
5	4	0.80	0.50
	9	1.02	0.82
	17	0.80	0.50
6	4	0.56	0.25
	9	0.56	0.25
	17	0.80	0.50
7	5	0.56	0.25
	6	0.56	0.25
	12	0.56	0.25
	18	0.56	0.25

The maximum hold-down forces are presented in Table 7.14 for all seismic tests. The maximum uplift measured was more than 170 kips, thus the need for specification of a high strength continuous tie-down system is apparent for this type of building to survive a major earthquake such as the ground motion used in seismic test 5.

Table 7.14: Maximum hold-down forces for all seismic tests (kips)

Story	Wall No.	Test 1		Test 2		Test 3		Test 4		Test 5	
		a	b	a	b	a	b	a	b	a	b
2	1	15.7	0.4	34.0	5.0	18.4	4.2	32.6	6.0	47.2	15.7
	2	12.5	11.0	28.7	20.4	7.9	8.6	23.8	21.4	39.2	33.9
	3	8.1	15.7	34.5	22.7	20.0	14.7	37.7	24.7	49.9	34.0
	4	19.0	41.6	23.7	121.9	7.6	52.0	18.1	111.7	29.2	**172.6**
	5	28.5	19.7	48.9	43.6	16.5	16.5	41.7	33.6	56.7	49.4
	6	34.1	18.1	70.1	37.0	33.3	14.5	66.8	31.9	82.1	44.7
	7	9.1	2.3	20.2	25.3	1.0	8.4	4.2	26.6	18.3	40.8
	8	5.0	55.2	3.4	100.7	3.5	51.0	16.8	96.7	16.5	129.2
	9	1.8	17.3	20.9	45.0	8.2	16.5	20.7	43.0	31.0	61.2
	10	8.2	3.9	30.7	12.0	6.3	4.1	28.7	13.3	50.4	23.9
	11	4.5	12.6	20.9	41.1	4.8	19.4	21.2	47.4	29.7	63.1
	12	7.1	6.8	15.3	25.0	9.0	12.5	20.2	27.1	26.3	42.3
	13	4.9	3.9	19.0	26.8	7.1	8.3	20.0	26.2	28.9	41.1
	14	6.5	19.1	8.8	44.9	3.6	14.6	8.7	33.9	11.8	48.0
	15	27.7	14.8	54.3	27.1	21.0	7.9	49.3	24.6	64.6	33.5
	16	17.9	3.4	39.2	14.8	17.3	4.7	44.0	12.5	51.7	21.4
	17	1.7	3.3	19.4	7.1	-0.5	16.6	2.5	40.8	4.6	56.8
3	4	15.2	33.8	80.9	110.2	35.6	49.9	69.3	109.6	85.9	135.4
	9	11.2	15.2	34.2	39.0	14.8	15.4	37.2	37.4	50.8	52.9
	17	1.1	3.5	18.6	7.0	-0.4	16.7	3.5	41.0	6.4	56.9
4	4	8.9	13.5	44.5	55.5	19.8	26.6	40.0	56.4	53.6	80.9
	9	5.8	6.8	19.6	21.9	9.0	9.0	20.3	21.5	29.0	33.0
	17	0.0	0.3	8.8	5.1	-0.3	5.2	3.0	16.5	5.1	23.5
5	4	4.7	6.2	19.2	26.7	8.2	12.8	16.5	28.9	23.8	44.6
	9	1.3	0.6	5.9	4.5	2.7	1.0	6.5	4.8	11.0	8.3
	17	-0.1	0.0	3.1	2.0	-0.1	0.5	1.8	4.6	2.9	7.2
6	4	2.7	3.3	11.3	7.8	4.9	4.5	9.0	9.1	12.8	15.7
	9	0.6	0.3	2.9	2.1	1.3	0.5	3.1	2.2	5.1	3.9
	17	0.0	0.0	0.9	1.4	0.0	0.2	0.6	2.8	1.0	4.8
7	5	2.0	0.9	3.1	2.7	1.8	1.5	3.5	2.8	5.0	4.7
	6	0.8	3.4	0.9	4.3	0.7	1.9	0.9	3.1	1.6	4.2
	12	1.5	1.6	5.4	2.1	1.8	0.7	5.3	2.7	8.0	5.5
	18	0.7	0.1	2.2	0.2	1.2	0.0	2.0	0.0	2.8	0.5

Note that the maximum hold-down forces shown in Appendix M and listed in Table 7.14 do not necessarily occur at the same time. In order to identify the pattern of the spatial distribution of tie-down forces at a specific time during the test, a "snap-shot" of the force distribution at several points in time during seismic test 5 are shown in Figure 7.11. From a series of time capture plots, one can see that it is not uncommon for the rods at two ends of a wall to act in unison rather than alternating in tension, especially for the walls on the exterior of the test specimen. The alternation in rod tension was observed to shift from the shear wall level to the system level, i.e. where the majority of rods on one side of the building go into tension while the rods on the other side are not in tension (stud packs go into compression). It is believed that this occurred partially as a result of boundary conditions enforced at the shear wall stud packs, i.e. framing into a wall perpendicular to the shear wall. Recall that the tie-down rods are not designed to go into compression and the wood stud packs at the ends of the shear walls take compression load while the rod is simply allowed to slip. The rocking alternation at wall level does occur in some of the interior walls.

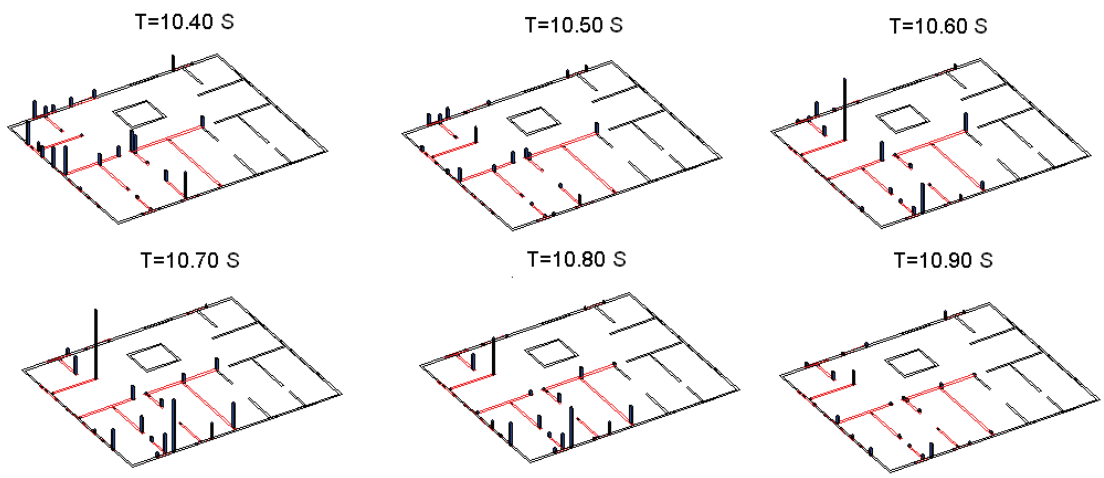

Figure 7.11: Time capture of rod forces during seismic test 5

7.9 Floor Diaphragm Out-of-plane Deformation

Relative vertical displacement between the 2nd story floor and ceiling was measured using LVDTs for 13 locations. The resulting deformation is presented in Appendix O. There is no apparent trend for the relative relationship of these deformations at different locations. The measured deformation for all locations was quite small. During seismic test 1 and 2, there was significant (relative) drifting of the origin for the measurements, indicating the building actually “settled” into a more stable stage after the initial shake, which was somewhat expected for new construction.

7.10 SMF moment connection strain measurement

Appendix S presents the strain measurements for 17 moment connections for the steel moment frame for all seismic tests conducted. The cross sectional area of the yielding plate and the basic geometry for each moment connection is shown in Figure 7.12 with specific dimensions listed in Table 15. Further analysis of the moment frame data was not conducted in this study.

Table 7.15: Dimensions for moment frame connections

Moment connection	H (inch)	B_p (inch)	t (inch)	A_p (inch^2)
1	16.95	4.80	0.63	3.00
2	17.59	4.80	0.63	3.00
3	17.59	4.80	0.63	3.00
4	17.59	4.80	0.63	3.00
5	17.59	4.80	0.63	3.00
6	17.59	4.80	0.63	3.00
7	17.05	3.60	0.63	2.25
8	17.05	3.60	0.63	2.25
9	17.59	6.00	0.63	3.75
10	17.59	6.00	0.63	3.75
11	16.95	5.00	0.63	3.13
12	16.95	5.00	0.63	3.13
13	16.95	5.00	0.63	3.13
14	17.59	4.80	0.63	3.00
15	16.95	4.80	0.63	3.00
16	16.83	5.00	0.50	2.50
17	17.47	5.00	0.50	2.50

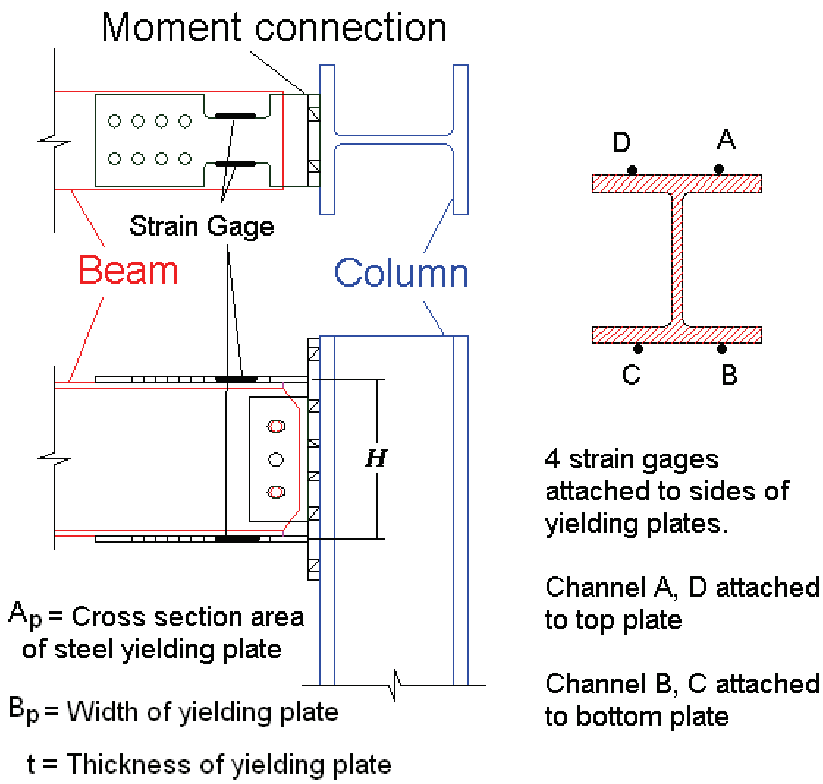

Figure 7.12: Geometry of the moment connection

Chapter 8 Summary and Conclusions

A series of five shake table tests on (1) a full-scale seven-story light-frame wood and steel hybrid building and (2) a full-scale six-story light-frame wood building were completed in July 2009 in Miki, Japan. The building was designed using a new PBSD philosophy developed within the NSF-funded NEESWood project. The building was constructed in Japan during a four-month period with construction materials shipped from the U.S. and Canada. Two phases of seismic testing were conducted. The first phase was the testing of 7-story hybrid structure with a steel moment frame at story 1. Two seismic tests were conducted during the first phase, with the maximum ground motion intensity corresponding approximately to a 665 year return period. During the second phase, the steel moment frame story was “locked down” with cross bracing members and the 6-story wood-only structure was subjected to three seismic tests, with maximum ground motion intensity corresponding approximately to the 2,475 year return period. The building performed very well with maximum averaged inter-story drifts on the order of 2% and suffered only minor damage, i.e. non-structural. Peak inter-story drifts for shear walls at one corner of the building slightly exceeded 3% due to the torsional response during the test. Based on the results of this test, the following conclusions can be drawn:

1.) It is feasible to design multi-story light-frame wood structure to survive major earthquakes and achieve expected performance levels using PBSD procedure developed in the NEESWood project.

2.) Design of a light-frame wood building using PBSD enabled better performance at all seismic intensities including the 2,475 year earthquake than has been observed in historical earthquakes and shake table tests for force-based designed buildings. However, this conclusion should note that these force-based design buildings were not specifically designed for MCE level events.

3.) Amplified accelerations were observed at the higher story levels but were felt to be reasonable given the height of the structure. Although there would be some contents damage, it is likely much of this could be prevented with proper precautions in a high seismic region.

4.) Although the floor plan of the Capstone test building was approximately symmetric and the seismic mass was evenly distributed, torsional response was still present during seismic tests. Inclusion of torsion is needed within PBSD, e.g. Direct Displacement Design, for mid-rise light-frame wood buildings.

5.) The tie-down system employed in the design of the specimen serves the critical role of transferring uplift forces down to the foundation and thereby preventing overturning. Although installed for each shear wall, correlation among the tie-down rods near the same floor plan region was observed during the tests, which means the rod acted as a system to provide overturning restraint to the entire floor plan as well as resisting racking motion for individual shear wall stack, depending on the boundary conditions.

Chapter 9 References

Christovasilis, I.P., Filiatrault, A., and Wanitkorkul, A. (2007). “Seismic testing of a full-scale two-story wood light-frame building: NEESWood benchmark test” NEESWood *Report No. NW-01*, Dept. of Civil, Structural and Environmental Engineering, University at Buffalo, State University of New York, Buffalo, available on-line at http://www.engr.colostate.edu/NEESWood/.

Collins, M., Kasal, B., Paevere, P. and Foliente, G.C.(2005). “Three-dimensional model of light frame wood buildings. I: Model description” *Journal of Structural Engineering*, v 131, n 4, p 676-683.

ICBO. (1988). “Uniform Building Code, 1988 ed.” International Conference of Building Officials, Whittier, CA.

Filiatrault, A., Christovasilis, I.P., Assawin Wanitkorkul, and John W. van de Lindt (2007) “Seismic Response of a Full-Scale Light-frame Wood Building: Experimental Study” *Journal of Structural Engineering,* In Press.

Folz, B. and Filiatrault, A. (2001) “Cyclic analysis of wood shear walls” *Journal of Structural Engineering*, v 127, n 4, p 433-441.

Folz, B. and Filiatrault, A. (2004) “Seismic analysis of woodframe structures. I: Model formulation” *Journal of Structural Engineering*, v 130, n 9, p 1353-1360.

Folz, B. and Filiatrault, A. (2004) “Seismic analysis of woodframe structures. II: Model implementation and verification” *Journal of Structural Engineering*, v 130, n 9, p 1361-1370.

Mosalam, K.M., C. Mochado, K.U. Gliniorz, C. Naito, E. Kurkel, and S.A. Mahin (2003) “Seismic evaluation of an asymmetric three-story woodframe building” CUREE Report W-19.

Pang, W.C., Rosowsky, D.V., Pei, S., and van de Lindt, J.W. (2007). “Evolutionary Parameter hysteretic Model for Wood Shear Walls.” *ASCE Journal of Structural Engineering*; 133(8); 1118-1129.

Pang, W.C., and Rosowsky, D.V. (2009) “Direct displacement procedure for performance-based seismic design of multistory woodframe structures” NEESWood *Report No. NW-02*, Zachry Dept. of Civil Engineering, Texas A&M University, College Station, available on-line at http://www.engr.colostate.edu/NEESWood/.

Pei S., and van de Lindt J.W. (2007). User’s manual for SAPWood for Windows, Version 1.0. SAPWood program user’s manual, available on-line at http://www.engr.colostate.edu/NEESWood/.

Pei S., and van de Lindt J.W. (2009). ”Coupled shear-bending formulation for seismic analysis of stacked wood shear wall systems”, *Earthquake Engineering and Structural Dynamics*, 38: 1631-1647.

Pei, S., Ni, C., van de Lindt, J.W., and Pryor, S.E. (2010). “Experimental Seismic Behavior of a Five-Story Double-Midply Wood Shear Wall in a Full Scale Building”, Canadian Journal of Civil Engineering, In Press.

Shinde, J. and Symans, M. (2010). “Integration of Seismic Protection Systems in Performance-based Seismic Design of Woodframed Structures” Neeswood *Report No. NW-06*, Rensselaer Polytechnic Institute, Troy, NY, available on-line at http://www.engr.colostate.edu/NEESWood/.

Tarabia, A.M. and Itani, R.Y. (1997) “Seismic response of light-frame wood buildings” *Journal of Structural Engineering*, v 123, n 11, p 1470-1477.

van de Lindt, J.W. and Liu, H. (2007) “Nonstructural elements in performance-based seismic design of wood frame structures” *Journal of Structural Engineering*, v 133, n 3, p 432-439.

MCEER Technical Reports

MCEER publishes technical reports on a variety of subjects written by authors funded through MCEER. These reports are available from both MCEER Publications and the National Technical Information Service (NTIS). Requests for reports should be directed to MCEER Publications, MCEER, University at Buffalo, State University of New York, 133A Ketter Hall, Buffalo, New York 14260. Reports can also be requested through NTIS, P.O. Box 1425, Springfield, Virginia 22151. NTIS accession numbers are shown in parenthesis, if available.

NCEER-87-0001 "First-Year Program in Research, Education and Technology Transfer," 3/5/87, (PB88-134275, A04, MF-A01).

NCEER-87-0002 "Experimental Evaluation of Instantaneous Optimal Algorithms for Structural Control," by R.C. Lin, T.T. Soong and A.M. Reinhorn, 4/20/87, (PB88-134341, A04, MF-A01).

NCEER-87-0003 "Experimentation Using the Earthquake Simulation Facilities at University at Buffalo," by A.M. Reinhorn and R.L. Ketter, to be published.

NCEER-87-0004 "The System Characteristics and Performance of a Shaking Table," by J.S. Hwang, K.C. Chang and G.C. Lee, 6/1/87, (PB88-134259, A03, MF-A01). This report is available only through NTIS (see address given above).

NCEER-87-0005 "A Finite Element Formulation for Nonlinear Viscoplastic Material Using a Q Model," by O. Gyebi and G. Dasgupta, 11/2/87, (PB88-213764, A08, MF-A01).

NCEER-87-0006 "Symbolic Manipulation Program (SMP) - Algebraic Codes for Two and Three Dimensional Finite Element Formulations," by X. Lee and G. Dasgupta, 11/9/87, (PB88-218522, A05, MF-A01).

NCEER-87-0007 "Instantaneous Optimal Control Laws for Tall Buildings Under Seismic Excitations," by J.N. Yang, A. Akbarpour and P. Ghaemmaghami, 6/10/87, (PB88-134333, A06, MF-A01). This report is only available through NTIS (see address given above).

NCEER-87-0008 "IDARC: Inelastic Damage Analysis of Reinforced Concrete Frame - Shear-Wall Structures," by Y.J. Park, A.M. Reinhorn and S.K. Kunnath, 7/20/87, (PB88-134325, A09, MF-A01). This report is only available through NTIS (see address given above).

NCEER-87-0009 "Liquefaction Potential for New York State: A Preliminary Report on Sites in Manhattan and Buffalo," by M. Budhu, V. Vijayakumar, R.F. Giese and L. Baumgras, 8/31/87, (PB88-163704, A03, MF-A01). This report is available only through NTIS (see address given above).

NCEER-87-0010 "Vertical and Torsional Vibration of Foundations in Inhomogeneous Media," by A.S. Veletsos and K.W. Dotson, 6/1/87, (PB88-134291, A03, MF-A01). This report is only available through NTIS (see address given above).

NCEER-87-0011 "Seismic Probabilistic Risk Assessment and Seismic Margins Studies for Nuclear Power Plants," by Howard H.M. Hwang, 6/15/87, (PB88-134267, A03, MF-A01). This report is only available through NTIS (see address given above).

NCEER-87-0012 "Parametric Studies of Frequency Response of Secondary Systems Under Ground-Acceleration Excitations," by Y. Yong and Y.K. Lin, 6/10/87, (PB88-134309, A03, MF-A01). This report is only available through NTIS (see address given above).

NCEER-87-0013 "Frequency Response of Secondary Systems Under Seismic Excitation," by J.A. HoLung, J. Cai and Y.K. Lin, 7/31/87, (PB88-134317, A05, MF-A01). This report is only available through NTIS (see address given above).

NCEER-87-0014 "Modelling Earthquake Ground Motions in Seismically Active Regions Using Parametric Time Series Methods," by G.W. Ellis and A.S. Cakmak, 8/25/87, (PB88-134283, A08, MF-A01). This report is only available through NTIS (see address given above).

NCEER-87-0015 "Detection and Assessment of Seismic Structural Damage," by E. DiPasquale and A.S. Cakmak, 8/25/87, (PB88-163712, A05, MF-A01). This report is only available through NTIS (see address given above).

NCEER-87-0016 "Pipeline Experiment at Parkfield, California," by J. Isenberg and E. Richardson, 9/15/87, (PB88-163720, A03, MF-A01). This report is available only through NTIS (see address given above).

NCEER-87-0017 "Digital Simulation of Seismic Ground Motion," by M. Shinozuka, G. Deodatis and T. Harada, 8/31/87, (PB88-155197, A04, MF-A01). This report is available only through NTIS (see address given above).

NCEER-87-0018 "Practical Considerations for Structural Control: System Uncertainty, System Time Delay and Truncation of Small Control Forces," J.N. Yang and A. Akbarpour, 8/10/87, (PB88-163738, A08, MF-A01). This report is only available through NTIS (see address given above).

NCEER-87-0019 "Modal Analysis of Nonclassically Damped Structural Systems Using Canonical Transformation," by J.N. Yang, S. Sarkani and F.X. Long, 9/27/87, (PB88-187851, A04, MF-A01).

NCEER-87-0020 "A Nonstationary Solution in Random Vibration Theory," by J.R. Red-Horse and P.D. Spanos, 11/3/87, (PB88-163746, A03, MF-A01).

NCEER-87-0021 "Horizontal Impedances for Radially Inhomogeneous Viscoelastic Soil Layers," by A.S. Veletsos and K.W. Dotson, 10/15/87, (PB88-150859, A04, MF-A01).

NCEER-87-0022 "Seismic Damage Assessment of Reinforced Concrete Members," by Y.S. Chung, C. Meyer and M. Shinozuka, 10/9/87, (PB88-150867, A05, MF-A01). This report is available only through NTIS (see address given above).

NCEER-87-0023 "Active Structural Control in Civil Engineering," by T.T. Soong, 11/11/87, (PB88-187778, A03, MF-A01).

NCEER-87-0024 "Vertical and Torsional Impedances for Radially Inhomogeneous Viscoelastic Soil Layers," by K.W. Dotson and A.S. Veletsos, 12/87, (PB88-187786, A03, MF-A01).

NCEER-87-0025 "Proceedings from the Symposium on Seismic Hazards, Ground Motions, Soil-Liquefaction and Engineering Practice in Eastern North America," October 20-22, 1987, edited by K.H. Jacob, 12/87, (PB88-188115, A23, MF-A01). This report is available only through NTIS (see address given above).

NCEER-87-0026 "Report on the Whittier-Narrows, California, Earthquake of October 1, 1987," by J. Pantelic and A. Reinhorn, 11/87, (PB88-187752, A03, MF-A01). This report is available only through NTIS (see address given above).

NCEER-87-0027 "Design of a Modular Program for Transient Nonlinear Analysis of Large 3-D Building Structures," by S. Srivastav and J.F. Abel, 12/30/87, (PB88-187950, A05, MF-A01). This report is only available through NTIS (see address given above).

NCEER-87-0028 "Second-Year Program in Research, Education and Technology Transfer," 3/8/88, (PB88-219480, A04, MF-A01).

NCEER-88-0001 "Workshop on Seismic Computer Analysis and Design of Buildings With Interactive Graphics," by W. McGuire, J.F. Abel and C.H. Conley, 1/18/88, (PB88-187760, A03, MF-A01). This report is only available through NTIS (see address given above).

NCEER-88-0002 "Optimal Control of Nonlinear Flexible Structures," by J.N. Yang, F.X. Long and D. Wong, 1/22/88, (PB88-213772, A06, MF-A01).

NCEER-88-0003 "Substructuring Techniques in the Time Domain for Primary-Secondary Structural Systems," by G.D. Manolis and G. Juhn, 2/10/88, (PB88-213780, A04, MF-A01).

NCEER-88-0004 "Iterative Seismic Analysis of Primary-Secondary Systems," by A. Singhal, L.D. Lutes and P.D. Spanos, 2/23/88, (PB88-213798, A04, MF-A01).

NCEER-88-0005 "Stochastic Finite Element Expansion for Random Media," by P.D. Spanos and R. Ghanem, 3/14/88, (PB88-213806, A03, MF-A01).

NCEER-88-0006 "Combining Structural Optimization and Structural Control," by F.Y. Cheng and C.P. Pantelides, 1/10/88, (PB88-213814, A05, MF-A01).

NCEER-88-0007 "Seismic Performance Assessment of Code-Designed Structures," by H.H-M. Hwang, J-W. Jaw and H-J. Shau, 3/20/88, (PB88-219423, A04, MF-A01). This report is only available through NTIS (see address given above).

NCEER-88-0008 "Reliability Analysis of Code-Designed Structures Under Natural Hazards," by H.H-M. Hwang, H. Ushiba and M. Shinozuka, 2/29/88, (PB88-229471, A07, MF-A01). This report is only available through NTIS (see address given above).

NCEER-88-0009 "Seismic Fragility Analysis of Shear Wall Structures," by J-W Jaw and H.H-M. Hwang, 4/30/88, (PB89-102867, A04, MF-A01).

NCEER-88-0010 "Base Isolation of a Multi-Story Building Under a Harmonic Ground Motion - A Comparison of Performances of Various Systems," by F-G Fan, G. Ahmadi and I.G. Tadjbakhsh, 5/18/88, (PB89-122238, A06, MF-A01). This report is only available through NTIS (see address given above).

NCEER-88-0011 "Seismic Floor Response Spectra for a Combined System by Green's Functions," by F.M. Lavelle, L.A. Bergman and P.D. Spanos, 5/1/88, (PB89-102875, A03, MF-A01).

NCEER-88-0012 "A New Solution Technique for Randomly Excited Hysteretic Structures," by G.Q. Cai and Y.K. Lin, 5/16/88, (PB89-102883, A03, MF-A01).

NCEER-88-0013 "A Study of Radiation Damping and Soil-Structure Interaction Effects in the Centrifuge," by K. Weissman, supervised by J.H. Prevost, 5/24/88, (PB89-144703, A06, MF-A01).

NCEER-88-0014 "Parameter Identification and Implementation of a Kinematic Plasticity Model for Frictional Soils," by J.H. Prevost and D.V. Griffiths, to be published.

NCEER-88-0015 "Two- and Three- Dimensional Dynamic Finite Element Analyses of the Long Valley Dam," by D.V. Griffiths and J.H. Prevost, 6/17/88, (PB89-144711, A04, MF-A01).

NCEER-88-0016 "Damage Assessment of Reinforced Concrete Structures in Eastern United States," by A.M. Reinhorn, M.J. Seidel, S.K. Kunnath and Y.J. Park, 6/15/88, (PB89-122220, A04, MF-A01). This report is only available through NTIS (see address given above).

NCEER-88-0017 "Dynamic Compliance of Vertically Loaded Strip Foundations in Multilayered Viscoelastic Soils," by S. Ahmad and A.S.M. Israil, 6/17/88, (PB89-102891, A04, MF-A01).

NCEER-88-0018 "An Experimental Study of Seismic Structural Response With Added Viscoelastic Dampers," by R.C. Lin, Z. Liang, T.T. Soong and R.H. Zhang, 6/30/88, (PB89-122212, A05, MF-A01). This report is available only through NTIS (see address given above).

NCEER-88-0019 "Experimental Investigation of Primary - Secondary System Interaction," by G.D. Manolis, G. Juhn and A.M. Reinhorn, 5/27/88, (PB89-122204, A04, MF-A01).

NCEER-88-0020 "A Response Spectrum Approach For Analysis of Nonclassically Damped Structures," by J.N. Yang, S. Sarkani and F.X. Long, 4/22/88, (PB89-102909, A04, MF-A01).

NCEER-88-0021 "Seismic Interaction of Structures and Soils: Stochastic Approach," by A.S. Veletsos and A.M. Prasad, 7/21/88, (PB89-122196, A04, MF-A01). This report is only available through NTIS (see address given above).

NCEER-88-0022 "Identification of the Serviceability Limit State and Detection of Seismic Structural Damage," by E. DiPasquale and A.S. Cakmak, 6/15/88, (PB89-122188, A05, MF-A01). This report is available only through NTIS (see address given above).

NCEER-88-0023 "Multi-Hazard Risk Analysis: Case of a Simple Offshore Structure," by B.K. Bhartia and E.H. Vanmarcke, 7/21/88, (PB89-145213, A05, MF-A01).

NCEER-88-0024 "Automated Seismic Design of Reinforced Concrete Buildings," by Y.S. Chung, C. Meyer and M. Shinozuka, 7/5/88, (PB89-122170, A06, MF-A01). This report is available only through NTIS (see address given above).

NCEER-88-0025 "Experimental Study of Active Control of MDOF Structures Under Seismic Excitations," by L.L. Chung, R.C. Lin, T.T. Soong and A.M. Reinhorn, 7/10/88, (PB89-122600, A04, MF-A01).

NCEER-88-0026 "Earthquake Simulation Tests of a Low-Rise Metal Structure," by J.S. Hwang, K.C. Chang, G.C. Lee and R.L. Ketter, 8/1/88, (PB89-102917, A04, MF-A01).

NCEER-88-0027 "Systems Study of Urban Response and Reconstruction Due to Catastrophic Earthquakes," by F. Kozin and H.K. Zhou, 9/22/88, (PB90-162348, A04, MF-A01).

NCEER-88-0028 "Seismic Fragility Analysis of Plane Frame Structures," by H.H-M. Hwang and Y.K. Low, 7/31/88, (PB89-131445, A06, MF-A01).

NCEER-88-0029 "Response Analysis of Stochastic Structures," by A. Kardara, C. Bucher and M. Shinozuka, 9/22/88, (PB89-174429, A04, MF-A01).

NCEER-88-0030 "Nonnormal Accelerations Due to Yielding in a Primary Structure," by D.C.K. Chen and L.D. Lutes, 9/19/88, (PB89-131437, A04, MF-A01).

NCEER-88-0031 "Design Approaches for Soil-Structure Interaction," by A.S. Veletsos, A.M. Prasad and Y. Tang, 12/30/88, (PB89-174437, A03, MF-A01). This report is available only through NTIS (see address given above).

NCEER-88-0032 "A Re-evaluation of Design Spectra for Seismic Damage Control," by C.J. Turkstra and A.G. Tallin, 11/7/88, (PB89-145221, A05, MF-A01).

NCEER-88-0033 "The Behavior and Design of Noncontact Lap Splices Subjected to Repeated Inelastic Tensile Loading," by V.E. Sagan, P. Gergely and R.N. White, 12/8/88, (PB89-163737, A08, MF-A01).

NCEER-88-0034 "Seismic Response of Pile Foundations," by S.M. Mamoon, P.K. Banerjee and S. Ahmad, 11/1/88, (PB89-145239, A04, MF-A01).

NCEER-88-0035 "Modeling of R/C Building Structures With Flexible Floor Diaphragms (IDARC2)," by A.M. Reinhorn, S.K. Kunnath and N. Panahshahi, 9/7/88, (PB89-207153, A07, MF-A01).

NCEER-88-0036 "Solution of the Dam-Reservoir Interaction Problem Using a Combination of FEM, BEM with Particular Integrals, Modal Analysis, and Substructuring," by C-S. Tsai, G.C. Lee and R.L. Ketter, 12/31/88, (PB89-207146, A04, MF-A01).

NCEER-88-0037 "Optimal Placement of Actuators for Structural Control," by F.Y. Cheng and C.P. Pantelides, 8/15/88, (PB89-162846, A05, MF-A01).

NCEER-88-0038 "Teflon Bearings in Aseismic Base Isolation: Experimental Studies and Mathematical Modeling," by A. Mokha, M.C. Constantinou and A.M. Reinhorn, 12/5/88, (PB89-218457, A10, MF-A01). This report is available only through NTIS (see address given above).

NCEER-88-0039 "Seismic Behavior of Flat Slab High-Rise Buildings in the New York City Area," by P. Weidlinger and M. Ettouney, 10/15/88, (PB90-145681, A04, MF-A01).

NCEER-88-0040 "Evaluation of the Earthquake Resistance of Existing Buildings in New York City," by P. Weidlinger and M. Ettouney, 10/15/88, to be published.

NCEER-88-0041 "Small-Scale Modeling Techniques for Reinforced Concrete Structures Subjected to Seismic Loads," by W. Kim, A. El-Attar and R.N. White, 11/22/88, (PB89-189625, A05, MF-A01).

NCEER-88-0042 "Modeling Strong Ground Motion from Multiple Event Earthquakes," by G.W. Ellis and A.S. Cakmak, 10/15/88, (PB89-174445, A03, MF-A01).

NCEER-88-0043 "Nonstationary Models of Seismic Ground Acceleration," by M. Grigoriu, S.E. Ruiz and E. Rosenblueth, 7/15/88, (PB89-189617, A04, MF-A01).

NCEER-88-0044 "SARCF User's Guide: Seismic Analysis of Reinforced Concrete Frames," by Y.S. Chung, C. Meyer and M. Shinozuka, 11/9/88, (PB89-174452, A08, MF-A01).

NCEER-88-0045 "First Expert Panel Meeting on Disaster Research and Planning," edited by J. Pantelic and J. Stoyle, 9/15/88, (PB89-174460, A05, MF-A01).

NCEER-88-0046 "Preliminary Studies of the Effect of Degrading Infill Walls on the Nonlinear Seismic Response of Steel Frames," by C.Z. Chrysostomou, P. Gergely and J.F. Abel, 12/19/88, (PB89-208383, A05, MF-A01).

NCEER-88-0047 "Reinforced Concrete Frame Component Testing Facility - Design, Construction, Instrumentation and Operation," by S.P. Pessiki, C. Conley, T. Bond, P. Gergely and R.N. White, 12/16/88, (PB89-174478, A04, MF-A01).

NCEER-89-0001 "Effects of Protective Cushion and Soil Compliancy on the Response of Equipment Within a Seismically Excited Building," by J.A. HoLung, 2/16/89, (PB89-207179, A04, MF-A01).

NCEER-89-0002 "Statistical Evaluation of Response Modification Factors for Reinforced Concrete Structures," by H.H-M. Hwang and J-W. Jaw, 2/17/89, (PB89-207187, A05, MF-A01).

NCEER-89-0003 "Hysteretic Columns Under Random Excitation," by G-Q. Cai and Y.K. Lin, 1/9/89, (PB89-196513, A03, MF-A01).

NCEER-89-0004 "Experimental Study of `Elephant Foot Bulge' Instability of Thin-Walled Metal Tanks," by Z-H. Jia and R.L. Ketter, 2/22/89, (PB89-207195, A03, MF-A01).

NCEER-89-0005 "Experiment on Performance of Buried Pipelines Across San Andreas Fault," by J. Isenberg, E. Richardson and T.D. O'Rourke, 3/10/89, (PB89-218440, A04, MF-A01). This report is available only through NTIS (see address given above).

NCEER-89-0006 "A Knowledge-Based Approach to Structural Design of Earthquake-Resistant Buildings," by M. Subramani, P. Gergely, C.H. Conley, J.F. Abel and A.H. Zaghw, 1/15/89, (PB89-218465, A06, MF-A01).

NCEER-89-0007 "Liquefaction Hazards and Their Effects on Buried Pipelines," by T.D. O'Rourke and P.A. Lane, 2/1/89, (PB89-218481, A09, MF-A01).

NCEER-89-0008 "Fundamentals of System Identification in Structural Dynamics," by H. Imai, C-B. Yun, O. Maruyama and M. Shinozuka, 1/26/89, (PB89-207211, A04, MF-A01).

NCEER-89-0009 "Effects of the 1985 Michoacan Earthquake on Water Systems and Other Buried Lifelines in Mexico," by A.G. Ayala and M.J. O'Rourke, 3/8/89, (PB89-207229, A06, MF-A01).

NCEER-89-R010 "NCEER Bibliography of Earthquake Education Materials," by K.E.K. Ross, Second Revision, 9/1/89, (PB90-125352, A05, MF-A01). This report is replaced by NCEER-92-0018.

NCEER-89-0011 "Inelastic Three-Dimensional Response Analysis of Reinforced Concrete Building Structures (IDARC-3D), Part I - Modeling," by S.K. Kunnath and A.M. Reinhorn, 4/17/89, (PB90-114612, A07, MF-A01). This report is available only through NTIS (see address given above).

NCEER-89-0012 "Recommended Modifications to ATC-14," by C.D. Poland and J.O. Malley, 4/12/89, (PB90-108648, A15, MF-A01).

NCEER-89-0013 "Repair and Strengthening of Beam-to-Column Connections Subjected to Earthquake Loading," by M. Corazao and A.J. Durrani, 2/28/89, (PB90-109885, A06, MF-A01).

NCEER-89-0014 "Program EXKAL2 for Identification of Structural Dynamic Systems," by O. Maruyama, C-B. Yun, M. Hoshiya and M. Shinozuka, 5/19/89, (PB90-109877, A09, MF-A01).

NCEER-89-0015 "Response of Frames With Bolted Semi-Rigid Connections, Part I - Experimental Study and Analytical Predictions," by P.J. DiCorso, A.M. Reinhorn, J.R. Dickerson, J.B. Radziminski and W.L. Harper, 6/1/89, to be published.

NCEER-89-0016 "ARMA Monte Carlo Simulation in Probabilistic Structural Analysis," by P.D. Spanos and M.P. Mignolet, 7/10/89, (PB90-109893, A03, MF-A01).

NCEER-89-P017 "Preliminary Proceedings from the Conference on Disaster Preparedness - The Place of Earthquake Education in Our Schools," Edited by K.E.K. Ross, 6/23/89, (PB90-108606, A03, MF-A01).

NCEER-89-0017 "Proceedings from the Conference on Disaster Preparedness - The Place of Earthquake Education in Our Schools," Edited by K.E.K. Ross, 12/31/89, (PB90-207895, A012, MF-A02). This report is available only through NTIS (see address given above).

NCEER-89-0018 "Multidimensional Models of Hysteretic Material Behavior for Vibration Analysis of Shape Memory Energy Absorbing Devices, by E.J. Graesser and F.A. Cozzarelli, 6/7/89, (PB90-164146, A04, MF-A01).

NCEER-89-0019 "Nonlinear Dynamic Analysis of Three-Dimensional Base Isolated Structures (3D-BASIS)," by S. Nagarajaiah, A.M. Reinhorn and M.C. Constantinou, 8/3/89, (PB90-161936, A06, MF-A01). This report has been replaced by NCEER-93-0011.

NCEER-89-0020 "Structural Control Considering Time-Rate of Control Forces and Control Rate Constraints," by F.Y. Cheng and C.P. Pantelides, 8/3/89, (PB90-120445, A04, MF-A01).

NCEER-89-0021 "Subsurface Conditions of Memphis and Shelby County," by K.W. Ng, T-S. Chang and H-H.M. Hwang, 7/26/89, (PB90-120437, A03, MF-A01).

NCEER-89-0022 "Seismic Wave Propagation Effects on Straight Jointed Buried Pipelines," by K. Elhmadi and M.J. O'Rourke, 8/24/89, (PB90-162322, A10, MF-A02).

NCEER-89-0023 "Workshop on Serviceability Analysis of Water Delivery Systems," edited by M. Grigoriu, 3/6/89, (PB90-127424, A03, MF-A01).

NCEER-89-0024 "Shaking Table Study of a 1/5 Scale Steel Frame Composed of Tapered Members," by K.C. Chang, J.S. Hwang and G.C. Lee, 9/18/89, (PB90-160169, A04, MF-A01).

NCEER-89-0025 "DYNA1D: A Computer Program for Nonlinear Seismic Site Response Analysis - Technical Documentation," by Jean H. Prevost, 9/14/89, (PB90-161944, A07, MF-A01). This report is available only through NTIS (see address given above).

NCEER-89-0026 "1:4 Scale Model Studies of Active Tendon Systems and Active Mass Dampers for Aseismic Protection," by A.M. Reinhorn, T.T. Soong, R.C. Lin, Y.P. Yang, Y. Fukao, H. Abe and M. Nakai, 9/15/89, (PB90-173246, A10, MF-A02). This report is available only through NTIS (see address given above).

NCEER-89-0027 "Scattering of Waves by Inclusions in a Nonhomogeneous Elastic Half Space Solved by Boundary Element Methods," by P.K. Hadley, A. Askar and A.S. Cakmak, 6/15/89, (PB90-145699, A07, MF-A01).

NCEER-89-0028 "Statistical Evaluation of Deflection Amplification Factors for Reinforced Concrete Structures," by H.H.M. Hwang, J-W. Jaw and A.L. Ch'ng, 8/31/89, (PB90-164633, A05, MF-A01).

NCEER-89-0029 "Bedrock Accelerations in Memphis Area Due to Large New Madrid Earthquakes," by H.H.M. Hwang, C.H.S. Chen and G. Yu, 11/7/89, (PB90-162330, A04, MF-A01).

NCEER-89-0030 "Seismic Behavior and Response Sensitivity of Secondary Structural Systems," by Y.Q. Chen and T.T. Soong, 10/23/89, (PB90-164658, A08, MF-A01).

NCEER-89-0031 "Random Vibration and Reliability Analysis of Primary-Secondary Structural Systems," by Y. Ibrahim, M. Grigoriu and T.T. Soong, 11/10/89, (PB90-161951, A04, MF-A01).

NCEER-89-0032 "Proceedings from the Second U.S. - Japan Workshop on Liquefaction, Large Ground Deformation and Their Effects on Lifelines, September 26-29, 1989," Edited by T.D. O'Rourke and M. Hamada, 12/1/89, (PB90-209388, A22, MF-A03).

NCEER-89-0033 "Deterministic Model for Seismic Damage Evaluation of Reinforced Concrete Structures," by J.M. Bracci, A.M. Reinhorn, J.B. Mander and S.K. Kunnath, 9/27/89, (PB91-108803, A06, MF-A01).

NCEER-89-0034 "On the Relation Between Local and Global Damage Indices," by E. DiPasquale and A.S. Cakmak, 8/15/89, (PB90-173865, A05, MF-A01).

NCEER-89-0035 "Cyclic Undrained Behavior of Nonplastic and Low Plasticity Silts," by A.J. Walker and H.E. Stewart, 7/26/89, (PB90-183518, A10, MF-A01).

NCEER-89-0036 "Liquefaction Potential of Surficial Deposits in the City of Buffalo, New York," by M. Budhu, R. Giese and L. Baumgrass, 1/17/89, (PB90-208455, A04, MF-A01).

NCEER-89-0037 "A Deterministic Assessment of Effects of Ground Motion Incoherence," by A.S. Veletsos and Y. Tang, 7/15/89, (PB90-164294, A03, MF-A01).

NCEER-89-0038 "Workshop on Ground Motion Parameters for Seismic Hazard Mapping," July 17-18, 1989, edited by R.V. Whitman, 12/1/89, (PB90-173923, A04, MF-A01).

NCEER-89-0039 "Seismic Effects on Elevated Transit Lines of the New York City Transit Authority," by C.J. Costantino, C.A. Miller and E. Heymsfield, 12/26/89, (PB90-207887, A06, MF-A01).

NCEER-89-0040 "Centrifugal Modeling of Dynamic Soil-Structure Interaction," by K. Weissman, Supervised by J.H. Prevost, 5/10/89, (PB90-207879, A07, MF-A01).

NCEER-89-0041 "Linearized Identification of Buildings With Cores for Seismic Vulnerability Assessment," by I-K. Ho and A.E. Aktan, 11/1/89, (PB90-251943, A07, MF-A01).

NCEER-90-0001 "Geotechnical and Lifeline Aspects of the October 17, 1989 Loma Prieta Earthquake in San Francisco," by T.D. O'Rourke, H.E. Stewart, F.T. Blackburn and T.S. Dickerman, 1/90, (PB90-208596, A05, MF-A01).

NCEER-90-0002 "Nonnormal Secondary Response Due to Yielding in a Primary Structure," by D.C.K. Chen and L.D. Lutes, 2/28/90, (PB90-251976, A07, MF-A01).

NCEER-90-0003 "Earthquake Education Materials for Grades K-12," by K.E.K. Ross, 4/16/90, (PB91-251984, A05, MF-A05). This report has been replaced by NCEER-92-0018.

NCEER-90-0004 "Catalog of Strong Motion Stations in Eastern North America," by R.W. Busby, 4/3/90, (PB90-251984, A05, MF-A01).

NCEER-90-0005 "NCEER Strong-Motion Data Base: A User Manual for the GeoBase Release (Version 1.0 for the Sun3)," by P. Friberg and K. Jacob, 3/31/90 (PB90-258062, A04, MF-A01).

NCEER-90-0006 "Seismic Hazard Along a Crude Oil Pipeline in the Event of an 1811-1812 Type New Madrid Earthquake," by H.H.M. Hwang and C-H.S. Chen, 4/16/90, (PB90-258054, A04, MF-A01).

NCEER-90-0007 "Site-Specific Response Spectra for Memphis Sheahan Pumping Station," by H.H.M. Hwang and C.S. Lee, 5/15/90, (PB91-108811, A05, MF-A01).

NCEER-90-0008 "Pilot Study on Seismic Vulnerability of Crude Oil Transmission Systems," by T. Ariman, R. Dobry, M. Grigoriu, F. Kozin, M. O'Rourke, T. O'Rourke and M. Shinozuka, 5/25/90, (PB91-108837, A06, MF-A01).

NCEER-90-0009 "A Program to Generate Site Dependent Time Histories: EQGEN," by G.W. Ellis, M. Srinivasan and A.S. Cakmak, 1/30/90, (PB91-108829, A04, MF-A01).

NCEER-90-0010 "Active Isolation for Seismic Protection of Operating Rooms," by M.E. Talbott, Supervised by M. Shinozuka, 6/8/9, (PB91-110205, A05, MF-A01).

NCEER-90-0011 "Program LINEARID for Identification of Linear Structural Dynamic Systems," by C-B. Yun and M. Shinozuka, 6/25/90, (PB91-110312, A08, MF-A01).

NCEER-90-0012 "Two-Dimensional Two-Phase Elasto-Plastic Seismic Response of Earth Dams," by A.N. Yiagos, Supervised by J.H. Prevost, 6/20/90, (PB91-110197, A13, MF-A02).

NCEER-90-0013 "Secondary Systems in Base-Isolated Structures: Experimental Investigation, Stochastic Response and Stochastic Sensitivity," by G.D. Manolis, G. Juhn, M.C. Constantinou and A.M. Reinhorn, 7/1/90, (PB91-110320, A08, MF-A01).

NCEER-90-0014 "Seismic Behavior of Lightly-Reinforced Concrete Column and Beam-Column Joint Details," by S.P. Pessiki, C.H. Conley, P. Gergely and R.N. White, 8/22/90, (PB91-108795, A11, MF-A02).

NCEER-90-0015 "Two Hybrid Control Systems for Building Structures Under Strong Earthquakes," by J.N. Yang and A. Danielians, 6/29/90, (PB91-125393, A04, MF-A01).

NCEER-90-0016 "Instantaneous Optimal Control with Acceleration and Velocity Feedback," by J.N. Yang and Z. Li, 6/29/90, (PB91-125401, A03, MF-A01).

NCEER-90-0017 "Reconnaissance Report on the Northern Iran Earthquake of June 21, 1990," by M. Mehrain, 10/4/90, (PB91-125377, A03, MF-A01).

NCEER-90-0018 "Evaluation of Liquefaction Potential in Memphis and Shelby County," by T.S. Chang, P.S. Tang, C.S. Lee and H. Hwang, 8/10/90, (PB91-125427, A09, MF-A01).

NCEER-90-0019 "Experimental and Analytical Study of a Combined Sliding Disc Bearing and Helical Steel Spring Isolation System," by M.C. Constantinou, A.S. Mokha and A.M. Reinhorn, 10/4/90, (PB91-125385, A06, MF-A01). This report is available only through NTIS (see address given above).

NCEER-90-0020 "Experimental Study and Analytical Prediction of Earthquake Response of a Sliding Isolation System with a Spherical Surface," by A.S. Mokha, M.C. Constantinou and A.M. Reinhorn, 10/11/90, (PB91-125419, A05, MF-A01).

NCEER-90-0021 "Dynamic Interaction Factors for Floating Pile Groups," by G. Gazetas, K. Fan, A. Kaynia and E. Kausel, 9/10/90, (PB91-170381, A05, MF-A01).

NCEER-90-0022 "Evaluation of Seismic Damage Indices for Reinforced Concrete Structures," by S. Rodriguez-Gomez and A.S. Cakmak, 9/30/90, PB91-171322, A06, MF-A01).

NCEER-90-0023 "Study of Site Response at a Selected Memphis Site," by H. Desai, S. Ahmad, E.S. Gazetas and M.R. Oh, 10/11/90, (PB91-196857, A03, MF-A01).

NCEER-90-0024 "A User's Guide to Strongmo: Version 1.0 of NCEER's Strong-Motion Data Access Tool for PCs and Terminals," by P.A. Friberg and C.A.T. Susch, 11/15/90, (PB91-171272, A03, MF-A01).

NCEER-90-0025 "A Three-Dimensional Analytical Study of Spatial Variability of Seismic Ground Motions," by L-L. Hong and A.H.-S. Ang, 10/30/90, (PB91-170399, A09, MF-A01).

NCEER-90-0026 "MUMOID User's Guide - A Program for the Identification of Modal Parameters," by S. Rodriguez-Gomez and E. DiPasquale, 9/30/90, (PB91-171298, A04, MF-A01).

NCEER-90-0027 "SARCF-II User's Guide - Seismic Analysis of Reinforced Concrete Frames," by S. Rodriguez-Gomez, Y.S. Chung and C. Meyer, 9/30/90, (PB91-171280, A05, MF-A01).

NCEER-90-0028 "Viscous Dampers: Testing, Modeling and Application in Vibration and Seismic Isolation," by N. Makris and M.C. Constantinou, 12/20/90 (PB91-190561, A06, MF-A01).

NCEER-90-0029 "Soil Effects on Earthquake Ground Motions in the Memphis Area," by H. Hwang, C.S. Lee, K.W. Ng and T.S. Chang, 8/2/90, (PB91-190751, A05, MF-A01).

NCEER-91-0001 "Proceedings from the Third Japan-U.S. Workshop on Earthquake Resistant Design of Lifeline Facilities and Countermeasures for Soil Liquefaction, December 17-19, 1990," edited by T.D. O'Rourke and M. Hamada, 2/1/91, (PB91-179259, A99, MF-A04).

NCEER-91-0002 "Physical Space Solutions of Non-Proportionally Damped Systems," by M. Tong, Z. Liang and G.C. Lee, 1/15/91, (PB91-179242, A04, MF-A01).

NCEER-91-0003 "Seismic Response of Single Piles and Pile Groups," by K. Fan and G. Gazetas, 1/10/91, (PB92-174994, A04, MF-A01).

NCEER-91-0004 "Damping of Structures: Part 1 - Theory of Complex Damping," by Z. Liang and G. Lee, 10/10/91, (PB92-197235, A12, MF-A03).

NCEER-91-0005 "3D-BASIS - Nonlinear Dynamic Analysis of Three Dimensional Base Isolated Structures: Part II," by S. Nagarajaiah, A.M. Reinhorn and M.C. Constantinou, 2/28/91, (PB91-190553, A07, MF-A01). This report has been replaced by NCEER-93-0011.

NCEER-91-0006 "A Multidimensional Hysteretic Model for Plasticity Deforming Metals in Energy Absorbing Devices," by E.J. Graesser and F.A. Cozzarelli, 4/9/91, (PB92-108364, A04, MF-A01).

NCEER-91-0007 "A Framework for Customizable Knowledge-Based Expert Systems with an Application to a KBES for Evaluating the Seismic Resistance of Existing Buildings," by E.G. Ibarra-Anaya and S.J. Fenves, 4/9/91, (PB91-210930, A08, MF-A01).

NCEER-91-0008 "Nonlinear Analysis of Steel Frames with Semi-Rigid Connections Using the Capacity Spectrum Method," by G.G. Deierlein, S-H. Hsieh, Y-J. Shen and J.F. Abel, 7/2/91, (PB92-113828, A05, MF-A01).

NCEER-91-0009 "Earthquake Education Materials for Grades K-12," by K.E.K. Ross, 4/30/91, (PB91-212142, A06, MF-A01). This report has been replaced by NCEER-92-0018.

NCEER-91-0010 "Phase Wave Velocities and Displacement Phase Differences in a Harmonically Oscillating Pile," by N. Makris and G. Gazetas, 7/8/91, (PB92-108356, A04, MF-A01).

NCEER-91-0011 "Dynamic Characteristics of a Full-Size Five-Story Steel Structure and a 2/5 Scale Model," by K.C. Chang, G.C. Yao, G.C. Lee, D.S. Hao and Y.C. Yeh," 7/2/91, (PB93-116648, A06, MF-A02).

NCEER-91-0012 "Seismic Response of a 2/5 Scale Steel Structure with Added Viscoelastic Dampers," by K.C. Chang, T.T. Soong, S-T. Oh and M.L. Lai, 5/17/91, (PB92-110816, A05, MF-A01).

NCEER-91-0013 "Earthquake Response of Retaining Walls; Full-Scale Testing and Computational Modeling," by S. Alampalli and A-W.M. Elgamal, 6/20/91, to be published.

NCEER-91-0014 "3D-BASIS-M: Nonlinear Dynamic Analysis of Multiple Building Base Isolated Structures," by P.C. Tsopelas, S. Nagarajaiah, M.C. Constantinou and A.M. Reinhorn, 5/28/91, (PB92-113885, A09, MF-A02).

NCEER-91-0015 "Evaluation of SEAOC Design Requirements for Sliding Isolated Structures," by D. Theodossiou and M.C. Constantinou, 6/10/91, (PB92-114602, A11, MF-A03).

NCEER-91-0016 "Closed-Loop Modal Testing of a 27-Story Reinforced Concrete Flat Plate-Core Building," by H.R. Somaprasad, T. Toksoy, H. Yoshiyuki and A.E. Aktan, 7/15/91, (PB92-129980, A07, MF-A02).

NCEER-91-0017 "Shake Table Test of a 1/6 Scale Two-Story Lightly Reinforced Concrete Building," by A.G. El-Attar, R.N. White and P. Gergely, 2/28/91, (PB92-222447, A06, MF-A02).

NCEER-91-0018 "Shake Table Test of a 1/8 Scale Three-Story Lightly Reinforced Concrete Building," by A.G. El-Attar, R.N. White and P. Gergely, 2/28/91, (PB93-116630, A08, MF-A02).

NCEER-91-0019 "Transfer Functions for Rigid Rectangular Foundations," by A.S. Veletsos, A.M. Prasad and W.H. Wu, 7/31/91, to be published.

NCEER-91-0020 "Hybrid Control of Seismic-Excited Nonlinear and Inelastic Structural Systems," by J.N. Yang, Z. Li and A. Danielians, 8/1/91, (PB92-143171, A06, MF-A02).

NCEER-91-0021 "The NCEER-91 Earthquake Catalog: Improved Intensity-Based Magnitudes and Recurrence Relations for U.S. Earthquakes East of New Madrid," by L. Seeber and J.G. Armbruster, 8/28/91, (PB92-176742, A06, MF-A02).

NCEER-91-0022 "Proceedings from the Implementation of Earthquake Planning and Education in Schools: The Need for Change - The Roles of the Changemakers," by K.E.K. Ross and F. Winslow, 7/23/91, (PB92-129998, A12, MF-A03).

NCEER-91-0023 "A Study of Reliability-Based Criteria for Seismic Design of Reinforced Concrete Frame Buildings," by H.H.M. Hwang and H-M. Hsu, 8/10/91, (PB92-140235, A09, MF-A02).

NCEER-91-0024 "Experimental Verification of a Number of Structural System Identification Algorithms," by R.G. Ghanem, H. Gavin and M. Shinozuka, 9/18/91, (PB92-176577, A18, MF-A04).

NCEER-91-0025 "Probabilistic Evaluation of Liquefaction Potential," by H.H.M. Hwang and C.S. Lee," 11/25/91, (PB92-143429, A05, MF-A01).

NCEER-91-0026 "Instantaneous Optimal Control for Linear, Nonlinear and Hysteretic Structures - Stable Controllers," by J.N. Yang and Z. Li, 11/15/91, (PB92-163807, A04, MF-A01).

NCEER-91-0027 "Experimental and Theoretical Study of a Sliding Isolation System for Bridges," by M.C. Constantinou, A. Kartoum, A.M. Reinhorn and P. Bradford, 11/15/91, (PB92-176973, A10, MF-A03).

NCEER-92-0001 "Case Studies of Liquefaction and Lifeline Performance During Past Earthquakes, Volume 1: Japanese Case Studies," Edited by M. Hamada and T. O'Rourke, 2/17/92, (PB92-197243, A18, MF-A04).

NCEER-92-0002 "Case Studies of Liquefaction and Lifeline Performance During Past Earthquakes, Volume 2: United States Case Studies," Edited by T. O'Rourke and M. Hamada, 2/17/92, (PB92-197250, A20, MF-A04).

NCEER-92-0003 "Issues in Earthquake Education," Edited by K. Ross, 2/3/92, (PB92-222389, A07, MF-A02).

NCEER-92-0004 "Proceedings from the First U.S. - Japan Workshop on Earthquake Protective Systems for Bridges," Edited by I.G. Buckle, 2/4/92, (PB94-142239, A99, MF-A06).

NCEER-92-0005 "Seismic Ground Motion from a Haskell-Type Source in a Multiple-Layered Half-Space," A.P. Theoharis, G. Deodatis and M. Shinozuka, 1/2/92, to be published.

NCEER-92-0006 "Proceedings from the Site Effects Workshop," Edited by R. Whitman, 2/29/92, (PB92-197201, A04, MF-A01).

NCEER-92-0007 "Engineering Evaluation of Permanent Ground Deformations Due to Seismically-Induced Liquefaction," by M.H. Baziar, R. Dobry and A-W.M. Elgamal, 3/24/92, (PB92-222421, A13, MF-A03).

NCEER-92-0008 "A Procedure for the Seismic Evaluation of Buildings in the Central and Eastern United States," by C.D. Poland and J.O. Malley, 4/2/92, (PB92-222439, A20, MF-A04).

NCEER-92-0009 "Experimental and Analytical Study of a Hybrid Isolation System Using Friction Controllable Sliding Bearings," by M.Q. Feng, S. Fujii and M. Shinozuka, 5/15/92, (PB93-150282, A06, MF-A02).

NCEER-92-0010 "Seismic Resistance of Slab-Column Connections in Existing Non-Ductile Flat-Plate Buildings," by A.J. Durrani and Y. Du, 5/18/92, (PB93-116812, A06, MF-A02).

NCEER-92-0011 "The Hysteretic and Dynamic Behavior of Brick Masonry Walls Upgraded by Ferrocement Coatings Under Cyclic Loading and Strong Simulated Ground Motion," by H. Lee and S.P. Prawel, 5/11/92, to be published.

NCEER-92-0012 "Study of Wire Rope Systems for Seismic Protection of Equipment in Buildings," by G.F. Demetriades, M.C. Constantinou and A.M. Reinhorn, 5/20/92, (PB93-116655, A08, MF-A02).

NCEER-92-0013 "Shape Memory Structural Dampers: Material Properties, Design and Seismic Testing," by P.R. Witting and F.A. Cozzarelli, 5/26/92, (PB93-116663, A05, MF-A01).

NCEER-92-0014 "Longitudinal Permanent Ground Deformation Effects on Buried Continuous Pipelines," by M.J. O'Rourke, and C. Nordberg, 6/15/92, (PB93-116671, A08, MF-A02).

NCEER-92-0015 "A Simulation Method for Stationary Gaussian Random Functions Based on the Sampling Theorem," by M. Grigoriu and S. Balopoulou, 6/11/92, (PB93-127496, A05, MF-A01).

NCEER-92-0016 "Gravity-Load-Designed Reinforced Concrete Buildings: Seismic Evaluation of Existing Construction and Detailing Strategies for Improved Seismic Resistance," by G.W. Hoffmann, S.K. Kunnath, A.M. Reinhorn and J.B. Mander, 7/15/92, (PB94-142007, A08, MF-A02).

NCEER-92-0017 "Observations on Water System and Pipeline Performance in the Limón Area of Costa Rica Due to the April 22, 1991 Earthquake," by M. O'Rourke and D. Ballantyne, 6/30/92, (PB93-126811, A06, MF-A02).

NCEER-92-0018 "Fourth Edition of Earthquake Education Materials for Grades K-12," Edited by K.E.K. Ross, 8/10/92, (PB93-114023, A07, MF-A02).

NCEER-92-0019 "Proceedings from the Fourth Japan-U.S. Workshop on Earthquake Resistant Design of Lifeline Facilities and Countermeasures for Soil Liquefaction," Edited by M. Hamada and T.D. O'Rourke, 8/12/92, (PB93-163939, A99, MF-E11).

NCEER-92-0020 "Active Bracing System: A Full Scale Implementation of Active Control," by A.M. Reinhorn, T.T. Soong, R.C. Lin, M.A. Riley, Y.P. Wang, S. Aizawa and M. Higashino, 8/14/92, (PB93-127512, A06, MF-A02).

NCEER-92-0021 "Empirical Analysis of Horizontal Ground Displacement Generated by Liquefaction-Induced Lateral Spreads," by S.F. Bartlett and T.L. Youd, 8/17/92, (PB93-188241, A06, MF-A02).

NCEER-92-0022 "IDARC Version 3.0: Inelastic Damage Analysis of Reinforced Concrete Structures," by S.K. Kunnath, A.M. Reinhorn and R.F. Lobo, 8/31/92, (PB93-227502, A07, MF-A02).

NCEER-92-0023 "A Semi-Empirical Analysis of Strong-Motion Peaks in Terms of Seismic Source, Propagation Path and Local Site Conditions, by M. Kamiyama, M.J. O'Rourke and R. Flores-Berrones, 9/9/92, (PB93-150266, A08, MF-A02).

NCEER-92-0024 "Seismic Behavior of Reinforced Concrete Frame Structures with Nonductile Details, Part I: Summary of Experimental Findings of Full Scale Beam-Column Joint Tests," by A. Beres, R.N. White and P. Gergely, 9/30/92, (PB93-227783, A05, MF-A01).

NCEER-92-0025 "Experimental Results of Repaired and Retrofitted Beam-Column Joint Tests in Lightly Reinforced Concrete Frame Buildings," by A. Beres, S. El-Borgi, R.N. White and P. Gergely, 10/29/92, (PB93-227791, A05, MF-A01).

NCEER-92-0026 "A Generalization of Optimal Control Theory: Linear and Nonlinear Structures," by J.N. Yang, Z. Li and S. Vongchavalitkul, 11/2/92, (PB93-188621, A05, MF-A01).

NCEER-92-0027 "Seismic Resistance of Reinforced Concrete Frame Structures Designed Only for Gravity Loads: Part I - Design and Properties of a One-Third Scale Model Structure," by J.M. Bracci, A.M. Reinhorn and J.B. Mander, 12/1/92, (PB94-104502, A08, MF-A02).

NCEER-92-0028 "Seismic Resistance of Reinforced Concrete Frame Structures Designed Only for Gravity Loads: Part II - Experimental Performance of Subassemblages," by L.E. Aycardi, J.B. Mander and A.M. Reinhorn, 12/1/92, (PB94-104510, A08, MF-A02).

NCEER-92-0029 "Seismic Resistance of Reinforced Concrete Frame Structures Designed Only for Gravity Loads: Part III - Experimental Performance and Analytical Study of a Structural Model," by J.M. Bracci, A.M. Reinhorn and J.B. Mander, 12/1/92, (PB93-227528, A09, MF-A01).

NCEER-92-0030 "Evaluation of Seismic Retrofit of Reinforced Concrete Frame Structures: Part I - Experimental Performance of Retrofitted Subassemblages," by D. Choudhuri, J.B. Mander and A.M. Reinhorn, 12/8/92, (PB93-198307, A07, MF-A02).

NCEER-92-0031 "Evaluation of Seismic Retrofit of Reinforced Concrete Frame Structures: Part II - Experimental Performance and Analytical Study of a Retrofitted Structural Model," by J.M. Bracci, A.M. Reinhorn and J.B. Mander, 12/8/92, (PB93-198315, A09, MF-A03).

NCEER-92-0032 "Experimental and Analytical Investigation of Seismic Response of Structures with Supplemental Fluid Viscous Dampers," by M.C. Constantinou and M.D. Symans, 12/21/92, (PB93-191435, A10, MF-A03). This report is available only through NTIS (see address given above).

NCEER-92-0033 "Reconnaissance Report on the Cairo, Egypt Earthquake of October 12, 1992," by M. Khater, 12/23/92, (PB93-188621, A03, MF-A01).

NCEER-92-0034 "Low-Level Dynamic Characteristics of Four Tall Flat-Plate Buildings in New York City," by H. Gavin, S. Yuan, J. Grossman, E. Pekelis and K. Jacob, 12/28/92, (PB93-188217, A07, MF-A02).

NCEER-93-0001 "An Experimental Study on the Seismic Performance of Brick-Infilled Steel Frames With and Without Retrofit," by J.B. Mander, B. Nair, K. Wojtkowski and J. Ma, 1/29/93, (PB93-227510, A07, MF-A02).

NCEER-93-0002 "Social Accounting for Disaster Preparedness and Recovery Planning," by S. Cole, E. Pantoja and V. Razak, 2/22/93, (PB94-142114, A12, MF-A03).

NCEER-93-0003 "Assessment of 1991 NEHRP Provisions for Nonstructural Components and Recommended Revisions," by T.T. Soong, G. Chen, Z. Wu, R-H. Zhang and M. Grigoriu, 3/1/93, (PB93-188639, A06, MF-A02).

NCEER-93-0004 "Evaluation of Static and Response Spectrum Analysis Procedures of SEAOC/UBC for Seismic Isolated Structures," by C.W. Winters and M.C. Constantinou, 3/23/93, (PB93-198299, A10, MF-A03).

NCEER-93-0005 "Earthquakes in the Northeast - Are We Ignoring the Hazard? A Workshop on Earthquake Science and Safety for Educators," edited by K.E.K. Ross, 4/2/93, (PB94-103066, A09, MF-A02).

NCEER-93-0006 "Inelastic Response of Reinforced Concrete Structures with Viscoelastic Braces," by R.F. Lobo, J.M. Bracci, K.L. Shen, A.M. Reinhorn and T.T. Soong, 4/5/93, (PB93-227486, A05, MF-A02).

NCEER-93-0007 "Seismic Testing of Installation Methods for Computers and Data Processing Equipment," by K. Kosar, T.T. Soong, K.L. Shen, J.A. HoLung and Y.K. Lin, 4/12/93, (PB93-198299, A07, MF-A02).

NCEER-93-0008 "Retrofit of Reinforced Concrete Frames Using Added Dampers," by A. Reinhorn, M. Constantinou and C. Li, to be published.

NCEER-93-0009 "Seismic Behavior and Design Guidelines for Steel Frame Structures with Added Viscoelastic Dampers," by K.C. Chang, M.L. Lai, T.T. Soong, D.S. Hao and Y.C. Yeh, 5/1/93, (PB94-141959, A07, MF-A02).

NCEER-93-0010 "Seismic Performance of Shear-Critical Reinforced Concrete Bridge Piers," by J.B. Mander, S.M. Waheed, M.T.A. Chaudhary and S.S. Chen, 5/12/93, (PB93-227494, A08, MF-A02).

NCEER-93-0011 "3D-BASIS-TABS: Computer Program for Nonlinear Dynamic Analysis of Three Dimensional Base Isolated Structures," by S. Nagarajaiah, C. Li, A.M. Reinhorn and M.C. Constantinou, 8/2/93, (PB94-141819, A09, MF-A02).

NCEER-93-0012 "Effects of Hydrocarbon Spills from an Oil Pipeline Break on Ground Water," by O.J. Helweg and H.H.M. Hwang, 8/3/93, (PB94-141942, A06, MF-A02).

NCEER-93-0013 "Simplified Procedures for Seismic Design of Nonstructural Components and Assessment of Current Code Provisions," by M.P. Singh, L.E. Suarez, E.E. Matheu and G.O. Maldonado, 8/4/93, (PB94-141827, A09, MF-A02).

NCEER-93-0014 "An Energy Approach to Seismic Analysis and Design of Secondary Systems," by G. Chen and T.T. Soong, 8/6/93, (PB94-142767, A11, MF-A03).

NCEER-93-0015 "Proceedings from School Sites: Becoming Prepared for Earthquakes - Commemorating the Third Anniversary of the Loma Prieta Earthquake," Edited by F.E. Winslow and K.E.K. Ross, 8/16/93, (PB94-154275, A16, MF-A02).

NCEER-93-0016 "Reconnaissance Report of Damage to Historic Monuments in Cairo, Egypt Following the October 12, 1992 Dahshur Earthquake," by D. Sykora, D. Look, G. Croci, E. Karaesmen and E. Karaesmen, 8/19/93, (PB94-142221, A08, MF-A02).

NCEER-93-0017 "The Island of Guam Earthquake of August 8, 1993," by S.W. Swan and S.K. Harris, 9/30/93, (PB94-141843, A04, MF-A01).

NCEER-93-0018 "Engineering Aspects of the October 12, 1992 Egyptian Earthquake," by A.W. Elgamal, M. Amer, K. Adalier and A. Abul-Fadl, 10/7/93, (PB94-141983, A05, MF-A01).

NCEER-93-0019 "Development of an Earthquake Motion Simulator and its Application in Dynamic Centrifuge Testing," by I. Krstelj, Supervised by J.H. Prevost, 10/23/93, (PB94-181773, A-10, MF-A03).

NCEER-93-0020 "NCEER-Taisei Corporation Research Program on Sliding Seismic Isolation Systems for Bridges: Experimental and Analytical Study of a Friction Pendulum System (FPS)," by M.C. Constantinou, P. Tsopelas, Y-S. Kim and S. Okamoto, 11/1/93, (PB94-142775, A08, MF-A02).

NCEER-93-0021 "Finite Element Modeling of Elastomeric Seismic Isolation Bearings," by L.J. Billings, Supervised by R. Shepherd, 11/8/93, to be published.

NCEER-93-0022 "Seismic Vulnerability of Equipment in Critical Facilities: Life-Safety and Operational Consequences," by K. Porter, G.S. Johnson, M.M. Zadeh, C. Scawthorn and S. Eder, 11/24/93, (PB94-181765, A16, MF-A03).

NCEER-93-0023 "Hokkaido Nansei-oki, Japan Earthquake of July 12, 1993, by P.I. Yanev and C.R. Scawthorn, 12/23/93, (PB94-181500, A07, MF-A01).

NCEER-94-0001 "An Evaluation of Seismic Serviceability of Water Supply Networks with Application to the San Francisco Auxiliary Water Supply System," by I. Markov, Supervised by M. Grigoriu and T. O'Rourke, 1/21/94, (PB94-204013, A07, MF-A02).

NCEER-94-0002 "NCEER-Taisei Corporation Research Program on Sliding Seismic Isolation Systems for Bridges: Experimental and Analytical Study of Systems Consisting of Sliding Bearings, Rubber Restoring Force Devices and Fluid Dampers," Volumes I and II, by P. Tsopelas, S. Okamoto, M.C. Constantinou, D. Ozaki and S. Fujii, 2/4/94, (PB94-181740, A09, MF-A02 and PB94-181757, A12, MF-A03).

NCEER-94-0003 "A Markov Model for Local and Global Damage Indices in Seismic Analysis," by S. Rahman and M. Grigoriu, 2/18/94, (PB94-206000, A12, MF-A03).

NCEER-94-0004 "Proceedings from the NCEER Workshop on Seismic Response of Masonry Infills," edited by D.P. Abrams, 3/1/94, (PB94-180783, A07, MF-A02).

NCEER-94-0005 "The Northridge, California Earthquake of January 17, 1994: General Reconnaissance Report," edited by J.D. Goltz, 3/11/94, (PB94-193943, A10, MF-A03).

NCEER-94-0006 "Seismic Energy Based Fatigue Damage Analysis of Bridge Columns: Part I - Evaluation of Seismic Capacity," by G.A. Chang and J.B. Mander, 3/14/94, (PB94-219185, A11, MF-A03).

NCEER-94-0007 "Seismic Isolation of Multi-Story Frame Structures Using Spherical Sliding Isolation Systems," by T.M. Al-Hussaini, V.A. Zayas and M.C. Constantinou, 3/17/94, (PB94-193745, A09, MF-A02).

NCEER-94-0008 "The Northridge, California Earthquake of January 17, 1994: Performance of Highway Bridges," edited by I.G. Buckle, 3/24/94, (PB94-193851, A06, MF-A02).

NCEER-94-0009 "Proceedings of the Third U.S.-Japan Workshop on Earthquake Protective Systems for Bridges," edited by I.G. Buckle and I. Friedland, 3/31/94, (PB94-195815, A99, MF-A06).

NCEER-94-0010 "3D-BASIS-ME: Computer Program for Nonlinear Dynamic Analysis of Seismically Isolated Single and Multiple Structures and Liquid Storage Tanks," by P.C. Tsopelas, M.C. Constantinou and A.M. Reinhorn, 4/12/94, (PB94-204922, A09, MF-A02).

NCEER-94-0011 "The Northridge, California Earthquake of January 17, 1994: Performance of Gas Transmission Pipelines," by T.D. O'Rourke and M.C. Palmer, 5/16/94, (PB94-204989, A05, MF-A01).

NCEER-94-0012 "Feasibility Study of Replacement Procedures and Earthquake Performance Related to Gas Transmission Pipelines," by T.D. O'Rourke and M.C. Palmer, 5/25/94, (PB94-206638, A09, MF-A02).

NCEER-94-0013 "Seismic Energy Based Fatigue Damage Analysis of Bridge Columns: Part II - Evaluation of Seismic Demand," by G.A. Chang and J.B. Mander, 6/1/94, (PB95-18106, A08, MF-A02).

NCEER-94-0014 "NCEER-Taisei Corporation Research Program on Sliding Seismic Isolation Systems for Bridges: Experimental and Analytical Study of a System Consisting of Sliding Bearings and Fluid Restoring Force/Damping Devices," by P. Tsopelas and M.C. Constantinou, 6/13/94, (PB94-219144, A10, MF-A03).

NCEER-94-0015 "Generation of Hazard-Consistent Fragility Curves for Seismic Loss Estimation Studies," by H. Hwang and J-R. Huo, 6/14/94, (PB95-181996, A09, MF-A02).

NCEER-94-0016 "Seismic Study of Building Frames with Added Energy-Absorbing Devices," by W.S. Pong, C.S. Tsai and G.C. Lee, 6/20/94, (PB94-219136, A10, A03).

NCEER-94-0017 "Sliding Mode Control for Seismic-Excited Linear and Nonlinear Civil Engineering Structures," by J. Yang, J. Wu, A. Agrawal and Z. Li, 6/21/94, (PB95-138483, A06, MF-A02).

NCEER-94-0018 "3D-BASIS-TABS Version 2.0: Computer Program for Nonlinear Dynamic Analysis of Three Dimensional Base Isolated Structures," by A.M. Reinhorn, S. Nagarajaiah, M.C. Constantinou, P. Tsopelas and R. Li, 6/22/94, (PB95-182176, A08, MF-A02).

NCEER-94-0019 "Proceedings of the International Workshop on Civil Infrastructure Systems: Application of Intelligent Systems and Advanced Materials on Bridge Systems," Edited by G.C. Lee and K.C. Chang, 7/18/94, (PB95-252474, A20, MF-A04).

NCEER-94-0020 "Study of Seismic Isolation Systems for Computer Floors," by V. Lambrou and M.C. Constantinou, 7/19/94, (PB95-138533, A10, MF-A03).

NCEER-94-0021 "Proceedings of the U.S.-Italian Workshop on Guidelines for Seismic Evaluation and Rehabilitation of Unreinforced Masonry Buildings," Edited by D.P. Abrams and G.M. Calvi, 7/20/94, (PB95-138749, A13, MF-A03).

NCEER-94-0022 "NCEER-Taisei Corporation Research Program on Sliding Seismic Isolation Systems for Bridges: Experimental and Analytical Study of a System Consisting of Lubricated PTFE Sliding Bearings and Mild Steel Dampers," by P. Tsopelas and M.C. Constantinou, 7/22/94, (PB95-182184, A08, MF-A02).

NCEER-94-0023 "Development of Reliability-Based Design Criteria for Buildings Under Seismic Load," by Y.K. Wen, H. Hwang and M. Shinozuka, 8/1/94, (PB95-211934, A08, MF-A02).

NCEER-94-0024 "Experimental Verification of Acceleration Feedback Control Strategies for an Active Tendon System," by S.J. Dyke, B.F. Spencer, Jr., P. Quast, M.K. Sain, D.C. Kaspari, Jr. and T.T. Soong, 8/29/94, (PB95-212320, A05, MF-A01).

NCEER-94-0025 "Seismic Retrofitting Manual for Highway Bridges," Edited by I.G. Buckle and I.F. Friedland, published by the Federal Highway Administration (PB95-212676, A15, MF-A03).

NCEER-94-0026 "Proceedings from the Fifth U.S.-Japan Workshop on Earthquake Resistant Design of Lifeline Facilities and Countermeasures Against Soil Liquefaction," Edited by T.D. O'Rourke and M. Hamada, 11/7/94, (PB95-220802, A99, MF-E08).

NCEER-95-0001 "Experimental and Analytical Investigation of Seismic Retrofit of Structures with Supplemental Damping: Part 1 - Fluid Viscous Damping Devices," by A.M. Reinhorn, C. Li and M.C. Constantinou, 1/3/95, (PB95-266599, A09, MF-A02).

NCEER-95-0002 "Experimental and Analytical Study of Low-Cycle Fatigue Behavior of Semi-Rigid Top-And-Seat Angle Connections," by G. Pekcan, J.B. Mander and S.S. Chen, 1/5/95, (PB95-220042, A07, MF-A02).

NCEER-95-0003 "NCEER-ATC Joint Study on Fragility of Buildings," by T. Anagnos, C. Rojahn and A.S. Kiremidjian, 1/20/95, (PB95-220026, A06, MF-A02).

NCEER-95-0004 "Nonlinear Control Algorithms for Peak Response Reduction," by Z. Wu, T.T. Soong, V. Gattulli and R.C. Lin, 2/16/95, (PB95-220349, A05, MF-A01).

NCEER-95-0005 "Pipeline Replacement Feasibility Study: A Methodology for Minimizing Seismic and Corrosion Risks to Underground Natural Gas Pipelines," by R.T. Eguchi, H.A. Seligson and D.G. Honegger, 3/2/95, (PB95-252326, A06, MF-A02).

NCEER-95-0006 "Evaluation of Seismic Performance of an 11-Story Frame Building During the 1994 Northridge Earthquake," by F. Naeim, R. DiSulio, K. Benuska, A. Reinhorn and C. Li, to be published.

NCEER-95-0007 "Prioritization of Bridges for Seismic Retrofitting," by N. Basöz and A.S. Kiremidjian, 4/24/95, (PB95-252300, A08, MF-A02).

NCEER-95-0008 "Method for Developing Motion Damage Relationships for Reinforced Concrete Frames," by A. Singhal and A.S. Kiremidjian, 5/11/95, (PB95-266607, A06, MF-A02).

NCEER-95-0009 "Experimental and Analytical Investigation of Seismic Retrofit of Structures with Supplemental Damping: Part II - Friction Devices," by C. Li and A.M. Reinhorn, 7/6/95, (PB96-128087, A11, MF-A03).

NCEER-95-0010 "Experimental Performance and Analytical Study of a Non-Ductile Reinforced Concrete Frame Structure Retrofitted with Elastomeric Spring Dampers," by G. Pekcan, J.B. Mander and S.S. Chen, 7/14/95, (PB96-137161, A08, MF-A02).

NCEER-95-0011 "Development and Experimental Study of Semi-Active Fluid Damping Devices for Seismic Protection of Structures," by M.D. Symans and M.C. Constantinou, 8/3/95, (PB96-136940, A23, MF-A04).

NCEER-95-0012 "Real-Time Structural Parameter Modification (RSPM): Development of Innervated Structures," by Z. Liang, M. Tong and G.C. Lee, 4/11/95, (PB96-137153, A06, MF-A01).

NCEER-95-0013 "Experimental and Analytical Investigation of Seismic Retrofit of Structures with Supplemental Damping: Part III - Viscous Damping Walls," by A.M. Reinhorn and C. Li, 10/1/95, (PB96-176409, A11, MF-A03).

NCEER-95-0014 "Seismic Fragility Analysis of Equipment and Structures in a Memphis Electric Substation," by J-R. Huo and H.H.M. Hwang, 8/10/95, (PB96-128087, A09, MF-A02).

NCEER-95-0015 "The Hanshin-Awaji Earthquake of January 17, 1995: Performance of Lifelines," Edited by M. Shinozuka, 11/3/95, (PB96-176383, A15, MF-A03).

NCEER-95-0016 "Highway Culvert Performance During Earthquakes," by T.L. Youd and C.J. Beckman, available as NCEER-96-0015.

NCEER-95-0017 "The Hanshin-Awaji Earthquake of January 17, 1995: Performance of Highway Bridges," Edited by I.G. Buckle, 12/1/95, to be published.

NCEER-95-0018 "Modeling of Masonry Infill Panels for Structural Analysis," by A.M. Reinhorn, A. Madan, R.E. Valles, Y. Reichmann and J.B. Mander, 12/8/95, (PB97-110886, MF-A01, A06).

NCEER-95-0019 "Optimal Polynomial Control for Linear and Nonlinear Structures," by A.K. Agrawal and J.N. Yang, 12/11/95, (PB96-168737, A07, MF-A02).

NCEER-95-0020 "Retrofit of Non-Ductile Reinforced Concrete Frames Using Friction Dampers," by R.S. Rao, P. Gergely and R.N. White, 12/22/95, (PB97-133508, A10, MF-A02).

NCEER-95-0021 "Parametric Results for Seismic Response of Pile-Supported Bridge Bents," by G. Mylonakis, A. Nikolaou and G. Gazetas, 12/22/95, (PB97-100242, A12, MF-A03).

NCEER-95-0022 "Kinematic Bending Moments in Seismically Stressed Piles," by A. Nikolaou, G. Mylonakis and G. Gazetas, 12/23/95, (PB97-113914, MF-A03, A13).

NCEER-96-0001 "Dynamic Response of Unreinforced Masonry Buildings with Flexible Diaphragms," by A.C. Costley and D.P. Abrams," 10/10/96, (PB97-133573, MF-A03, A15).

NCEER-96-0002 "State of the Art Review: Foundations and Retaining Structures," by I. Po Lam, to be published.

NCEER-96-0003 "Ductility of Rectangular Reinforced Concrete Bridge Columns with Moderate Confinement," by N. Wehbe, M. Saiidi, D. Sanders and B. Douglas, 11/7/96, (PB97-133557, A06, MF-A02).

NCEER-96-0004 "Proceedings of the Long-Span Bridge Seismic Research Workshop," edited by I.G. Buckle and I.M. Friedland, to be published.

NCEER-96-0005 "Establish Representative Pier Types for Comprehensive Study: Eastern United States," by J. Kulicki and Z. Prucz, 5/28/96, (PB98-119217, A07, MF-A02).

NCEER-96-0006 "Establish Representative Pier Types for Comprehensive Study: Western United States," by R. Imbsen, R.A. Schamber and T.A. Osterkamp, 5/28/96, (PB98-118607, A07, MF-A02).

NCEER-96-0007 "Nonlinear Control Techniques for Dynamical Systems with Uncertain Parameters," by R.G. Ghanem and M.I. Bujakov, 5/27/96, (PB97-100259, A17, MF-A03).

NCEER-96-0008 "Seismic Evaluation of a 30-Year Old Non-Ductile Highway Bridge Pier and Its Retrofit," by J.B. Mander, B. Mahmoodzadegan, S. Bhadra and S.S. Chen, 5/31/96, (PB97-110902, MF-A03, A10).

NCEER-96-0009 "Seismic Performance of a Model Reinforced Concrete Bridge Pier Before and After Retrofit," by J.B. Mander, J.H. Kim and C.A. Ligozio, 5/31/96, (PB97-110910, MF-A02, A10).

NCEER-96-0010 "IDARC2D Version 4.0: A Computer Program for the Inelastic Damage Analysis of Buildings," by R.E. Valles, A.M. Reinhorn, S.K. Kunnath, C. Li and A. Madan, 6/3/96, (PB97-100234, A17, MF-A03).

NCEER-96-0011 "Estimation of the Economic Impact of Multiple Lifeline Disruption: Memphis Light, Gas and Water Division Case Study," by S.E. Chang, H.A. Seligson and R.T. Eguchi, 8/16/96, (PB97-133490, A11, MF-A03).

NCEER-96-0012 "Proceedings from the Sixth Japan-U.S. Workshop on Earthquake Resistant Design of Lifeline Facilities and Countermeasures Against Soil Liquefaction, Edited by M. Hamada and T. O'Rourke, 9/11/96, (PB97-133581, A99, MF-A06).

NCEER-96-0013 "Chemical Hazards, Mitigation and Preparedness in Areas of High Seismic Risk: A Methodology for Estimating the Risk of Post-Earthquake Hazardous Materials Release," by H.A. Seligson, R.T. Eguchi, K.J. Tierney and K. Richmond, 11/7/96, (PB97-133565, MF-A02, A08).

NCEER-96-0014 "Response of Steel Bridge Bearings to Reversed Cyclic Loading," by J.B. Mander, D-K. Kim, S.S. Chen and G.J. Premus, 11/13/96, (PB97-140735, A12, MF-A03).

NCEER-96-0015 "Highway Culvert Performance During Past Earthquakes," by T.L. Youd and C.J. Beckman, 11/25/96, (PB97-133532, A06, MF-A01).

NCEER-97-0001 "Evaluation, Prevention and Mitigation of Pounding Effects in Building Structures," by R.E. Valles and A.M. Reinhorn, 2/20/97, (PB97-159552, A14, MF-A03).

NCEER-97-0002 "Seismic Design Criteria for Bridges and Other Highway Structures," by C. Rojahn, R. Mayes, D.G. Anderson, J. Clark, J.H. Hom, R.V. Nutt and M.J. O'Rourke, 4/30/97, (PB97-194658, A06, MF-A03).

NCEER-97-0003 “Proceedings of the U.S.-Italian Workshop on Seismic Evaluation and Retrofit,” Edited by D.P. Abrams and G.M. Calvi, 3/19/97, (PB97-194666, A13, MF-A03).

NCEER-97-0004 "Investigation of Seismic Response of Buildings with Linear and Nonlinear Fluid Viscous Dampers," by A.A. Seleemah and M.C. Constantinou, 5/21/97, (PB98-109002, A15, MF-A03).

NCEER-97-0005 "Proceedings of the Workshop on Earthquake Engineering Frontiers in Transportation Facilities," edited by G.C. Lee and I.M. Friedland, 8/29/97, (PB98-128911, A25, MR-A04).

NCEER-97-0006 "Cumulative Seismic Damage of Reinforced Concrete Bridge Piers," by S.K. Kunnath, A. El-Bahy, A. Taylor and W. Stone, 9/2/97, (PB98-108814, A11, MF-A03).

NCEER-97-0007 "Structural Details to Accommodate Seismic Movements of Highway Bridges and Retaining Walls," by R.A. Imbsen, R.A. Schamber, E. Thorkildsen, A. Kartoum, B.T. Martin, T.N. Rosser and J.M. Kulicki, 9/3/97, (PB98-108996, A09, MF-A02).

NCEER-97-0008 "A Method for Earthquake Motion-Damage Relationships with Application to Reinforced Concrete Frames," by A. Singhal and A.S. Kiremidjian, 9/10/97, (PB98-108988, A13, MF-A03).

NCEER-97-0009 "Seismic Analysis and Design of Bridge Abutments Considering Sliding and Rotation," by K. Fishman and R. Richards, Jr., 9/15/97, (PB98-108897, A06, MF-A02).

NCEER-97-0010 "Proceedings of the FHWA/NCEER Workshop on the National Representation of Seismic Ground Motion for New and Existing Highway Facilities," edited by I.M. Friedland, M.S. Power and R.L. Mayes, 9/22/97, (PB98-128903, A21, MF-A04).

NCEER-97-0011 "Seismic Analysis for Design or Retrofit of Gravity Bridge Abutments," by K.L. Fishman, R. Richards, Jr. and R.C. Divito, 10/2/97, (PB98-128937, A08, MF-A02).

NCEER-97-0012 "Evaluation of Simplified Methods of Analysis for Yielding Structures," by P. Tsopelas, M.C. Constantinou, C.A. Kircher and A.S. Whittaker, 10/31/97, (PB98-128929, A10, MF-A03).

NCEER-97-0013 "Seismic Design of Bridge Columns Based on Control and Repairability of Damage," by C-T. Cheng and J.B. Mander, 12/8/97, (PB98-144249, A11, MF-A03).

NCEER-97-0014 "Seismic Resistance of Bridge Piers Based on Damage Avoidance Design," by J.B. Mander and C-T. Cheng, 12/10/97, (PB98-144223, A09, MF-A02).

NCEER-97-0015 “Seismic Response of Nominally Symmetric Systems with Strength Uncertainty,” by S. Balopoulou and M. Grigoriu, 12/23/97, (PB98-153422, A11, MF-A03).

NCEER-97-0016 “Evaluation of Seismic Retrofit Methods for Reinforced Concrete Bridge Columns,” by T.J. Wipf, F.W. Klaiber and F.M. Russo, 12/28/97, (PB98-144215, A12, MF-A03).

NCEER-97-0017 “Seismic Fragility of Existing Conventional Reinforced Concrete Highway Bridges,” by C.L. Mullen and A.S. Cakmak, 12/30/97, (PB98-153406, A08, MF-A02).

NCEER-97-0018 “Loss Asssessment of Memphis Buildings,” edited by D.P. Abrams and M. Shinozuka, 12/31/97, (PB98-144231, A13, MF-A03).

NCEER-97-0019 “Seismic Evaluation of Frames with Infill Walls Using Quasi-static Experiments,” by K.M. Mosalam, R.N. White and P. Gergely, 12/31/97, (PB98-153455, A07, MF-A02).

NCEER-97-0020 “Seismic Evaluation of Frames with Infill Walls Using Pseudo-dynamic Experiments,” by K.M. Mosalam, R.N. White and P. Gergely, 12/31/97, (PB98-153430, A07, MF-A02).

NCEER-97-0021 “Computational Strategies for Frames with Infill Walls: Discrete and Smeared Crack Analyses and Seismic Fragility,” by K.M. Mosalam, R.N. White and P. Gergely, 12/31/97, (PB98-153414, A10, MF-A02).

NCEER-97-0022 "Proceedings of the NCEER Workshop on Evaluation of Liquefaction Resistance of Soils," edited by T.L. Youd and I.M. Idriss, 12/31/97, (PB98-155617, A15, MF-A03).

MCEER-98-0001 "Extraction of Nonlinear Hysteretic Properties of Seismically Isolated Bridges from Quick-Release Field Tests," by Q. Chen, B.M. Douglas, E.M. Maragakis and I.G. Buckle, 5/26/98, (PB99-118838, A06, MF-A01).

MCEER-98-0002 "Methodologies for Evaluating the Importance of Highway Bridges," by A. Thomas, S. Eshenaur and J. Kulicki, 5/29/98, (PB99-118846, A10, MF-A02).

MCEER-98-0003 "Capacity Design of Bridge Piers and the Analysis of Overstrength," by J.B. Mander, A. Dutta and P. Goel, 6/1/98, (PB99-118853, A09, MF-A02).

MCEER-98-0004 "Evaluation of Bridge Damage Data from the Loma Prieta and Northridge, California Earthquakes," by N. Basoz and A. Kiremidjian, 6/2/98, (PB99-118861, A15, MF-A03).

MCEER-98-0005 "Screening Guide for Rapid Assessment of Liquefaction Hazard at Highway Bridge Sites," by T. L. Youd, 6/16/98, (PB99-118879, A06, not available on microfiche).

MCEER-98-0006 "Structural Steel and Steel/Concrete Interface Details for Bridges," by P. Ritchie, N. Kauhl and J. Kulicki, 7/13/98, (PB99-118945, A06, MF-A01).

MCEER-98-0007 "Capacity Design and Fatigue Analysis of Confined Concrete Columns," by A. Dutta and J.B. Mander, 7/14/98, (PB99-118960, A14, MF-A03).

MCEER-98-0008 "Proceedings of the Workshop on Performance Criteria for Telecommunication Services Under Earthquake Conditions," edited by A.J. Schiff, 7/15/98, (PB99-118952, A08, MF-A02).

MCEER-98-0009 "Fatigue Analysis of Unconfined Concrete Columns," by J.B. Mander, A. Dutta and J.H. Kim, 9/12/98, (PB99-123655, A10, MF-A02).

MCEER-98-0010 "Centrifuge Modeling of Cyclic Lateral Response of Pile-Cap Systems and Seat-Type Abutments in Dry Sands," by A.D. Gadre and R. Dobry, 10/2/98, (PB99-123606, A13, MF-A03).

MCEER-98-0011 "IDARC-BRIDGE: A Computational Platform for Seismic Damage Assessment of Bridge Structures," by A.M. Reinhorn, V. Simeonov, G. Mylonakis and Y. Reichman, 10/2/98, (PB99-162919, A15, MF-A03).

MCEER-98-0012 "Experimental Investigation of the Dynamic Response of Two Bridges Before and After Retrofitting with Elastomeric Bearings," by D.A. Wendichansky, S.S. Chen and J.B. Mander, 10/2/98, (PB99-162927, A15, MF-A03).

MCEER-98-0013 "Design Procedures for Hinge Restrainers and Hinge Sear Width for Multiple-Frame Bridges," by R. Des Roches and G.L. Fenves, 11/3/98, (PB99-140477, A13, MF-A03).

MCEER-98-0014 "Response Modification Factors for Seismically Isolated Bridges," by M.C. Constantinou and J.K. Quarshie, 11/3/98, (PB99-140485, A14, MF-A03).

MCEER-98-0015 "Proceedings of the U.S.-Italy Workshop on Seismic Protective Systems for Bridges," edited by I.M. Friedland and M.C. Constantinou, 11/3/98, (PB2000-101711, A22, MF-A04).

MCEER-98-0016 "Appropriate Seismic Reliability for Critical Equipment Systems: Recommendations Based on Regional Analysis of Financial and Life Loss," by K. Porter, C. Scawthorn, C. Taylor and N. Blais, 11/10/98, (PB99-157265, A08, MF-A02).

MCEER-98-0017 "Proceedings of the U.S. Japan Joint Seminar on Civil Infrastructure Systems Research," edited by M. Shinozuka and A. Rose, 11/12/98, (PB99-156713, A16, MF-A03).

MCEER-98-0018 "Modeling of Pile Footings and Drilled Shafts for Seismic Design," by I. PoLam, M. Kapuskar and D. Chaudhuri, 12/21/98, (PB99-157257, A09, MF-A02).

MCEER-99-0001 "Seismic Evaluation of a Masonry Infilled Reinforced Concrete Frame by Pseudodynamic Testing," by S.G. Buonopane and R.N. White, 2/16/99, (PB99-162851, A09, MF-A02).

MCEER-99-0002 "Response History Analysis of Structures with Seismic Isolation and Energy Dissipation Systems: Verification Examples for Program SAP2000," by J. Scheller and M.C. Constantinou, 2/22/99, (PB99-162869, A08, MF-A02).

MCEER-99-0003 "Experimental Study on the Seismic Design and Retrofit of Bridge Columns Including Axial Load Effects," by A. Dutta, T. Kokorina and J.B. Mander, 2/22/99, (PB99-162877, A09, MF-A02).

MCEER-99-0004 "Experimental Study of Bridge Elastomeric and Other Isolation and Energy Dissipation Systems with Emphasis on Uplift Prevention and High Velocity Near-source Seismic Excitation," by A. Kasalanati and M. C. Constantinou, 2/26/99, (PB99-162885, A12, MF-A03).

MCEER-99-0005 "Truss Modeling of Reinforced Concrete Shear-flexure Behavior," by J.H. Kim and J.B. Mander, 3/8/99, (PB99-163693, A12, MF-A03).

MCEER-99-0006 "Experimental Investigation and Computational Modeling of Seismic Response of a 1:4 Scale Model Steel Structure with a Load Balancing Supplemental Damping System," by G. Pekcan, J.B. Mander and S.S. Chen, 4/2/99, (PB99-162893, A11, MF-A03).

MCEER-99-0007 "Effect of Vertical Ground Motions on the Structural Response of Highway Bridges," by M.R. Button, C.J. Cronin and R.L. Mayes, 4/10/99, (PB2000-101411, A10, MF-A03).

MCEER-99-0008 "Seismic Reliability Assessment of Critical Facilities: A Handbook, Supporting Documentation, and Model Code Provisions," by G.S. Johnson, R.E. Sheppard, M.D. Quilici, S.J. Eder and C.R. Scawthorn, 4/12/99, (PB2000-101701, A18, MF-A04).

MCEER-99-0009 "Impact Assessment of Selected MCEER Highway Project Research on the Seismic Design of Highway Structures," by C. Rojahn, R. Mayes, D.G. Anderson, J.H. Clark, D'Appolonia Engineering, S. Gloyd and R.V. Nutt, 4/14/99, (PB99-162901, A10, MF-A02).

MCEER-99-0010 "Site Factors and Site Categories in Seismic Codes," by R. Dobry, R. Ramos and M.S. Power, 7/19/99, (PB2000-101705, A08, MF-A02).

MCEER-99-0011 "Restrainer Design Procedures for Multi-Span Simply-Supported Bridges," by M.J. Randall, M. Saiidi, E. Maragakis and T. Isakovic, 7/20/99, (PB2000-101702, A10, MF-A02).

MCEER-99-0012 "Property Modification Factors for Seismic Isolation Bearings," by M.C. Constantinou, P. Tsopelas, A. Kasalanati and E. Wolff, 7/20/99, (PB2000-103387, A11, MF-A03).

MCEER-99-0013 "Critical Seismic Issues for Existing Steel Bridges," by P. Ritchie, N. Kauhl and J. Kulicki, 7/20/99, (PB2000-101697, A09, MF-A02).

MCEER-99-0014 "Nonstructural Damage Database," by A. Kao, T.T. Soong and A. Vender, 7/24/99, (PB2000-101407, A06, MF-A01).

MCEER-99-0015 "Guide to Remedial Measures for Liquefaction Mitigation at Existing Highway Bridge Sites," by H.G. Cooke and J. K. Mitchell, 7/26/99, (PB2000-101703, A11, MF-A03).

MCEER-99-0016 "Proceedings of the MCEER Workshop on Ground Motion Methodologies for the Eastern United States," edited by N. Abrahamson and A. Becker, 8/11/99, (PB2000-103385, A07, MF-A02).

MCEER-99-0017 "Quindío, Colombia Earthquake of January 25, 1999: Reconnaissance Report," by A.P. Asfura and P.J. Flores, 10/4/99, (PB2000-106893, A06, MF-A01).

MCEER-99-0018 "Hysteretic Models for Cyclic Behavior of Deteriorating Inelastic Structures," by M.V. Sivaselvan and A.M. Reinhorn, 11/5/99, (PB2000-103386, A08, MF-A02).

MCEER-99-0019 "Proceedings of the 7th U.S.- Japan Workshop on Earthquake Resistant Design of Lifeline Facilities and Countermeasures Against Soil Liquefaction," edited by T.D. O'Rourke, J.P. Bardet and M. Hamada, 11/19/99, (PB2000-103354, A99, MF-A06).

MCEER-99-0020 "Development of Measurement Capability for Micro-Vibration Evaluations with Application to Chip Fabrication Facilities," by G.C. Lee, Z. Liang, J.W. Song, J.D. Shen and W.C. Liu, 12/1/99, (PB2000-105993, A08, MF-A02).

MCEER-99-0021 "Design and Retrofit Methodology for Building Structures with Supplemental Energy Dissipating Systems," by G. Pekcan, J.B. Mander and S.S. Chen, 12/31/99, (PB2000-105994, A11, MF-A03).

MCEER-00-0001 "The Marmara, Turkey Earthquake of August 17, 1999: Reconnaissance Report," edited by C. Scawthorn; with major contributions by M. Bruneau, R. Eguchi, T. Holzer, G. Johnson, J. Mander, J. Mitchell, W. Mitchell, A. Papageorgiou, C. Scaethorn, and G. Webb, 3/23/00, (PB2000-106200, A11, MF-A03).

MCEER-00-0002 "Proceedings of the MCEER Workshop for Seismic Hazard Mitigation of Health Care Facilities," edited by G.C. Lee, M. Ettouney, M. Grigoriu, J. Hauer and J. Nigg, 3/29/00, (PB2000-106892, A08, MF-A02).

MCEER-00-0003 "The Chi-Chi, Taiwan Earthquake of September 21, 1999: Reconnaissance Report," edited by G.C. Lee and C.H. Loh, with major contributions by G.C. Lee, M. Bruneau, I.G. Buckle, S.E. Chang, P.J. Flores, T.D. O'Rourke, M. Shinozuka, T.T. Soong, C-H. Loh, K-C. Chang, Z-J. Chen, J-S. Hwang, M-L. Lin, G-Y. Liu, K-C. Tsai, G.C. Yao and C-L. Yen, 4/30/00, (PB2001-100980, A10, MF-A02).

MCEER-00-0004 "Seismic Retrofit of End-Sway Frames of Steel Deck-Truss Bridges with a Supplemental Tendon System: Experimental and Analytical Investigation," by G. Pekcan, J.B. Mander and S.S. Chen, 7/1/00, (PB2001-100982, A10, MF-A02).

MCEER-00-0005 "Sliding Fragility of Unrestrained Equipment in Critical Facilities," by W.H. Chong and T.T. Soong, 7/5/00, (PB2001-100983, A08, MF-A02).

MCEER-00-0006 "Seismic Response of Reinforced Concrete Bridge Pier Walls in the Weak Direction," by N. Abo-Shadi, M. Saiidi and D. Sanders, 7/17/00, (PB2001-100981, A17, MF-A03).

MCEER-00-0007 "Low-Cycle Fatigue Behavior of Longitudinal Reinforcement in Reinforced Concrete Bridge Columns," by J. Brown and S.K. Kunnath, 7/23/00, (PB2001-104392, A08, MF-A02).

MCEER-00-0008 "Soil Structure Interaction of Bridges for Seismic Analysis," I. PoLam and H. Law, 9/25/00, (PB2001-105397, A08, MF-A02).

MCEER-00-0009 "Proceedings of the First MCEER Workshop on Mitigation of Earthquake Disaster by Advanced Technologies (MEDAT-1), edited by M. Shinozuka, D.J. Inman and T.D. O'Rourke, 11/10/00, (PB2001-105399, A14, MF-A03).

MCEER-00-0010 "Development and Evaluation of Simplified Procedures for Analysis and Design of Buildings with Passive Energy Dissipation Systems, Revision 01," by O.M. Ramirez, M.C. Constantinou, C.A. Kircher, A.S. Whittaker, M.W. Johnson, J.D. Gomez and C. Chrysostomou, 11/16/01, (PB2001-105523, A23, MF-A04).

MCEER-00-0011 "Dynamic Soil-Foundation-Structure Interaction Analyses of Large Caissons," by C-Y. Chang, C-M. Mok, Z-L. Wang, R. Settgast, F. Waggoner, M.A. Ketchum, H.M. Gonnermann and C-C. Chin, 12/30/00, (PB2001-104373, A07, MF-A02).

MCEER-00-0012 "Experimental Evaluation of Seismic Performance of Bridge Restrainers," by A.G. Vlassis, E.M. Maragakis and M. Saiid Saiidi, 12/30/00, (PB2001-104354, A09, MF-A02).

MCEER-00-0013 "Effect of Spatial Variation of Ground Motion on Highway Structures," by M. Shinozuka, V. Saxena and G. Deodatis, 12/31/00, (PB2001-108755, A13, MF-A03).

MCEER-00-0014 "A Risk-Based Methodology for Assessing the Seismic Performance of Highway Systems," by S.D. Werner, C.E. Taylor, J.E. Moore, II, J.S. Walton and S. Cho, 12/31/00, (PB2001-108756, A14, MF-A03).

MCEER-01-0001 “Experimental Investigation of P-Delta Effects to Collapse During Earthquakes,” by D. Vian and M. Bruneau, 6/25/01, (PB2002-100534, A17, MF-A03).

MCEER-01-0002 “Proceedings of the Second MCEER Workshop on Mitigation of Earthquake Disaster by Advanced Technologies (MEDAT-2),” edited by M. Bruneau and D.J. Inman, 7/23/01, (PB2002-100434, A16, MF-A03).

MCEER-01-0003 “Sensitivity Analysis of Dynamic Systems Subjected to Seismic Loads,” by C. Roth and M. Grigoriu, 9/18/01, (PB2003-100884, A12, MF-A03).

MCEER-01-0004 “Overcoming Obstacles to Implementing Earthquake Hazard Mitigation Policies: Stage 1 Report,” by D.J. Alesch and W.J. Petak, 12/17/01, (PB2002-107949, A07, MF-A02).

MCEER-01-0005 “Updating Real-Time Earthquake Loss Estimates: Methods, Problems and Insights,” by C.E. Taylor, S.E. Chang and R.T. Eguchi, 12/17/01, (PB2002-107948, A05, MF-A01).

MCEER-01-0006 “Experimental Investigation and Retrofit of Steel Pile Foundations and Pile Bents Under Cyclic Lateral Loadings,” by A. Shama, J. Mander, B. Blabac and S. Chen, 12/31/01, (PB2002-107950, A13, MF-A03).

MCEER-02-0001 “Assessment of Performance of Bolu Viaduct in the 1999 Duzce Earthquake in Turkey” by P.C. Roussis, M.C. Constantinou, M. Erdik, E. Durukal and M. Dicleli, 5/8/02, (PB2003-100883, A08, MF-A02).

MCEER-02-0002 “Seismic Behavior of Rail Counterweight Systems of Elevators in Buildings,” by M.P. Singh, Rildova and L.E. Suarez, 5/27/02. (PB2003-100882, A11, MF-A03).

MCEER-02-0003 “Development of Analysis and Design Procedures for Spread Footings,” by G. Mylonakis, G. Gazetas, S. Nikolaou and A. Chauncey, 10/02/02, (PB2004-101636, A13, MF-A03, CD-A13).

MCEER-02-0004 “Bare-Earth Algorithms for Use with SAR and LIDAR Digital Elevation Models,” by C.K. Huyck, R.T. Eguchi and B. Houshmand, 10/16/02, (PB2004-101637, A07, CD-A07).

MCEER-02-0005 “Review of Energy Dissipation of Compression Members in Concentrically Braced Frames,” by K.Lee and M. Bruneau, 10/18/02, (PB2004-101638, A10, CD-A10).

MCEER-03-0001 “Experimental Investigation of Light-Gauge Steel Plate Shear Walls for the Seismic Retrofit of Buildings” by J. Berman and M. Bruneau, 5/2/03, (PB2004-101622, A10, MF-A03, CD-A10).

MCEER-03-0002 “Statistical Analysis of Fragility Curves,” by M. Shinozuka, M.Q. Feng, H. Kim, T. Uzawa and T. Ueda, 6/16/03, (PB2004-101849, A09, CD-A09).

MCEER-03-0003 “Proceedings of the Eighth U.S.-Japan Workshop on Earthquake Resistant Design f Lifeline Facilities and Countermeasures Against Liquefaction,” edited by M. Hamada, J.P. Bardet and T.D. O'Rourke, 6/30/03, (PB2004-104386, A99, CD-A99).

MCEER-03-0004 “Proceedings of the PRC-US Workshop on Seismic Analysis and Design of Special Bridges,” edited by L.C. Fan and G.C. Lee, 7/15/03, (PB2004-104387, A14, CD-A14).

MCEER-03-0005 “Urban Disaster Recovery: A Framework and Simulation Model,” by S.B. Miles and S.E. Chang, 7/25/03, (PB2004-104388, A07, CD-A07).

MCEER-03-0006 “Behavior of Underground Piping Joints Due to Static and Dynamic Loading,” by R.D. Meis, M. Maragakis and R. Siddharthan, 11/17/03, (PB2005-102194, A13, MF-A03, CD-A00).

MCEER-04-0001 “Experimental Study of Seismic Isolation Systems with Emphasis on Secondary System Response and Verification of Accuracy of Dynamic Response History Analysis Methods,” by E. Wolff and M. Constantinou, 1/16/04 (PB2005-102195, A99, MF-E08, CD-A00).

MCEER-04-0002 “Tension, Compression and Cyclic Testing of Engineered Cementitious Composite Materials,” by K. Kesner and S.L. Billington, 3/1/04, (PB2005-102196, A08, CD-A08).

MCEER-04-0003 "Cyclic Testing of Braces Laterally Restrained by Steel Studs to Enhance Performance During Earthquakes," by O.C. Celik, J.W. Berman and M. Bruneau, 3/16/04, (PB2005-102197, A13, MF-A03, CD-A00).

MCEER-04-0004 "Methodologies for Post Earthquake Building Damage Detection Using SAR and Optical Remote Sensing: Application to the August 17, 1999 Marmara, Turkey Earthquake," by C.K. Huyck, B.J. Adams, S. Cho, R.T. Eguchi, B. Mansouri and B. Houshmand, 6/15/04, (PB2005-104888, A10, CD-A00).

MCEER-04-0005 "Nonlinear Structural Analysis Towards Collapse Simulation: A Dynamical Systems Approach," by M.V. Sivaselvan and A.M. Reinhorn, 6/16/04, (PB2005-104889, A11, MF-A03, CD-A00).

MCEER-04-0006 "Proceedings of the Second PRC-US Workshop on Seismic Analysis and Design of Special Bridges," edited by G.C. Lee and L.C. Fan, 6/25/04, (PB2005-104890, A16, CD-A00).

MCEER-04-0007 "Seismic Vulnerability Evaluation of Axially Loaded Steel Built-up Laced Members," by K. Lee and M. Bruneau, 6/30/04, (PB2005-104891, A16, CD-A00).

MCEER-04-0008 "Evaluation of Accuracy of Simplified Methods of Analysis and Design of Buildings with Damping Systems for Near-Fault and for Soft-Soil Seismic Motions," by E.A. Pavlou and M.C. Constantinou, 8/16/04, (PB2005-104892, A08, MF-A02, CD-A00).

MCEER-04-0009 "Assessment of Geotechnical Issues in Acute Care Facilities in California," by M. Lew, T.D. O'Rourke, R. Dobry and M. Koch, 9/15/04, (PB2005-104893, A08, CD-A00).

MCEER-04-0010 "Scissor-Jack-Damper Energy Dissipation System," by A.N. Sigaher-Boyle and M.C. Constantinou, 12/1/04 (PB2005-108221).

MCEER-04-0011 "Seismic Retrofit of Bridge Steel Truss Piers Using a Controlled Rocking Approach," by M. Pollino and M. Bruneau, 12/20/04 (PB2006-105795).

MCEER-05-0001 "Experimental and Analytical Studies of Structures Seismically Isolated with an Uplift-Restraint Isolation System," by P.C. Roussis and M.C. Constantinou, 1/10/05 (PB2005-108222).

MCEER-05-0002 "A Versatile Experimentation Model for Study of Structures Near Collapse Applied to Seismic Evaluation of Irregular Structures," by D. Kusumastuti, A.M. Reinhorn and A. Rutenberg, 3/31/05 (PB2006-101523).

MCEER-05-0003 "Proceedings of the Third PRC-US Workshop on Seismic Analysis and Design of Special Bridges," edited by L.C. Fan and G.C. Lee, 4/20/05, (PB2006-105796).

MCEER-05-0004 "Approaches for the Seismic Retrofit of Braced Steel Bridge Piers and Proof-of-Concept Testing of an Eccentrically Braced Frame with Tubular Link," by J.W. Berman and M. Bruneau, 4/21/05 (PB2006-101524).

MCEER-05-0005 "Simulation of Strong Ground Motions for Seismic Fragility Evaluation of Nonstructural Components in Hospitals," by A. Wanitkorkul and A. Filiatrault, 5/26/05 (PB2006-500027).

MCEER-05-0006 "Seismic Safety in California Hospitals: Assessing an Attempt to Accelerate the Replacement or Seismic Retrofit of Older Hospital Facilities," by D.J. Alesch, L.A. Arendt and W.J. Petak, 6/6/05 (PB2006-105794).

MCEER-05-0007 "Development of Seismic Strengthening and Retrofit Strategies for Critical Facilities Using Engineered Cementitious Composite Materials," by K. Kesner and S.L. Billington, 8/29/05 (PB2006-111701).

MCEER-05-0008 "Experimental and Analytical Studies of Base Isolation Systems for Seismic Protection of Power Transformers," by N. Murota, M.Q. Feng and G-Y. Liu, 9/30/05 (PB2006-111702).

MCEER-05-0009 "3D-BASIS-ME-MB: Computer Program for Nonlinear Dynamic Analysis of Seismically Isolated Structures," by P.C. Tsopelas, P.C. Roussis, M.C. Constantinou, R. Buchanan and A.M. Reinhorn, 10/3/05 (PB2006-111703).

MCEER-05-0010 "Steel Plate Shear Walls for Seismic Design and Retrofit of Building Structures," by D. Vian and M. Bruneau, 12/15/05 (PB2006-111704).

MCEER-05-0011 "The Performance-Based Design Paradigm," by M.J. Astrella and A. Whittaker, 12/15/05 (PB2006-111705).

MCEER-06-0001 "Seismic Fragility of Suspended Ceiling Systems," H. Badillo-Almaraz, A.S. Whittaker, A.M. Reinhorn and G.P. Cimellaro, 2/4/06 (PB2006-111706).

MCEER-06-0002 "Multi-Dimensional Fragility of Structures," by G.P. Cimellaro, A.M. Reinhorn and M. Bruneau, 3/1/06 (PB2007-106974, A09, MF-A02, CD A00).

MCEER-06-0003 "Built-Up Shear Links as Energy Dissipators for Seismic Protection of Bridges," by P. Dusicka, A.M. Itani and I.G. Buckle, 3/15/06 (PB2006-111708).

MCEER-06-0004 "Analytical Investigation of the Structural Fuse Concept," by R.E. Vargas and M. Bruneau, 3/16/06 (PB2006-111709).

MCEER-06-0005 "Experimental Investigation of the Structural Fuse Concept," by R.E. Vargas and M. Bruneau, 3/17/06 (PB2006-111710).

MCEER-06-0006 "Further Development of Tubular Eccentrically Braced Frame Links for the Seismic Retrofit of Braced Steel Truss Bridge Piers," by J.W. Berman and M. Bruneau, 3/27/06 (PB2007-105147).

MCEER-06-0007 "REDARS Validation Report," by S. Cho, C.K. Huyck, S. Ghosh and R.T. Eguchi, 8/8/06 (PB2007-106983).

MCEER-06-0008 "Review of Current NDE Technologies for Post-Earthquake Assessment of Retrofitted Bridge Columns," by J.W. Song, Z. Liang and G.C. Lee, 8/21/06 (PB2007-106984).

MCEER-06-0009 "Liquefaction Remediation in Silty Soils Using Dynamic Compaction and Stone Columns," by S. Thevanayagam, G.R. Martin, R. Nashed, T. Shenthan, T. Kanagalingam and N. Ecemis, 8/28/06 (PB2007-106985).

MCEER-06-0010 "Conceptual Design and Experimental Investigation of Polymer Matrix Composite Infill Panels for Seismic Retrofitting," by W. Jung, M. Chiewanichakorn and A.J. Aref, 9/21/06 (PB2007-106986).

MCEER-06-0011 "A Study of the Coupled Horizontal-Vertical Behavior of Elastomeric and Lead-Rubber Seismic Isolation Bearings," by G.P. Warn and A.S. Whittaker, 9/22/06 (PB2007-108679).

MCEER-06-0012 "Proceedings of the Fourth PRC-US Workshop on Seismic Analysis and Design of Special Bridges: Advancing Bridge Technologies in Research, Design, Construction and Preservation," Edited by L.C. Fan, G.C. Lee and L. Ziang, 10/12/06 (PB2007-109042).

MCEER-06-0013 "Cyclic Response and Low Cycle Fatigue Characteristics of Plate Steels," by P. Dusicka, A.M. Itani and I.G. Buckle, 11/1/06 06 (PB2007-106987).

MCEER-06-0014 "Proceedings of the Second US-Taiwan Bridge Engineering Workshop," edited by W.P. Yen, J. Shen, J-Y. Chen and M. Wang, 11/15/06 (PB2008-500041).

MCEER-06-0015 "User Manual and Technical Documentation for the REDARS^{TM} Import Wizard," by S. Cho, S. Ghosh, C.K. Huyck and S.D. Werner, 11/30/06 (PB2007-114766).

MCEER-06-0016 "Hazard Mitigation Strategy and Monitoring Technologies for Urban and Infrastructure Public Buildings: Proceedings of the China-US Workshops," edited by X.Y. Zhou, A.L. Zhang, G.C. Lee and M. Tong, 12/12/06 (PB2008-500018).

MCEER-07-0001 "Static and Kinetic Coefficients of Friction for Rigid Blocks," by C. Kafali, S. Fathali, M. Grigoriu and A.S. Whittaker, 3/20/07 (PB2007-114767).

MCEER-07-0002 "Hazard Mitigation Investment Decision Making: Organizational Response to Legislative Mandate," by L.A. Arendt, D.J. Alesch and W.J. Petak, 4/9/07 (PB2007-114768).

MCEER-07-0003 "Seismic Behavior of Bidirectional-Resistant Ductile End Diaphragms with Unbonded Braces in Straight or Skewed Steel Bridges," by O. Celik and M. Bruneau, 4/11/07 (PB2008-105141).

MCEER-07-0004 "Modeling Pile Behavior in Large Pile Groups Under Lateral Loading," by A.M. Dodds and G.R. Martin, 4/16/07(PB2008-105142).

MCEER-07-0005 "Experimental Investigation of Blast Performance of Seismically Resistant Concrete-Filled Steel Tube Bridge Piers," by S. Fujikura, M. Bruneau and D. Lopez-Garcia, 4/20/07 (PB2008-105143).

MCEER-07-0006 "Seismic Analysis of Conventional and Isolated Liquefied Natural Gas Tanks Using Mechanical Analogs," by I.P. Christovasilis and A.S. Whittaker, 5/1/07.

MCEER-07-0007 "Experimental Seismic Performance Evaluation of Isolation/Restraint Systems for Mechanical Equipment – Part 1: Heavy Equipment Study," by S. Fathali and A. Filiatrault, 6/6/07 (PB2008-105144).

MCEER-07-0008 "Seismic Vulnerability of Timber Bridges and Timber Substructures," by A.A. Sharma, J.B. Mander, I.M. Friedland and D.R. Allicock, 6/7/07 (PB2008-105145).

MCEER-07-0009 "Experimental and Analytical Study of the XY-Friction Pendulum (XY-FP) Bearing for Bridge Applications," by C.C. Marin-Artieda, A.S. Whittaker and M.C. Constantinou, 6/7/07 (PB2008-105191).

MCEER-07-0010 "Proceedings of the PRC-US Earthquake Engineering Forum for Young Researchers," Edited by G.C. Lee and X.Z. Qi, 6/8/07 (PB2008-500058).

MCEER-07-0011 "Design Recommendations for Perforated Steel Plate Shear Walls," by R. Purba and M. Bruneau, 6/18/07, (PB2008-105192).

MCEER-07-0012 "Performance of Seismic Isolation Hardware Under Service and Seismic Loading," by M.C. Constantinou, A.S. Whittaker, Y. Kalpakidis, D.M. Fenz and G.P. Warn, 8/27/07, (PB2008-105193).

MCEER-07-0013 "Experimental Evaluation of the Seismic Performance of Hospital Piping Subassemblies," by E.R. Goodwin, E. Maragakis and A.M. Itani, 9/4/07, (PB2008-105194).

MCEER-07-0014 "A Simulation Model of Urban Disaster Recovery and Resilience: Implementation for the 1994 Northridge Earthquake," by S. Miles and S.E. Chang, 9/7/07, (PB2008-106426).

MCEER-07-0015 "Statistical and Mechanistic Fragility Analysis of Concrete Bridges," by M. Shinozuka, S. Banerjee and S-H. Kim, 9/10/07, (PB2008-106427).

MCEER-07-0016 "Three-Dimensional Modeling of Inelastic Buckling in Frame Structures," by M. Schachter and AM. Reinhorn, 9/13/07, (PB2008-108125).

MCEER-07-0017 "Modeling of Seismic Wave Scattering on Pile Groups and Caissons," by I. Po Lam, H. Law and C.T. Yang, 9/17/07 (PB2008-108150).

MCEER-07-0018 "Bridge Foundations: Modeling Large Pile Groups and Caissons for Seismic Design," by I. Po Lam, H. Law and G.R. Martin (Coordinating Author), 12/1/07 (PB2008-111190).

MCEER-07-0019 "Principles and Performance of Roller Seismic Isolation Bearings for Highway Bridges," by G.C. Lee, Y.C. Ou, Z. Liang, T.C. Niu and J. Song, 12/10/07 (PB2009-110466).

MCEER-07-0020 "Centrifuge Modeling of Permeability and Pinning Reinforcement Effects on Pile Response to Lateral Spreading," by L.L Gonzalez-Lagos, T. Abdoun and R. Dobry, 12/10/07 (PB2008-111191).

MCEER-07-0021 "Damage to the Highway System from the Pisco, Perú Earthquake of August 15, 2007," by J.S. O'Connor, L. Mesa and M. Nykamp, 12/10/07, (PB2008-108126).

MCEER-07-0022 "Experimental Seismic Performance Evaluation of Isolation/Restraint Systems for Mechanical Equipment – Part 2: Light Equipment Study," by S. Fathali and A. Filiatrault, 12/13/07 (PB2008-111192).

MCEER-07-0023 "Fragility Considerations in Highway Bridge Design," by M. Shinozuka, S. Banerjee and S.H. Kim, 12/14/07 (PB2008-111193).

MCEER-07-0024 "Performance Estimates for Seismically Isolated Bridges," by G.P. Warn and A.S. Whittaker, 12/30/07 (PB2008-112230).

MCEER-08-0001 "Seismic Performance of Steel Girder Bridge Superstructures with Conventional Cross Frames," by L.P. Carden, A.M. Itani and I.G. Buckle, 1/7/08, (PB2008-112231).

MCEER-08-0002 "Seismic Performance of Steel Girder Bridge Superstructures with Ductile End Cross Frames with Seismic Isolators," by L.P. Carden, A.M. Itani and I.G. Buckle, 1/7/08 (PB2008-112232).

MCEER-08-0003 "Analytical and Experimental Investigation of a Controlled Rocking Approach for Seismic Protection of Bridge Steel Truss Piers," by M. Pollino and M. Bruneau, 1/21/08 (PB2008-112233).

MCEER-08-0004 "Linking Lifeline Infrastructure Performance and Community Disaster Resilience: Models and Multi-Stakeholder Processes," by S.E. Chang, C. Pasion, K. Tatebe and R. Ahmad, 3/3/08 (PB2008-112234).

MCEER-08-0005 "Modal Analysis of Generally Damped Linear Structures Subjected to Seismic Excitations," by J. Song, Y-L. Chu, Z. Liang and G.C. Lee, 3/4/08 (PB2009-102311).

MCEER-08-0006 "System Performance Under Multi-Hazard Environments," by C. Kafali and M. Grigoriu, 3/4/08 (PB2008-112235).

MCEER-08-0007 "Mechanical Behavior of Multi-Spherical Sliding Bearings," by D.M. Fenz and M.C. Constantinou, 3/6/08 (PB2008-112236).

MCEER-08-0008 "Post-Earthquake Restoration of the Los Angeles Water Supply System," by T.H.P. Tabucchi and R.A. Davidson, 3/7/08 (PB2008-112237).

MCEER-08-0009 "Fragility Analysis of Water Supply Systems," by A. Jacobson and M. Grigoriu, 3/10/08 (PB2009-105545).

MCEER-08-0010 "Experimental Investigation of Full-Scale Two-Story Steel Plate Shear Walls with Reduced Beam Section Connections," by B. Qu, M. Bruneau, C-H. Lin and K-C. Tsai, 3/17/08 (PB2009-106368).

MCEER-08-0011 "Seismic Evaluation and Rehabilitation of Critical Components of Electrical Power Systems," S. Ersoy, B. Feizi, A. Ashrafi and M. Ala Saadeghvaziri, 3/17/08 (PB2009-105546).

MCEER-08-0012 "Seismic Behavior and Design of Boundary Frame Members of Steel Plate Shear Walls," by B. Qu and M. Bruneau, 4/26/08 . (PB2009-106744).

MCEER-08-0013 "Development and Appraisal of a Numerical Cyclic Loading Protocol for Quantifying Building System Performance," by A. Filiatrault, A. Wanitkorkul and M. Constantinou, 4/27/08 (PB2009-107906).

MCEER-08-0014 "Structural and Nonstructural Earthquake Design: The Challenge of Integrating Specialty Areas in Designing Complex, Critical Facilities," by W.J. Petak and D.J. Alesch, 4/30/08 (PB2009-107907).

MCEER-08-0015 "Seismic Performance Evaluation of Water Systems," by Y. Wang and T.D. O'Rourke, 5/5/08 (PB2009-107908).

MCEER-08-0016 "Seismic Response Modeling of Water Supply Systems," by P. Shi and T.D. O'Rourke, 5/5/08 (PB2009-107910).

MCEER-08-0017 "Numerical and Experimental Studies of Self-Centering Post-Tensioned Steel Frames," by D. Wang and A. Filiatrault, 5/12/08 (PB2009-110479).

MCEER-08-0018 "Development, Implementation and Verification of Dynamic Analysis Models for Multi-Spherical Sliding Bearings," by D.M. Fenz and M.C. Constantinou, 8/15/08 (PB2009-107911).

MCEER-08-0019 "Performance Assessment of Conventional and Base Isolated Nuclear Power Plants for Earthquake Blast Loadings," by Y.N. Huang, A.S. Whittaker and N. Luco, 10/28/08 (PB2009-107912).

MCEER-08-0020 "Remote Sensing for Resilient Multi-Hazard Disaster Response – Volume I: Introduction to Damage Assessment Methodologies," by B.J. Adams and R.T. Eguchi, 11/17/08 (PB2010-102695).

MCEER-08-0021 "Remote Sensing for Resilient Multi-Hazard Disaster Response – Volume II: Counting the Number of Collapsed Buildings Using an Object-Oriented Analysis: Case Study of the 2003 Bam Earthquake," by L. Gusella, C.K. Huyck and B.J. Adams, 11/17/08 (PB2010-100925).

MCEER-08-0022 "Remote Sensing for Resilient Multi-Hazard Disaster Response – Volume III: Multi-Sensor Image Fusion Techniques for Robust Neighborhood-Scale Urban Damage Assessment," by B.J. Adams and A. McMillan, 11/17/08 (PB2010-100926).

MCEER-08-0023 "Remote Sensing for Resilient Multi-Hazard Disaster Response – Volume IV: A Study of Multi-Temporal and Multi-Resolution SAR Imagery for Post-Katrina Flood Monitoring in New Orleans," by A. McMillan, J.G. Morley, B.J. Adams and S. Chesworth, 11/17/08 (PB2010-100927).

MCEER-08-0024 "Remote Sensing for Resilient Multi-Hazard Disaster Response – Volume V: Integration of Remote Sensing Imagery and VIEWS^{TM} Field Data for Post-Hurricane Charley Building Damage Assessment," by J.A. Womble, K. Mehta and B.J. Adams, 11/17/08 (PB2009-115532).

MCEER-08-0025 "Building Inventory Compilation for Disaster Management: Application of Remote Sensing and Statistical Modeling," by P. Sarabandi, A.S. Kiremidjian, R.T. Eguchi and B. J. Adams, 11/20/08 (PB2009-110484).

MCEER-08-0026 "New Experimental Capabilities and Loading Protocols for Seismic Qualification and Fragility Assessment of Nonstructural Systems," by R. Retamales, G. Mosqueda, A. Filiatrault and A. Reinhorn, 11/24/08 (PB2009-110485).

MCEER-08-0027 "Effects of Heating and Load History on the Behavior of Lead-Rubber Bearings," by I.V. Kalpakidis and M.C. Constantinou, 12/1/08 (PB2009-115533).

MCEER-08-0028 "Experimental and Analytical Investigation of Blast Performance of Seismically Resistant Bridge Piers," by S.Fujikura and M. Bruneau, 12/8/08 (PB2009-115534).

MCEER-08-0029 "Evolutionary Methodology for Aseismic Decision Support," by Y. Hu and G. Dargush, 12/15/08.

MCEER-08-0030 "Development of a Steel Plate Shear Wall Bridge Pier System Conceived from a Multi-Hazard Perspective," by D. Keller and M. Bruneau, 12/19/08 (PB2010-102696).

MCEER-09-0001 "Modal Analysis of Arbitrarily Damped Three-Dimensional Linear Structures Subjected to Seismic Excitations," by Y.L. Chu, J. Song and G.C. Lee, 1/31/09 (PB2010-100922).

MCEER-09-0002 "Air-Blast Effects on Structural Shapes," by G. Ballantyne, A.S. Whittaker, A.J. Aref and G.F. Dargush, 2/2/09 (PB2010-102697).

MCEER-09-0003 "Water Supply Performance During Earthquakes and Extreme Events," by A.L. Bonneau and T.D. O'Rourke, 2/16/09 (PB2010-100923).

MCEER-09-0004 "Generalized Linear (Mixed) Models of Post-Earthquake Ignitions," by R.A. Davidson, 7/20/09 (PB2010-102698).

MCEER-09-0005 "Seismic Testing of a Full-Scale Two-Story Light-Frame Wood Building: NEESWood Benchmark Test," by I.P. Christovasilis, A. Filiatrault and A. Wanitkorkul, 7/22/09.

MCEER-09-0006 "IDARC2D Version 7.0: A Program for the Inelastic Damage Analysis of Structures," by A.M. Reinhorn, H. Roh, M. Sivaselvan, S.K. Kunnath, R.E. Valles, A. Madan, C. Li, R. Lobo and Y.J. Park, 7/28/09 (PB2010-103199).

MCEER-09-0007 "Enhancements to Hospital Resiliency: Improving Emergency Planning for and Response to Hurricanes," by D.B. Hess and L.A. Arendt, 7/30/09 (PB2010-100924).

MCEER-09-0008 "Assessment of Base-Isolated Nuclear Structures for Design and Beyond-Design Basis Earthquake Shaking," by Y.N. Huang, A.S. Whittaker, R.P. Kennedy and R.L. Mayes, 8/20/09 (PB2010-102699).

MCEER-09-0009 "Quantification of Disaster Resilience of Health Care Facilities," by G.P. Cimellaro, C. Fumo, A.M Reinhorn and M. Bruneau, 9/14/09.

MCEER-09-0010 "Performance-Based Assessment and Design of Squat Reinforced Concrete Shear Walls," by C.K. Gulec and A.S. Whittaker, 9/15/09 (PB2010-102700).

MCEER-09-0011 "Proceedings of the Fourth US-Taiwan Bridge Engineering Workshop," edited by W.P. Yen, J.J. Shen, T.M. Lee and R.B. Zheng, 10/27/09 (PB2010-500009).

MCEER-09-0012 "Proceedings of the Special International Workshop on Seismic Connection Details for Segmental Bridge Construction," edited by W. Phillip Yen and George C. Lee, 12/21/09.

MCEER-10-0001 "Direct Displacement Procedure for Performance-Based Seismic Design of Multistory Woodframe Structures," by W. Pang and D. Rosowsky, 4/26/10.

MCEER-10-0002 "Simplified Direct Displacement Design of Six-Story NEESWood Capstone Building and Pre-Test Seismic Performance Assessment," by W. Pang, D. Rosowsky, J. van de Lindt and S. Pei, 5/28/10.

MCEER-10-0003 "Integration of Seismic Protection Systems in Performance-Based Seismic Design of Woodframed Structures," by J.K. Shinde and M.D. Symans, 6/18/10.

MCEER-10-0004 "Modeling and Seismic Evaluation of Nonstructural Components: Testing Frame for Experimental Evaluation of Suspended Ceiling Systems," by A.M. Reinhorn, K.P. Ryu and G. Maddaloni, 6/30/10.

MCEER-10-0005 "Analytical Development and Experimental Validation of a Structural-Fuse Bridge Pier Concept," by S. El-Bahey and M. Bruneau, 10/1/10.

MCEER-10-0006 "A Framework for Defining and Measuring Resilience at the Community Scale: The PEOPLES Resilience Framework," by C.S. Renschler, A.E. Frazier, L.A. Arendt, G.P. Cimellaro, A.M. Reinhorn and M. Bruneau, 10/8/10.

MCEER-10-0007 "Impact of Horizontal Boundary Elements Design on Seismic Behavior of Steel Plate Shear Walls," by R. Purba and M. Bruneau, 11/14/10.

MCEER-10-0008 "Seismic Testing of a Full-Scale Mid-Rise Building: The NEESWood Capstone Test," by S. Pei, J.W. van de Lindt, S.E. Pryor, H. Shimizu, H. Isoda and D.R. Rammer, 12/1/10.

Appendix A

Architectural and Structural Drawings of Capstone Test Building

ABBREVIATIONS

Abbr.	Meaning	Abbr.	Meaning
AB	ANCHOR BOLT	INSUL	INSULATION
ADH	ADHESIVE	INT	INTERIOR
ALT	ALTERNATE	JNT	JOINT
ARCH	ARCHITECTURAL	JST	JOIST
AWS	AMERICAN WELDING SOCIETY	LOCN	LOCATION
@	AT	LP	LOW POINT
BLDG	BUILDING	MATL	MATERIAL
BLK	BLOCK	MAX	MAXIMUM
BLKG	BLOCKING	MECH	MECHANICAL
BM	BEAM	MFG	MANUFACTURER
B.O.	BOTTOM OF	MIN	MINIMUM
B.O.C.	BOTTOM OF CONCRETE	MCL	MICROLAM
B.O.S.	BOTTOM OF STEEL	MNL	MINILAM
BS	BOTH SIDES	(N)	NEW
BRG	BEARING	NA	NOT APPLICABLE
BOTT	BOTTOM	N.I.C.	NOT IN CONTRACT
BTWN	BETWEEN	"NO., #"	NUMBER
CL ℄	CENTERLINE	N.T.S.	NOT TO SCALE
CLG	CEILING	OC	ON CENTER
CLR	CLEAR	O/	OVER
COL	COLUMN		
CONC	CONCRETE	OPP	OPPOSITE
CONN	CONNECTION	OPNG	OPENING
CONSTR	CONSTRUCTION	OSB	ORIENTED STRAND BOARD
CONT	CONTINOUS	P.D.F.	POWER DRIVEN FASTENER
CP	COMPLETE PENETRATION	PERP	PERPENDICULAR
CTR	CENTER	PERIM	PERIMETER
DBL	DOUBLE	PL, ℞	PLATE
DET	DETAIL	PLWD	PLYWOOD
DF	DOUGLAS FIR	POST TEN	POST TENSIONED
DF/L	DOUGLAS FIR-LARCH	PTDF	PRESSURE TREATED DOUGLAS FIR
DIA	DIAMETER	REF	REFERENCE
DIAG	DIAGONAL	REINF	REINFORCING
DIM	DIMENSION	REQ'D	REQUIRED
DWG	DRAWING	RET	RETAINING
(E)	EXISTING	RM	ROOM
EA	EACH	R.O.	ROUGH OPENING
EF	EACH FACE	RDWD	REDWOOD
ELEC	ELECTRICAL	S.A.D.	SEE ARCHITECTURAL DRAWINGS
"ELEV, EL"	ELEVATION	SCHED	SCHEDULE
EN	EDGE NAIL	SEL STRUCT	SELECT STRUCTURAL
EQUIP	EQUIPMENT	SHT	SHEET
EW	EACH WAY	SHTG	SHEATHING
EXP BOLT	EXPANSION BOLT	SIM	SIMILAR
EXP JNT	EXPANSION JOINT	SPEC	SPECIFICATIONS
EXT	EXTERIOR	SQ	SQUARE
FNDN	FOUNDATION	SS	STAINLESS STEEL
FIN FLR	FINISHED FLOOR	STD	STANDARD
FLR	FLOOR	STRUCT	STRUCTURAL
F.O.	FACE OF	T & B	TOP AND BOTTOM
F.O.B.	FACE OF BLOCK (BRICK)	T & G	TONGUE AND GROOVE
F.O.C.	FACE OF CONCRETE	TN	TOE NAIL
F.O.S.	FACE OF STEEL	T.O.	TOP OF
FRMG	FRAMING	T.O.C.	TOP OF CONCRETE
F.S.	FAR SIDE	T.O.S.	TOP OF STEEL
FT	FOOT	TS	TUBE STEEL
FTG	FOOTING	TSW	TOP SEAM WELD
"GA, ga"	GAGE	TYP	TYPICAL
GALV	GALVANIZED	UON	UNLESS OTHERWISE NOTED
G.E.T.	GABLE END TRUSS	VERT	VERTICAL
GR BM	GRADE BEAM	W.P.	WORKING POINT OR WATER PROOFING
GL	GLULAM	WT	WEIGHT
GYP BD	GYPSUM BOARD	WWF	WELDED WIRE FABRIC
HDR	HEADER	w/	WITH
HGR	HANGER	XS	EXTRA STRONG
HORIZ	HORIZONTAL		
H.S.	HIGH STRENGTH		

GENERAL NOTES

SCOPE
The scope of work depicted in these drawings involves a new multi-family residential building.

CODE
Design conducted following Performance Based Seismic Design Procedures. The 2006 International Building Code (IBC) should be used as minimum requirements. All work shall conform to applicable requirements of the PBSD or this code, whichever is more strict.

LOADS

Equivalent total seismic masses (including half of wall weight above and below the diaphragm)
Roof 27 psf
Floor 5 46 psf
Floor 4 43 psf
Floor 3 42 psf
Floor 2 43 psf
Floor 1 45 psf

COORDINATION
Details shown are typical, similar details apply to similar conditions. Contractor shall review drawings as to layout, details, dimensions and elevations. All questions, discrepancies and conflicts shall be reported to the Engineer for adjustment prior to proceeding with work. If conditions arise that are not addressed by available details, contact Engineer for direction. No substitutions are to be made without Engineer's approval.

TEMPORARY SHORING AND BRACING
The contractor shall be responsible to provide all temporary support and bracing of the structure required for construction of the depicted work.

CUTTING AND PATCHING
Do not cut, bore or notch structural elements except as shown on the drawings or as specifically approved by the Engineer.

ROUGH CARPENTRY
Structural lumber shall conform to the following WCLIB minimum grades and shall be Douglas fir unless otherwise noted:

Joists and rafters	No. 2 or TJI (see below)
Headers	LSL (see bleow)
Top and bottom plates	STUD
Studs	STUD
Posts	No. 2
Misc framing	STUD

Moisture content for structural framing shall be "dry" (19% maximum moisture content).

Foundation sill plates shall be Douglas fir-Larch or Hem-Fir treated in accordance with AWPA C-2. Field cuts and holes shall be field treated in accordance with AWPA M-4.

First story bearing wall studs shall be 2-2x6 at 16" o.c. maximum. Other bearing and non-bearing wall studs shall be 2x6 @ 16" max.

ROOF I-JOISTS
Roof I-Joists are to be Trus Joist 14" LPI 20. Install per plans and Trus Joist Specifier's Guide.

FLOOR I-JOISTS
Floor I-Joists are to be Trus Joist 9-1/2" LPI 20. Install per plans and Trus Joist Specifier's Guide.

GLULAM BEAMS
Glulam beams are to be DF/DF 20F-1.5E, produced in accordance with ANSI/AITC A190.1 and ASTM D 3737.

LVL BEAMS & HEADERS
LVL beams and headers are to be Timberstrand 1.55E, built up from 1-3/4 plys.

SHEATHING
Wall sheathing shall be 15/32" or 1/2" rated sheathing, exterior exposure, conforming to Voluntary Product Standard PS1 or PS2
See shear wall schedule for sheathing edge fastening. Block all sheathing joints.
Provide Structural I sheathing where required by shear wal schedule.
Field nail at not less than 12" on center.

Roof sheathing shall be 19/32" or 5/8" rated sheathing, exterior exposure, conforming to Voluntary Product Standard PS1 or PS2 with a minimum span rating of 32/16. Lay face grain across rafters and stagger adjacent sheets. Fasten with 10d common nails at 6" on center all supported edges, 12" on center other supports. See details for additional enge nailing locations.

SHEATHING cont.

Floor sheathing shall be 3/4" rated sheathing, T & G exterior exposure, conforming to Voluntary Product Standard PS1 or PS2 with a minimum span rating of 48/24, or single floor sheathing with a span rating of 24 oc. Lay face grain across joists and stagger adjacent sheets. Fasten with 10d common nails at 6" on center all supported edges, 12" on center other supports and additional locations specified in details.
Glue floor sheathing with liquid nails or equivalent.

Sheathing minimum dimension shall not be less than 24 inches for wall, floor & roof.

Provide 1/8 inch gap at all panel ends and edges.

FASTENERS
Unless otherwise noted, all nails other than 16d shall be common nails.

10d common nail dimensions in accordance with ASTM F1667
Flat head, diamond point, L=3", D=0.148"
Submit specifications for gun nails for approval prior to use.

Unless otherwise noted, 16d nails shall be vinyl coated sinker nails.
Flat head, diamond point, L=3.5", D=0.135"

Hot-dipped galvanized box nails to be used in lieu of common nails at pressure treated sills. Only hot-dipped galvanized nails shall be permitted in any pressure-treated wood.

Tie down system shall be per shear wall schedule and details.

Connector devices, unless otherwise noted, are Simpson Strong-Tie.

The following minimum fastening shall be provided as a minimum for all new construction:
Joist or sill to girder – toe nail 3-8d
Bridging to joist – toe nail each end 2-8d
Sole plate to joist or blocking – toe nail each end 2-8d
Top plate to stud – end nail 3-16d
Stud to sole plate – toe nail 3- 16d end or 4-8d toe
Double studs – face nail 16d @ 12"
Doubled top plates – face nail – 16d @ 6"
Top plates – laps at intersections – face nail 3-16d
Ceiling joists – to plate – toe nail 3-8d
Continuous header to stud – toe nail 4-8d
Ceiling joists – laps over partitions – face nail 2-16d
Ceiling joists to parallel rafters – face nail 3-16d
Rafter to plate – toe nail 3-8d
Corner studs and angles (built up corners) 16d @ 12"
Built-up corners and beams 16d @ 12" at top and bottom, 2-16d each end.

SPECIAL INSPECTIONS
Special inspections shall be provided in accordance with IBC Chapter 17. Owner is responsible to retain a special inspection agency to provide required inspections.

SHEAR WALL NOTES:
1. LOCATE TIE DOWN STUD OR POST AND PROVIDE PLYWOOD EDGE NAILING TO STUD OR POST, AS WELL AS ALL PANEL EDGES.

2. ADD 3x STUD OR 2-2x INTERCONNECTED WITH 16 NAILS SPACED TO MATCH PANEL EDGE NAIL SPACING AT ABUTTING PANEL EDGES

3. NAILS SHALL BE CONSIDERED OVERDRIVEN WHEN THE TOP OF THE HEAD OF THE NAIL IS MORE THAN 1/32" BELOW THE FACE OF PLWD SHEATHGING. REPLACE EACH OVERDRIVEN NAIL WITH A NEW NAIL.

4. WHERE MORE THAT 30 PERCENT OF EDGE NAILING ON ANY SHEATHING PANEL IS OVERDRIVEN, REMOVE SHEATHING, REPLACE ANY SPLIT FRAMING MEMBERS, AND ADD NEW SHEATHING.

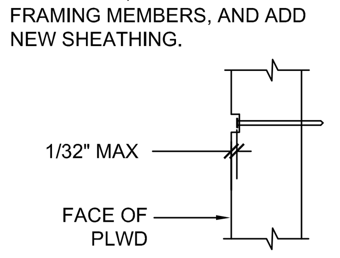

1 S0.1 SHEAR WALL NOTES
N.T.S.

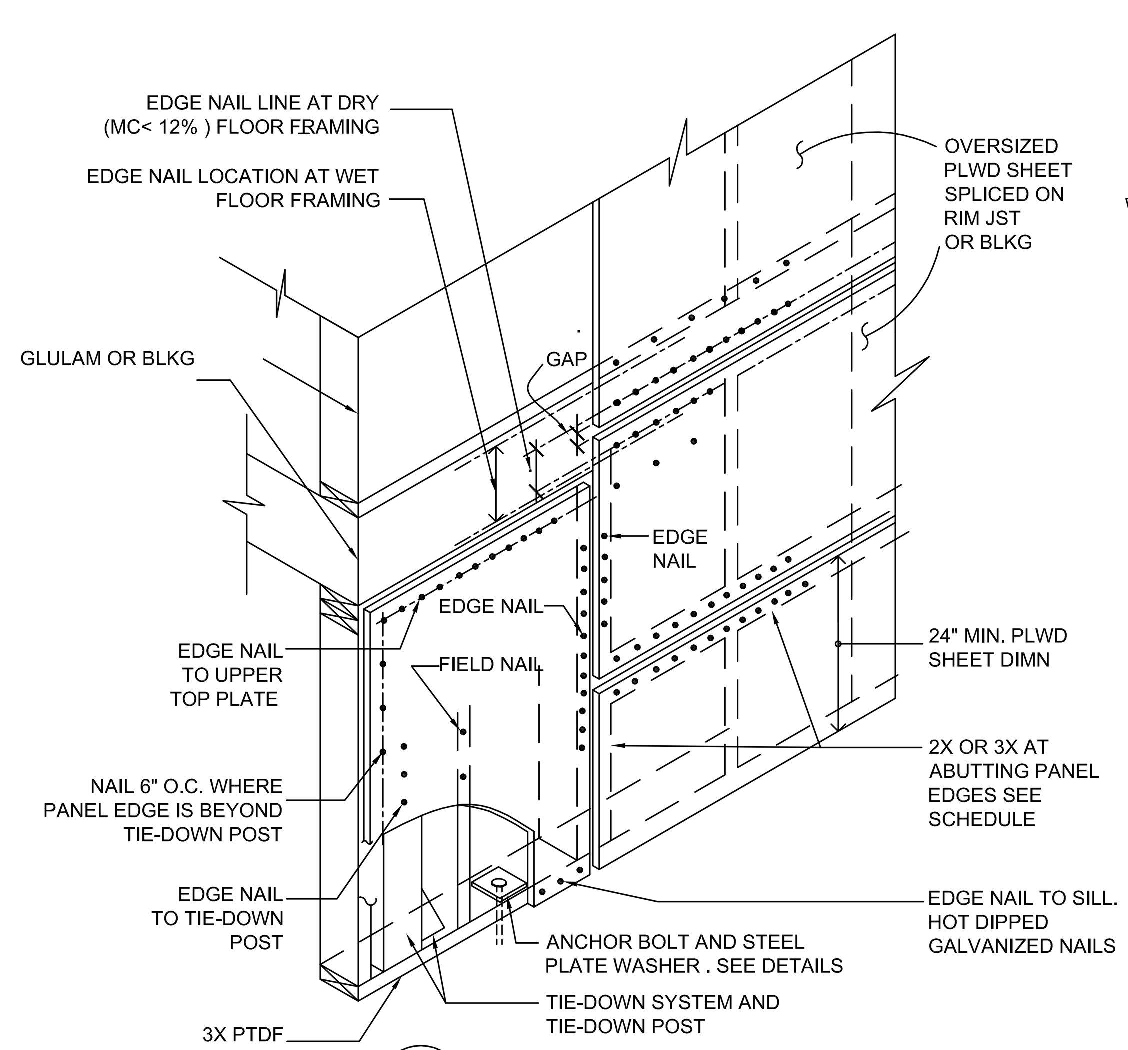

2 S0.1 TYP. SHEAR WALL ELEVATION
NTS

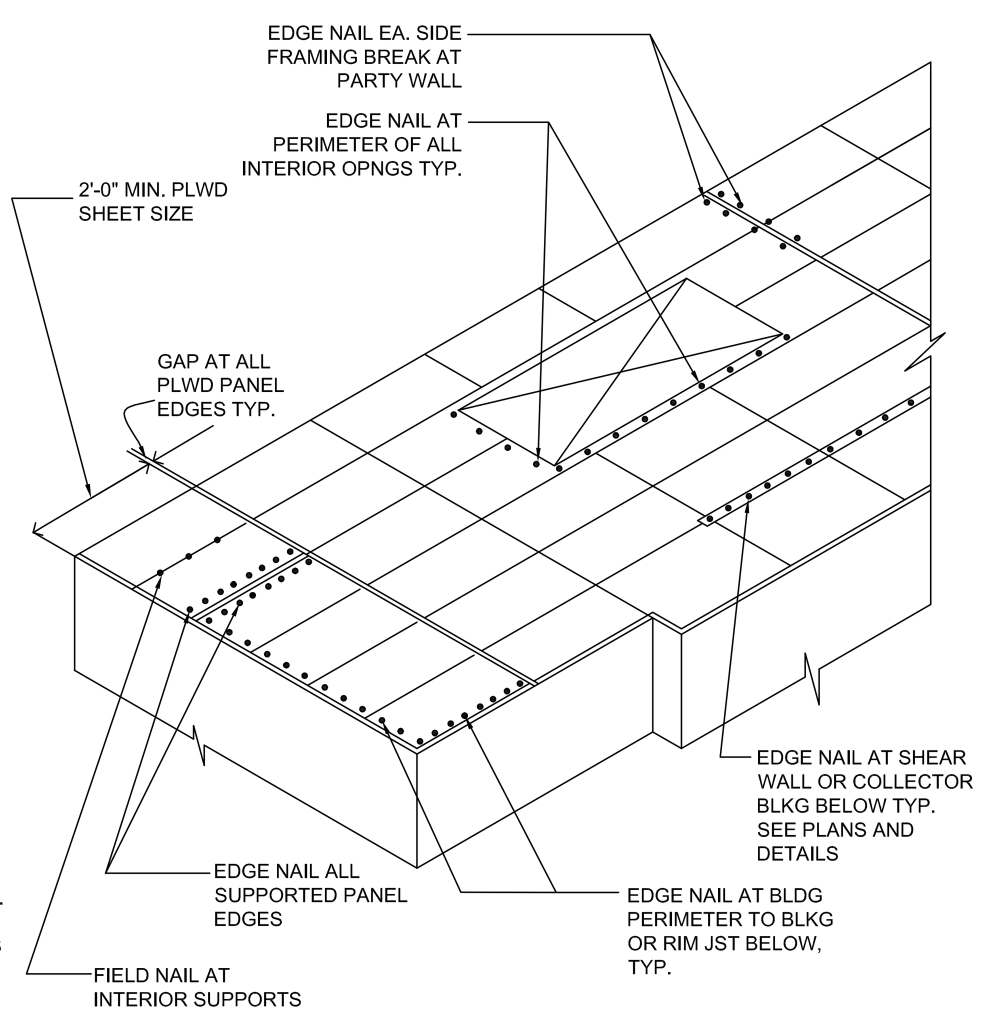

3 S0.1 TYP. UNBLOCKED DIAPHRAGM
NTS

JOHN VAN DE LINDT
ANDRE FILIATRAULT
RACHEL DAVIDSON
DAVID ROSSOWSKY
MICHAEL D. SYMANS

NEESwood capstone

(performanced-based design)

colorado state university
fort collins, colorado

CAPSTONE TEAM:
COLORADO STATE UNIVERSITY:
JOHN VAN DE LINDT
KIMBERLY CRONIN p.e.
shiling pei

www.engr.colostate.edu/NEESWood/

REVISIONS :
01/06/09 - 90% complete
01/15/09 - 100% complete

SHEET NO :
A1.00

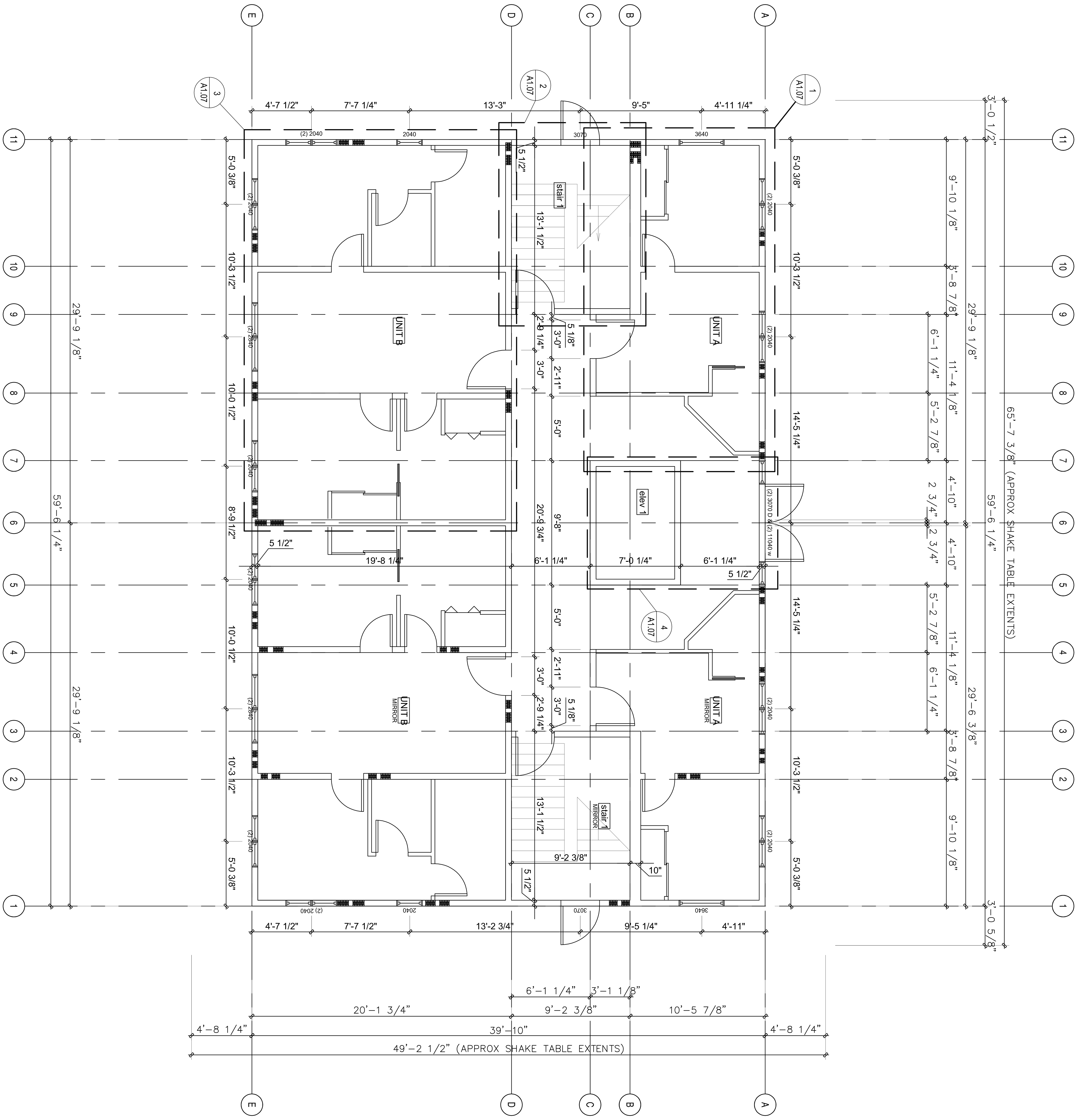

FIRST FLOOR PLAN

NEESwood capstone

(performanced-based design)

colorado state university
fort collins, colorado

CAPSTONE TEAM:
COLORADO STATE UNIVERSITY:
JOHN VAN DE LINDT
KIMBERLY CRONIN p.e.
shiling pei

www.engr.colostate.edu/NEESWood/

REVISIONS:
01/06/09 - 90% complete
01/14/09 - 100% complete

SHEET NO:
A1.01

NEESWOOD
JOHN VAN DE LINDT
ANDRE FILIATRAULT
RACHEL DAVIDSON
DAVID ROSOWSKY
MICHAEL D. SYMANS

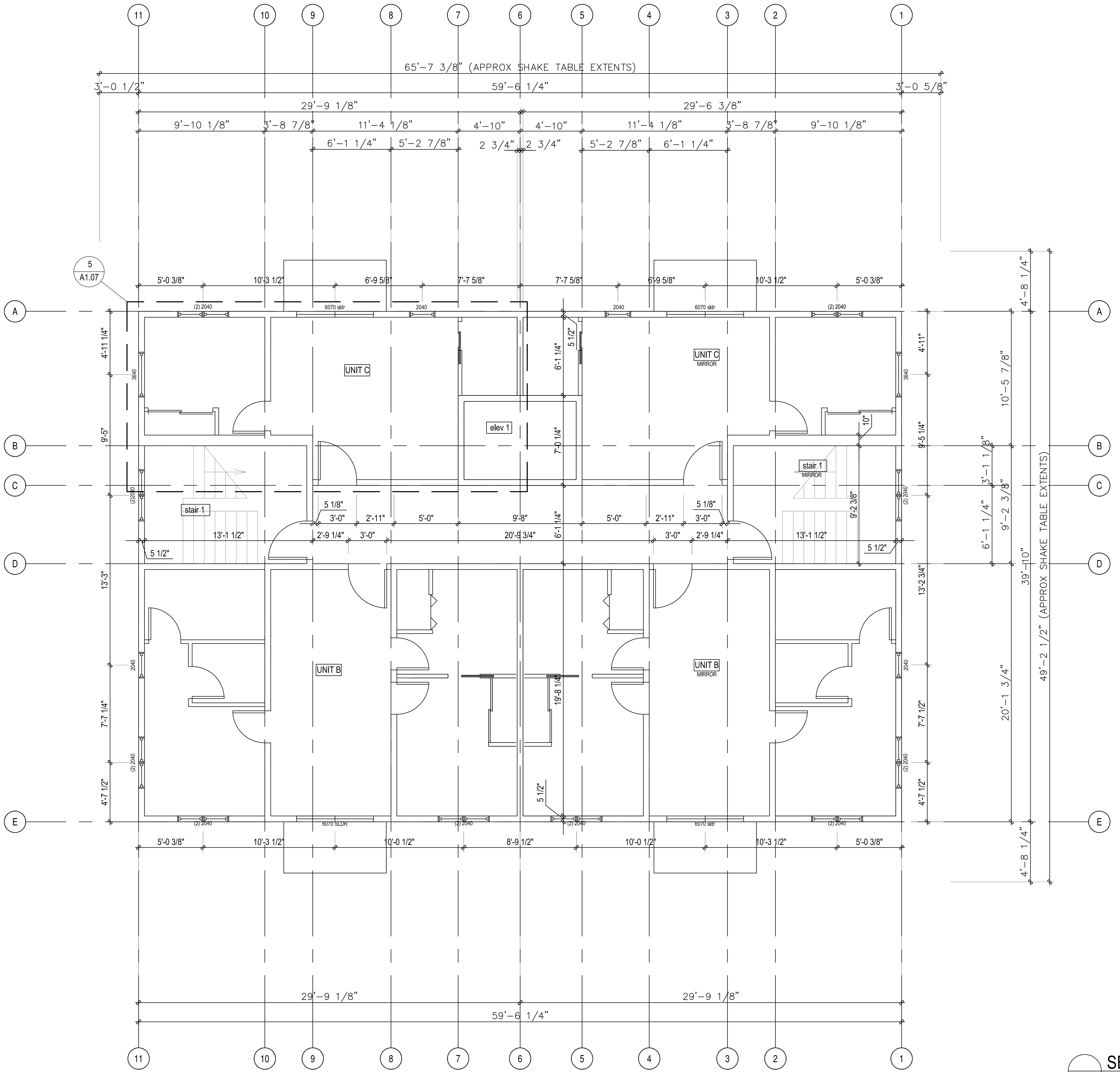

SECOND FLOOR PLAN

JOHN VAN DE LINDT
ANDRE FILIATRAULT
RACHEL DAVIDSON
DAVID ROSSOWSKY
MICHAEL D. SYMANS

NEESwood capstone
(performanced–based design)
colorado state university
fort collins, colorado

CAPSTONE TEAM:
COLORADO STATE UNIVERSITY:
JOHN VAN DE LINDT
KIMBERLY CRONIN p.e.
shiling pei

www.engr.colostate.edu/NEESWood/

REVISIONS :
01/06/09 - 90% complete
01/14/09 - 100% complete

SHEET NO :
A1.02

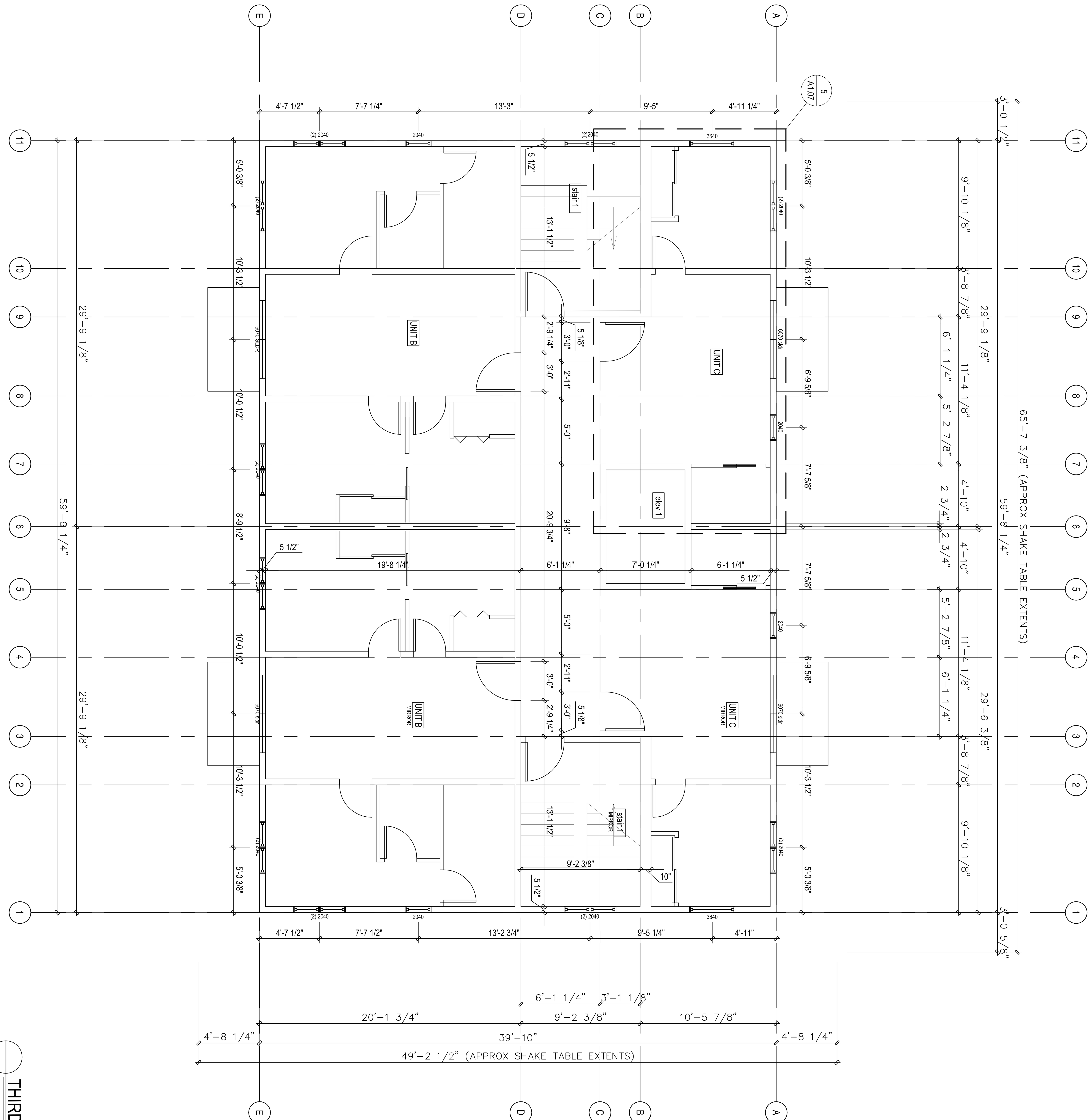

THIRD FLOOR PLAN

SHEET NO: A1.03

REVISIONS :
01/06/09 - 90% complete
01/14/09 - 100% complete

CAPSTONE TEAM:
COLORADO STATE UNIVERSITY:
JOHN VAN DE LINDT
KIMBERLY CRONIN p.e.
shiling pei

www.engr.colostate.edu/NEESWood/

NEESwood capstone

(performanced-based design)

colorado state university
fort collins, colorado

NEESWOOD
JOHN VAN DE LINDT
ANDRE FILIATRAULT
RACHEL DAVIDSON
DAVID ROSOWSKY
MICHAEL D. SYMANS

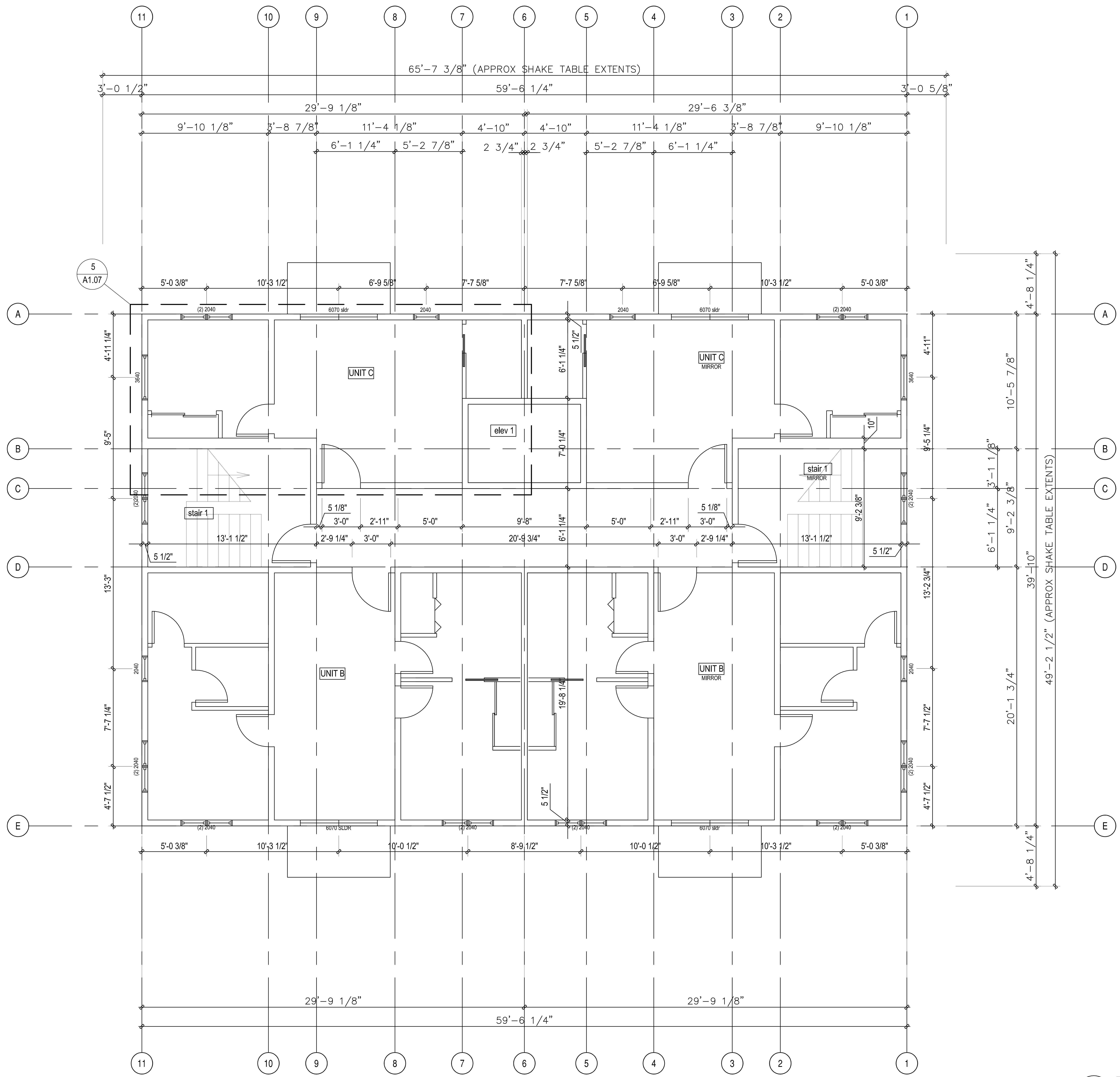

FOURTH FLOOR PLAN

NEESWOOD

JOHN VAN DE LINDT
ANDRE FILIATRAULT
RACHEL DAVIDSON
DAVID ROSSOWSKY
MICHAEL D. SYMANS

NEESwood capstone

(performanced-based design)

colorado state university
fort collins, colorado

CAPSTONE TEAM:

COLORADO STATE UNIVERSITY:
JOHN VAN DE LINDT
KIMBERLY CRONIN p.e.
shiling pei

www.engr.colostate.edu/NEESWood/

REVISIONS :

01/06/09 - 90% complete
01/14/09 - 100% complete

SHEET NO :

A1.04

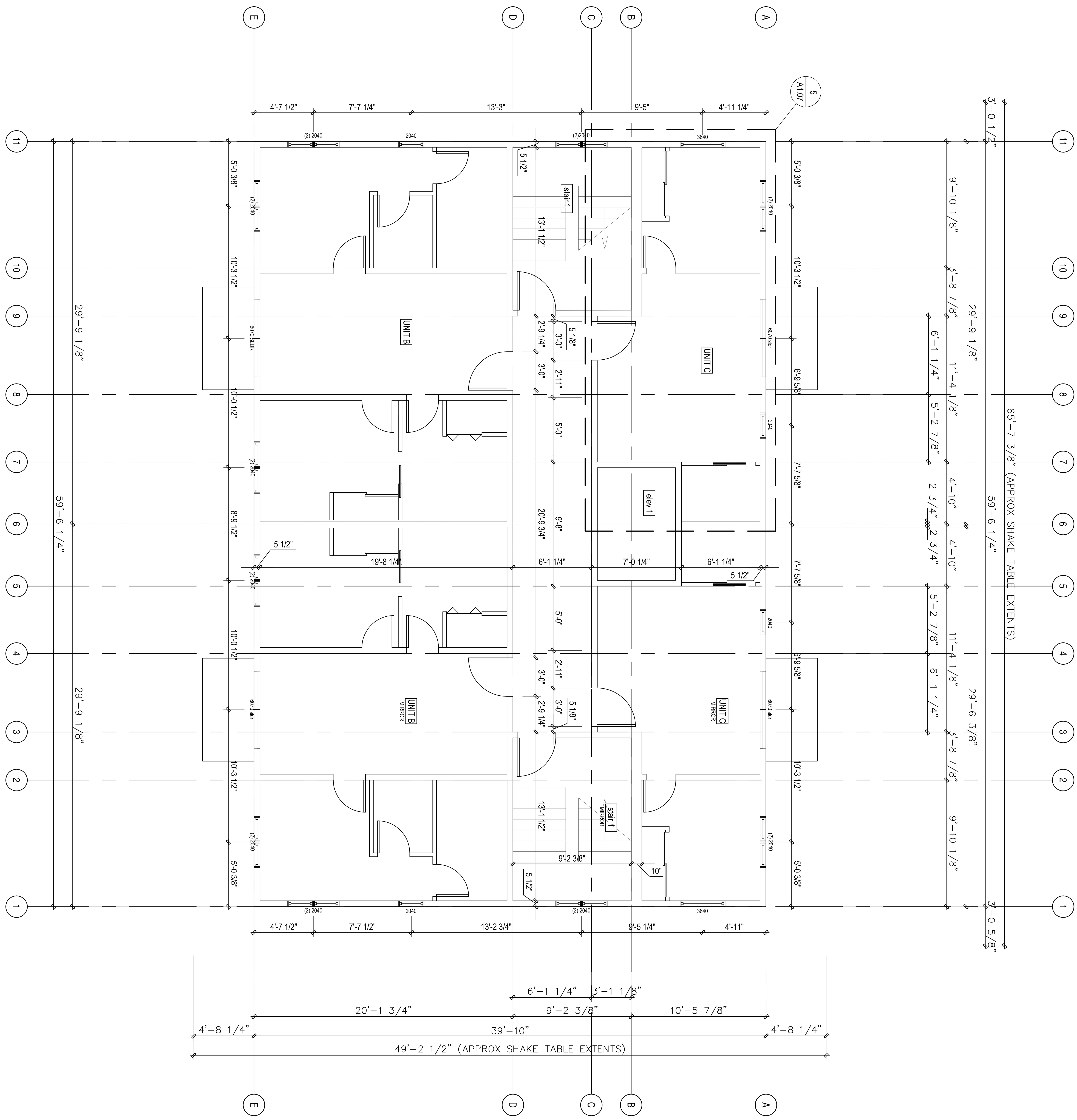

FIFTH FLOOR PLAN

SHEET NO.:
A1.05

REVISIONS:
01/06/09 - 90% complete
01/14/09 - 100% complete

www.engr.colostate.edu/NEESWood/

CAPSTONE TEAM:
COLORADO STATE UNIVERSITY:
JOHN VAN DE LINDT
KIMBERLY CRONIN p.e.
shiling pei

NEESwood capstone

(performanced-based design)

colorado state university
fort collins, colorado

JOHN VAN DE LINDT
ANDRE FILIATRAULT
RACHEL DAVIDSON
DAVID ROSOWSKY
MICHAEL D. SYMANS

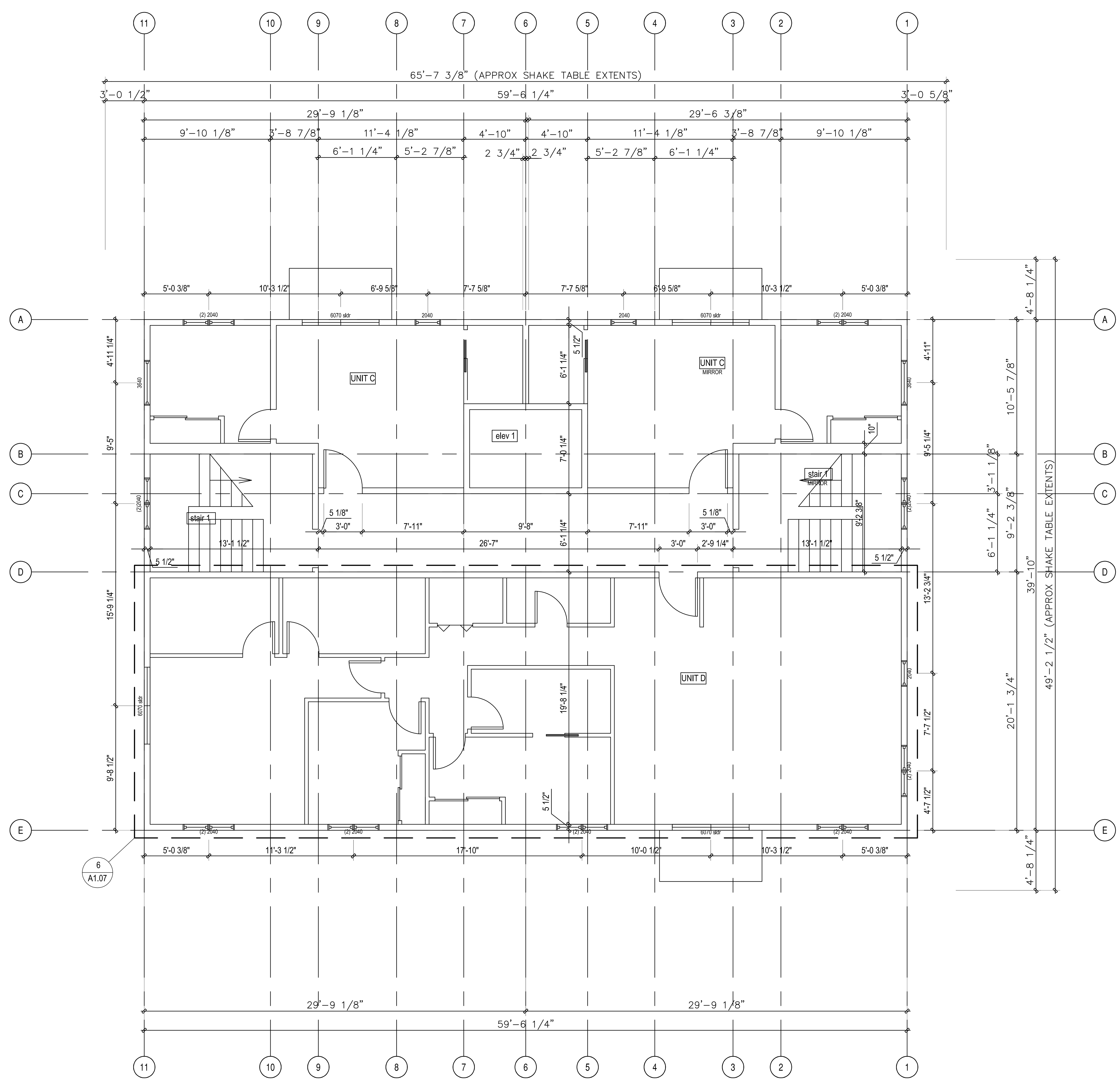

SIXTH FLOOR PLAN

JOHN VAN DE LINDT
ANDRE FILIATRAULT
RACHEL DAVIDSON
DAVID ROSOWSKY
MICHAEL D. SYMANS

NEESwood capstone

(performanced–based design)

colorado state university
fort collins, colorado

CAPSTONE TEAM:

COLORADO STATE UNIVERSITY:
JOHN VAN DE LINDT
KIMBERLY CRONIN p.e.
shiling pei

www.engr.colostate.edu/NEESWood/

REVISIONS :

01/06/09 - 90% complete
01/14/09 - 100% complete

SHEET NO :

A1.06

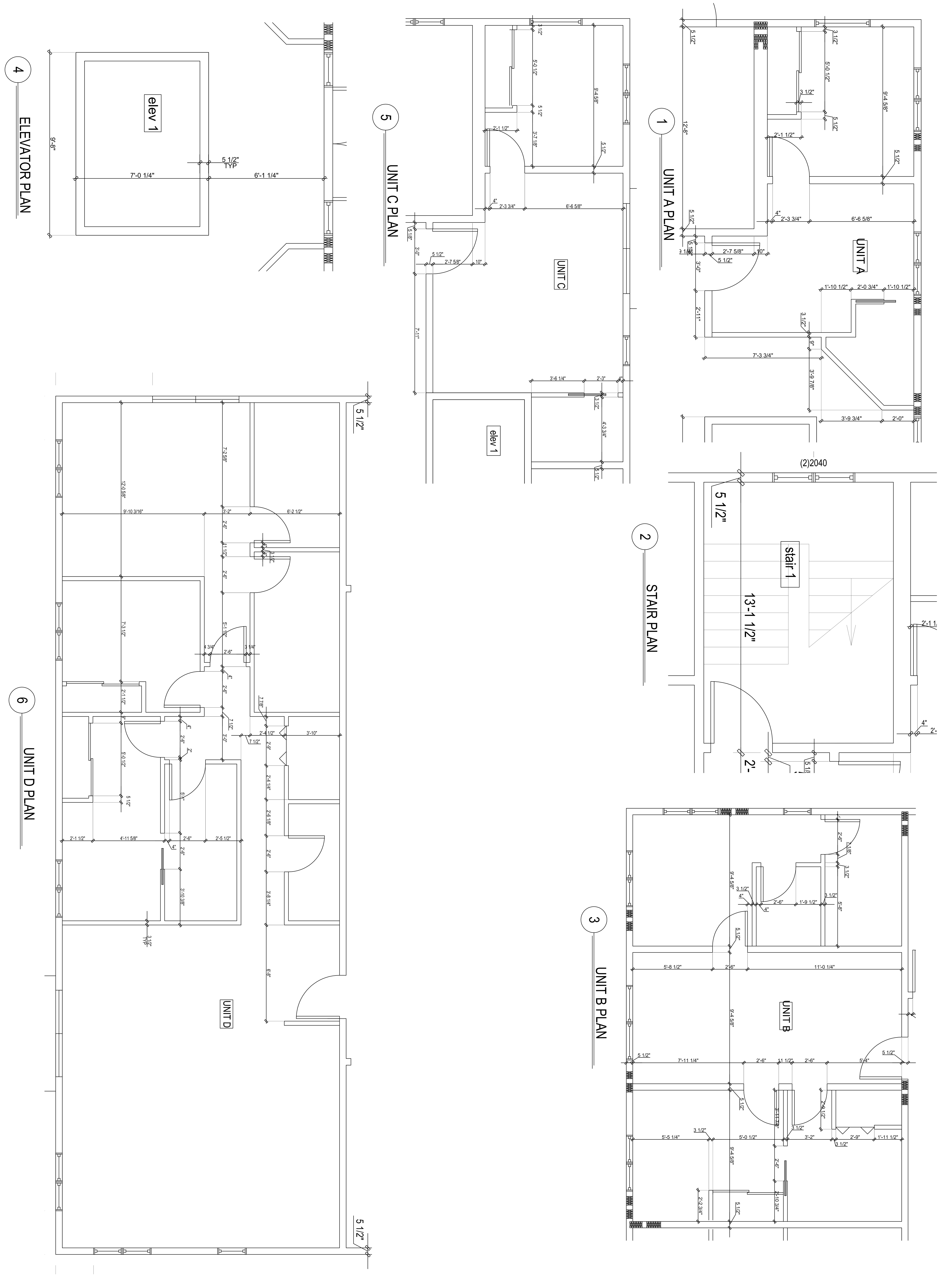

SHEET NO : A1.07

REVISIONS :
01/06/09 - 90% complete
01/14/09 - 100% complete

CAPSTONE TEAM:
COLORADO STATE UNIVERSITY:
JOHN VAN DE LINDT
KIMBERLY CRONIN p.e.
shiling pei

www.engr.colostate.edu/NEESwood/

NEESwood capstone

(performanced-based design)

colorado state university
fort collins, colorado

NEESWOOD
JOHN VAN DE LINDT
ANDRE FILIATRAULT
RACHEL DAVIDSON
DAVID ROSOWSKY
MICHAEL D SYMANS

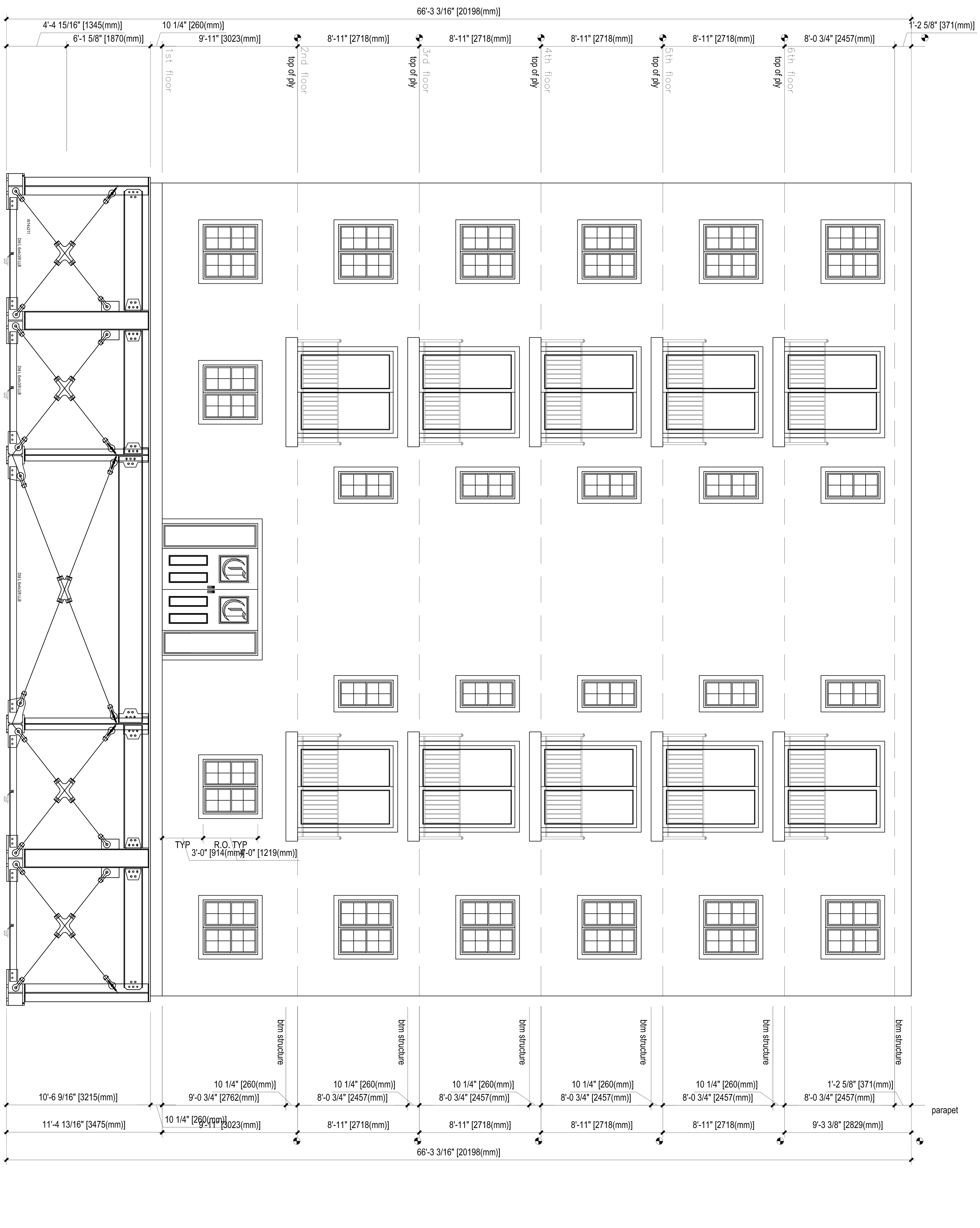

WEST ELEVATION

SHEET NO. :
A2.01

REVISIONS :
01/06/09 - 90% complete
01/14/09 - 100% complete

CAPSTONE TEAM:
COLORADO STATE UNIVERSITY:
JOHN VAN DE LINDT
KIMBERLY CRONIN p.e.
shiling pei

www.engr.colostate.edu/NEESwood/

NEESwood capstone
(performanced—based design)
colorado state university
fort collins, colorado

JOHN VAN DE LINDT
ANDRE FILIATRAULT
RACHEL DAVIDSON
DAVID ROSSOWSKY
MICHAEL D. SYMANS

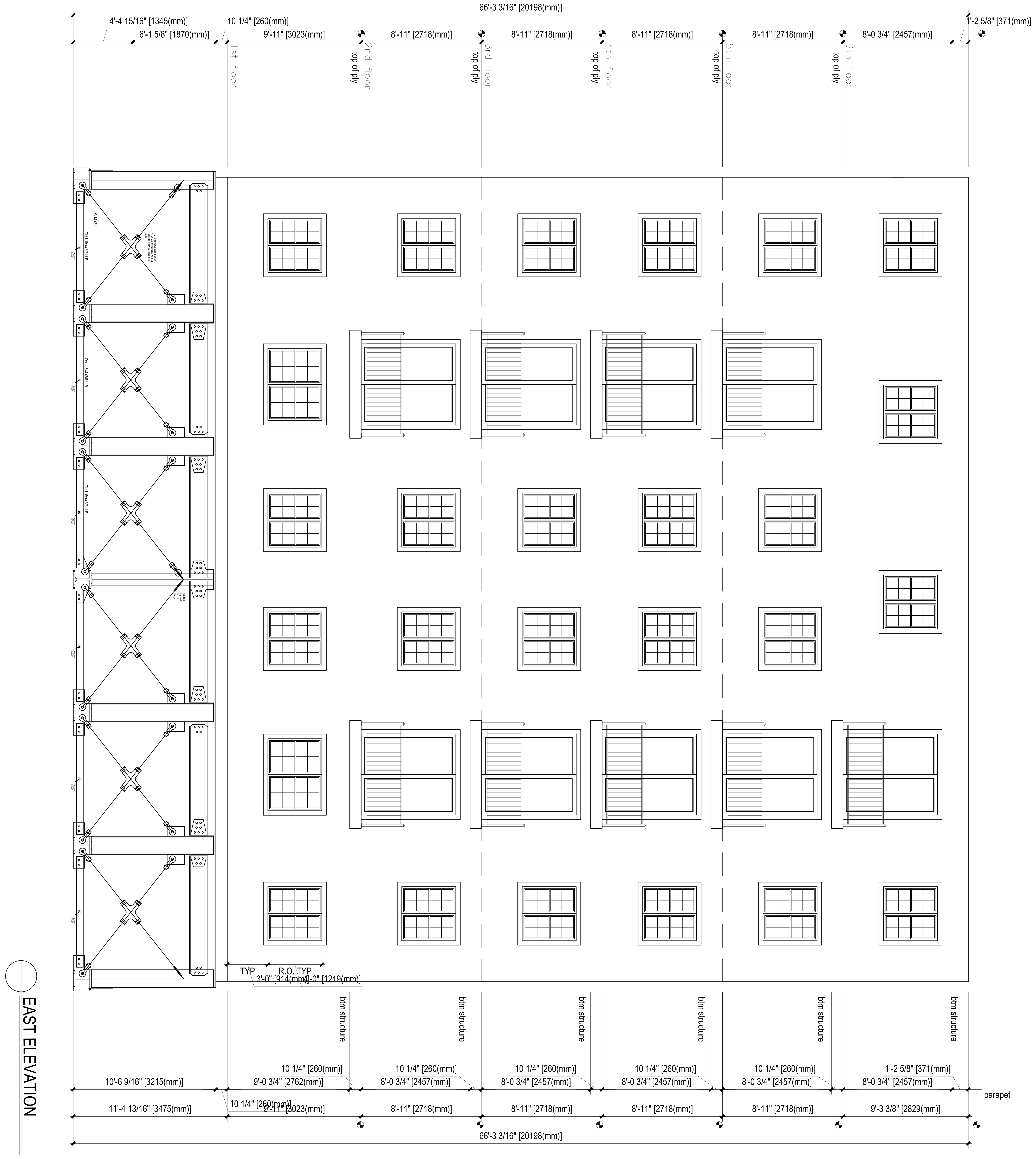

SHEET NO : A2.02

REVISIONS :
01/06/09 - 90% complete
01/14/09 - 100% complete

www.engr.colostate.edu/NEESWood/

CAPSTONE TEAM:
COLORADO STATE UNIVERSITY:
JOHN VAN DE LINDT
KIMBERLY CRONIN p.e.
shiling pei

NEESwood capstone

(performanced-based design)

colorado state university
fort collins, colorado

JOHN VAN DE LINDT
ANDRE FILIATRAULT
RACHEL DAVIDSON
DAVID ROSSOWSKY
MICHAEL D. SYMANS

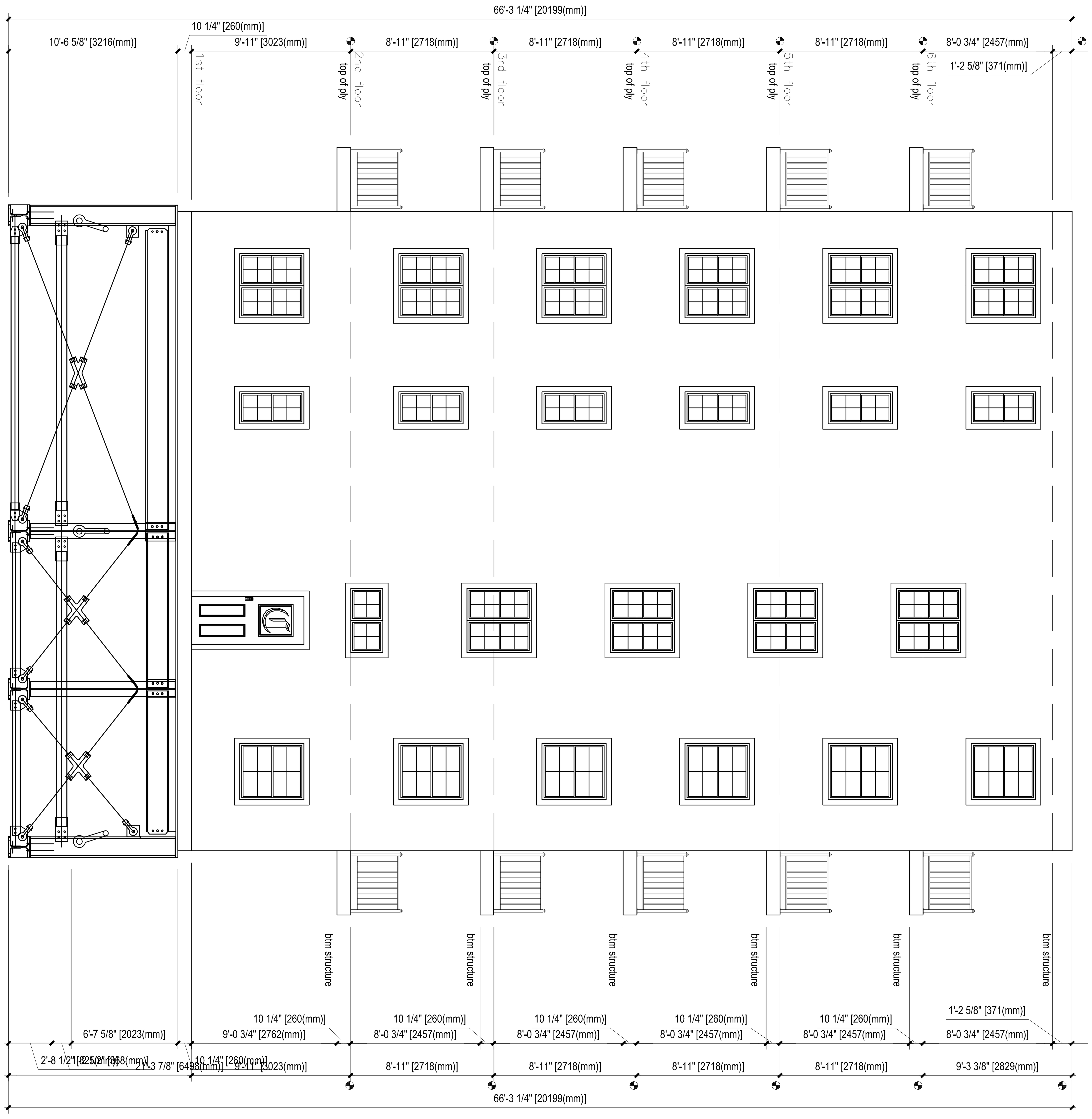

NORTH ELEVATION

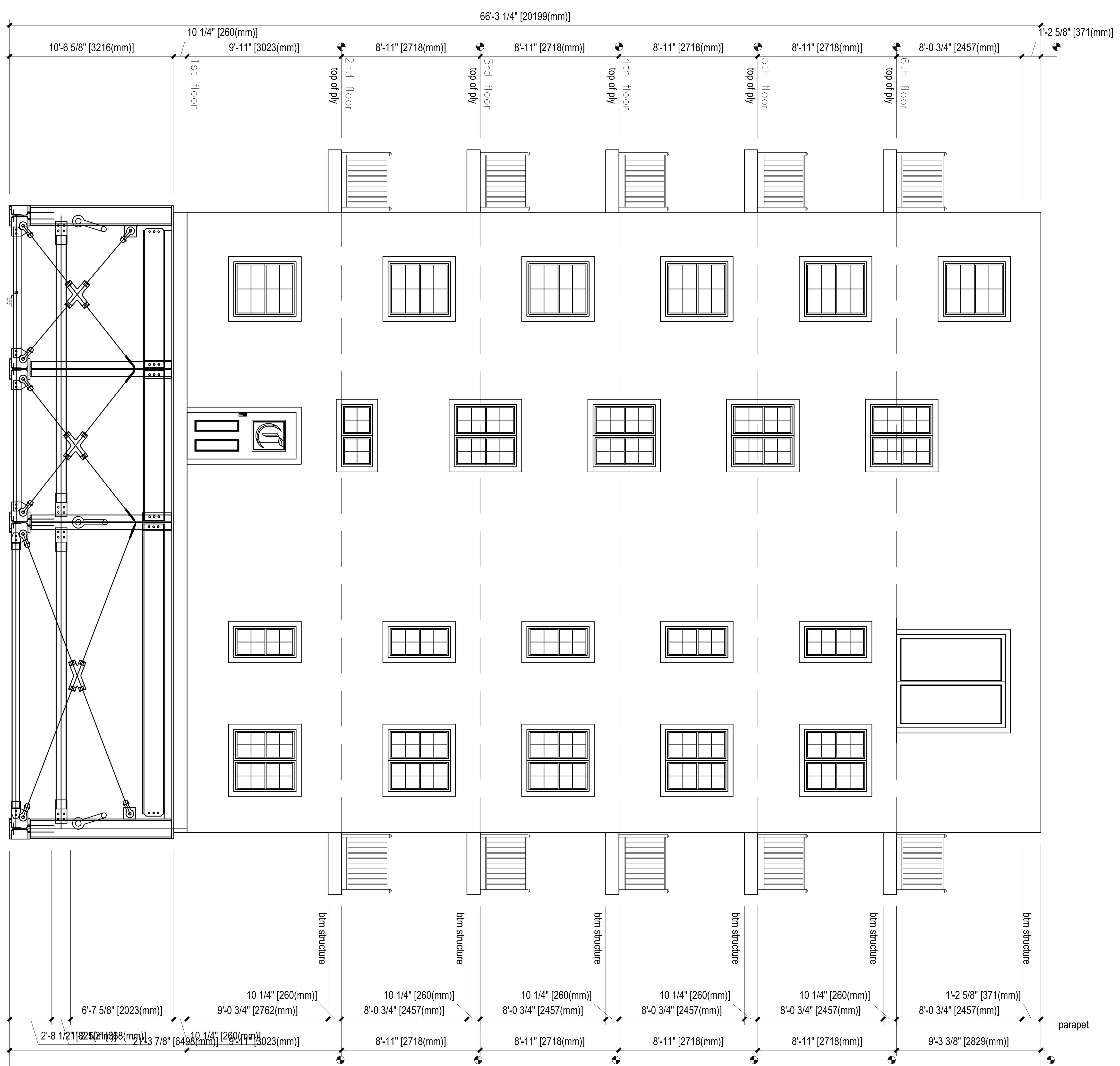

SOUTH ELEVATION

SHEET NO :

A2.03

REVISIONS :

01/06/09 - 90% complete

01/14/09 - 100% complete

CAPSTONE TEAM:

COLORADO STATE UNIVERSITY:

JOHN VAN DE LINDT

KIMBERLY CRONIN p.e.

shiling pei

www.engr.colostate.edu/NEESWood/

NEESwood capstone

(performanced–based design)

colorado state university

fort collins, colorado

NEESWOOD

JOHN VAN DE LINDT

ANDRE FILIATRAULT

RACHEL DAVIDSON

DAVID ROSOWSKY

MICHAEL D. SYMANS

A-A

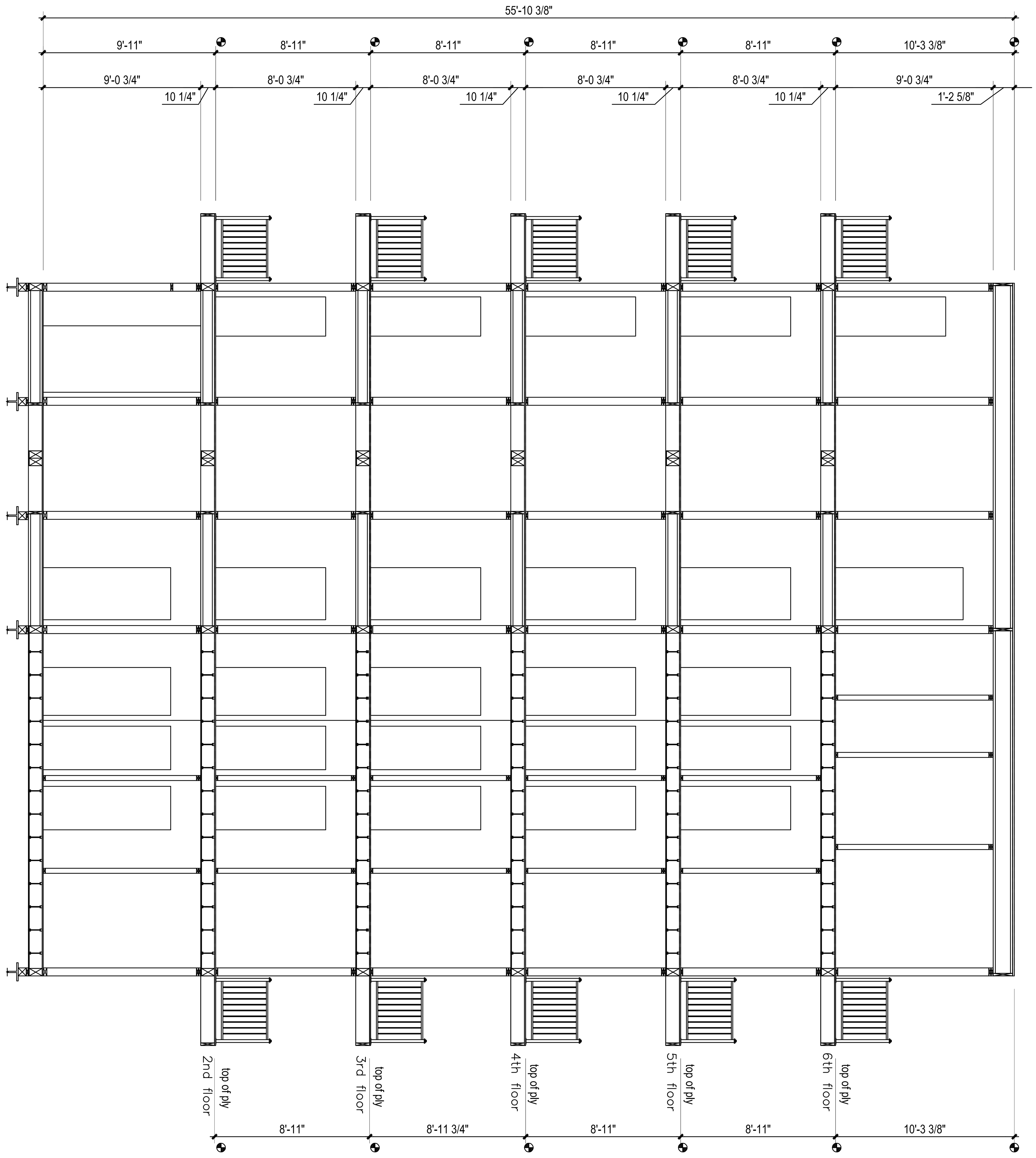

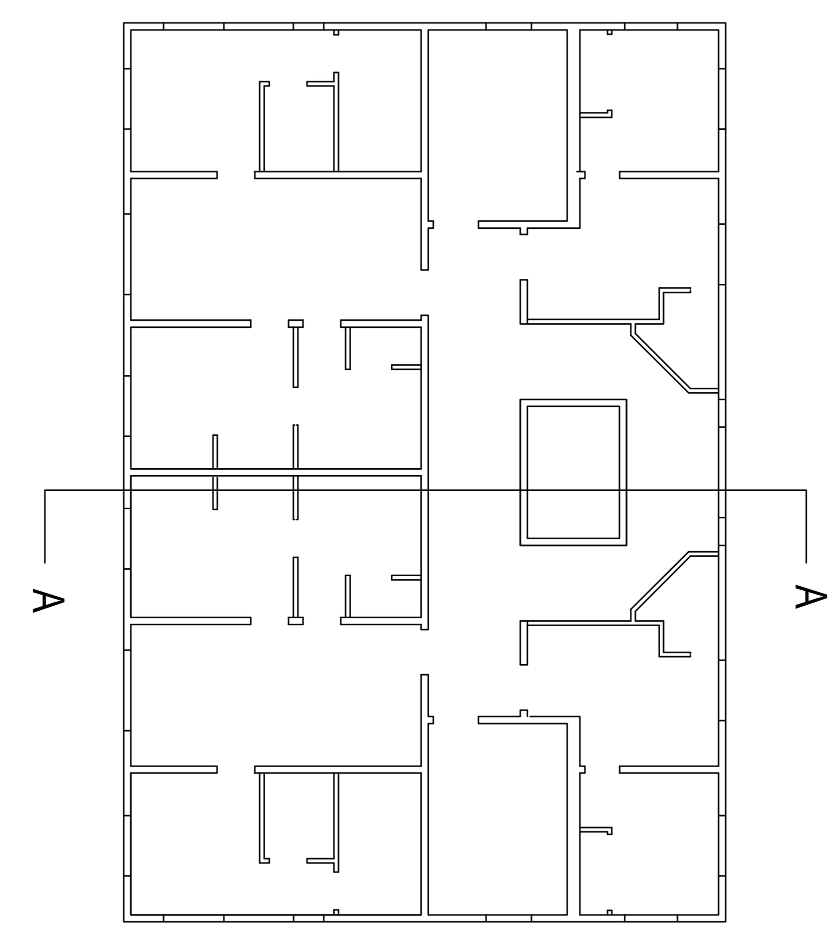

B-B

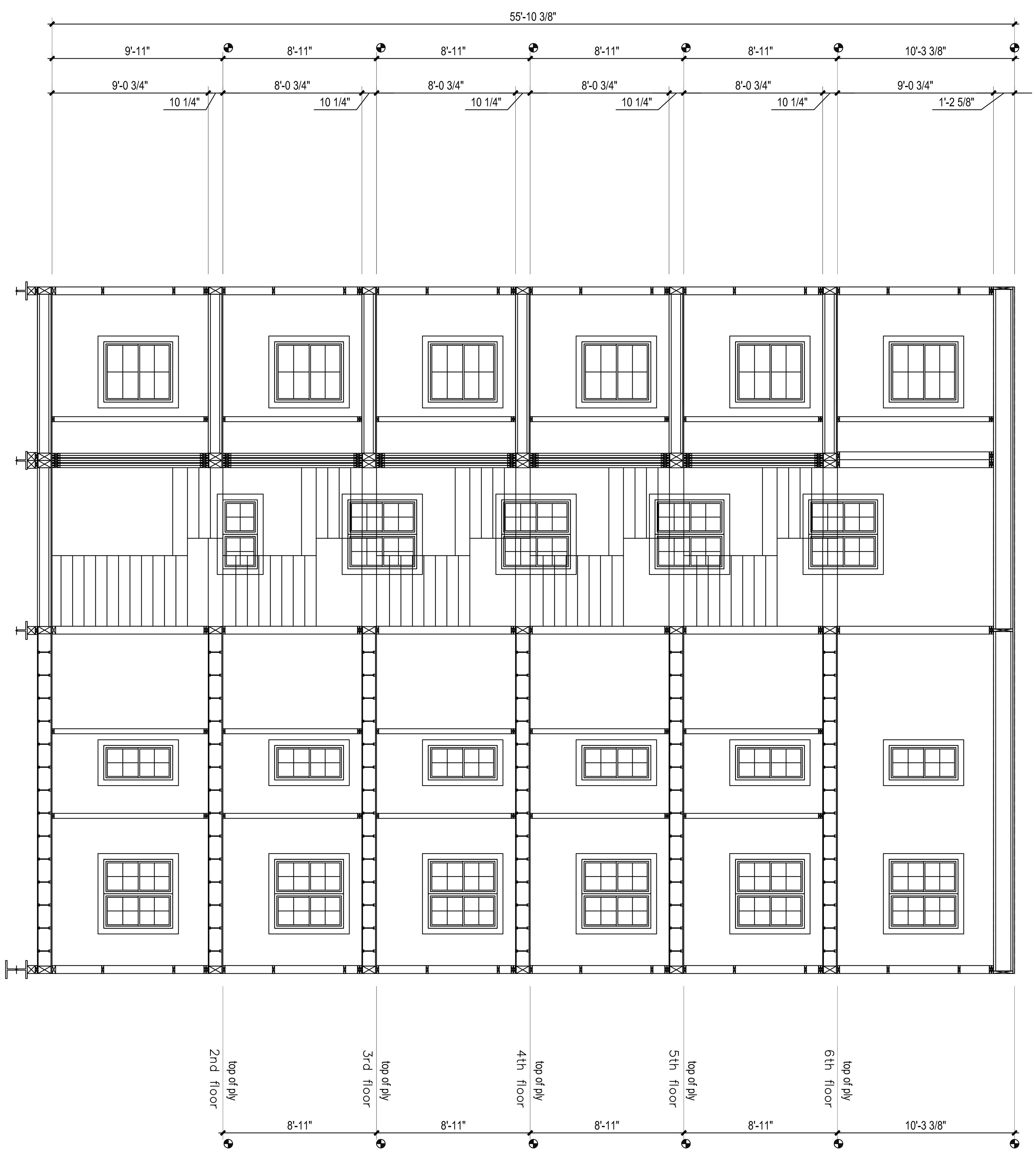

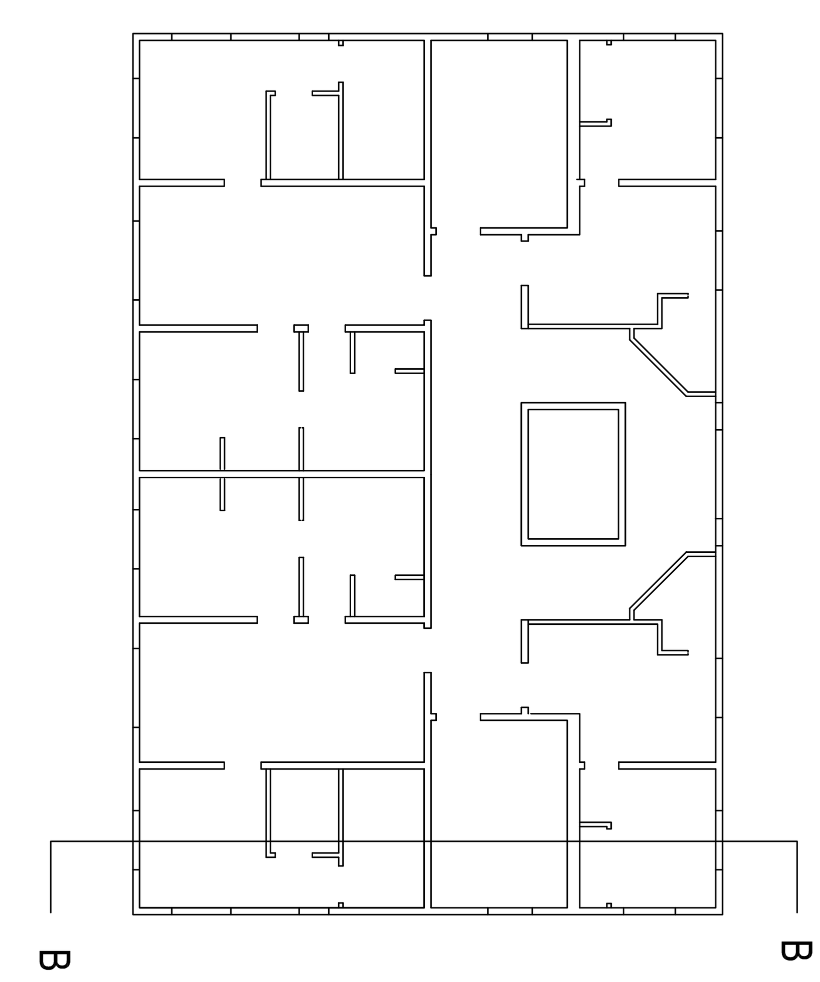

SHEET NO :

A3.01

REVISIONS :

01/06/09 - 90% complete

www.engr.colostate.edu/NEESWood/

CAPSTONE TEAM:

COLORADO STATE UNIVERSITY:
JOHN VAN DE LINDT
KIMBERLY CRONIN p.e.
shiling pei

NEESwood capstone

(performanced–based design)

colorado state university
fort collins, colorado

JOHN VAN DE LINDT
ANDRE FILIATRAULT
RACHEL DAVIDSON
DAVID ROSSOWSKY
MICHAEL D. SYMANS

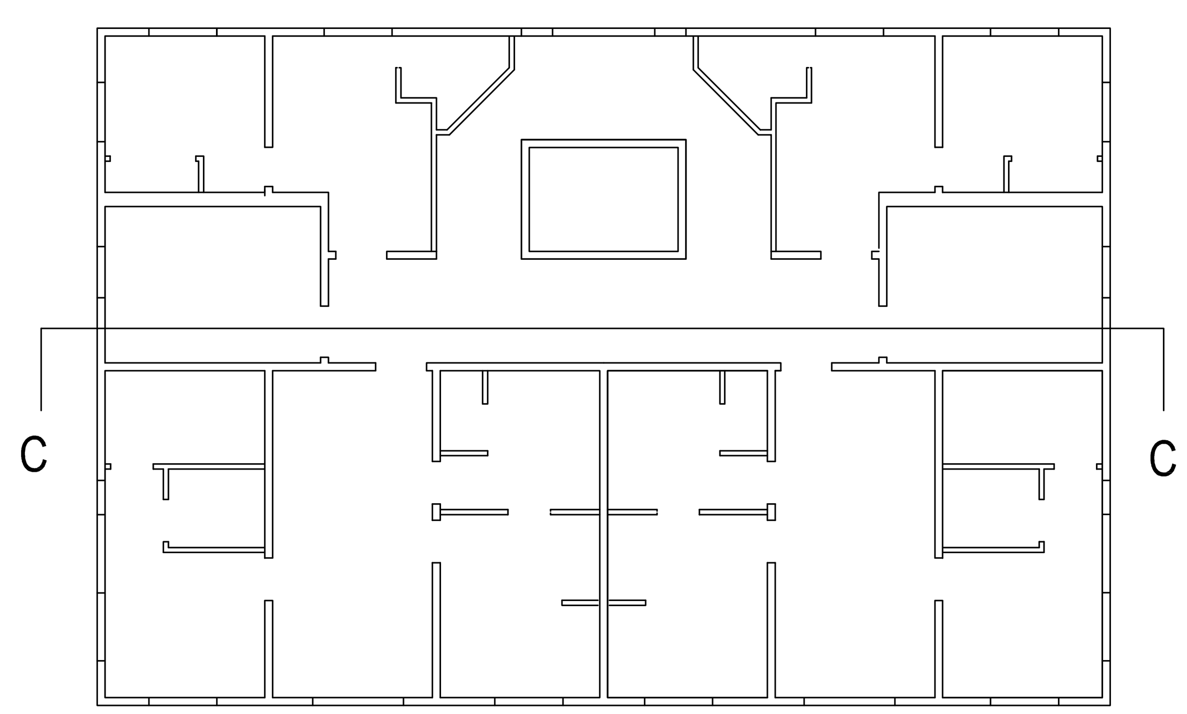

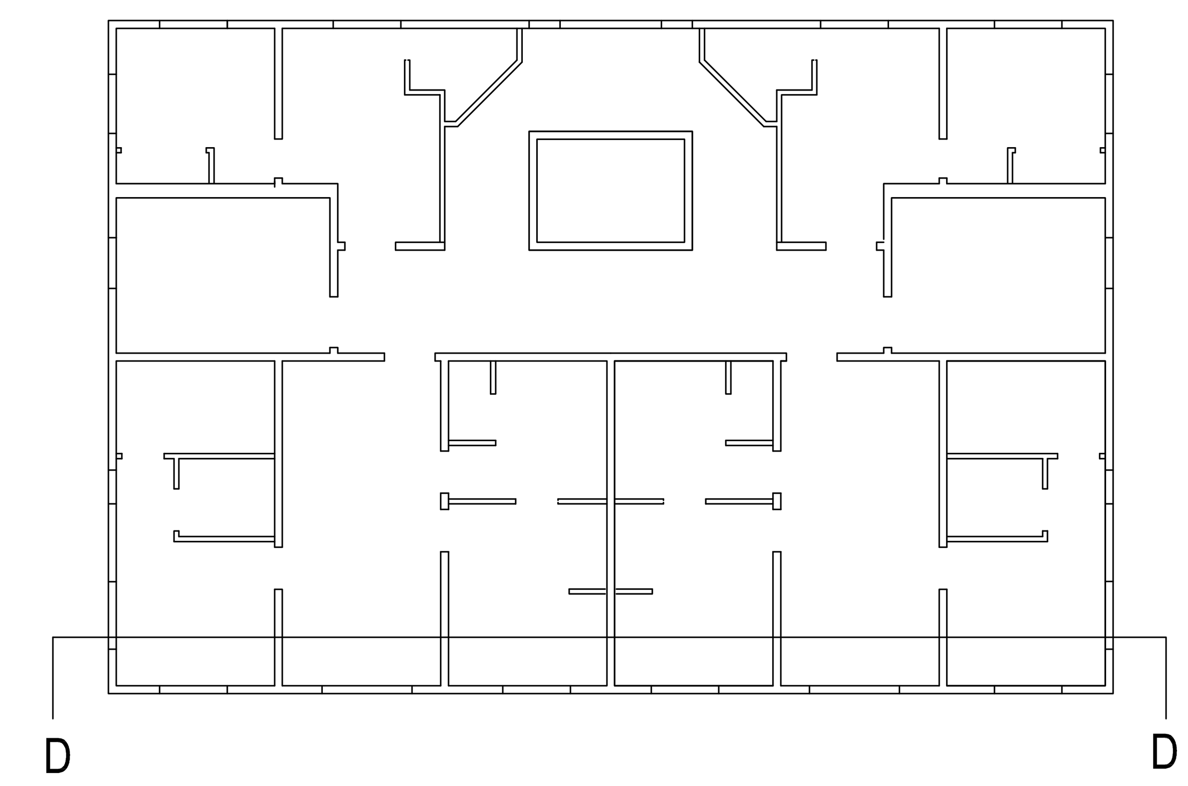

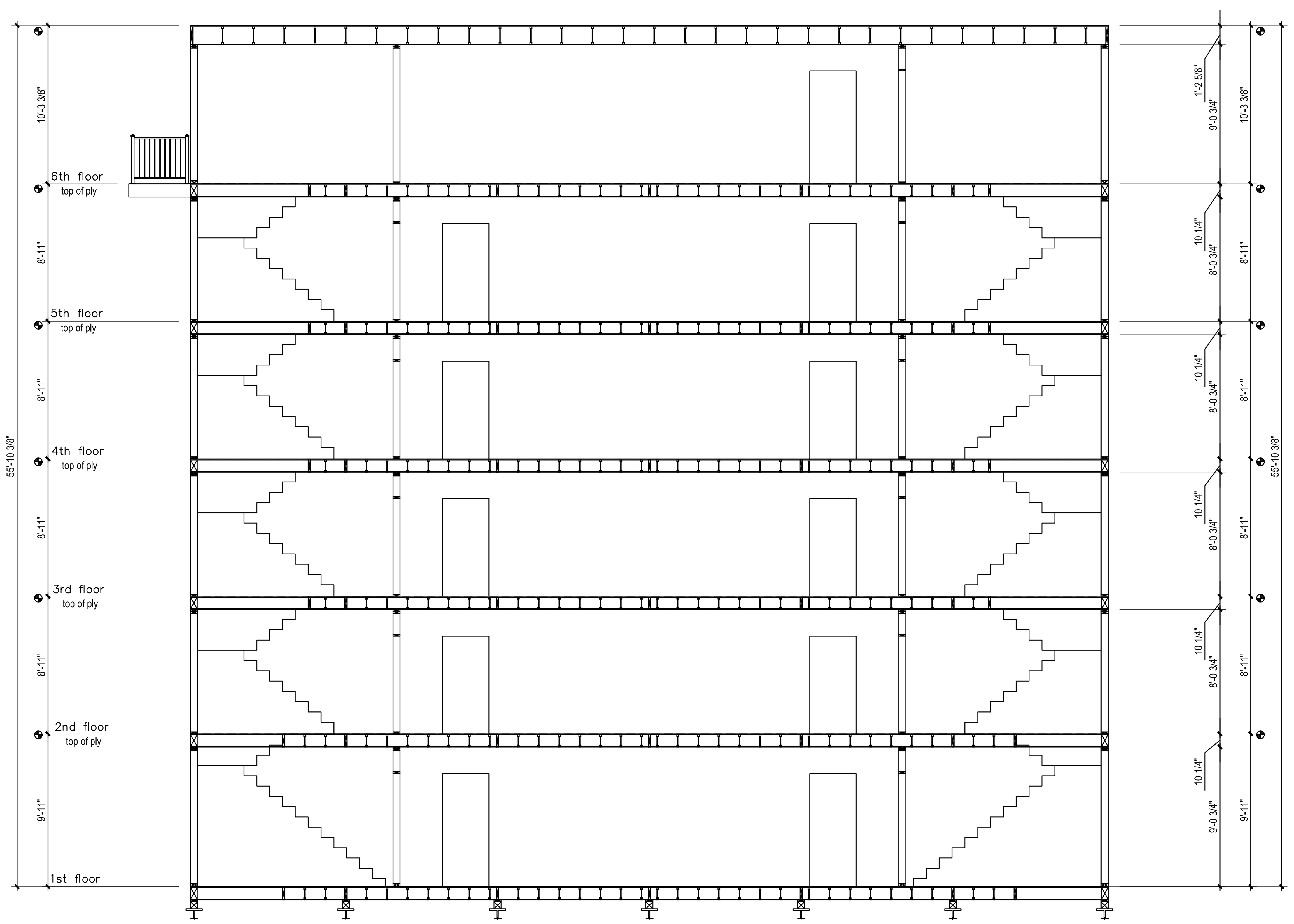

C-C

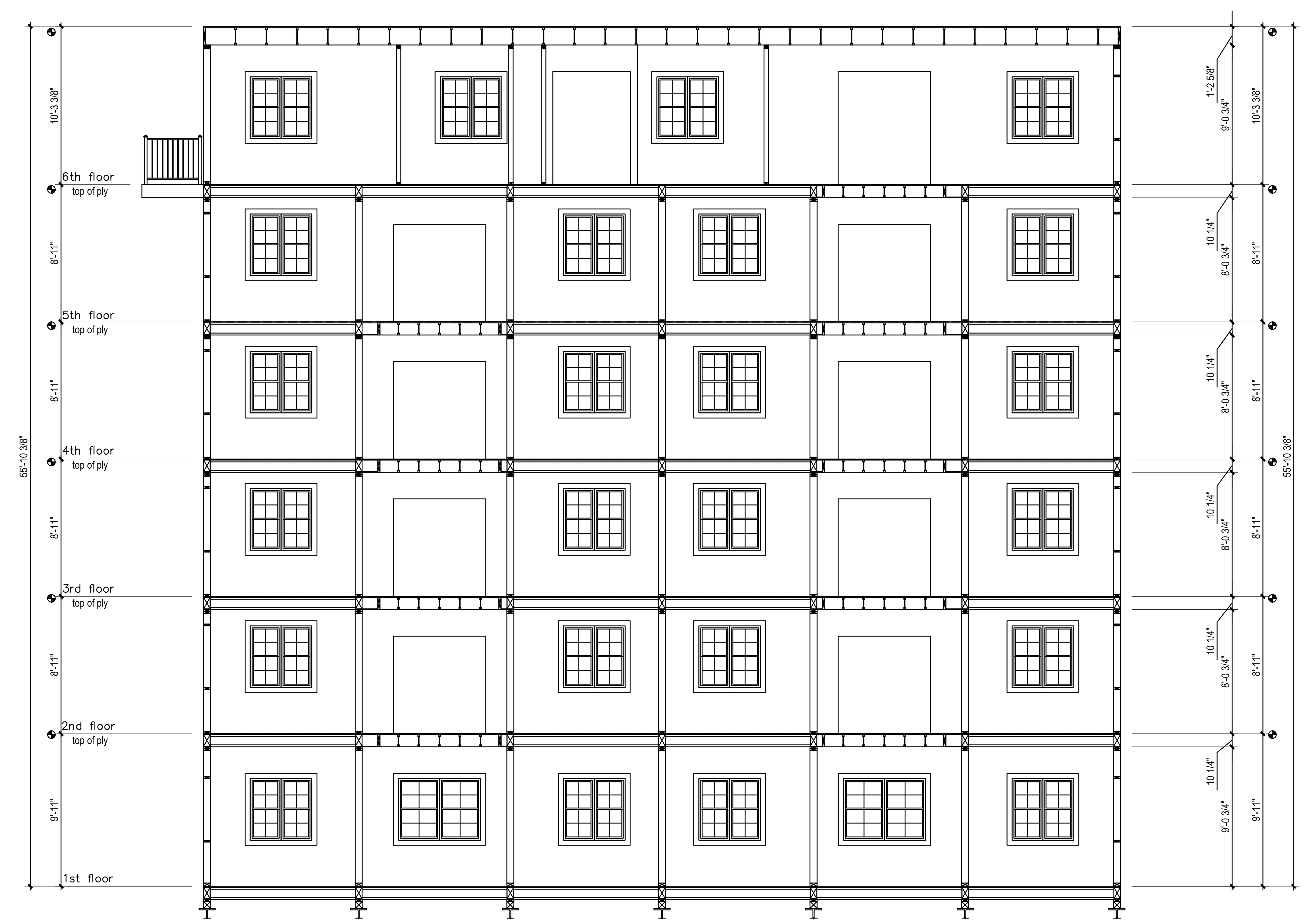

D-D

JOHN VAN DE LINDT
ANDRE FILIATRAULT
RACHEL DAVIDSON
DAVID ROSSOWSKY
MICHAEL D. SYMANS

NEESwood capstone

(performanced—based design)

colorado state university
fort collins, colorado

CAPSTONE TEAM:

COLORADO STATE UNIVERSITY:
JOHN VAN DE LINDT
KIMBERLY CRONIN p.e.
shiling pei

www.engr.colostate.edu/NEESWood/

REVISIONS :

01/06/09 - 90% complete

SHEET NO :

A3.02

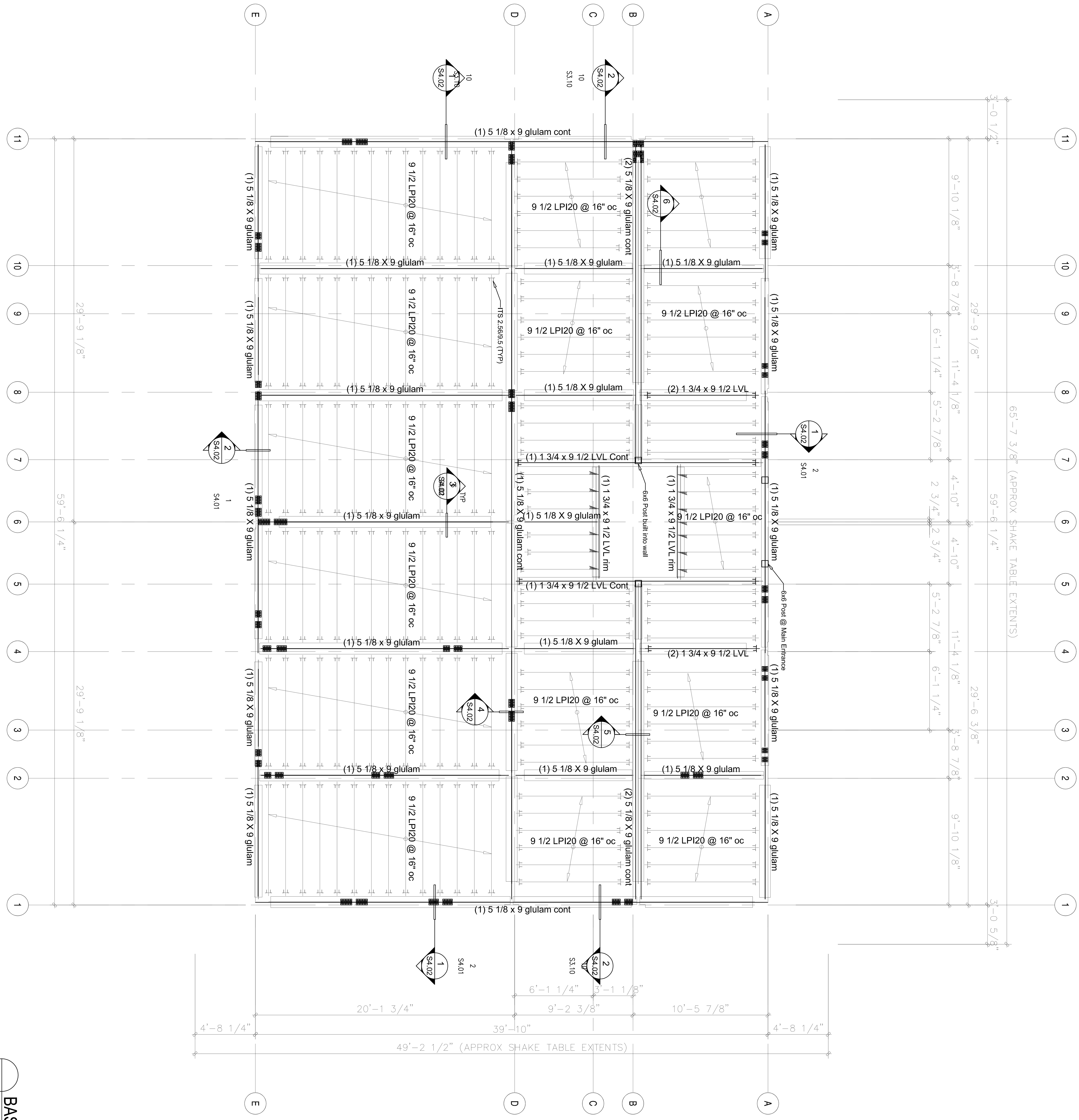

BASE FLOOR PLAN

NEESwood capstone

(performanced-based design)

colorado state university
fort collins, colorado

JOHN VAN DE LINDT
ANDRE FILIATRAULT
RACHEL DAVIDSON
DAVID ROSOWSKY
MICHAEL D. SYMANS

CAPSTONE TEAM:
COLORADO STATE UNIVERSITY:
JOHN VAN DE LINDT
KIMBERLY CRONIN P.E.
SHILING PEI

www.engr.colostate.edu/NEESWood/

REVISIONS :
01/06/09 - 90% complete
01/14/09 - 100% complete

SHEET NO :
S1.01

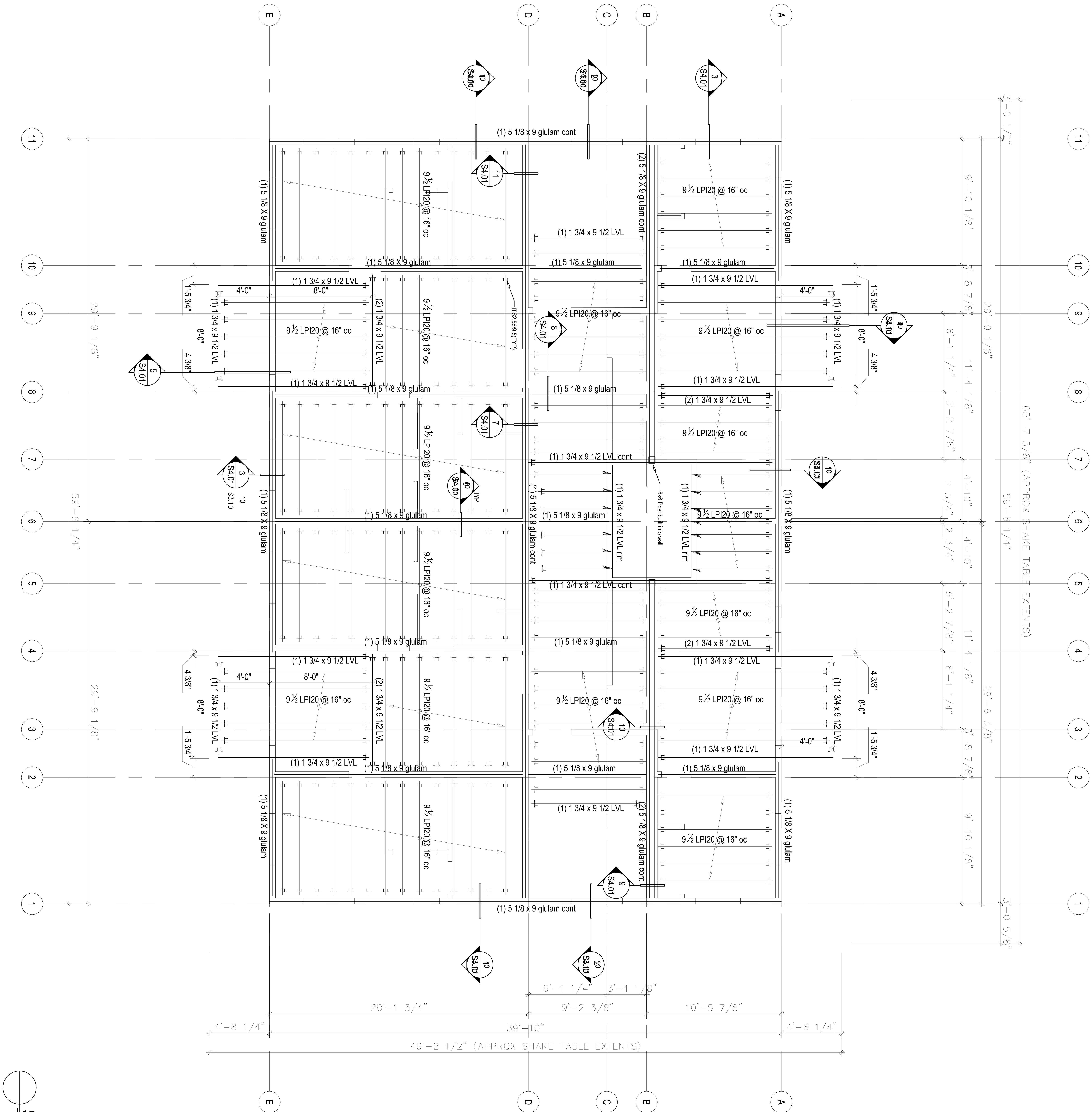

SECOND FLOOR PLAN

SHEET NO :

S1.02

REVISIONS :

01/06/09 - 90% complete

01/14/09 - 100% complete

www.engr.colostate.edu/NEESWood/

CAPSTONE TEAM:

COLORADO STATE UNIVERSITY:

JOHN VAN DE LINDT

KIMBERLY CRONIN P.E.

SHILING PEI

NEESwood capstone

(performanced-based design)

colorado state university

fort collins, colorado

NEESWOOD

JOHN VAN DE LINDT

ANDRE FILIATRAULT

RACHEL DAVIDSON

DAVID ROSOWSKY

MICHAEL D. SYMANS

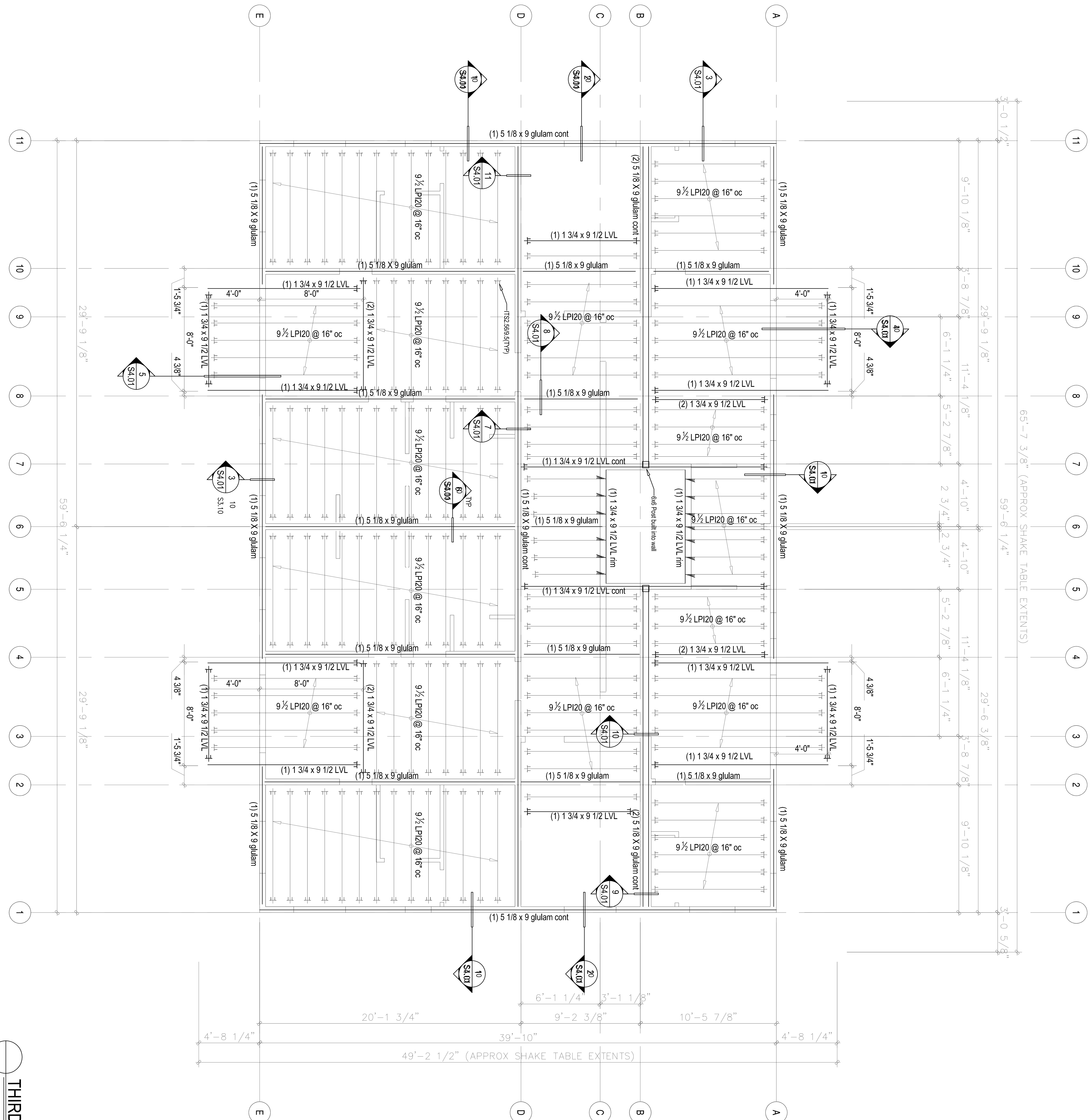

THIRD FLOOR PLAN

NEESwood capstone

(performanced-based design)

colorado state university
fort collins, colorado

JOHN VAN DE LINDT
ANDRE FILIATRAULT
RACHEL DAVIDSON
DAVID ROSOWSKY
MICHAEL D. SYMANS

CAPSTONE TEAM:
COLORADO STATE UNIVERSITY:
JOHN VAN DE LINDT
KIMBERLY CROWN P.E.
SHILING PEI

www.engr.colostate.edu/NEESWood/

REVISIONS:
01/06/09 - 90% complete
01/14/09 - 100% complete

SHEET NO:
S1.03

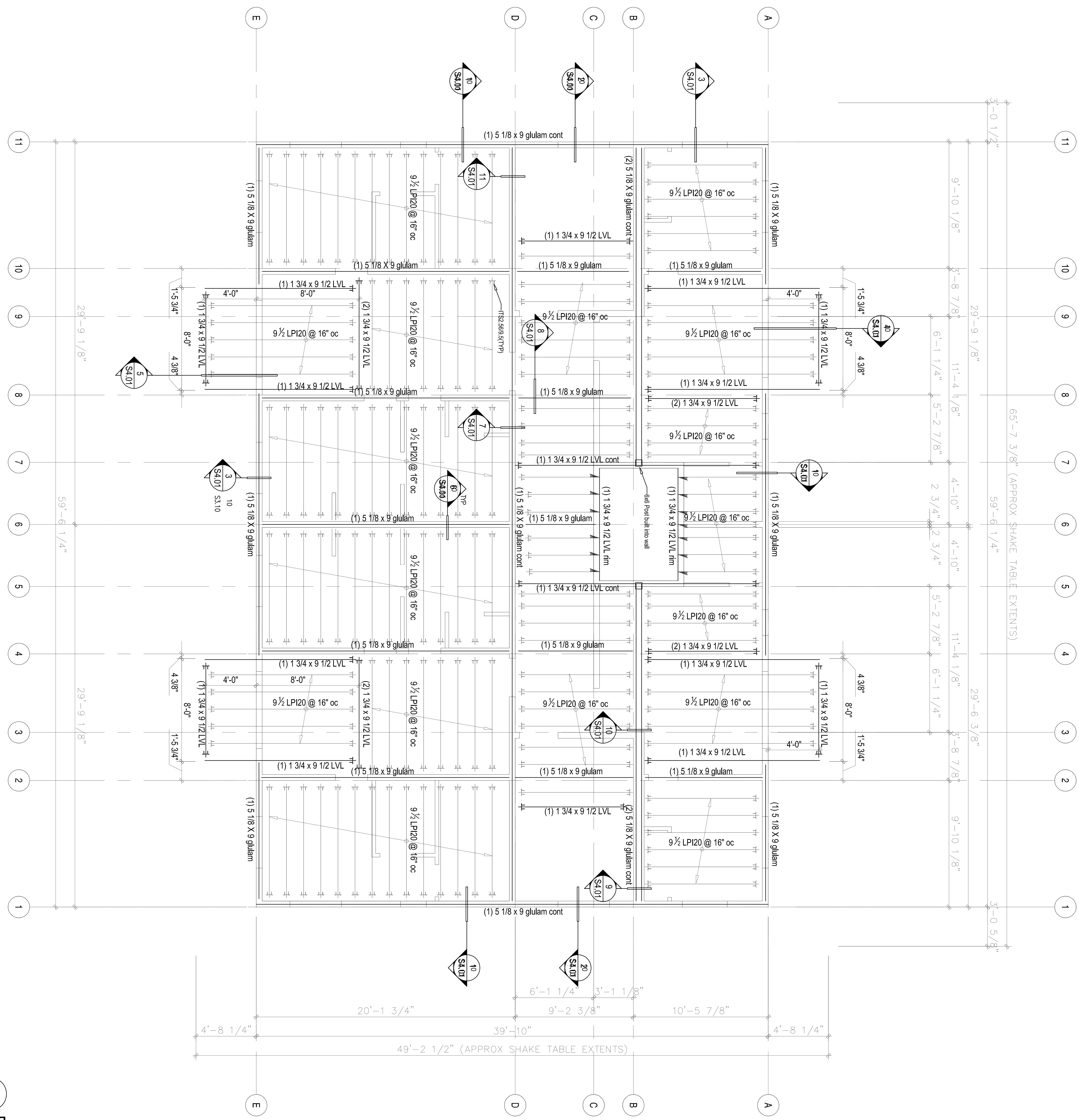

FOURTH FLOOR PLAN

NEESwood capstone

(performanced-based design)

colorado state university
fort collins, colorado

CAPSTONE TEAM:
COLORADO STATE UNIVERSITY:
JOHN VAN DE LINDT
KIMBERLY CRONIN P.E.
SHILING PEI

www.engr.colostate.edu/NEESWood/

REVISIONS:
01/06/09 - 90% complete
01/14/09 - 100% complete

SHEET NO:
S1.04

JOHN VAN DE LINDT
ANDRE FILIATRAULT
RACHEL DAVIDSON
DAVID ROSOWSKY
MICHAEL D. SYMANS

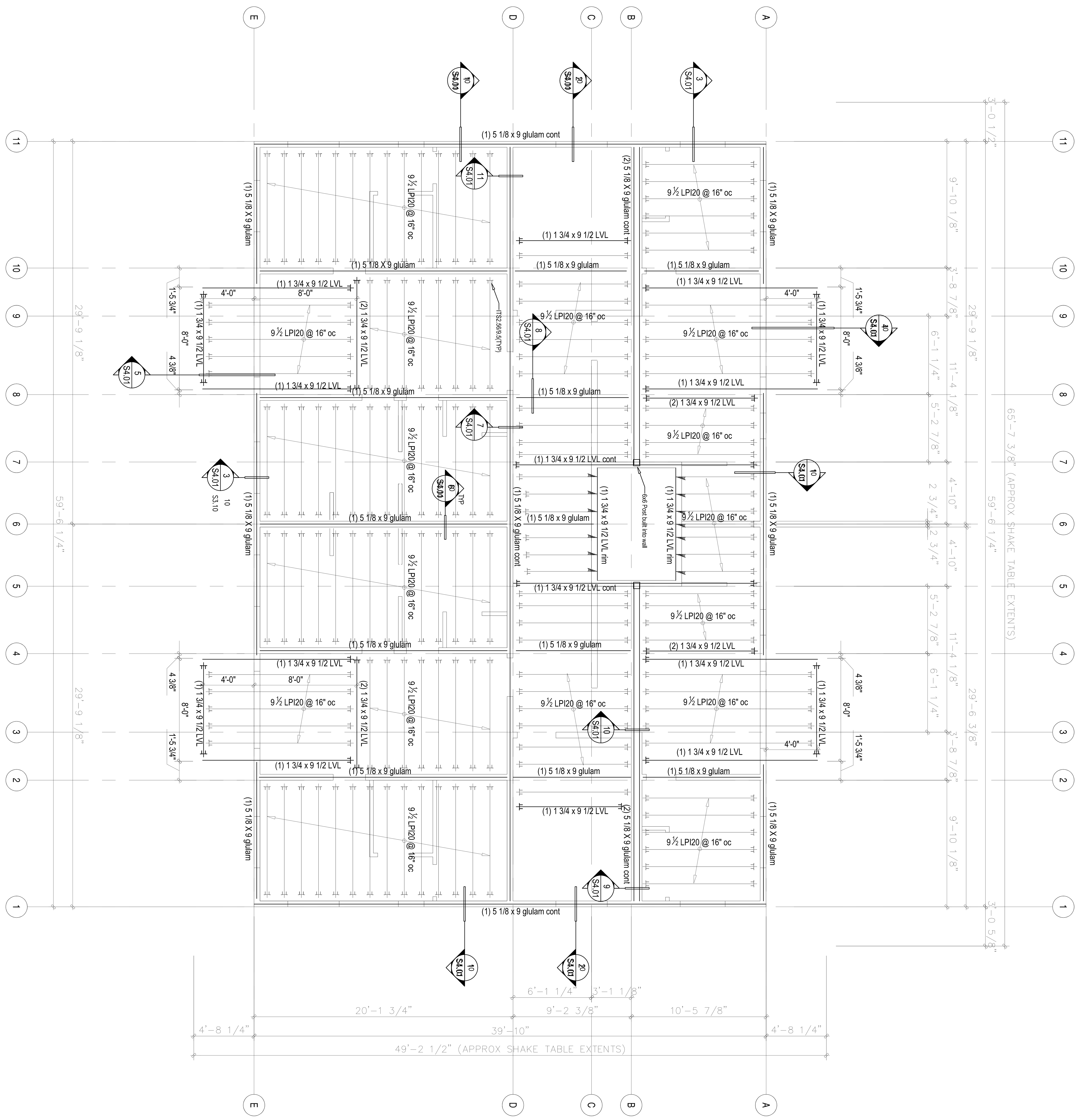

FIFTH FLOOR PLAN

SHEET NO:
S1.05

REVISIONS:
01/06/09 - 90% complete
01/14/09 - 100% complete

www.engr.colostate.edu/NEESWood/

CAPSTONE TEAM:
COLORADO STATE UNIVERSITY:
JOHN VAN DE LINDT
KIMBERLY CRONIN P.E.
SHILING PEI

NEESwood capstone

(performanced-based design)

colorado state university
fort collins, colorado

NEESWOOD
JOHN VAN DE LINDT
ANDRE FILIATRAULT
RACHEL DAVIDSON
DAVID ROSOWSKY
MICHAEL D. SYMANS

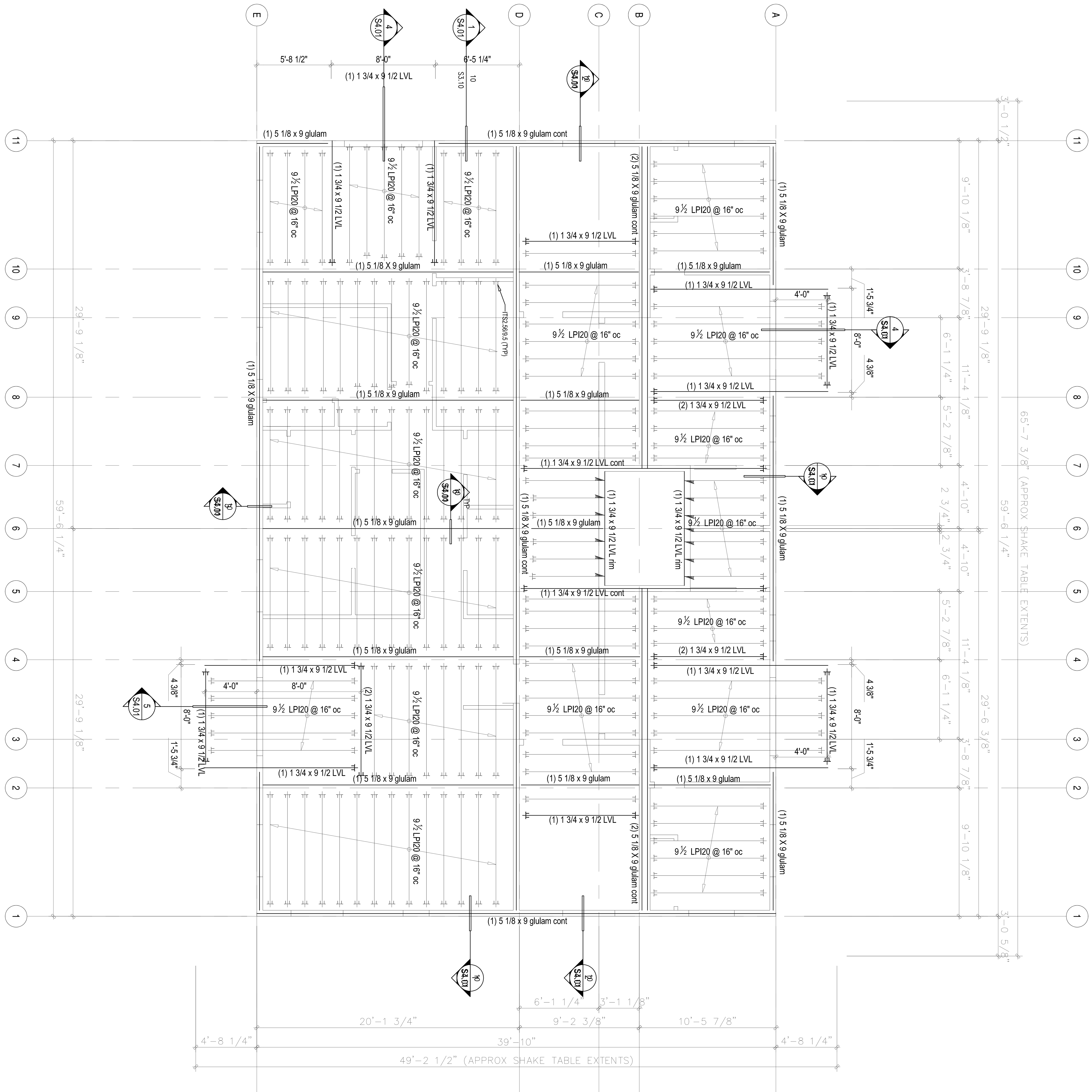

SIXTH FLOOR PLAN

NEESwood capstone

(performanced-based design)

colorado state university
fort collins, colorado

CAPSTONE TEAM:
COLORADO STATE UNIVERSITY:
JOHN VAN DE LINDT
KIMBERLY CRONIN P.E.
SHILING PEI

www.engr.colostate.edu/NEESWood/

REVISIONS :
01/06/09 - 90% complete
01/14/09 - 100% complete

SHEET NO :
S1.06

NEESWOOD
JOHN VAN DE LINDT
ANDRE FILIATRAULT
RACHEL DAVIDSON
DAVID ROSOWSKY
MICHAEL D. SYMANS

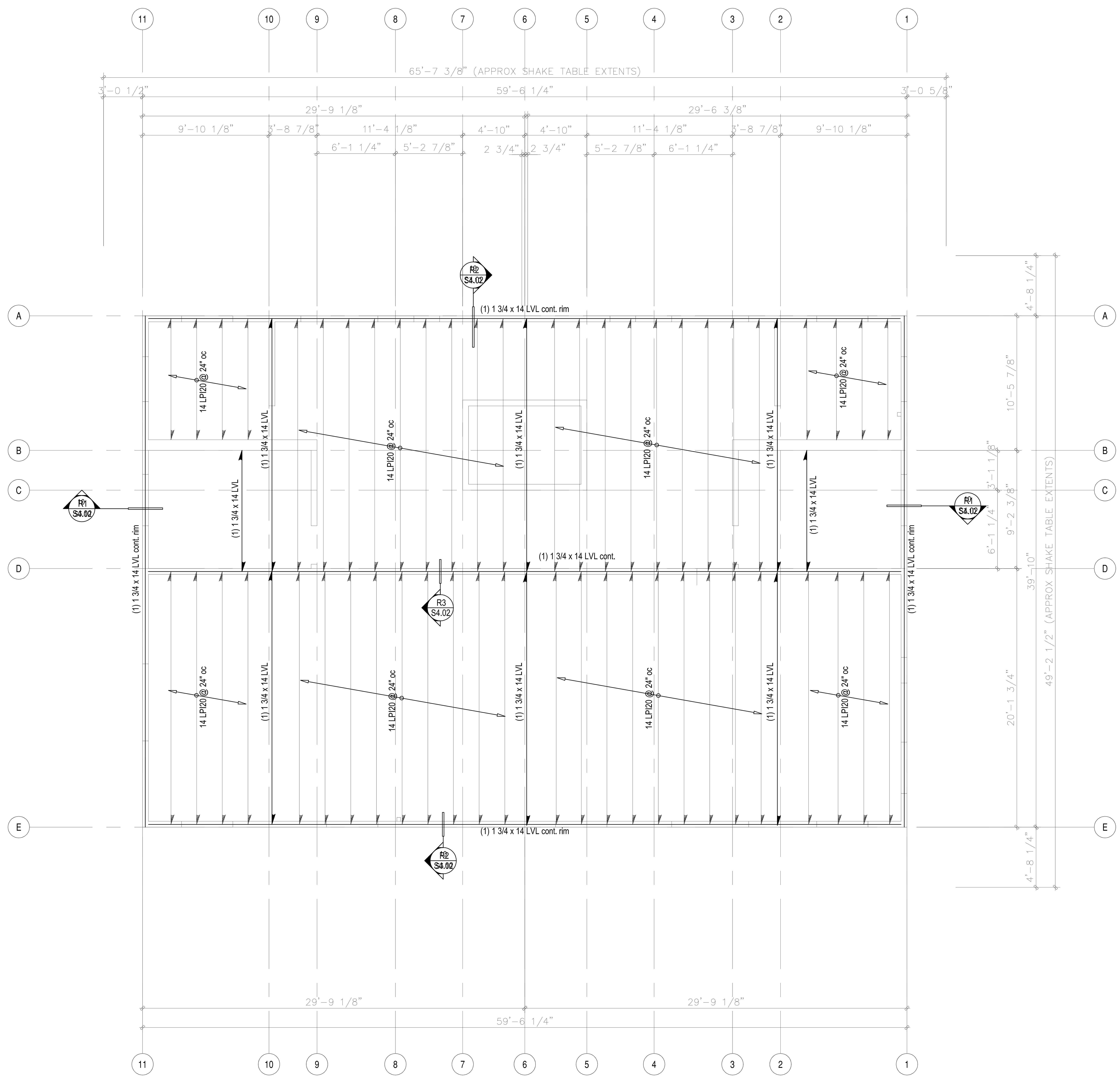

ROOF FRAMING PLAN

NEESwood capstone

(performanced–based design)

colorado state university
fort collins, colorado

JOHN VAN DE LINDT
ANDRE FILIATRAULT
RACHEL DAVIDSON
DAVID ROSSOWSKY
MICHAEL D. SYMANS

CAPSTONE TEAM:

COLORADO STATE UNIVERSITY:
JOHN VAN DE LINDT
KIMBERLY CRONIN P.E.
SHILING PEI

www.engr.colostate.edu/NEESWood/

REVISIONS :

01/06/09 - 90% complete
01/14/09 - 100% complete
05/19/09 - Revision

SHEET NO :

S1.07

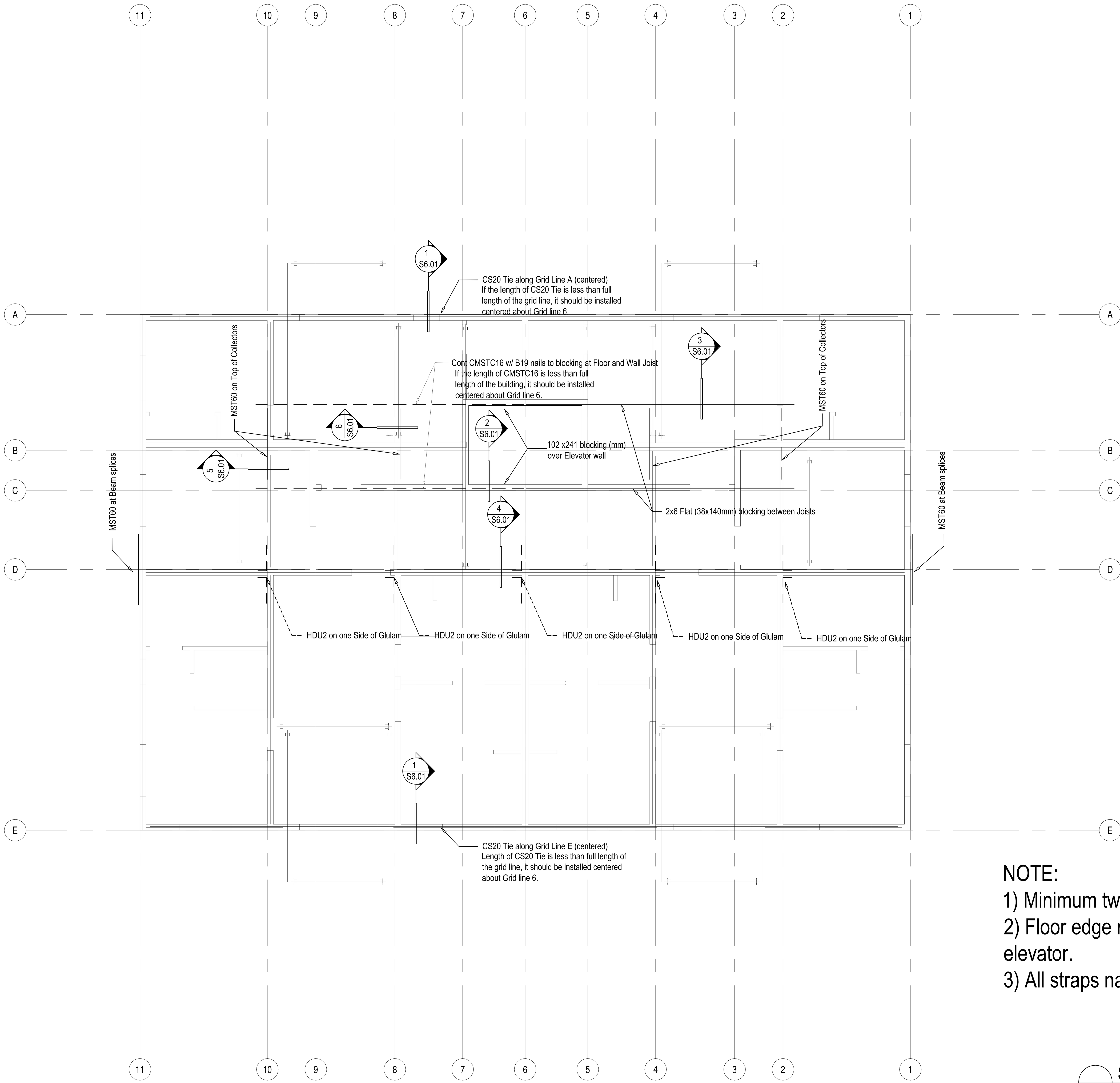

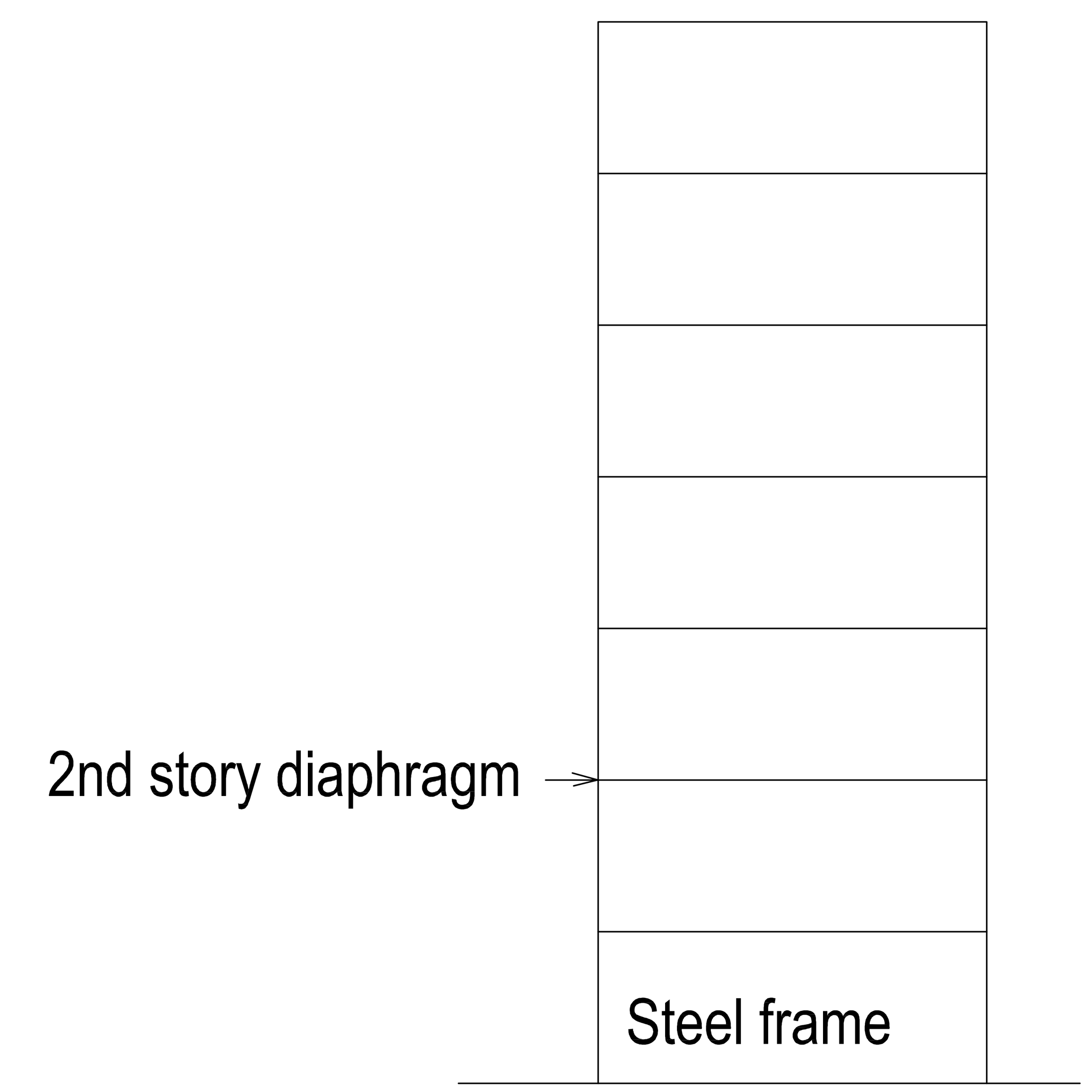

NOTE:
1) Minimum two rows of floor edge nailing for all collectors.
2) Floor edge nail to full length of joist (or LVL) around elevator.
3) All straps nailed using B19 (10d) nail.

SECOND FLOOR TENSION TIE

NEESWOOD

Colorado State University — JOHN VAN DE LINDT
University at Buffalo — ANDRE FILIATRAULT
University of Delaware — RACHEL DAVIDSON
Texas A&M Engineering — DAVID ROSSOWSKY
Rensselaer — MICHAEL D. SYMANS

NEESwood capstone
(performanced–based design)
colorado state university
fort collins, colorado

CAPSTONE TEAM:
COLORADO STATE UNIVERSITY:
JOHN VAN DE LINDT
KIMBERLY CRONIN P.E.
SHILING PEI

www.engr.colostate.edu/NEESWood/

REVISIONS :
01/06/09 - 90% complete
01/14/09 - 100% complete
04/02/09 - Revision

SHEET NO :
S2.02

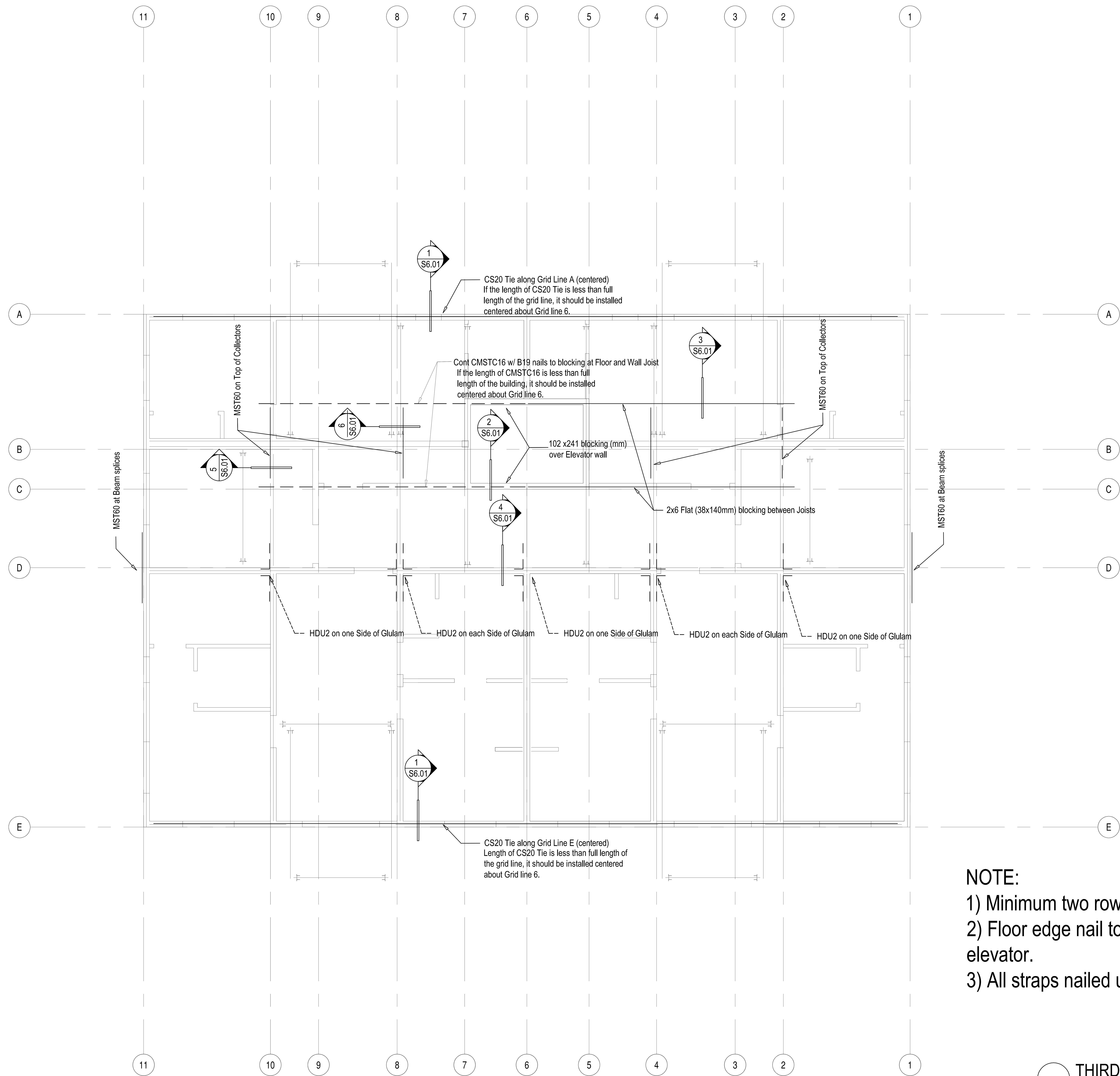

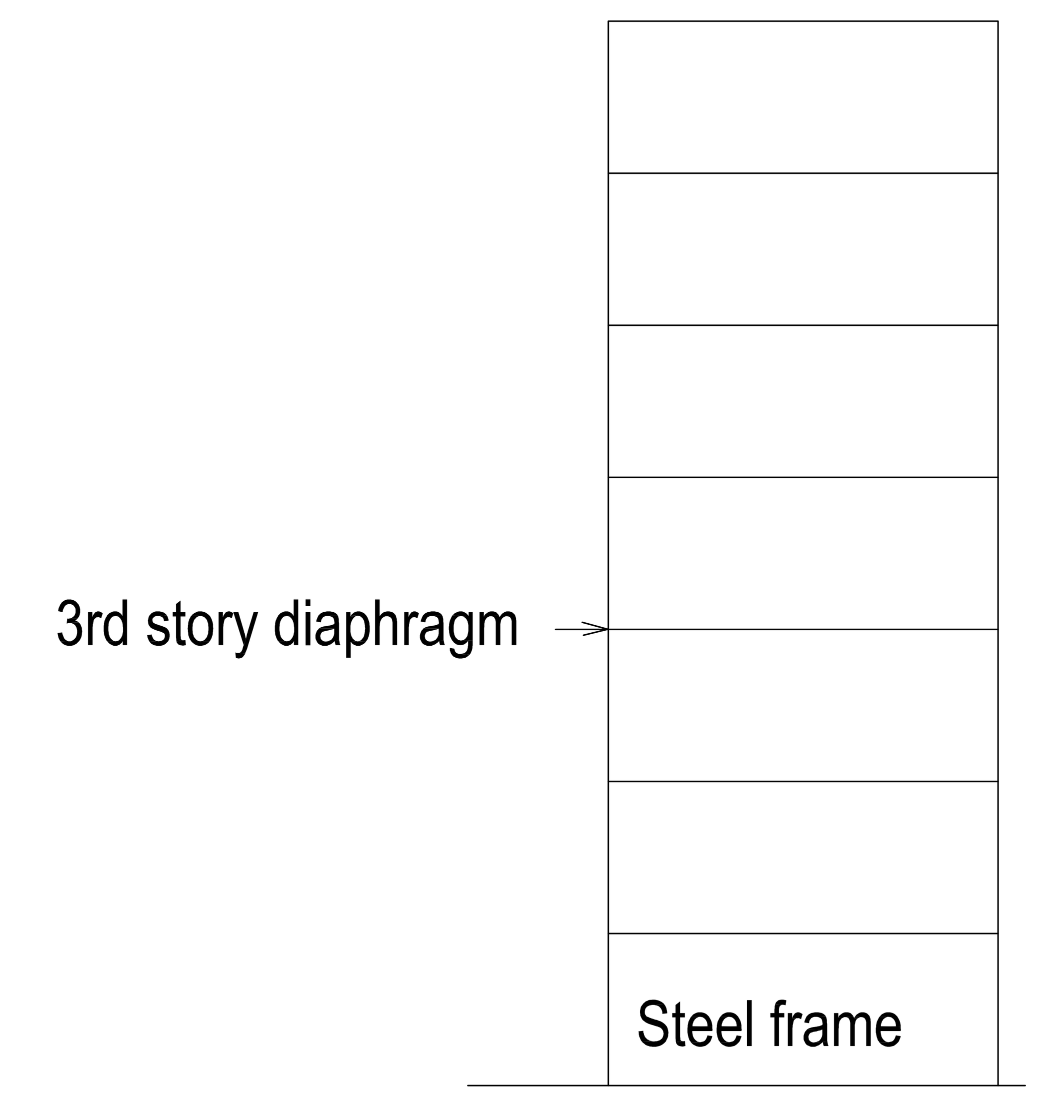

NOTE:
1) Minimum two rows of floor edge nailing for all collectors.
2) Floor edge nail to full length of joist (or LVL) around elevator.
3) All straps nailed using B19 (10d) nail.

THIRD FLOOR TENSION TIE

NEESWOOD
JOHN VAN DE LINDT
ANDRE FILIATRAULT
RACHEL DAVIDSON
DAVID ROSSOWSKY
MICHAEL D. SYMANS

NEESwood capstone
(performanced—based design)
colorado state university
fort collins, colorado

CAPSTONE TEAM:
COLORADO STATE UNIVERSITY:
JOHN VAN DE LINDT
KIMBERLY CRONIN P.E.
SHILING PEI
www.engr.colostate.edu/NEESWood/

REVISIONS :
01/06/09 - 90% complete
01/14/09 - 100% complete
04/02/09 - Revision

SHEET NO :
S2.03

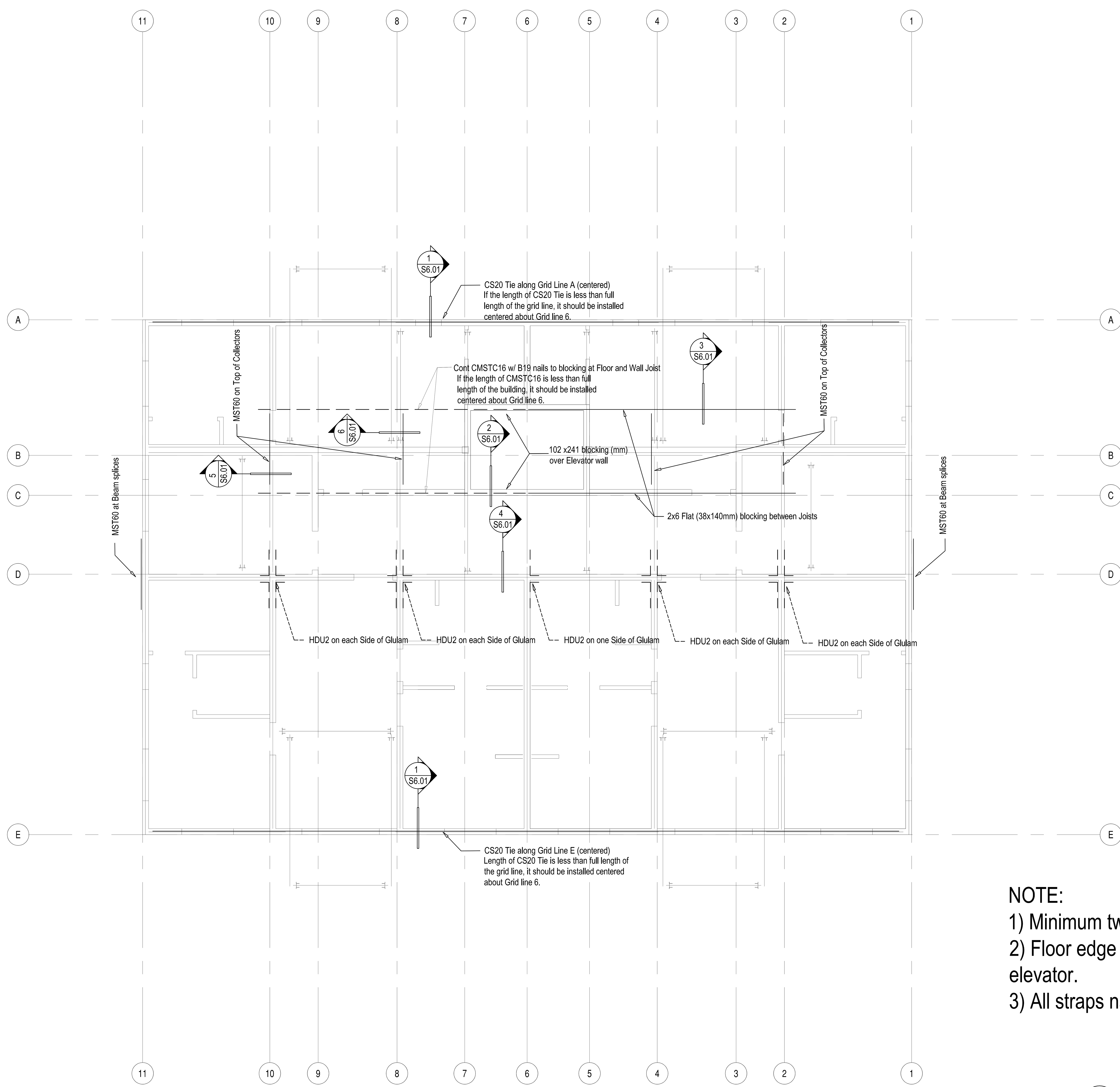

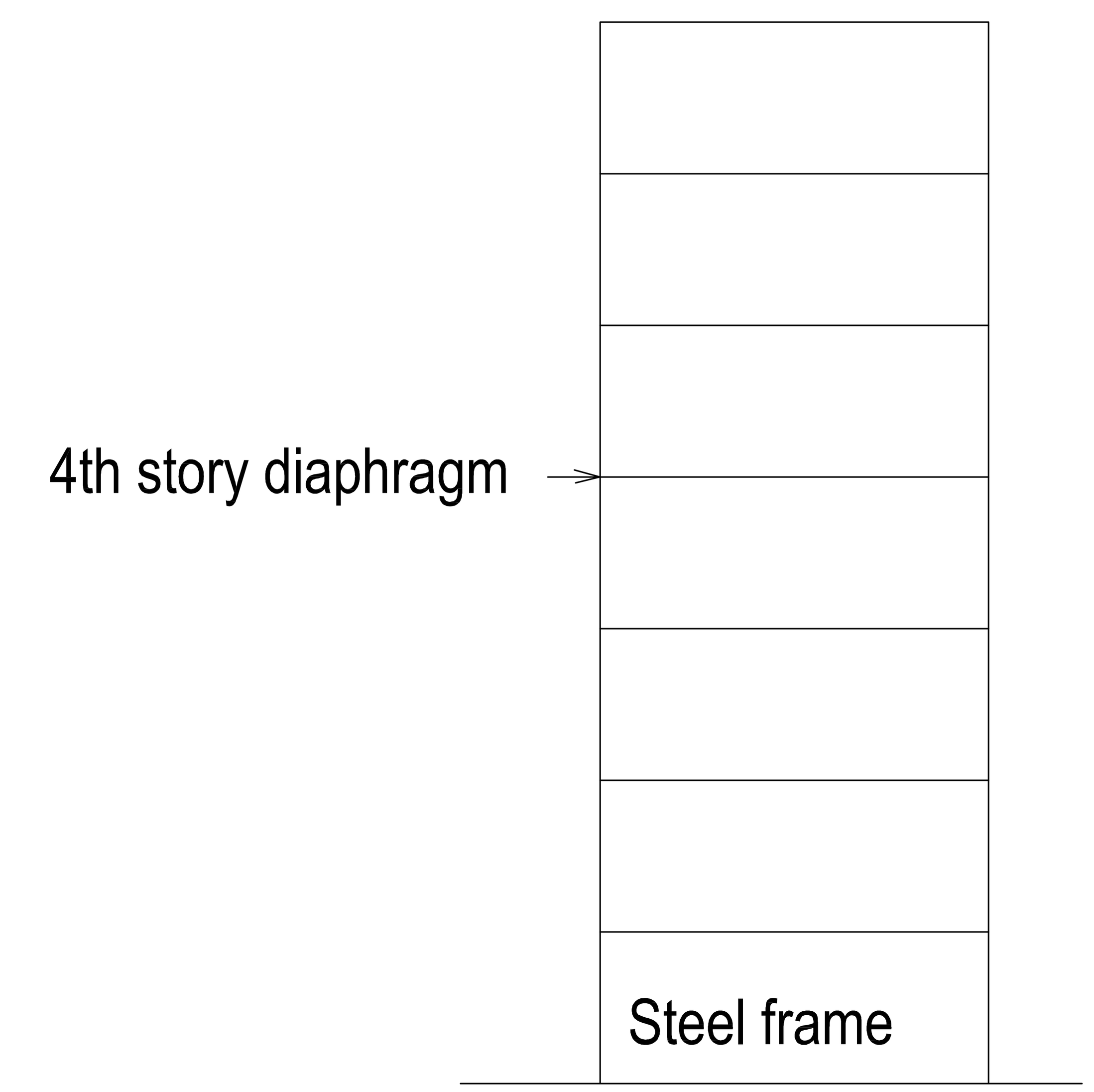

NOTE:
1) Minimum two rows of floor edge nailing for all collectors.
2) Floor edge nail to full length of joist (or LVL) around elevator.
3) All straps nailed using B19 (10d) nail.

FOURTH FLOOR TENSION TIE

NEESWOOD

JOHN VAN DE LINDT
ANDRE FILIATRAULT
RACHEL DAVIDSON
DAVID ROSSOWSKY
MICHAEL D. SYMANS

NEESwood capstone
(performanced−based design)
colorado state university
fort collins, colorado

CAPSTONE TEAM:
COLORADO STATE UNIVERSITY:
JOHN VAN DE LINDT
KIMBERLY CRONIN P.E.
SHILING PEI
www.engr.colostate.edu/NEESWood/

REVISIONS :
01/06/09 - 90% complete
01/14/09 - 100% complete
04/02/09 - Revision

SHEET NO :
S2.04

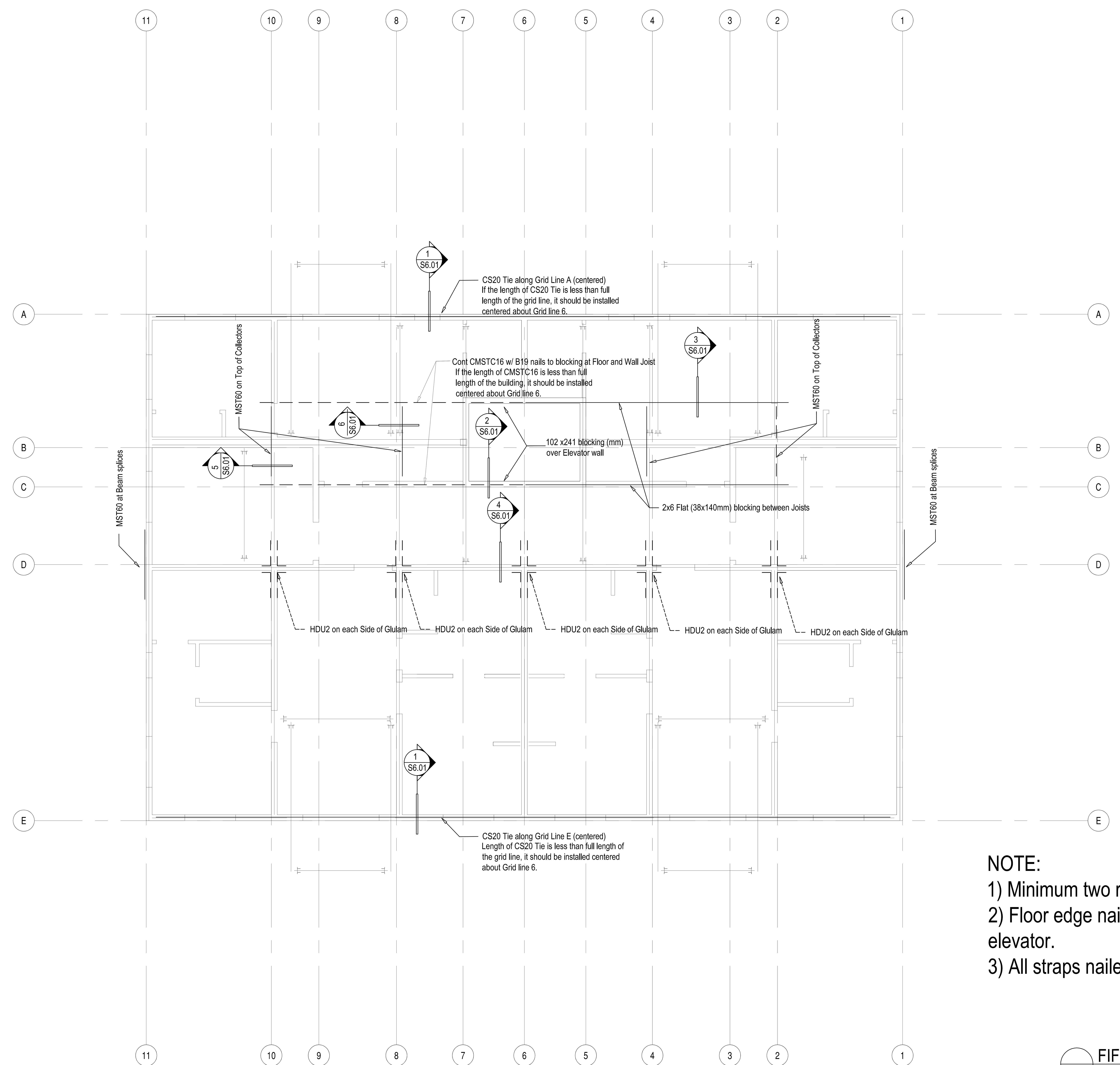

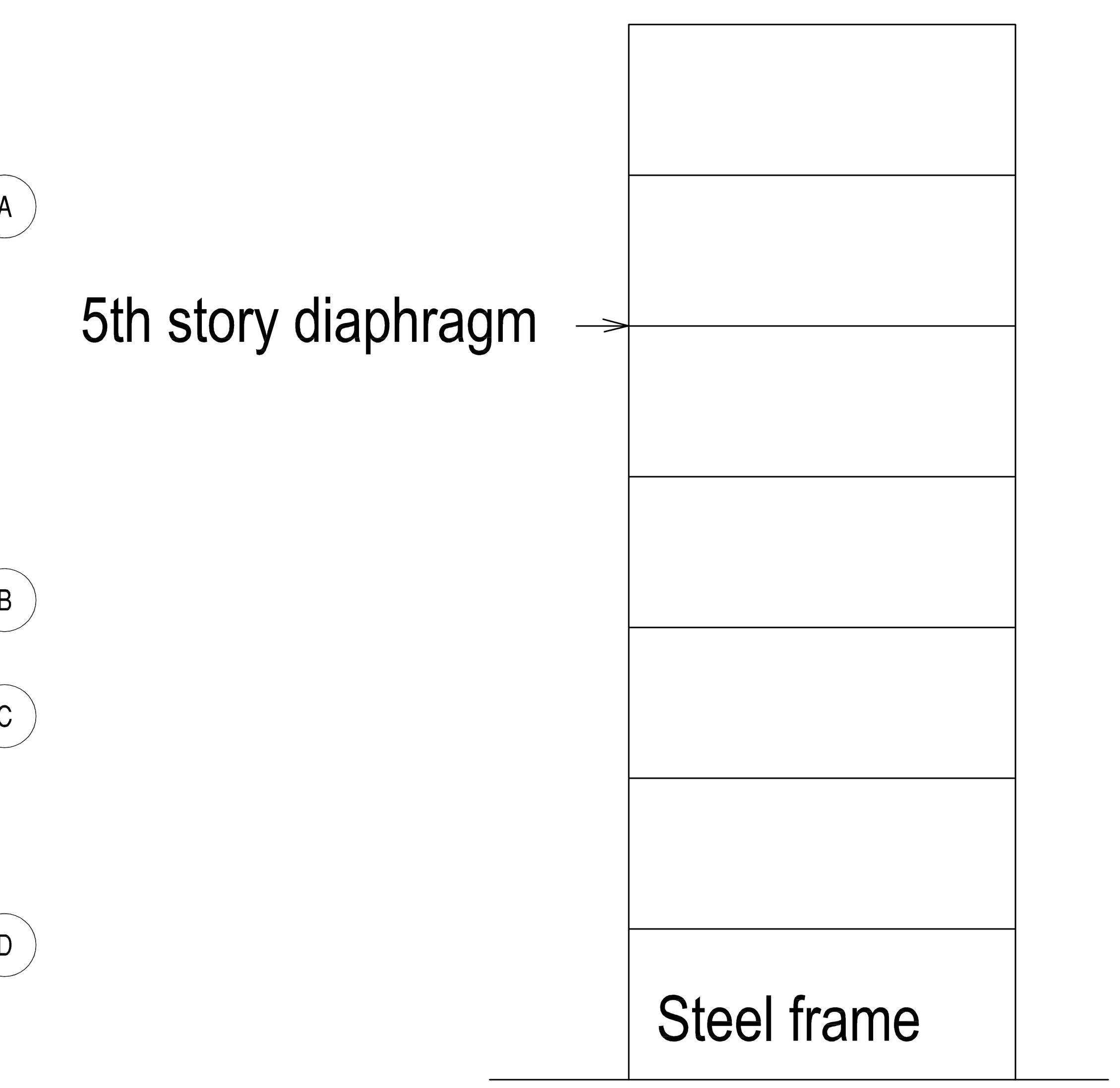

NOTE:

1) Minimum two rows of floor edge nailing for all collectors.
2) Floor edge nail to full length of joist (or LVL) around elevator.
3) All straps nailed using B19 (10d) nail.

FIFTH FLOOR TENSION TIE

NEESWOOD
Colorado State University — JOHN VAN DE LINDT
University at Buffalo — ANDRE FILIATRAULT
University of Delaware — RACHEL DAVIDSON
TEXAS A&M ENGINEERING — DAVID ROSSOWSKY
Rensselaer — MICHAEL D. SYMANS

NEESwood capstone

(performanced–based design)

colorado state university
fort collins, colorado

CAPSTONE TEAM:

COLORADO STATE UNIVERSITY:
JOHN VAN DE LINDT
KIMBERLY CRONIN P.E.
SHILING PEI

www.engr.colostate.edu/NEESWood/

REVISIONS :
01/06/09 - 90% complete
01/14/09 - 100% complete
04/02/09 - Revision

SHEET NO :
S2.05

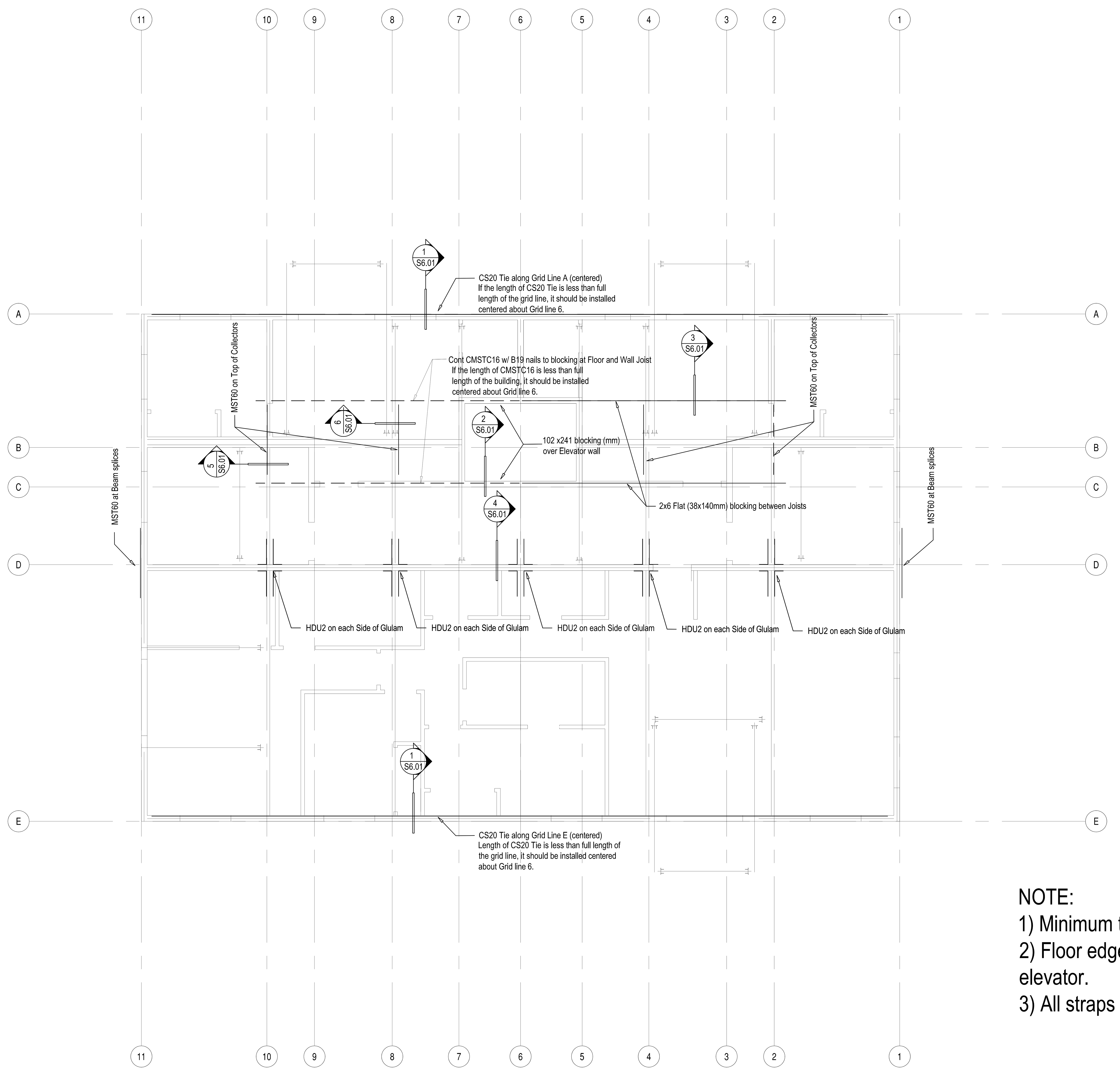

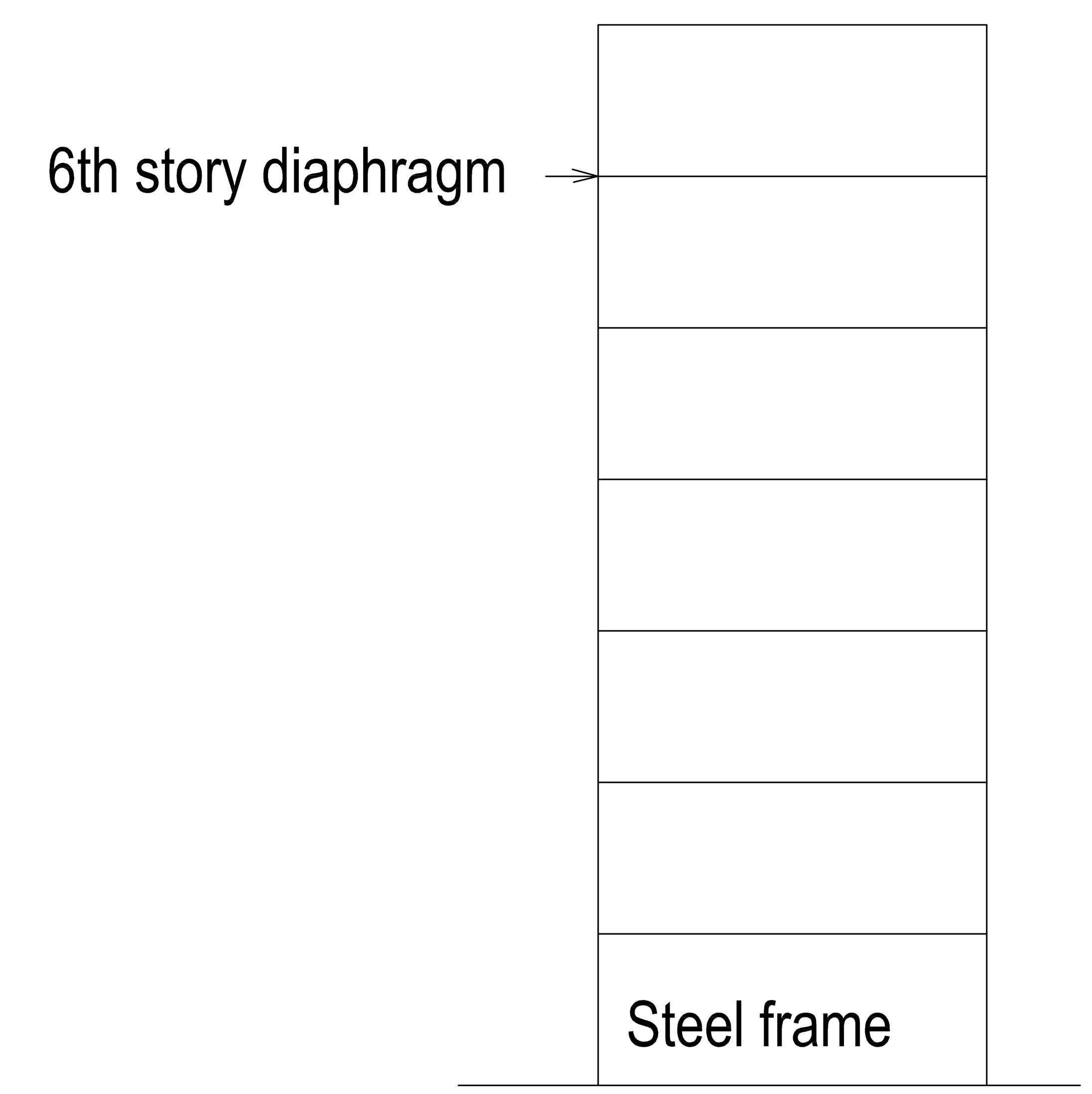

NOTE:

1) Minimum two rows of floor edge nailing for all collectors.
2) Floor edge nail to full length of joist (or LVL) around elevator.
3) All straps nailed using B19 (10d) nail.

SIXTH FLOOR TENSION TIE

JOHN VAN DE LINDT
ANDRE FILIATRAULT
RACHEL DAVIDSON
DAVID ROSSOWSKY
MICHAEL D. SYMANS

NEESwood capstone
(performanced–based design)
colorado state university
fort collins, colorado

CAPSTONE TEAM:
COLORADO STATE UNIVERSITY:
JOHN VAN DE LINDT
KIMBERLY CRONIN P.E.
SHILING PEI
www.engr.colostate.edu/NEESWood/

REVISIONS :
01/06/09 - 90% complete
01/14/09 - 100% complete
04/02/09 - Revision

SHEET NO :
S2.06

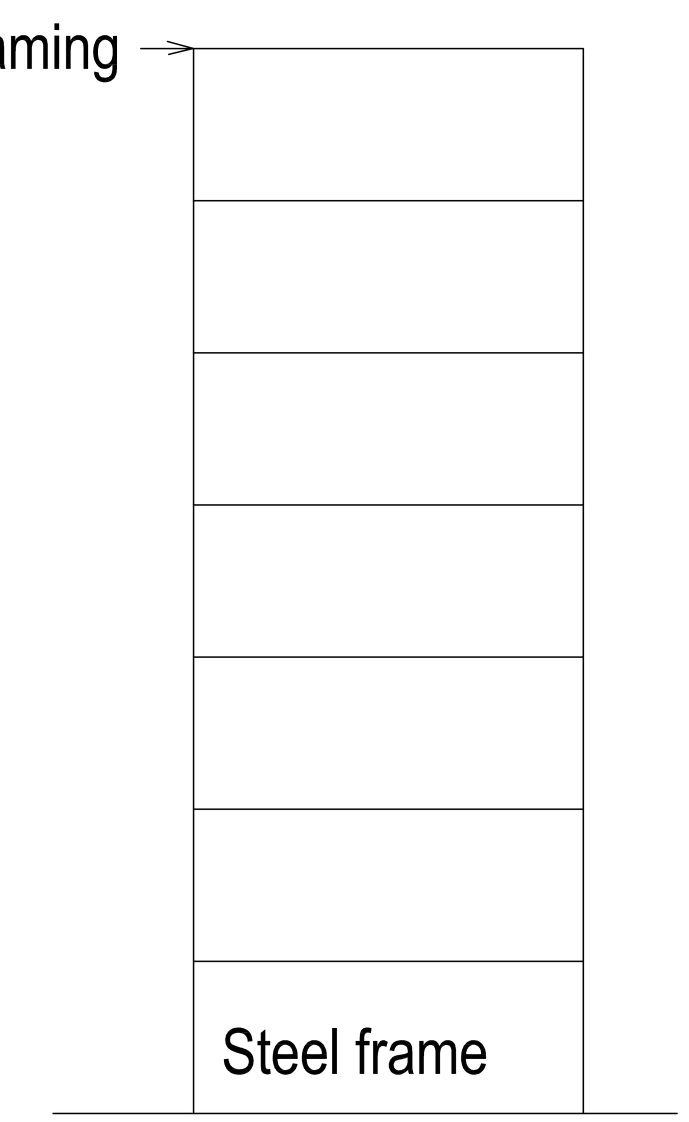

NOTE:
1) Minimum two rows of floor edge nailing for all collectors.
2) Floor edge nail to full length of joist (or LVL) around elevator.
3) All straps nailed using B19 (10d) nail.

ROOF TENSION TIE

NEESWOOD
Colorado State University — JOHN VAN DE LINDT
University at Buffalo — ANDRE FILIATRAULT
University of Delaware — RACHEL DAVIDSON
Texas A&M Engineering — DAVID ROSSOWSKY
Rensselaer — MICHAEL D. SYMANS

NEESwood capstone
(performanced−based design)
colorado state university
fort collins, colorado

CAPSTONE TEAM:
COLORADO STATE UNIVERSITY:
JOHN VAN DE LINDT
KIMBERLY CRONIN P.E.
SHILING PEI
www.engr.colostate.edu/NEESWood/

REVISIONS :
01/06/09 - 90% complete
01/14/09 - 100% complete
04/02/09 - Revision

SHEET NO :
S2.07

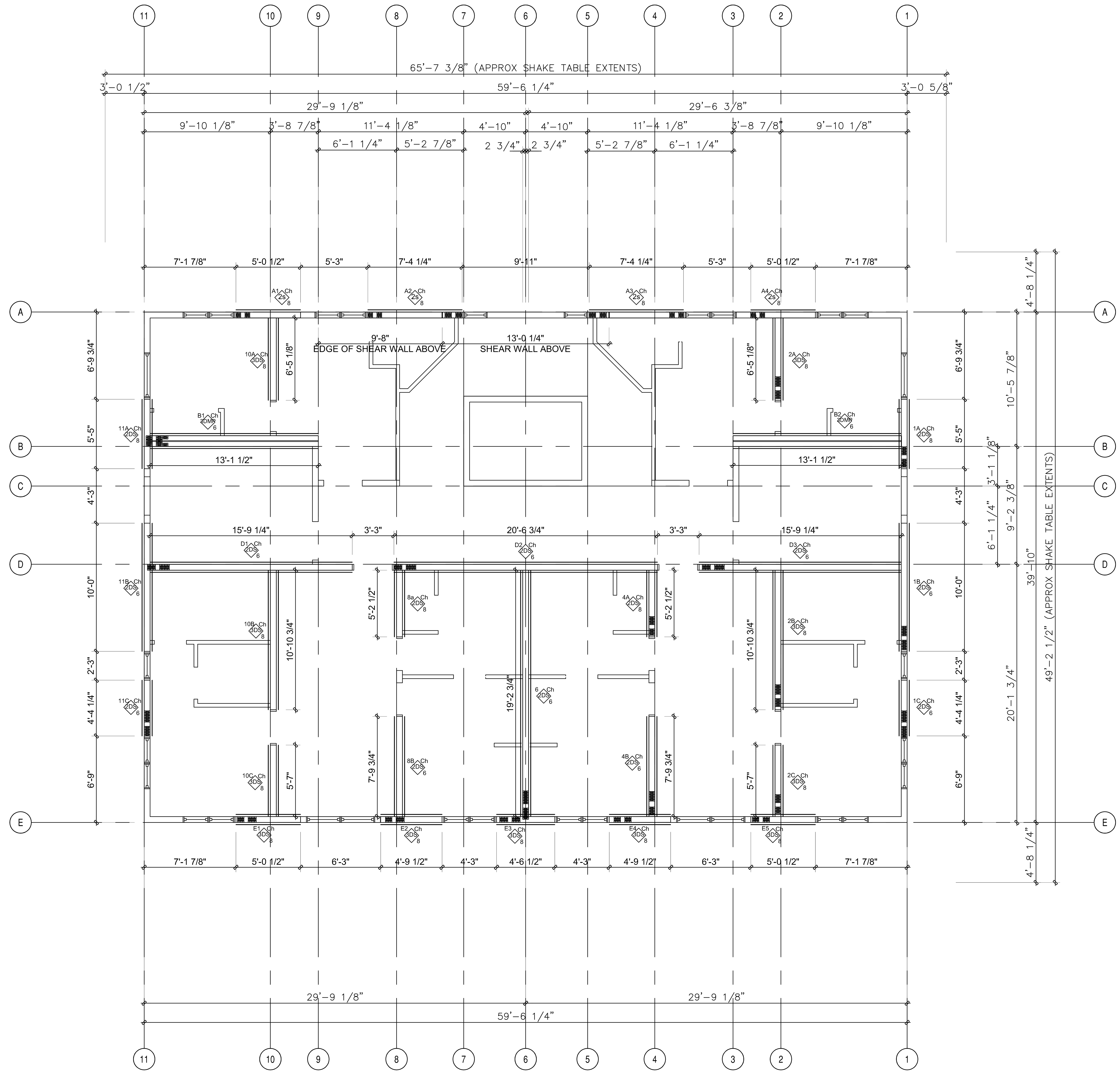

FIRST FLOOR PLAN

SHEAR WALL SCHEDULE

- TOP PLATE CONNECTION
  - Ch Custom channel connector (full wall length)
  - Sd 1/4"x6" sds screws @ 3" oc through top plates
- shear wall callout
- (2) rows of 1/4"x6" sds screws @ sill
  - 6" oc
  - 8" oc
- SHEAR WALL TYPE
  - S SINGLE SIDE SHEATHED
  - DS DOUBLE SIDE SHEATHED
  - MP MID PLY SHEATHED
  - DMP DOUBLE MID PLY SHEATHED
- SPACING OF EDGE SHEATHING NAILS (10d)
- shear wall location

NEESWOOD
Colorado State University
JOHN VAN DE LINDT
University at Buffalo
ANDRE FILIATRAULT
University of Delaware
RACHEL DAVIDSON
TEXAS A&M ENGINEERING
DAVID ROSSOWSKY
Rensselaer
MICHAEL D. SYMANS

NEESwood capstone

(performanced-based design)

colorado state university
fort collins, colorado

CAPSTONE TEAM:
COLORADO STATE UNIVERSITY:
JOHN VAN DE LINDT
KIMBERLY CRONIN P.E.
SHILING PEI

www.engr.colostate.edu/NEESWood/

REVISIONS :
01/06/09 - 90% complete
01/14/09 - 100% complete

SHEET NO :
s3.01

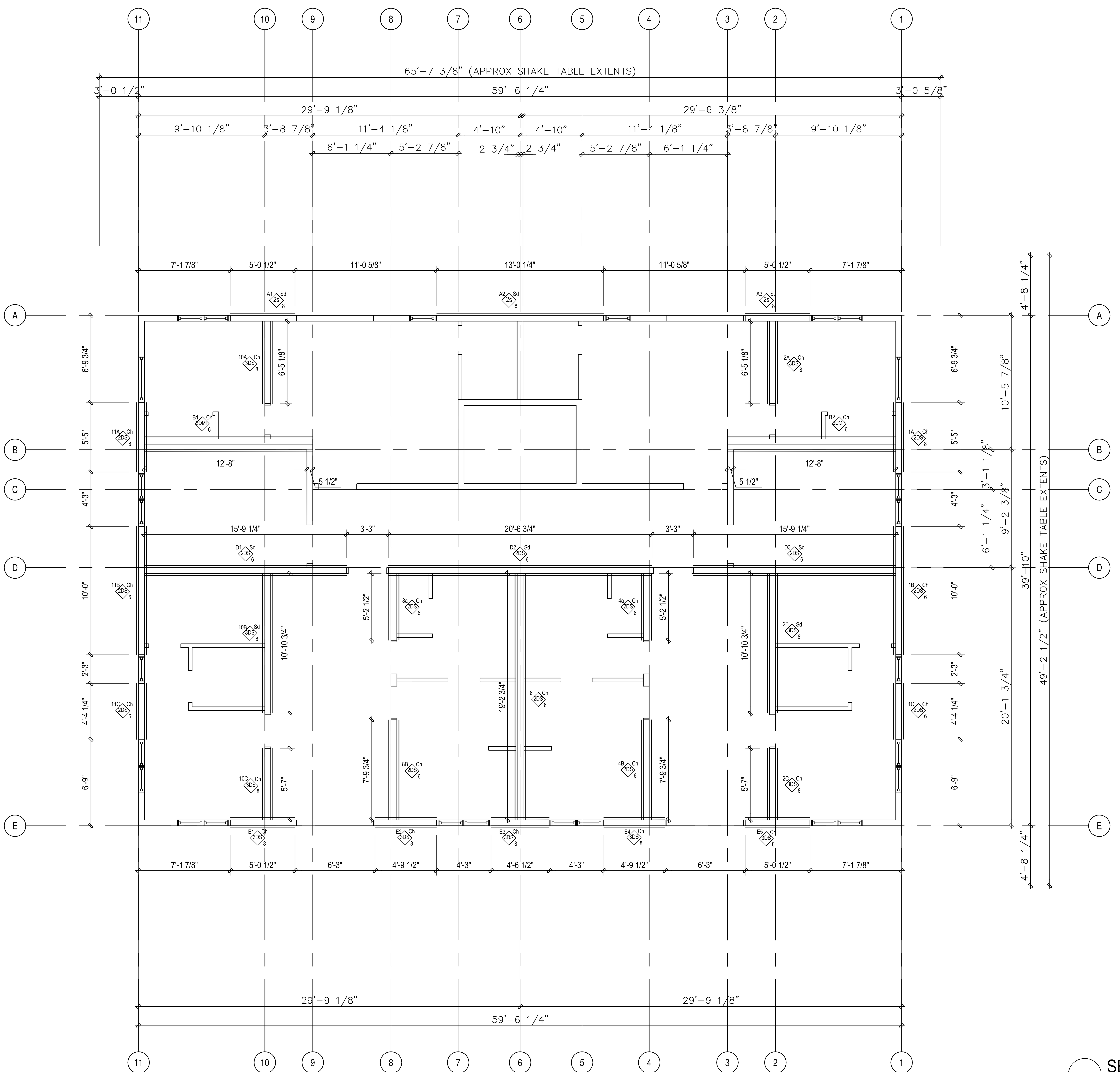

SECOND FLOOR PLAN

SHEAR WALL SCHEDULE

- TOP PLATE CONNECTION
  - Ch — Custom channel connector (full wall length)
  - Sd — 1/4"x6" sds screws @ 3" oc through top plates
- shear wall callout
- (2) rows of 1/4"x4" sds screws @ sill
  - 6" oc
  - 8" oc
- SHEAR WALL TYPE
  - S — SINGLE SIDE SHEATHED
  - DS — DOUBLE SIDE SHEATHED
  - MP — MID PLY SHEATHED
  - DMP — DOUBLE MID PLY SHEATHED
- SPACING OF EDGE SHEATHING NAILS (10d)
- shear wall location

NEESWOOD

Colorado State University — JOHN VAN DE LINDT

University at Buffalo — ANDRE FILIATRAULT

University of Delaware — RACHEL DAVIDSON

TEXAS A&M ENGINEERING — DAVID ROSSOWSKY

Rensselaer — MICHAEL D. SYMANS

NEESwood capstone

(performanced–based design)

colorado state university
fort collins, colorado

CAPSTONE TEAM:

COLORADO STATE UNIVERSITY:
JOHN VAN DE LINDT
KIMBERLY CRONIN P.E.
SHILING PEI

www.engr.colostate.edu/NEESWood/

REVISIONS :

01/06/09 - 90% complete
01/14/09 - 100% complete

SHEET NO :

s3.02

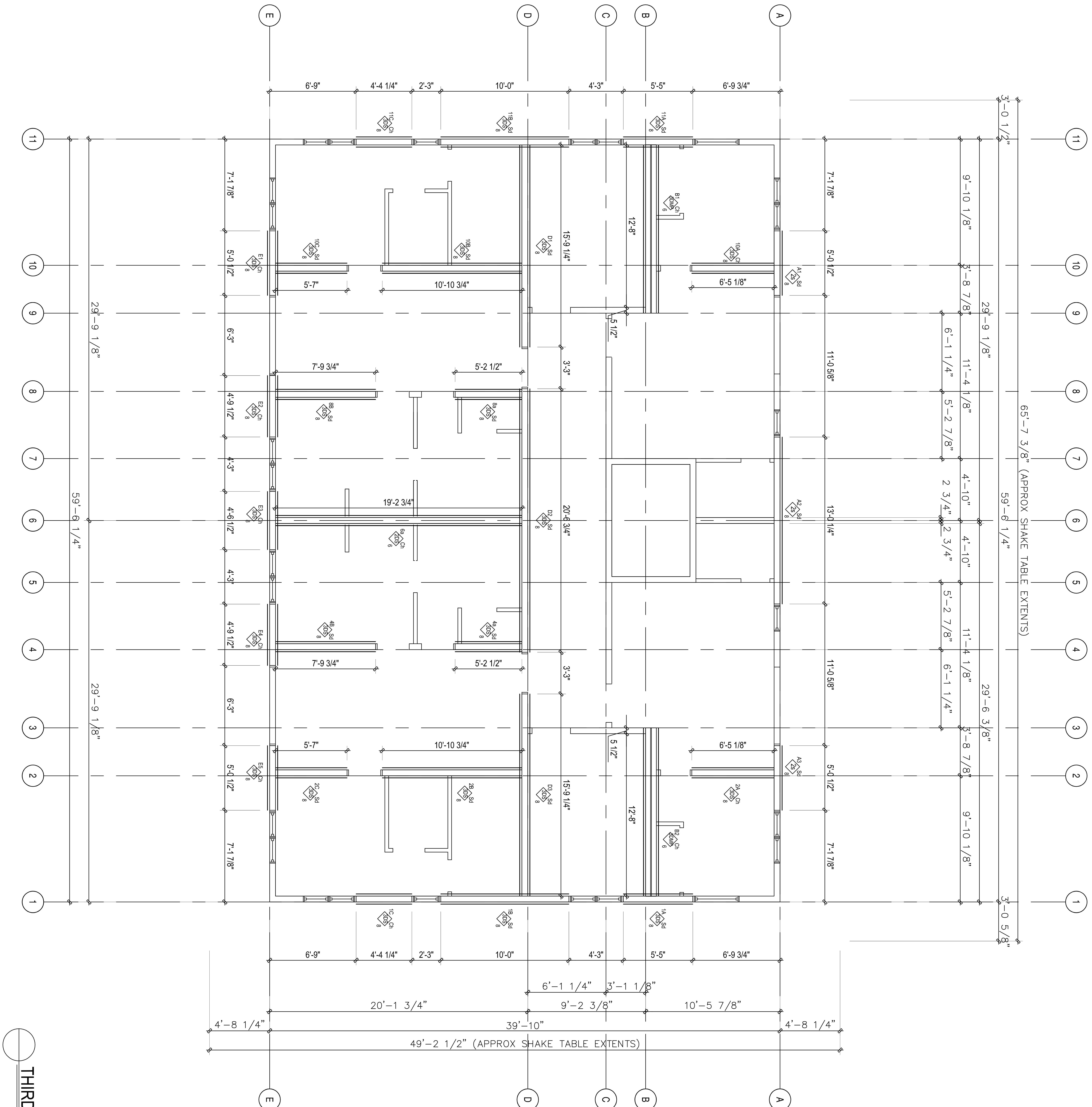

THIRD FLOOR PLAN

SHEAR WALL SCHEDULE

TOP PLATE CONNECTION
- Ch Custom channel connector (full wall length)
- Sd 1/4"x6" sds screws @ 3" oc through top plates

shear wall callout

(2) rows of 1/4"x4" sds screws @ sill
- 6" oc
- 8" oc

SHEAR WALL TYPE
- S SINGLE SIDE SHEATHED
- DS DOUBLE SIDE SHEATHED
- MP MID PLY SHEATHED
- DMP DOUBLE MID PLY SHEATHED

SPACING OF EDGE SHEATHING NAILS (10d)

shear wall location

SHEET NO: s3.03

REVISIONS:
01/06/09 - 90% complete
01/14/09 - 100% complete

CAPSTONE TEAM:
COLORADO STATE UNIVERSITY:
JOHN VAN DE LINDT
KIMBERLY CRONIN P.E.
SHILING PEI

www.engr.colostate.edu/NEESWood/

NEESwood capstone

(performanced-based design)

colorado state university
fort collins, colorado

JOHN VAN DE LINDT
ANDRE FILIATRAULT
RACHEL DAVIDSON
DAVID ROSOWSKY
MICHAEL D. SYMANS

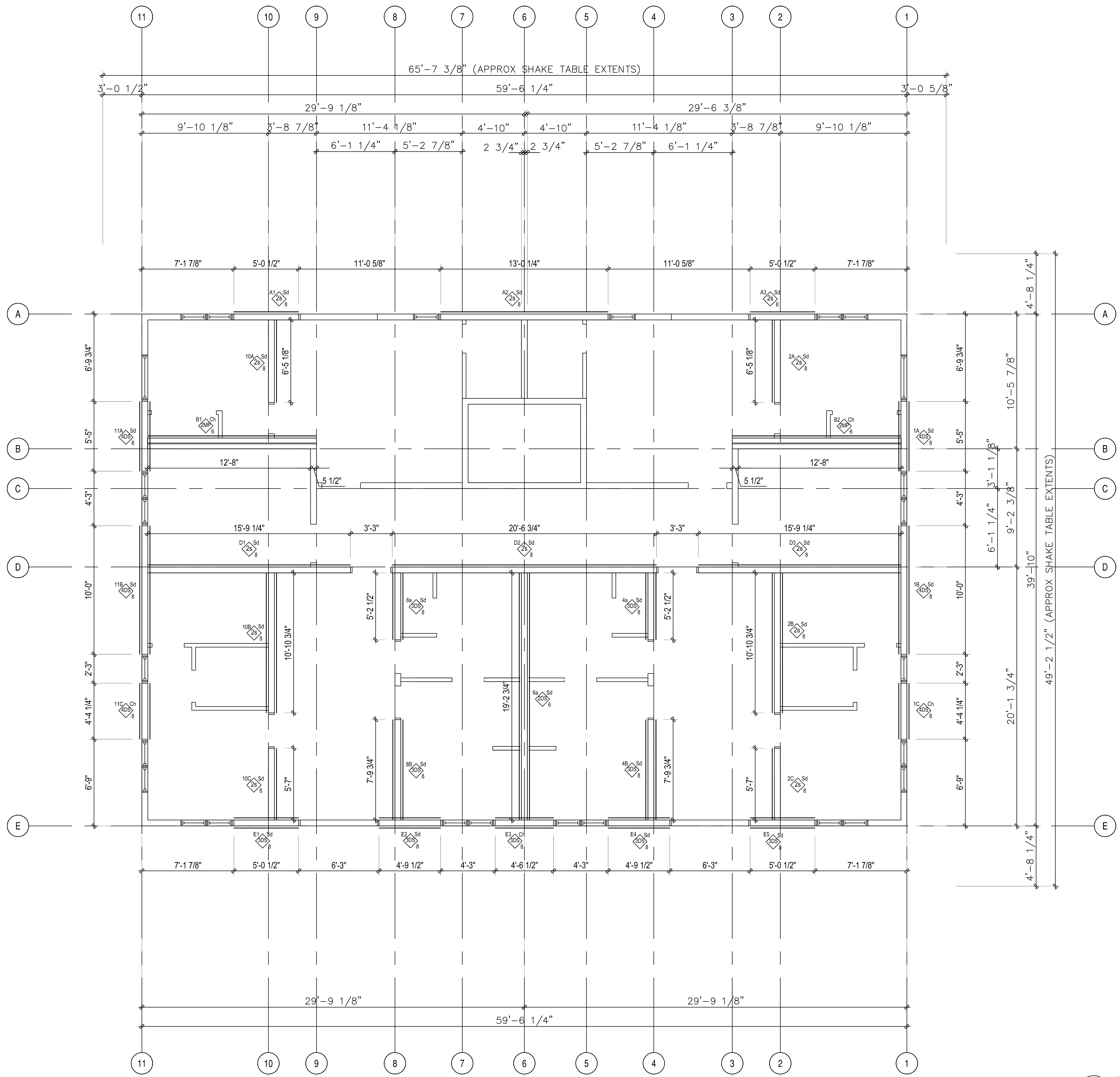

FOURTH FLOOR PLAN

SHEAR WALL SCHEDULE

- TOP PLATE CONNECTION
  - Ch — Custom channel connector (full wall length)
  - Sd — 1/4"x6" sds screws @ 3" oc through top plates
- shear wall callout
- (2) rows of 1/4"x4" sds screws @ sill
  - 6" oc
  - 8" oc
- SHEAR WALL TYPE
  - S — SINGLE SIDE SHEATHED
  - DS — DOUBLE SIDE SHEATHED
  - MP — MID PLY SHEATHED
  - DMP — DOUBLE MID PLY SHEATHED
- SPACING OF EDGE SHEATHING NAILS (10d)
- shear wall location

NEESWOOD

Colorado State University — JOHN VAN DE LINDT

University at Buffalo — ANDRE FILIATRAULT

University of Delaware — RACHEL DAVIDSON

TEXAS A&M ENGINEERING — DAVID ROSSOWSKY

Rensselaer — MICHAEL D. SYMANS

NEESwood capstone

(performanced-based design)

colorado state university
fort collins, colorado

CAPSTONE TEAM:

COLORADO STATE UNIVERSITY:
JOHN VAN DE LINDT
KIMBERLY CRONIN P.E.
SHILING PEI

www.engr.colostate.edu/NEESWood/

REVISIONS :

01/06/09 - 90% complete
01/14/09 - 100% complete

SHEET NO :

s3.04

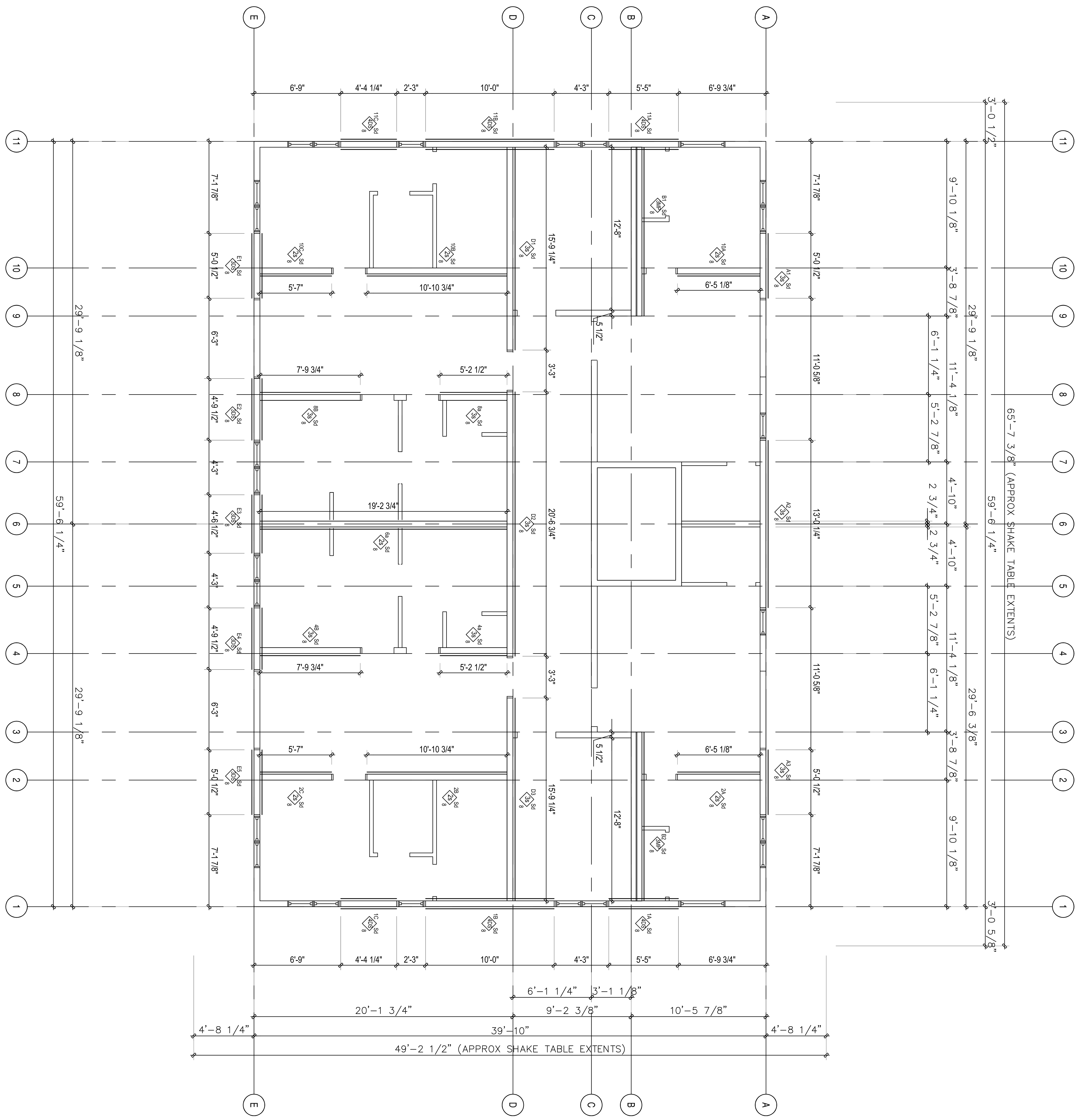

FIFTH FLOOR PLAN

SHEAR WALL SCHEDULE

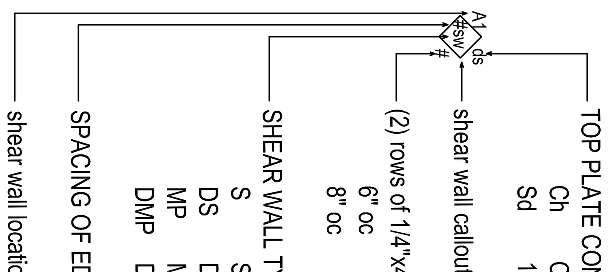

- TOP PLATE CONNECTION
  - Ch Custom channel connector (full wall length)
  - Sd 1/4"x6" sds screws @ 3" oc through top plates
- shear wall callout
- (2) rows of 1/4"x4" sds screws @ sill
  - 6" oc
  - 8" oc
- SHEAR WALL TYPE
  - S SINGLE SIDE SHEATHED
  - DS DOUBLE SIDE SHEATHED
  - MP MID PLY SHEATHED
  - DMP DOUBLE MID PLY SHEATHED
- SPACING OF EDGE SHEATHING NAILS (10d)
- shear wall location

SHEET NO.:
s3.05

REVISIONS :
01/06/09 - 90% complete
01/14/09 - 100% complete

www.engr.colostate.edu/NEESWood/

CAPSTONE TEAM:
COLORADO STATE UNIVERSITY:
JOHN VAN DE LINDT
KIMBERLY CRONIN P.E.
SHILING PEI

NEESwood capstone

(performanced-based design)

colorado state university
fort collins, colorado

NEESWOOD
JOHN VAN DE LINDT
ANDRE FILIATRAULT
RACHEL DAVIDSON
DAVID ROSOWSKY
MICHAEL D. SYMANS

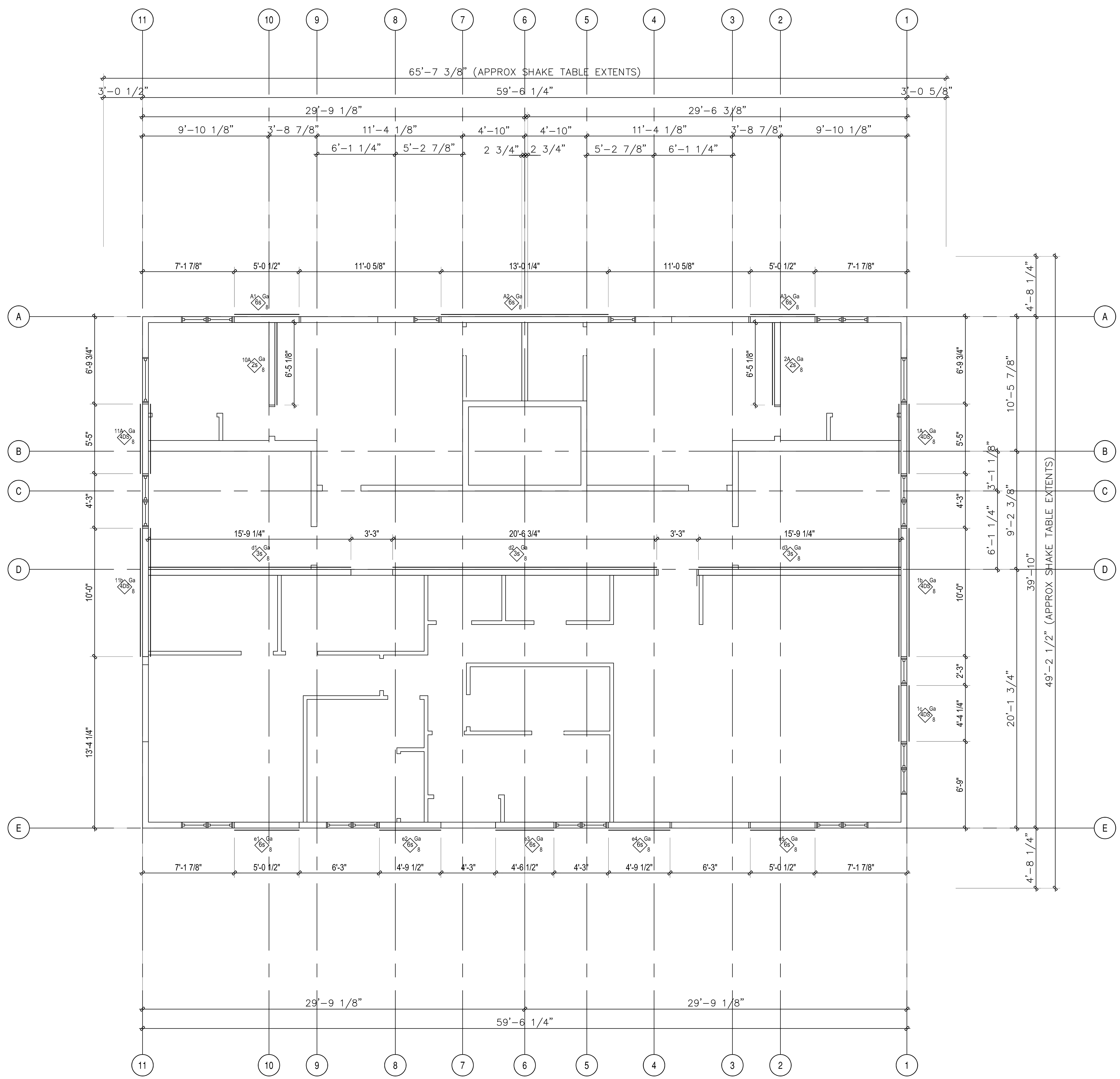

SHEAR WALL SCHEDULE

- TOP PLATE CONNECTION
  - Ga Custom
- shear wall callout
- (2) rows of 1/4"x4" sds screws @ sill
  - 6" oc
  - 8" oc
- SHEAR WALL TYPE
  - S SINGLE SIDE SHEATHED
  - DS DOUBLE SIDE SHEATHED
  - MP MID PLY SHEATHED
  - DMP DOUBLE MID PLY SHEATHED
- SPACING OF EDGE SHEATHING NAILS (10d)
- shear wall location

SIXTH FLOOR PLAN

NEESWOOD

Colorado State University — JOHN VAN DE LINDT

University at Buffalo — ANDRE FILIATRAULT

University of Delaware — RACHEL DAVIDSON

TEXAS A&M ENGINEERING — DAVID ROSSOWSKY

Rensselaer — MICHAEL D. SYMANS

NEESwood capstone

(performanced-based design)

colorado state university
fort collins, colorado

CAPSTONE TEAM:

COLORADO STATE UNIVERSITY:
JOHN VAN DE LINDT
KIMBERLY CRONIN P.E.
SHILING PEI

www.engr.colostate.edu/NEESWood/

REVISIONS :

01/06/09 - 90% complete
01/14/09 - 100% complete

SHEET NO :

s3.06

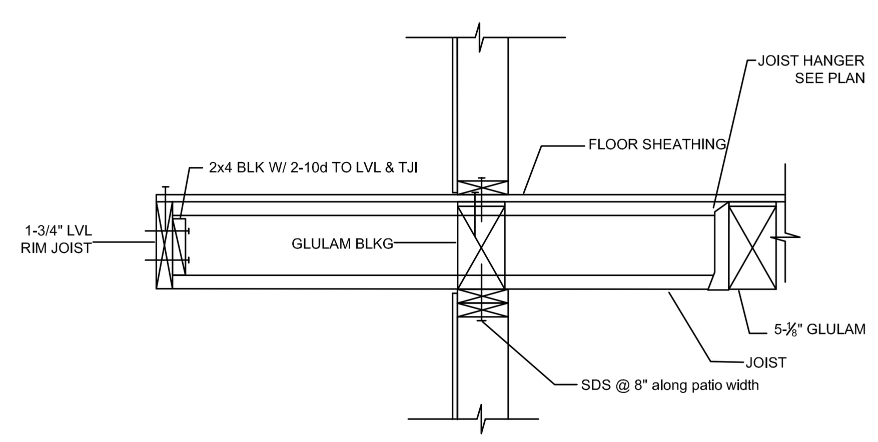

BALCONY CANT FROM GLULAM

13 DETAIL
SCALE: |F" = 1'-0"

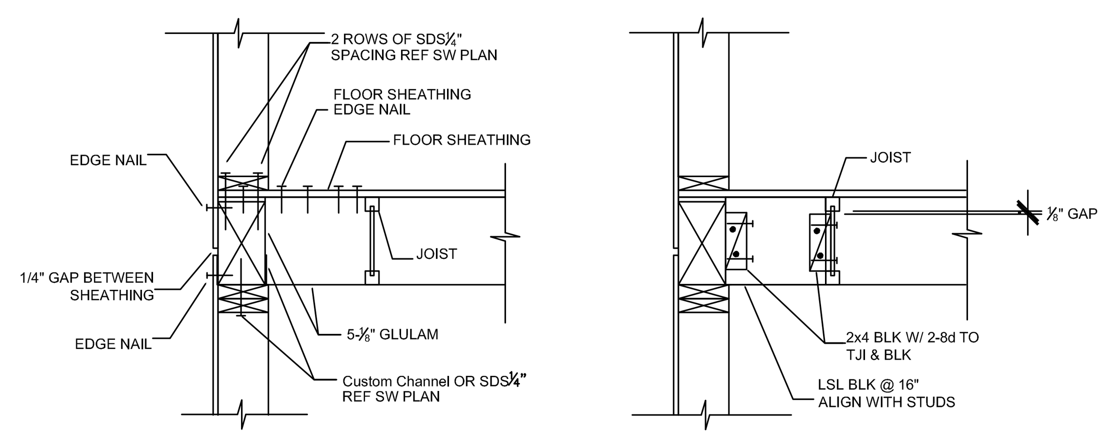

Exterior Wall Joist-Parallel

9 DETAIL
SCALE: |F" = 1'-0"

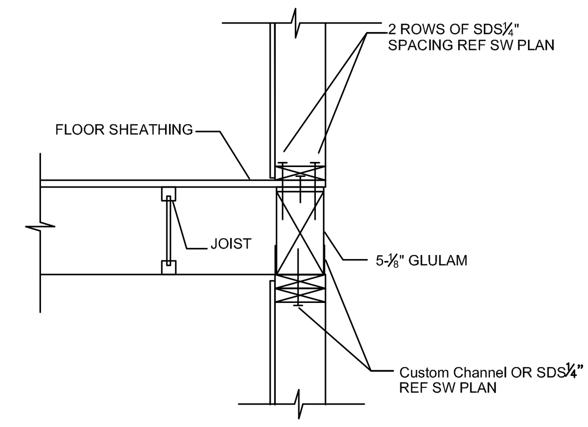

Interior Wall (Stairwell)

5 DETAIL
SCALE: |F" = 1'-0"

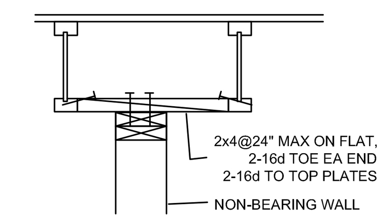

TYP NON-BEARING WALL JOIST-PARALLEL
SCALE: |F" = 1'-0"

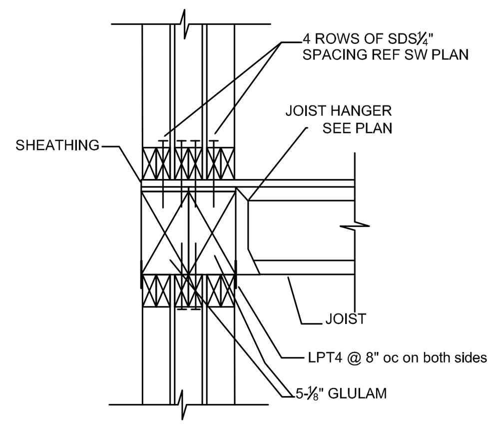

Double Mid-Ply Detail-Stairwell

14 DETAIL
SCALE: |F" = 1'-0"

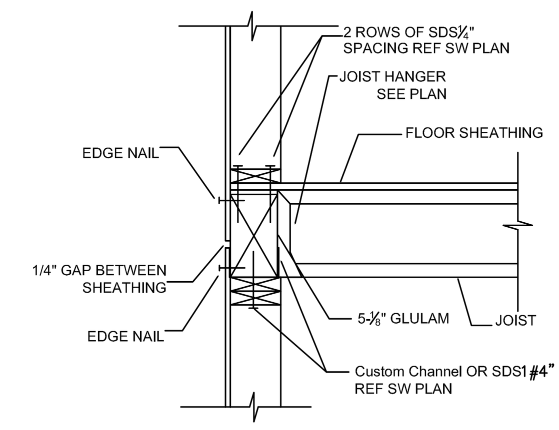

Exterior Wall Joist-Perp

10 DETAIL
SCALE: |F" = 1'-0"

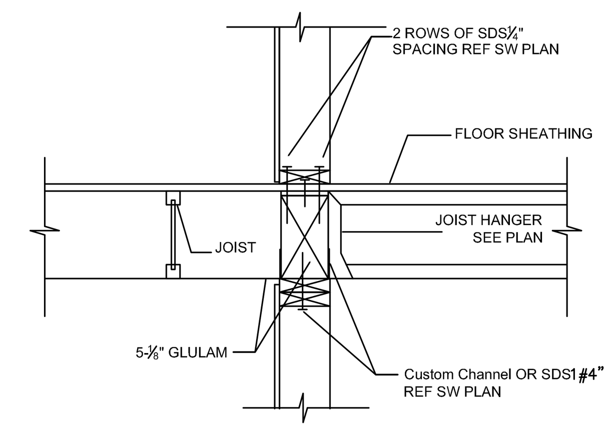

Interior Wall Joist-Perp/Parallel

6 DETAIL
SCALE: |F" = 1'-0"

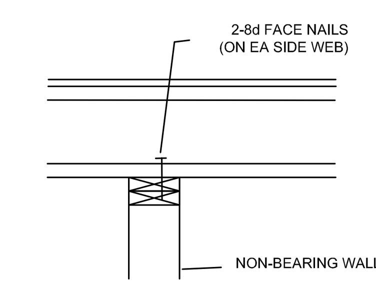

2 TYP NON-BEARING WALL JOIST-PERP
SCALE: |F" = 1'-0"

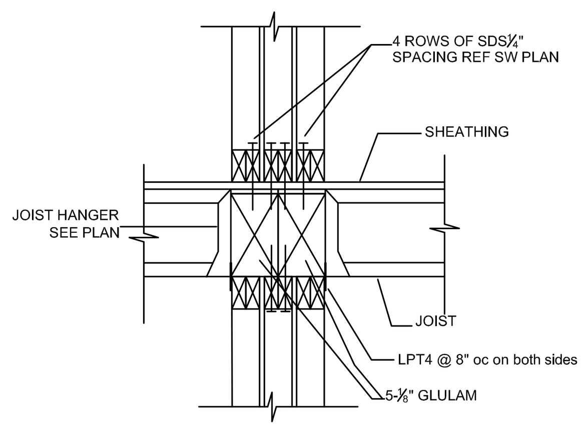

Double Mid-Ply Detail

15 DETAIL
SCALE: |F" = 1'-0"

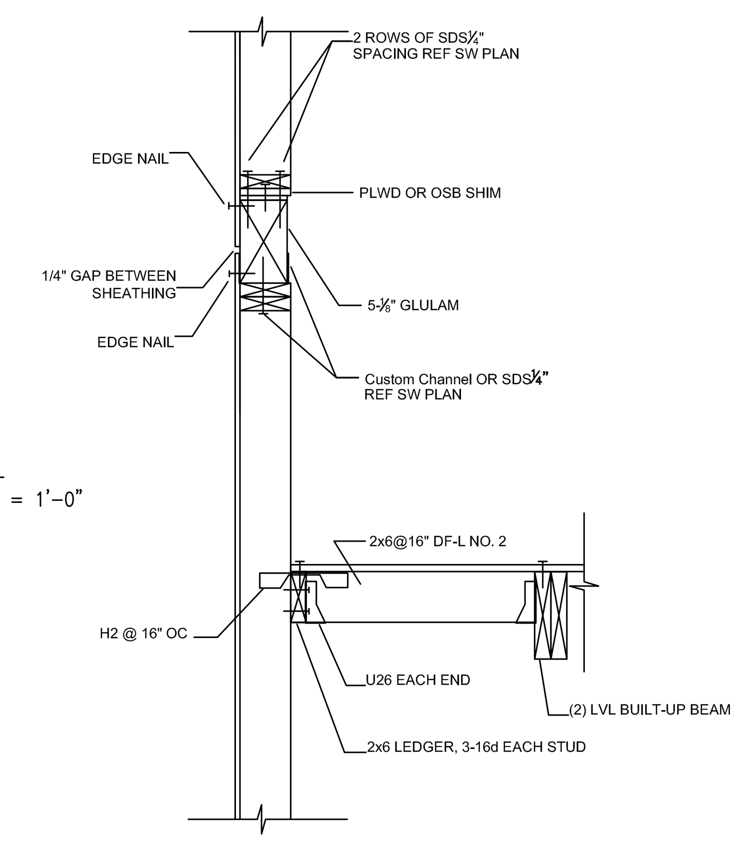

STAIR LANDING

11 DETAIL
SCALE: |F" = 1'-0"

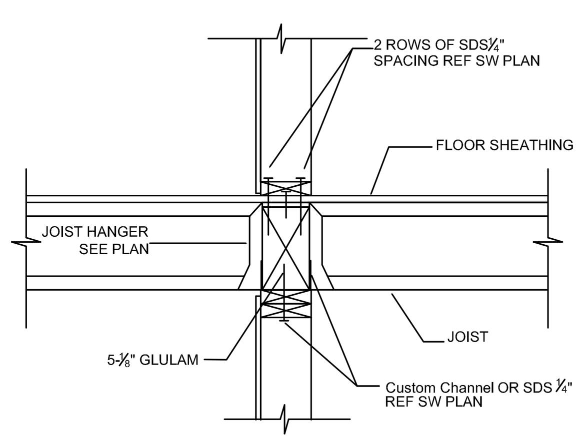

Interior Wall Joist-Perp

7 DETAIL
SCALE: |F" = 1'-0"

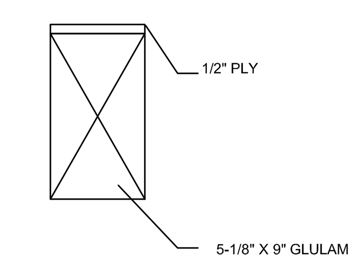

3 TYP GLULAM BUILT-UP SECTION
SCALE: |F" = 1'-0"

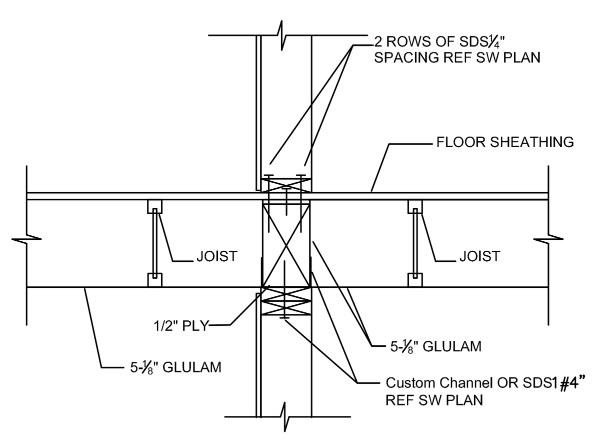

Interior Wall Joist-Parallel

16 DETAIL
SCALE: |F" = 1'-0"

12 DETAIL
SCALE: |F" = 1'-0"

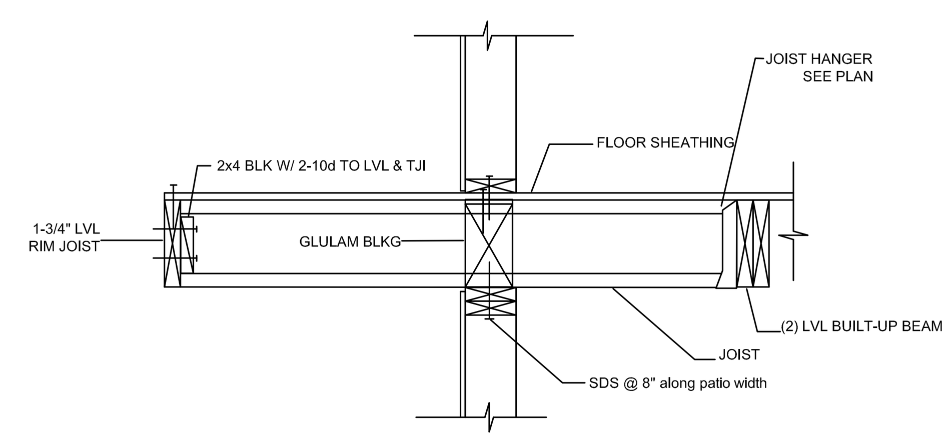

BALCONY CANT FROM LVL

8 DETAIL
SCALE: |F" = 1'-0"

4 DETAIL
SCALE: |F" = 1'-0"

NEESWOOD
Colorado State University
JOHN VAN DE LINDT
University at Buffalo
ANDRE FILIATRAULT
University of Delaware
RACHEL DAVIDSON
TEXAS A&M ENGINEERING
DAVID ROSSOWSKY
Rensselaer
MICHAEL D. SYMANS

NEESwood capstone
(performanced–based design)

colorado state university
fort collins, colorado

CAPSTONE TEAM:

COLORADO STATE UNIVERSITY:
JOHN VAN DE LINDT
KIMBERLY CRONIN P.E.
SHILING PEI

www.engr.colostate.edu/NEESWood/

REVISIONS :
01/06/09 - 90% complete
01/14/09 - 100% complete

SHEET NO :
S4.01

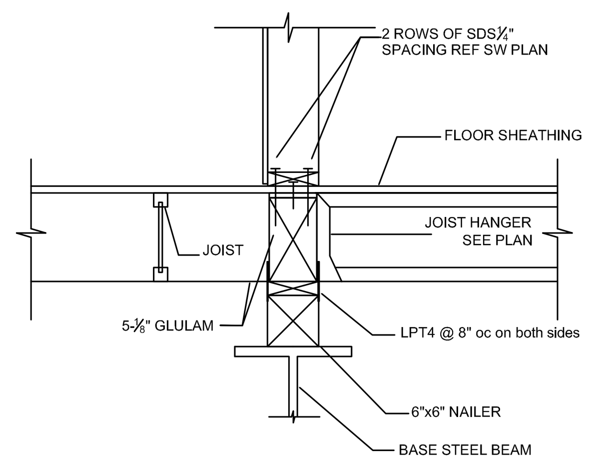

Base Interior Wall Joist-Perp/Parallel

13 S4.02 DETAIL
SCALE: 1" = 1'-0"

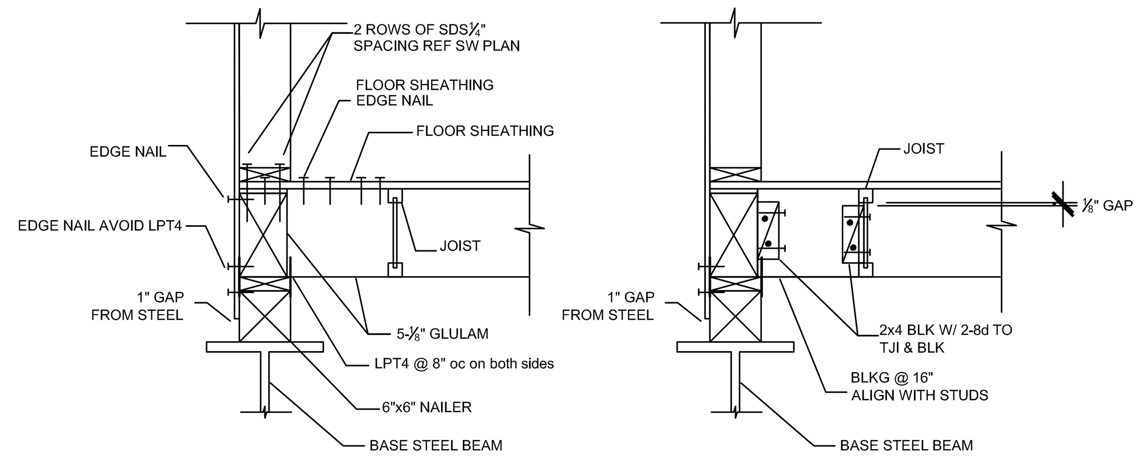

Base Exterior Wall Joist-Parallel

9 S4.02 DETAIL
SCALE: 1" = 1'-0"

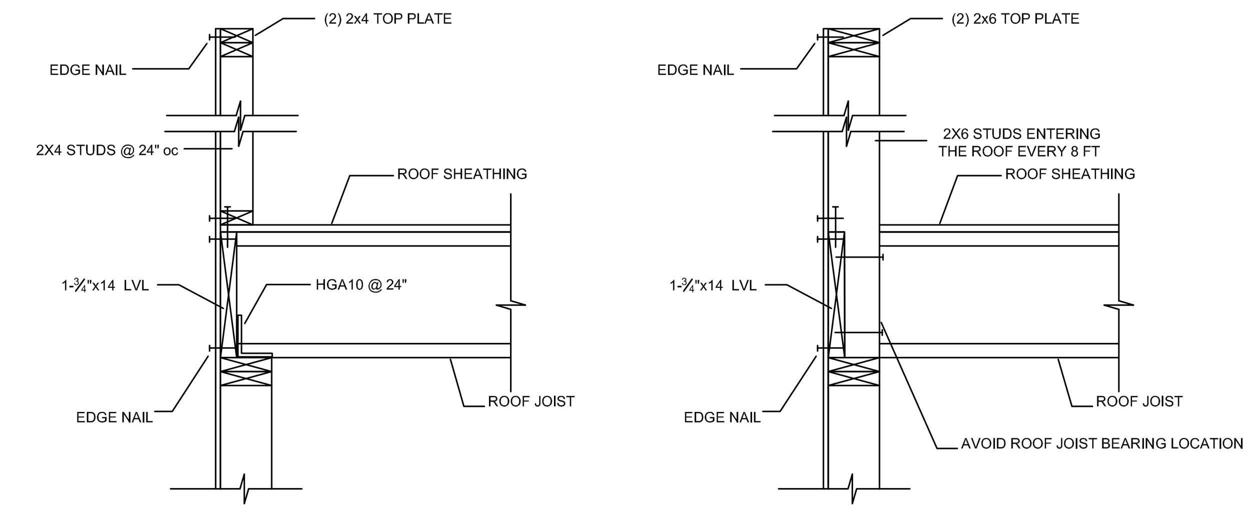

Roof Exterior Wall Joist-Perp

5 S4.02 DETAIL
SCALE: 1" = 1'-0"

SCALE: 1" = 1'-0"

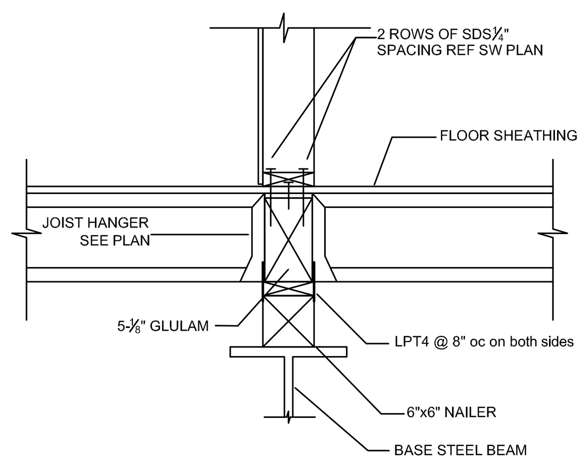

Base Interior Wall Joist-Perp

14 S4.02 DETAIL
SCALE: 1" = 1'-0"

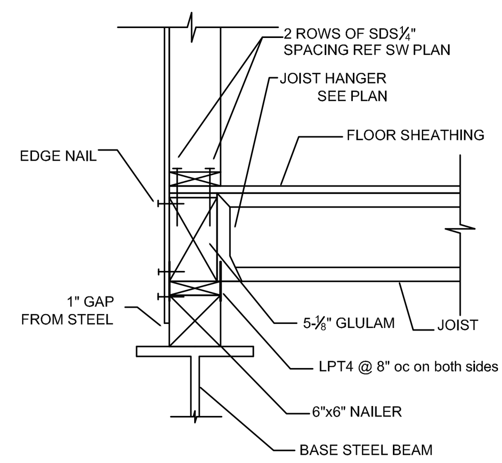

Base Exterior Wall Joist-Perp

10 S4.02 DETAIL
SCALE: 1" = 1'-0"

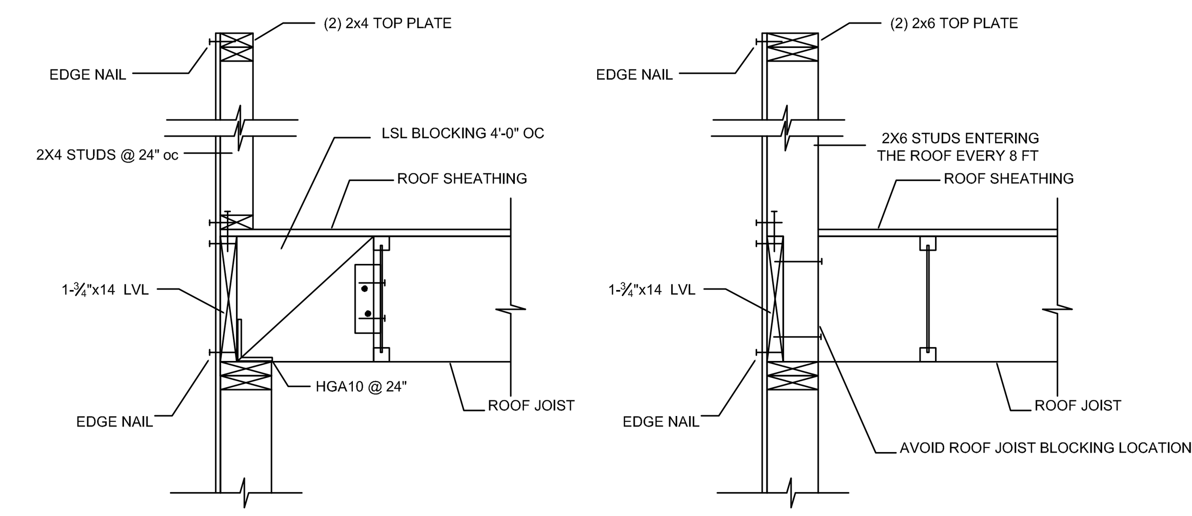

Roof Exterior Wall Joist-Parallel

6 S4.02 DETAIL
SCALE: 1" = 1'-0"

2 DETAIL
SCALE: 1" = 1'-0"

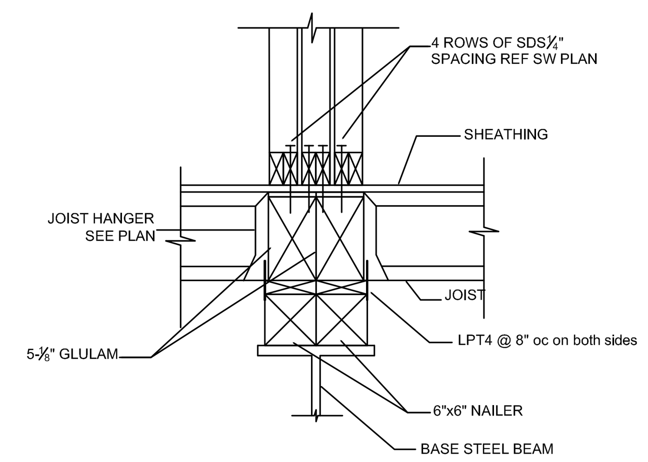

Base Double Midply Wall

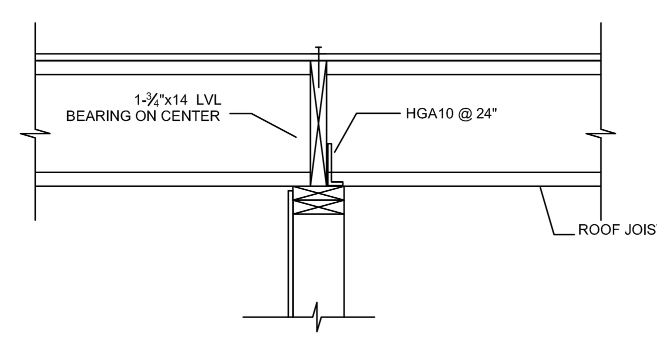

Roof Interior Wall

15 DETAIL
SCALE: 1" = 1'-0"

11 S4.02 DETAIL
SCALE: 1" = 1'-0"

7 S4.02 DETAIL
SCALE: 1" = 1'-0"

3 DETAIL
SCALE: 1" = 1'-0"

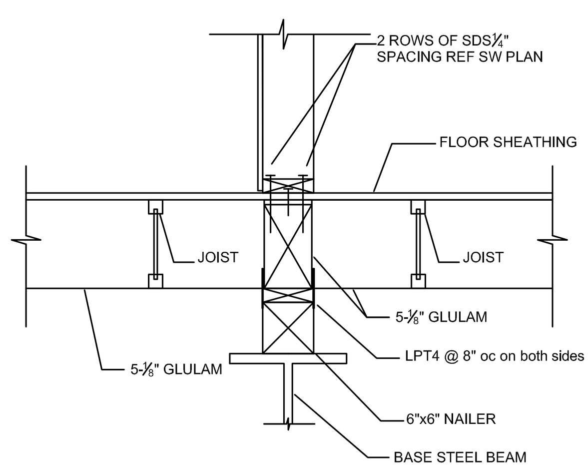

Base Interior Wall Joist-Parallel

16 DETAIL
SCALE: 1" = 1'-0"

12 S4.02 DETAIL
SCALE: 1" = 1'-0"

8 DETAIL
SCALE: 1" = 1'-0"

4 DETAIL
SCALE: 1" = 1'-0"

NEESWOOD

Colorado State University
JOHN VAN DE LINDT
University at Buffalo
ANDRE FILIATRAULT
University of Delaware
RACHEL DAVIDSON
TEXAS A&M ENGINEERING
DAVID ROSSOWSKY
Rensselaer
MICHAEL D. SYMANS

NEESwood capstone
(performanced–based design)
colorado state university
fort collins, colorado

CAPSTONE TEAM:
COLORADO STATE UNIVERSITY:
JOHN VAN DE LINDT
KIMBERLY CRONIN P.E.
SHILING PEI

www.engr.colostate.edu/NEESWood/

REVISIONS :
01/06/09 - 90% complete
01/14/09 - 100% complete

SHEET NO :
S4.02

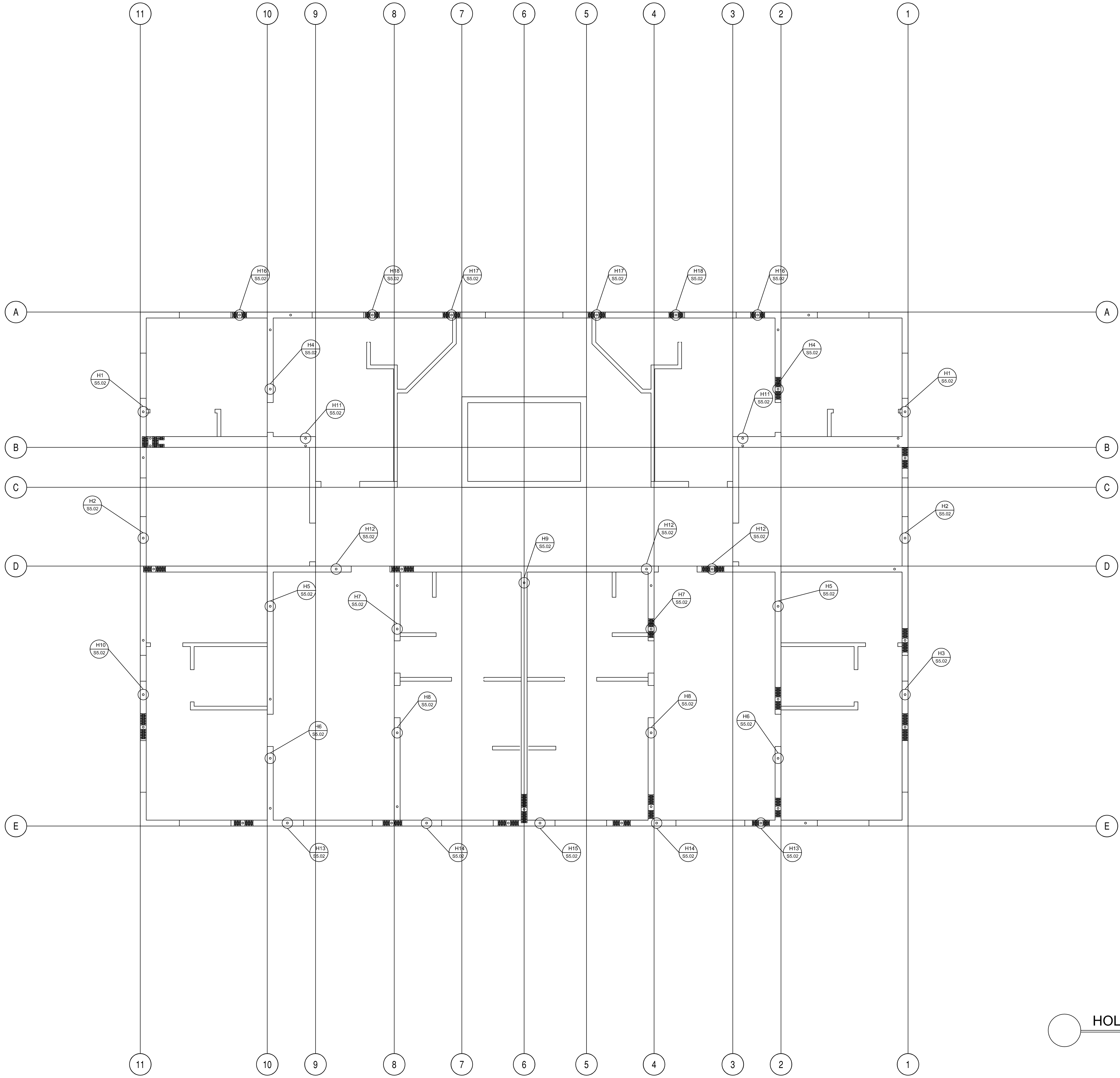

HOLD-DOWN SYSTEM

JOHN VAN DE LINDT

ANDRE FILIATRAULT

RACHEL DAVIDSON

DAVID ROSSOWSKY

MICHAEL D. SYMANS

NEESwood capstone

(performanced–based design)

colorado state university
fort collins, colorado

CAPSTONE TEAM:

COLORADO STATE UNIVERSITY:
JOHN VAN DE LINDT
KIMBERLY CRONIN P.E.
SHILING PEI

www.engr.colostate.edu/NEESWood/

REVISIONS :

01/06/09 - 90% complete
01/14/09 - 100% complete

SHEET NO :

S5.01

Direction: End of the Wall

Direction: Center of the Wall

	Base	St2	St3	St4	St5	St6
H1	1-3/4(H150) SPEC	1-3/4(H) SPEC	SR9H-12	SR9H-12	SR7H-12	SR5H-10
H2	1-3/4(H150) SPEC	1-3/4(H) SPEC	SR9H-12 11C: (SR10H-12)	SR9H-12	SR7H-12	SR5H-10
H3	1-3/4(H150) SPEC	1-3/4(H) SPEC	SR10H-12	SR9H-12	SR7H-12	SR5H-10
H4	1-3/4(H) SPEC	SR10H-12	SR9H-12	SR7H-12	SR7H-12	SR5H-10
H5	1-3/4(H150) SPEC	SR10H-12 10B:(1-3/4(H) SPEC)	SR9H-12	SR7H-12	SR5-10 10B:(SR5-12)	
H6	1-3/4(H) SPEC	SR10H-12 10C:(SR9H-12)	SR9-12	SR7-12	SR5-10 10C:(SR5-12)	
H7	1-3/4(H) SPEC	SR9H-12 8A:(SR10H-12)	SR9H-12	SR7-12	SR5-10	
H8	1-3/4(H150) SPEC	1-3/4(H) SPEC	SR9H-12	SR7H-12	SR5-10	
H9	1-3/4(H150) SPEC	1-3/4(H) SPEC	SR9H-12	SR9-12	SR5H-12	
H10	1-3/4(H150) SPEC	1-3/4(H) SPEC	SR9H-12	SR7H-12	SR7H-12	
H11	1-3/4(H) SPEC	SR9H-12	SR7H-12	SR7-12	SR5-12	
H12	1-3/4(H) SPEC	SR10H-12	SR9H-12	SR7H-12	SR5H-12	SR5-10
H13	1-3/4(H150) SPEC	1-3/4(H) SPEC	SR10H-12	SR9-12	SR5H-12	SR5-10
H14	1-3/4(H150) SPEC	1-3/4(H) SPEC	SR9H-12	SR7H-12	SR5H-12	SR5-10
H15	2 (H150) SPEC	1-3/4(H) SPEC	SR10H-12	SR9H-12	SR7-12	SR5-10
H16	SR10H-12	SR9H-12	SR7H-12	SR7-12	SR5-12	SR5-10
H17	1-3/4(H) SPEC	SR9H-12	SR7H-12	SR7-12	SR5-12	SR5-10
H18	SR10H-12					

Roof

NOTE:
ALL HOLD-DOWN RODS SHIFT 1" PER-STORY TOWARDS THE EDGE OF WALLS FOR STORY 1-5.
ALL HOLD-DOWN CONFIGURATION SYMMETRIC ABOUT THE CENTER OF WALL.
THE STUDS SHOWN ARE THE MINIMUM NUMBER OF STUDS REQUIRED, THE NUMBER CAN BE EXCEEDED IN CONSTRUCTION IF NEEDED FOR FRAMING.

NEESWOOD
JOHN VAN DE LINDT
ANDRE FILIATRAULT
RACHEL DAVIDSON
DAVID ROSSOWSKY
MICHAEL D. SYMANS

NEESwood capstone
(performanced–based design)
colorado state university
fort collins, colorado

CAPSTONE TEAM:
COLORADO STATE UNIVERSITY:
JOHN VAN DE LINDT
KIMBERLY CRONIN P.E.
SHILING PEI
www.engr.colostate.edu/NEESWood/

REVISIONS :
01/06/09 - 90% complete
01/14/09 - 100% complete

SHEET NO :
S5.02

Strap hardware detail for floor framing

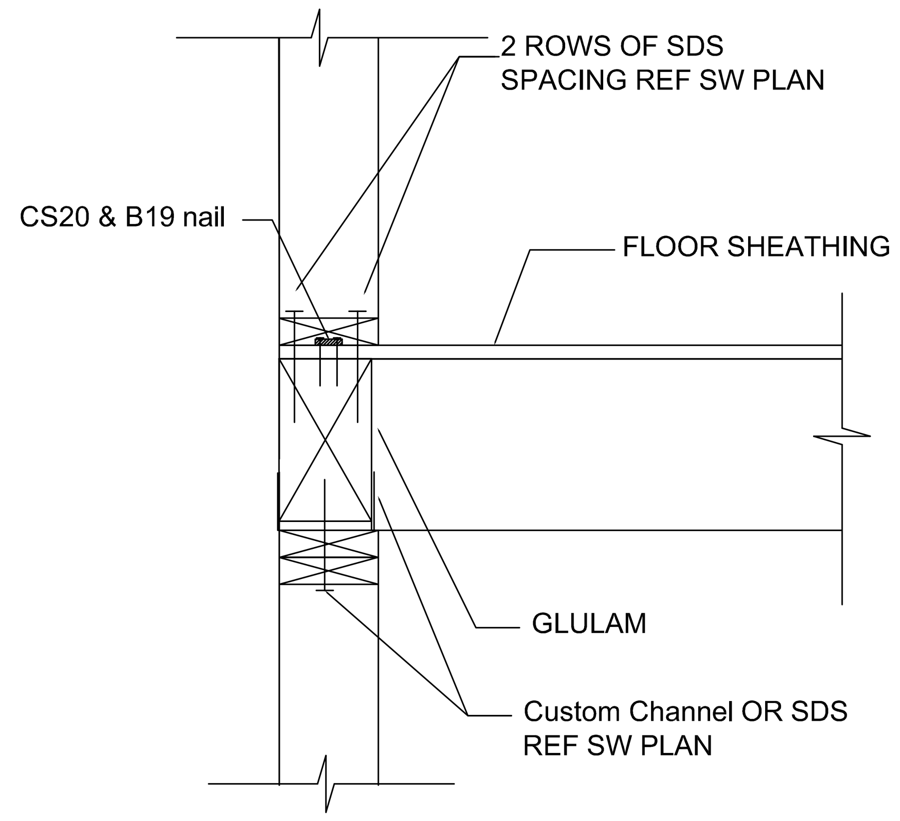

1 DETAIL S6.01

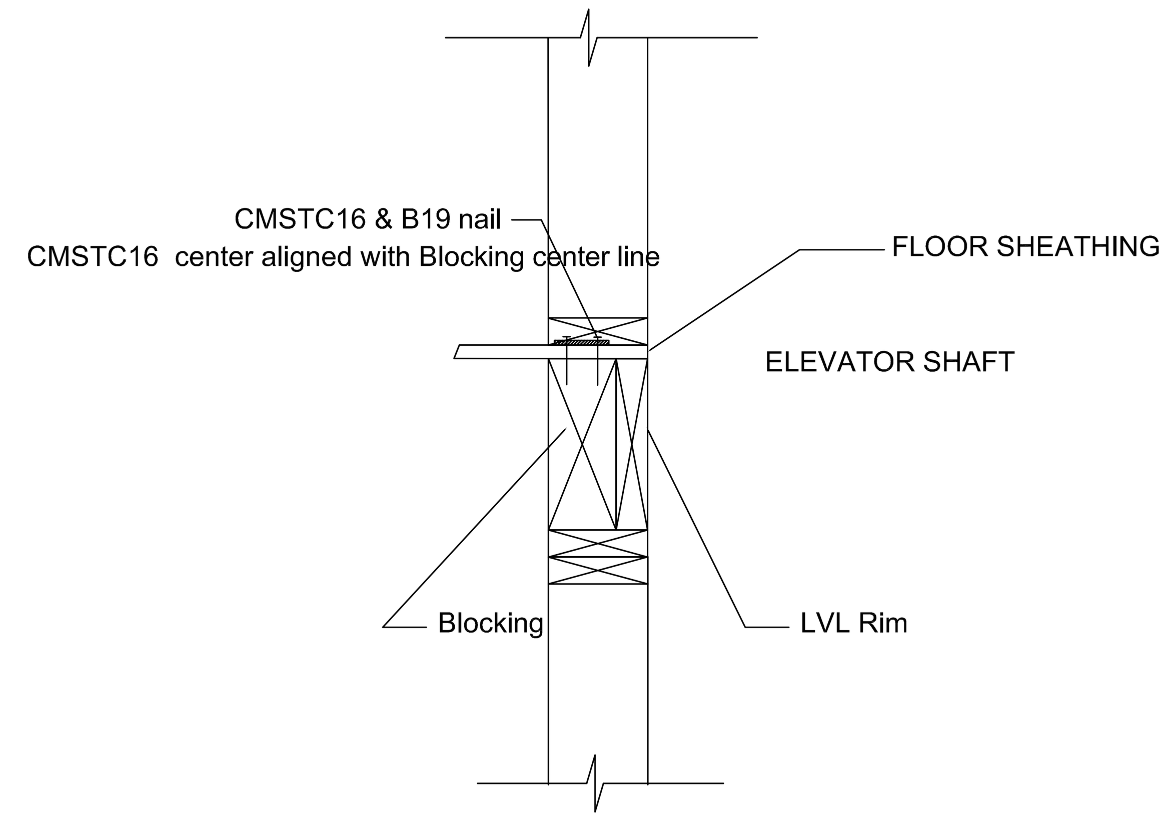

2 DETAIL S6.01

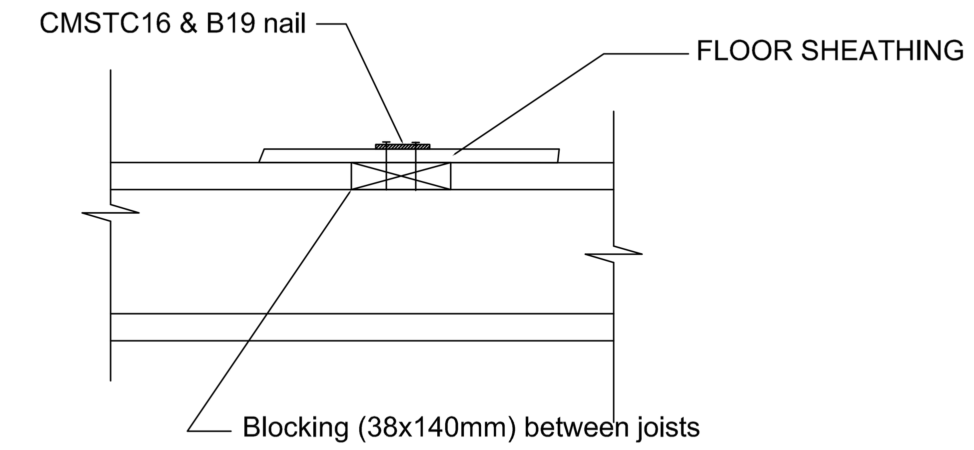

3 DETAIL S6.01

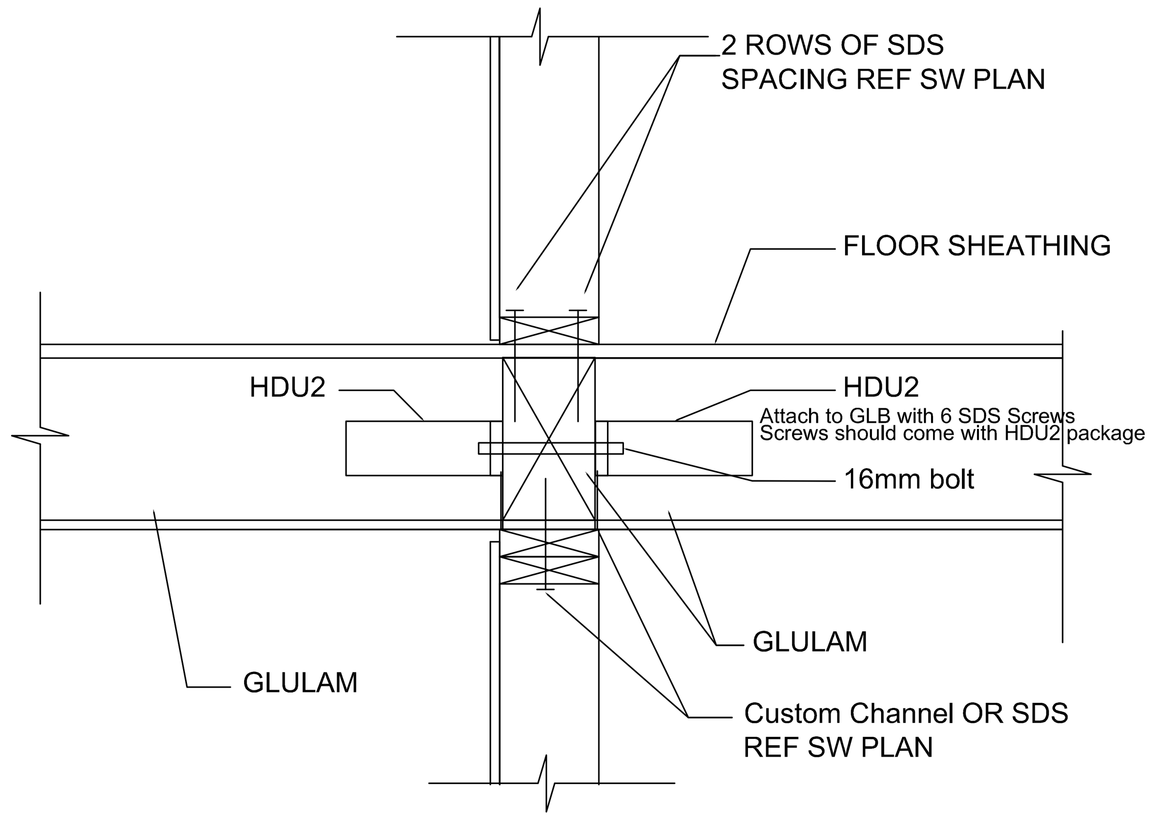

4 DETAIL S6.01

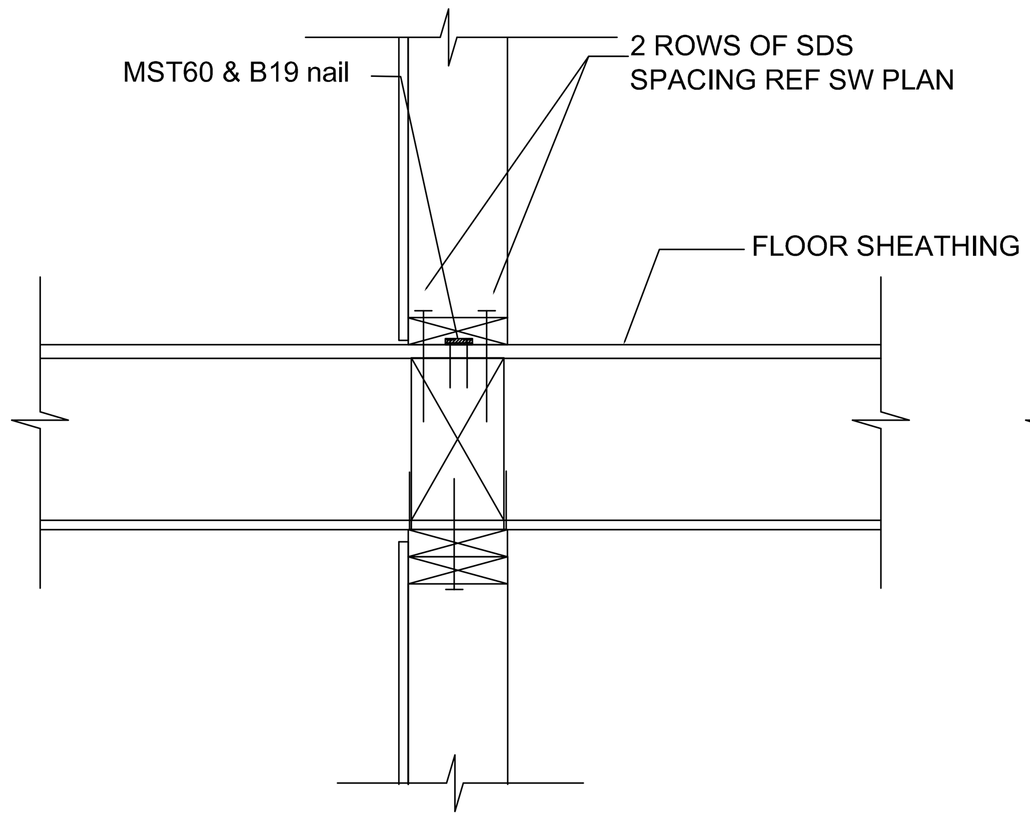

5 DETAIL S6.01

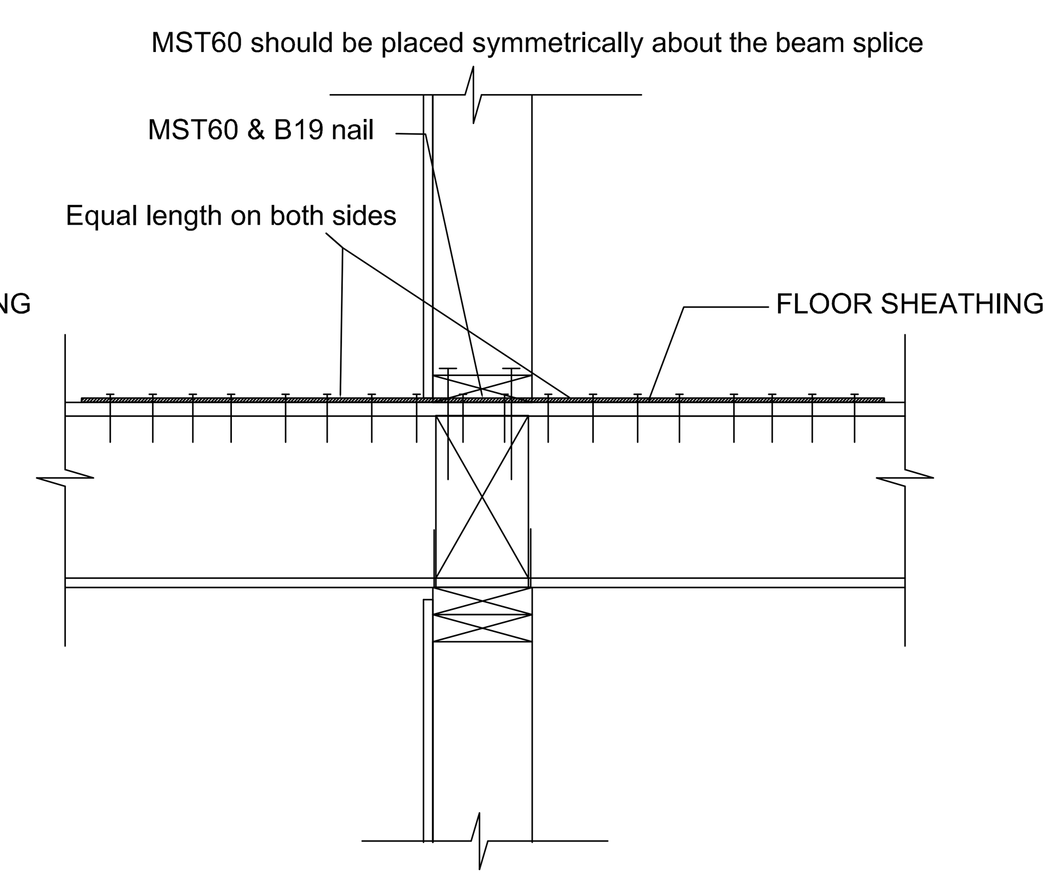

5 (a) DETAIL S6.01

Detail 5(a) is detail 5 viewed from the perpendicular angle

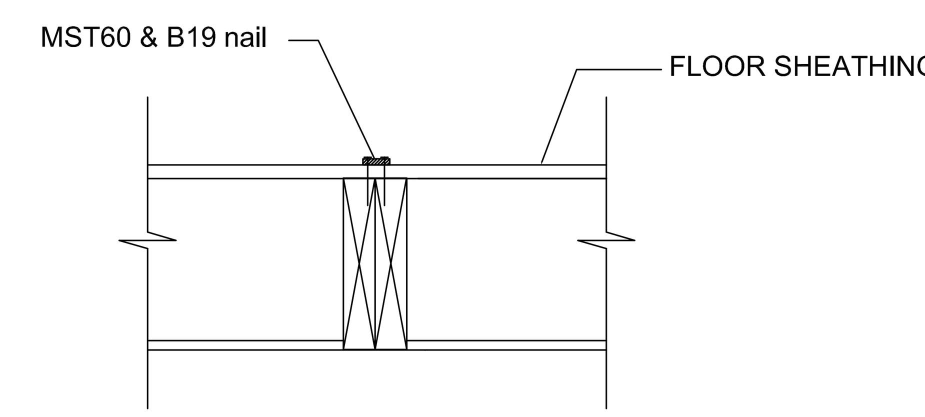

6 DETAIL S6.01

NEESWOOD

JOHN VAN DE LINDT
ANDRE FILIATRAULT
RACHEL DAVIDSON
DAVID ROSSOWSKY
MICHAEL D. SYMANS

NEESwood capstone

(performanced–based design)

colorado state university
fort collins, colorado

CAPSTONE TEAM:

COLORADO STATE UNIVERSITY:
JOHN VAN DE LINDT
KIMBERLY CRONIN P.E.
SHILING PEI

www.engr.colostate.edu/NEESWood/

REVISIONS :

04/02/09 - 100% complete

SHEET NO :

S6.01

Steel Floor Plan (Dec 08)

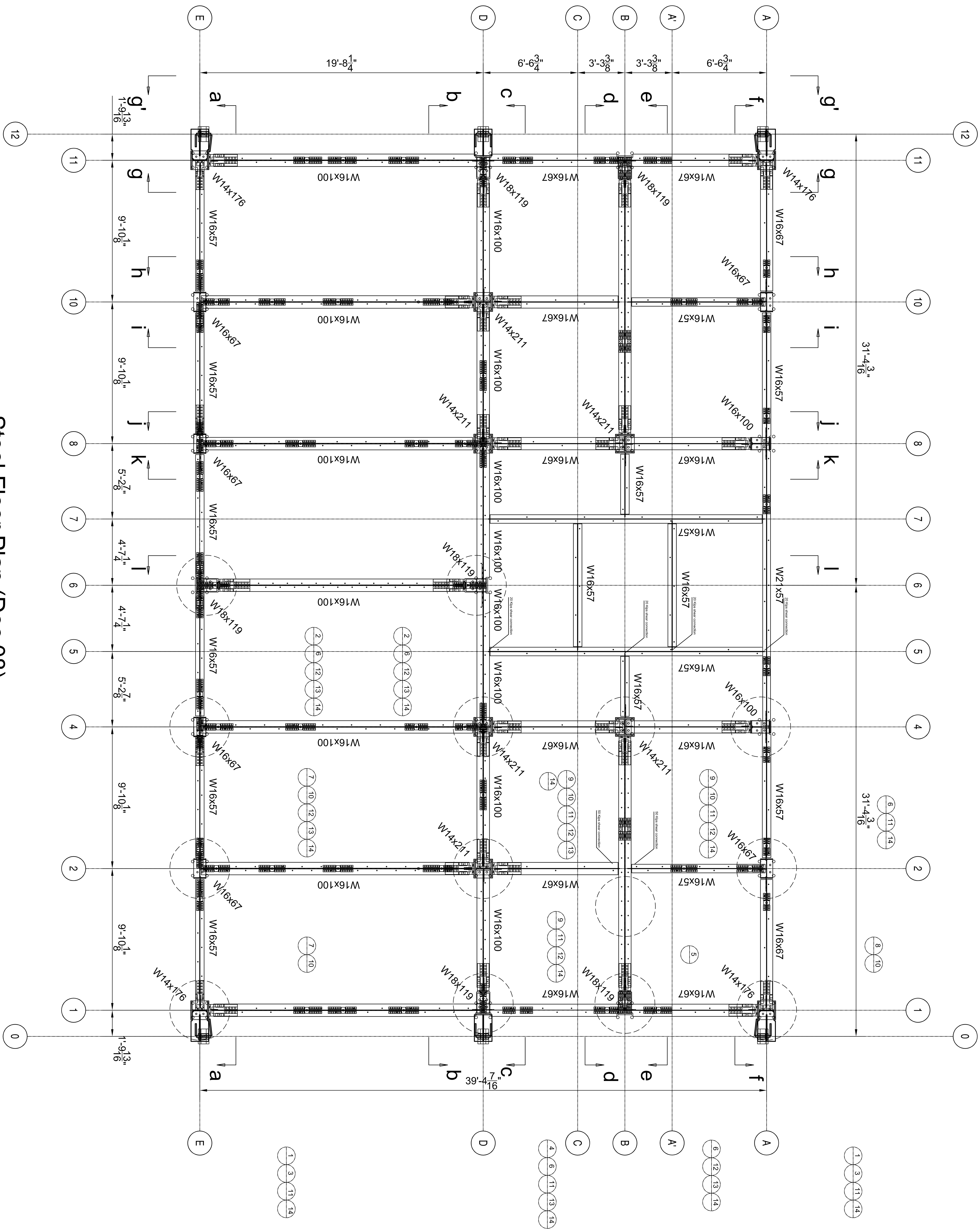

Drawing Name: Floor Plan	Project Name: NEESWood Capstone - Simpson		Revision: 1 of 1
Drawn By:	Reviewed By:	Date:	Sheet:

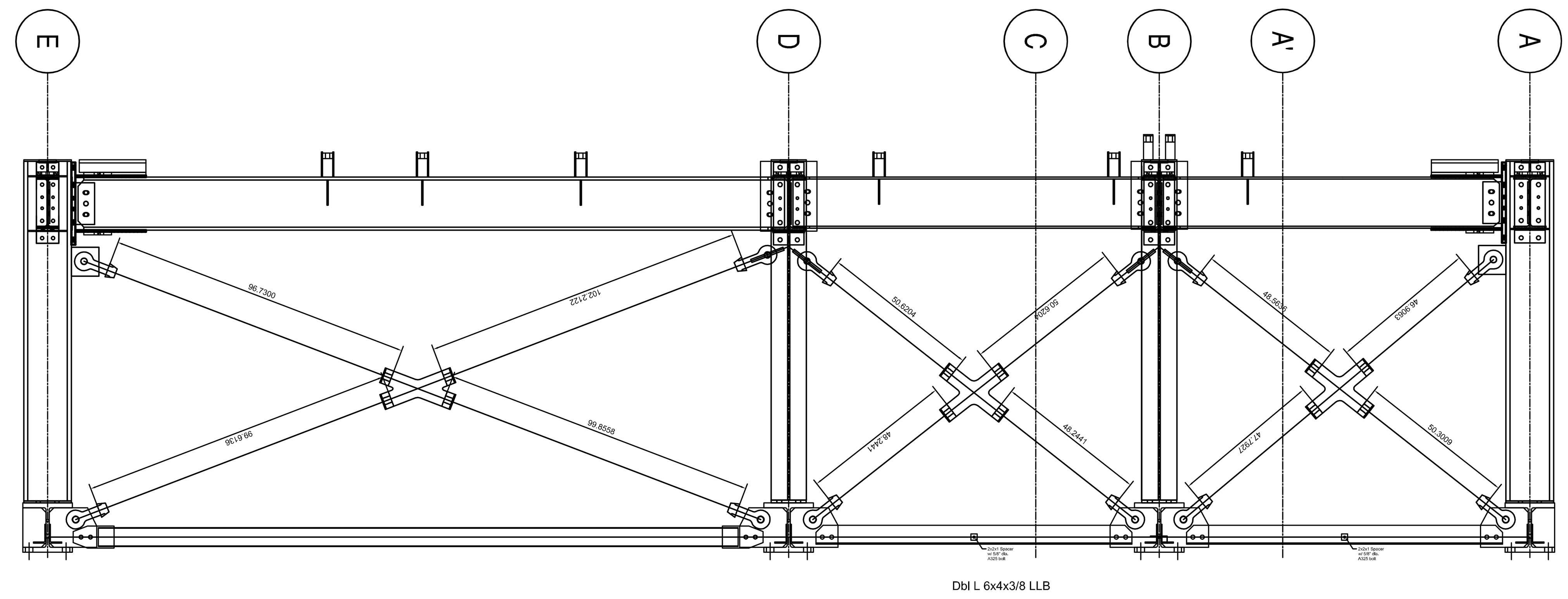

g-g

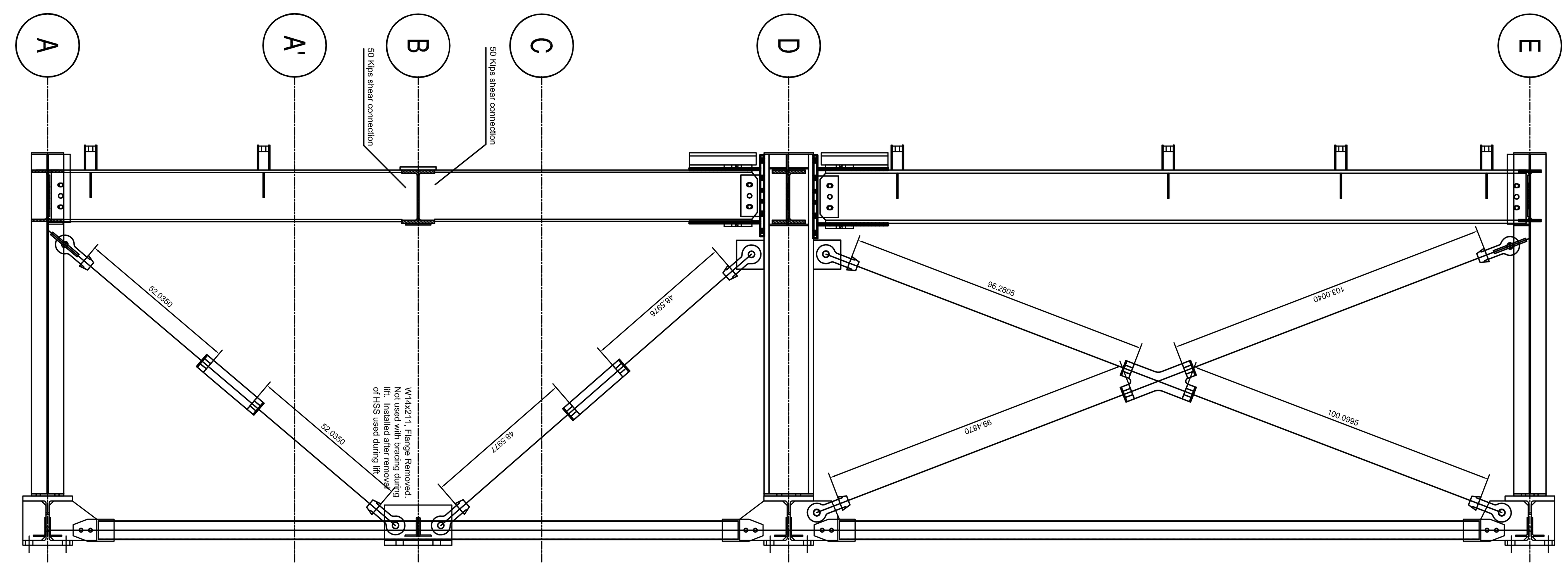

h-h

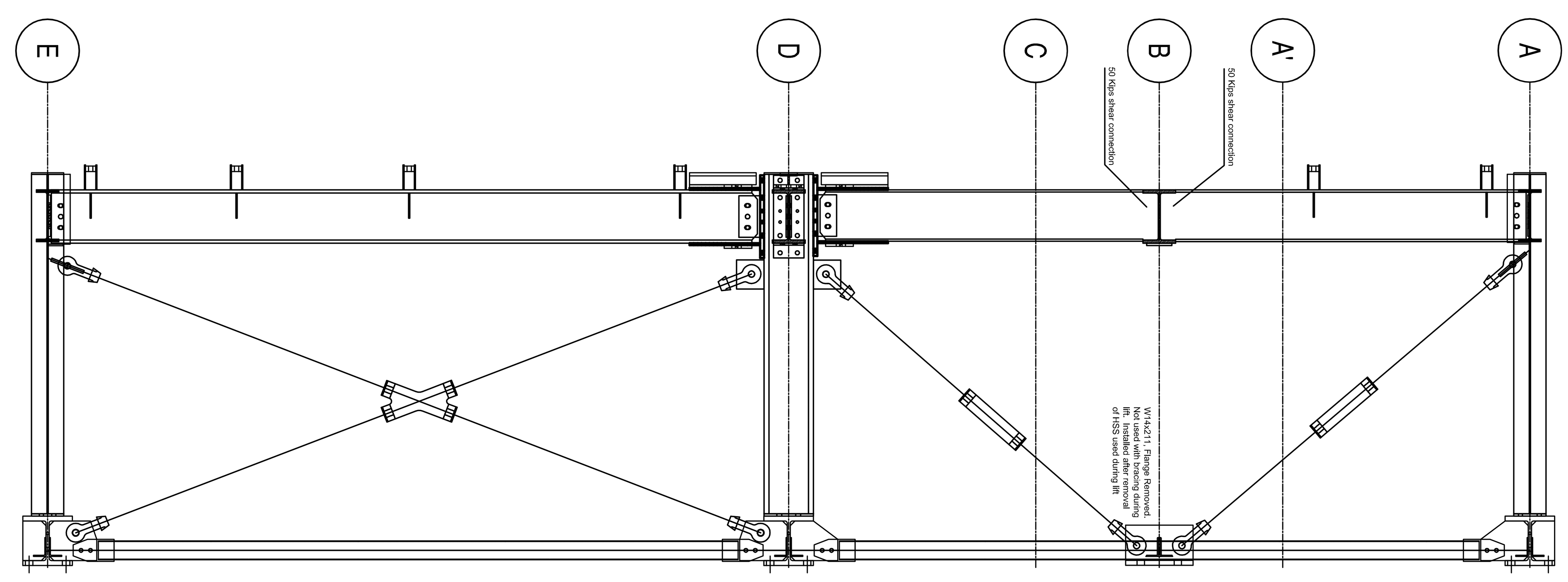

i-i

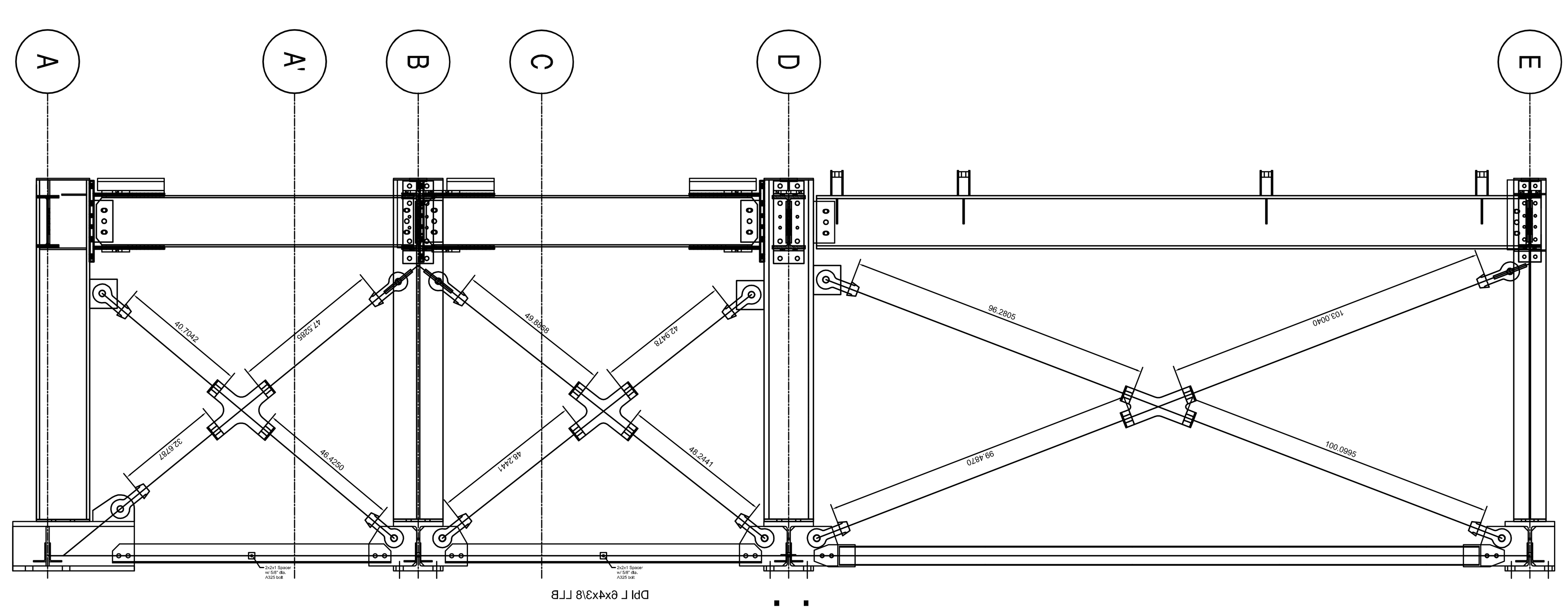

j-j

Drawing Name: Floor Plan	Project Name: NEESWood Capstone - Simpson		Revision: 1 of 1
Drawn By:	Reviewed By:	Date:	Sheet:

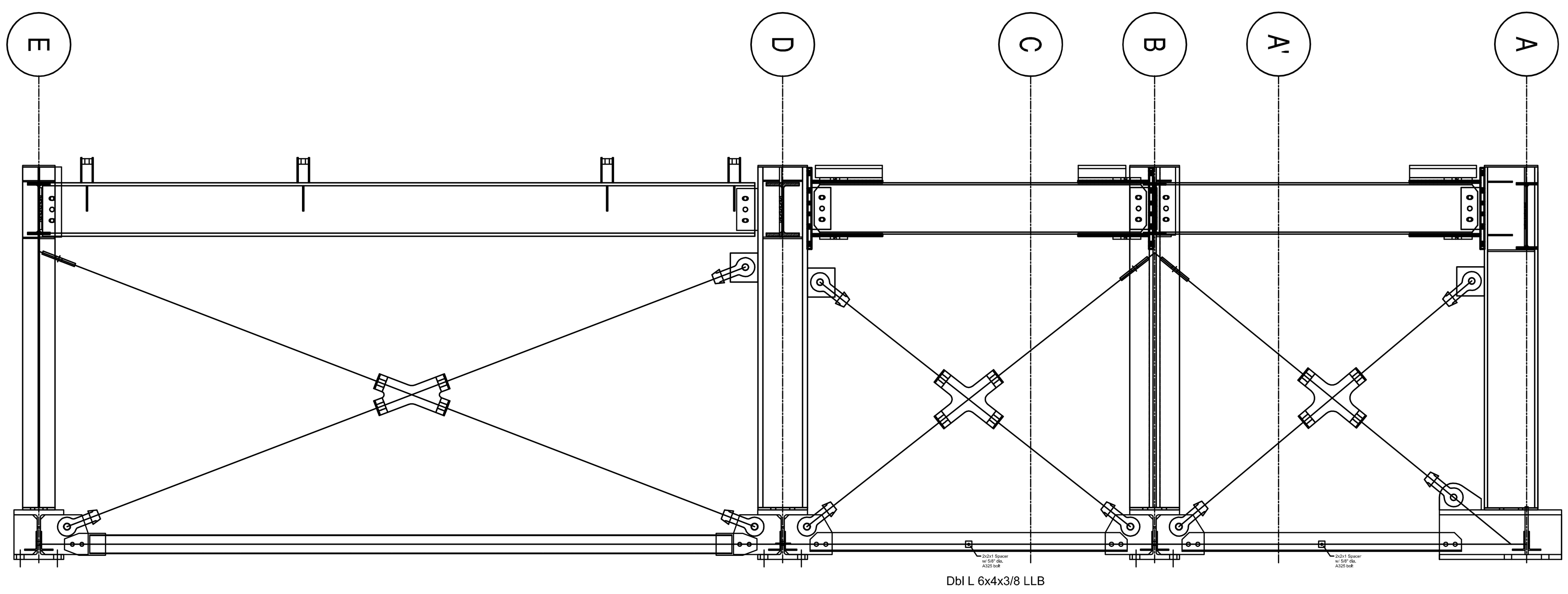

k-k

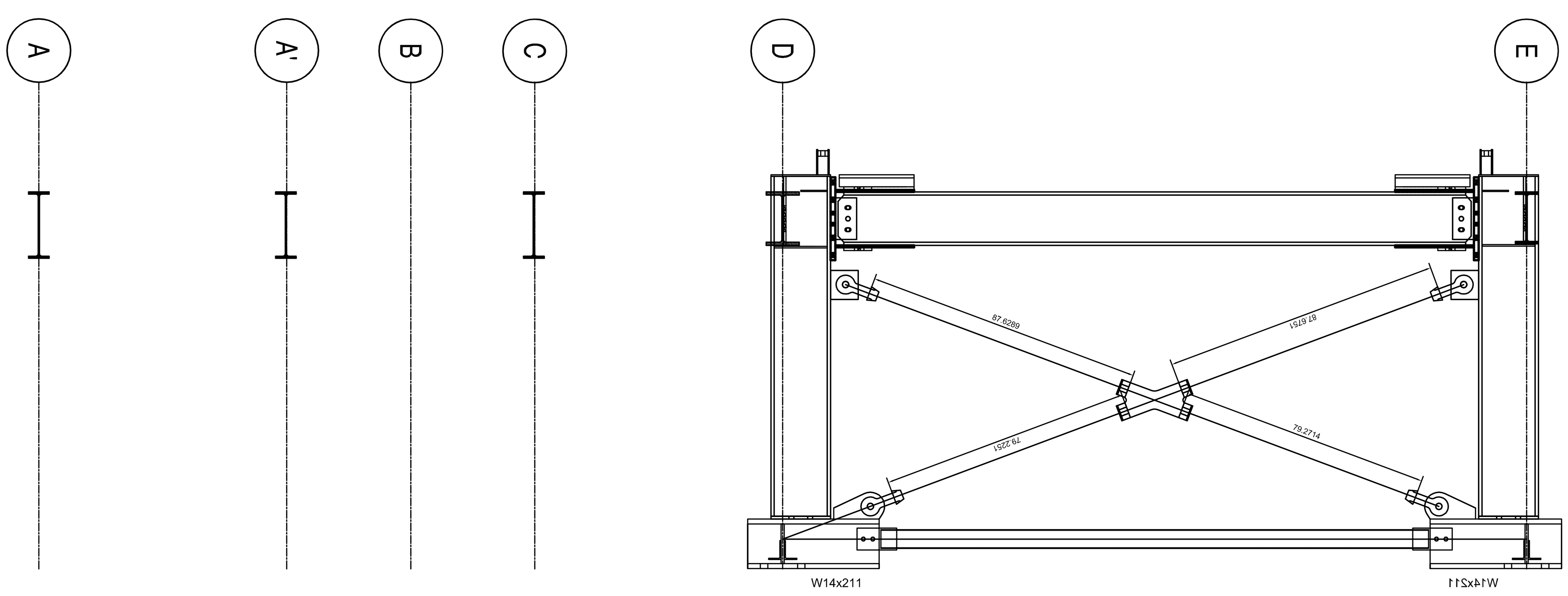

l-l

B:\TGLab_Marketing_Tools\SimpsonLogo.jpg	Drawing Name: Floor Plan	Project Name: NEESWood Capstone - Simpson	Revision: 1 of 1
	Drawn By:	Reviewed By: Date:	Sheet:

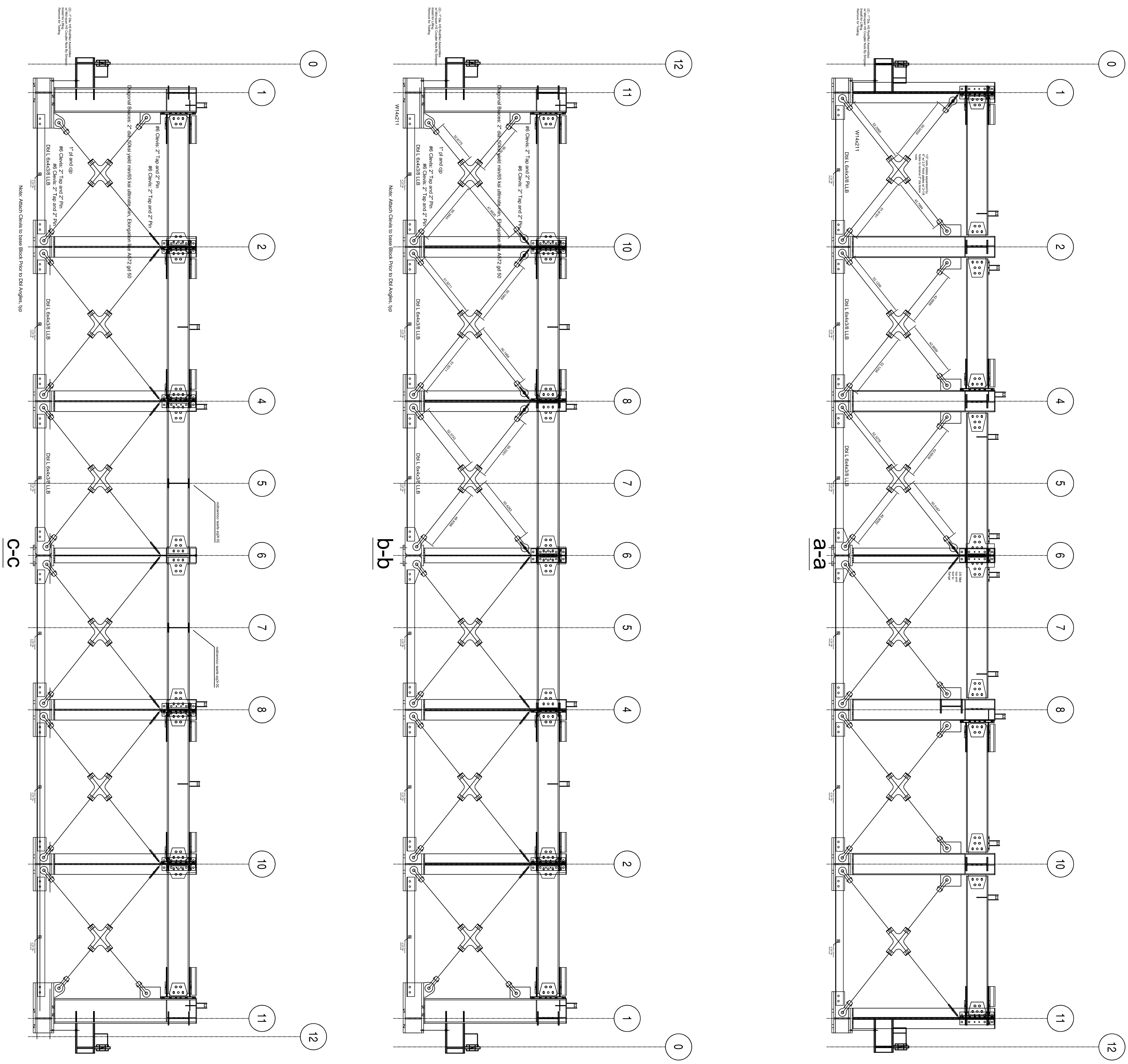

Drawing Name:
Floor Plan

Project Name:
NEESWood Capstone - Simpson

Revision:
1 of 1

Drawn By:

Reviewed By:

Date:

Sheet:

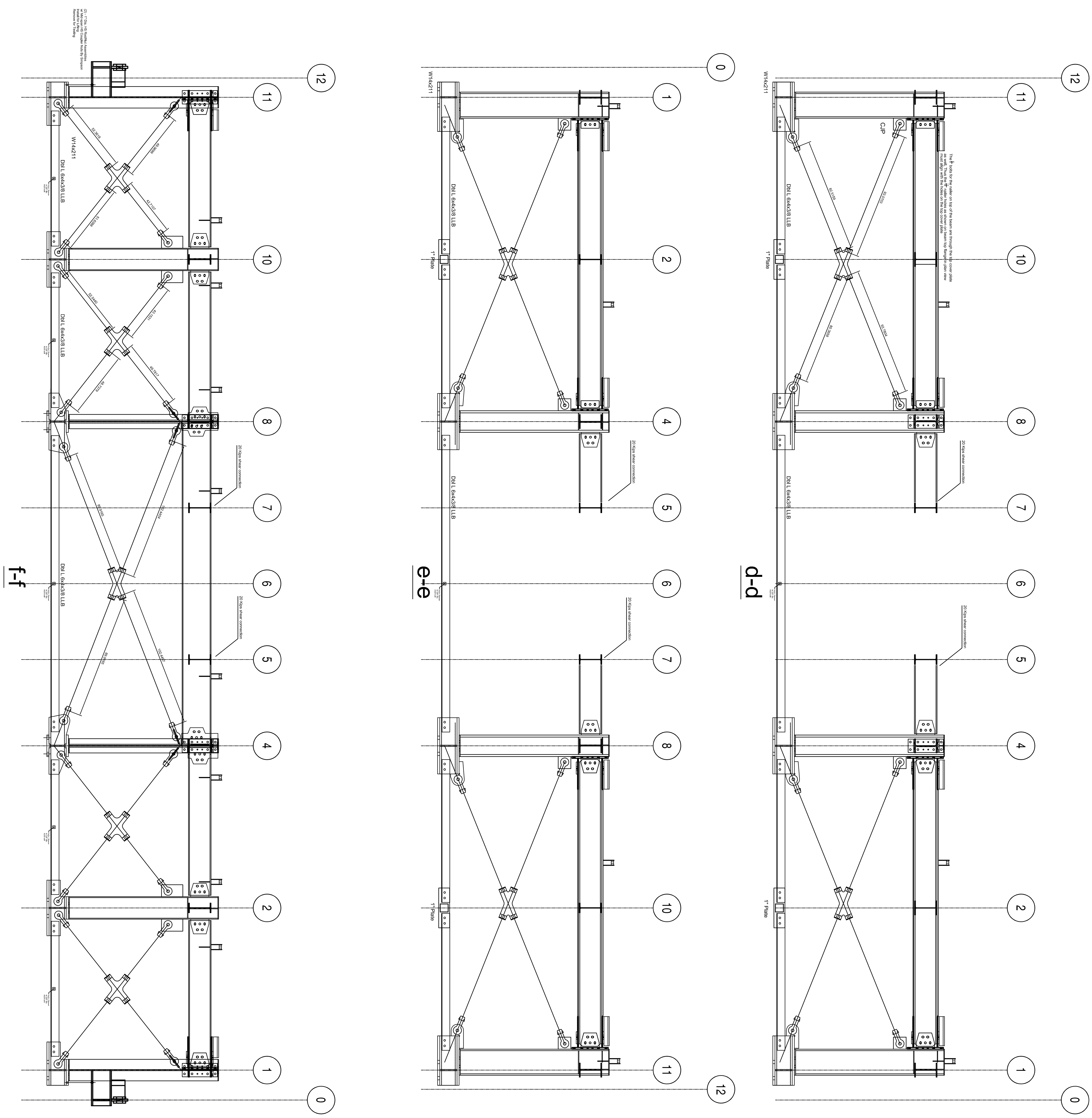

Drawing Name: Floor Plan	Project Name: NEESWood Capstone - Simpson		Revision: 1 of 1
Drawn By:	Reviewed By:	Date:	Sheet:

Appendix B

Structural drawings of wall assemblies

Appendix B

Notes for wall assembly drawing

The wall assembly drawings include both the framing drawing and sheathing panel layout. The shaded panel is the wall segment that needs to be nailed using the nailing patter specified in the title of each drawing:

- 2/12: 2” edge nail spacing, 12” field nail spacing
- 2/12-D: 2” edge nail spacing, 12” field nail spacing, double sided
- 3/12: 3” edge nail spacing, 12” field nail spacing
- 3/12-D: 3” edge nail spacing, 12” field nail spacing, double sided
- 4/12: 4” edge nail spacing, 12” field nail spacing
- 4/12-D: 4” edge nail spacing, 12” field nail spacing, double sided
- 6/12: 6” edge nail spacing, 12” field nail spacing
- 6/12-D: 6” edge nail spacing, 12” field nail spacing, double sided

The rest of sheathing panels were attached using 6/12 nailing pattern.

All of the framing was constructed with 2x6 dimension lumber (with the exception of Midply walls).

Appendix B

Wall assembly for Story 2

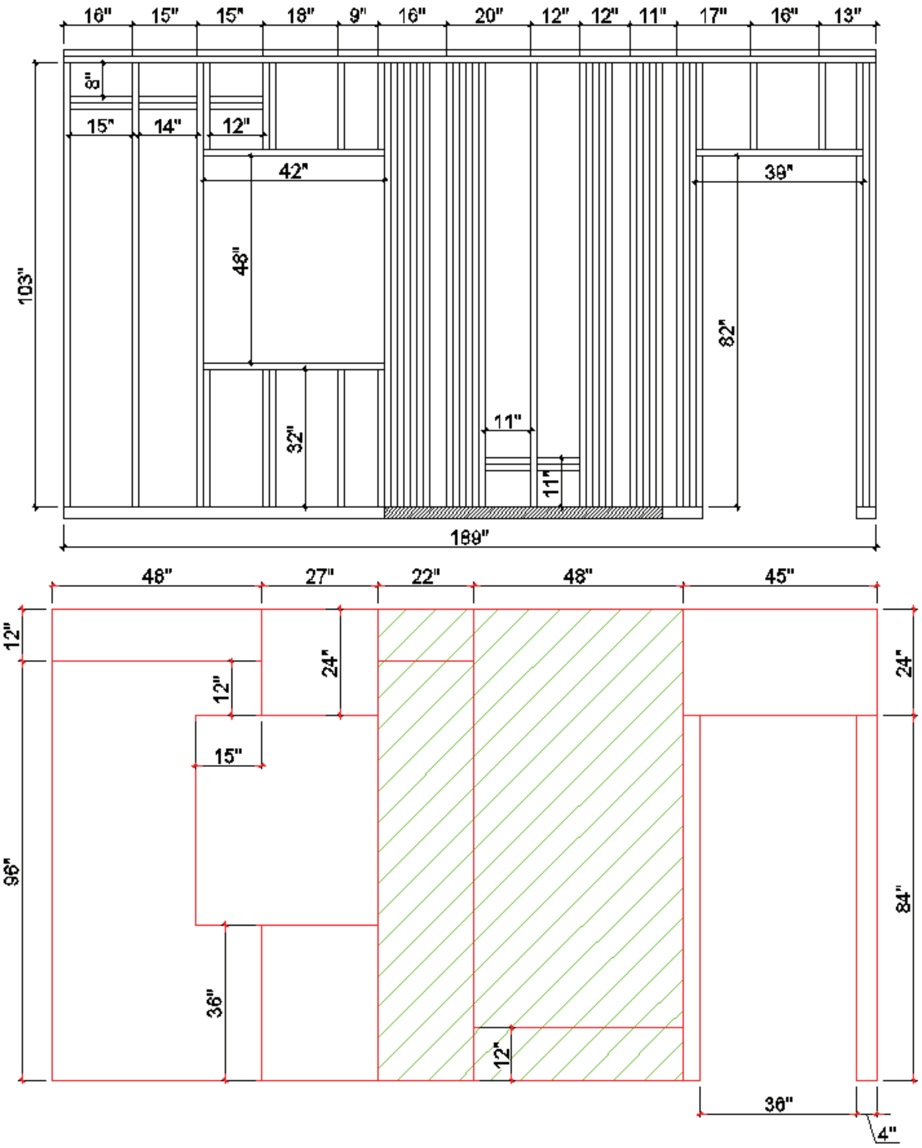

Figure B.1: Assembly for story 2, wall 1A, 11A, 2/12-D

Appendix B

Wall assembly for Story 2

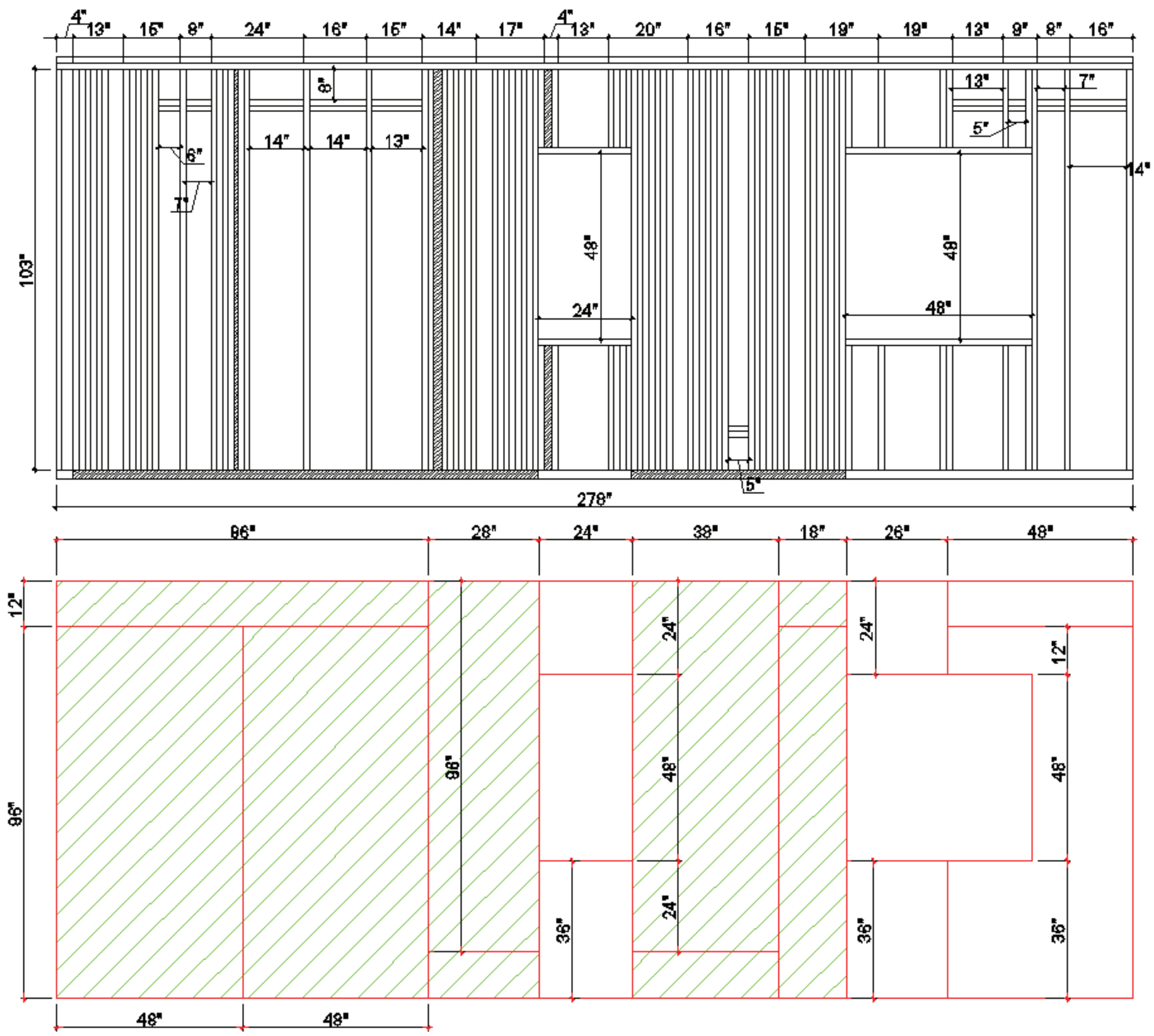

Figure B.2: Assembly for story 2, wall 1B-C, 11B-C, 2/12-D

Appendix B

Wall assembly for Story 2

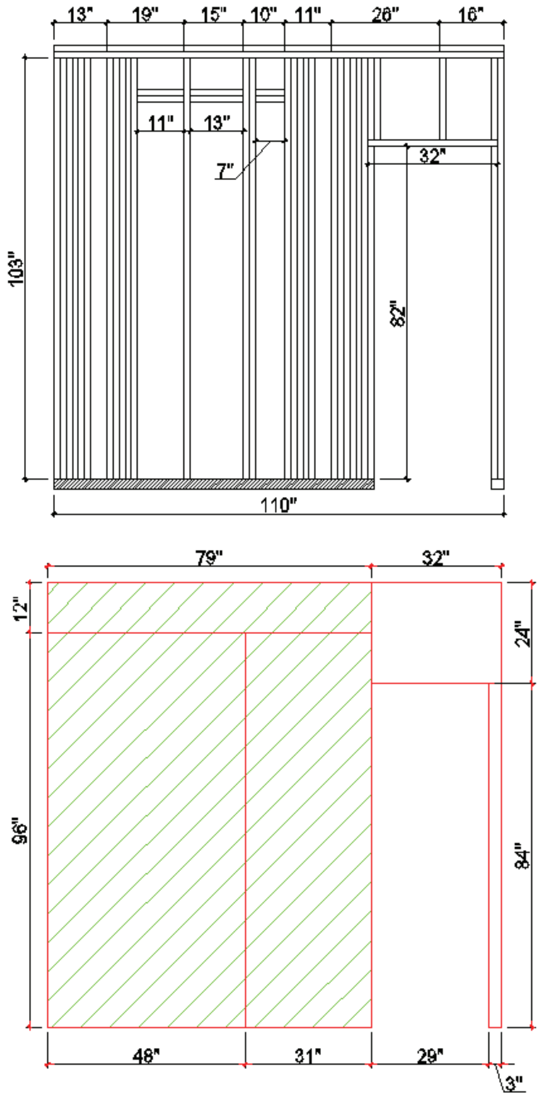

Figure B.3: Assembly for story 2, wall 2A, 10A, 3/12-D

Appendix B

Wall assembly for Story 2

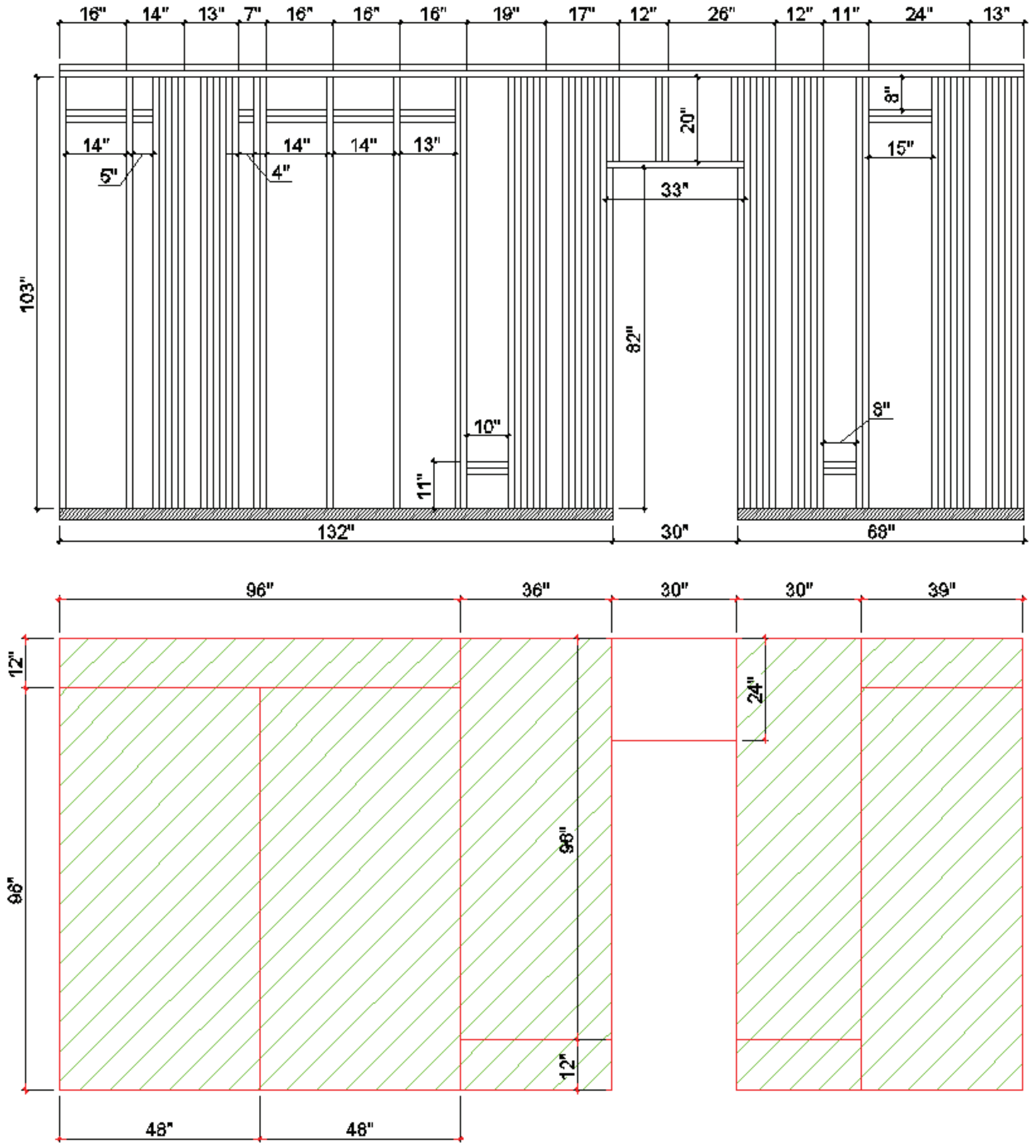

Figure B.4: Assembly for story 2, wall 2B-C, 10B-C, 3/12-D

Appendix B

Wall assembly for Story 2

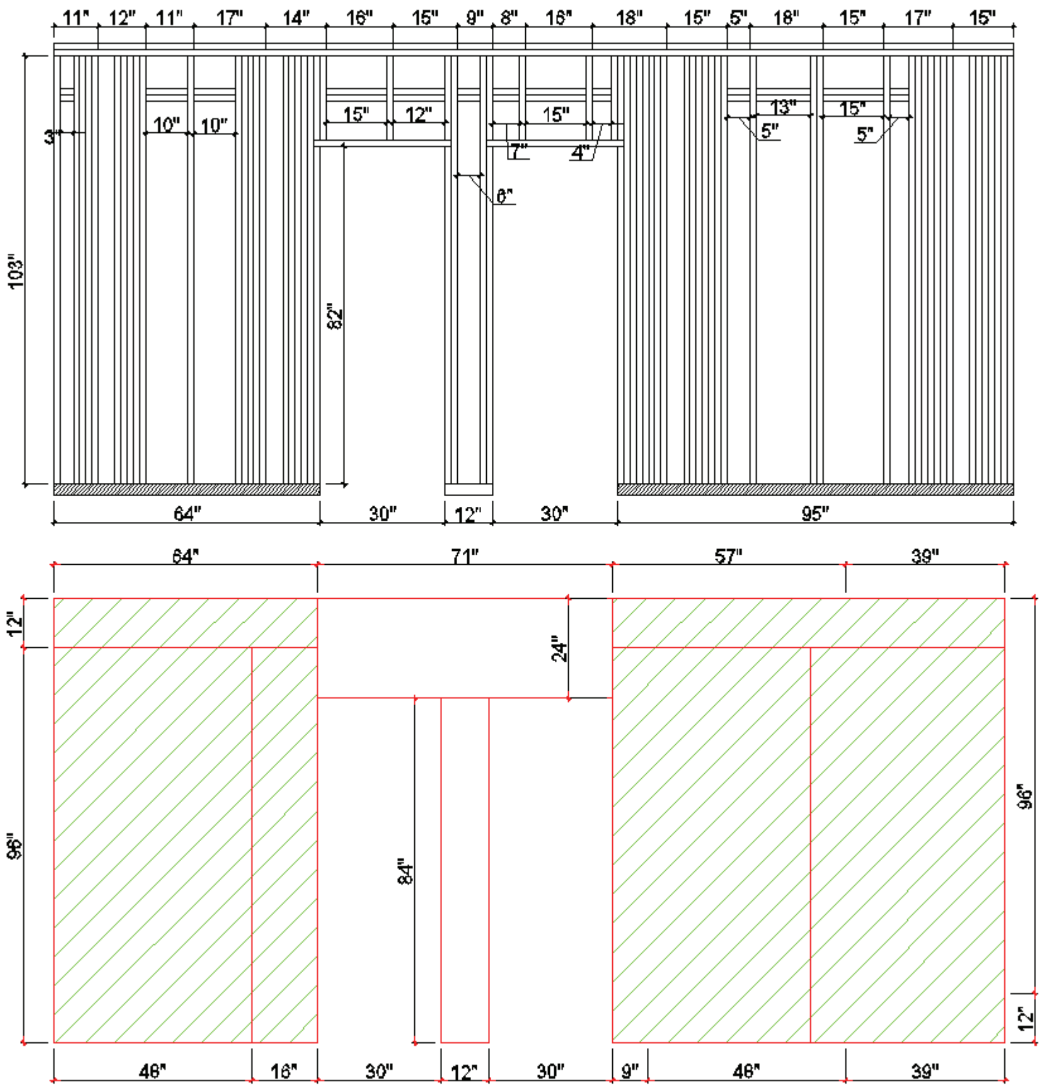

Figure B.5: Assembly for story 2, wall 4A-B, 8A-B, 2/12-D

Appendix B

Wall assembly for Story 2

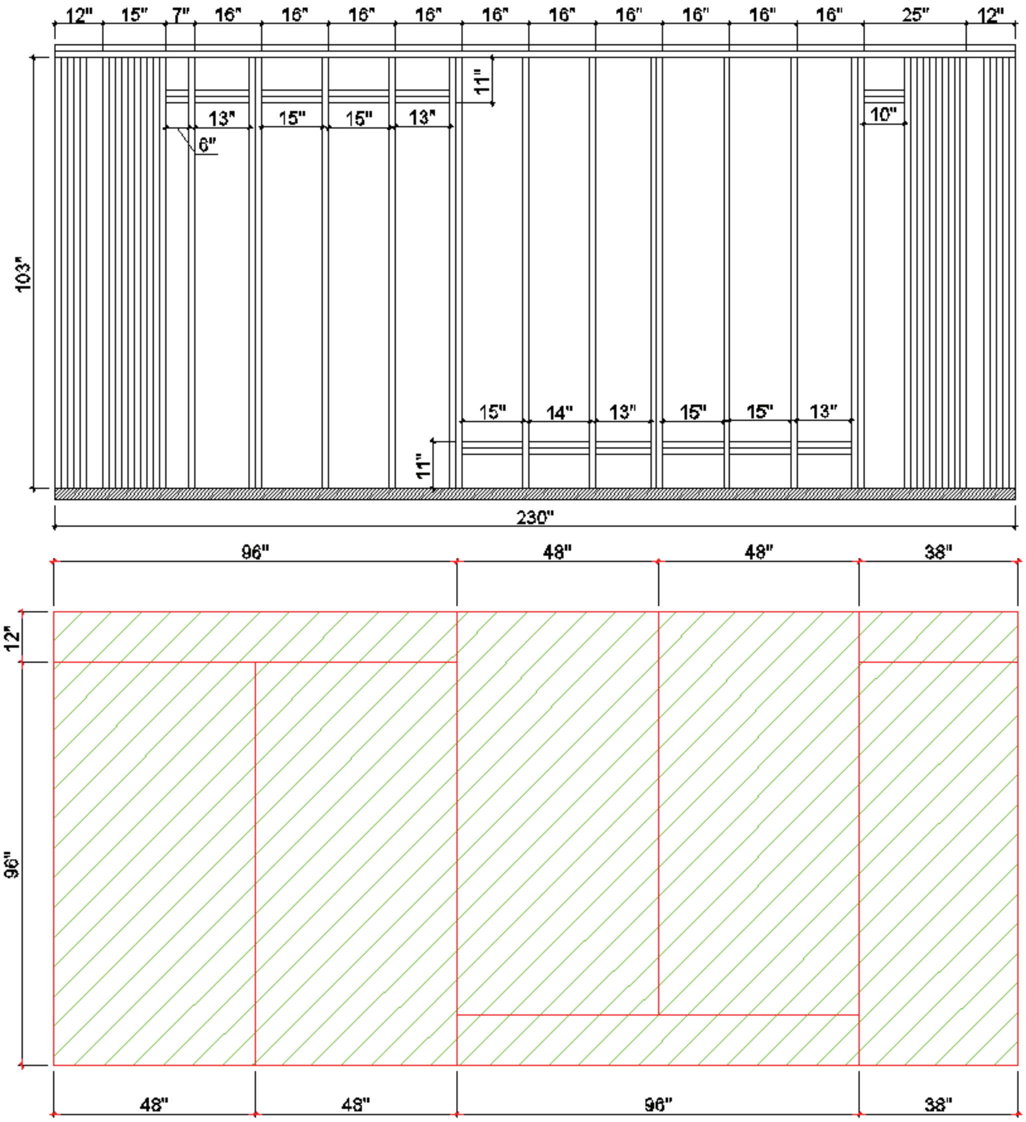

Figure B.6: Assembly for story 2, wall 6, 2/12-D

Appendix B

Wall assembly for Story 2

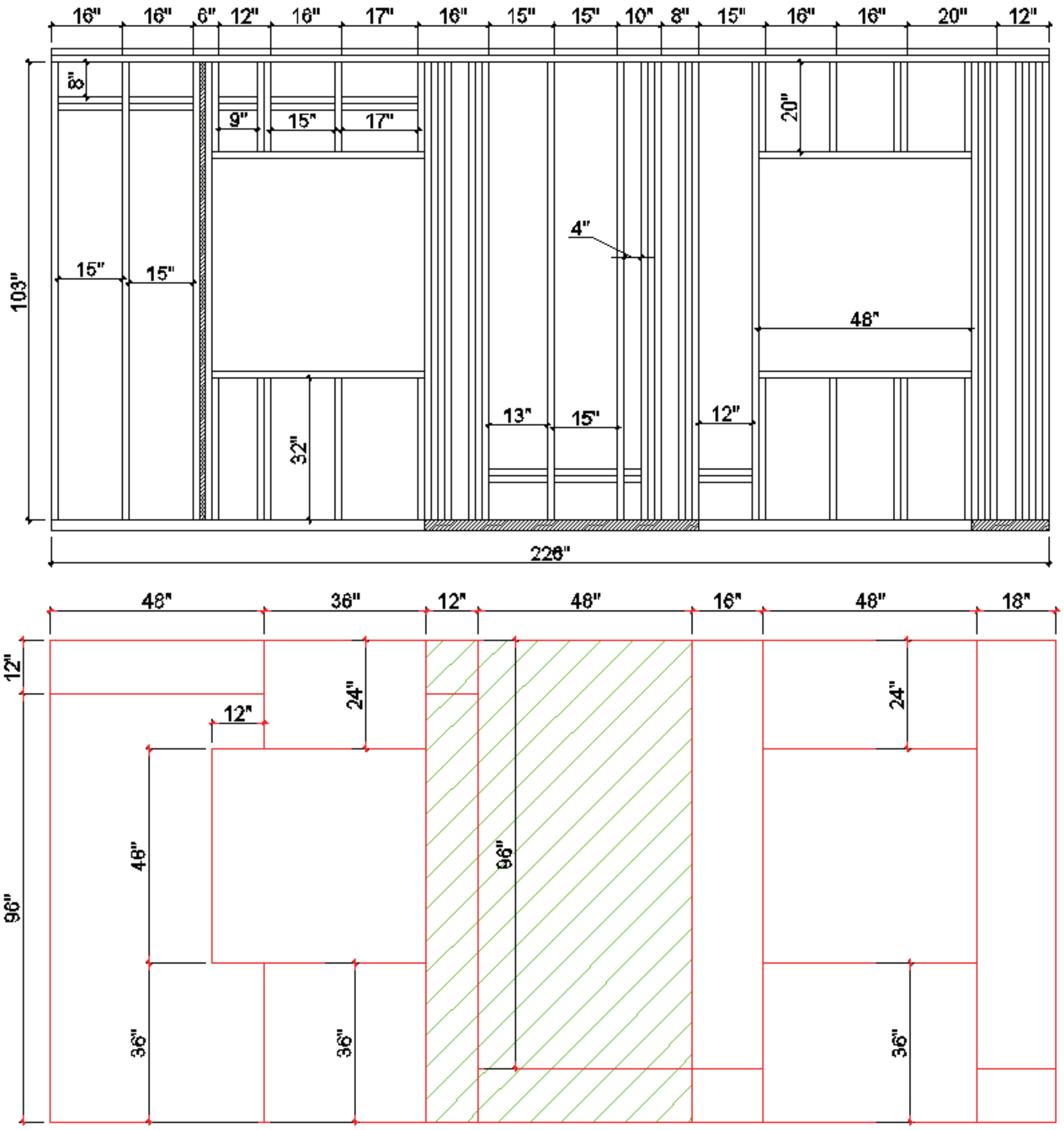

Figure B.7: Assembly for story 2, wall A1, A3, 2/12

Appendix B

Wall assembly for Story 2

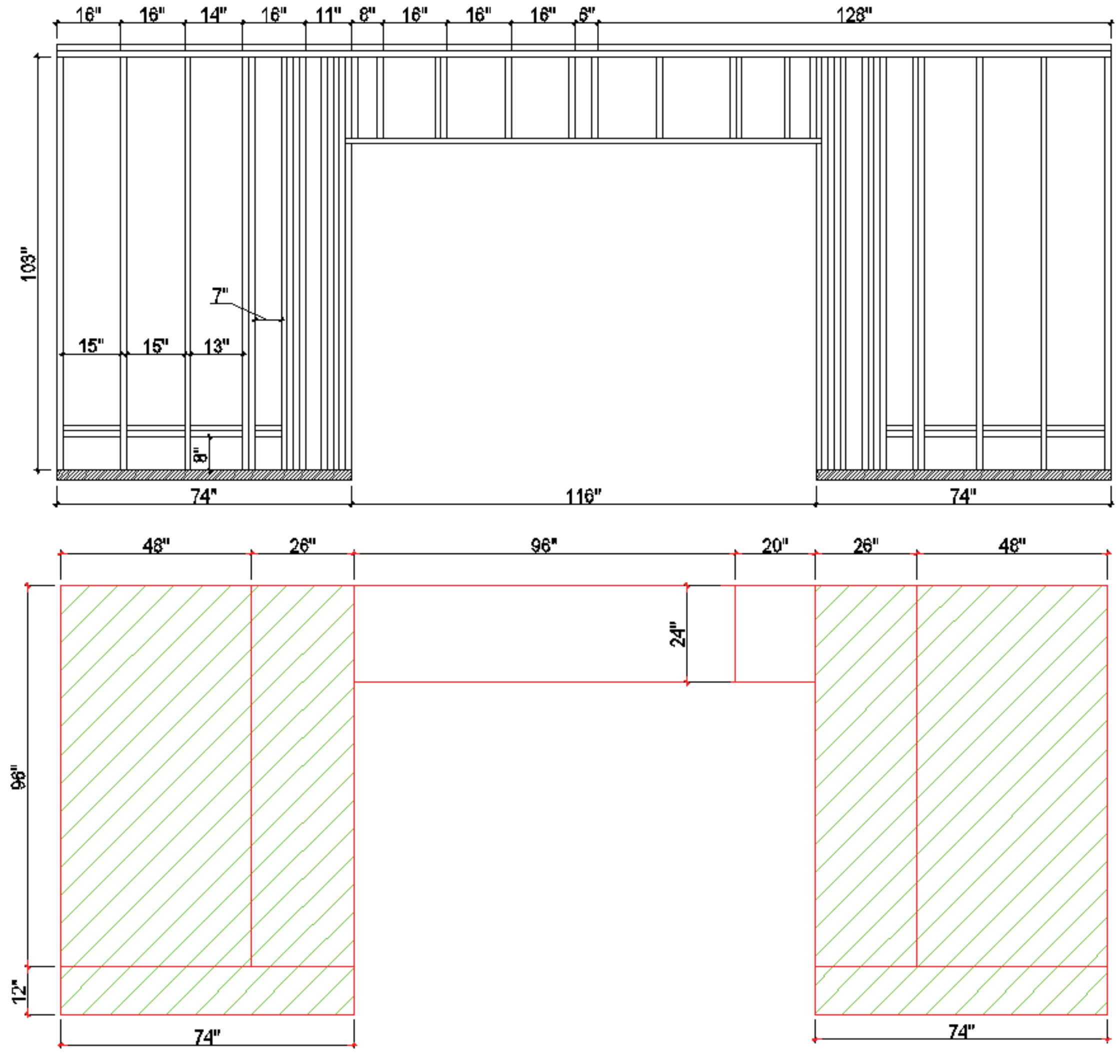

Figure B.8: Assembly for story 2, wall A2, 2/12

Appendix B

Wall assembly for Story 2

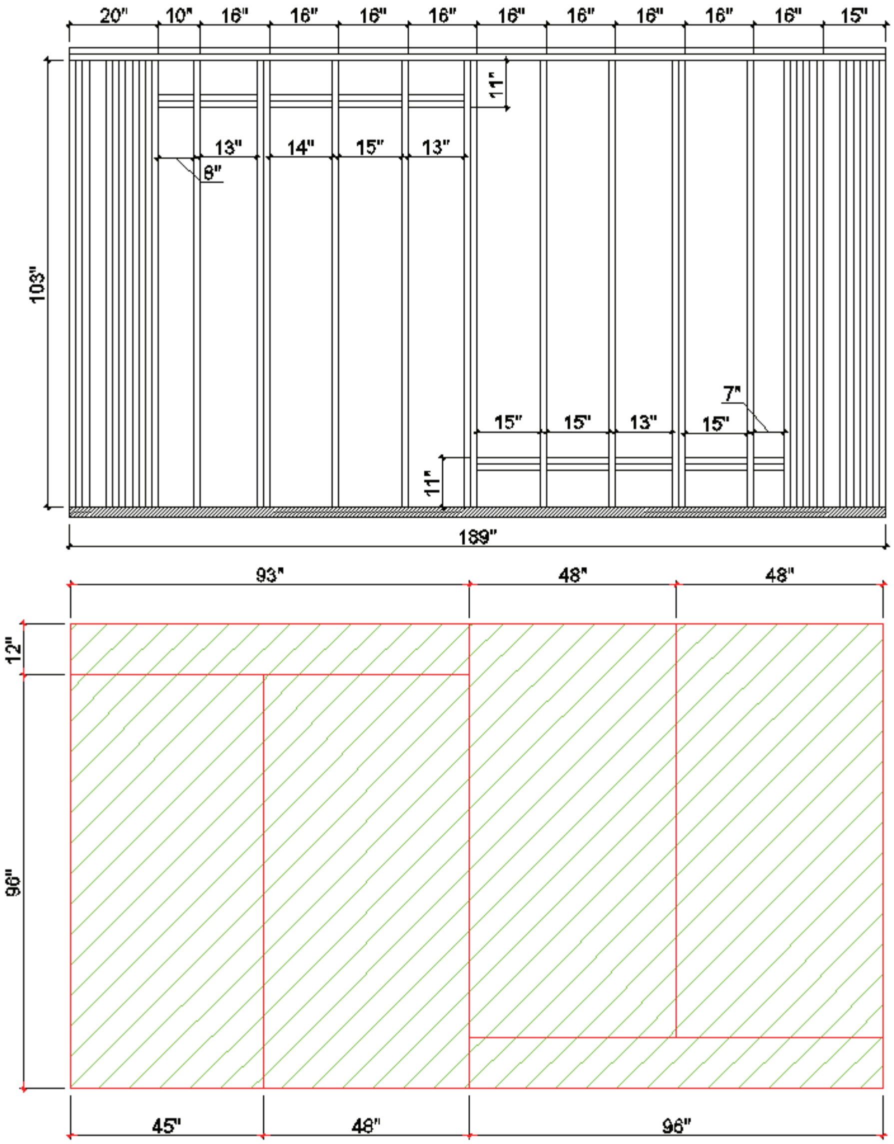

Figure B.9: Assembly for story 2, wall D1, D3, 2/12-D

Appendix B

Wall assembly for Story 2

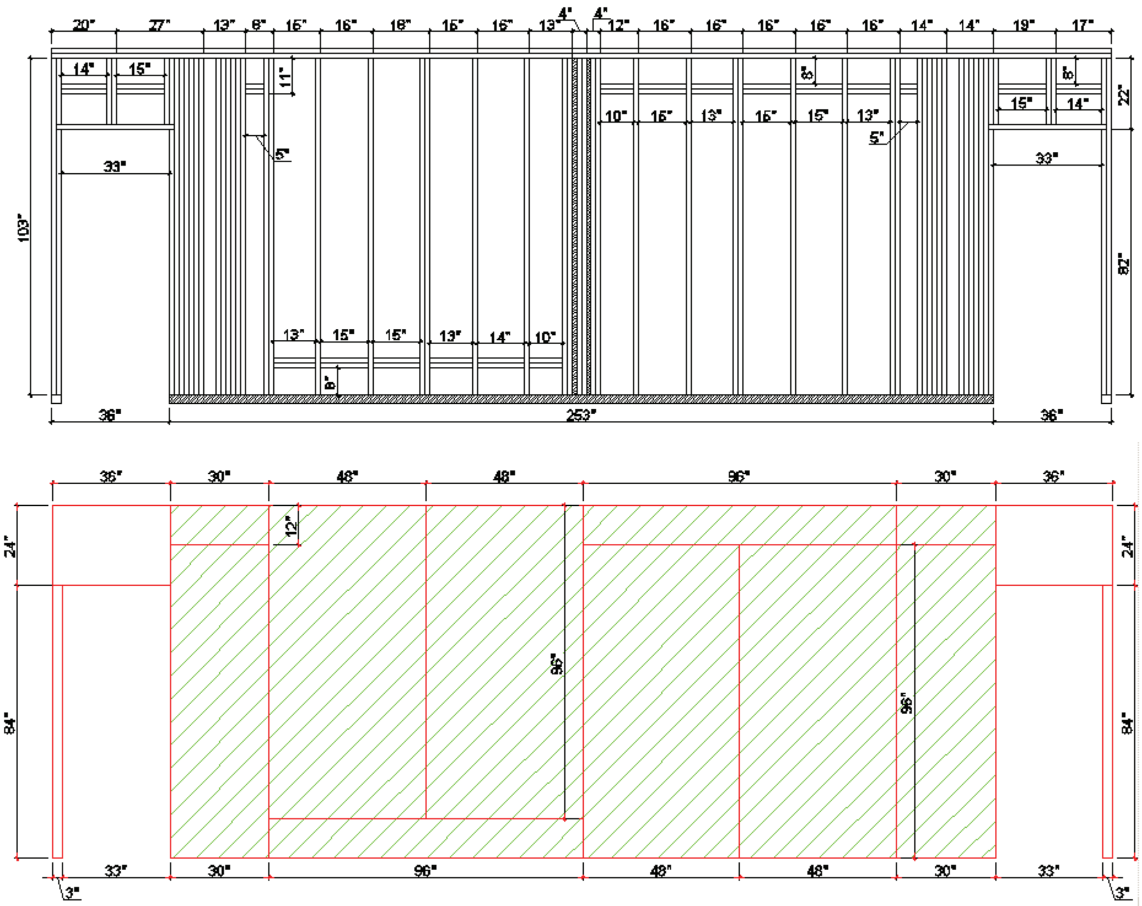

Figure B.10: Assembly for story 2, wall D2, 2/12-D

Appendix B

Wall assembly for Story 2

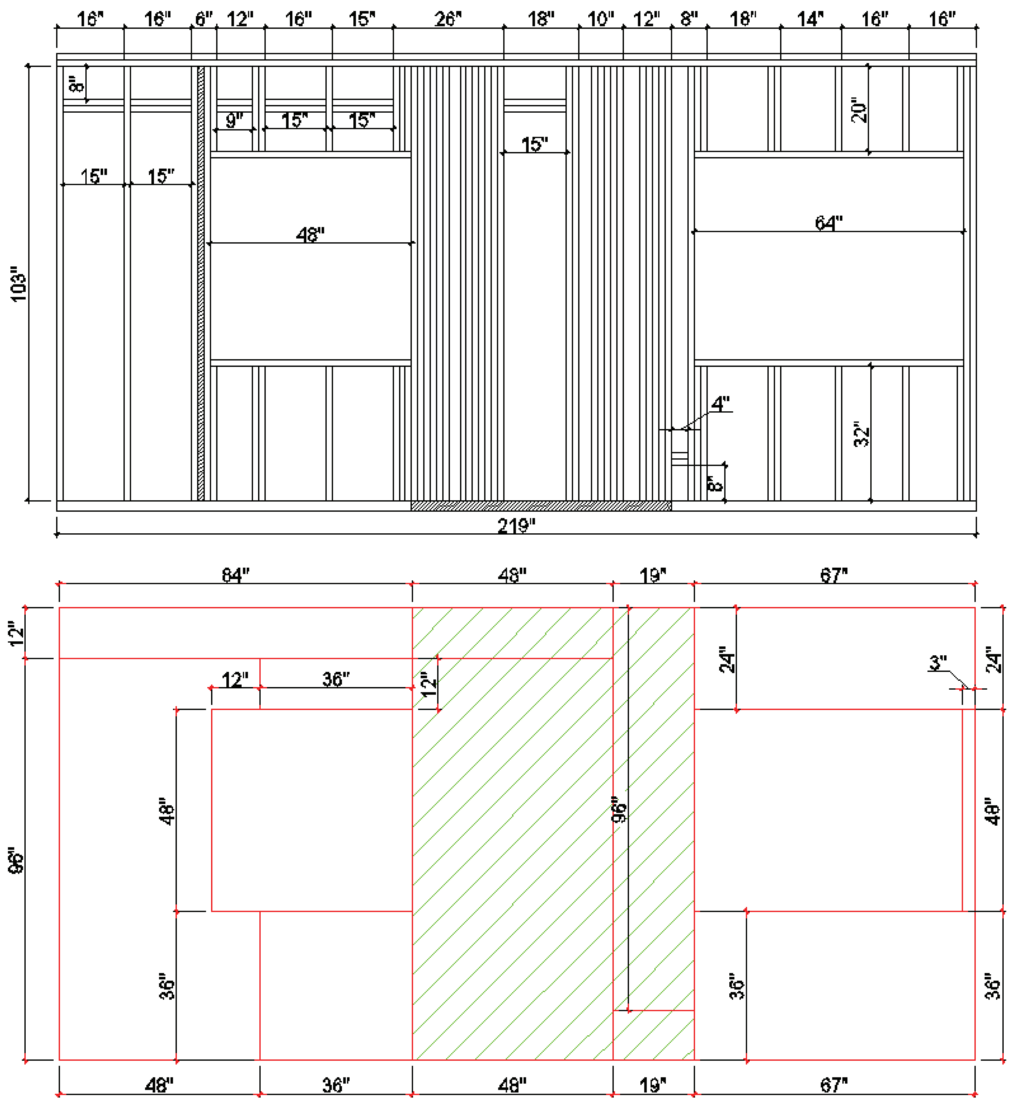

Figure B.11: Assembly for story 2, wall E1, E5, 3/12-D

Appendix B

Wall assembly for Story 2

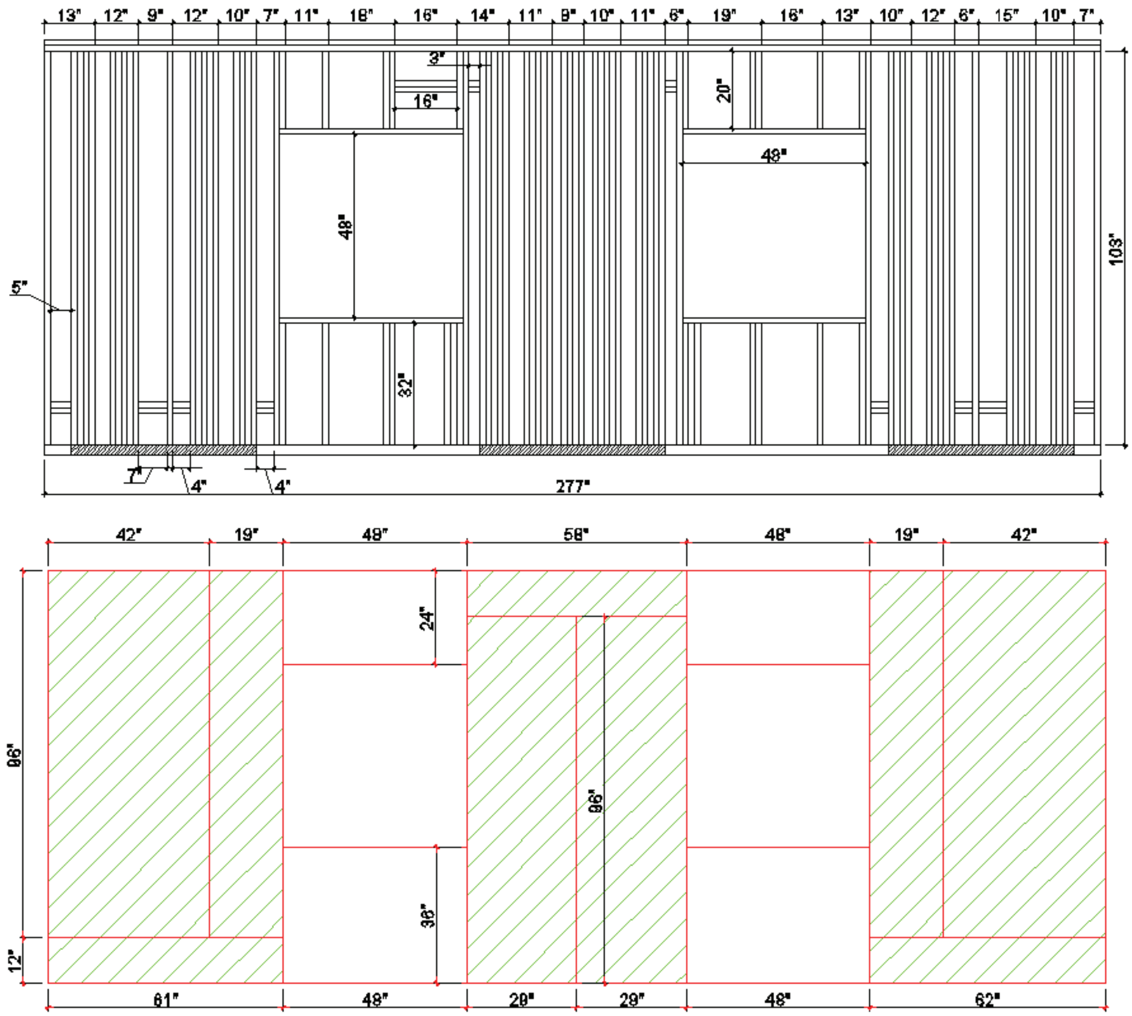

Figure B.12: Assembly for story 2, wall E2, E3, E4, 3/12-D

Appendix B

Wall assembly for Story 2

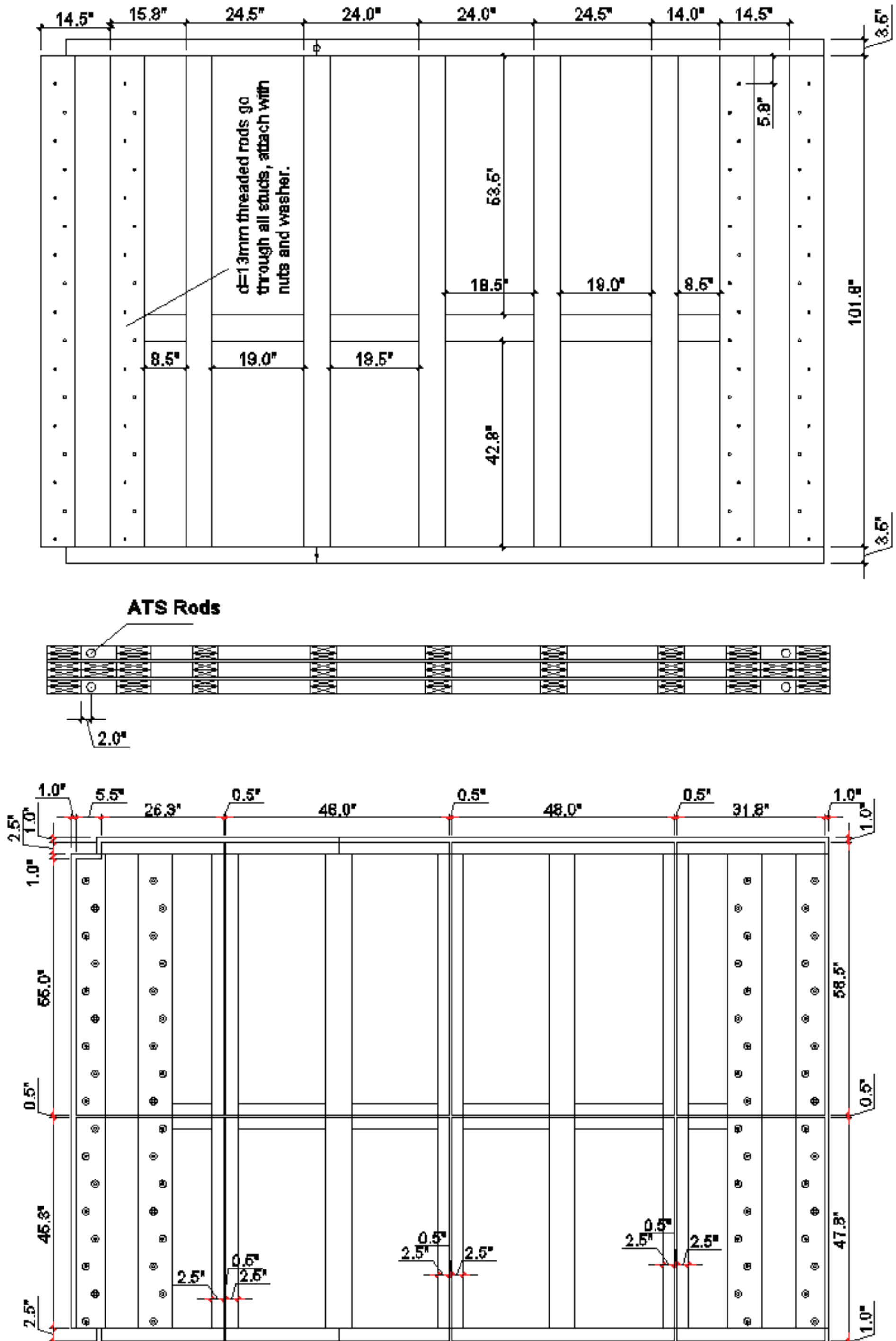

Figure B.13: Assembly for story 2, wall B1, B2, 3/12 Double Midply

Appendix B

Wall assembly for Story 3

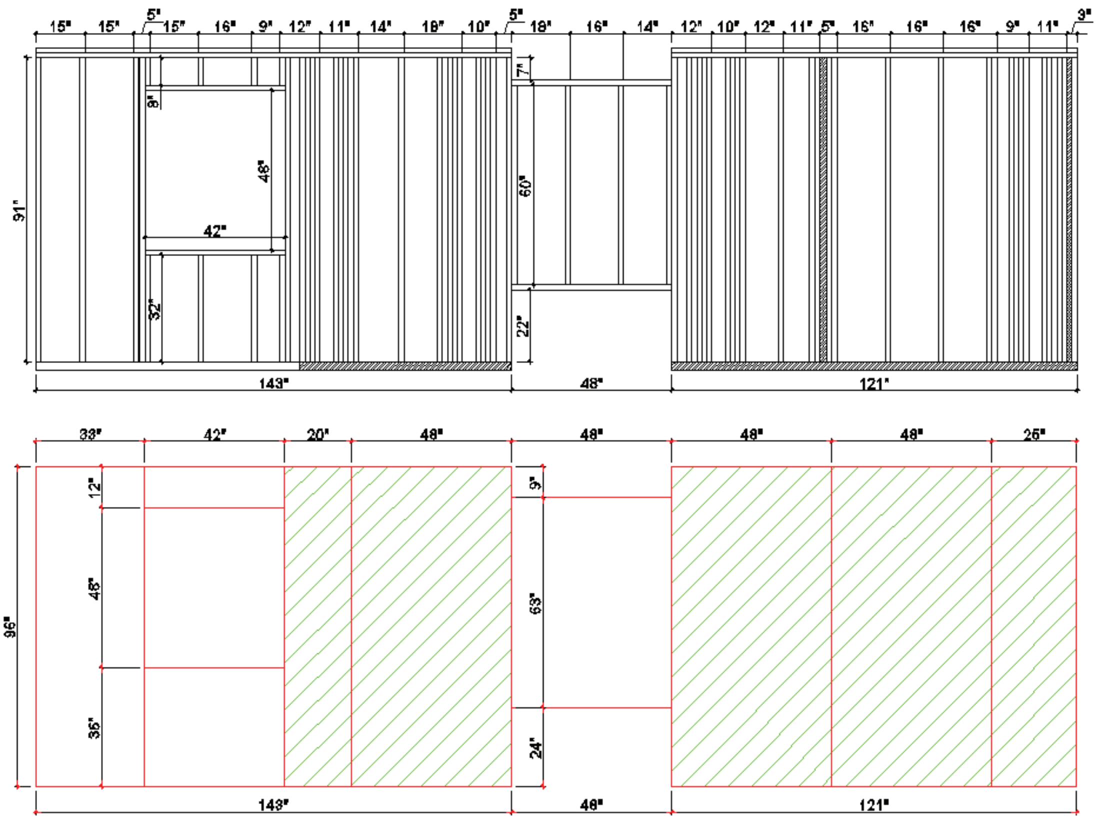

Figure B.14: Assembly for story 3, wall 1AB, 11AB, 2/12-D

Appendix B

Wall assembly for Story 3

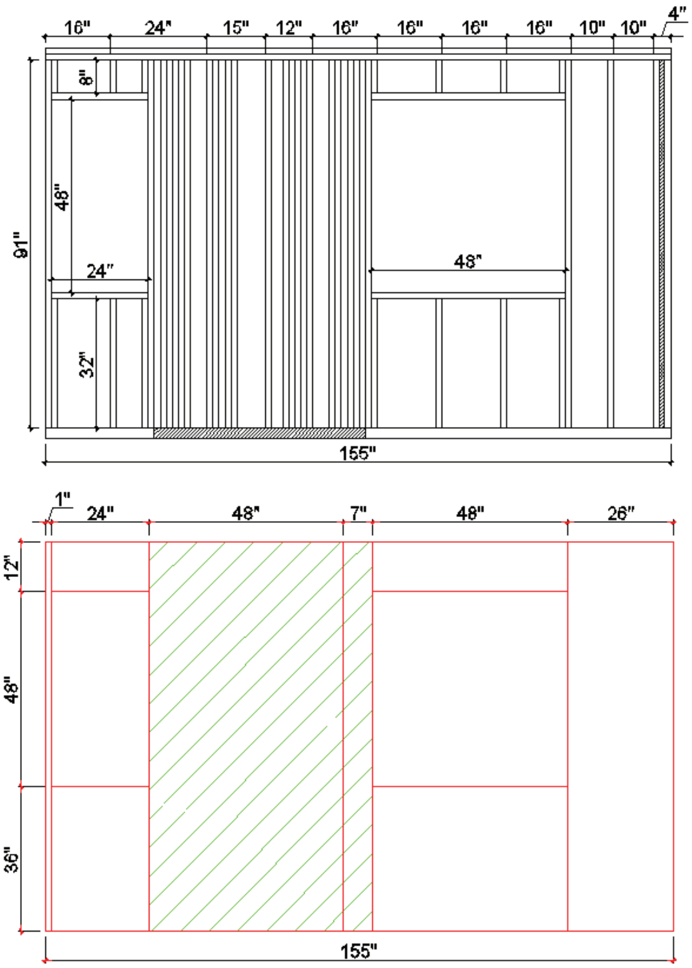

Figure B.15: Assembly for story 3, wall 1C, 11C, 2/12-D

Appendix B

Wall assembly for Story 3

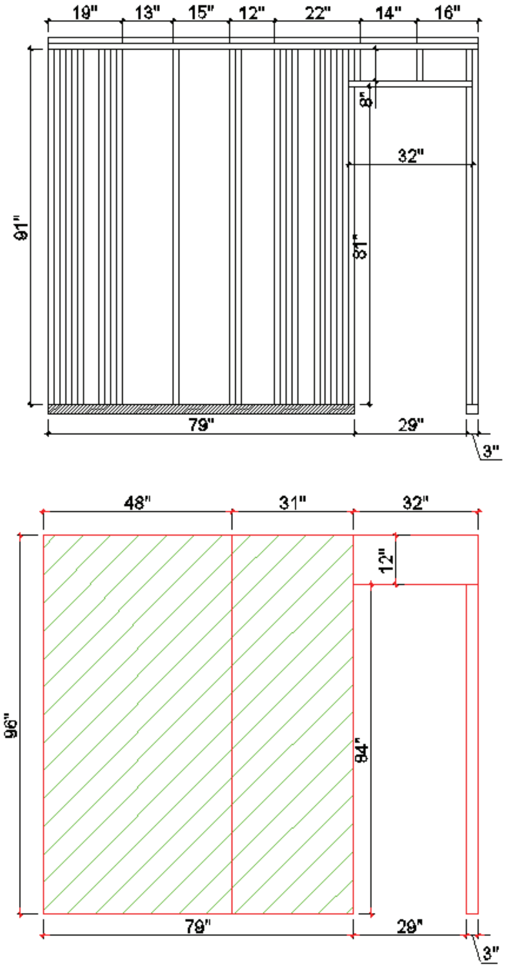

Figure B.16: Assembly for story 3, wall 2A, 10A, 3/12-D

Appendix B

Wall assembly for Story 3

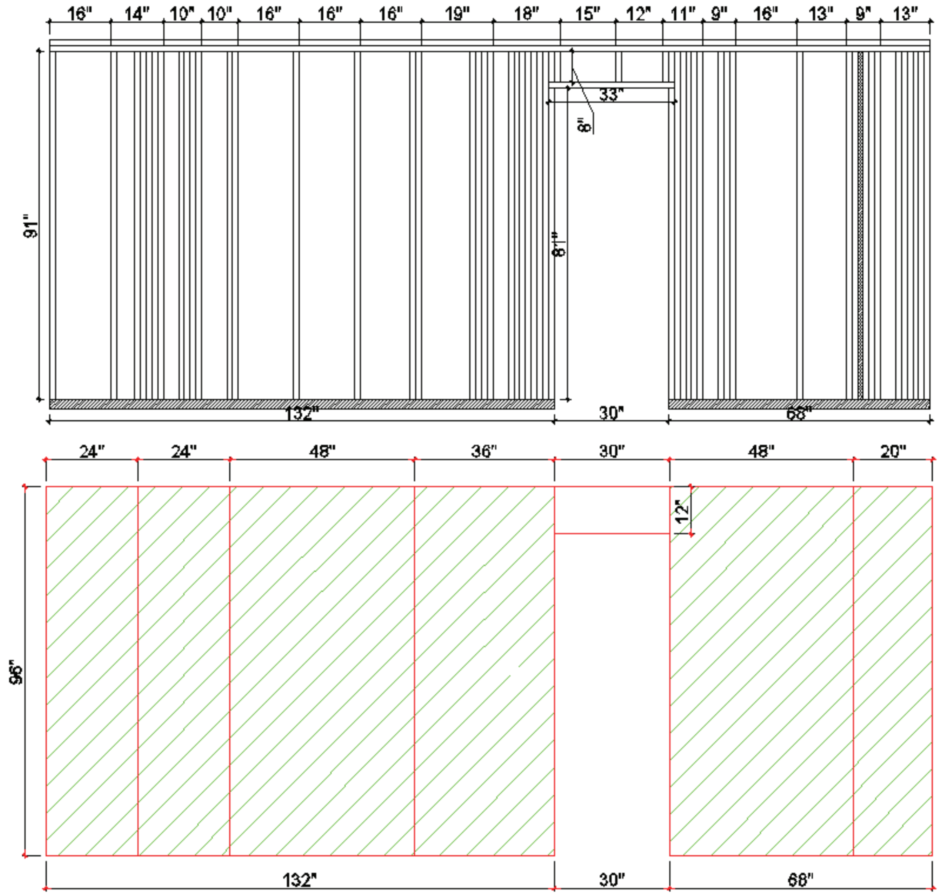

Figure B.17: Assembly for story 3, wall 2B-C, 10B-C, 3/12-D

Appendix B

Wall assembly for Story 3

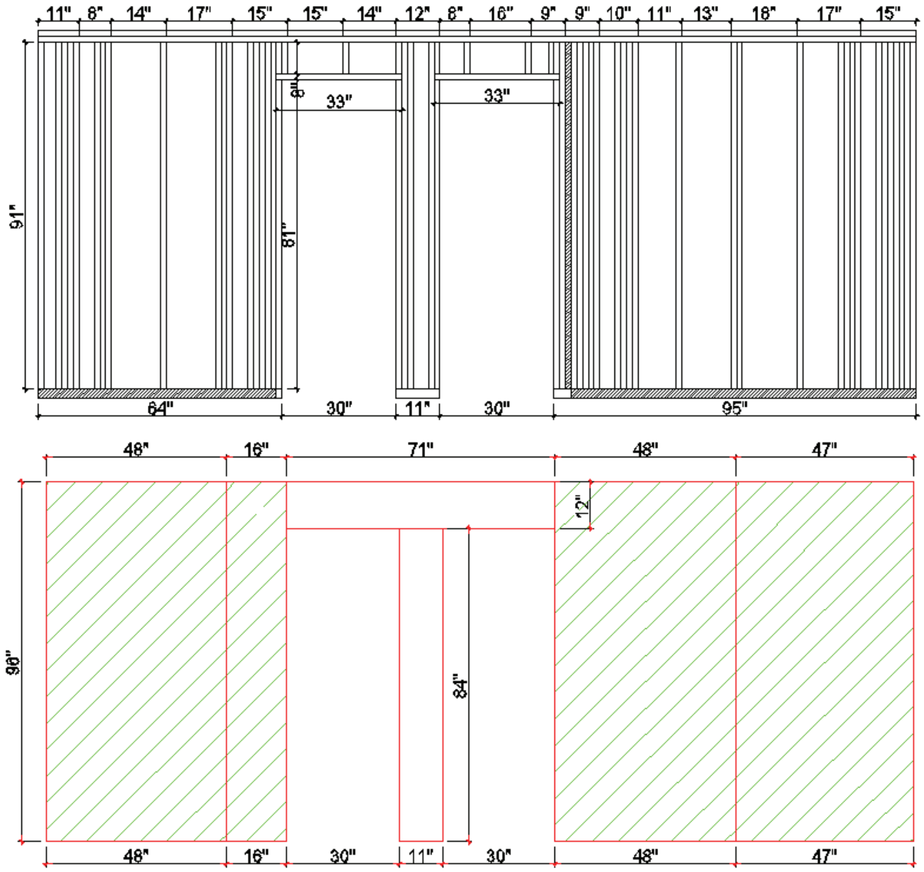

Figure B.18: Assembly for story 3, wall 4A-B, 8A-B, 2/12-D

Appendix B

Wall assembly for Story 3

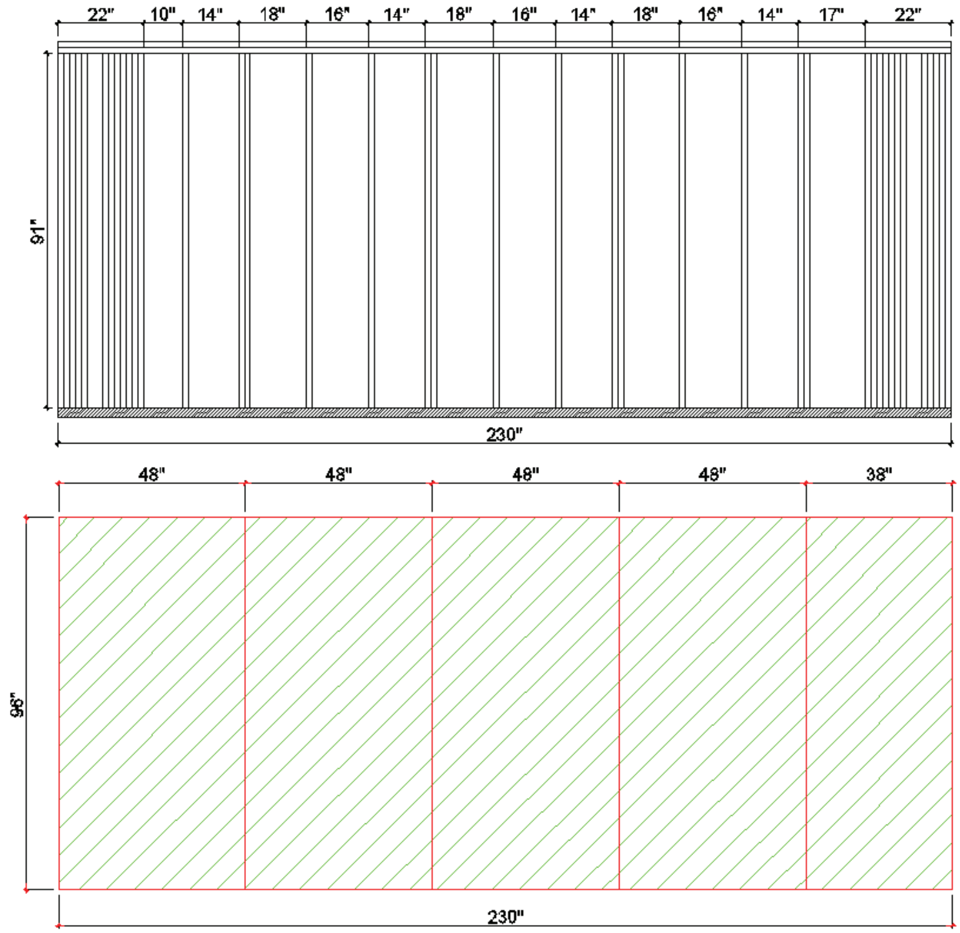

Figure B.19: Assembly for story 3, wall 6, 2/12-D

Appendix B

Wall assembly for Story 3

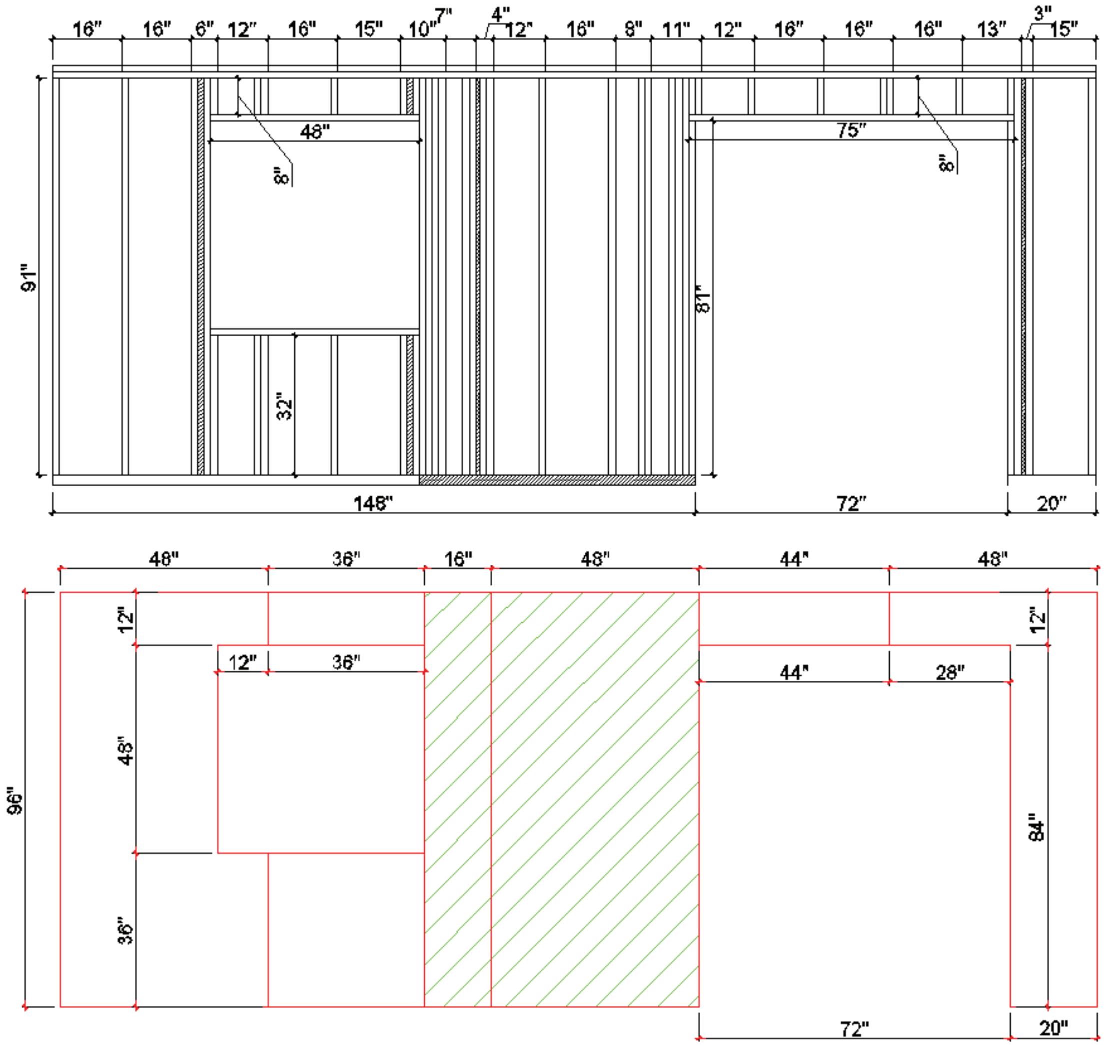

Figure B.20: Assembly for story 3, wall A1, A3, 2/12

Appendix B

Wall assembly for Story 3

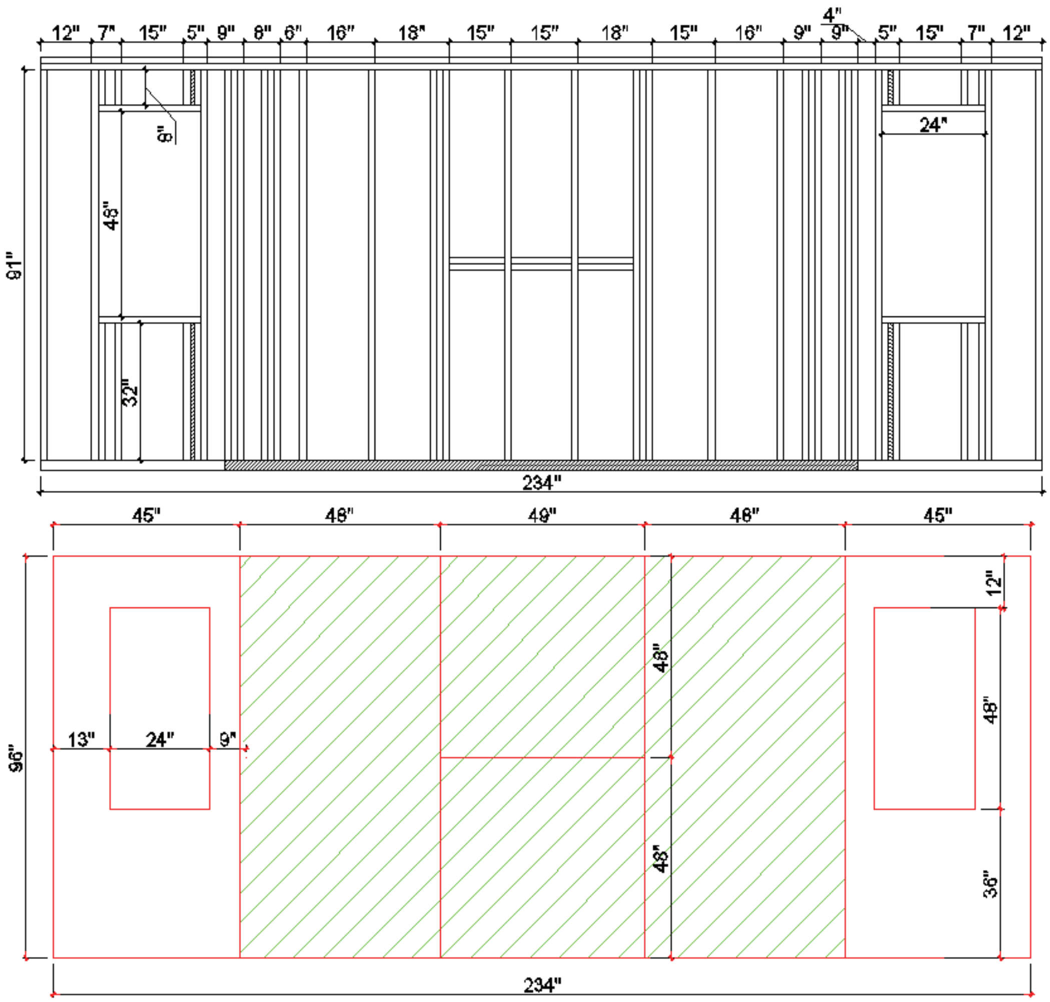

Figure B.21: Assembly for story 3, wall A2, 2/12

Appendix B

Wall assembly for Story 3

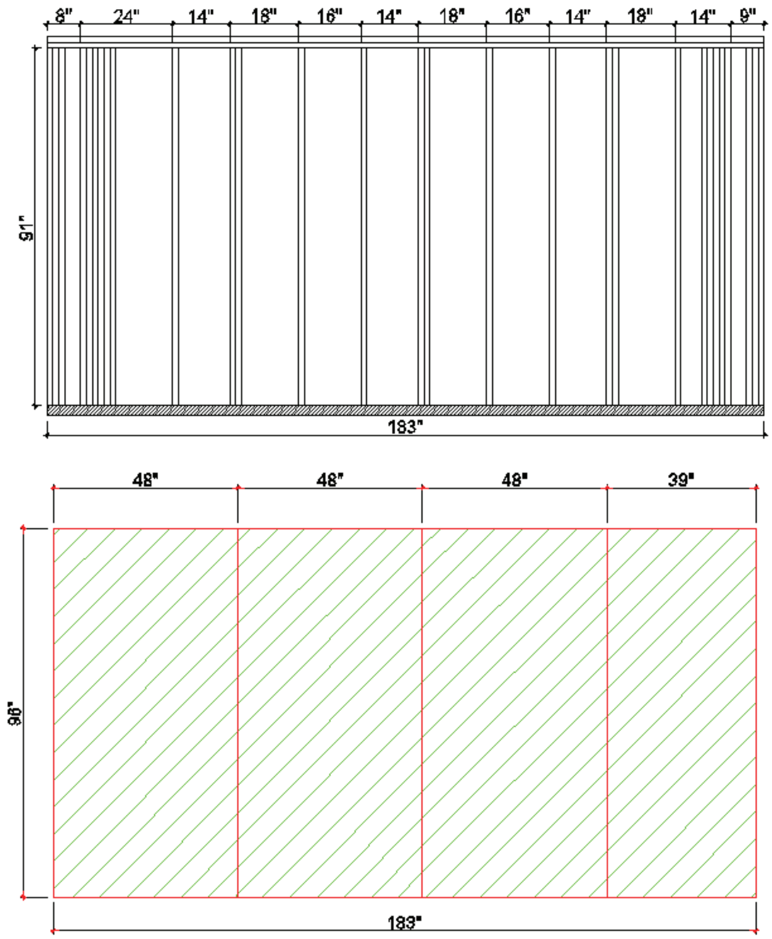

Figure B.22: Assembly for story 3, wall D1, D3, 2/12-D

Appendix B

Wall assembly for Story 3

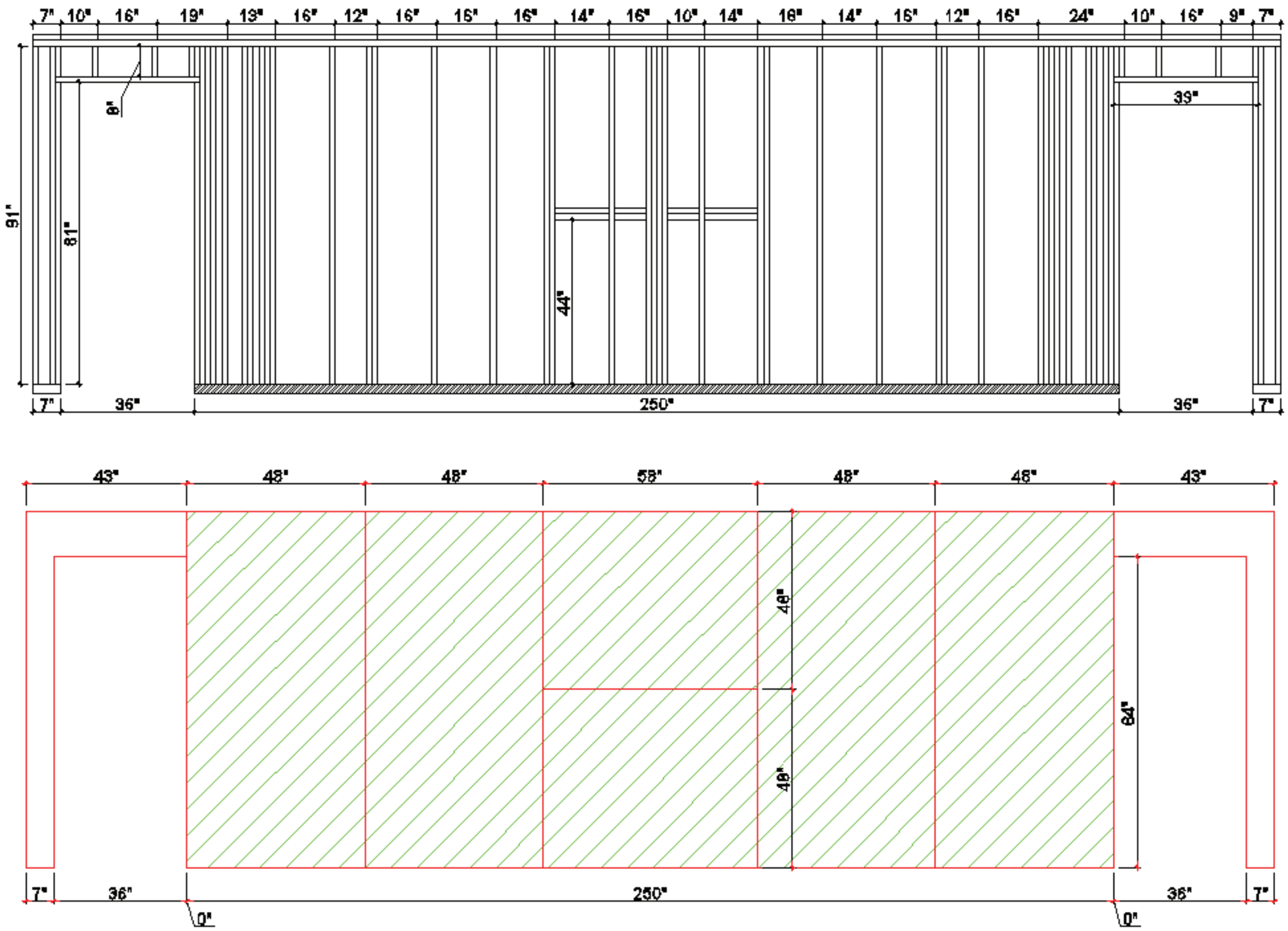

Figure B.23: Assembly for story 3, wall D2, 2/12-D

Appendix B

Wall assembly for Story 3

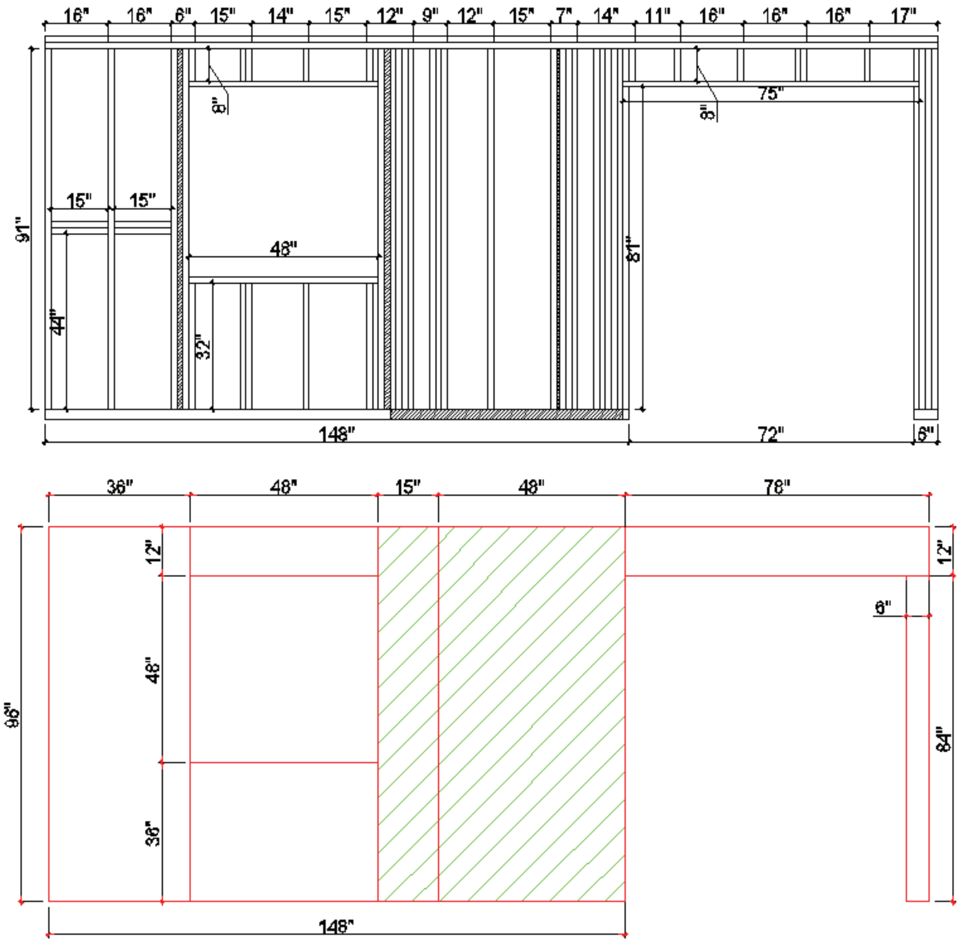

Figure B.24: Assembly for story 3, wall E1, E5, 3/12-D

Appendix B

Wall assembly for Story 3

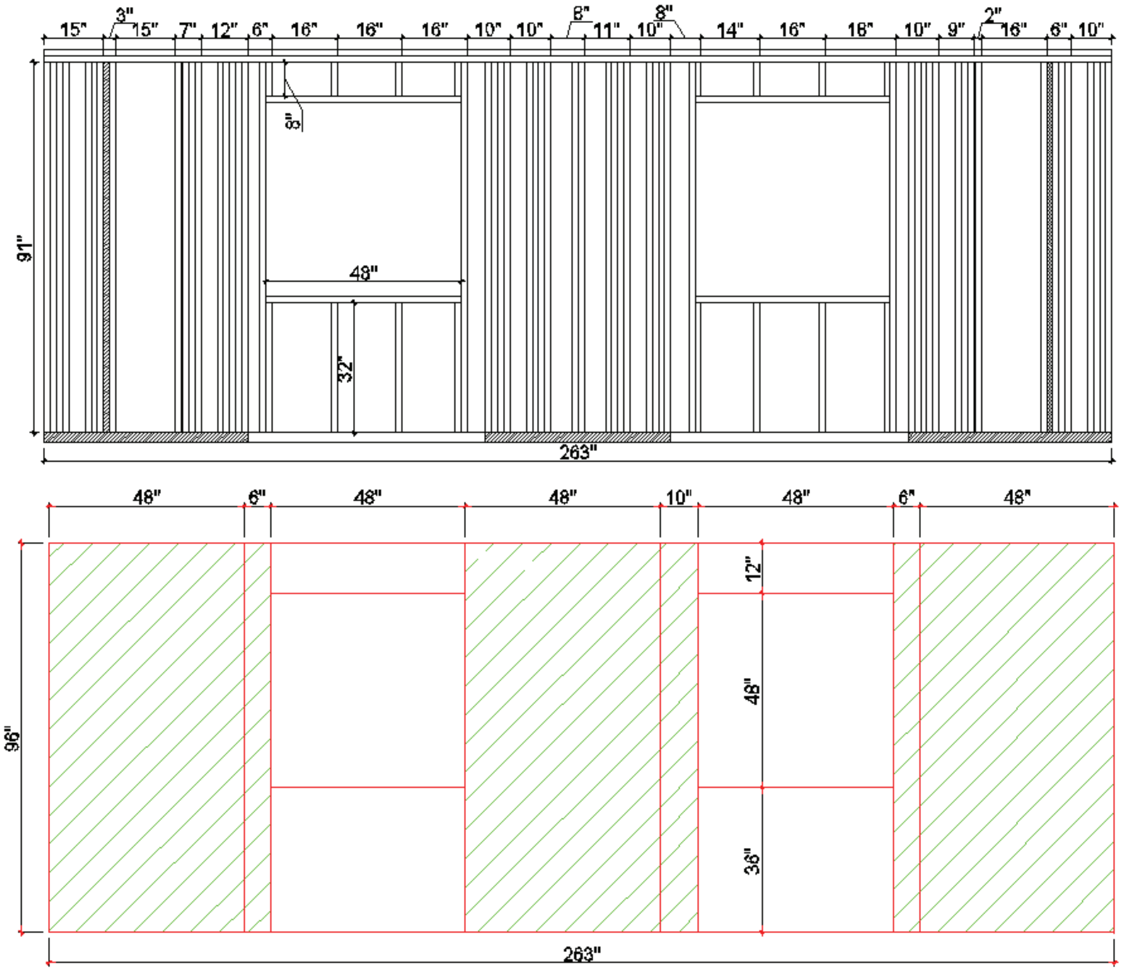

Figure B.25: Assembly for story 3, wall E2, E3, E4, 3/12-D

Appendix B

Wall assembly for Story 3

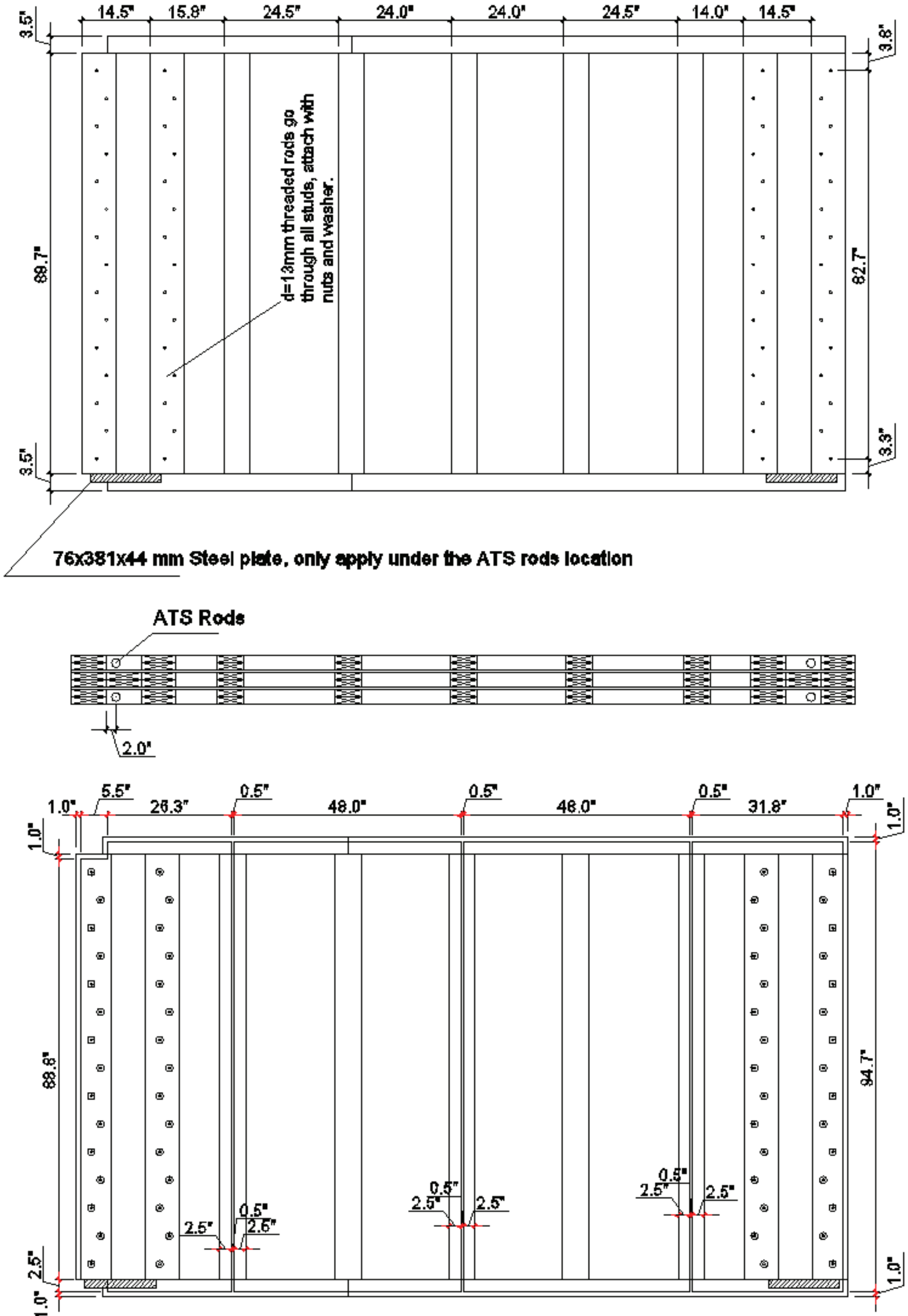

Figure B.26: Assembly for story 3, wall B1, B2, 3/12 Double Midply

Appendix B

Wall assembly for Story 4

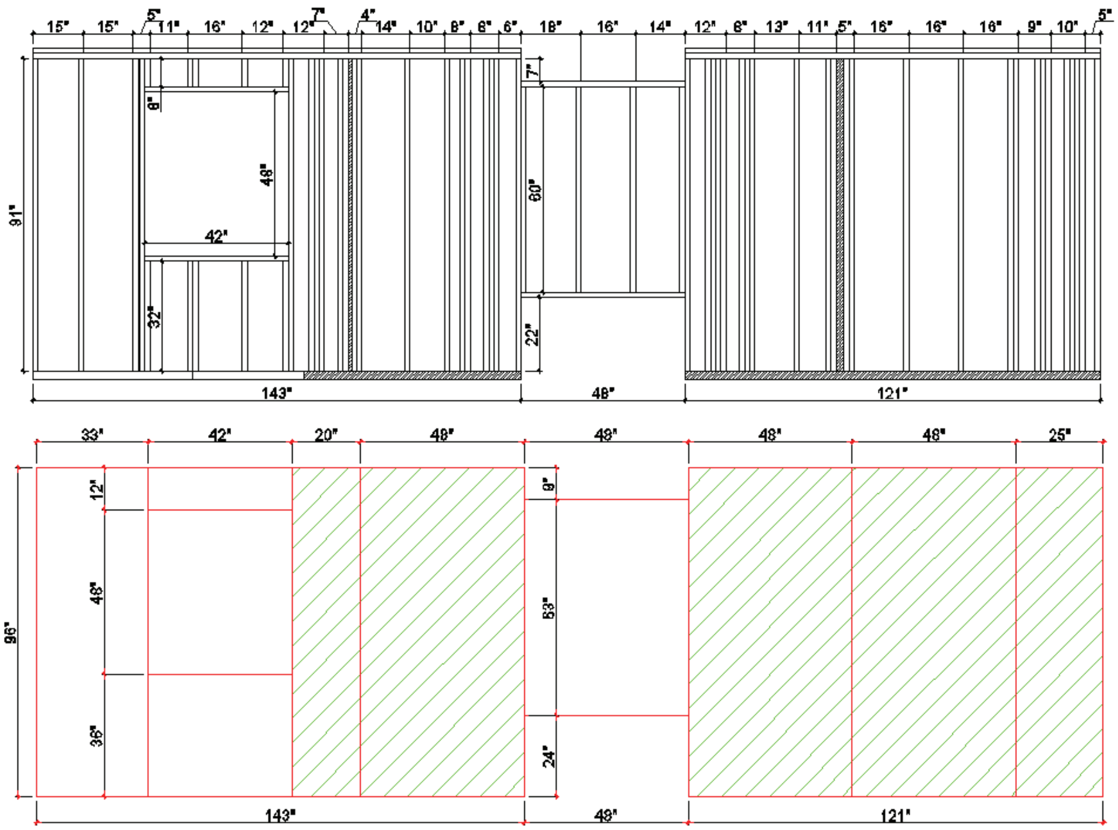

Figure B.27: Assembly for story 4, wall 1AB, 11AB, 3/12-D

Appendix B

Wall assembly for Story 4

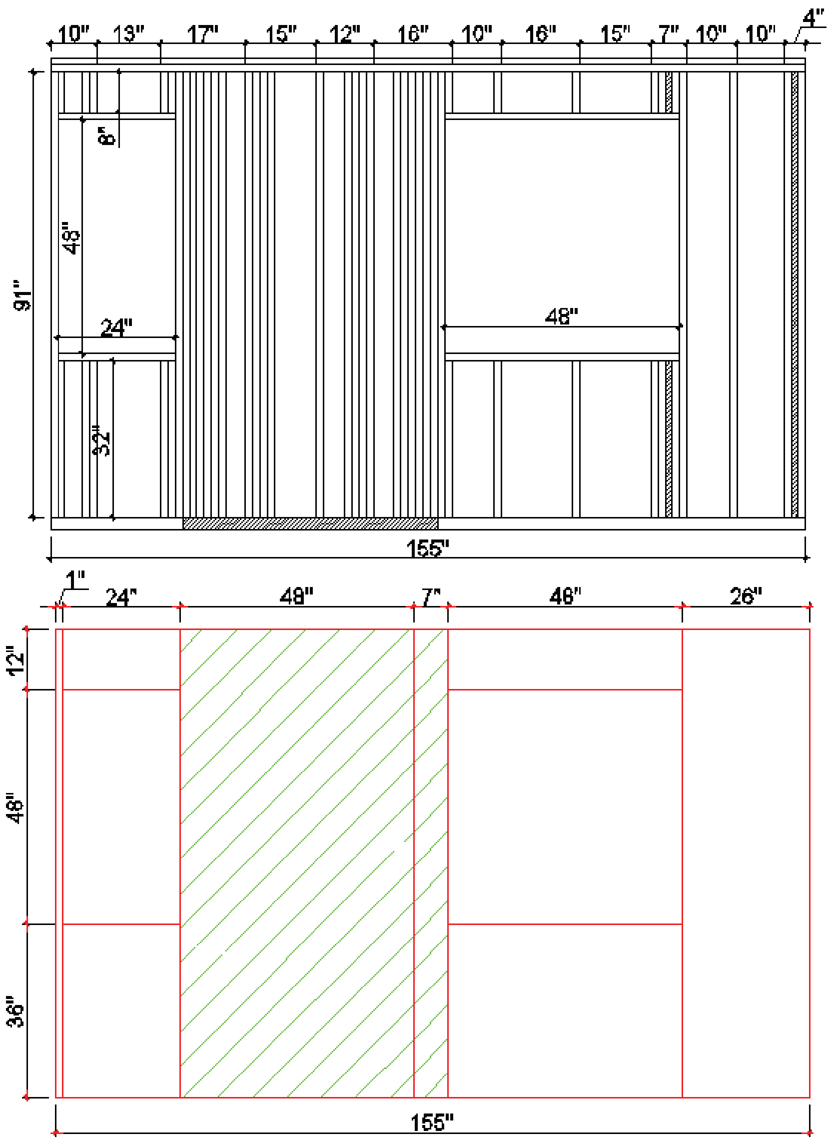

Figure B.28: Assembly for story 4, wall 1C, 11C, 3/12-D

Appendix B

Wall assembly for Story 4

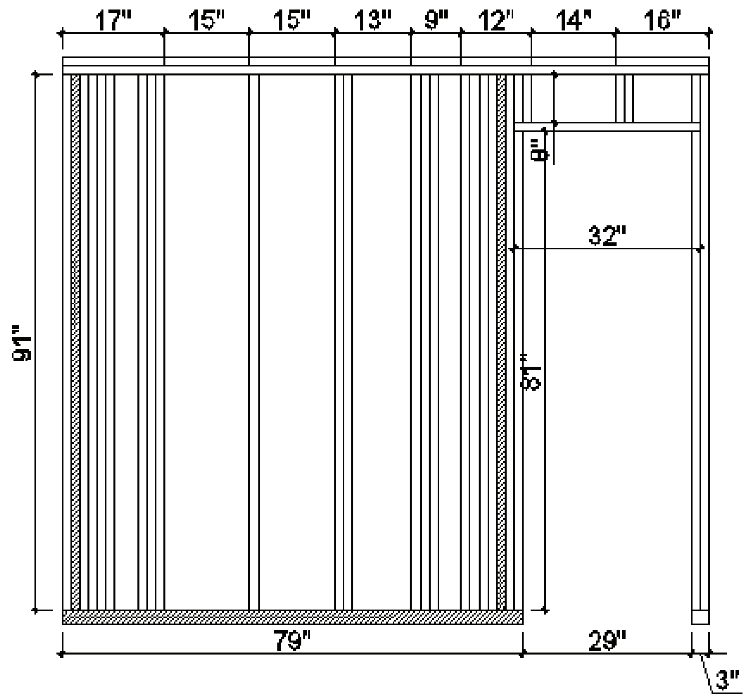

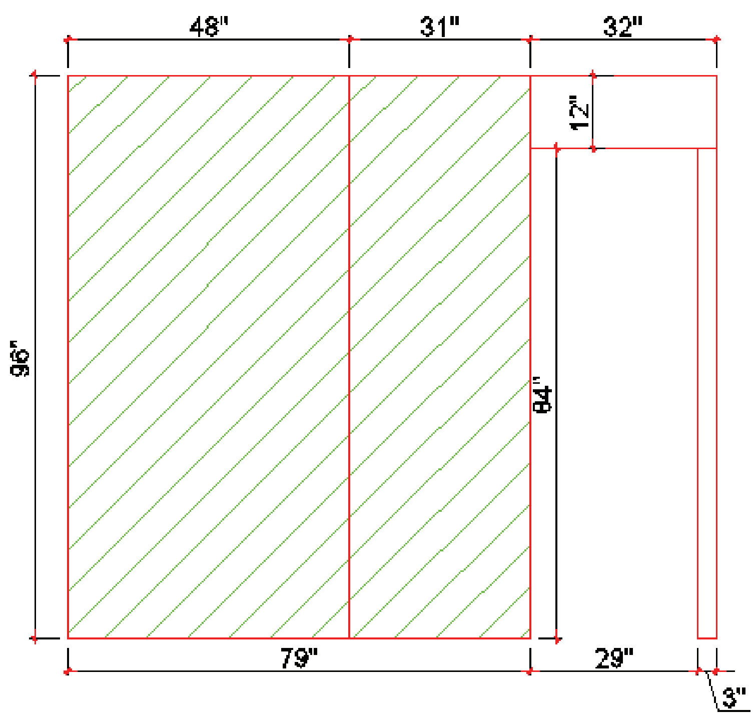

Figure B.29: Assembly for story 4, wall 2A, 10A, 3/12-D

Appendix B

Wall assembly for Story 4

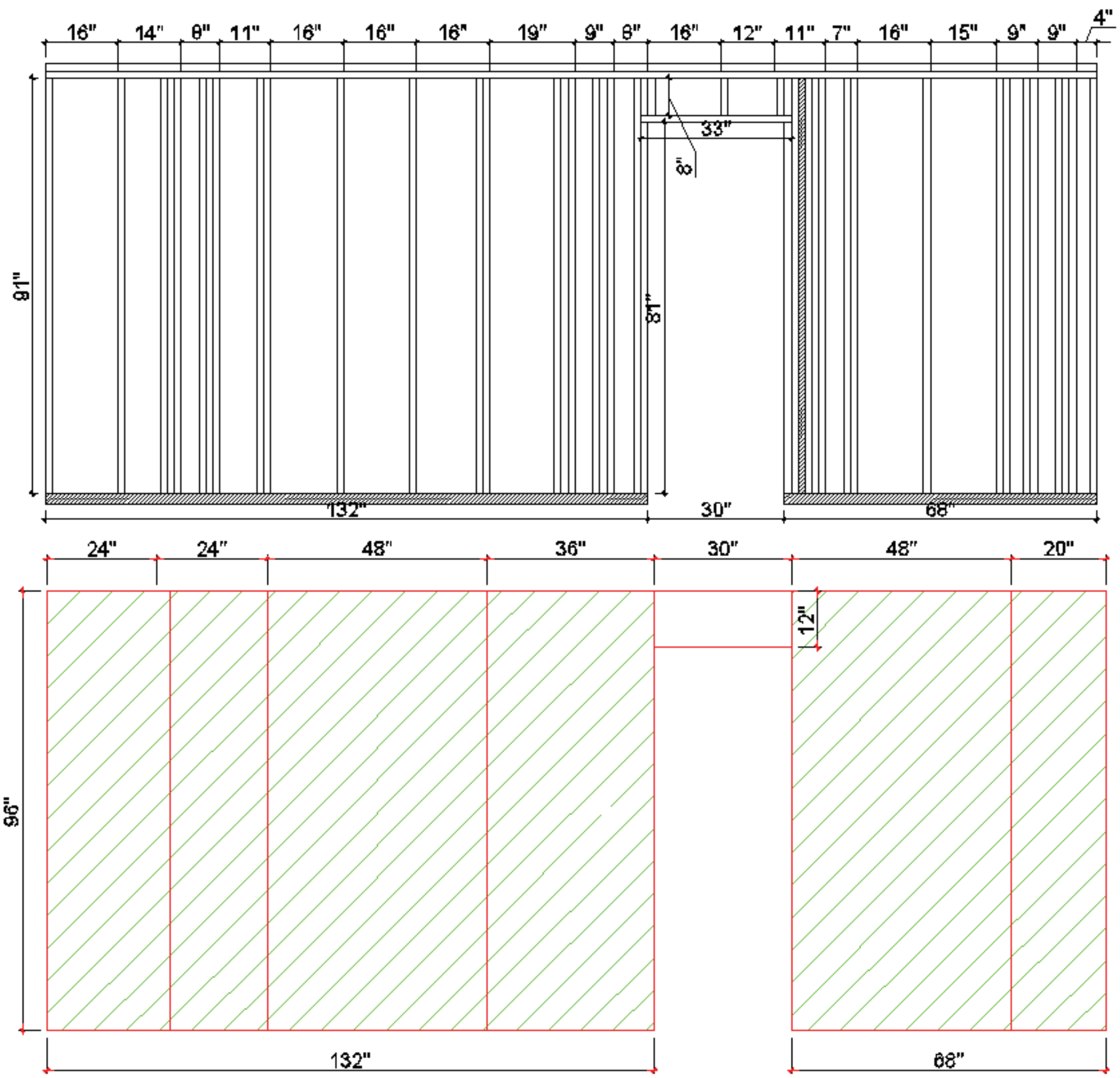

Figure B.30: Assembly for story 4, wall 2BC, 10BC, 3/12-D

Appendix B

Wall assembly for Story 4

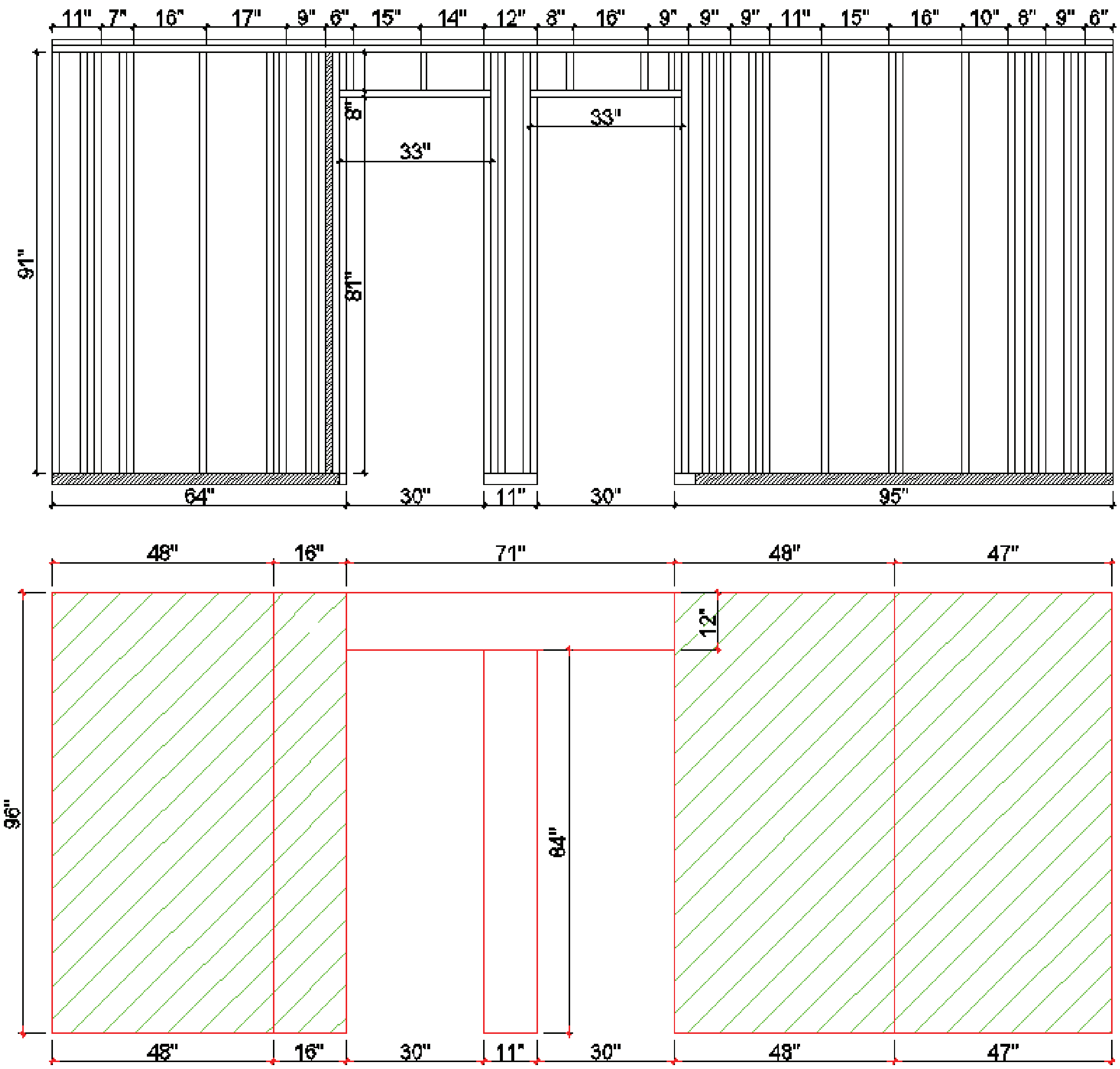

Figure B.31: Assembly for story 4, wall 4A-B, 8A-B, 3/12-D

Appendix B

Wall assembly for Story 4

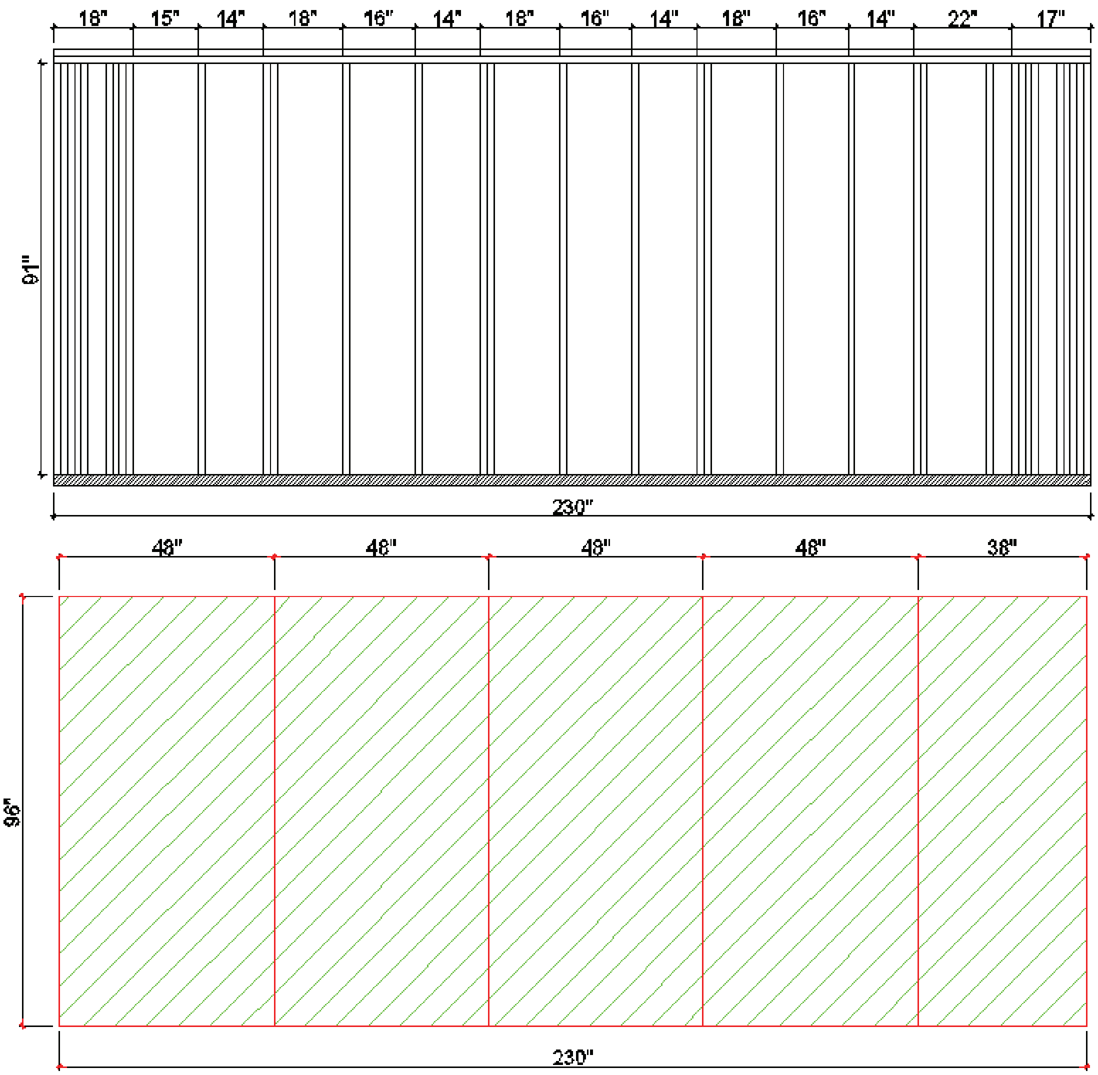

Figure B.32: Assembly for story 4, wall 6, 2/12-D

Appendix B

Wall assembly for Story 4

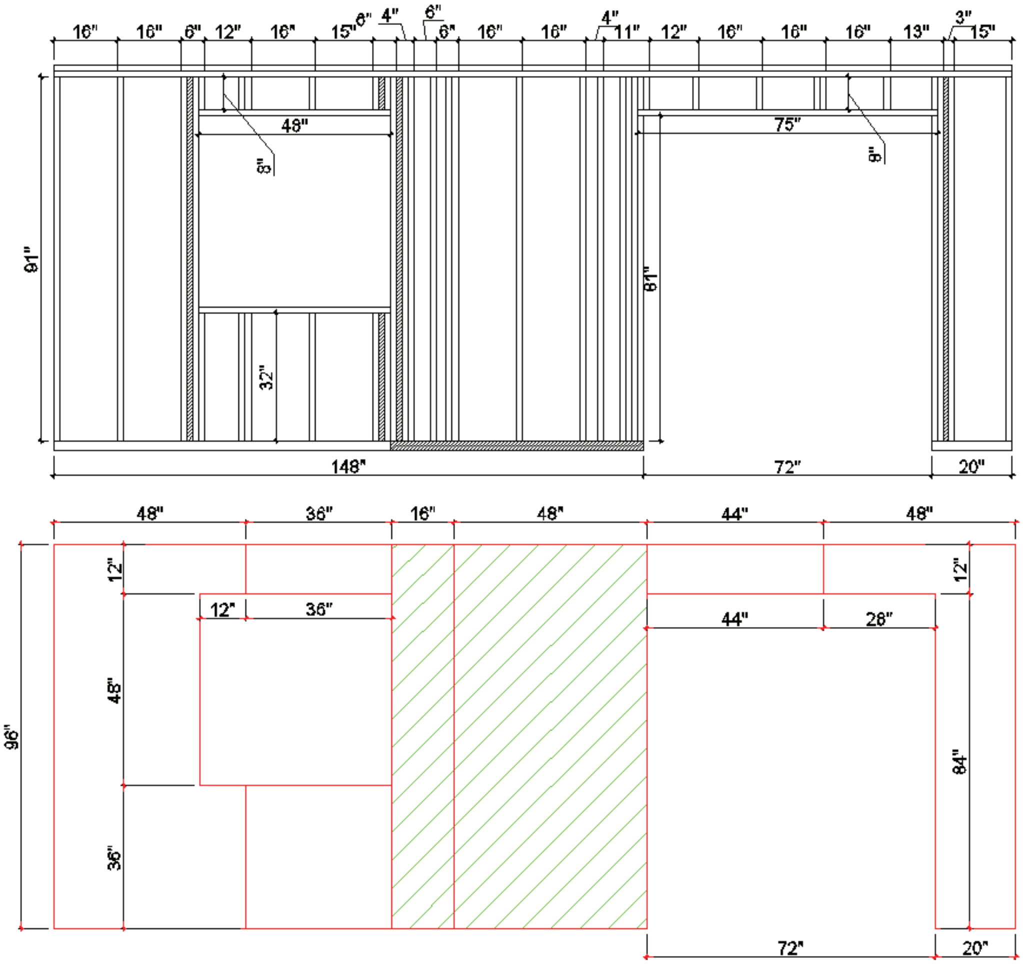

Figure B.33: Assembly for story 4, wall A1, A3, 2/12

Appendix B

Wall assembly for Story 4

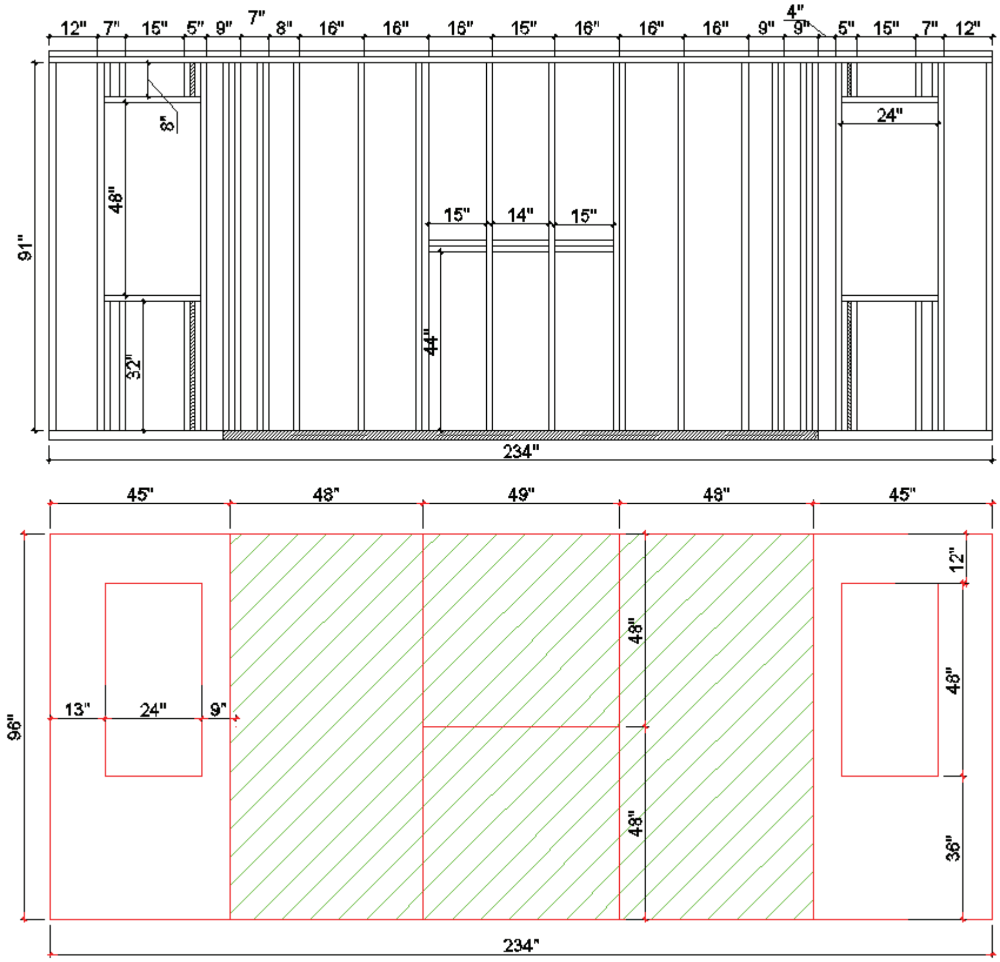

Figure B.34: Assembly for story 4, wall A2, 2/12

Appendix B

Wall assembly for Story 4

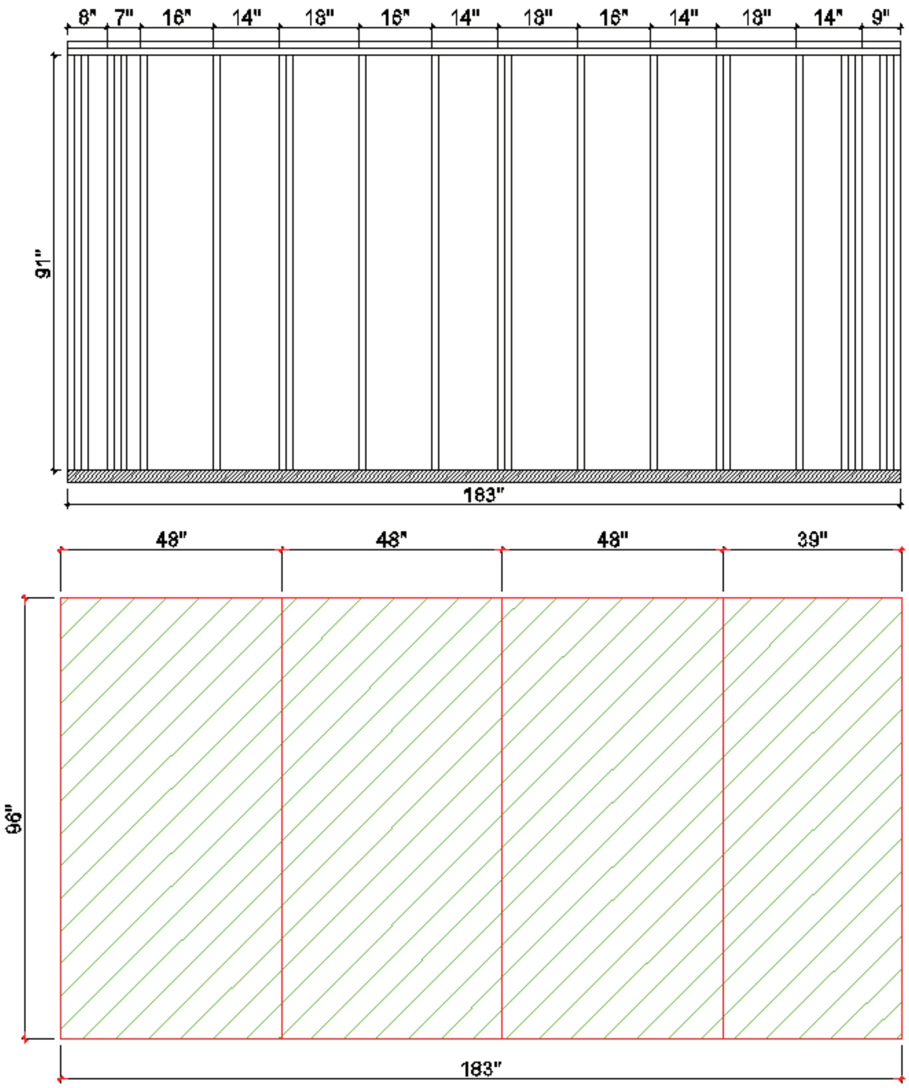

Figure B.35: Assembly for story 4, wall D1, D3, 3/12-D

Appendix B

Wall assembly for Story 4

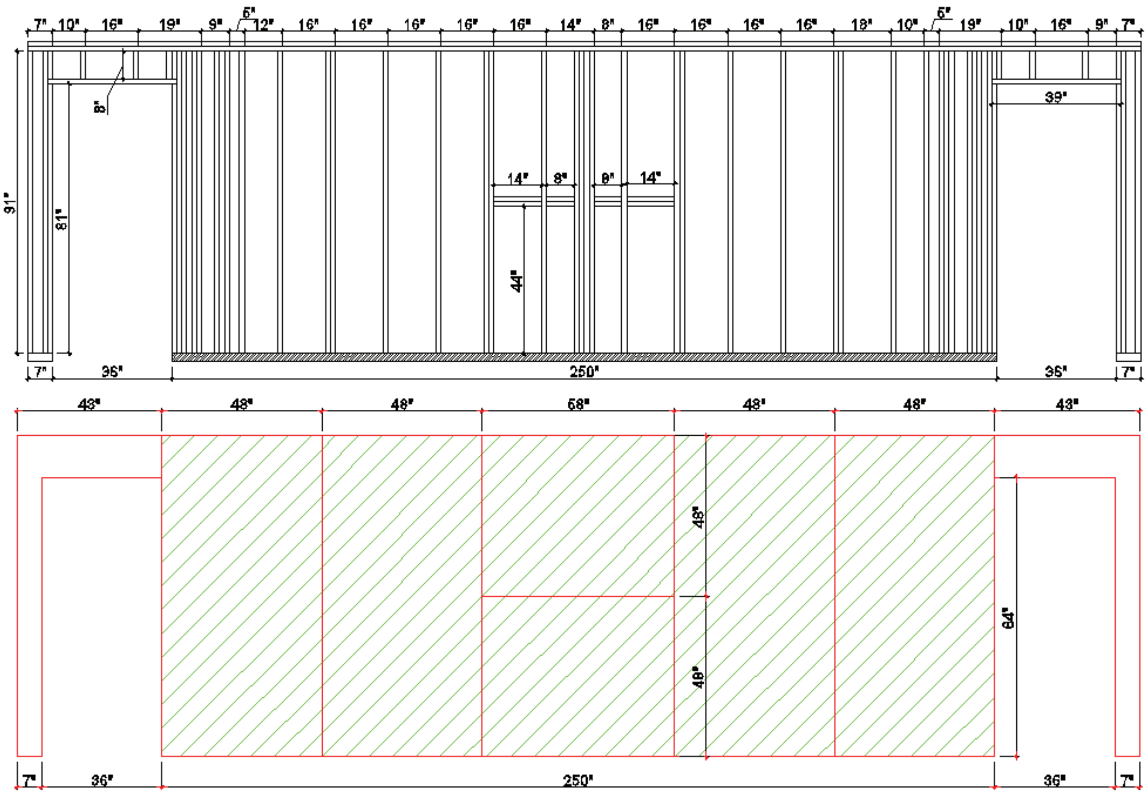

Figure B.36: Assembly for story 4, wall D2, 3/12-D

Appendix B

Wall assembly for Story 4

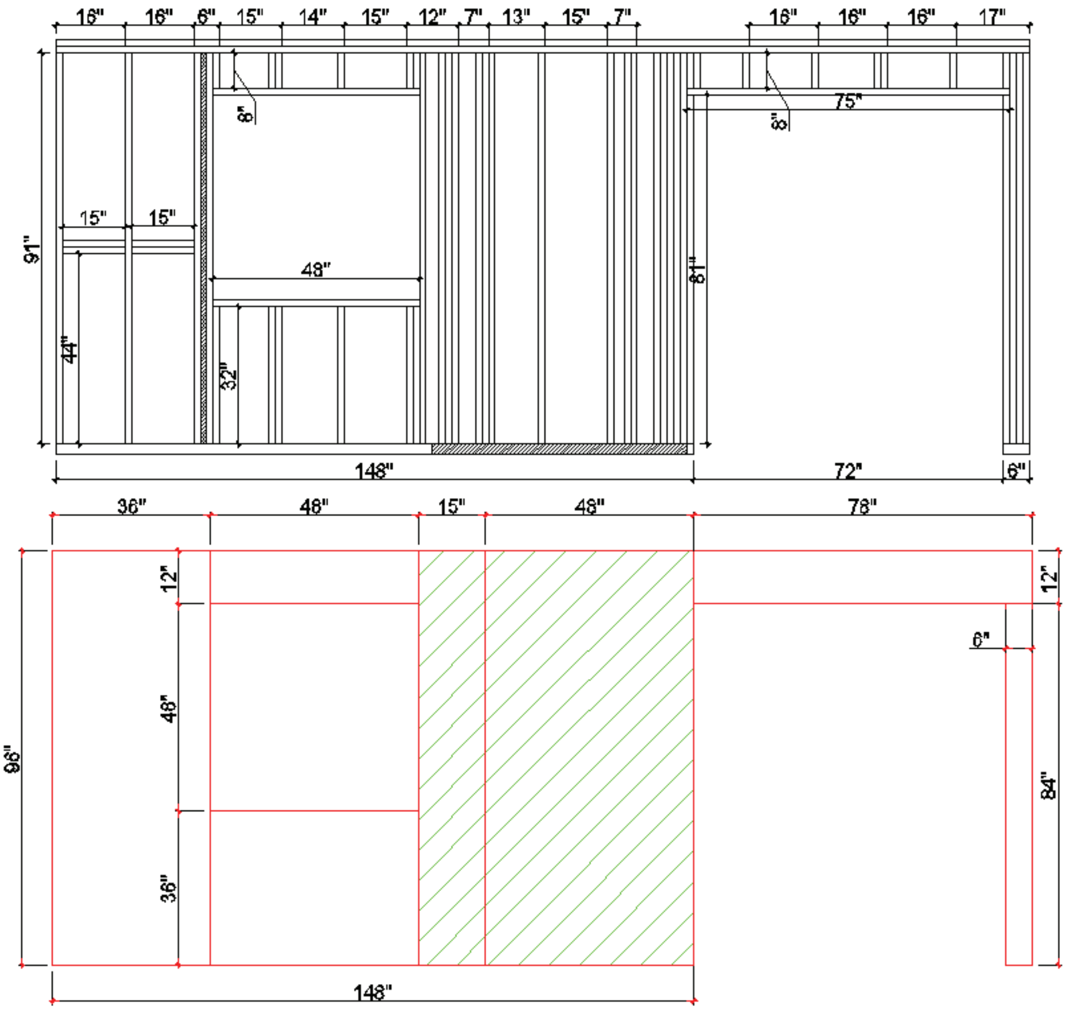

Figure B.37: Assembly for story 4, wall E1, E5, 3/12-D

Appendix B

Wall assembly for Story 4

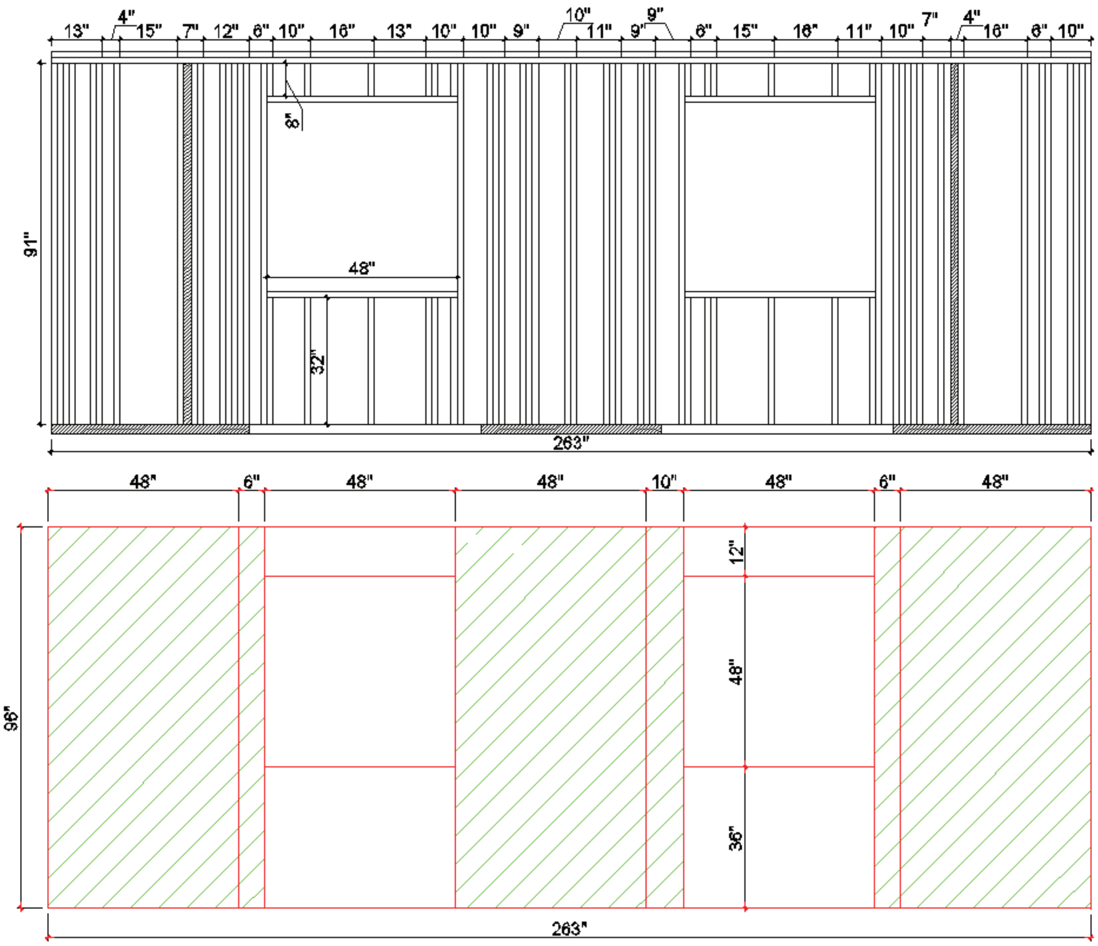

Figure B.38: Assembly for story 4, wall E2, E3, E4, 3/12-D

Appendix B

Wall assembly for Story 4

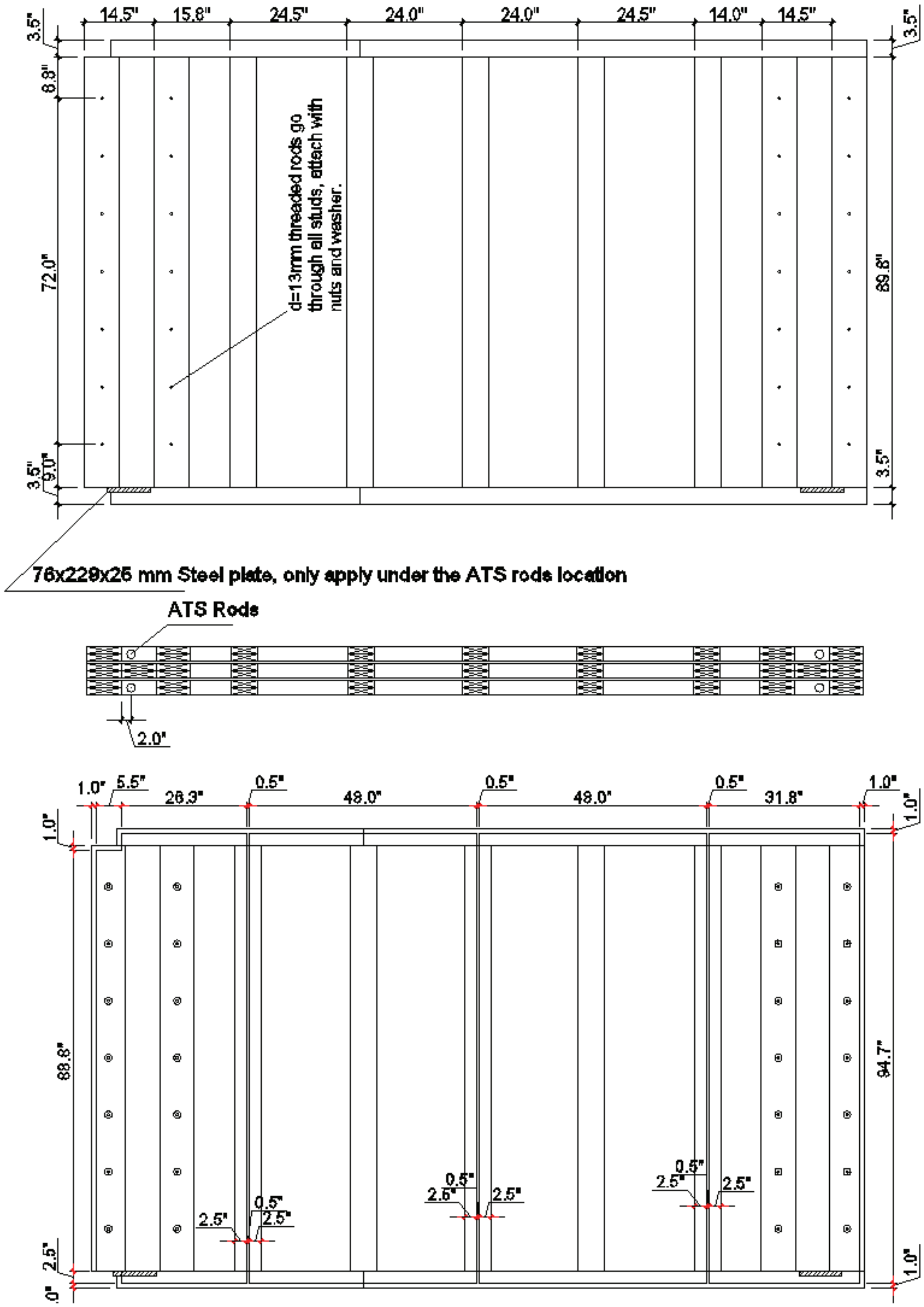

Figure B.39: Assembly for story 4, wall B1, B2, 3/12 Double Midply

Appendix B

Wall assembly for Story 5

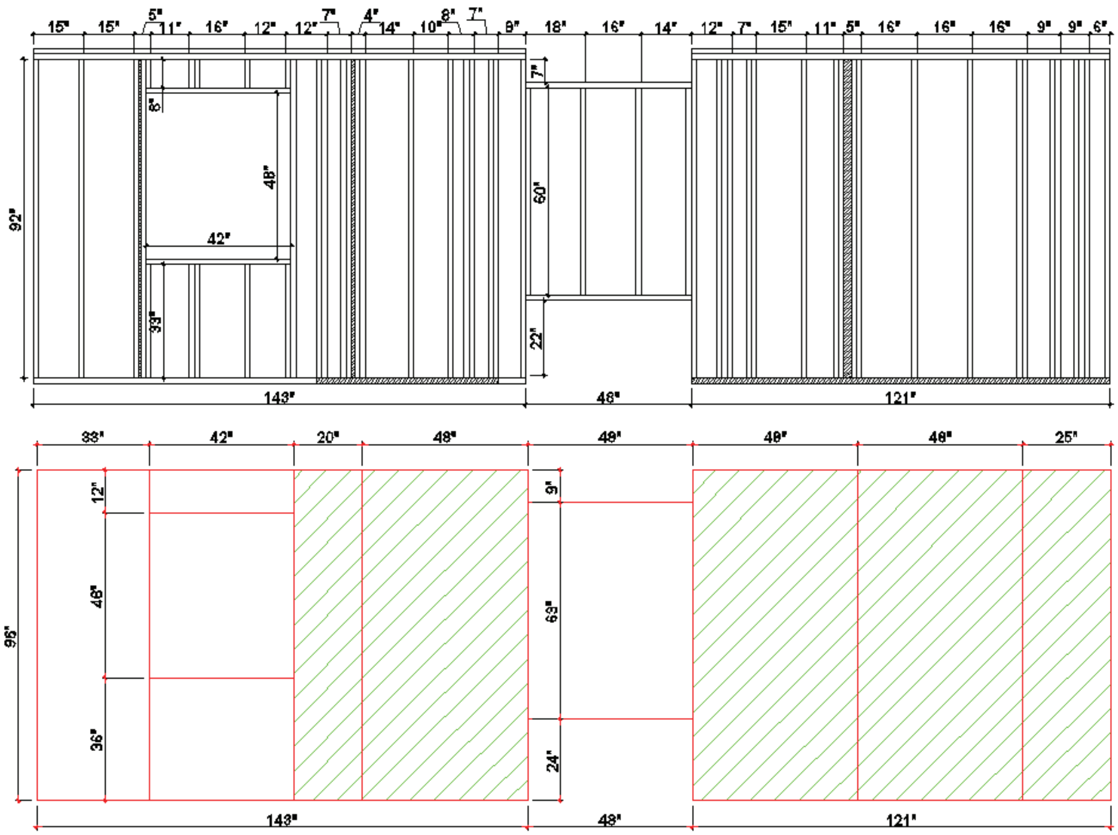

Figure B.40: Assembly for story 5, wall 1AB, 11AB, 4/12-D

Appendix B

Wall assembly for Story 5

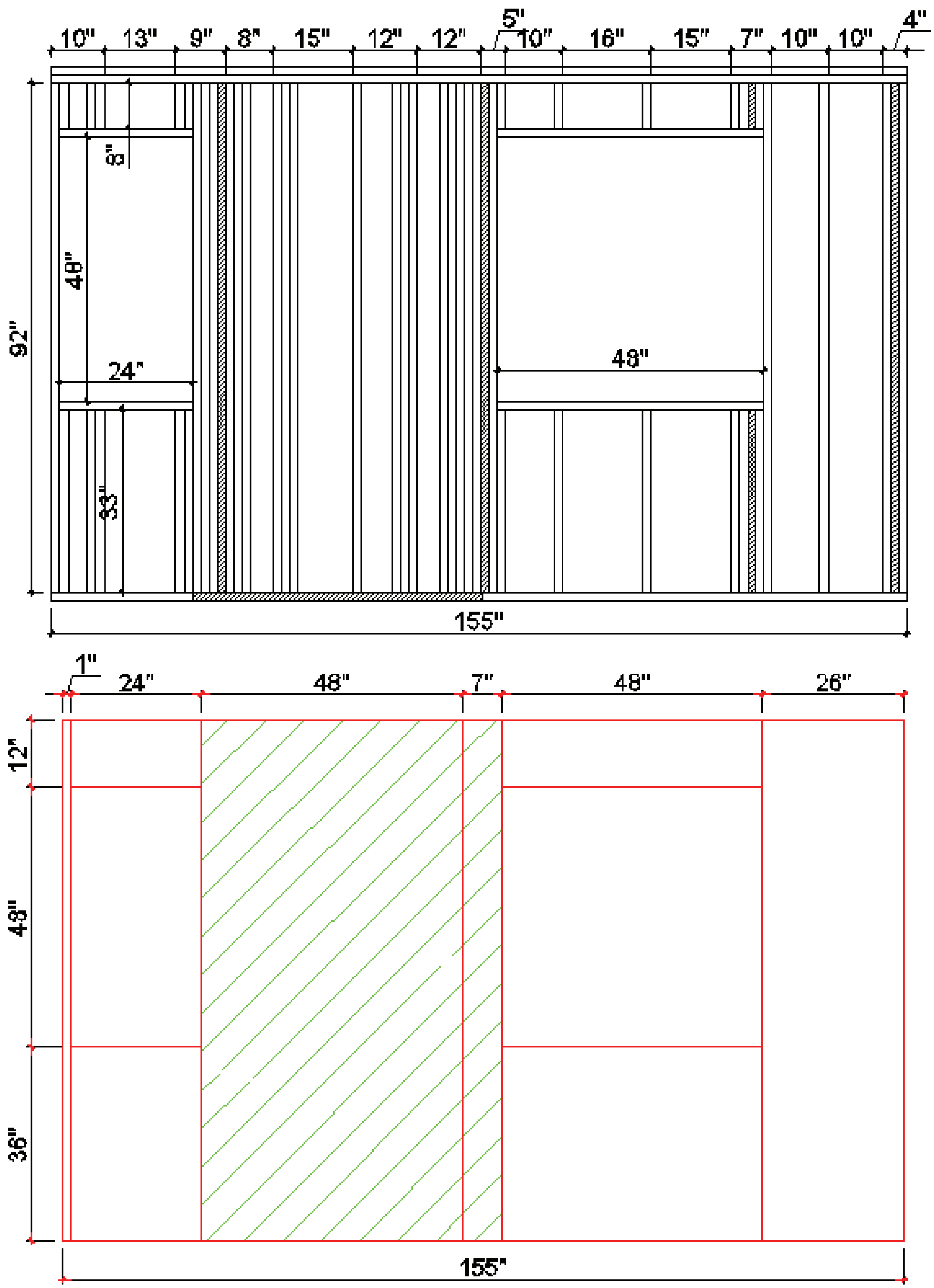

Figure B.41: Assembly for story 5, wall 1C, 11C, 4/12-D

Appendix B

Wall assembly for Story 5

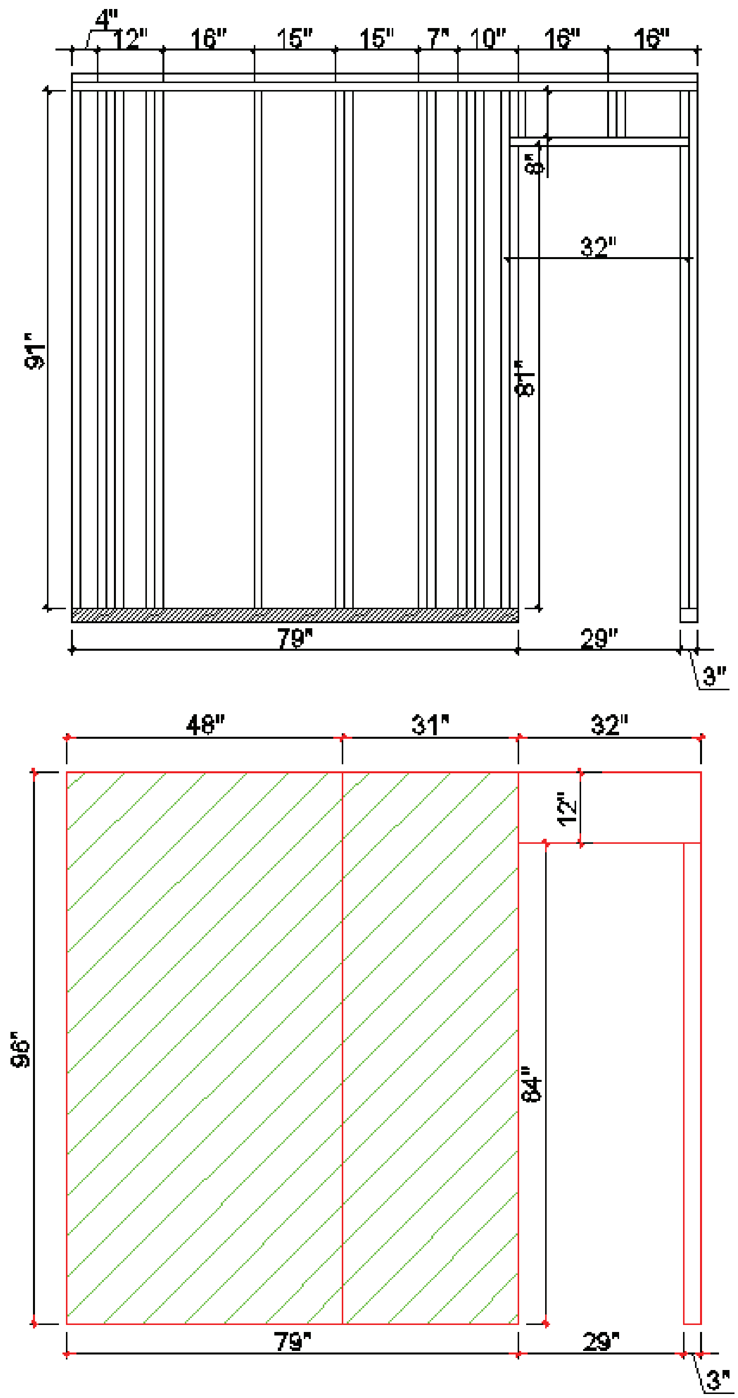

Figure B.42: Assembly for story 5, wall 2A, 10A, 2/12

Appendix B

Wall assembly for Story 5

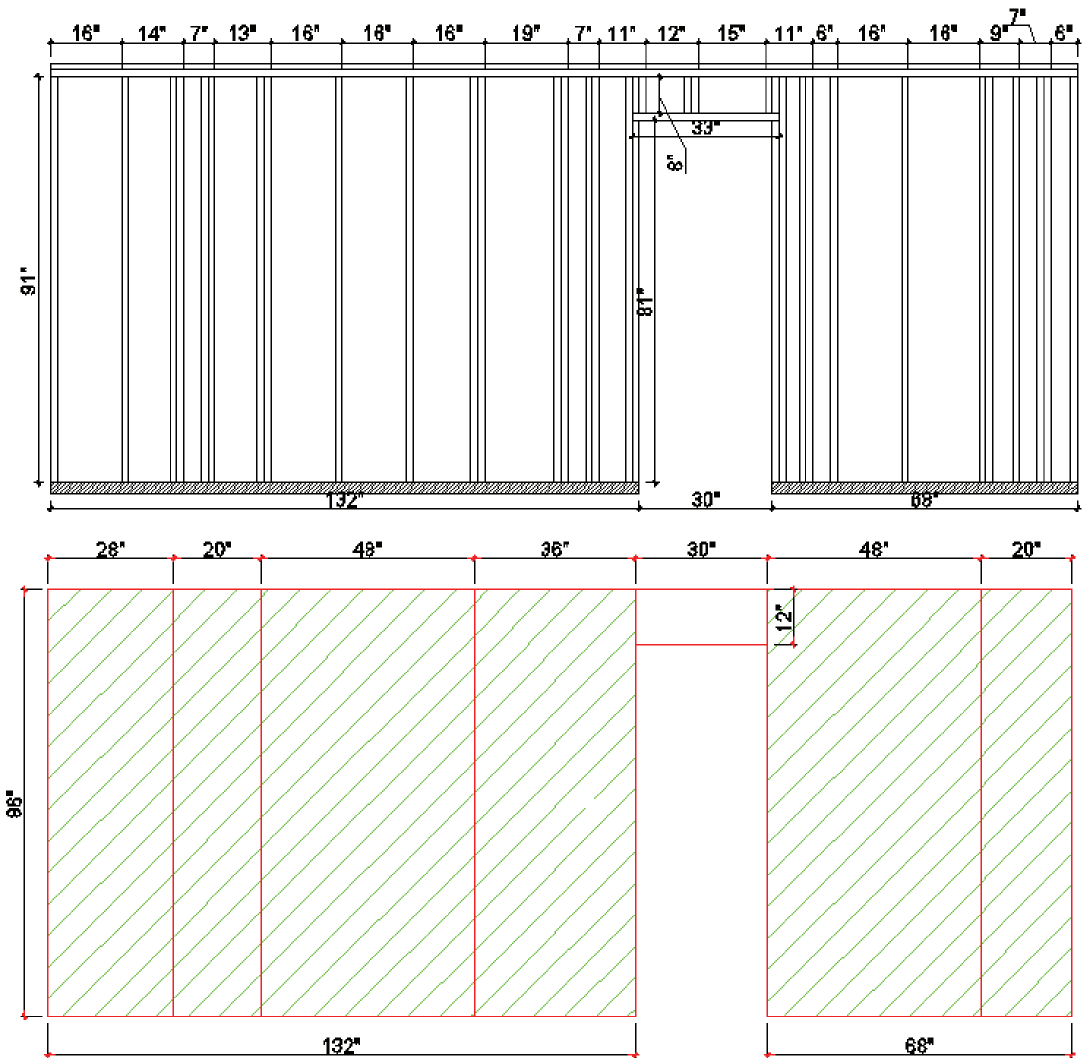

Figure B.43: Assembly for story 5, wall 2BC, 10BC, 2/12

Appendix B

Wall assembly for Story 5

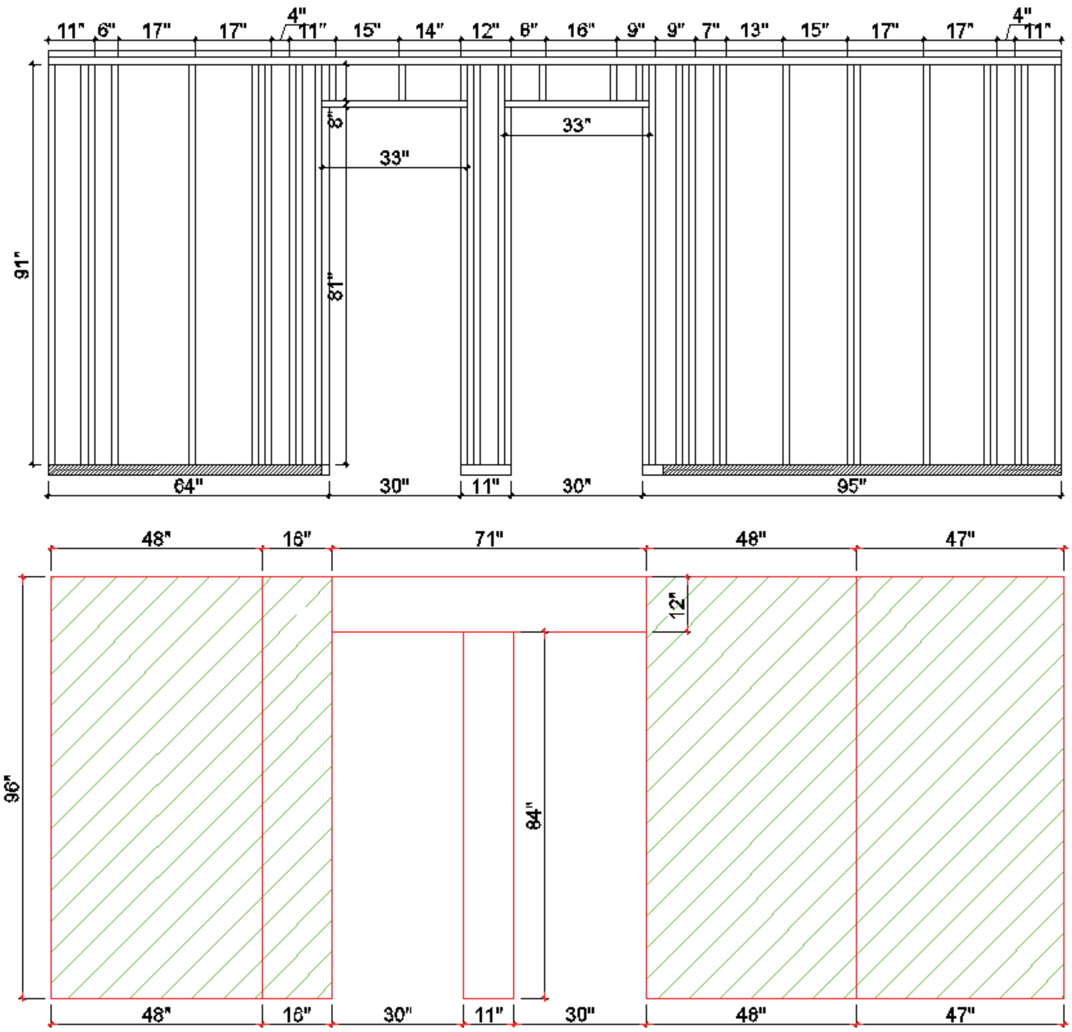

Figure B.44: Assembly for story 5, wall 4A-B, 8A-B, 3/12-D

Appendix B

Wall assembly for Story 5

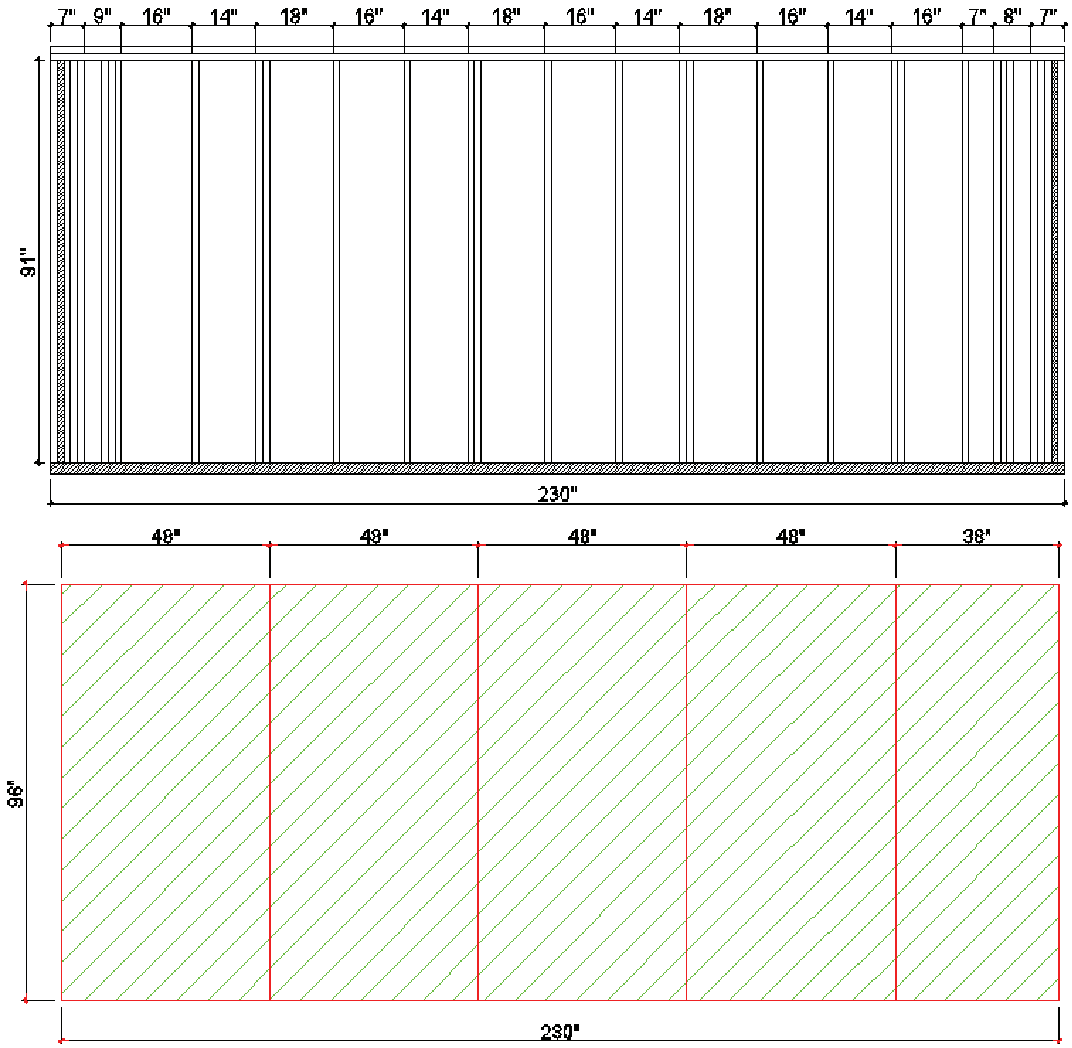

Figure B.45: Assembly for story 5, wall 6, 2/12-D

Appendix B

Wall assembly for Story 5

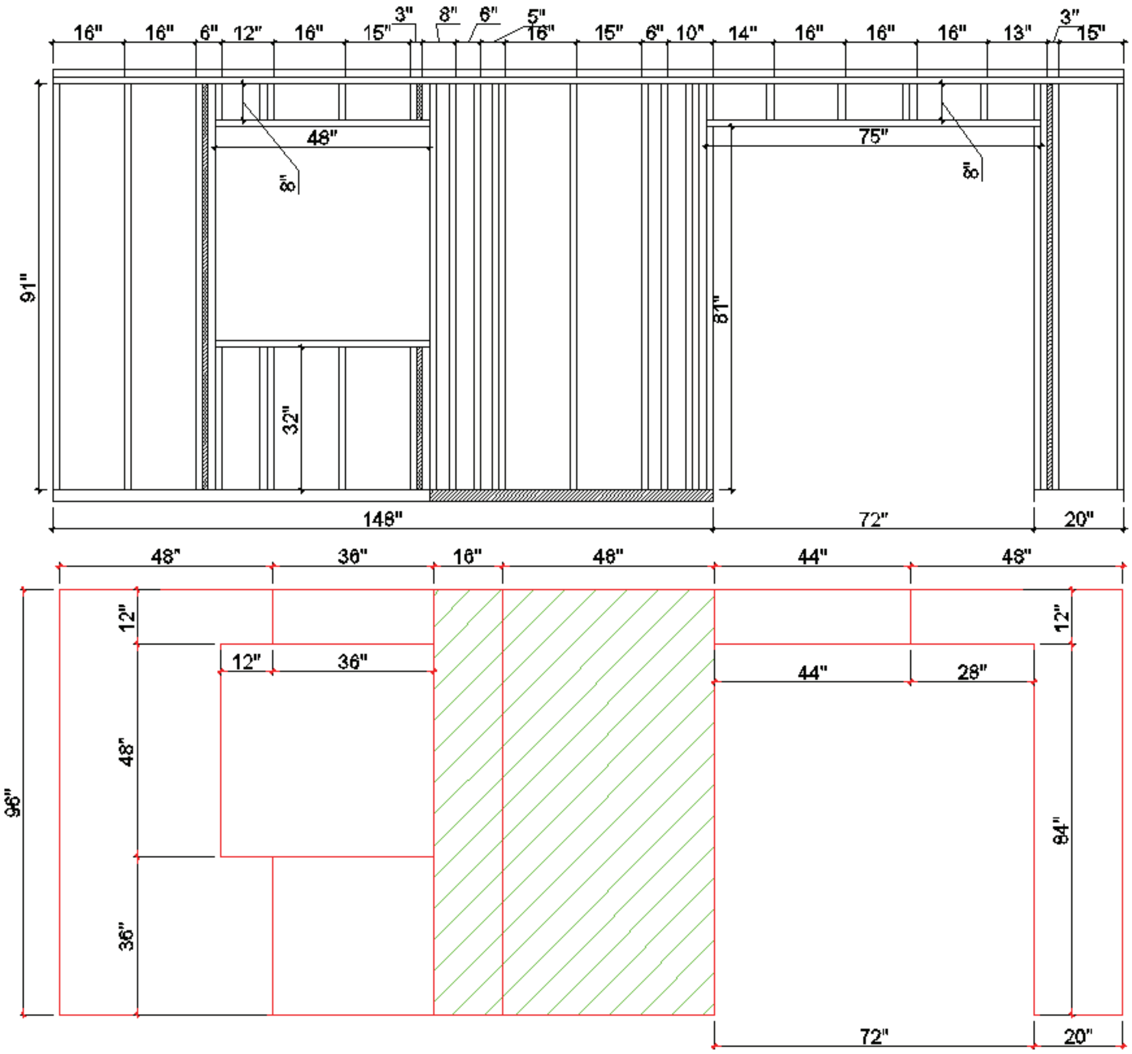

Figure B.46: Assembly for story 5, wall A1, A3, 2/12

Appendix B

Wall assembly for Story 5

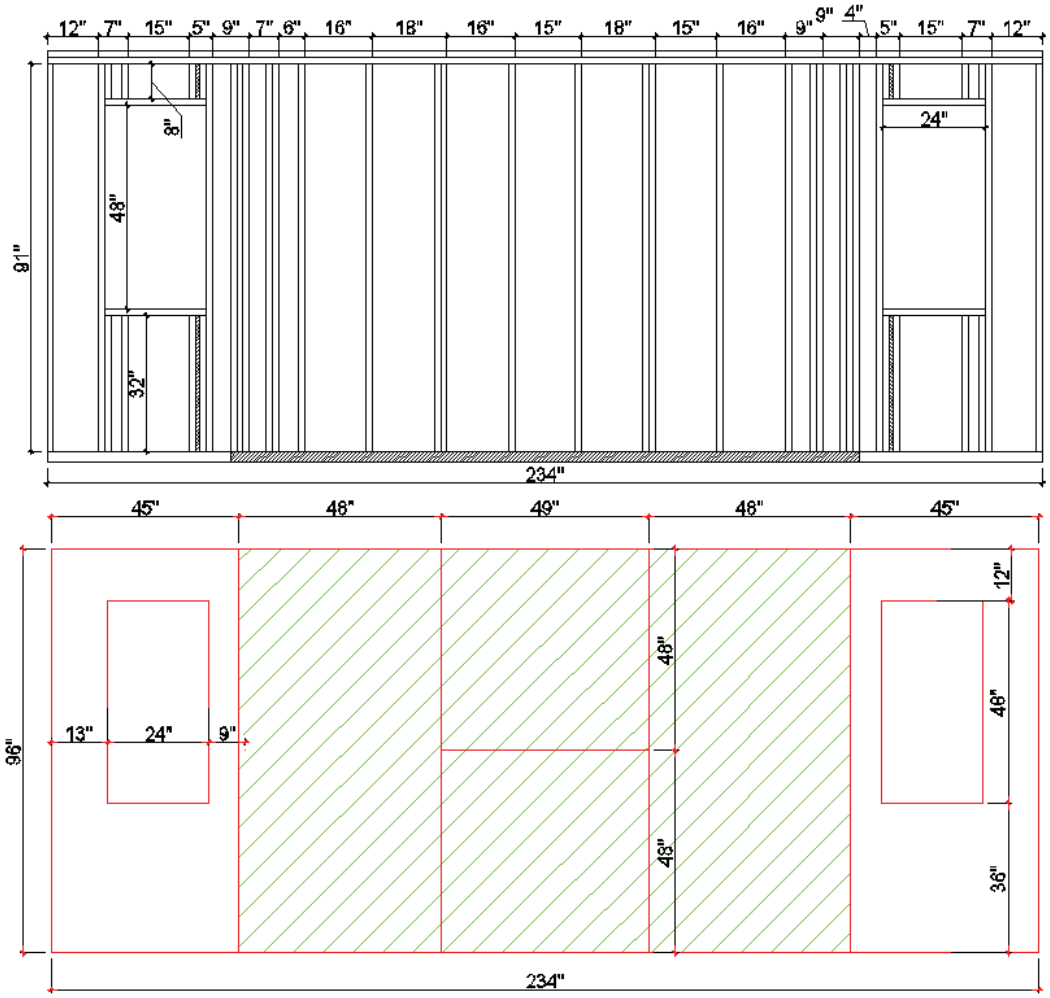

Figure B.47: Assembly for story 5, wall A2, 2/12

Appendix B

Wall assembly for Story 5

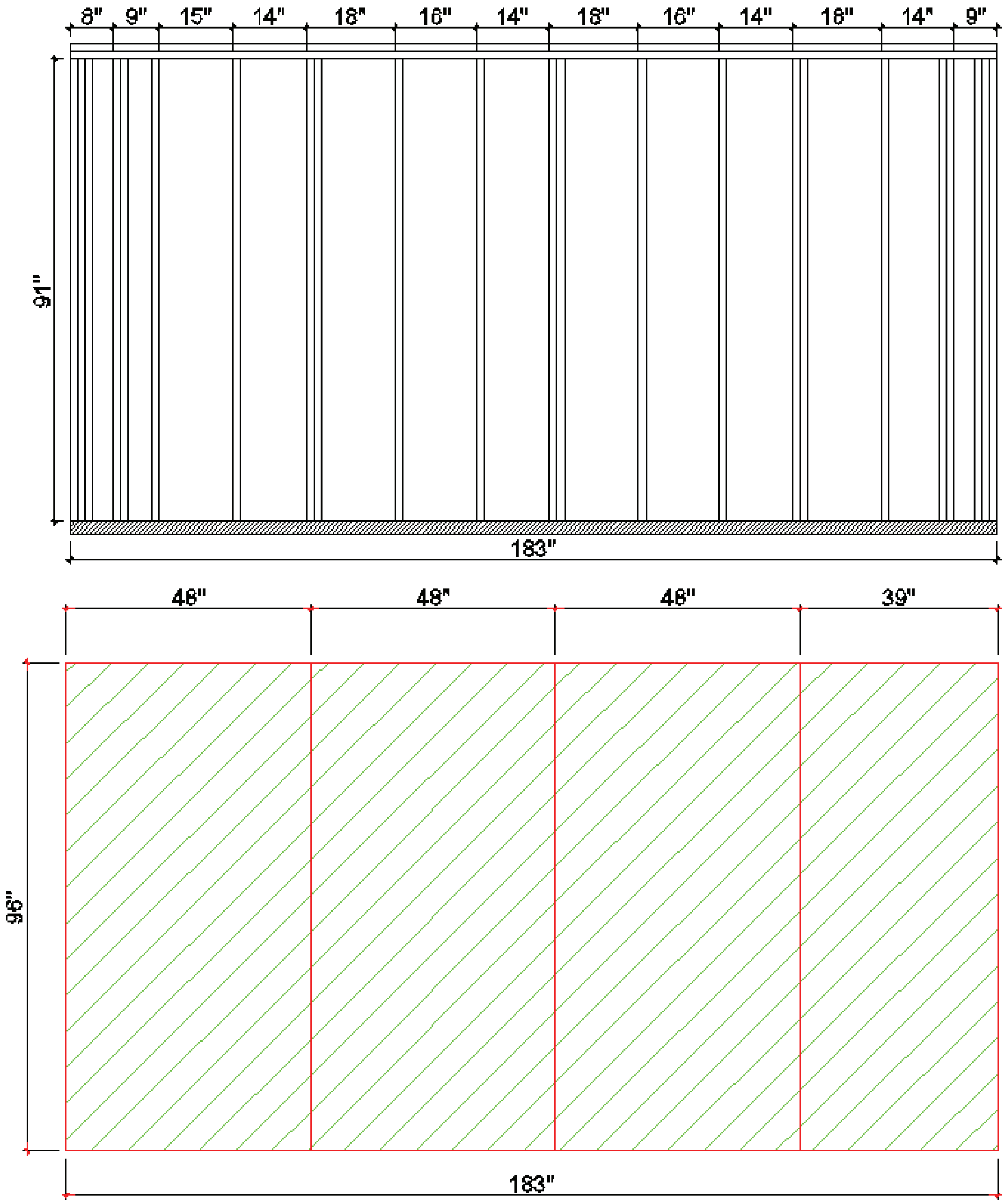

Figure B.48: Assembly for story 5, wall D1, D3, 2/12

Appendix B

Wall assembly for Story 5

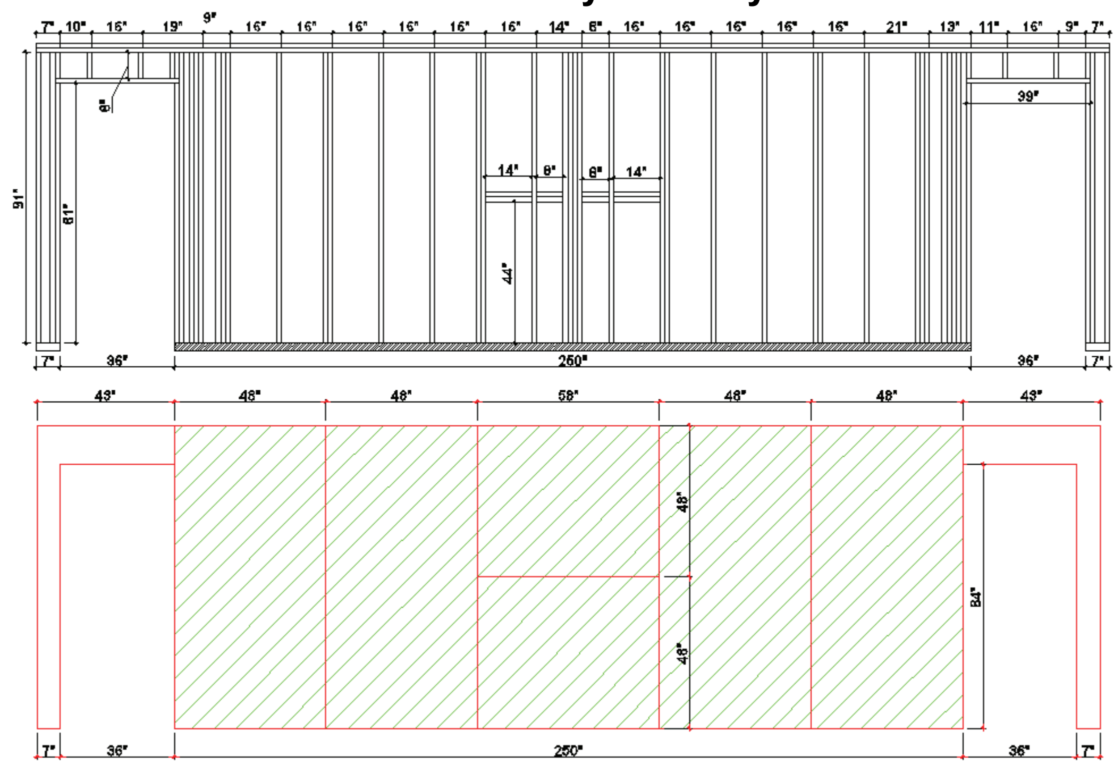

Figure B.49: Assembly for story 5, wall D2, 2/12

Appendix B

Wall assembly for Story 5

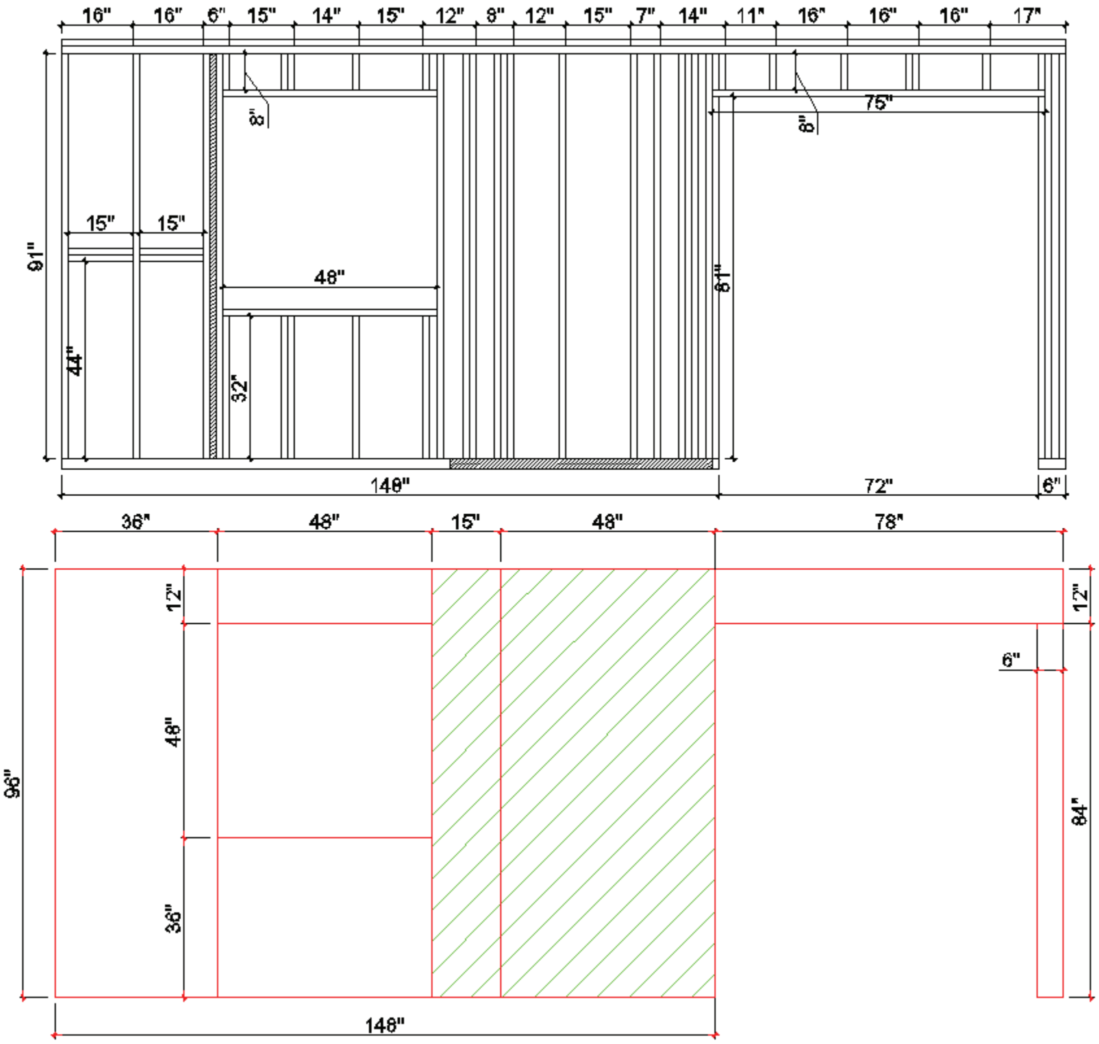

Figure B.50: Assembly for story 5, wall E1, E5, 3/12-D

Appendix B

Wall assembly for Story 5

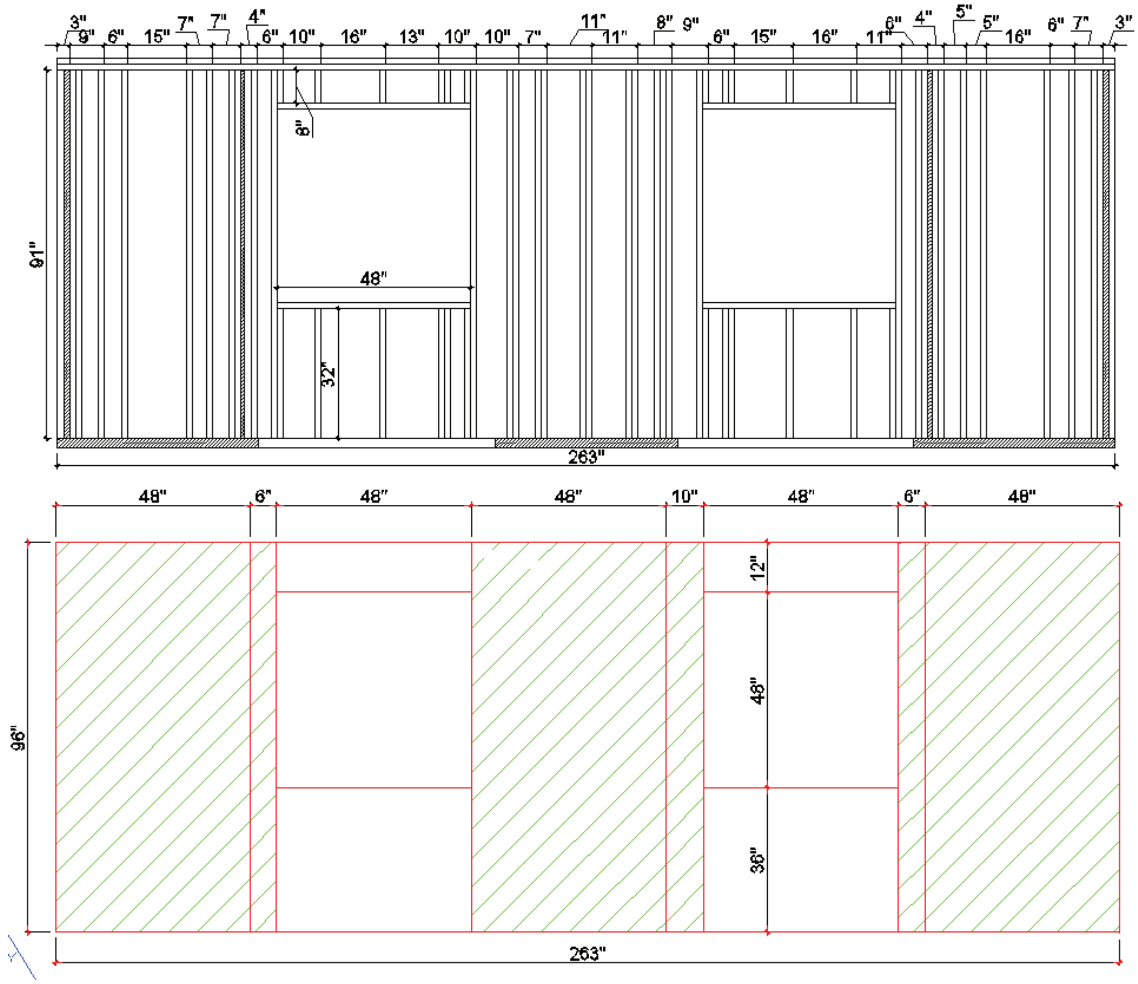

Figure B.51: Assembly for story 5, wall E2, E3, E4, 3/12-D

Appendix B

Wall assembly for Story 5

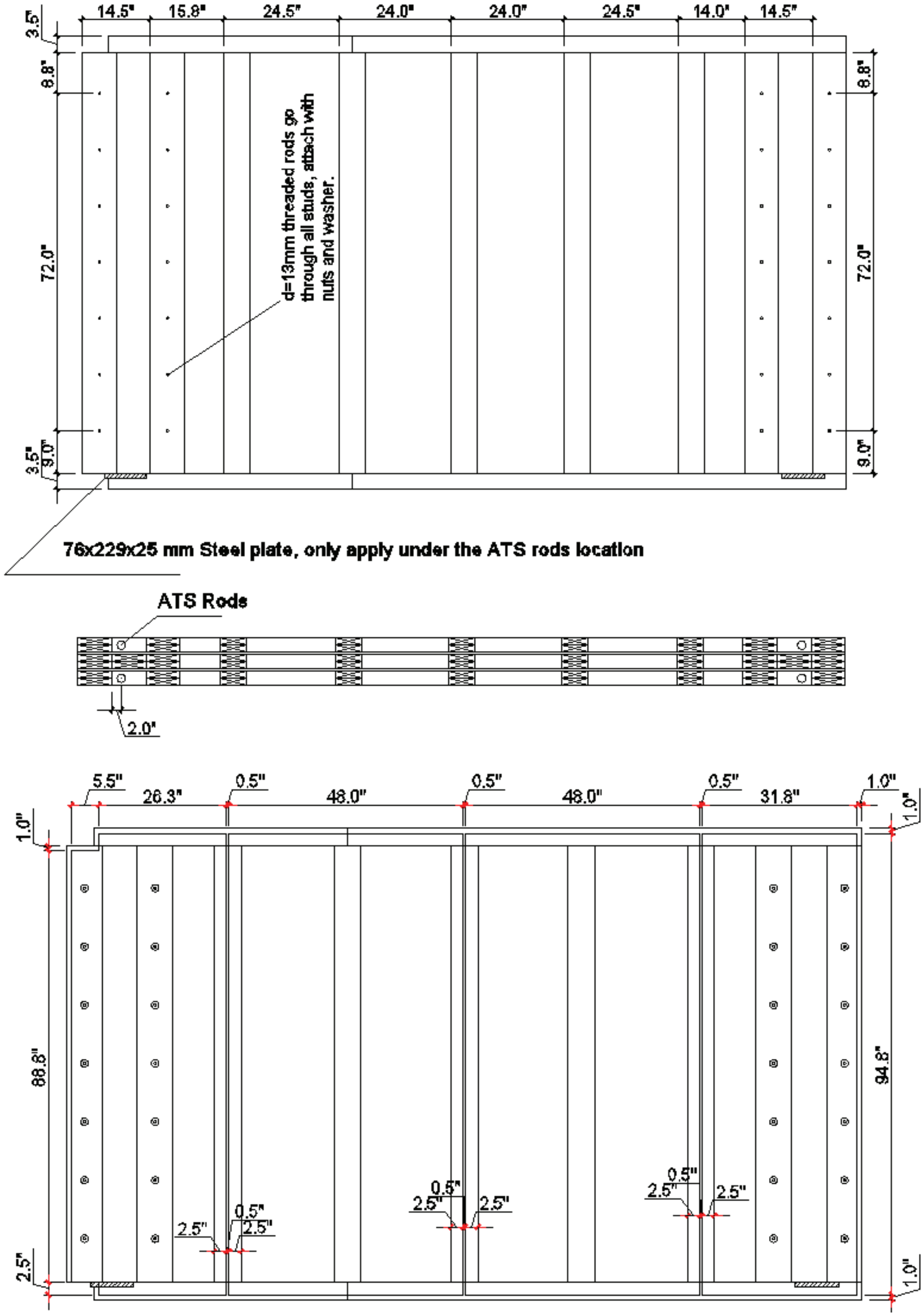

Figure B.52: Assembly for story 5, wall B1, B2, 4/12 Double Midply

Appendix B

Wall assembly for Story 6

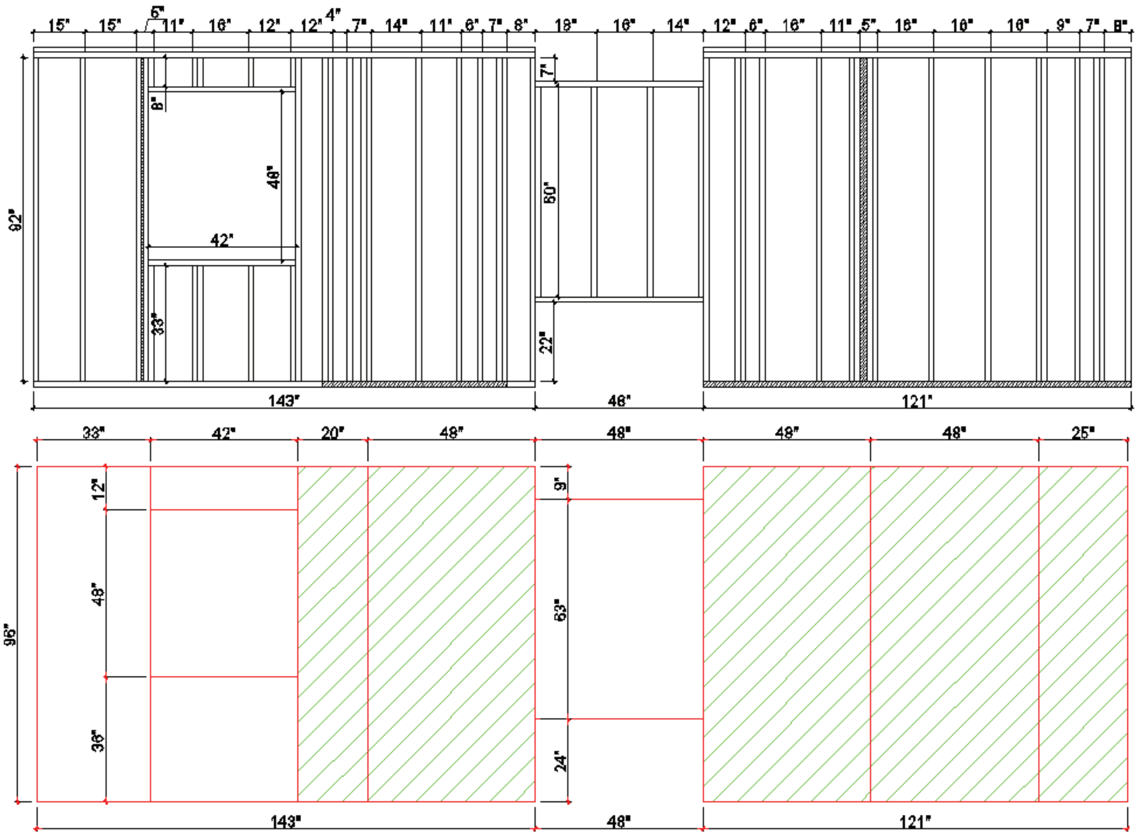

Figure B.53: Assembly for story 6, wall 1AB, 11AB, 4/12-D

Appendix B

Wall assembly for Story 6

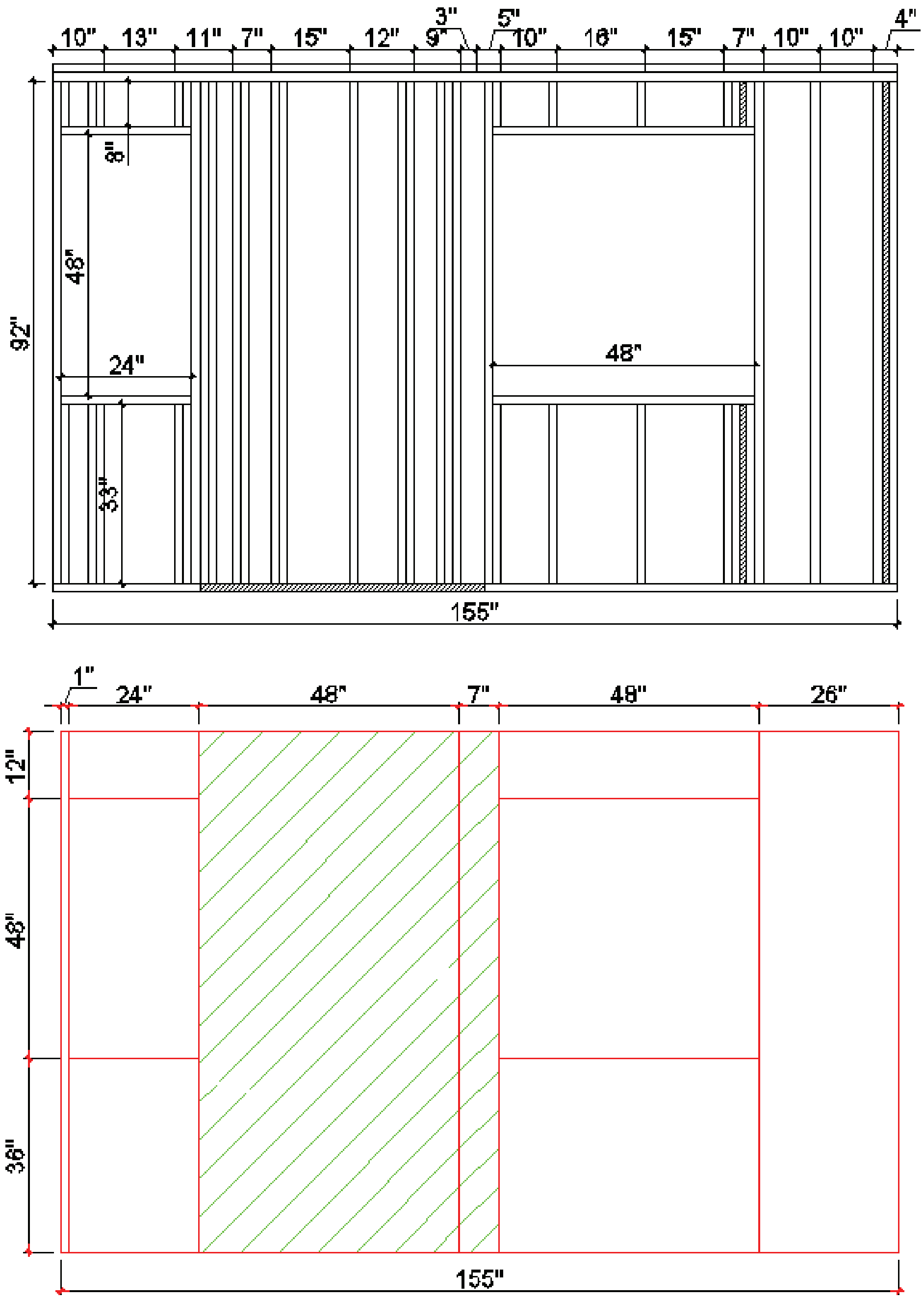

Figure B.54: Assembly for story 6, wall 1C, 11C, 4/12-D

Appendix B

Wall assembly for Story 6

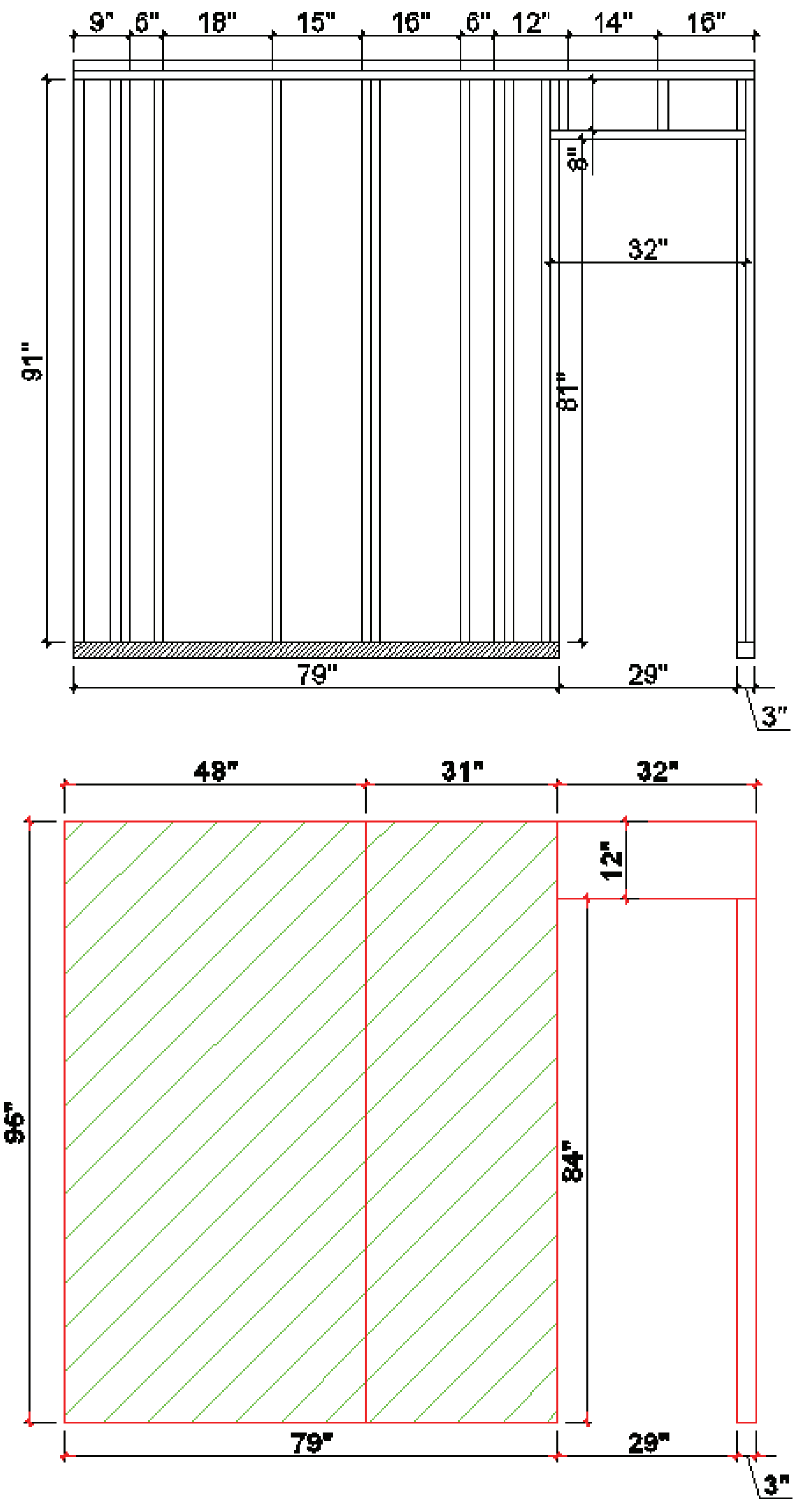

Figure B.55: Assembly for story 6, wall 2A, 10A, 2/12

Appendix B

Wall assembly for Story 6

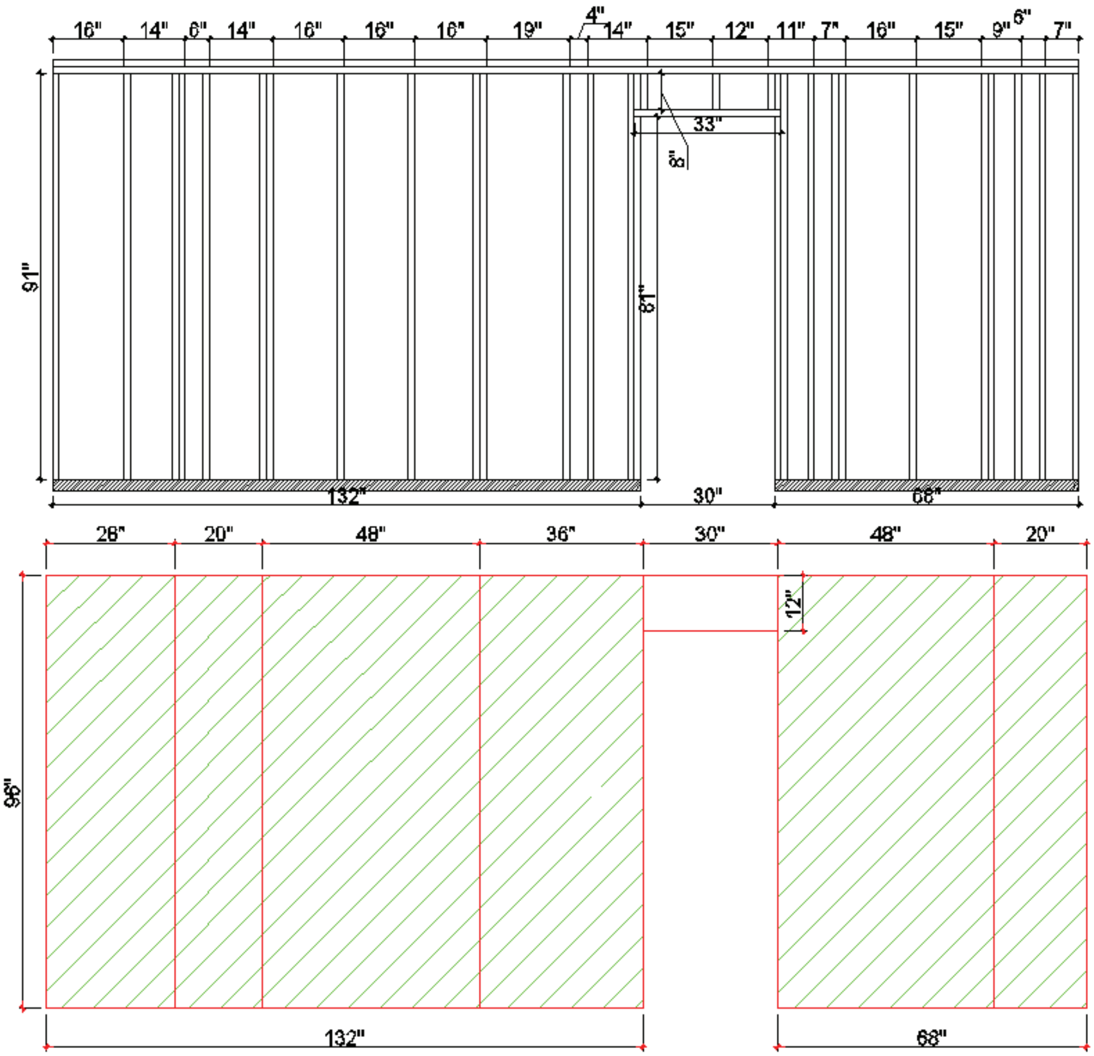

Figure B.56: Assembly for story 6, wall 2BC, 10BC, 2/12

Appendix B

Wall assembly for Story 6

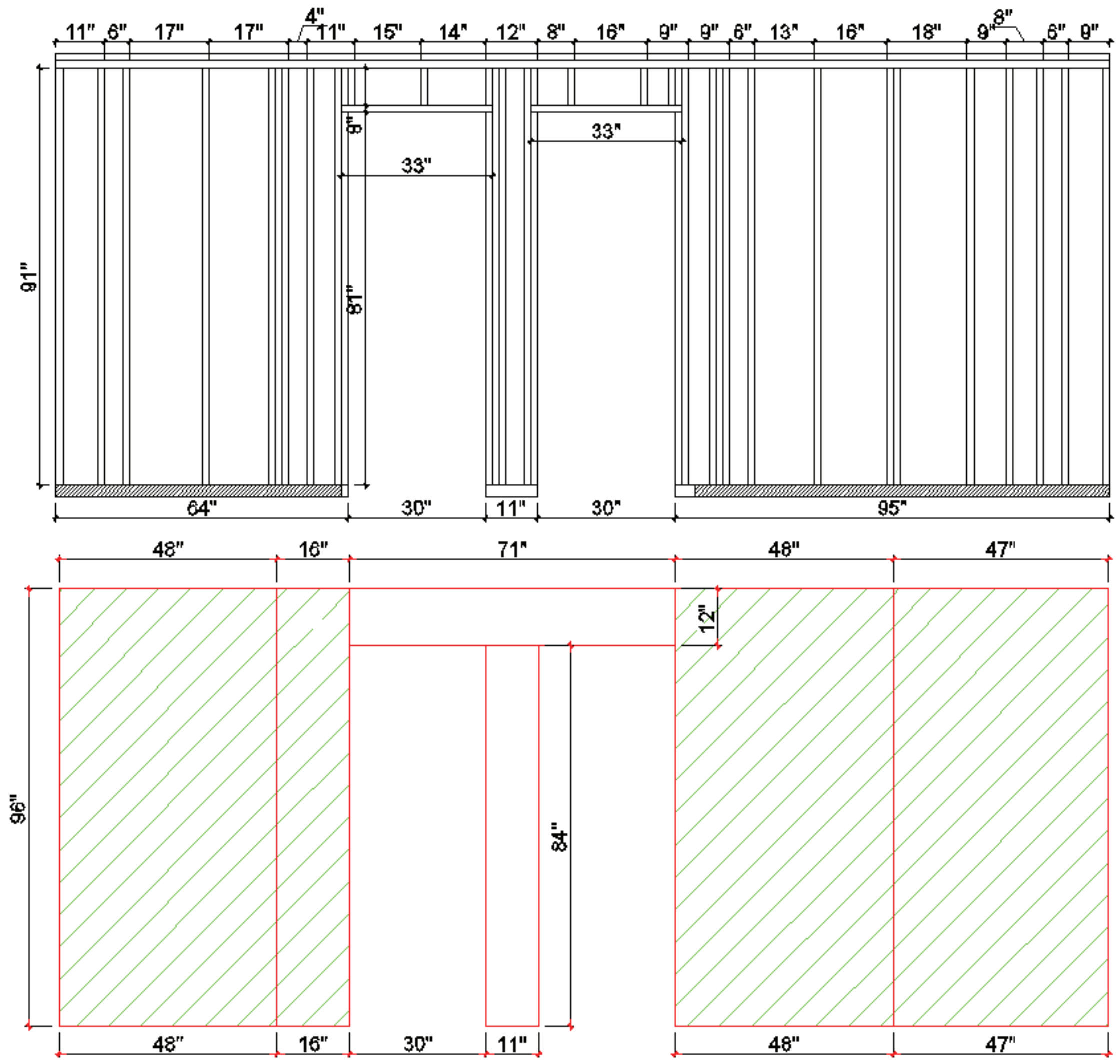

Figure B.57: Assembly for story 6, wall 4AB, 8AB, 3/12

Appendix B

Wall assembly for Story 6

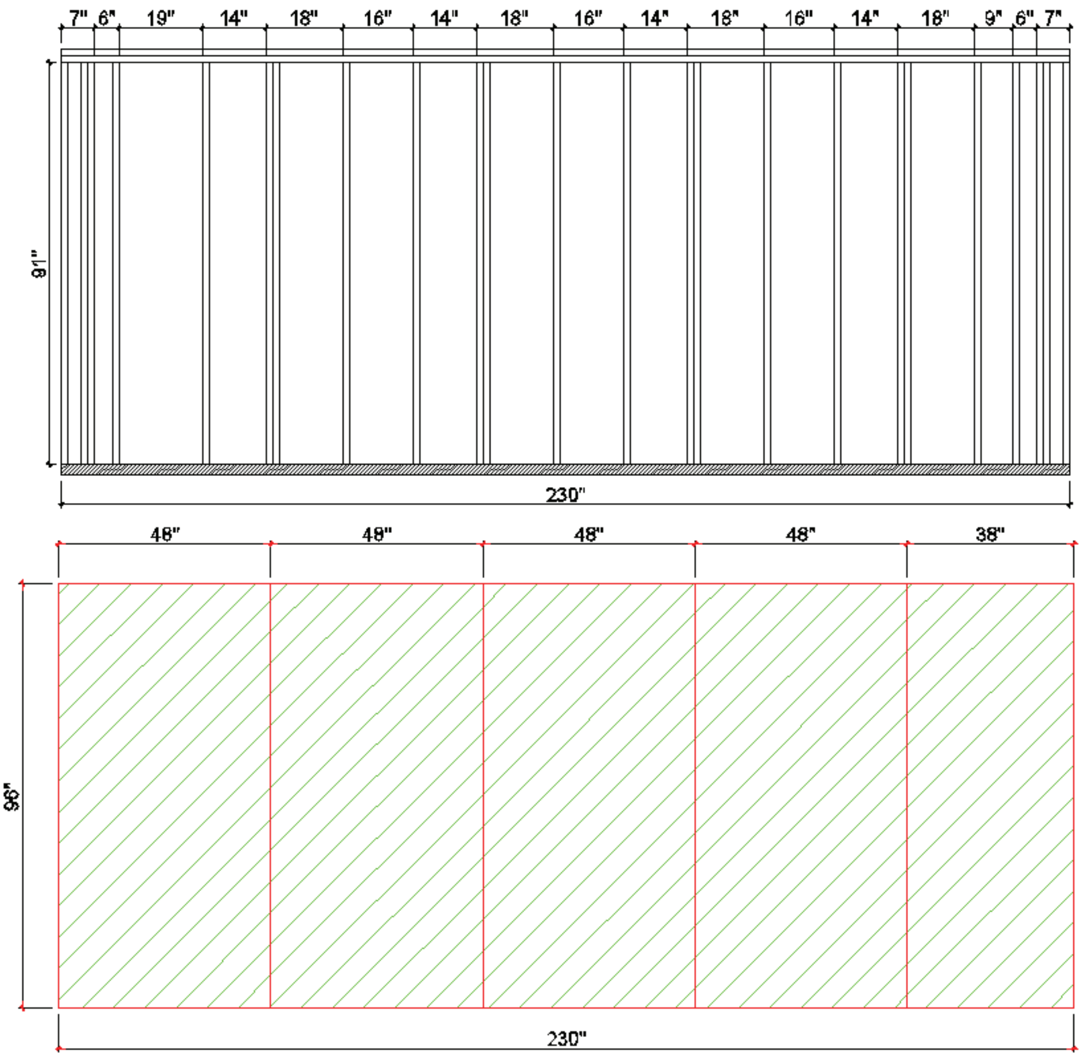

Figure B.58: Assembly for story 6, wall 6, 2/12

Appendix B

Wall assembly for Story 6

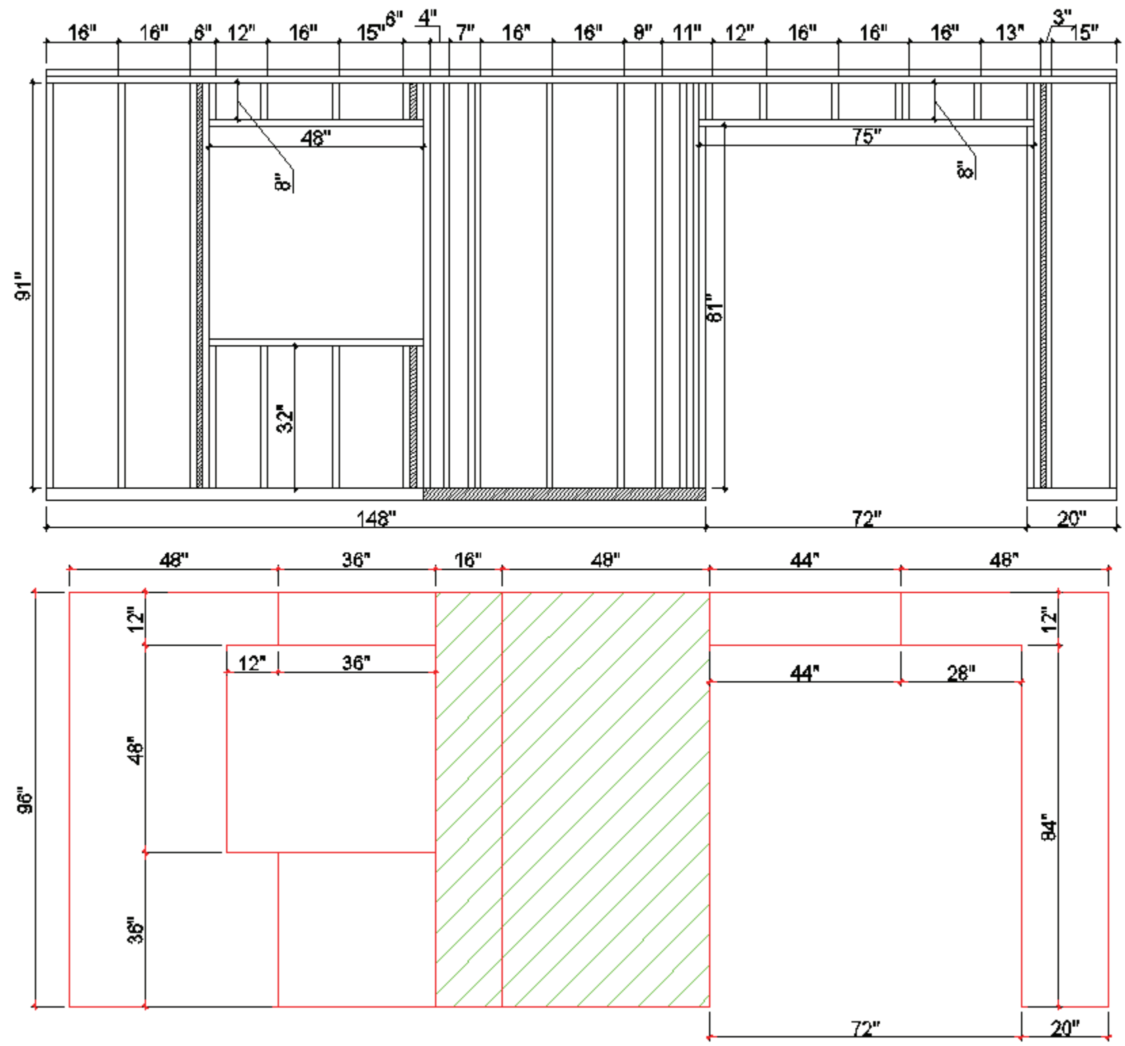

Figure B.59: Assembly for story 6, wall A1, A3, 3/12

Appendix B

Wall assembly for Story 6

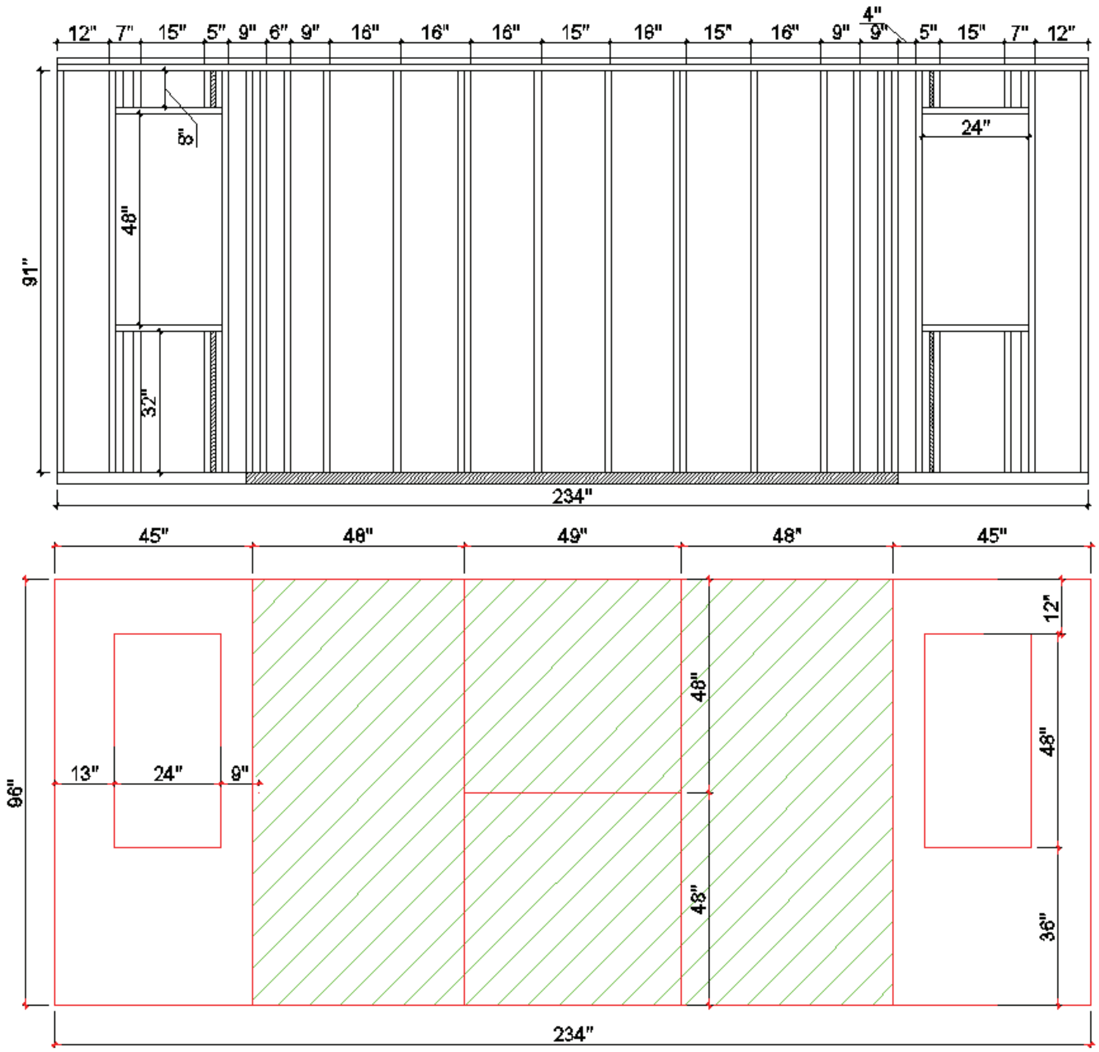

Figure B.60: Assembly for story 6, wall A2, 3/12

Appendix B

Wall assembly for Story 6

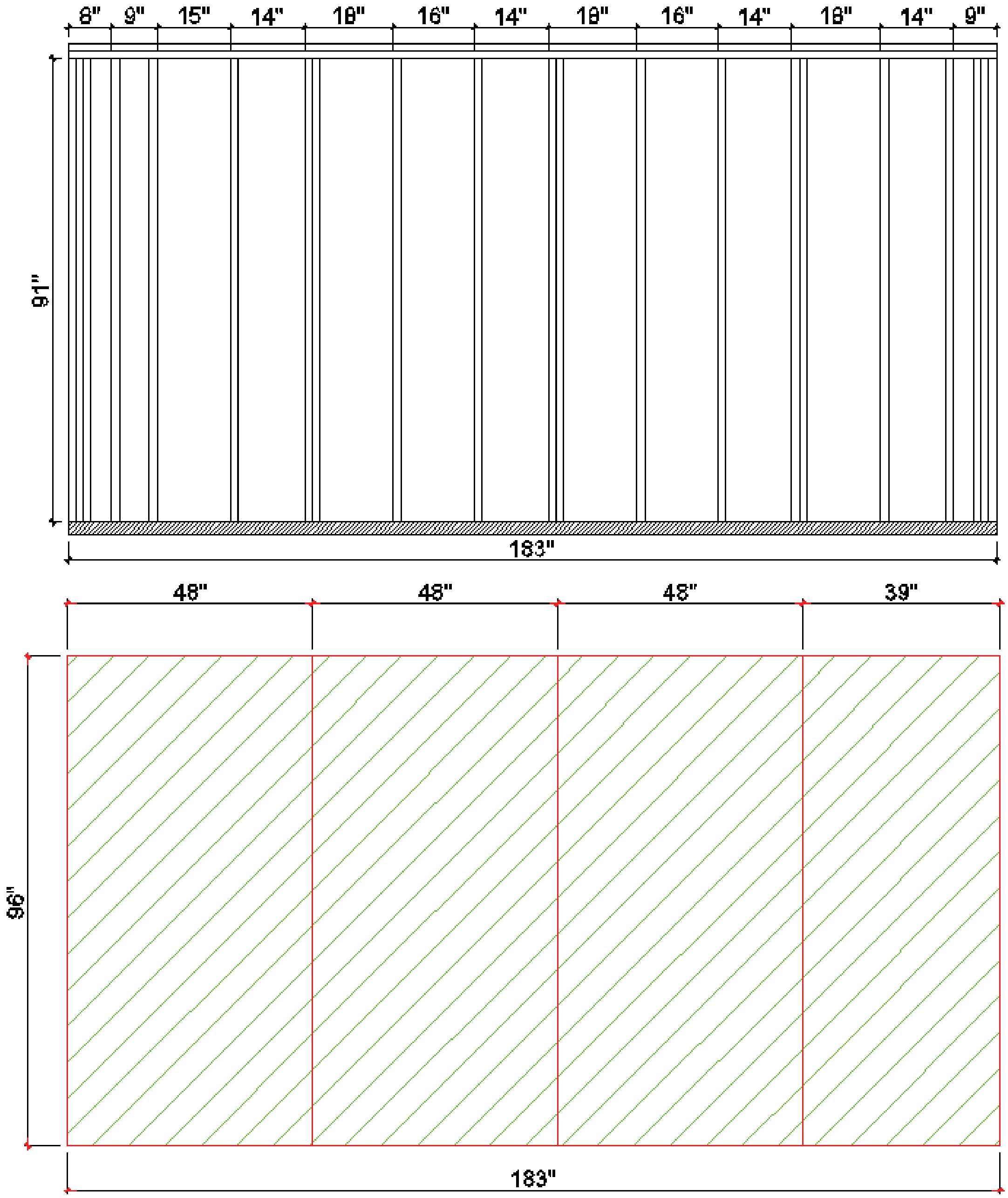

Figure B.61: Assembly for story 6, wall D1, D3, 3/12

Appendix B

Wall assembly for Story 6

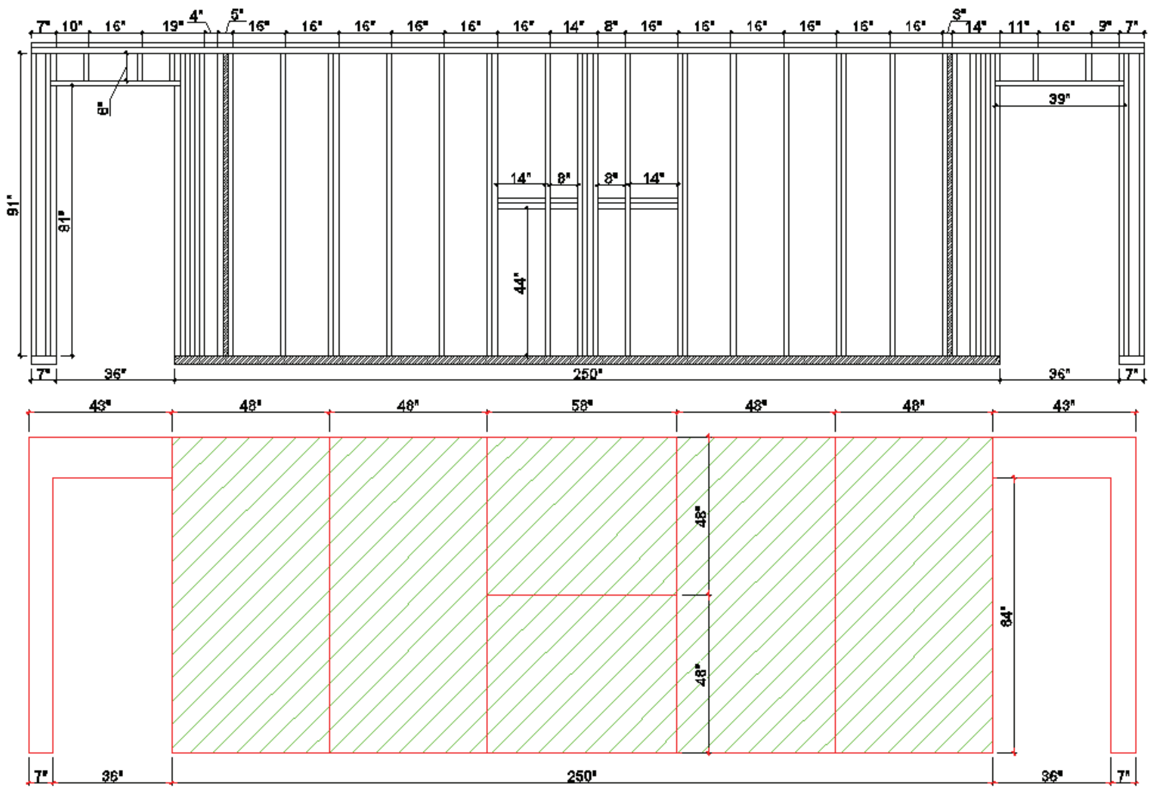

Figure B.62: Assembly for story 6, wall D2, 3/12

Appendix B

Wall assembly for Story 6

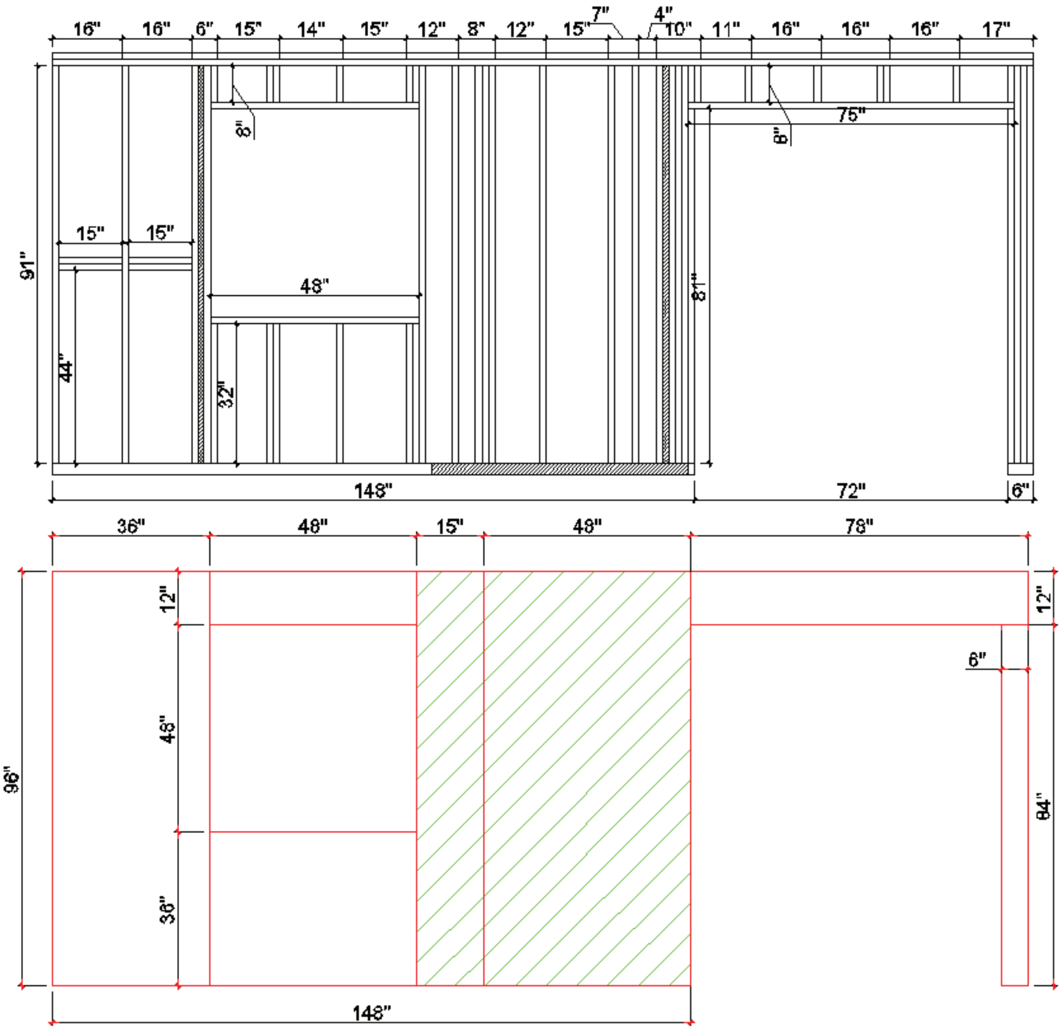

Figure B.63: Assembly for story 6, wall E1, E5, 3/12-D

Appendix B

Wall assembly for Story 6

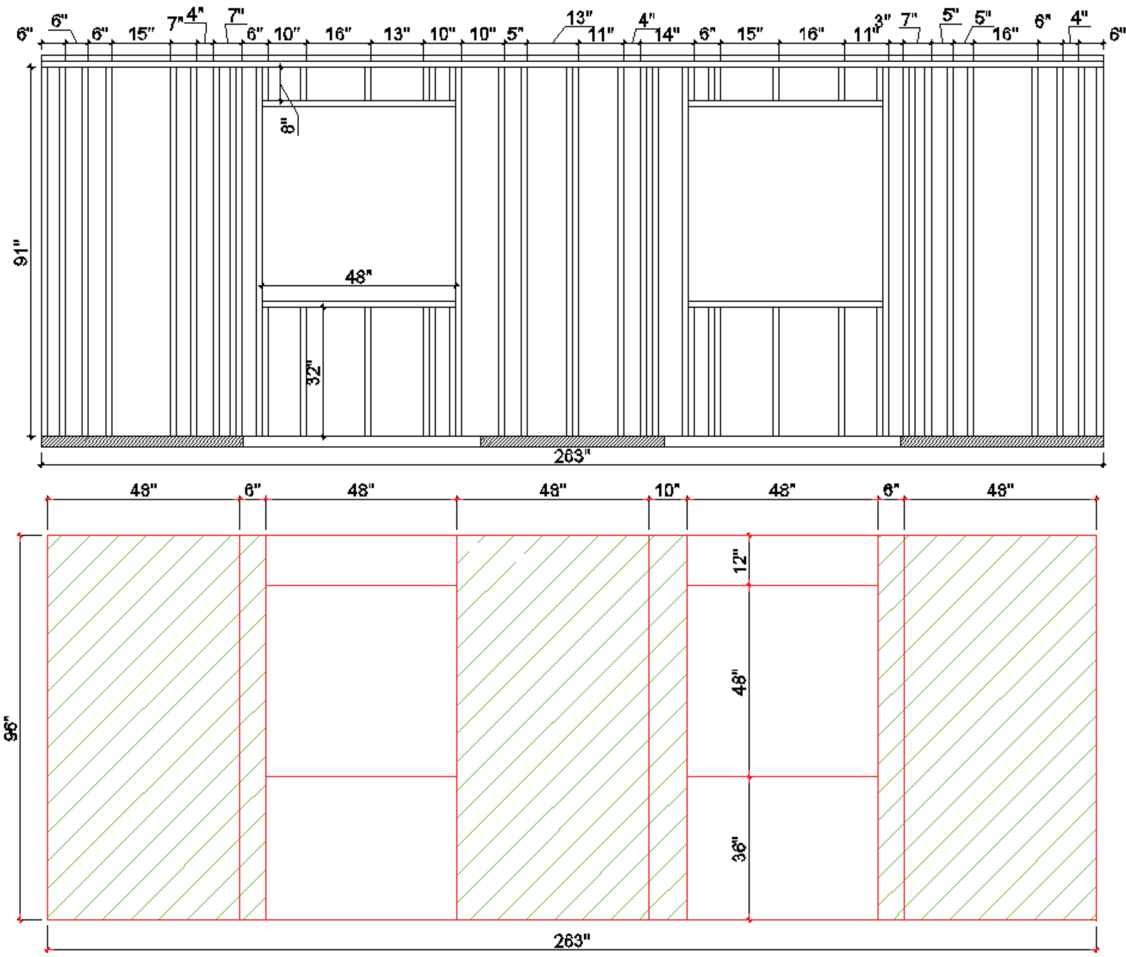

Figure B.64: Assembly for story 6, wall E2, E3, E4, 3/12-D

Appendix B

Wall assembly for Story 6

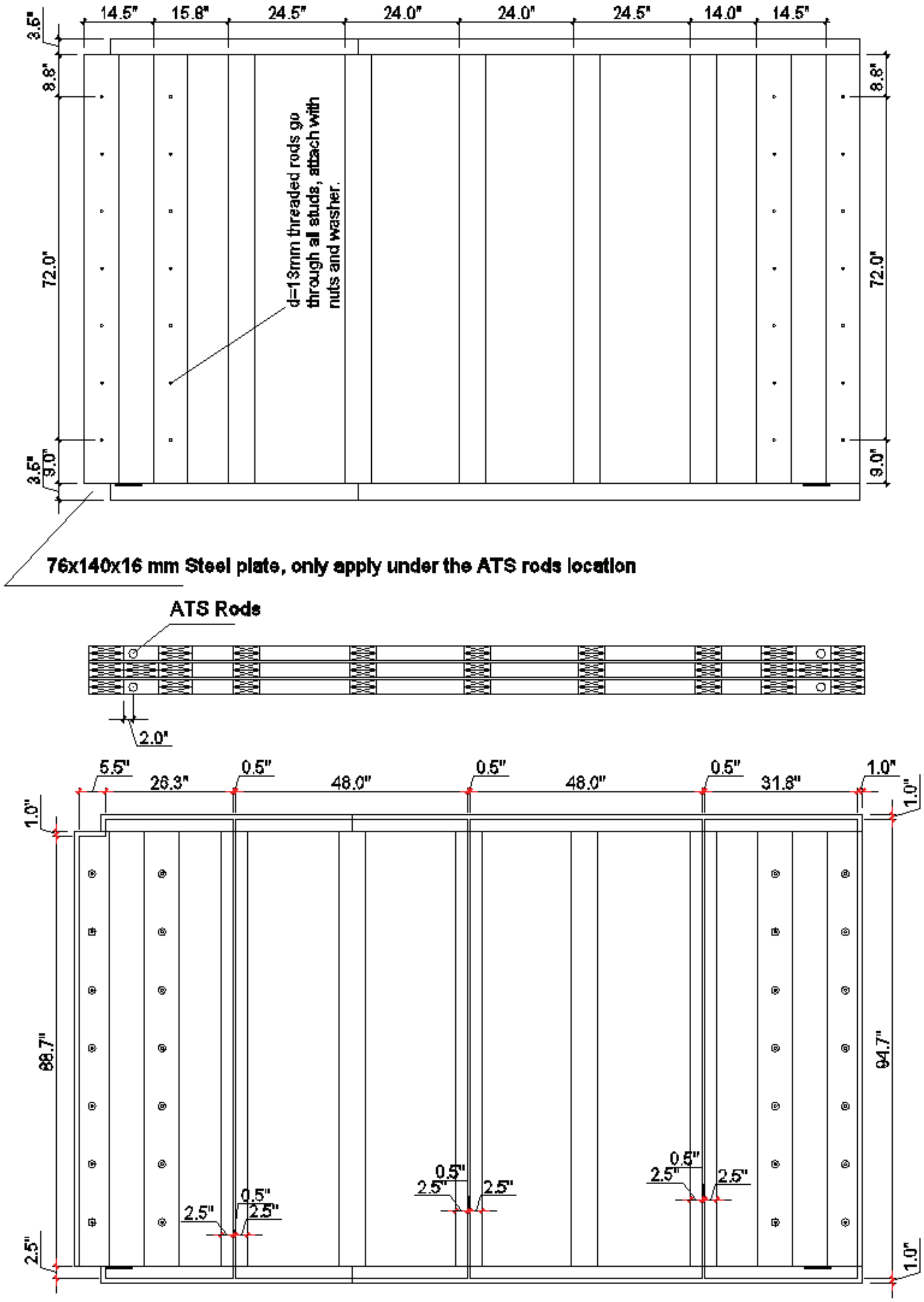

Figure B.65: Assembly for story 6, wall B1, B2, 6/12 Double Midply

Appendix B

Wall assembly for Story 7

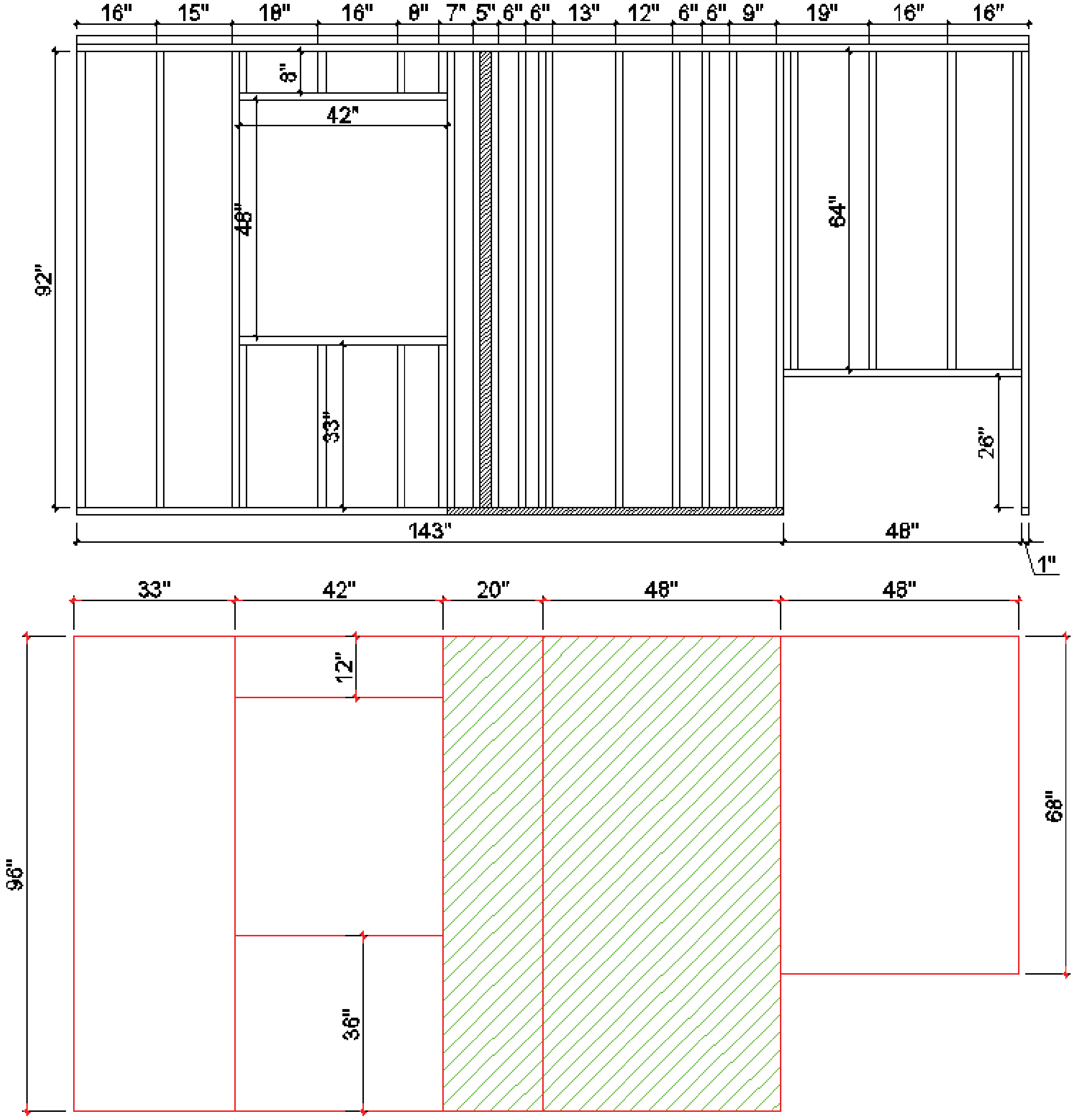

Figure B.66: Assembly for story 7, wall 1A, 4/12-D

Appendix B

Wall assembly for Story 7

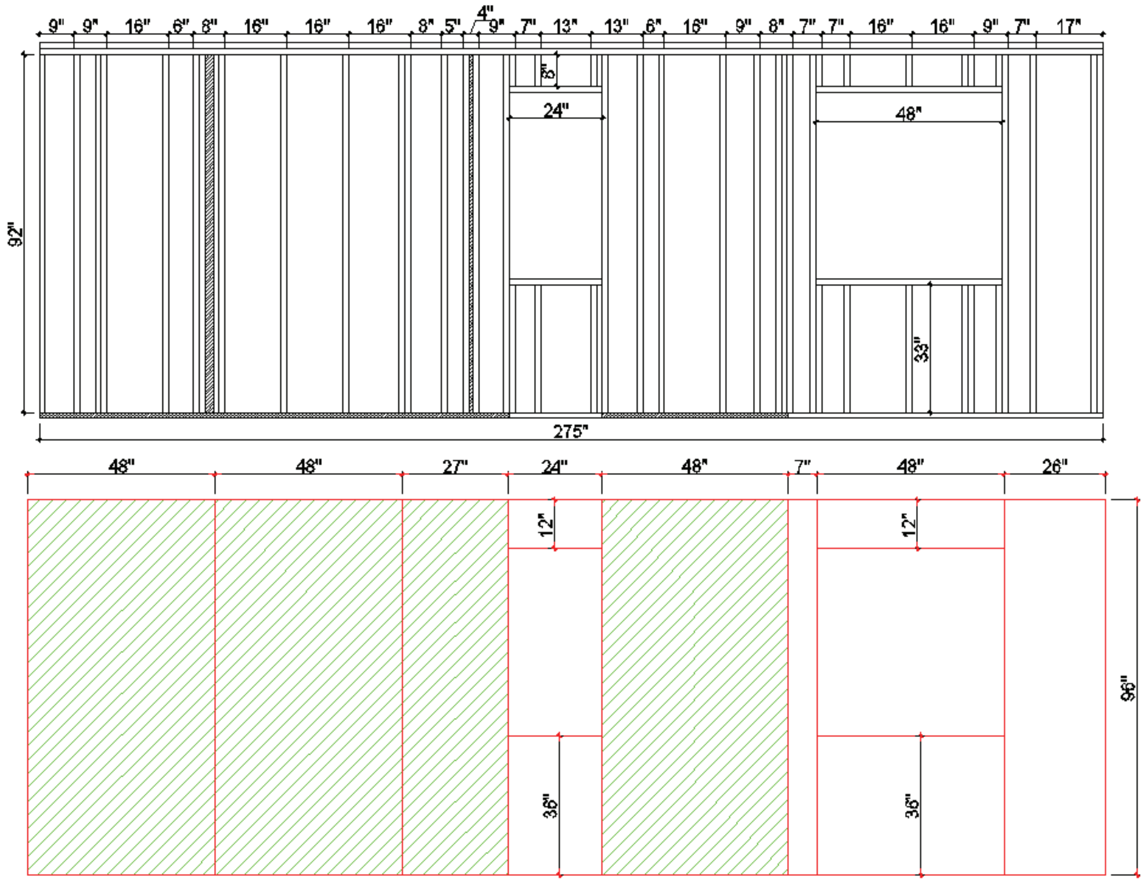

Figure B.67: Assembly for story 7, wall 1BC, 4/12-D

Appendix B

Wall assembly for Story 7

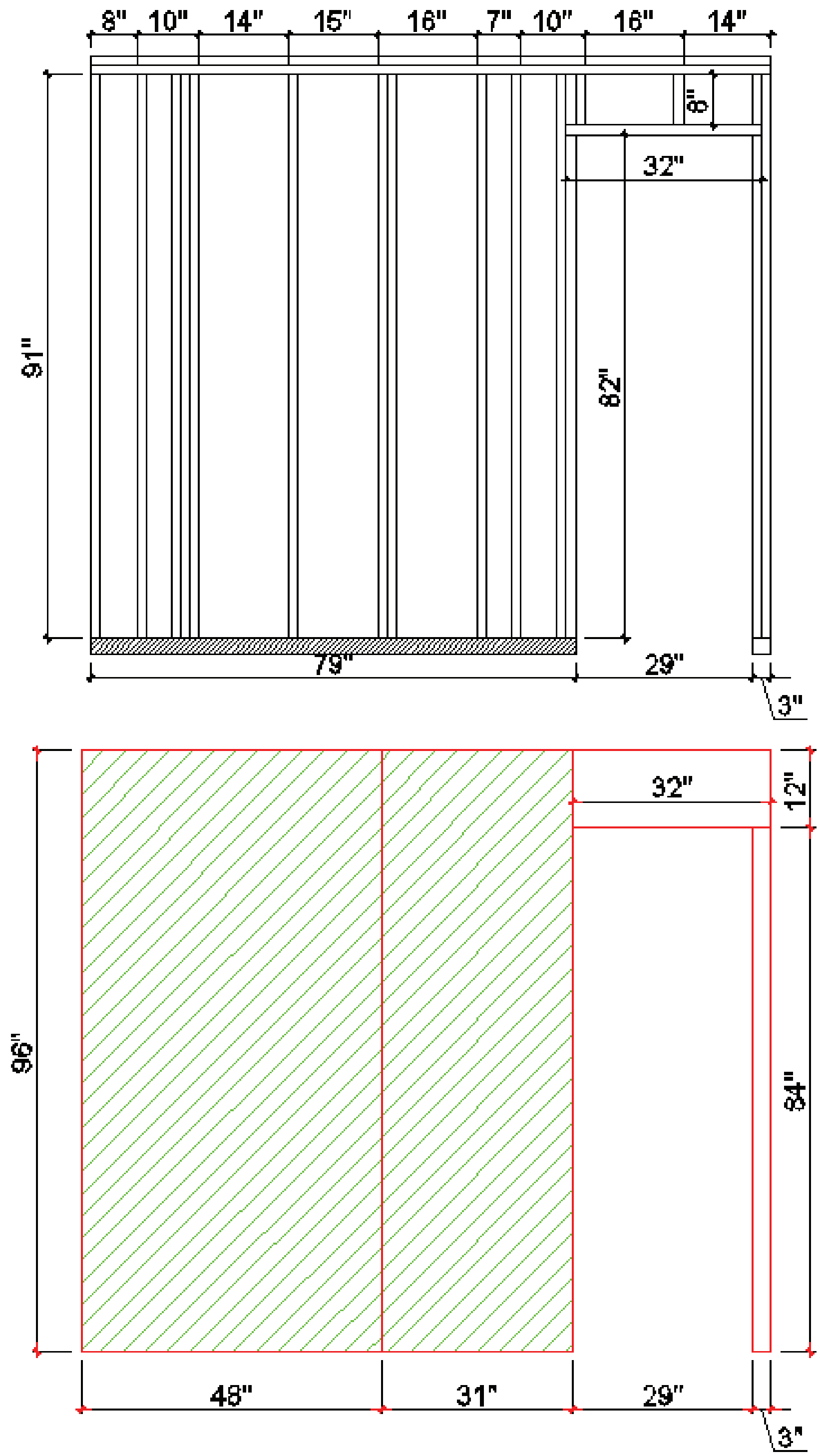

Figure B.68: Assembly for story 7, wall 2A, 10A, 2/12

Appendix B

Wall assembly for Story 7

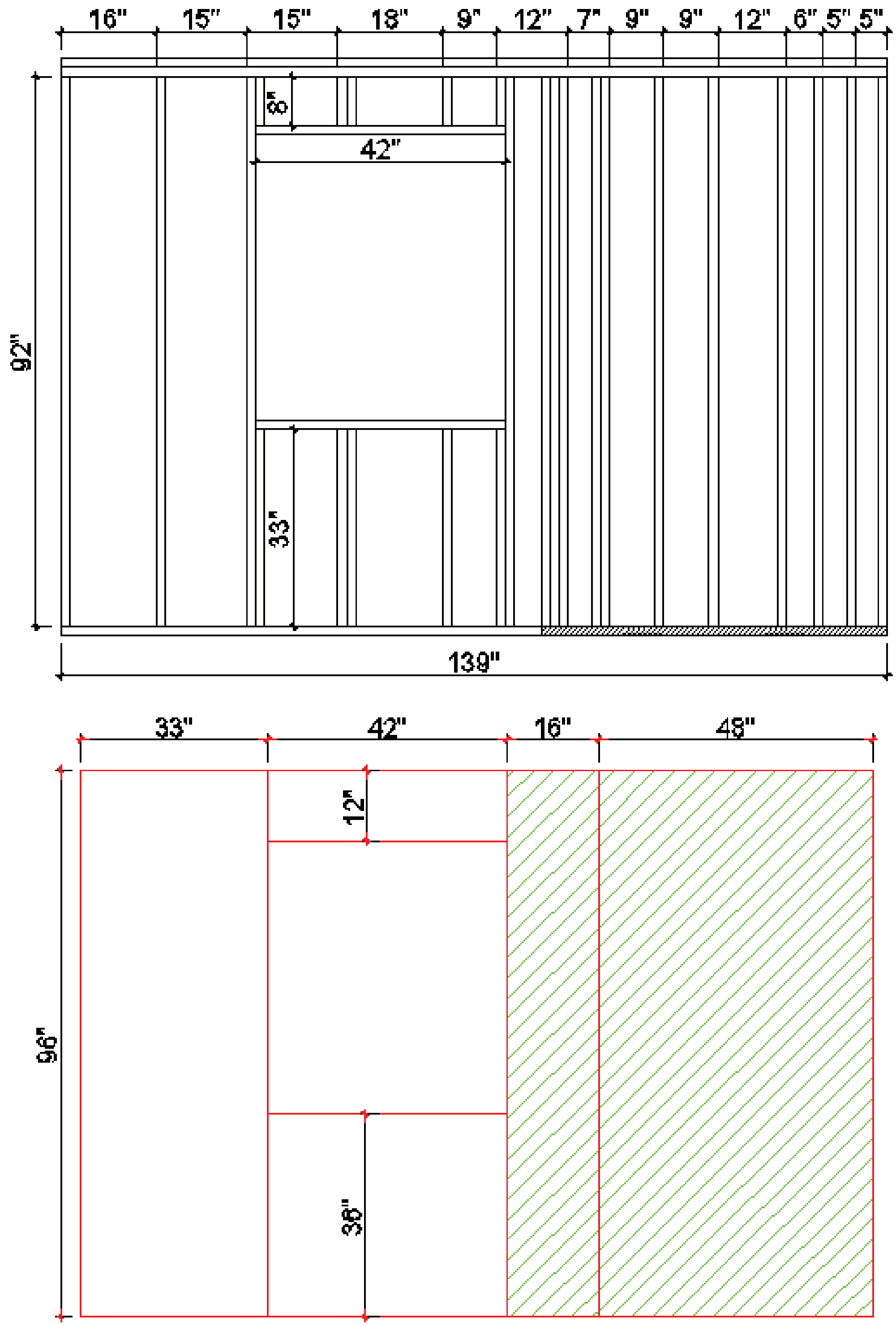

Figure B.69: Assembly for story 7, wall 11A, 4/12-D

Appendix B

Wall assembly for Story 7

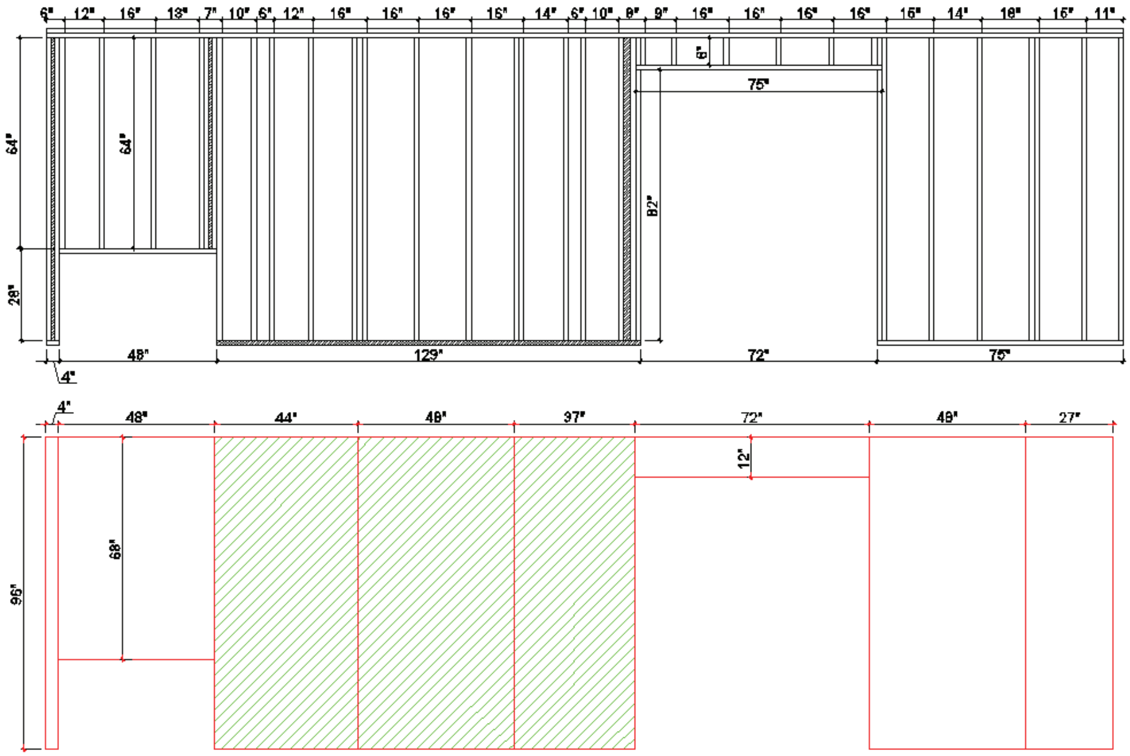

Figure B.70: Assembly for story 7, wall 11B, 4/12-D

Appendix B

Wall assembly for Story 7

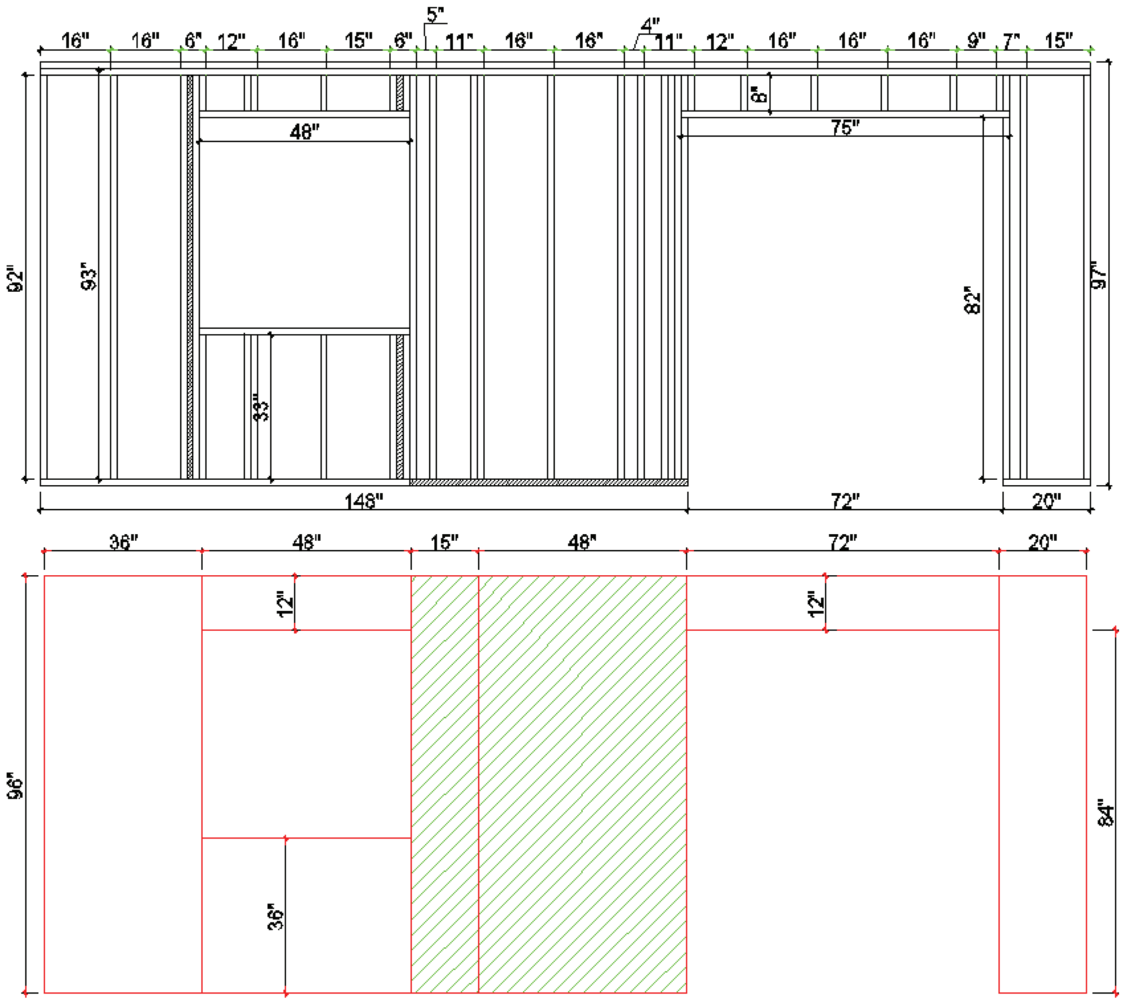

Figure B.71: Assembly for story 7, wall A1, A3, 6/12

Appendix B

Wall assembly for Story 7

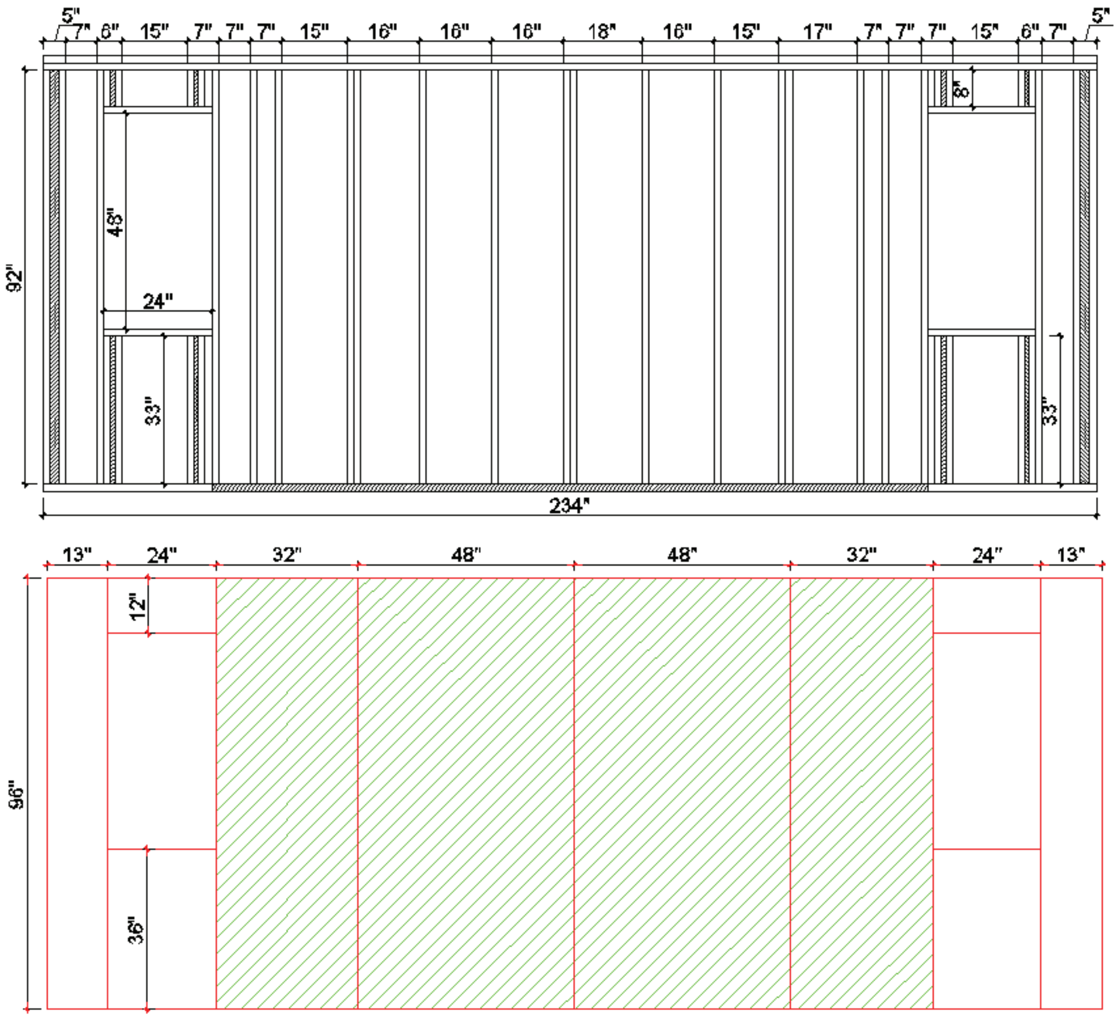

Figure B.72: Assembly for story 7, wall A2, 6/12

Appendix B

Wall assembly for Story 7

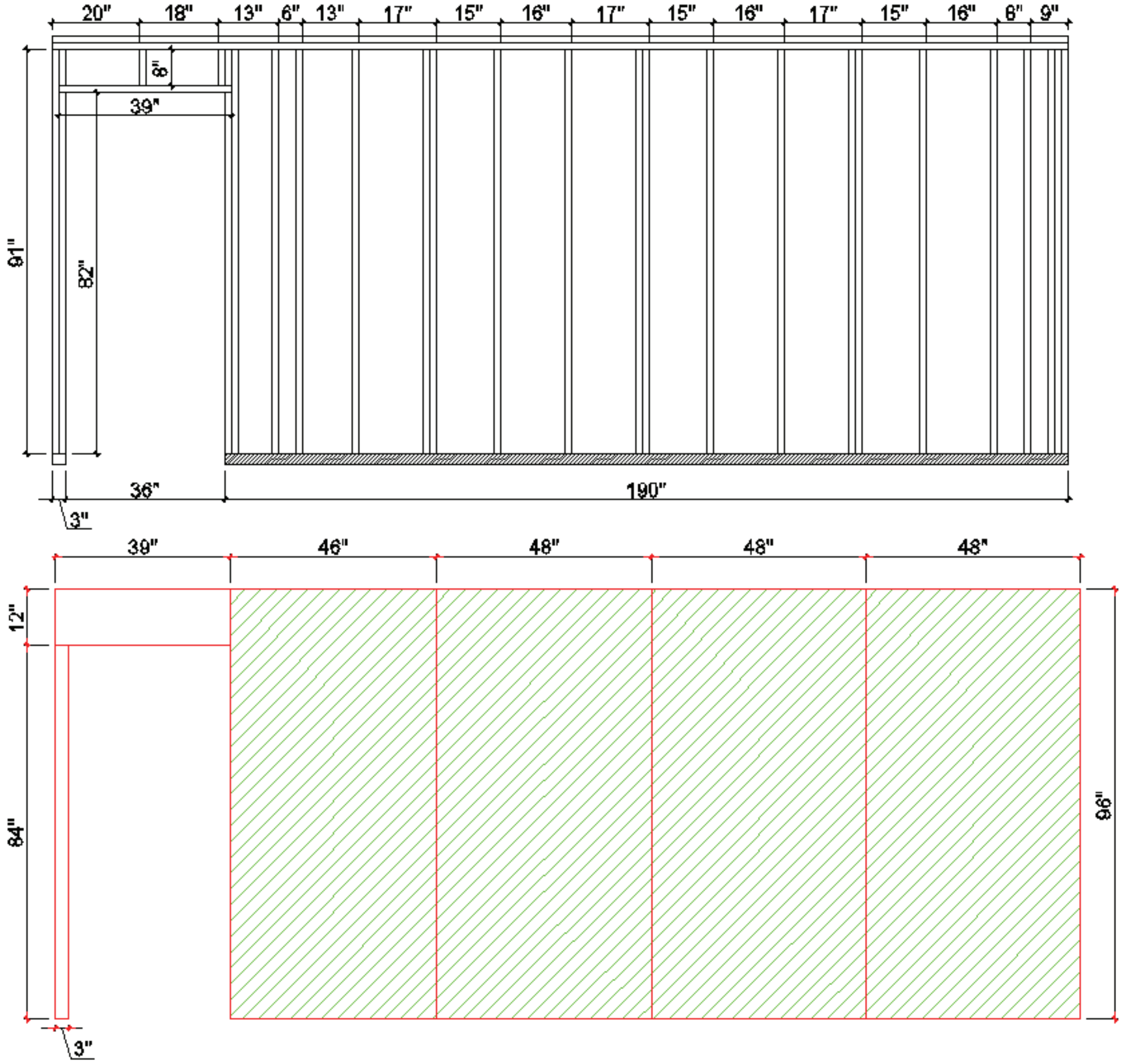

Figure B.73: Assembly for story 7, wall D3, 3/12

Appendix B

Wall assembly for Story 7

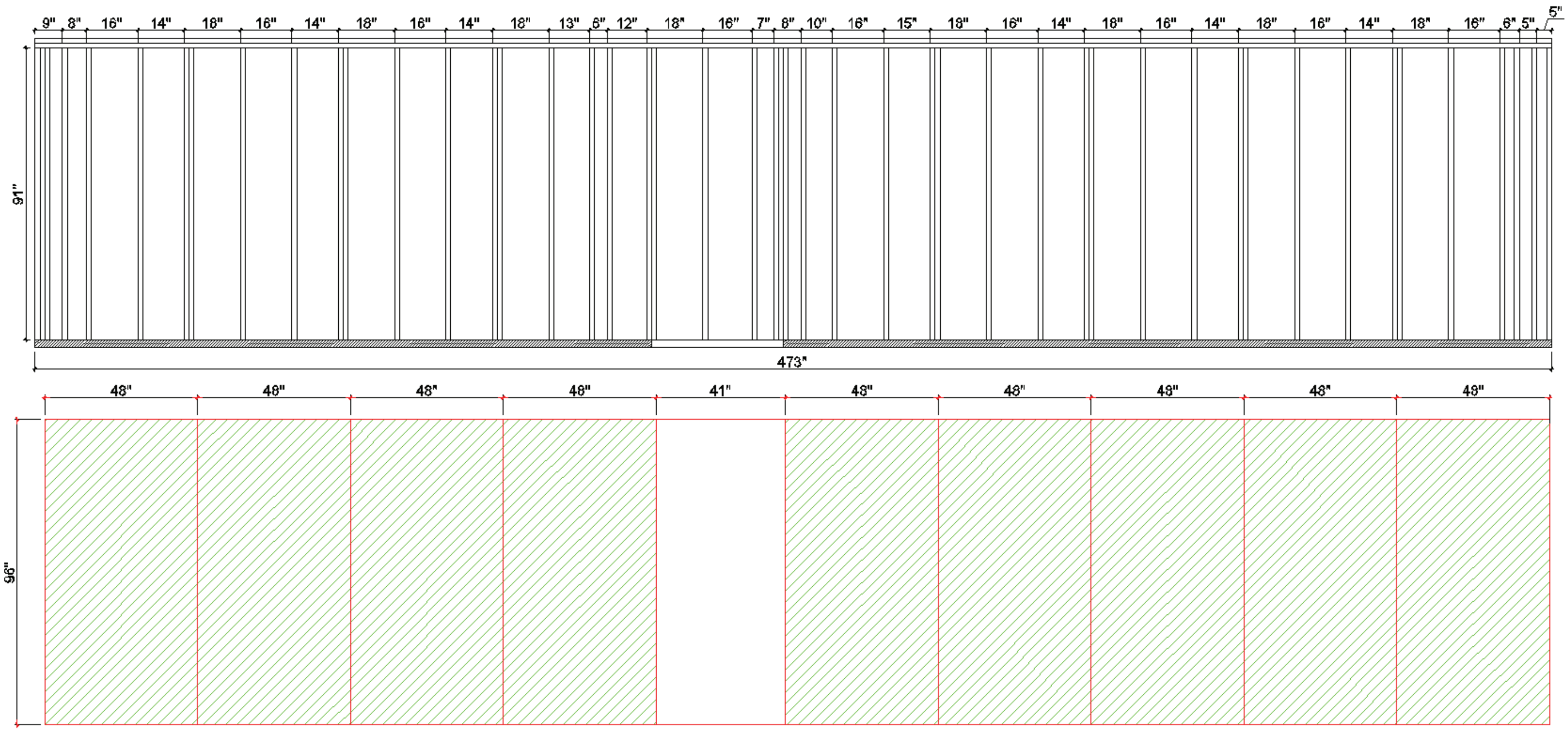

Figure B.74: Assembly for story 7, wall D1, D2, 3/12

Appendix B

Wall assembly for Story 7

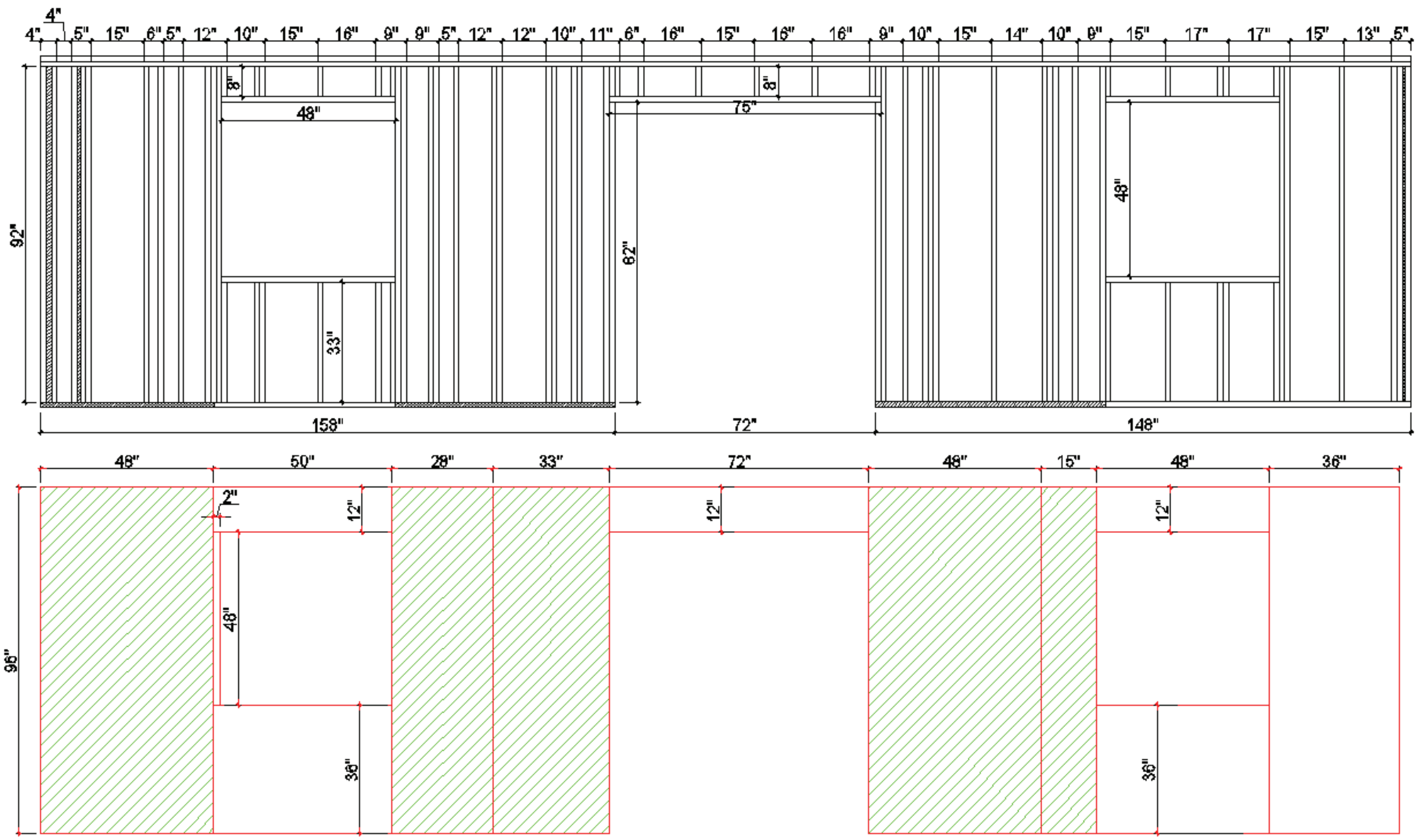

Figure B.75: Assembly for story 7, wall E3, E4, E5, 6/12

Appendix B

Wall assembly for Story 7

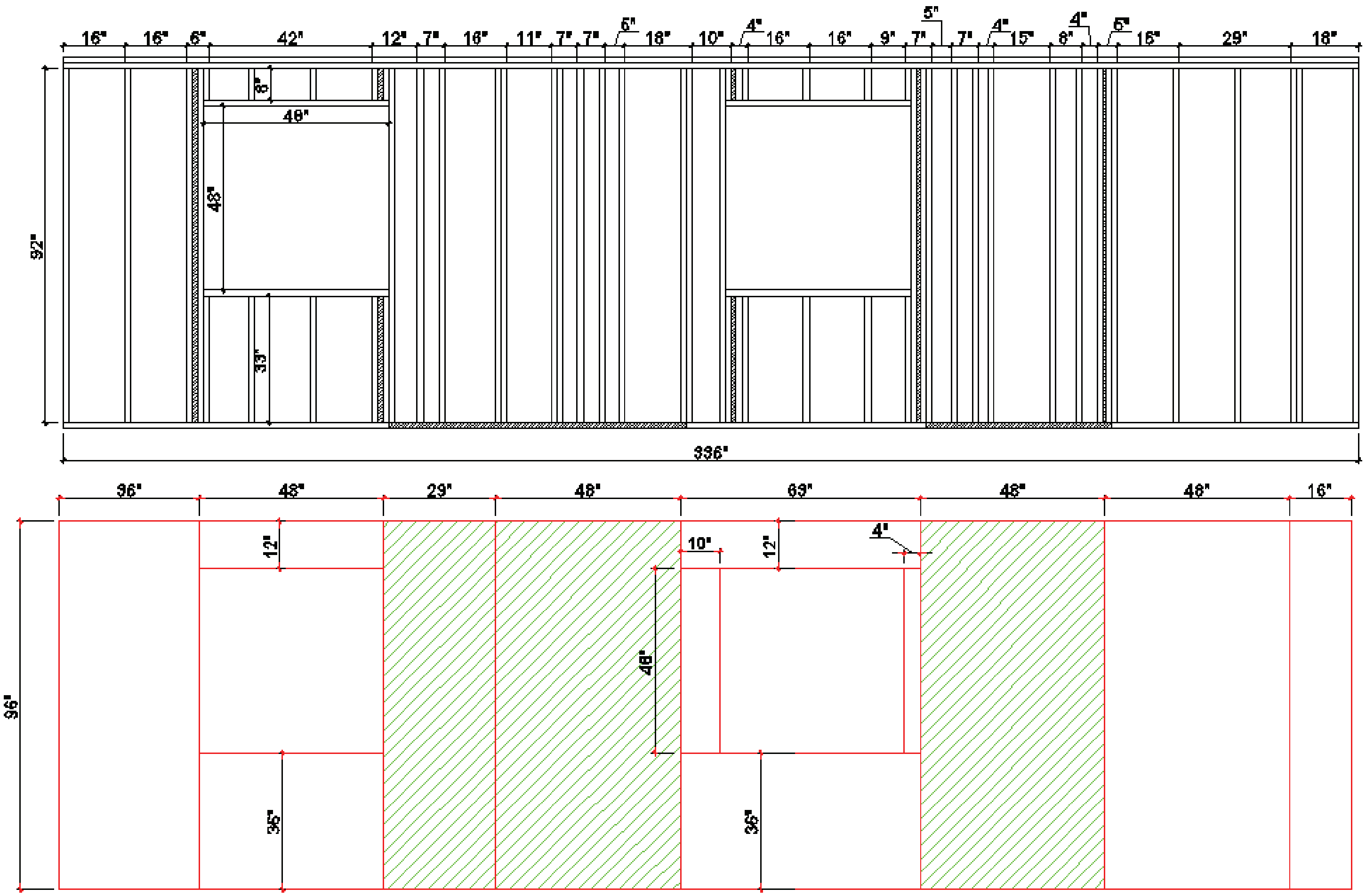

Figure B.76: Assembly for story 7, wall E1, E2, 6/12

Appendix C

Description of shake table tests

Appendix C

Test ID	Test Type	Test Level	PGA (g)			Test Date	Comments
			X	Y	Z		
W1	White Noise	N/A	0.05	0.05	0.05	6-30-09	SMF free
1	Seismic	1	**0.19**	**0.22**	**0.26**		53% original
W2	White Noise	N/A	0.05	0.05	0.05		
W3	White Noise	N/A	0.05	0.05	0.05		Re-tighten tie-down
2	Seismic	2+	**0.50**	**0.58**	**0.69**		140% original
W4	White Noise	N/A	0.05	0.05	0.05		
W5	White Noise	N/A	0.05	0.05	0.05	7-4-09	SMF locked
3	Seismic	1	**0.19**	**0.22**	**0.26**		53% original
W6	White Noise	N/A	0.05	0.05	0.05		
4	Seismic	2	**0.43**	**0.50**	**0.59**		120% original
W7	White Noise	N/A	0.05	0.05	0.05		
W8	White Noise	N/A	0.05	0.05	0.05	7-14-09	
5	Seismic	3	**0.64**	**0.76**	**0.88**		180% original
W9	White Noise	N/A	0.05	0.05	0.05		

Appendix D

Instrumentation Setup for the Test specimen

Appendix D

Table D.1: Summary of instrumentation for Capstone specimen

Measurement	Location	Type	Number
Absolute acceleration	Each Floor	3D-acceleration	38
Diagonal shear wall drift	Selected shear walls	LVDT	33
Out of plane diaphragm deformation	Third floor diaphragm	LVDT	13
Shear wall end stud uplift	Selected shear walls	LVDT	8
ATS hold-down strain	Selected shear walls	Strain gage	78
Absolute displacement	Building exterior	3D Optical tracking	50

Table D.2: List of instrumentation channels (With the sequence in data files)

No.	Channel name	Unit	Location/Notes
1	129-1A001X	Gal	Table center acceleration
2	130-1A002Y	Gal	Table center acceleration
3	131-1A003Z	Gal	Table center acceleration
4	132-2A001X	Gal	2nd floor location 1 acceleration
5	133-2A002Y	Gal	2nd floor location 1 acceleration
6	134-2A003Z	Gal	2nd floor location 1 acceleration
7	135-2A004X	Gal	2nd floor location 2 acceleration
8	136-2A005Y	Gal	2nd floor location 2 acceleration
9	137-2A006Z	Gal	2nd floor location 2 acceleration
10	138-2A007X	Gal	2nd floor location 3 acceleration
11	139-2A008Y	Gal	2nd floor location 3 acceleration
12	140-2A009Z	Gal	2nd floor location 3 acceleration
13	141-2A010X	Gal	2nd floor location 4 acceleration
14	142-2A011Y	Gal	2nd floor location 4 acceleration
15	143-2A012Z	Gal	2nd floor location 4 acceleration
16	144-2A013X	Gal	2nd floor location 5 acceleration
17	145-2A014Y	Gal	2nd floor location 5 acceleration
18	146-2A015Z	Gal	2nd floor location 5 acceleration
19	147-2D201Z	mm	2nd floor Wall B1 stud uplift (end B)
20	148-2D202Z	mm	2nd floor Wall 10A stud uplift (end A)
21	149-2D203Z	mm	2nd floor Wall 10A stud uplift (end B)
22	150-2D204Z	mm	2nd floor Wall B1 stud uplift (end A)
23	151-7D201Z	mm	7th floor Wall D2 stud uplift (end B)
24	152-7D202Z	mm	7th floor Wall 10A stud uplift (end A)
25	153-7D203Z	mm	7th floor Wall 10A stud uplift (end B)
26	154-7D204Z	mm	7th floor Wall D2 stud uplift (end A)
27	155-1SS01Y	mu	SMF moment connection strain Location 1 gage 1
28	156-1SS02Y	mu	SMF moment connection strain Location 1 gage 2
29	157-1SS03Y	mu	SMF moment connection strain Location 1 gage 3
30	158-1SS04Y	mu	SMF moment connection strain Location 1 gage 4

Appendix D

Table D.2: List of instrumentation channels (cont'd)

31	159-1SS61X	mu	SMF moment connection strain Location 16 gage 1
32	160-1SS62X	mu	SMF moment connection strain Location 16 gage 2
33	161-1SS63X	mu	SMF moment connection strain Location 16 gage 3
34	162-1SS64X	mu	SMF moment connection strain Location 16 gage 4
35	163-1SS05Y	mu	SMF moment connection strain Location 2 gage 1
36	164-1SS06Y	mu	SMF moment connection strain Location 2 gage 2
37	165-1SS07Y	mu	SMF moment connection strain Location 2 gage 3
38	166-1SS08Y	mu	SMF moment connection strain Location 2 gage 4
39	167-1SS41X	mu	SMF moment connection strain Location 11 gage 1
40	168-1SS42X	mu	SMF moment connection strain Location 11 gage 2
41	169-1SS43X	mu	SMF moment connection strain Location 11 gage 3
42	170-1SS44X	mu	SMF moment connection strain Location 11 gage 4
43	171-1SS09Y	mu	SMF moment connection strain Location 3 gage 1
44	172-1SS10Y	mu	SMF moment connection strain Location 3 gage 2
45	173-1SS11Y	mu	SMF moment connection strain Location 3 gage 3
46	174-1SS12Y	mu	SMF moment connection strain Location 3 gage 4
47	175-1SS21Y	mu	SMF moment connection strain Location 6 gage 1
48	176-1SS22Y	mu	SMF moment connection strain Location 6 gage 2
49	177-1SS23Y	mu	SMF moment connection strain Location 6 gage 3
50	178-1SS24Y	mu	SMF moment connection strain Location 6 gage 4
51	193-3A001X	Gal	3rd floor location 1 acceleration
52	194-3A002Y	Gal	3rd floor location 1 acceleration
53	195-3A003Z	Gal	3rd floor location 1 acceleration
54	196-3A004X	Gal	3rd floor location 2 acceleration
55	197-3A005Y	Gal	3rd floor location 2 acceleration
56	198-3A006Z	Gal	3rd floor location 2 acceleration
57	199-3A007X	Gal	3rd floor location 3 acceleration
58	200-3A008Y	Gal	3rd floor location 3 acceleration
59	201-3A009Z	Gal	3rd floor location 3 acceleration
60	202-3A010X	Gal	3rd floor location 4 acceleration
61	203-3A011Y	Gal	3rd floor location 4 acceleration
62	204-3A012Z	Gal	3rd floor location 4 acceleration
63	205-3A013X	Gal	3rd floor location 5 acceleration
64	206-3A014Y	Gal	3rd floor location 5 acceleration
65	207-3A015Z	Gal	3rd floor location 5 acceleration
66	208-2D101Z	mm	Floor diaphragm out-of-plane deformation between 2nd and 3rd floor (Location 1)
67	209-2D102Z	mm	Floor diaphragm out-of-plane deformation between 2nd and 3rd floor (Location 2)
68	210-2D103Z	mm	Floor diaphragm out-of-plane deformation between 2nd and 3rd floor (Location 3)
69	211-2D104Z	mm	Floor diaphragm out-of-plane deformation between 2nd and 3rd floor (Location 4)
70	212-2D105Z	mm	Floor diaphragm out-of-plane deformation between 2nd and 3rd floor (Location 5)

Appendix D

Table D.2: List of instrumentation channels (cont'd)

71	213-2D106Z	mm	Floor diaphragm out-of-plane deformation between 2nd and 3rd floor (Location 6)
72	214-2D107Z	mm	Floor diaphragm out-of-plane deformation between 2nd and 3rd floor (Location 7)
73	215-2D108Z	mm	Floor diaphragm out-of-plane deformation between 2nd and 3rd floor (Location 8)
74	216-2D109Z	mm	Floor diaphragm out-of-plane deformation between 2nd and 3rd floor (Location 9)
75	217-2D110Z	mm	Floor diaphragm out-of-plane deformation between 2nd and 3rd floor (Location 10)
76	218-2D111Z	mm	Floor diaphragm out-of-plane deformation between 2nd and 3rd floor (Location 11)
77	219-2D112Z	mm	Floor diaphragm out-of-plane deformation between 2nd and 3rd floor (Location 12)
78	220-2D113Z	mm	Floor diaphragm out-of-plane deformation between 2nd and 3rd floor (Location 13)
79	221-1SS13Y	mu	SMF moment connection strain Location 4 gage 1
80	222-1SS14Y	mu	SMF moment connection strain Location 4 gage 2
81	223-1SS15Y	mu	SMF moment connection strain Location 4 gage 3
82	224-1SS16Y	mu	SMF moment connection strain Location 4 gage 4
83	225-1SS33X	mu	SMF moment connection strain Location 9 gage 1
84	226-1SS34X	mu	SMF moment connection strain Location 9 gage 2
85	227-1SS35X	mu	SMF moment connection strain Location 9 gage 3
86	228-1SS36X	mu	SMF moment connection strain Location 9 gage 4
87	229-1SS17Y	mu	SMF moment connection strain Location 5 gage 1
88	230-1SS18Y	mu	SMF moment connection strain Location 5 gage 2
89	231-1SS19Y	mu	SMF moment connection strain Location 5 gage 3
90	232-1SS20Y	mu	SMF moment connection strain Location 5 gage 4
91	233-1SS45X	mu	SMF moment connection strain Location 12 gage 1
92	234-1SS46X	mu	SMF moment connection strain Location 12 gage 2
93	235-1SS47X	mu	SMF moment connection strain Location 12 gage 3
94	236-1SS48X	mu	SMF moment connection strain Location 12 gage 4
95	237-1SS25Y	mu	SMF moment connection strain Location 7 gage 1
96	238-1SS26Y	mu	SMF moment connection strain Location 7 gage 2
97	239-1SS27Y	mu	SMF moment connection strain Location 7 gage 3
98	240-1SS28Y	mu	SMF moment connection strain Location 7 gage 4
99	241-1SS37X	mu	SMF moment connection strain Location 10 gage 1
100	242-1SS38X	mu	SMF moment connection strain Location 10 gage 2
101	243-1SS39X	mu	SMF moment connection strain Location 10 gage 3
102	244-1SS40X	mu	SMF moment connection strain Location 10 gage 4
103	245-1A004X	Gal	SMF Center Acceleration (Accelerometer attached to Steel beam)
104	246-1A005Y	Gal	SMF Center Acceleration (Accelerometer attached to Steel beam)
105	247-1A006Z	Gal	SMF Center Acceleration (Accelerometer attached to Steel beam)
106	257-4A001X	Gal	4th floor location 1 acceleration
107	258-4A002Y	Gal	4th floor location 1 acceleration

Table D.2: List of instrumentation channels (cont'd)

108	259-4A003Z	Gal	4th floor location 1 acceleration
109	260-4A004X	Gal	4th floor location 2 acceleration
110	261-4A005Y	Gal	4th floor location 2 acceleration
111	262-4A006Z	Gal	4th floor location 2 acceleration
112	263-4A007X	Gal	4th floor location 3 acceleration
113	264-4A008Y	Gal	4th floor location 3 acceleration
114	265-4A009Z	Gal	4th floor location 3 acceleration
115	266-4A010X	Gal	4th floor location 4 acceleration
116	267-4A011Y	Gal	4th floor location 4 acceleration
117	268-4A012Z	Gal	4th floor location 4 acceleration
118	269-4A013X	Gal	4th floor location 5 acceleration
119	270-4A014Y	Gal	4th floor location 5 acceleration
120	271-4A015Z	Gal	4th floor location 5 acceleration
121	272-2D001Y	mm	2nd story diagonal string gage measurement, Wall ID 1
122	273-2D002Y	mm	2nd story diagonal string gage measurement, Wall ID 2
123	274-2D003Y	mm	2nd story diagonal string gage measurement, Wall ID 3
124	275-2D004Y	mm	2nd story diagonal string gage measurement, Wall ID 4
125	276-2D005Y	mm	2nd story diagonal string gage measurement, Wall ID 5
126	277-2D006Y	mm	2nd story diagonal string gage measurement, Wall ID 6
127	278-2D007Y	mm	2nd story diagonal string gage measurement, Wall ID 7
128	279-2D008Y	mm	2nd story diagonal string gage measurement, Wall ID 8
129	280-2D009X	mm	2nd story diagonal string gage measurement, Wall ID 9
130	281-2D010X	mm	2nd story diagonal string gage measurement, Wall ID 10
131	282-2D011X	mm	2nd story diagonal string gage measurement, Wall ID 11
132	283-2D012X	mm	2nd story diagonal string gage measurement, Wall ID 12
133	284-2D013X	mm	2nd story diagonal string gage measurement, Wall ID 13
134	285-2D014X	mm	2nd story diagonal string gage measurement, Wall ID 14
135	286-2D015X	mm	2nd story diagonal string gage measurement, Wall ID 15
136	287-2D016X	mm	2nd story diagonal string gage measurement, Wall ID 16
137	288-2D017X	mm	2nd story diagonal string gage measurement, Wall ID 17
138	289-3D001Y	mm	3rd story diagonal string gage measurement, Wall ID 4
139	290-3D002X	mm	3rd story diagonal string gage measurement, Wall ID 9
140	291-3D003X	mm	3rd story diagonal string gage measurement, Wall ID 17
141	292-4D001Y	mm	4th story diagonal string gage measurement, Wall ID 4
142	293-4D002X	mm	4th story diagonal string gage measurement, Wall ID 9
143	294-4D003X	mm	4th story diagonal string gage measurement, Wall ID 17
144	295-5D001Y	mm	5th story diagonal string gage measurement, Wall ID 4
145	296-5D002X	mm	5th story diagonal string gage measurement, Wall ID 9
146	297-5D003X	mm	5th story diagonal string gage measurement, Wall ID 17
147	298-6D001Y	mm	6th story diagonal string gage measurement, Wall ID 4
148	299-6D002X	mm	6th story diagonal string gage measurement, Wall ID 9
149	300-6D003X	mm	6th story diagonal string gage measurement, Wall ID 17
150	301-7D001Y	mm	7th story diagonal string gage measurement, Wall ID 18

Appendix D

Table D.2: List of instrumentation channels (cont'd)

151	302-7D002Y	mm	7th story diagonal string gage measurement, Wall ID 5
152	303-7D003Y	mm	7th story diagonal string gage measurement, Wall ID 6
153	304-7D004X	mm	7th story diagonal string gage measurement, Wall ID 12
154	305-8A016X	Gal	Accelerometer attached to one of seismic weight steel plates on the roof
155	306-8A017Y	Gal	Accelerometer attached to one of seismic weight steel plates on the roof
156	307-8A018Z	Gal	Accelerometer attached to one of seismic weight steel plates on the roof
157	321-5A001X	Gal	5th floor location 1 acceleration
158	322-5A002Y	Gal	5th floor location 1 acceleration
159	323-5A003Z	Gal	5th floor location 1 acceleration
160	324-5A004X	Gal	5th floor location 2 acceleration
161	325-5A005Y	Gal	5th floor location 2 acceleration
162	326-5A006Z	Gal	5th floor location 2 acceleration
163	327-5A007X	Gal	5th floor location 3 acceleration
164	328-5A008Y	Gal	5th floor location 3 acceleration
165	329-5A009Z	Gal	5th floor location 3 acceleration
166	330-5A010X	Gal	5th floor location 4 acceleration
167	331-5A011Y	Gal	5th floor location 4 acceleration
168	332-5A012Z	Gal	5th floor location 4 acceleration
169	333-5A013X	Gal	5th floor location 5 acceleration
170	334-5A014Y	Gal	5th floor location 5 acceleration
171	335-5A015Z	Gal	5th floor location 5 acceleration
172	336-7A001X	Gal	7th floor location 1 acceleration
173	337-7A002Y	Gal	7th floor location 1 acceleration
174	338-7A003Z	Gal	7th floor location 1 acceleration
175	339-7A004X	Gal	7th floor location 2 acceleration
176	340-7A005Y	Gal	7th floor location 2 acceleration
177	341-7A006Z	Gal	7th floor location 2 acceleration
178	342-7A007X	Gal	7th floor location 3 acceleration
179	343-7A008Y	Gal	7th floor location 3 acceleration
180	344-7A009Z	Gal	7th floor location 3 acceleration
181	345-7A010X	Gal	7th floor location 4 acceleration
182	346-7A011Y	Gal	7th floor location 4 acceleration
183	347-7A012Z	Gal	7th floor location 4 acceleration
184	348-7A013X	Gal	7th floor location 5 acceleration
185	349-7A014Y	Gal	7th floor location 5 acceleration
186	350-7A015Z	Gal	7th floor location 5 acceleration
187	351-1SS29Y	mu	SMF moment connection strain Location 8 gage 1
188	352-1SS30Y	mu	SMF moment connection strain Location 8 gage 2
189	353-1SS31Y	mu	SMF moment connection strain Location 8 gage 3
190	354-1SS32Y	mu	SMF moment connection strain Location 8 gage 4
191	355-1SS65X	mu	SMF moment connection strain Location 17 gage 1
192	356-1SS66X	mu	SMF moment connection strain Location 17 gage 2

Appendix D

Table D.2: List of instrumentation channels (cont'd)

193	357-1SS67X	mu	SMF moment connection strain Location 17 gage 3
194	358-1SS68X	mu	SMF moment connection strain Location 17 gage 4
195	359-1SS49X	mu	SMF moment connection strain Location 13 gage 1
196	360-1SS50X	mu	SMF moment connection strain Location 13 gage 2
197	361-1SS51X	mu	SMF moment connection strain Location 13 gage 3
198	362-1SS52X	mu	SMF moment connection strain Location 13 gage 4
199	363-1SS53X	mu	SMF moment connection strain Location 14 gage 1
200	364-1SS54X	mu	SMF moment connection strain Location 14 gage 2
201	365-1SS55X	mu	SMF moment connection strain Location 14 gage 3
202	366-1SS56X	mu	SMF moment connection strain Location 14 gage 4
203	367-1SS57X	mu	SMF moment connection strain Location 15 gage 1
204	368-1SS58X	mu	SMF moment connection strain Location 15 gage 2
205	369-1SS59X	mu	SMF moment connection strain Location 15 gage 3
206	370-1SS60X	mu	SMF moment connection strain Location 15 gage 4
207	385-6A001X	Gal	6th floor location 1 acceleration
208	386-6A002Y	Gal	6th floor location 1 acceleration
209	387-6A003Z	Gal	6th floor location 1 acceleration
210	388-6A004X	Gal	6th floor location 2 acceleration
211	389-6A005Y	Gal	6th floor location 2 acceleration
212	390-6A006Z	Gal	6th floor location 2 acceleration
213	391-6A007X	Gal	6th floor location 3 acceleration
214	392-6A008Y	Gal	6th floor location 3 acceleration
215	393-6A009Z	Gal	6th floor location 3 acceleration
216	394-6A010X	Gal	6th floor location 4 acceleration
217	395-6A011Y	Gal	6th floor location 4 acceleration
218	396-6A012Z	Gal	6th floor location 4 acceleration
219	397-6A013X	Gal	6th floor location 5 acceleration
220	398-6A014Y	Gal	6th floor location 5 acceleration
221	399-6A015Z	Gal	6th floor location 5 acceleration
222	400-2SA01Y	mu	2nd story ATS rod strain 1B
223	401-2SA02Y	mu	2nd story ATS rod strain 1A
224	402-2SA11Y	mu	2nd story ATS rod strain 5B
225	403-2SA03Y	mu	2nd story ATS rod strain 2B
226	404-2SA04Y	mu	2nd story ATS rod strain 2A
227	405-2SA05Y	mu	2nd story ATS rod strain 3B
228	406-2SA06Y	mu	2nd story ATS rod strain 3A
229	407-2SA07Y	mu	2nd story ATS rod strain 4aB
230	408-2SA08Y	mu	2nd story ATS rod strain 4aA
231	409-2SA09Y	mu	2nd story ATS rod strain 4bB
232	410-2SA25X	mu	2nd story ATS rod strain 12A
233	411-2SA26X	mu	2nd story ATS rod strain 12B
234	412-2SA31X	mu	2nd story ATS rod strain 15A

Appendix D

Table D.2: List of instrumentation channels (cont'd)

235	413-2SA10Y	mu	2nd story ATS rod strain 4bA
236	414-2SA13Y	mu	2nd story ATS rod strain 6B
237	415-2SA14Y	mu	2nd story ATS rod strain 6A
238	416-2SA32X	mu	2nd story ATS rod strain 15B
239	417-2SA33X	mu	2nd story ATS rod strain 16A
240	418-2SA12Y	mu	2nd story ATS rod strain 5A
241	419-2SA21X	mu	2nd story ATS rod strain 10A
242	420-2SA22X	mu	2nd story ATS rod strain 10B
243	421-2SA23X	mu	2nd story ATS rod strain 11A
244	422-2SA19X	mu	2nd story ATS rod strain 9A
245	423-2SA15Y	mu	2nd story ATS rod strain 7B
246	424-2SA24X	mu	2nd story ATS rod strain 11B
247	425-2SA20X	mu	2nd story ATS rod strain 9B
248	426-2SA16Y	mu	2nd story ATS rod strain 7A
249	427-2SA17Y	mu	2nd story ATS rod strain 8B
250	428-2SA27X	mu	2nd story ATS rod strain 13A
251	429-2SA28X	mu	2nd story ATS rod strain 13B
252	430-2SA29X	mu	2nd story ATS rod strain 14A
253	431-2SA30X	mu	2nd story ATS rod strain 14B
254	432-2SA18Y	mu	2nd story ATS rod strain 8A
255	433-2SA34X	mu	2nd story ATS rod strain 16B
256	434-2SA35X	mu	2nd story ATS rod strain 17A
257	435-2SA36X	mu	2nd story ATS rod strain 17B
258	449-8A001X	Gal	Roof location 1 acceleration
259	450-8A002Y	Gal	Roof location 1 acceleration
260	451-8A003Z	Gal	Roof location 1 acceleration
261	452-8A004X	Gal	Roof location 2 acceleration
262	453-8A005Y	Gal	Roof location 2 acceleration
263	454-8A006Z	Gal	Roof location 2 acceleration
264	455-8A007X	Gal	Roof location 3 acceleration
265	456-8A008Y	Gal	Roof location 3 acceleration
266	457-8A009Z	Gal	Roof location 3 acceleration
267	458-8A010X	Gal	Roof location 4 acceleration
268	459-8A011Y	Gal	Roof location 4 acceleration
269	460-8A012Z	Gal	Roof location 4 acceleration
270	461-8A013X	Gal	Roof location 5 acceleration
271	462-8A014Y	Gal	Roof location 5 acceleration
272	463-8A015Z	Gal	Roof location 5 acceleration
273	464-3SA01Y	mu	3rd story ATS rod strain 4aB
274	465-3SA02Y	mu	3rd story ATS rod strain 4aA
275	466-3SA03Y	mu	3rd story ATS rod strain 4bB

Appendix D

Table D.2: List of instrumentation channels (cont'd)

276	467-3SA04Y	mu	3rd story ATS rod strain 4bA
277	468-3SA05X	mu	3rd story ATS rod strain 9A
278	469-3SA06X	mu	3rd story ATS rod strain 9B
279	470-3SA07X	mu	3rd story ATS rod strain 17A
280	471-3SA08X	mu	3rd story ATS rod strain 17B
281	472-4SA01Y	mu	4th story ATS rod strain 4aB
282	473-4SA02Y	mu	4th story ATS rod strain 4aA
283	474-4SA03Y	mu	4th story ATS rod strain 4bB
284	475-4SA04Y	mu	4th story ATS rod strain 4bA
285	476-4SA05X	mu	4th story ATS rod strain 9A
286	477-4SA06X	mu	4th story ATS rod strain 9B
287	478-4SA07X	mu	4th story ATS rod strain 17A
288	479-4SA08X	mu	4th story ATS rod strain 17B
289	480-5SA01Y	mu	5th story ATS rod strain 4aB
290	481-5SA02Y	mu	5th story ATS rod strain 4aA
291	482-5SA03Y	mu	5th story ATS rod strain 4bB
292	483-5SA04Y	mu	5th story ATS rod strain 4bA
293	484-5SA05X	mu	5th story ATS rod strain 9A
294	485-5SA06X	mu	5th story ATS rod strain 9B
295	486-5SA07X	mu	5th story ATS rod strain 17A
296	487-5SA08X	mu	5th story ATS rod strain 17B
297	488-6SA01Y	mu	6th story ATS rod strain 4aB
298	489-6SA02Y	mu	6th story ATS rod strain 4aA
299	490-6SA03Y	mu	6th story ATS rod strain 4bB
300	491-6SA04Y	mu	6th story ATS rod strain 4bA
301	492-6SA05X	mu	6th story ATS rod strain 9A
302	493-6SA06X	mu	6th story ATS rod strain 9B
303	494-6SA07X	mu	6th story ATS rod strain 17A
304	495-6SA08X	mu	6th story ATS rod strain 17B
305	496-7SA01Y	mu	7th story ATS rod strain 18B
306	497-7SA02Y	mu	7th story ATS rod strain 18A
307	498-7SA03Y	mu	7th story ATS rod strain 5B
308	499-7SA04Y	mu	7th story ATS rod strain 5A
309	500-7SA05Y	mu	7th story ATS rod strain 6B
310	501-7SA06Y	mu	7th story ATS rod strain 6A
311	502-7SA07X	mu	7th story ATS rod strain 12A
312	503-7SA08X	mu	7th story ATS rod strain 12B
313	504-7SA09X	mu	7th story ATS rod strain 15A
314	505-7SA10X	mu	7th story ATS rod strain 15B
315	897-Target X	gal	Table target acceleration
316	898-Target Y	gal	Table target acceleration
317	899-Target Z	gal	Table target acceleration

Appendix D

Table D.2: List of instrumentation channels (cont'd)

318	900-Acc ref X	gal	Table reference acceleration
319	901-Acc ref Y	gal	Table reference acceleration
320	902-Acc ref Z	gal	Table reference acceleration
321	903-Acc ref Roll	deg/s^2	Table reference rotational acceleration
322	904-Acc ref Pitch	deg/s^2	Table reference rotational acceleration
323	905-Acc ref Yaw	deg/s^2	Table reference rotational acceleration
324	906-Drive X	gal	Table driving acceleration
325	907-Drive Y	gal	Table driving acceleration
326	908-Drive Z	gal	Table driving acceleration
327	909-Drive Roll	deg/s^2	Table driving rotational acceleration
328	910-Drive Pitch	deg/s^2	Table driving rotational acceleration
329	911-Drive Yaw	deg/s^2	Table driving rotational acceleration
330	912-Dis ref X	mm	Table reference displacement
331	913-Dis ref Y	mm	Table reference displacement
332	914-Dis ref Z	mm	Table reference displacement
333	915-Dis ref Roll	deg	Table reference rotation
334	916-Dis ref Pitch	deg	Table reference rotation
335	917-Dis ref Yaw	deg	Table reference rotation
336	918-Vel ref X	cm/s	Table reference velocity
337	919-Vel ref Y	cm/s	Table reference velocity
338	920-Vel ref Z	cm/s	Table reference velocity
339	921-Vel ref Roll	deg/s	Table reference rotational velocity
340	922-Vel ref Pitch	deg/s	Table reference rotational velocity
341	923-Vel ref Yaw	deg/s	Table reference rotational velocity
342	924-Dis fbk X	mm	Table feedback displacement
343	925-Dis fbk Y	mm	Table feedback displacement
344	926-Dis fbk Z	mm	Table feedback displacement
345	927-Dis fbk Roll	deg	Table feedback rotation
346	928-Dis fbk Pitch	deg	Table feedback rotation
347	929-Dis fbk Yaw	deg	Table feedback rotation
348	930-Dis fbk X(r)	mm	Table feedback displacement (raw)
349	931-Dis fbk Y(r)	mm	Table feedback displacement (raw)
350	932-Dis fbk Z(r)	mm	Table feedback displacement (raw)
351	933-Dis fbk Roll(r)	deg	Table feedback rotation (raw)
352	934-Dis fbk Pitch(r)	deg	Table feedback rotation (raw)
353	935-Dis fbk Yaw(r)	deg	Table feedback rotation (raw)
354	936-Vel fbk X	cm/s	Table feedback velocity
355	937-Vel fbk Y	cm/s	Table feedback velocity
356	938-Vel fbk Z	cm/s	Table feedback velocity

Appendix D

Table D.2: List of instrumentation channels (cont'd)

357	939-Vel fbk Roll	deg/s	Table feedback rotational velocity
358	940-Vel fbk Pitch	deg/s	Table feedback rotational velocity
359	941-Vel fbk Yaw	deg/s	Table feedback rotational velocity
360	942-Acc fbk X	gal	Table feedback acceleration
361	943-Acc fbk Y	gal	Table feedback acceleration
362	944-Acc fbk Z	gal	Table feedback acceleration
363	945-Acc fbk Roll	deg/s^2	Table feedback rotational acceleration
364	946-Acc fbk Pitch	deg/s^2	Table feedback rotational acceleration
365	947-Acc fbk Yaw	deg/s^2	Table feedback rotational acceleration
366	948-Acc fbk X(r)	gal	Table feedback acceleration (raw)
367	949-Acc fbk Y(r)	gal	Table feedback acceleration (raw)
368	950-Acc fbk Z(r)	gal	Table feedback acceleration (raw)
369	951-Acc fbk Roll(r)	deg/s^2	Table feedback rotational acceleration (raw)
370	952-Acc fbk Pitch(r)	deg/s^2	Table feedback rotational acceleration (raw)
371	953-Acc fbk Yaw(r)	deg/s^2	Table feedback rotational acceleration (raw)
372	954-Force fbk X	Kn	Table feedback force
373	955-Force fbk Y	Kn	Table feedback force
374	956-Force fbk Z	Kn	Table feedback force
375	957-Force fbk Roll	kN-m	Tabel feedback moment
376	958-Force fbk Pitch	kN-m	Tabel feedback moment
377	959-Force fbk Yaw	kN-m	Tabel feedback moment

Appendix D

Location for acceleration measurements

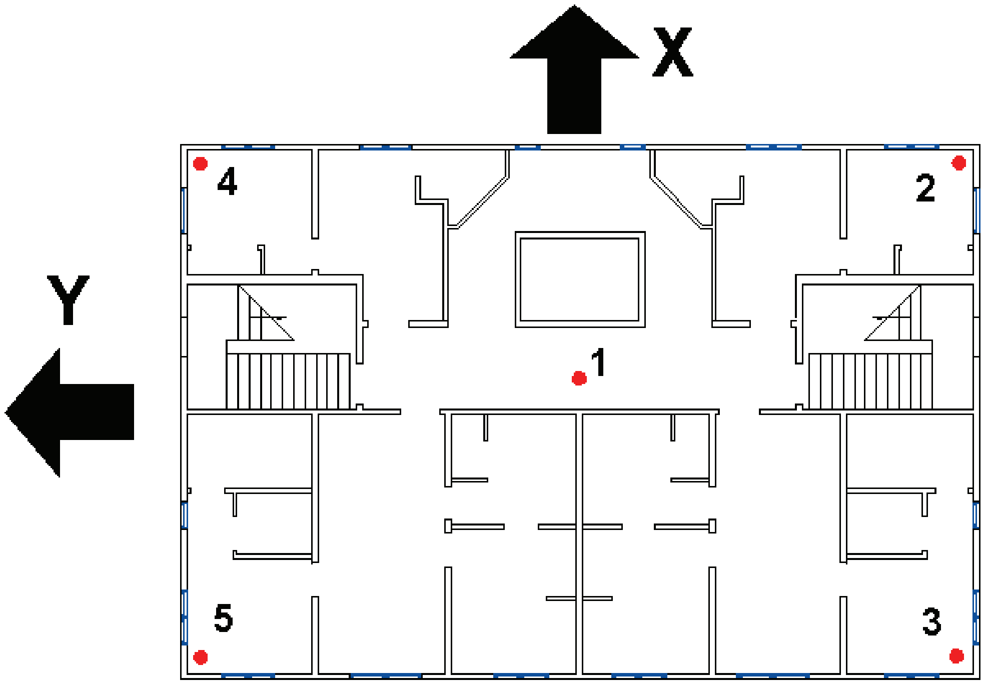

Figure D.1: Absolute acceleration sensor location at story 2 (Identical for all other stories)

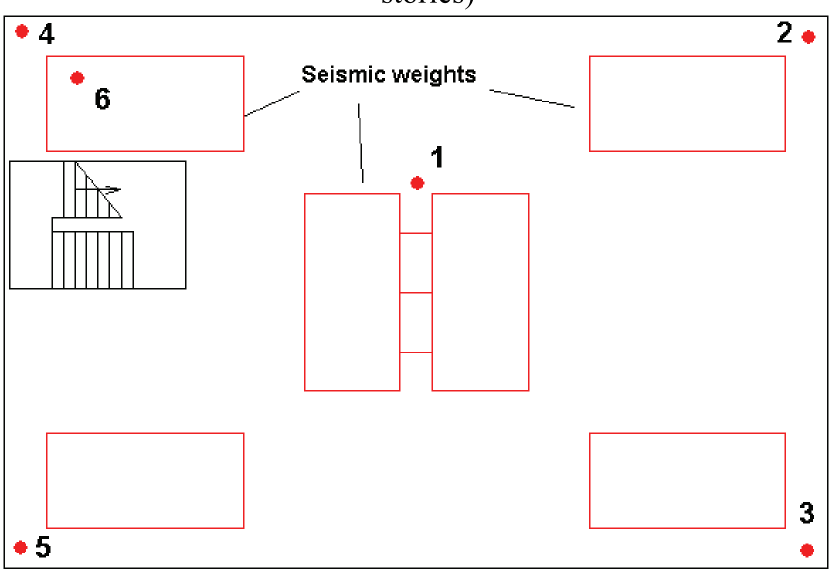

Figure D.2: Absolute acceleration sensor location at roof (location 6 is on the seismic weight steel plate)

Appendix D

Location for Diagonal string gage measurements

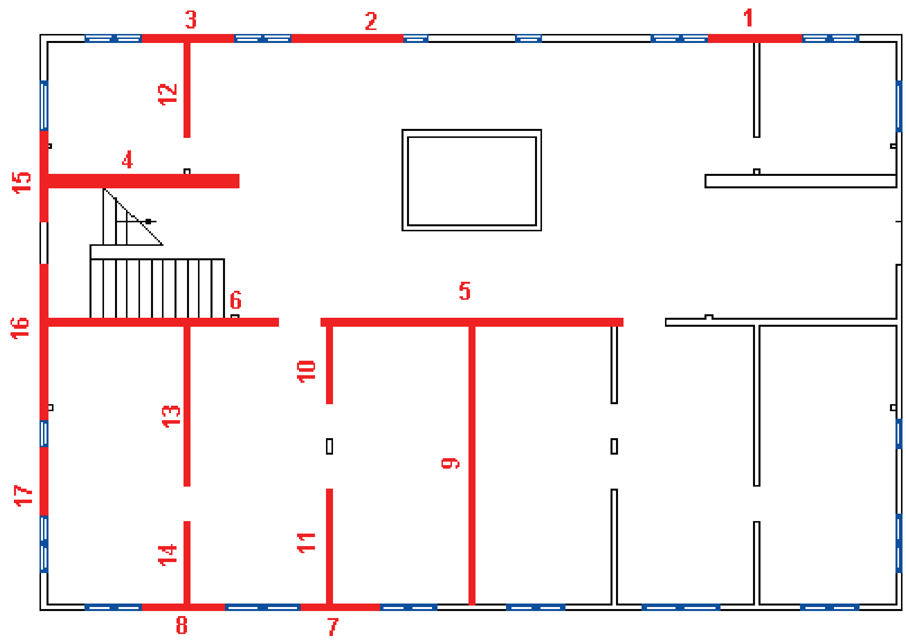

Figure D.3: Shear wall numbering for diagonal gage in story 2

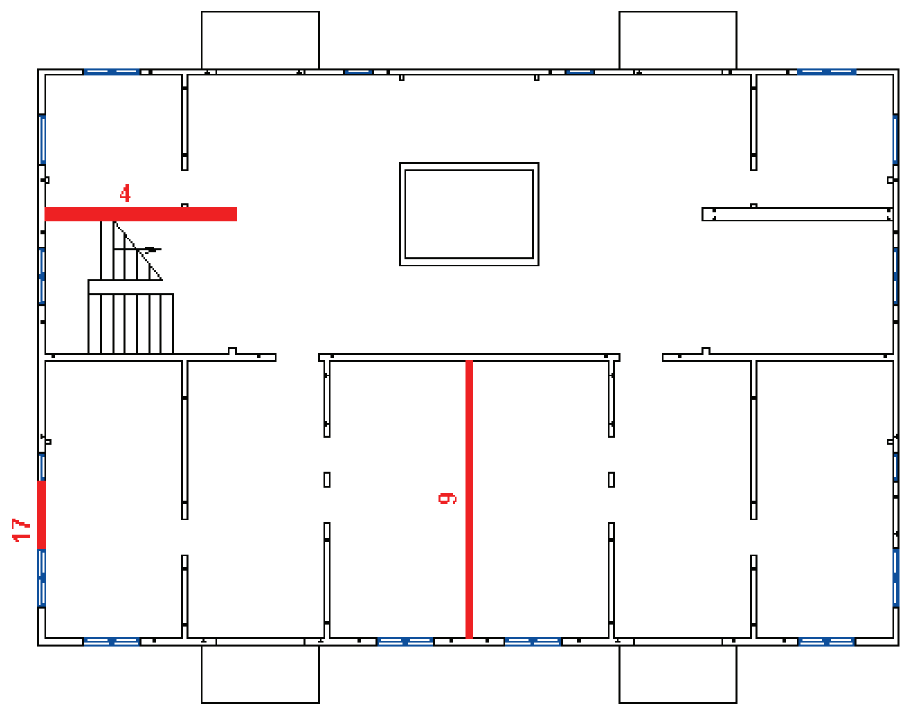

Figure D.4: Shear wall numbering for diagonal gage in story 3~6

Appendix D

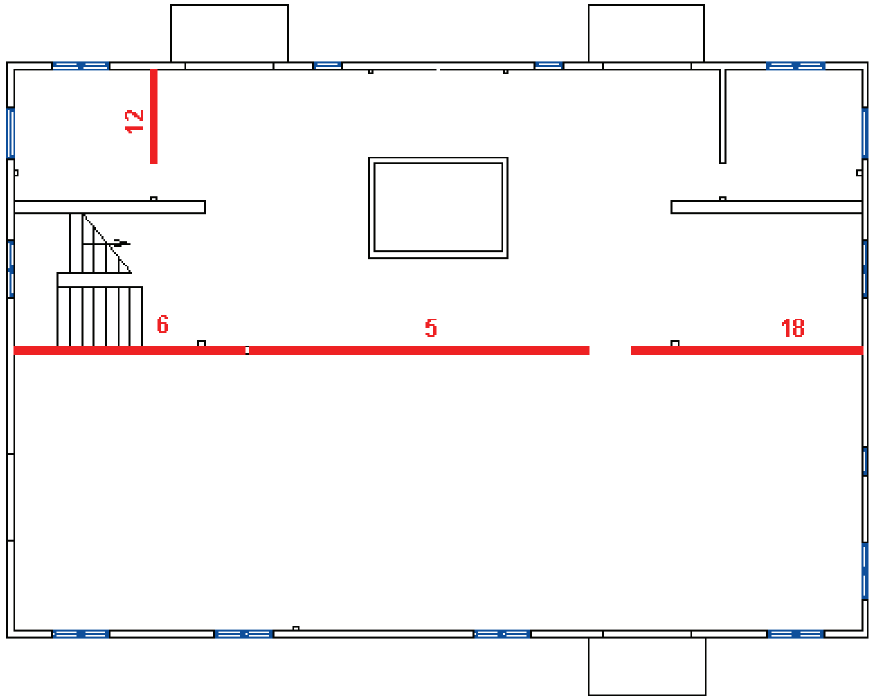

Figure D.5: Shear wall numbering for diagonal gage in story 7

Figure D.6: Photo of a diagonal gage set up

Appendix D

Location for ATS strain measurements

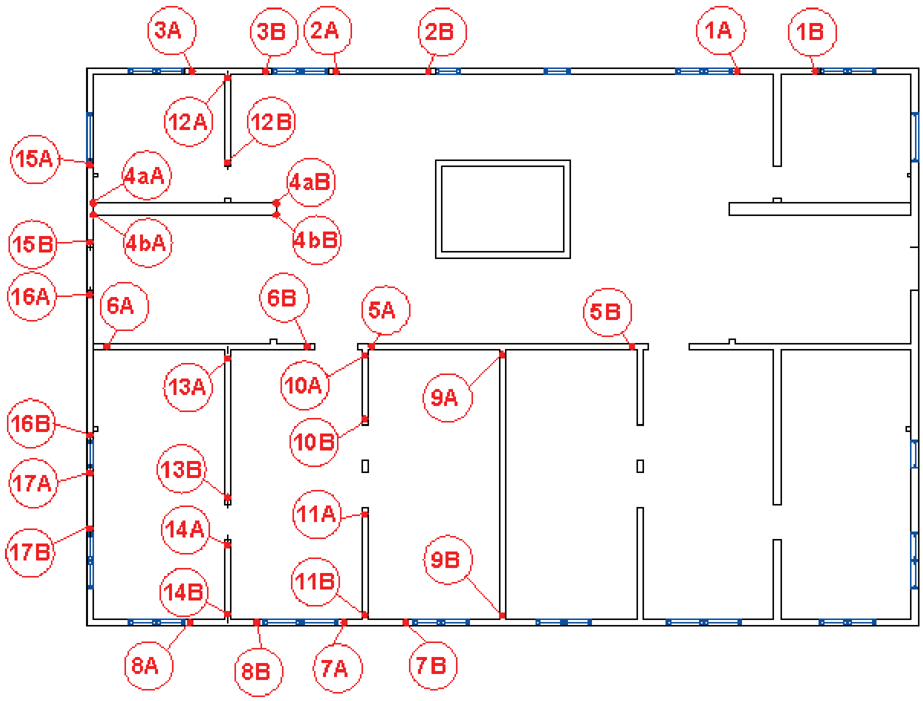

Figure D.7: ATS rod number for story 2

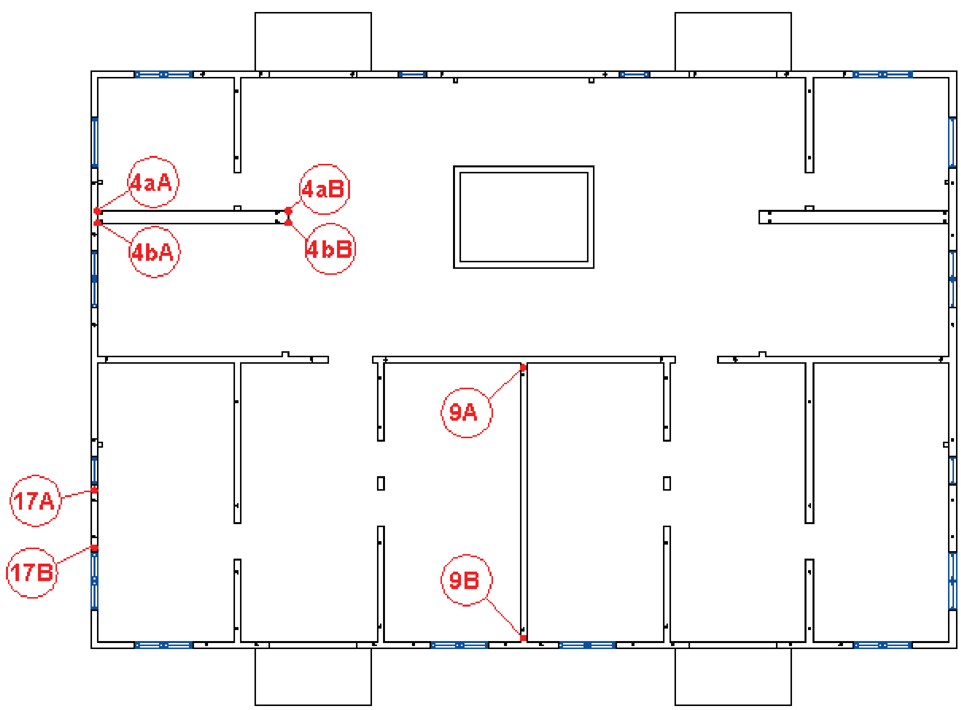

Figure D.8: ATS rod number for story 3~6

Appendix D

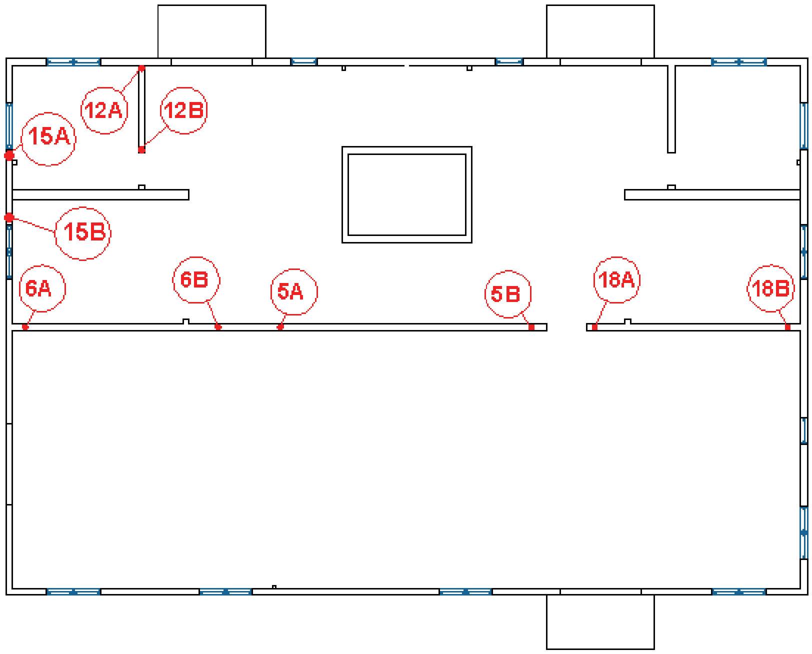

Figure D.9: ATS rod number for story 7

Figure D.10: Photo of the strain gage on ATS rod

Appendix D

Location for shear wall end stud uplift measurements

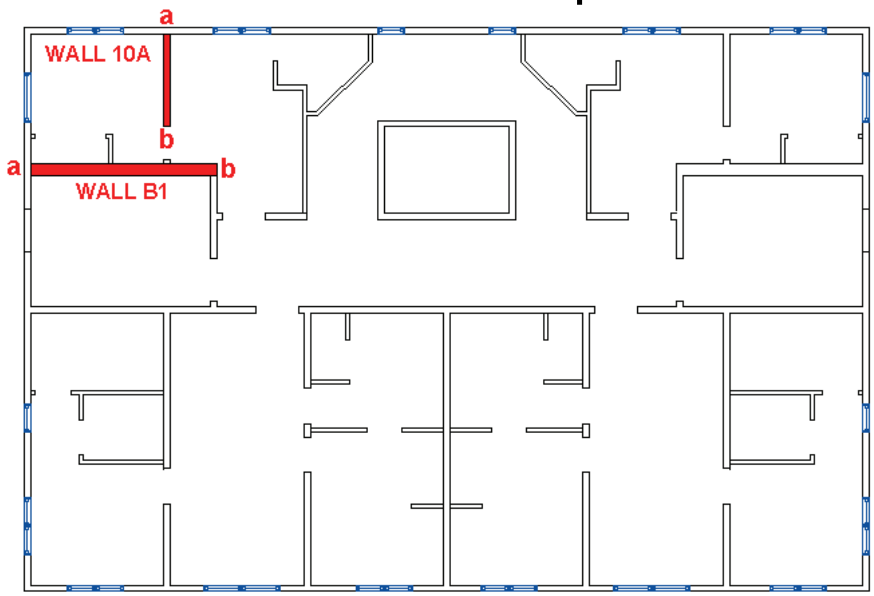

Figure D.11: Story 2 wall stud uplift measurement location

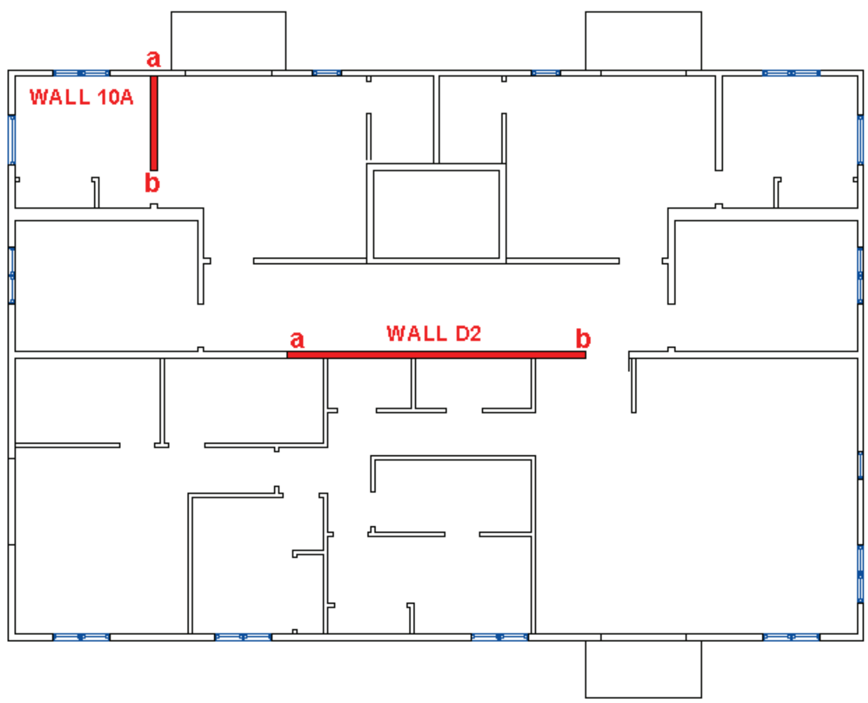

Figure D.12: Story 7 wall stud uplift measurement location

Appendix D

Figure D.13: Photo of shear wall stud uplift measurement set up

Appendix D

Out-of-plane diaphragm displacement measurement

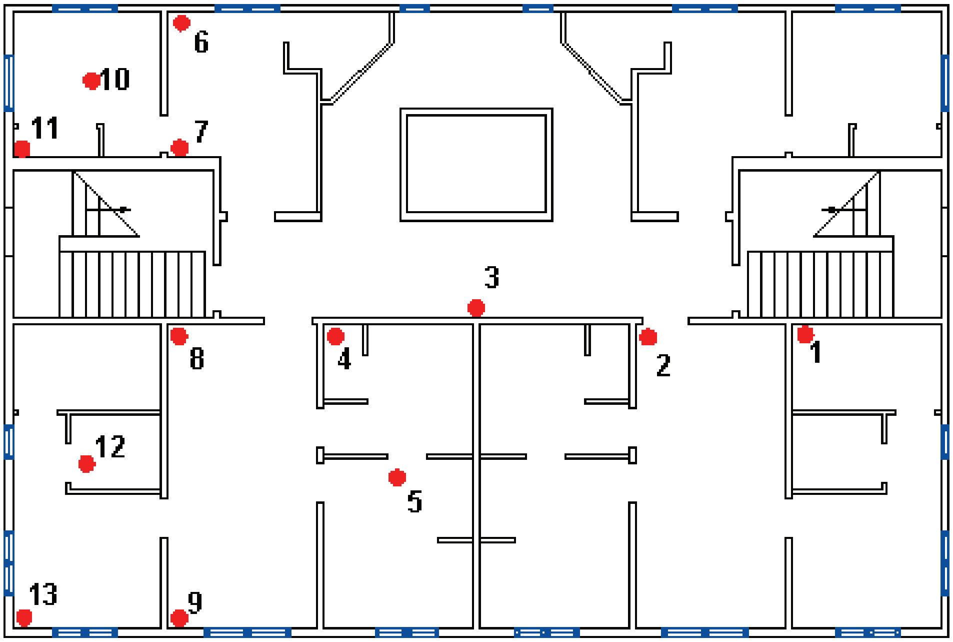

Figure D.14: Floor out-of-plane displacement measurement location

Figure D.15: Photo of floor out-of-plane displacement measurement set up

Appendix D

SMF strain measurement

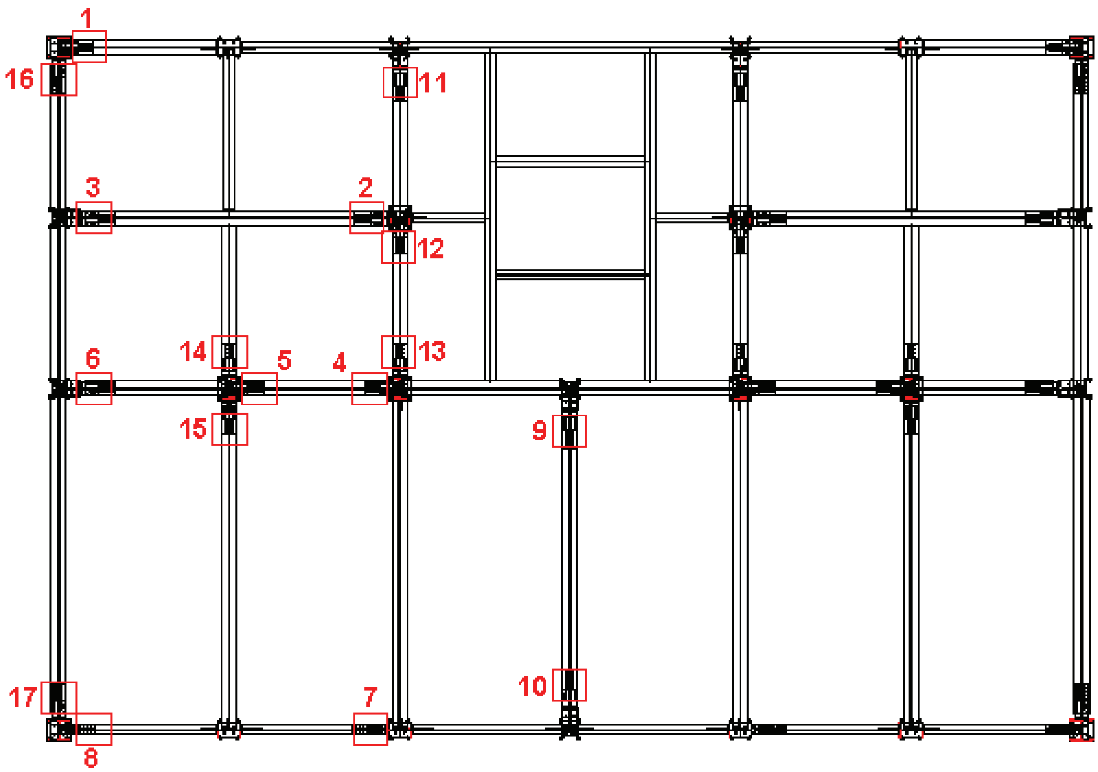

Figure D.16: Location for SMF moment connection strain measurement

Appendix D

Optical tracking measurement

Figure D.17: Location for optical tracking measurement, side A

Appendix D

Optical tracking measurement

Figure D.18: Location for optical tracking measurement, side B

Appendix D

Figure D.19: Photo of optical tracking marker

Appendix E

Optical tracking measurement using LED markers

Appendix E

Optical tracking marker location

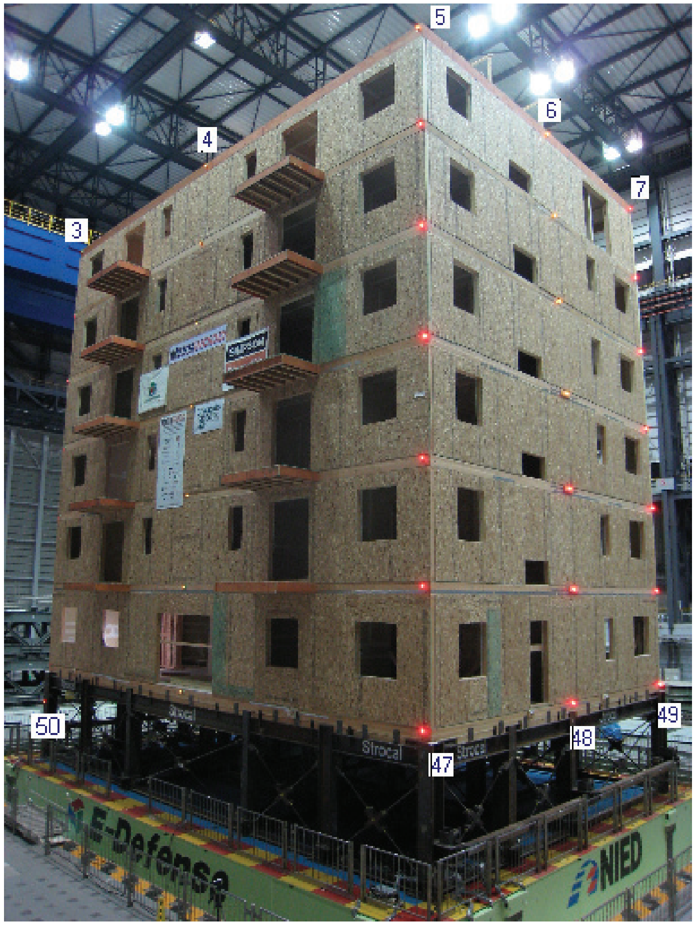

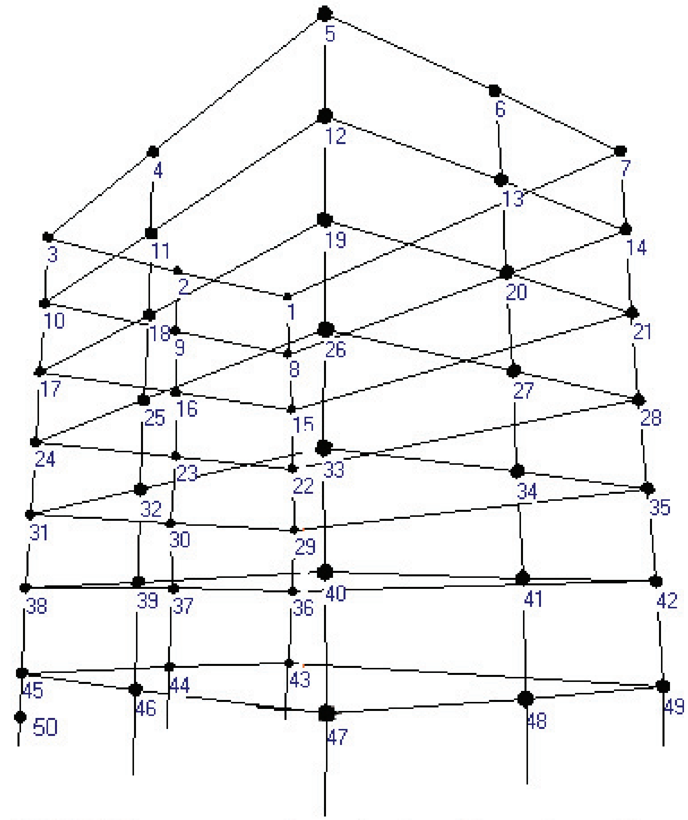

50 LED Sensors on the exterior of specimen, 7 sensors for each story diaphragm, one on the SMF.

Figure E.1. LED sensors for optical tracking of absolute displacements on the exterior of the specimen

Appendix E

Seismic test 1, Optical tracking displacement (1~5)

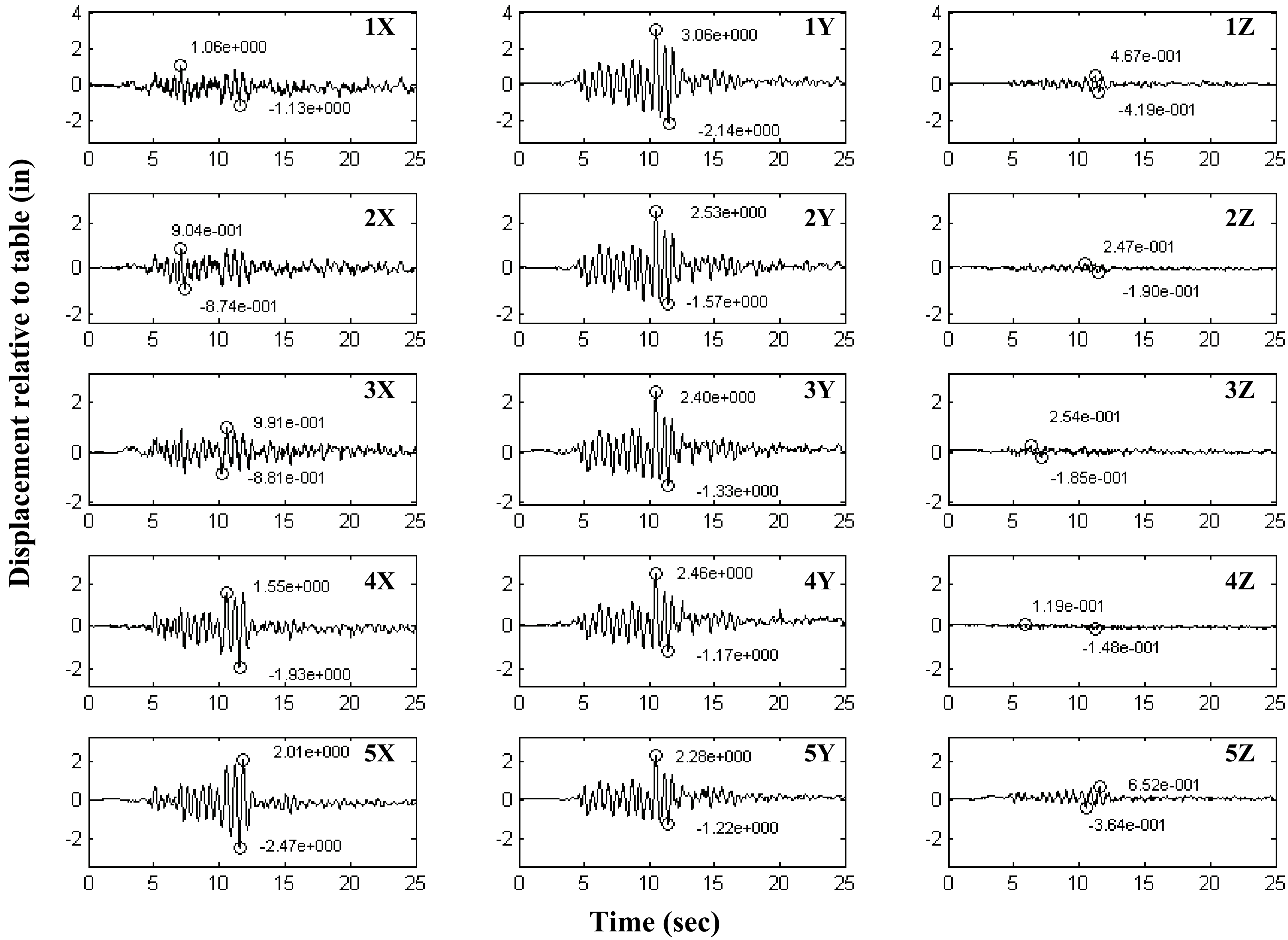

Figure E.2: Displacement of optical tracking markers (1~5) relative to table during Seismic test 1

Appendix E

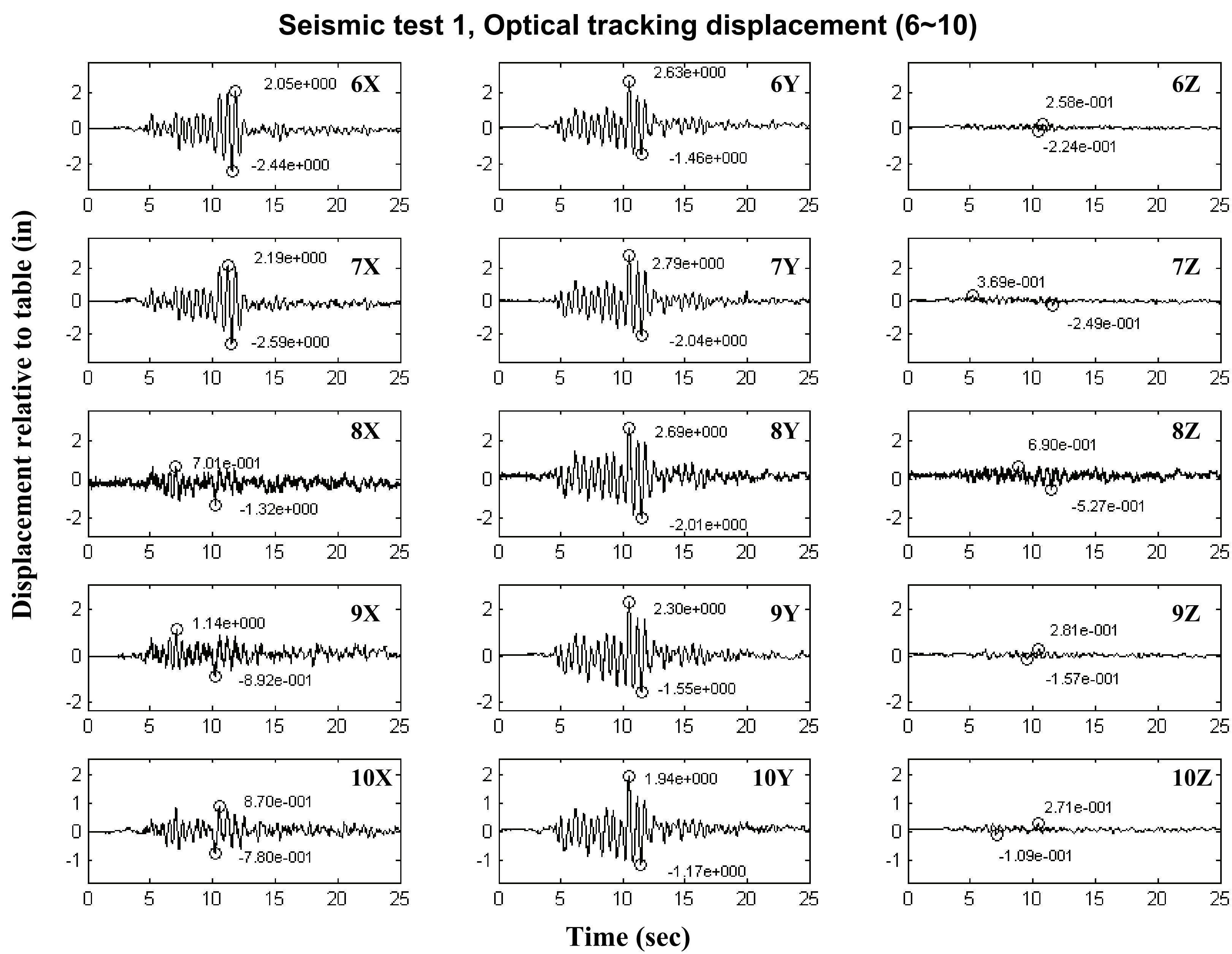

Figure E.3: Displacement of optical tracking markers (6~10) relative to table during Seismic test 1

Appendix E

Seismic test 1, Optical tracking displacement (11~15)

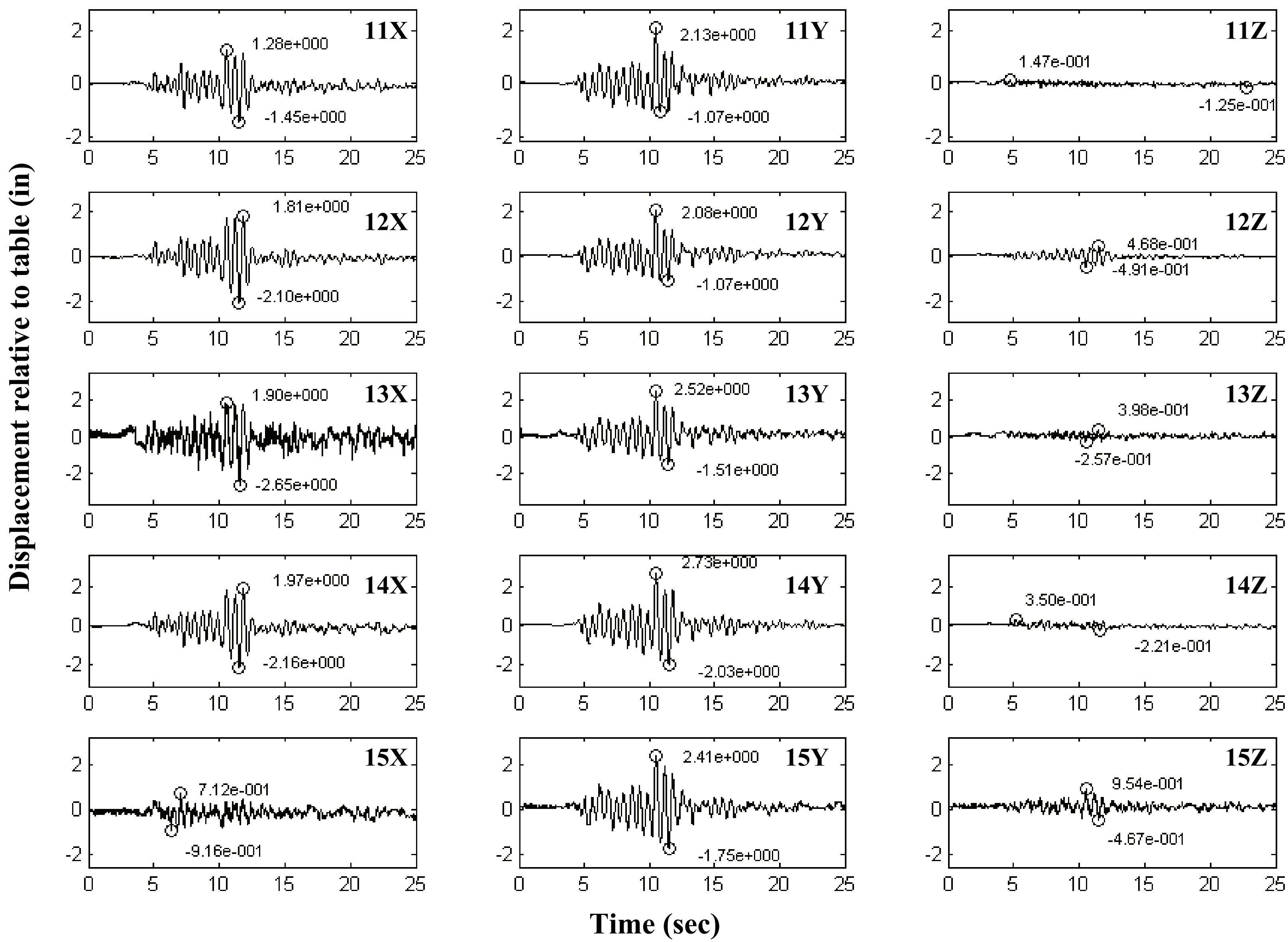

Figure E.4: Displacement of optical tracking markers (11~15) relative to table during Seismic test 1

Appendix E

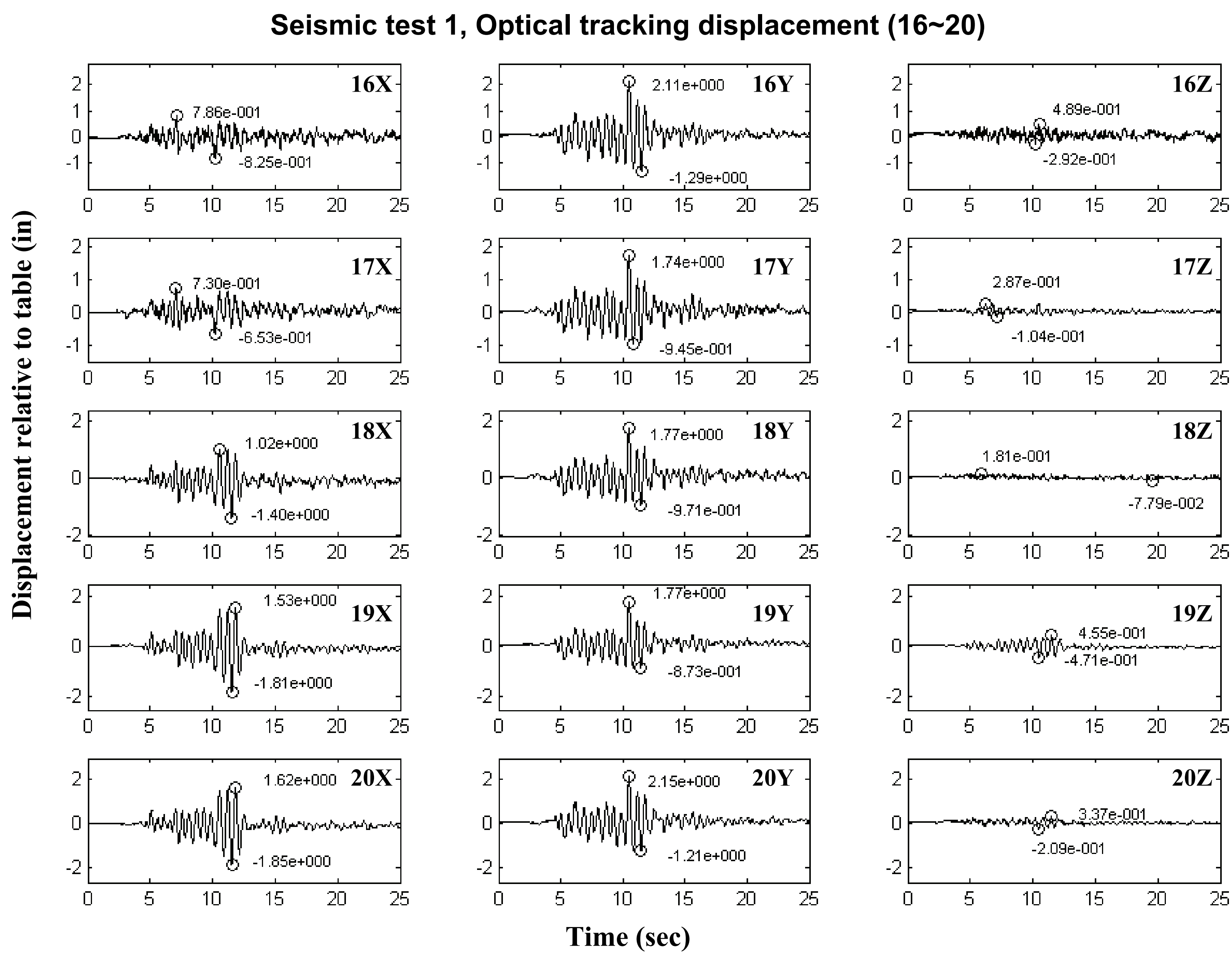

Figure E.5: Displacement of optical tracking markers (16~20) relative to table during Seismic test 1

Appendix E

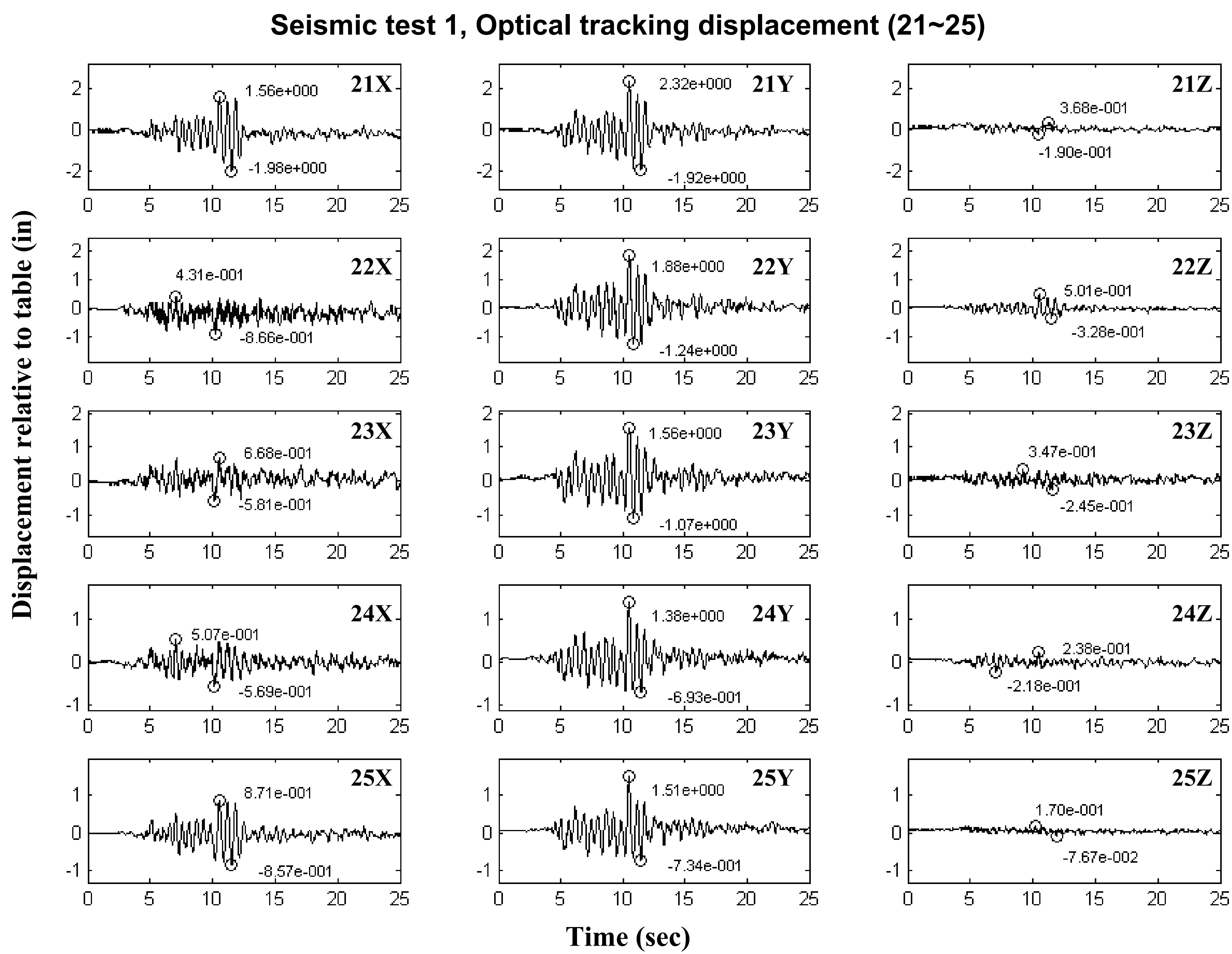

Figure E.6: Displacement of optical tracking markers (21~25) relative to table during Seismic test 1

Appendix E

Seismic test 1, Optical tracking displacement (26~30)

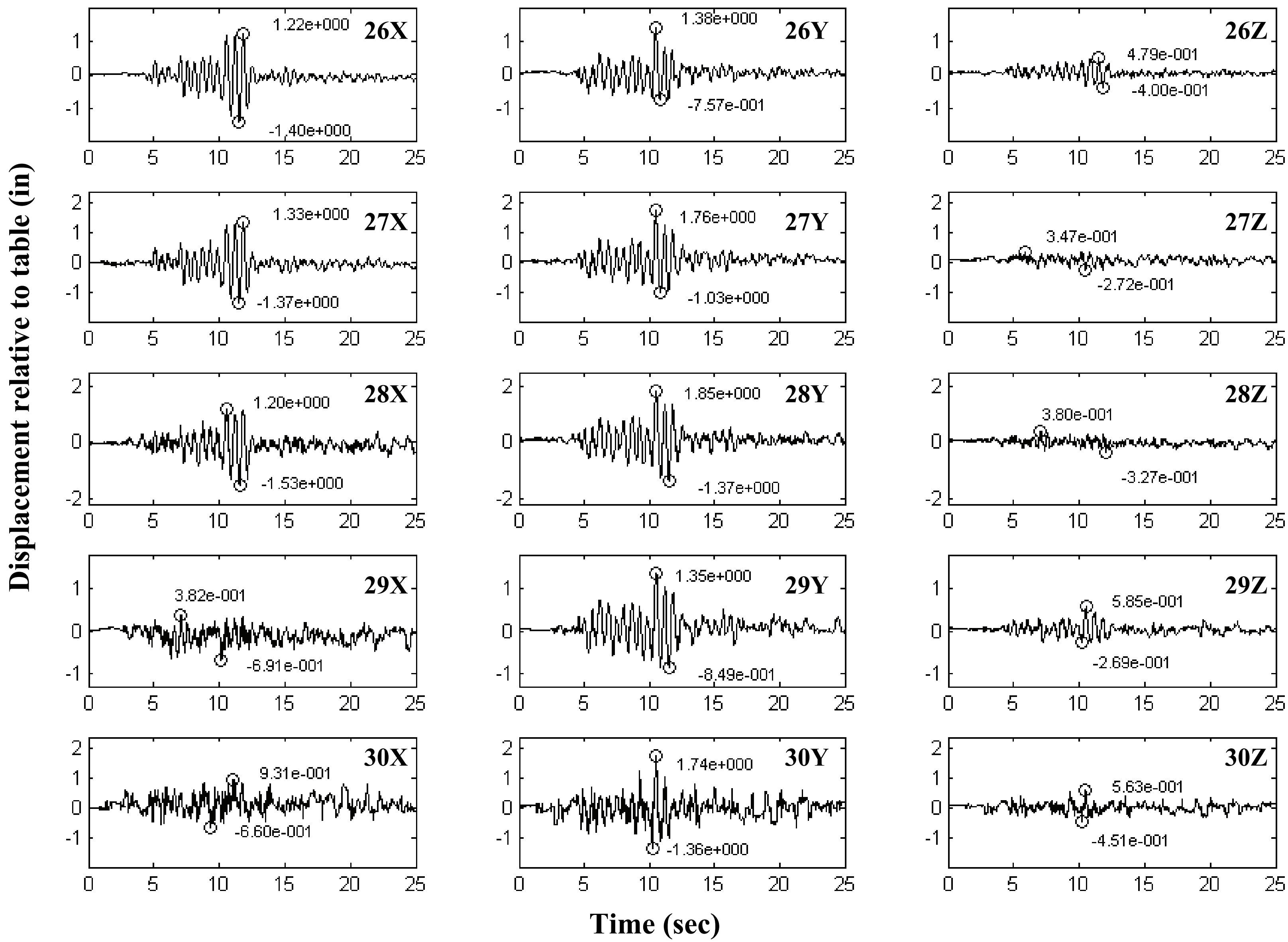

Figure E.7: Displacement of optical tracking markers (26~30) relative to table during Seismic test 1

Appendix E

Seismic test 1, Optical tracking displacement (31~35)

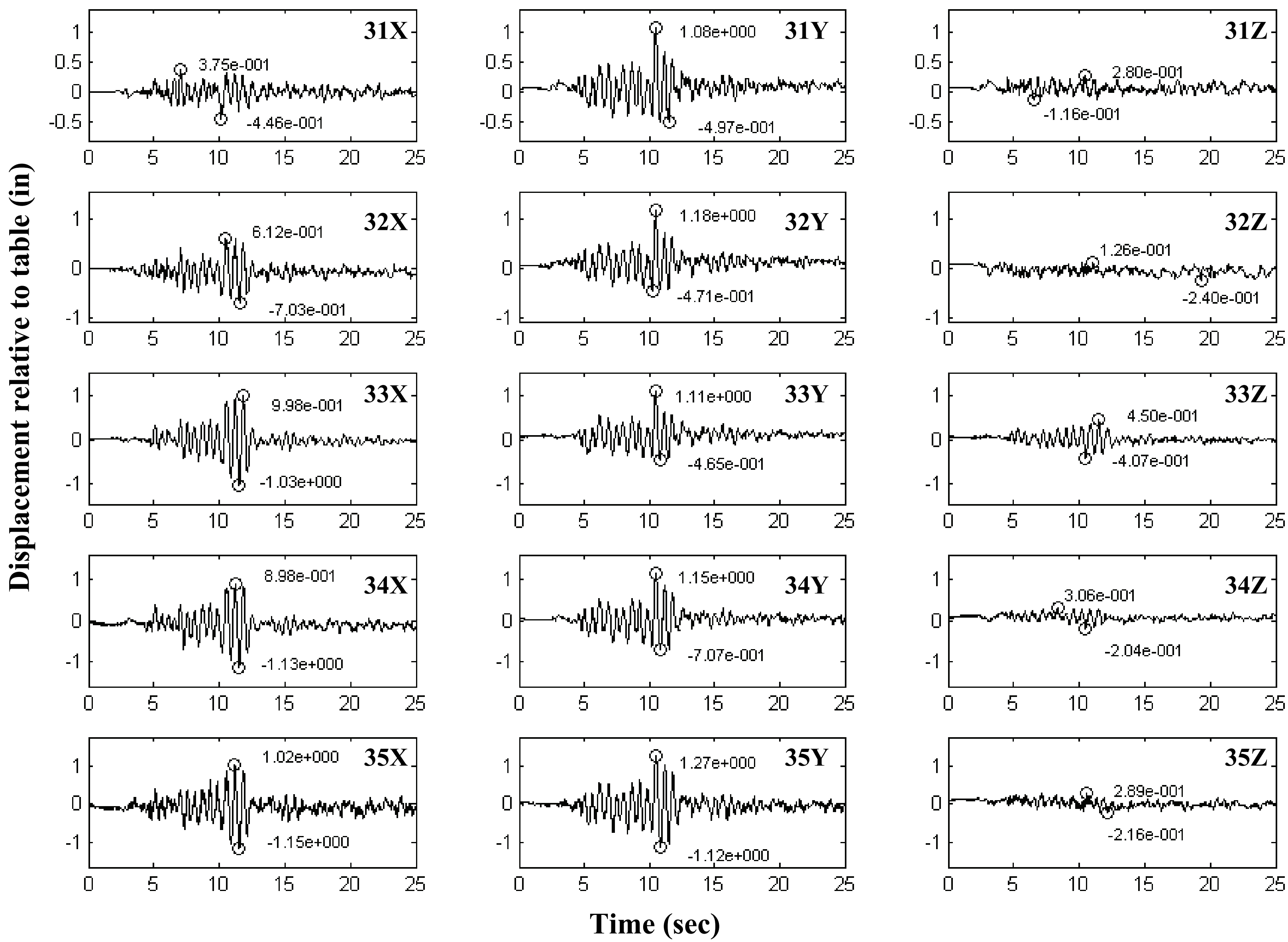

Figure E.8: Displacement of optical tracking markers (31~35) relative to table during Seismic test 1

Seismic test 1, Optical tracking displacement (36~40)

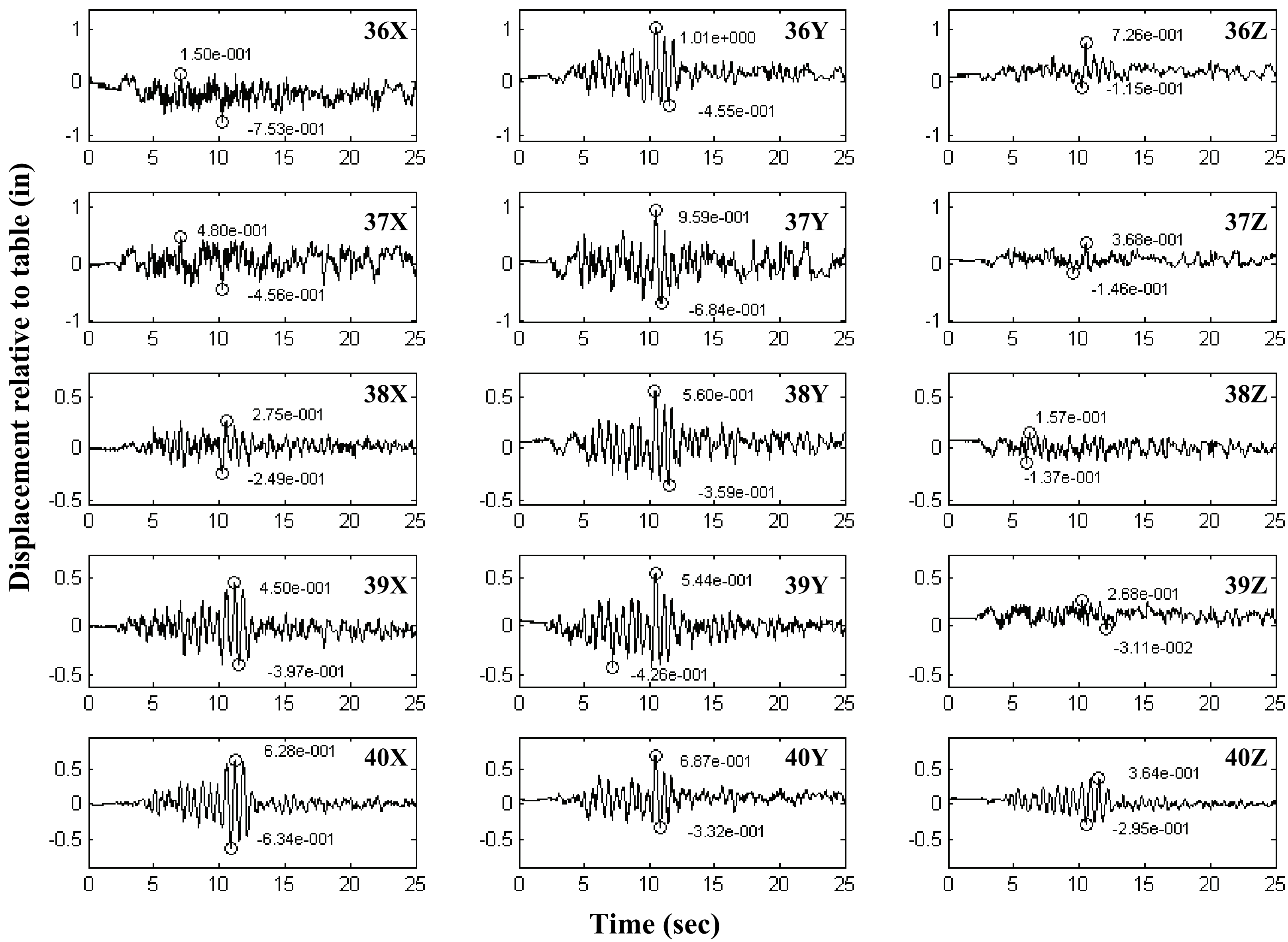

Figure E.9: Displacement of optical tracking markers (36~40) relative to table during Seismic test 1

Seismic test 1, Optical tracking displacement (41~45)

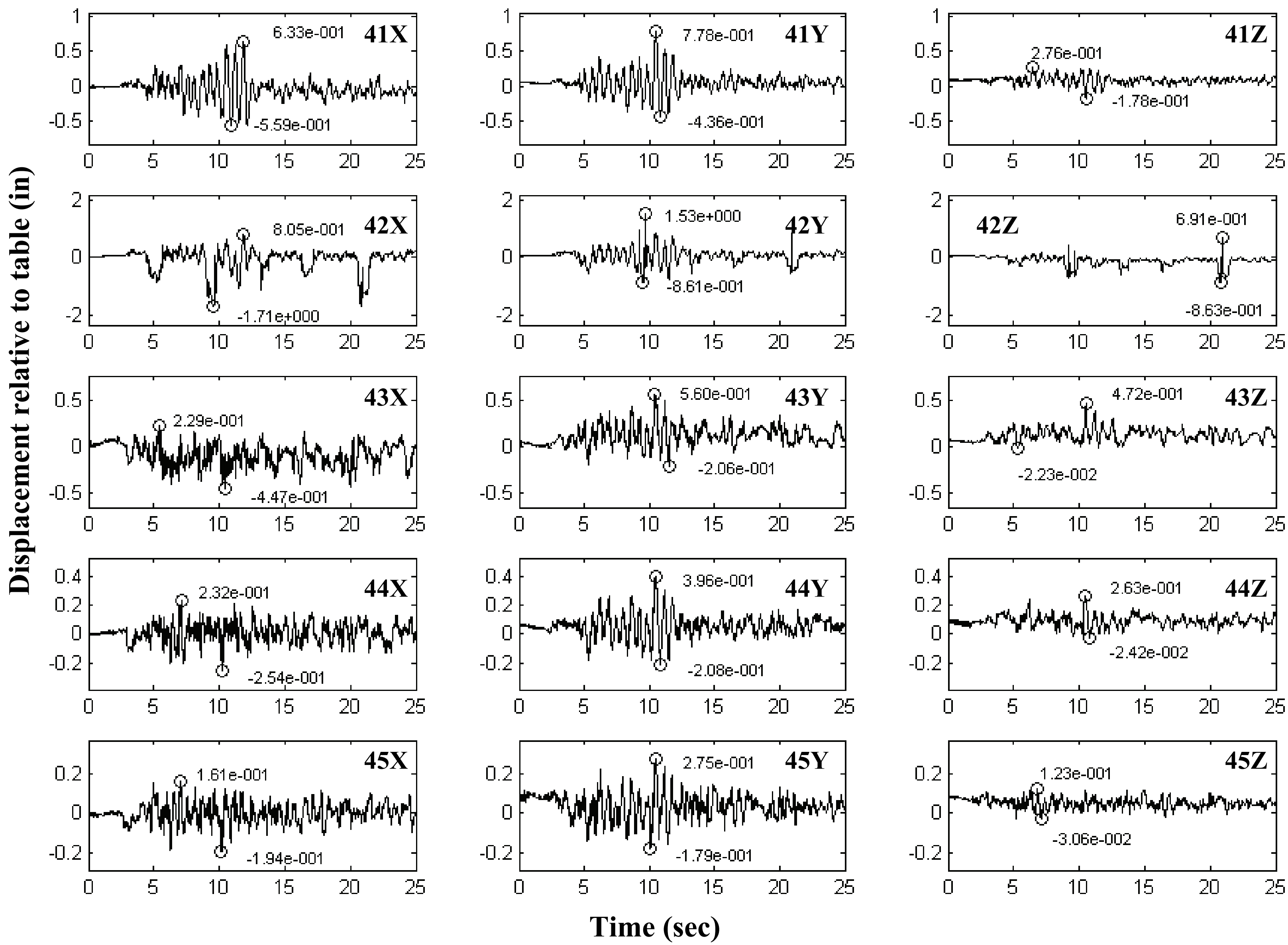

Figure E.10: Displacement of optical tracking markers (41~45) relative to table during Seismic test 1

Appendix E

Seismic test 1, Optical tracking displacement (46~50)

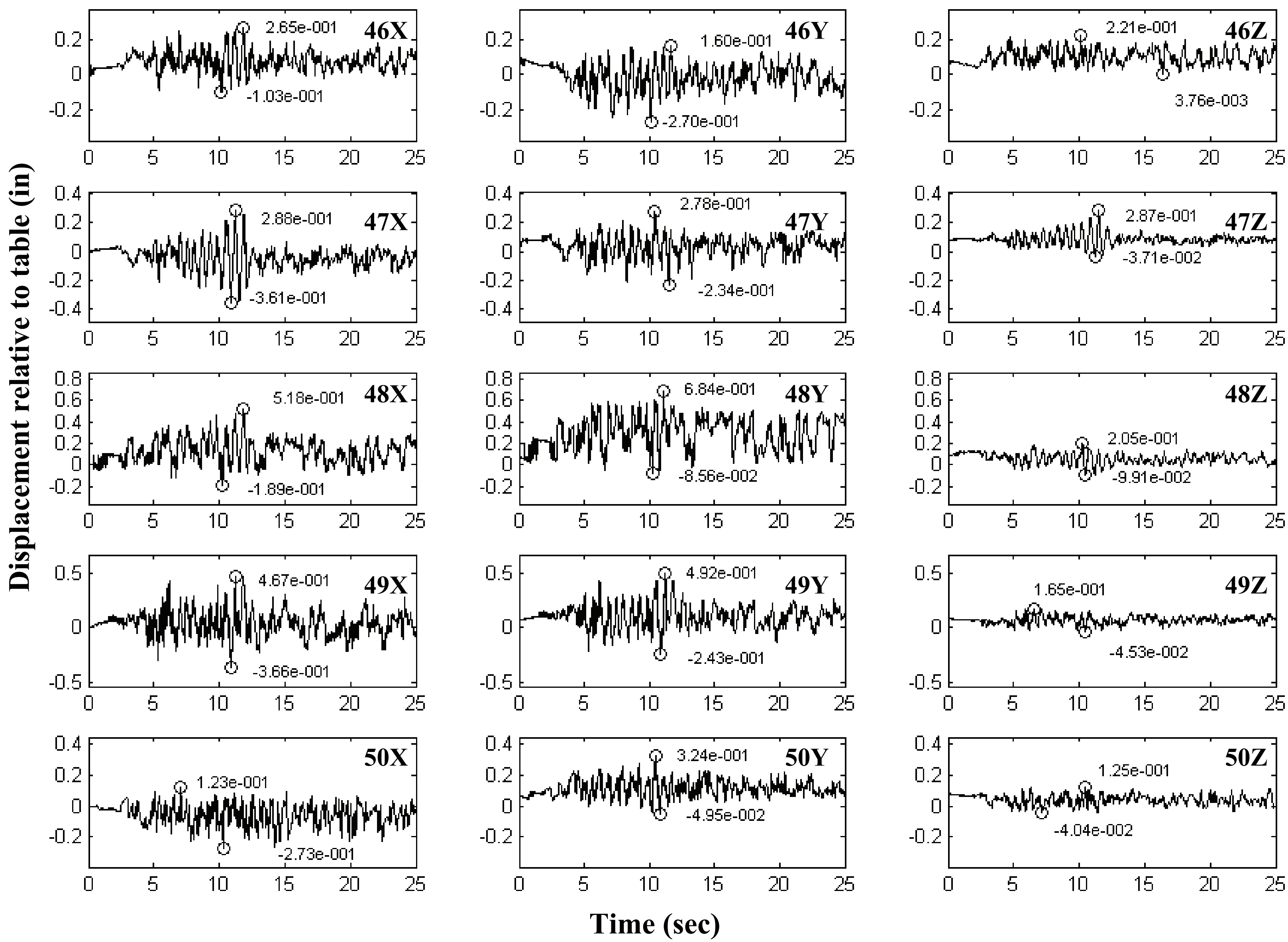

Figure E.11: Displacement of optical tracking markers (46~50) relative to table during Seismic test 1

Appendix E

Seismic test 2, Optical tracking displacement (1~5)

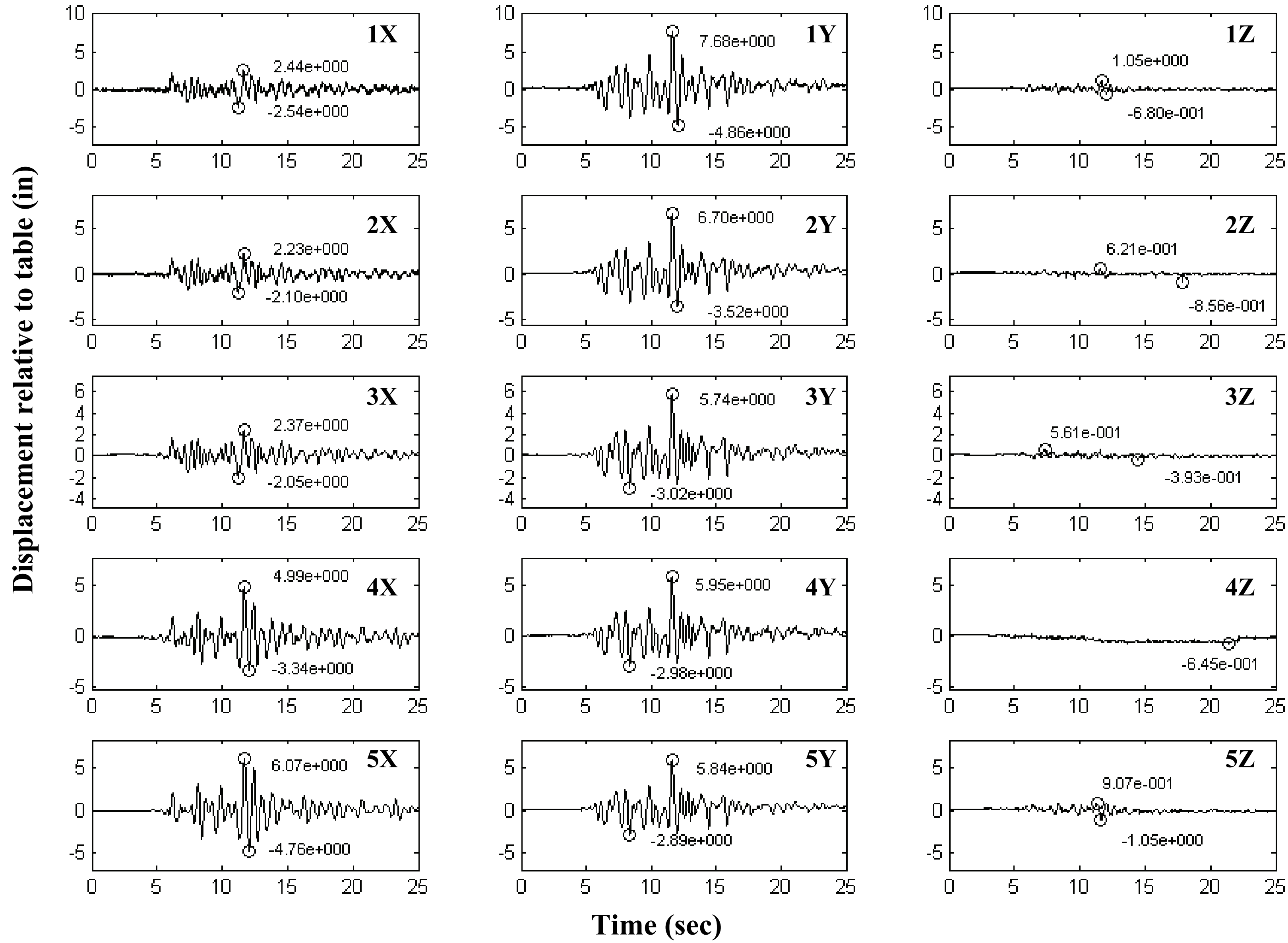

Figure E.12: Displacement of optical tracking markers (1~5) relative to table during Seismic test 2

Appendix E

Seismic test 2, Optical tracking displacement (6~10)

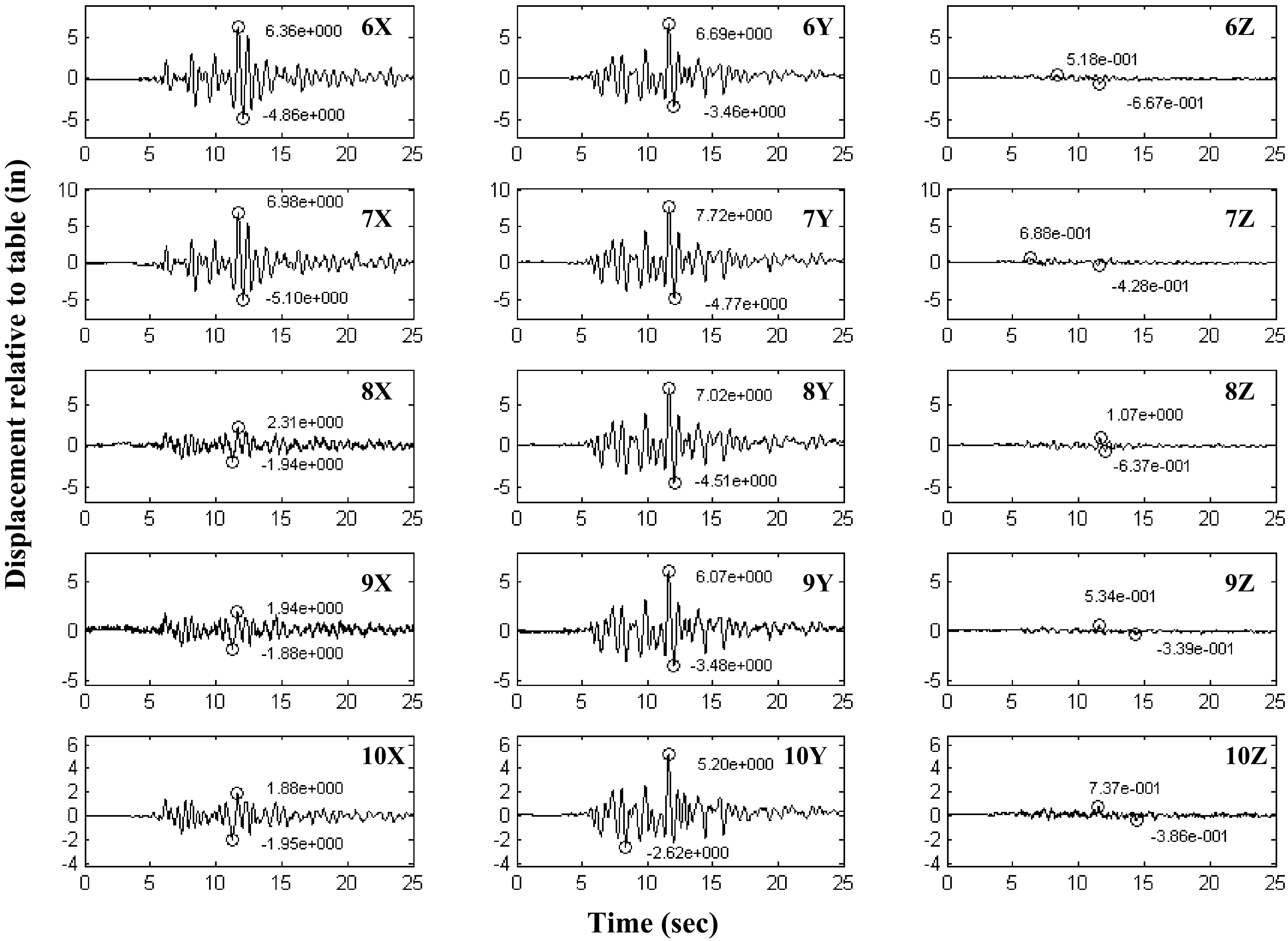

Figure E.13: Displacement of optical tracking markers (6~10) relative to table during Seismic test 2

Appendix E

Seismic test 2, Optical tracking displacement (11~15)

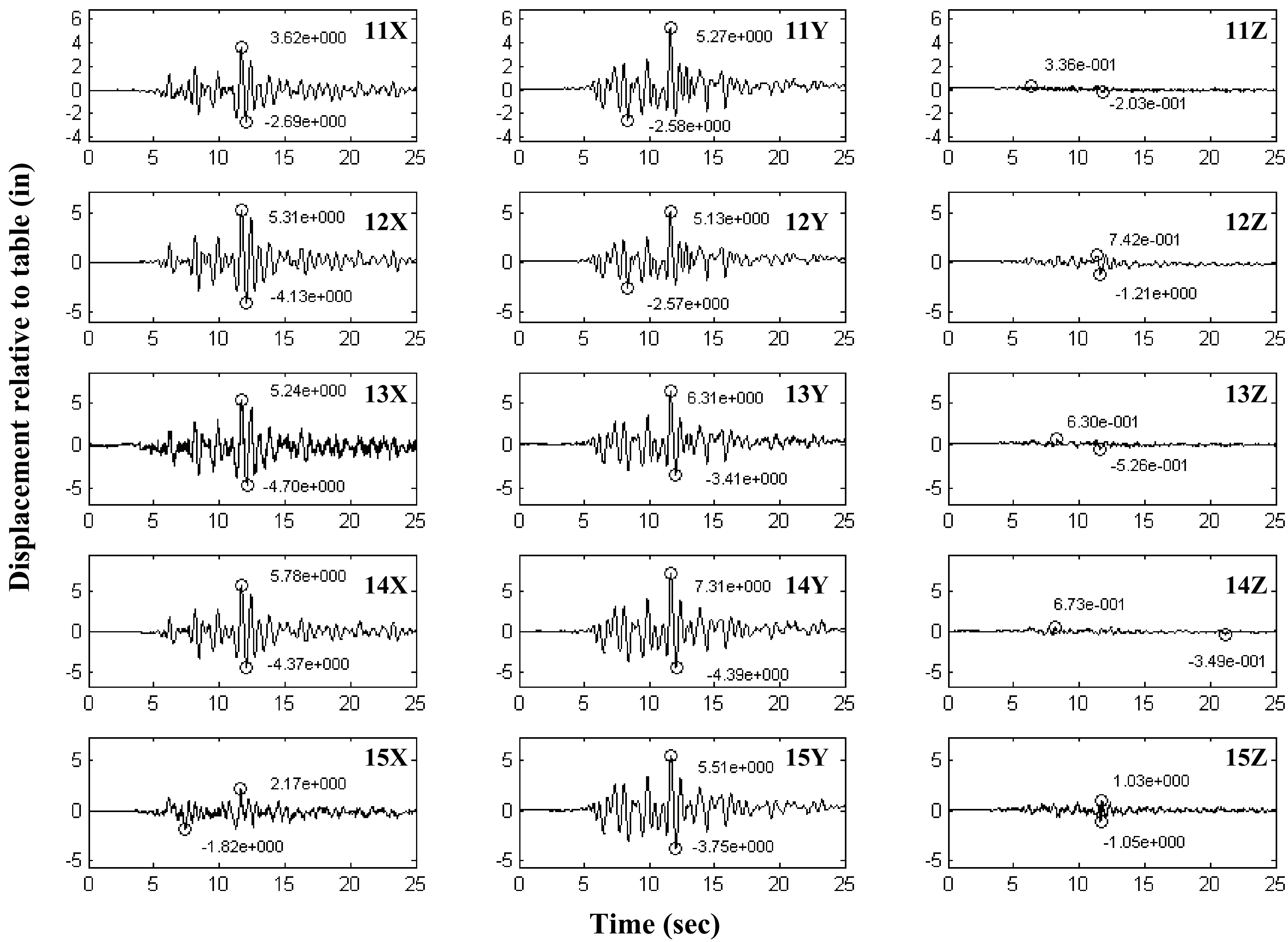

Figure E.14: Displacement of optical tracking markers (11~15) relative to table during Seismic test 2

Appendix E

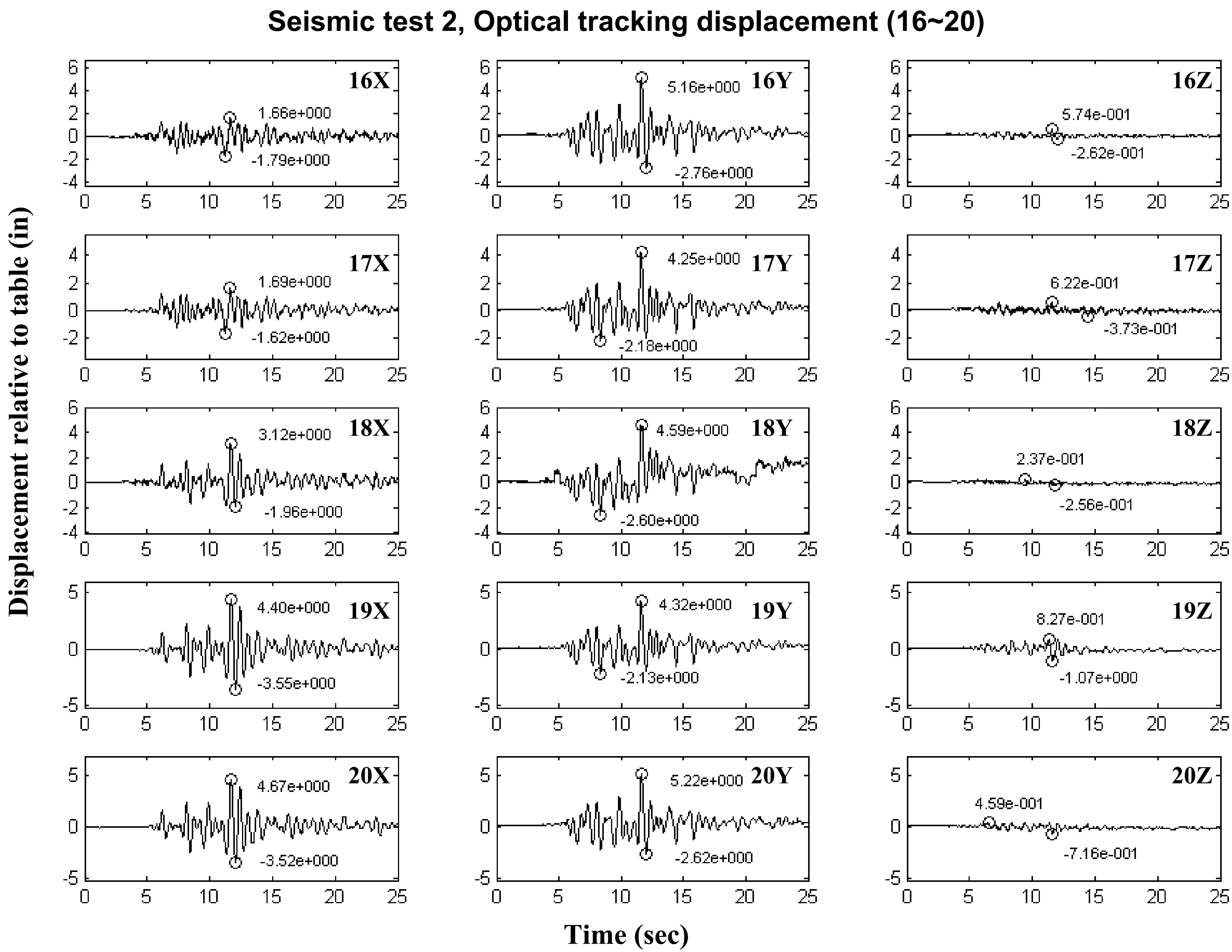

Figure E.15: Displacement of optical tracking markers (16~20) relative to table during Seismic test 2

Appendix E

Seismic test 2, Optical tracking displacement (21~25)

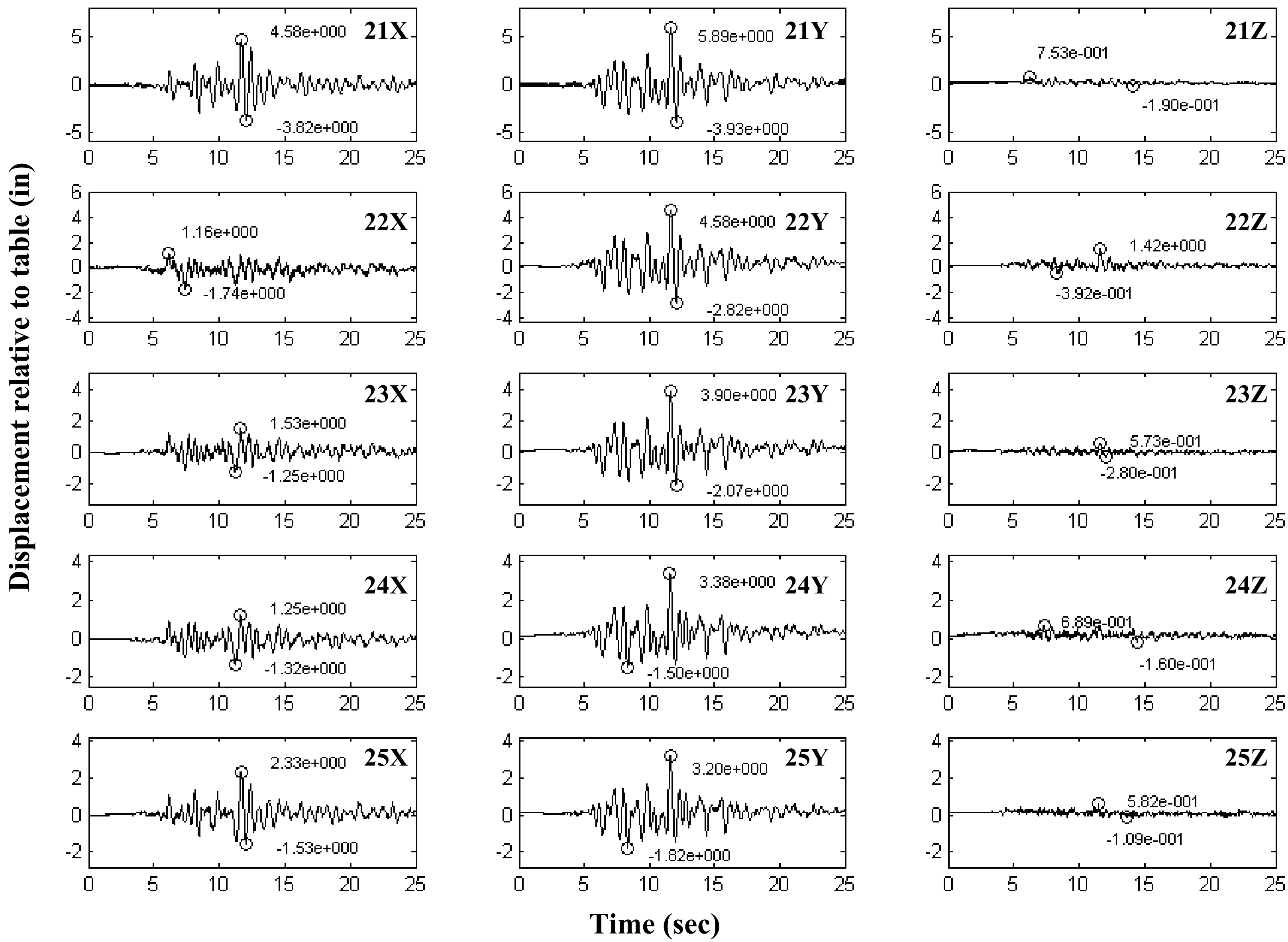

Figure E.16: Displacement of optical tracking markers (21~25) relative to table during Seismic test 2

Appendix E

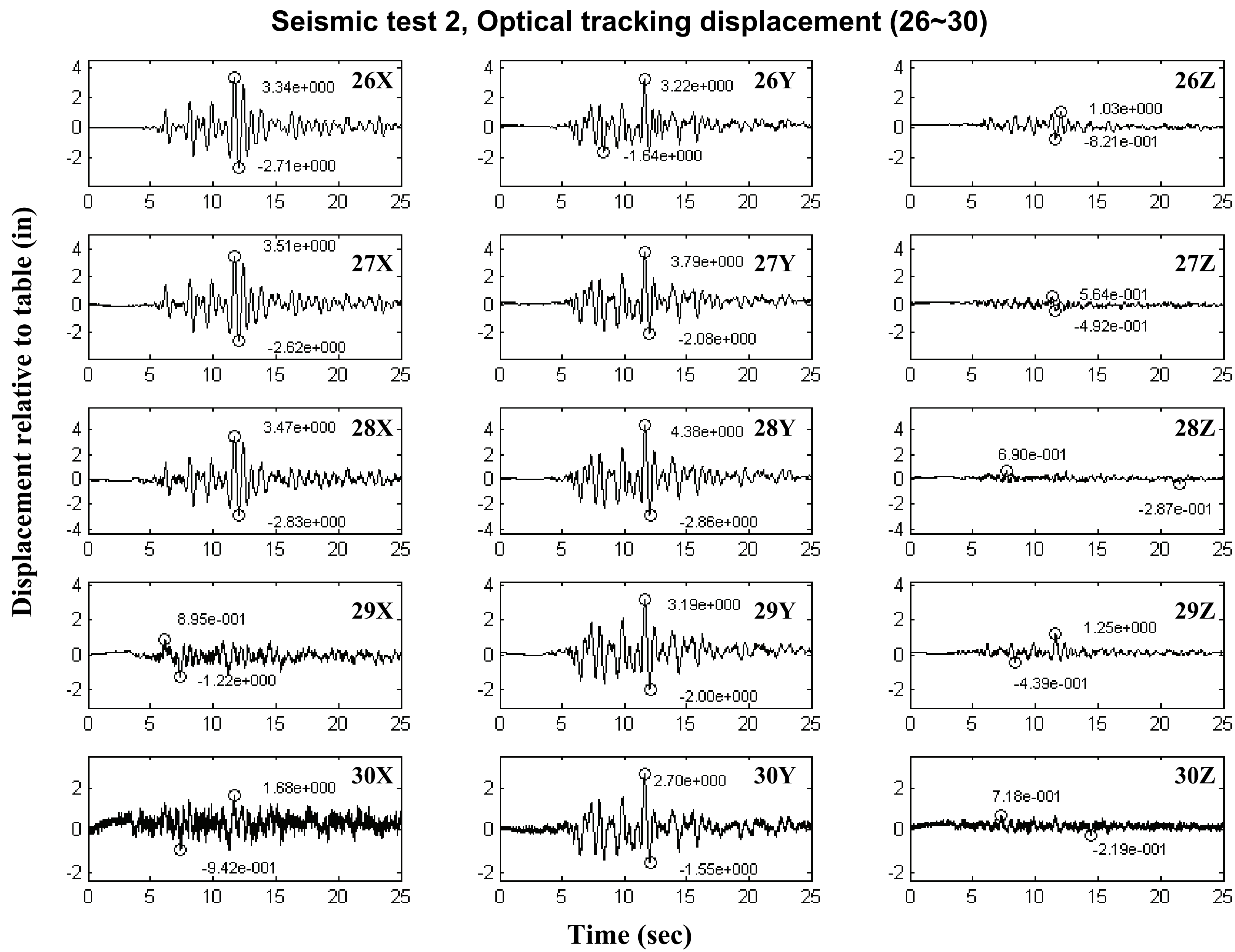

Figure E.17: Displacement of optical tracking markers (26~30) relative to table during Seismic test 2

Appendix E

Seismic test 2, Optical tracking displacement (31~35)

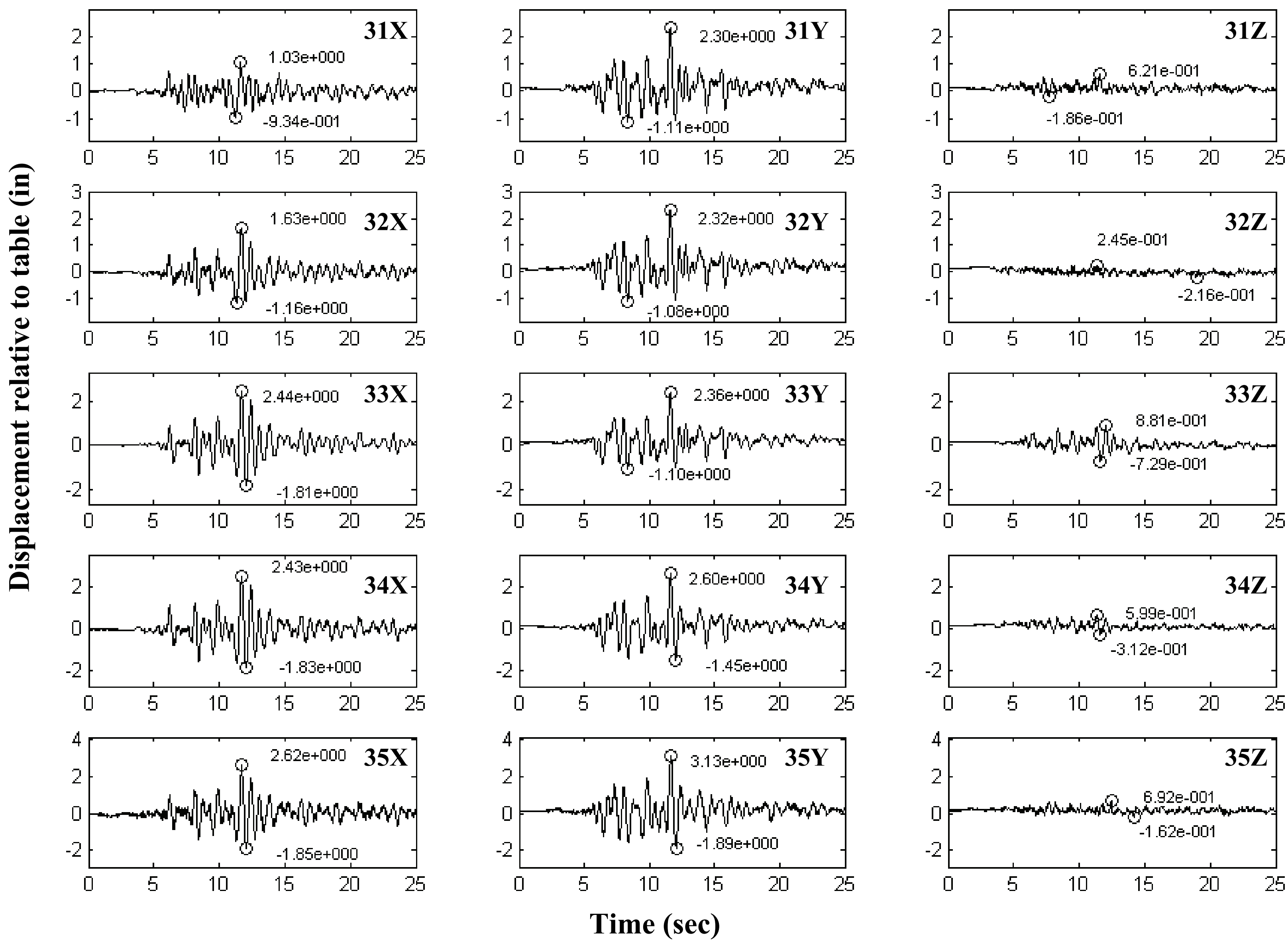

Figure E.18: Displacement of optical tracking markers (31~35) relative to table during Seismic test 2

Seismic test 2, Optical tracking displacement (36~40)

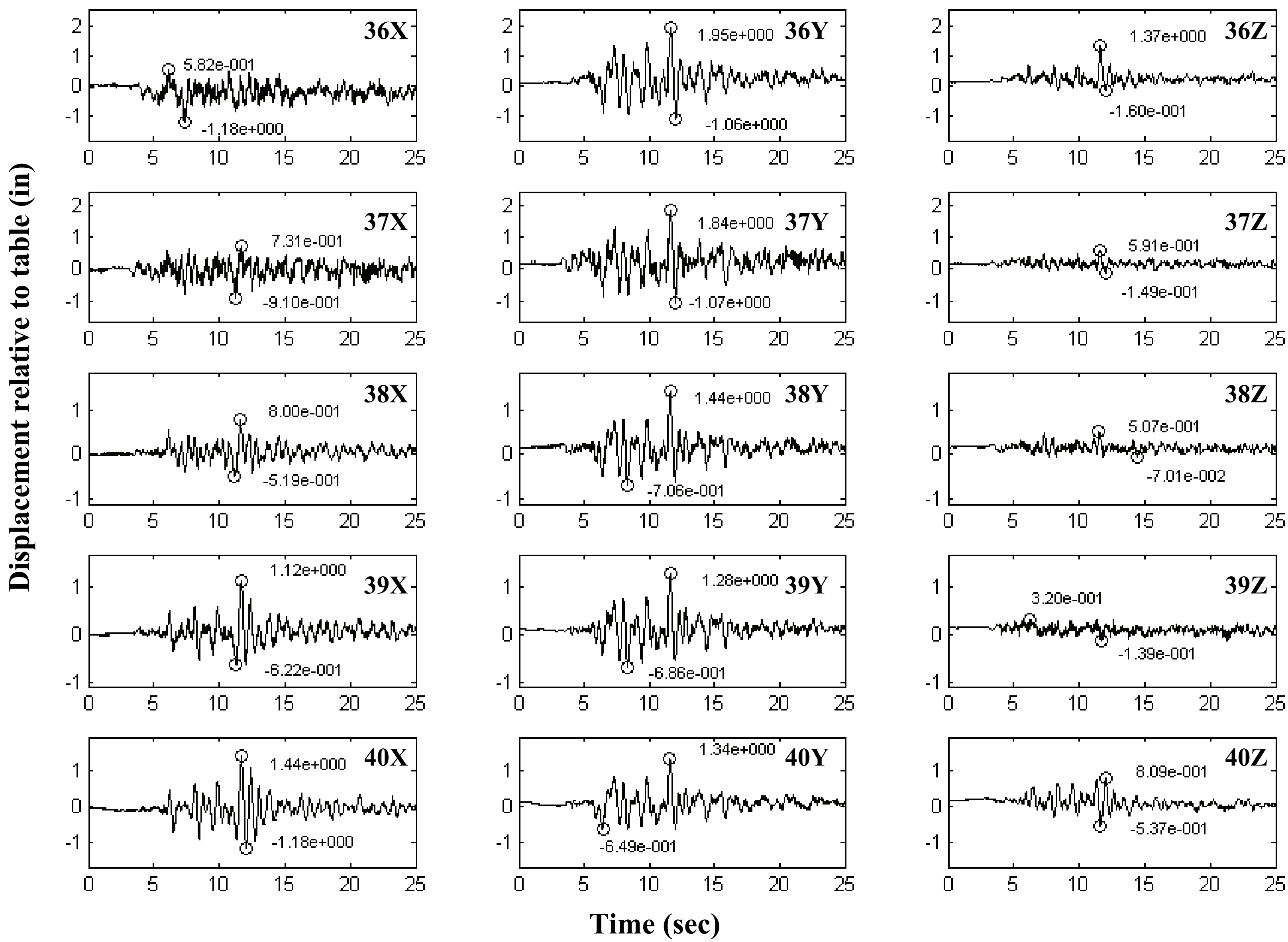

Figure E.19: Displacement of optical tracking markers (36~40) relative to table during Seismic test 2

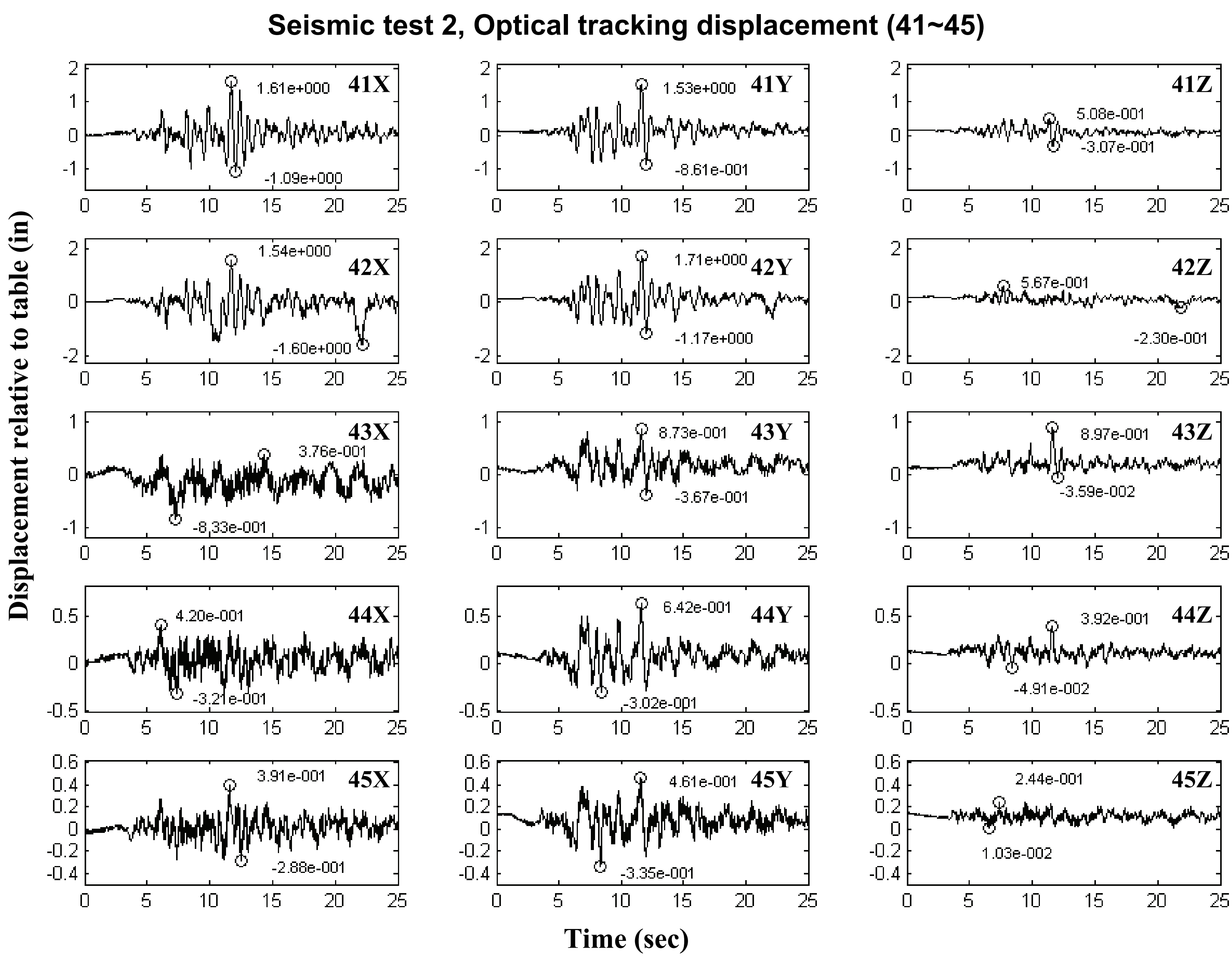

Figure E.20: Displacement of optical tracking markers (41~45) relative to table during Seismic test 2

Appendix E

Seismic test 2, Optical tracking displacement (46~50)

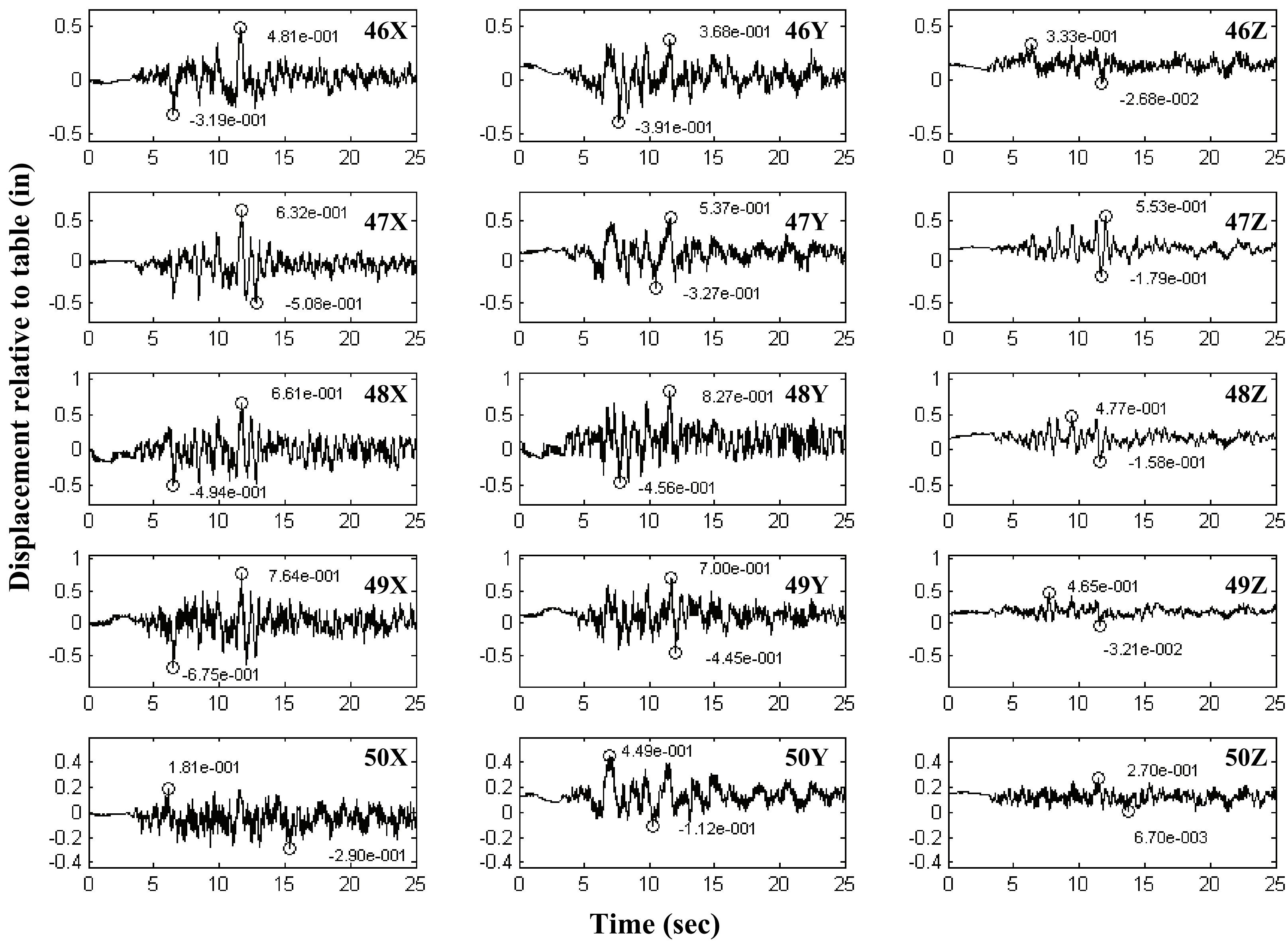

Figure E.21: Displacement of optical tracking markers (46~50) relative to table during Seismic test 2

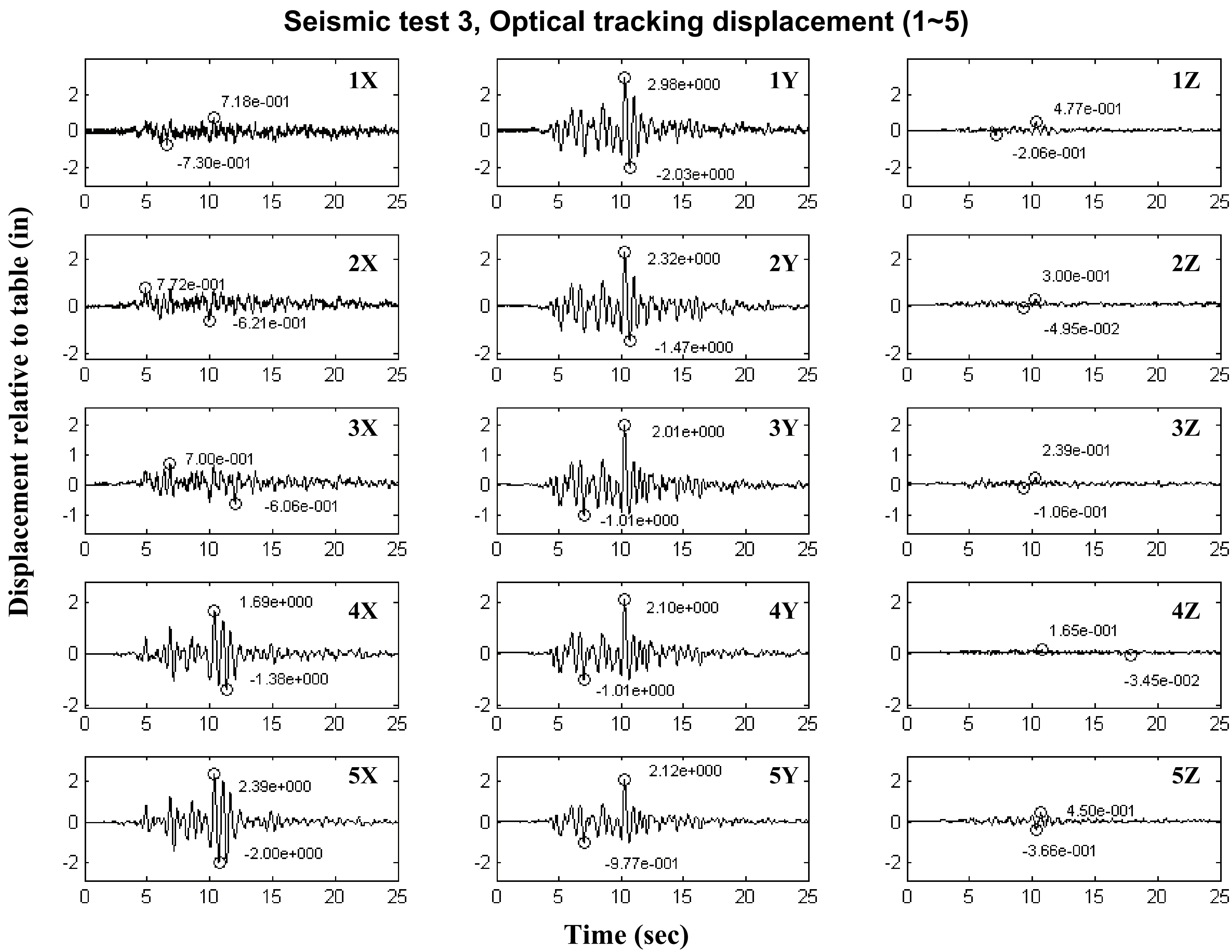

Figure E.22: Displacement of optical tracking markers (1~5) relative to table during Seismic test 3

Appendix E

Seismic test 3, Optical tracking displacement (6~10)

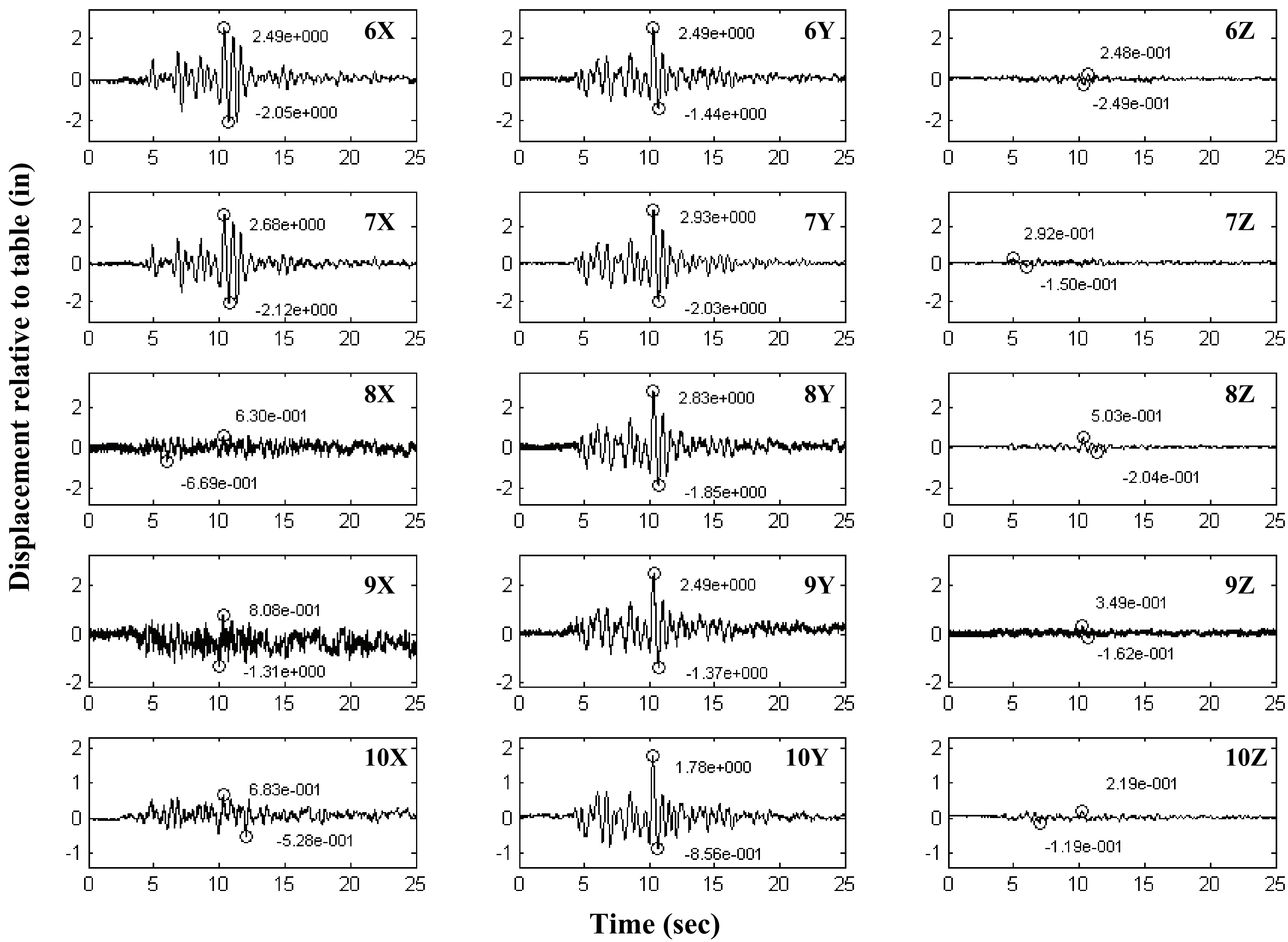

Figure E.23: Displacement of optical tracking markers (6~10) relative to table during Seismic test 3

Appendix E

Seismic test 3, Optical tracking displacement (11~15)

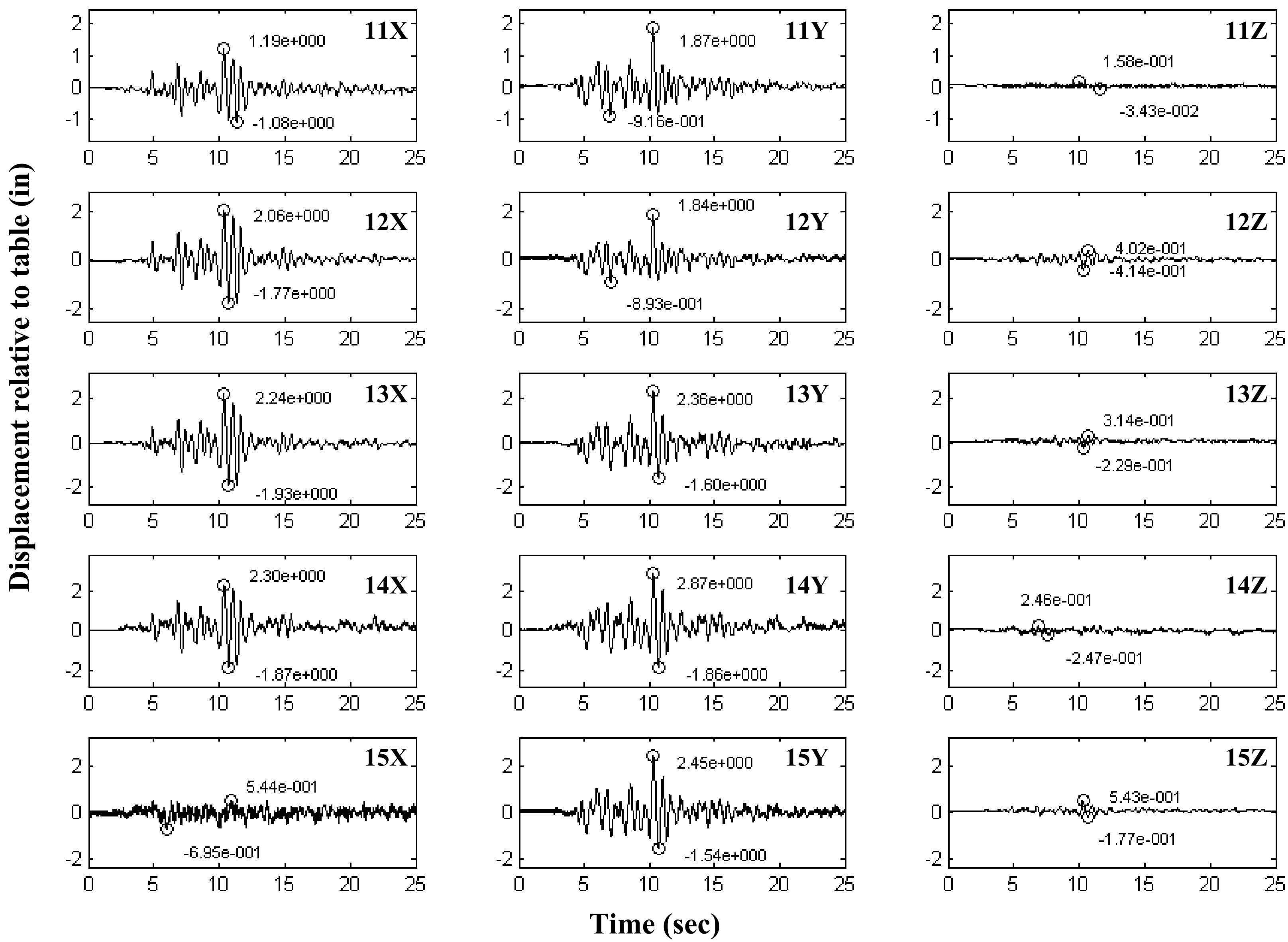

Figure E.24: Displacement of optical tracking markers (11~15) relative to table during Seismic test 3

Appendix E

Seismic test 3, Optical tracking displacement (16~20)

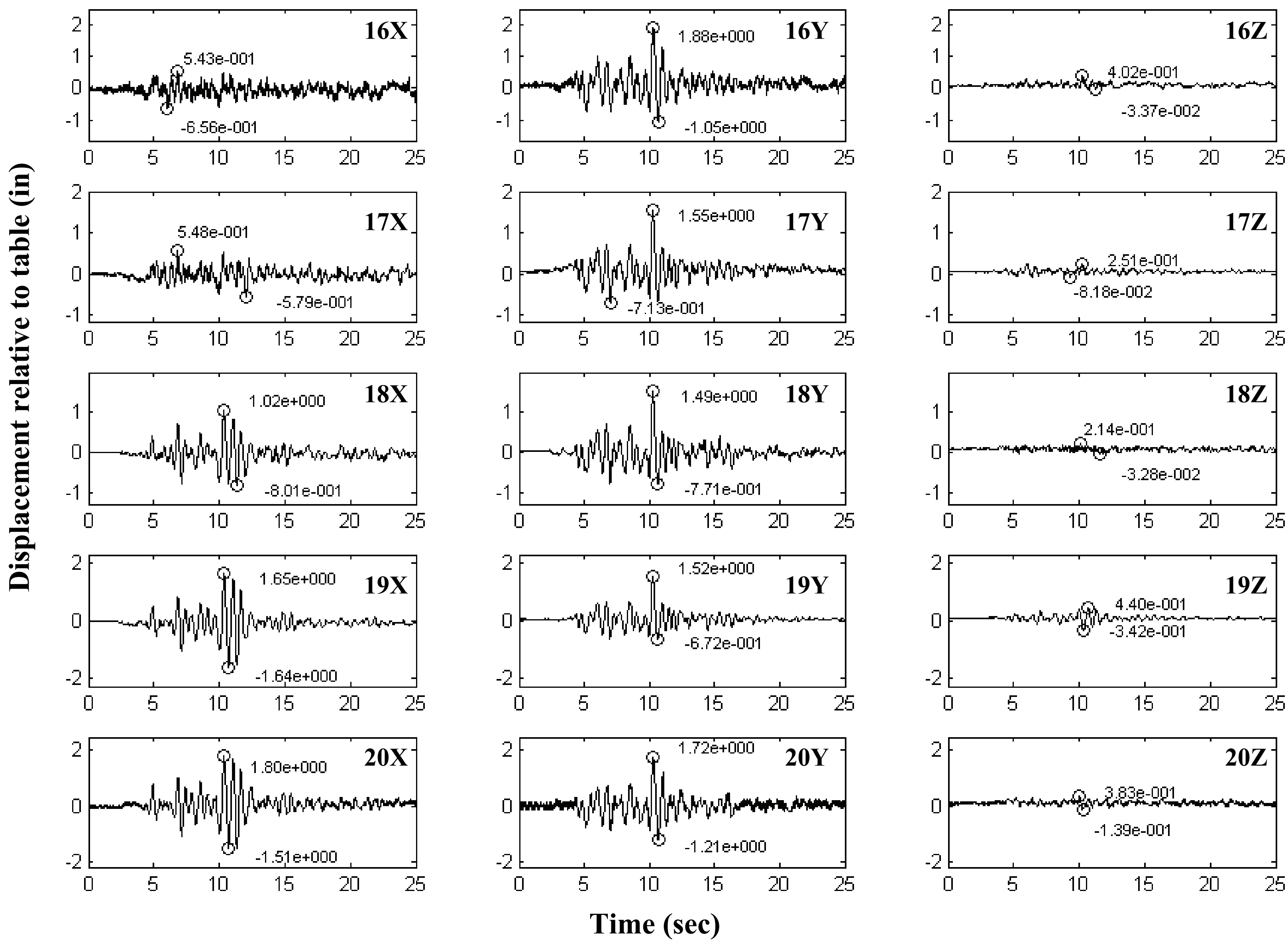

Figure E.25: Displacement of optical tracking markers (16~20) relative to table during Seismic test 3

Appendix E

Seismic test 3, Optical tracking displacement (21~25)

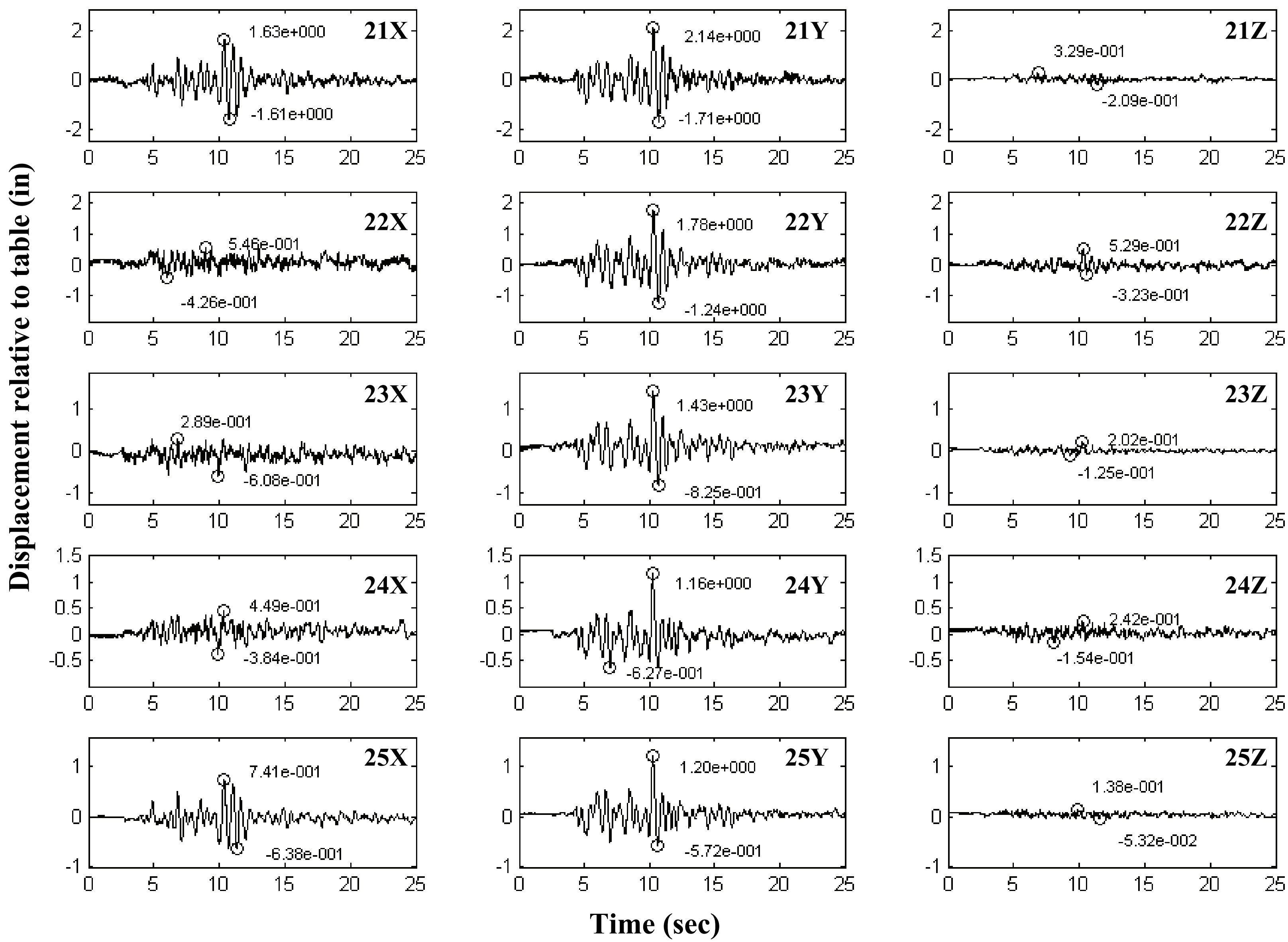

Figure E.26: Displacement of optical tracking markers (21~25) relative to table during Seismic test 3

Appendix E

Seismic test 3, Optical tracking displacement (26~30)

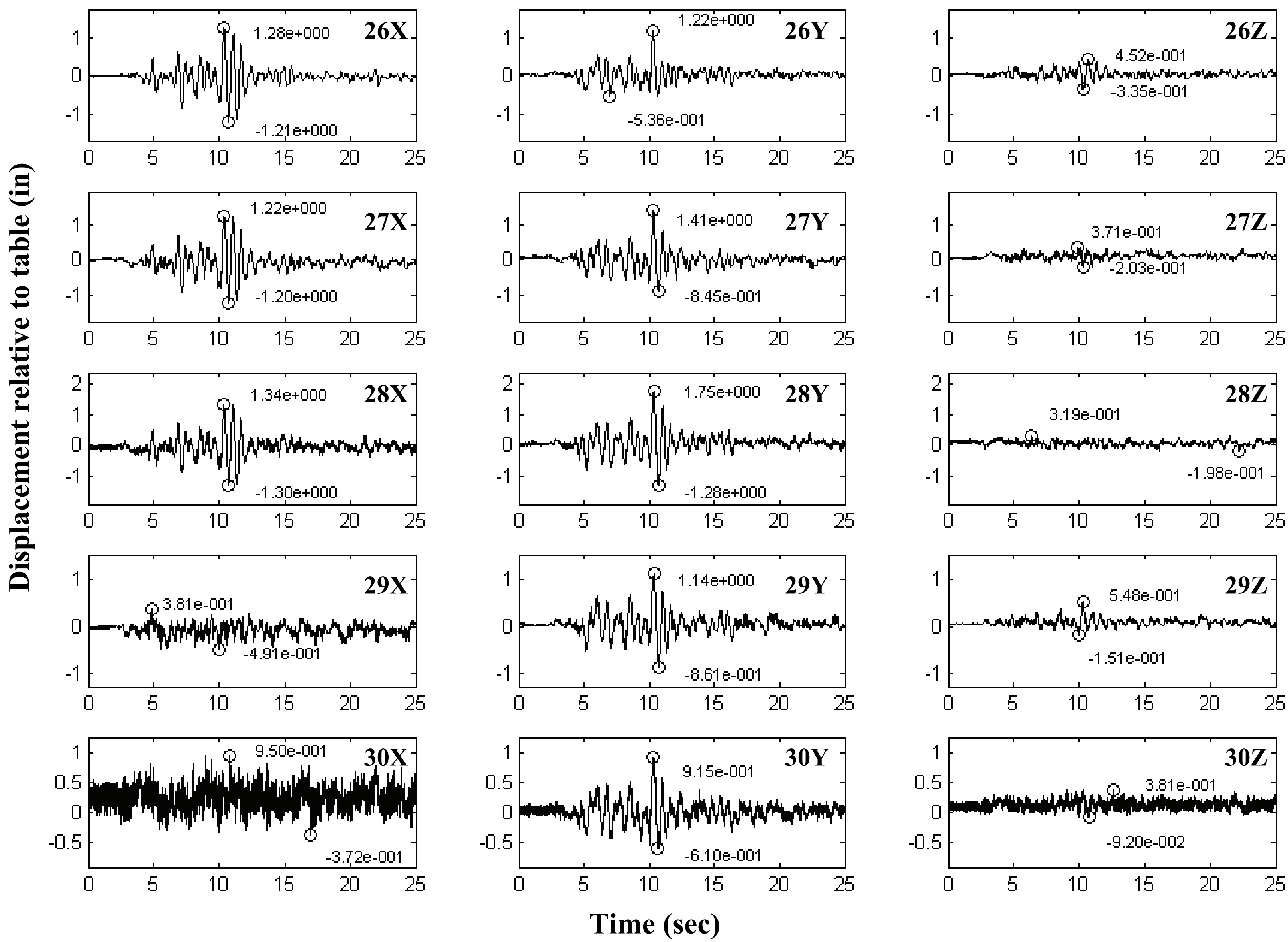

Figure E.27: Displacement of optical tracking markers (26~30) relative to table during Seismic test 3

Seismic test 3, Optical tracking displacement (31~35)

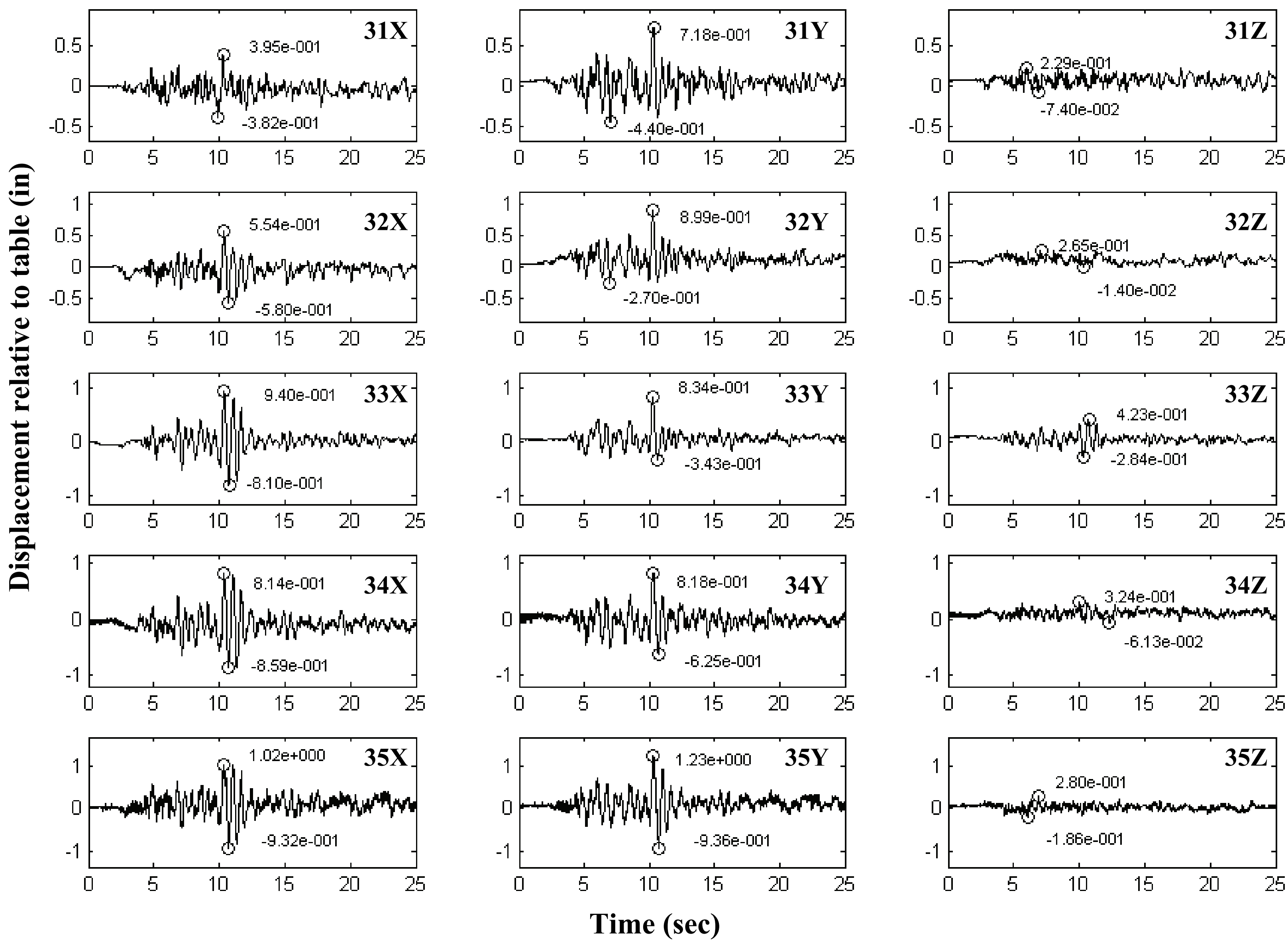

Figure E.28: Displacement of optical tracking markers (31~35) relative to table during Seismic test 3

Seismic test 3, Optical tracking displacement (36~40)

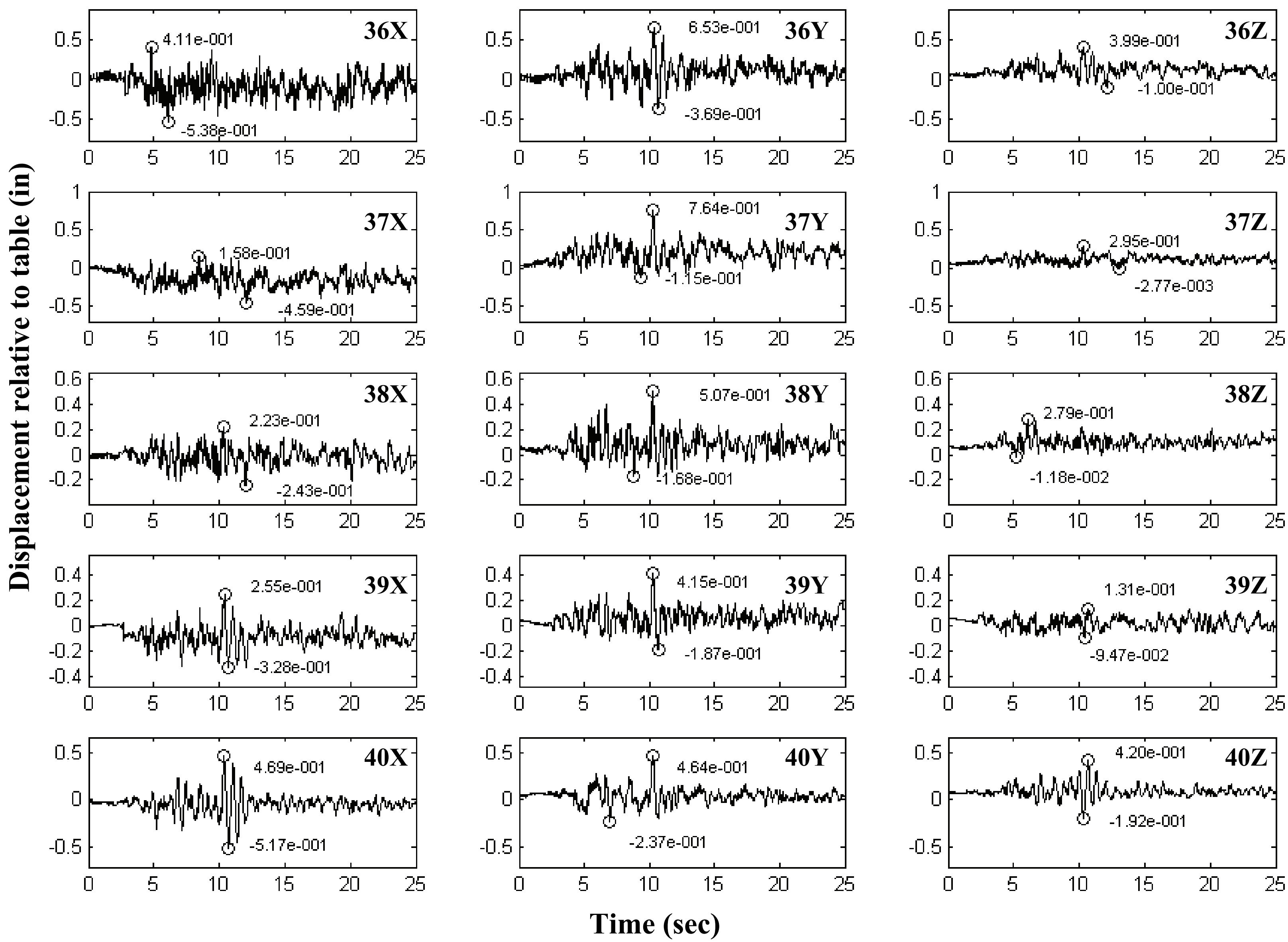

Figure E.29: Displacement of optical tracking markers (36~40) relative to table during Seismic test 3

Seismic test 3, Optical tracking displacement (41~45)

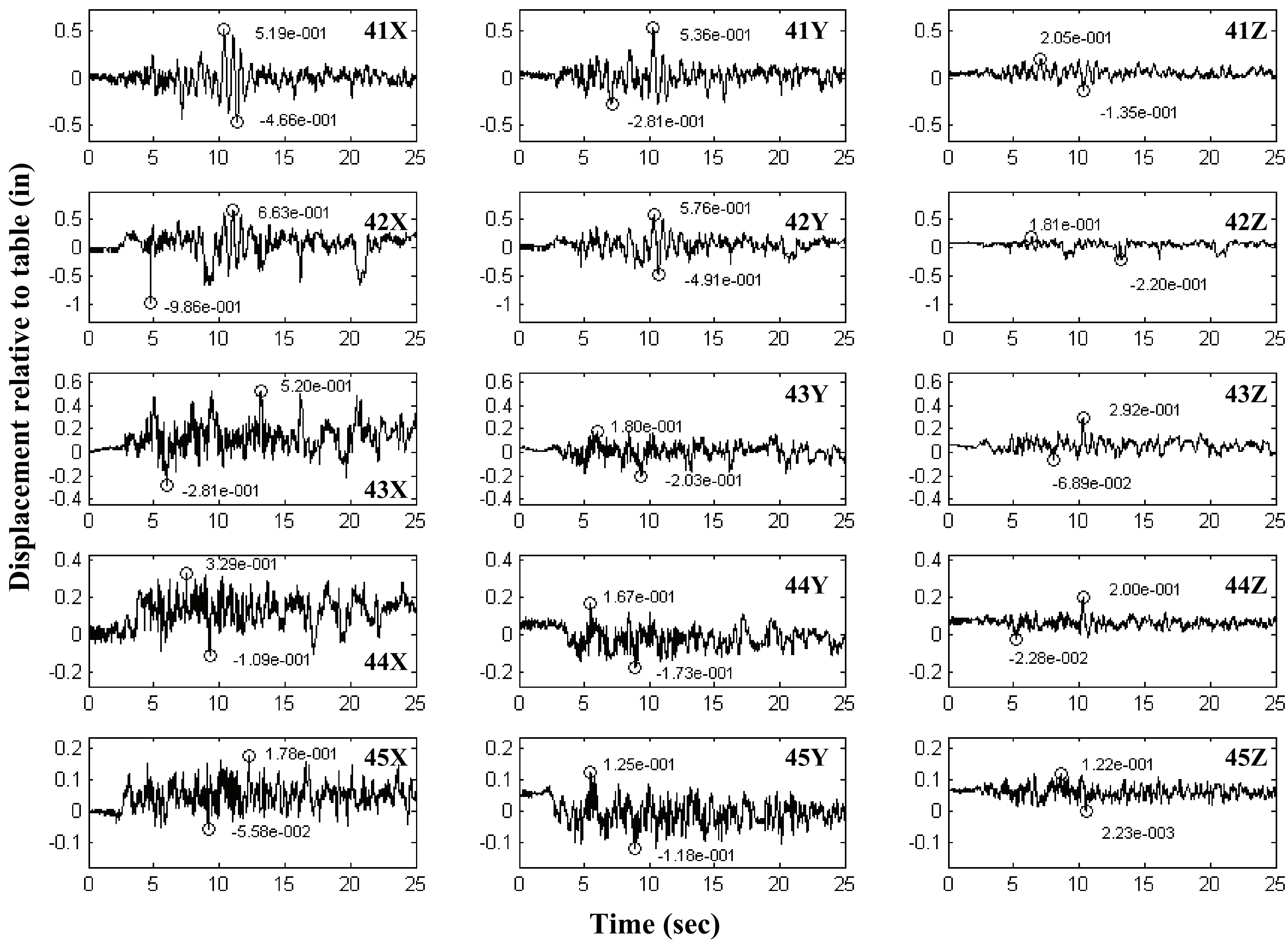

Figure E.30: Displacement of optical tracking markers (41~45) relative to table during Seismic test 3

Seismic test 3, Optical tracking displacement (46~50)

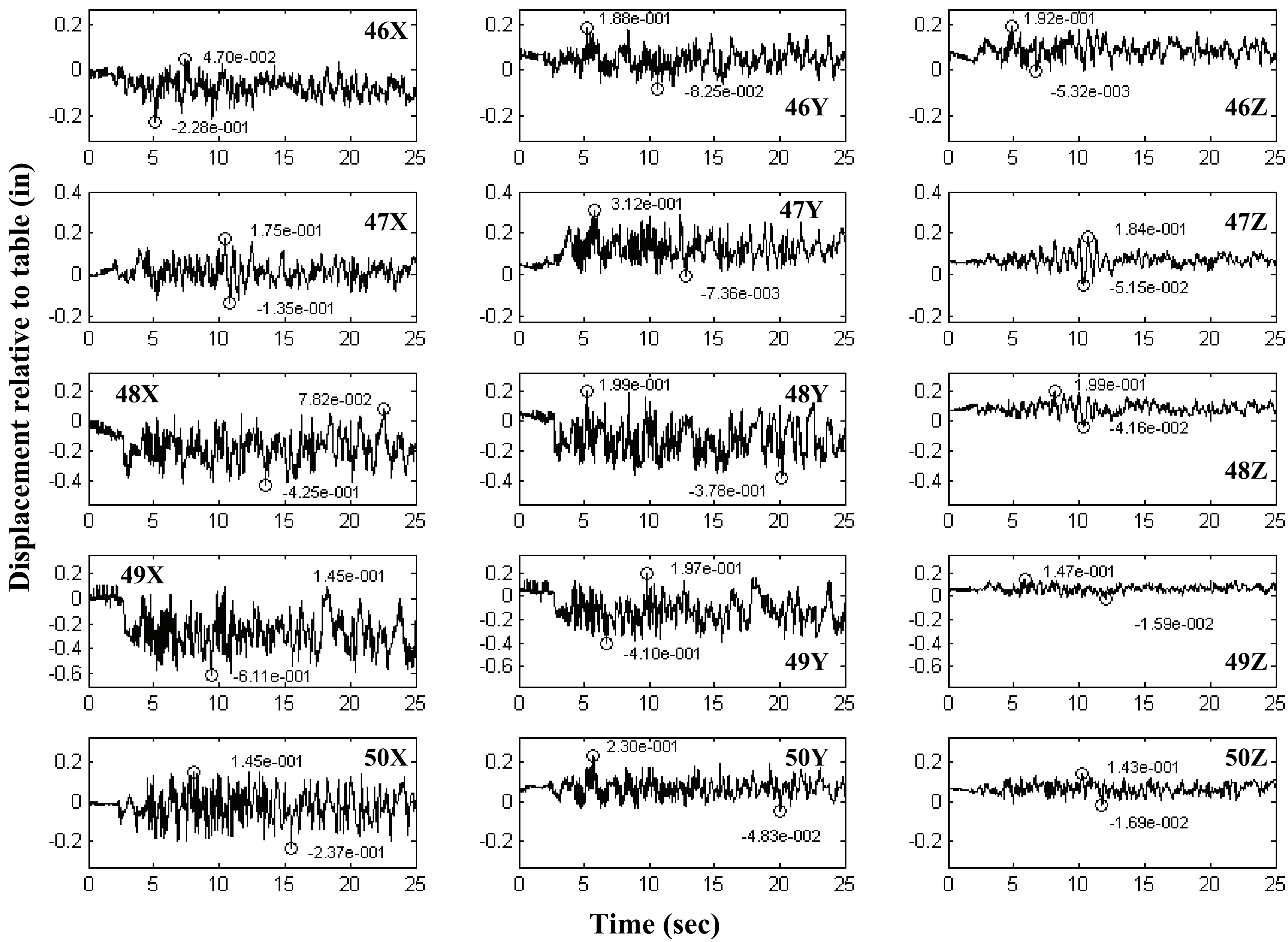

Figure E.31: Displacement of optical tracking markers (46~50) relative to table during Seismic test 3

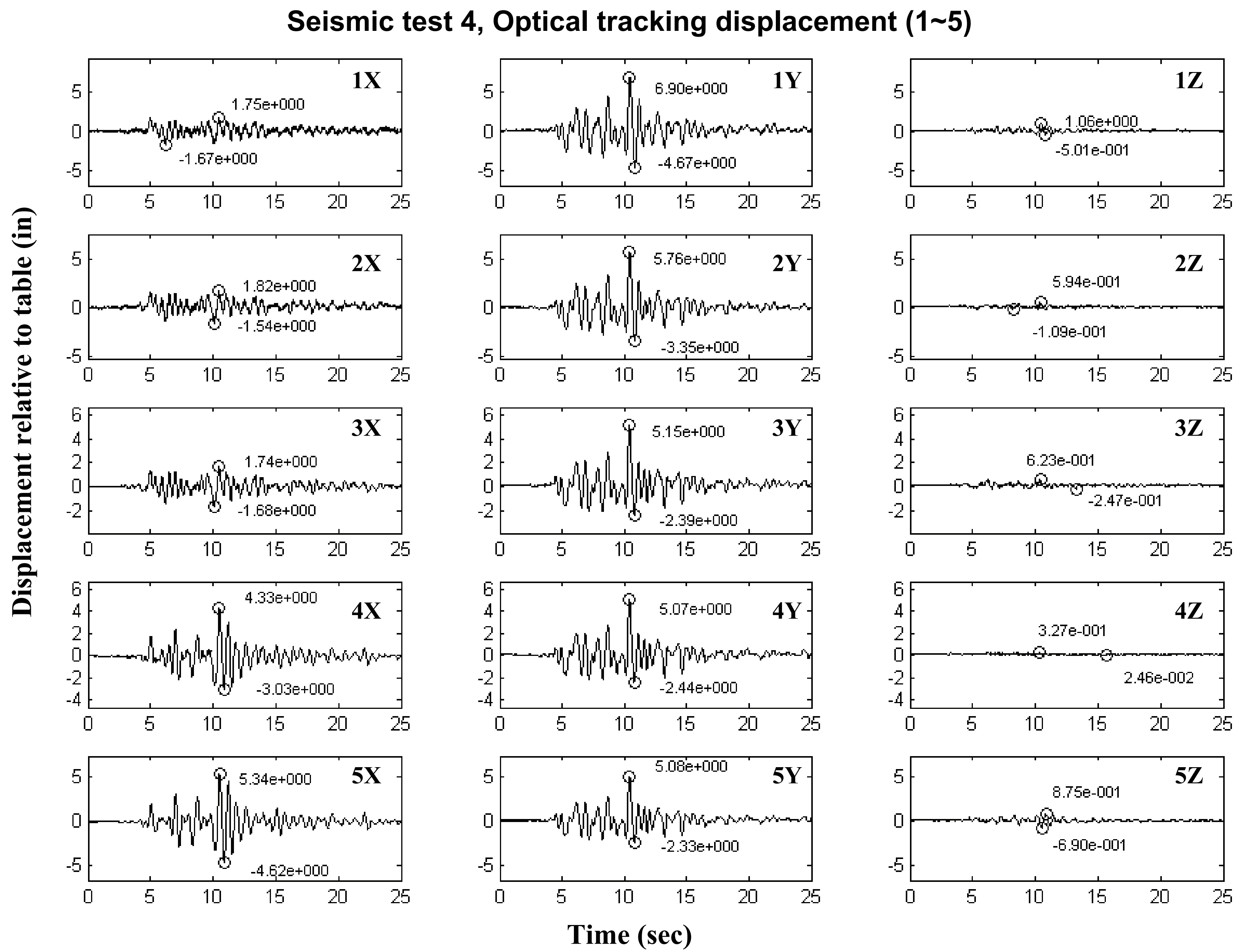

Figure E.32: Displacement of optical tracking markers (1~5) relative to table during Seismic test 4

Appendix E

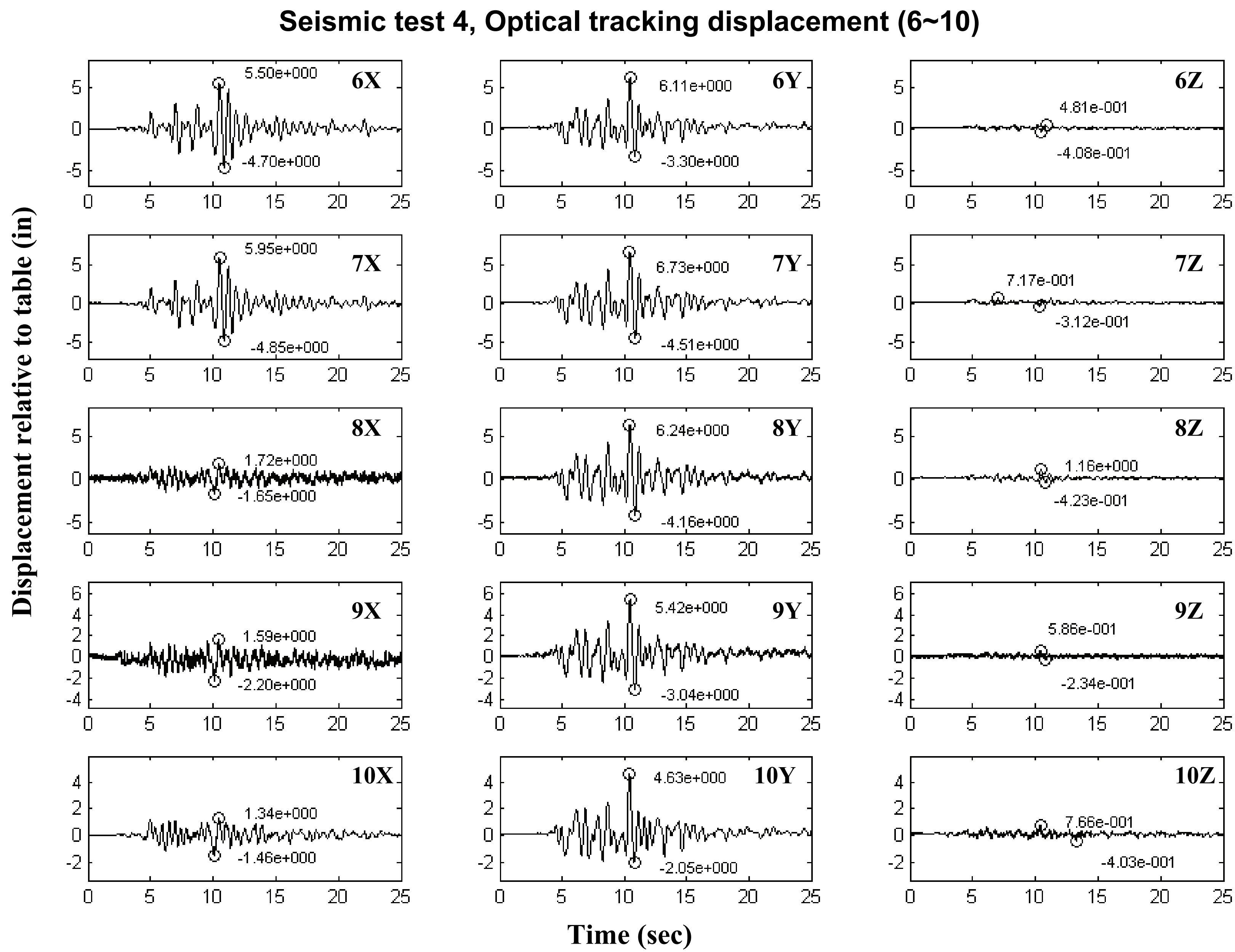

Figure E.33: Displacement of optical tracking markers (6~10) relative to table during Seismic test 4

Appendix E

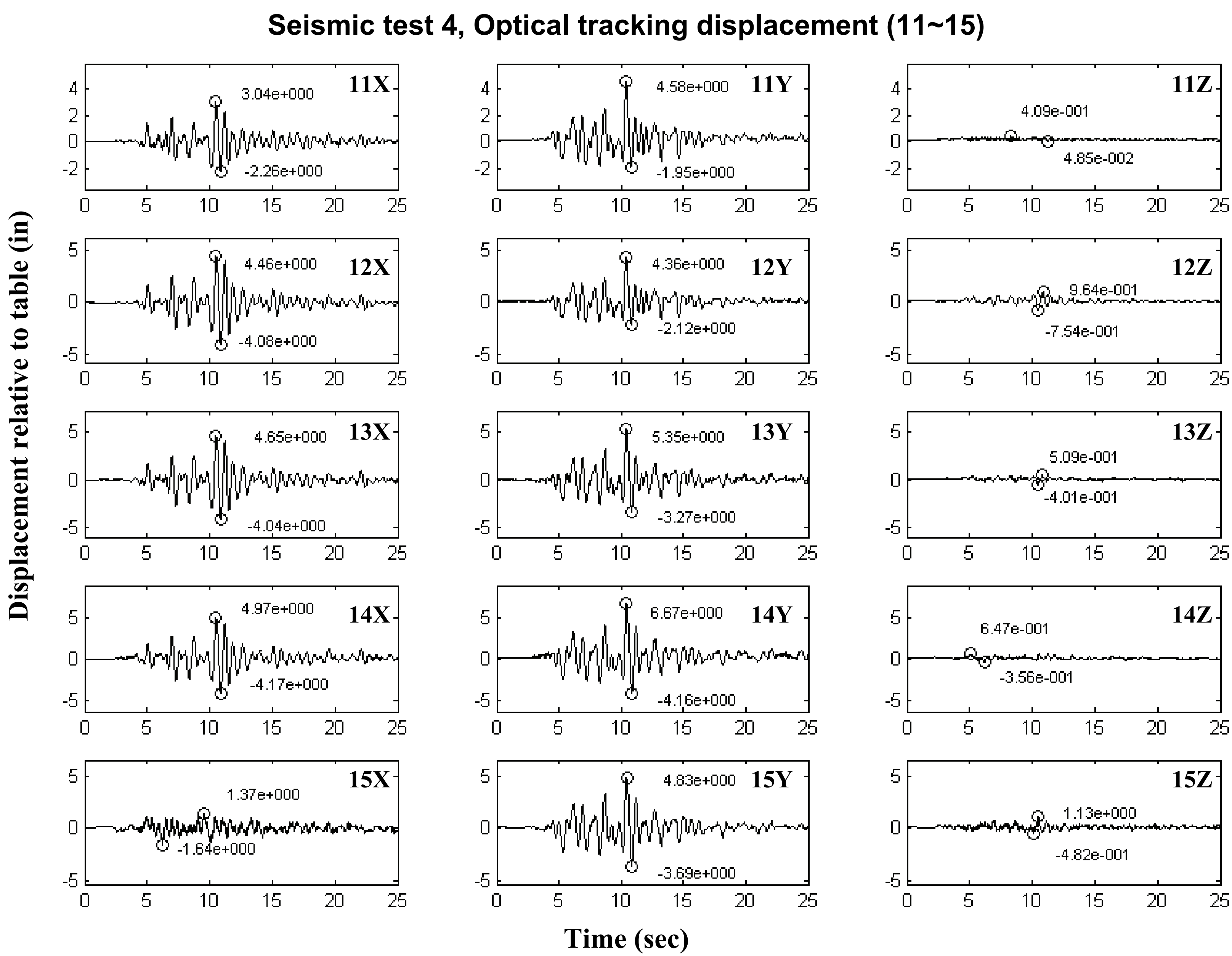

Figure E.34: Displacement of optical tracking markers (11~15) relative to table during Seismic test 4

Seismic test 4, Optical tracking displacement (16~20)

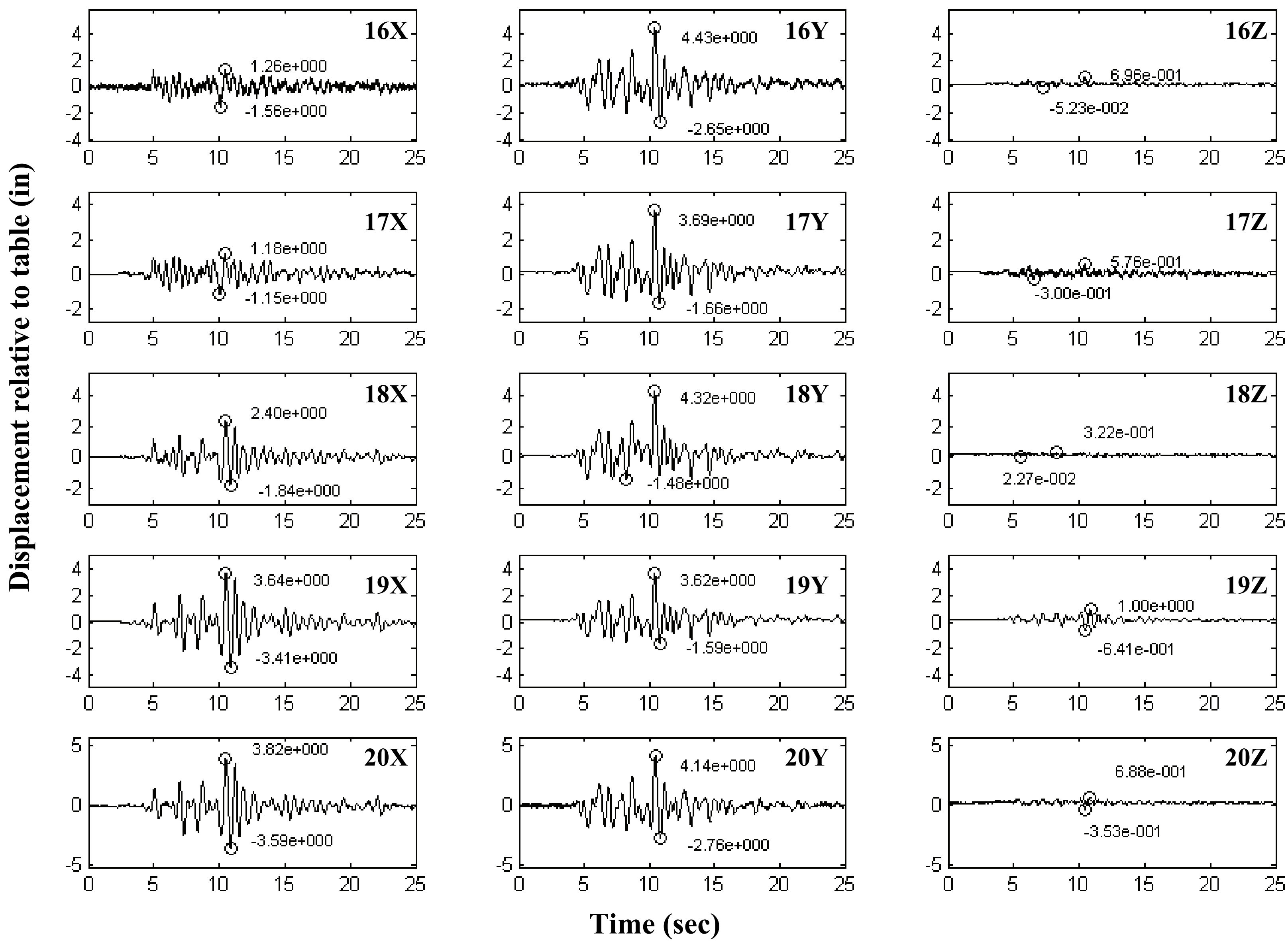

Figure E.35: Displacement of optical tracking markers (16~20) relative to table during Seismic test 4

Seismic test 4, Optical tracking displacement (21~25)

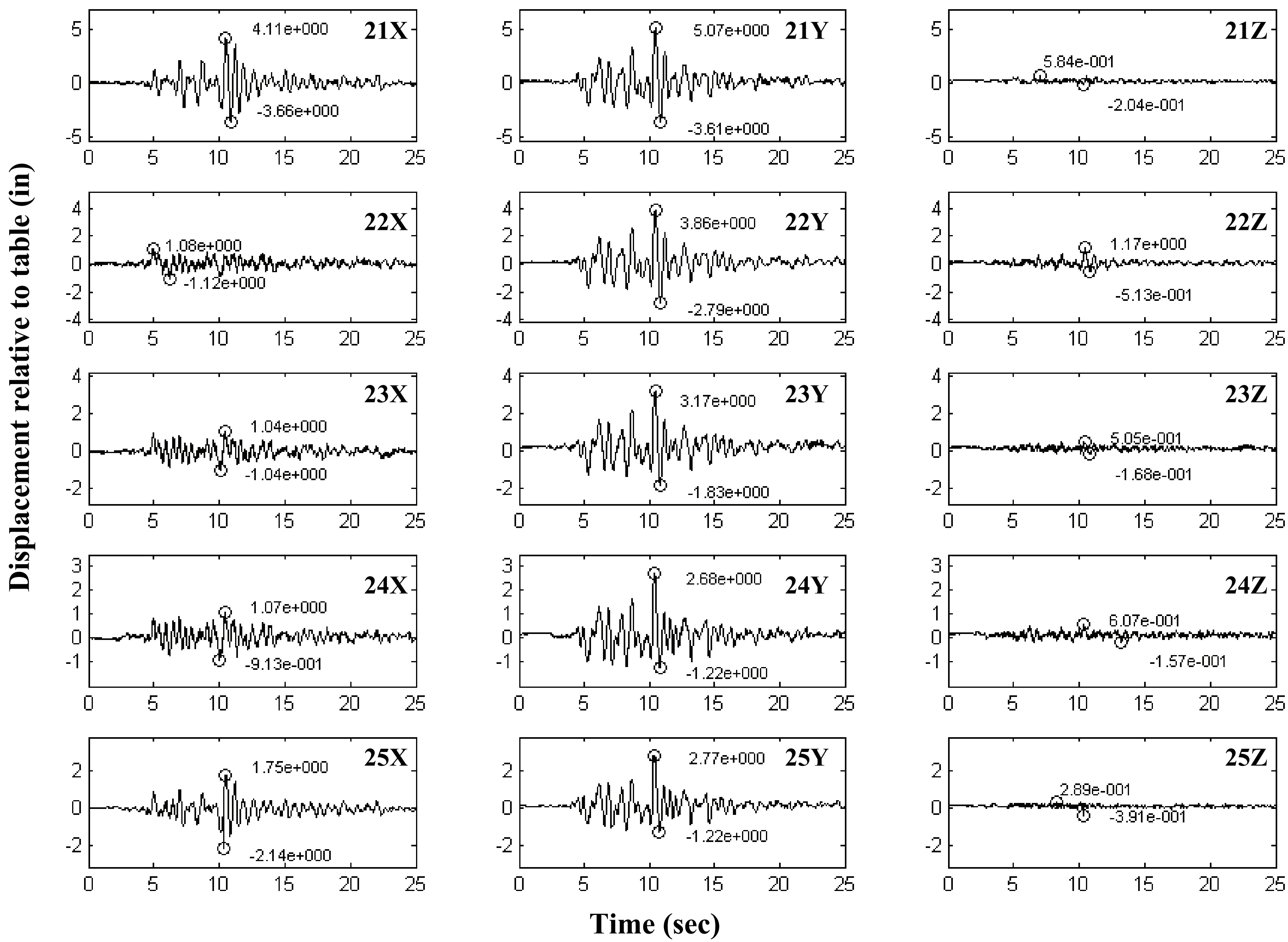

Figure E.36: Displacement of optical tracking markers (21~25) relative to table during Seismic test 4

Seismic test 4, Optical tracking displacement (26~30)

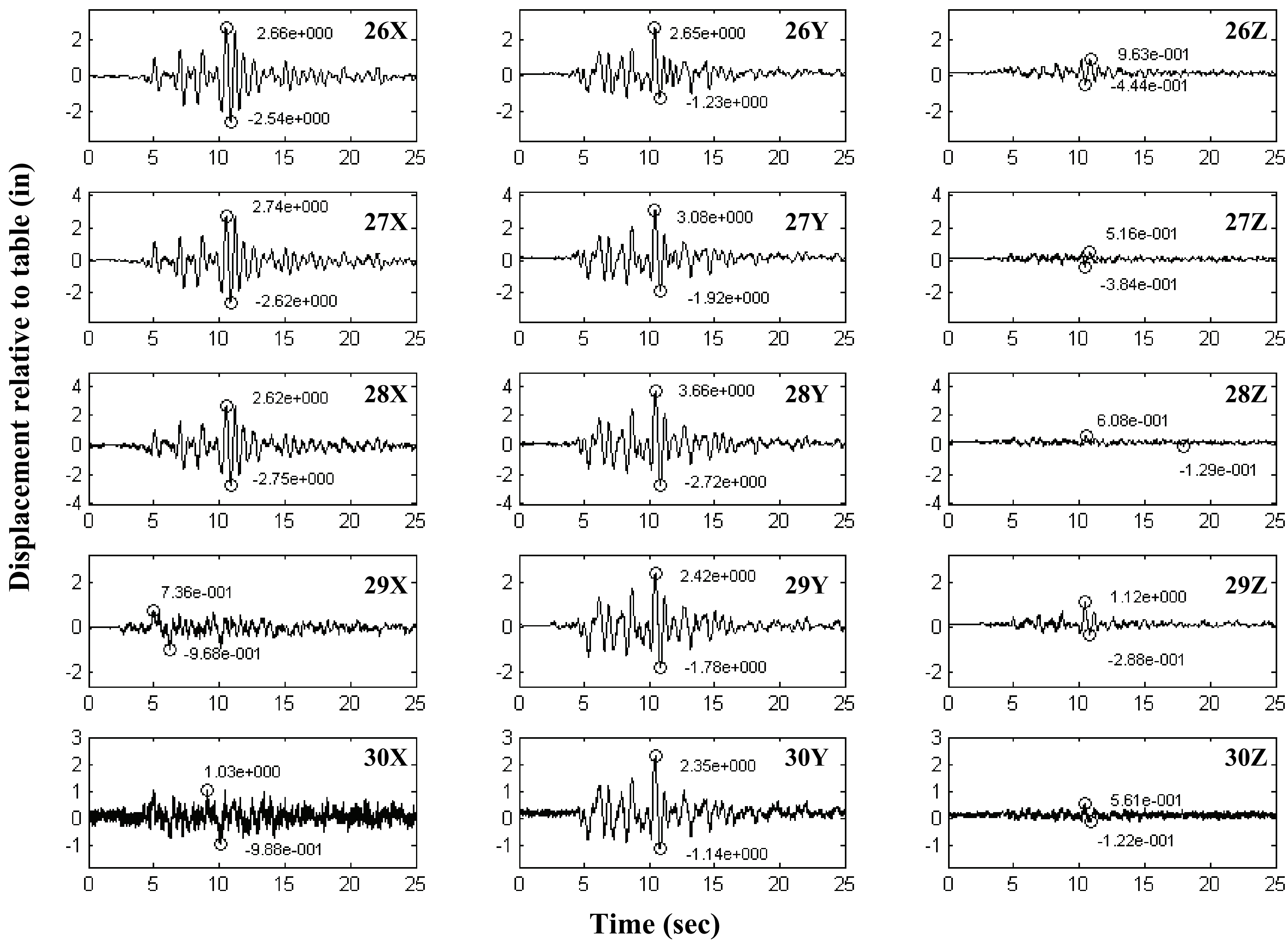

Figure E.37: Displacement of optical tracking markers (26~30) relative to table during Seismic test 4

Appendix E

Seismic test 4, Optical tracking displacement (31~35)

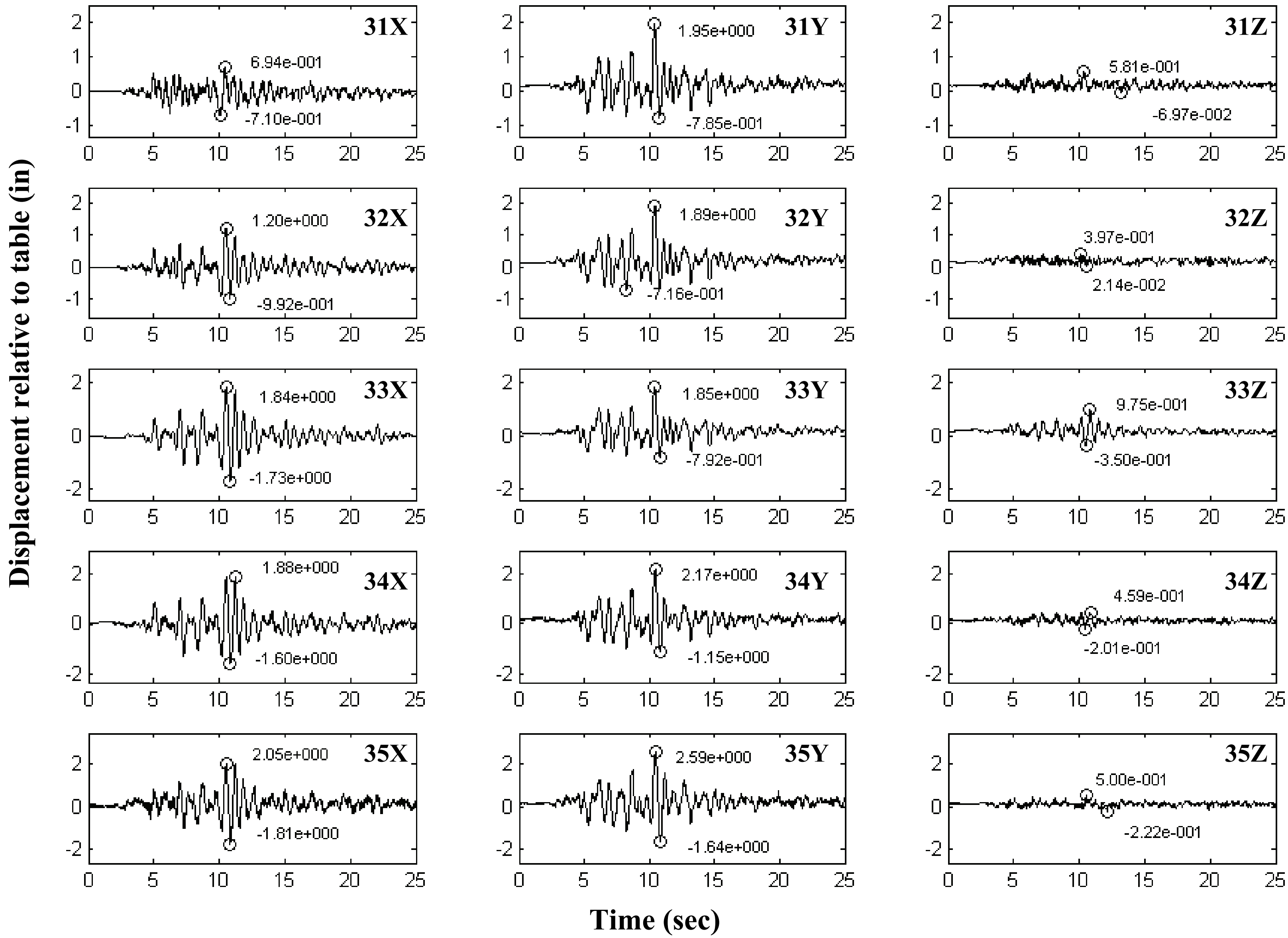

Figure E.38: Displacement of optical tracking markers (31~35) relative to table during Seismic test 4

Seismic test 4, Optical tracking displacement (36~40)

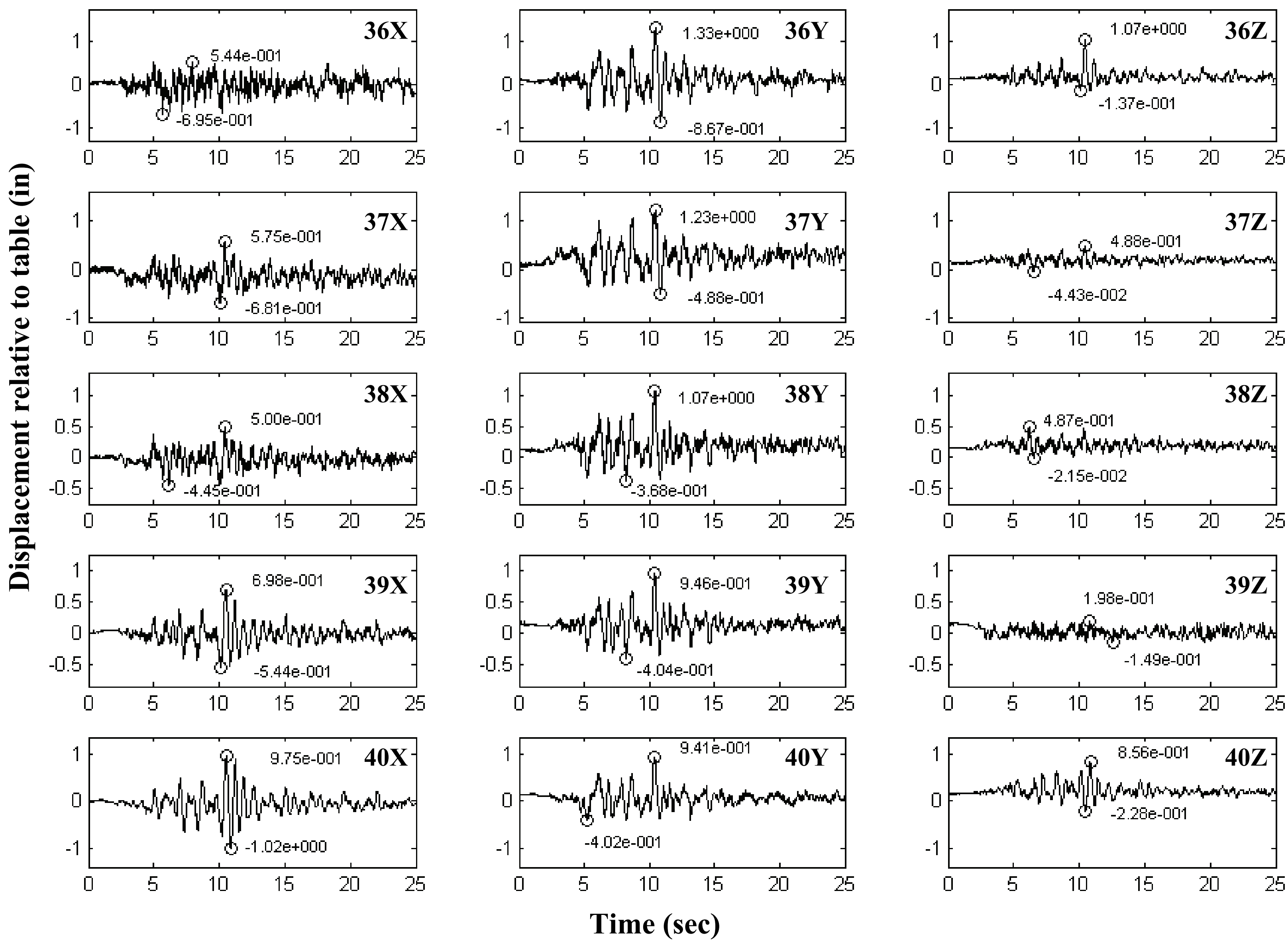

Figure E.39: Displacement of optical tracking markers (36~40) relative to table during Seismic test 4

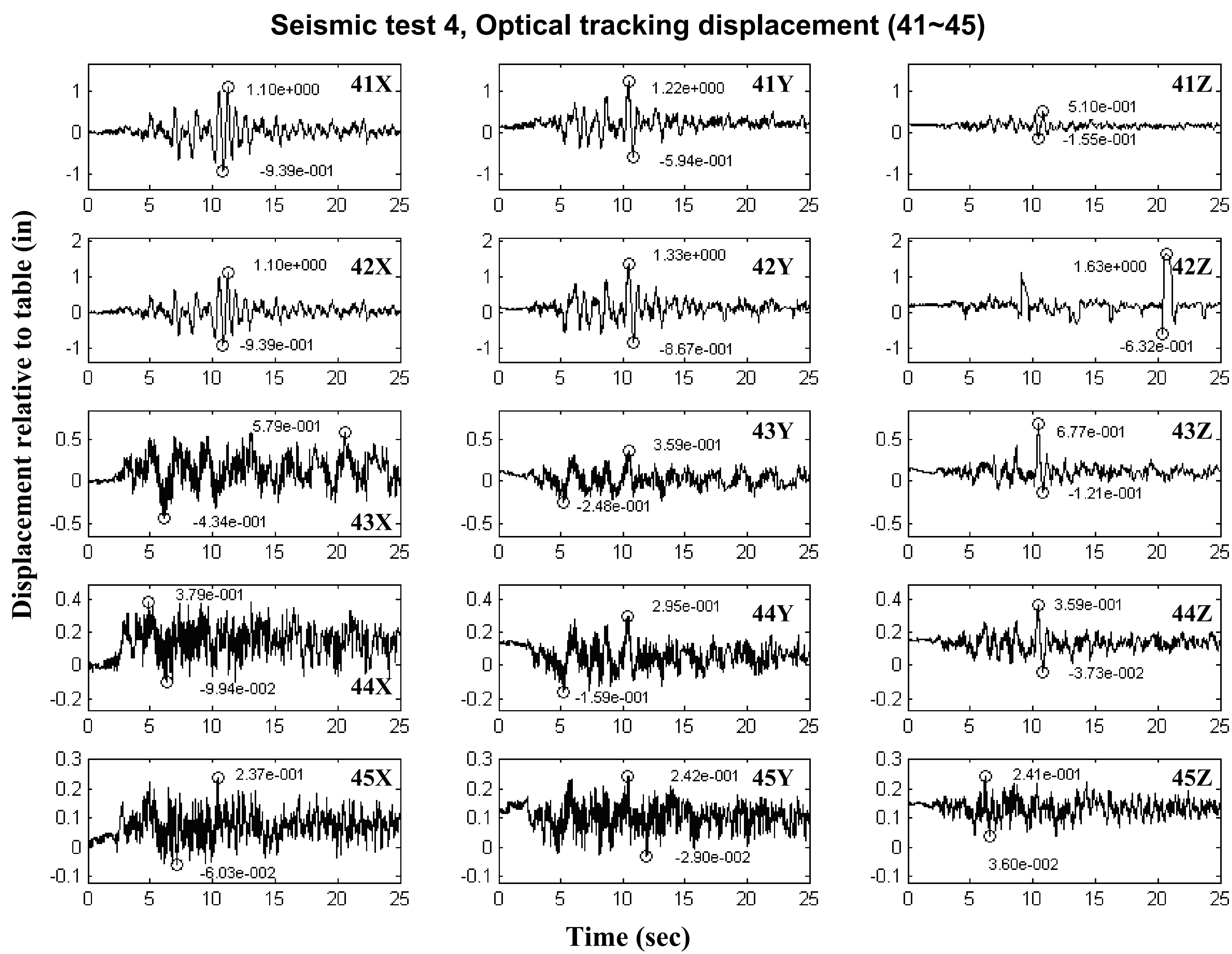

Figure E.40: Displacement of optical tracking markers (41~45) relative to table during Seismic test 4

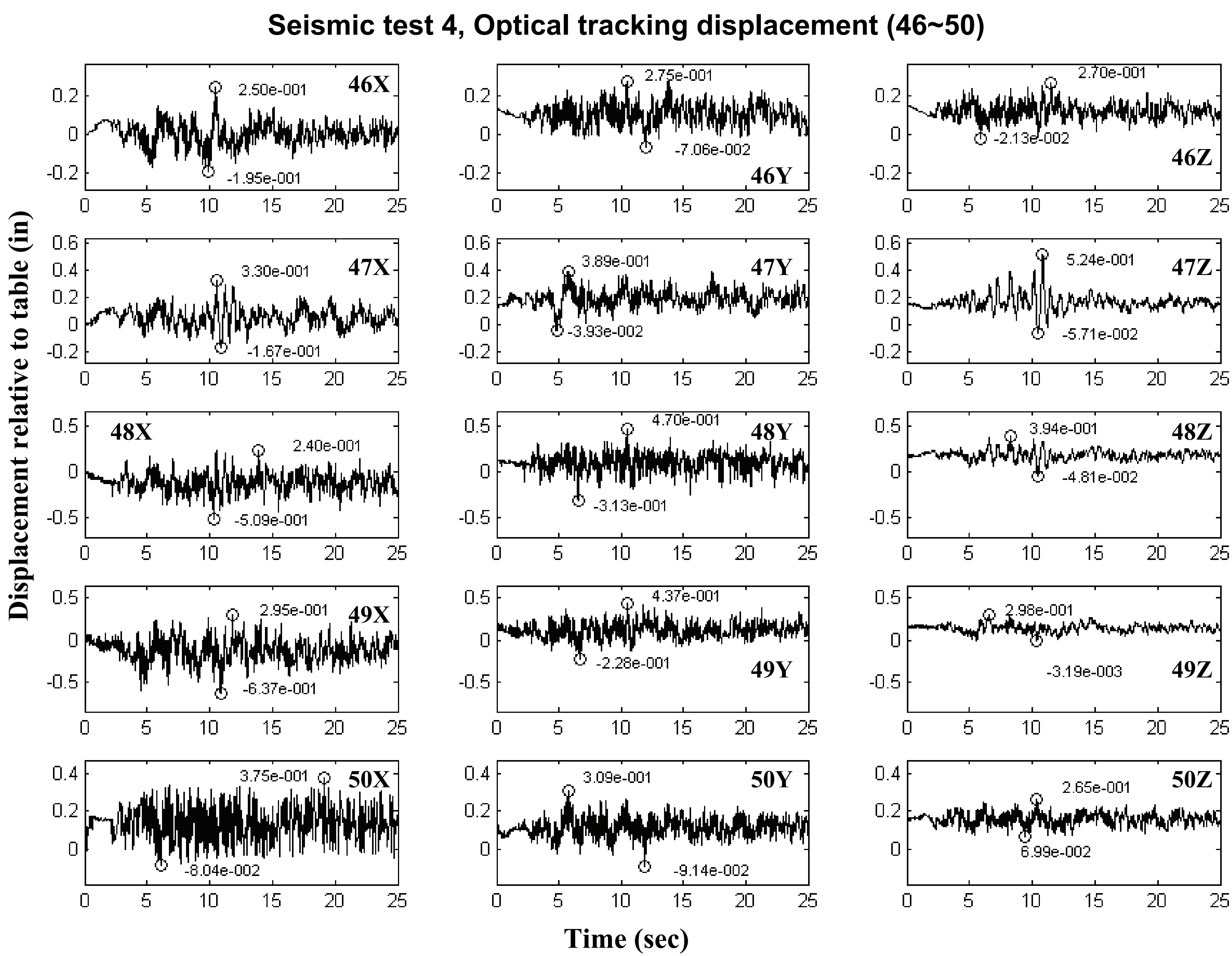

Figure E.41: Displacement of optical tracking markers (46~50) relative to table during Seismic test 4

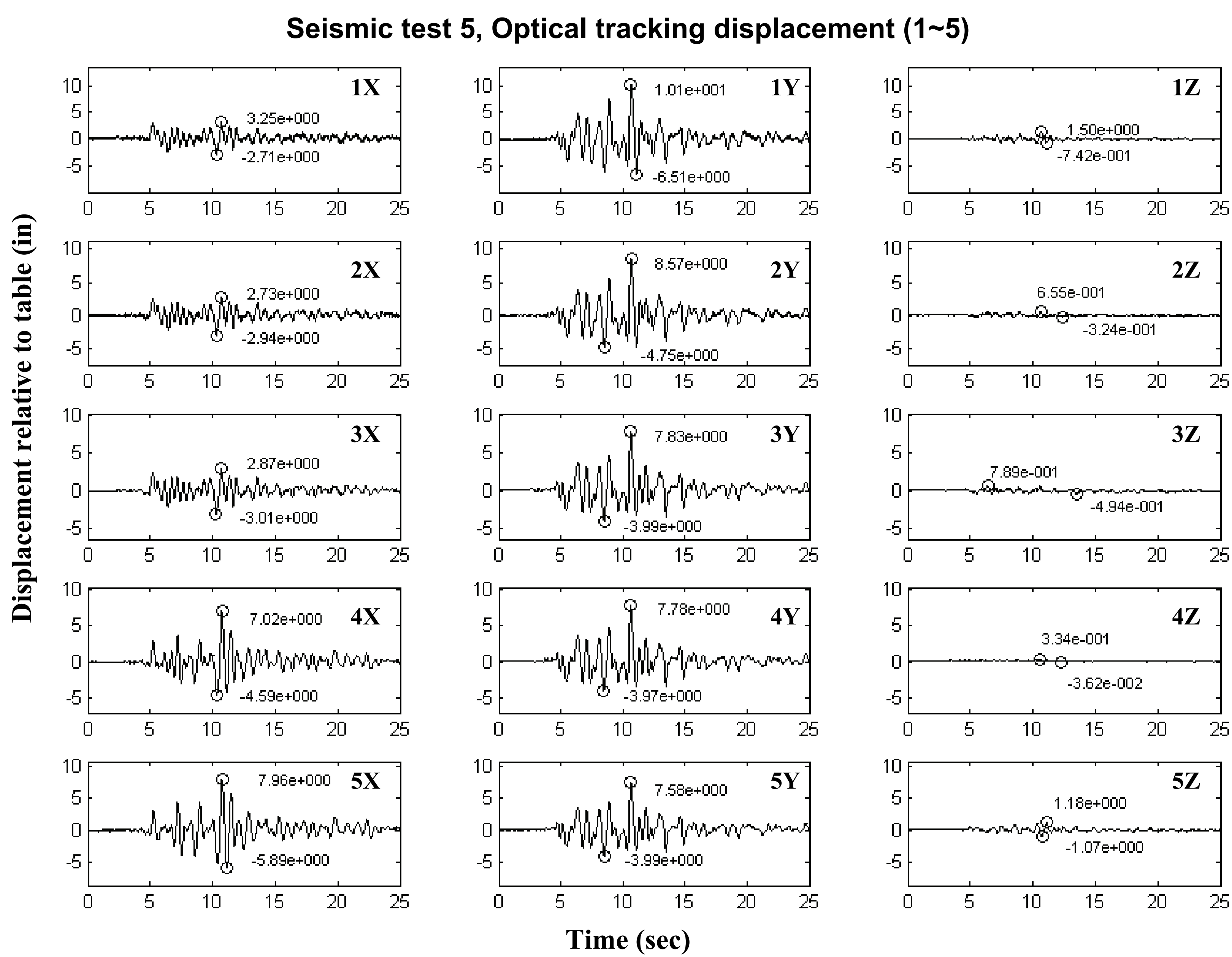

Figure E.42: Displacement of optical tracking markers (1~5) relative to table during Seismic test 5

Seismic test 5, Optical tracking displacement (6~10)

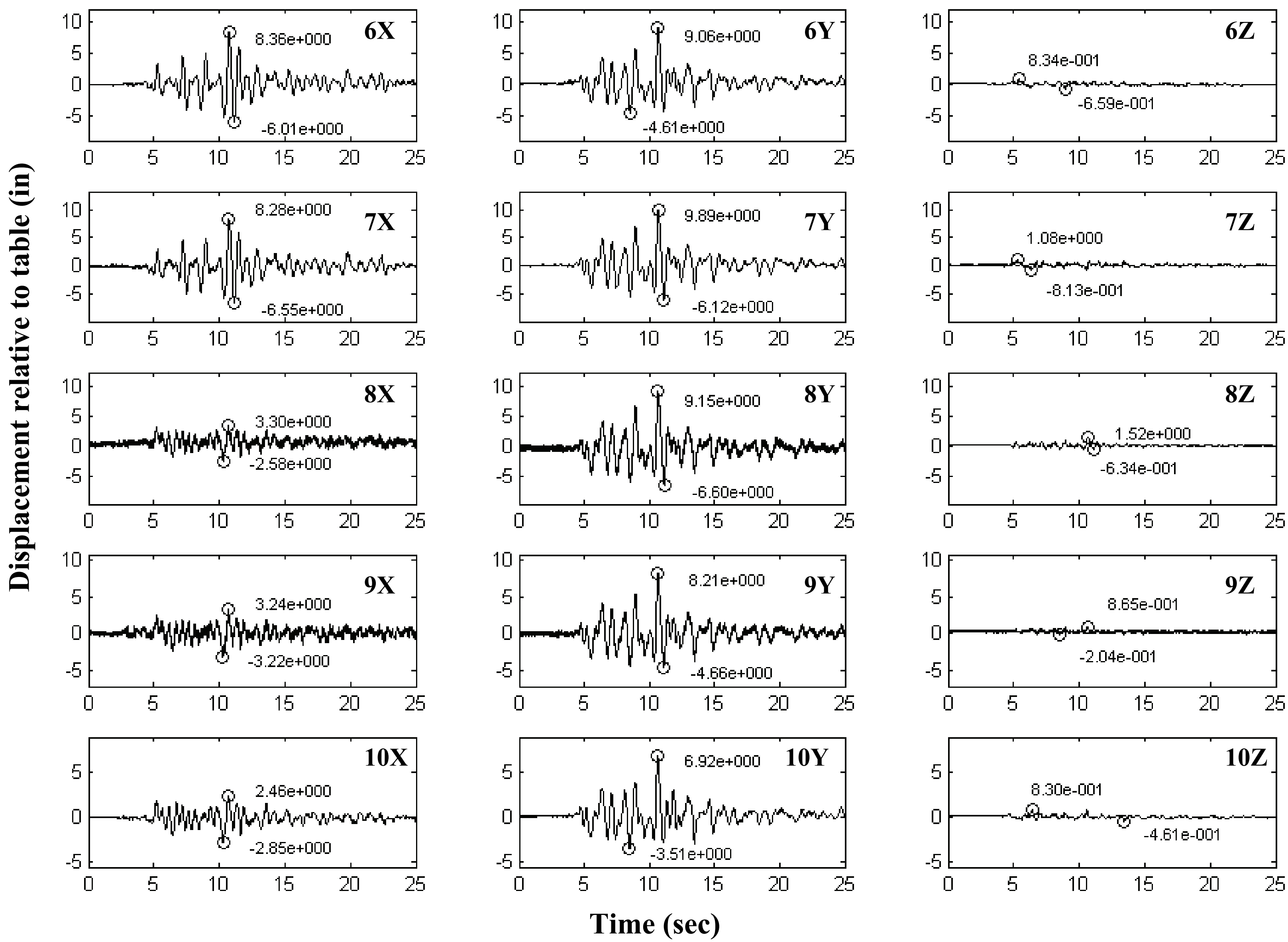

Figure E.43: Displacement of optical tracking markers (6~10) relative to table during Seismic test 5

Seismic test 5, Optical tracking displacement (11~15)

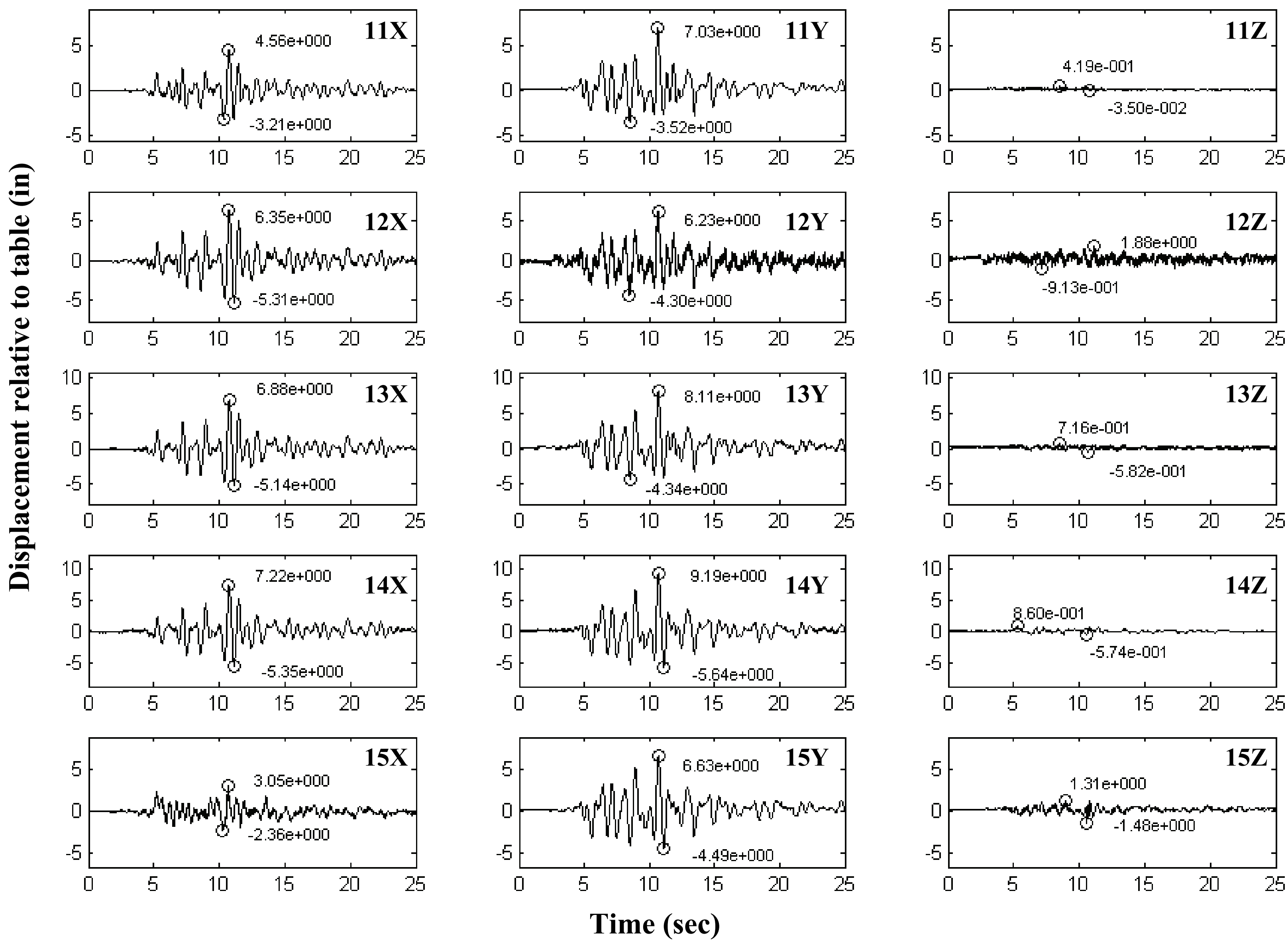

Figure E.44: Displacement of optical tracking markers (11~15) relative to table during Seismic test 5

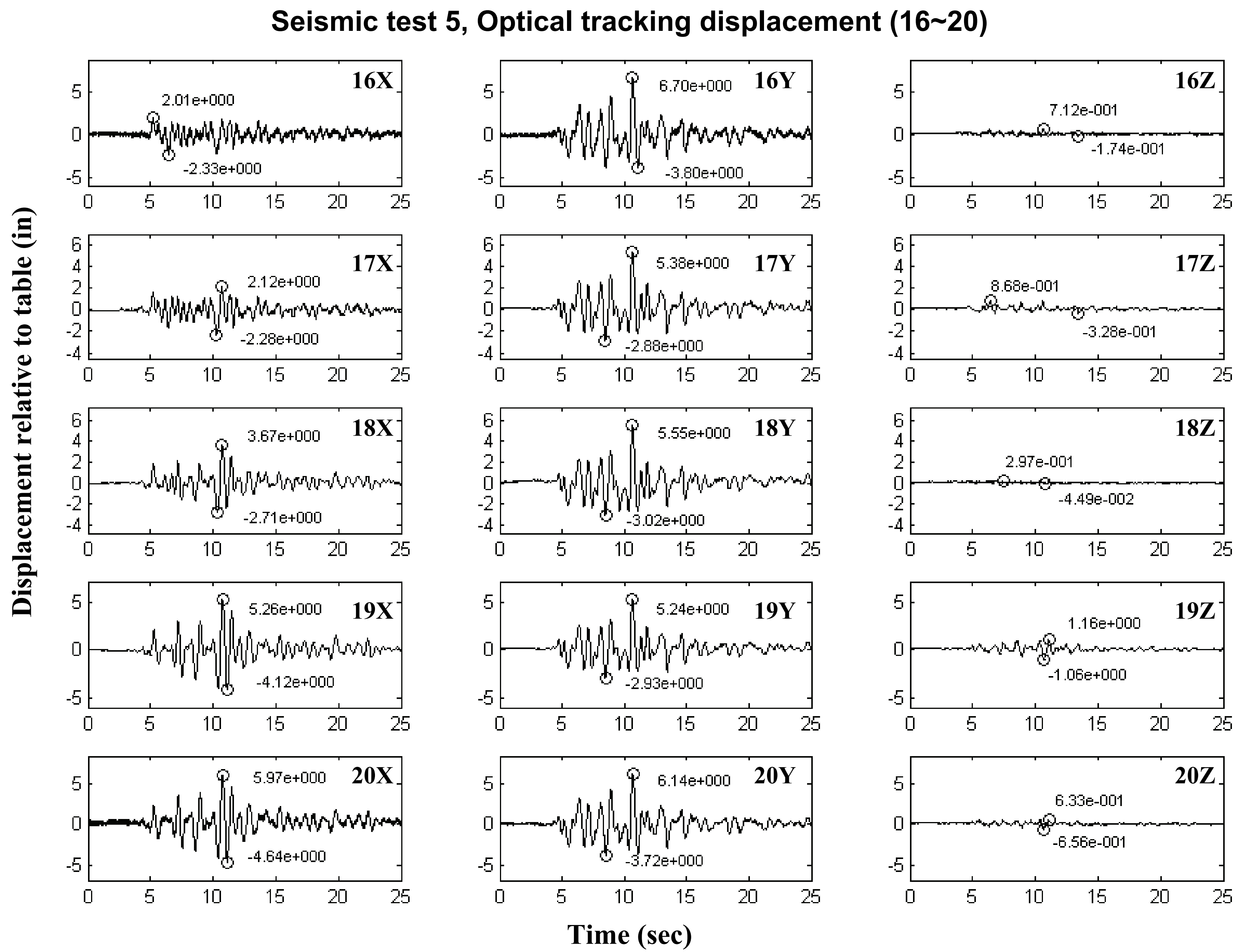

Figure E.45: Displacement of optical tracking markers (16~20) relative to table during Seismic test 5

Seismic test 5, Optical tracking displacement (21~25)

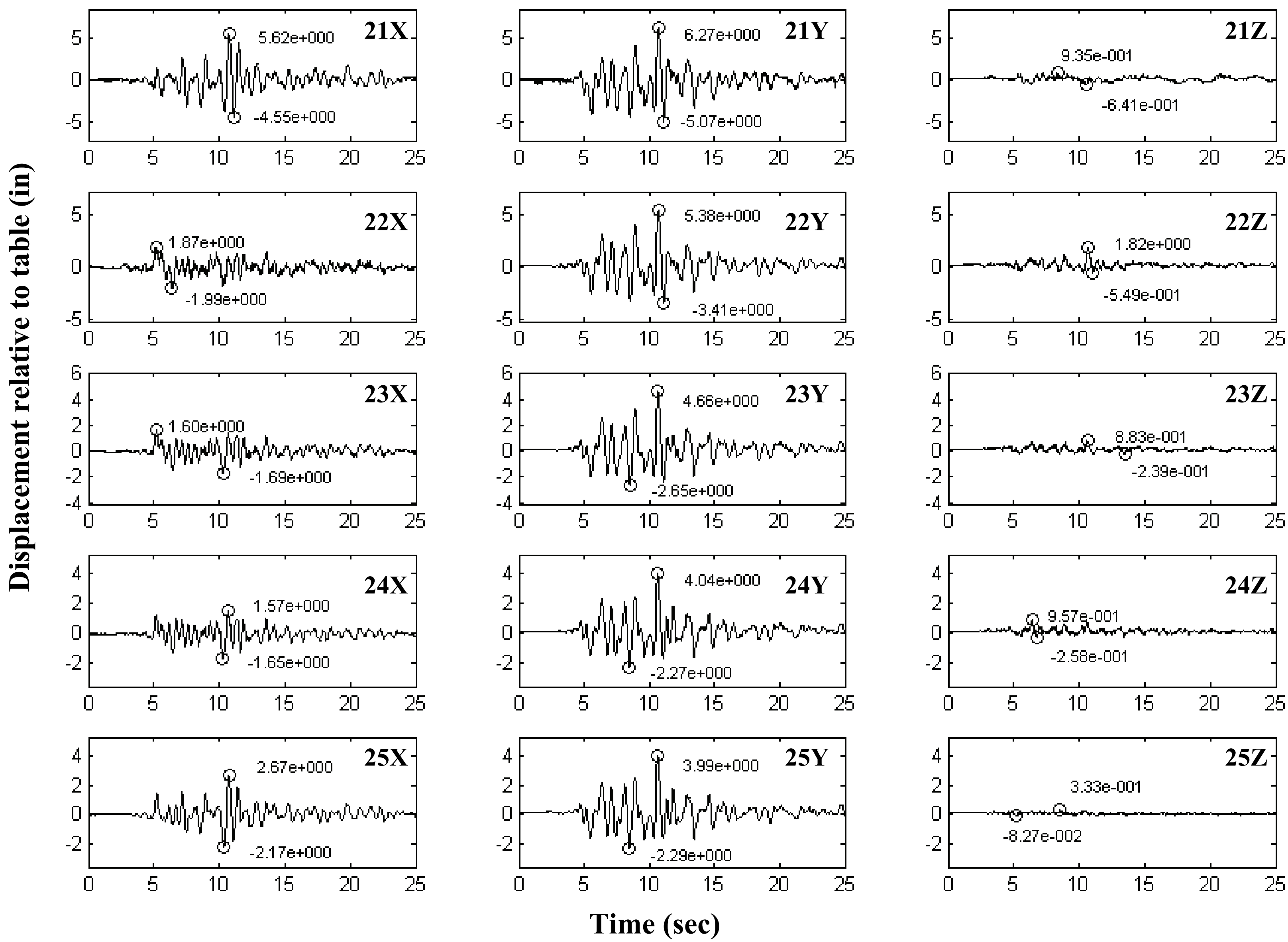

Figure E.46: Displacement of optical tracking markers (21~25) relative to table during Seismic test 5

Seismic test 5, Optical tracking displacement (26~30)

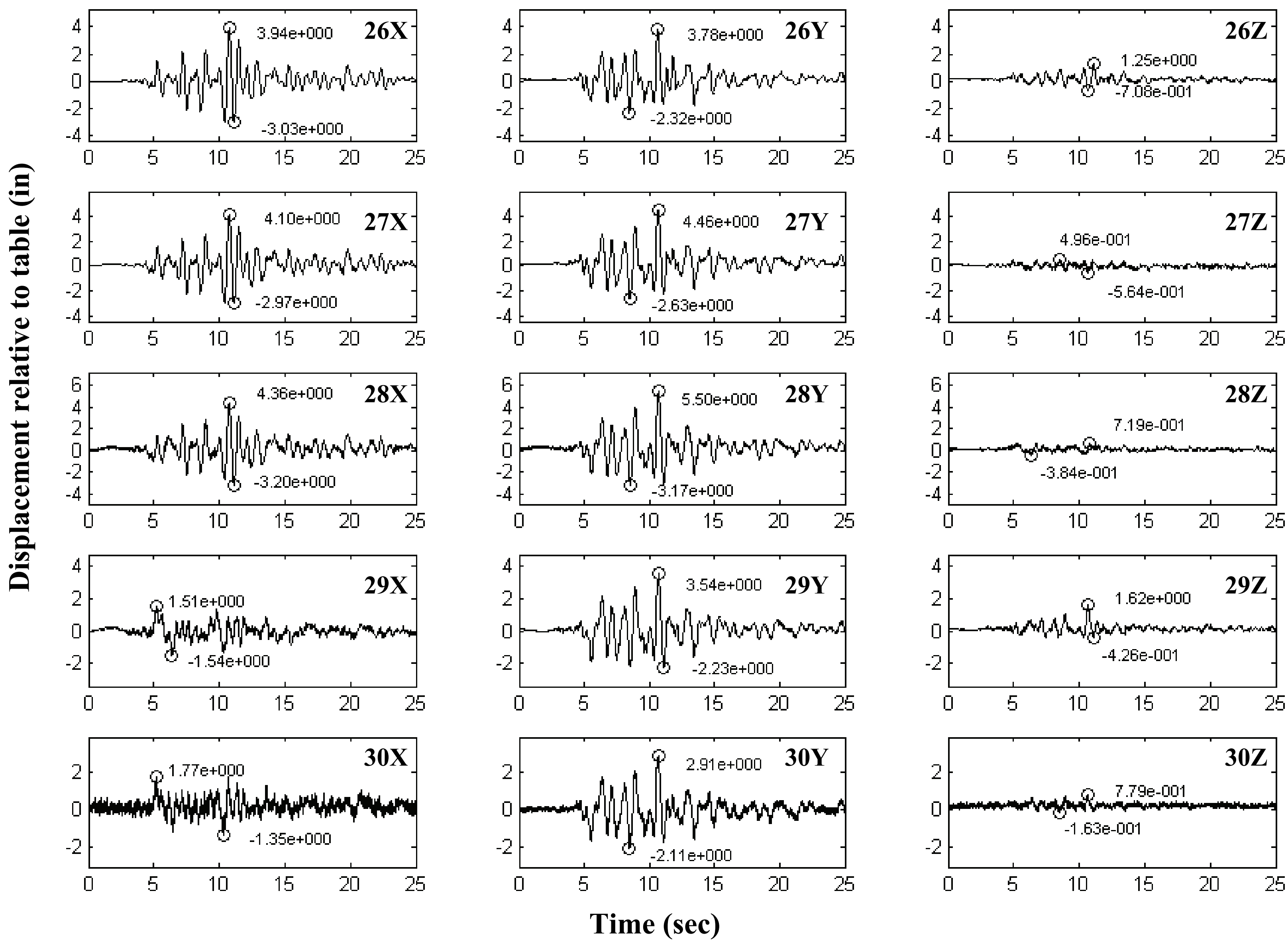

Figure E.47: Displacement of optical tracking markers (26~30) relative to table during Seismic test 5

Appendix E

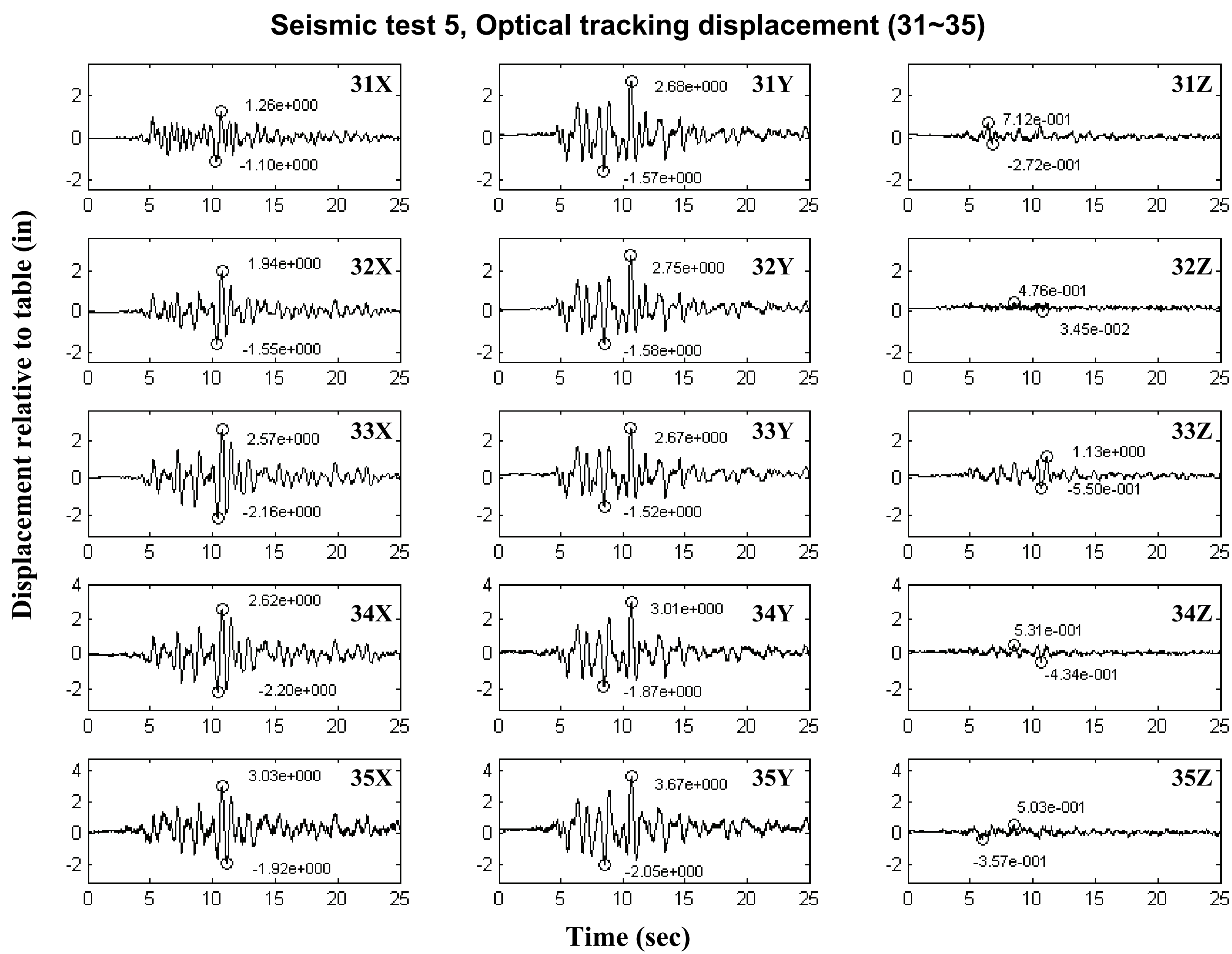

Figure E.48: Displacement of optical tracking markers (31~35) relative to table during Seismic test 5

Appendix E

Seismic test 5, Optical tracking displacement (36~40)

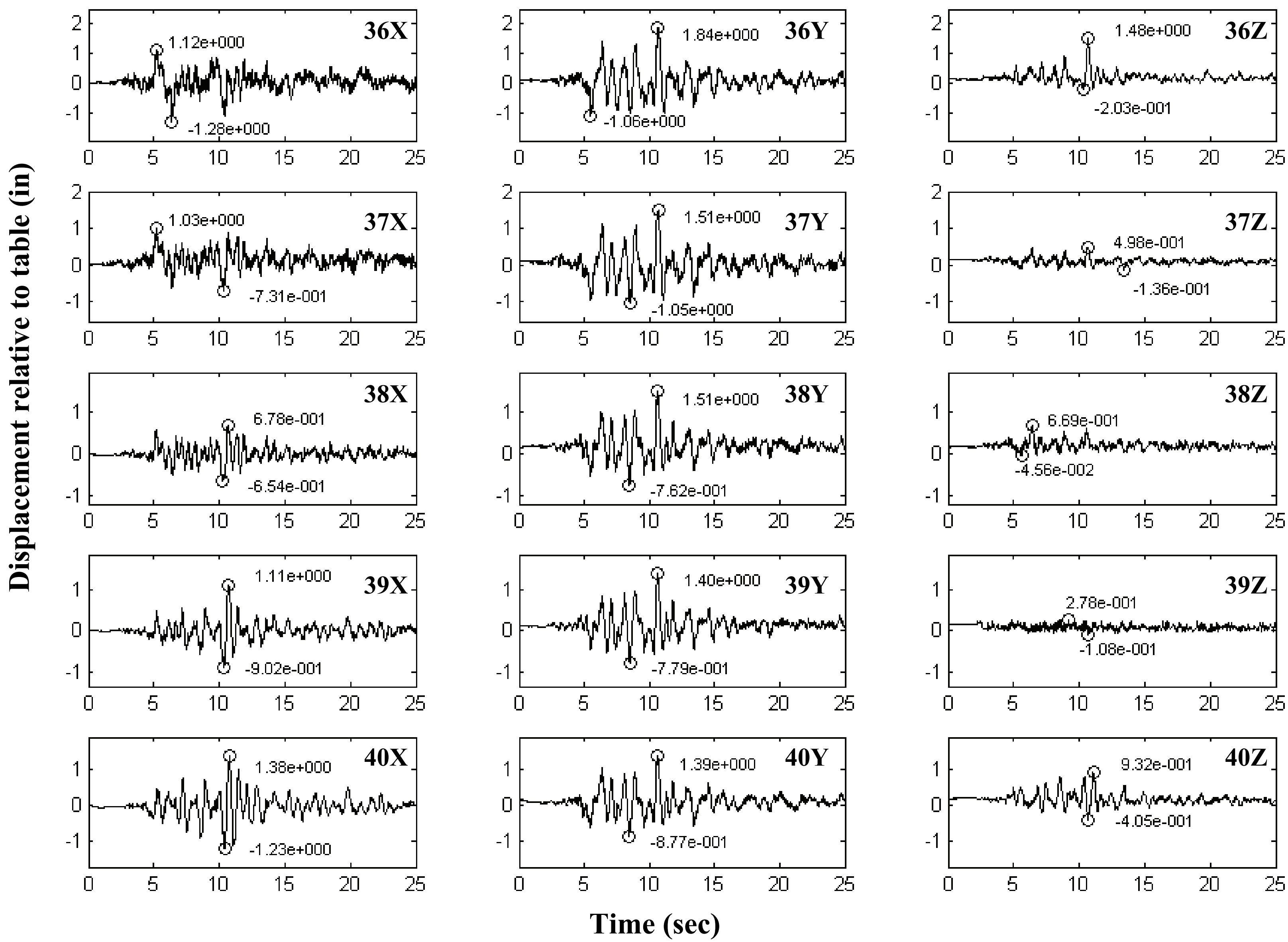

Figure E.49: Displacement of optical tracking markers (36~40) relative to table during Seismic test 5

Seismic test 5, Optical tracking displacement (41~45)

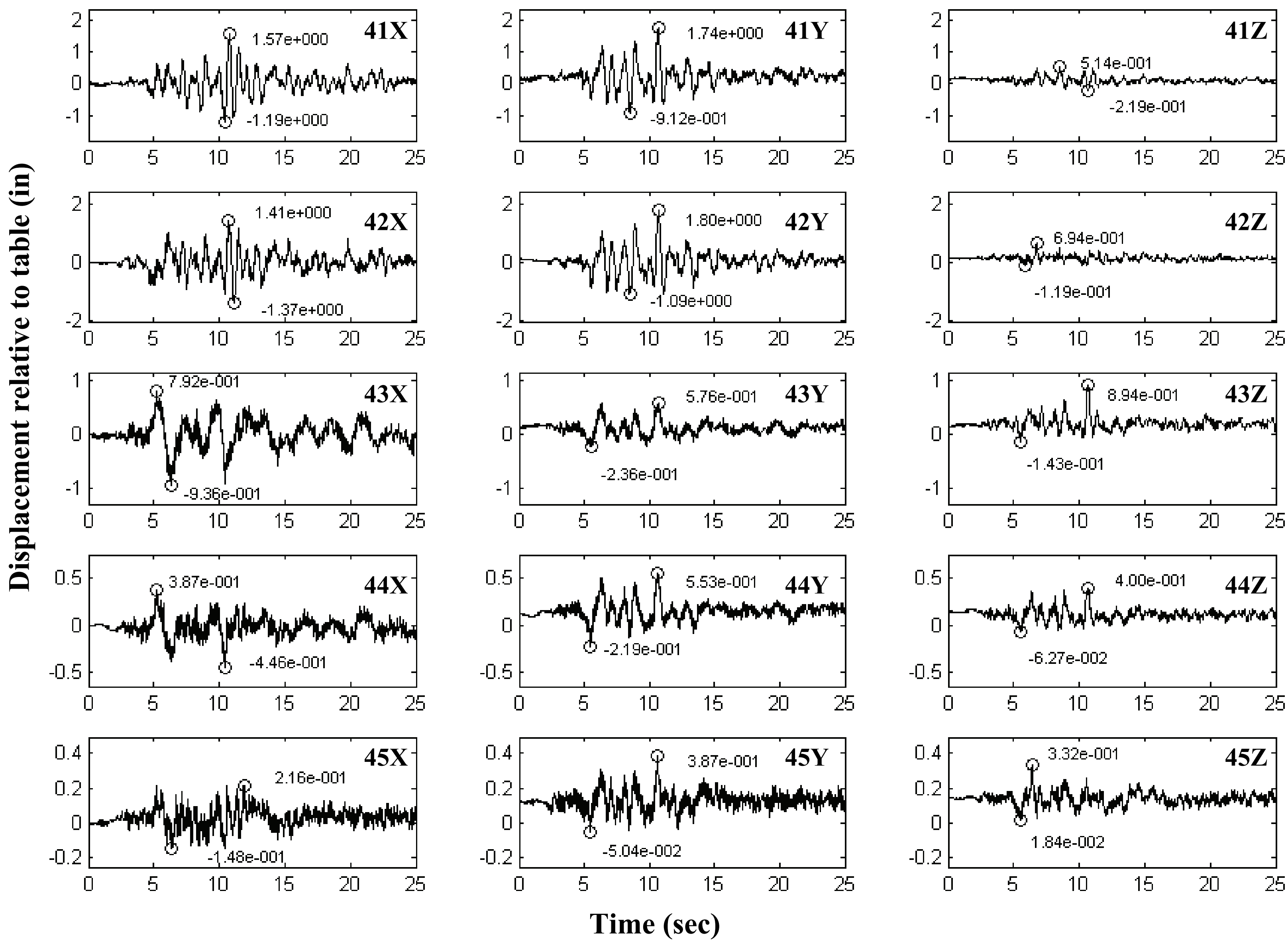

Figure E.50: Displacement of optical tracking markers (41~45) relative to table during Seismic test 5

Seismic test 5, Optical tracking displacement (46~50)

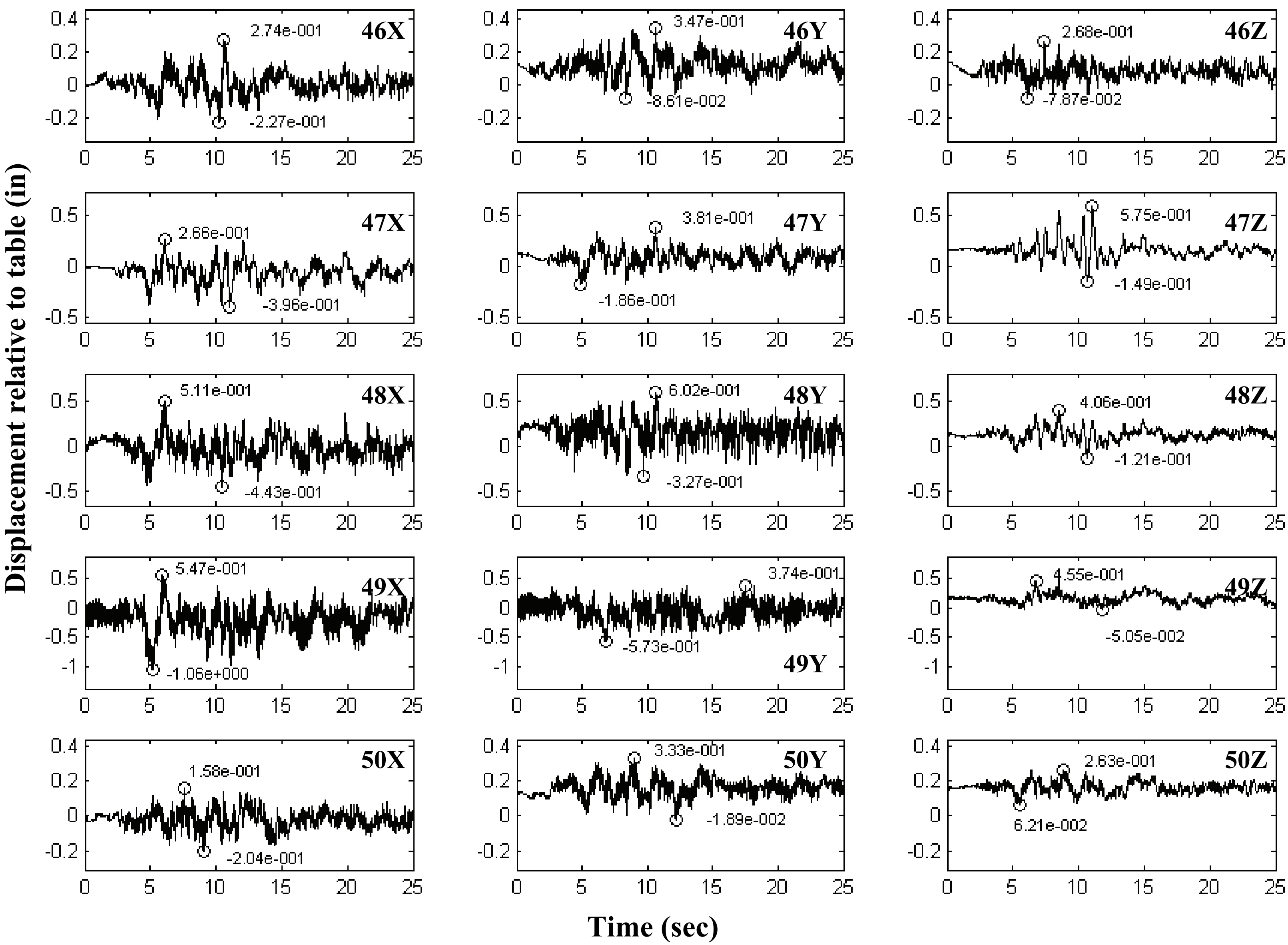

Figure E.51: Displacement of optical tracking markers (46~50) relative to table during Seismic test 5

Appendix F

Supplemental weight layout and total weight of test specimen

Appendix F

Seismic weight of the Capstone test building

Table F.1: Summary of seismic weight of Capstone specimen (lb)

Story	FBD target	Dead weight	Supplement weight	Total as-built weight
2	N/A	99559	40789	140348
3	112849	65761	40275	106036
4	106551	61378	40068	101446
5	106551	58885	41222	100107
6	106551	56321	44577	100898
7	113489	50639	57796	108435
Roof	68678	29677	35194	64871

*10% wood building material weight were added as the hardware weight
*FBD stands for Force-Based Design, it was not conducted for hybrid building
*Seismic weight at each story includes half of the wall weight above and below the story (story 2 weight including 53000 lb contribution from SMF)
*Wood specimen weighs total 628352 lb
*Hybrid specimen weighs total 810431 lb

Appendix F

Supplement seismic weights used during the tests

- Type A: Steel plate (big)

Dimension: 83x169x1 in
Unit weight: 3889 lb

- Type B: Steel I beam

Unit weight: 992 lb

- Type C: Steel plate (small)

Dimension: 35x35x3.15 in
Unit weight: 1076 lb

Appendix F

Supplement seismic weights used during the tests

- Type D: Drywall panels
  Standard 4x8 ft 1/2" Drywall panels. Approximately 2 lb/ft^2.

- Type O: OSB panels
  Standard 4x8 ft 15/32" OSB panels. Approximately 1.6 lb/ft^2.

- Type E: Gusset steel plates

Dimension: Various
Total weight: See Figure F.2

Appendix F

Supplement seismic weights layout (Story 2~3)

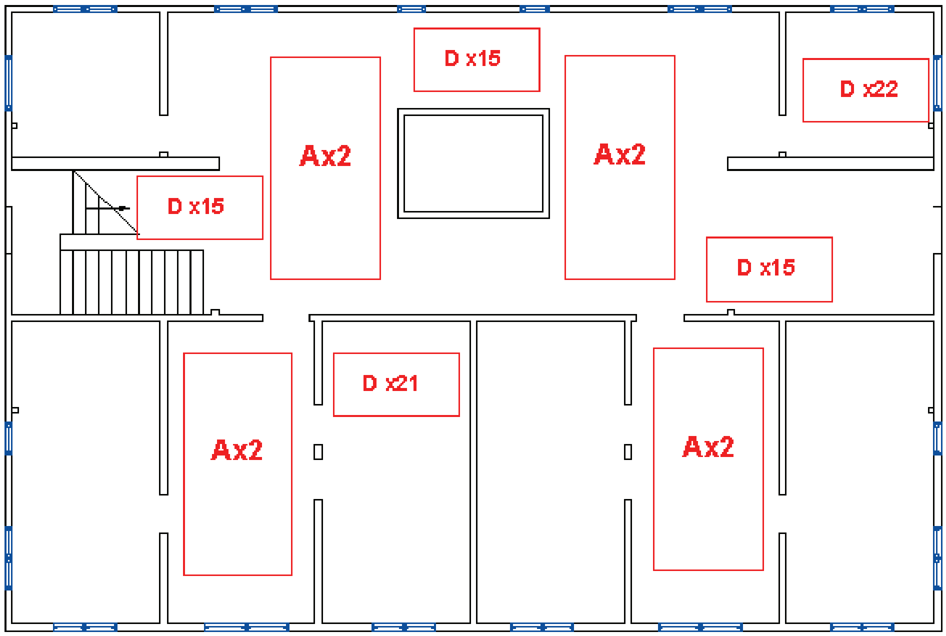

Figure F.1: Supplement weight layout on story 2

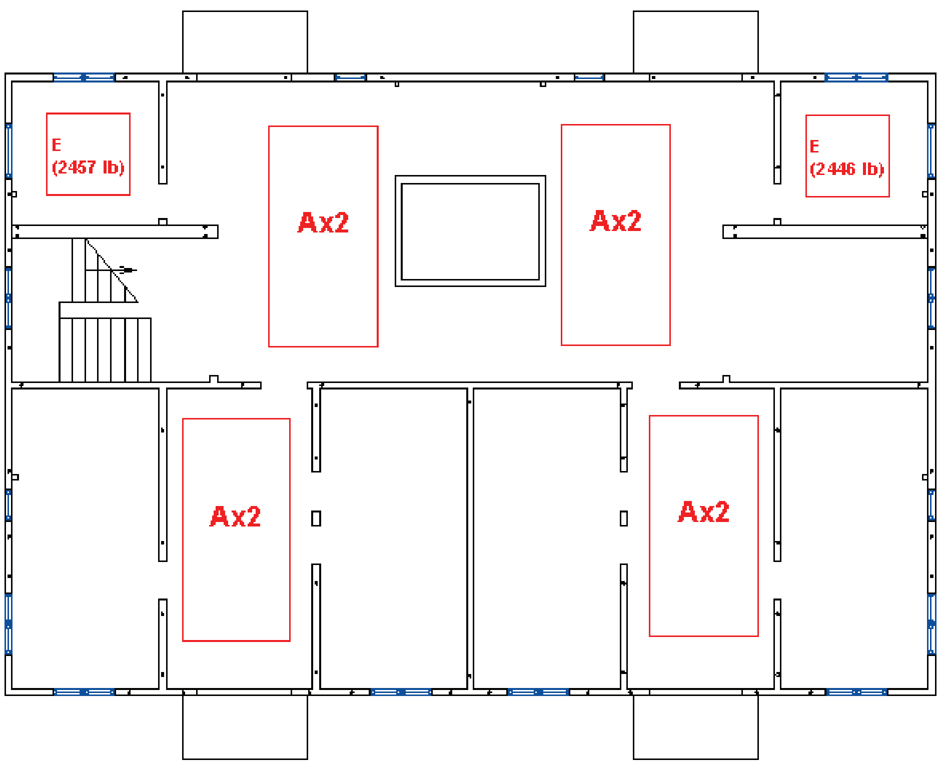

Figure F.2: Supplement weight layout on story 3

Appendix F

Supplement seismic weights layout (Story 4~5)

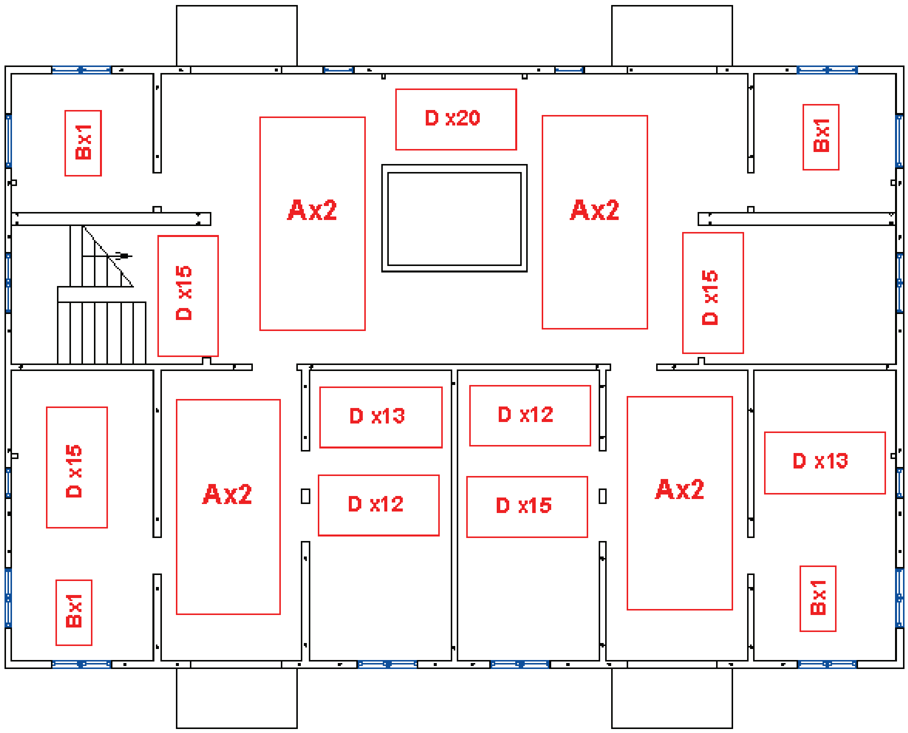

Figure F.3: Supplement weight layout on story 4

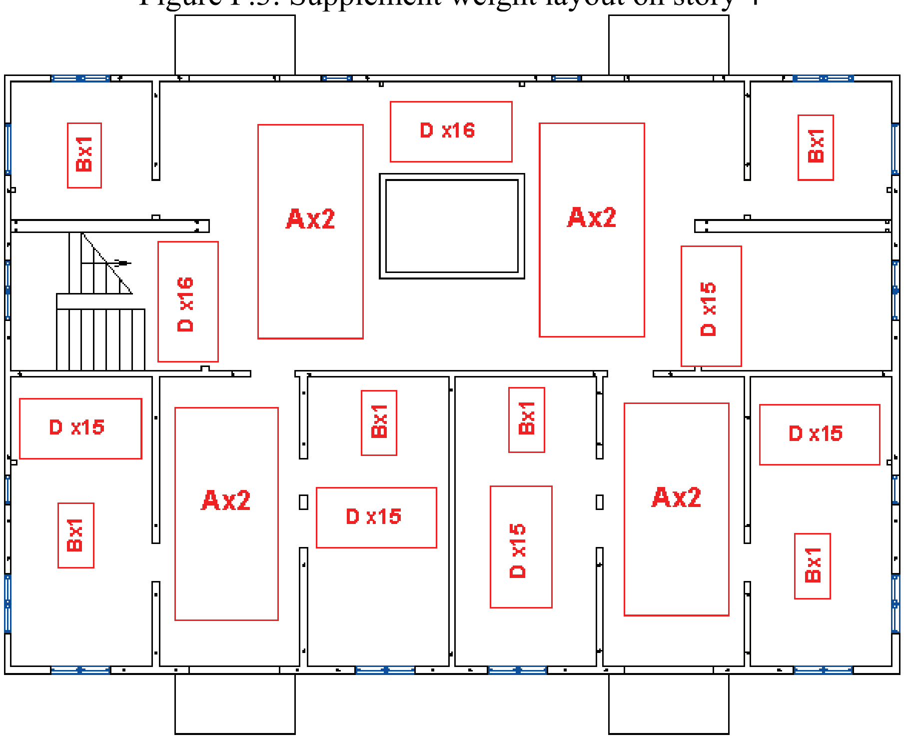

Figure F.4: Supplement weight layout on story 5

Appendix F

Supplement seismic weights layout (Story 6~7)

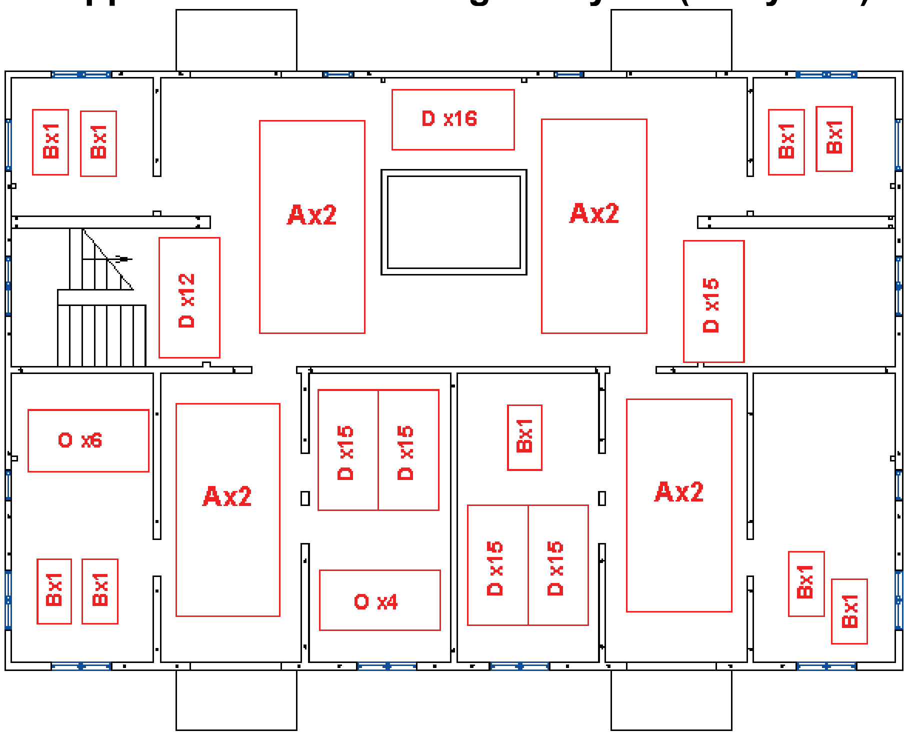

Figure F.5: Supplement weight layout on story 6

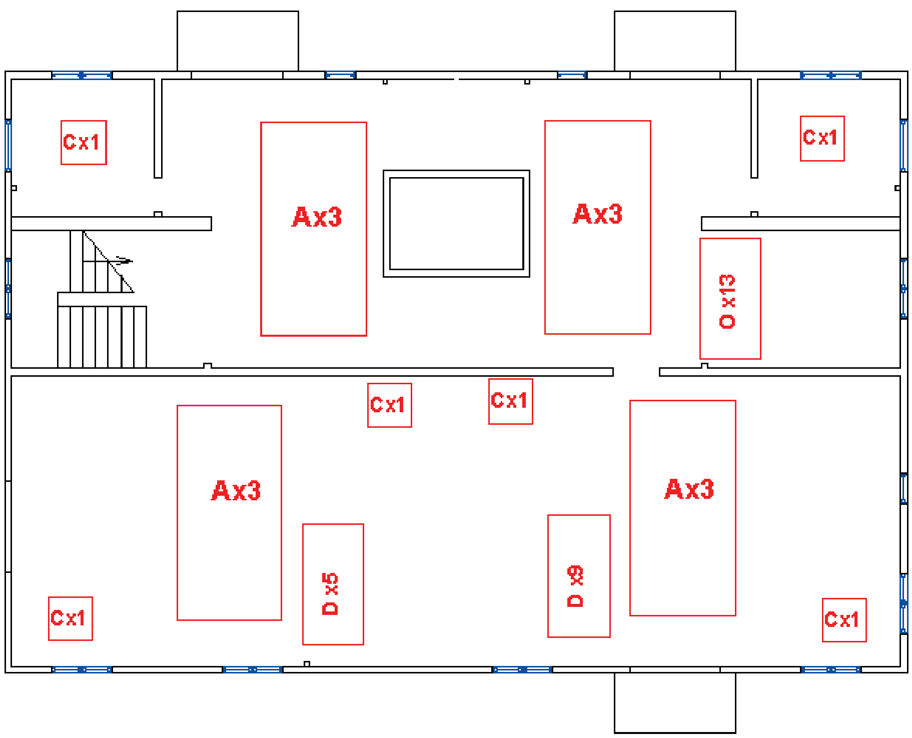

Figure F.6: Supplement weight layout on story 7

Appendix F

Supplement seismic weights layout (Roof)

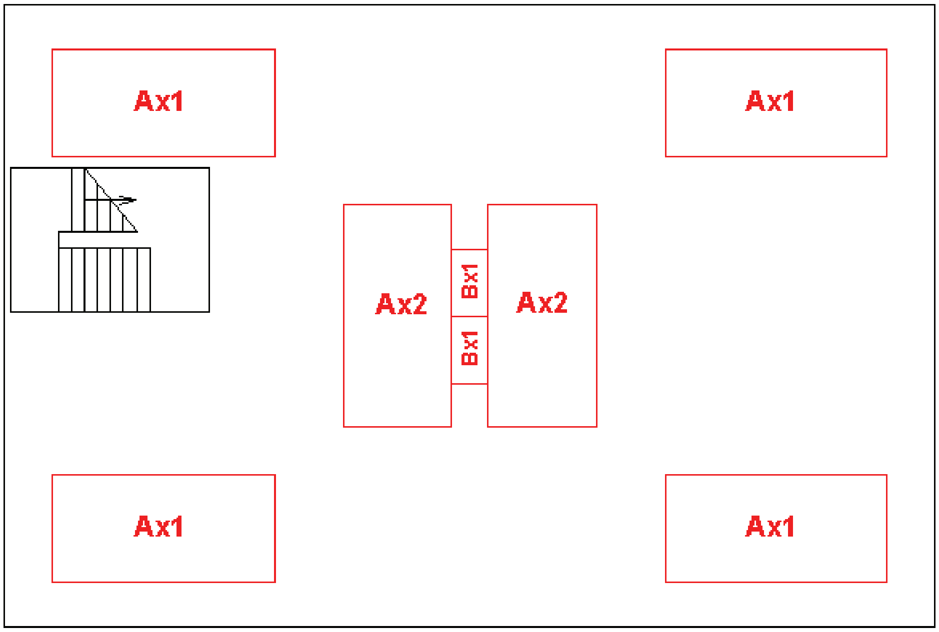

Figure F.7: Supplement weight layout on the roof

Appendix G

Building fundamental periods

Appendix G

Building fundamental periods

Table G.1: Summary of fundamental period estimation from white noise tests

Test ID	Natural Period (sec)		
	X	Y	Z
WN1	0.42	0.41	0.13
1	Test Level 1-Seismic (SMF)		
WN2	0.48	0.48	0.13
WN3	0.48	0.48	0.13
2	Test Level 2 plus-Seismic (SMF)		
WN4	0.48	0.49	0.14
SMF Tie down			
WN5	0.41	0.42	0.13
ST3	Test Level 1-Seismic		
WN6	0.41	0.42	0.13
ST4	Test Level 2-Seismic		
WN7	0.41	0.42	0.13
WN8	0.41	0.42	0.13
ST5	Test Level 3-Seismic		
WN9	0.47	0.49	0.14

*Fundamental periods estimated based on spectral analysis of roof average acceleration record.

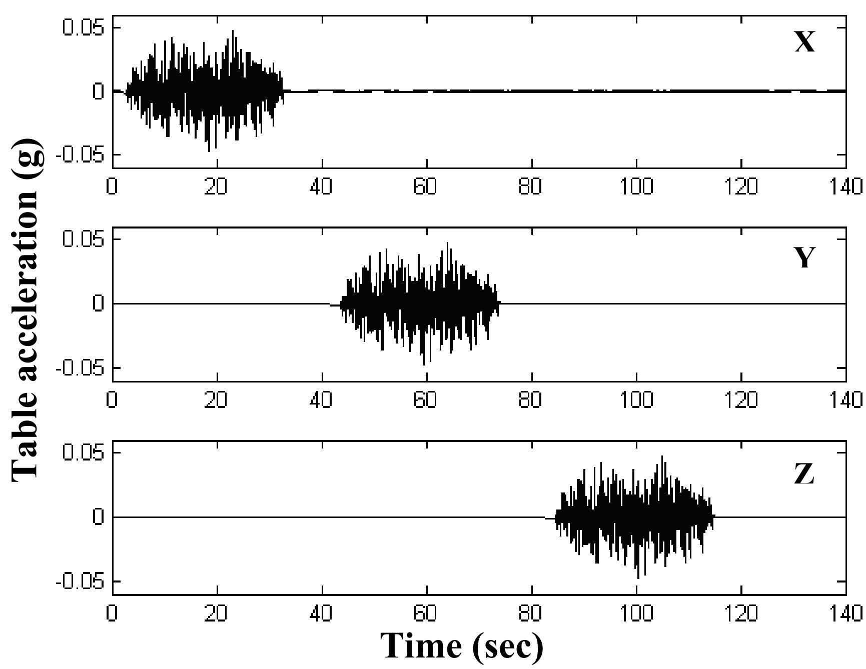

Figure G.1: Input white noise record used in the test

Appendix H

Fidelity of shake table motions

Appendix H

Seismic Test 1

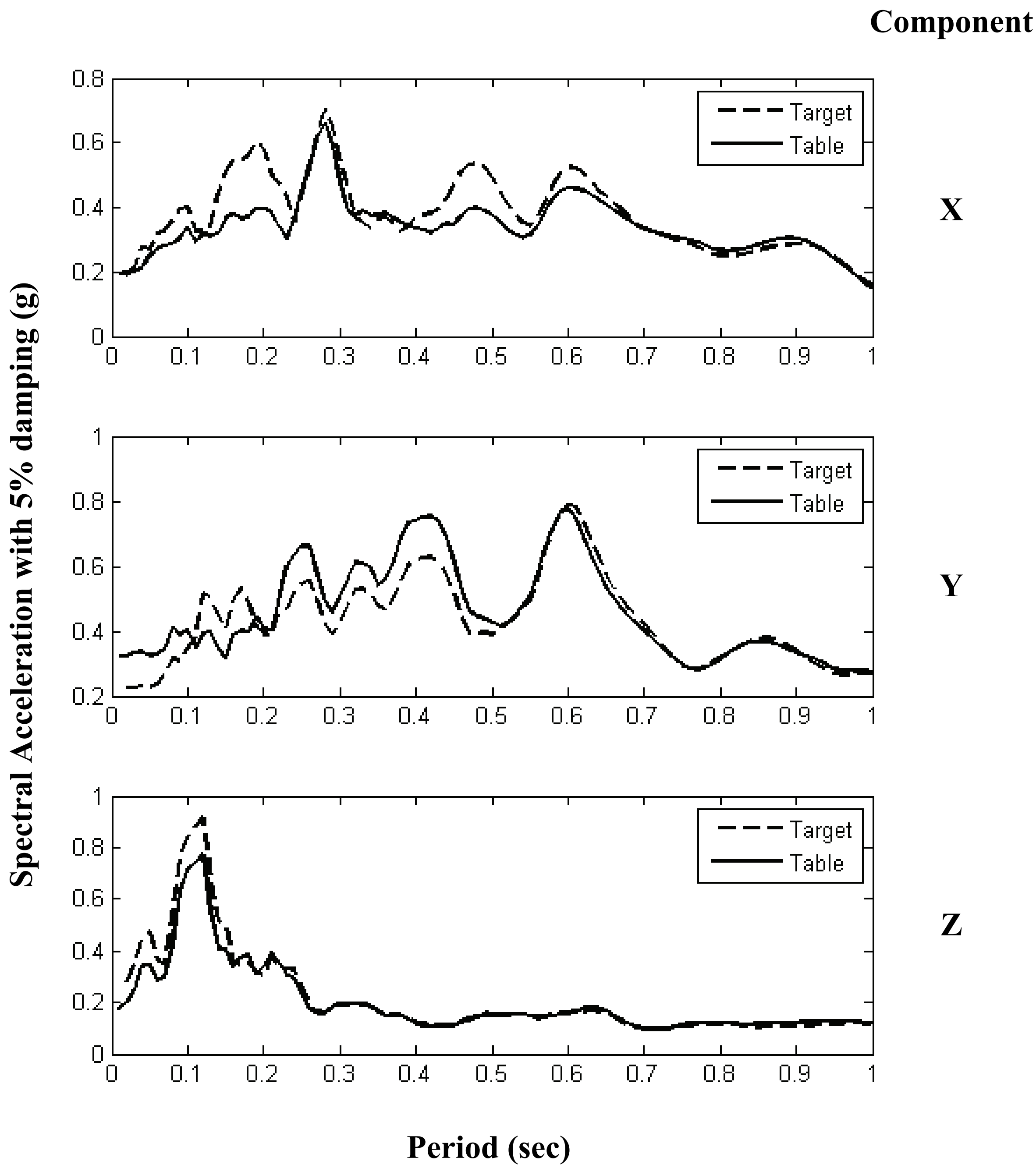

Figure H.1: Response spectra of ground motion input and table feedback for Seismic Test 1

Appendix H

Seismic Test 2

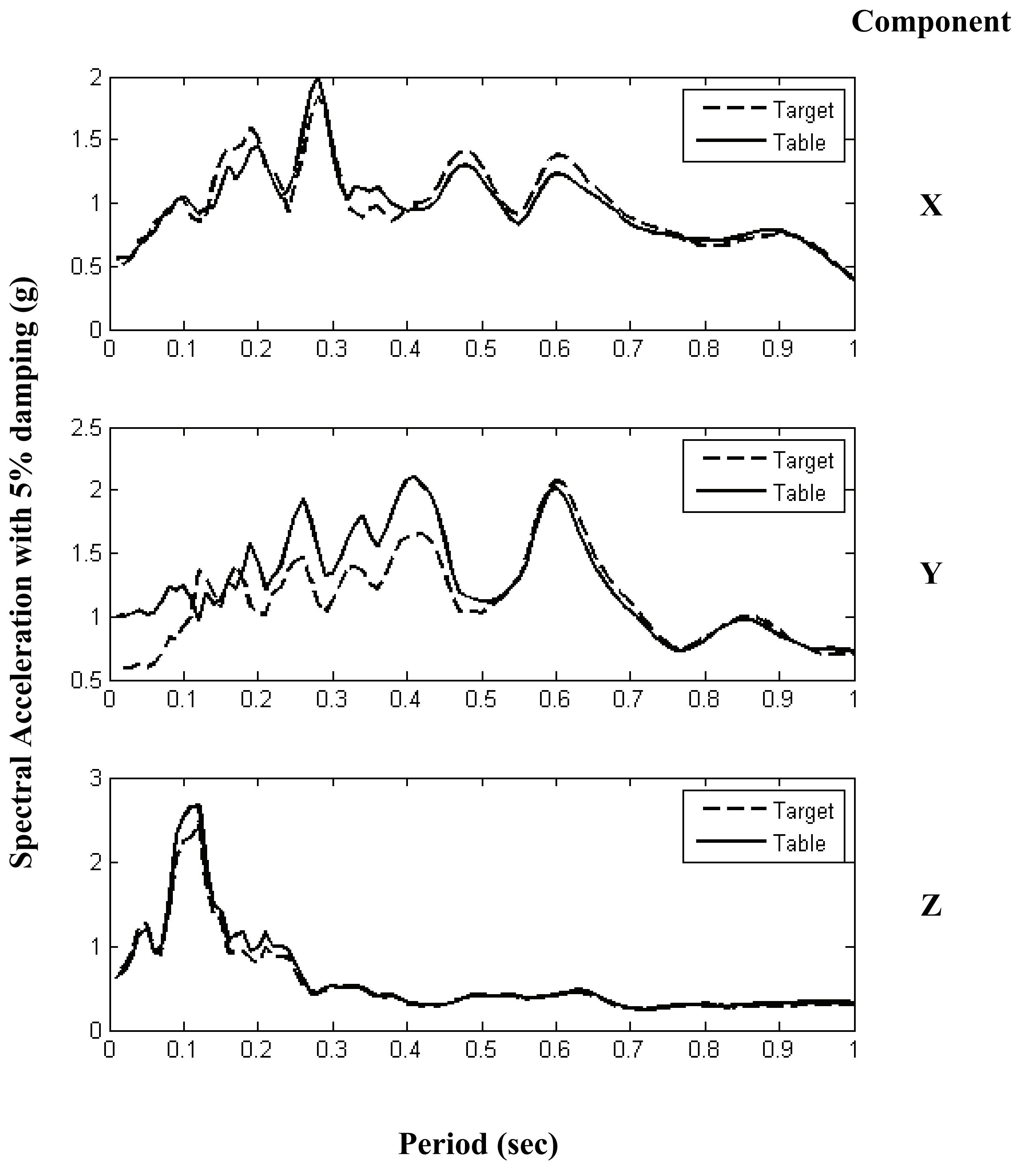

Figure H.2: Response spectra of ground motion input and table feedback for Seismic Test 2

Appendix H

Seismic Test 3

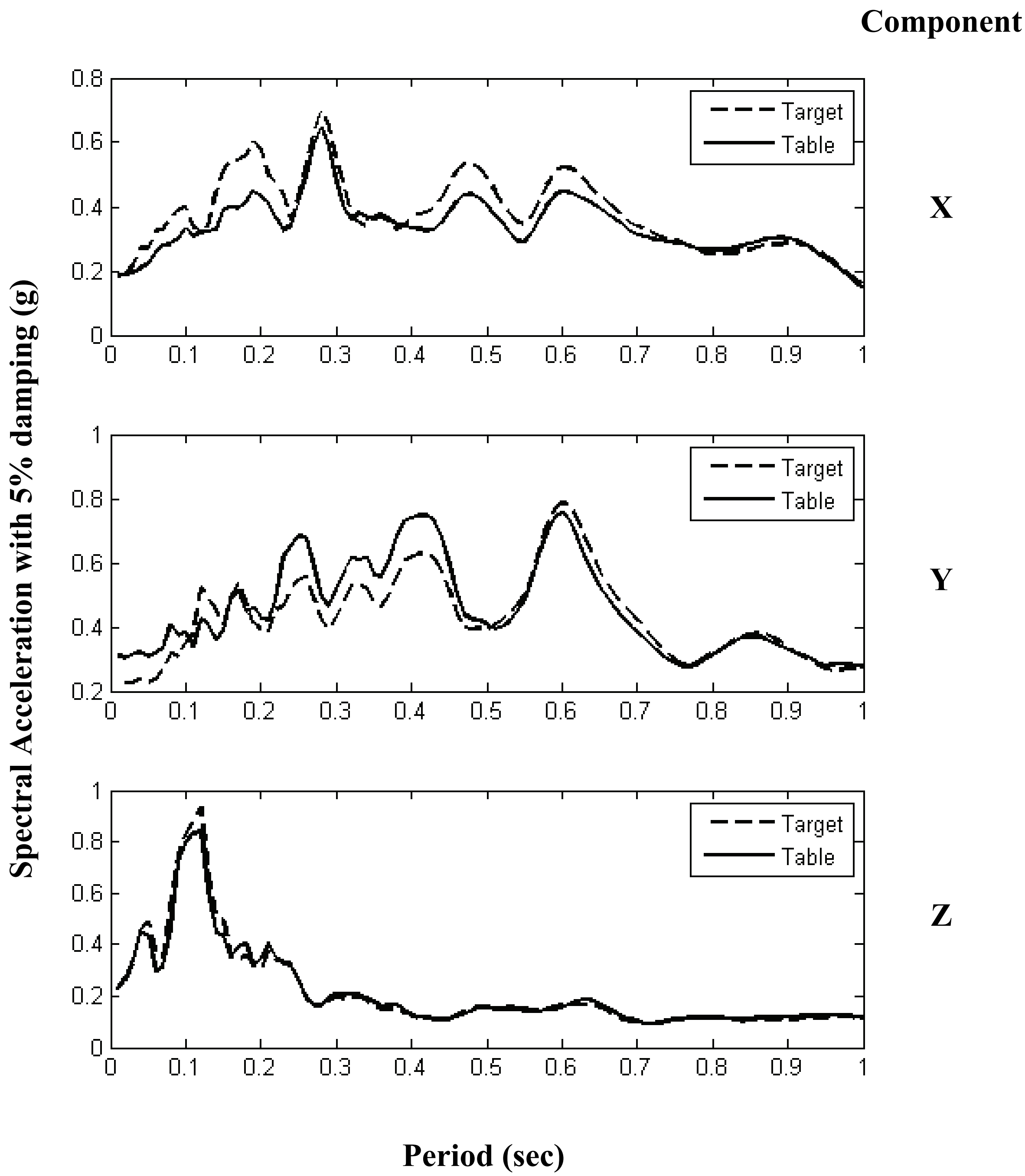

Figure H.3: Response spectra of ground motion input and table feedback for Seismic Test 3

Appendix H

Seismic Test 4

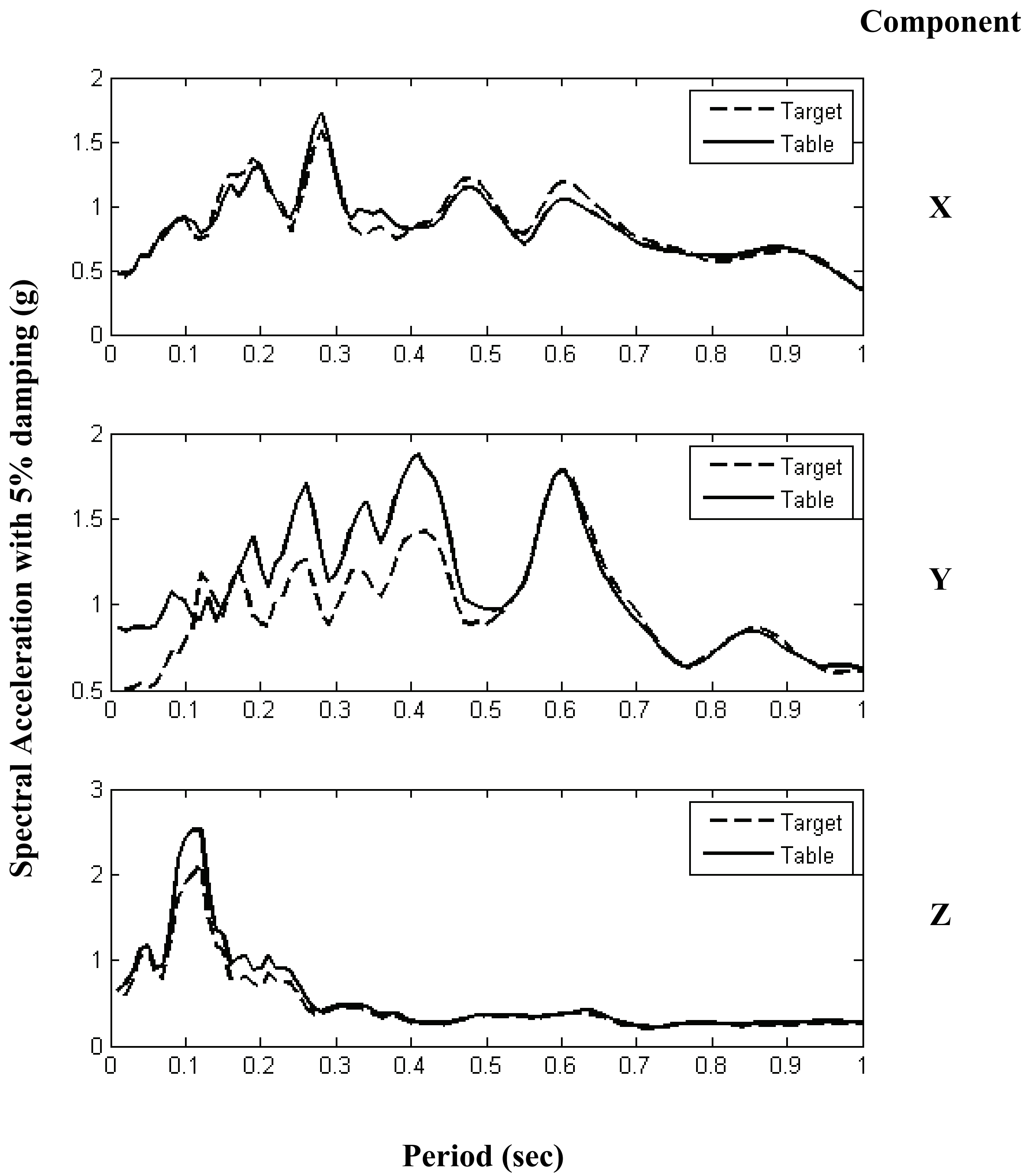

Figure H.4: Response spectra of ground motion input and table feedback for Seismic Test 4

Appendix H

Seismic Test 5

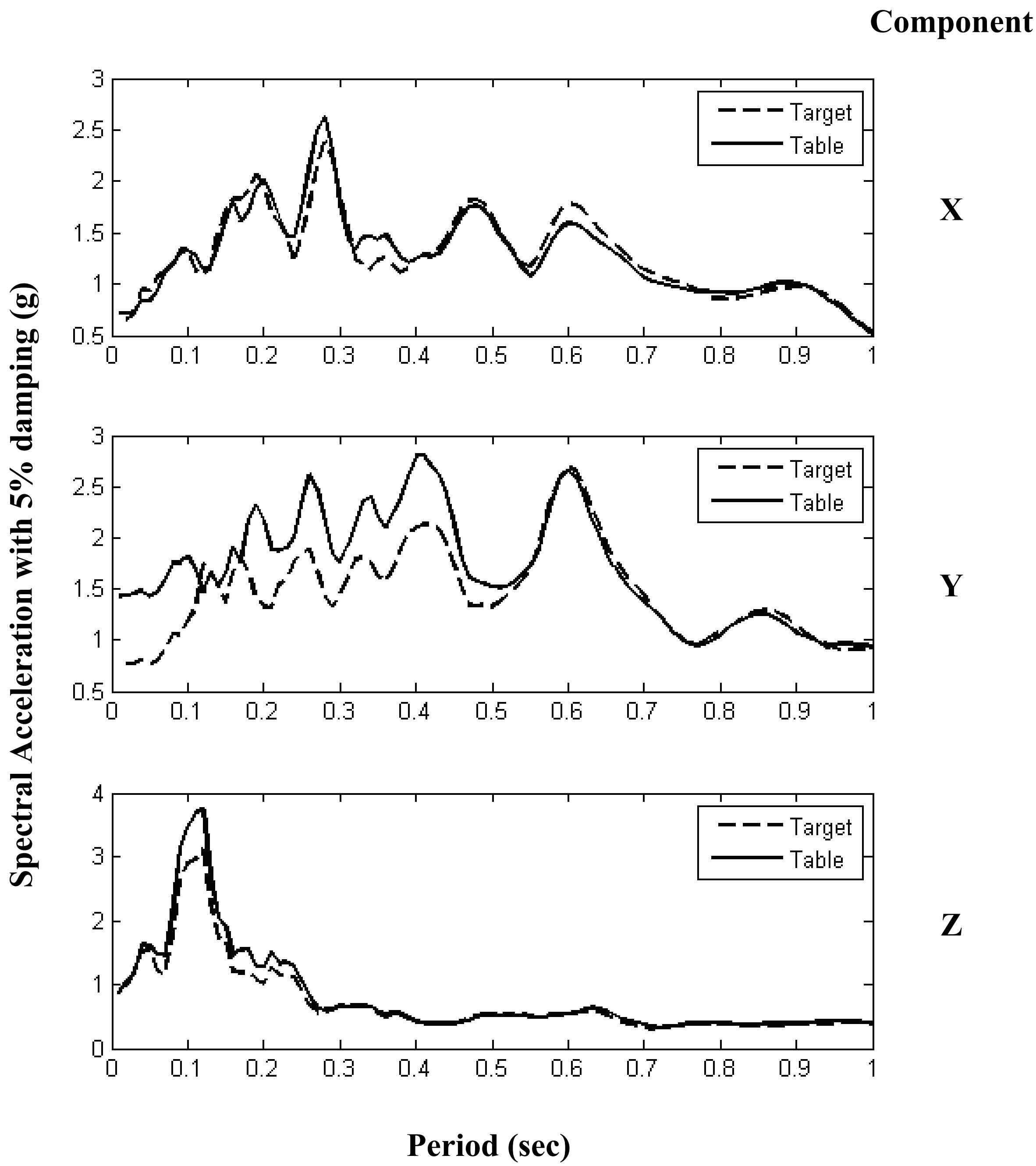

Figure H.5: Response spectra of ground motion input and table feedback for Seismic Test 5

Appendix I

Selected visual damage identification photos

Appendix I

Selected damage photo for Seismic Test 1

Figure I.1: Minor crack on Wall E4, Story 2 (over window opening)

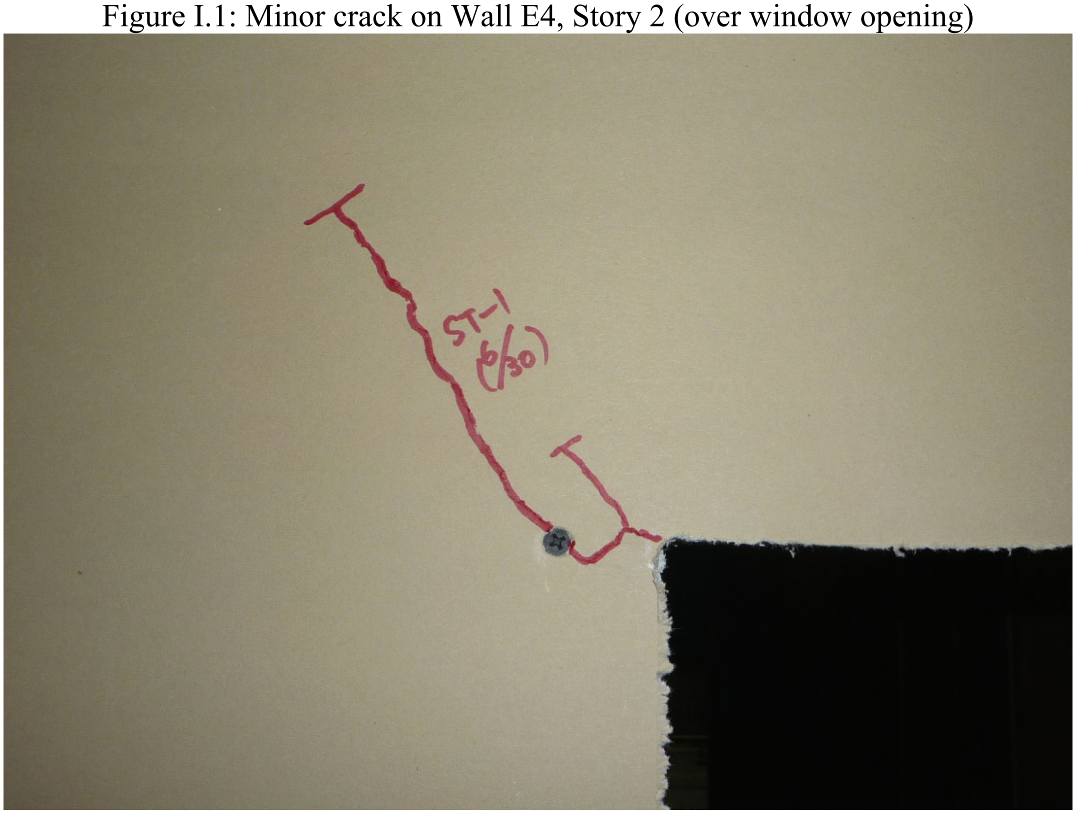

Figure I.2: Minor crack on Wall D1, Story 4 (over door opening)

Appendix I

Selected damage photo for Seismic Test 2

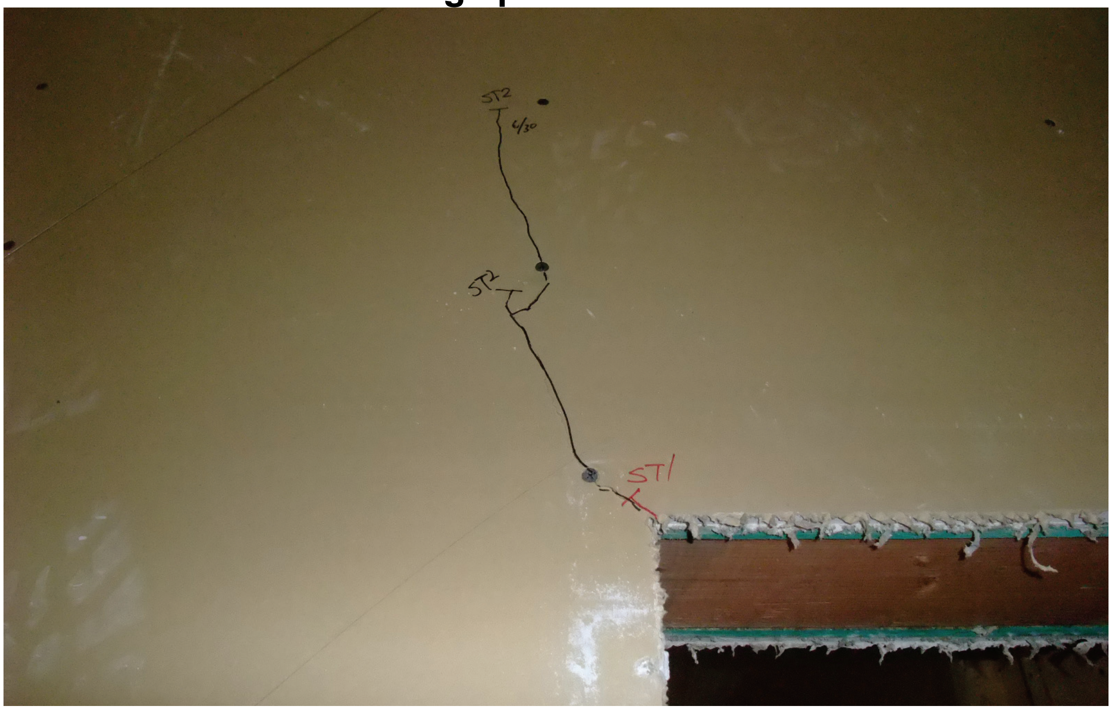

Figure I.3: Crack on Wall 10A, Story 2 (over door opening)

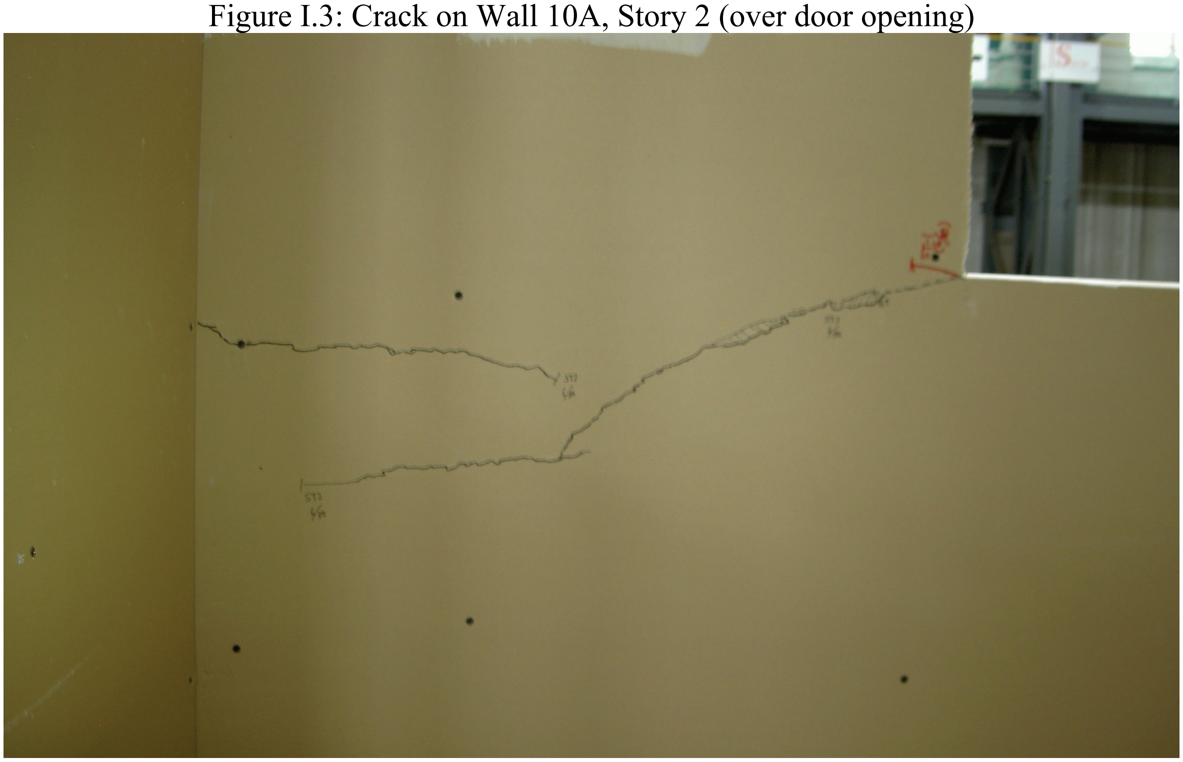

Figure I.4: Minor crack on Wall A2, Story 3 (over window opening)

Appendix I

Selected damage photo for Seismic Test 2

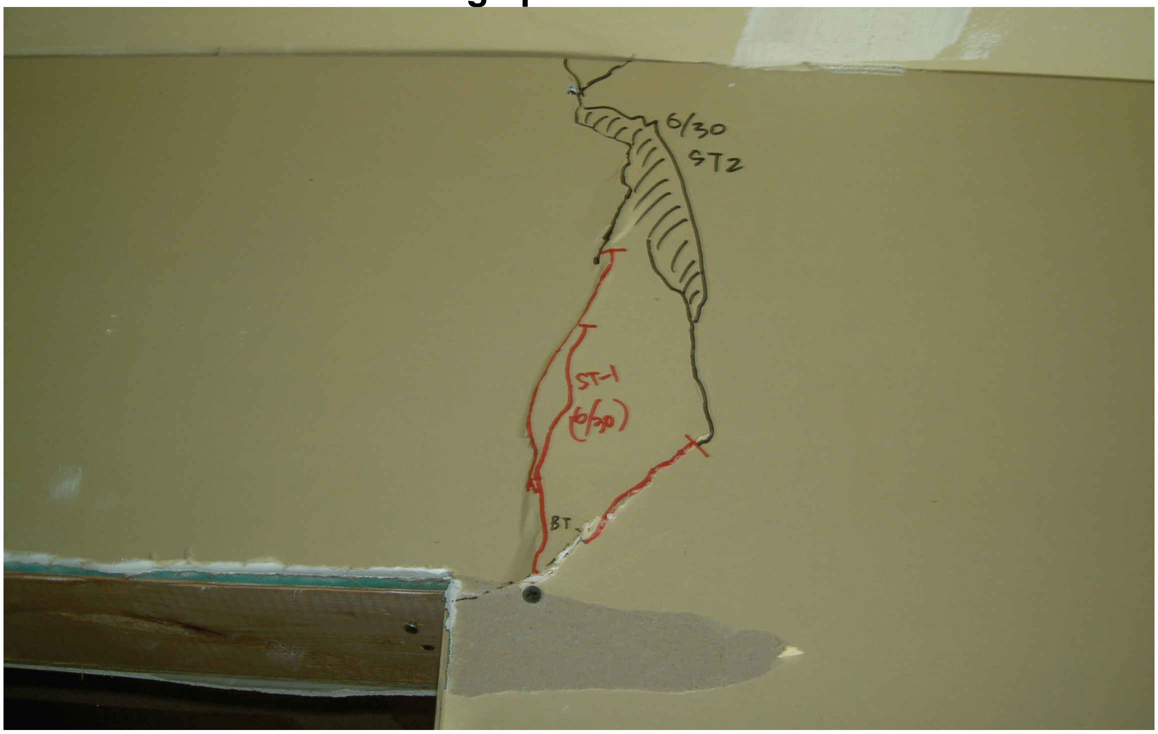

Figure I.5: Crack on Wall D1, Story 4 (over door opening)

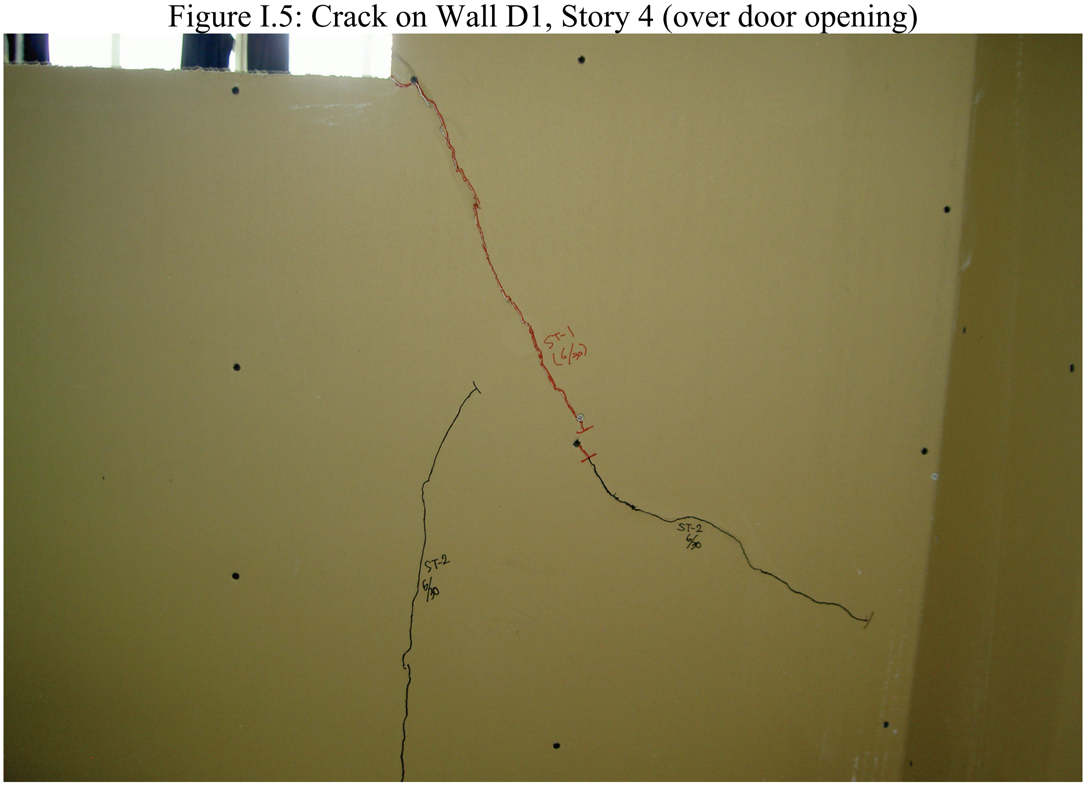

Figure I.6: Minor crack on Wall E3, Story 5 (over window opening)

Appendix I

Selected damage photo for Seismic Test 2

Figure I.7: Crack on Wall 2A, Story 7 (over door opening)

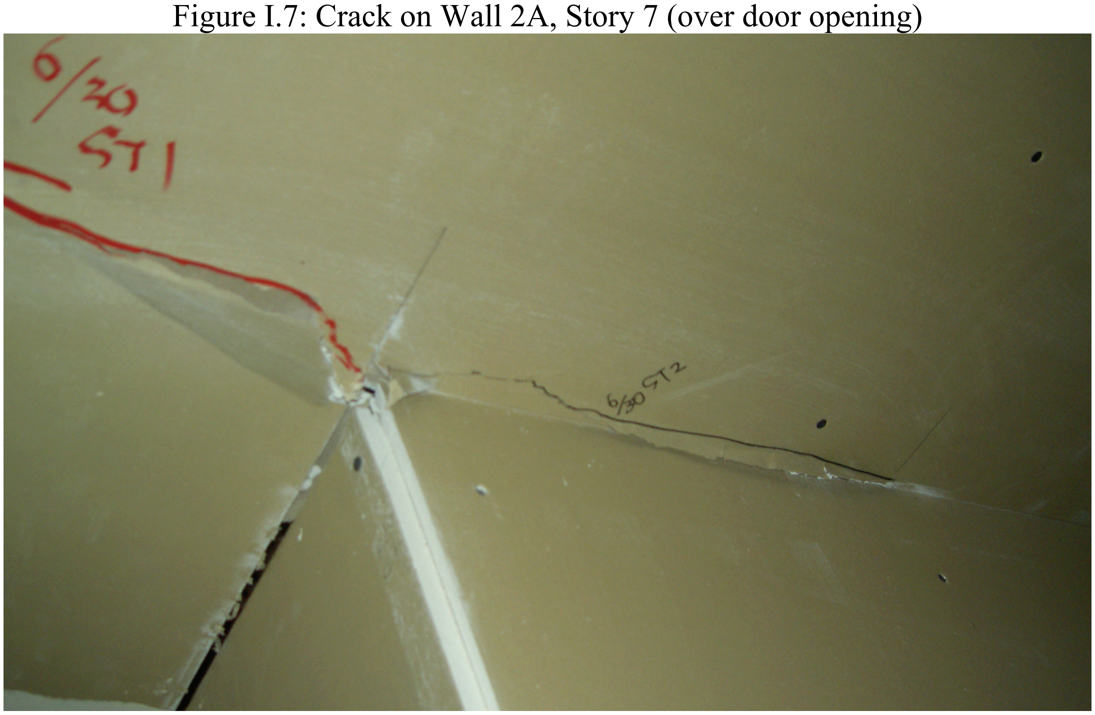

Figure I.8: Crack on ceiling near elevator shaft, Story 7

Appendix I

Selected damage photo for Seismic Test 3

Figure I.9: Crack on Wall B1 stud, Story 2 (Midply-wall)

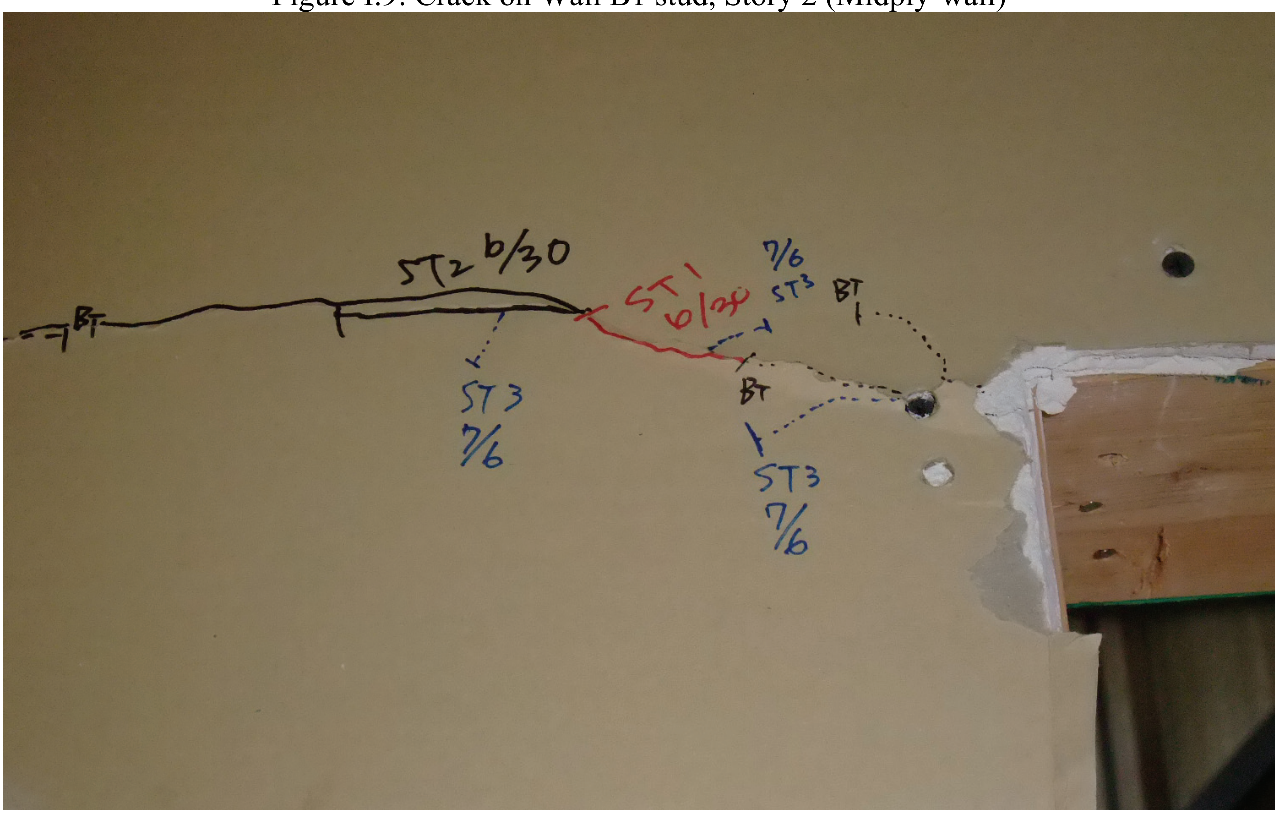

Figure I.10: Crack on Wall A3, Story 2 (over window opening)

Appendix I

Selected damage photo for Seismic Test 3

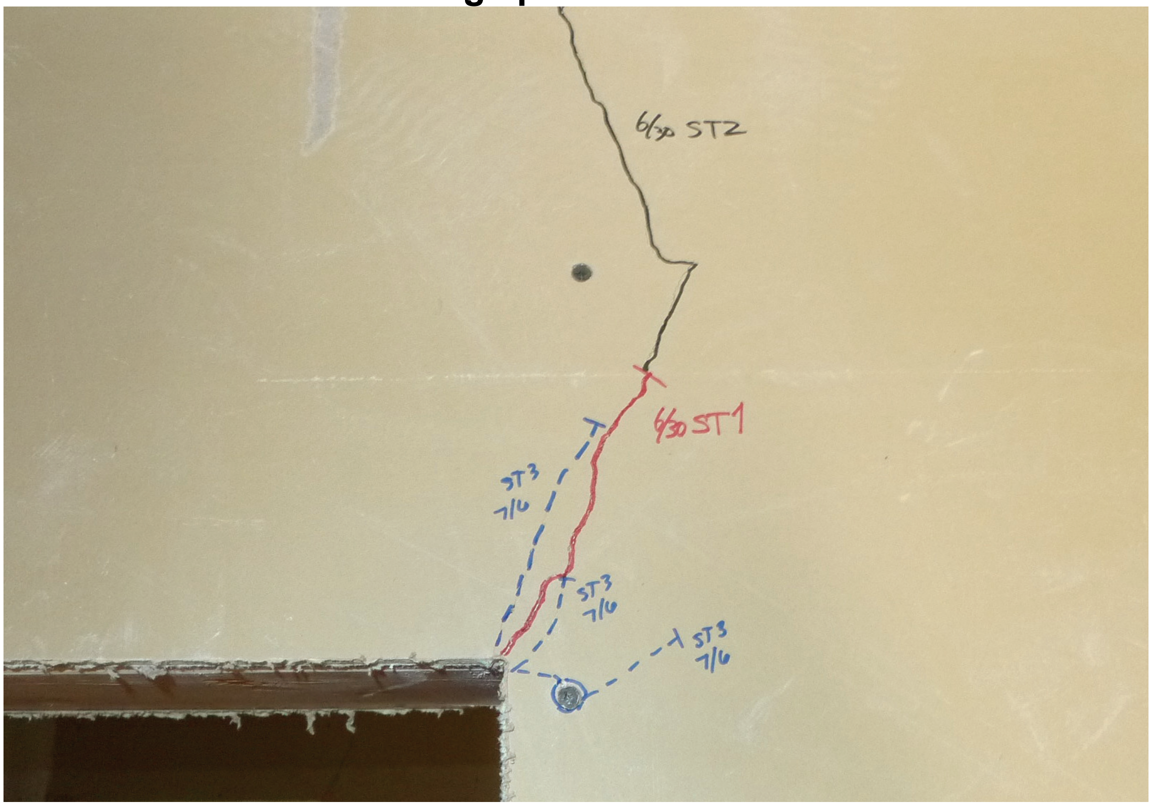

Figure I.11: Crack on Wall 10C, Story 4 (over door opening)

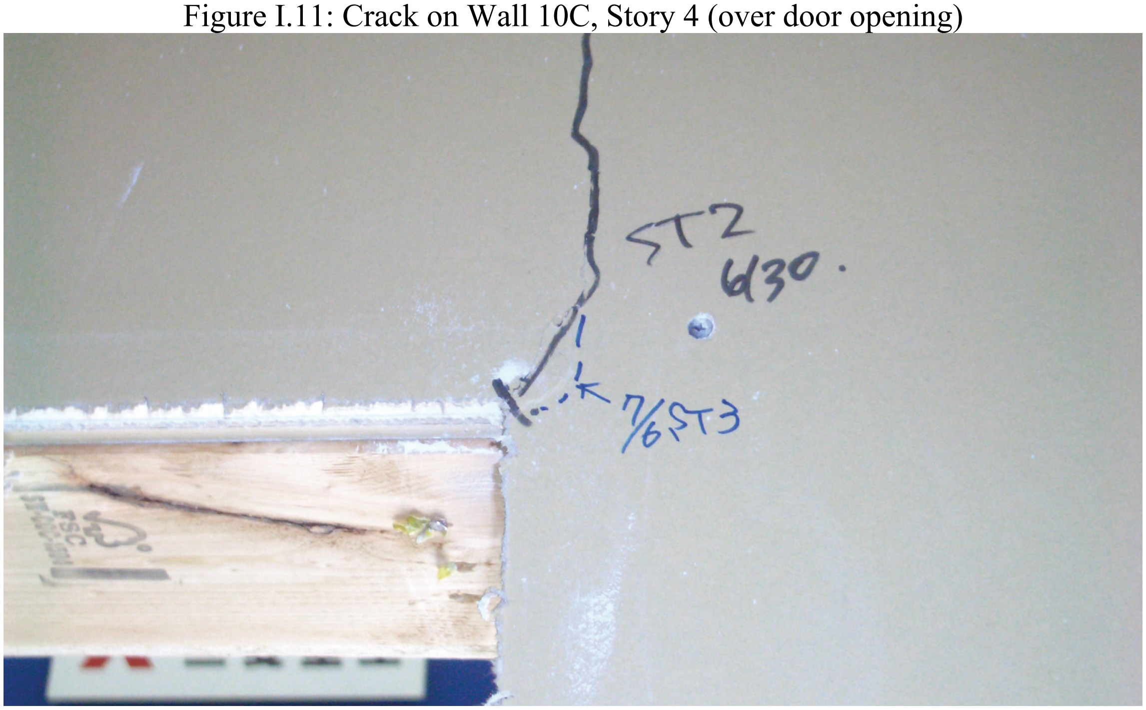

Figure I.12: Crack on Wall 11B, Story 7 (over window opening)

Appendix I

Selected damage photo for Seismic Test 4

Figure I.13: Crack on Wall D1, Story 3 (corner crashing)

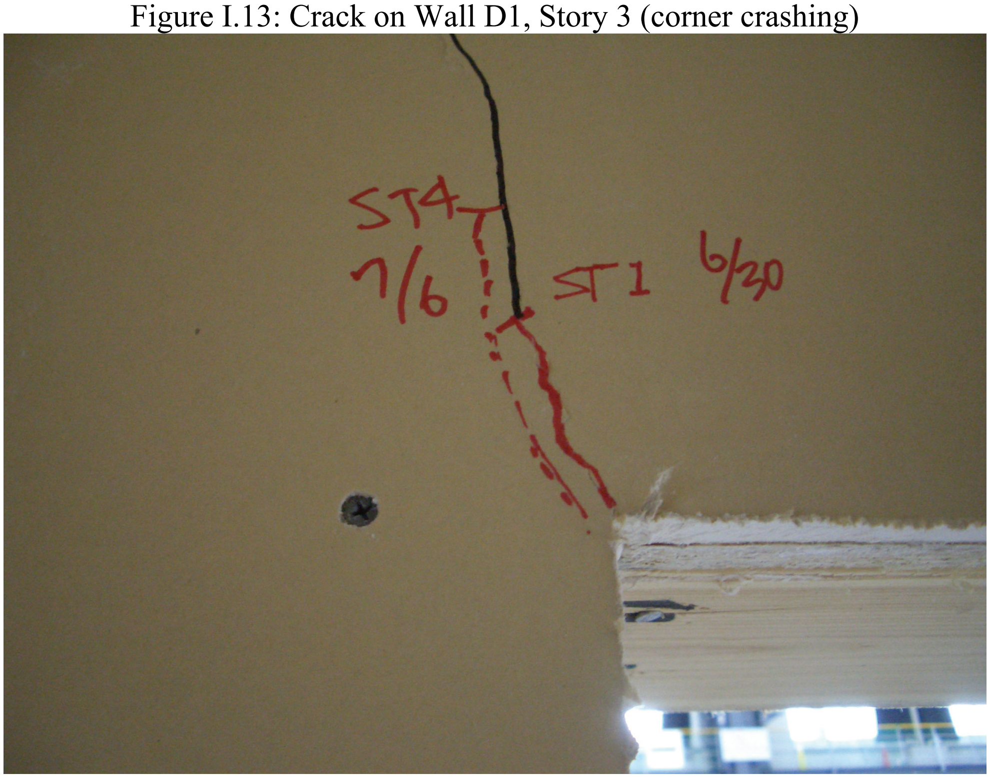

Figure I.14: Crack on Wall E1, Story 3 (over window opening)

Appendix I

Selected damage photo for Seismic Test 4

Figure I.15: Crack on ceiling, Story 5 (near Wall B1)

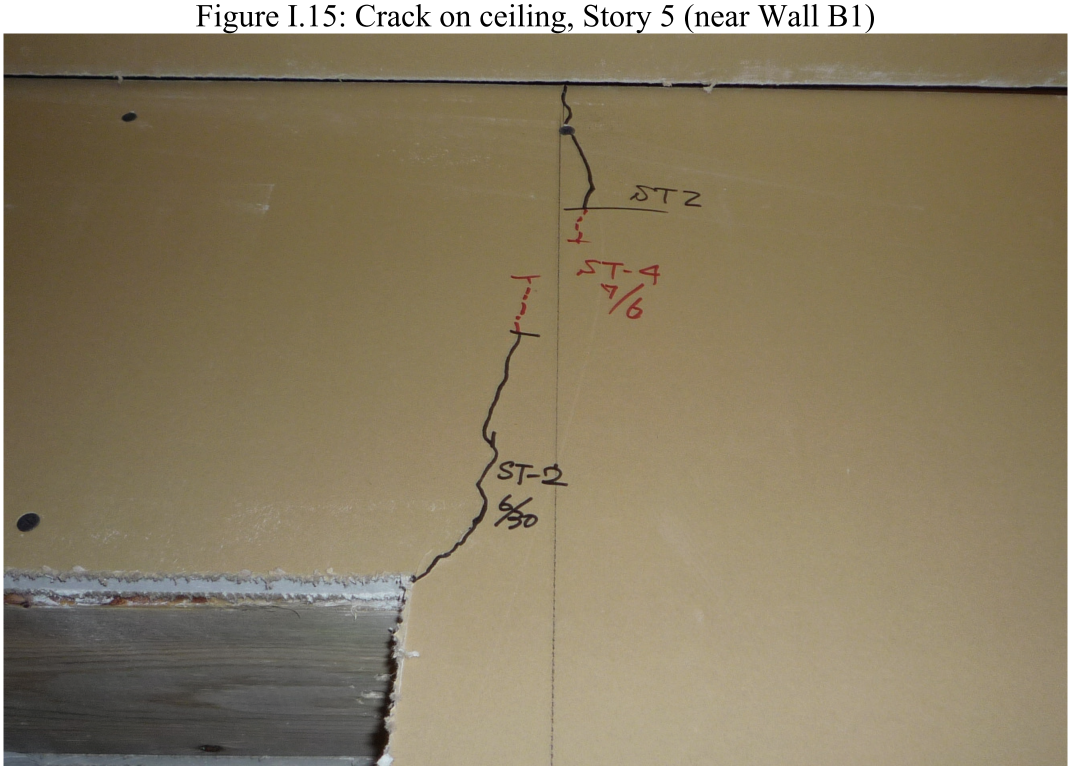

Figure I.16: Crack on Wall 2A, Story 5 (over door opening)

Appendix I

Selected damage photo for Seismic Test 5

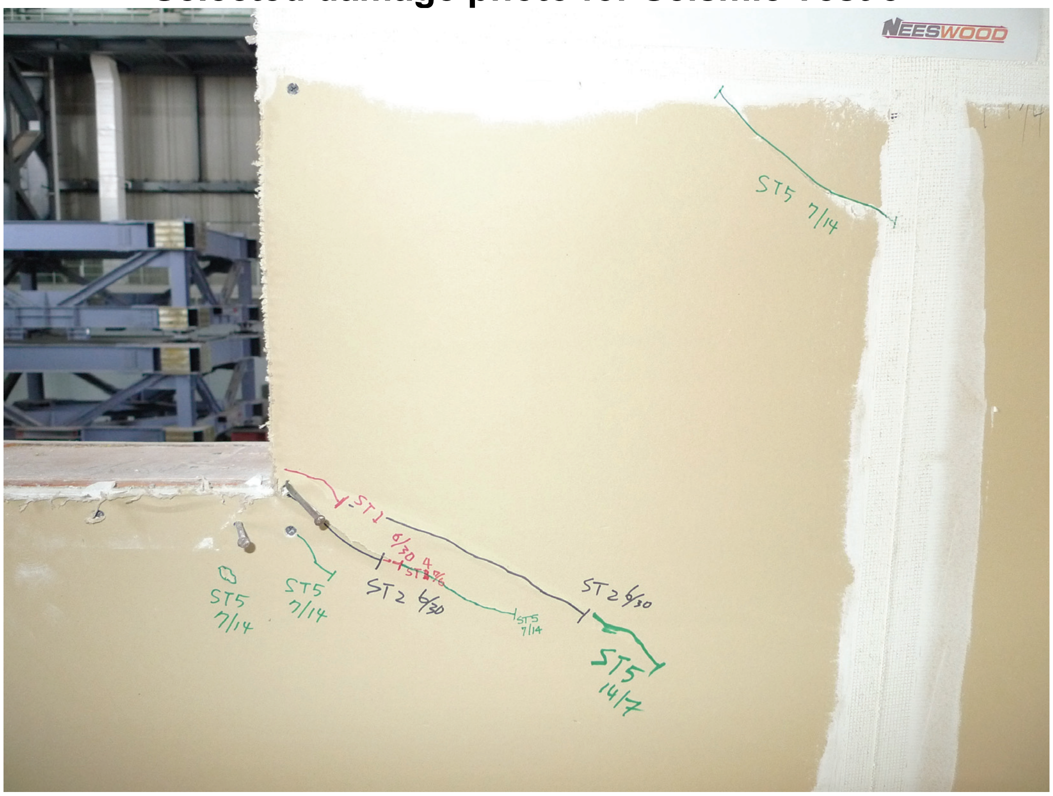

Figure I.17: Crack on Wall E1, Story 2 (over window opening)

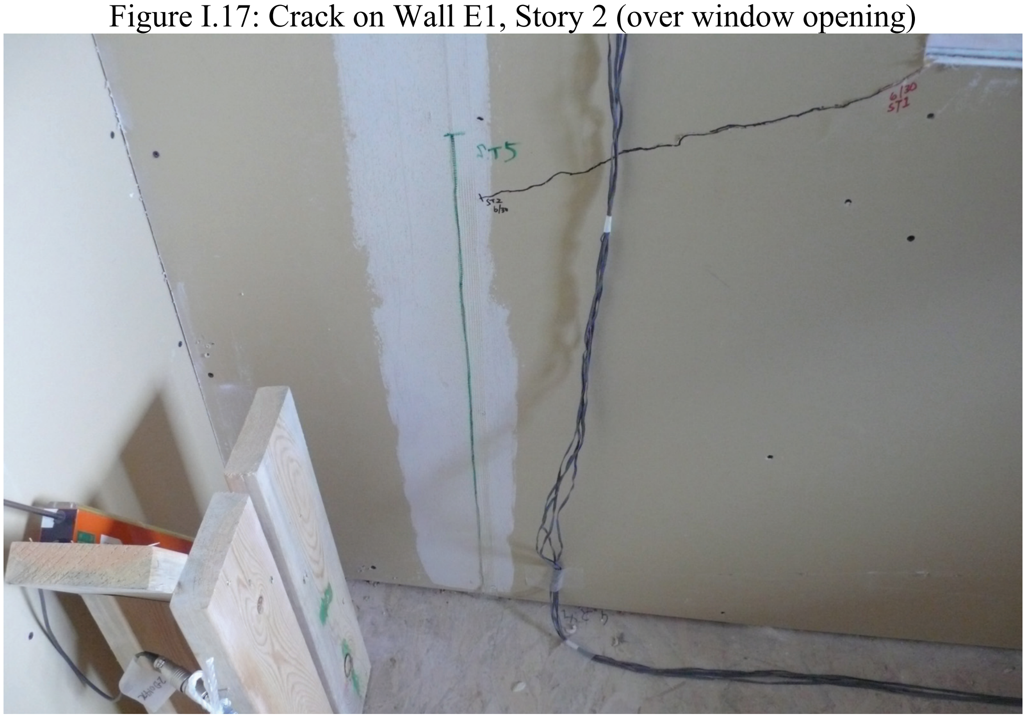

Figure I.18: Crack on Wall E5, Story 2 (along panel edge)

Appendix I

Selected damage photo for Seismic Test 5

Figure I.19: Nail withdraw on Wall B1, Story 3 (Midply end post)

Figure I.20: Crack on Wall B1 stud, Story 4 (Midply wall)

Appendix I

Selected damage photo for Seismic Test 5

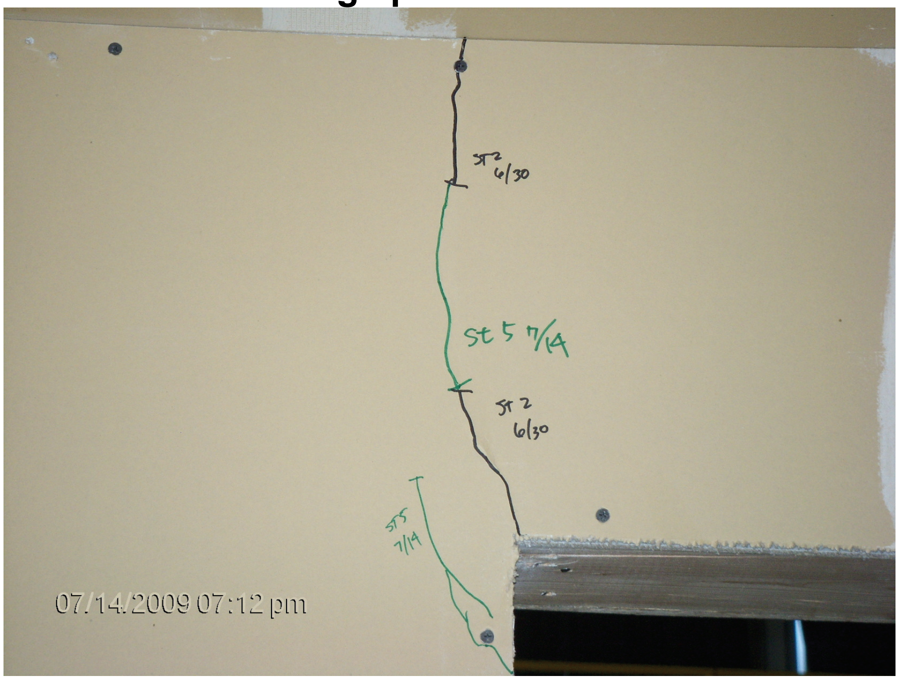

Figure I.21: Crack on Wall A3, Story 4 (over window opening)

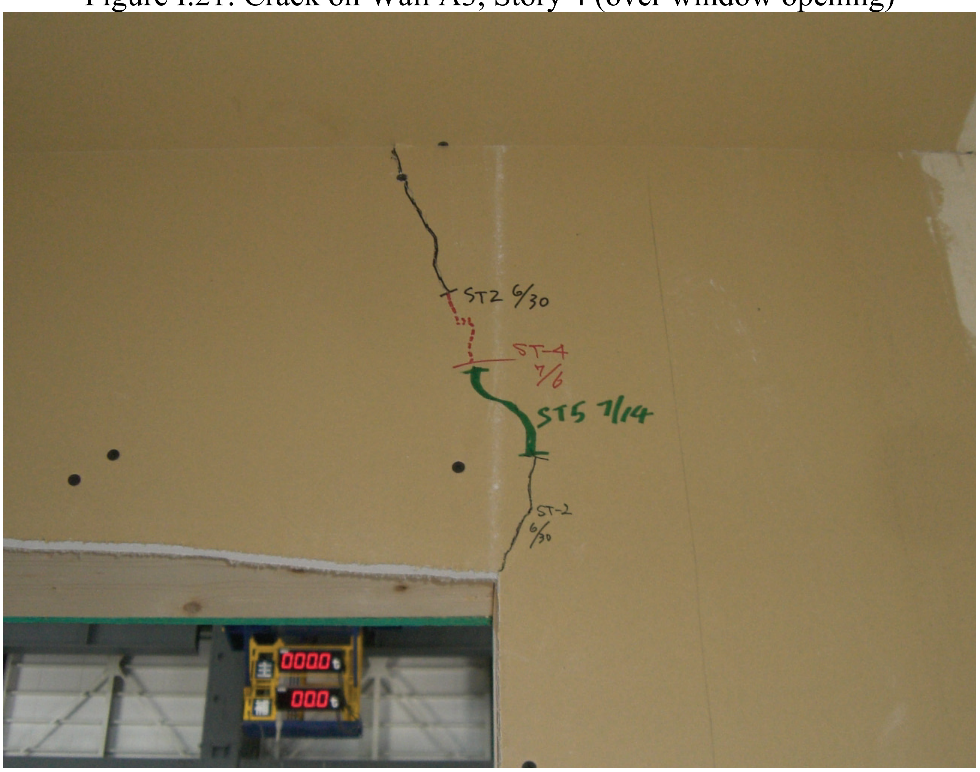

Figure I.22: Crack on Wall E1, Story 5 (over window opening)

Appendix I

Selected damage photo for Seismic Test 5

Figure I.23: Crack on Wall D2, Story 6 (corner crashing)

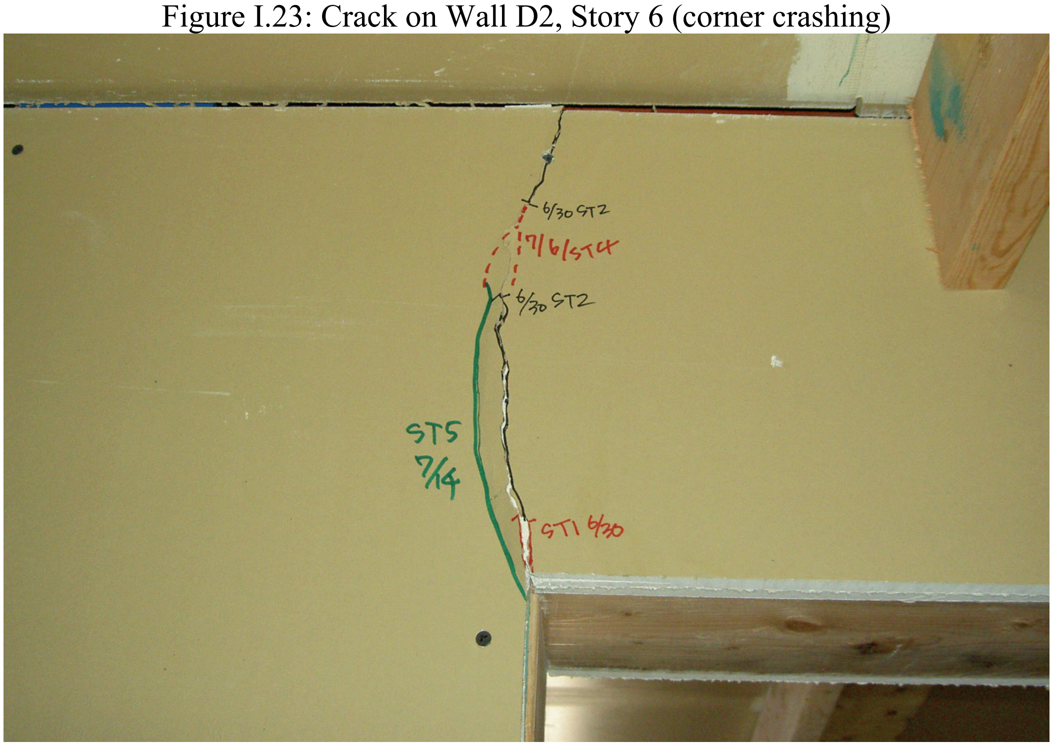

Figure I.24: Crack on Wall 2A, Story 7 (over door opening)

Appendix J

Seismic Test Results: Inter-story Drift Time History

Appendix J

Seismic Test 1

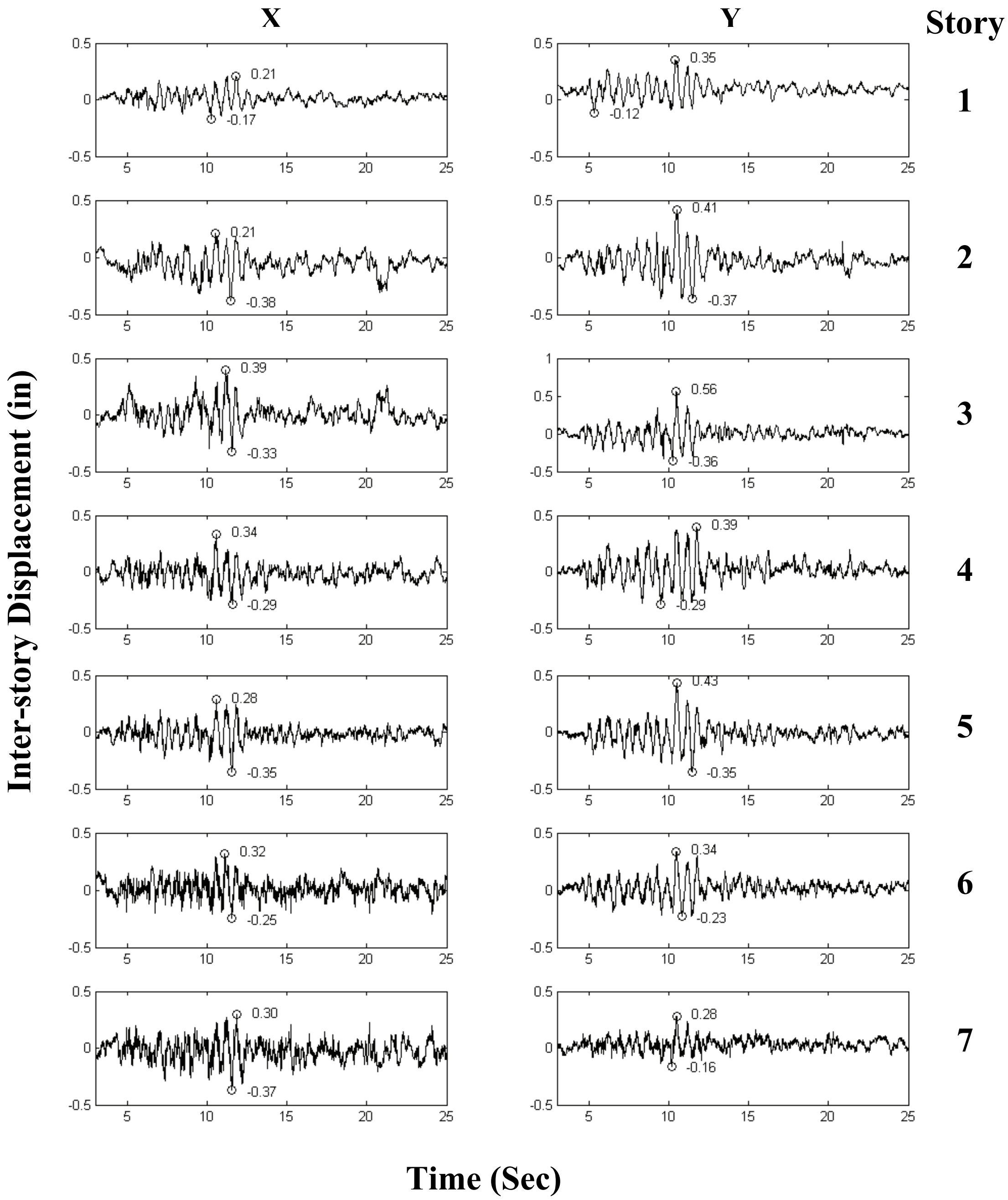

Figure J.1: Relative floor averaged inter-story drift time histories for Seismic Test 1

*Average measurements obtained by averaging all 7 optical tracking point data on the same floor

Appendix J

Seismic Test 2

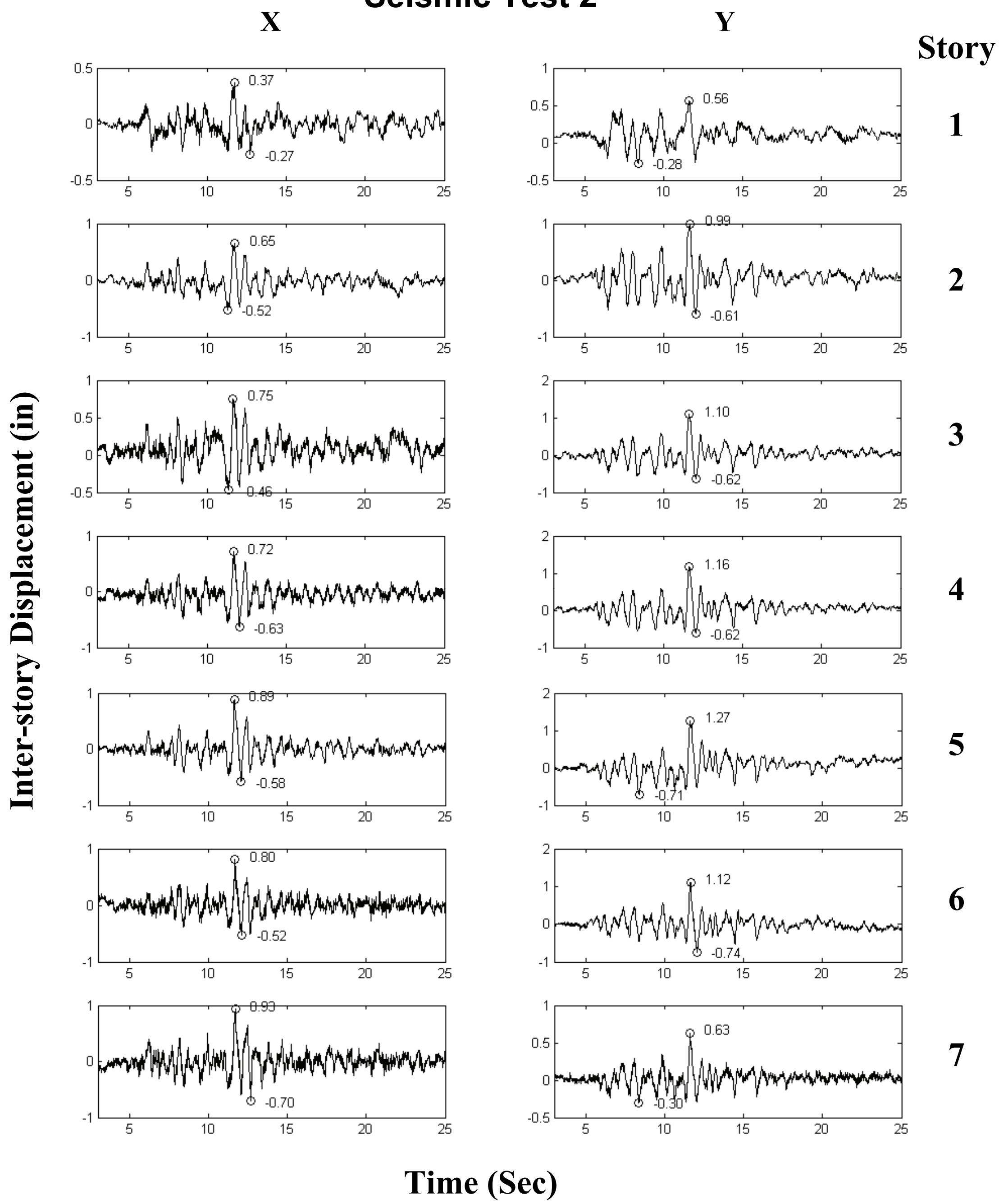

Figure J.2: Relative floor averaged inter-story drift time histories for Seismic Test 2

*Average measurements obtained by averaging all 7 optical tracking point data on the same floor

Appendix J

Seismic Test 3

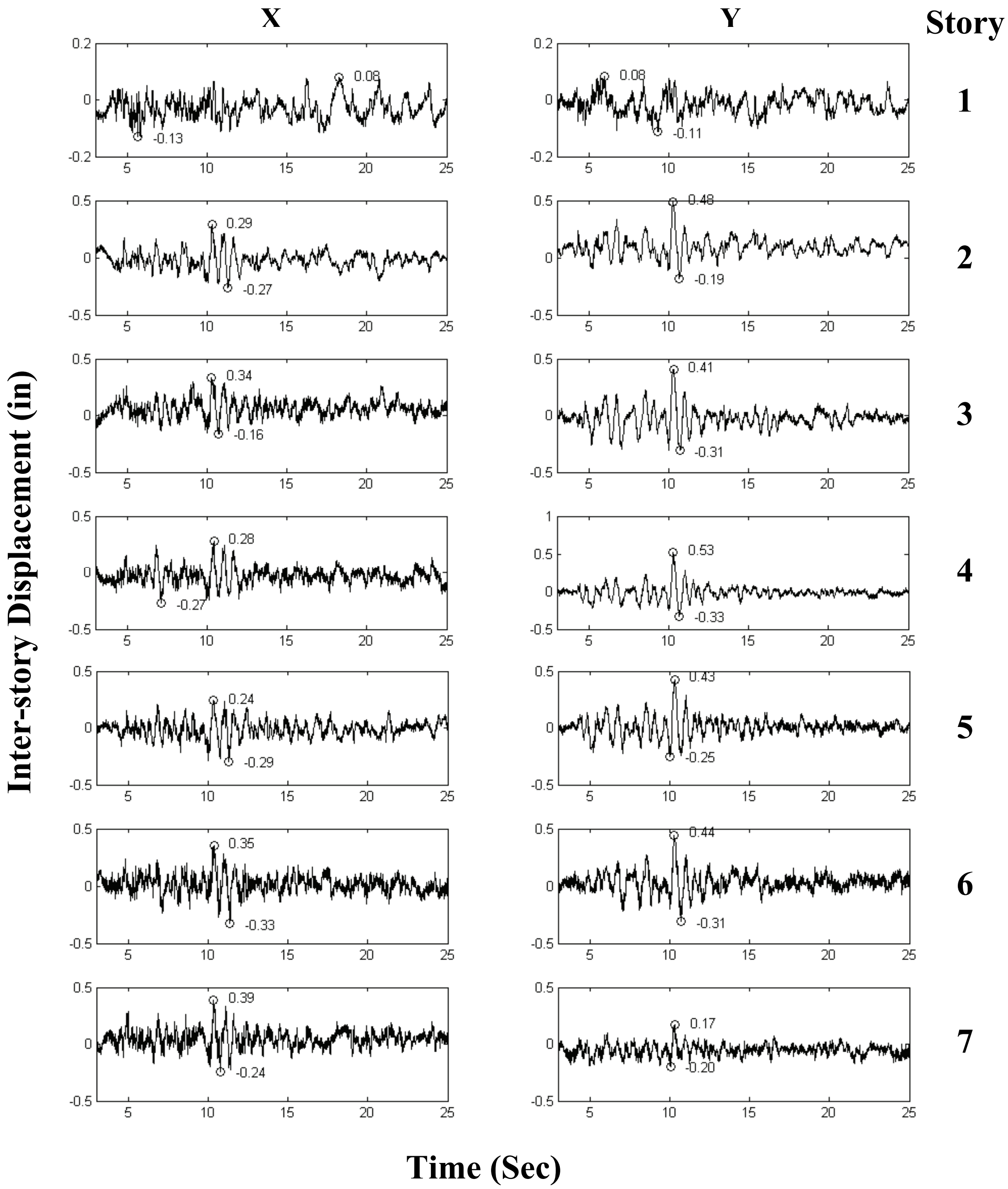

Figure J.3: Relative floor averaged inter-story drift time histories for Seismic Test 3

*Average measurements obtained by averaging all 7 optical tracking point data on the same floor

Appendix J

Seismic Test 4

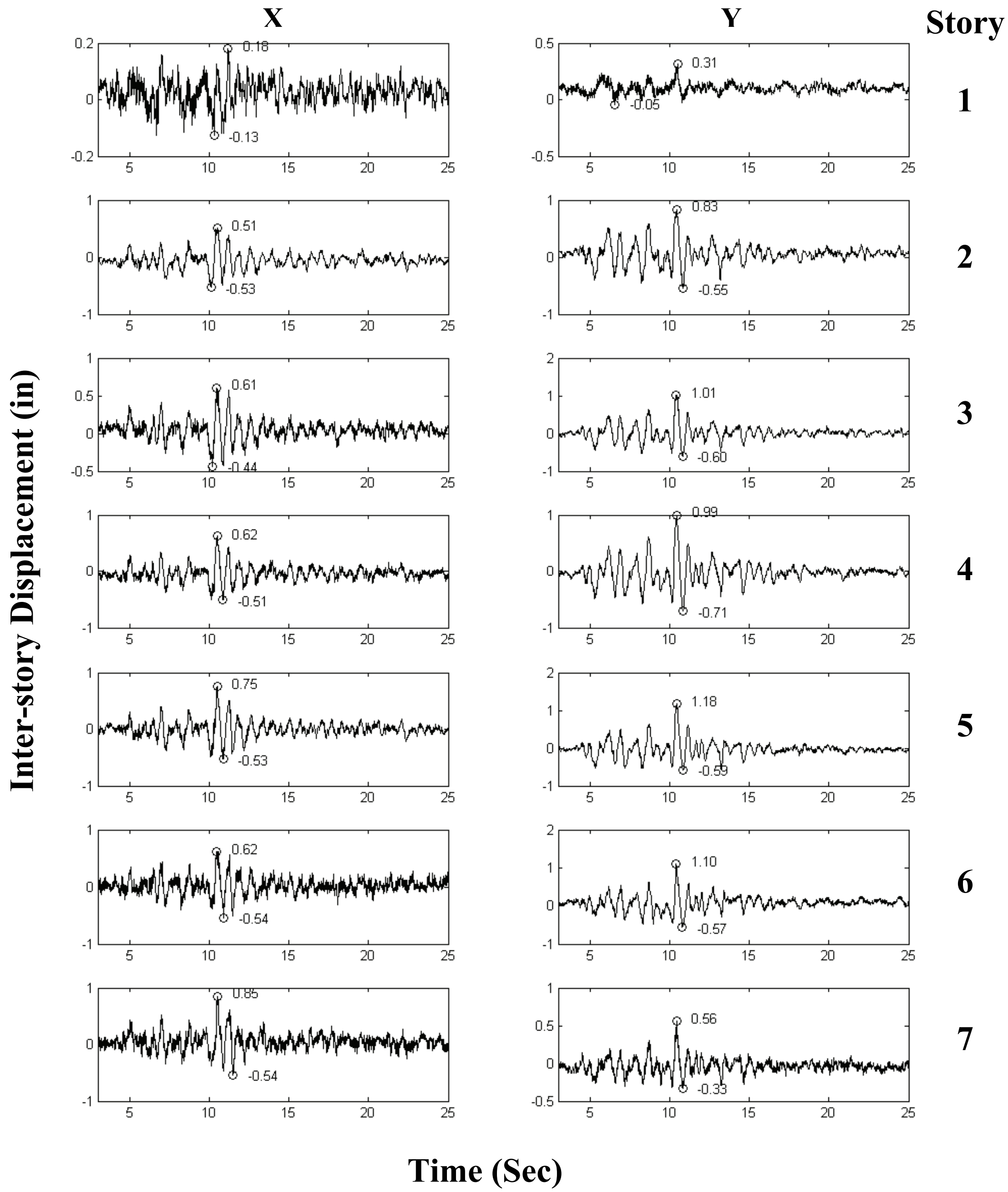

Figure J.4: Relative floor averaged inter-story drift time histories for Seismic Test 4

*Average measurements obtained by averaging all 7 optical tracking point data on the same floor

Appendix J

Seismic Test 5

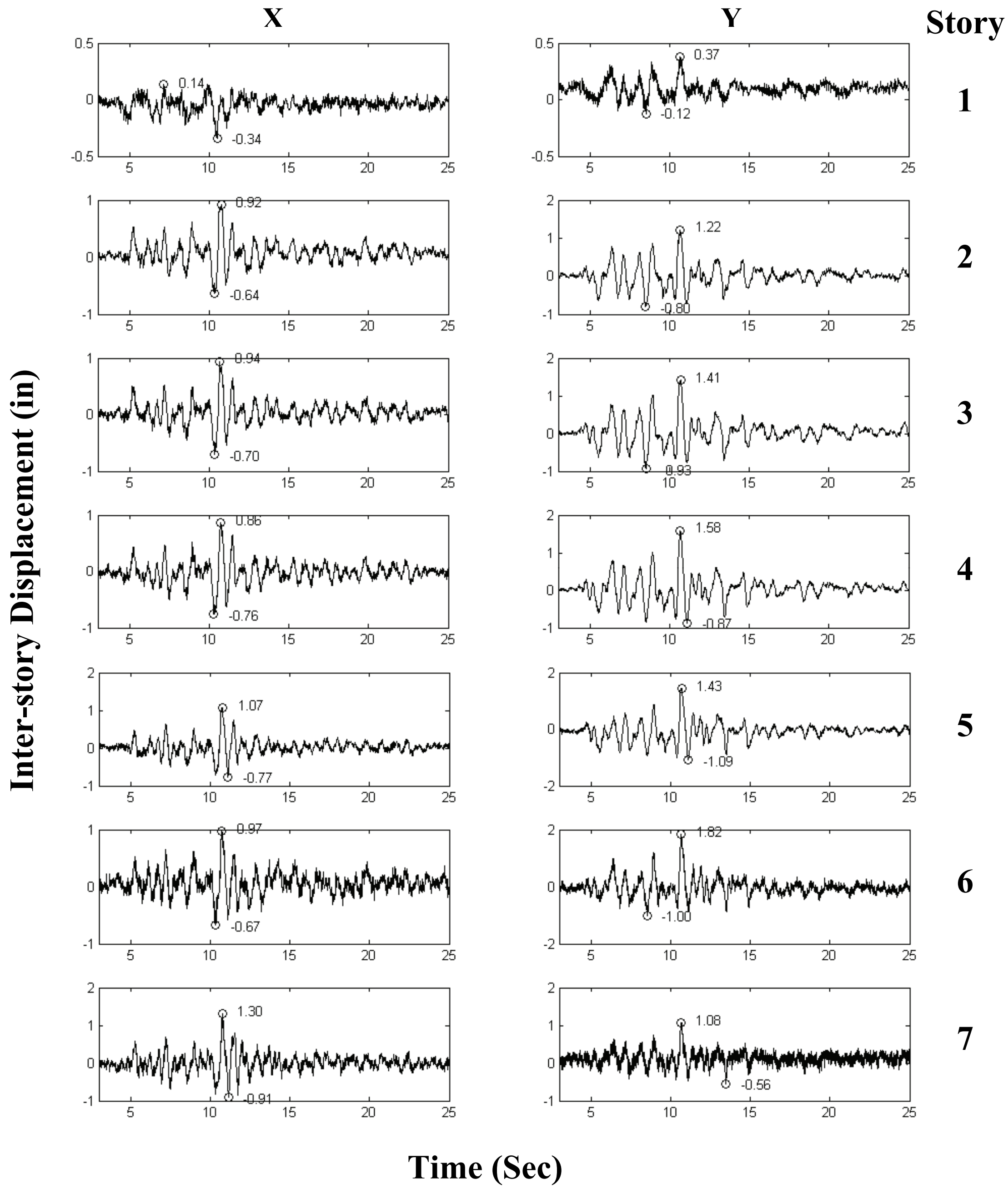

Figure J.5: Relative floor averaged inter-story drift time histories for Seismic Test 5

*Average measurements obtained by averaging all 7 optical tracking point data on the same floor

Appendix K

Seismic Test Results: Absolute Acceleration Time history

Appendix K

Absolute acceleration sensor location (Identical for all stories)

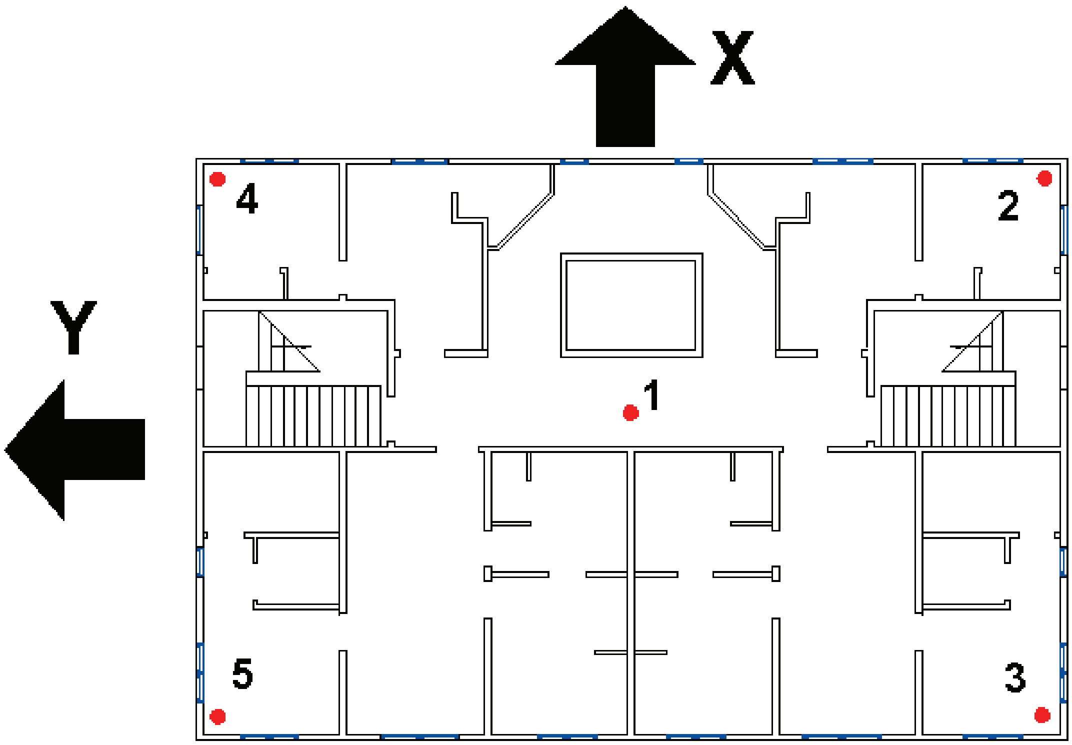

Appendix K

Seismic test 1, Story 2 absolute acceleration

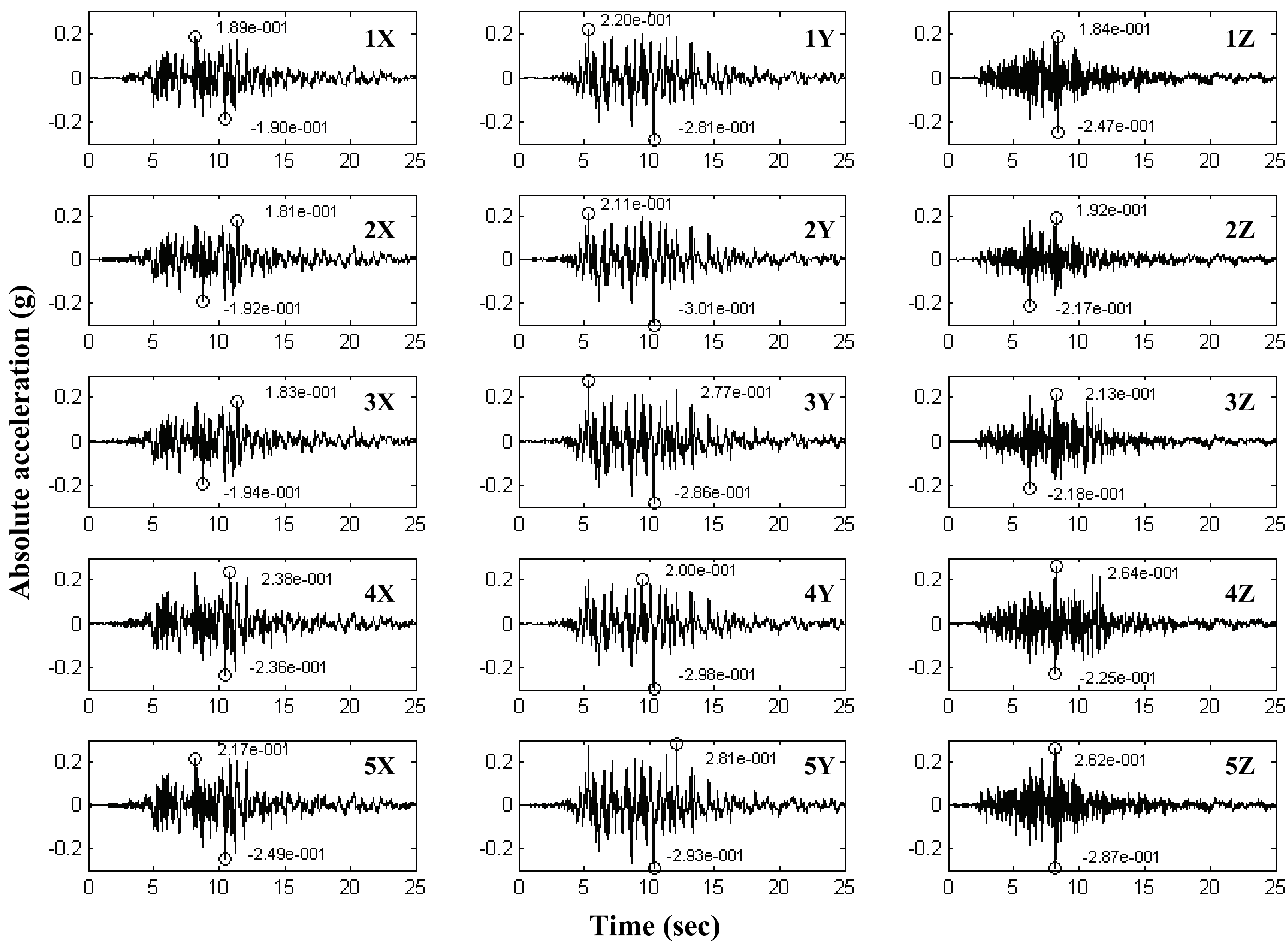

Figure K.1: Absolute acceleration at story 2 locations during Seismic test 1

Appendix K

Seismic test 1, Story 3 absolute acceleration

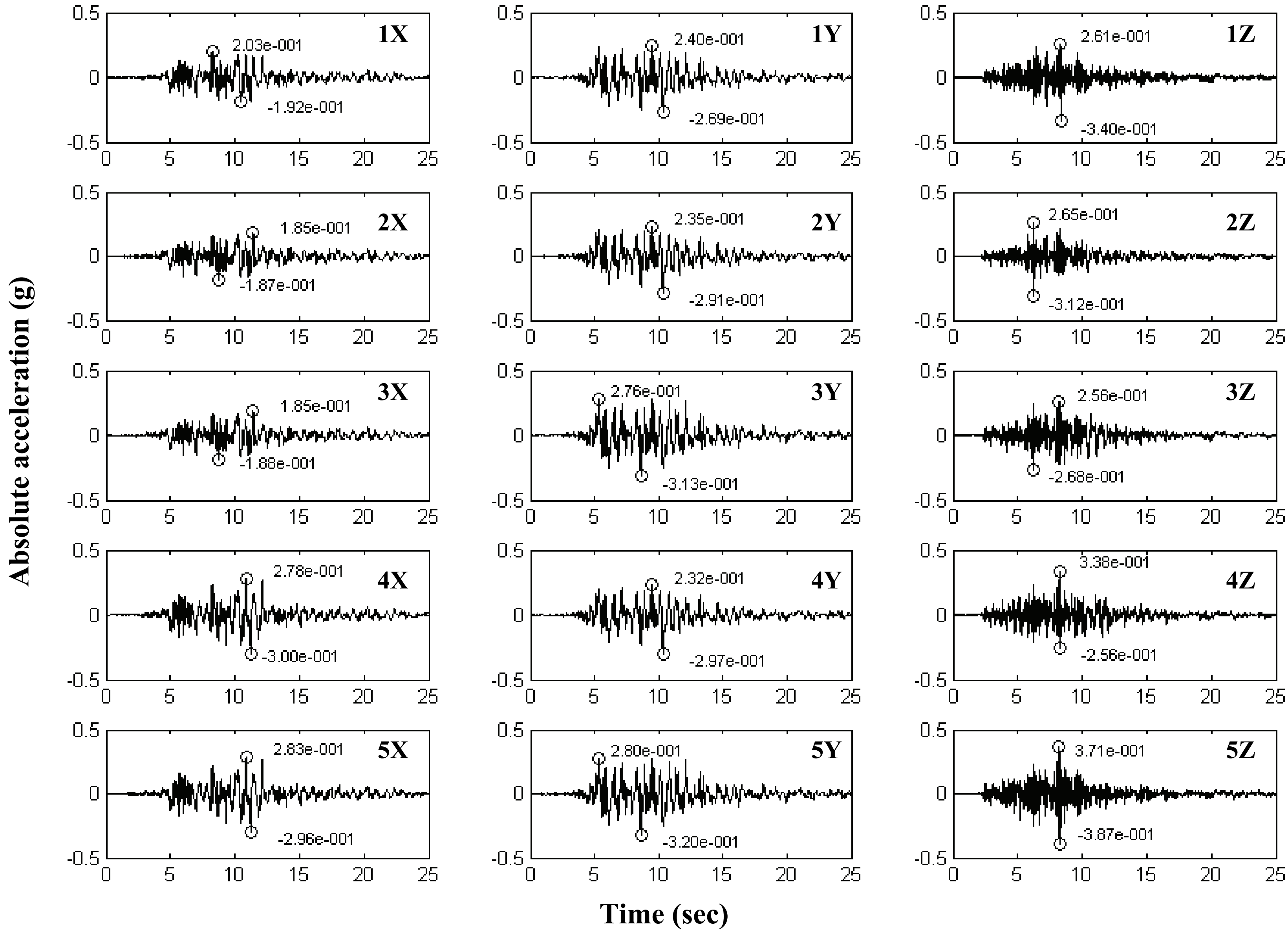

Figure K.2: Absolute acceleration at story 3 locations during Seismic test 1

Appendix K

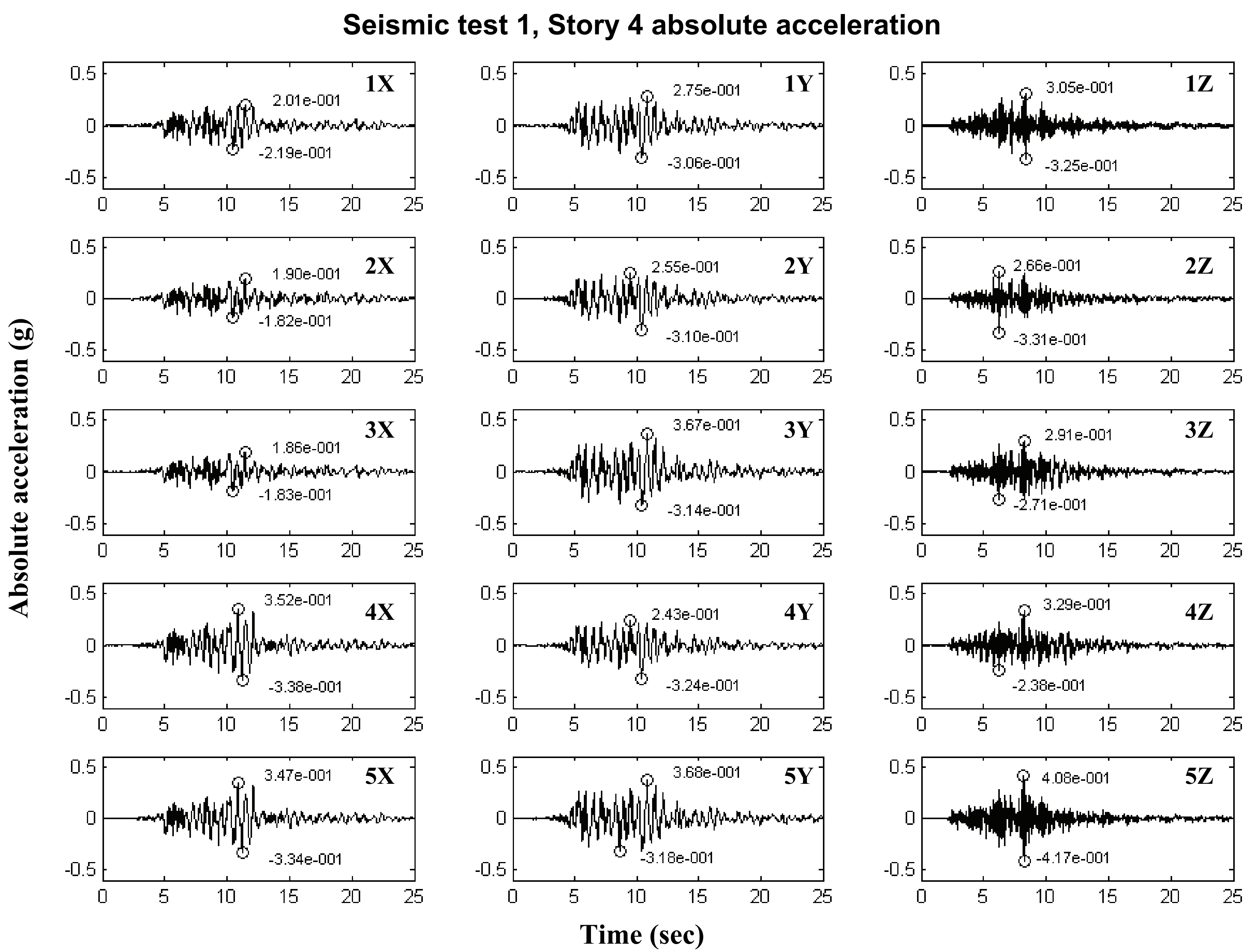

Figure K.3: Absolute acceleration at story 4 locations during Seismic test 1

Appendix K

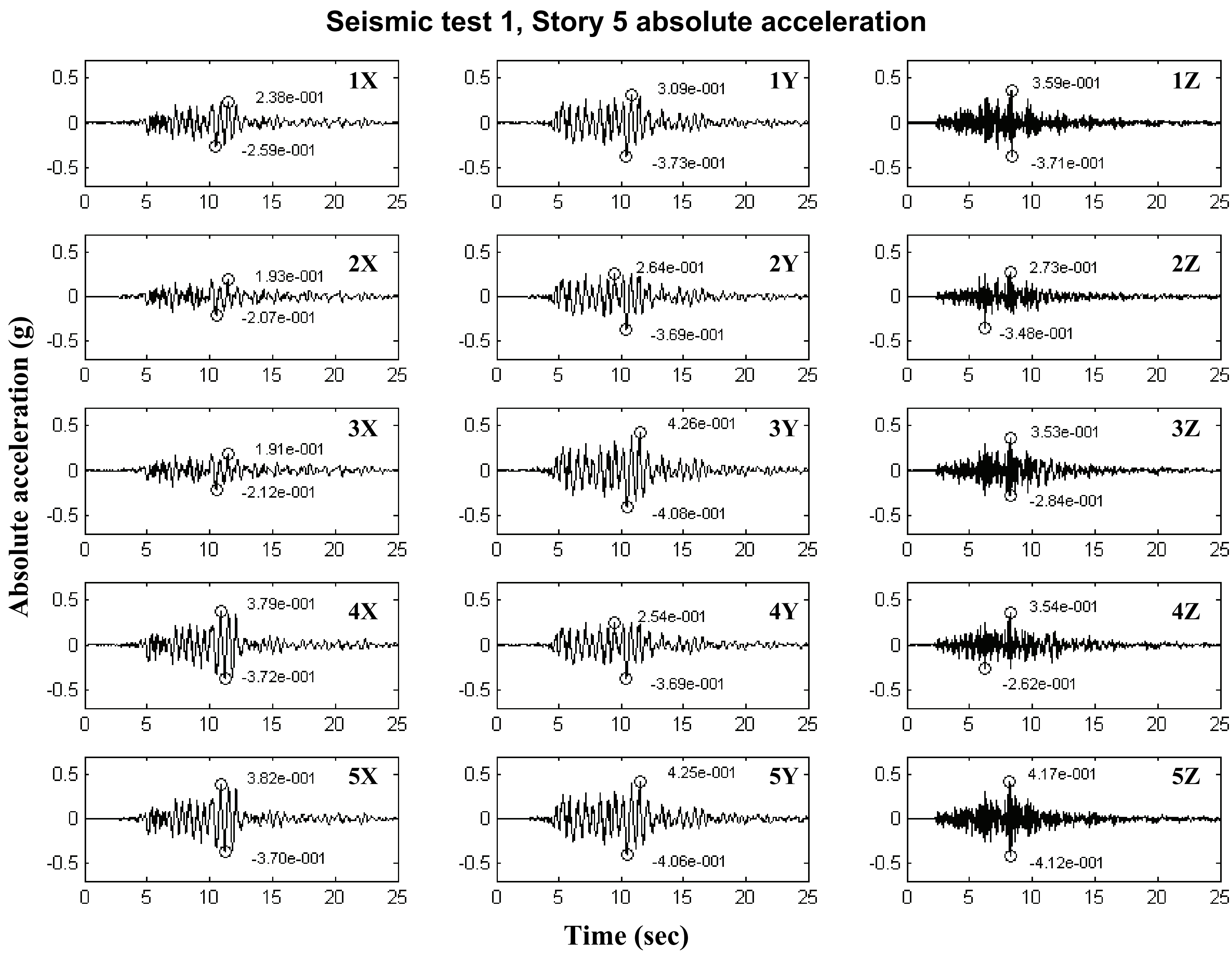

Figure K.4: Absolute acceleration at story 5 locations during Seismic test 1

Appendix K

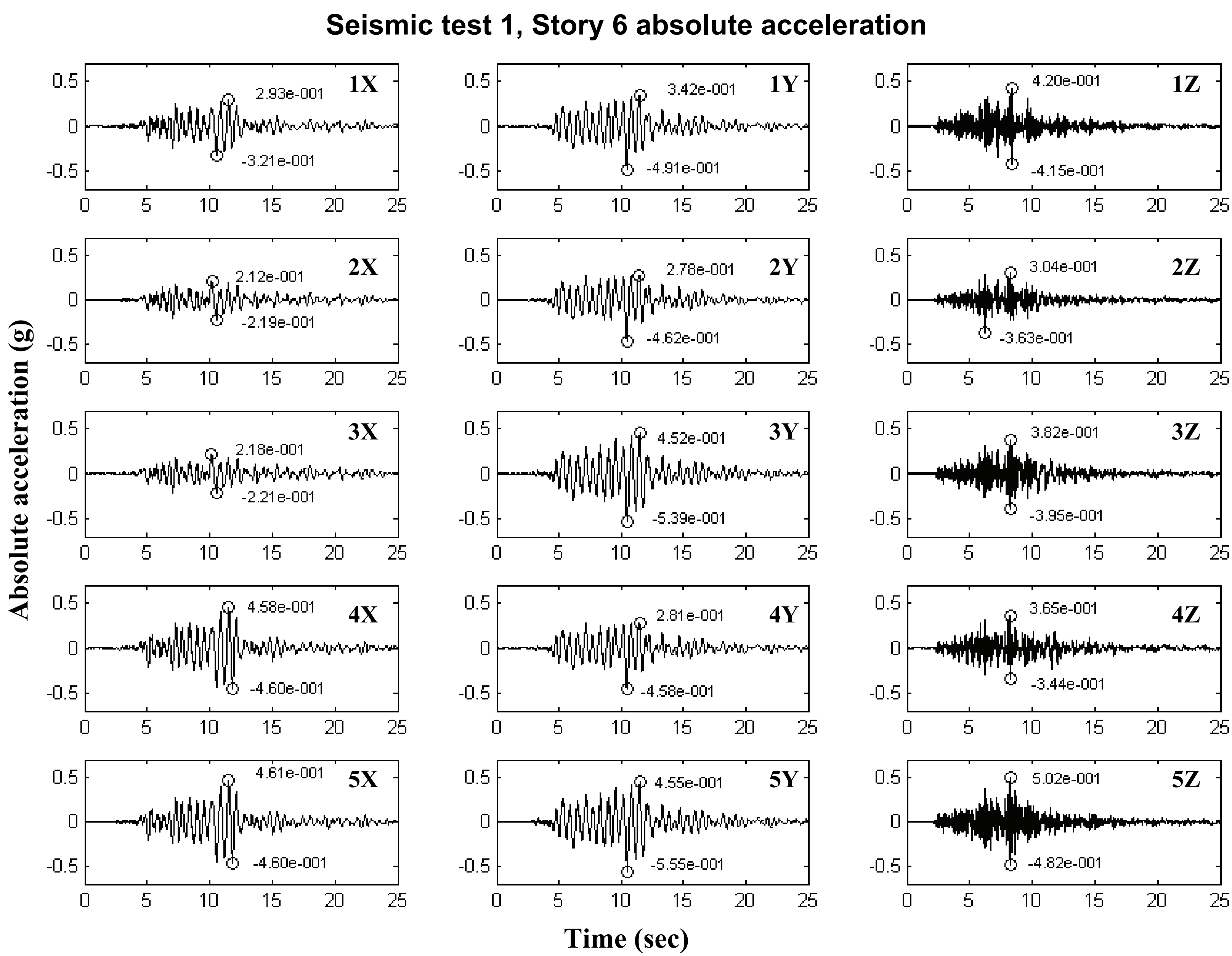

Figure K.5: Absolute acceleration at story 6 locations during Seismic test 1

Appendix K

Seismic test 1, Story 7 absolute acceleration

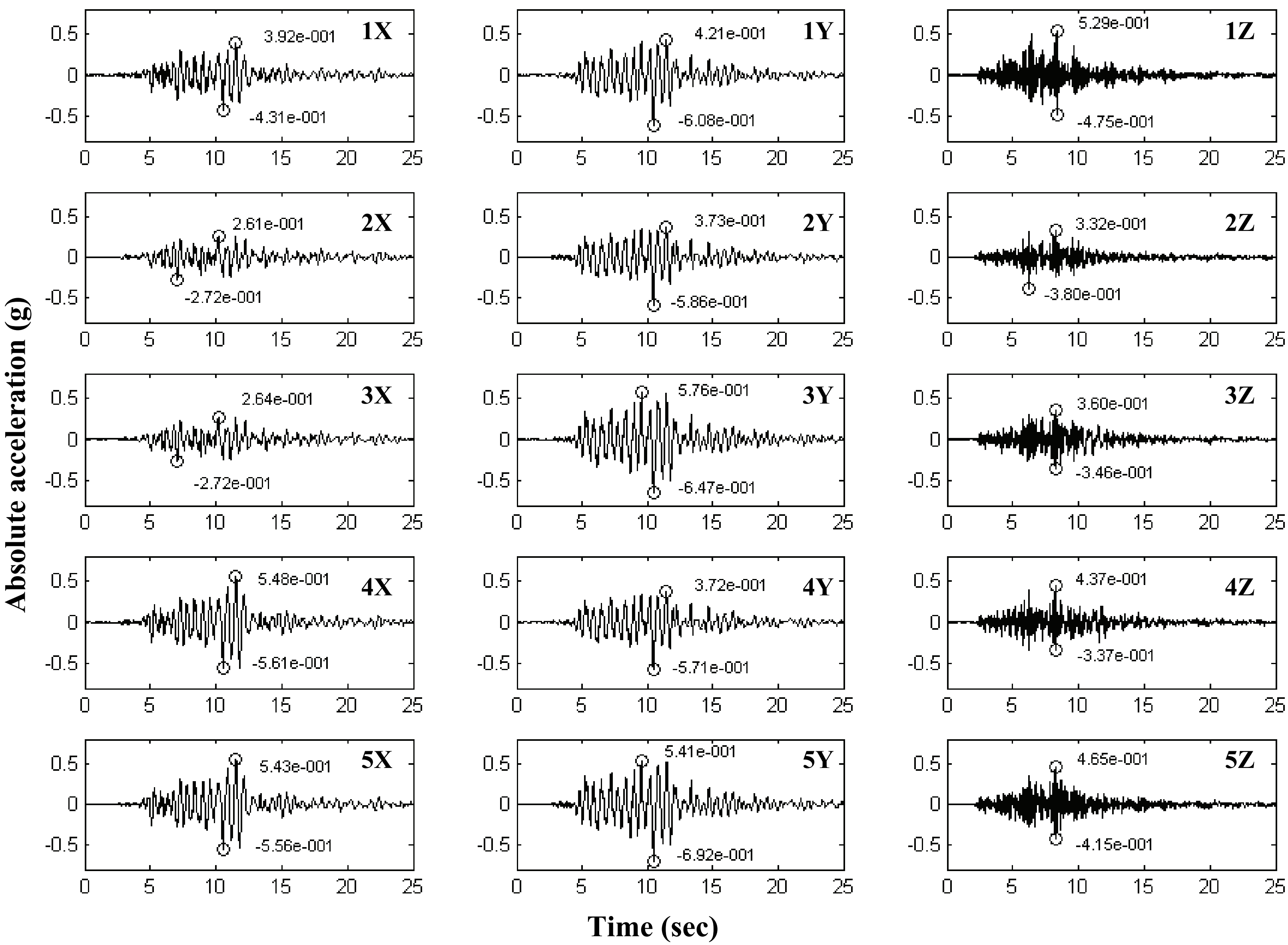

Figure K.6: Absolute acceleration at story 7 locations during Seismic test 1

Appendix K

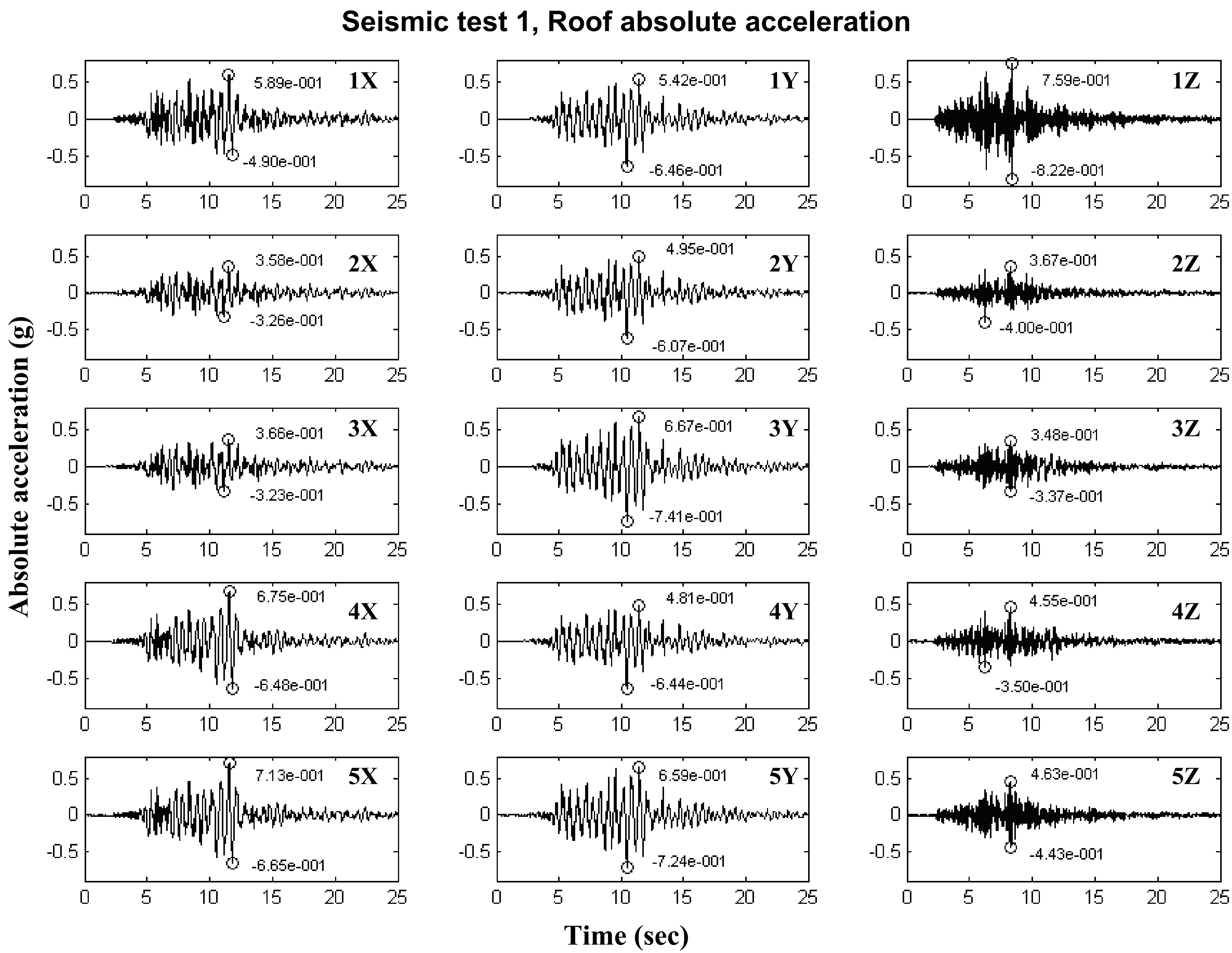

Figure K.7: Absolute acceleration at roof locations during Seismic test 1

Appendix K

Seismic test 2, Story 2 absolute acceleration

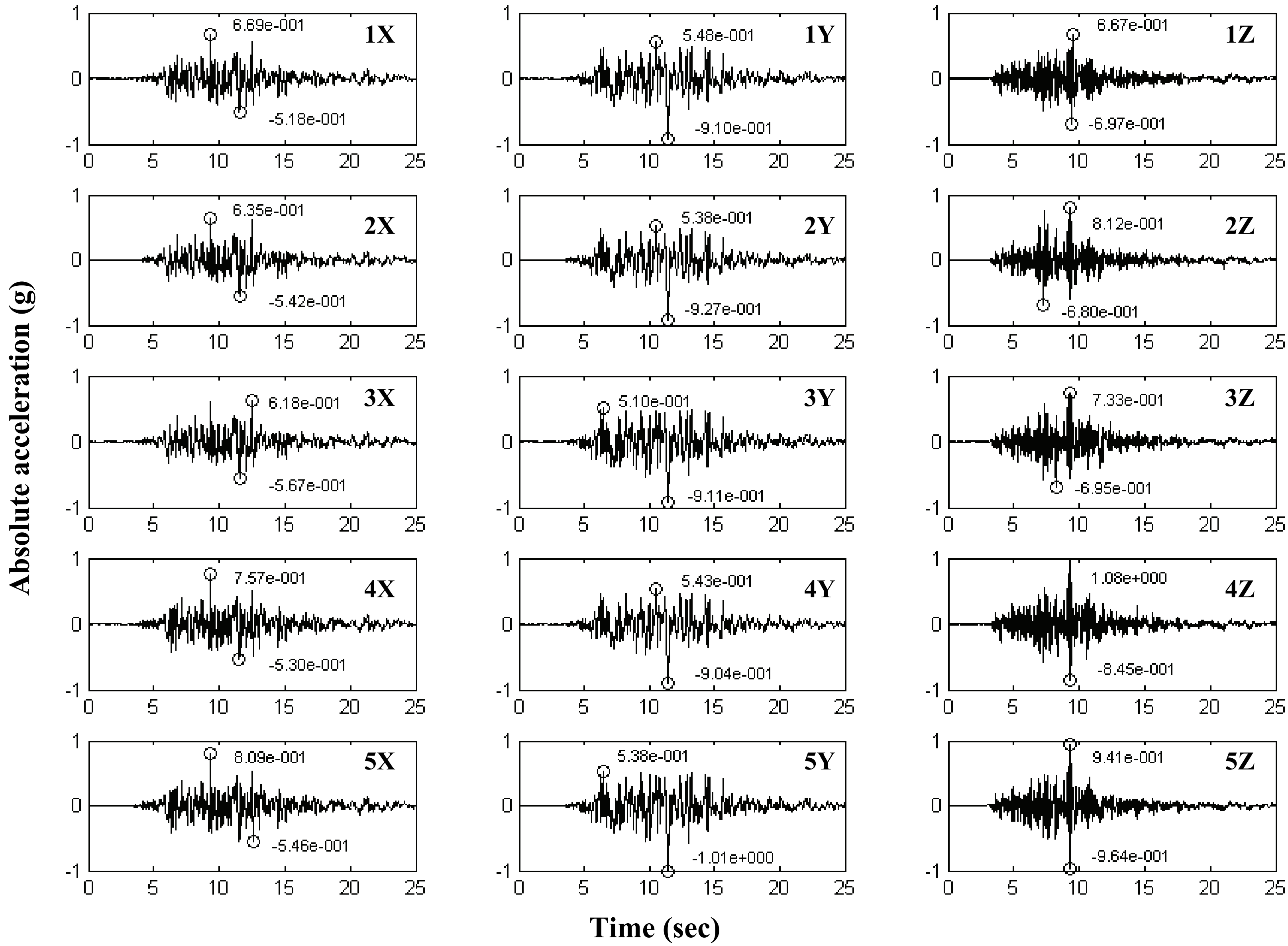

Figure K.8: Absolute acceleration at story 2 locations during Seismic test 2

Appendix K

Seismic test 2, Story 3 absolute acceleration

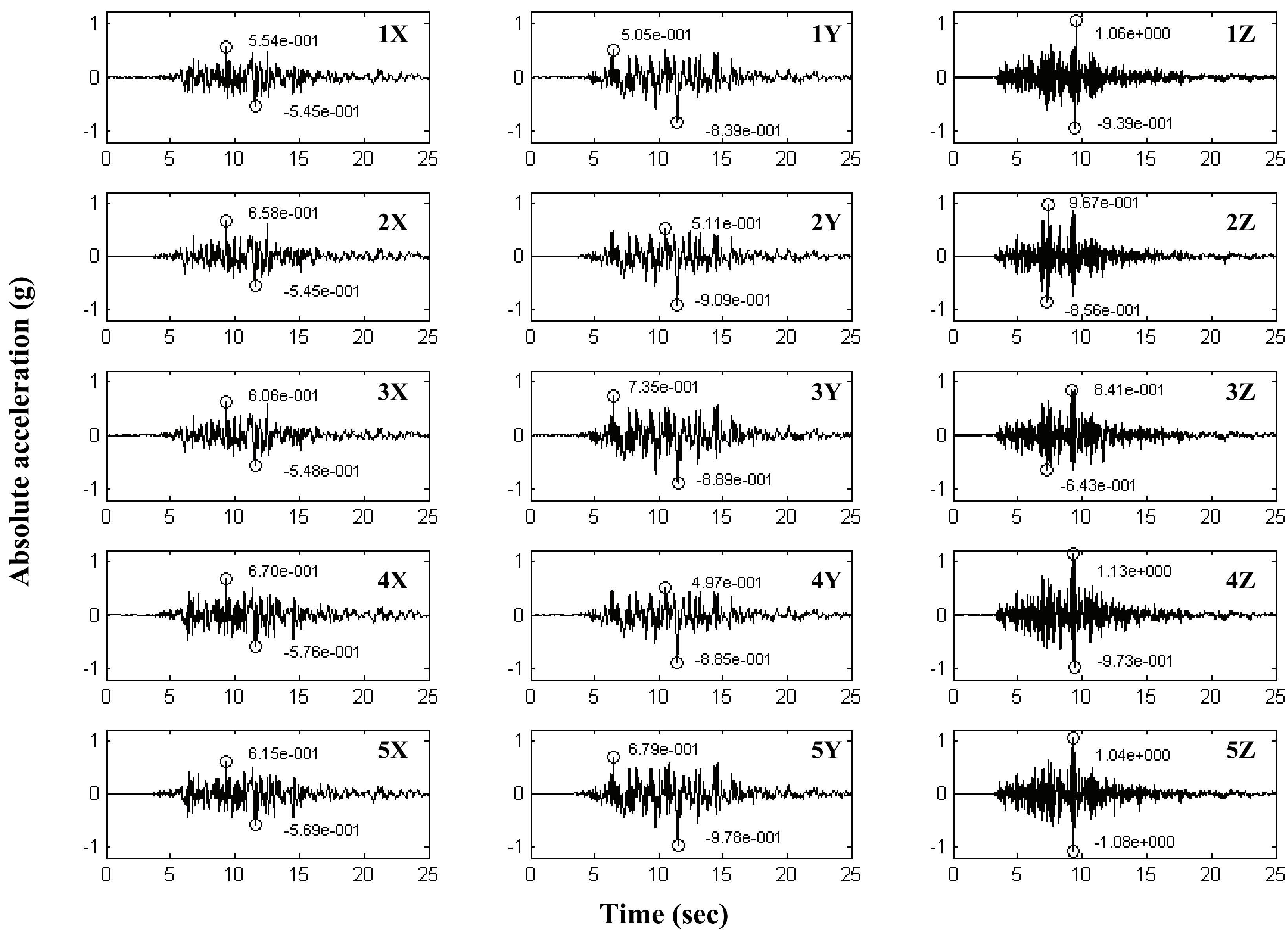

Figure K.9: Absolute acceleration at story 3 locations during Seismic test 2

Appendix K

Seismic test 2, Story 4 absolute acceleration

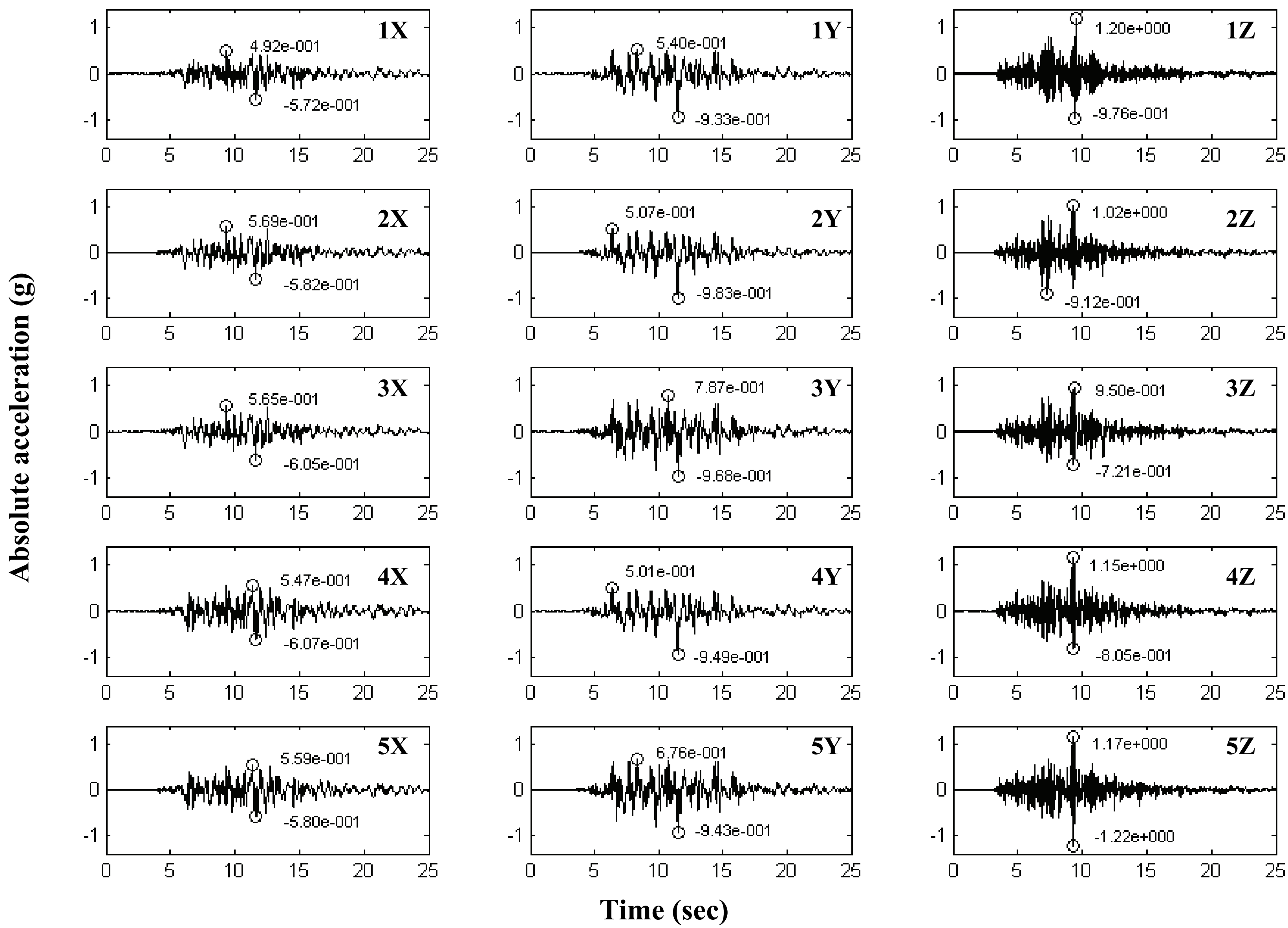

Figure K.10: Absolute acceleration at story 4 locations during Seismic test 2

Appendix K

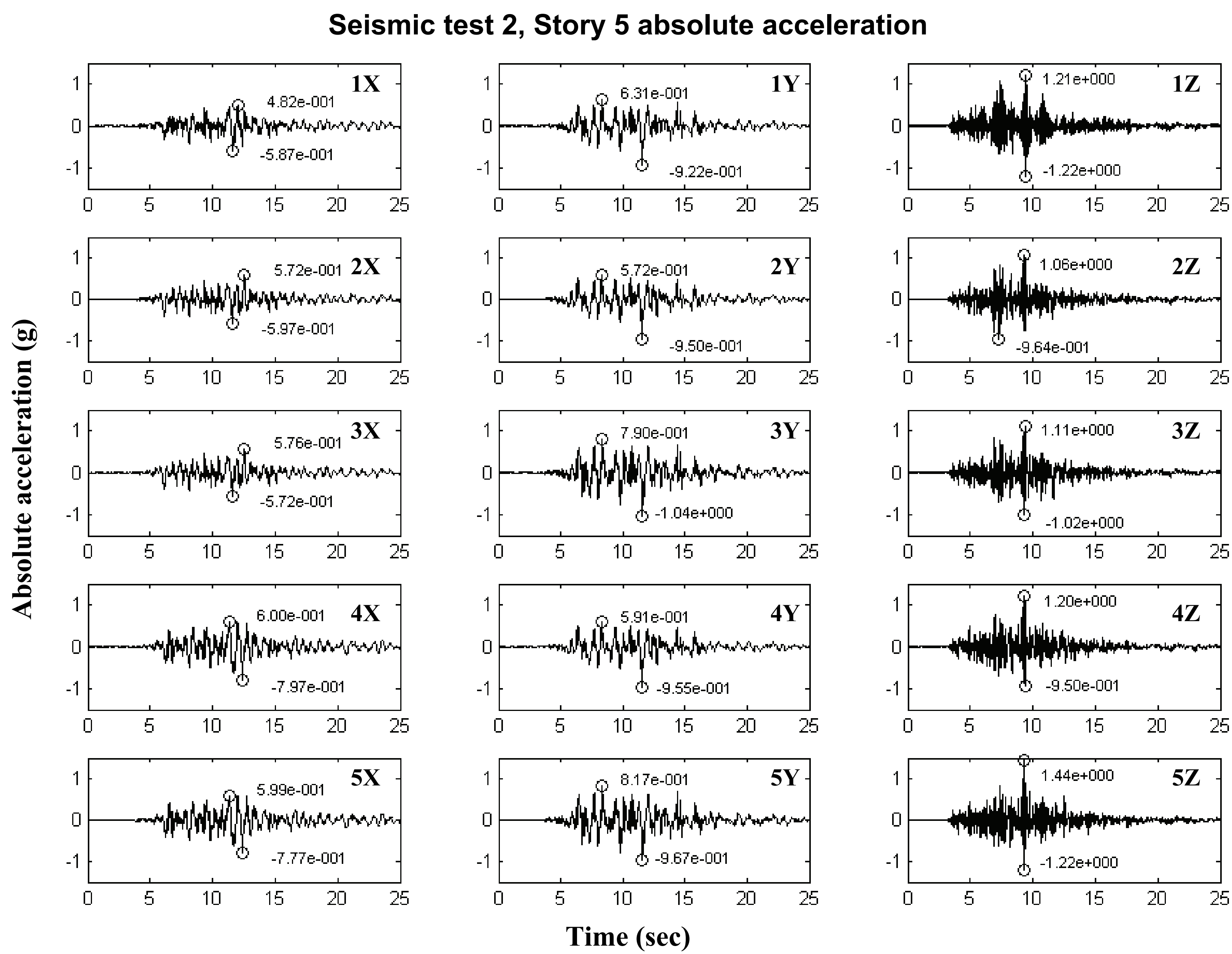

Figure K.11: Absolute acceleration at story 5 locations during Seismic test 2

Appendix K

Seismic test 2, Story 6 absolute acceleration

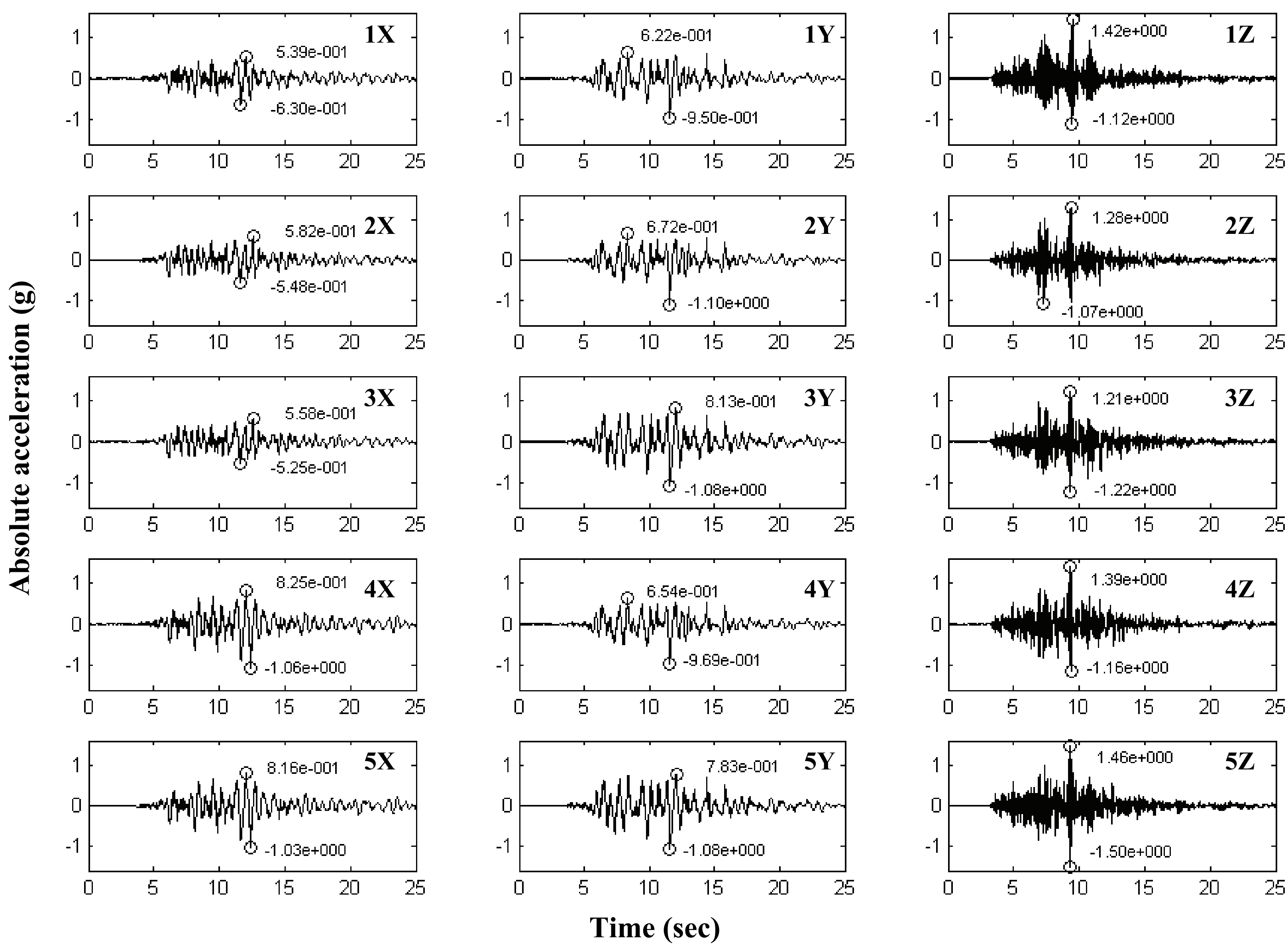

Figure K.12: Absolute acceleration at story 6 locations during Seismic test 2

Appendix K

Seismic test 2, Story 7 absolute acceleration

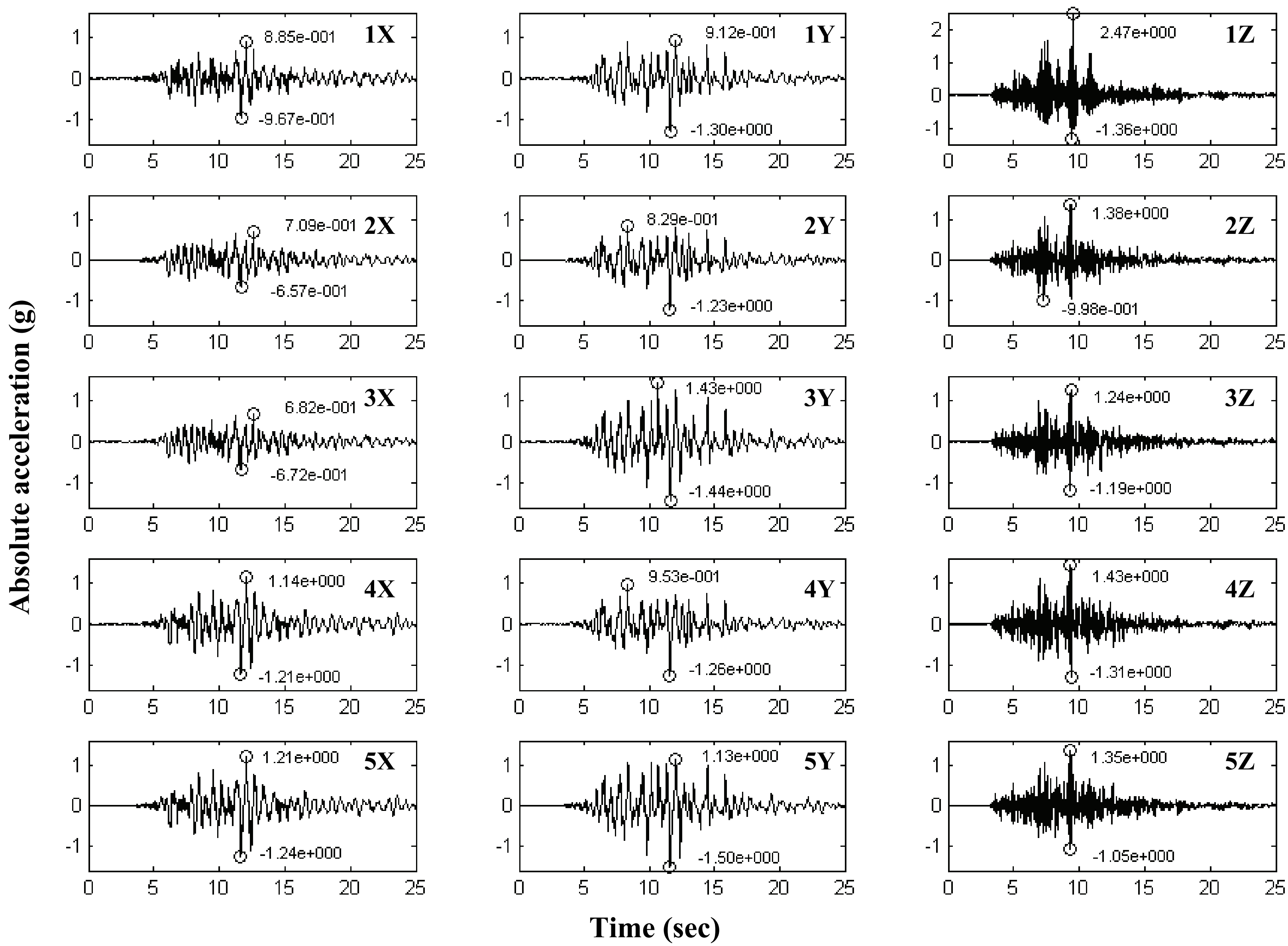

Figure K.13: Absolute acceleration at story 7 locations during Seismic test 2

Appendix K

Seismic test 2, Roof absolute acceleration

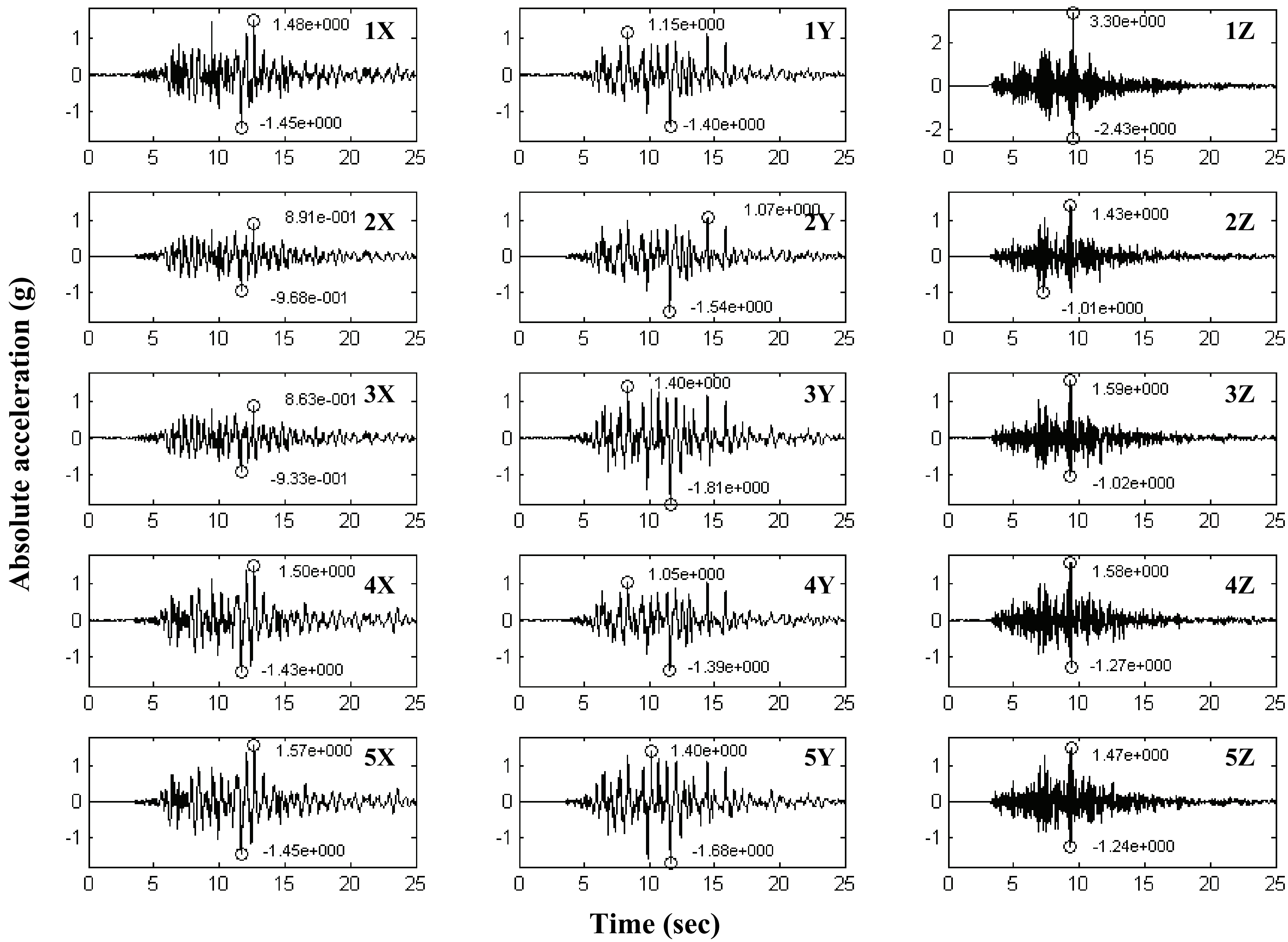

Figure K.14: Absolute acceleration at roof locations during Seismic test 2

Appendix K

Seismic test 3, Story 2 absolute acceleration

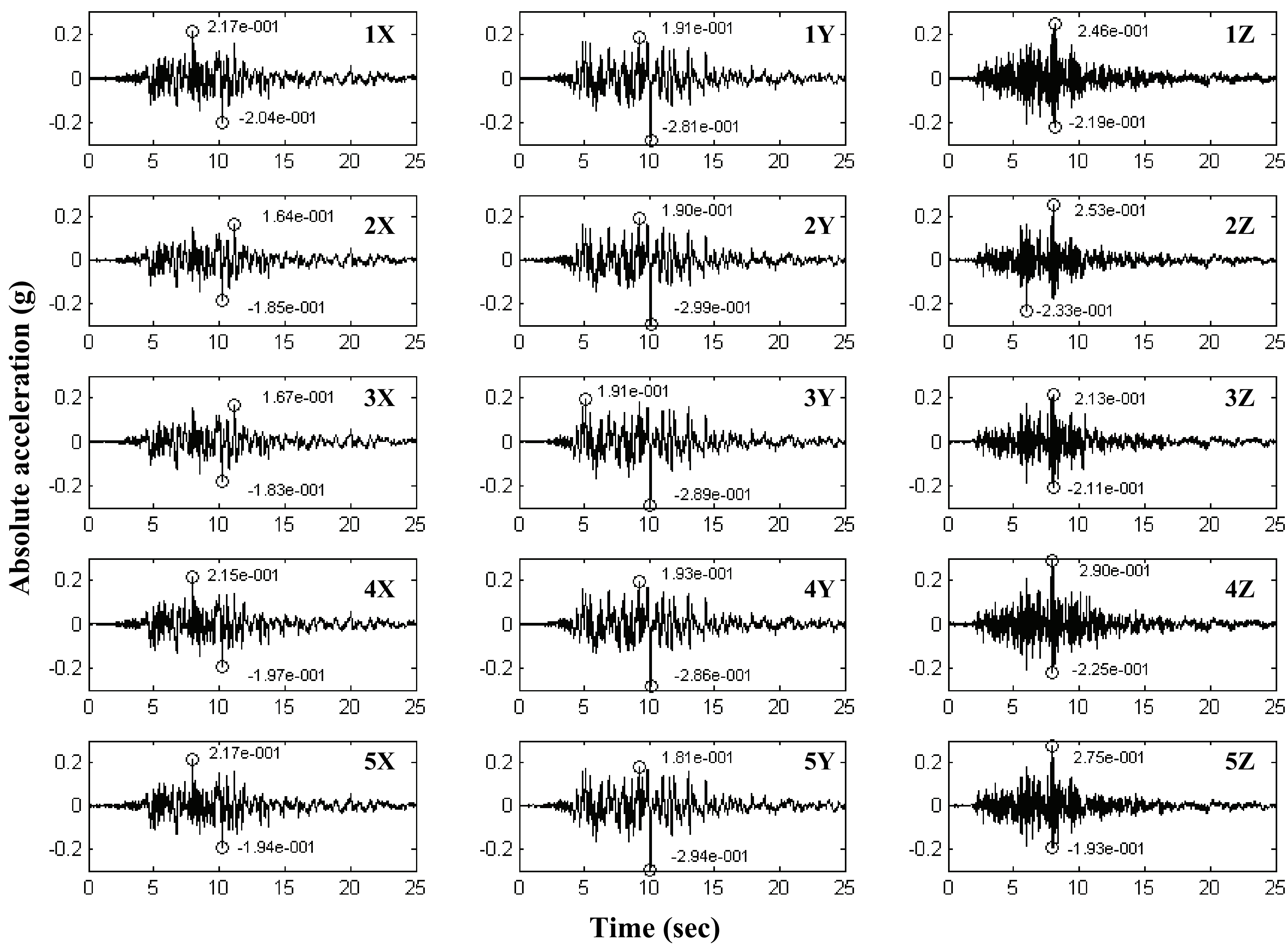

Figure K.15: Absolute acceleration at story 2 locations during Seismic test 3

Appendix K

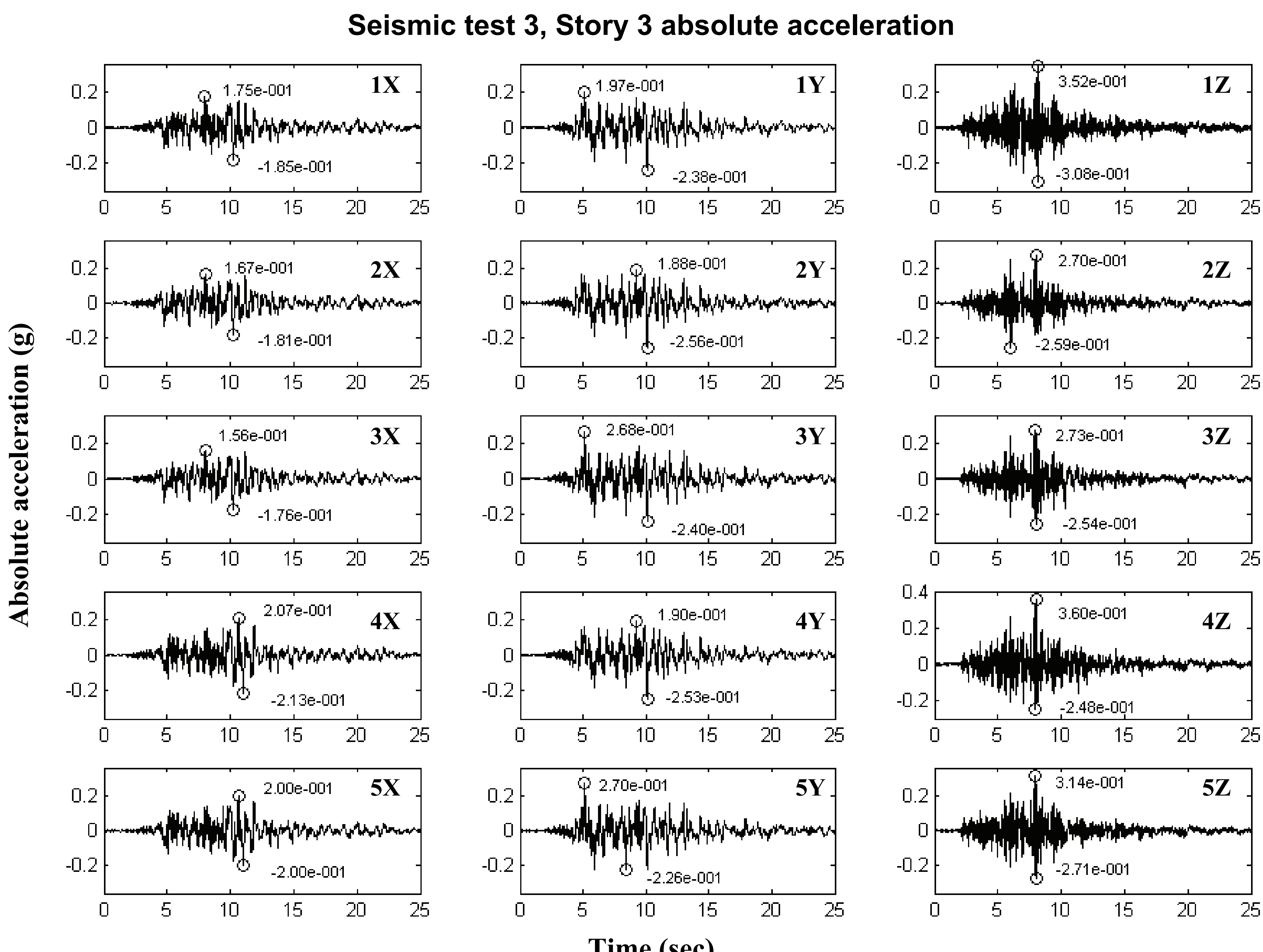

Figure K.16: Absolute acceleration at story 3 locations during Seismic test 3

Appendix K

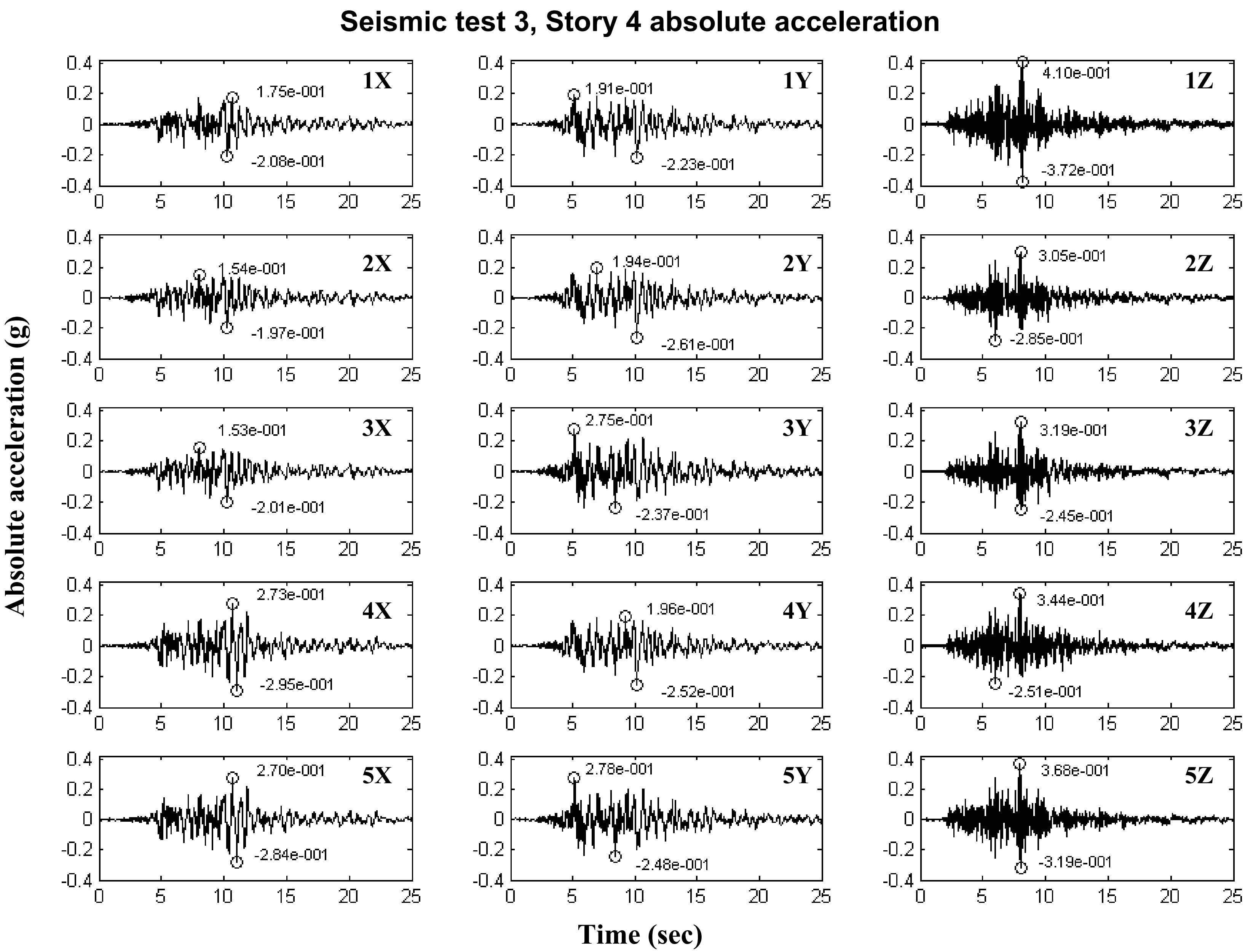

Figure K.17: Absolute acceleration at story 4 locations during Seismic test 3

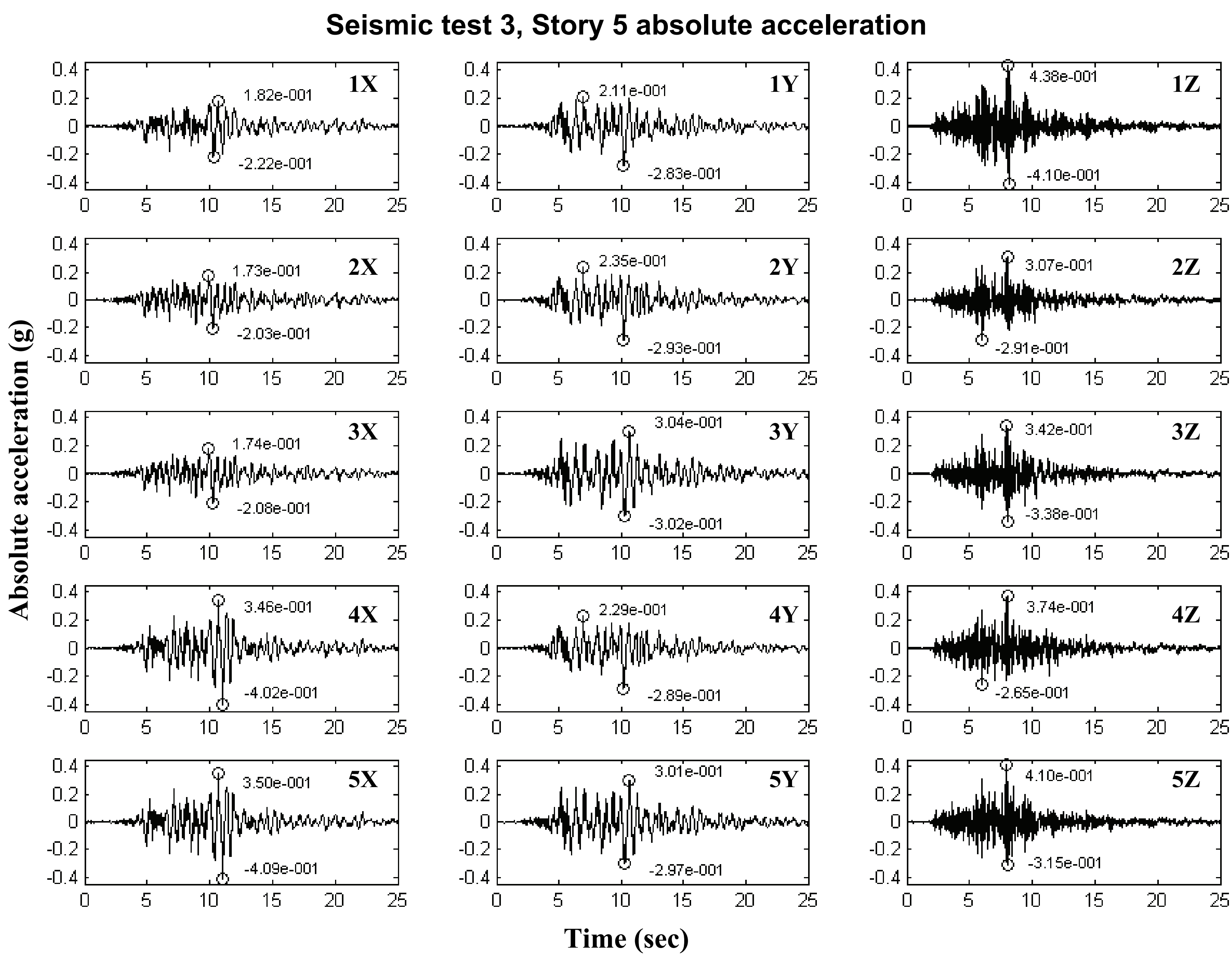

Figure K.18: Absolute acceleration at story 5 locations during Seismic test 3

Appendix K

Seismic test 3, Story 6 absolute acceleration

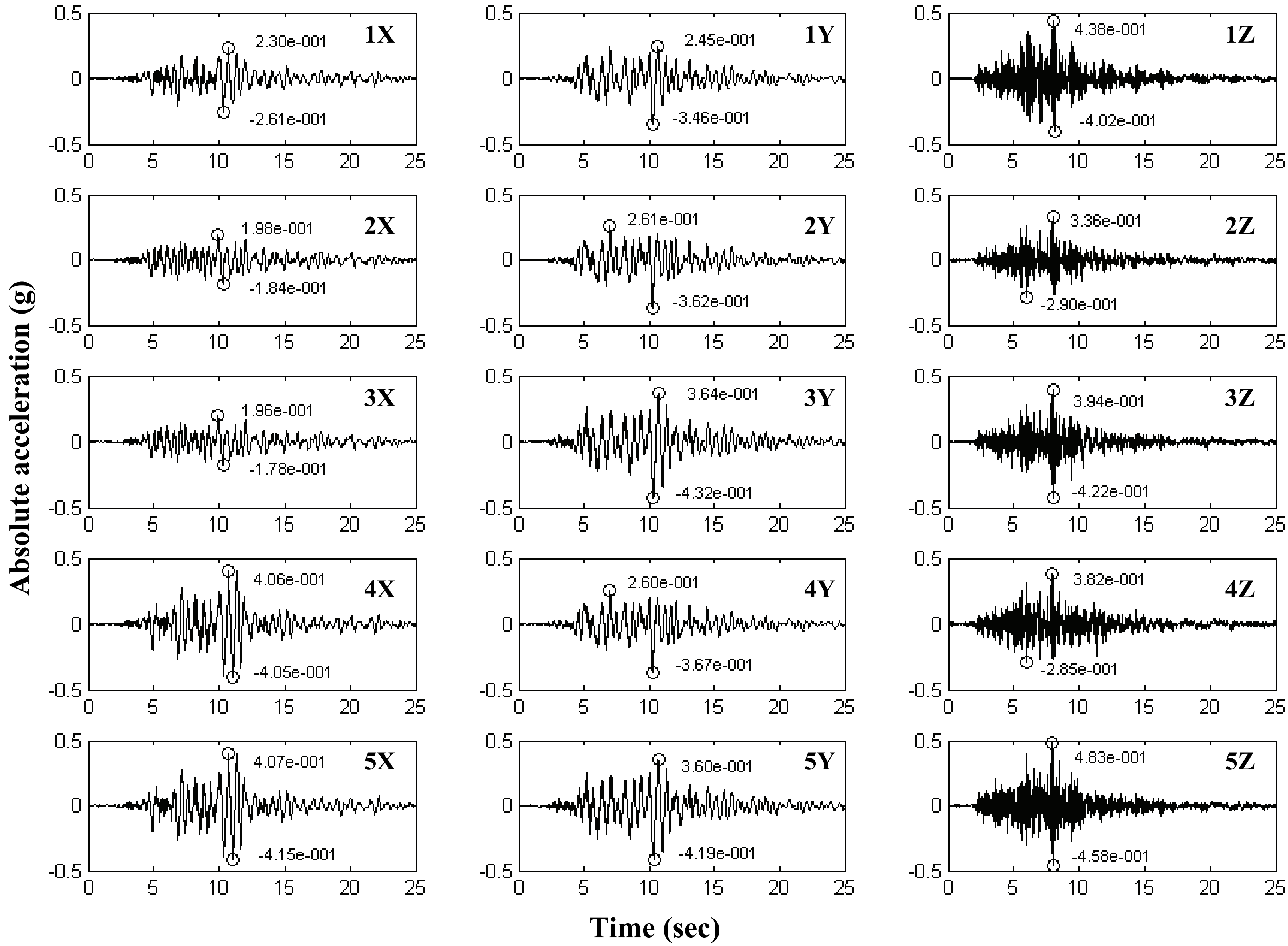

Figure K.19: Absolute acceleration at story 6 locations during Seismic test 3

Appendix K

Seismic test 3, Story 7 absolute acceleration

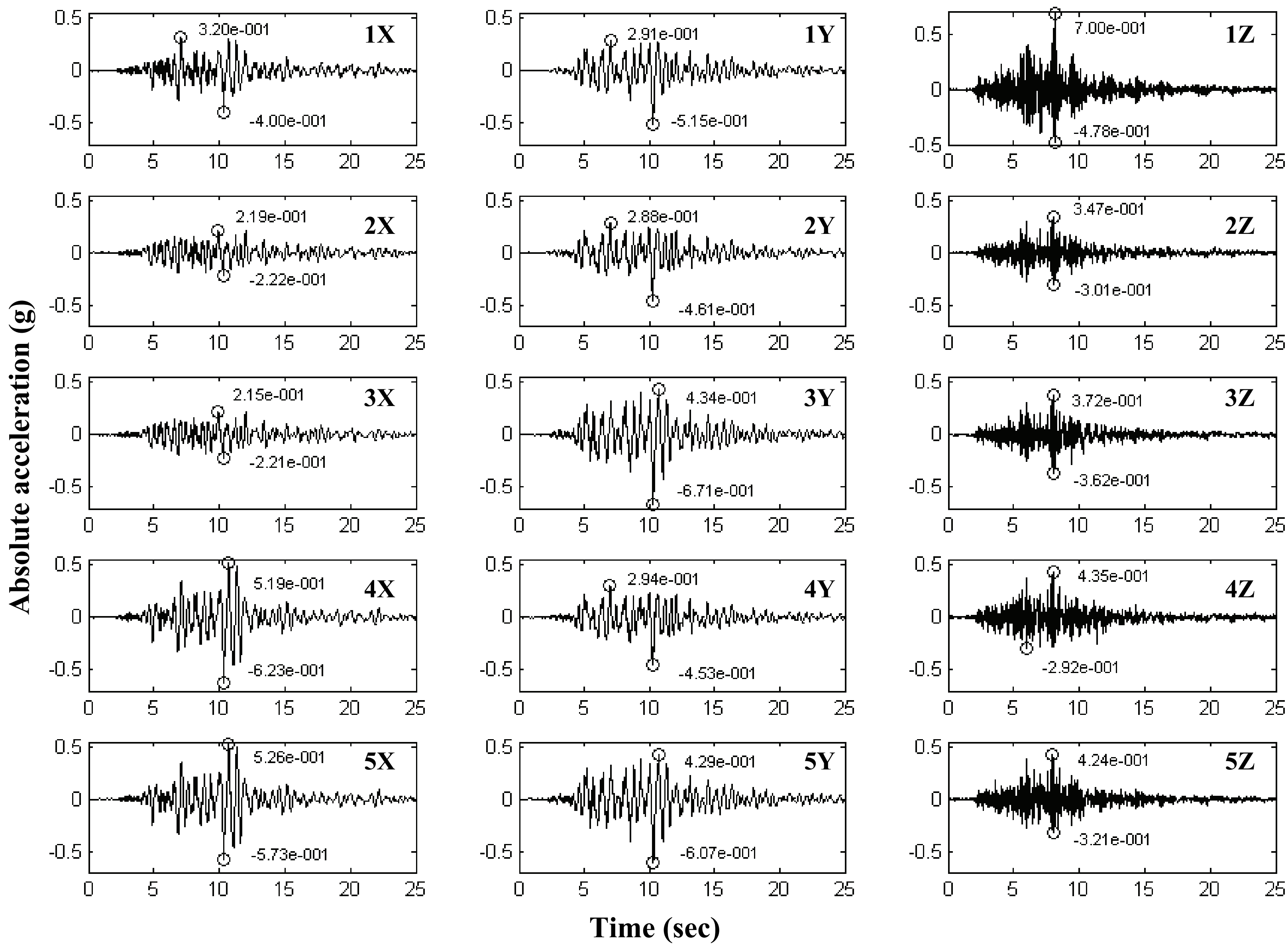

Figure K.20: Absolute acceleration at story 7 locations during Seismic test 3

Appendix K

Seismic test 3, Roof absolute acceleration

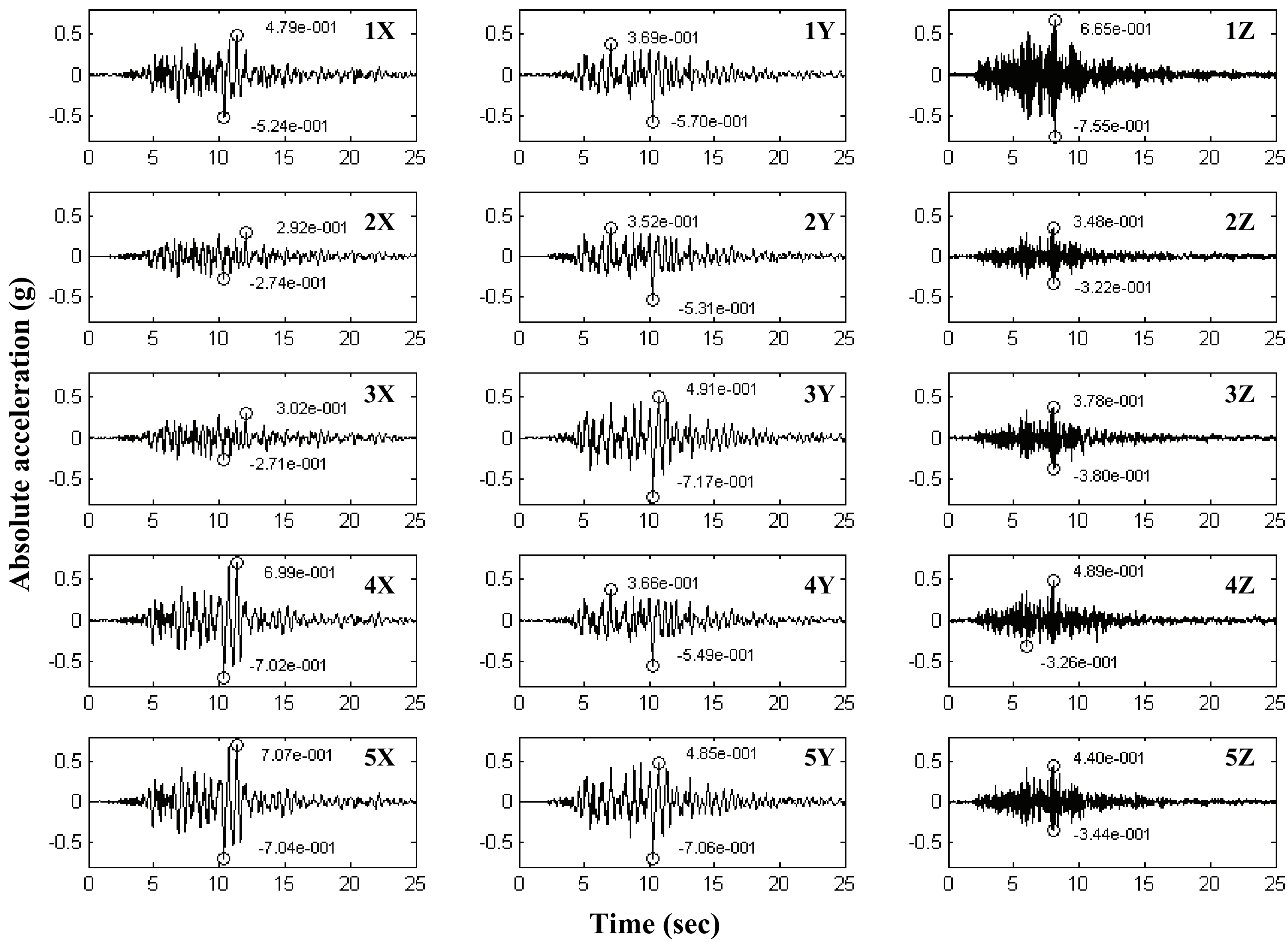

Figure K.21: Absolute acceleration at roof locations during Seismic test 3

Appendix K

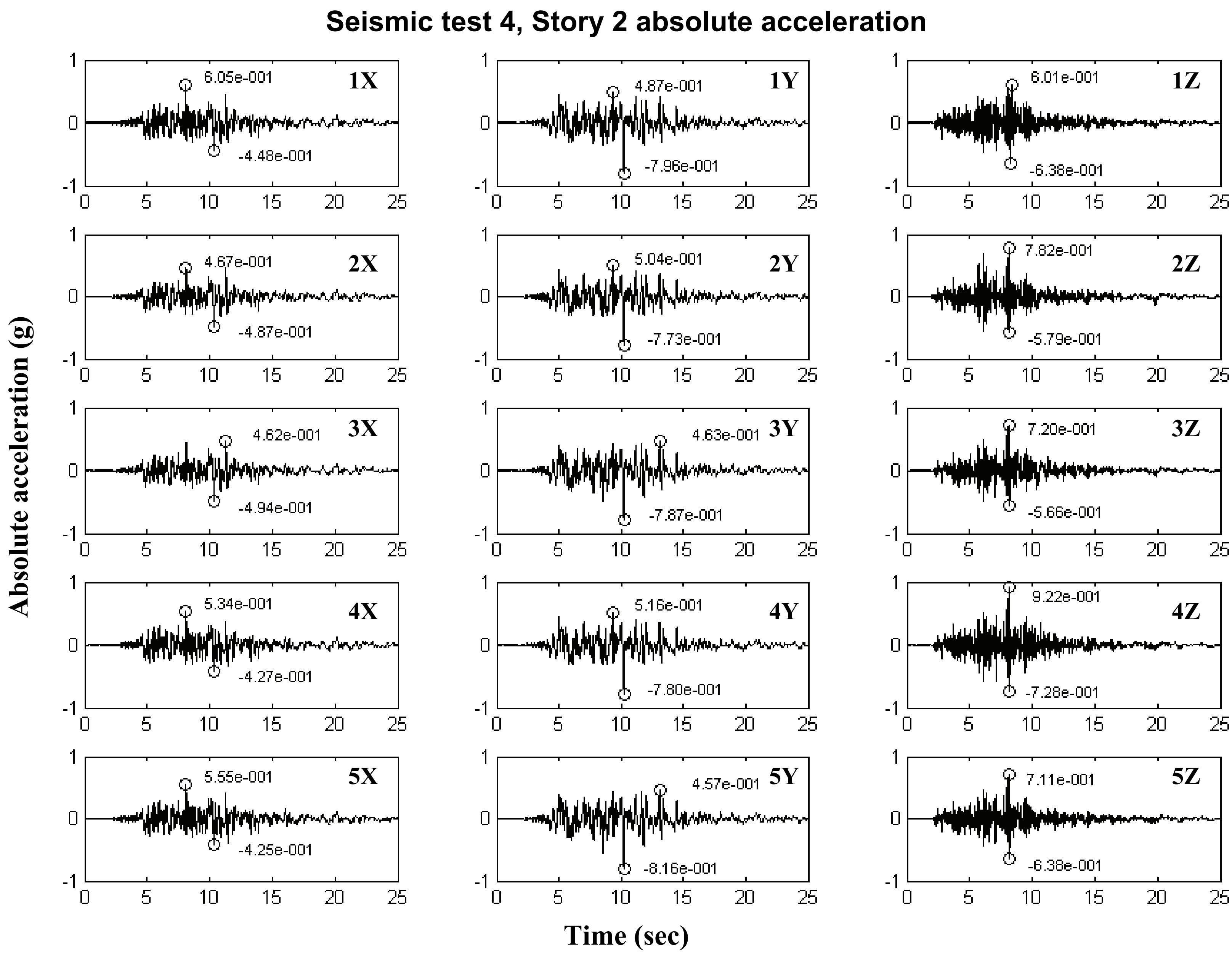

Figure K.22: Absolute acceleration at story 2 locations during Seismic test 4

Appendix K

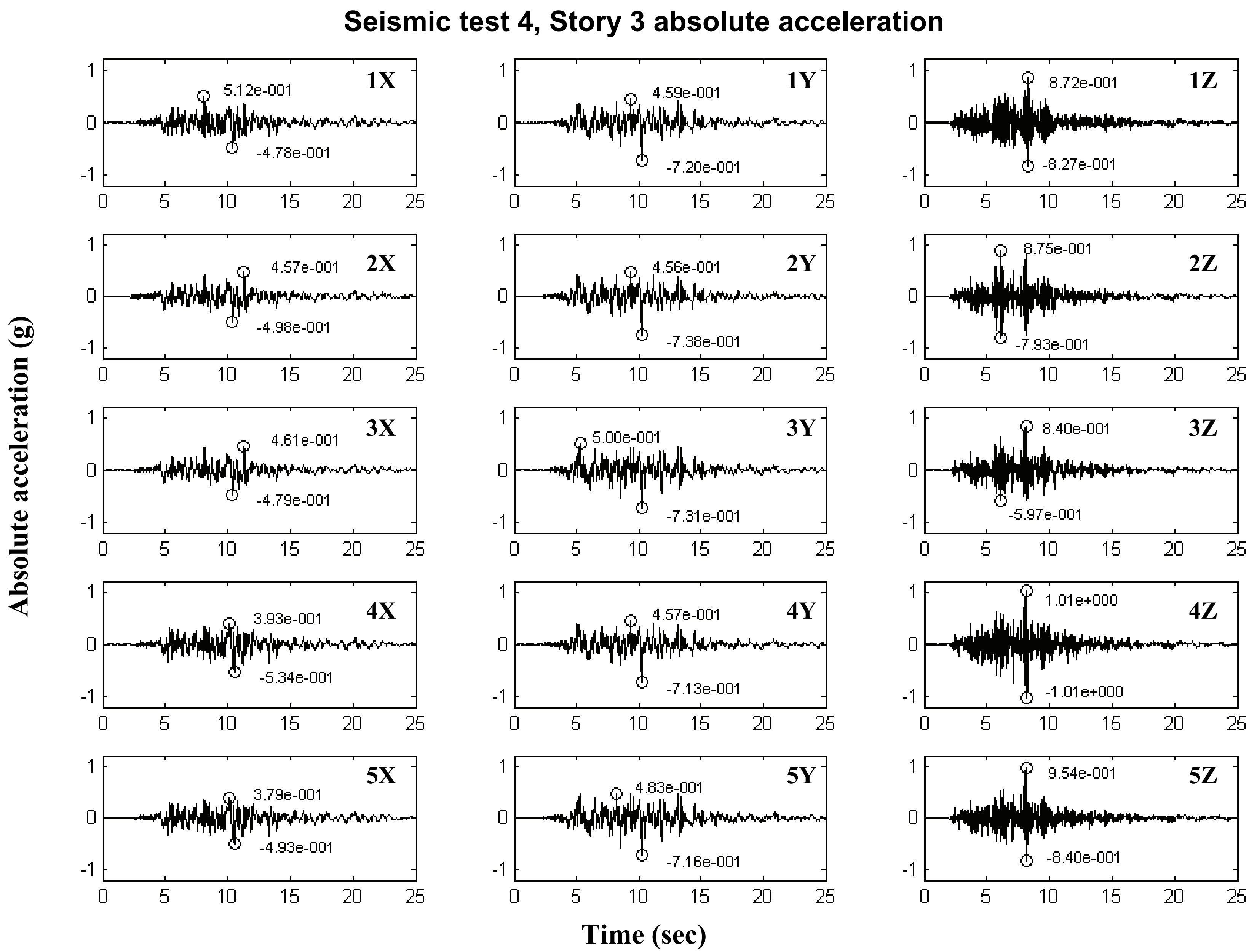

Figure K.23: Absolute acceleration at story 3 locations during Seismic test 4

Appendix K

Seismic test 4, Story 4 absolute acceleration

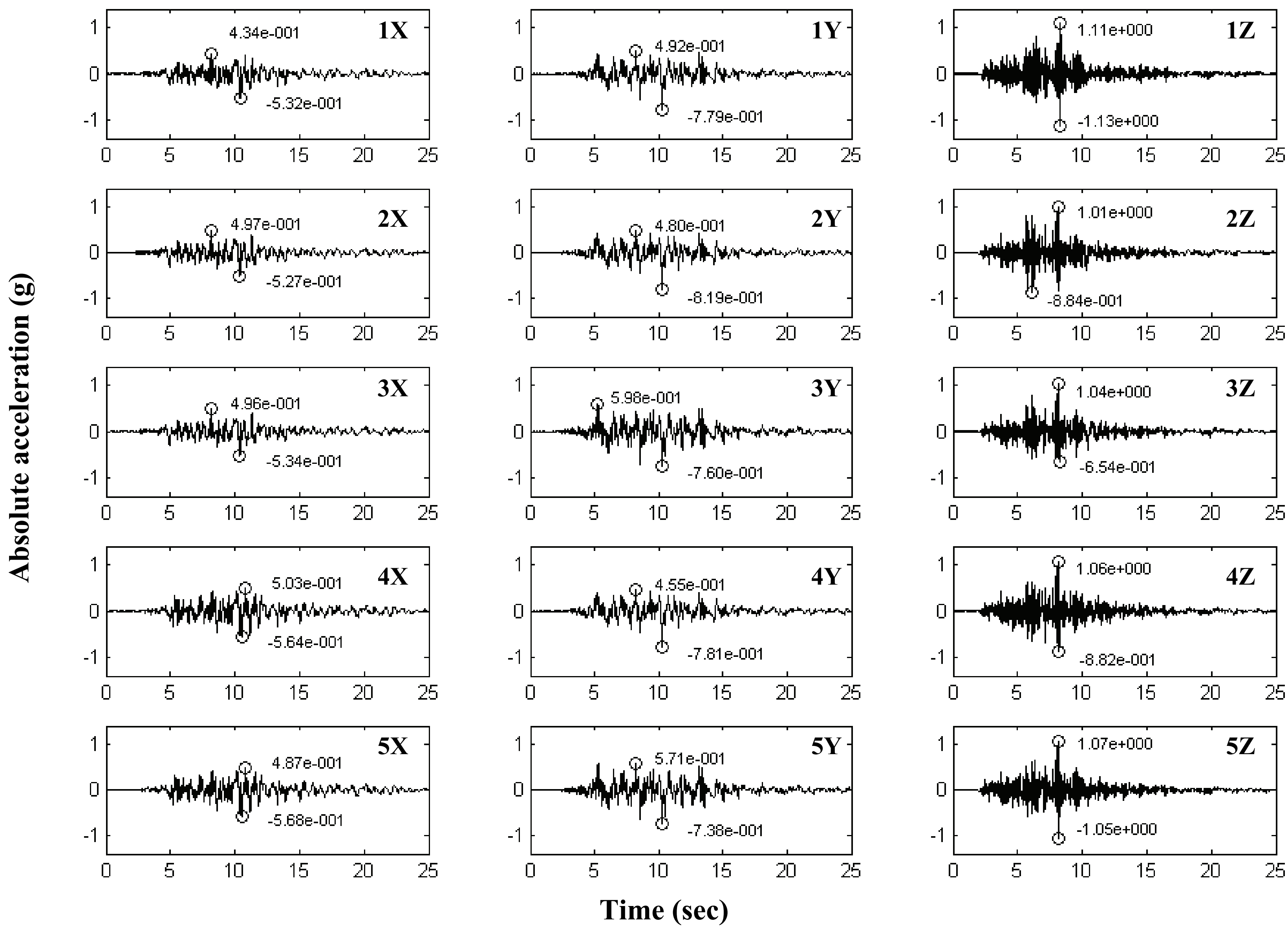

Figure K.24: Absolute acceleration at story 4 locations during Seismic test 4

Appendix K

Seismic test 4, Story 5 absolute acceleration

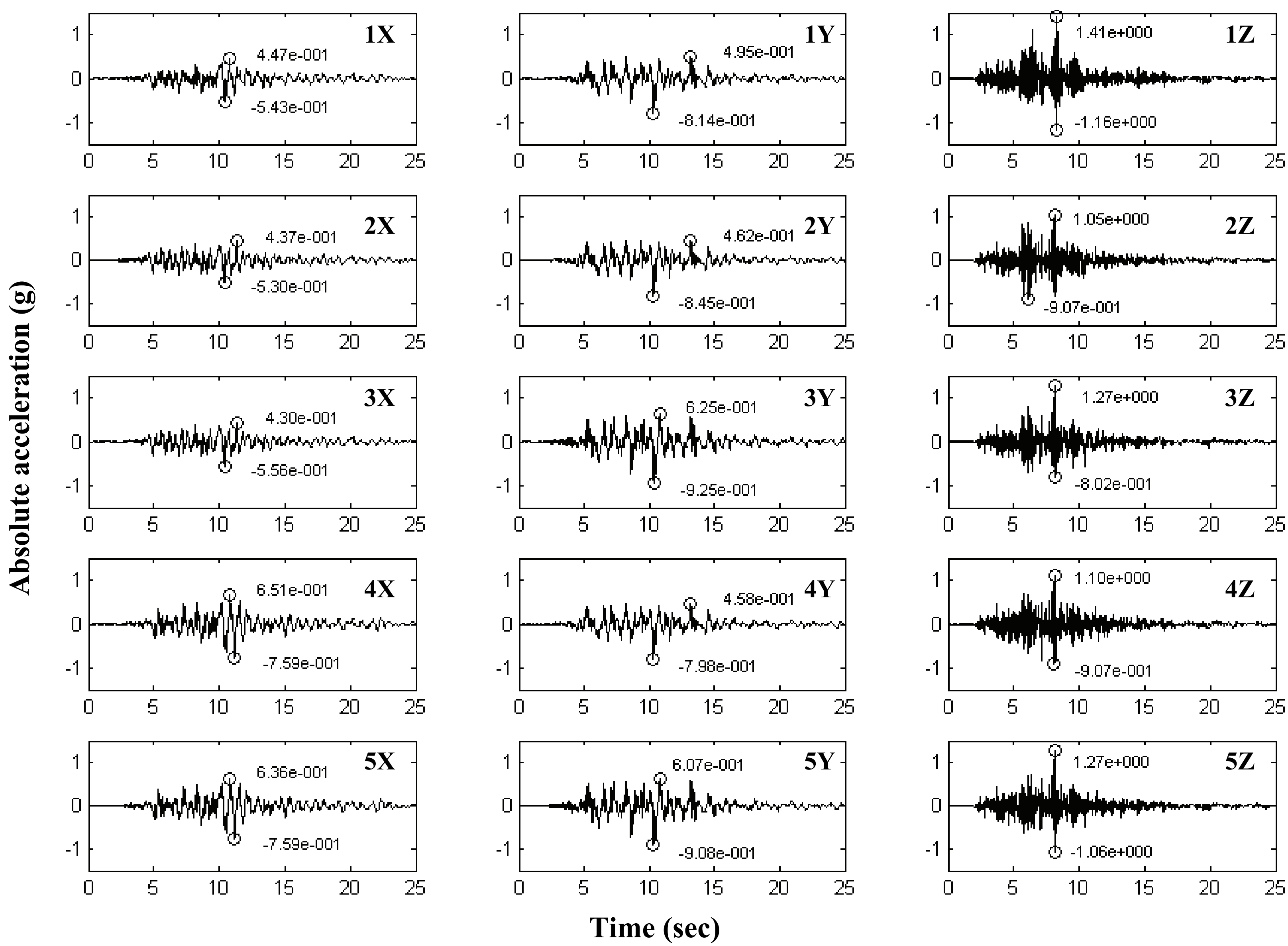

Figure K.25: Absolute acceleration at story 5 locations during Seismic test 4

Appendix K

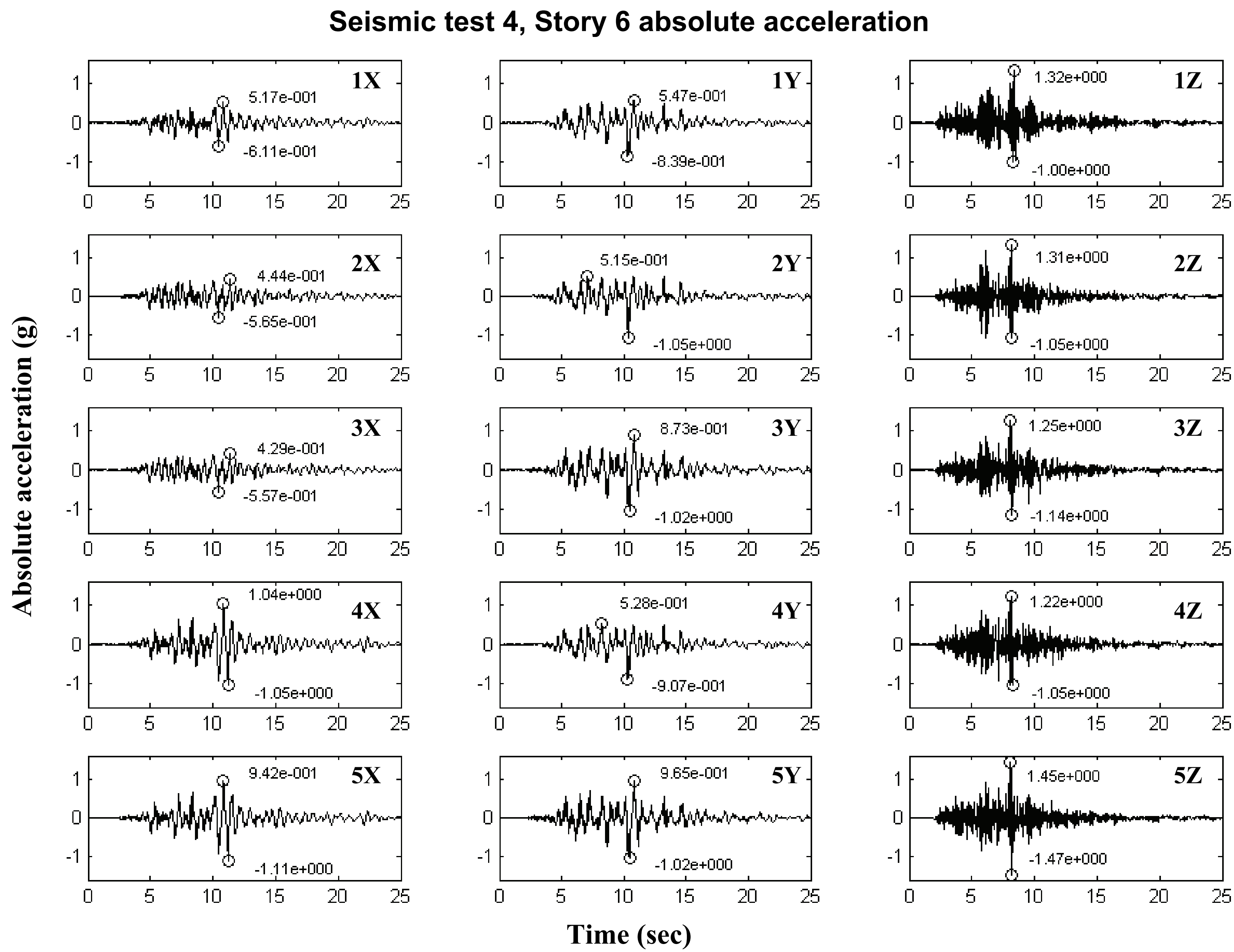

Figure K.26: Absolute acceleration at story 6 locations during Seismic test 4

Appendix K

Seismic test 4, Story 7 absolute acceleration

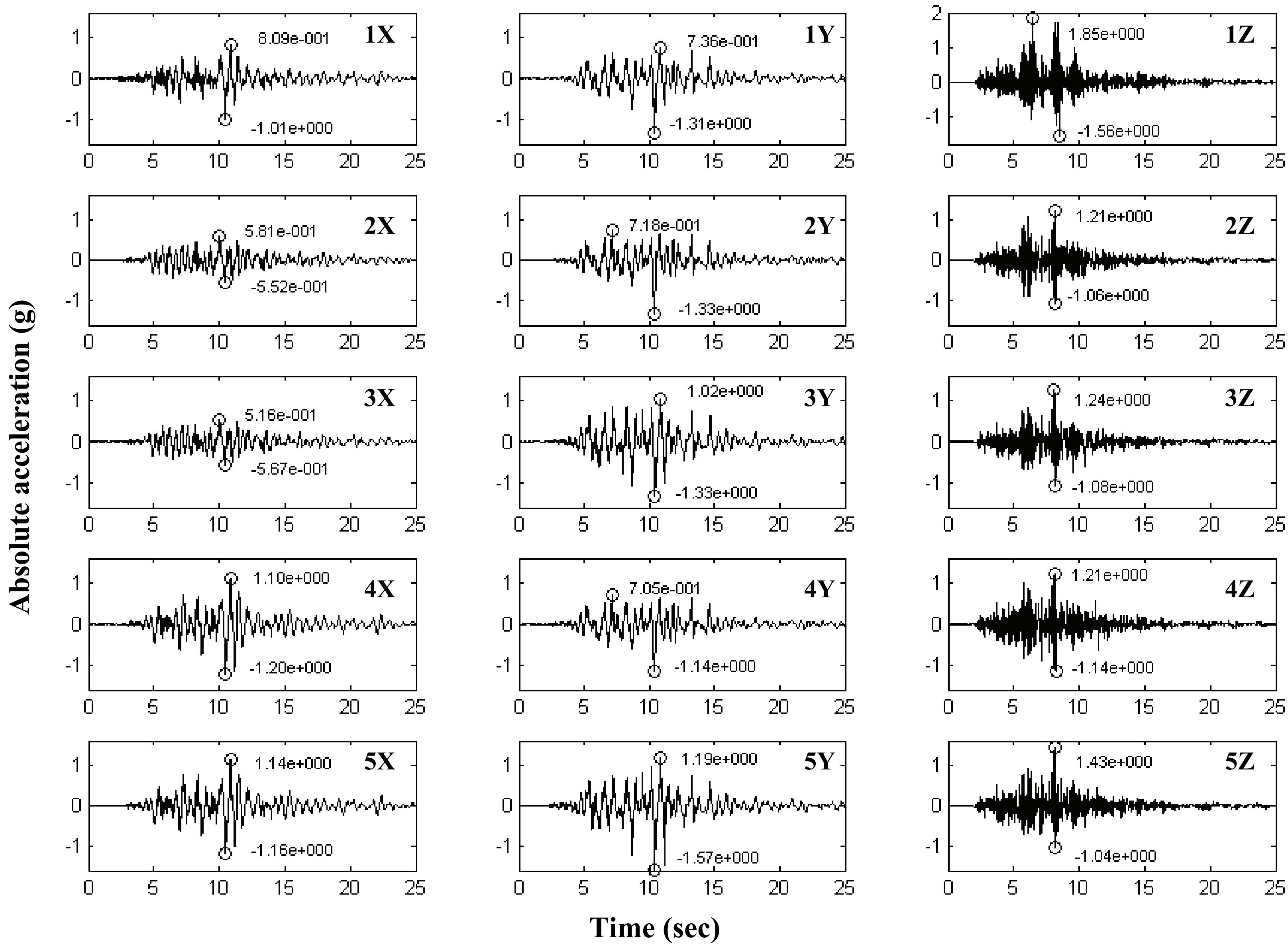

Figure K.27: Absolute acceleration at story 7 locations during Seismic test 4

Appendix K

Seismic test 4, Roof absolute acceleration

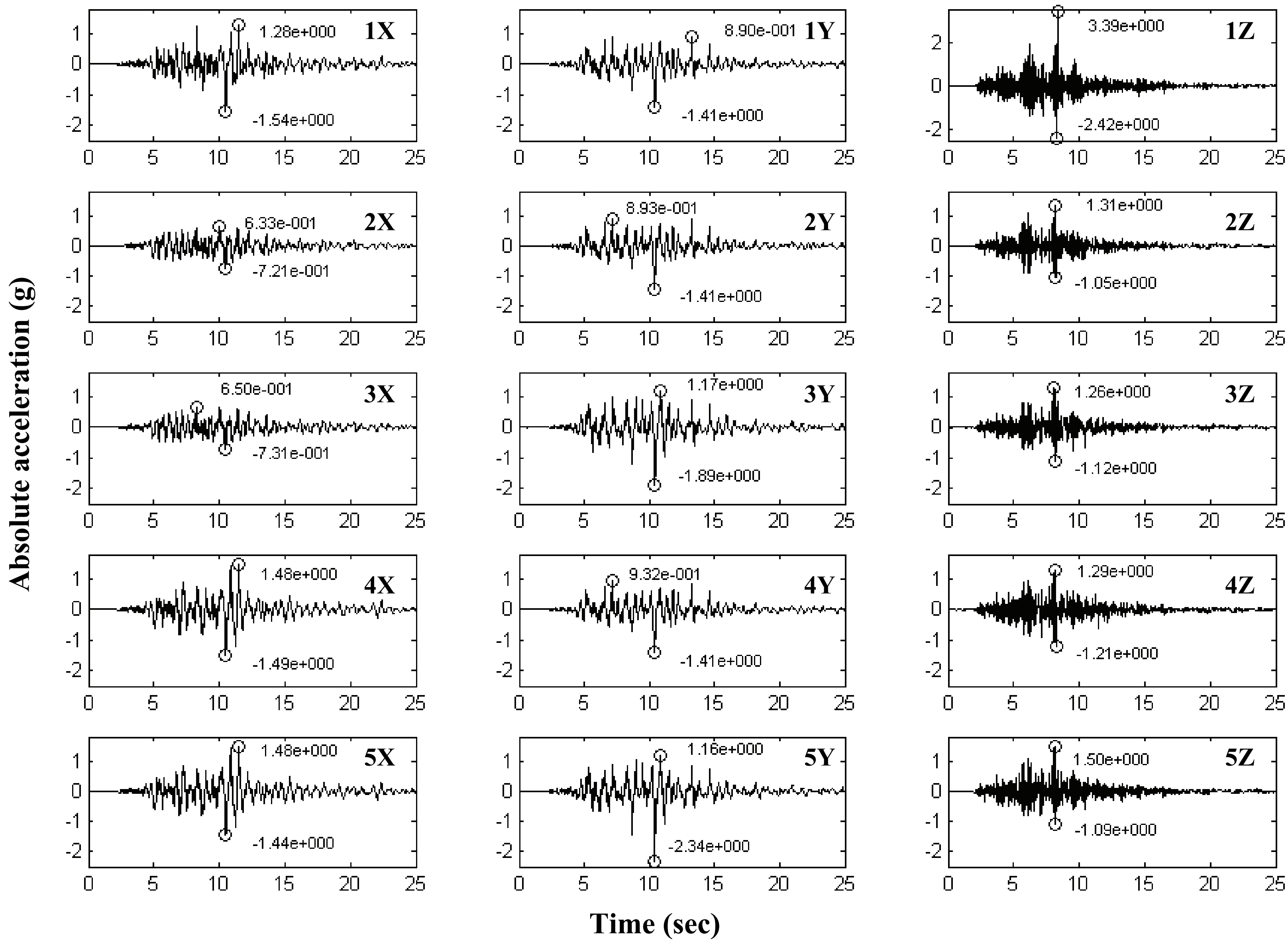

Figure K.28: Absolute acceleration at roof locations during Seismic test 4

Appendix K

Seismic test 5, Story 2 absolute acceleration

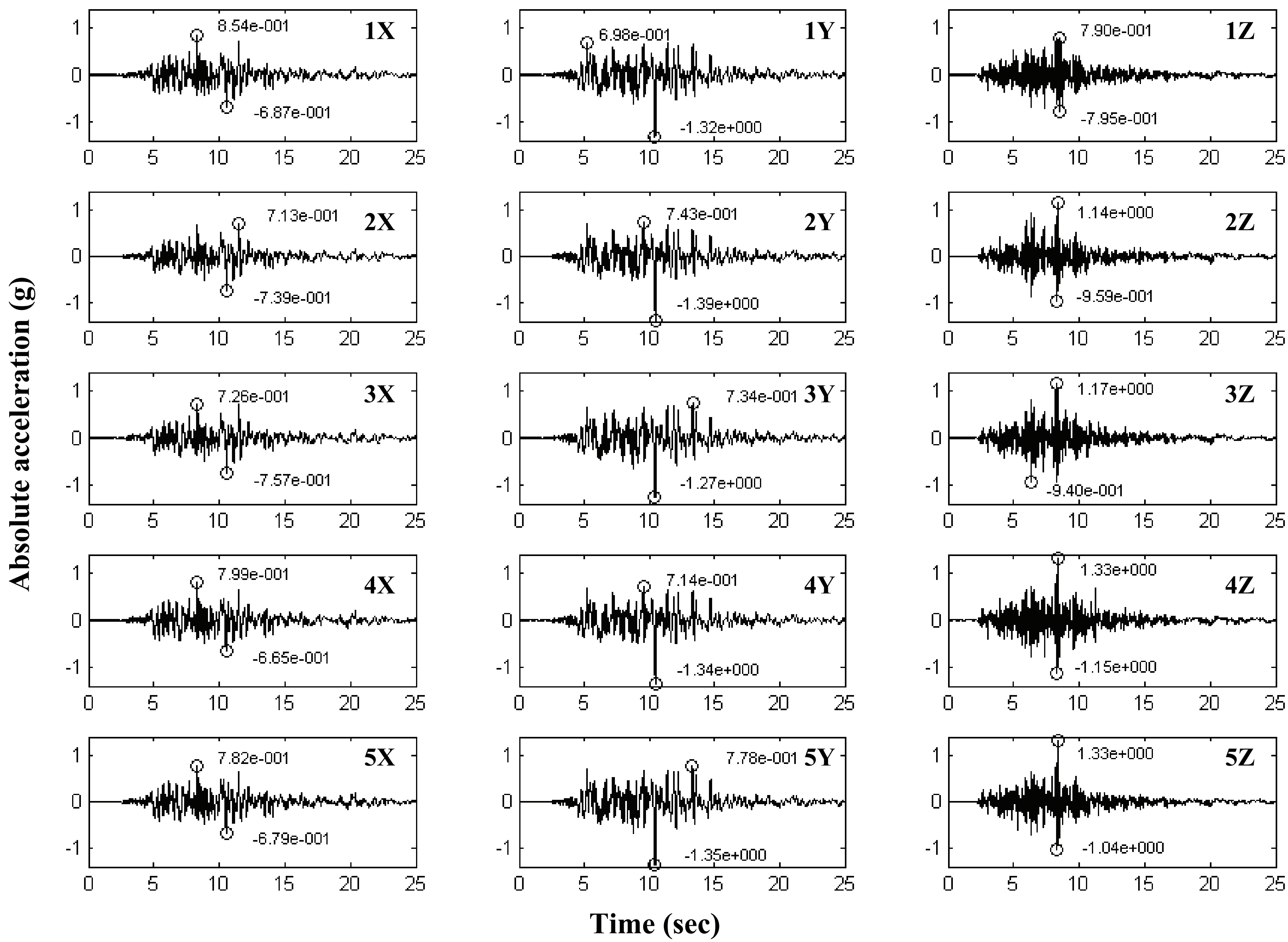

Figure K.29: Absolute acceleration at story 2 locations during Seismic test 5

Appendix K

Seismic test 5, Story 3 absolute acceleration

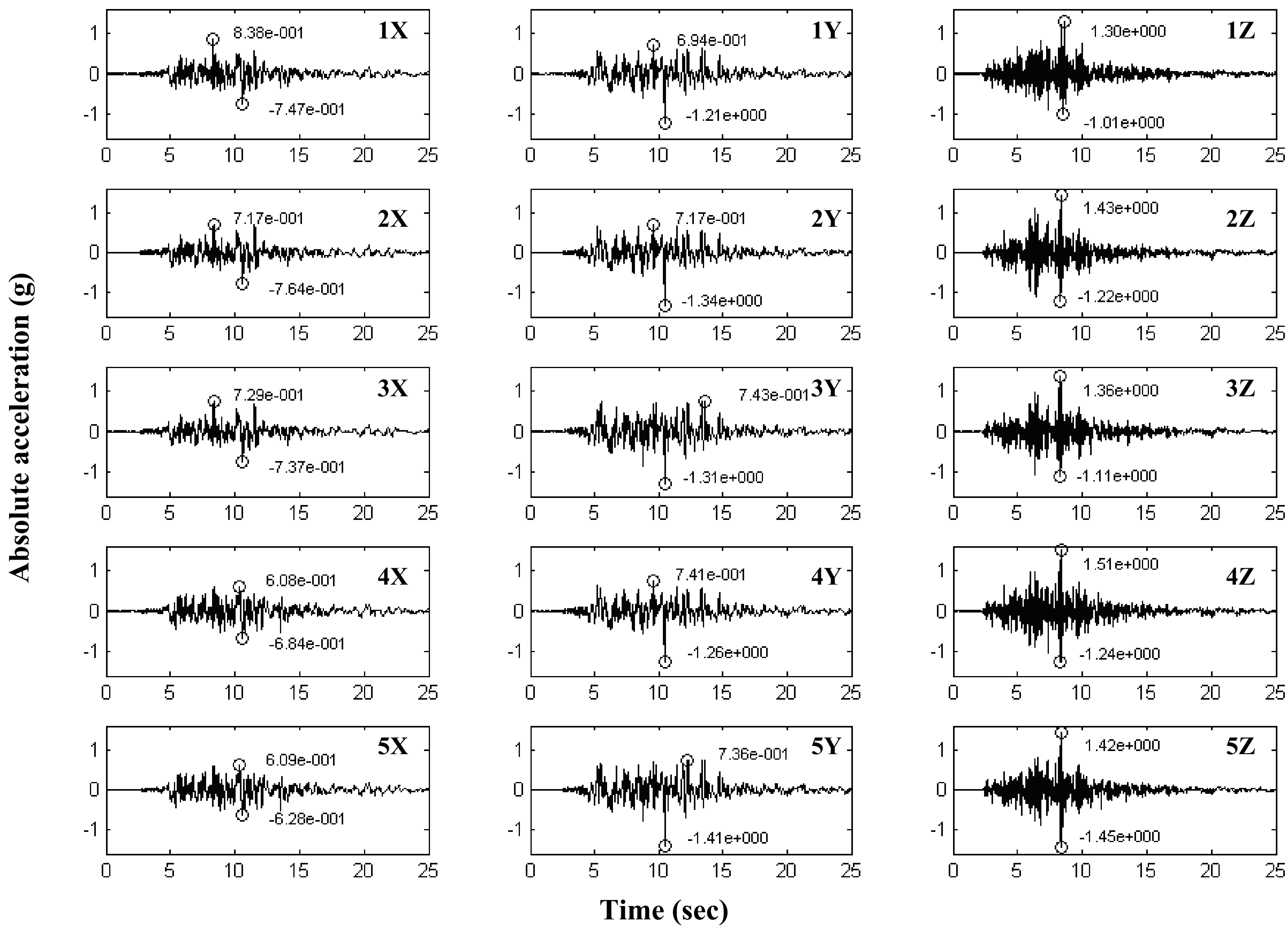

Figure K.30: Absolute acceleration at story 3 locations during Seismic test 5

Appendix K

Seismic test 5, Story 4 absolute acceleration

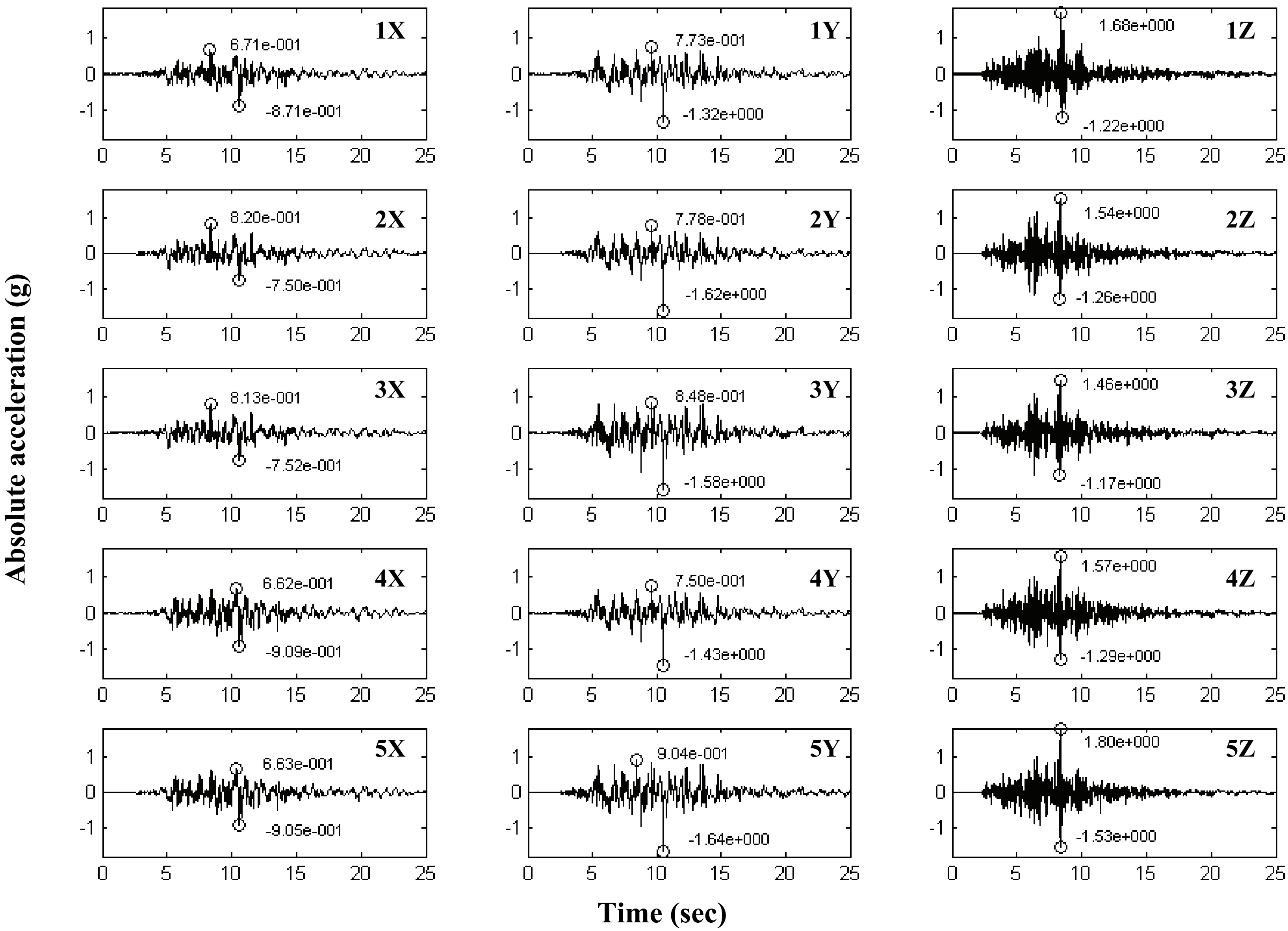

Figure K.31: Absolute acceleration at story 4 locations during Seismic test 5

Appendix K

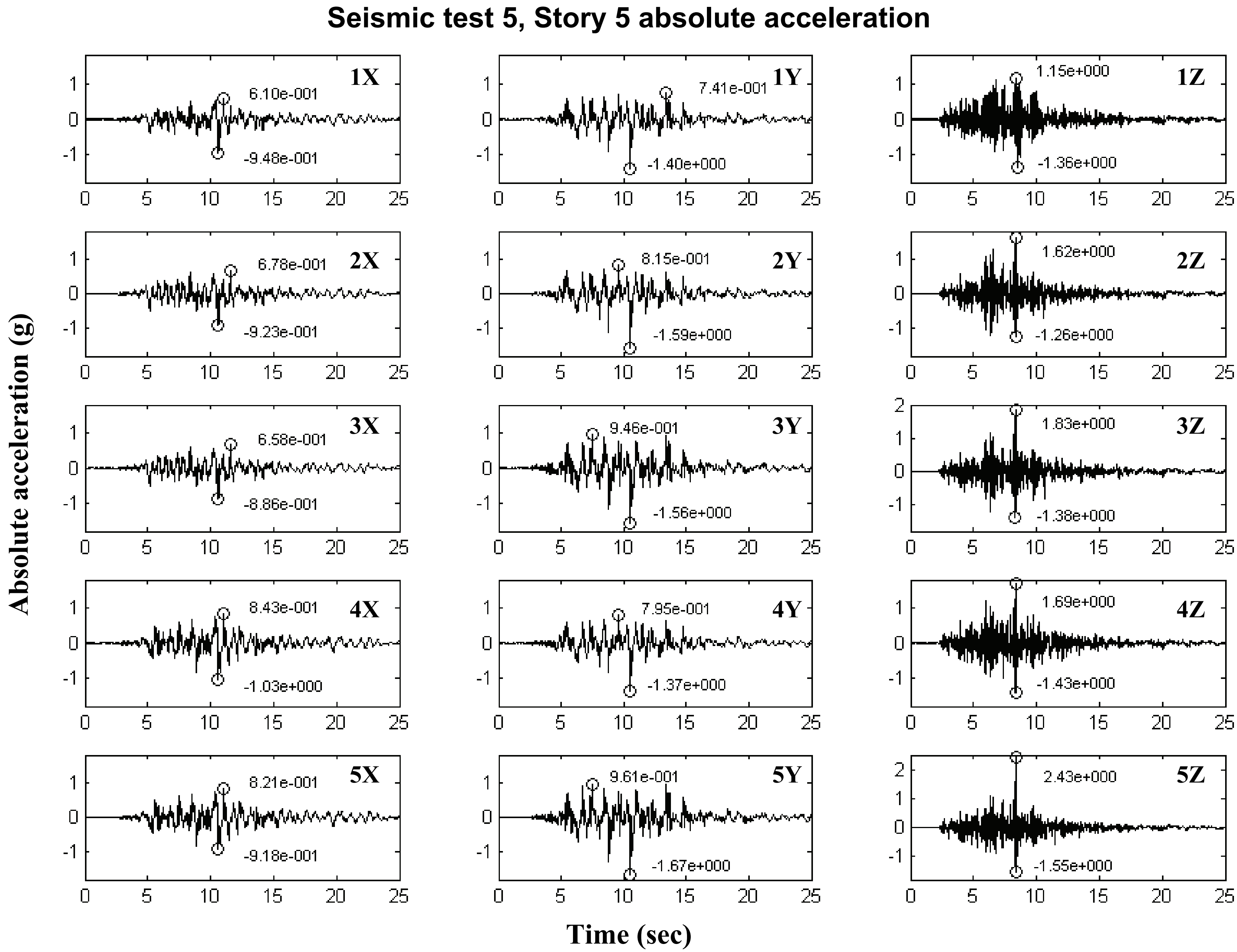

Figure K.32: Absolute acceleration at story 5 locations during Seismic test 5

Appendix K

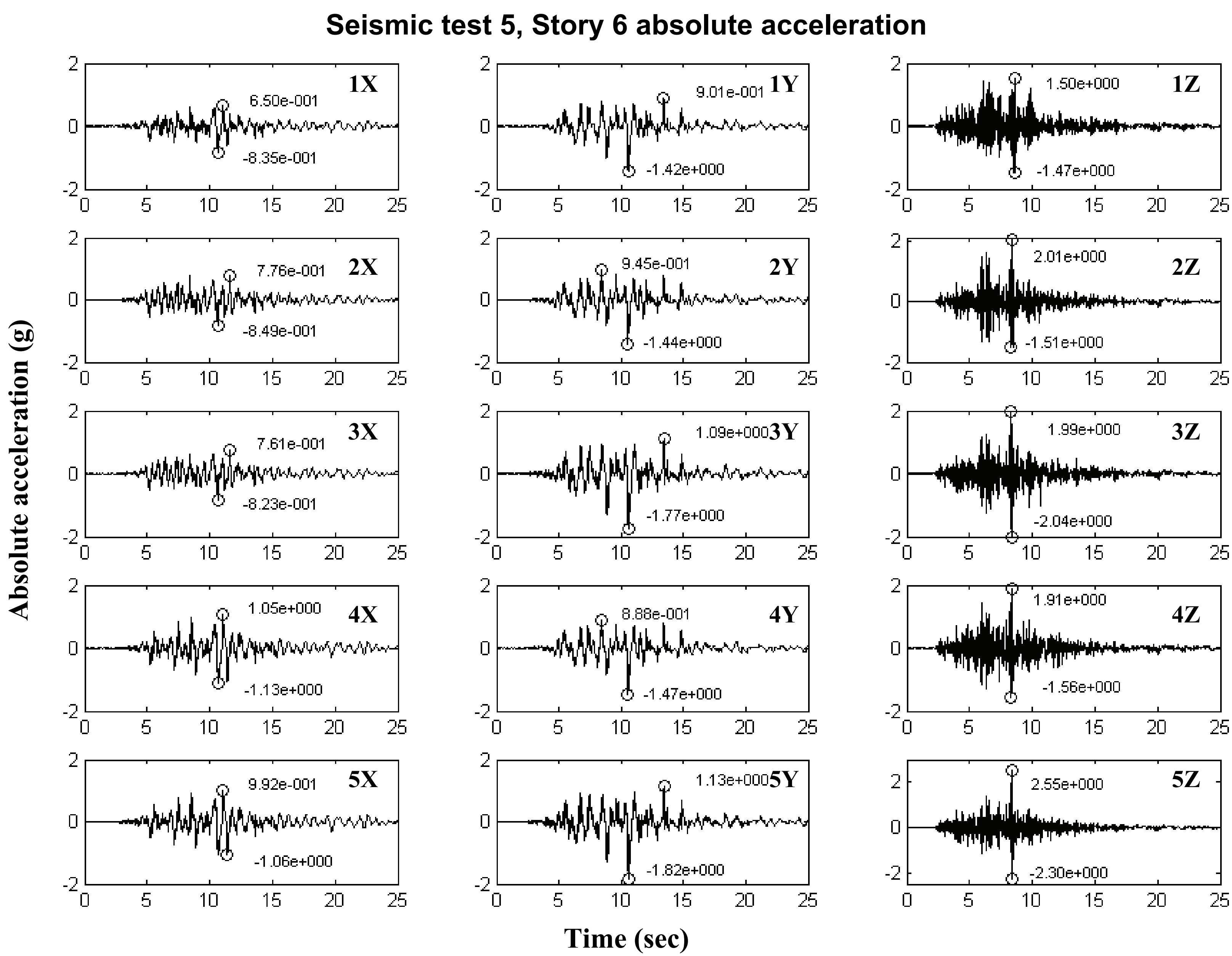

Figure K.33: Absolute acceleration at story 6 locations during Seismic test 5

Appendix K

Seismic test 5, Story 7 absolute acceleration

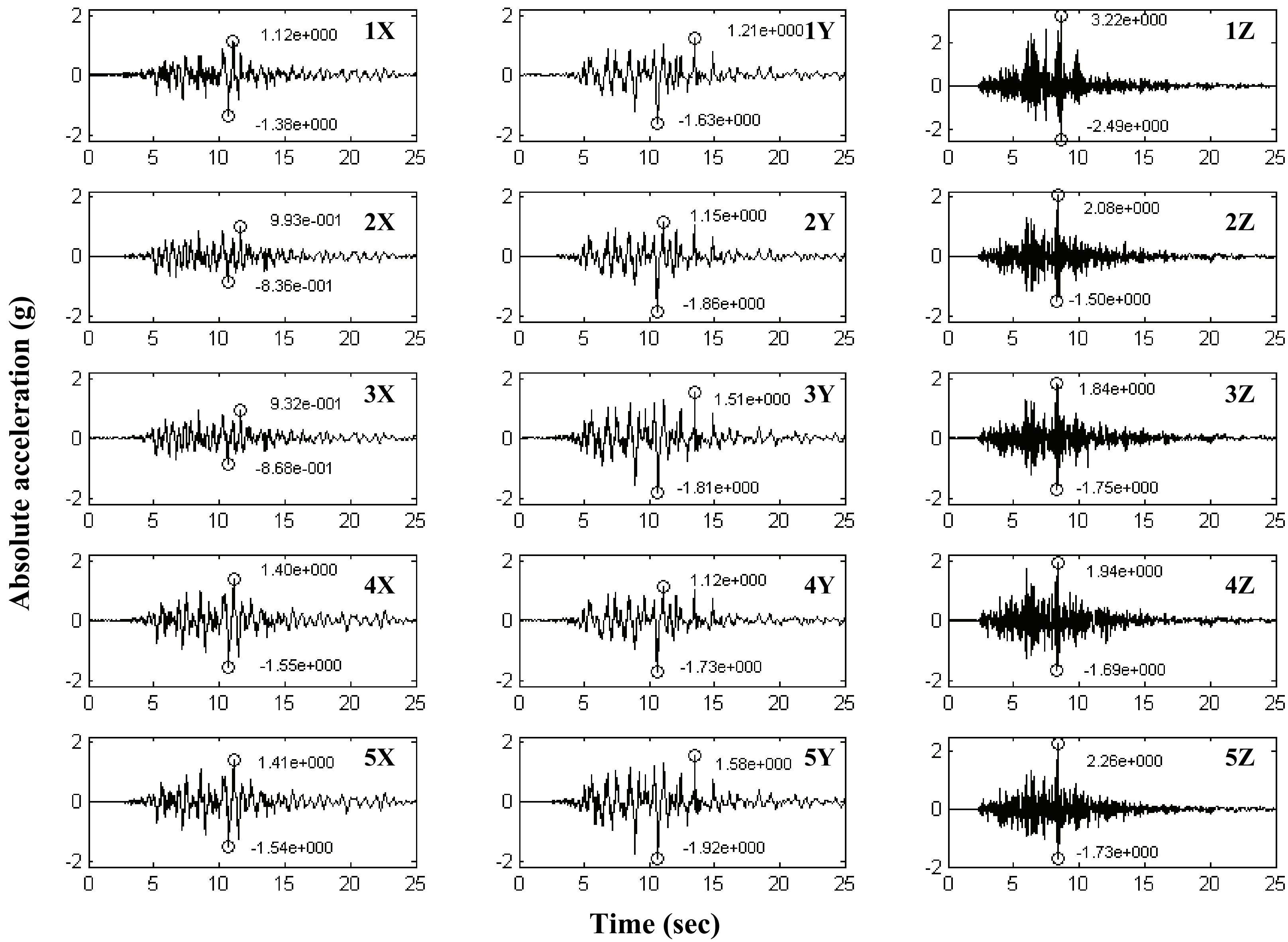

Figure K.34: Absolute acceleration at story 7 locations during Seismic test 5

Appendix K

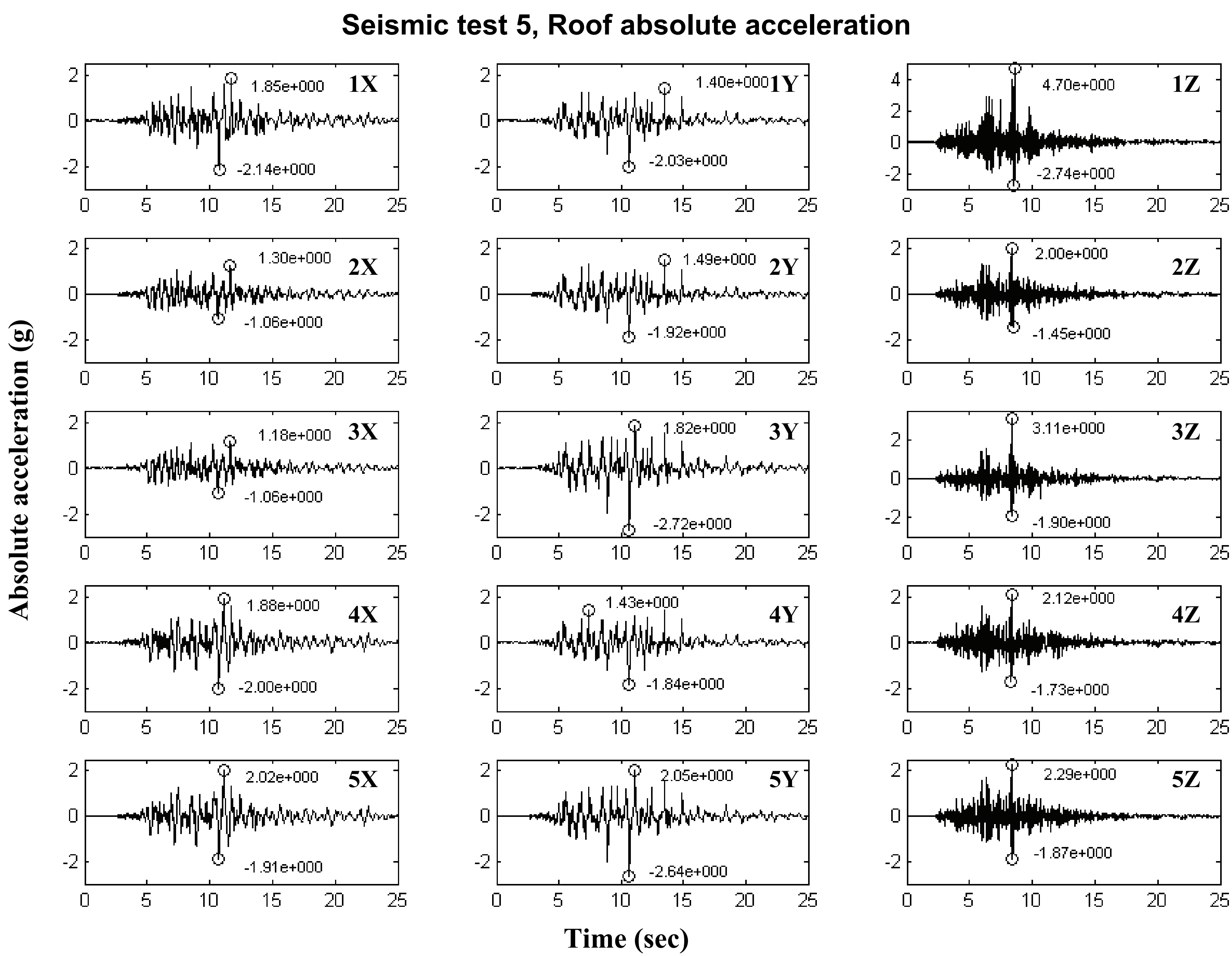

Figure K.35: Absolute acceleration at roof locations during Seismic test 5

Appendix L

Seismic Test Results: Wall deformation from diagonal string potentiometer measurements

Appendix L

Numbering of shear walls with diagonal gages

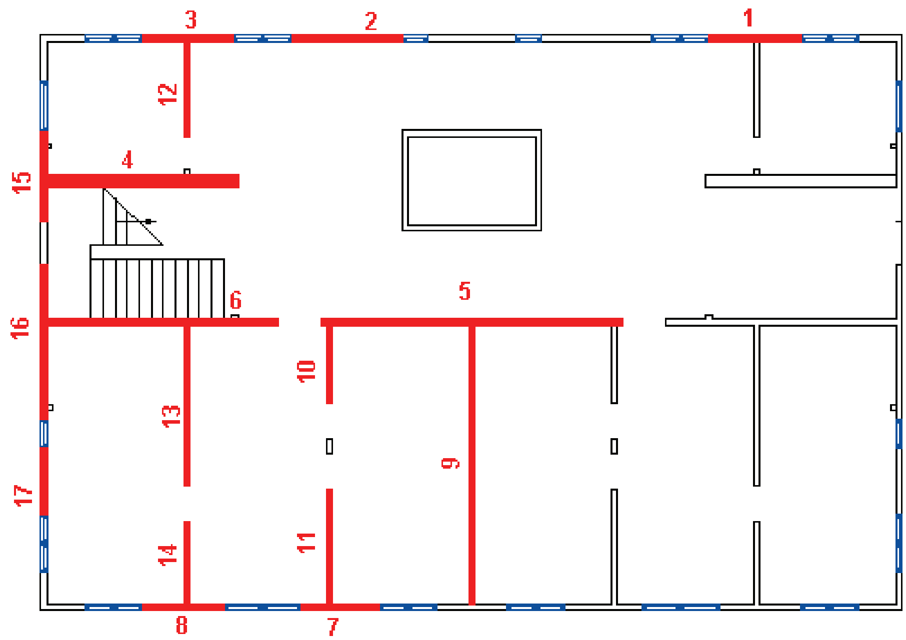

Figure L.1: Shear wall number for story 2

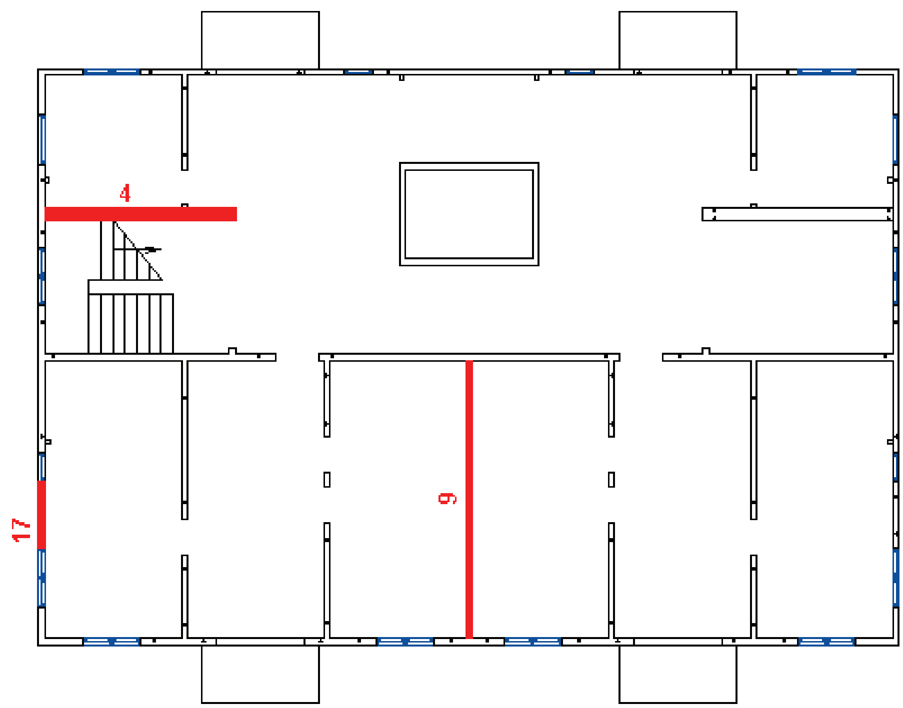

Figure L.2: Shear wall number for story 3~6

Appendix L

Numbering of shear walls with diagonal gages

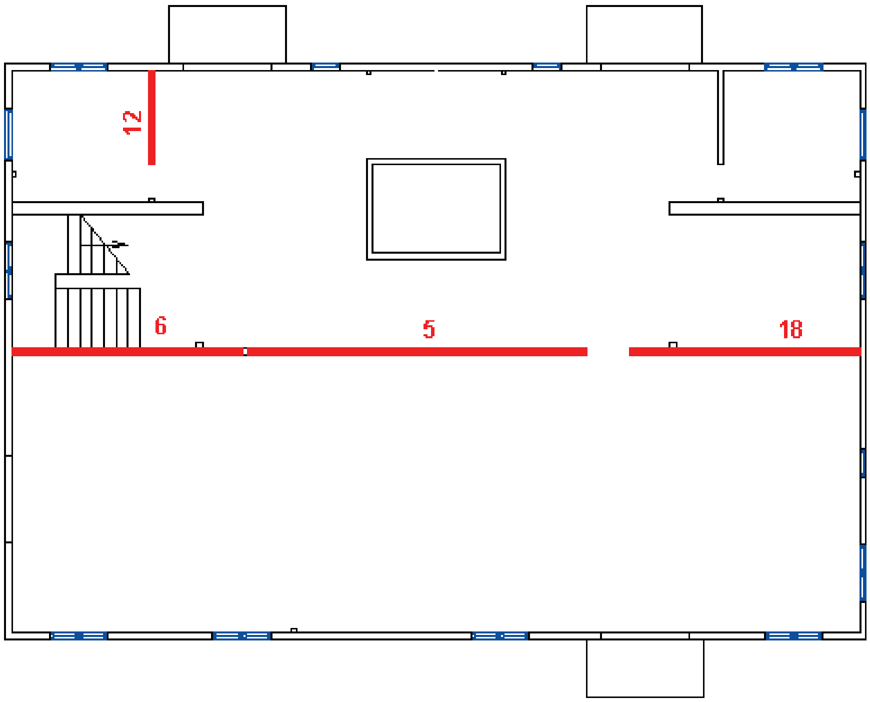

Figure L.3: Shear wall number for story 7

Appendix L

Shear wall displacement (Part 1) Seismic Test 1

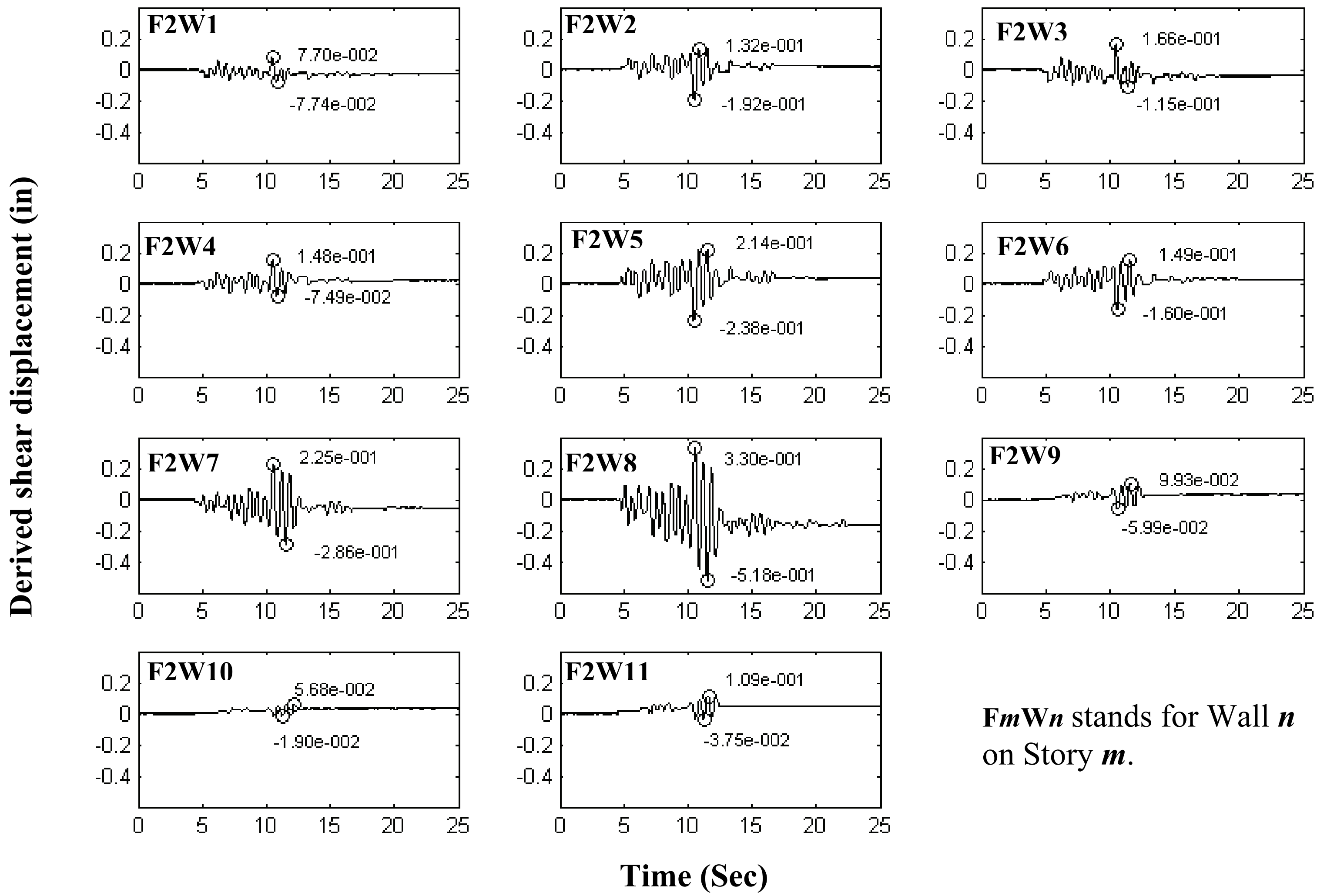

F*m*W*n* stands for Wall ***n*** on Story ***m***.

Figure L.4: Shear wall displacement derived from diagonal gage measurement for Seismic Test 1 (Part 1)

Appendix L

Shear wall displacement (Part 2) Seismic Test 1

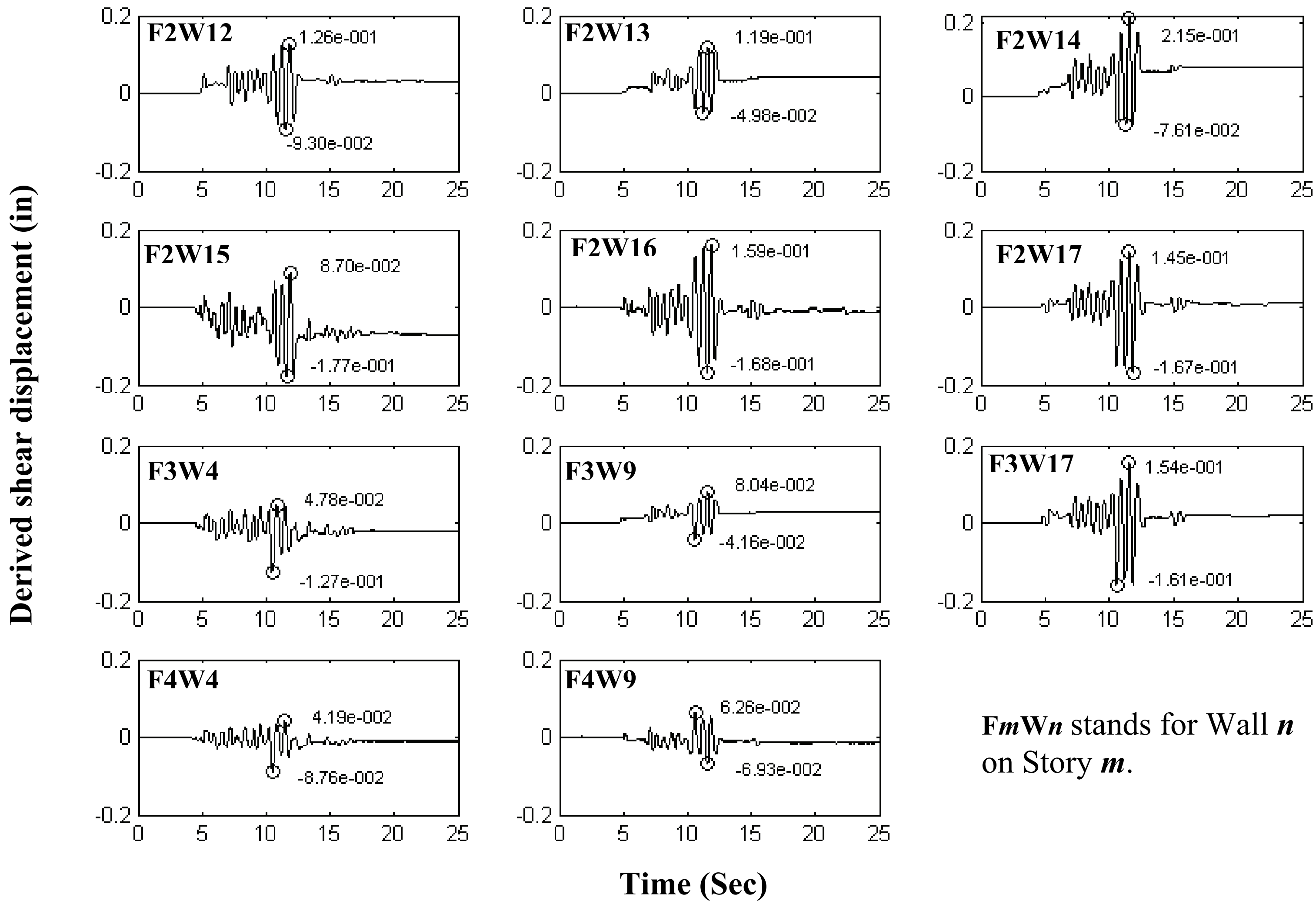

Figure L.5: Shear wall displacement derived from diagonal gage measurement for Seismic Test 1 (Part 2)

Appendix L

Shear wall displacement (Part 3) Seismic Test 1

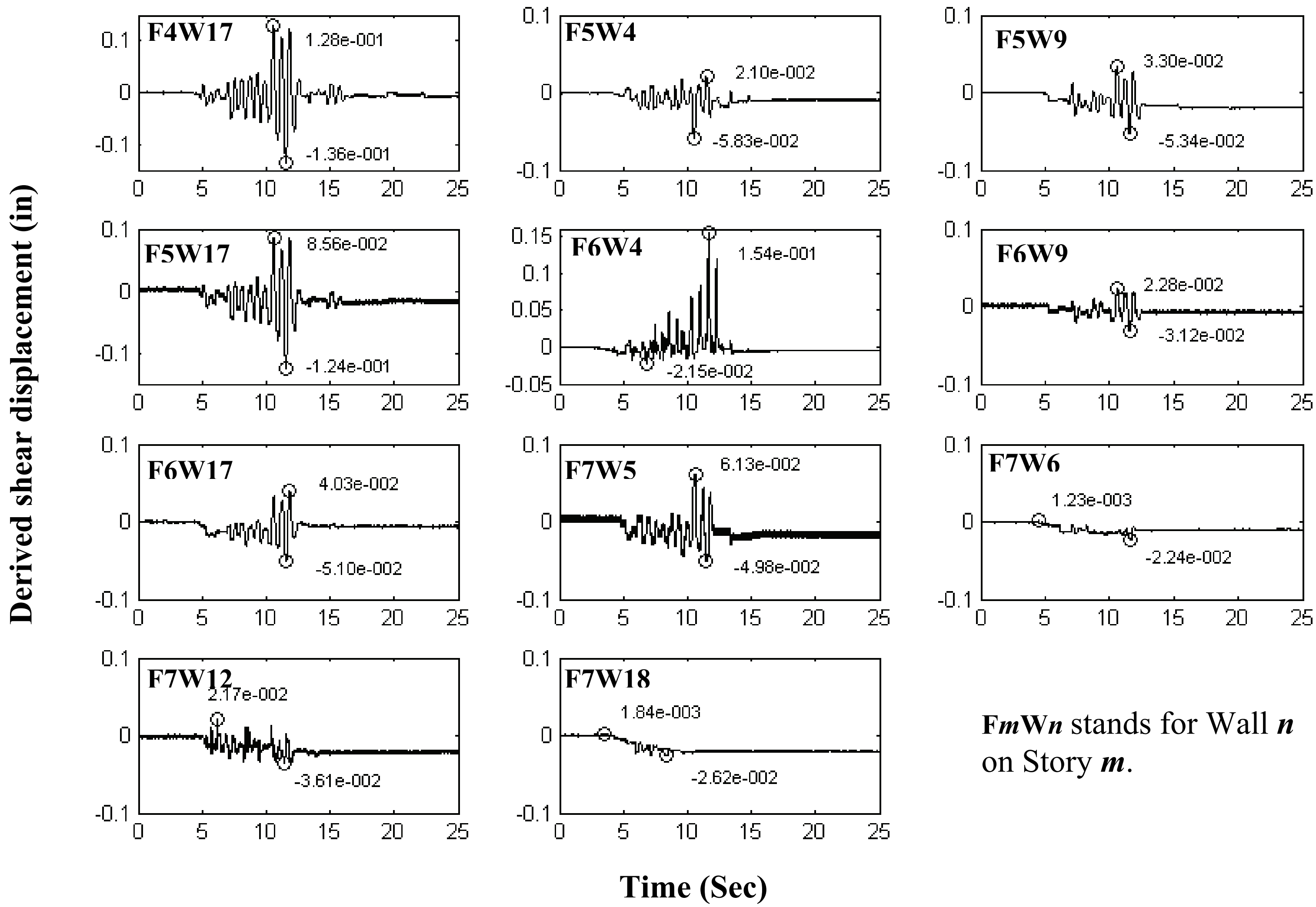

Figure L.6: Shear wall displacement derived from diagonal gage measurement for Seismic Test 1 (Part 3)

Appendix L

Shear wall displacement (Part 1) Seismic Test 2

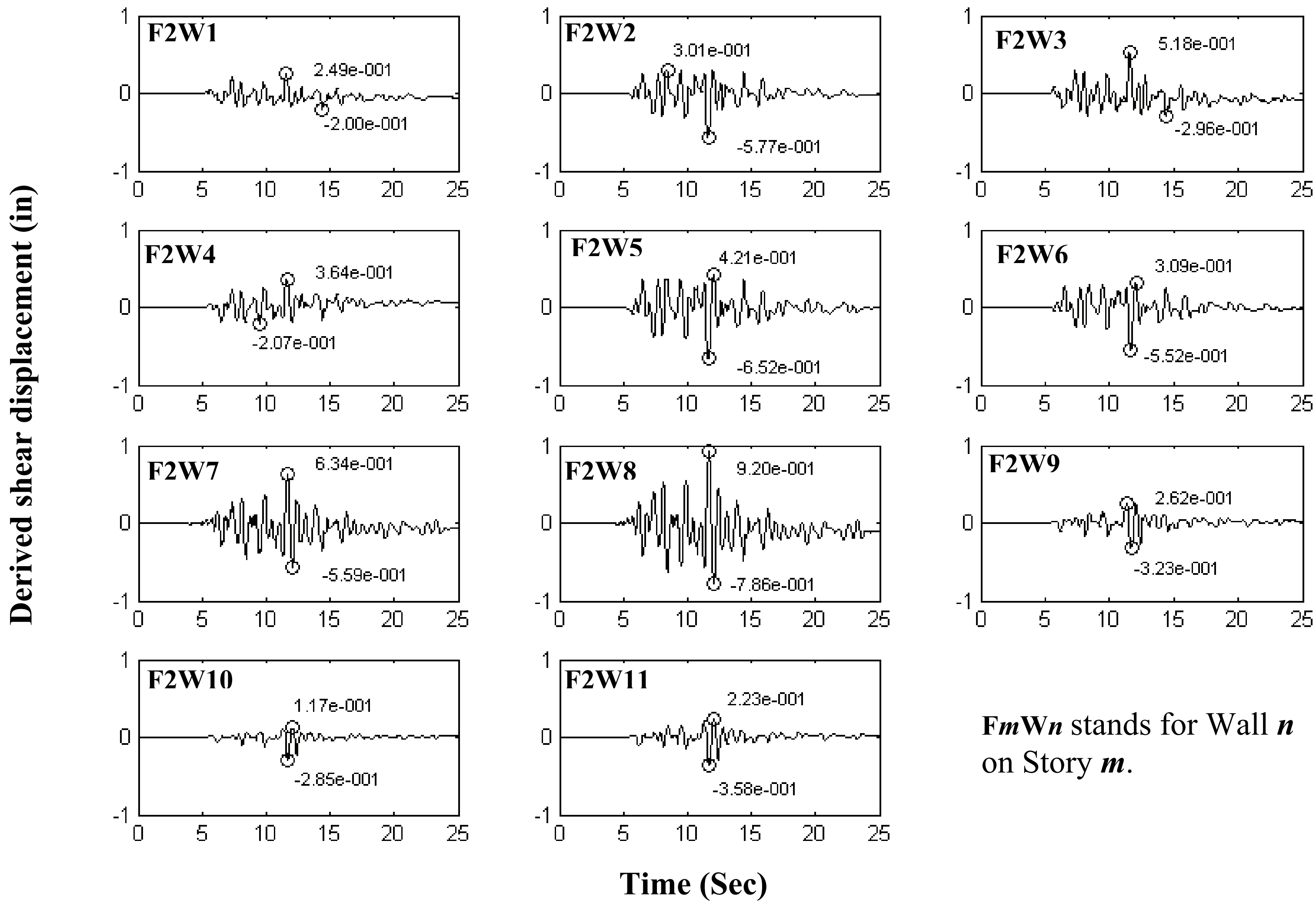

F*m*W*n* stands for Wall ***n*** on Story ***m***.

Figure L.7: Shear wall displacement derived from diagonal gage measurement for Seismic Test 2 (Part 1)

Appendix L

Shear wall displacement (Part 2) Seismic Test 2

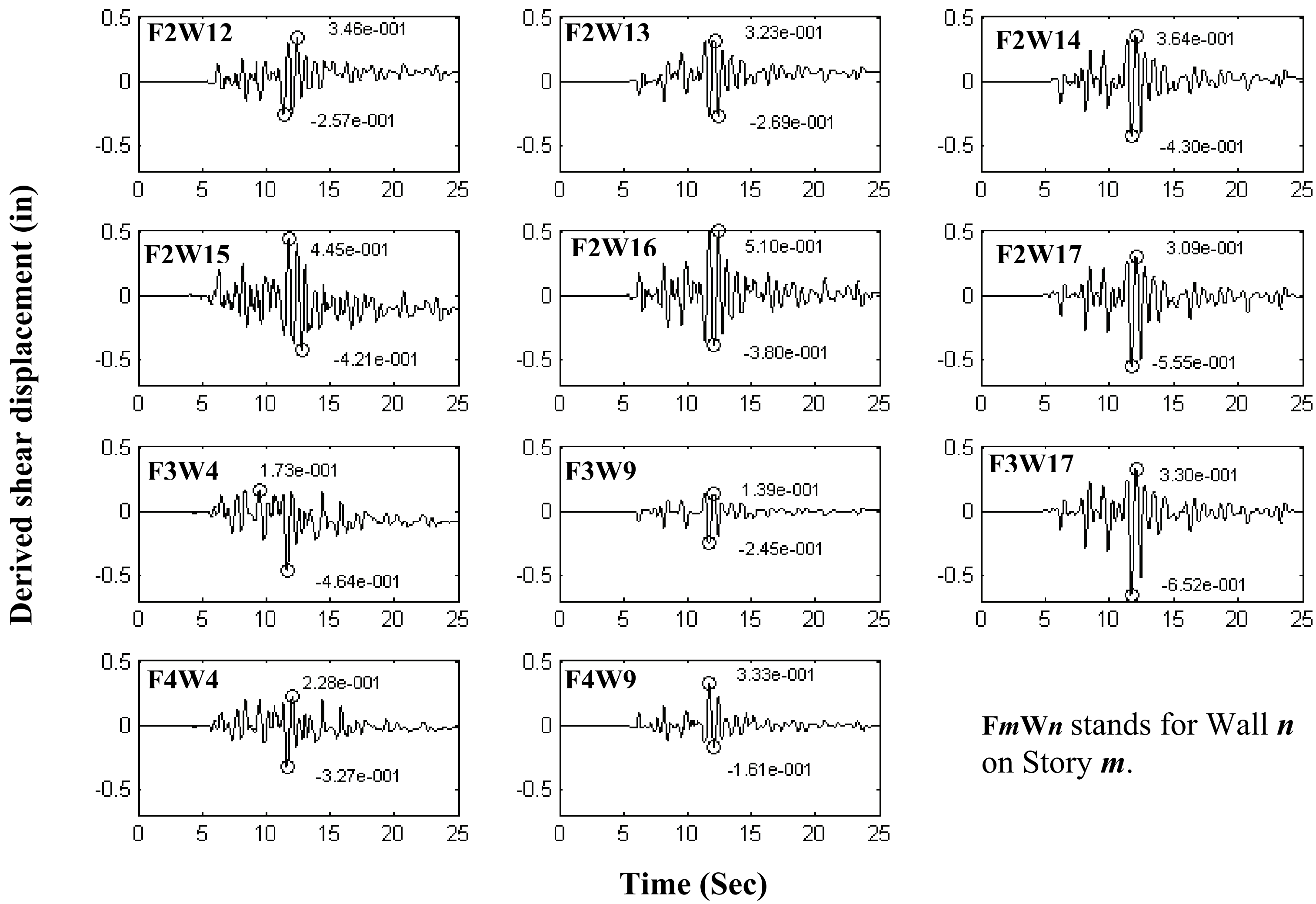

Figure L.8: Shear wall displacement derived from diagonal gage measurement for Seismic Test 2 (Part 2)

Appendix L

Shear wall displacement (Part 3) Seismic Test 2

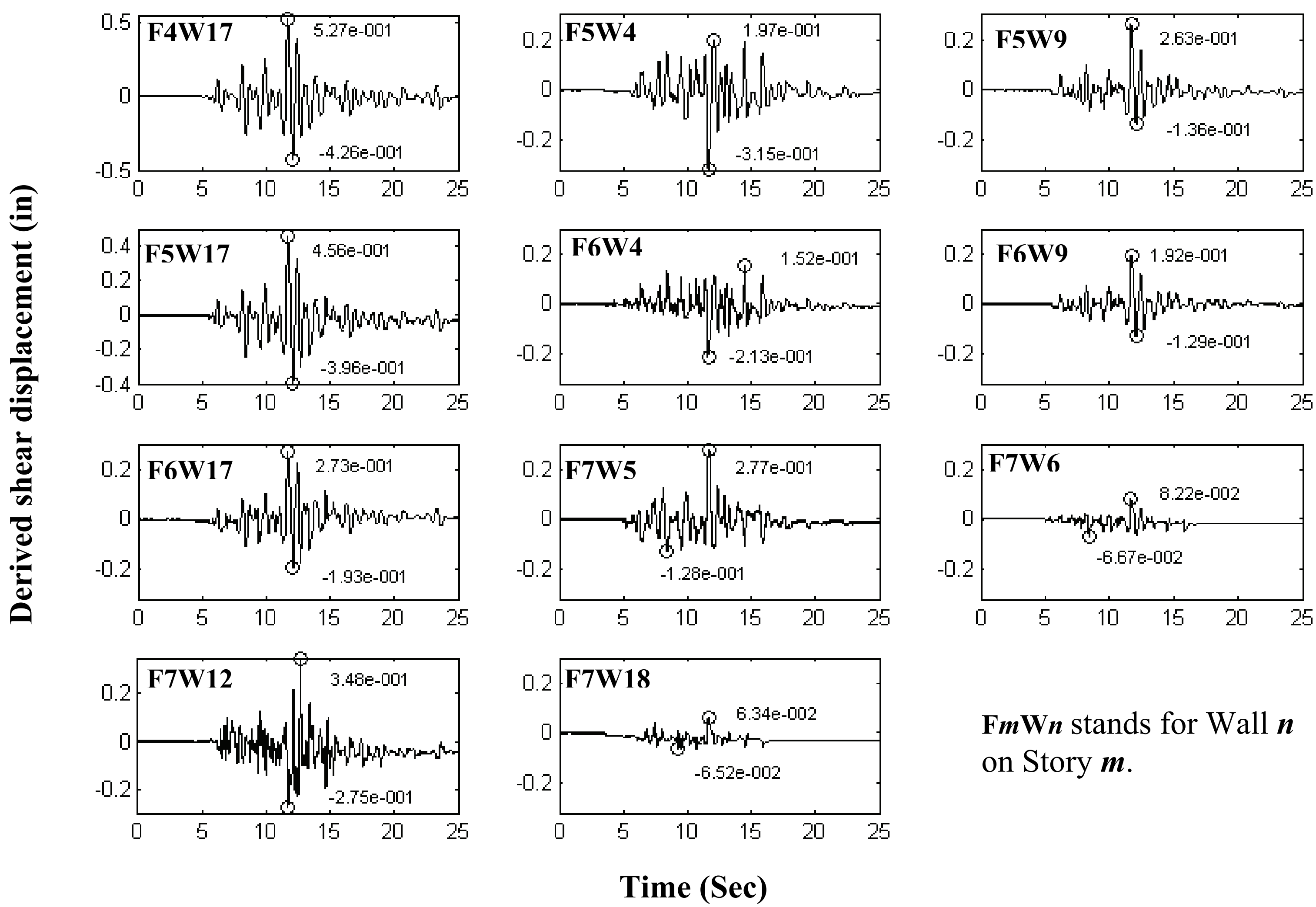

Figure L.9: Shear wall displacement derived from diagonal gage measurement for Seismic Test 2 (Part 3)

Appendix L

Shear wall displacement (Part 1) Seismic Test 3

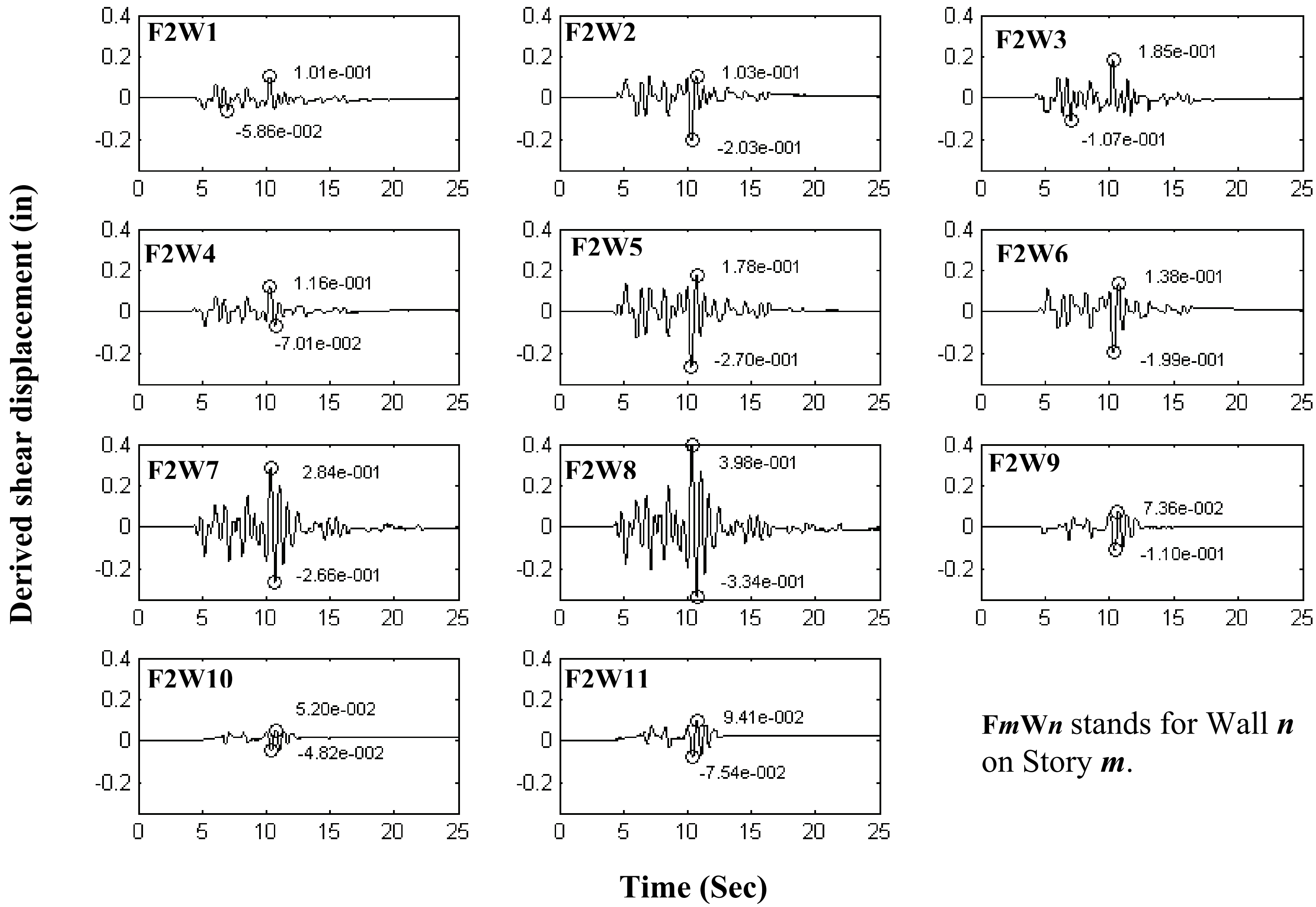

F*m*W*n* stands for Wall ***n*** on Story ***m***.

Figure L.10: Shear wall displacement derived from diagonal gage measurement for Seismic Test 3 (Part 1)

Appendix L

Shear wall displacement (Part 2) Seismic Test 3

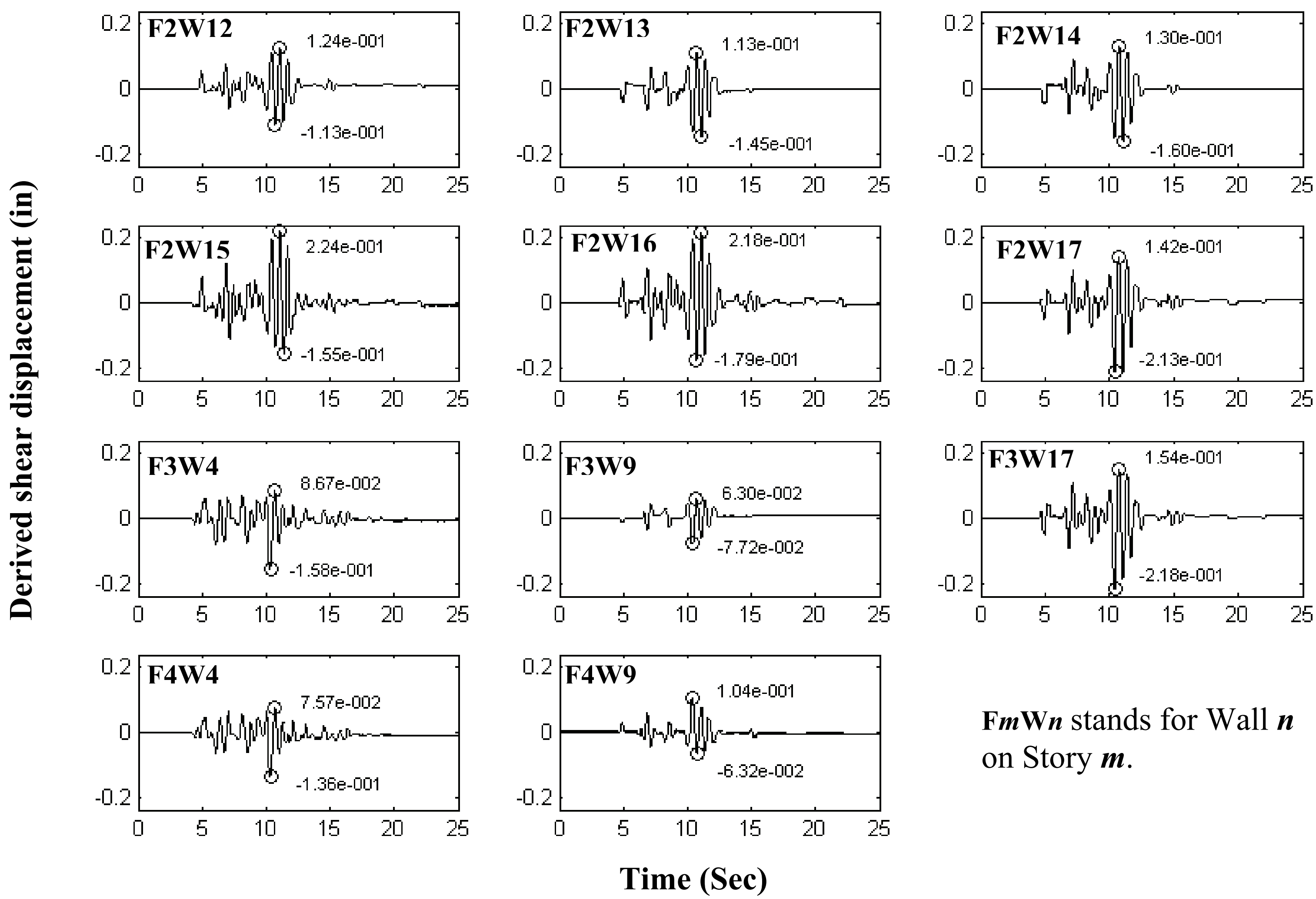

Figure L.11: Shear wall displacement derived from diagonal gage measurement for Seismic Test 3 (Part 2)

Appendix L

Shear wall displacement (Part 3) Seismic Test 3

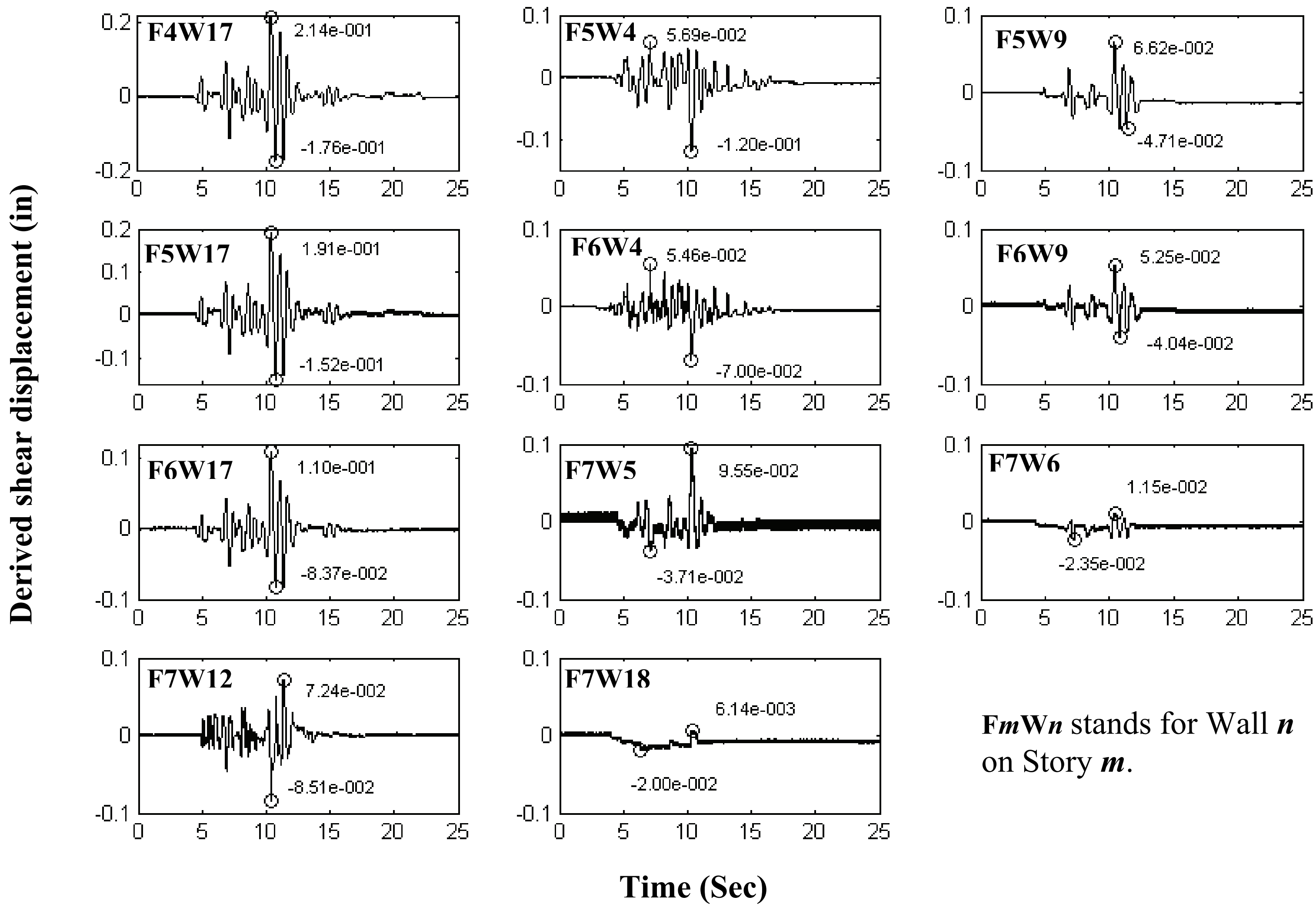

Figure L.12: Shear wall displacement derived from diagonal gage measurement for Seismic Test 3 (Part 3)

Appendix L

Shear wall displacement (Part 1) Seismic Test 4

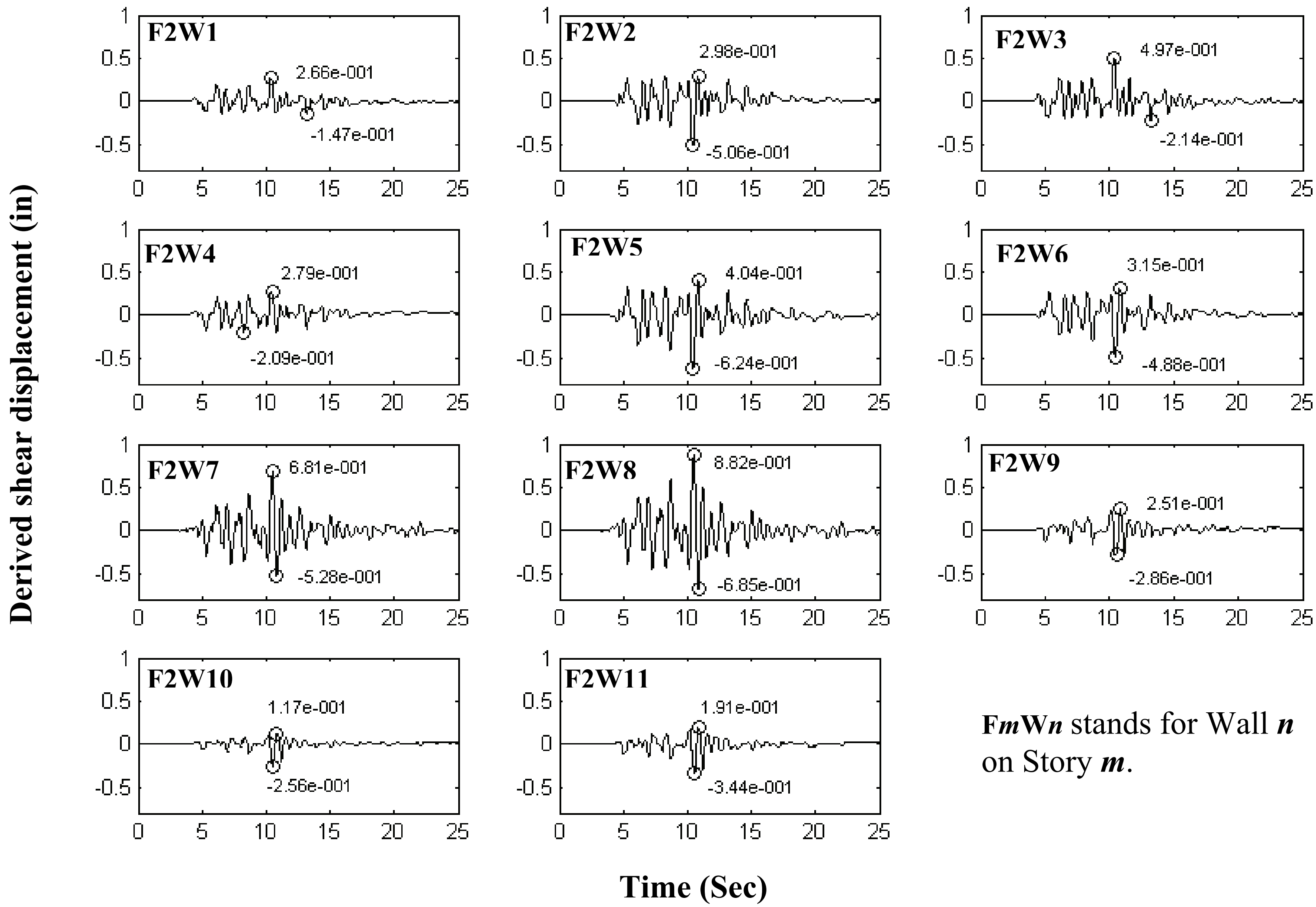

Figure L.13: Shear wall displacement derived from diagonal gage measurement for Seismic Test 4 (Part 1)

Appendix L

Shear wall displacement (Part 2) Seismic Test 4

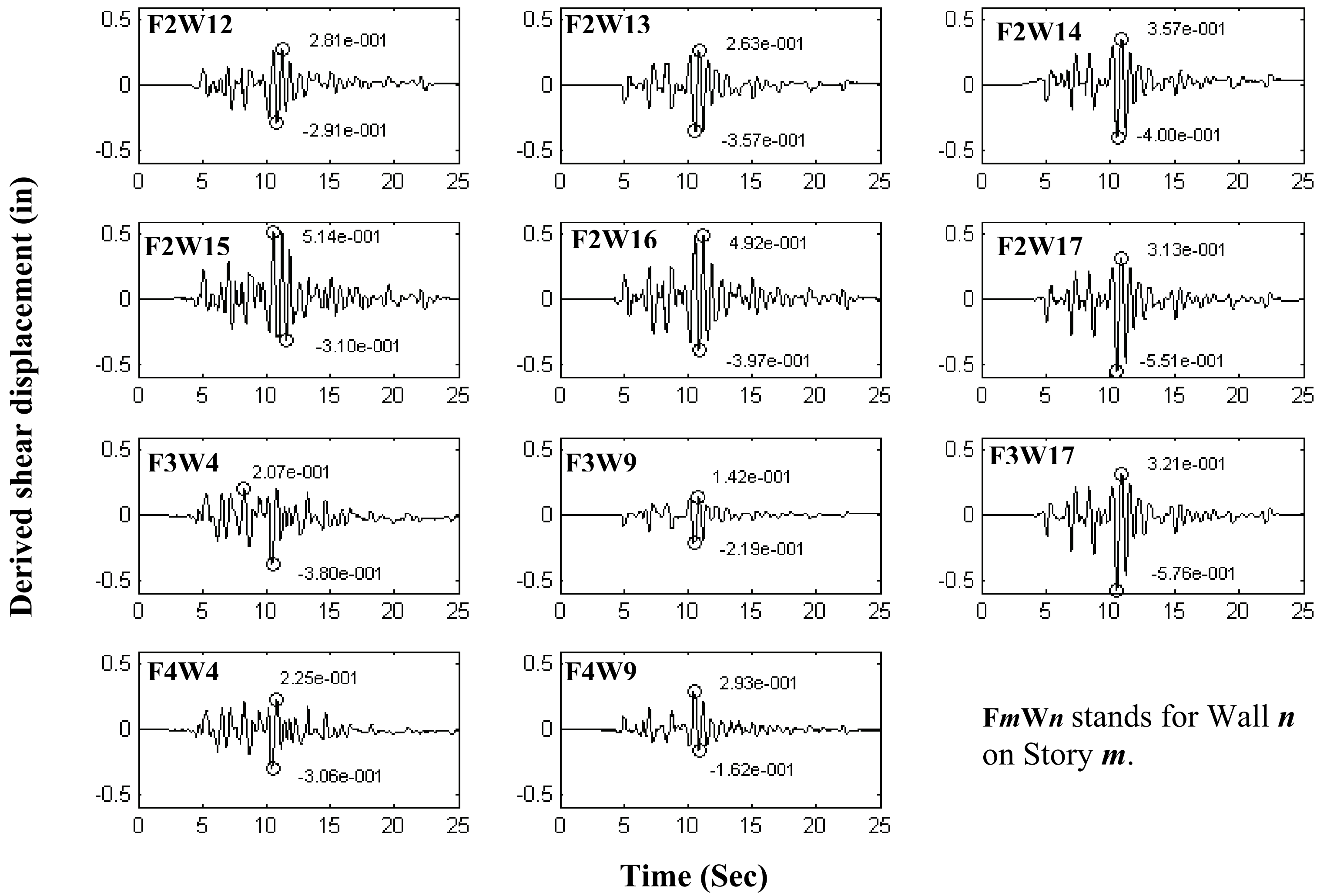

F*m*W*n* stands for Wall ***n*** on Story ***m***.

Figure L.14: Shear wall displacement derived from diagonal gage measurement for Seismic Test 4 (Part 2)

Appendix L

Shear wall displacement (Part 3) Seismic Test 4

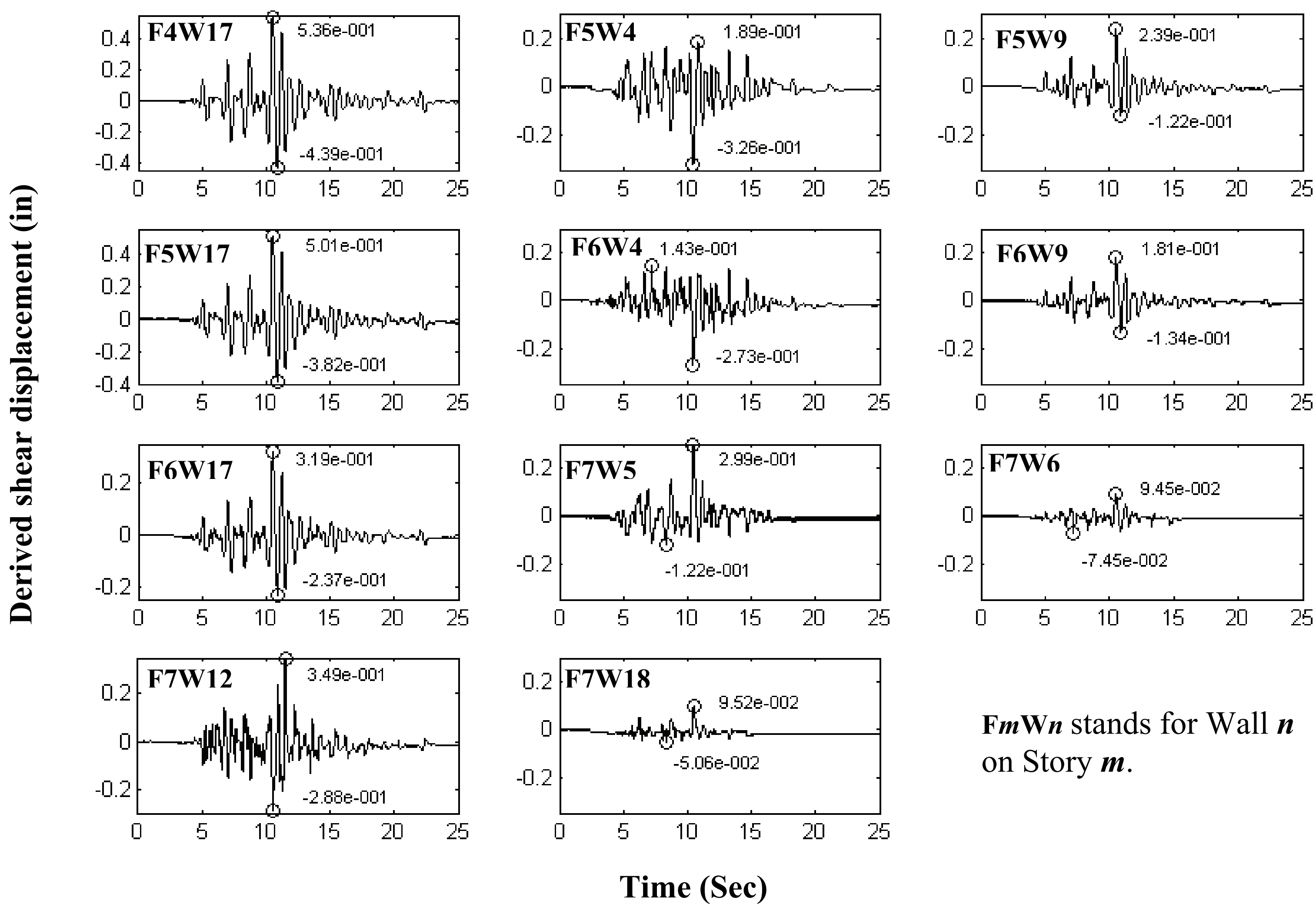

Figure L.15: Shear wall displacement derived from diagonal gage measurement for Seismic Test 4 (Part 3)

Appendix L

Shear wall displacement (Part 1) Seismic Test 5

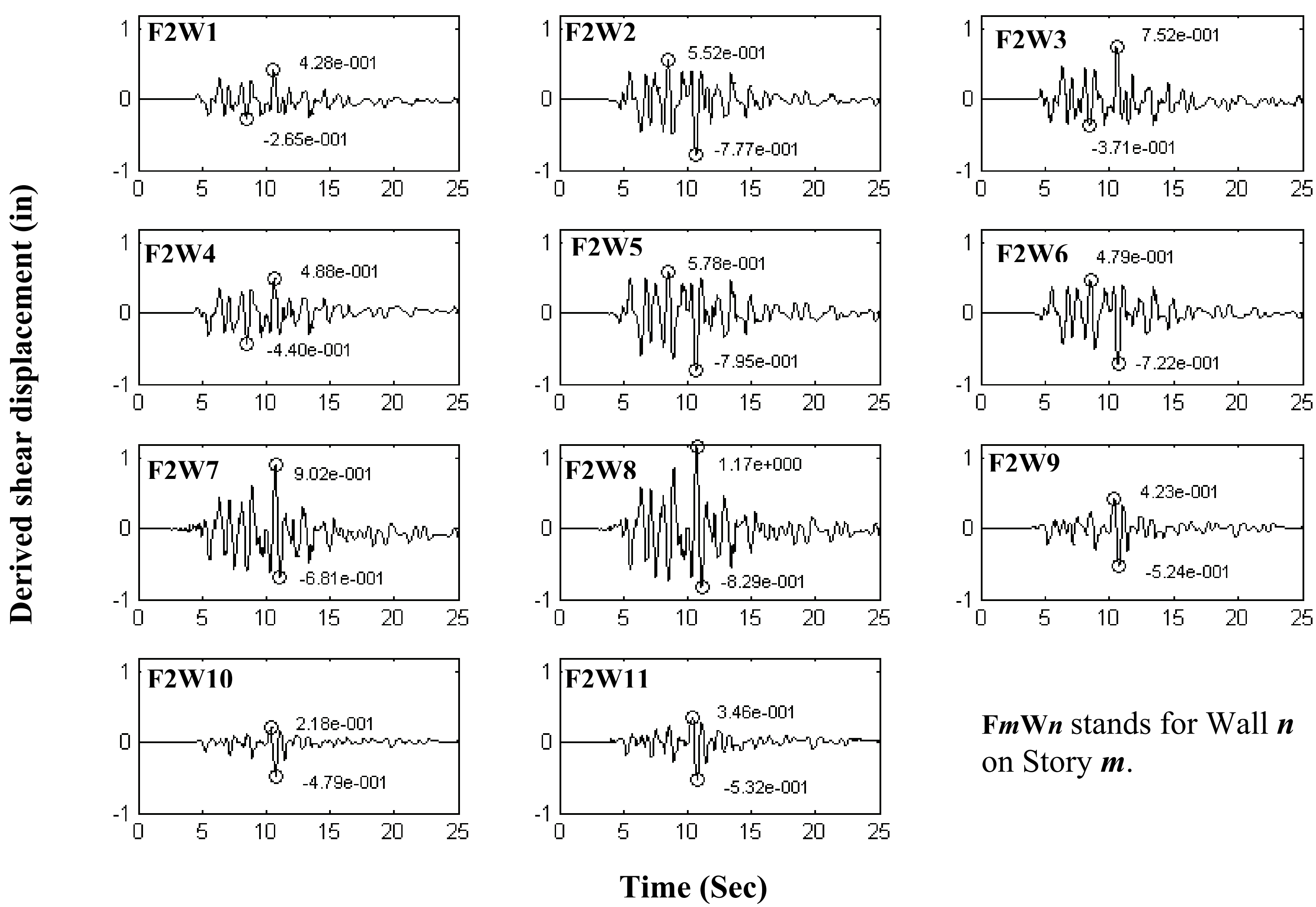

Figure L.16: Shear wall displacement derived from diagonal gage measurement for Seismic Test 5 (Part 1)

Appendix L

Shear wall displacement (Part 2) Seismic Test 5

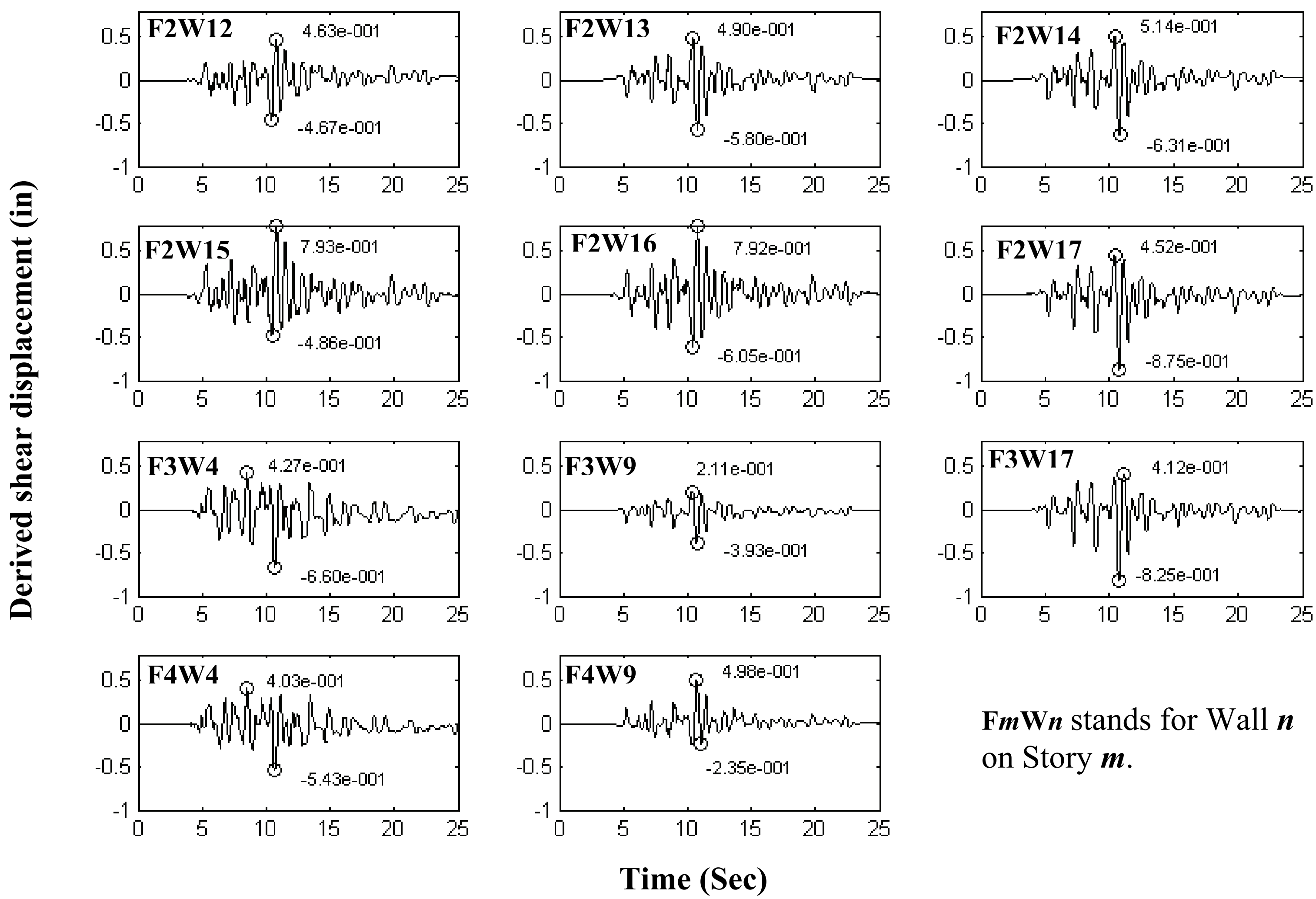

F*m*W*n* stands for Wall ***n*** on Story ***m***.

Figure L.17: Shear wall displacement derived from diagonal gage measurement for Seismic Test 5 (Part 2)

Appendix L

Shear wall displacement (Part 3) Seismic Test 5

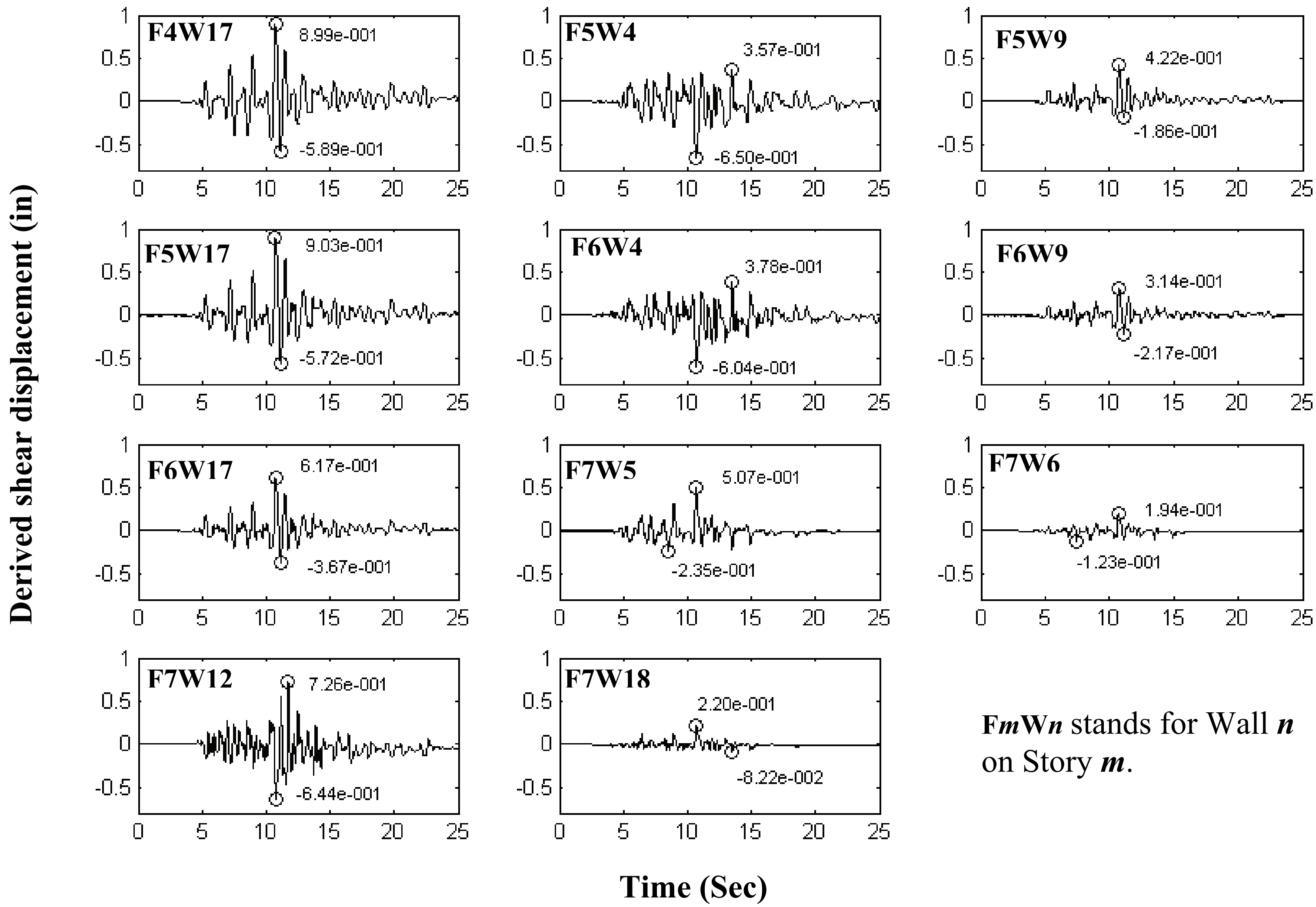

Figure L.18: Shear wall displacement derived from diagonal gage measurement for Seismic Test 5 (Part 3)

Appendix M

Seismic Test Results: Differential ATS rod force measurements

Appendix M

ATS anchor rod numbering (Story 2)

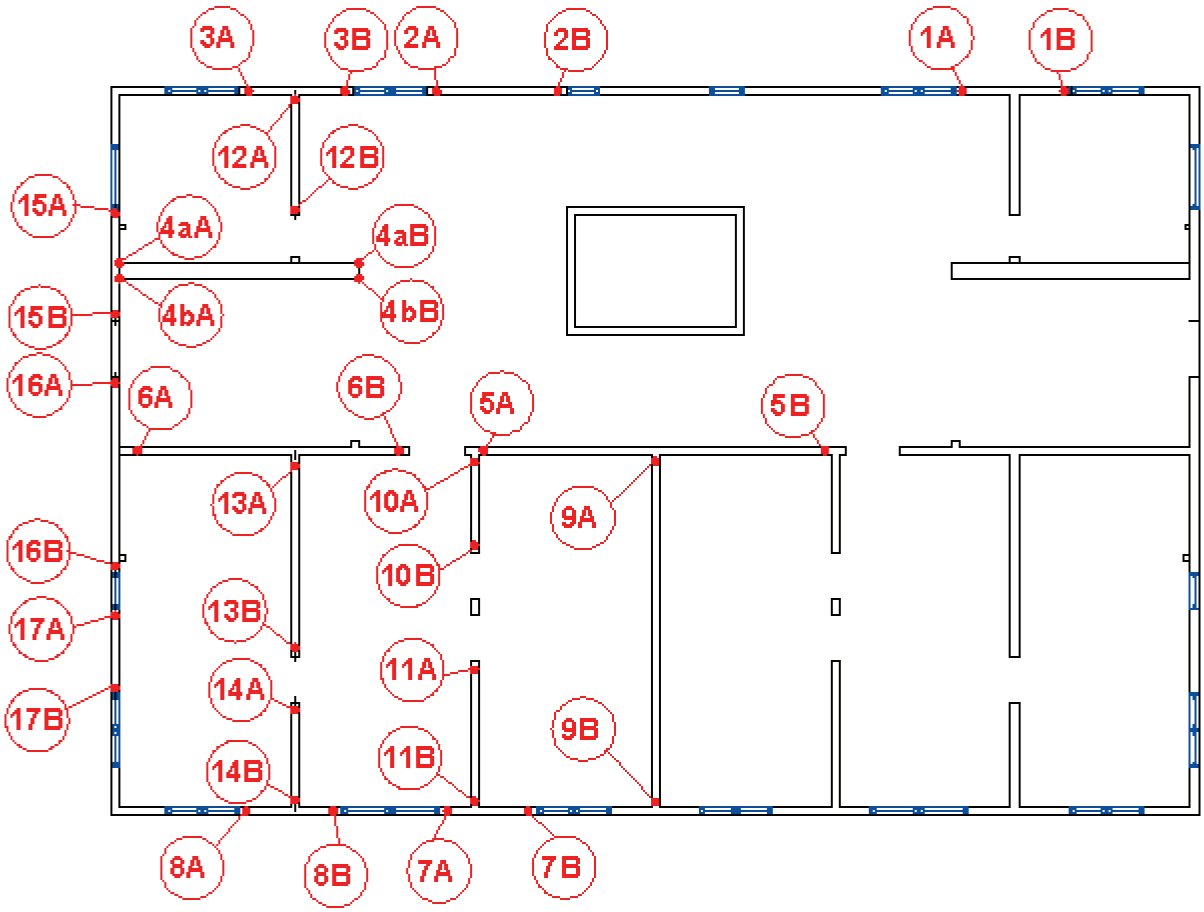

Figure M.1: ATS rod number for story 2

Appendix M

ATS anchor rod numbering (Story 3~6)

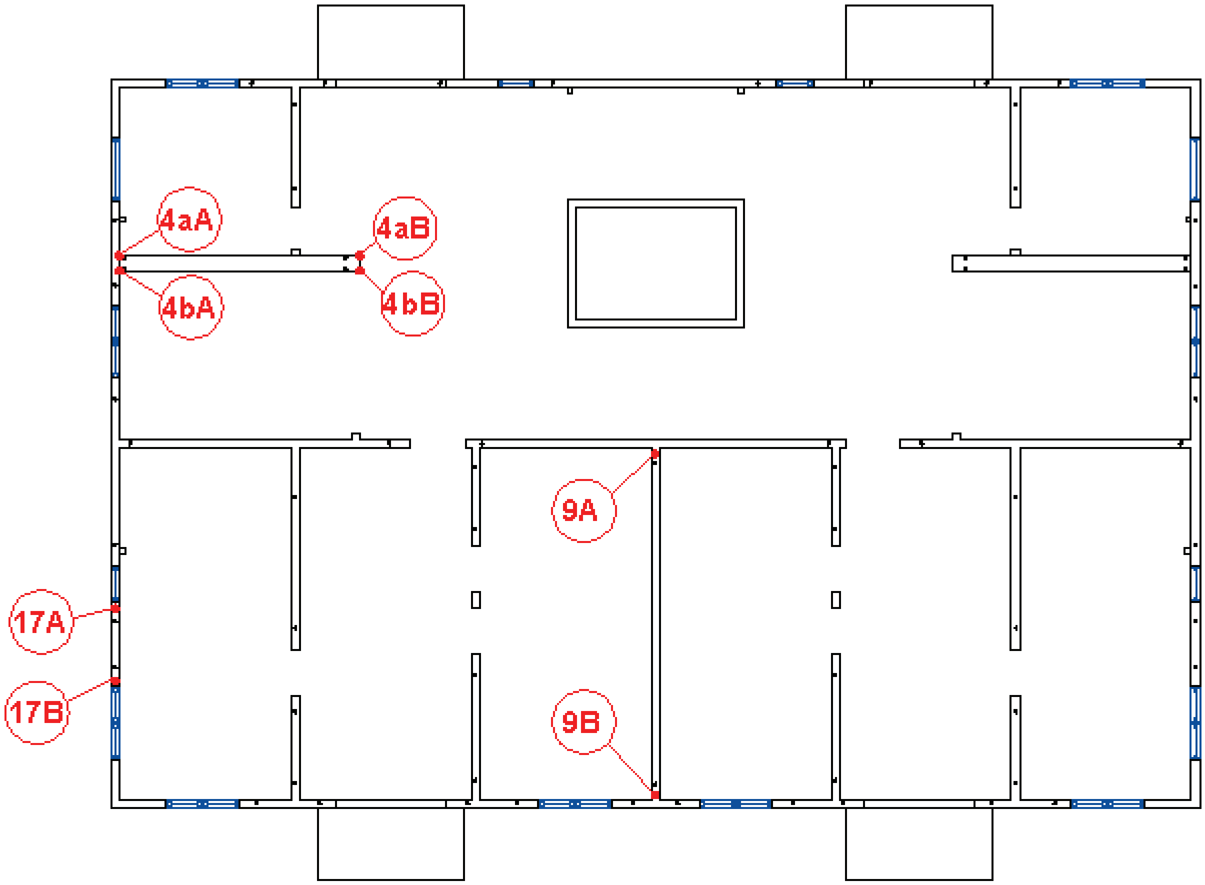

Figure M.2: ATS rod number for story 3~6

Appendix M

ATS anchor rod numbering (Story 7)

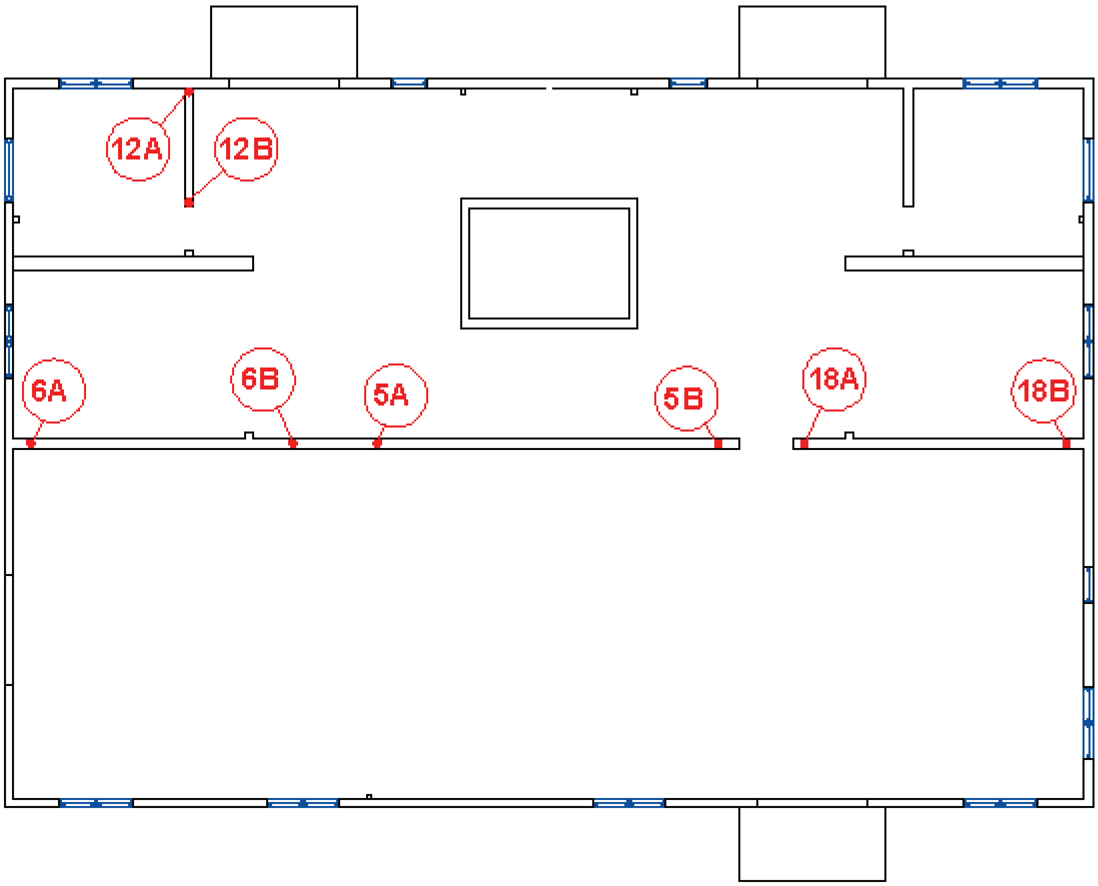

Figure M.3: ATS rod number for story 7

Appendix M

ATS rod forces for Seismic Test 1 (Part 1)

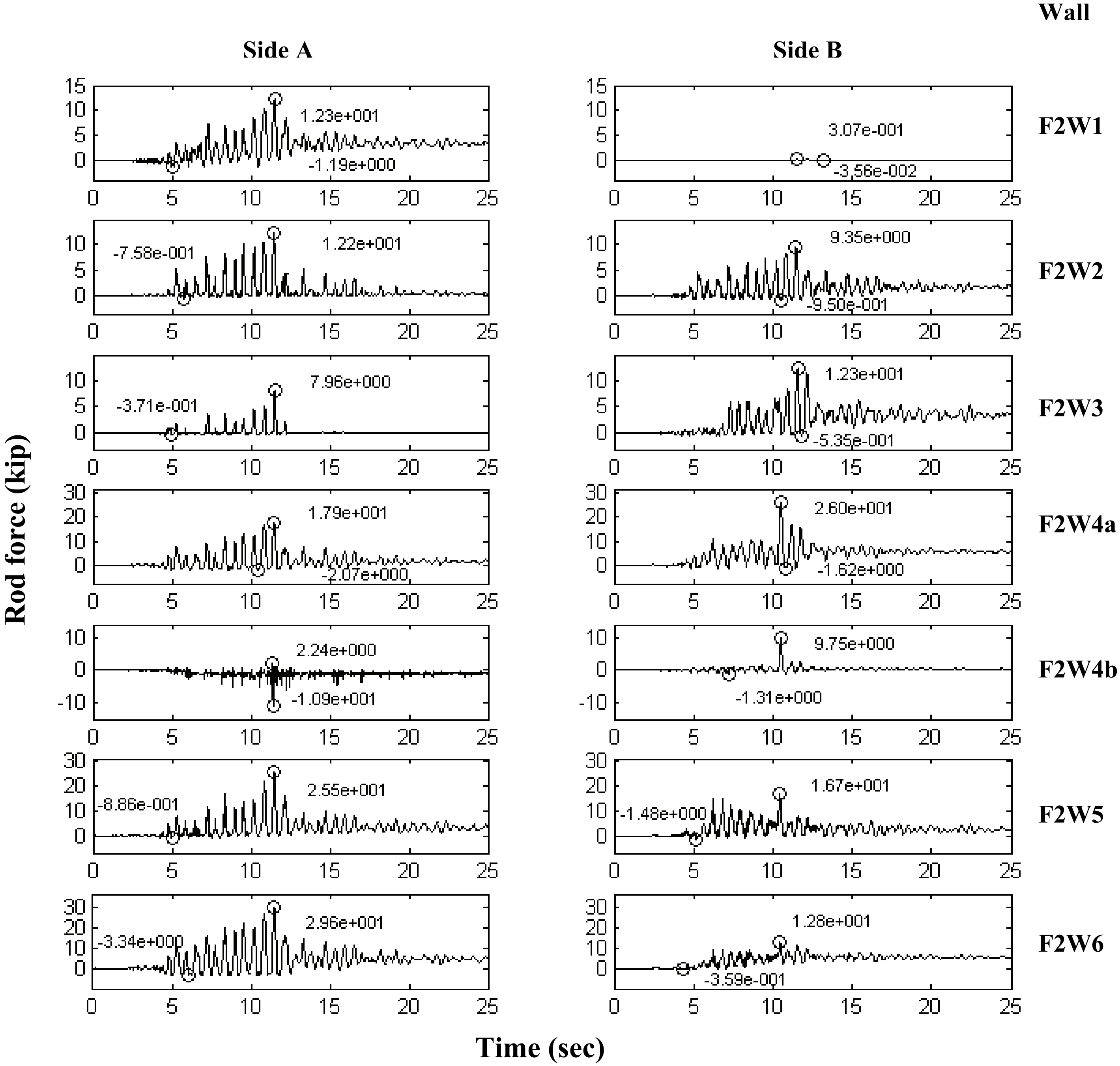

Figure M.4: ATS rod forces for Seismic Test 1 (Part 1)

Appendix M

ATS rod forces for Seismic Test 1 (Part 2)

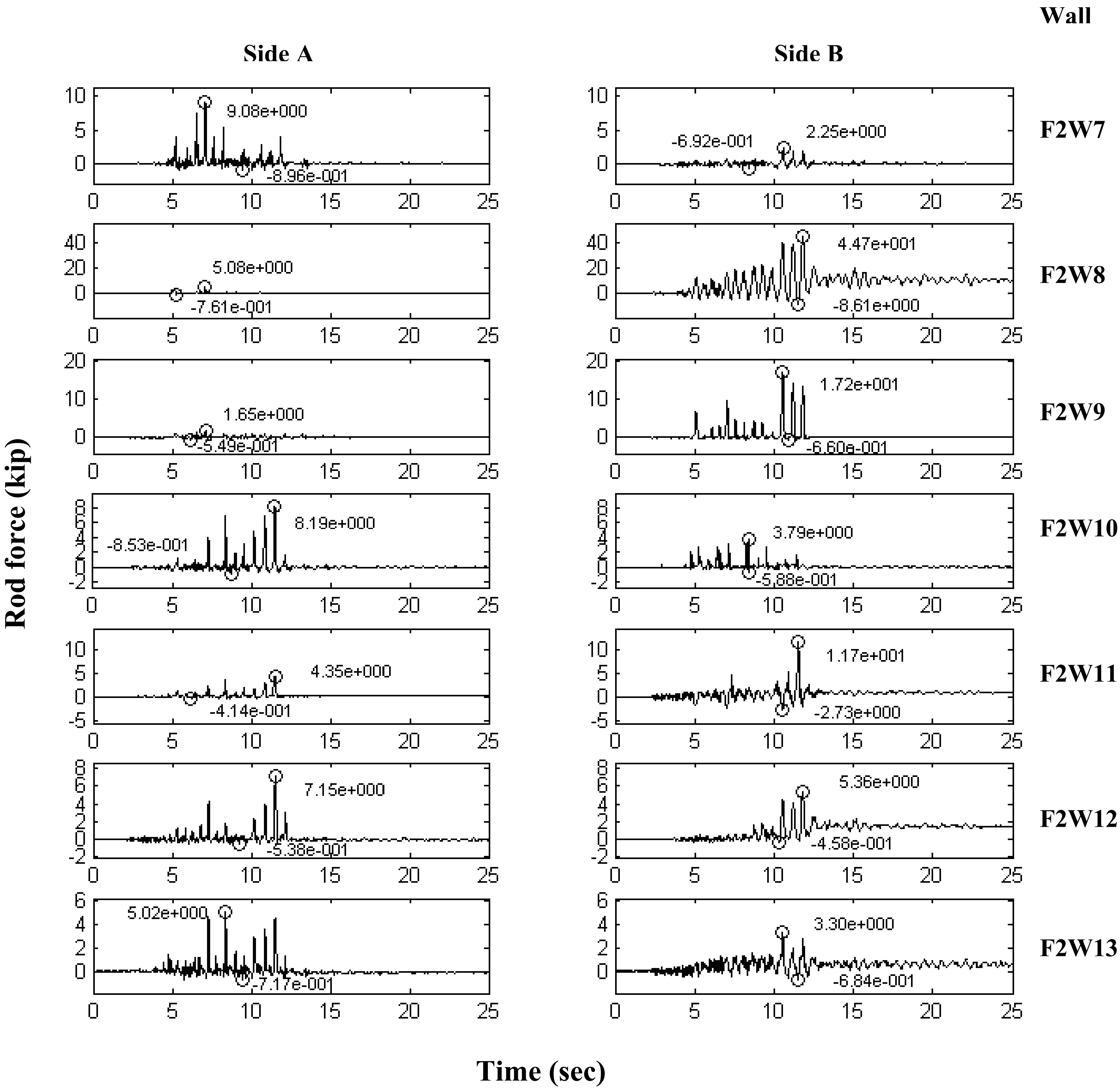

Figure M.5: ATS rod forces for Seismic Test 1 (Part 2)

Appendix M

ATS rod forces for Seismic Test 1 (Part 3)

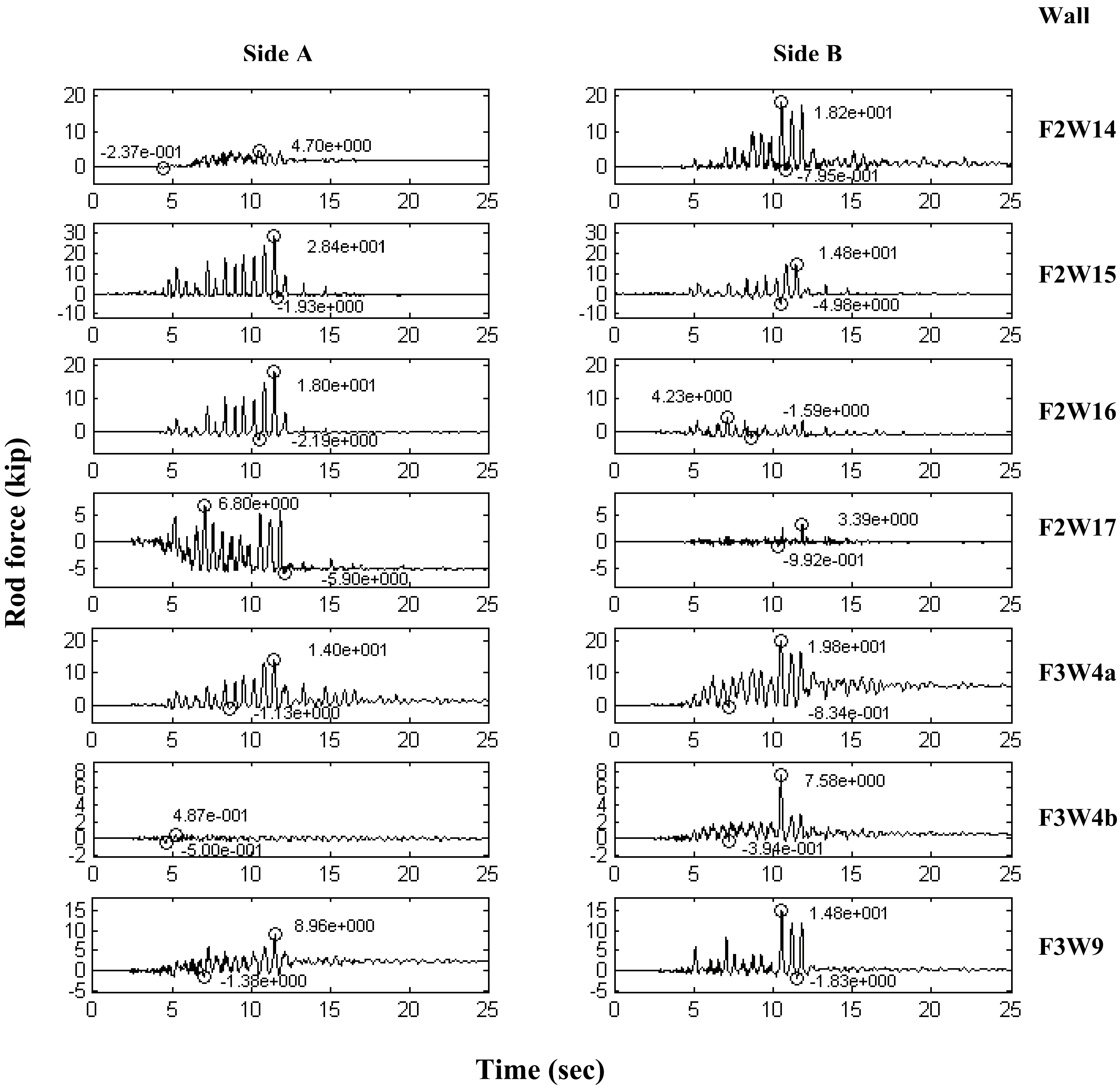

Figure M.6: ATS rod forces for Seismic Test 1 (Part 3)

Appendix M

ATS rod forces for Seismic Test 1 (Part 4)

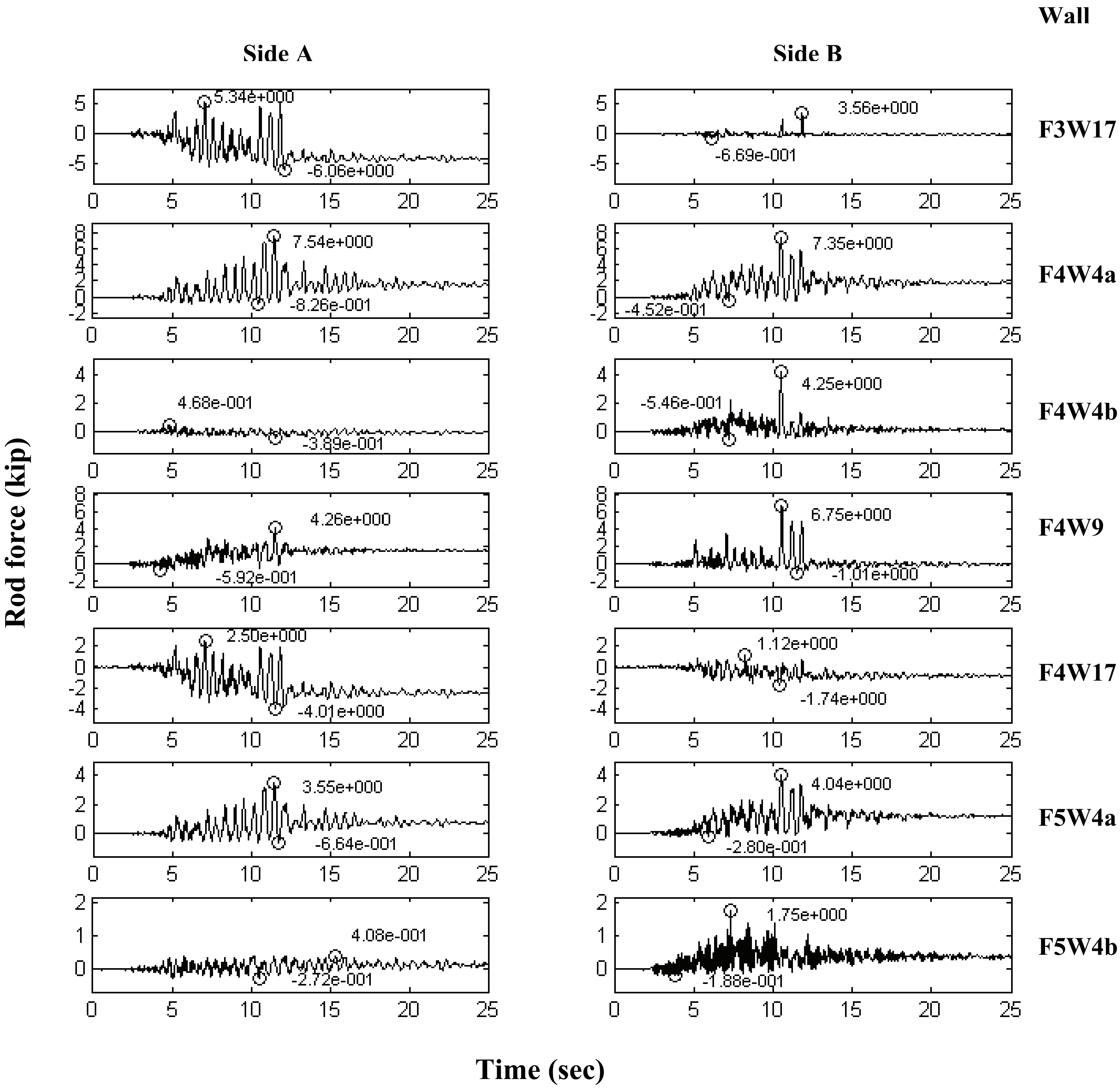

Figure M.7: ATS rod forces for Seismic Test 1 (Part 4)

Appendix M

ATS rod forces for Seismic Test 1 (Part 5)

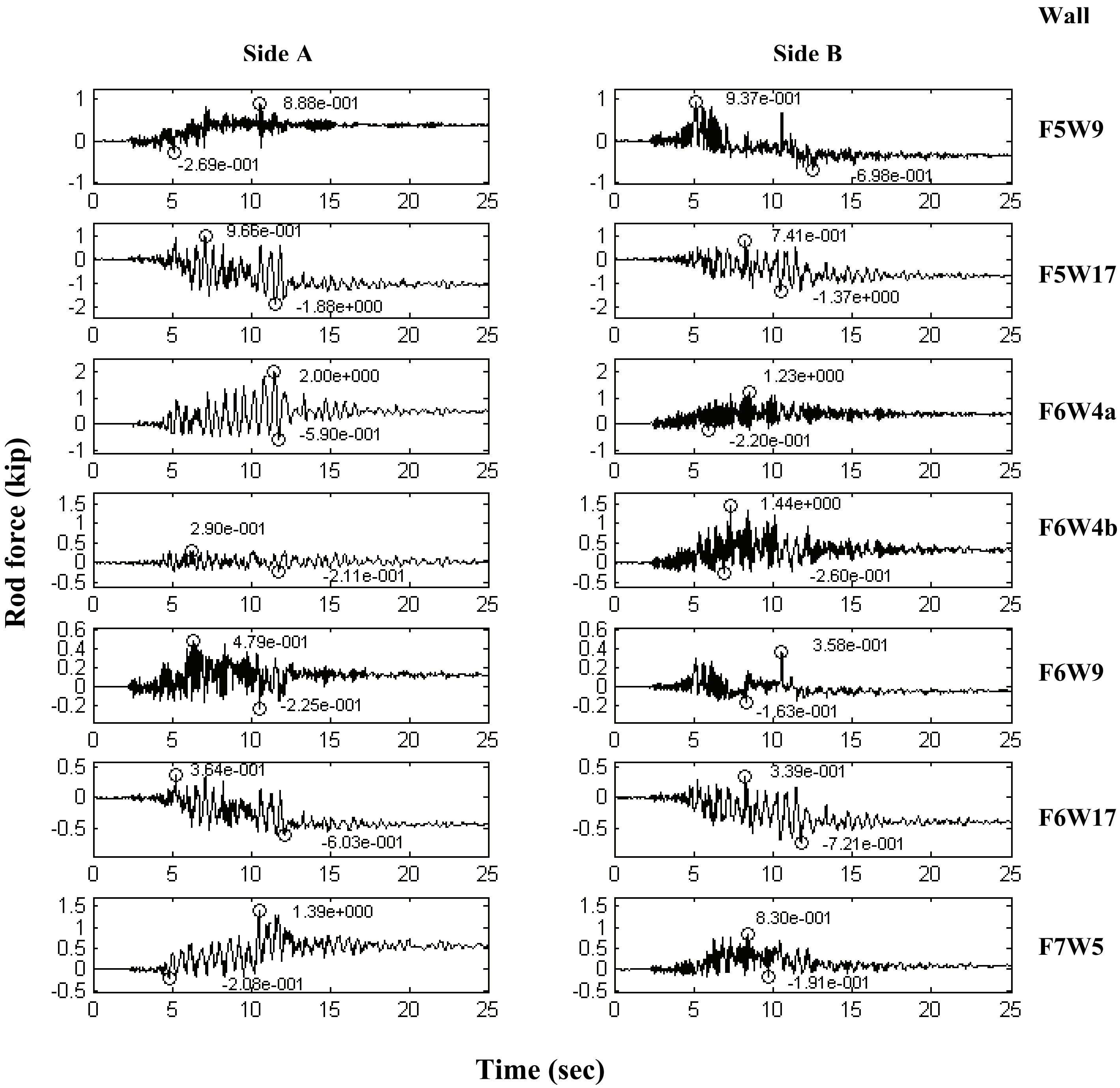

Figure M.8: ATS rod forces for Seismic Test 1 (Part 5)

Appendix M

ATS rod forces for Seismic Test 1 (Part 6)

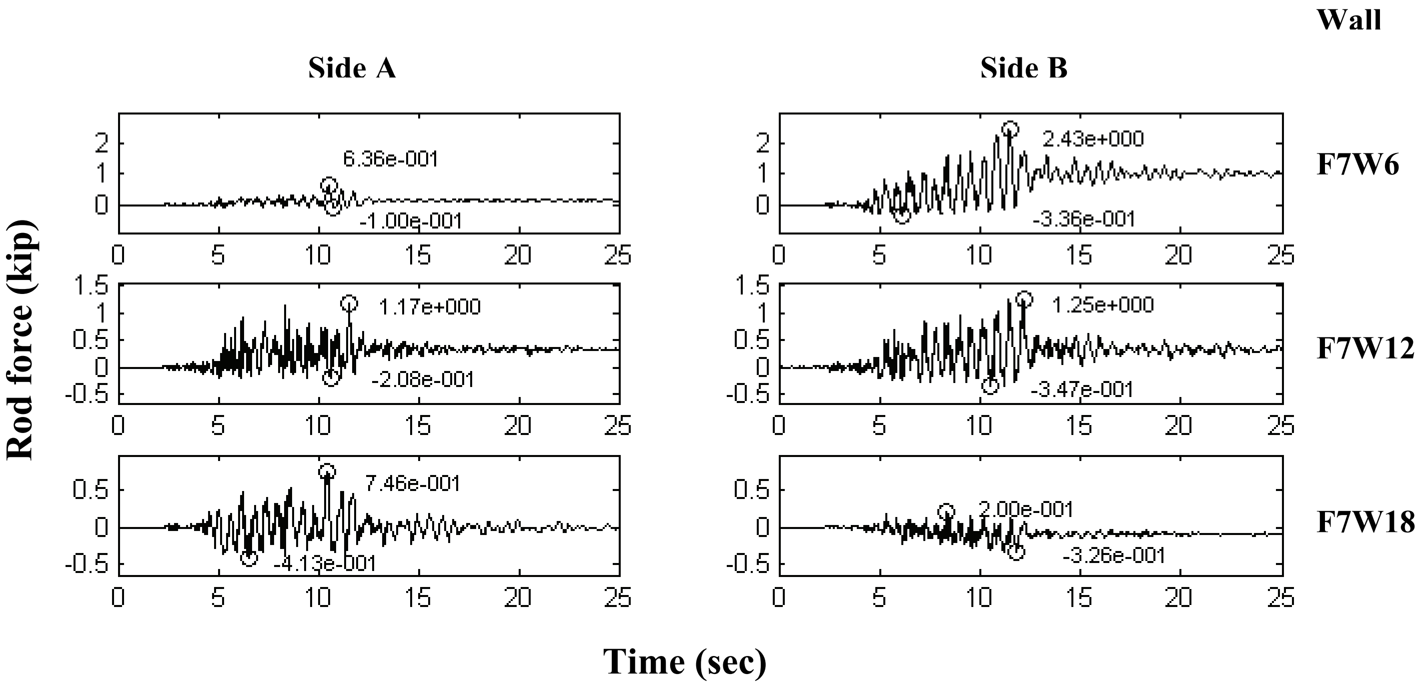

Figure M.9: ATS rod forces for Seismic Test 1 (Part 6)

Appendix M

ATS rod forces for Seismic Test 2 (Part 1)

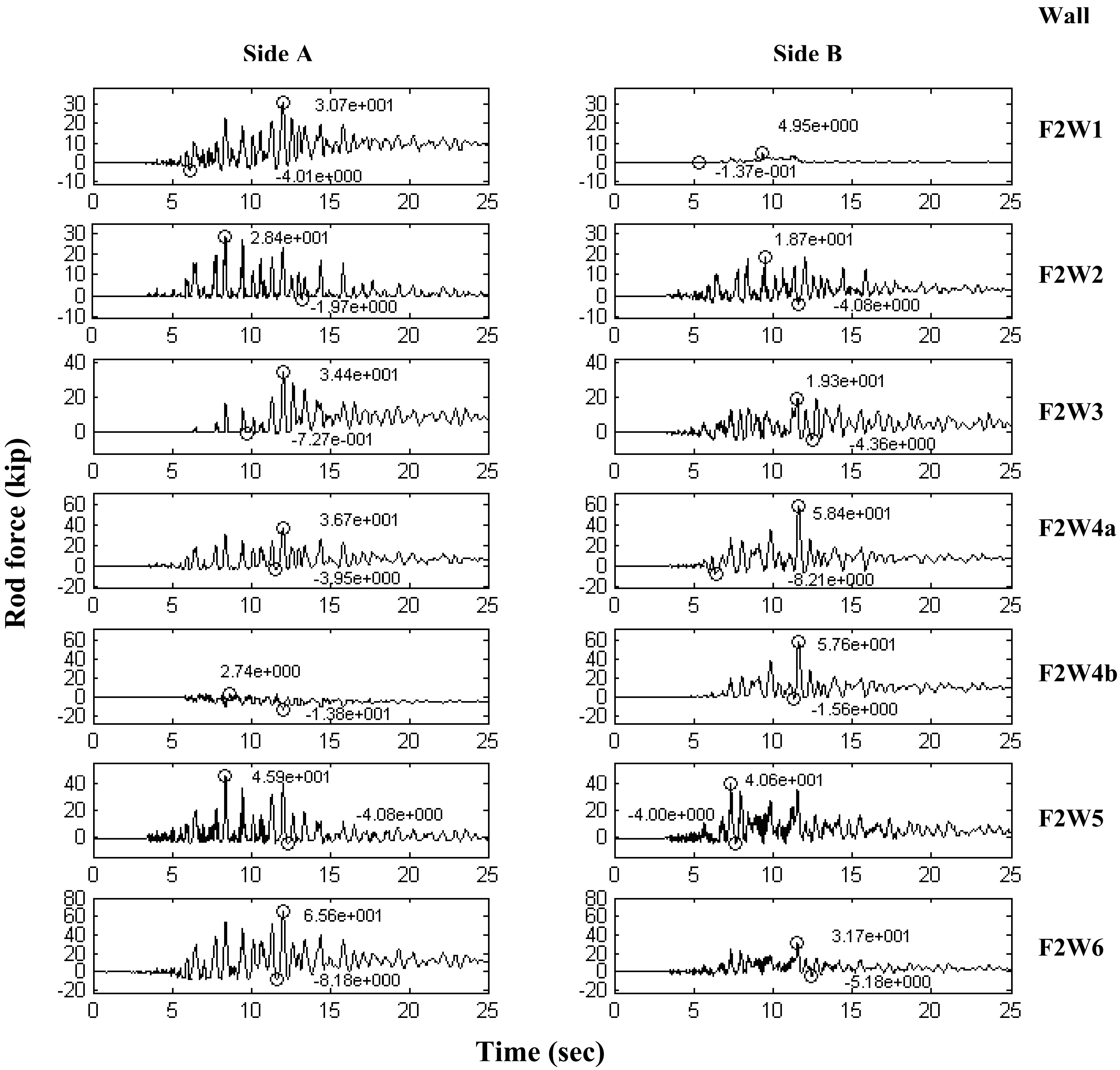

Figure M.10: ATS rod forces for Seismic Test 2 (Part 1)

Appendix M

ATS rod forces for Seismic Test 2 (Part 2)

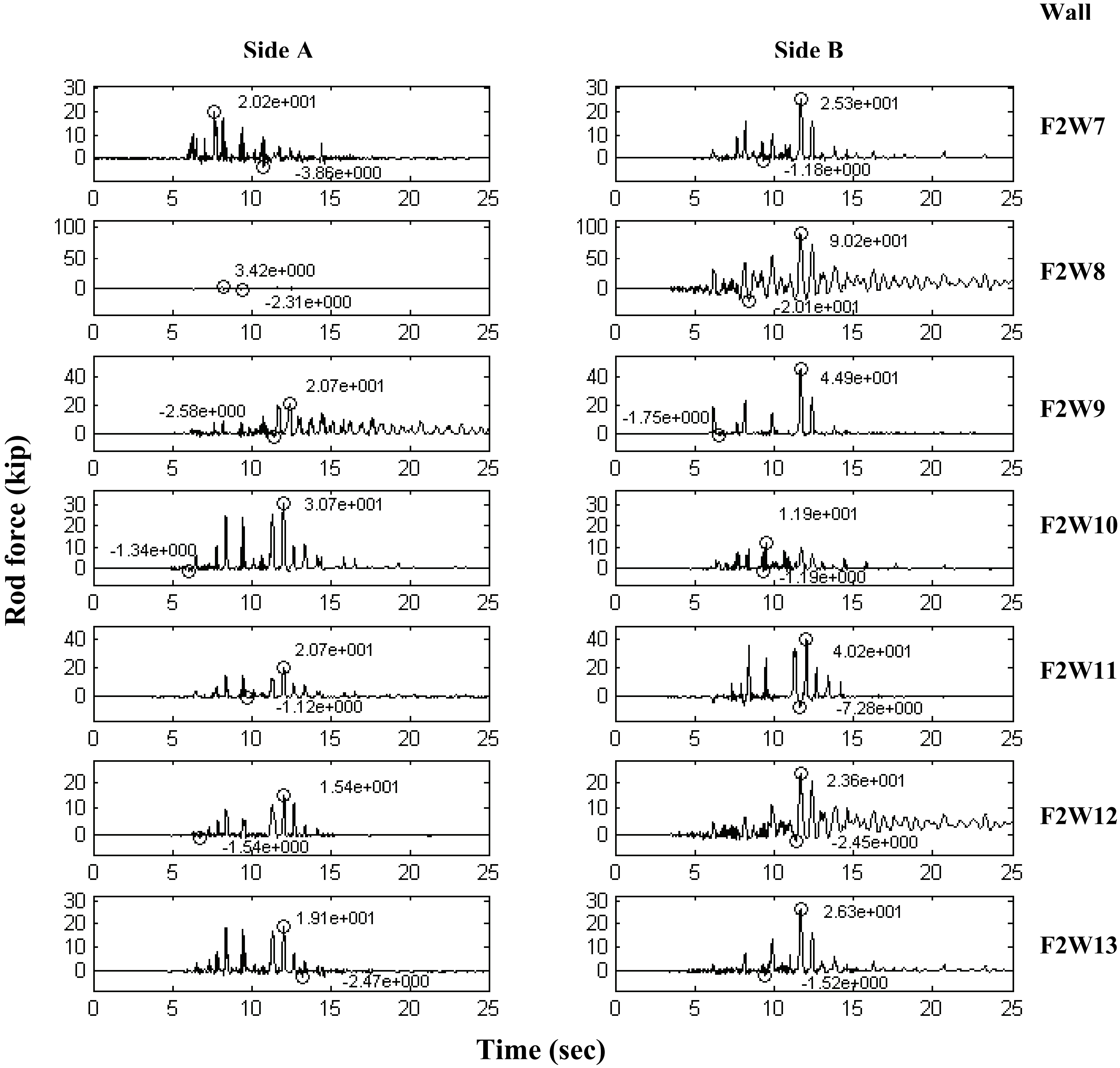

Figure M.11: ATS rod forces for Seismic Test 2 (Part 2)

Appendix M

ATS rod forces for Seismic Test 2 (Part 3)

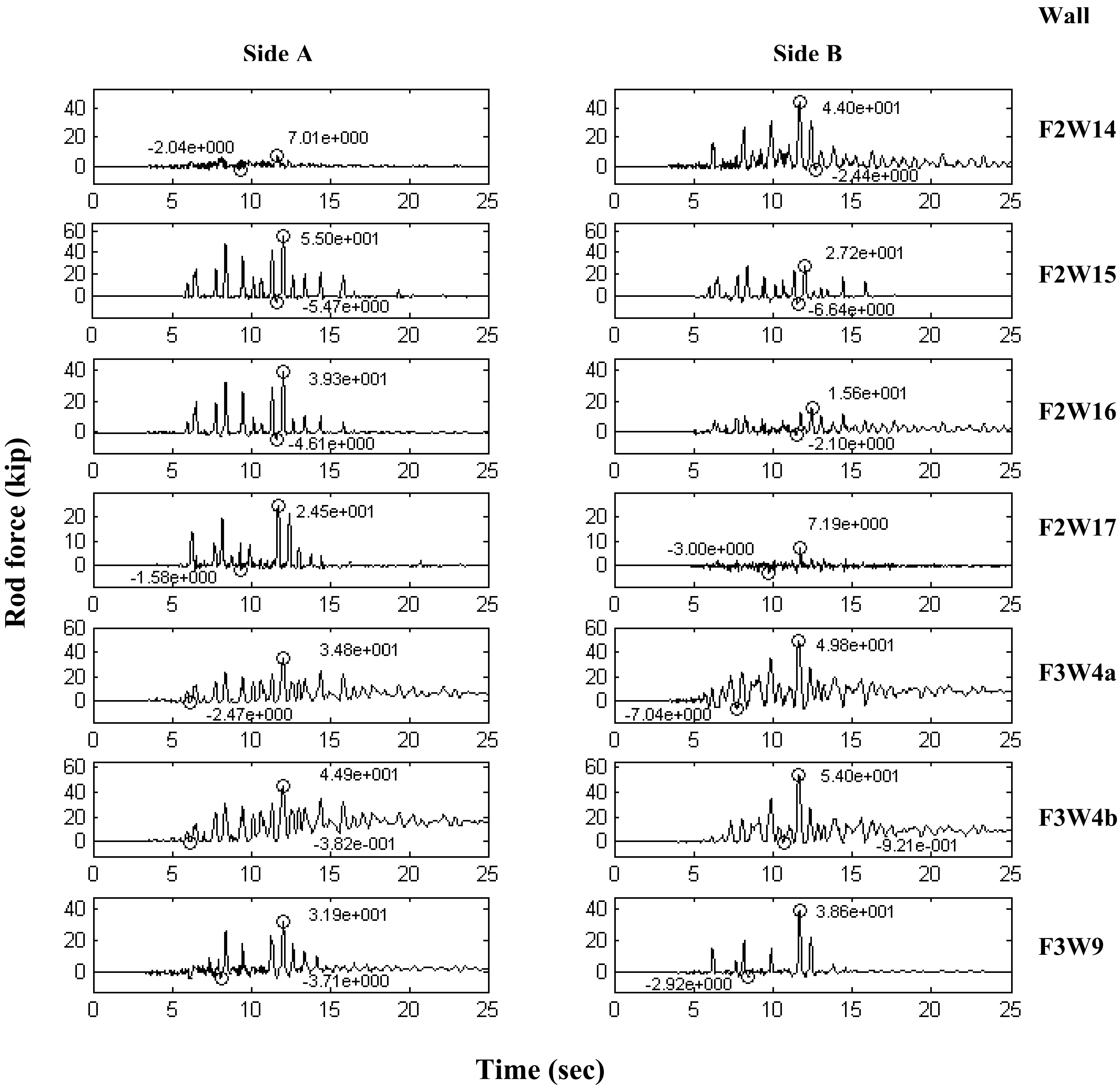

Figure M.12: ATS rod forces for Seismic Test 2 (Part 3)

Appendix M

ATS rod forces for Seismic Test 2 (Part 4)

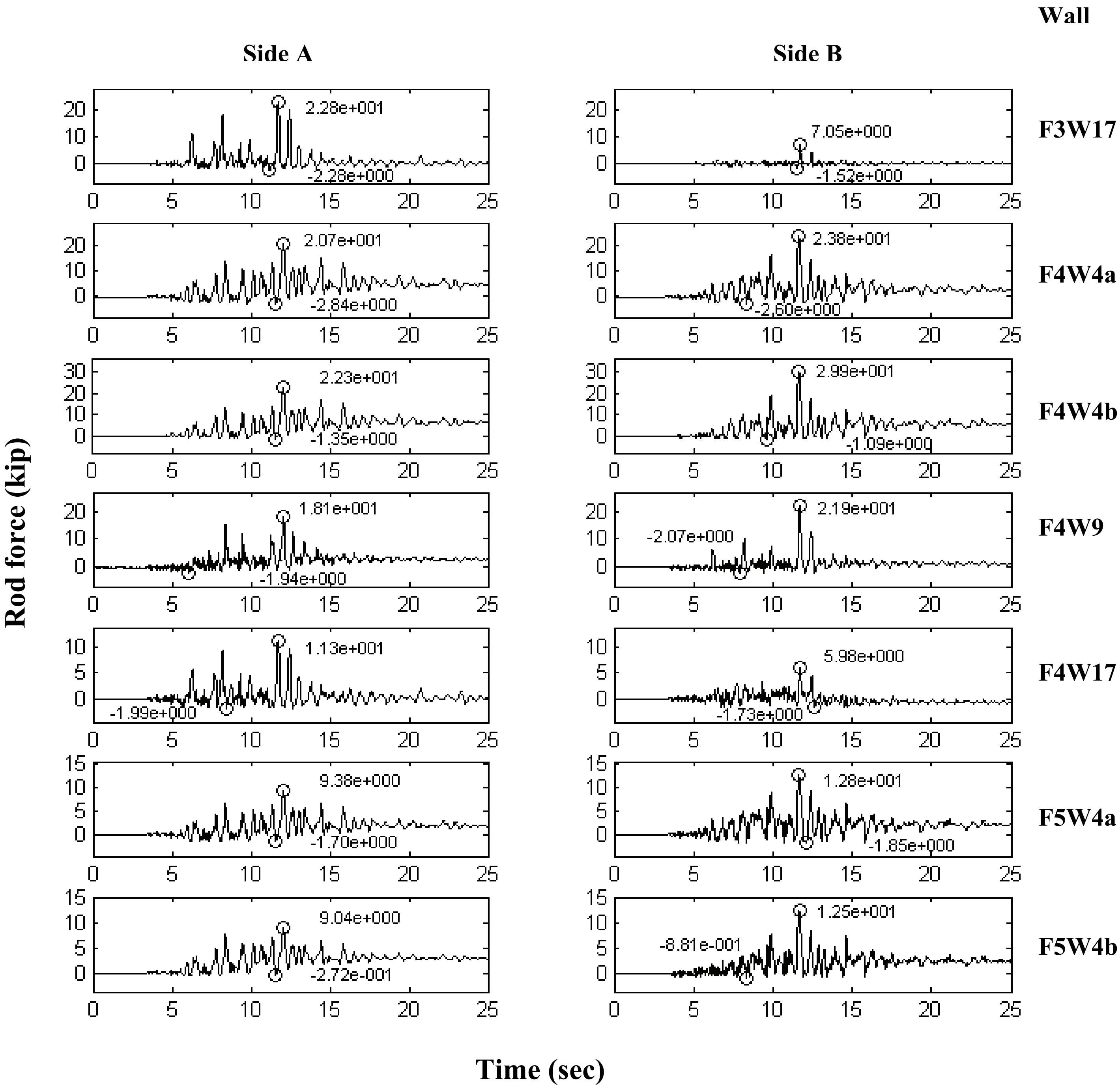

Figure M.13: ATS rod forces for Seismic Test 2 (Part 4)

Appendix M

ATS rod forces for Seismic Test 2 (Part 5)

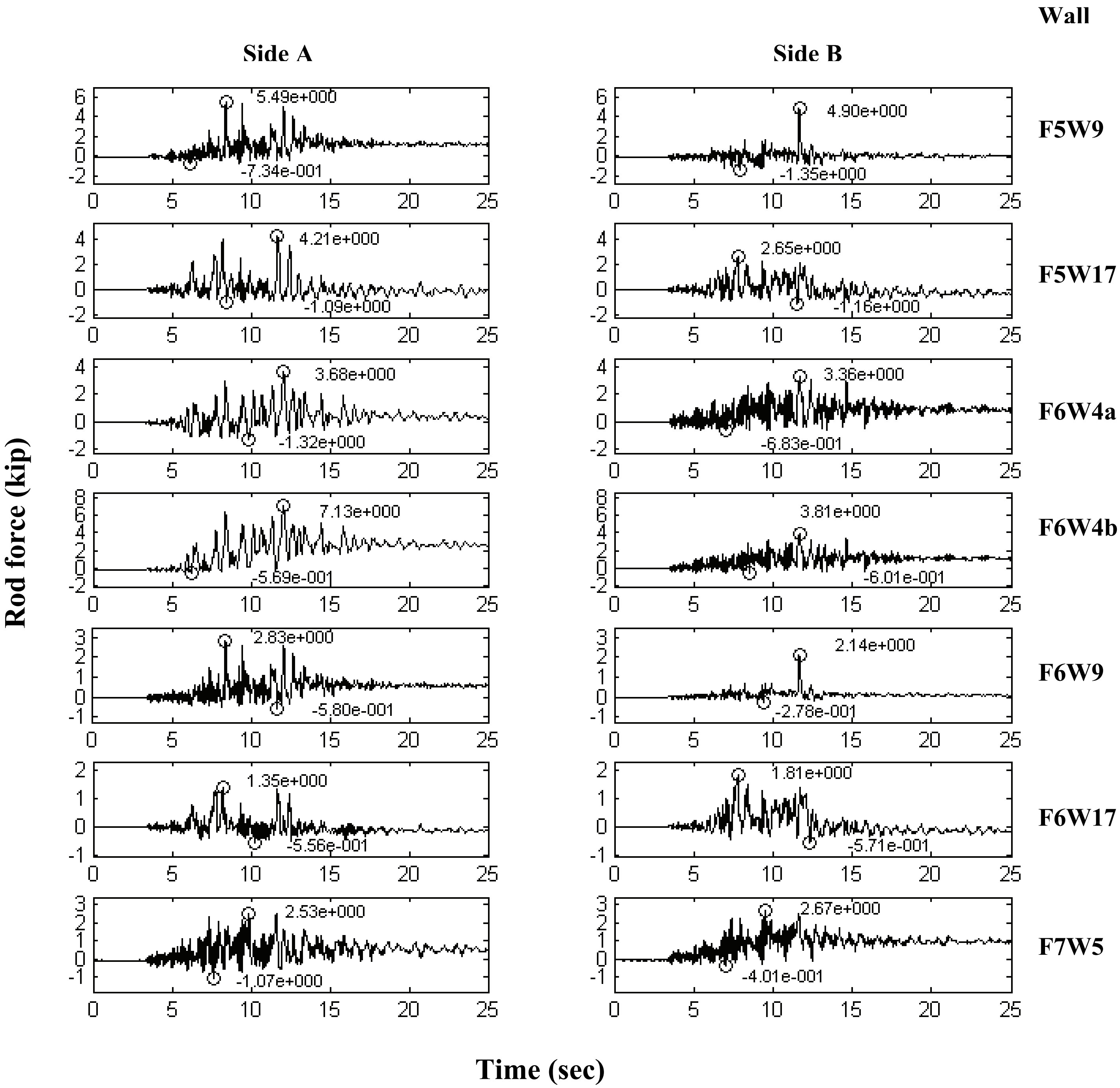

Figure M.14: ATS rod forces for Seismic Test 2 (Part 5)

Appendix M

ATS rod forces for Seismic Test 2 (Part 6)

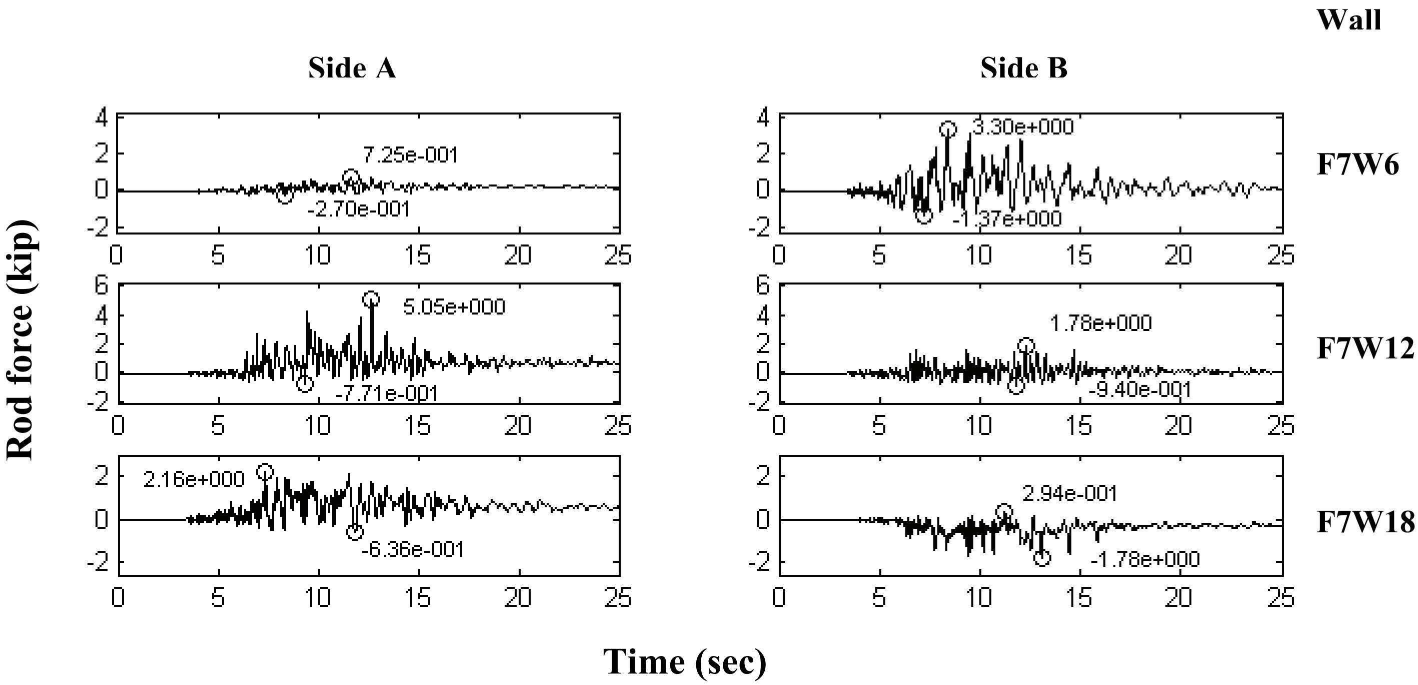

Figure M.15: ATS rod forces for Seismic Test 2 (Part 6)

Appendix M

ATS rod forces for Seismic Test 3 (Part 1)

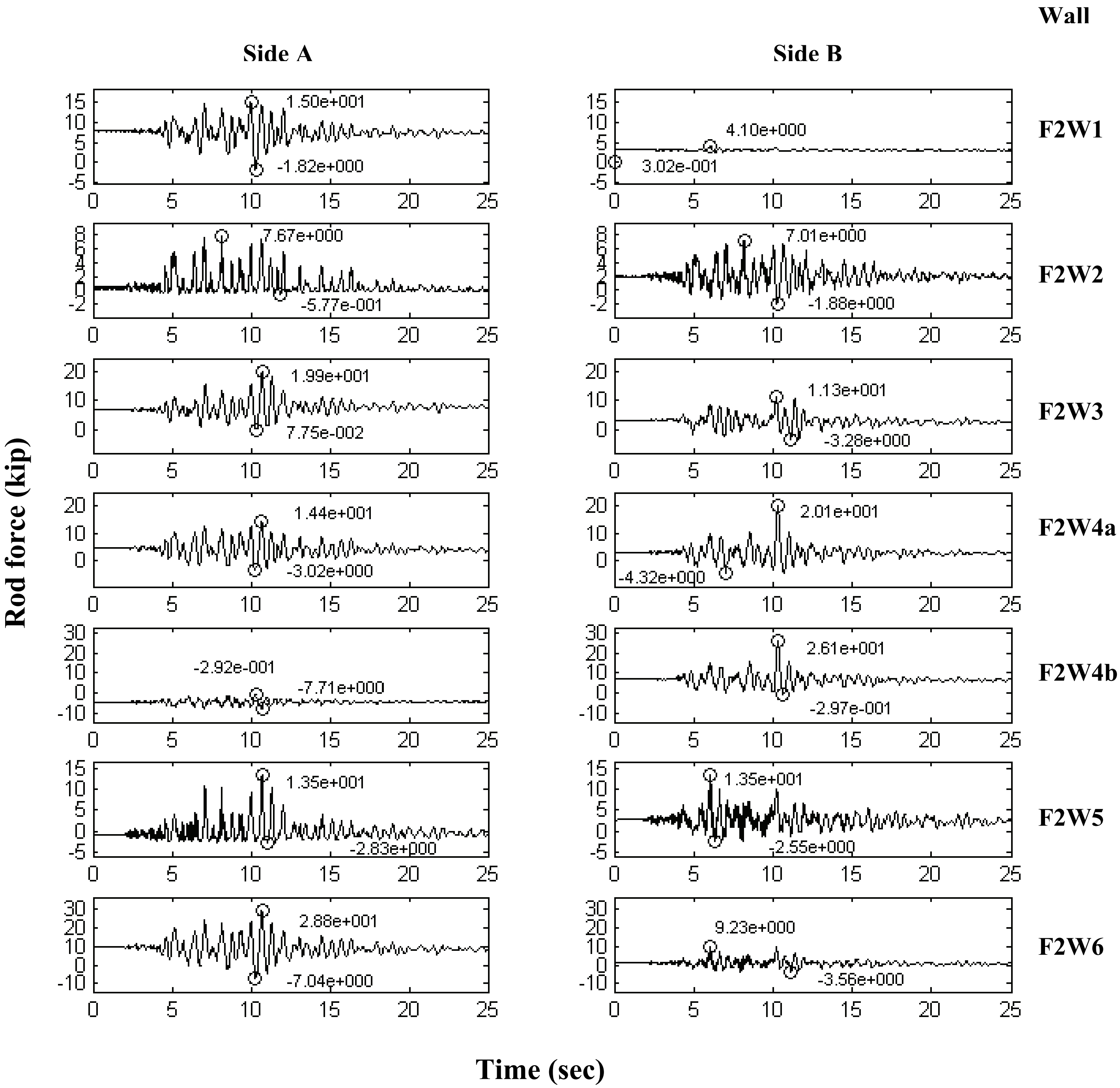

Figure M.16: ATS rod forces for Seismic Test 3 (Part 1)

Appendix M

ATS rod forces for Seismic Test 3 (Part 2)

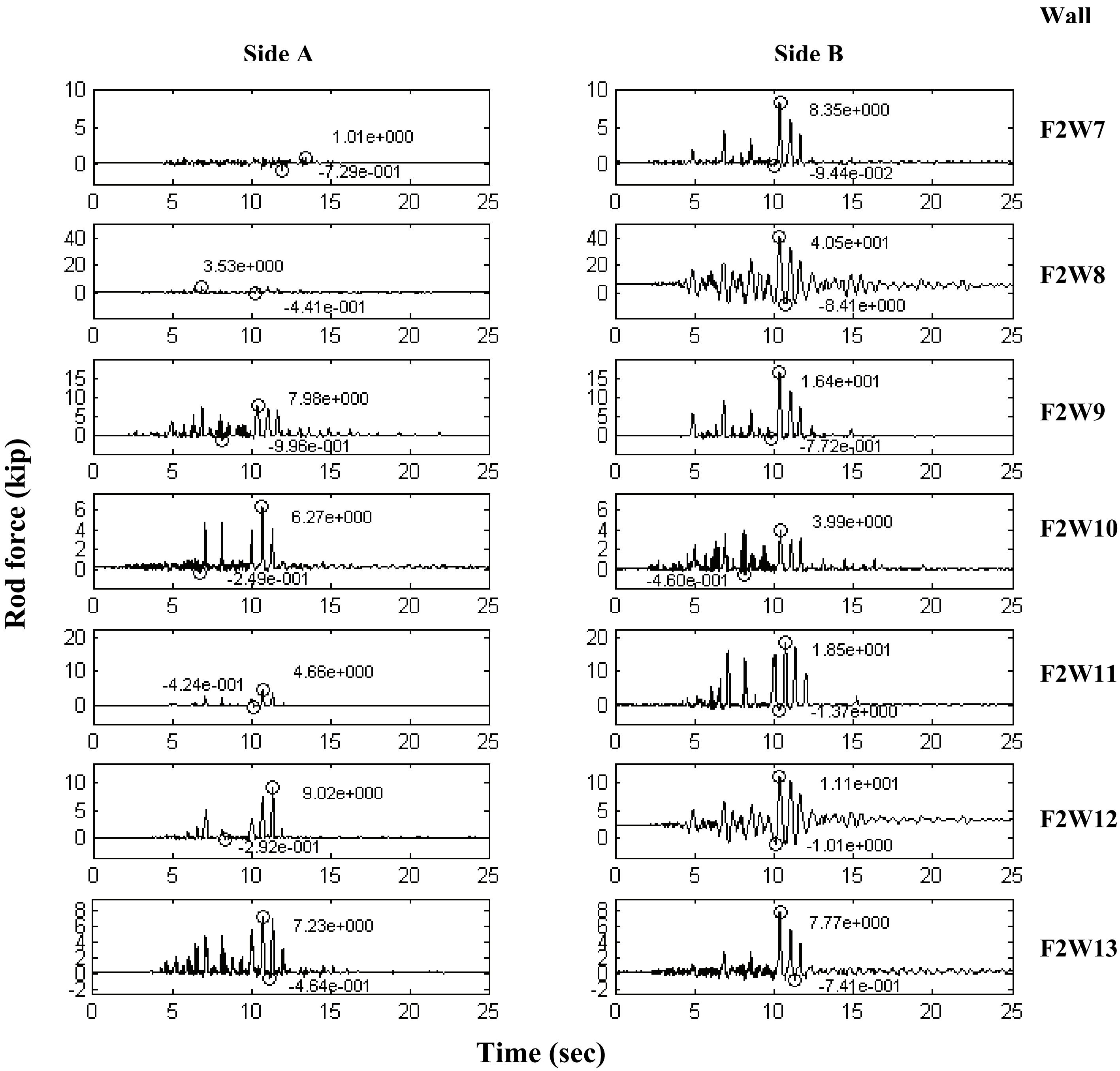

Figure M.17: ATS rod forces for Seismic Test 3 (Part 2)

Appendix M

ATS rod forces for Seismic Test 3 (Part 3)

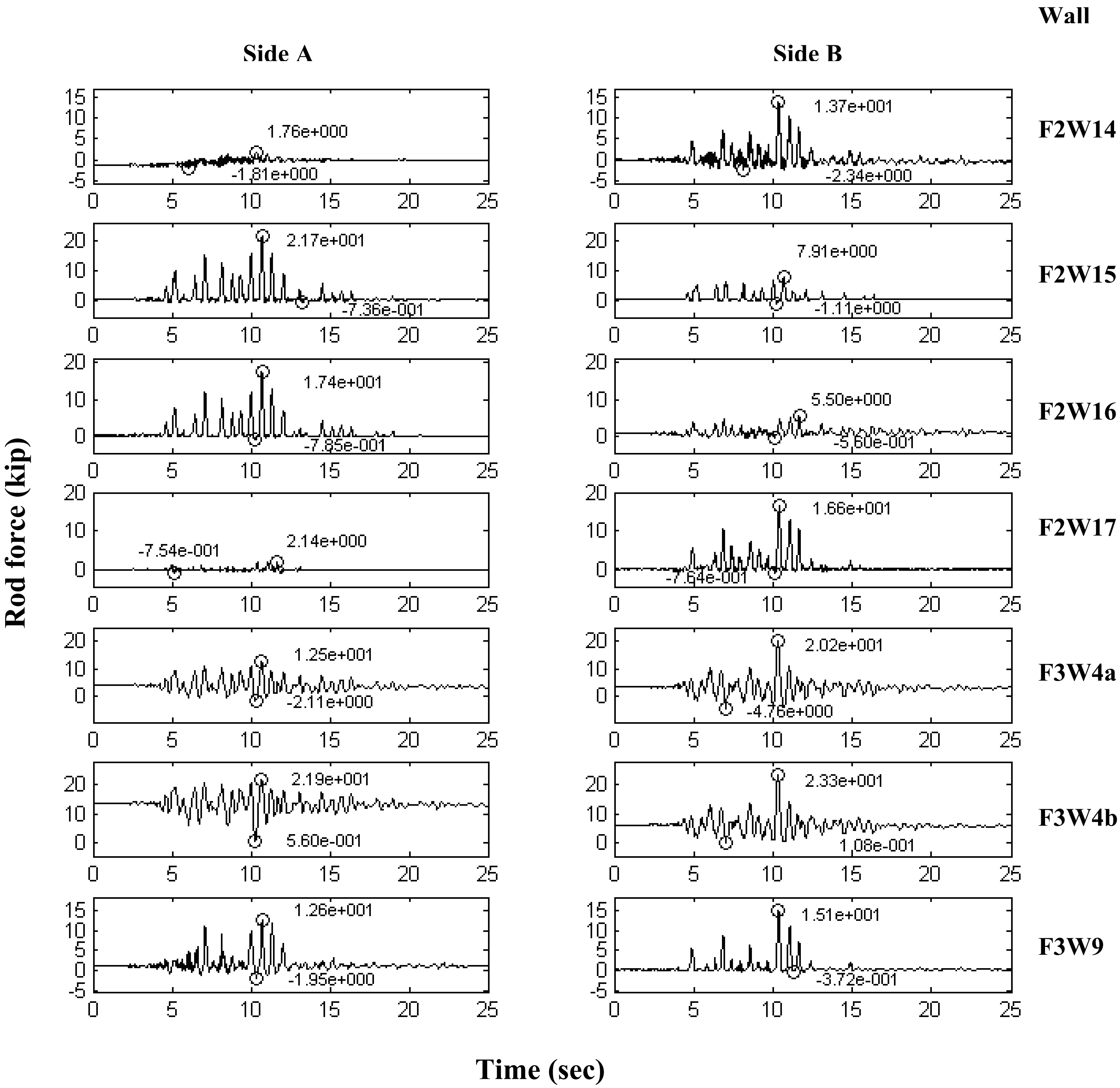

Figure M.18: ATS rod forces for Seismic Test 3 (Part 3)

Appendix M

ATS rod forces for Seismic Test 3 (Part 4)

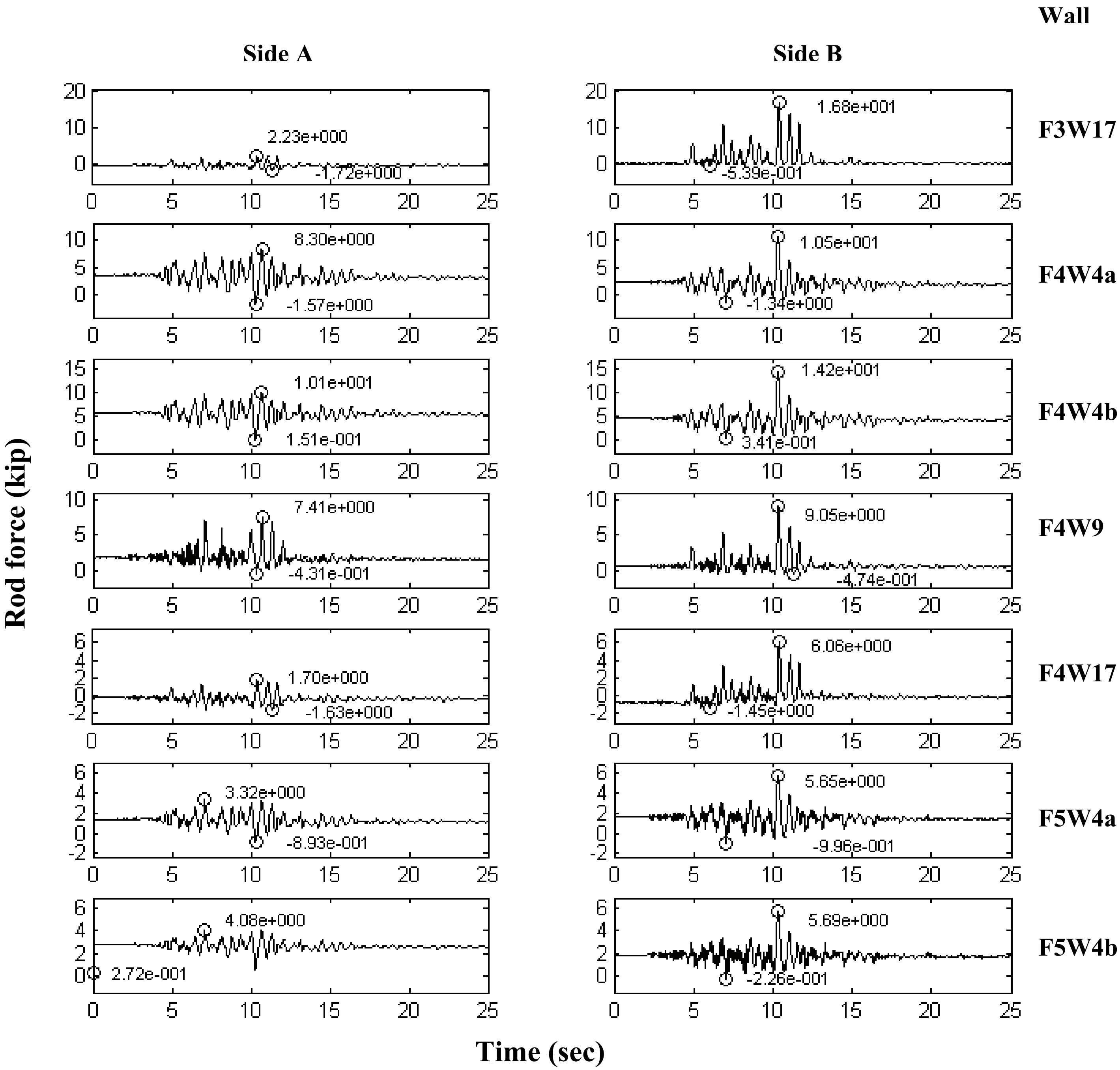

Figure M.19: ATS rod forces for Seismic Test 3 (Part 4)

Appendix M

ATS rod forces for Seismic Test 3 (Part 5)

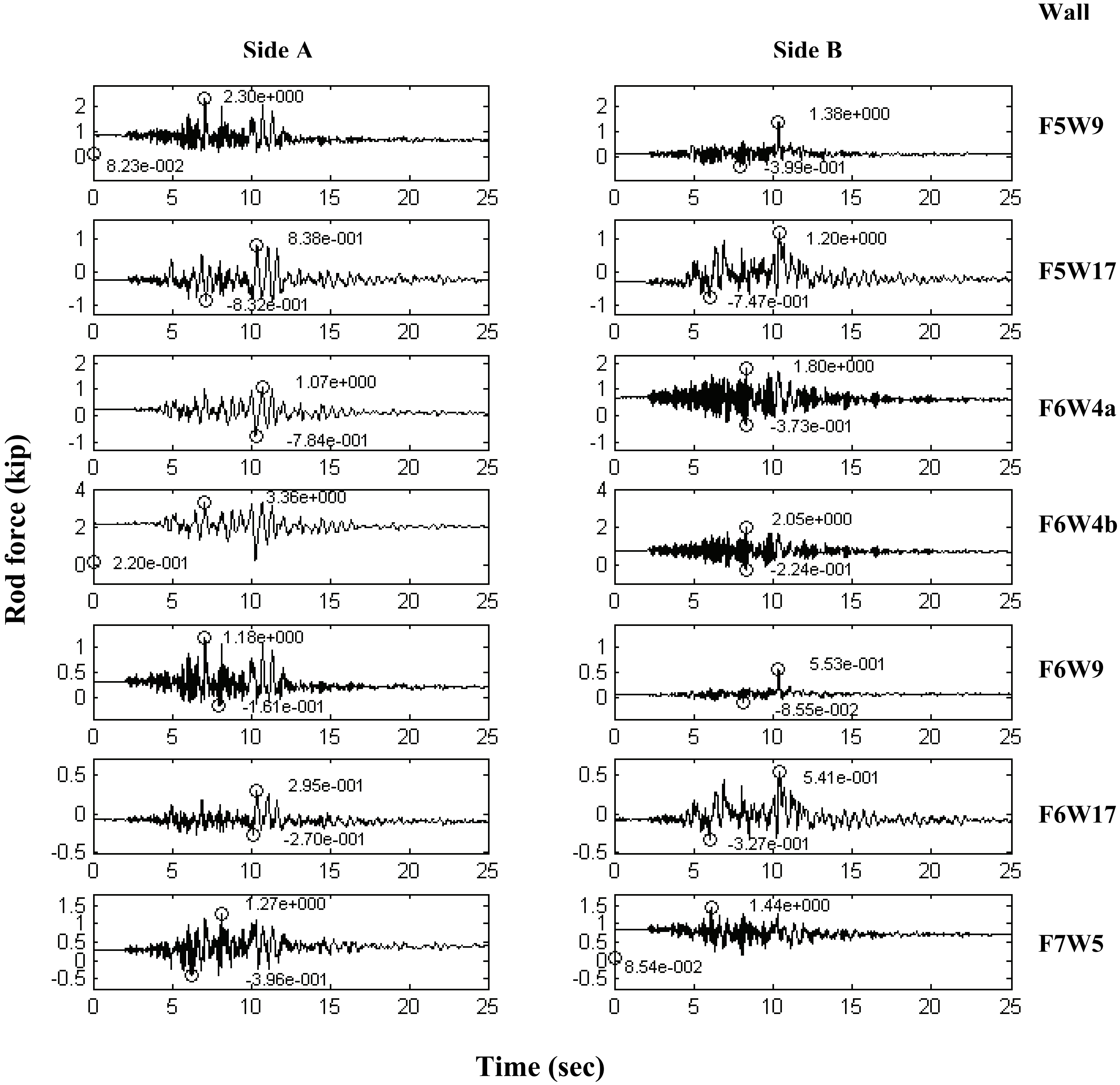

Figure M.20: ATS rod forces for Seismic Test 3 (Part 5)

Appendix M

ATS rod forces for Seismic Test 3 (Part 6)

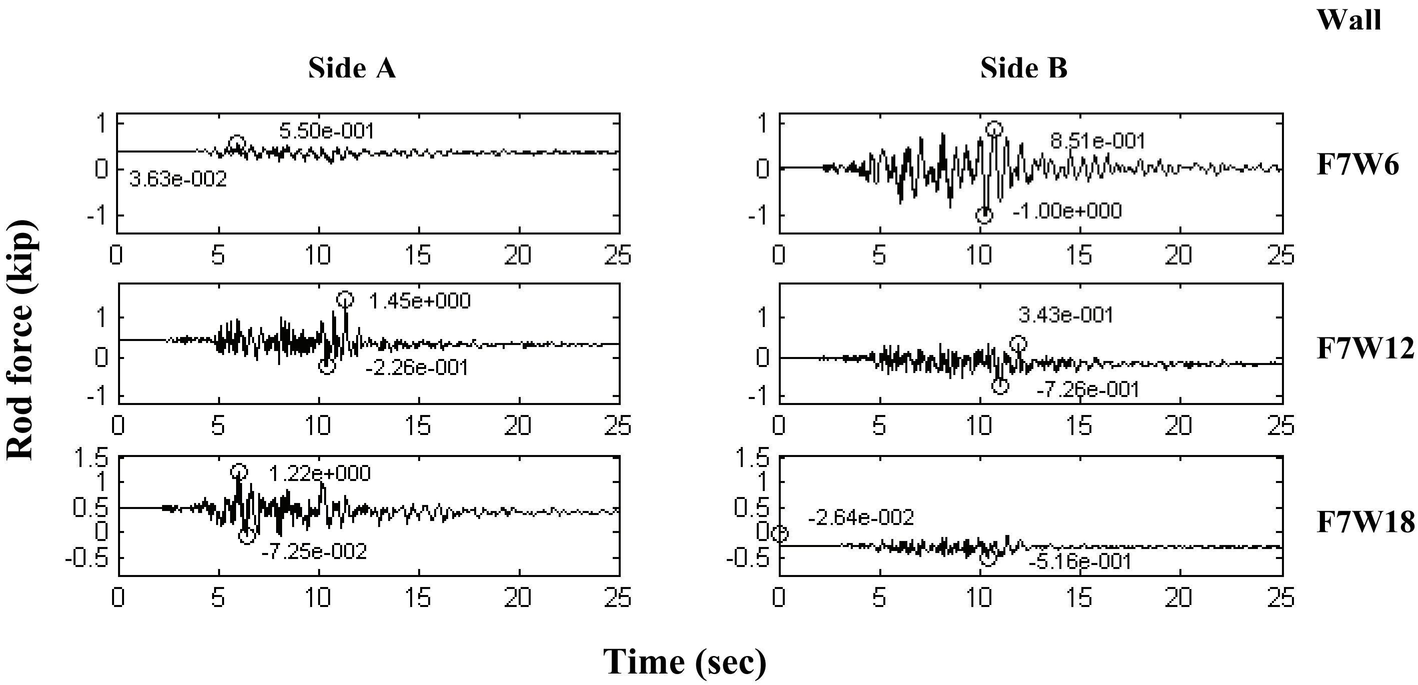

Figure M.21: ATS rod forces for Seismic Test 3 (Part 6)

Appendix M

ATS rod forces for Seismic Test 4 (Part 1)

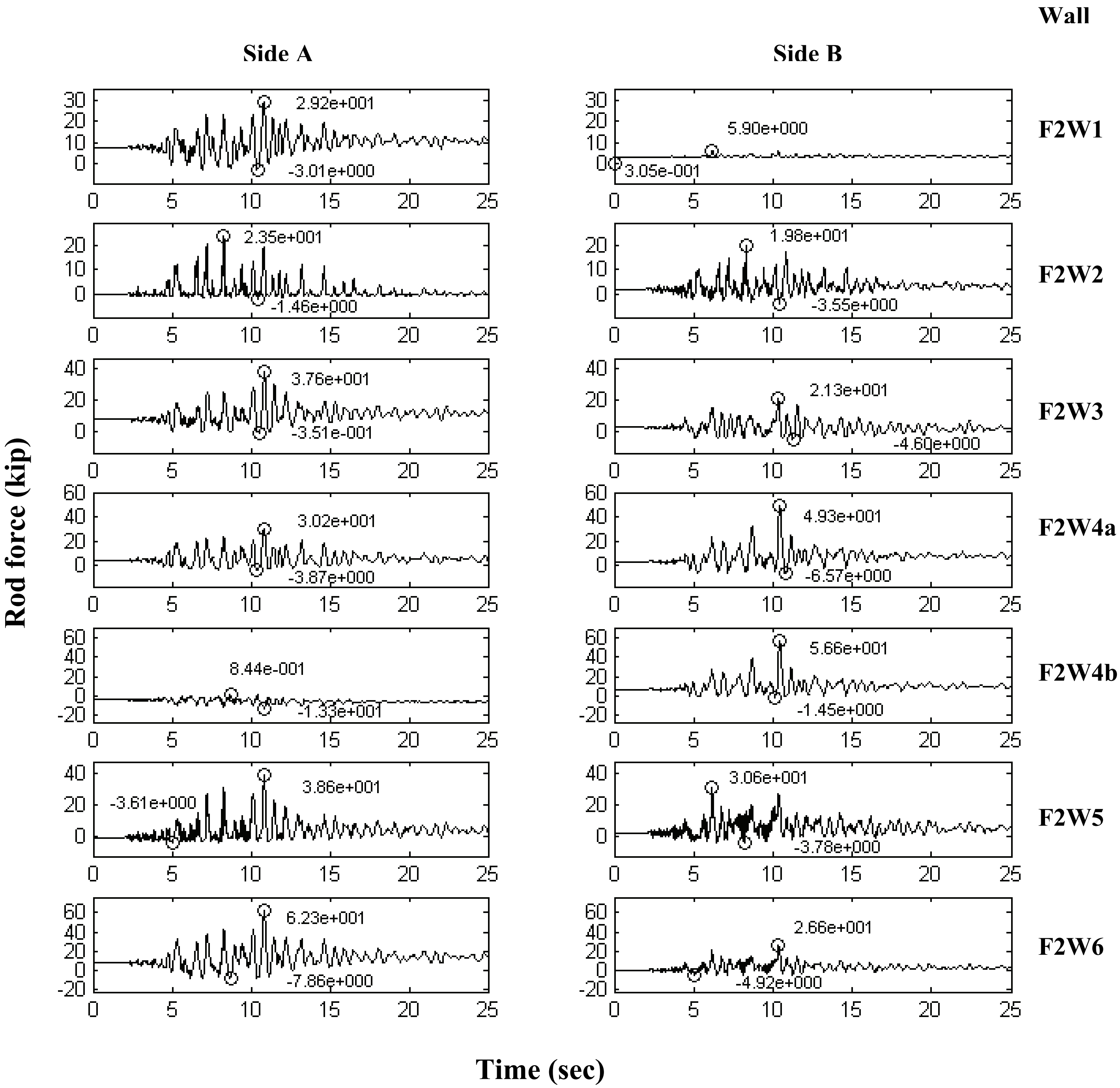

Figure M.22: ATS rod forces for Seismic Test 4 (Part 1)

Appendix M

ATS rod forces for Seismic Test 4 (Part 2)

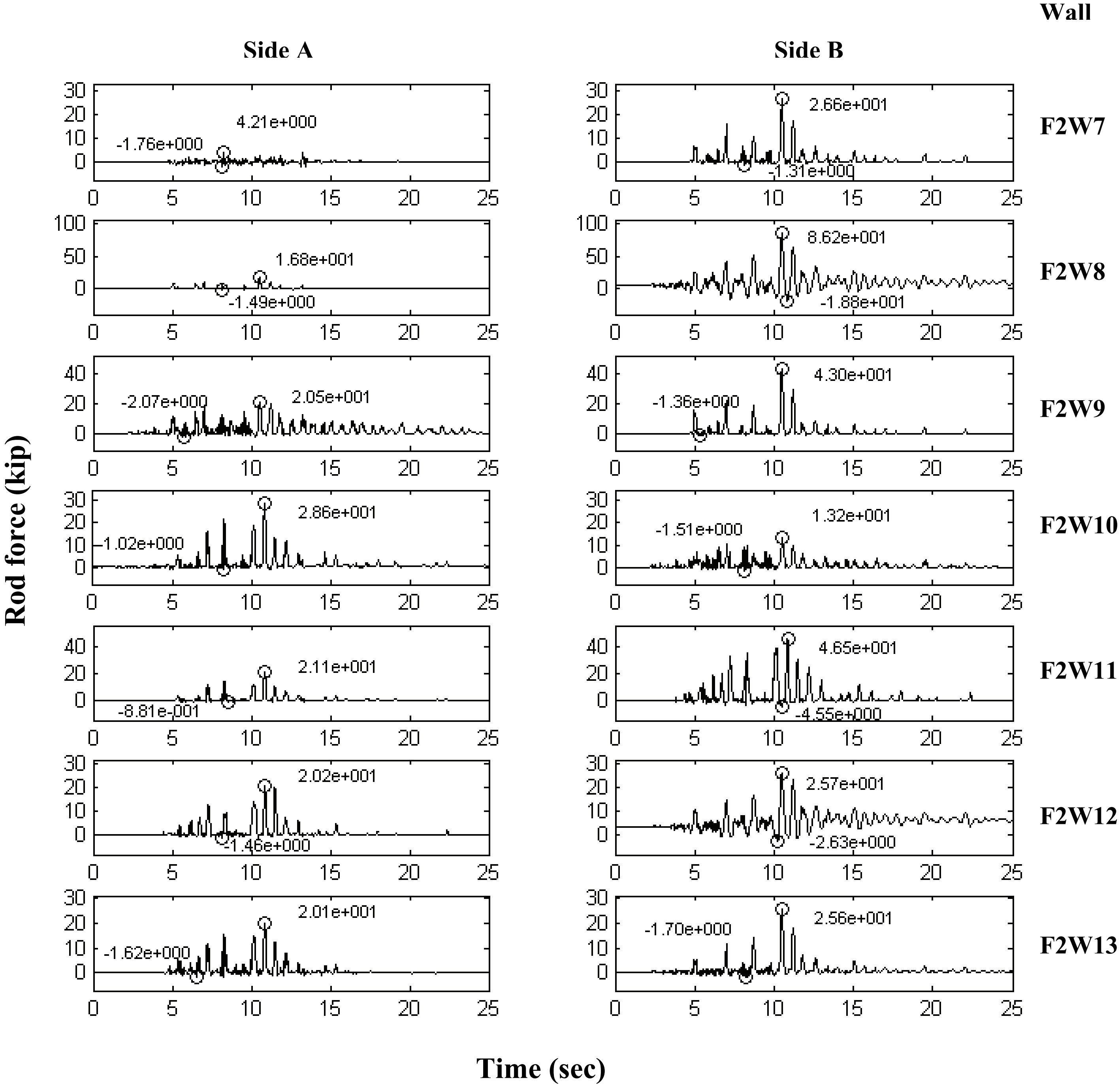

Figure M.23: ATS rod forces for Seismic Test 4 (Part 2)

Appendix M

ATS rod forces for Seismic Test 4 (Part 3)

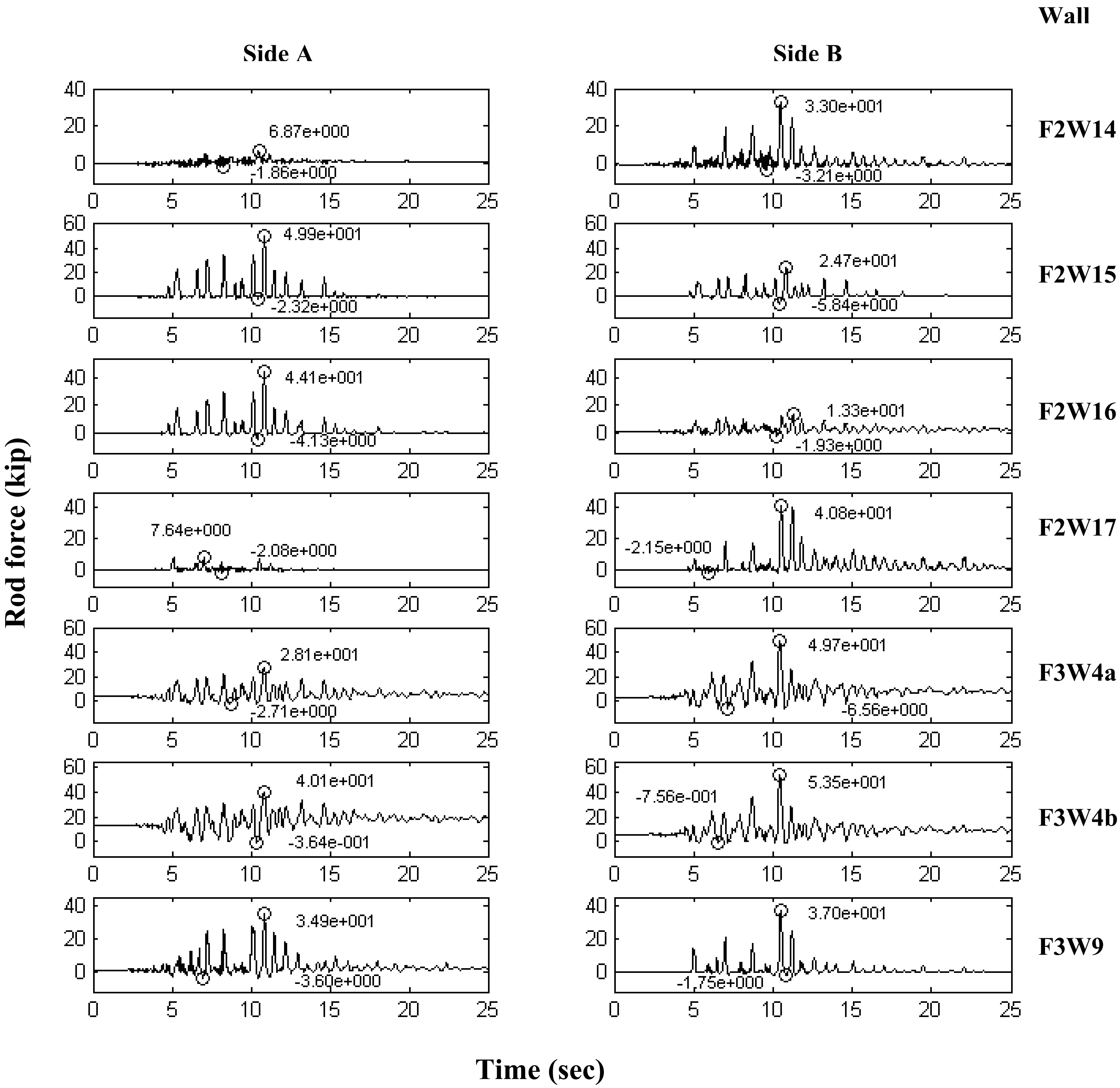

Figure M.24: ATS rod forces for Seismic Test 4 (Part 3)

Appendix M

ATS rod forces for Seismic Test 4 (Part 4)

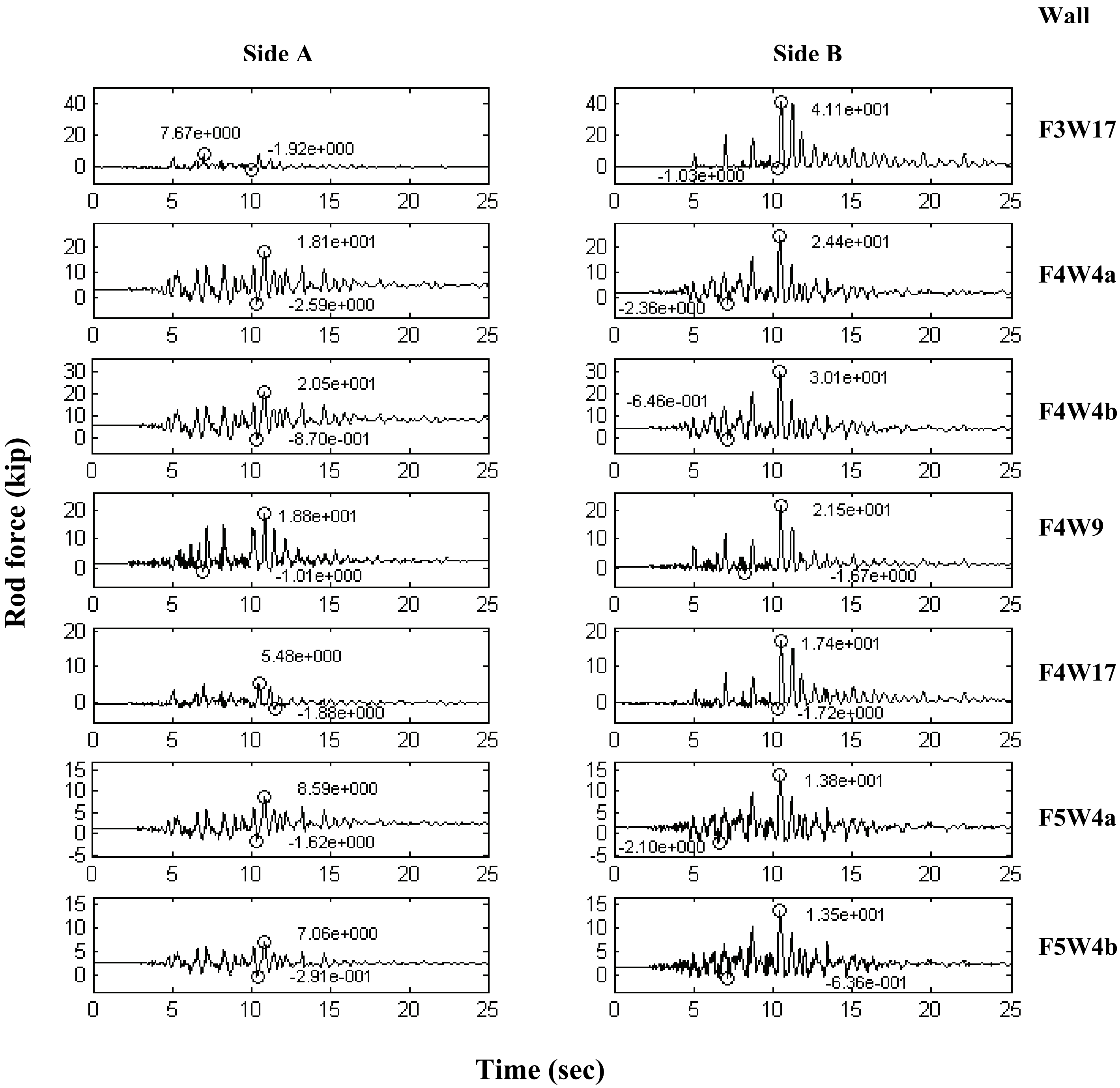

Figure M.25: ATS rod forces for Seismic Test 4 (Part 4)

Appendix M

ATS rod forces for Seismic Test 4 (Part 5)

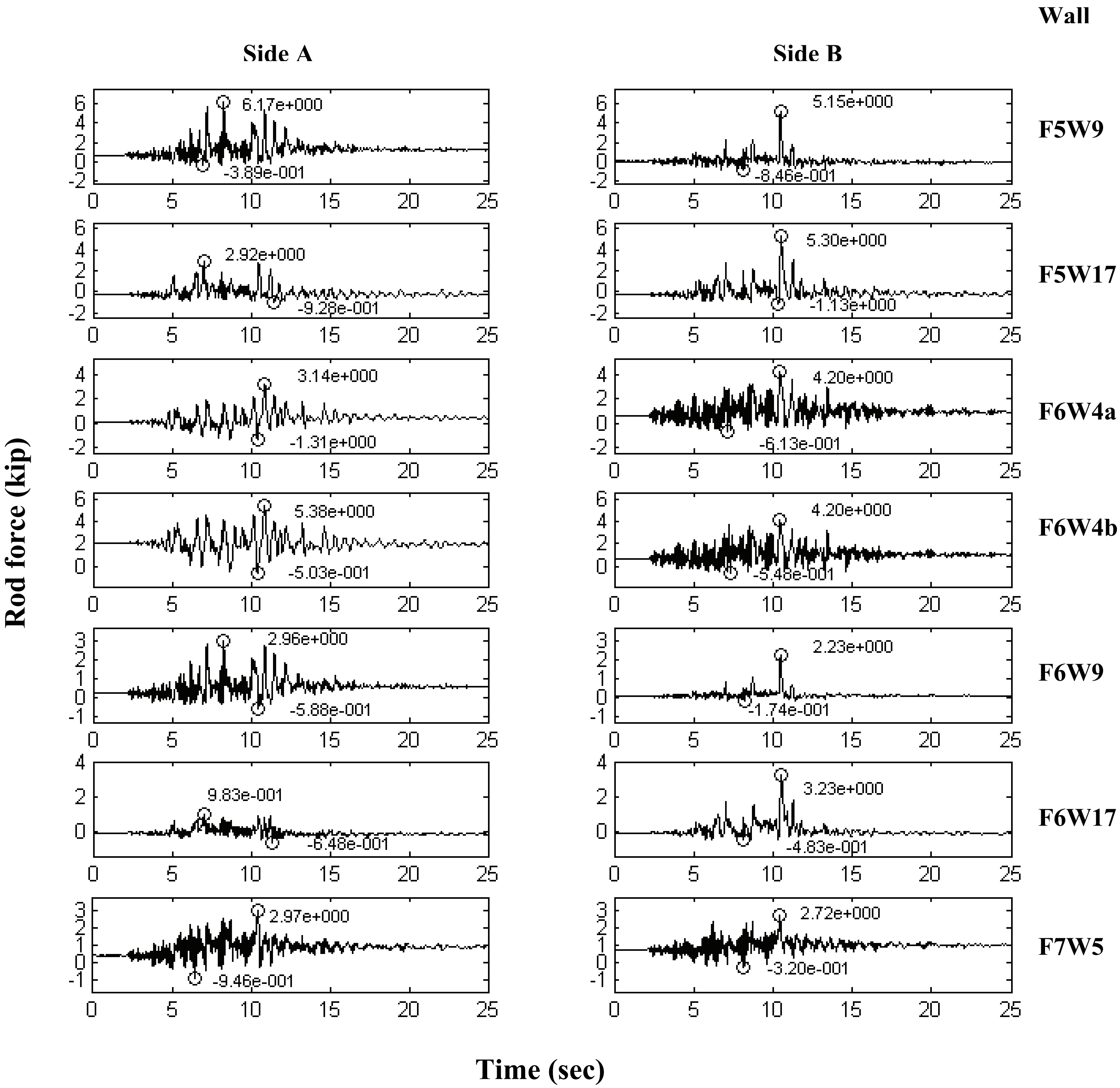

Figure M.26: ATS rod forces for Seismic Test 4 (Part 5)

Appendix M

ATS rod forces for Seismic Test 4 (Part 6)

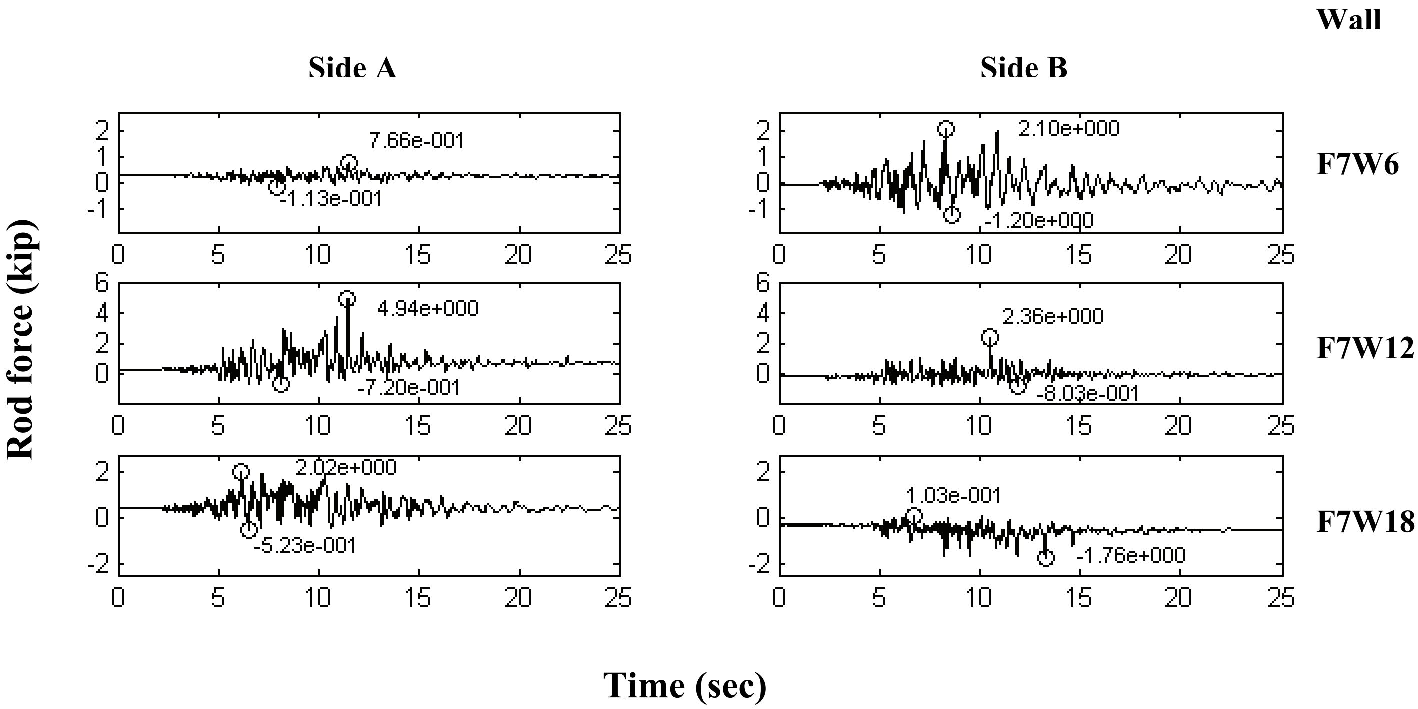

Figure M.27: ATS rod forces for Seismic Test 4 (Part 6)

Appendix M

ATS rod forces for Seismic Test 5 (Part 1)

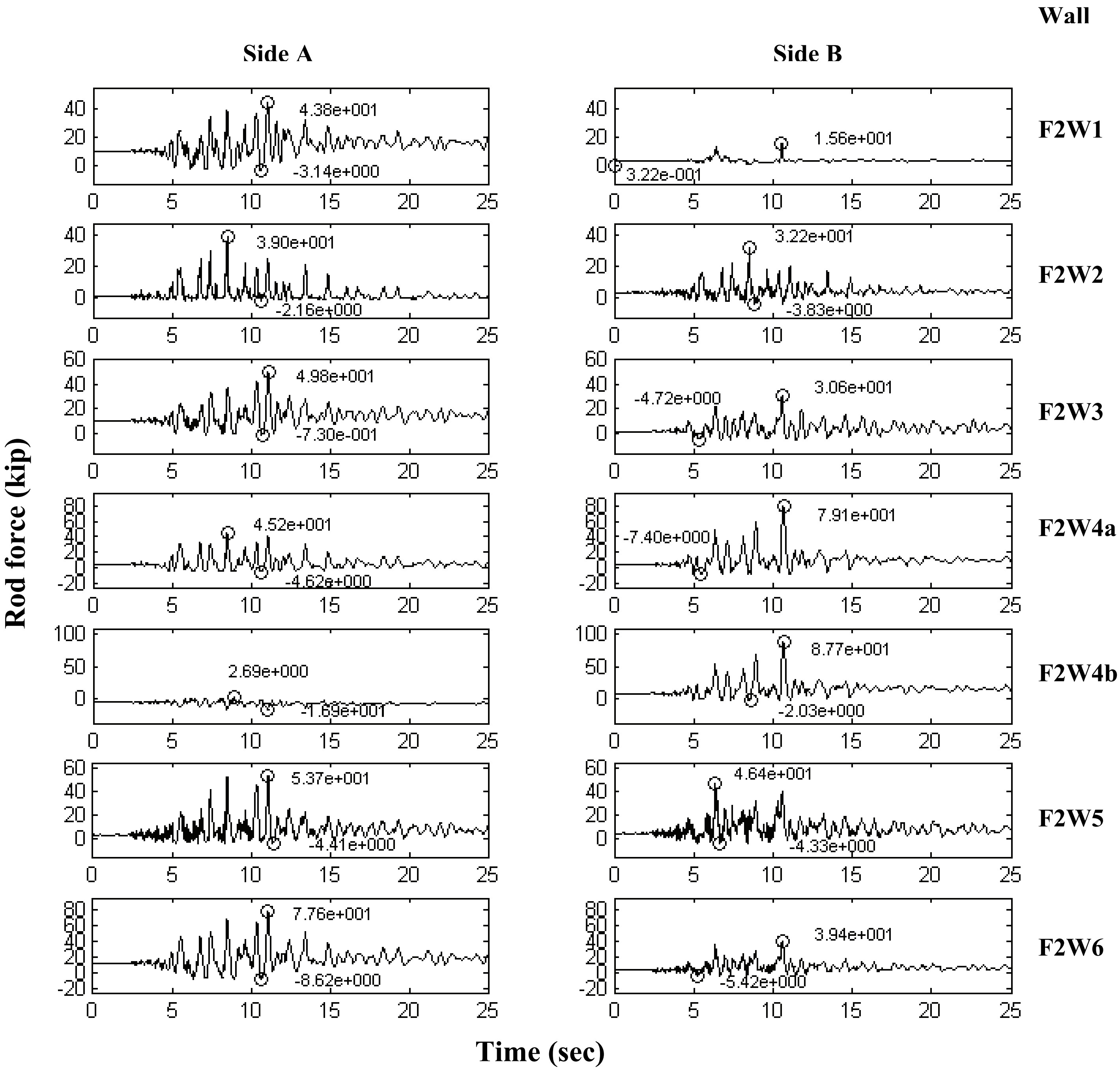

Figure M.28: ATS rod forces for Seismic Test 5 (Part 1)

Appendix M

ATS rod forces for Seismic Test 5 (Part 2)

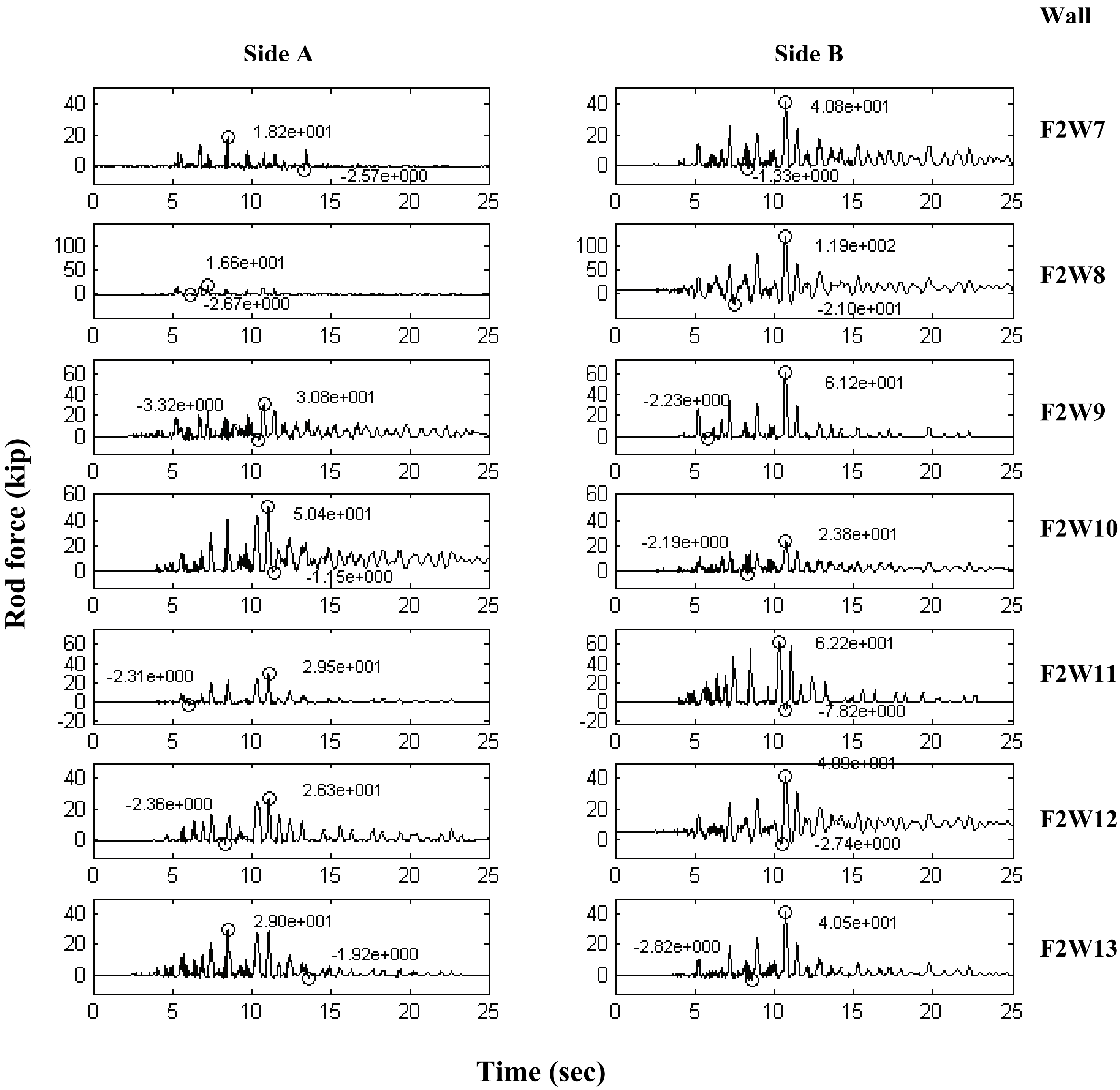

Figure M.29: ATS rod forces for Seismic Test 5 (Part 2)

Appendix M

ATS rod forces for Seismic Test 5 (Part 3)

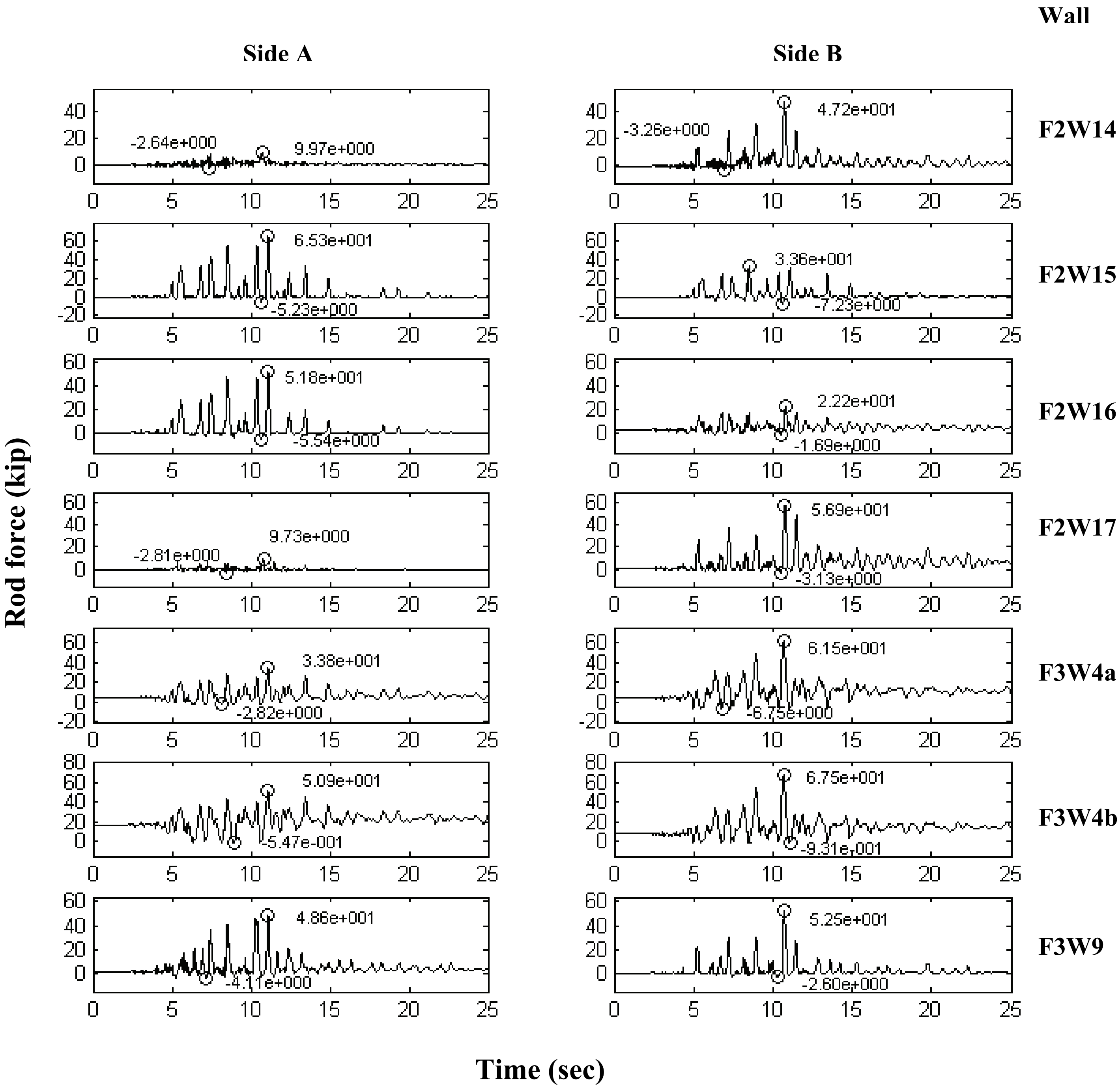

Figure M.30: ATS rod forces for Seismic Test 5 (Part 3)

Appendix M

ATS rod forces for Seismic Test 5 (Part 4)

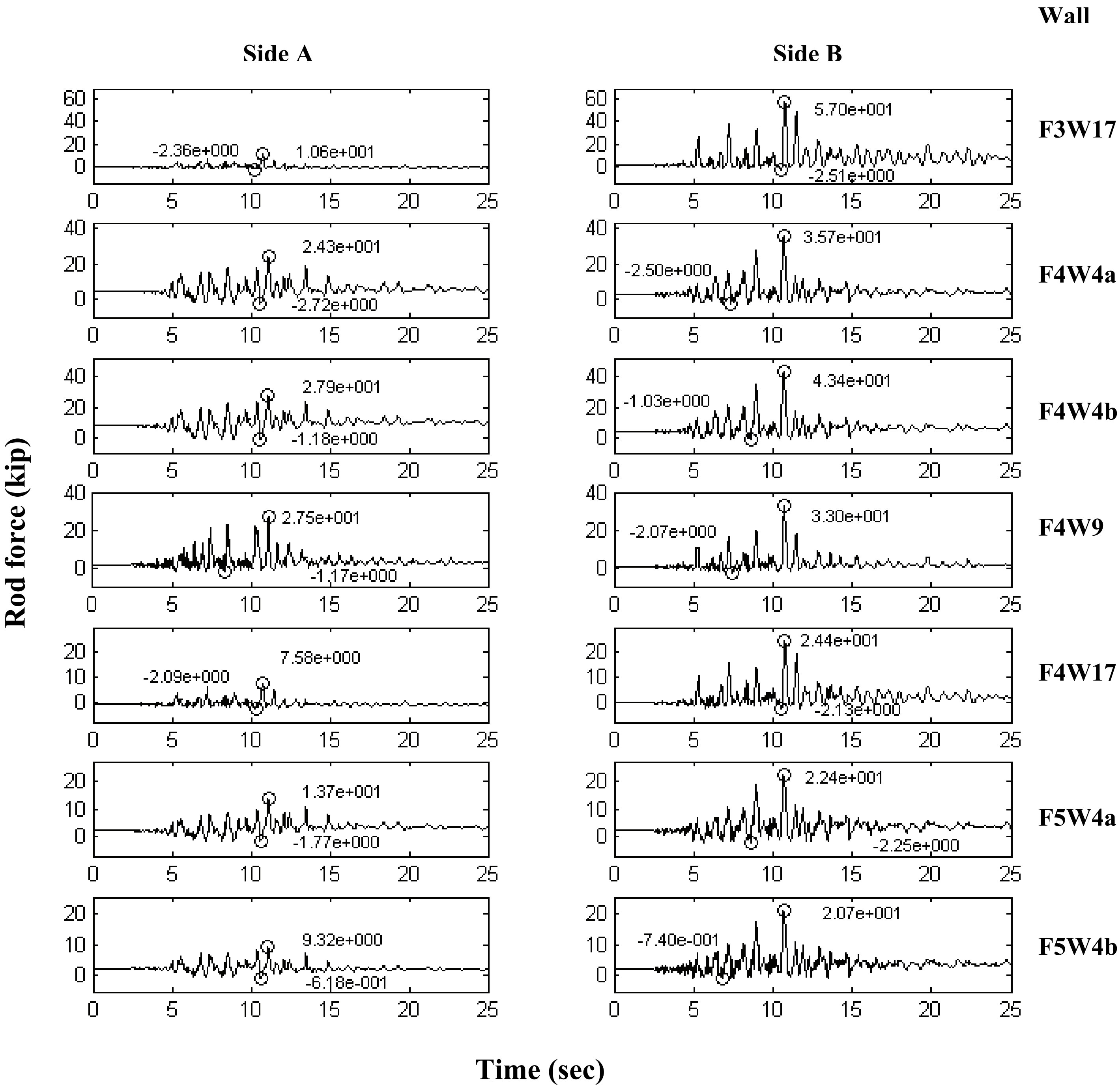

Figure M.31: ATS rod forces for Seismic Test 5 (Part 4)

Appendix M

ATS rod forces for Seismic Test 5 (Part 5)

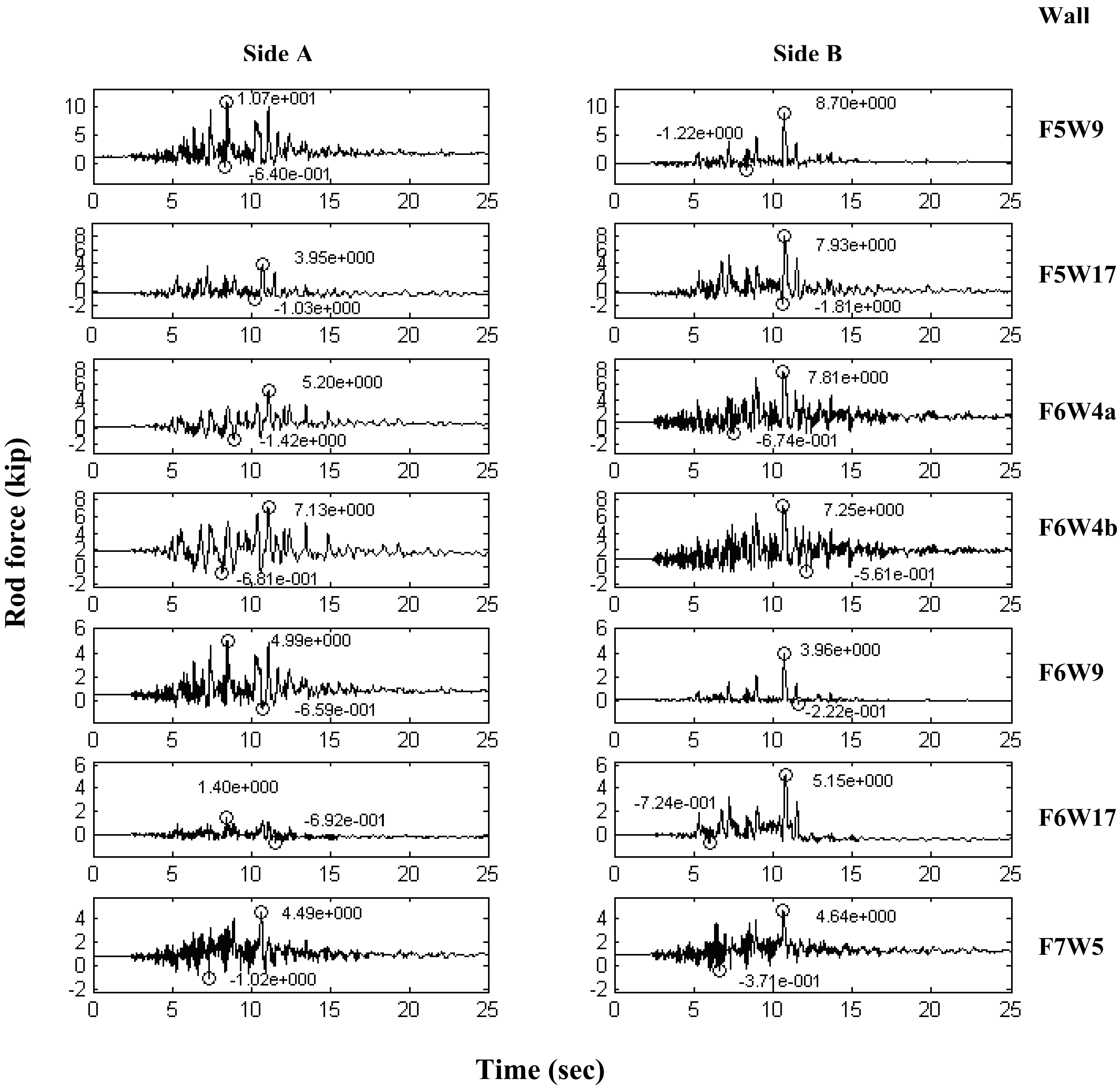

Figure M.32: ATS rod forces for Seismic Test 5 (Part 5)

Appendix M

ATS rod forces for Seismic Test 5 (Part 6)

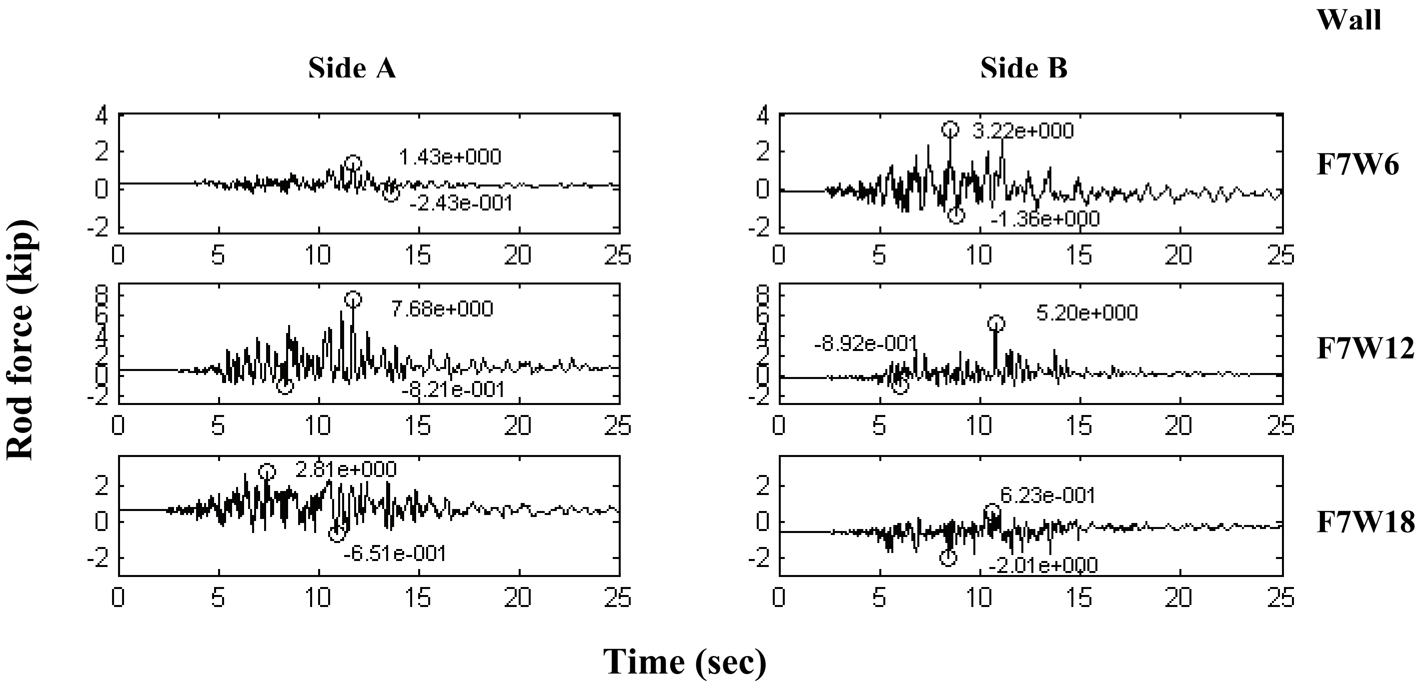

Figure M.33: ATS rod forces for Seismic Test 5 (Part 6)

Appendix M

Maximum ATS rod forces at Story 2 for Seismic Test 1

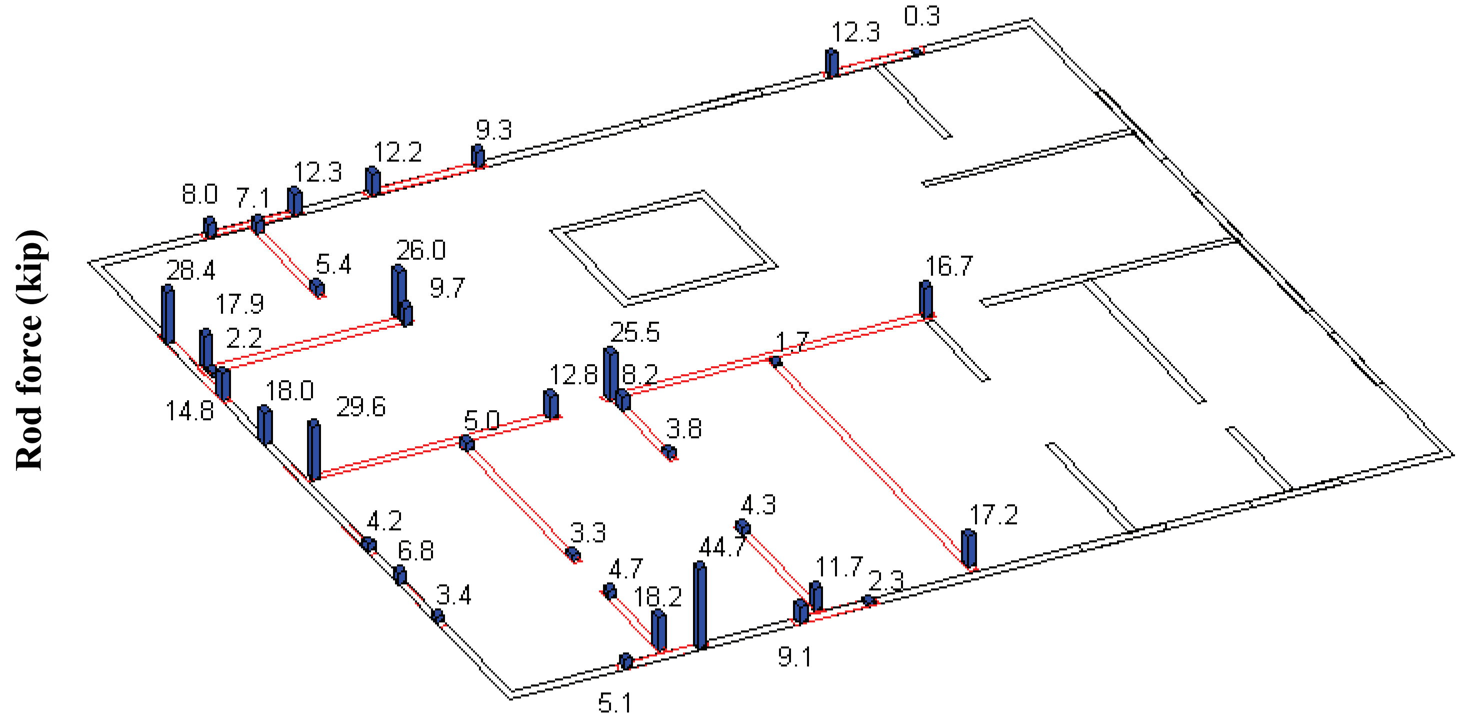

Figure M.34: Maximum ATS rod forces at Story 2 for Seismic Test 1

Appendix M

Maximum ATS rod forces at Story 2 for Seismic Test 2

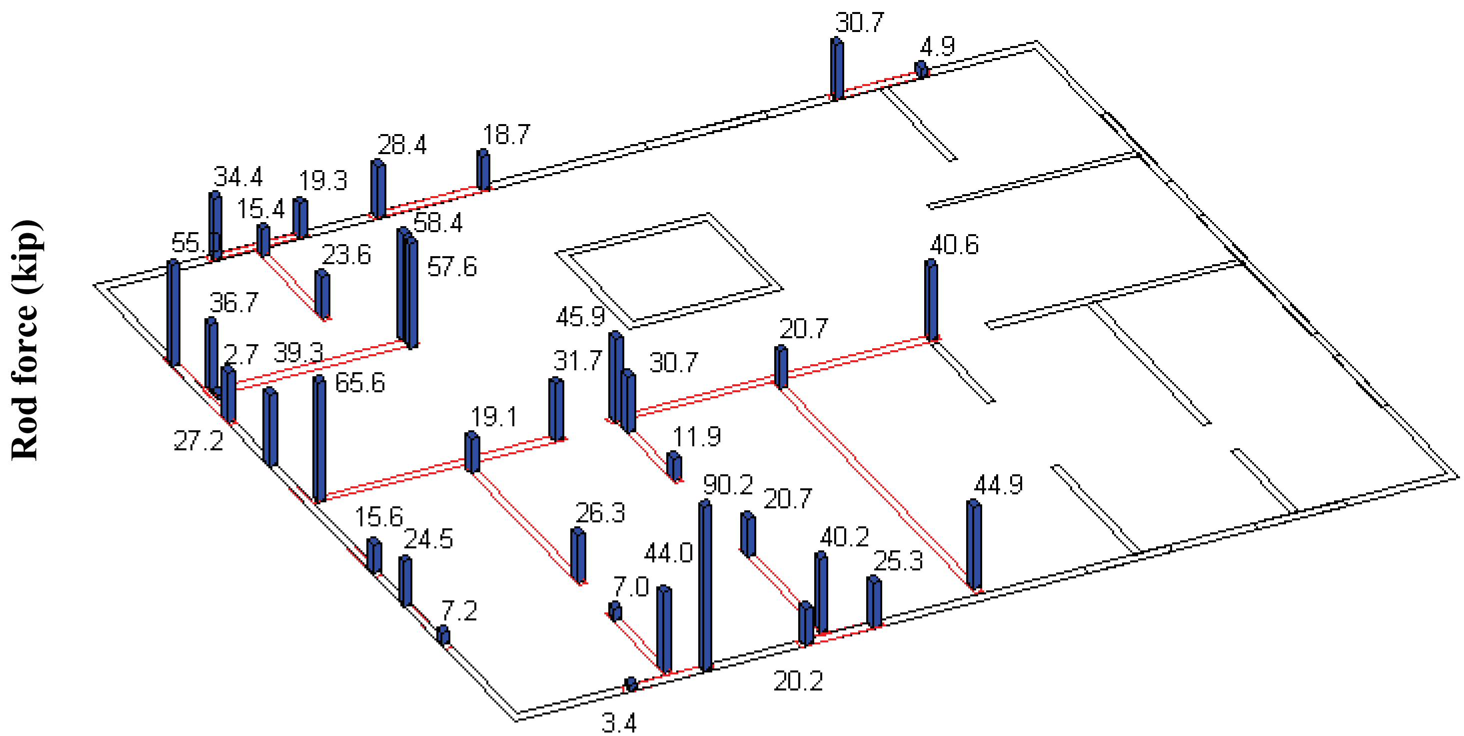

Figure M.35: Maximum ATS rod forces at Story 2 for Seismic Test 2

Appendix M

Maximum ATS rod forces at Story 2 for Seismic Test 3

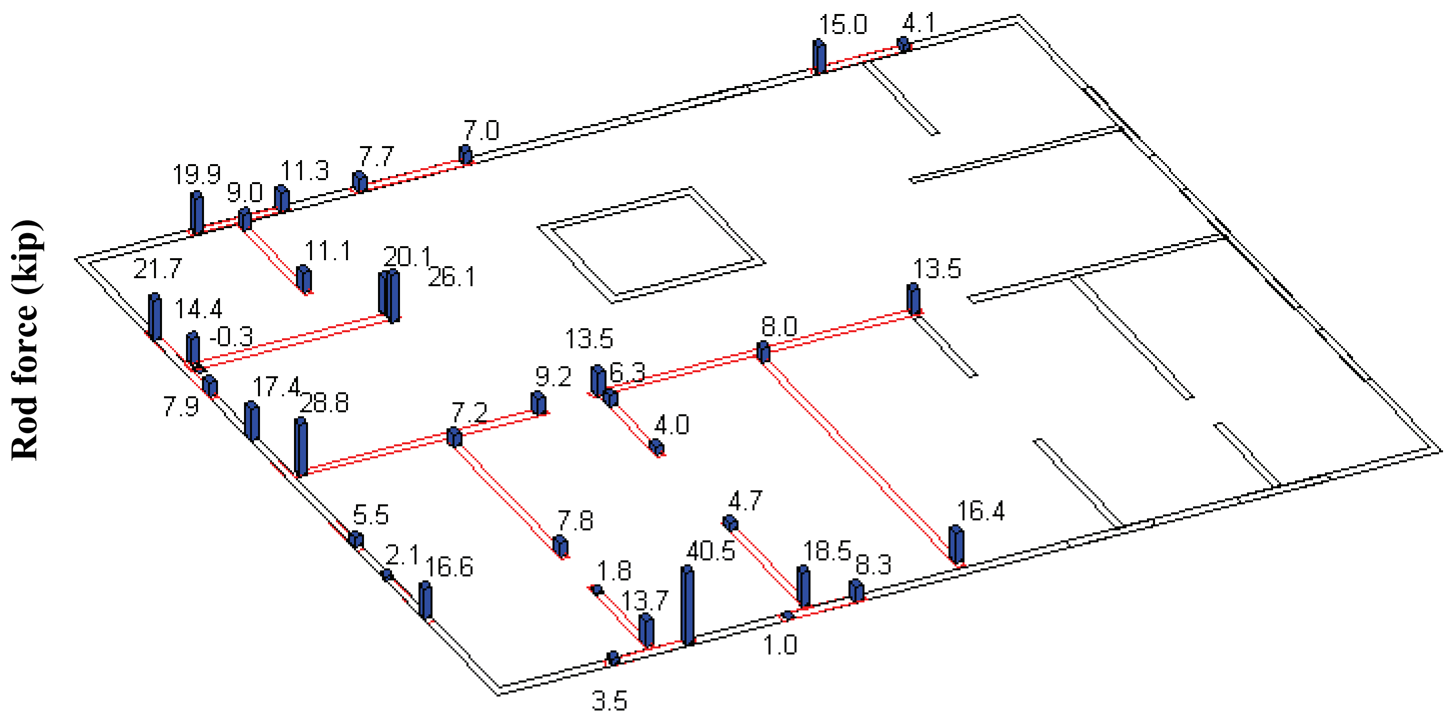

Figure M.36: Maximum ATS rod forces at Story 2 for Seismic Test 3

Appendix M

Maximum ATS rod forces at Story 2 for Seismic Test 4

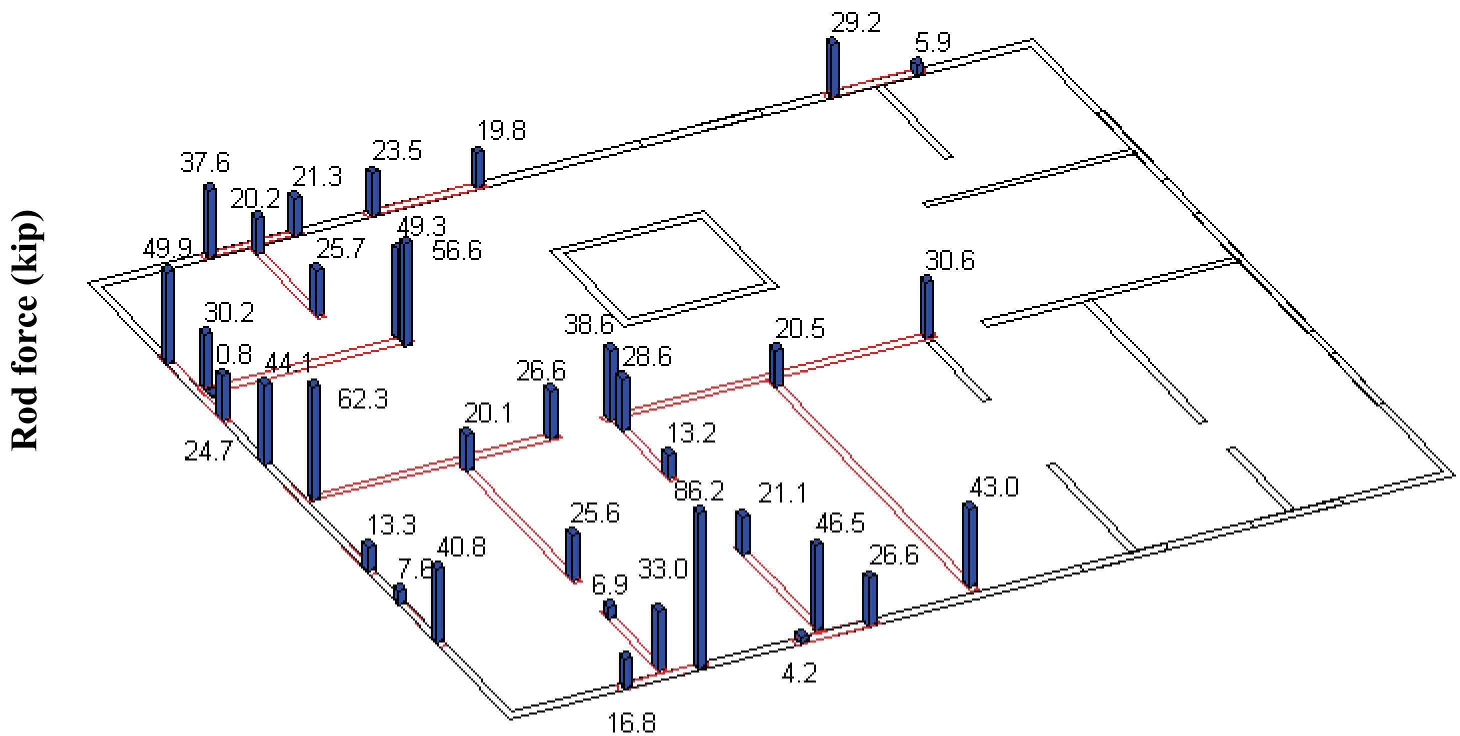

Figure M.37: Maximum ATS rod forces at Story 2 for Seismic Test 4

Appendix M

Maximum ATS rod forces at Story 2 for Seismic Test 5

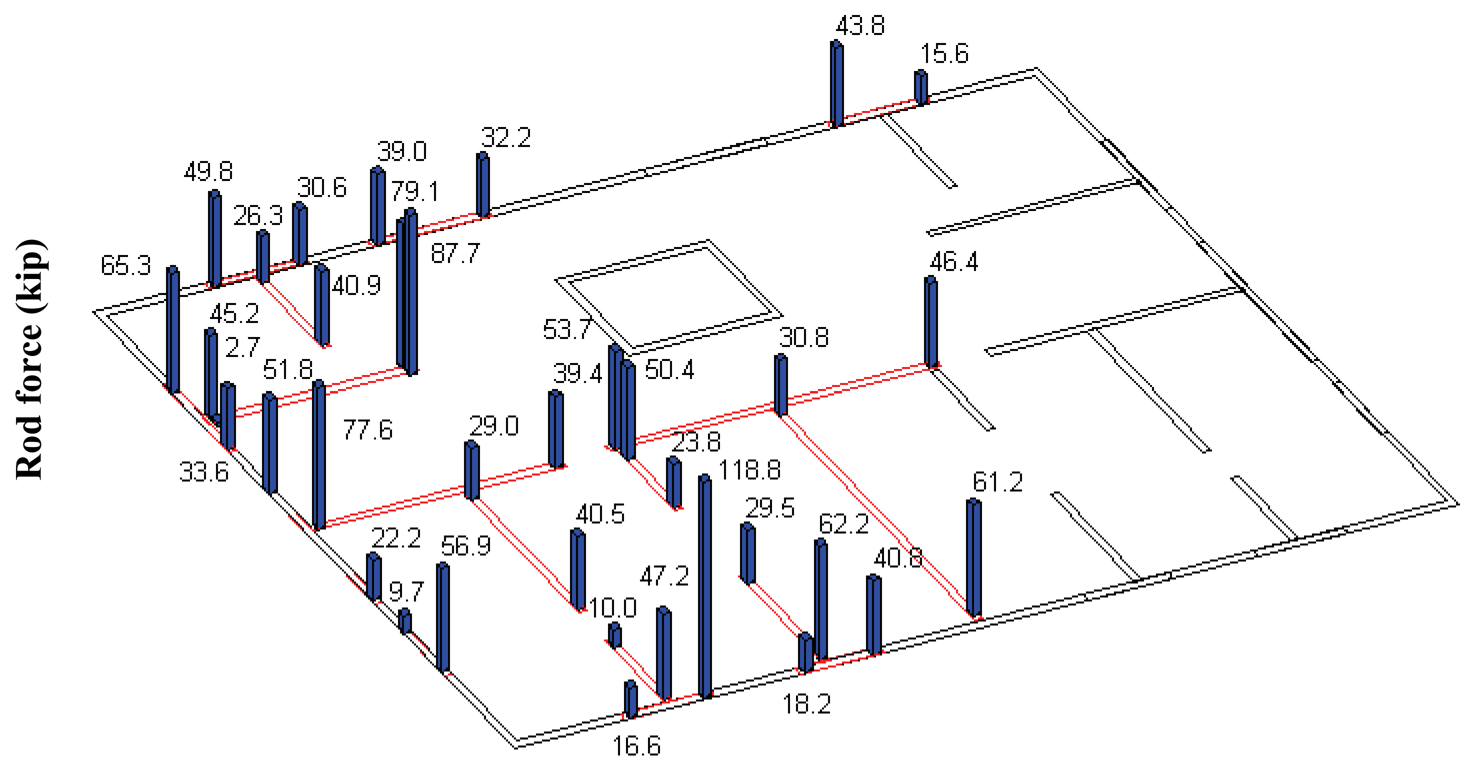

Figure M.38: Maximum ATS rod forces at Story 2 for Seismic Test 5

Appendix N

Seismic Test Results: Selected shearwall stud uplift measurements

Appendix N

Story 2 wall end stud uplift for Seismic test 1

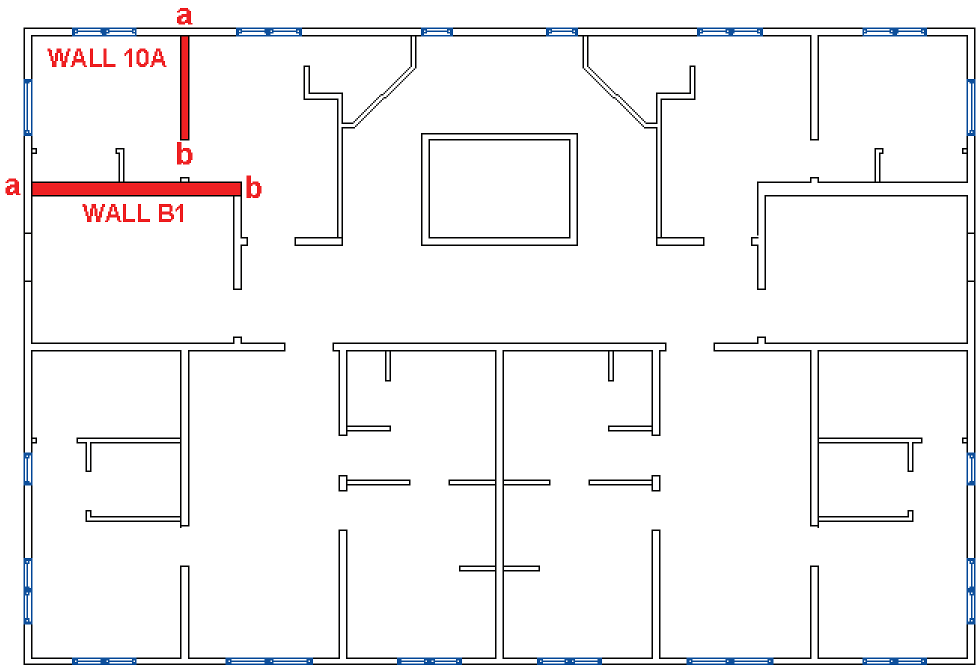

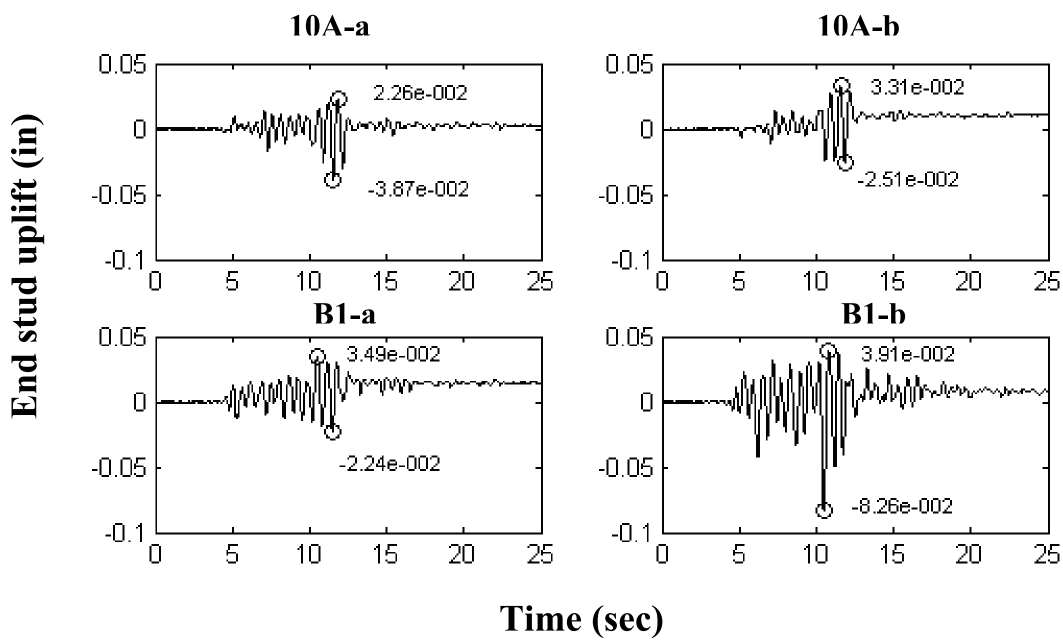

Figure N.1: Wall end stud uplift at story 2 for Seismic test 1

Appendix N

Story 7 wall end stud uplift for Seismic test 1

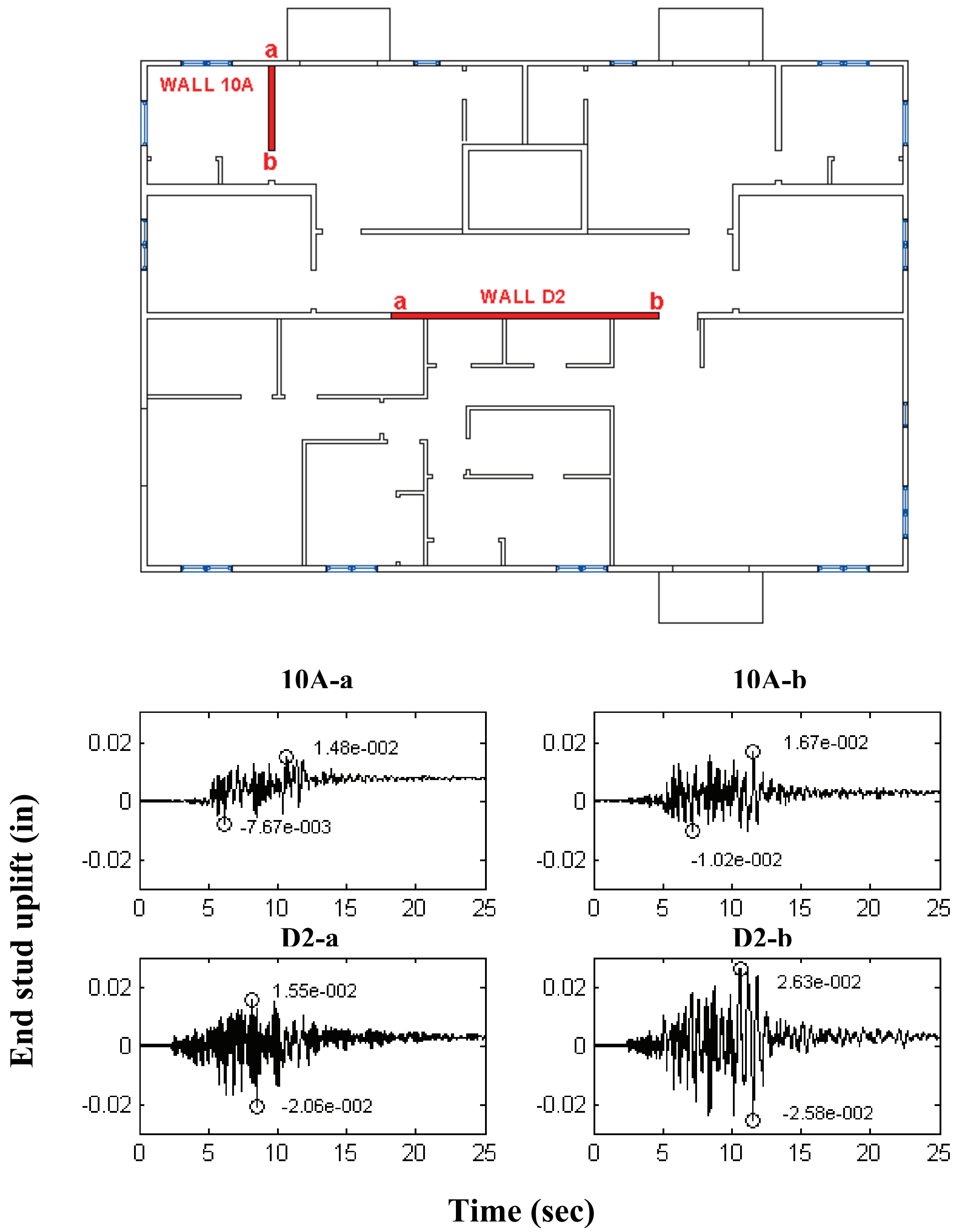

Figure N.2: Wall end stud uplift at story 7 for Seismic test 1

Appendix N

Story 2 wall end stud uplift for Seismic test 2

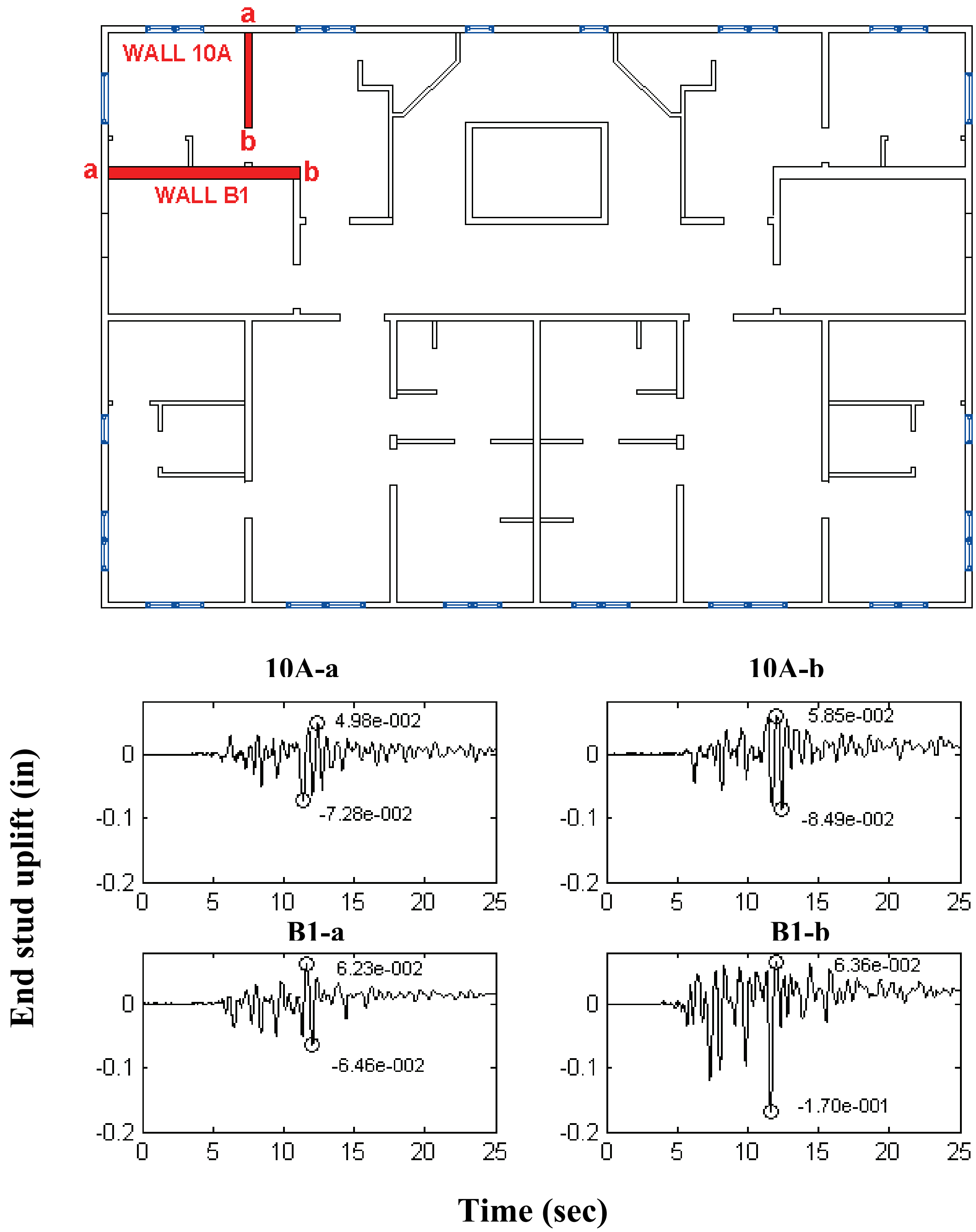

Figure N.3: Wall end stud uplift at story 2 for Seismic test 2

Appendix N

Story 7 wall end stud uplift for Seismic test 2

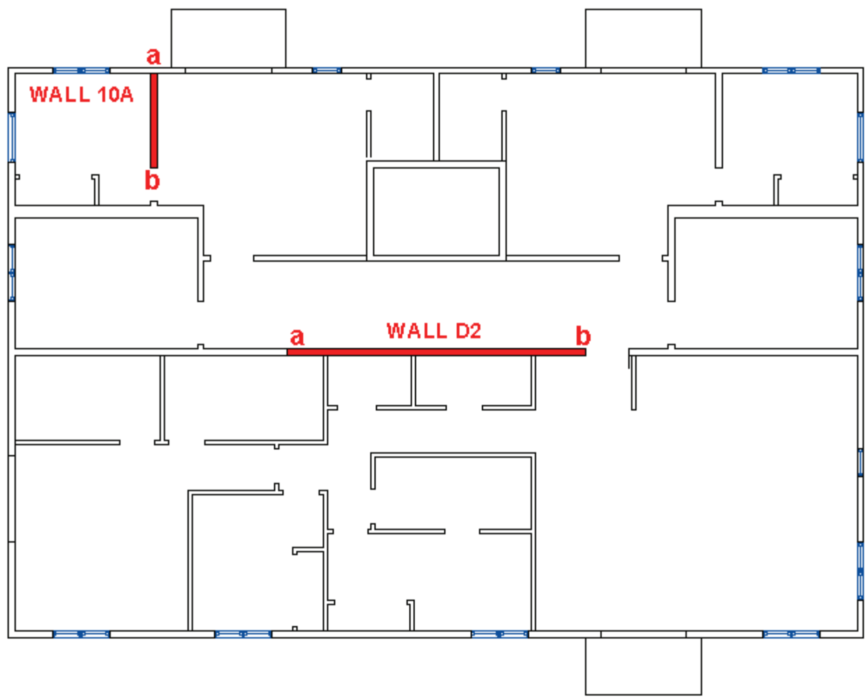

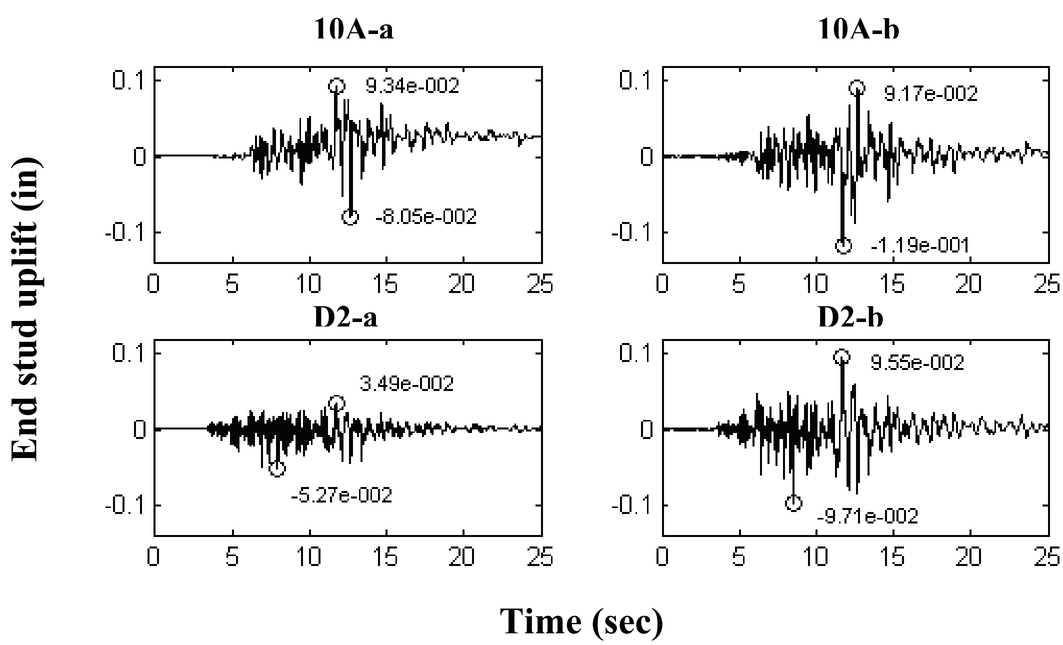

Figure N.4: Wall end stud uplift at story 7 for Seismic test 2

Appendix N

Story 2 wall end stud uplift for Seismic test 3

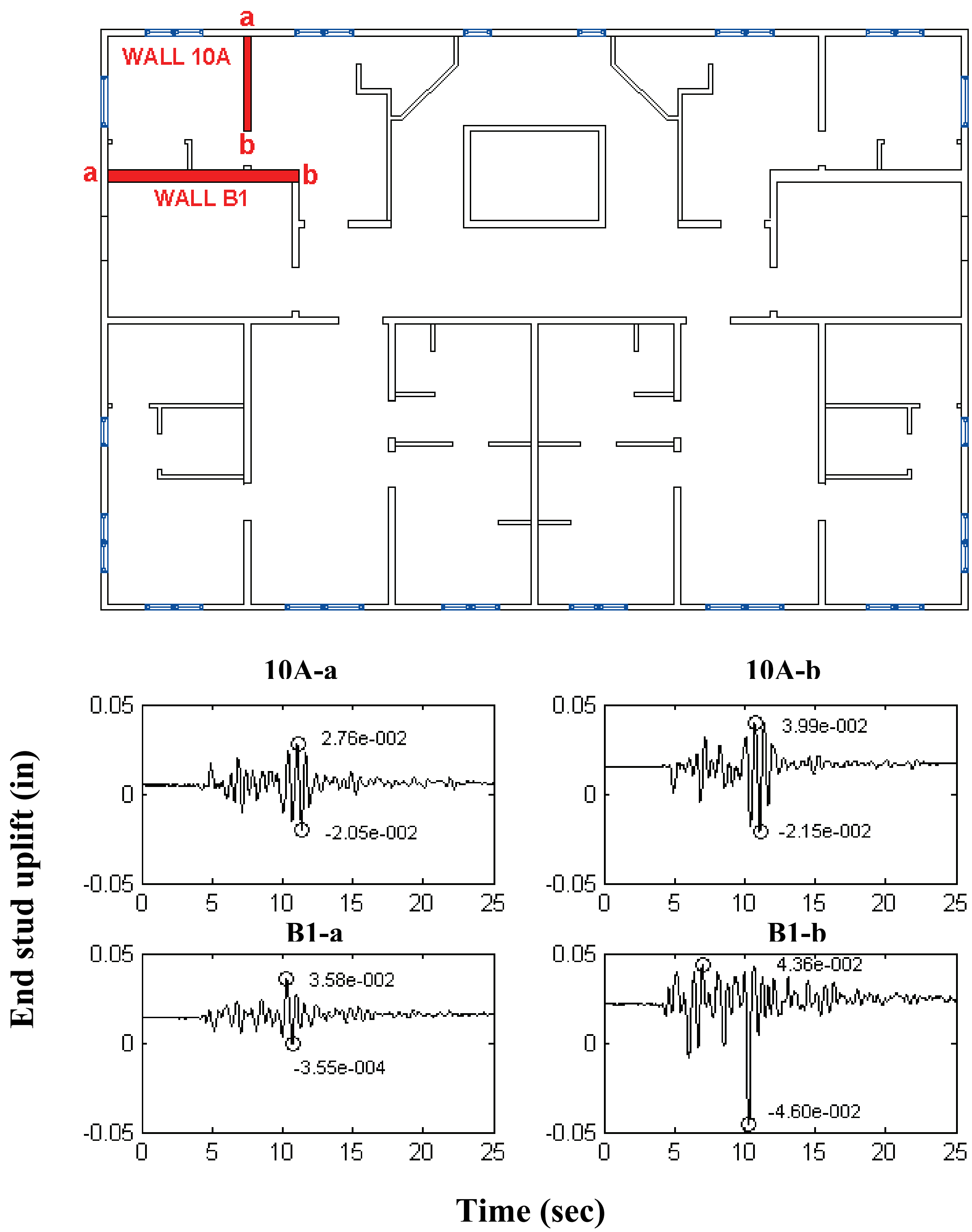

Figure N.5: Wall end stud uplift at story 2 for Seismic test 3

Appendix N

Story 7 wall end stud uplift for Seismic test 3

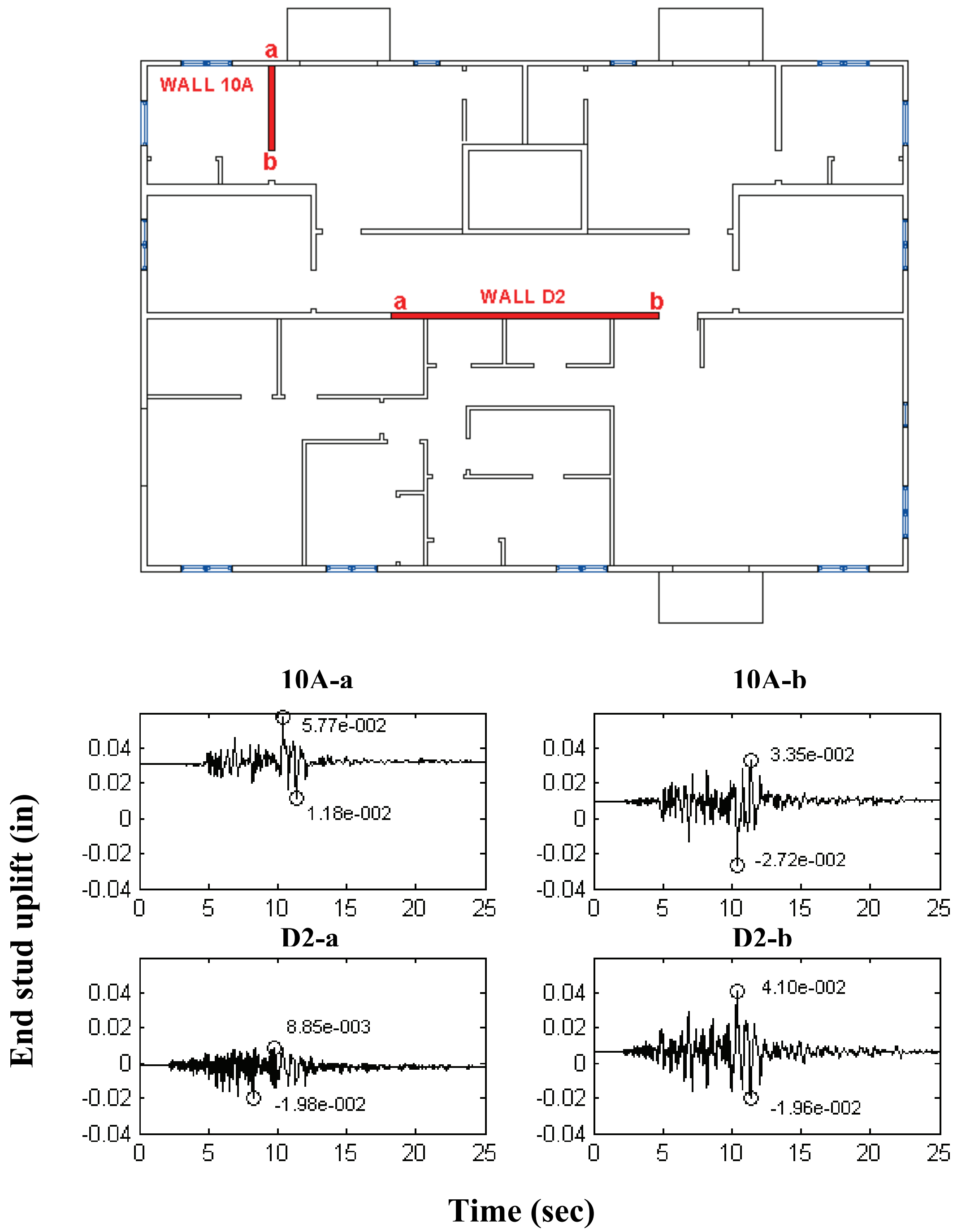

Figure N.6: Wall end stud uplift at story 7 for Seismic test 3

Appendix N

Story 2 wall end stud uplift for Seismic test 4

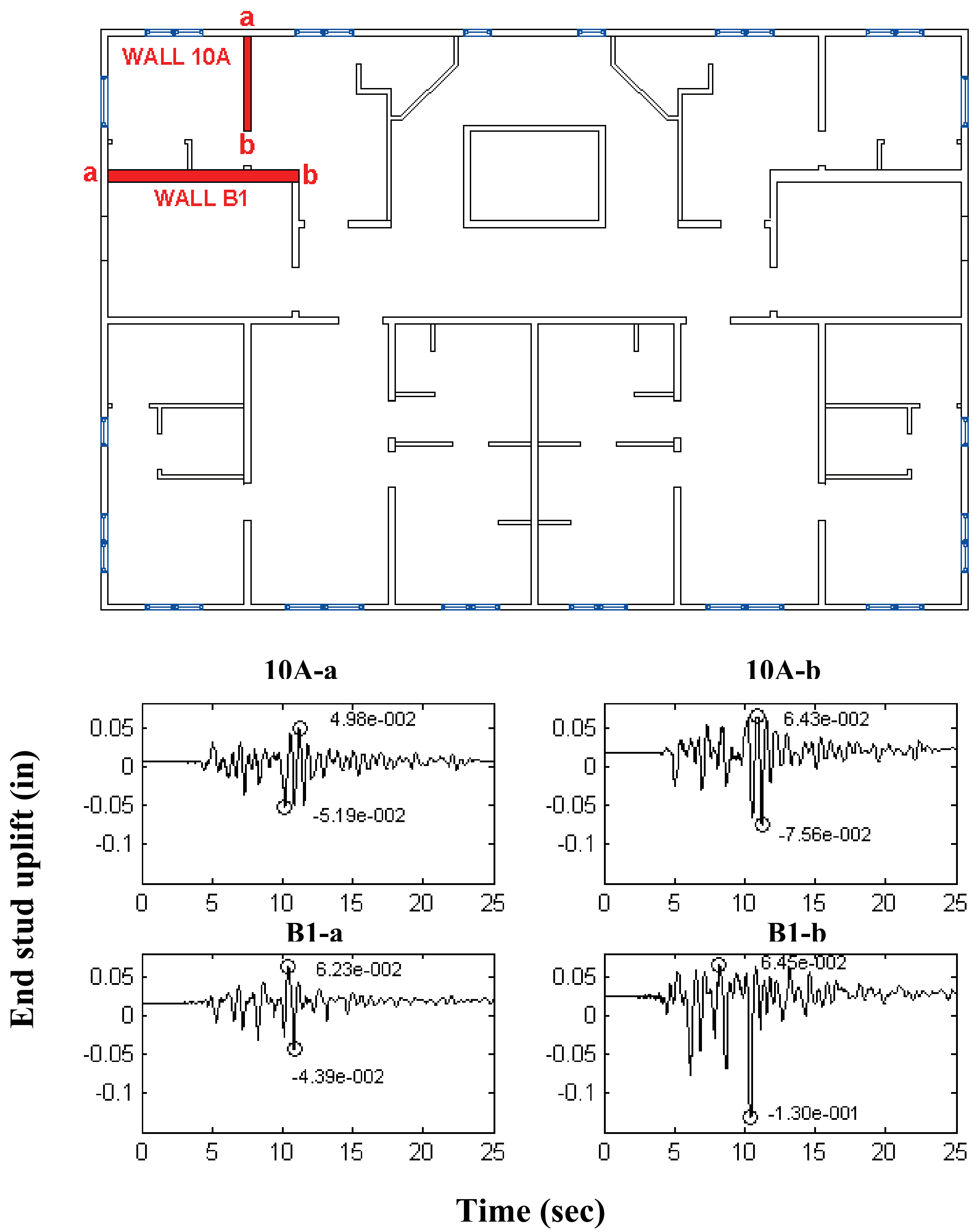

Figure N.7: Wall end stud uplift at story 2 for Seismic test 4

Appendix N

Story 7 wall end stud uplift for Seismic test 4

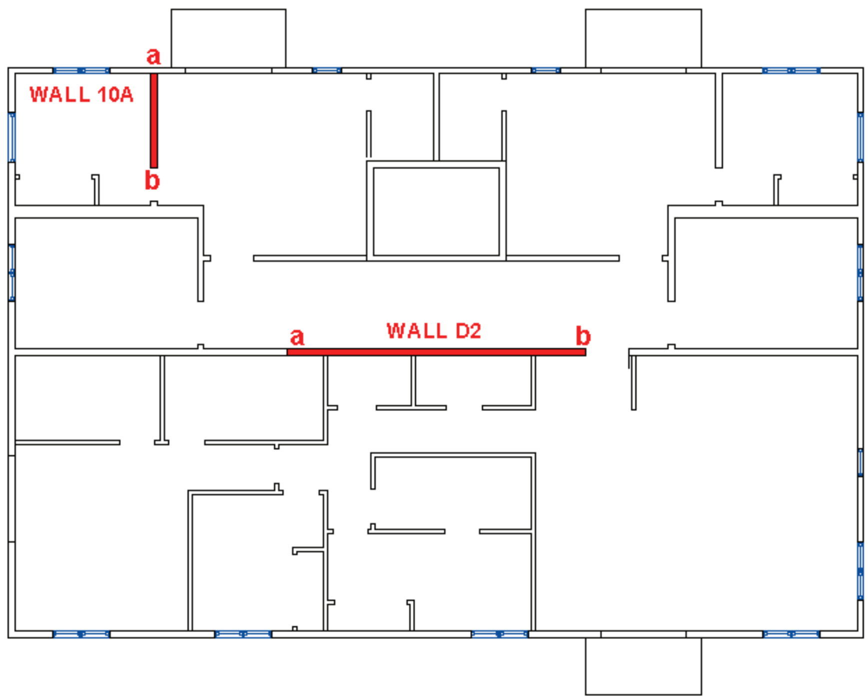

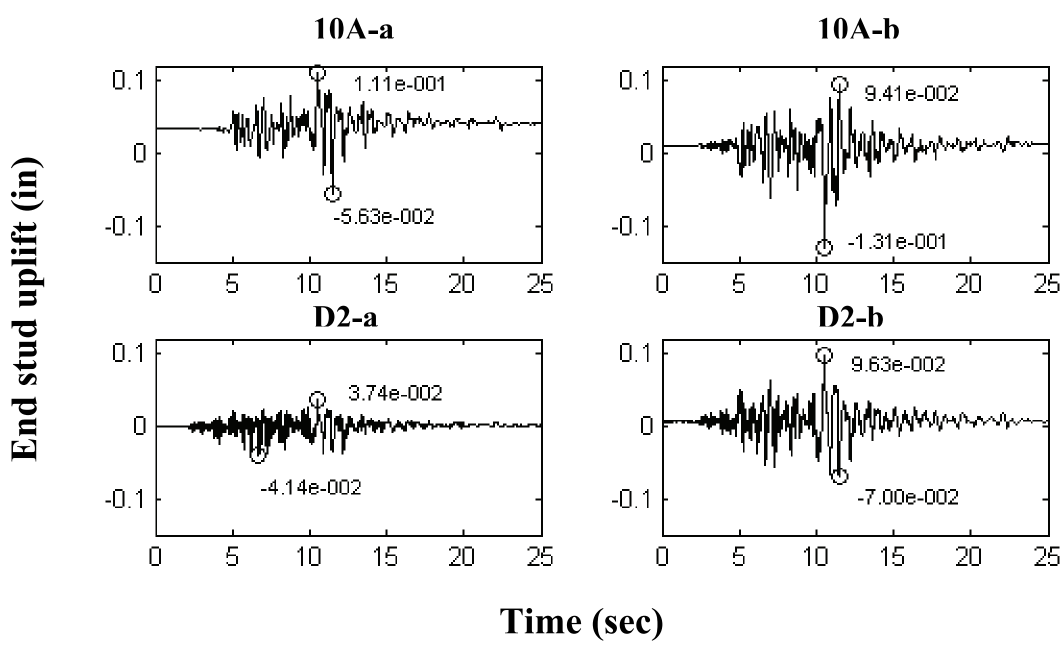

Figure N.8: Wall end stud uplift at story 7 for Seismic test 4

Appendix N

Story 2 wall end stud uplift for Seismic test 5

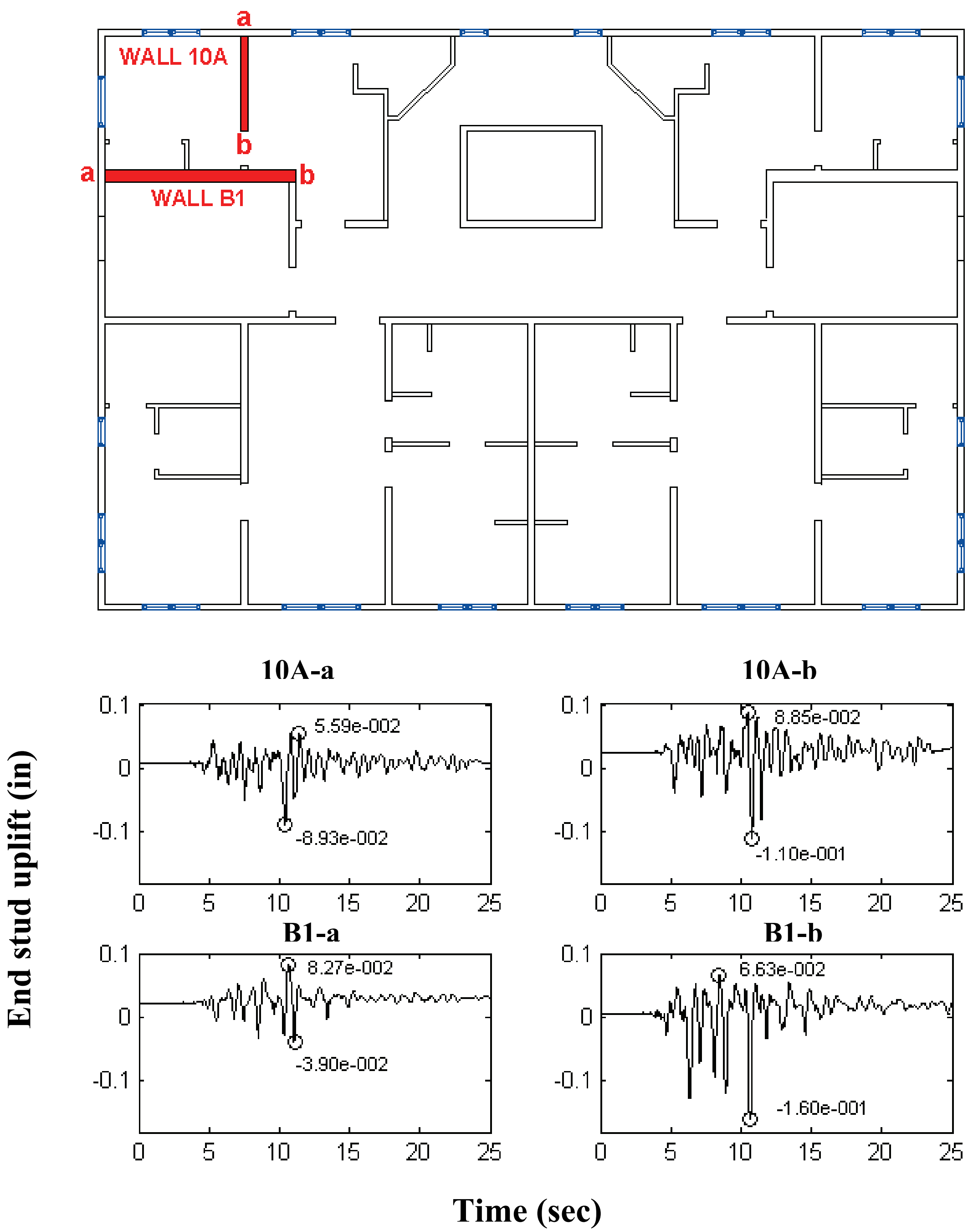

Figure N.9: Wall end stud uplift at story 2 for Seismic test 5

Appendix N

Story 7 wall end stud uplift for Seismic test 5

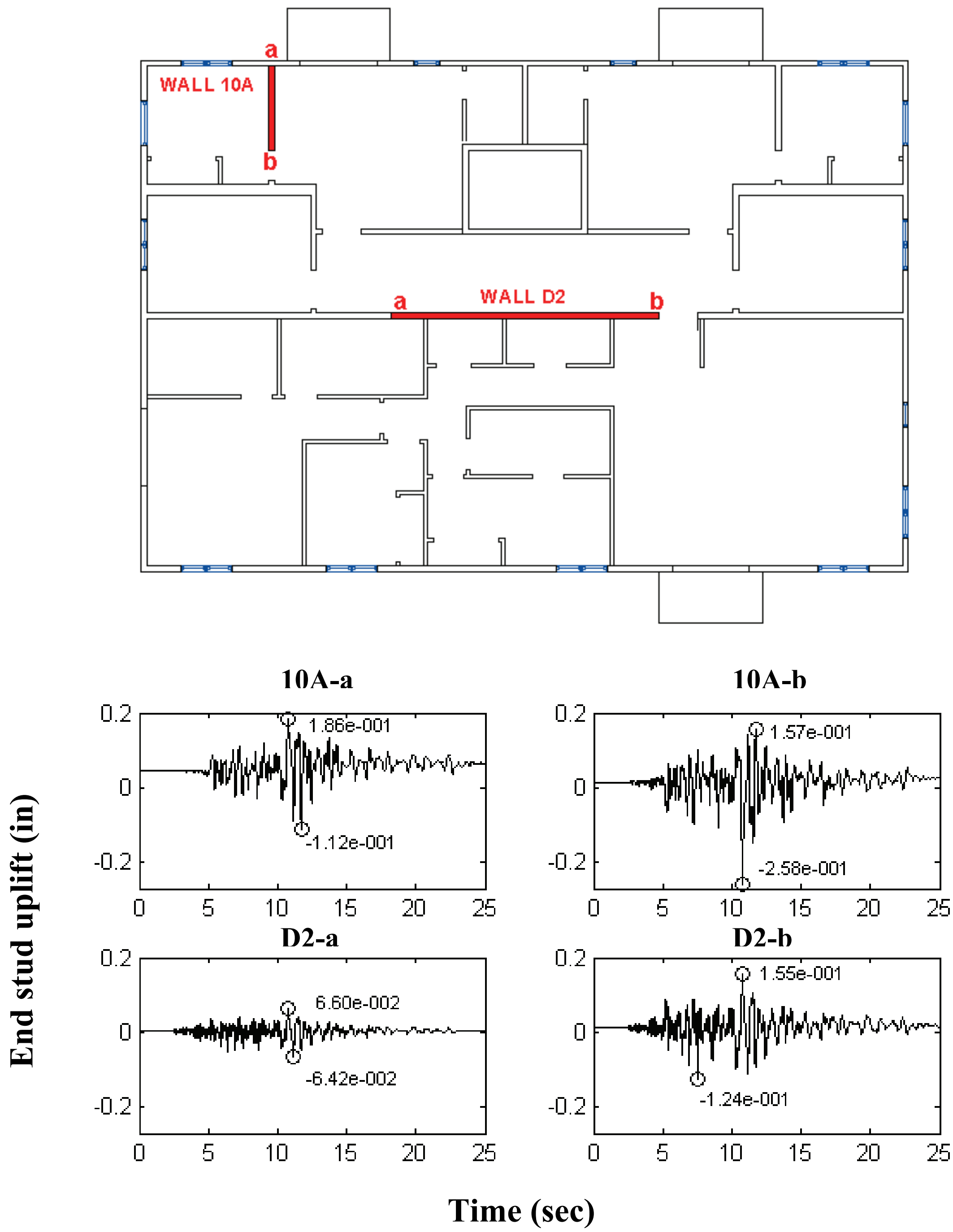

Figure N.10: Wall end stud uplift at story 7 for Seismic test 5

Appendix O

Out of plane diaphragm measurements for selected locations

Appendix O

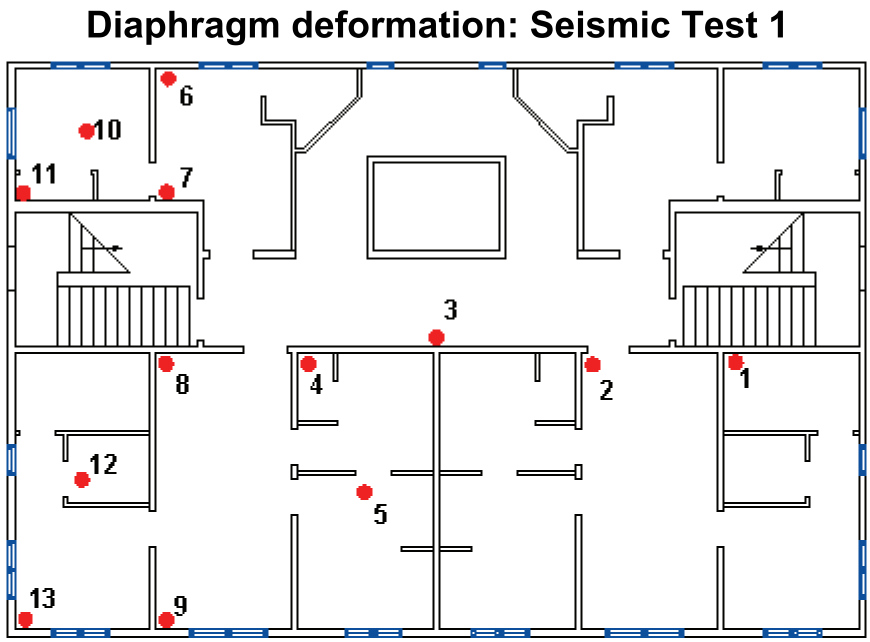

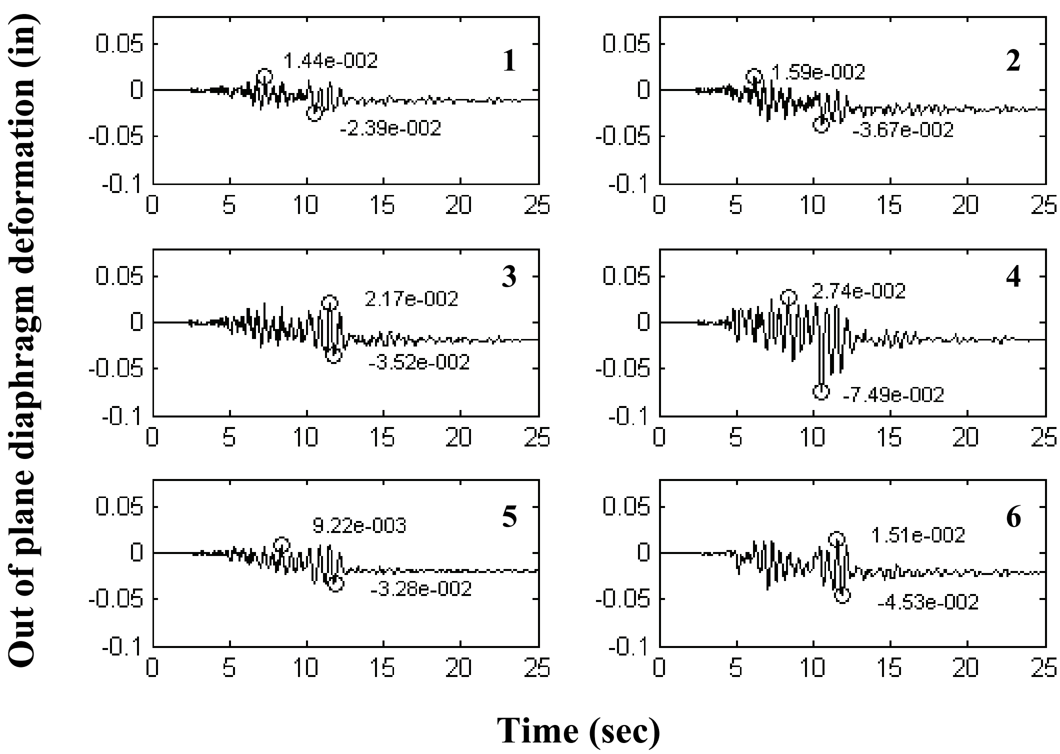

Figure O.1: Out of plane diaphragm deformation at story 2 for Seismic Test 1 (Points 1~6)

Appendix O

Diaphragm deformation: Seismic Test 1

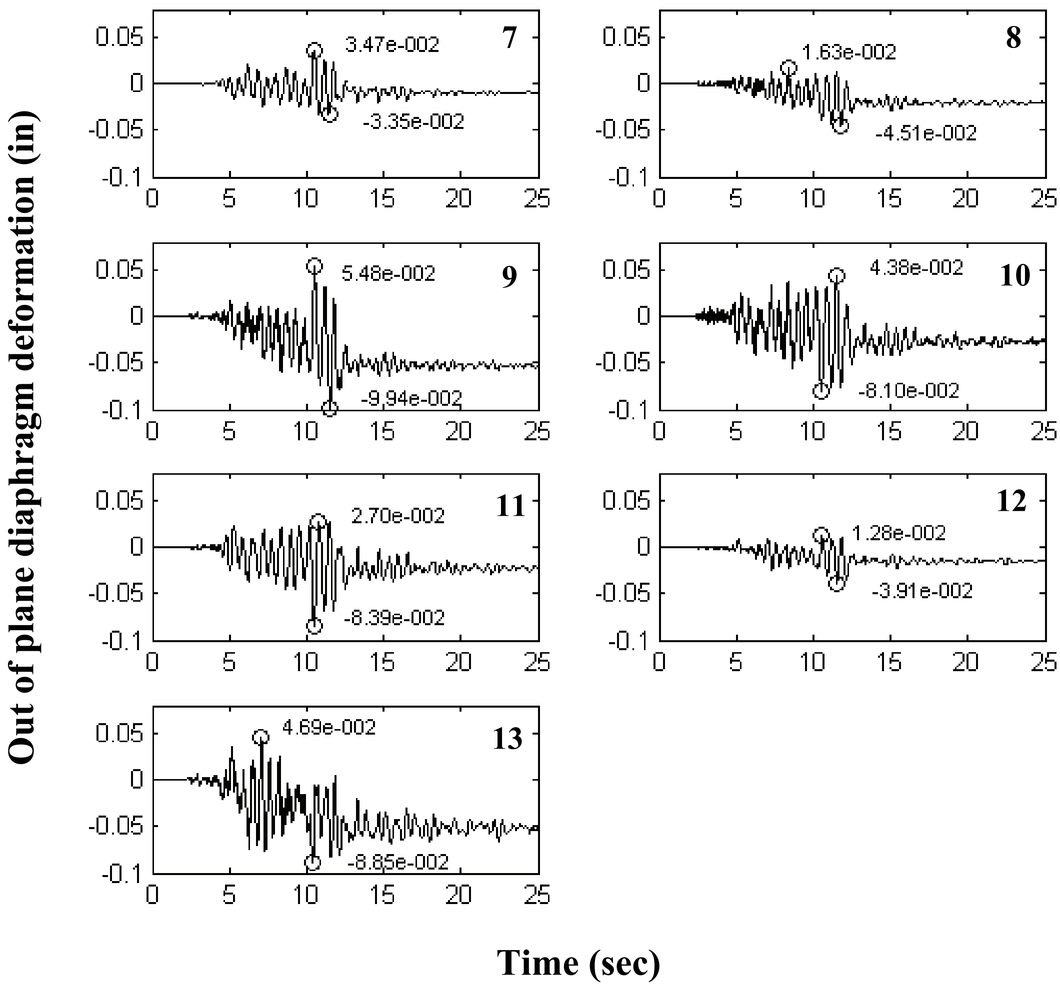

Figure O.2: Out of plane diaphragm deformation at story 2 for Seismic Test 1 (Points 7~13)

Appendix O

Diaphragm deformation: Seismic Test 2

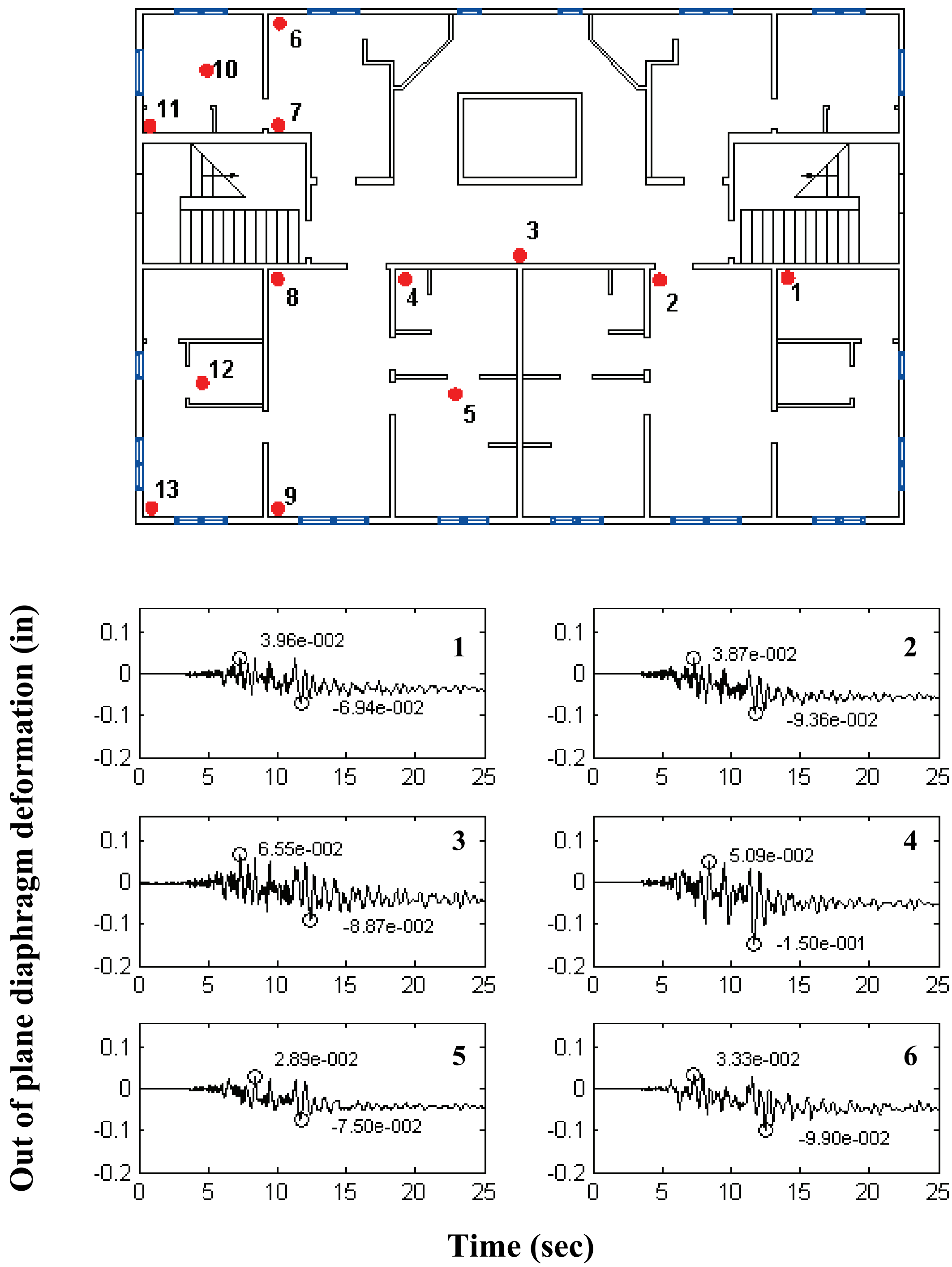

Figure O.3: Out of plane diaphragm deformation at story 2 for Seismic Test 2 (Points 1~6)

Appendix O

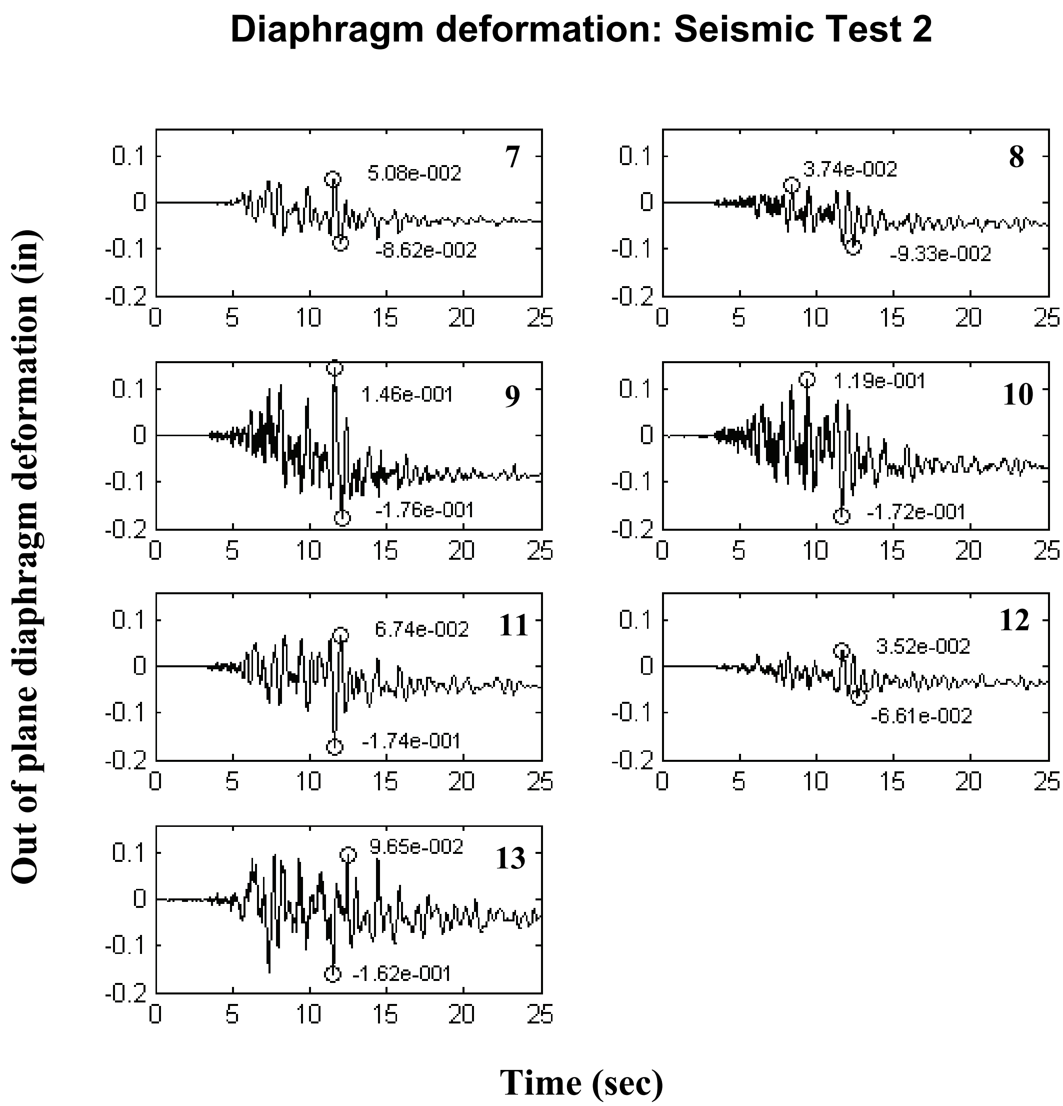

Figure O.4: Out of plane diaphragm deformation at story 2 for Seismic Test 2 (Points 7~13)

Appendix O

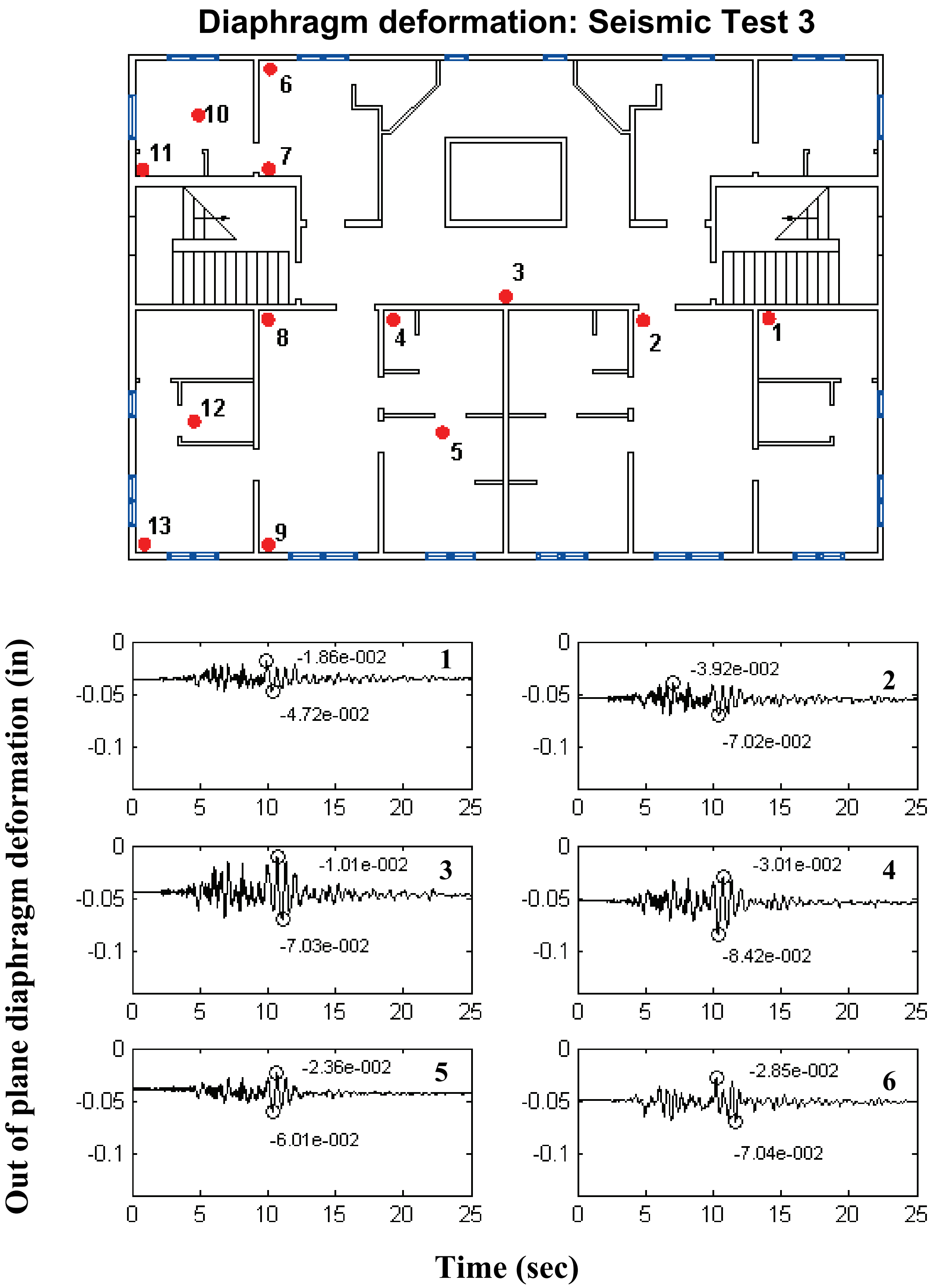

Figure O.5: Out of plane diaphragm deformation at story 2 for Seismic Test 3 (Points 1~6)

Appendix O

Diaphragm deformation: Seismic Test 3

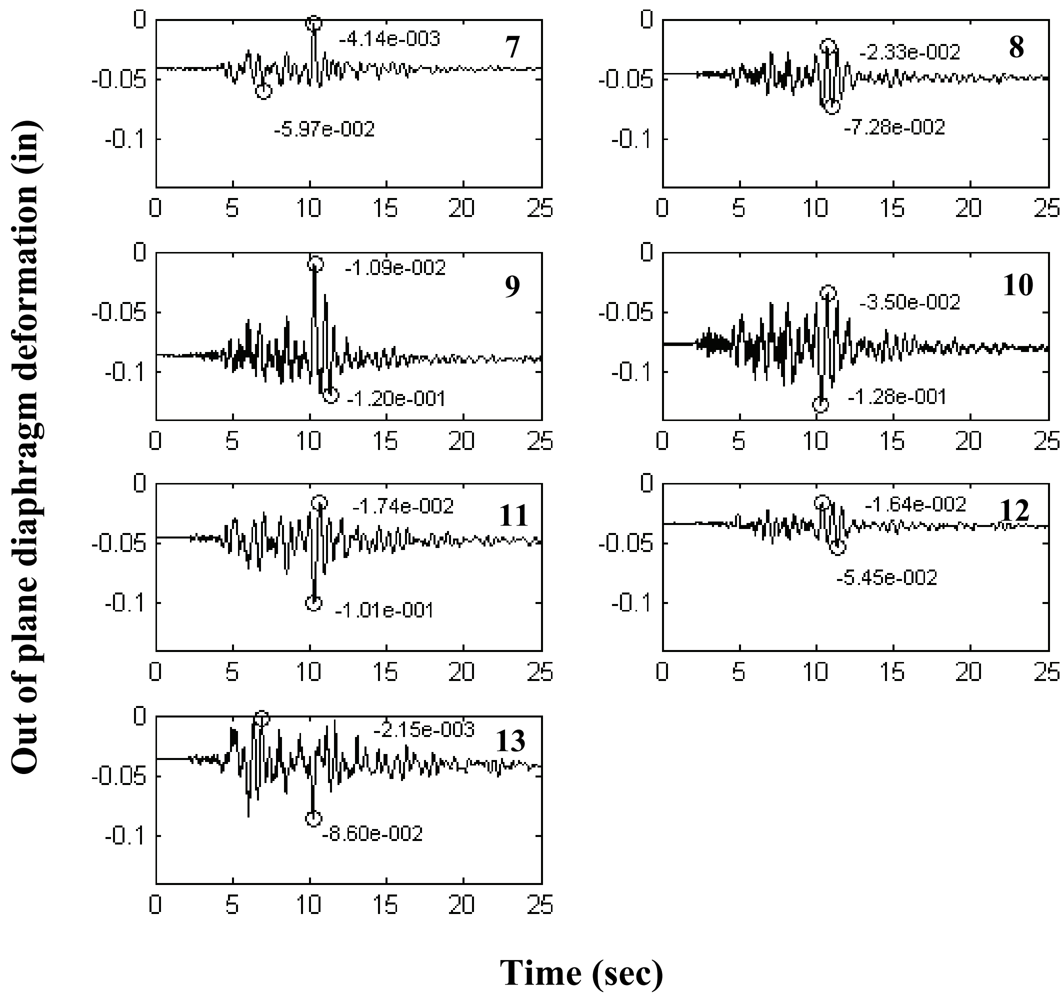

Figure O.6: Out of plane diaphragm deformation at story 2 for Seismic Test 3 (Points 7~13)

Appendix O

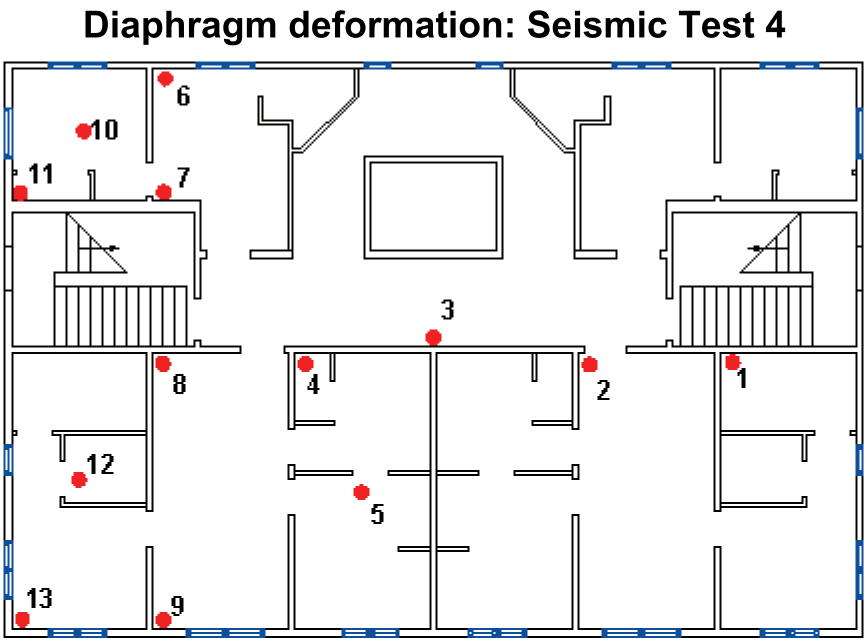

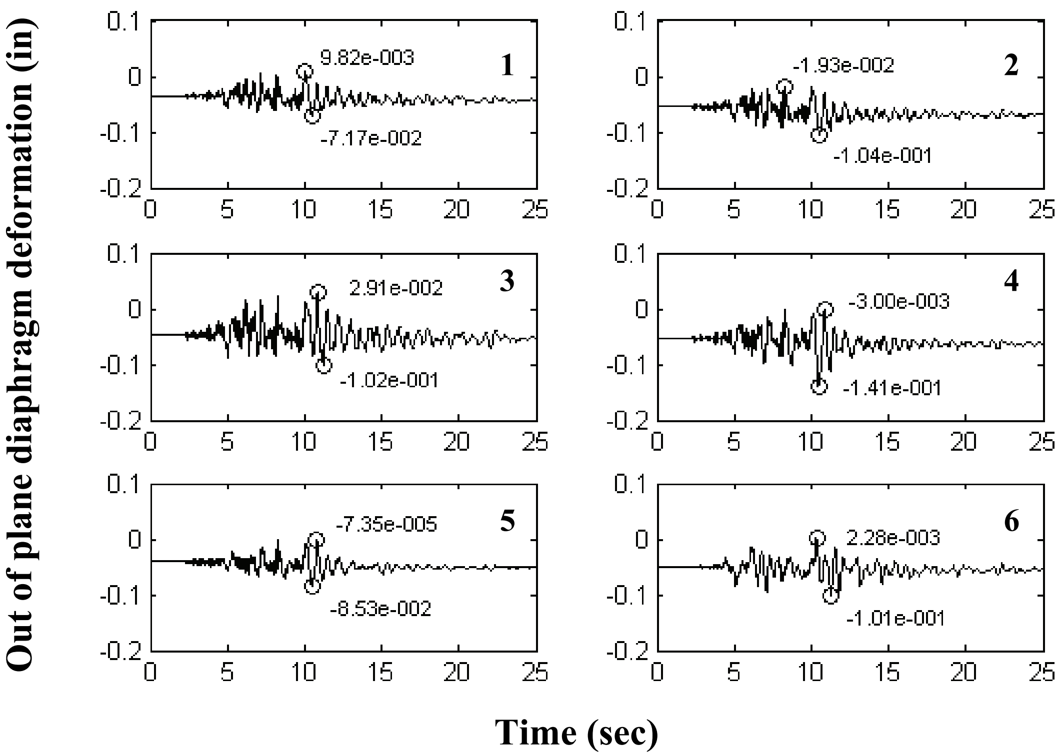

Figure O.7: Out of plane diaphragm deformation at story 2 for Seismic Test 4 (Points 1~6)

Appendix O

Diaphragm deformation: Seismic Test 4

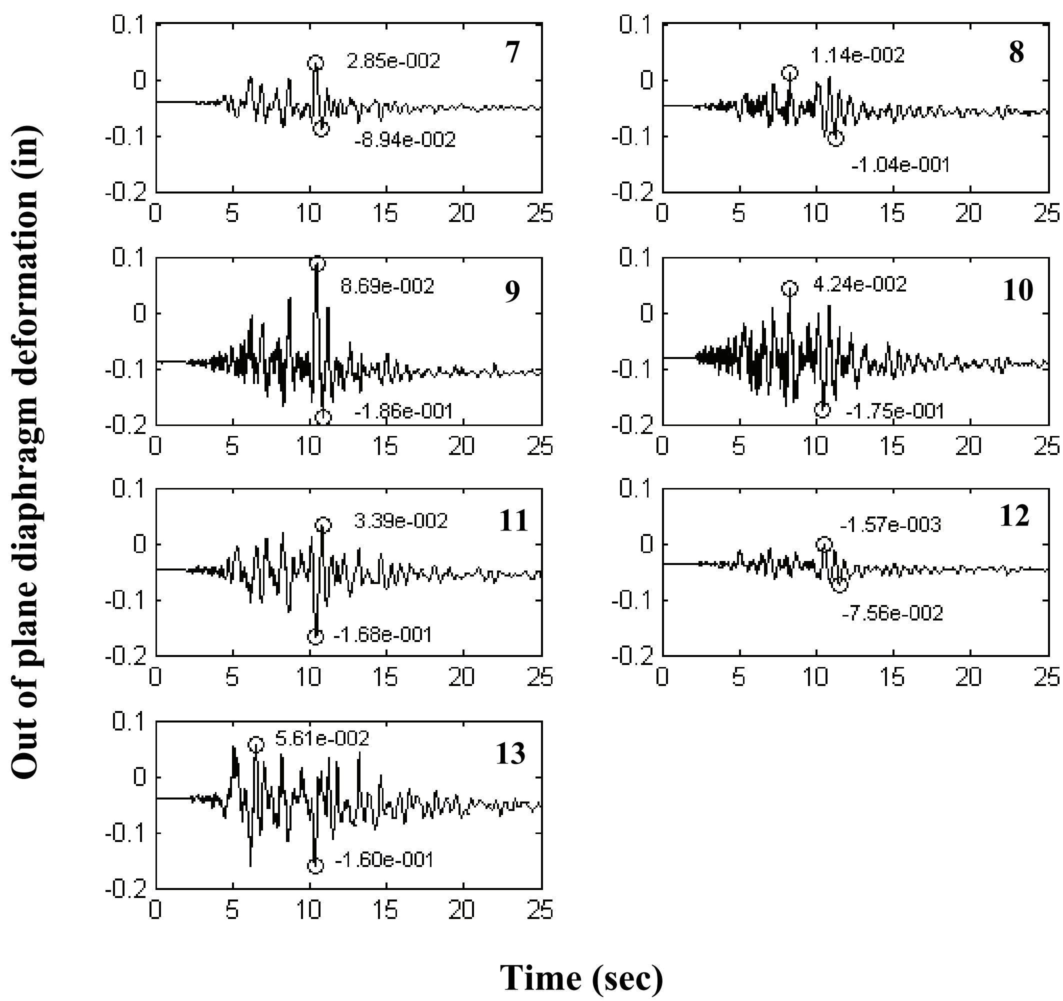

Figure O.8: Out of plane diaphragm deformation at story 2 for Seismic Test 4 (Points 7~13)

Appendix O

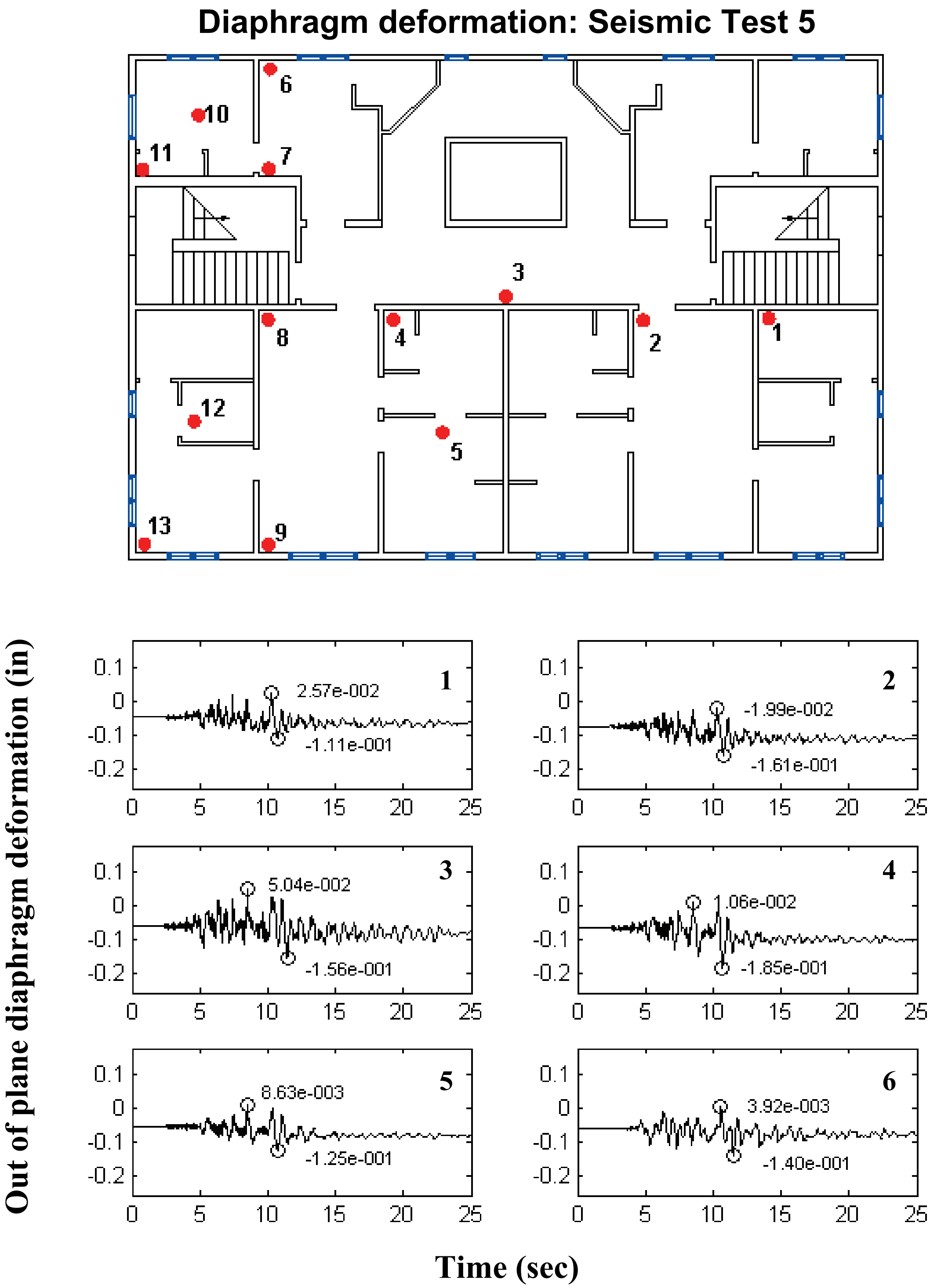

Figure O.9: Out of plane diaphragm deformation at story 2 for Seismic Test 5 (Points 1~6)

Appendix O

Diaphragm deformation: Seismic Test 5

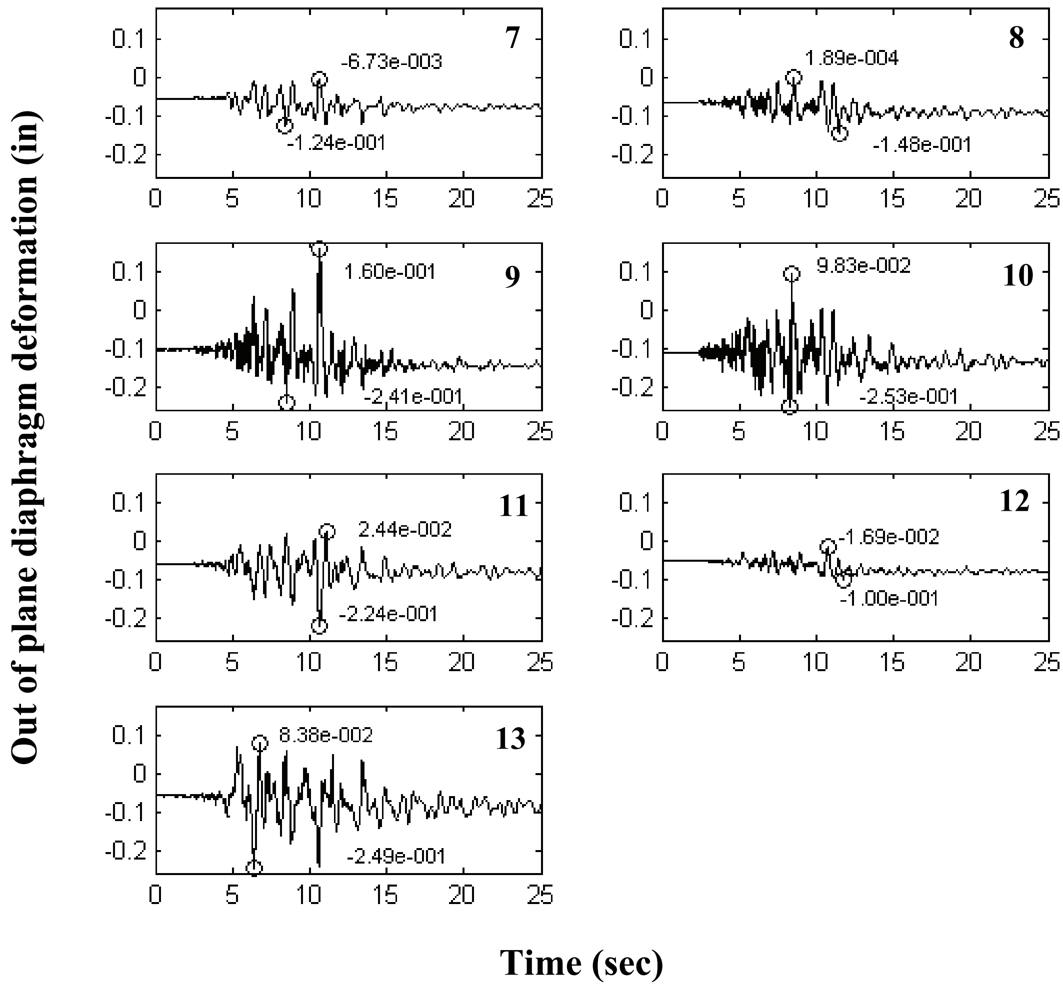

Figure O.10: Out of plane diaphragm deformation at story 2 for Seismic Test 5 (Points 7~13)

Appendix P

Base shear force-displacement hysteresis loops

Appendix P

Seismic Test 1 and 2 with SMF

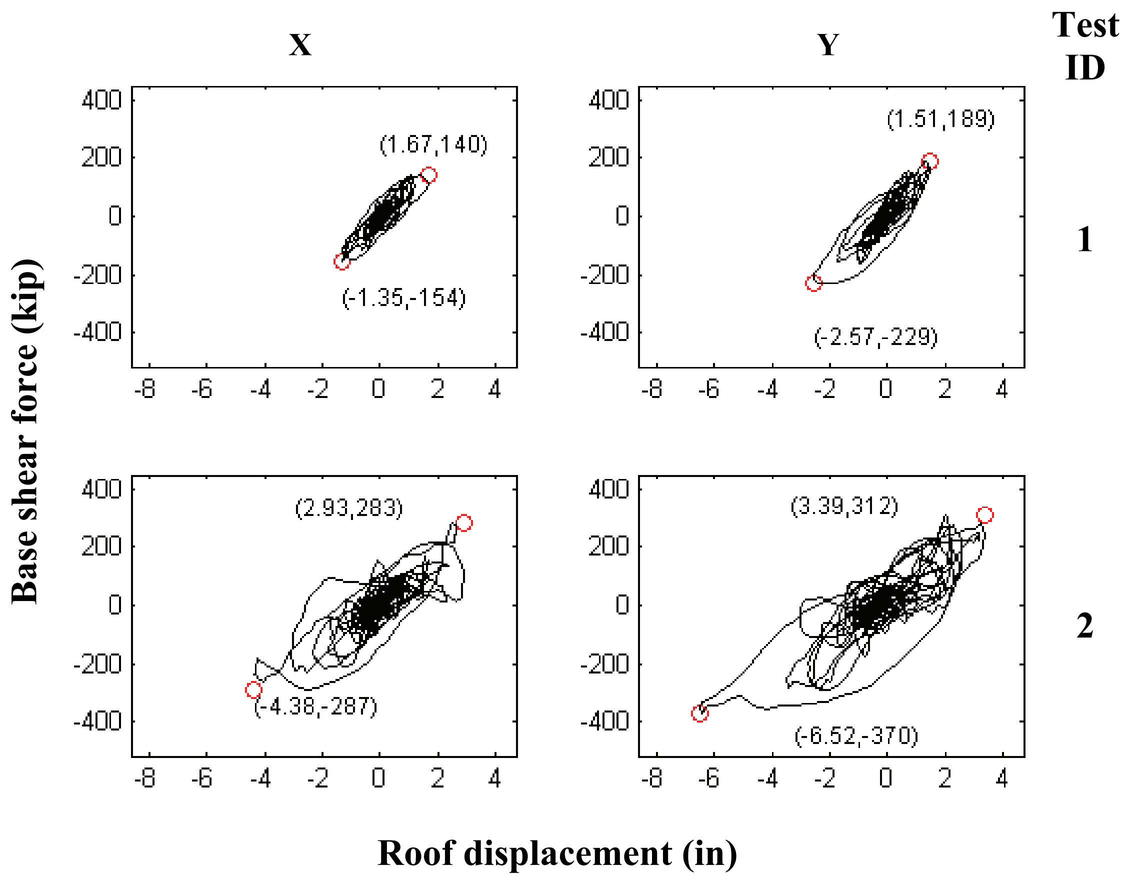

Figure P.1: Base shear vs. Roof displacement hysteresis loop for Seismic Test 1 & 2

*Base shear calculated from seismic mass and recorded absolute acceleration at each story

Appendix P

Seismic Test 3, 4, and 5 without SMF

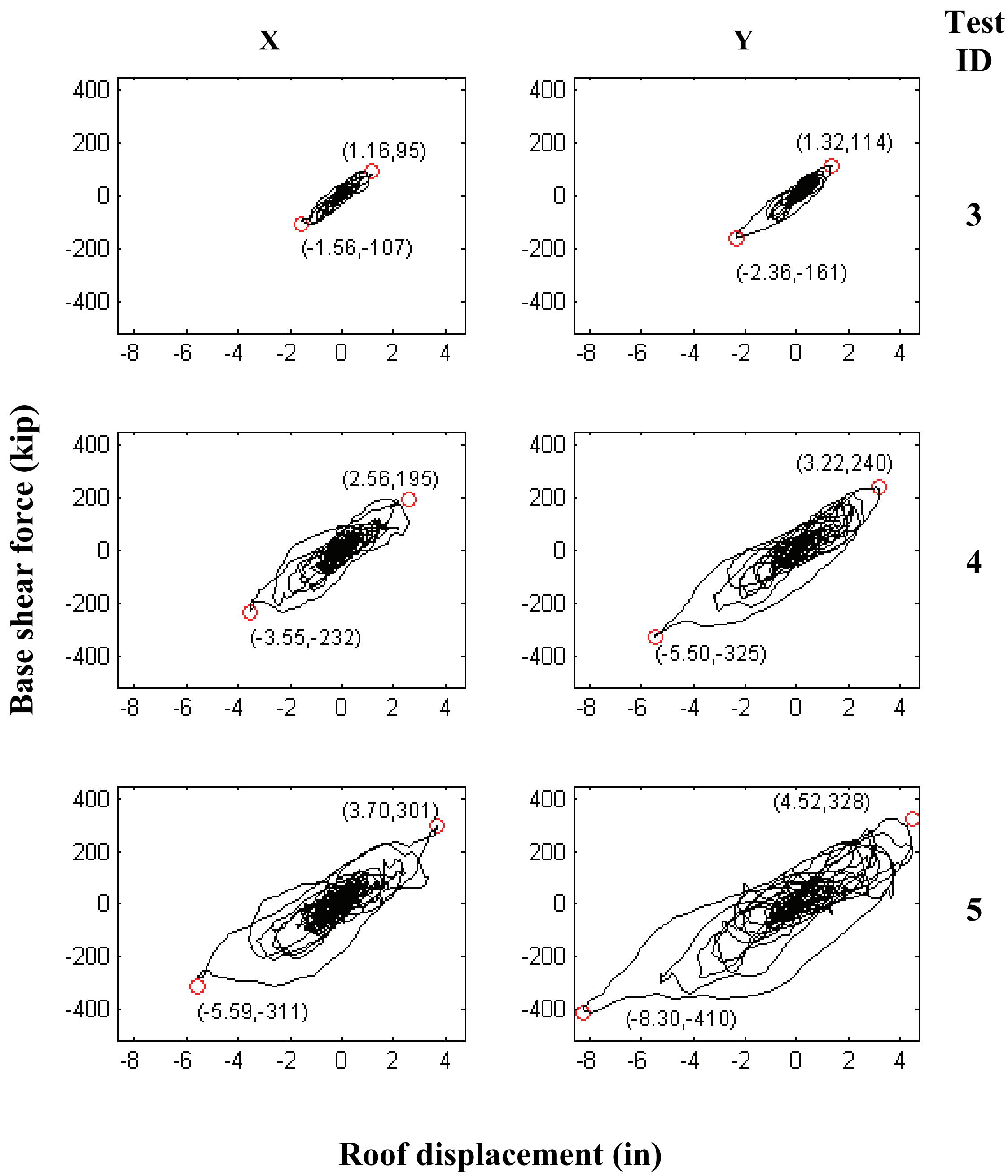

Figure P.2: Base shear vs. Roof displacement hysteresis loop for Seismic Test 3, 4, and 5

*Base shear calculated from seismic mass and recorded absolute acceleration at each story

Appendix Q

Inter-story shear force-displacement hysteresis loops

Appendix Q

Story 1 (SMF) hysteresis

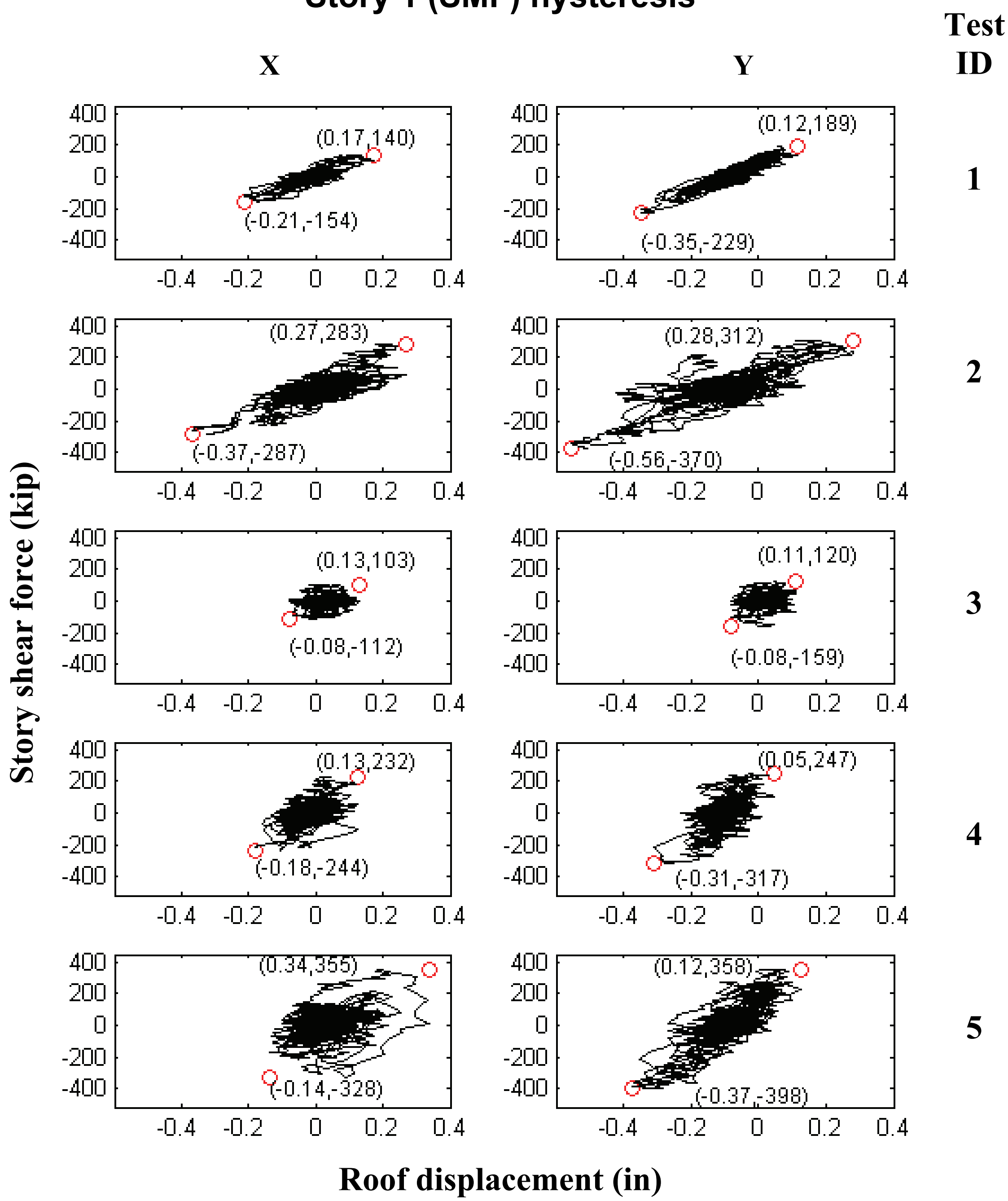

Figure Q.1: Story shear vs. inter-story displacement hysteresis loop for story 1 (SMF)

Appendix Q

Story 2 hysteresis

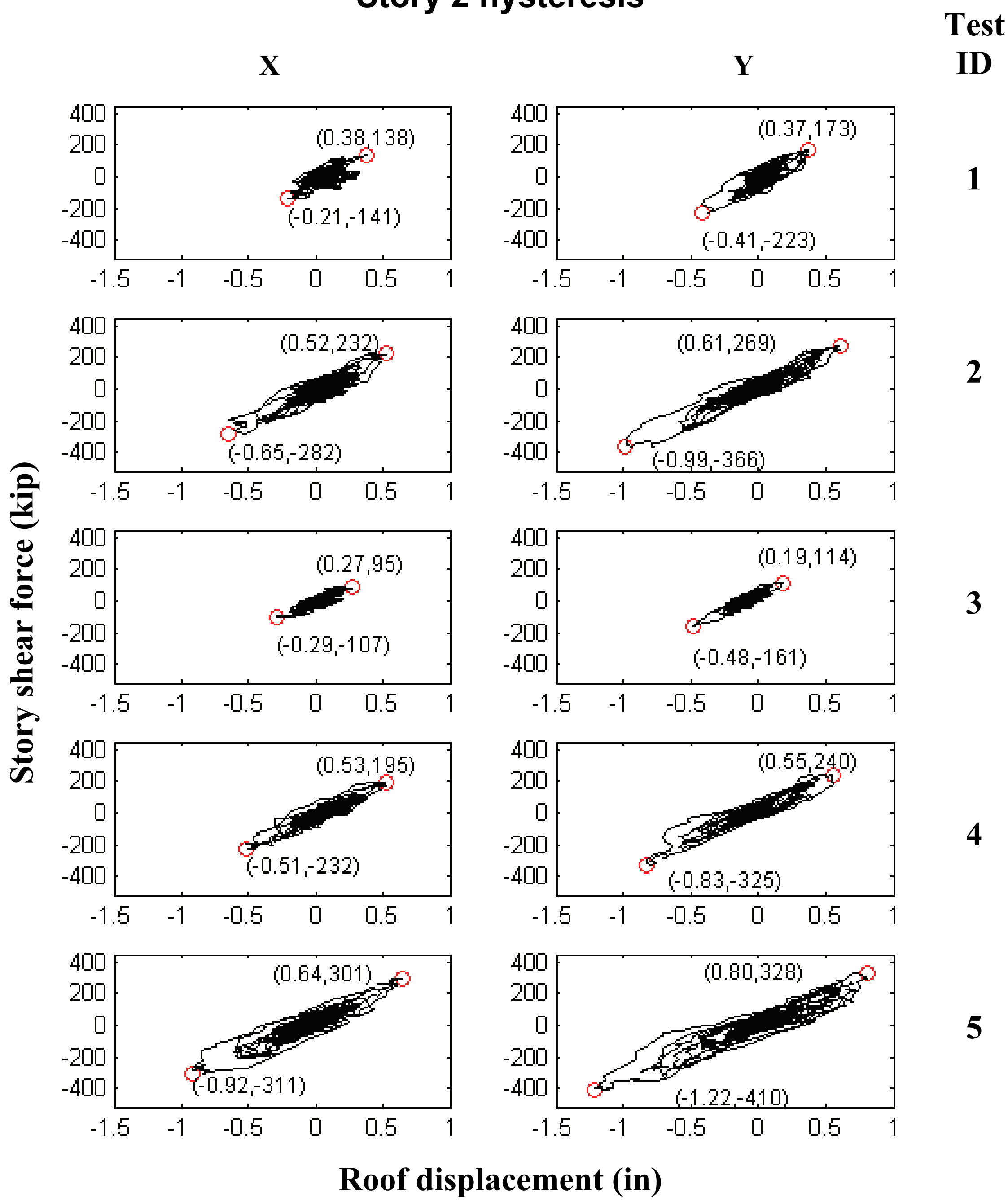

Figure Q.2: Story shear vs. inter-story displacement hysteresis loop for story 2

Appendix Q

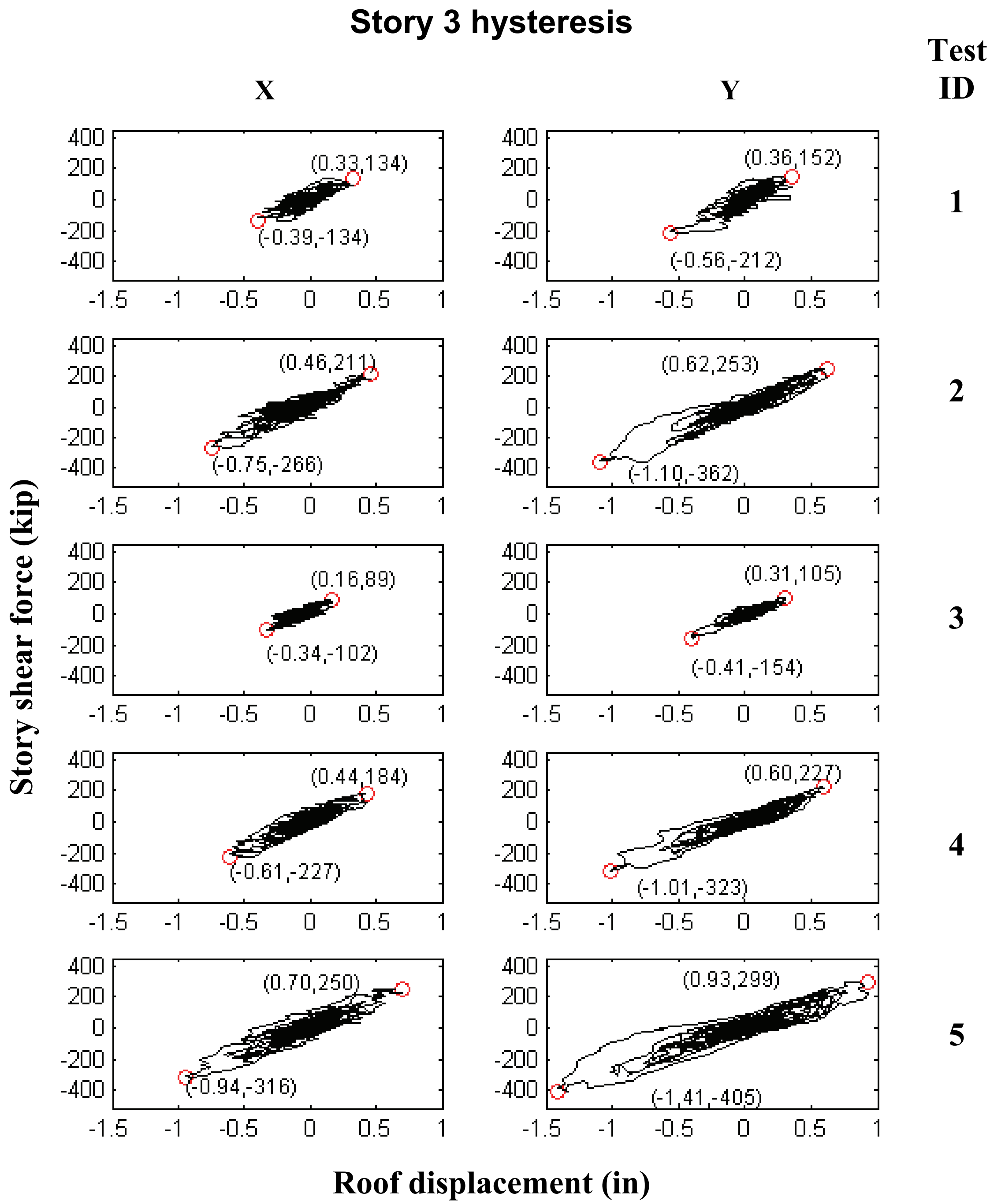

Figure Q.3: Story shear vs. inter-story displacement hysteresis loop for story 3

Appendix Q

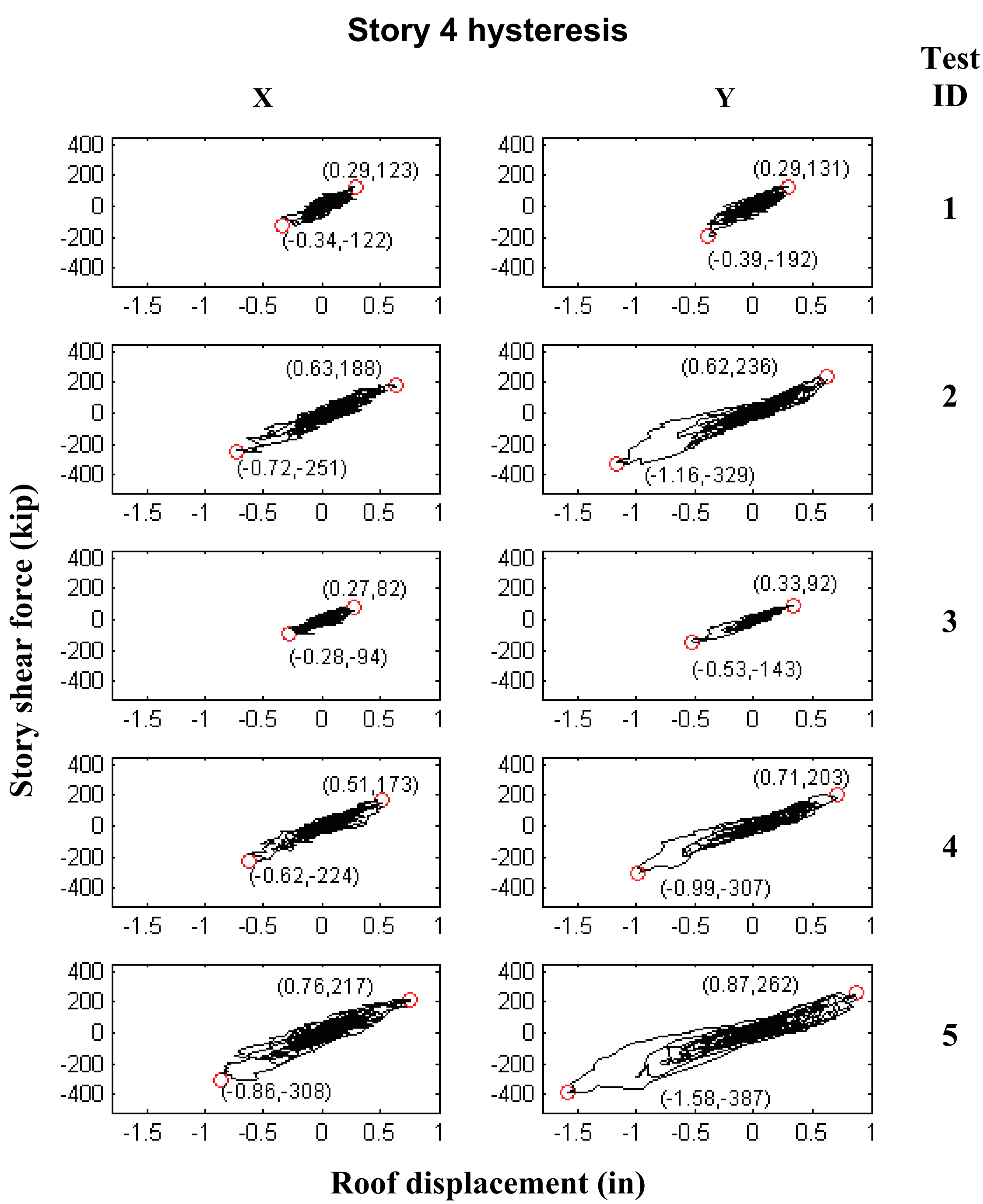

Figure Q.4: Story shear vs. inter-story displacement hysteresis loop for story 4

Appendix Q

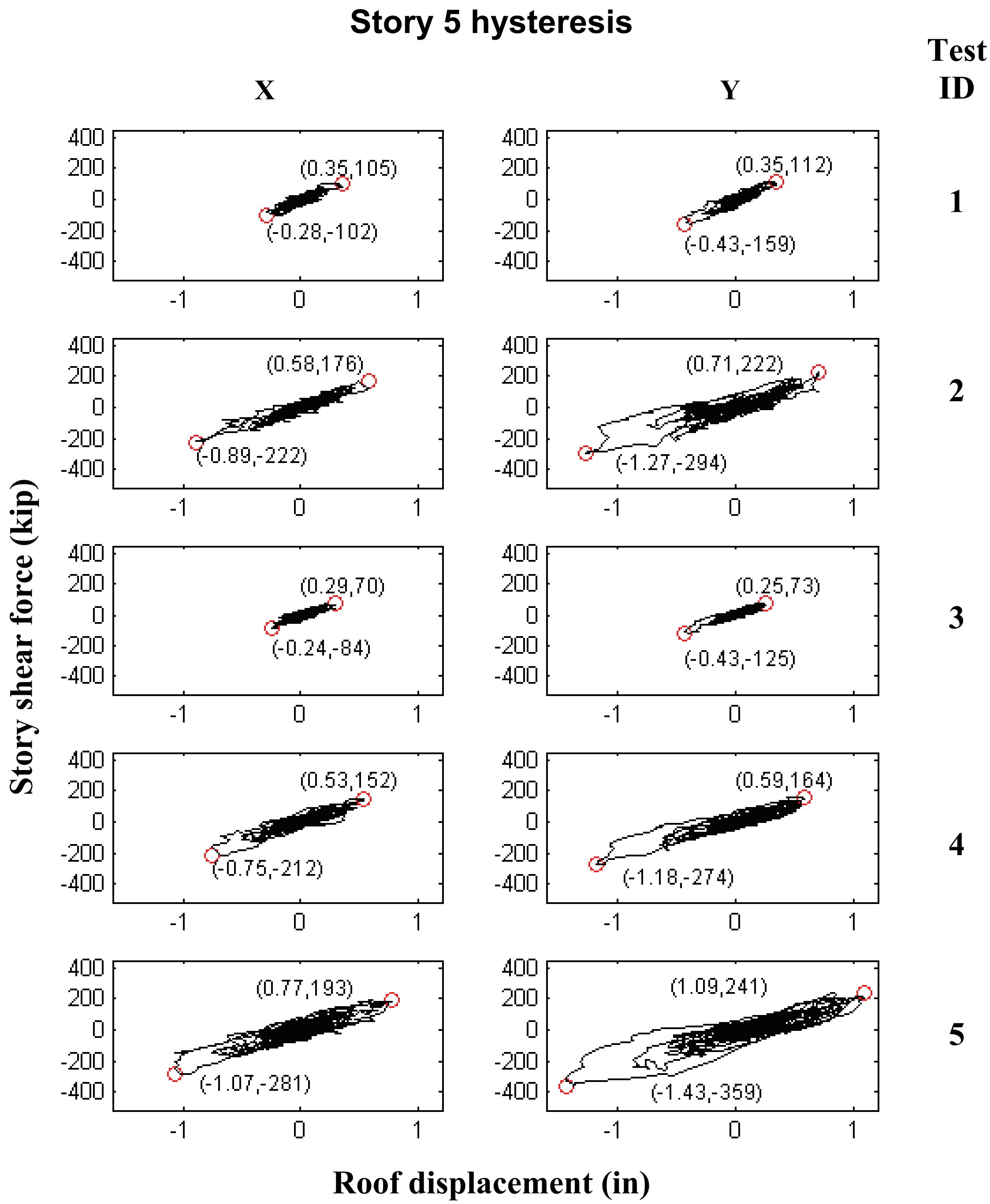

Figure Q.5: Story shear vs. inter-story displacement hysteresis loop for story 5

Appendix Q

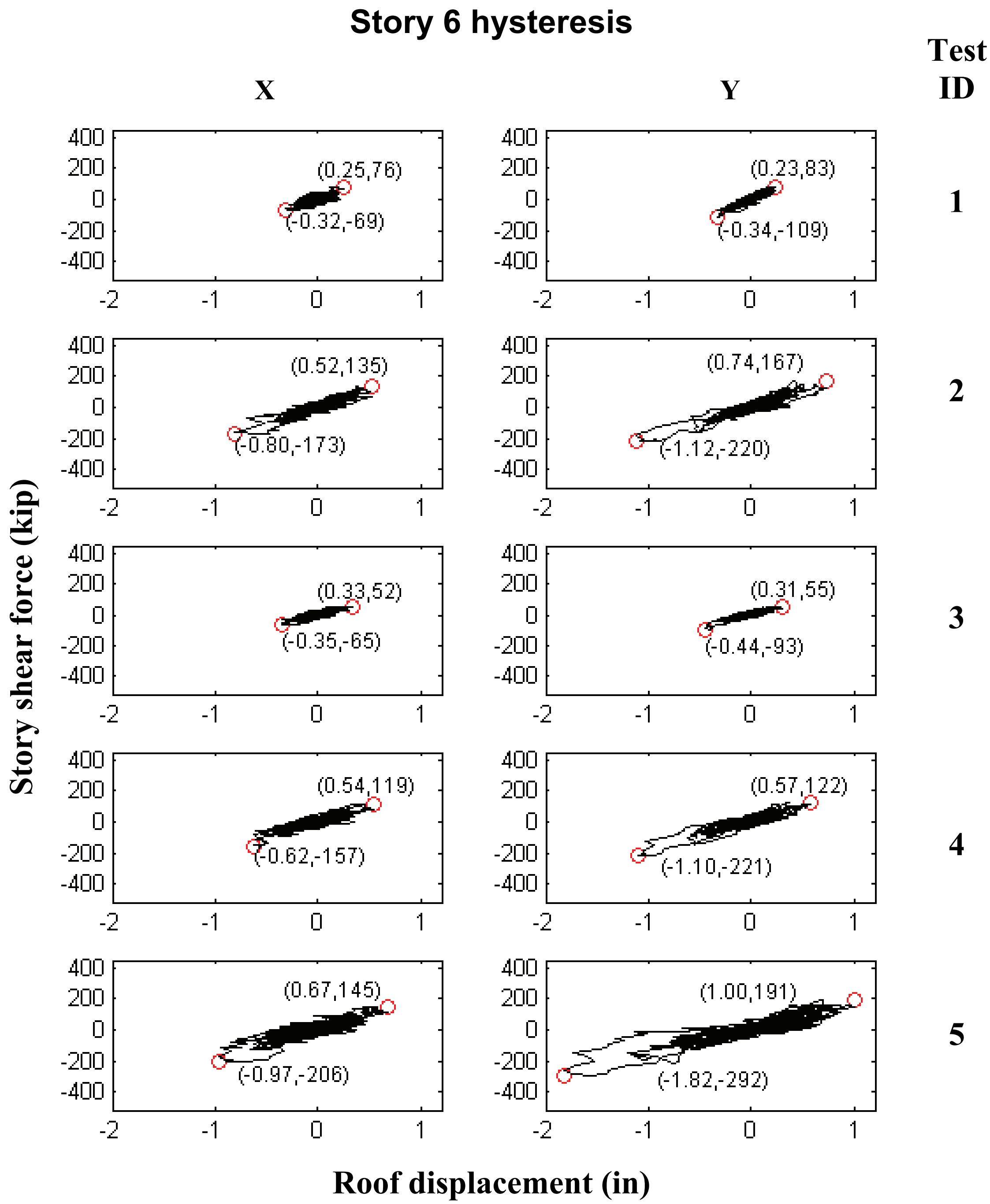

Figure Q.6: Story shear vs. inter-story displacement hysteresis loop for story 6

Appendix Q

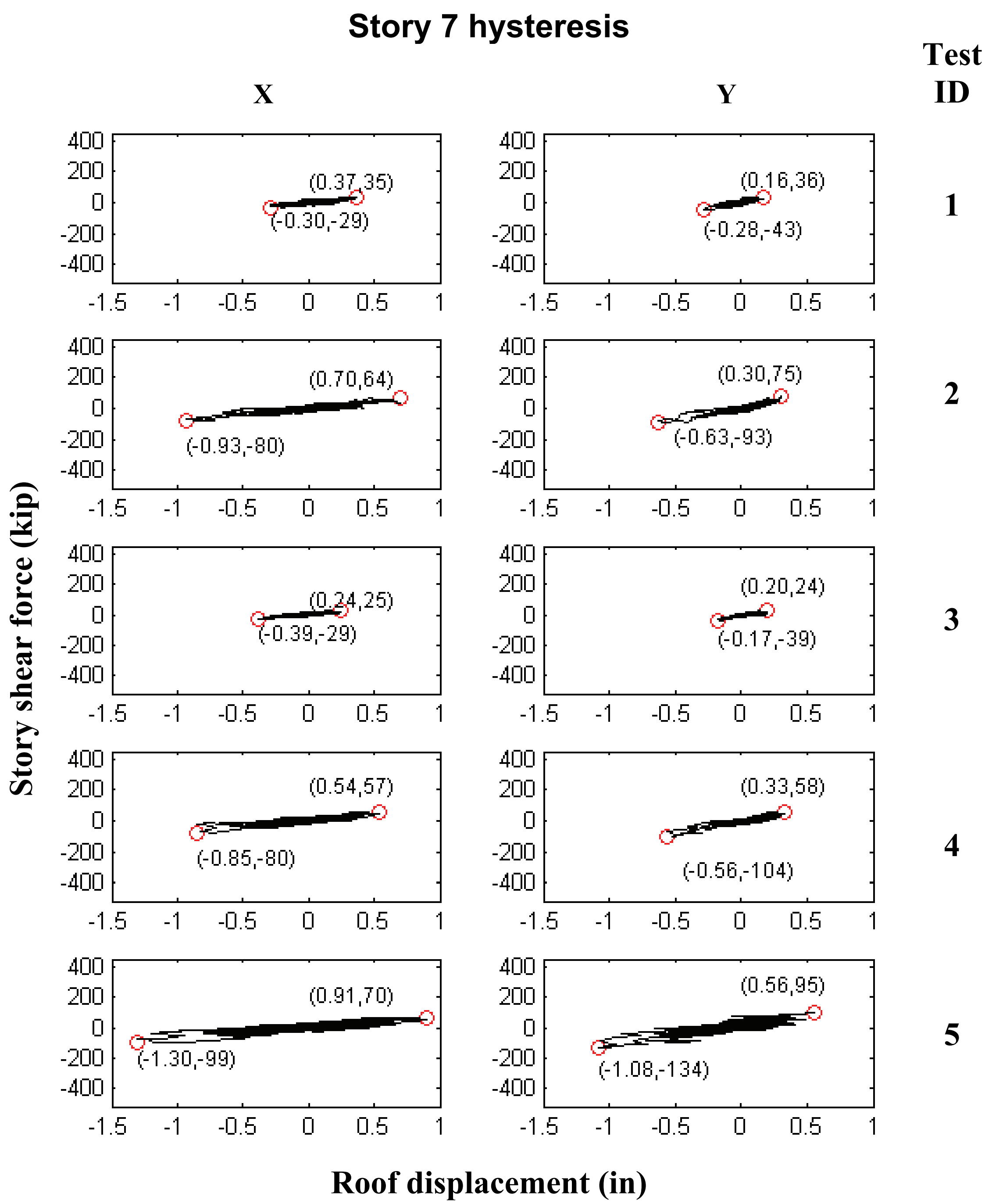

Figure Q.7: Story shear vs. inter-story displacement hysteresis loop for story 7

Appendix R

Global and Inter-story torsion responses

Appendix R

Global Torsion Response at Roof Level

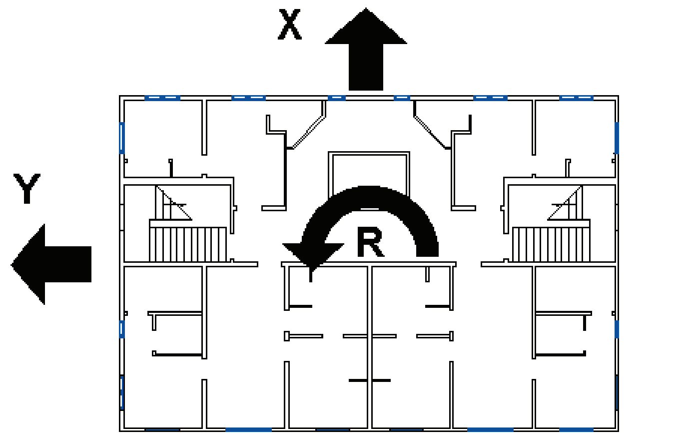

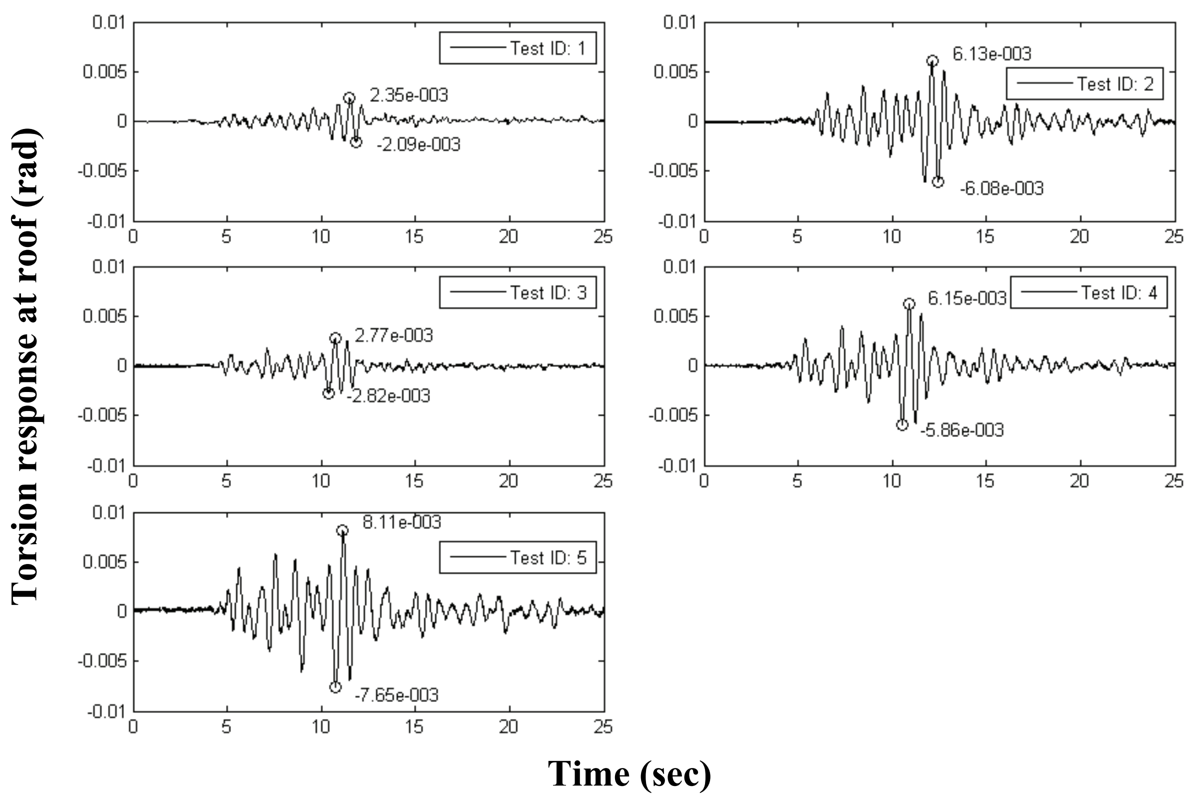

Figure R.1: Global torsion response of the building relative to shake table at roof level

*Torsion response calculated based on optical tracking measurements at roof corners

Appendix R

Inter-story torsion responses: Seismic Test 1

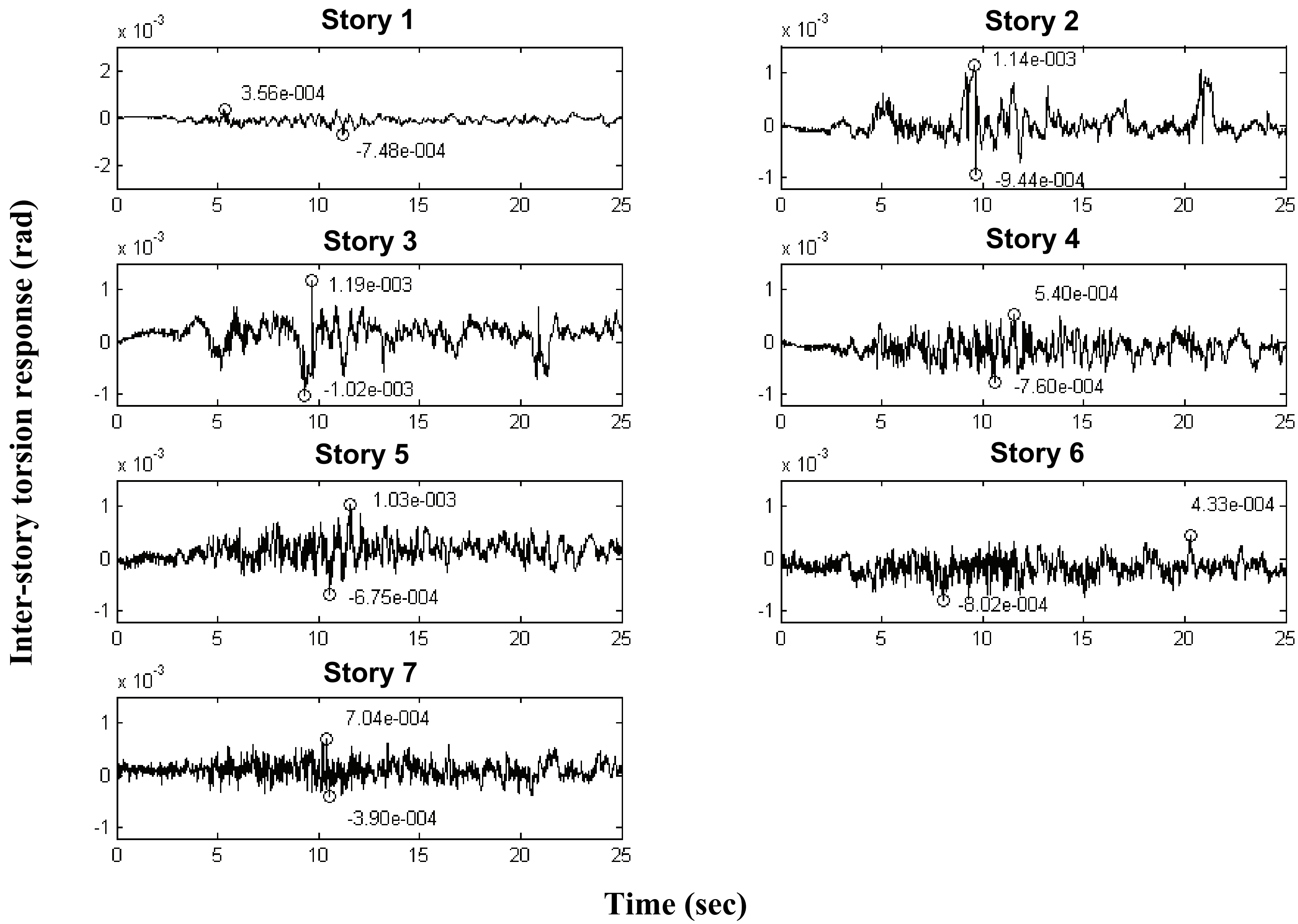

Figure R.2: Inter-story torsion responses during Seismic Test 1

Appendix R

Inter-story torsion responses: Seismic Test 2

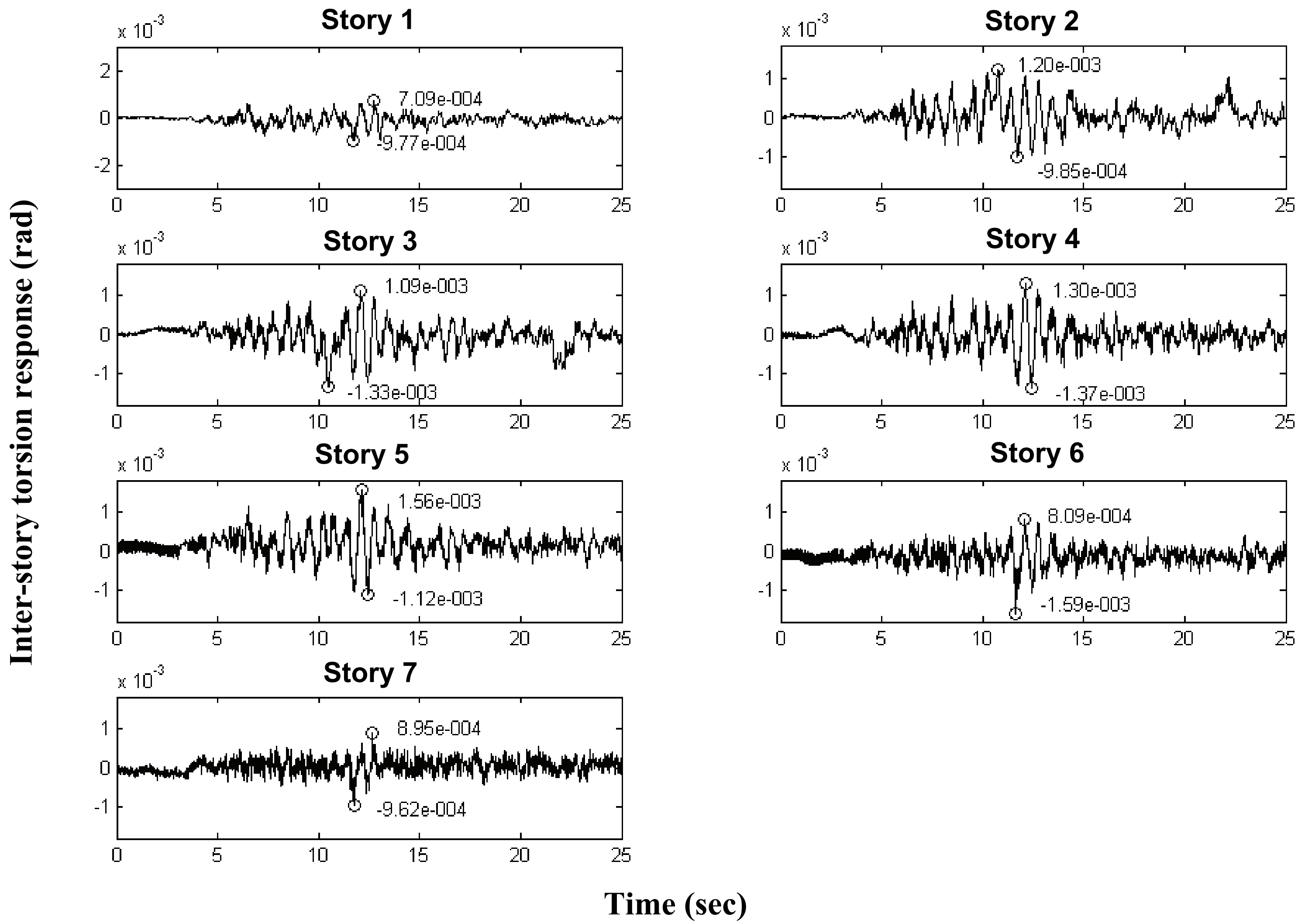

Figure R.3: Inter-story torsion responses during Seismic Test 2

Appendix R

Inter-story torsion responses: Seismic Test 3

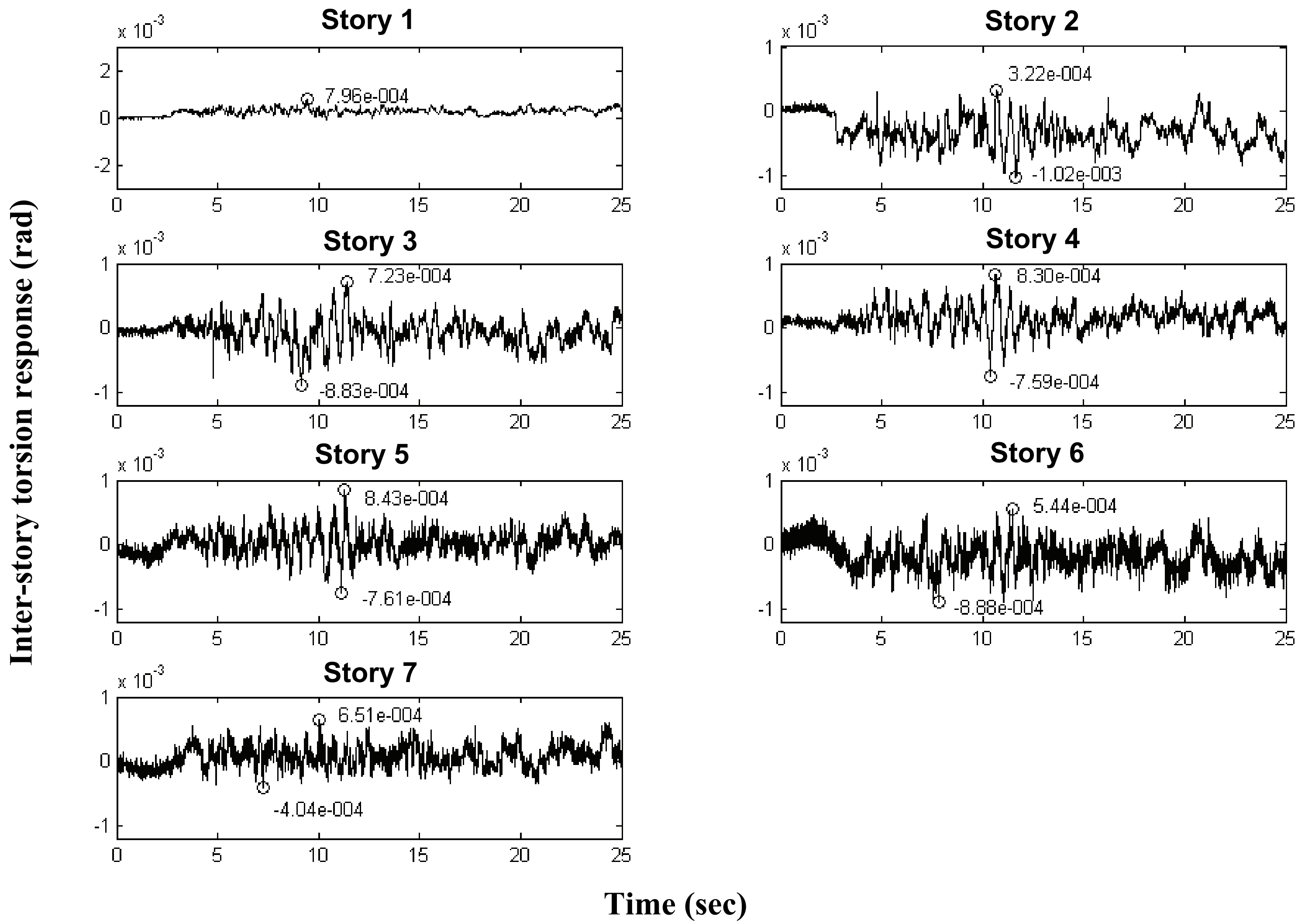

Figure R.4: Inter-story torsion responses during Seismic Test 3

Appendix R

Inter-story torsion responses: Seismic Test 4

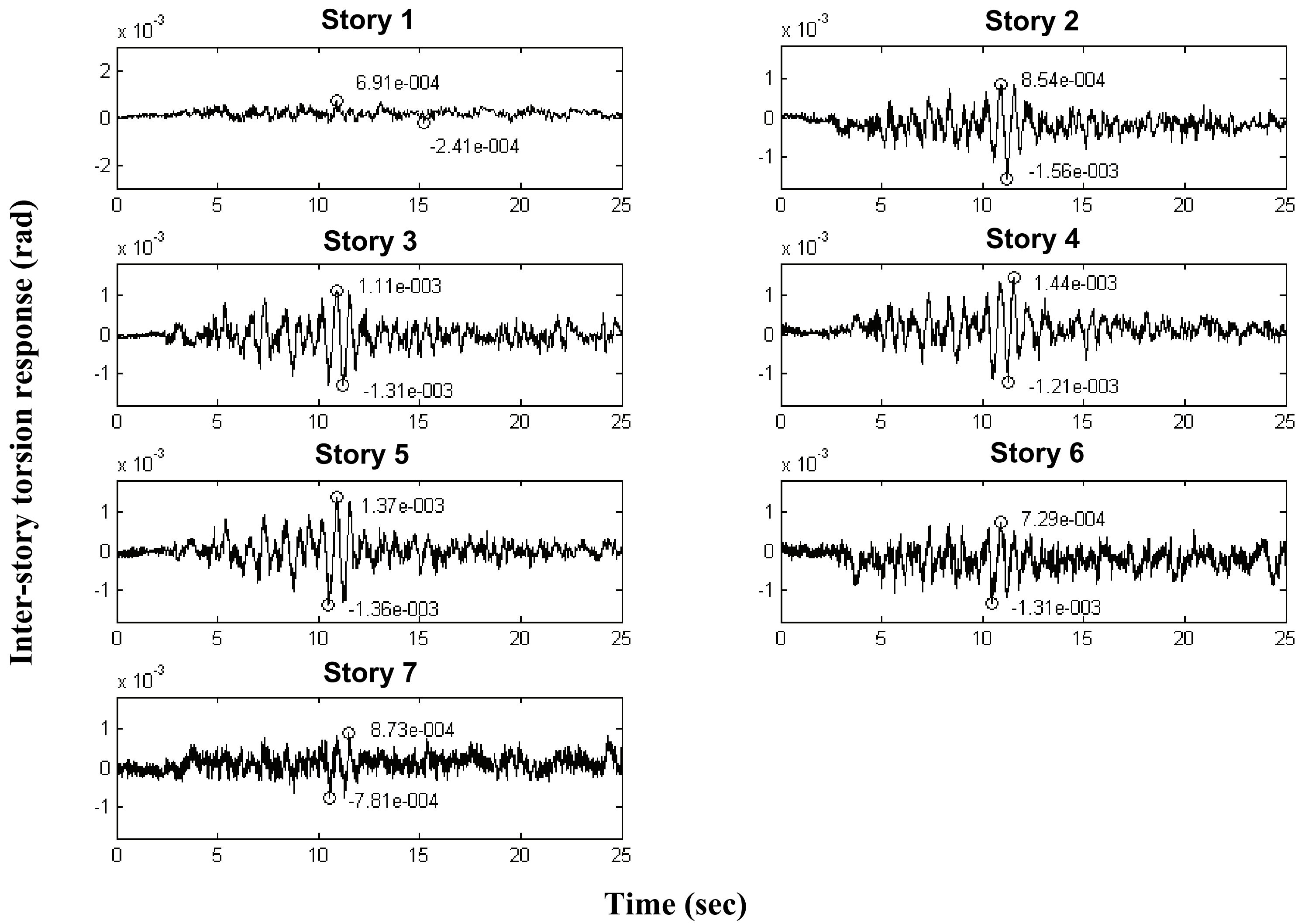

Figure R.5: Inter-story torsion responses during Seismic Test 4

Appendix R

Inter-story torsion responses: Seismic Test 5

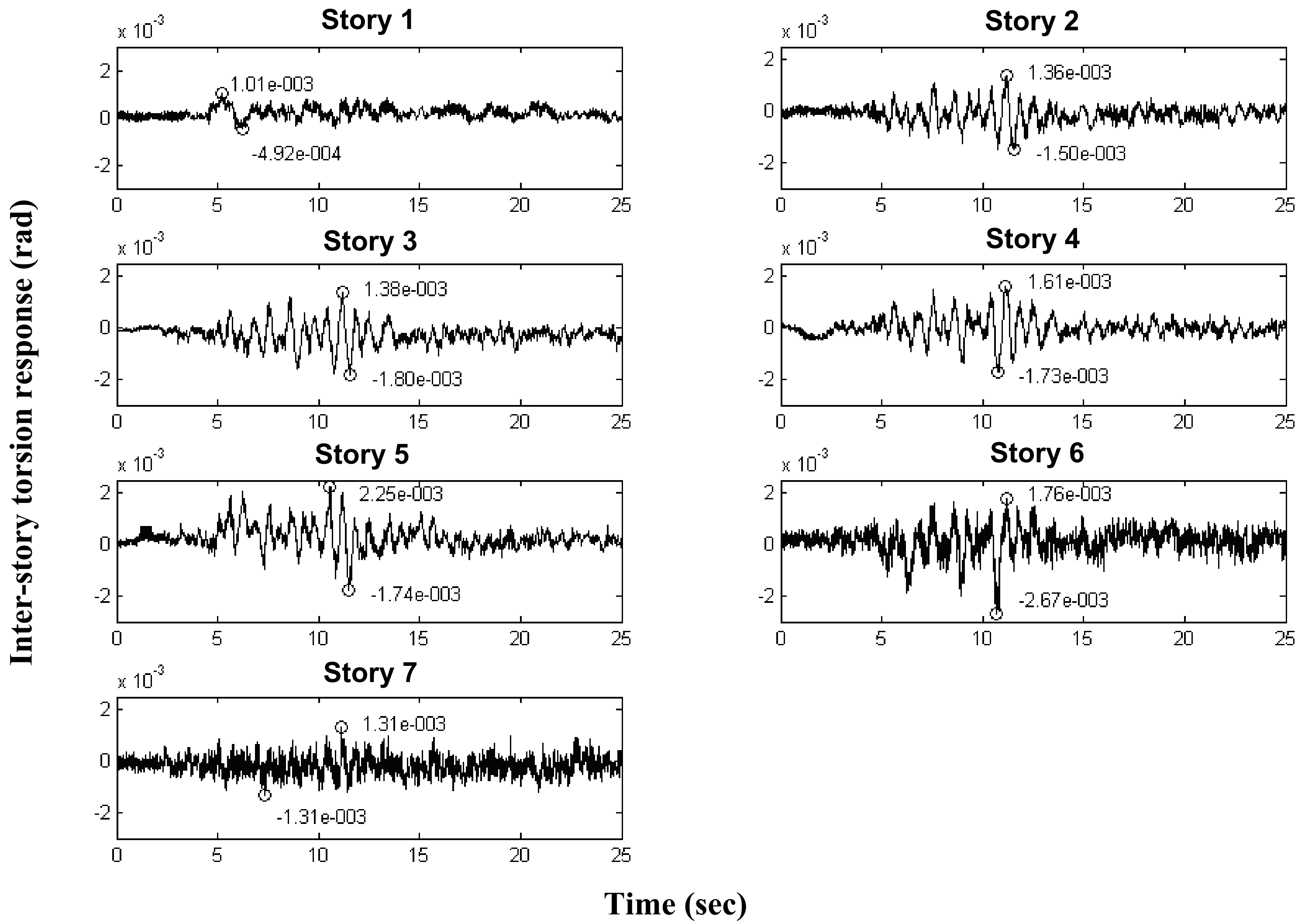

Figure R.6: Inter-story torsion responses during Seismic Test 5

Appendix S

Strain measurements for SMF moment connections

Appendix S

Location ID (LOC) for the moment connections

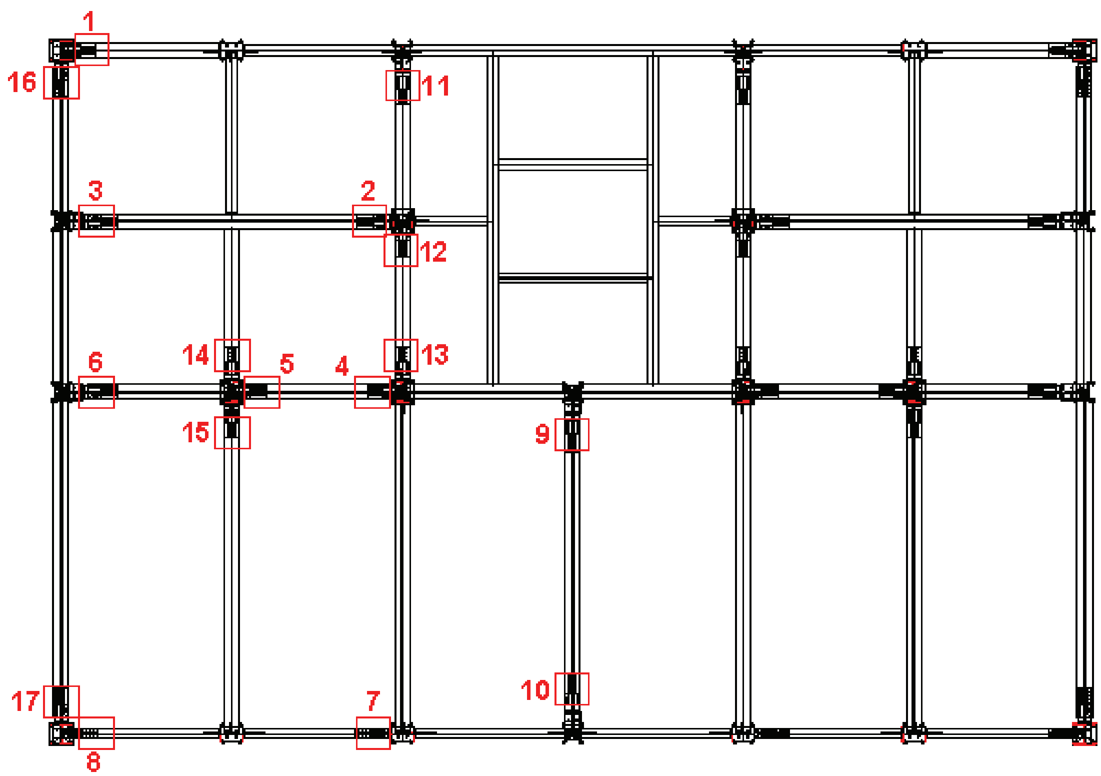

Figure S.1: Location ID for moment connections (each connection contains 4 strain measurements)

Appendix S

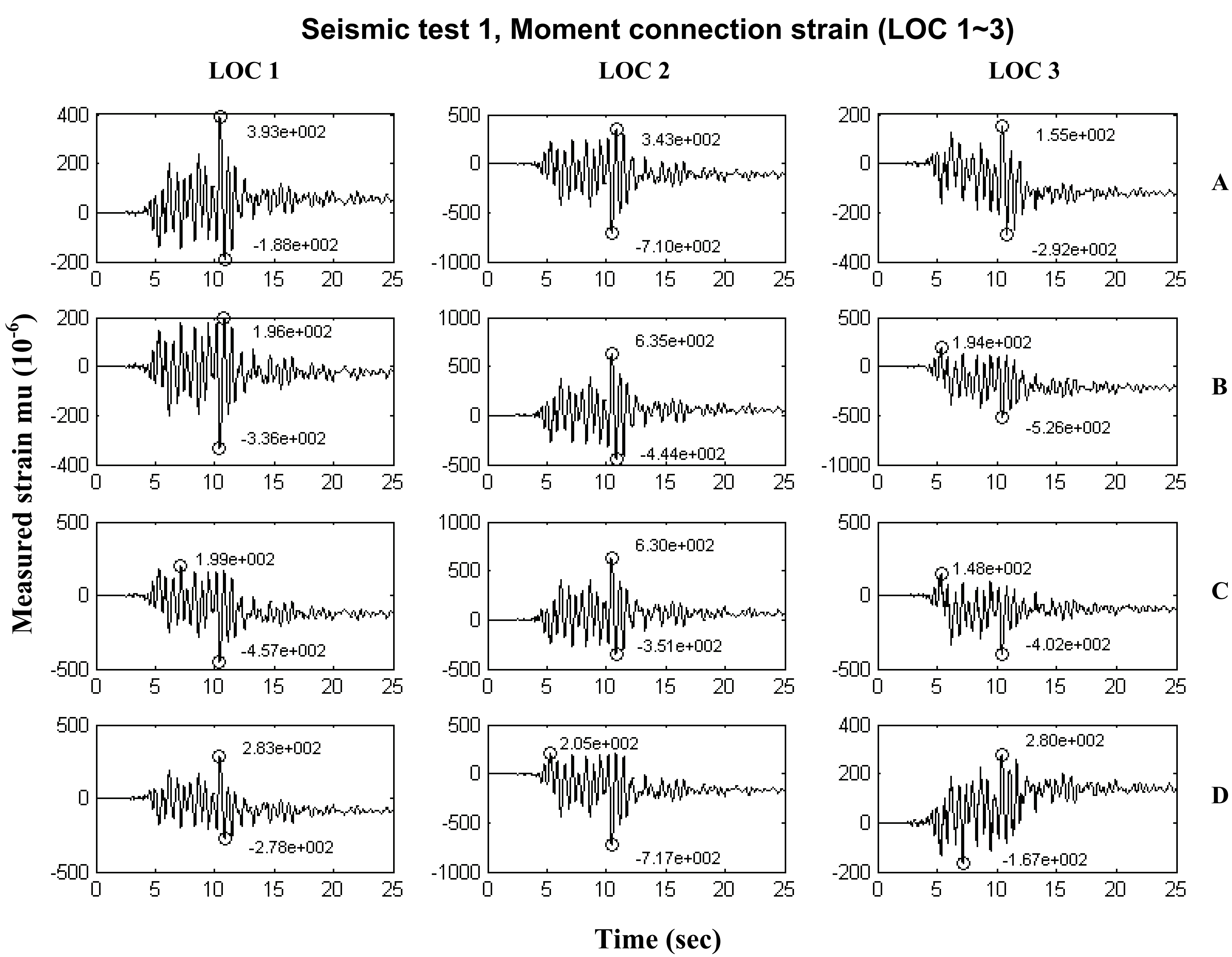

Figure S.2: Moment connection strain for LOC 1~3 during Seismic test 1

Appendix S

Seismic test 1, Moment connection strain (LOC 4~6)

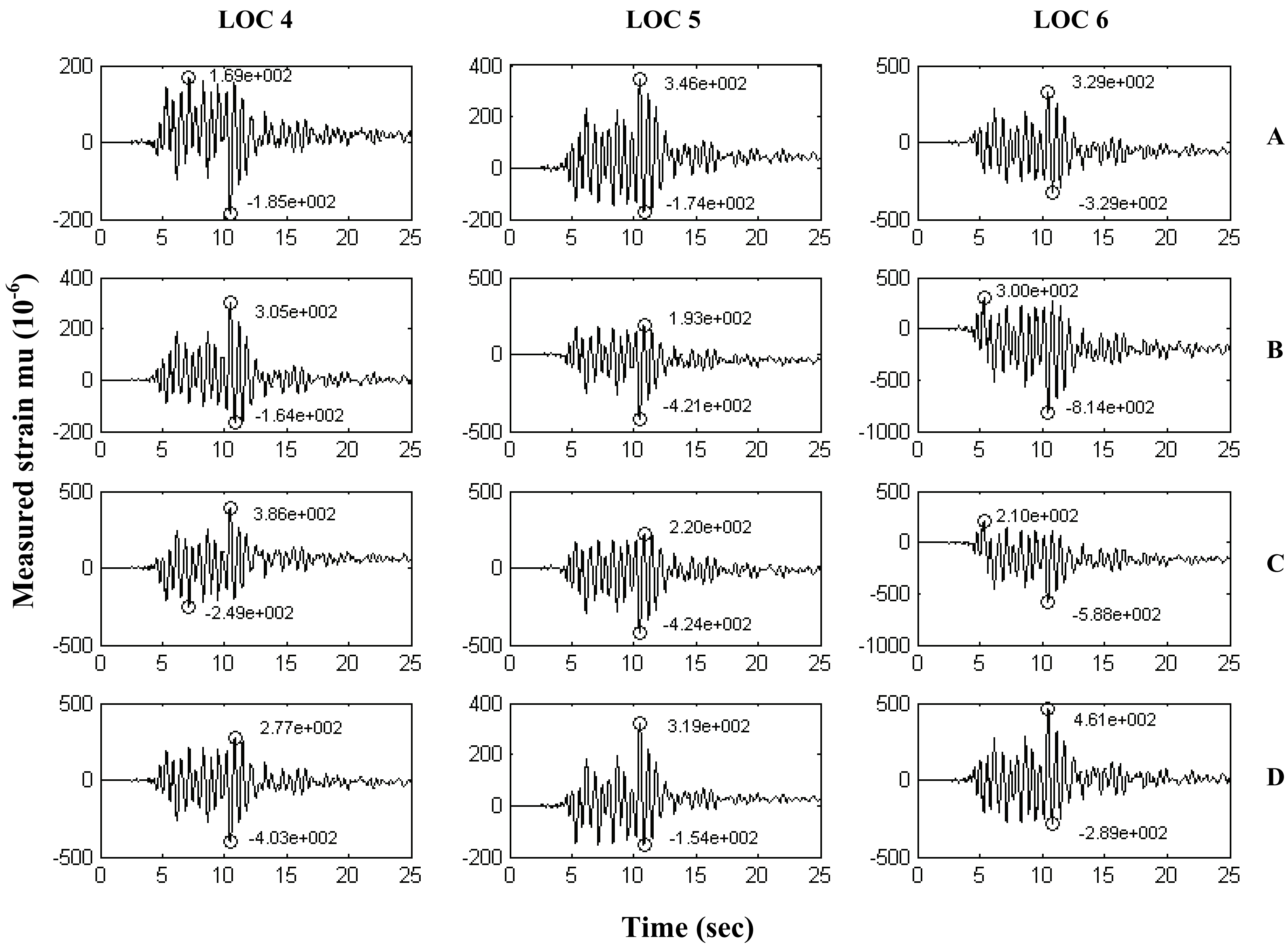

Figure S.3: Moment connection strain for LOC 4~6 during Seismic test 1

Appendix S

Seismic test 1, Moment connection strain (LOC 7~9)

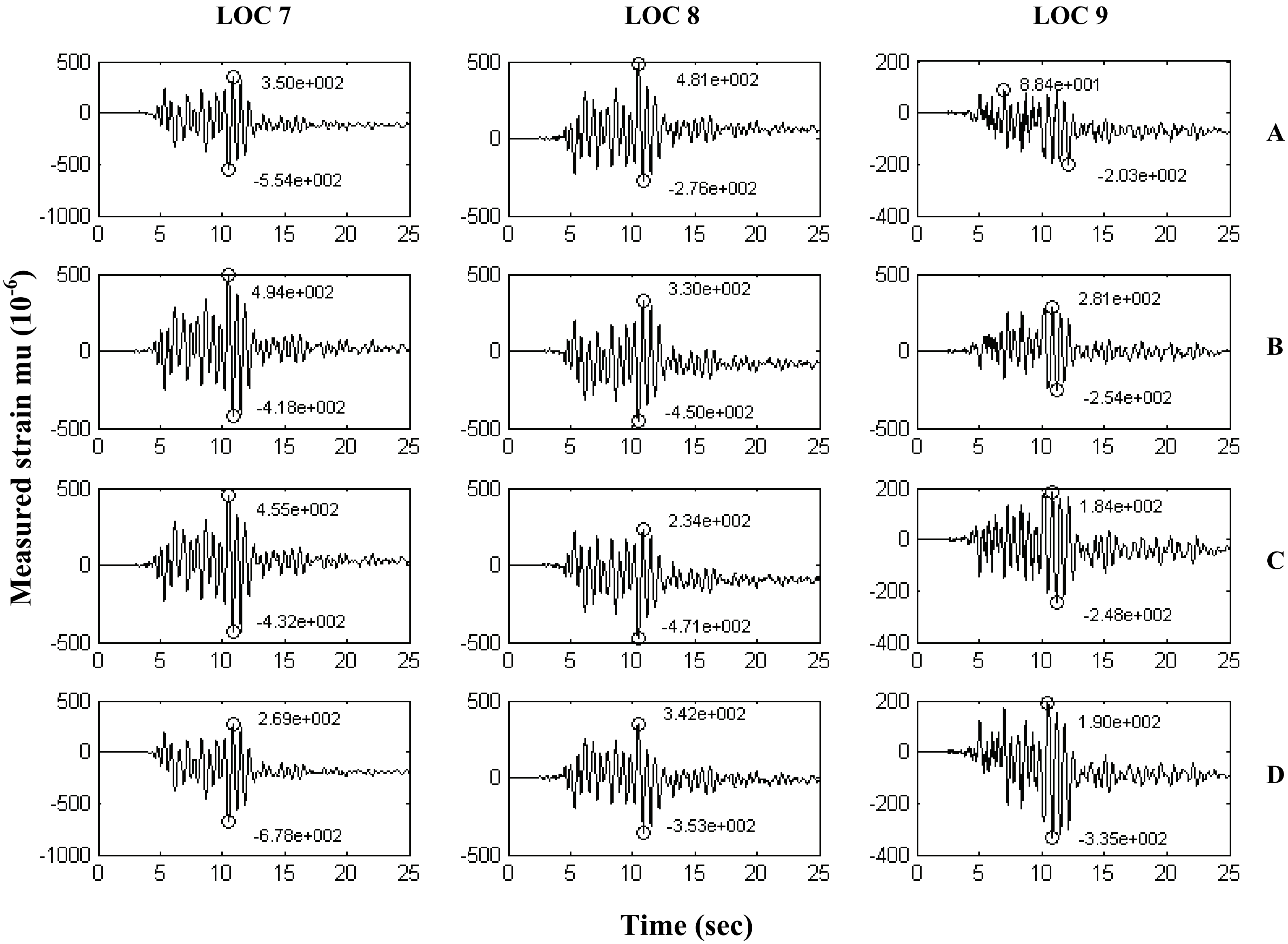

Figure S.4: Moment connection strain for LOC 7~9 during Seismic test 1

Appendix S

Seismic test 1, Moment connection strain (LOC 10~12)

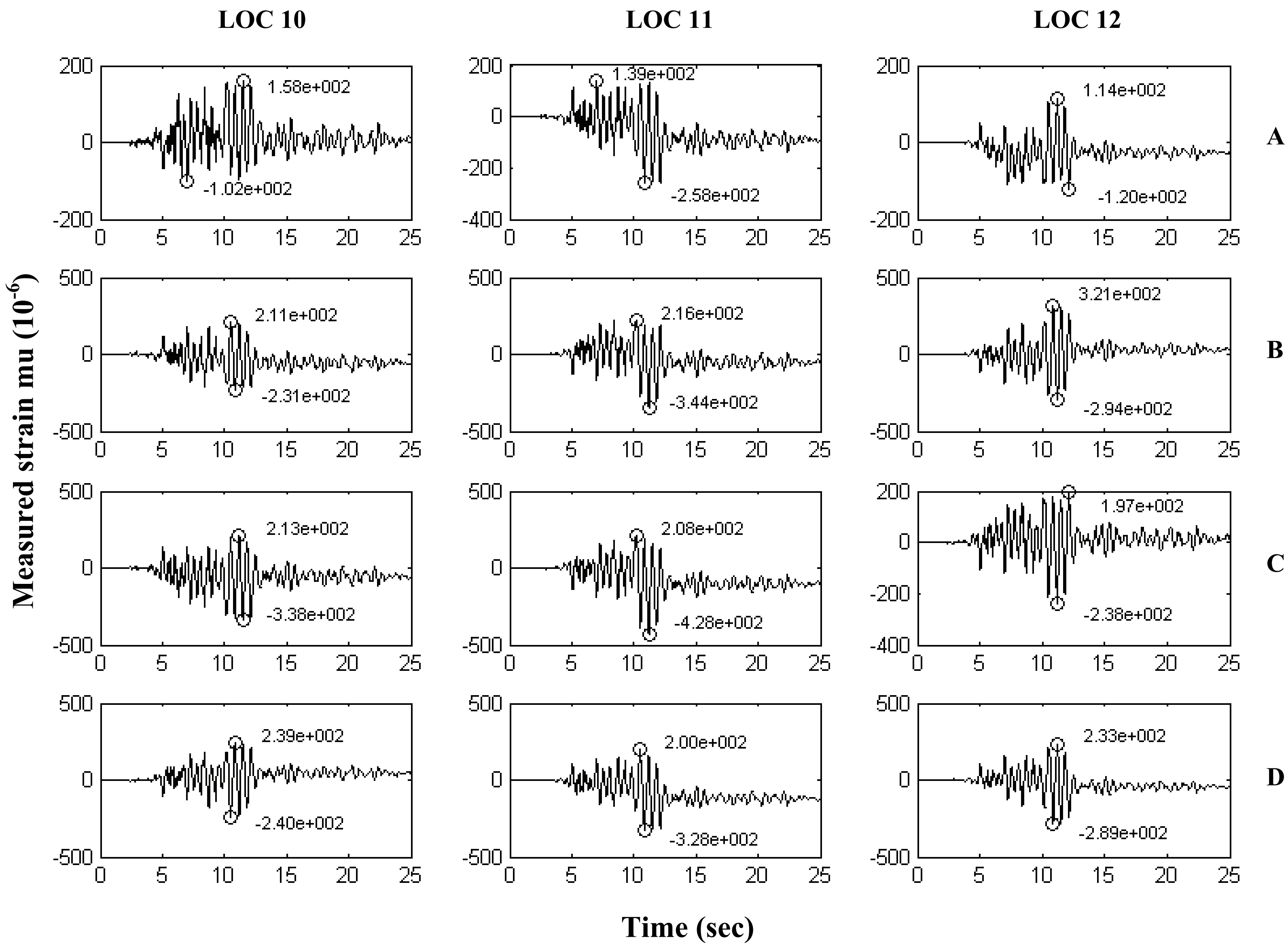

Figure S.5: Moment connection strain for LOC 10~12 during Seismic test 1

Appendix S

Seismic test 1, Moment connection strain (LOC 13~15)

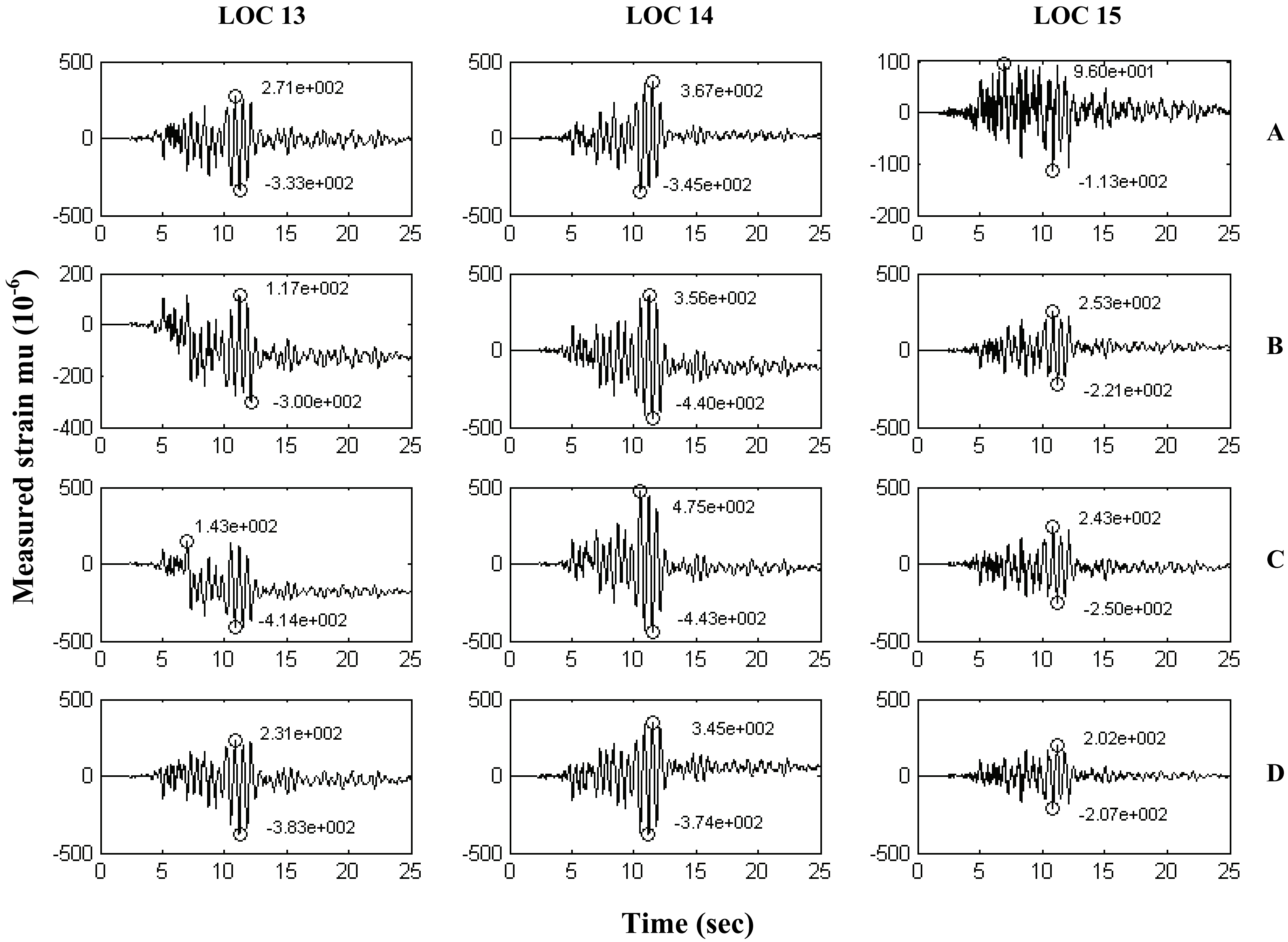

Figure S.6: Moment connection strain for LOC 13~15 during Seismic test 1

Appendix S

Seismic test 1, Moment connection strain (LOC 16~17)

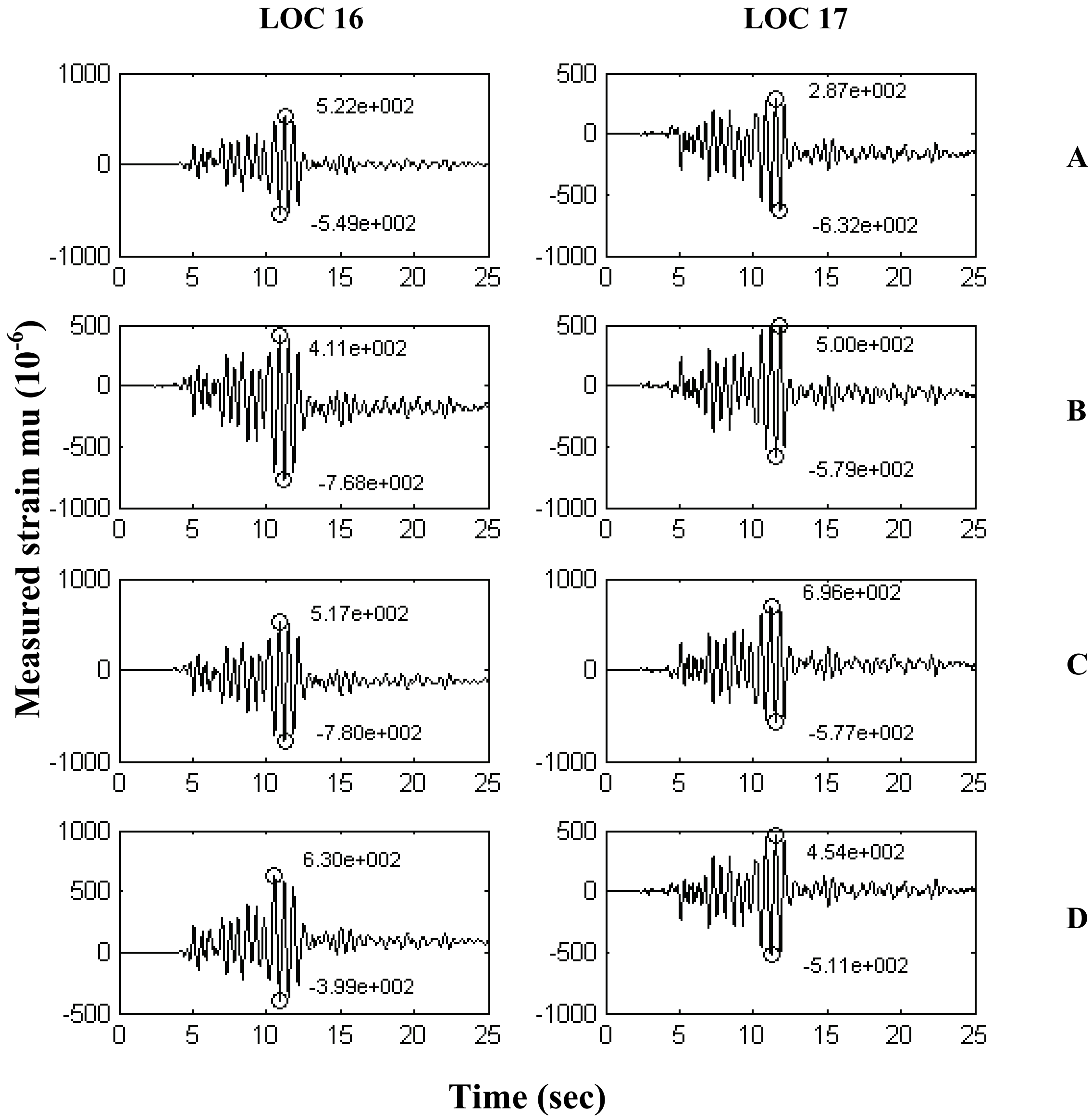

Figure S.7: Moment connection strain for LOC 16~17 during Seismic test 1

Appendix S

Seismic test 2, Moment connection strain (LOC 1~3)

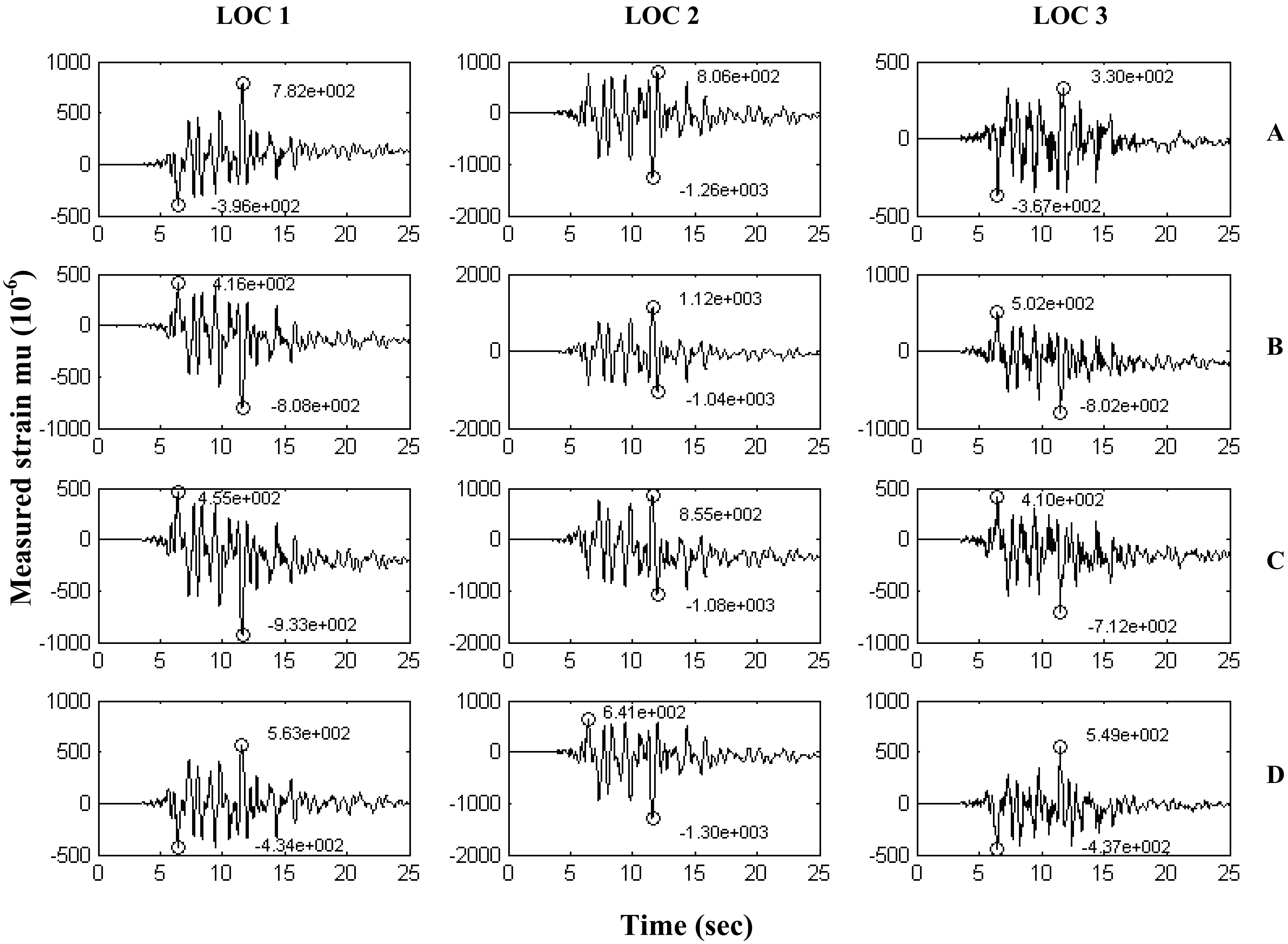

Figure S.8: Moment connection strain for LOC 1~3 during Seismic test 2

Appendix S

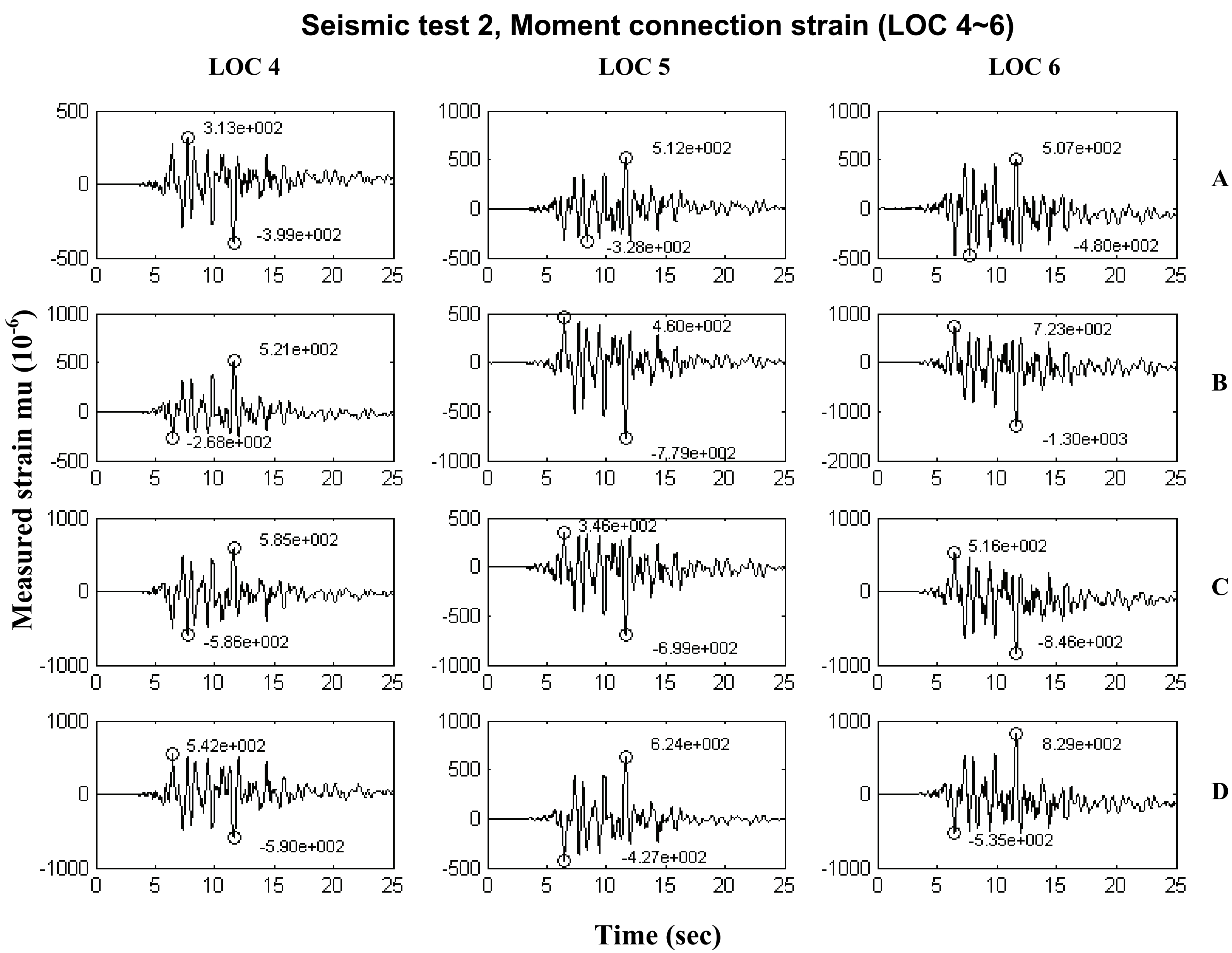

Figure S.9: Moment connection strain for LOC 4~6 during Seismic test 2

Appendix S

Seismic test 2, Moment connection strain (LOC 7~9)

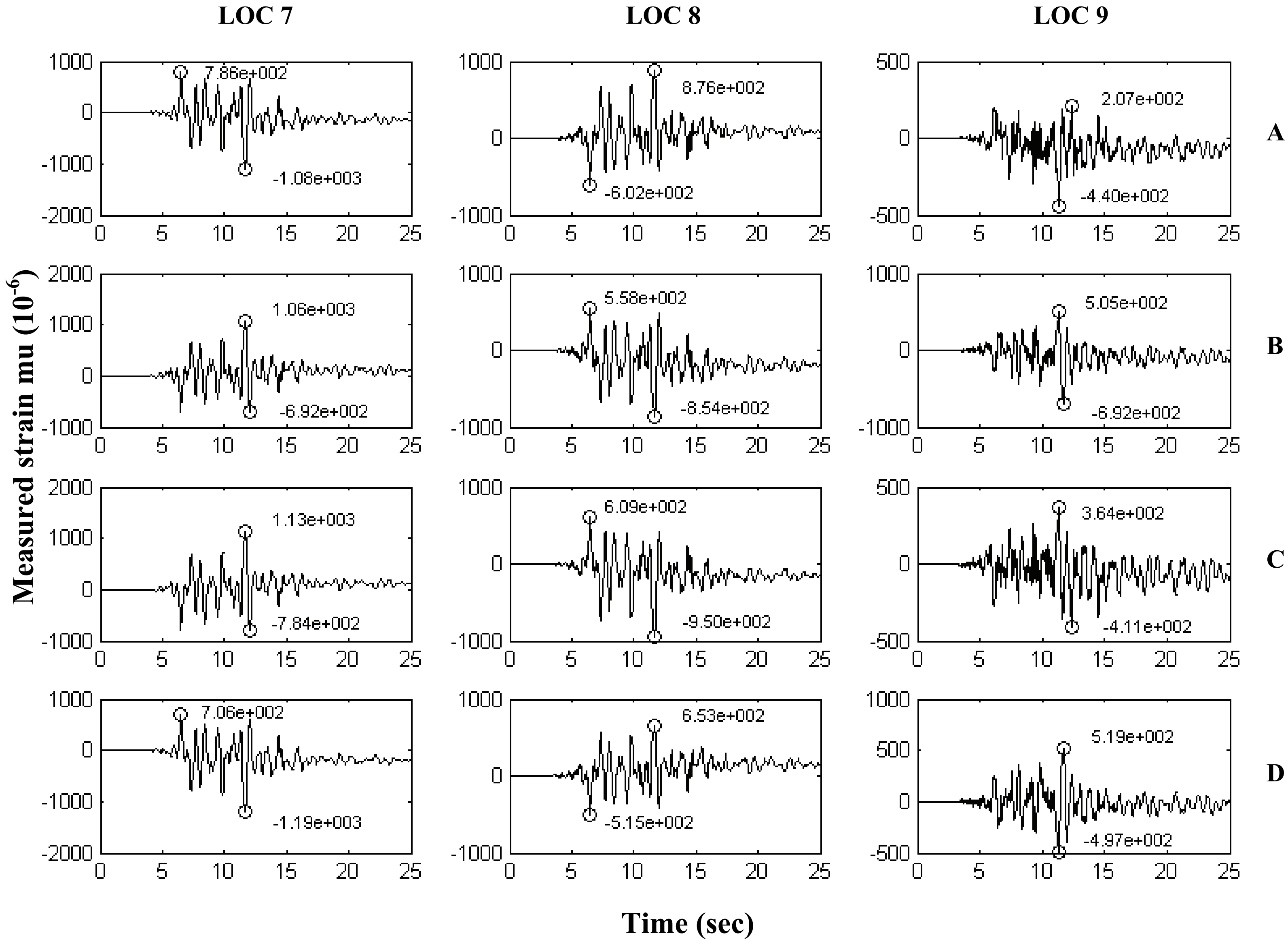

Figure S.10: Moment connection strain for LOC 7~9 during Seismic test 2

Appendix S

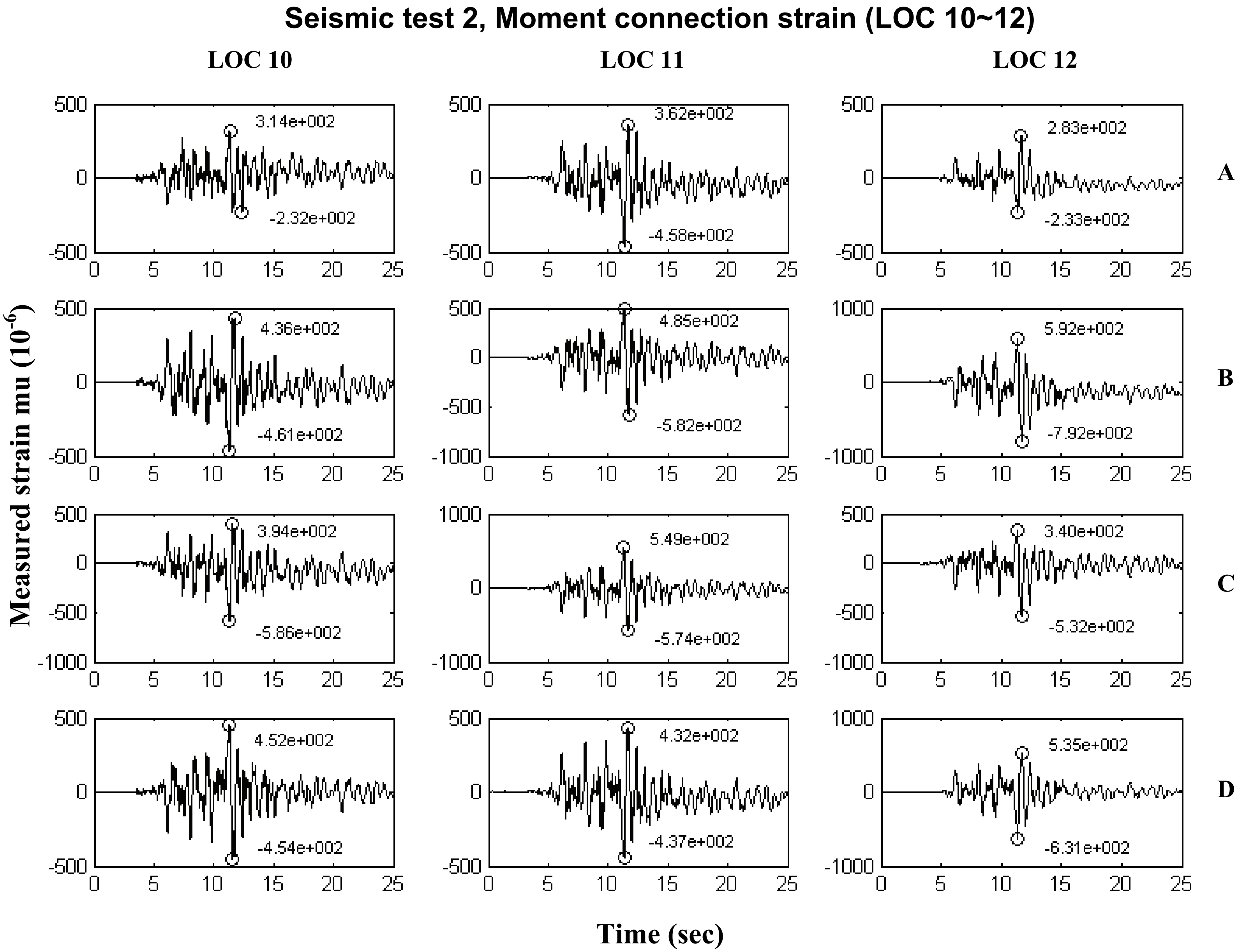

Figure S.11: Moment connection strain for LOC 10~12 during Seismic test 2

Appendix S

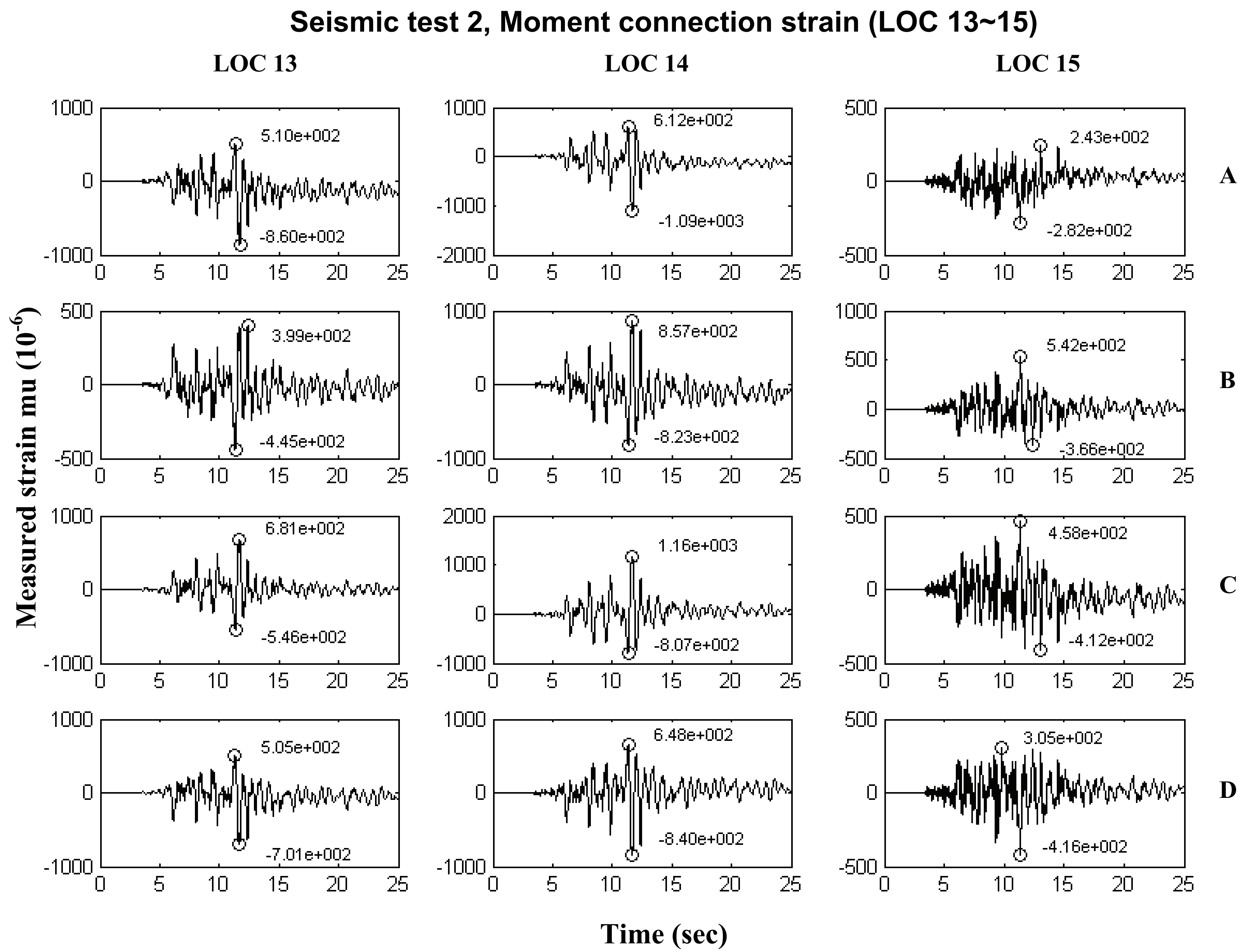

Figure S.12: Moment connection strain for LOC 13~15 during Seismic test 2

Seismic test 2, Moment connection strain (LOC 16~17)

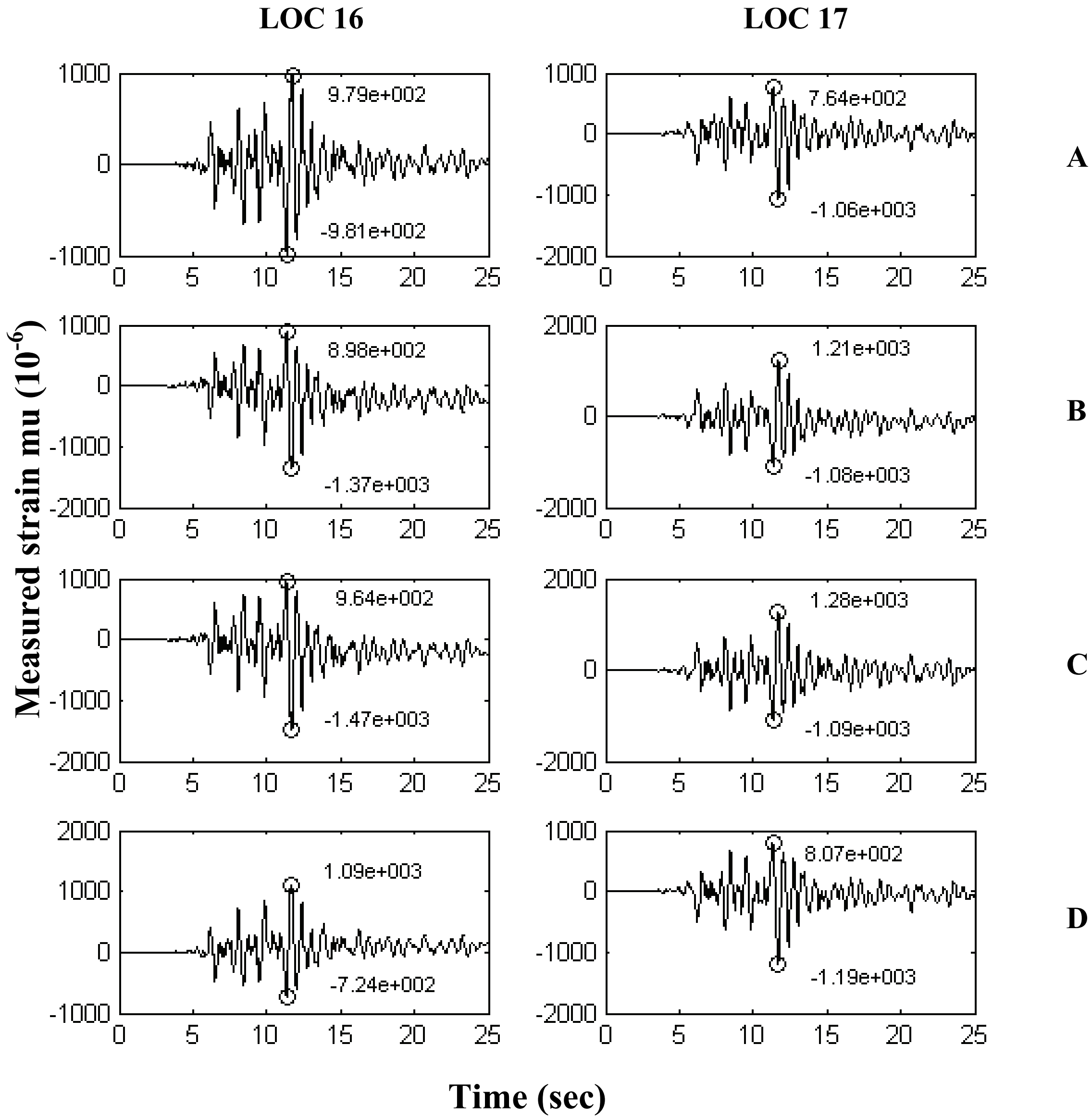

Figure S.13: Moment connection strain for LOC 16~17 during Seismic test 2

Appendix S

Seismic test 3, Moment connection strain (LOC 1~3)

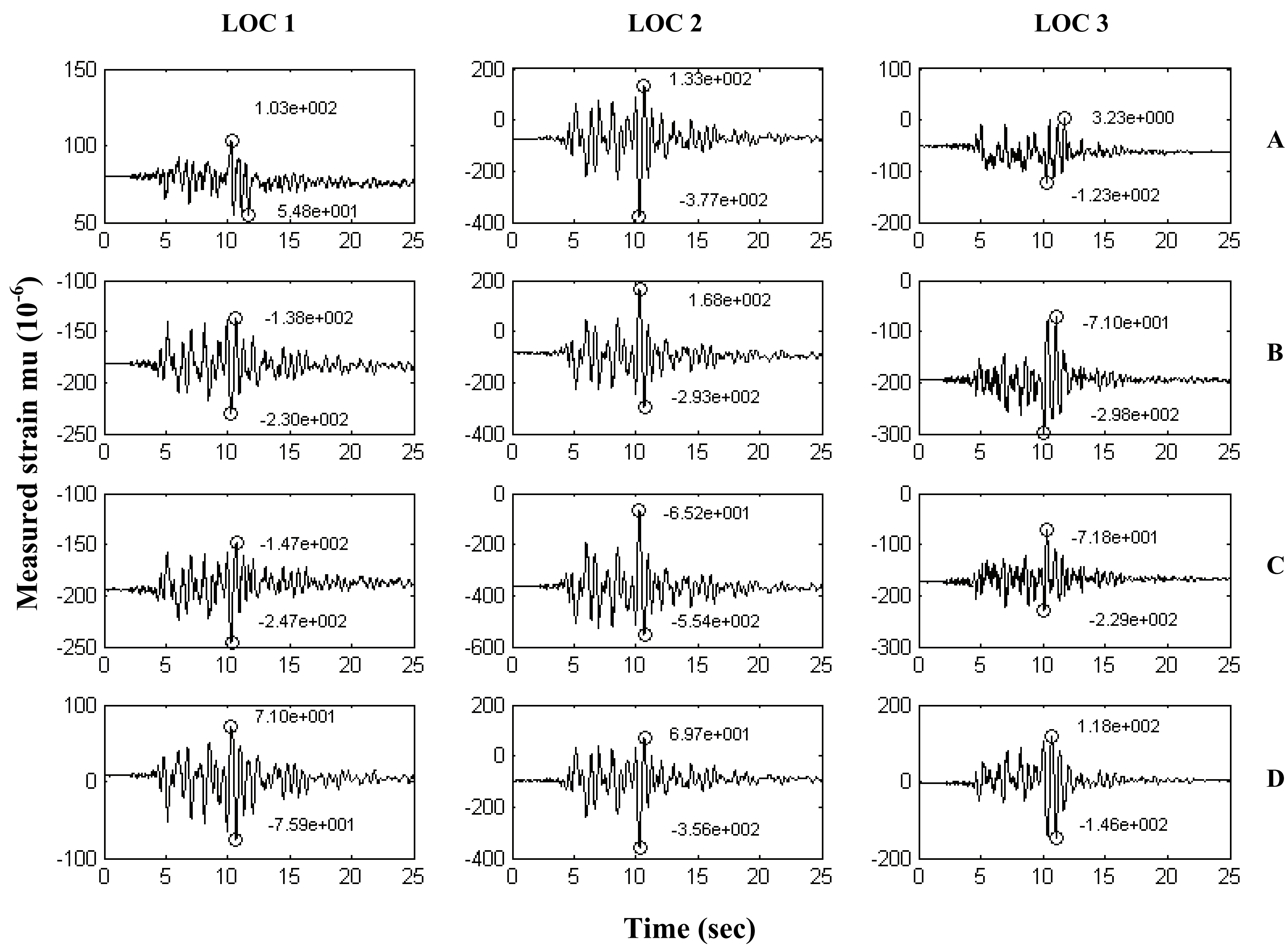

Figure S.14: Moment connection strain for LOC 1~3 during Seismic test 3

Appendix S

Seismic test 3, Moment connection strain (LOC 4~6)

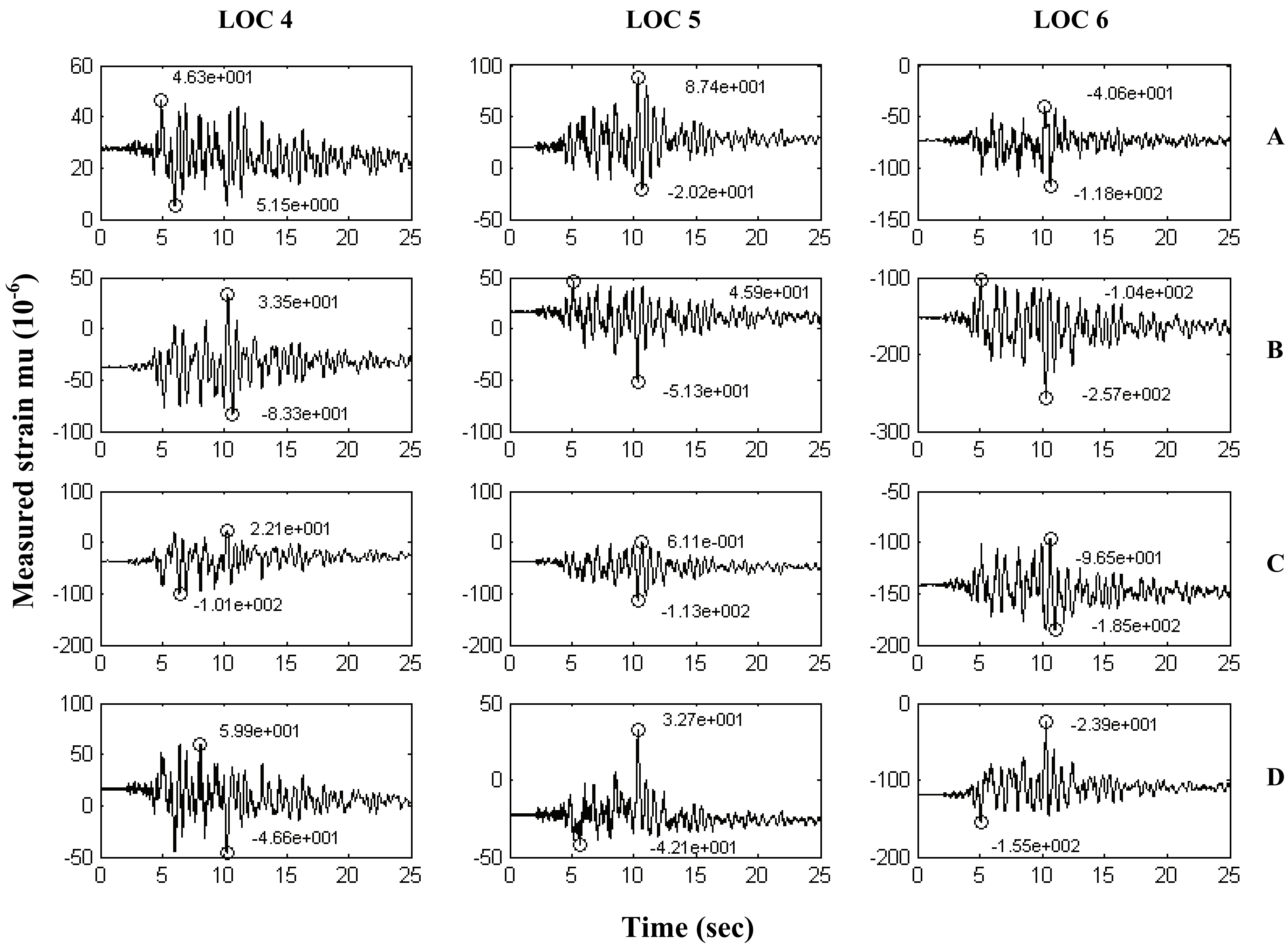

Figure S.15: Moment connection strain for LOC 4~6 during Seismic test 3

Appendix S

Seismic test 3, Moment connection strain (LOC 7~9)

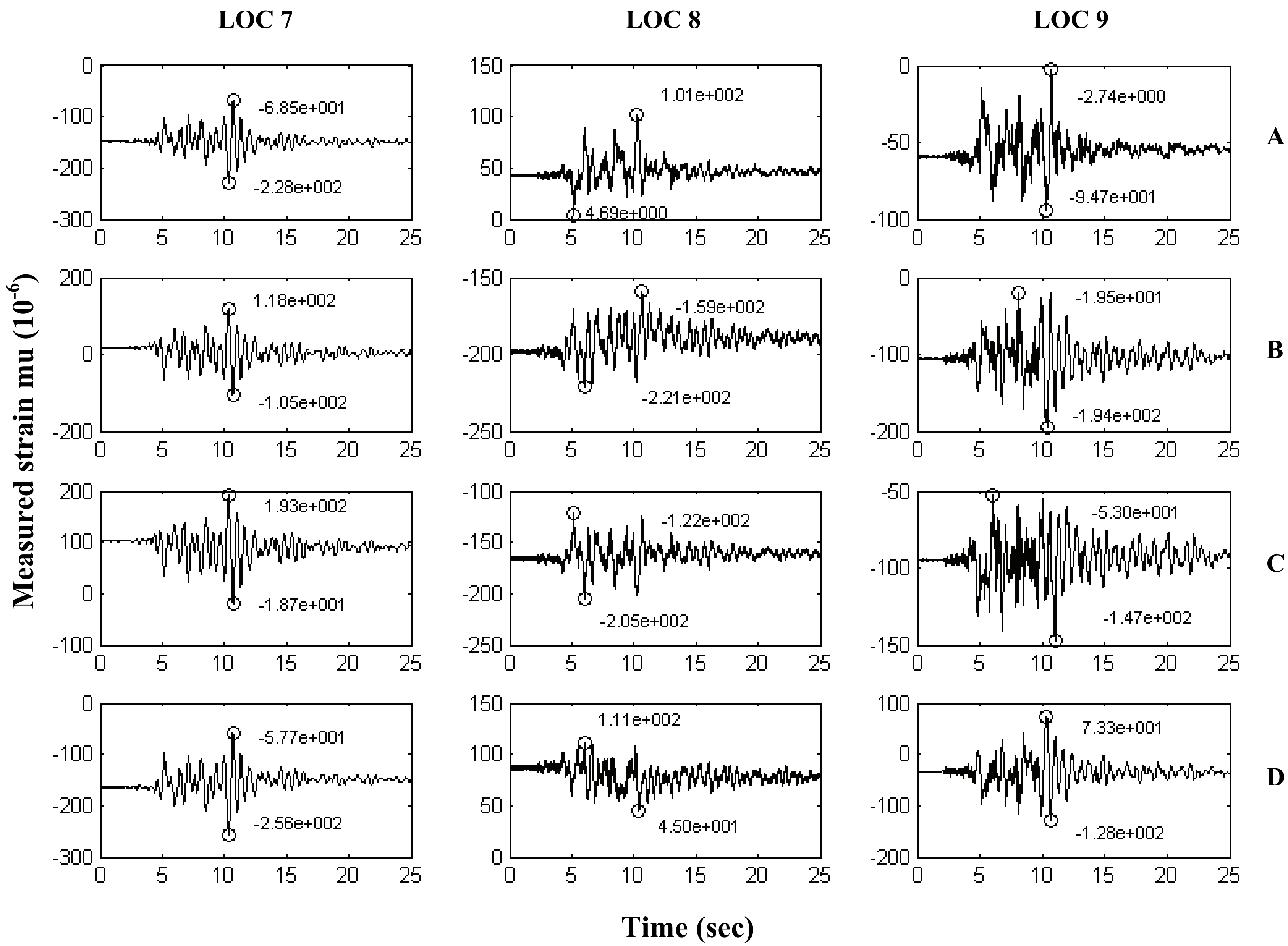

Figure S.16: Moment connection strain for LOC 7~9 during Seismic test 3

Appendix S

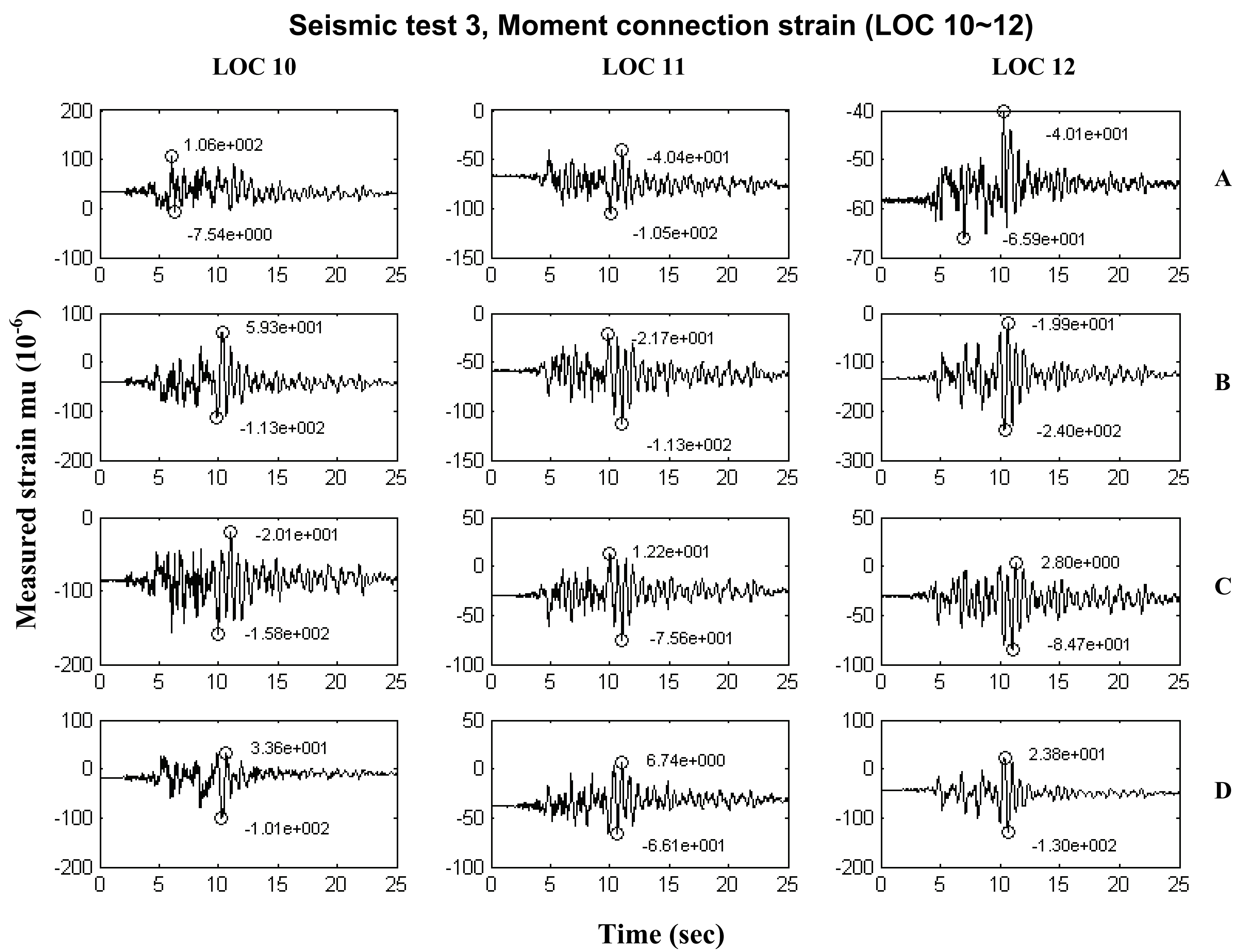

Figure S.17: Moment connection strain for LOC 10~12 during Seismic test 3

Appendix S

Seismic test 3, Moment connection strain (LOC 13~15)

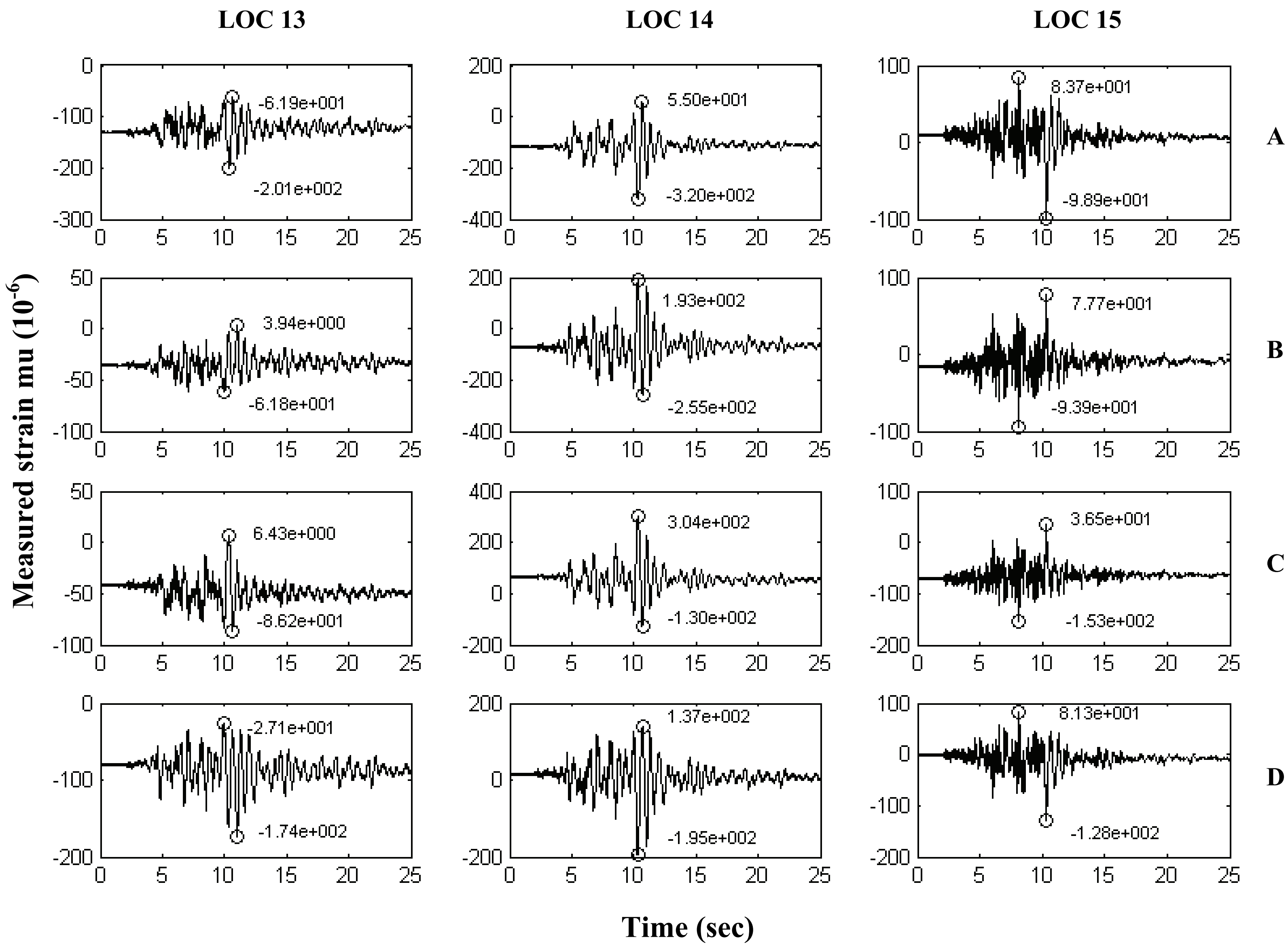

Figure S.18: Moment connection strain for LOC 13~15 during Seismic test 3

Appendix S

Seismic test 3, Moment connection strain (LOC 16~17)

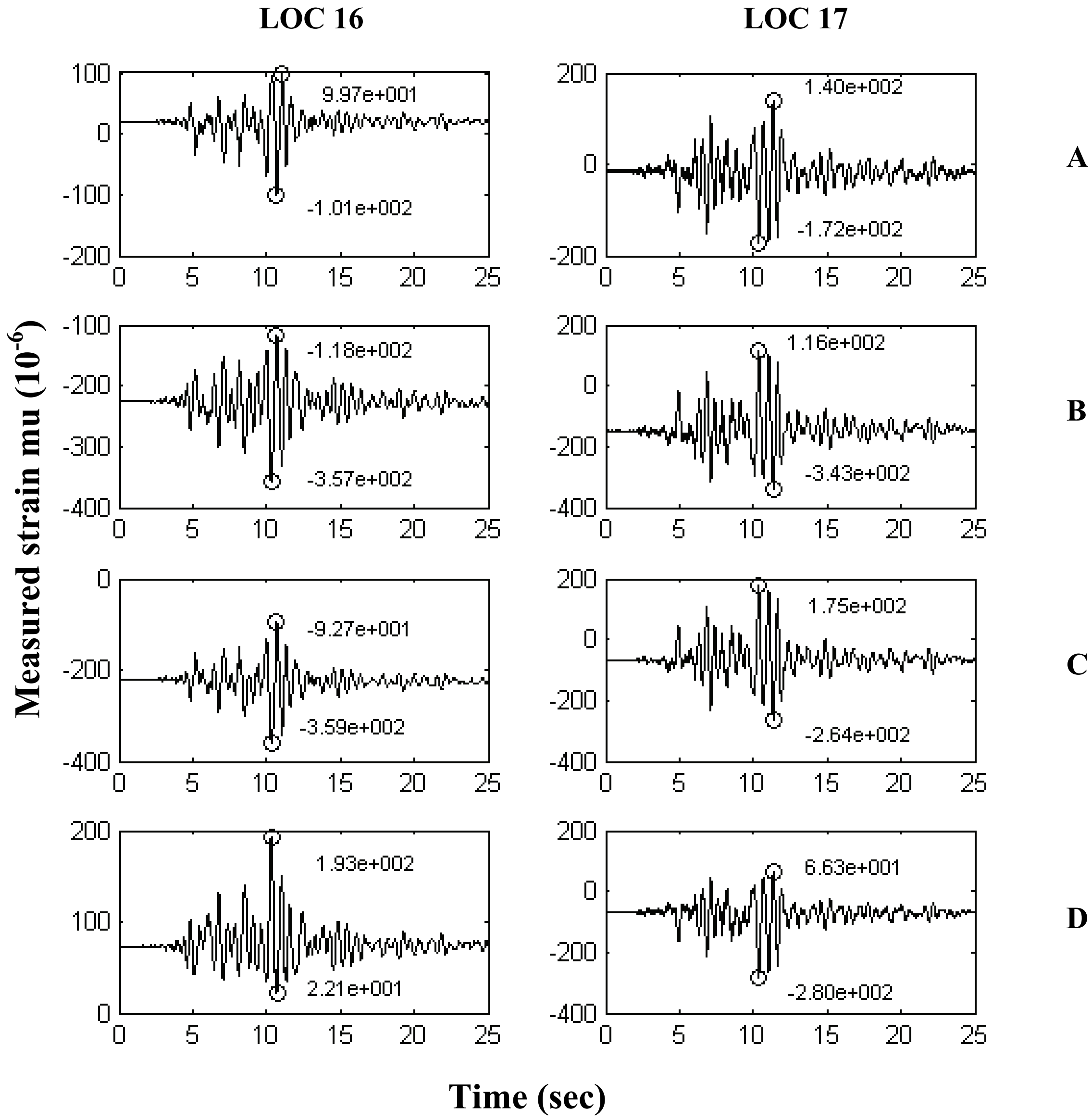

Figure S.19: Moment connection strain for LOC 16~17 during Seismic test 3

Appendix S

Seismic test 4, Moment connection strain (LOC 1~3)

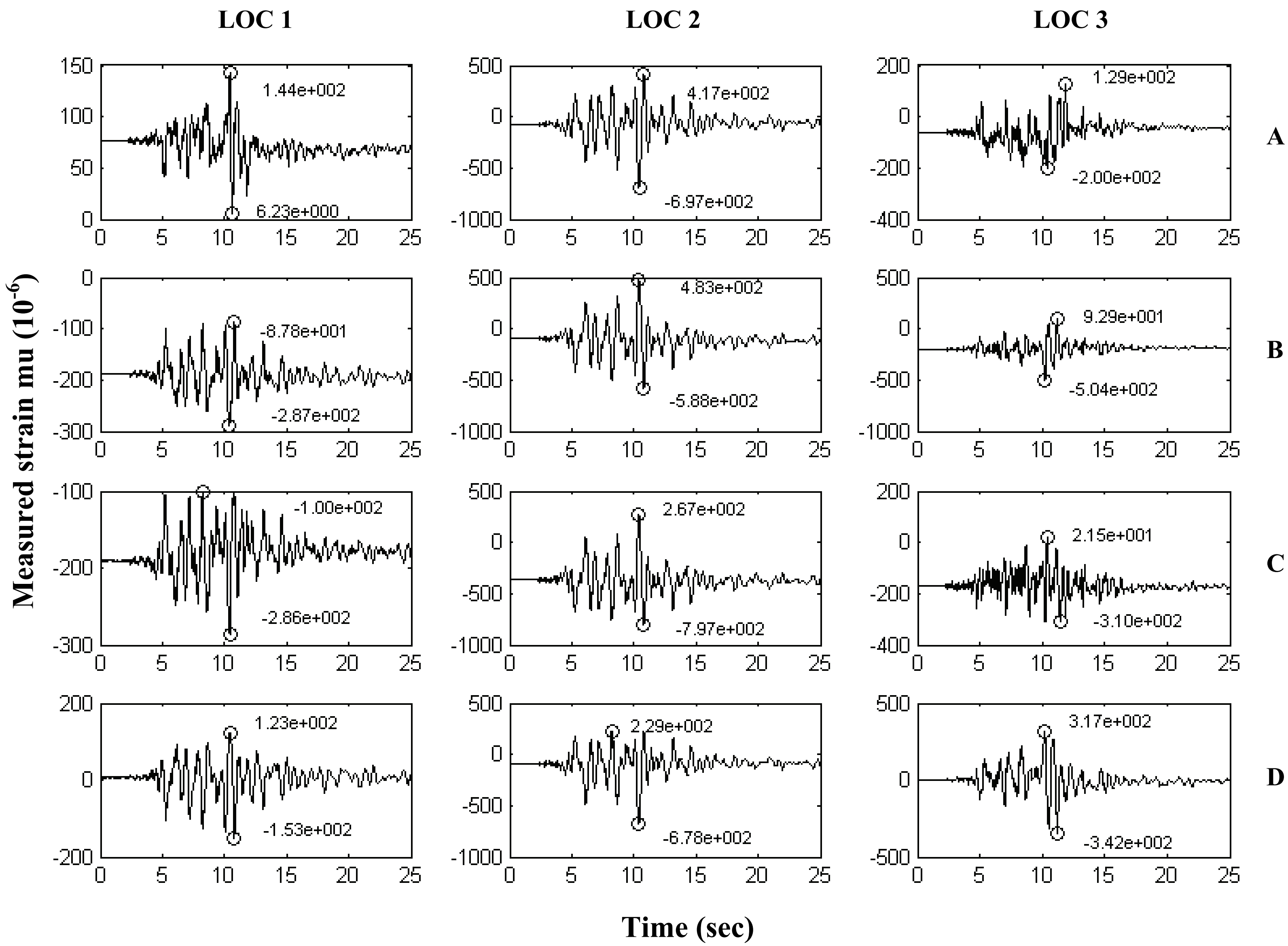

Figure S.20: Moment connection strain for LOC 1~3 during Seismic test 4

Appendix S

Seismic test 4, Moment connection strain (LOC 4~6)

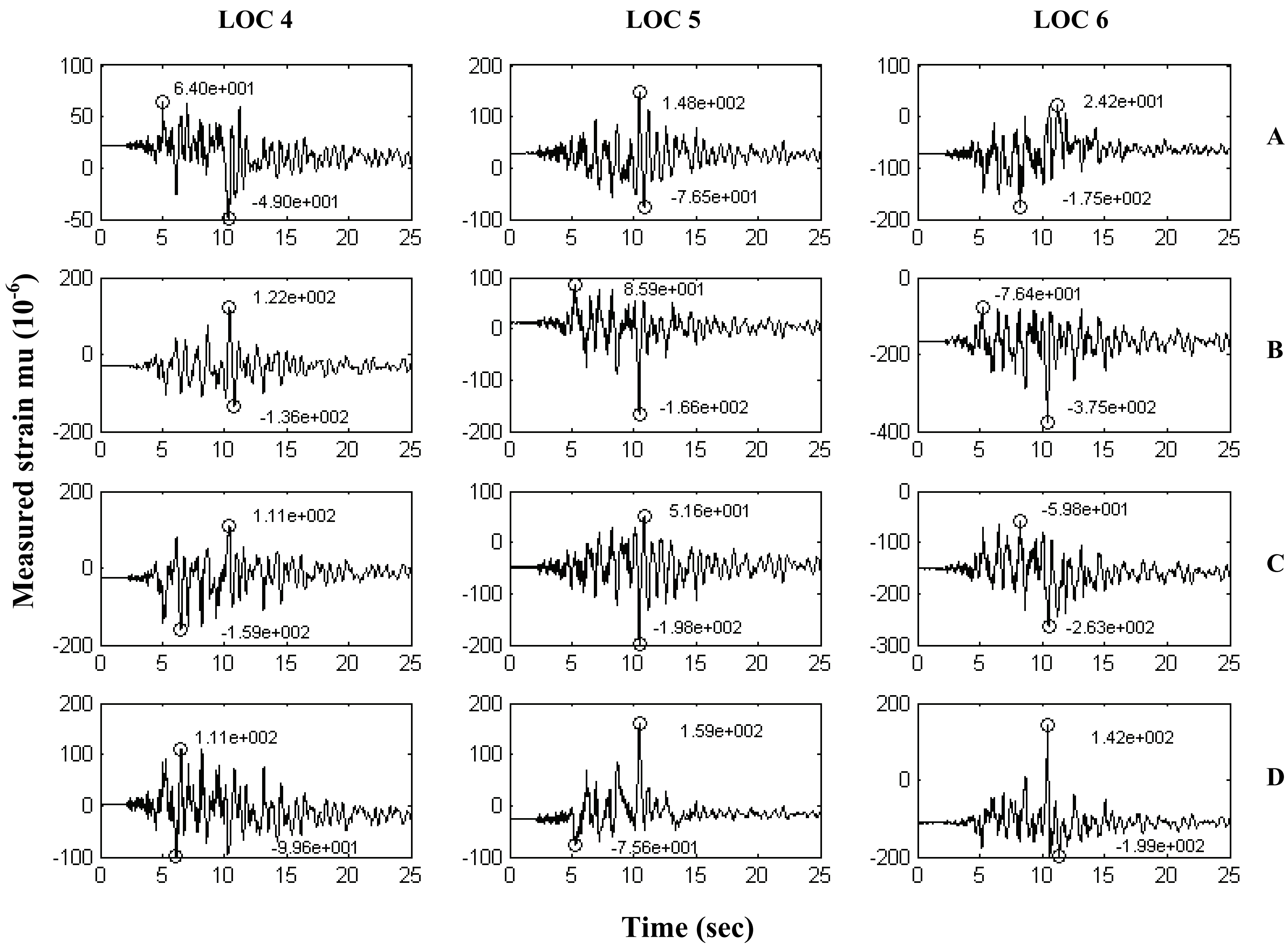

Figure S.21: Moment connection strain for LOC 4~6 during Seismic test 4

Appendix S

Seismic test 4, Moment connection strain (LOC 7~9)

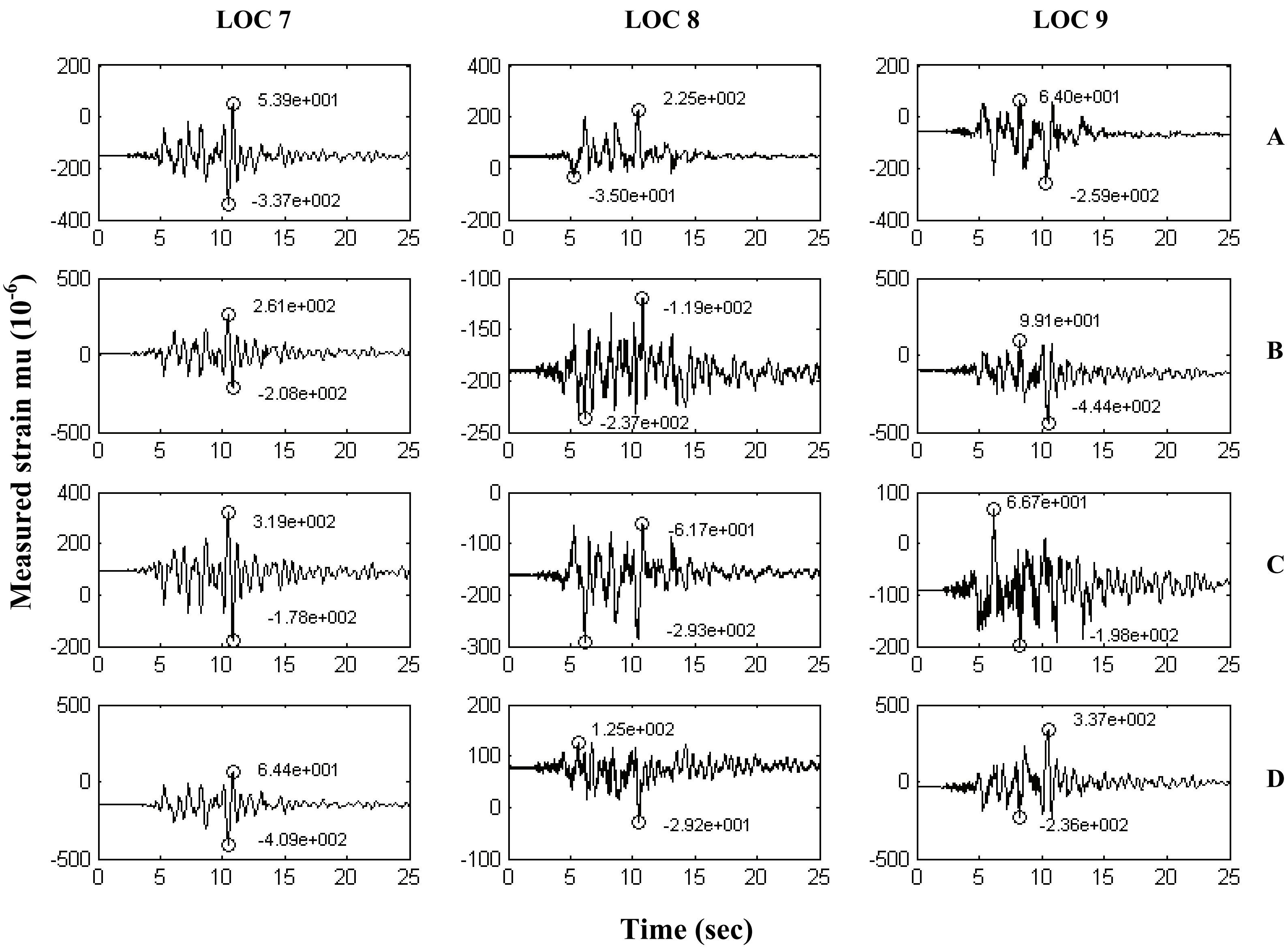

Figure S.22: Moment connection strain for LOC 7~9 during Seismic test 4

Appendix S

Seismic test 4, Moment connection strain (LOC 10~12)

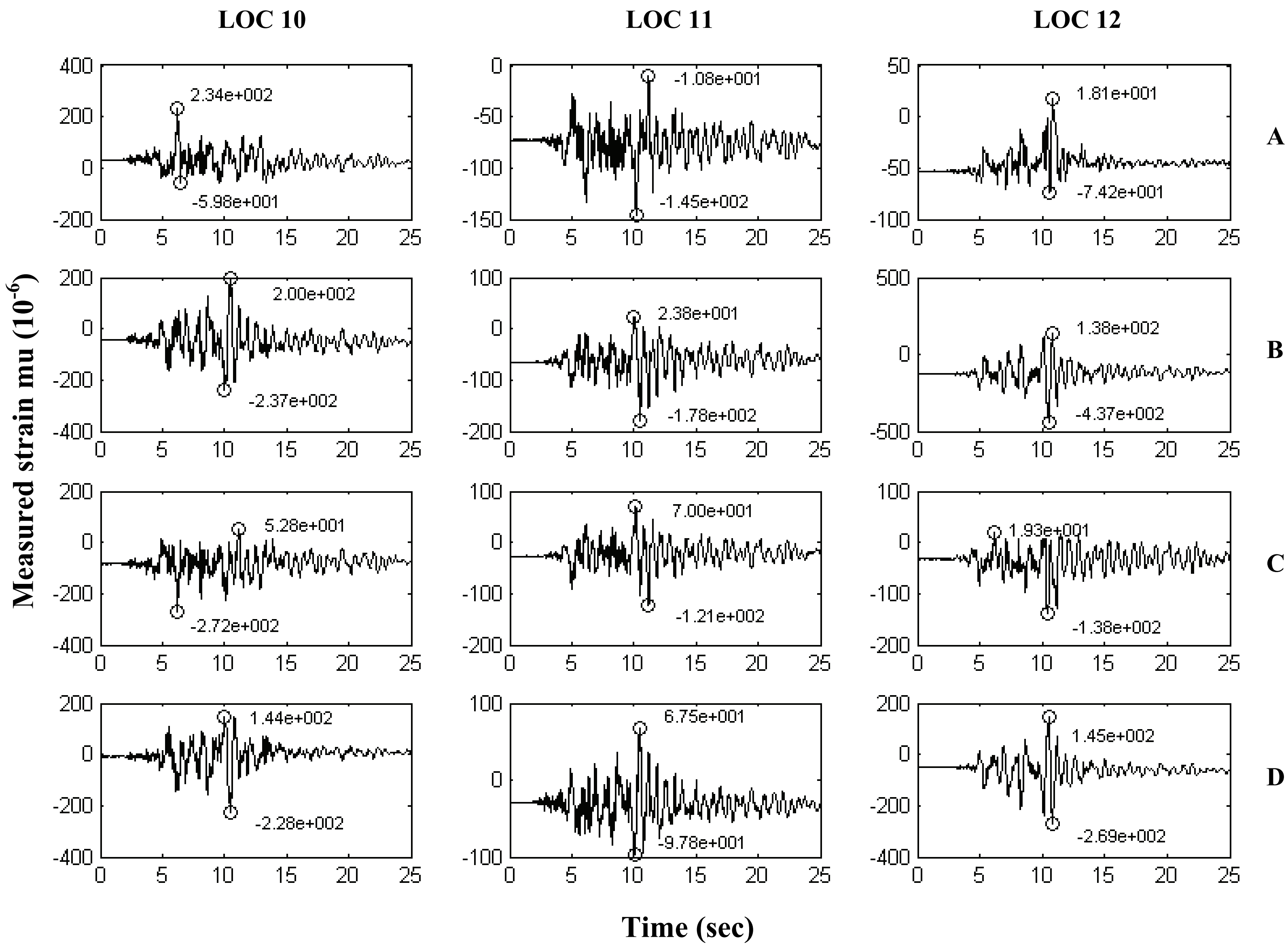

Figure S.23: Moment connection strain for LOC 10~12 during Seismic test 4

Appendix S

Seismic test 4, Moment connection strain (LOC 13~15)

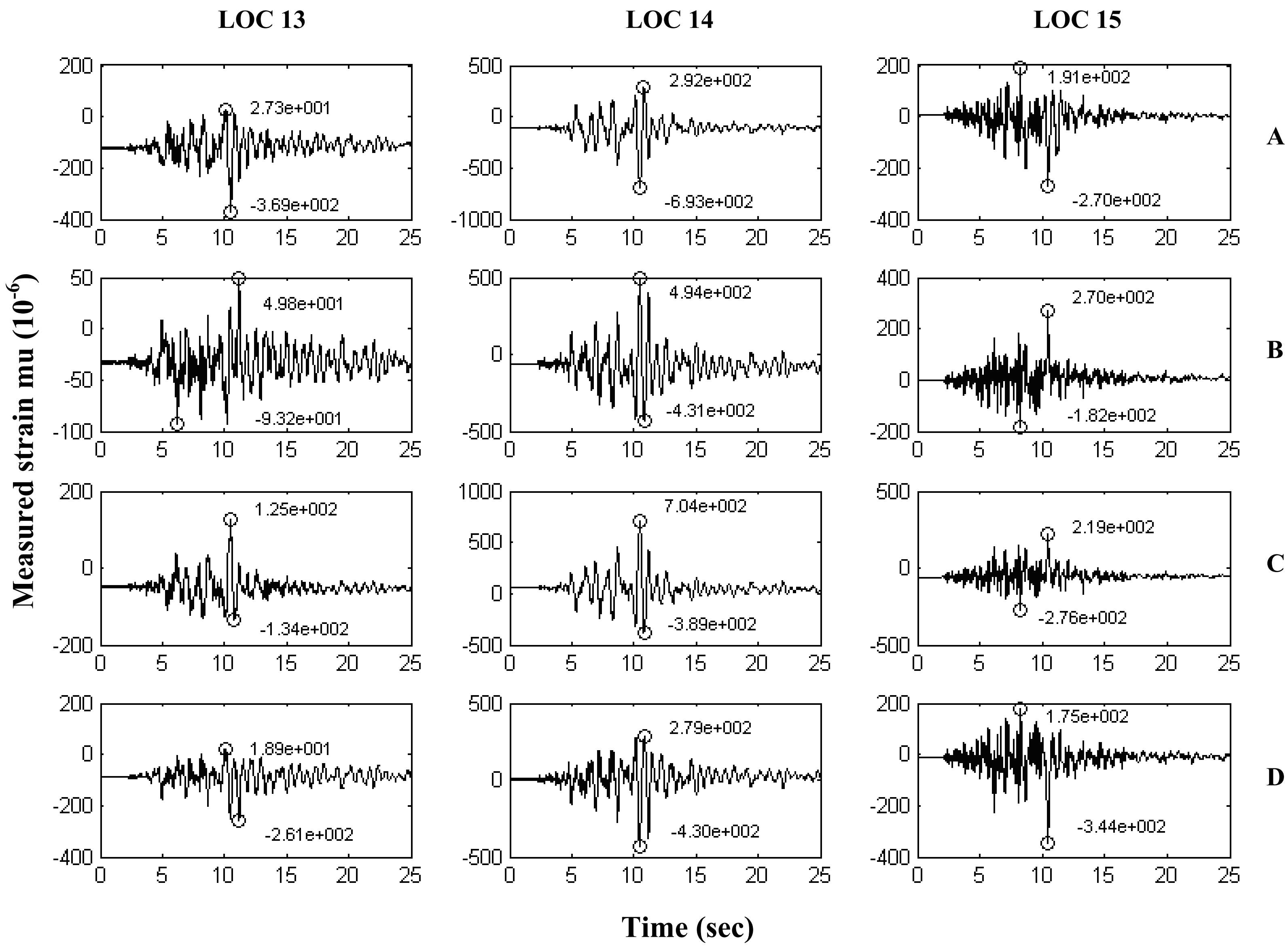

Figure S.24: Moment connection strain for LOC 13~15 during Seismic test 4

Appendix S

Seismic test 4, Moment connection strain (LOC 16~17)

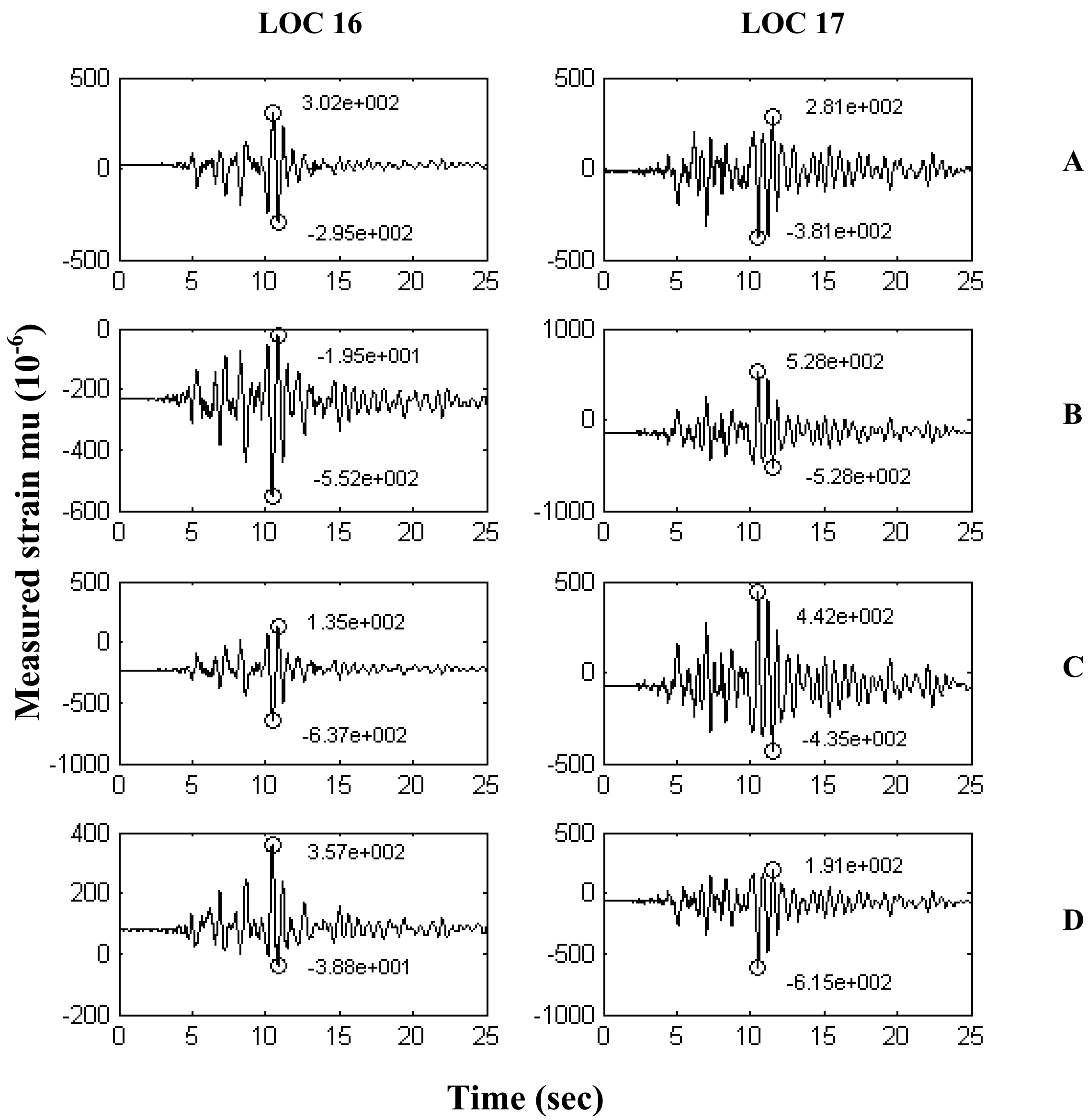

Figure S.25: Moment connection strain for LOC 16~17 during Seismic test 4

Appendix S

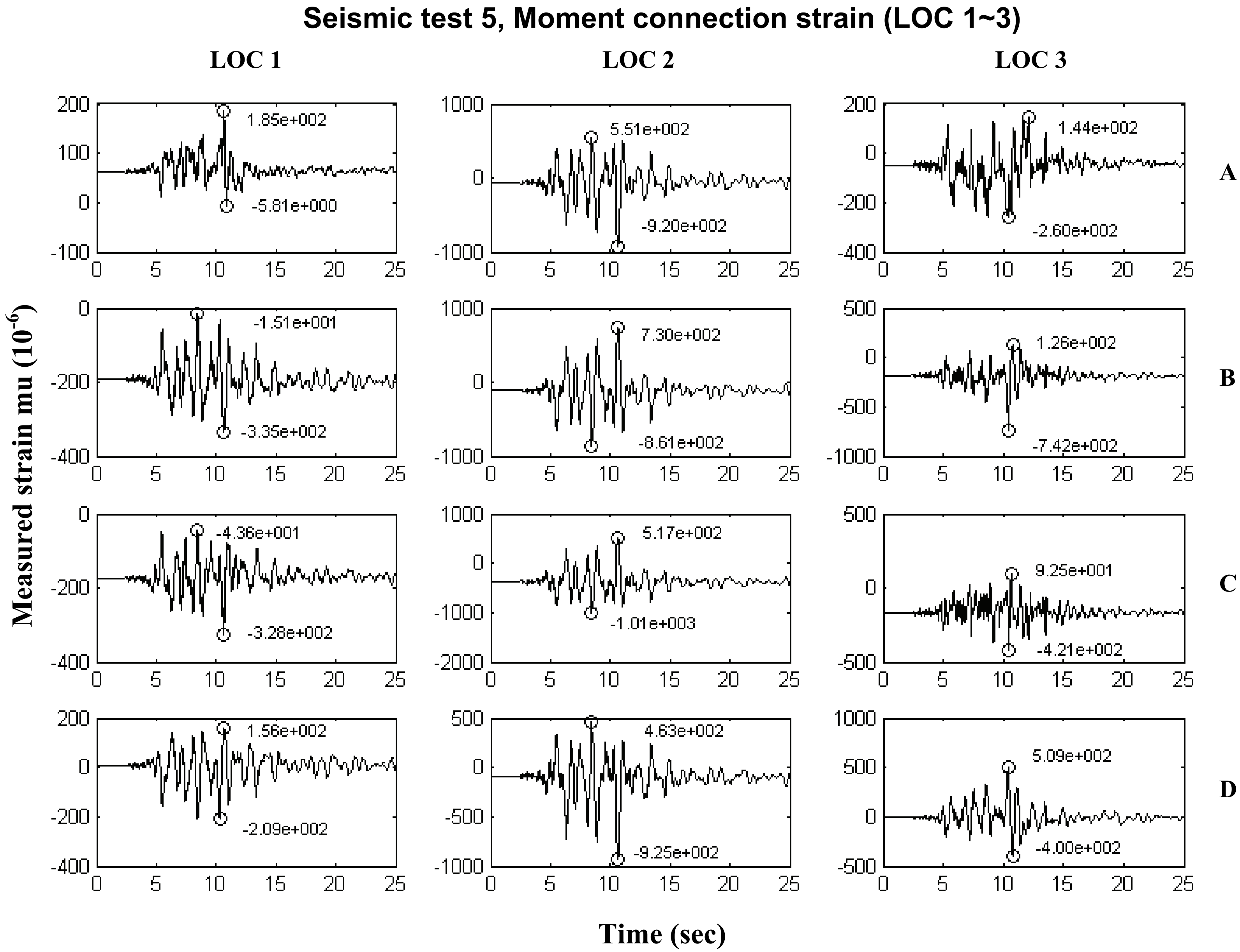

Figure S.26: Moment connection strain for LOC 1~3 during Seismic test 5

Appendix S

Seismic test 5, Moment connection strain (LOC 4~6)

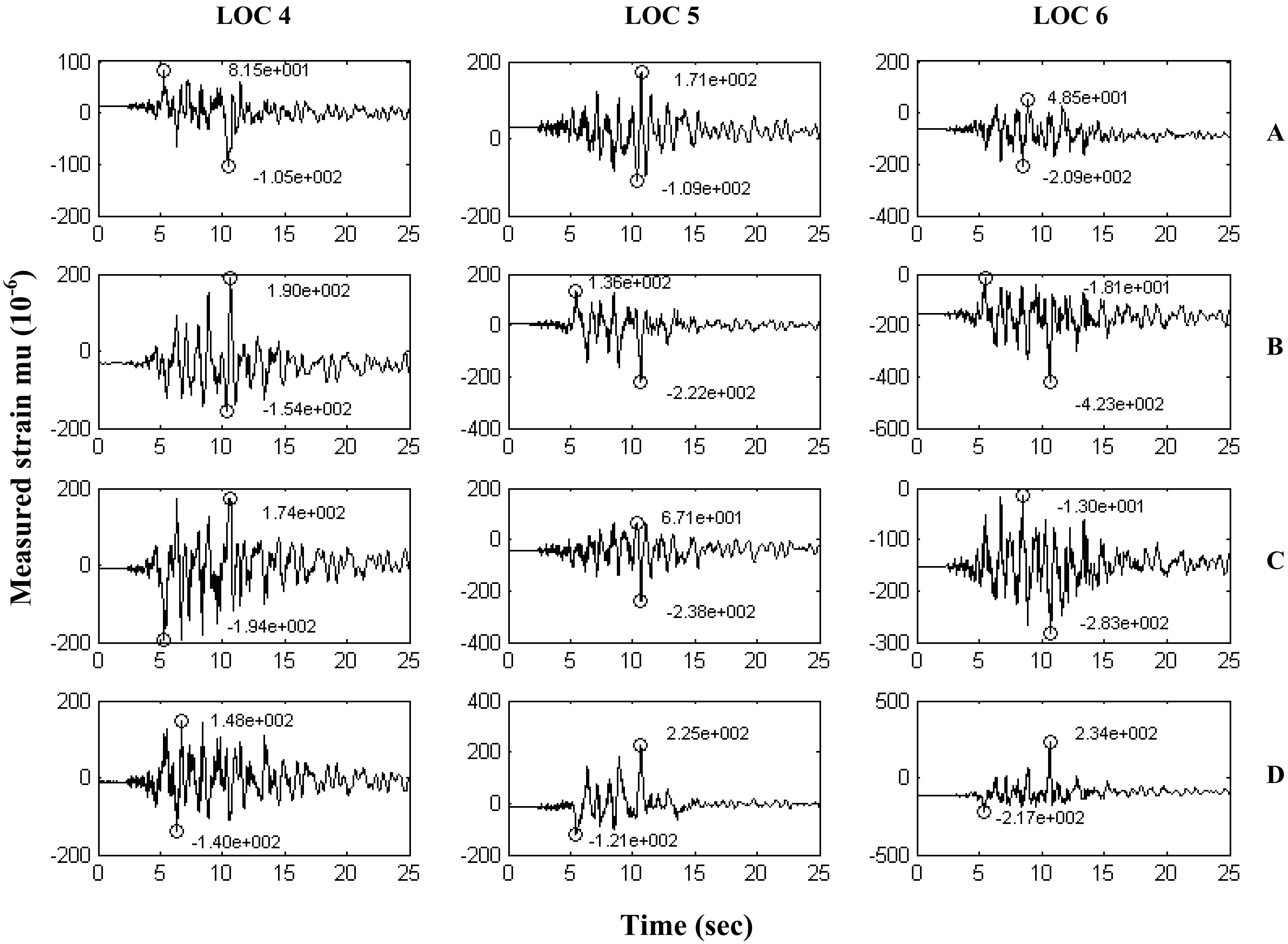

Figure S.27: Moment connection strain for LOC 4~6 during Seismic test 5

Appendix S

Seismic test 5, Moment connection strain (LOC 7~9)

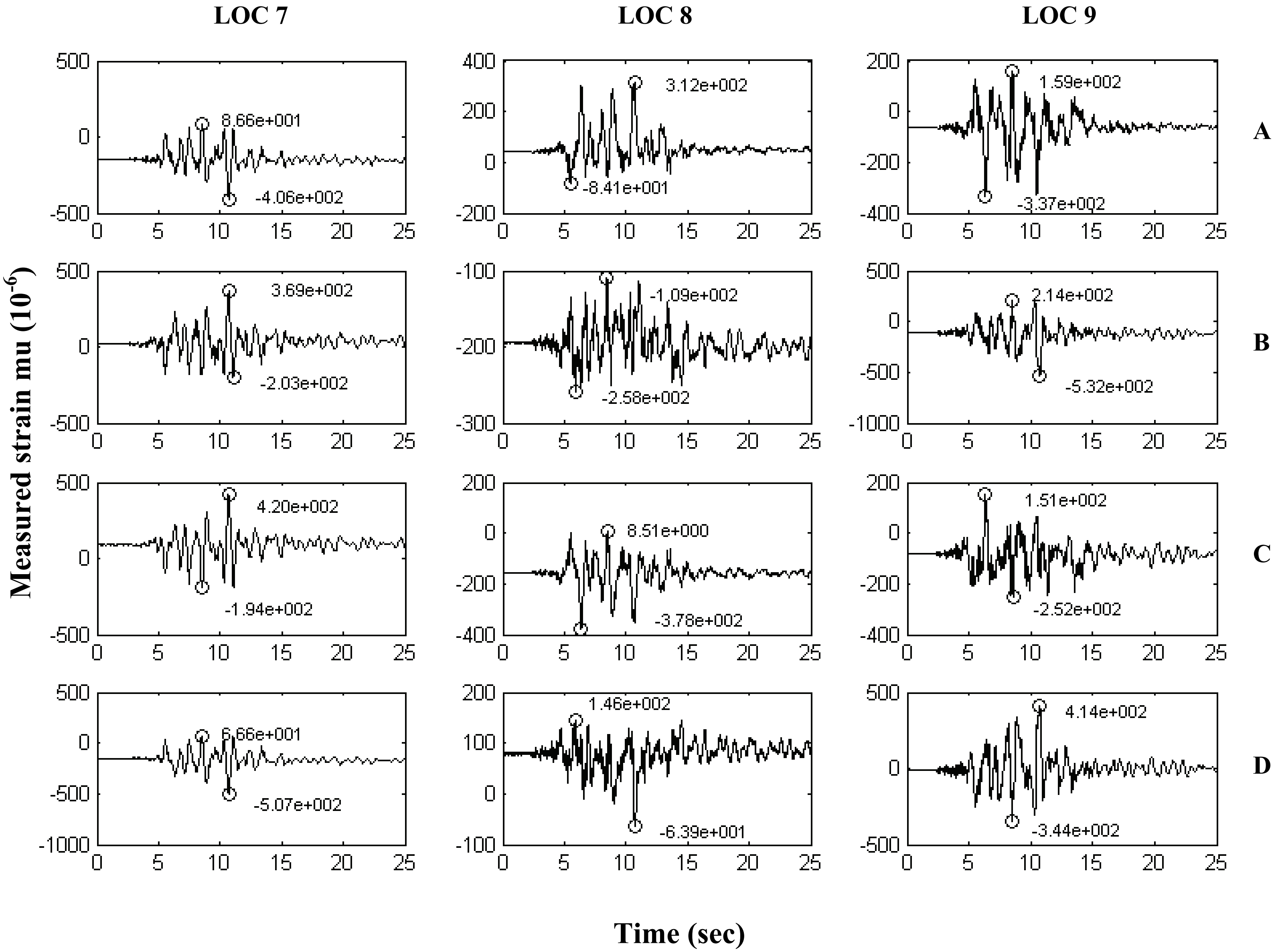

Figure S.28: Moment connection strain for LOC 7~9 during Seismic test 5

Appendix S

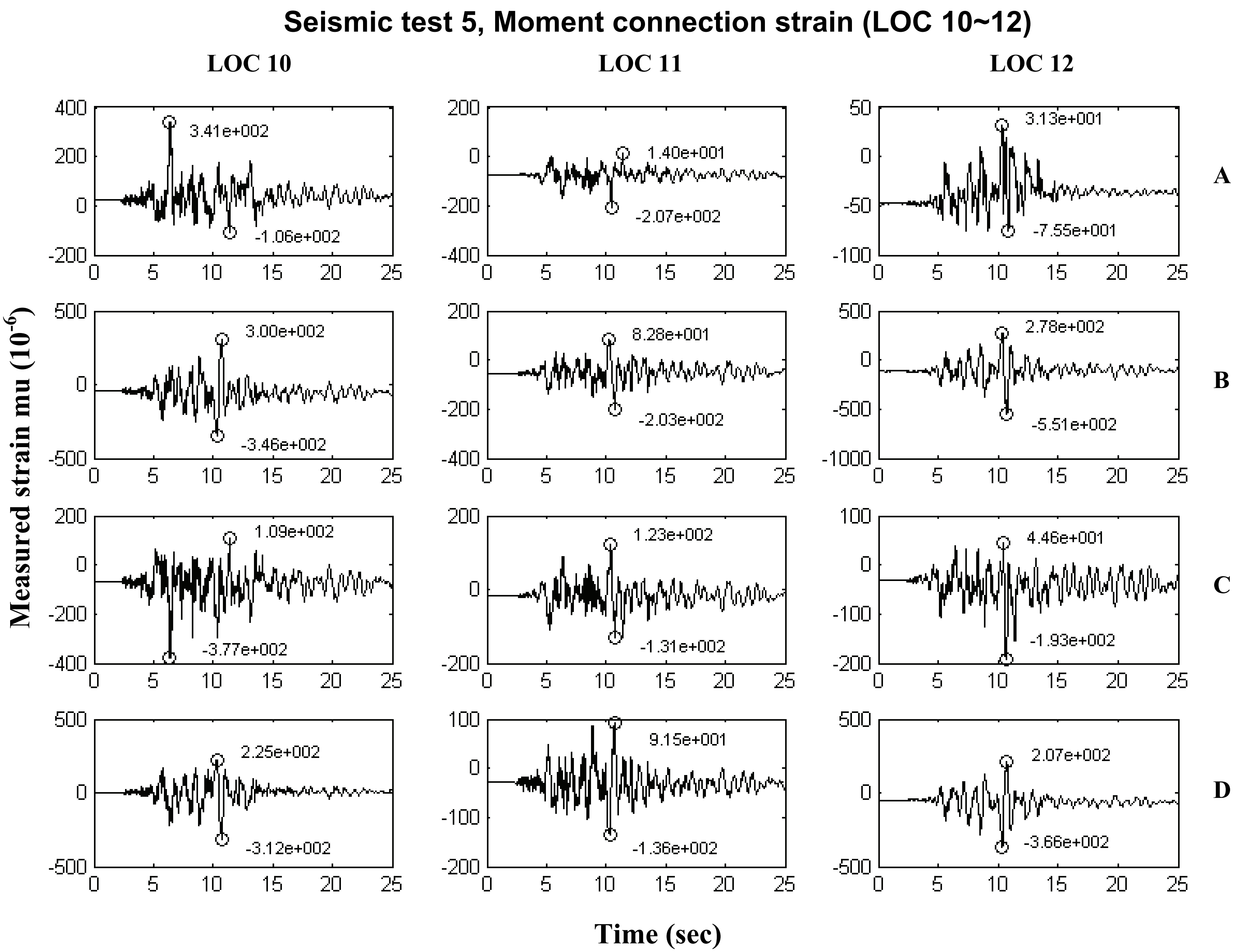

Figure S.29: Moment connection strain for LOC 10~12 during Seismic test 5

Appendix S

Seismic test 5, Moment connection strain (LOC 13~15)

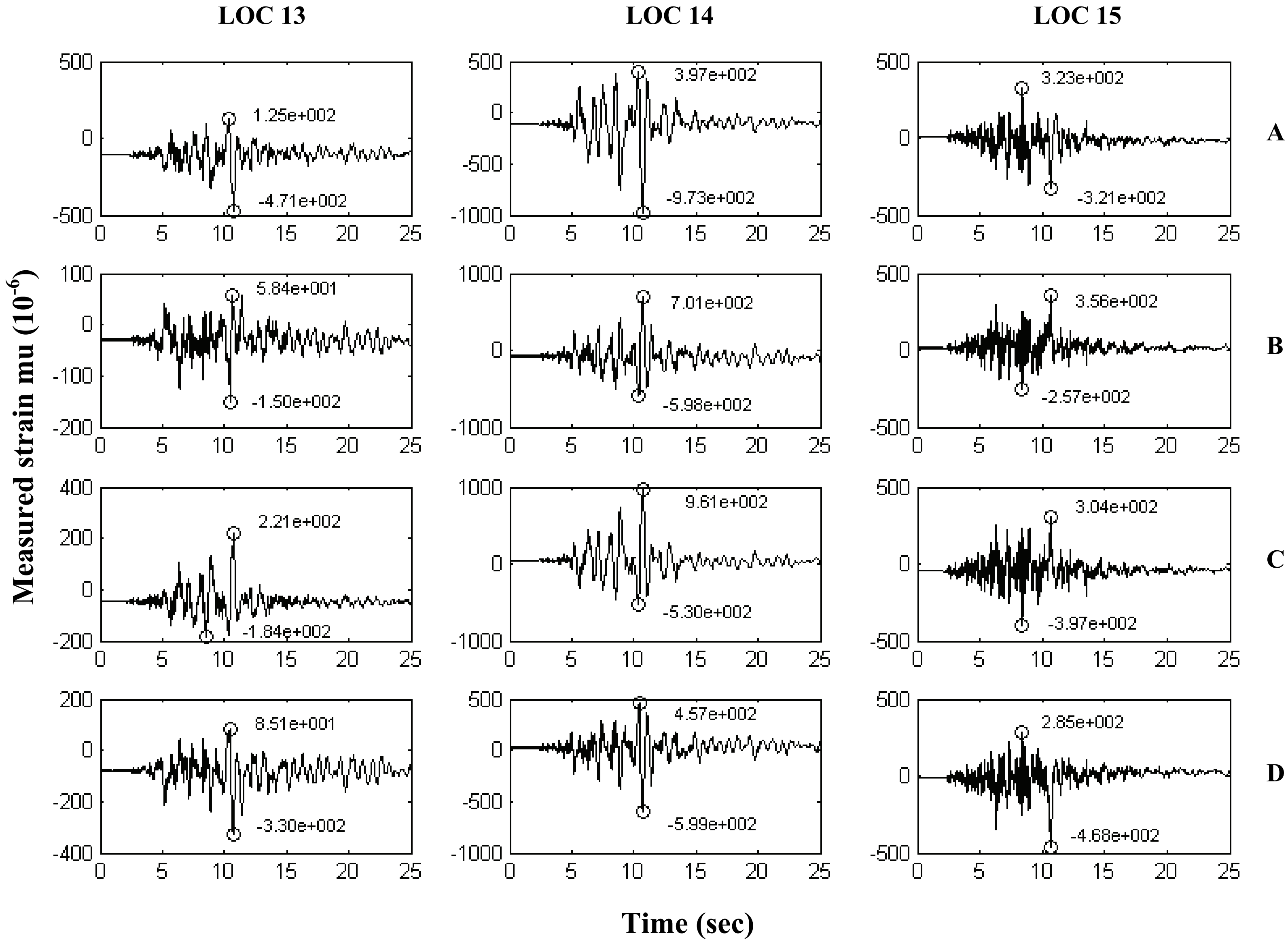

Figure S.30: Moment connection strain for LOC 13~15 during Seismic test 5

Appendix S

Seismic test 5, Moment connection strain (LOC 16~17)

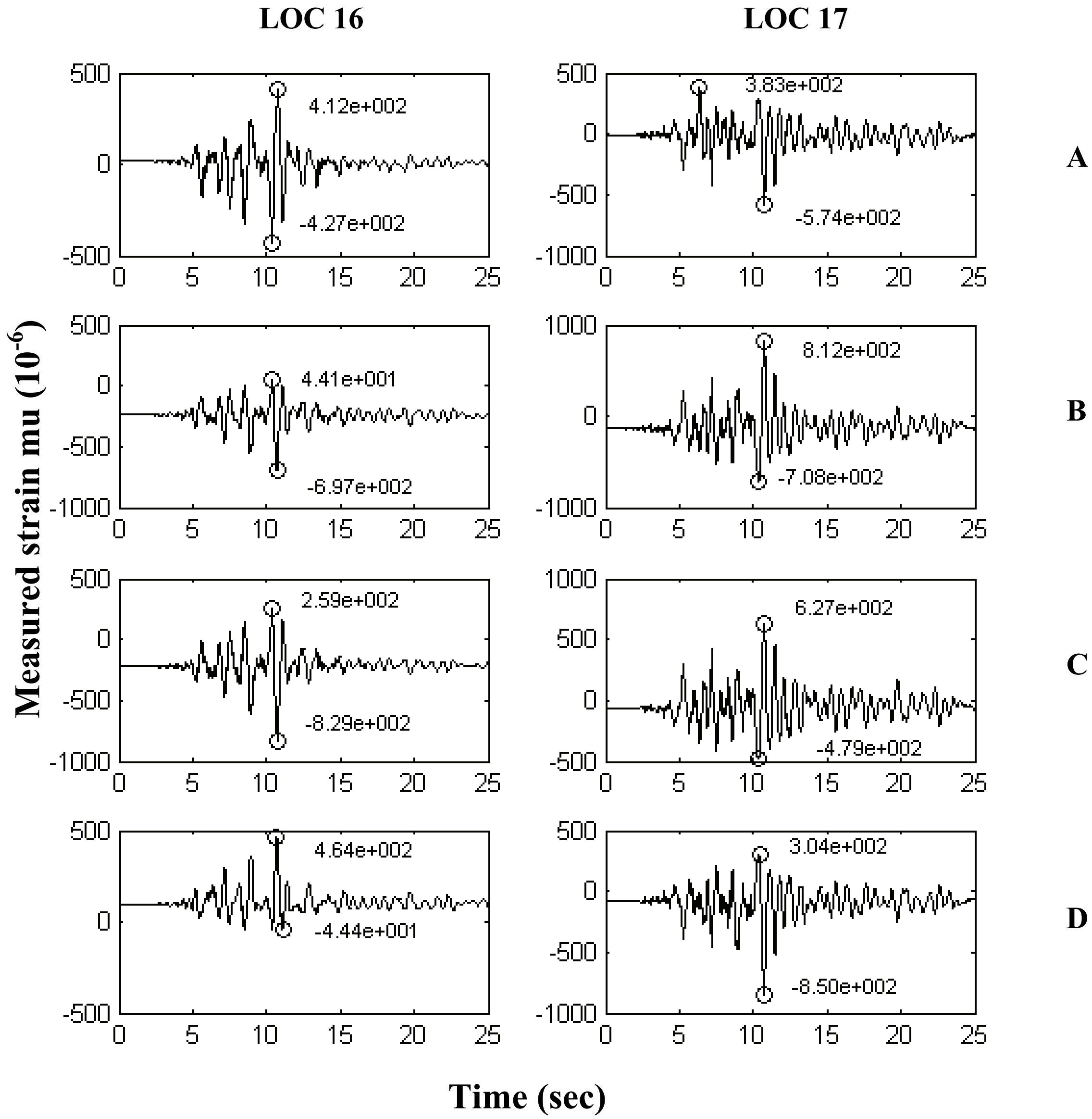

Figure S.31: Moment connection strain for LOC 16~17 during Seismic test 5

MCEER
EARTHQUAKE ENGINEERING TO EXTREME EVENTS

University at Buffalo, The State University of New York
Red Jacket Quadrangle ▪ Buffalo, New York 14261
Phone: (716) 645-3391 ▪ Fax: (716) 645-3399
E-mail: *mceer@buffalo.edu* ▪ WWW Site *http://mceer.buffalo.edu*

University at Buffalo *The State University of New York*

ISSN 1520-295X